

DEVELOPMENT OF LARGE HIGH-STRENGTH REINFORCING BARS WITH STANDARD HOOKS AND HEADS

By
Ali Banaeipour, David Darwin
Matthew O'Reilly, Rémy D. Lequesne
Andres Lepage, Matthew Blessent

A Report on Research Sponsored by



**CHARLES PANKOW
FOUNDATION**

Charles Pankow Foundation Research Grant Agreement #05-18, D17
ACI Foundation, BarSplice Products,
Headed Reinforcement Corporation, nVENT Lenton,
CRSI Education and Research Foundation,
Precast/Prestressed Concrete Institute,
Commercial Metals Company, Nucor Corporation

Structural Engineering and Engineering Materials
SM Report No. 153
July 2023



THE UNIVERSITY OF KANSAS CENTER FOR RESEARCH, INC.
2385 Irving Hill Road, Lawrence, Kansas 66045-7563

**DEVELOPMENT OF LARGE HIGH-STRENGTH REINFORCING BARS WITH
STANDARD HOOKS AND HEADS**

By
Ali Banaeipour
David Darwin
Matthew O'Reilly
Rémy D. Lequesne
Andres Lepage
Matthew Blessent

A Report on Research Sponsored by



**CHARLES PANKOW
FOUNDATION**

Charles Pankow Foundation Research Grant Agreement #05-18, D17

**ACI Foundation, BarSplice Products,
Headed Reinforcement Corporation, nVENT Lenton,
CRSI Education and Research Foundation,
Precast/Prestressed Concrete Institute,
Commercial Metals Company, Nucor Corporation**

Structural Engineering and Engineering Materials

SM Report No. 153

THE UNIVERSITY OF KANSAS CENTER FOR RESEARCH, INC.

LAWRENCE, KANSAS

July 2023

ABSTRACT

Hooked and headed reinforcing bars are viable alternatives for development of reinforcing steel when member geometry does not allow for a straight deformed bar to fully develop its yield strength. Current design provisions in ACI 318-19 Building Code impose limitations on the use of hooked and headed bars larger than No. 11 (that is, No. 14 and No. 18 bars), mainly due to a lack of experimental data. This research continues a comprehensive study of the anchorage and development of high-strength hooked and headed bars to expand the available data to include No. 14 and No. 18 bars. Forty-two large-scale simulated beam-column joint specimens containing No. 11, No. 14 and No. 18 hooked and headed bars are tested. Of the 42 specimens, 12 contain hooked bars and 30 contain headed bars. The effects of bar size, bar spacing, bar location, embedment length, confining transverse reinforcement in the joint region, placement of bars within the cross-section, concrete compressive strength, compression strut angle, and effective beam depth on anchorage strength are investigated. Two loading conditions are used. In loading condition A, the joint shear is 80% of the total applied force to the bars, simulating the forces in an exterior beam-column joint with the beam located at the midheight of the column. The joint shear is reduced to ~69% of the total applied force in loading condition B. All hooked bar specimens and 15 headed bar specimens are tested under loading condition A, while the other 15 headed bar specimens are tested using loading condition B. Concrete compressive strengths range from 6,390 to 15,770 psi for hooked bars and from 5,310 to 16,210 psi for headed bars. Bar stress at failure ranges from 87,300 to 130,600 psi for hooked bars and from 54,900 to 148,300 psi for headed bars. Center-to-center bar spacing, s , ranges from $3.5d_b$ to $10.6d_b$ for hooked bars and from $2.7d_b$ to $10.6d_b$ for headed bars, where d_b is the nominal hooked or headed bar diameter. Confining reinforcement, A_{th} , or parallel ties, A_{tt} , in the joint region ranges from 0 to $0.465A_{hs}$ and 0 to $0.827A_{hs}$ for hooked and headed bars, respectively, where A_{th} or A_{tt} equal the total cross-sectional area of tie legs within $10d_b$ from the top of the bars and A_{hs} is the total area of the bars being developed. Headed bars with net bearing areas between 4.2 and 4.4 times the bar area are used.

The test results are compared with the current provisions for the development length of hooked and headed bars in Chapter 25 of ACI 318-19. Descriptive equations to characterize anchorage strength of hooked and headed bars developed previously for No. 11 and smaller bars are evaluated. New descriptive equations are developed to represent the anchorage strength for bars as large as No. 18. The equations are compared with the test results in the current study and available in the literature. New design provisions for development length are developed for hooked

and headed bars and evaluated with respect to test results and ACI 318-19 provisions.

The descriptive equations for hooked and headed bars developed in this study accurately account for concrete compressive strength, confining reinforcement, and bar spacing. The ability of the equations to accurately represent anchorage strength is insensitive to variations in compression strut angle and effective beam depth. While the contribution of confining reinforcement to anchorage strength increases with bar size, the effect of increasing confining reinforcement for headed bars is much lower than for hooked bars and much lower for headed bars than observed in prior studies. Under loading condition A, all hooked bar specimens, even those without confining reinforcement, carried the joint shear and exhibited an anchorage failure, whereas shear-like failures were observed in some headed bar specimens under similar conditions. These observations reveal the distinct role of the tail of the hook in helping to carry the joint shear, and indicate the difference in joint shear under loading conditions A and B is a key factor in the type of failure and anchorage strength of headed bars. Larger headed bars need confining reinforcement on the order of $0.5A_{hs}$ to carry the joint shear demand under loading condition A.

The development length provisions in ACI 318-19 are unnecessarily conservative for No. 14 and No. 18 hooked and headed bars. For both hooked and headed bars, providing confining reinforcement below the minimum amounts required by ACI 318-19 contributes to anchorage strength. Similar to No. 11 and smaller hooked and headed bars, the effect on anchorage strength of concrete compressive strength is best represented by the 0.25 power for design. The bar location factor ψ_o of 1.25 in ACI 318-19, applied to bars terminating inside column longitudinal reinforcement (column core) with side cover < 2.5 in. or bars with side cover $< 6d_b$, can be safely reduced to 1.15 for design. The proposed design equations for hooked and headed bars are applicable to concrete with compressive strengths up to 16,000 psi, steel with yield strengths up to 120,000 psi, and bars as large as No. 18. The proposed modification factors for confining reinforcement (expressed as A_{th}/A_{hs} or A_{tl}/A_{hs}) and bar spacing (expressed as s/d_b), in the form of a single expression or simplified expressions that address the effects of confining reinforcement and bar spacing independently, provide more flexibility for designers to take advantage of a range of values for A_{th}/A_{hs} or A_{tl}/A_{hs} and s/d_b and, ultimately, permit the use of shorter development lengths than the provisions in ACI 318-19 for all bar sizes.

Keywords: anchorage, beam-column joint, bond, development length, headed bar, high-strength concrete, high-strength steel, hooked bar, large-scale testing

ACKNOWLEDGEMENTS

This report is based on a thesis presented by Ali Banaeipour in partial fulfillment of the requirements for the Ph.D. degree from the University of Kansas. Support for the study was provided by the Charles Pankow Foundation under Research Grant Agreement #05-18, the ACI Foundation, BarSplice Products, Headed Reinforcement Corporation, nVENT Lenton, the CRSI Education and Research Foundation, the Precast/Prestressed Concrete Institute, Commercial Metals Company, and Nucor Corporation.

Additional support was provided by Dayton Superior, Midwest Concrete Materials, and Grace Construction Products. Thanks are due to Jack Moehle, Amy Trygstad, Javeed Munshi, and Andrew Taylor who served on the advisory panel.

TABLE OF CONTENTS

ABSTRACT	iii
ACKNOWLEDGEMENTS	v
TABLE OF CONTENTS	vii
LIST OF FIGURES	xi
LIST OF TABLES	xxiv
CHAPTER 1: INTRODUCTION.....	1
1.1 GENERAL	1
1.2 BACKGROUND AND PREVIOUS RESEARCH	3
1.2.1 Reinforcing Bars with Standard Hooks	3
1.2.2 Headed Reinforcing Bars	14
1.3 CURRENT CODE PROVISIONS AND DESIGN GUIDELINES	29
1.3.1 Reinforcing Bars with Standard Hooks	30
1.3.2 Headed Reinforcing Bars	36
1.4 OBJECTIVE AND SCOPE	43
CHAPTER 2: EXPERIMENTAL WORK.....	45
2.1 MATERIAL PROPERTIES	45
2.1.1 Hooked and Headed Bars	45
2.1.2 Reinforcing Steel Properties	46
2.1.3 Concrete Properties	47
2.2 TEST SPECIMENS	48
2.2.1 Specimen Design.....	48
2.2.2 Test Parameters	52
2.2.3 Specimen Designation.....	53
2.2.4 Specimen Fabrication.....	54
2.2.5 Specimen Instrumentation.....	58
2.3 TESTING APPARATUS.....	59
2.3.1 Loading Conditions.....	59

2.3.2 Reaction Frame	61
2.3.3 Bearing Plates	67
2.3.4 Bar Displacement Measurement	68
2.3.5 Load Cells	69
2.3.6 Testing Procedure	69
2.3.7 Summary of Test Program	71
CHAPTER 3: TEST RESULTS	73
3.1 CRACKING PATTERNS.....	73
3.1.1 Hooked Bars.....	73
3.1.2 Headed Bars	75
3.2 FAILURE MODES.....	79
3.2.1 Hooked Bars.....	79
3.2.2 Headed Bars	81
3.3 STRAIN DEVELOPED IN REINFORCEMENT	87
3.3.1 Ties.....	87
3.3.2 Hooked Bars.....	90
3.3.3 Headed Bars	92
3.4 ANCHORAGE STRENGTH.....	93
CHAPTER 4: ANALYSIS AND DISCUSSION: HOOKED BARS	96
4.1 COMPARISON OF TEST RESULTS WITH ACI 318-19.....	96
4.2 COMPARISON OF TEST RESULTS WITH DESCRIPTIVE EQUATIONS DEVELOPED BY AJAAM ET AL. (2017, 2018)	99
4.3 NEW DESCRIPTIVE EQUATIONS	101
4.3.1 Widely-spaced Bars Without Confining Reinforcement	101
4.3.2 Closely-spaced Bars Without Confining Reinforcement.....	103
4.3.3 Widely-spaced Bars with Confining Reinforcement	107
4.3.4 Closely-spaced Bars with Confining Reinforcement.....	109
4.3.5 Summary	111

4.4 EVALUATING DESCRIPTIVE EQUATIONS	113
4.4.1 Bar Location.....	113
4.4.2 Confining Reinforcement.....	118
4.4.3 Bar Spacing	121
4.4.4 Strut Angle	122
4.4.5 Effective Beam Depth.....	125
4.4.6 Embedment Length	127
4.5 SPECIMENS NOT USED TO DEVELOP DESCRIPTIVE EQUATIONS	128
CHAPTER 5: ANALYSIS AND DISCUSSION: HEADED BARS	136
5.1 COMPARISON OF TEST RESULTS WITH ACI 318-19	136
5.2 COMPARISON OF TEST RESULTS WITH DESCRIPTIVE EQUATIONS DEVELOPED BASED ON TESTS OF NO. 5 THROUGH NO. 11 HEADED BARS.....	139
5.3 NEW DESCRIPTIVE EQUATIONS	143
5.3.1 Widely-spaced Bars Without Parallel Ties	144
5.3.2 Closely-spaced Bars Without Parallel Ties.....	145
5.3.3 Widely-Spaced Bars with Parallel Ties	148
5.3.4 Closely-Spaced Bars with Parallel Ties	150
5.3.5 Summary	153
5.4 EVALUATING NEW DESCRIPTIVE EQUATIONS FOR NO. 14 AND NO. 18 BARS...	155
5.5 EFFECT OF TEST PARAMETERS	161
5.5.1 Loading Condition	161
5.5.2 Parallel tie Reinforcement.....	171
5.5.3 Bar Spacing	174
5.5.4 Placement of Bars Within the Cross-section.....	175
5.5.5 Compression Strut Angle	178
5.5.6 Effective Beam Depth.....	179
5.5.7 Embedment Length	181
5.5.8 Bar Location.....	182

5.6 BEAM-COLUMN JOINT SPECIMENS NOT USED TO DEVELOP DESCRIPTIVE EQUATIONS	187
CHAPTER 6: DESIGN APPROACH.....	193
6.1 HOOKED BARS	193
6.1.1 Simplified Descriptive Equations	193
6.1.2 Design Equation for Development Length	198
6.1.3 Evaluating Proposed Design Equation.....	206
6.2 HEADED BARS.....	217
6.2.1 Simplified Descriptive Equations	217
6.2.2 Design Equation for Development Length	223
6.2.3 Evaluating Proposed Design Equation.....	228
6.3 COMPARISONS WITH ACI 318-19.....	237
6.3.1 Concrete Compressive Strength.....	237
6.3.2 Required Development Length	239
CHAPTER 7: SUMMARY, CONCLUSIONS, AND FUTURE WORK.....	247
7.1 SUMMARY	247
7.2 CONCLUSIONS.....	248
7.3 FUTURE WORK.....	251
REFERENCES.....	252
APPENDIX A: NOTATION.....	257
APPENDIX B: HOOKED BAR BEAM-COLUMN JOINT SPECIMENS	261
B.1 DRAWINGS AND REINFORCEMENT LAYOUTS FOR NO. 14 AND NO. 18 BAR SPECIMENS TESTED IN CURRENT STUDY	262
B.2 DETAILED PROPERTIES AND TEST RESULTS FOR NO. 14 AND NO. 18 BAR SPECIMENS TESTED IN CURRENT STUDY	274
B.3 SPECIMENS TESTED AT THE UNIVERSITY OF KANSAS.....	278
B.4 SPECIMENS TESTED IN OTHER STUDIES	314
APPENDIX C: HEADED BAR BEAM-COLUMN JOINT SPECIMENS.....	323

C.1 DRAWINGS AND REINFORCEMENT LAYOUTS FOR NO. 14 AND NO. 18 BAR SPECIMENS TESTED IN CURRENT STUDY	324
C.2 DETAILED PROPERTIES AND TEST RESULTS FOR NO. 14 AND NO. 18 BAR SPECIMENS TESTED IN CURRENT STUDY	352
C.3 SPECIMENS TESTED AT THE UNIVERSITY OF KANSAS	360
C.4 SPECIMENS TESTED IN OTHER STUDIES	383

LIST OF FIGURES

Figure 1.1. Anchorage mechanism of hooked bars (adapted from Marques and Jirsa 1975).....	4
Figure 1.2 Crack progression observed in the beam-column joint specimens containing hooked bars (Sperry et al. 2015b, 2017a). Breakout failure is preceded by bond slip of the straight portion of the bars and cracking of the concrete	4
Figure 1.3 Schematic of test specimens used by Marques and Jirsa (1975); Type 1: Hooked bars inside column core without confining reinforcement, Type 2 and 4: Hooked bars outside column core without confining reinforcement, Type 3: Hooked bars outside column core with No. 3 ties, and Type 5: Hooked bars outside column core with No. 3 ties plus cross-tie	6
Figure 1.4 Strut angle as defined by Joh et al. (1995)	7
Figure 1.5 Schematic of specimens (a) side view (b) cross-section without confining reinforcement, and (c) cross-section with confining reinforcement, where ℓ_{eh} is the embedment length and d_b is bar diameter.....	10
Figure 1.6 Schematic of the reaction frame (Sperry et al. 2015b)	11
Figure 1.7 Primary failure modes observed in hooked bar specimens (Sperry et al. 2015b)	12
Figure 1.8 Steel congestion in an external beam-column joint caused by staggered hooked bars (https://www.sefindia.org)	14
Figure 1.9 Different types of headed bars (Shao et al. 2016)	15
Figure 1.10 Previous limits on headed bar obstructions (ASTM A970/M970-16)	15
Figure 1.11 Current dimensional limits for obstructions or interruptions in headed bars (ASTM A970/M970-18)	16
Figure 1.12 Anchorage and bond of headed bars (Shao et al. 2016)	16

Figure 1.13 Crack progression observed in the beam-column joint specimens containing headed bars. Breakout failure is preceded by bond slip along the straight portion of the bars and cracking of the concrete (Shao et al. 2016, Ghimire et al. 2019a)	17
Figure 1.14 (a) Side view of specimen proportions used by Chun et al. (2017a) and Chun and Lee (2019); (b) Side view of the specimen proportions used by Sim and Chun (2022b); (c) Side view of the specimen proportions used by Sim and Chun (2022a)	20
Figure 1.15 Schematic of headed bar specimens (a) side view (b) cross-section, where h and w are column height and width, respectively, and ℓ_{eh} is the embedment length (Shao et al. 2016).....	23
Figure 1.16 The loading frame and test setup of headed bar specimens (Shao et al. 2016)	24
Figure 1.17 Concrete breakout (a) cone-shaped (b) back cover spalling (Shao et al. 2016)	25
Figure 1.18 Side-face blowout (a) side view (b) back view (Shao et al. 2016).....	26
Figure 1.19 Confining reinforcement contributing to anchorage strength of headed bars anchored in beam-column joints (Shao et al. 2016, Ghimire et al. 2019)	28
Figure 1.20 ACI 318-14 provisions for ties or stirrups placed perpendicular (left) or parallel (right) to the hooked bar being developed (ACI 318-14)	30
Figure 1.21 Ratio of test-to-calculated stress $f_{su}/f_{s,ACI}$ versus f_{cm} for hooked bars without confining reinforcement (Sperry et al. 2015b)	31
Figure 1.22 Ratio of test-to-calculated stress $f_{su}/f_{s,ACI}$ versus f_{cm} for hooked bars with No. 3 ties spaced at $3d_b$ in the joint region (Sperry et al. 2015b).....	32
Figure 1.23 Confining reinforcement placed parallel (left) or perpendicular (right) to the hooked bar being developed as defined in ACI 318-19 (from ACI 318-19).....	35
Figure 1.24 Ratio of test-to-calculated stress $f_{su}/f_{s,ACI}$ versus f_{cm} for two widely-spaced headed bars without confining reinforcement, where $f_{s,ACI}$ is based on ACI 318-14 (from Shao et al. 2016) .	37
Figure 1.25 Ratio of test-to-calculated stress $f_{su}/f_{s,ACI}$ versus f_{cm} for two widely-spaced headed bars with No. 3 hoops spaced at $3d_b$, where $f_{s,ACI}$ is based on ACI 318-14 (Shao et al. 2016)	38
Figure 1.26 Bars located outside (left) or inside (right) of the column core.....	40
Figure 1.27 Parallel tie reinforcement that contribute to anchorage strength of headed bars as defined in ACI 318-19 (ACI 318-19)	41
Figure 2.1 Different types of headed bars used in the study	45
Figure 2.2 Schematic of the specimens with hooked bars, side view (left) and top view (right)	49
Figure 2.3 Schematic of the specimens with headed bars, side view (left) and top view (right)	50

Figure 2.4 Dimensional proportions of the specimens; For specimens with No. 14 bar, $x_{mid} = 28.56$ in. and $h_0 = 14$ ft, and for specimens with No. 18 bar, $x_{mid} = 38.15$ in. and $h_0 = 18$ ft	51
Figure 2.5 Double overlapping tie configuration.....	53
Figure 2.6 Example specimen designation	54
Figure 2.7 Cross-sectional dimensions and variable callouts of specimens	54
Figure 2.8 Vertical formwork for No. 14 bar specimens and sawhorses to hold the bars	55
Figure 2.9 Clamping system to brace the vertical forms for No. 14 bar specimens	56
Figure 2.10 Horizontal formwork for No. 18 bar specimens.....	56
Figure 2.11 A typical reinforcement cage (steel cage)	57
Figure 2.12 No. 14 hooked (left) and headed (right) bars tied to steel cages	57
Figure 2.13 No. 18 hooked (left) and headed (right) bars tied to steel cages	58
Figure 2.14 Side view (left and middle) and top view (right) of strain gauge locations	59
Figure 2.15 Forces applied to specimens by the reaction frame during the test.....	60
Figure 2.16 Side elevation of the reaction frame for the No. 14 bar setup	62
Figure 2.17 End-elevation of the reaction frame for the No. 14 bar setup	63
Figure 2.18 The reaction frame (No. 14 bar setup) and applied forces	64
Figure 2.19 Plan view and cross-section of the built-up section	65
Figure 2.20 Load cells, washer plates, and couplers for No. 14 bar test setup	66
Figure 2.21 Alternative test setup used in widely-spaced No. 18 bar specimens	67
Figure 2.22 Setup for using the LVDTs.....	68
Figure 2.23 Load cell for No. 14 and No. 18 bars	69
Figure 3.1 Example of cracking pattern in hooked bar specimens (front face, specimen H14-15): (a) Horizontal cracks likely initiating due to bar slip, (b) Cracks radiating from the hooked bars, and (c) Cracks radiated from the hooked bars connected to each other along with local concrete damage	74
Figure 3.2 Example of cracking pattern in hooked bar specimens (side face, specimen H14-15): (a) Vertical crack likely initiating due to bar slip, (b) and (c) Cracks propagating and branching towards upper and lower bearing members, (d) Cone-shaped cracking pattern near failure (see arrows.)	75
Figure 3.3 Example of cracking pattern in headed bar specimens (side face, specimen 18-3): (a) Vertical crack likely initiating due to bar slip, (b) Cracks branching towards bearing members, (c)	

First diagonal crack due to shear in joint, (d) and (e) Cracks propagating throughout the joint, (f) Cone-shaped cracking pattern after failure. (Note: Extension of diagonal cracks along the back face of the specimen towards the top of the column are marked by dashed lines.).....	77
Figure 3.4 Example of cracking pattern in headed bar specimens (top face, specimen 18-3): (a) Crack between bars likely initiating due to bar slip, (b) Cracks branching towards bearing members, (c) First diagonal crack due to shear in joint, (d) and (e) Cracks propagating throughout the joint	78
Figure 3.5 Side view of a concrete breakout failure in hooked bars with tail kickout (H14-7)...	80
Figure 3.6 Side view of a side-splitting failure for hooked bars (H14-8).....	81
Figure 3.7 Primarily concrete breakout failure (top: specimen 14-10, bottom: specimen 18-5). (Note: Dashed lines highlight the cracks extending beyond the joint and along the back face of the column or towards the upper bearing member)	82
Figure 3.8 Primarily side-splitting failure (left: specimen 14-3, right: specimen 18-4)	83
Figure 3.9 Combination of concrete breakout and side splitting (specimen 14-15).....	84
Figure 3.10 Concrete breakout accompanied by side splitting and compression failure of concrete between bearing face of the head and lower bearing member (specimen 14-16B).....	84
Figure 3.11 Shear-like failure in headed-bar specimen 14-16. (Note: The specimen shows no indication of a breakout or side-splitting failure.)	85
Figure 3.12 Examples of strain developed in parallel ties in hooked bar specimen H14-2 (left) and headed bar specimen 14-6 (right)	88
Figure 3.13 Specimens H14-2 at failure showing location of ties and strain gauges	89
Figure 3.14 Parallel ties trapping the first diagonal cracks and their strain gauge labels in the headed bar specimen 14-6.....	90
Figure 3.15 Strain developed in one hooked bar in specimens H14-2 (left) and H14-15 (right). (Note: T1 was mounted just before the bend in the tail, and T2 mounted 1 in. from the front face of the column).....	91
Figure 3.16 Strain developed in one headed bar in specimen 14-16C (left) and 18-8 (right) (Note: T1 was mounted 1.5 in. from the bearing face of the head, and T2 was mounted 1 in. from the column front face).....	92

Figure 4.1 Ratio of test/calculated bar stress (ACI), $f_s/f_{s,ACI}$ versus concrete compressive strength f_{cm} for No. 14 and No. 18 hooked bar specimens (using values of ψ_r permitted for No. 11 and smaller bars, as shown in Table 4.1).....	99
Figure 4.2 Ratio of test-to-calculated bar force at failure T/T_c versus concrete compressive strength for hooked bar specimens with widely-spaced bars (center-to-center spacing $\geq 6d_b$) without confining reinforcement.....	102
Figure 4.3 Test-to-calculated bar force at failure T/T_c versus ratio of center-to-center spacing to bar diameter s/d_b for widely- and closely-spaced hooked bars without confining reinforcement	104
Figure 4.4 Ratio of test-to-calculated failure load T/T_c versus concrete compressive strength for hooked bar specimens having widely- and closely-spaced bars without confining reinforcement	106
Figure 4.5 Ratio of test-to-calculated bar force at failure T/T_h versus concrete compressive strength for hooked bar specimens having widely-spaced ($s/d_b \geq 6d_b$) bars with confining reinforcement	108
Figure 4.6 Test-to-calculated bar force at failure T/T_h versus ratio of center-to-center spacing to bar diameter s/d_b for widely- and closely-spaced hooked bars with confining reinforcement ...	109
Figure 4.7 Ratio of test-to-calculated bar force at failure T/T_h versus concrete compressive strength for hooked bar specimens having widely- and closely-spaced bars with confining reinforcement	111
Figure 4.8 Measured versus calculated bar force at failure based on new descriptive equations for hooked bars, Eq. (4.5) and (4.7).....	112
Figure 4.9 Confining reinforcement layouts in specimens with hooked bars placed outside the column core: (a) hooks outside the confining ties (Chun et al. 2017b), (b) hooks inside confining ties (Chun et al. 2017b), and (c) hooks inside confining ties (Sperry et al. 2015b).....	116
Figure 4.10 Test-to-calculated ratio T/T_h based on new descriptive equations, Eq. (4.5) and (4.7), for hooked bars versus confining reinforcement ratio A_{th}/A_{hs}	118
Figure 4.11 Comparing anchorage strength of No. 14 hooked bars for confining reinforcement. T/T_h ratios shown based on Eq. (4.5) and (4.7). Center-to center spacing is $3.5d_b$ for specimens H14-7 and H14-8 (closely-spaced), and $10.6d_b$ for all other specimens (widely-spaced).....	120

Figure 4.12 Comparing anchorage strength of No. 18 hooked bars for confining reinforcement. T/T_h ratios shown on top of each bar. Hooked bars have center-to-center spacing of $6d_b$	120
Figure 4.13 Test-to-calculated ratio T/T_h versus ratio of center-to-center spacing to bar diameter s/d_b based on Eq. (4.5) and (4.7), for hooked bar specimens used to develop the equations	122
Figure 4.14 Definition of compression strut angle (θ) for hooked bars.....	123
Figure 4.15 Test-to-calculated T/T_h ratio based on Eq. (4.5) and (4.7) versus compression strut angle θ for hooked bar specimens used to develop descriptive equations (not including specimens with $d_{eff}/\ell_{eh} > 1.5$).....	124
Figure 4.16 ℓ_{eh}/d_b versus compression strut angle θ for hooked bar specimens used to develop descriptive equations, Eq. (4.5) and (4.7)	125
Figure 4.17 Effective beam depth d_{eff} for hooked bars (Ajaam et al. 2017)	126
Figure 4.18 Test-to-calculated T/T_h ratio based on Eq. (4.5) and (4.7) versus effective beam depth to embedment length d_{eff}/ℓ_{eh} ratio for hooked bar specimens used to develop descriptive equations plus specimens with $d_{eff}/\ell_{eh} > 1.5$	127
Figure 4.19 Test-to-calculated T/T_h ratio based on Eq. (4.5) and (4.7) versus embedment length to bar diameter ℓ_{eh}/d_b ratio for hooked bar specimens used to develop descriptive equations	128
Figure 4.20 Schematic of the forces applied to specimens by (a) Marques and Jirsa (1975) and (b) University of Kansas studies (Searle et al. 2014, Sperry et al. 2015a, 2015b, 2017a, 2017b, 2018, Yasso et al. 2017, Ajaam et al. 2017, 2018) (Note: drawings are not to scale)	131
Figure 4.21 No. 11 hooked bar specimen proportions and applied forces: (a) University of Kansas (Searle et al. 2014, Sperry et al. 2015a, 2015b, 2017a, 2017b, 2018, Yasso et al. 2017, Ajaam et al. 2017, 2018), and (b) Marques and Jirsa (1975) (Note: T is the total applied force, and the force in the lower tension member is neglected)	134
Figure 5.1 Ratio of test/calculated bar stress $f_s/f_{s,ACI}$ applying the ACI 318-19 provisions to No. 14 and No. 18 headed bar specimens versus concrete compressive strength f_{cm} , excluding specimens that failed in shear	138
Figure 5.2 Test versus calculated force per bar at failure for No. 14 and No. 18 headed bar specimens based on descriptive equations by Shao et. al (2016)	143
Figure 5.3 Ratio of test-to-calculated bar force at failure T/T_c , with T_c based on Eq. (5.4), versus concrete compressive strength for headed bar specimens with widely-spaced bars without parallel ties	144

Figure 5.4 Test-to-calculated bar force at failure T/T_c versus ratio of center-to-center spacing to bar diameter s/d_b for widely- and closely-spaced headed bars without parallel ties with T_c based on Eq. (5.4)	146
Figure 5.5 Ratio of test-to-calculated bar force at failure T/T_c , based on Eq. (5.5), versus concrete compressive strength for headed bar specimens with widely- and closely-spaced bars without parallel ties	147
Figure 5.6 Ratio of test-to-calculated bar force at failure T/T_h versus concrete compressive strength for headed bar specimens with widely-spaced bars with parallel ties with T_h based on Eq. (5.6)	149
Figure 5.7 Test-to-calculated bar force at failure T/T_h versus ratio of center-to-center spacing to bar diameter s/d_b for widely- and closely-spaced headed bars with parallel ties with T_h based on Eq. (5.6)	151
Figure 5.8 Ratio of test-to-calculated bar force at failure T/T_h versus concrete compressive strength for headed bar specimens with widely- and closely-spaced bars with parallel ties with T_h based on Eq. (5.7)	152
Figure 5.9 Measured versus calculated bar force at failure using new descriptive equations for all headed bar specimens, excluding those with a shear-like failure, with the calculated bar force, T_h , based on Eq. (5.5) or (5.7)	155
Figure 5.10 Measured versus calculated bar force at failure using new descriptive equations for No. 14 and No. 18 headed bar specimens, excluding those with a shear-like failure, with the calculated bar force, T_h , based on Eq. (5.5) or (5.7)	158
Figure 5.11 Ratio of test/calculated ratio T/T_h versus concrete compressive strength f_{cm} for No. 14 and No. 18 headed bar specimens, with the calculated bar force, T_h , based on Eq. (5.5) or (5.7)	159
Figure 5.12 Ratio of test/calculated ratio T/T_h versus parallel tie reinforcement ratio A_{tl}/A_{hs} for No. 14 and No. 18 headed bar specimens, with the calculated bar force, T_h , based on Eq. (5.5) or (5.7)	160
Figure 5.13 Ratio of test/calculated ratio T/T_h versus ratio of center-to-center spacing to bar diameter s/d_b for No. 14 and No. 18 headed bar specimens, with the calculated bar force, T_h , based on Eq. (5.5) or (5.7)	161

Figure 5.14 Shear-like failure observed in specimen 14-16 ($A_{tt}/A_{hs} = 0.178$) tested under loading condition A: (a) after failure and (b) after dissection	163
Figure 5.15 Anchorage failure observed in specimen 14-15 ($A_{tt}/A_{hs} = 0$) tested under loading condition B.....	164
Figure 5.16 Additional No. 11 longitudinal bars in specimen 14-16A.....	165
Figure 5.17 Shear-like failure observed in specimen 14-16A ($A_{tt}/A_{hs} = 0.178$) tested under loading condition A.....	165
Figure 5.18 Shear-like failure observed in specimen 14-1A ($A_{tt}/A_{hs} = 0$) tested under loading condition B.....	166
Figure 5.19 Anchorage failure observed in specimen 14-2A ($A_{tt}/A_{hs} = 0.267$) tested under loading condition B.....	166
Figure 5.20 Anchorage failure observed in specimen 14-16B ($A_{tt}/A_{hs} = 0.178$) tested under loading condition B.....	167
Figure 5.21 Anchorage failure observed in specimen 14-16C ($A_{tt}/A_{hs} = 0.356$) tested under loading condition B.....	168
Figure 5.22 Double overlapping No. 5 ties in specimen 14-16D; (a) top view, (b) front view.	169
Figure 5.23 Anchorage failure observed in specimen 14-16D ($A_{tt}/A_{hs} = 0.827$) tested under loading condition A (after removal of loose concrete)	169
Figure 5.24 Anchorage failure observed in specimen 14-16E ($A_{tt}/A_{hs} = 0.551$).....	170
Figure 5.25 Comparing anchorage strength of headed bars with and without parallel ties (Note: L.C. = Loading Condition, and the number below L.C. denotes $A_{tt,ACI}/A_{hs}$)	171
Figure 5.26 Double No. 5 ties used in specimen 14-16F	172
Figure 5.27 Comparing side splitting failure modes of specimens 14-16E with parallel ties with middle legs (top) and 14-16F with only external legs (bottom), both with $A_{tt}/A_{hs} = 0.551$	173
Figure 5.28 Comparing the anchorage strength (average force per bar at failure) of No. 14 and No. 18 headed bars based on bar spacing	174
Figure 5.29 Concrete breakout observed in specimen 14-17 ($A_{tt}/A_{hs} = 0.551$) with increased side cover to the bar and decreased bar spacing.....	175
Figure 5.30 Comparing failure modes of specimen 18-1 with 3.5 in. side cover to the bar (top, side splitting) with specimen 18-5 with 6.5 in. side cover to the bar (bottom, concrete breakout), both with $A_{tt}/A_{hs} = 0.543$	176

Figure 5.31 Comparing failure modes of specimen 18-2 with 3.5 in. side cover to the bar (top) with specimen 18-6 with 6.5 in. side cover to the bar (bottom), both with $A_{tl}/A_{hs} = 0.543$	177
Figure 5.32 Compression strut angle (θ) for headed bars (x_{mid} is 28.56 and 38.15 in. for No. 14 and No. 18 bars, respectively, and ℓ_{eh} is the embedment length)	178
Figure 5.33 Comparison of strut angle θ versus test-to-calculated ratio T/T_h based on Eq. (5.5) and (5.7) for large (No. 11, No. 14, and No. 18) headed bars for specimens with $d_{eff}/\ell_{eh} < 1.5$	179
Figure 5.34 Effective beam depth d_{eff} for headed bars (Shao et al. 2016)	180
Figure 5.35 Comparison of d_{eff}/ℓ_{eh} versus test-to-calculated ratio T/T_h based on Eq. (5.5) and (5.7) for large (No. 11, No. 14, and No. 18) headed bars.....	181
Figure 5.36 Comparison of ℓ_{eh}/d_b versus test-to-calculated ratio T/T_h for based on Eq. (5.5) and (5.7) for large (No. 11, No. 14, and No. 18) headed bars	182
Figure 5.37 Parallel tie layouts in specimens with headed bars placed outside the column core tested by Chun et al. (2017) and Sim and Chun (2022a, 2022b): (a) heads outside parallel ties (“unconfined”), (b) heads inside parallel ties (“confined”), and (c) heads outside parallel ties but “confined” by hairpin transverse reinforcement	184
Figure 5.38 Specimen proportions and applied forces: (a) current study; (b) Bashandy 1996 (Note: the bottom drawing is not to scale, L.C. = Loading condition, V_J = Joint Shear)	191
Figure 5.39 Schematic of the reinforcement layouts used by Bashandy (1996): (a) Headed bars outside the column core and parallel ties (specimens T10, T12, and T13); (b) Headed bars inside the column core and parallel ties (specimens T14 and T25); and (c) Headed bars inside column core but ties were not wrapped around column longitudinal bars (rest of the specimens).....	192
Figure 6.1 Test-to-calculated bar force at failure T/T_c based on simplified Eq. (6.2) versus ratio of center-to-center spacing to bar diameter s/d_b for widely- and closely-spaced hooked bars without confining reinforcement used to develop descriptive equations, Eq. (4.5) and (4.7)	194
Figure 6.2 Ratio of test-to-calculated bar force at failure T/T_c based on simplified descriptive equation Eq. (6.3) versus concrete compressive strength f_{cm} for hooked bar specimens with widely- and closely-spaced bars without confining reinforcement used to develop descriptive equations, Eq. (4.5) and (4.7).....	195
Figure 6.3 Test-to-calculated bar force at failure T/T_h based on simplified Eq. (6.5) versus ratio of center-to-center spacing to bar diameter s/d_b for widely- and closely-spaced hooked bars with confining reinforcement used to develop descriptive equations, Eq. (4.5) and (4.7)	196

Figure 6.4 Ratio of test-to-calculated bar force at failure T/T_c based on simplified Eq. (6.6) versus concrete compressive strength for hooked bars with widely- and closely-spaced bars with confining reinforcement used to develop descriptive equations, Eq. (4.5) and (4.6)	197
Figure 6.5 Test-to-calculated bar force at failure T/T_c based on Eq. (6.19) versus ratio of center-to-center spacing to bar diameter s/d_b for widely- and closely-spaced headed bars without parallel ties	218
Figure 6.6 Ratio of test-to-calculated bar force at failure T/T_c based on simplified descriptive equation, Eq. (6.20), versus concrete compressive strength f_{cm} for headed bar specimens with widely- and closely-spaced bars without parallel ties used to develop descriptive equations, Eq. (5.5) and (5.7)	219
Figure 6.7 Test-to-calculated bar force at failure T/T_c based on Eq. (6.22) versus ratio of center-to-center spacing to bar diameter s/d_b for widely- and closely-spaced headed bars with parallel ties used to develop descriptive equations, Eq. (5.5) and (5.7)	221
Figure 6.8 Ratio of test-to-calculated bar force at failure T/T_c based on simplified descriptive equation, Eq. (6.23), versus concrete compressive strength f_{cm} for headed bar specimens with widely- and closely-spaced bars with parallel ties used to develop descriptive equations, Eq. (5.5) and (5.7)	222
Figure 6.9 Ratio $f_{s,Descriptive}/f_{s,calc}$ versus concrete compressive strength f_{cm} for No. 8 bars headed bars with $s = 6d_b$ and $A_{tl}/A_{hs} = 0$ for ACI 318-19 and proposed design provisions	239
Figure 6.10 Required development lengths of No. 8 hooked bars for $f'_c =$ (a) 4000 psi, (b) 10,000 psi, and (c) 16,000 psi as a function of s/d_b and A_{th}/A_{hs} based on based on ACI 318-19 and the proposed provisions using the full expression for ψ_r , Eq. (6.14)	241
Figure 6.11 Required development lengths of No. 8 hooked bars for $f'_c =$ (a) 4000 psi, (b) 10,000 psi, and (c) 16,000 psi as a function of s/d_b and A_{th}/A_{hs} based on ACI 318-19 and the proposed provisions using the simplified expressions for ψ_r , Eq. (6.15)	242
Figure 6.12 Required development lengths of No. 8 headed bars for $f'_c =$ (a) 4000 psi, (b) 10,000 psi, and (c) 16,000 psi as a function of s/d_b and A_{tl}/A_{hs} based on ACI 318-19 and the proposed provisions using the full expression for ψ_p , Eq. (6.29)	244

Figure 6.13 Required development lengths of No. 8 headed bars for $f'_c =$ (a) 4000 psi, (b) 10,000 psi, and (c) 16,000 psi as a function of s/d_b and A_{tt}/A_{hs} based on ACI 318-19 and the proposed provisions using the simplified expressions for ψ_p , Eq. (6.30).....	245
Figure B.1 Details of reinforcement layout for No. 14 hooked bar specimen H14-1: (a) elevation, (b) cross-section	262
Figure B.2 Details of reinforcement layout for No. 14 hooked bar specimen H14-2: (a) elevation, (b) cross-section	263
Figure B.3 Details of reinforcement layout for No. 14 hooked bar specimen H14-3: (a) elevation, (b) cross-section	264
Figure B.4 Details of reinforcement layout for No. 14 hooked bar specimen H14-3: (a) elevation, (b) cross-section	265
Figure B.5 Details of reinforcement layout for No. 14 hooked bar specimen H14-15: (a) elevation, (b) cross-section	266
Figure B.6 Details of reinforcement layout for No. 14 hooked bar specimen H14-16: (a) elevation, (b) cross-section	267
Figure B.7 Details of reinforcement layout for No. 14 hooked bar specimen H14-7: (a) elevation, (b) cross-section	268
Figure B.8 Details of reinforcement layout for No. 14 hooked bar specimen H14-8: (a) elevation, (b) cross-section	269
Figure B.9 Details of reinforcement layout for No. 18 hooked bar specimen H18-1: (a) elevation, (b) cross-section	270
Figure B.10 Details of reinforcement layout for No. 18 hooked bar specimen H18-2: (a) elevation, (b) cross-section	271
Figure B.11 Details of reinforcement layout for No. 18 hooked bar specimen H18-3: (a) elevation, (b) cross-section	272
Figure B.12 Details of reinforcement layout for No. 18 hooked bar specimen H18-4: (a) elevation, (b) cross-section	273
Figure C.1 Details of reinforcement layout for No. 14 headed bar specimen 14-2: (a) elevation, (b) cross-section	324
Figure C.2 Details of reinforcement layout for No. 14 headed bar specimen 14-3: (a) elevation, (b) cross-section	325

Figure C.3 Details of reinforcement layout for No. 14 headed bar specimen 14-4: (a) elevation, (b) cross-section	326
Figure C.4 Details of reinforcement layout for No. 14 headed bar specimen 14-15: (a) elevation, (b) cross-section	327
Figure C.5 Details of reinforcement layout for No. 14 headed bar specimen 14-16: (a) elevation, (b) cross-section	328
Figure C.6 Details of reinforcement layout for No. 14 headed bar specimen 14-16A: (a) elevation, (b) cross-section	329
Figure C.7 Details of reinforcement layout for No. 14 headed bar specimen 14-1A: (a) elevation, (b) cross-section	330
Figure C.8 Details of reinforcement layout for No. 14 headed bar specimen 14-2A: (a) elevation, (b) cross-section	331
Figure C.9 Details of reinforcement layout for No. 14 headed bar specimen 14-16B: (a) elevation, (b) cross-section	332
Figure C.10 Details of reinforcement layout for No. 14 headed bar specimen 14-16C: (a) elevation, (b) cross-section	333
Figure C.11 Details of reinforcement layout for No. 14 headed bar specimen 14-16D: (a) elevation, (b) cross-section	334
Figure C.12 Details of reinforcement layout for No. 14 headed bar specimen 14-16E: (a) elevation, (b) cross-section	335
Figure C.13 Details of reinforcement layout for No. 14 headed bar specimen 14-16F: (a) elevation, (b) cross-section	336
Figure C.14 Details of reinforcement layout for No. 14 headed bar specimen 14-17: (a) elevation, (b) cross-section	337
Figure C.15 Details of reinforcement layout for No. 14 headed bar specimen 14-5: (a) elevation, (b) cross-section	338
Figure C.16 Details of reinforcement layout for No. 14 headed bar specimen 14-6: (a) elevation, (b) cross-section	339
Figure C.17 Details of reinforcement layout for No. 14 headed bar specimen 14-7: (a) elevation, (b) cross-section	340

Figure C.18 Details of reinforcement layout for No. 14 headed bar specimen 14-8: (a) elevation, (b) cross-section	341
Figure C.19 Details of reinforcement layout for No. 14 headed bar specimen 14-9: (a) elevation, (b) cross-section	342
Figure C.20 Details of reinforcement layout for No. 14 headed bar specimen 14-10: (a) elevation, (b) cross-section	343
Figure C.21 Details of reinforcement layout for No. 18 headed bar specimen 18-1: (a) elevation, (b) cross-section	344
Figure C.22 Details of reinforcement layout for No. 18 headed bar specimen 18-2: (a) elevation, (b) cross-section	345
Figure C.23 Details of reinforcement layout for No. 18 headed bar specimen 18-3: (a) elevation, (b) cross-section	346
Figure C.24 Details of reinforcement layout for No. 18 headed bar specimen 18-4: (a) elevation, (b) cross-section	347
Figure C.25 Details of reinforcement layout for No. 18 headed bar specimen 18-5: (a) elevation, (b) cross-section	348
Figure C.26 Details of reinforcement layout for No. 18 headed bar specimen 18-6: (a) elevation, (b) cross-section	349
Figure C.27 Details of reinforcement layout for No. 18 headed bar specimen 18-7: (a) elevation, (b) cross-section	350
Figure C.28 Details of reinforcement layout for No. 18 headed bar specimen 18-8: (a) elevation, (b) cross-section	351

LIST OF TABLES

Table 1.1 Standard hook requirements (ACI 318-19).....	3
Table 1.2 Values for the confinement and bar spacing factor, ψ_{cs} , as proposed by Ajaam et al. (2017) for hooked bars ^[1]	33
Table 1.3 Modification factors for hooked bars as given in Table 25.4.3.2 of ACI 318-19	34
Table 1.4 Values for the confinement and bar spacing factor, ψ_{cs} , as proposed by Shao et al. (2016) for headed bars	39
Table 1.5 Modification factors for headed bars as given in Table 25.4.4.3 of ACI 318-19	41
Table 2.1 Dimensions of the headed bars	46
Table 2.2 Physical properties of reinforcing steel.....	47
Table 2.3 Concrete mixture proportions	48
Table 2.4 Values of forces applied to the specimens under the two loading conditions	61
Table 2.5 Test program and the main parameters for No. 11, No. 14, and No. 18 bar specimens	71
Table 2.6 Summary of the test program and number of specimens.....	72
Table 3.1 Summary of hooked bar specimens with different failure types.....	86
Table 3.2 Summary of headed bar specimens with different failure types	86
Table 3.3 Summary of anchorage strength results for hooked bar specimens	94
Table 3.4 Summary of anchorage strength results for headed bar specimens	95
Table 4.1 Comparison of No. 14 and No. 18 hooked bar test results with descriptive equations by Ajaam et al. (2018), Eq. (1.1) and (1.2), also Eq. (4.2) and (4.3), and ACI 318-19. Eq. (4.1).....	97
Table 4.2 Summary of test-to-calculated ratio for No. 14 and No. 18 hooked bars based on descriptive equations by Ajaam et a. (2017, 2018), Eq. (4.2) and (4.3)	100
Table 4.3 Statistical parameters of T/T_c ratio using Eq. (4.4) for hooked bar specimens with widely-spaced bars (center-to-center spacing $\geq 6d_b$) without confining reinforcement	103
Table 4.4 Statistical parameters of T/T_c ratio using Eq. (4.5) for hooked bar specimens with closely-spaced ($s/d_b < 6d_b$) bars without confining reinforcement	105
Table 4.5 Statistical parameters of T/T_c ratio using Eq. (4.5) for hooked bar specimens with widely- and closely-spaced bars without confining reinforcement	106

Table 4.6 Statistical parameters of T/T_h ratio using Eq. (4.6) for hooked bar specimens with widely-spaced ($s/d_b \geq 6d_b$) bars with confining reinforcement.....	108
Table 4.7 Statistical parameters of T/T_h ratio using Eq. (4.7) for hooked bar specimens with closely-spaced bars with confining reinforcement	110
Table 4.8 Statistical parameters of T/T_h ratio using Eq. (4.7) for hooked bar specimens with widely- and closely-spaced bars with confining reinforcement	110
Table 4.9 Statistical parameters of T/T_h ratio using Eq. (4.5) and (4.7) for all hooked bar specimens used to develop the descriptive equations.....	111
Table 4.10 Summary of test-to-calculated ratio T/T_h using Eq. (4.5) and (4.7) for No. 14 and No. 18 hooked bar specimens tested in this study	113
Table 4.11 Test-to-calculated T/T_h ratio based on Eq. (4.5) and (4.7) for specimens with hooked bars placed outside column core (Ajaam et al. 2017).....	114
Table 4.12 Test-to-calculated ratio T/T_h based on Eq. (4.5) and (4.7) for specimens with No. 14 and No. 18 hooked bars placed outside column core by Chun et al. (2017b)	116
Table 4.13 Test-to-calculated T/T_h ratio based on Eq. (4.5) and (4.7) for specimens tested outside University of Kansas and not used to develop Eq. (4.5) and (4.7)	129
Table 4.14 Bar stresses and slip at failure for No. 7 and No. 11 hooked bar specimens by Marques and Jirsa (1975) along with T/T_h based on descriptive equations, Eq. (4.5) and (4.7)	135
Table 5.1 Comparison of No. 14 and No. 18 headed bar test results with descriptive equations by Shao et al. (2016), Eq. (1.5) and (1.6), also (5.2) and (5.3), and ACI 318-19	137
Table 5.2 Summary of test-to-calculated ratio T/T_h for No. 14 and No. 18 headed bars based on bar size and parallel ties with T_h based on Eq. (5.2) or (5.3), excluding specimens that failed in shear	141
Table 5.3 Summary of test-to-calculated ratio T/T_h for No. 14 and No. 18 headed bars tested under loading condition A (all with parallel ties) with T_h based on Eq. (5.3), excluding specimens that failed in shear.....	141
Table 5.4 Summary of test-to-calculated ratio T/T_h for No. 14 and No. 18 headed bars with parallel ties and tested under loading condition B with T_h based on Eq. (5.3)	142
Table 5.5 Statistical parameters for T/T_c ratio for headed bar specimens with widely-spaced bars without parallel ties with T_c based on Eq. (5.4)	145

Table 5.6 Statistical parameters of T/T_c ratio for headed bar specimens with closely-spaced bars without parallel ties with T_c based on Eq. (5.5)	147
Table 5.7 Statistical parameters of T/T_c , with T_c based on Eq. (5.5), for headed bar specimens with widely- and closely-spaced bars without parallel ties.....	148
Table 5.8 Statistical parameters of T/T_h ratio for headed bar specimens with widely-spaced bars with parallel ties with T_h based on Eq. (5.6)	150
Table 5.9 Statistical parameters of T/T_h ratio for headed bar specimens with closely-spaced bars with parallel ties with T_h based on Eq. (5.7)	152
Table 5.10 Statistical parameters of T/T_h ratio for headed bar specimens with widely- and closely-spaced bars with parallel ties with T_h based on Eq. (5.7)	153
Table 5.11 Statistical parameters of T/T_h ratio for all headed bar specimens with T_h based on Eq. (5.5) or (5.7).....	153
Table 5.12 Summary of T/T_h values for No. 14 and No. 18 headed bars specimens tested in this study based on the developed descriptive equations, Eq. (5.5) and (5.7)	154
Table 5.13 Summary of test-to-calculated ratio T/T_h for No. 14 and No. 18 headed bars based on bar size and parallel ties, with T_h based on Eq. (5.5) or (5.7), excluding specimens that failed in shear	156
Table 5.14 Summary of test-to-calculated ratio T/T_h for No. 14 and No. 18 headed bars tested under loading condition A (all with parallel ties) with T_h based on Eq. (5.7), excluding specimens that failed in shear	156
Table 5.15 Summary of test-to-calculated ratio T/T_h for No. 14 and No. 18 headed bars with parallel ties and tested under loading condition B with T_h based on Eq. (5.7)	157
Table 5.16 Details and test-to-calculated T/T_h ratios of the specimens tested by Chun et al. (2017) and Sim and Chun (2022a, 2022b) with headed bars outside column core	184
Table 5.17 Test-to-calculated ratio T/T_h based on Eq. (5.5) and (5.7) for beam-column joint specimens tested by Bashandy (1996) (values converted from SI units)	189
Table 6.1 Statistical parameters of T/T_c ratio using Eq. (6.3) for hooked bar specimens with widely- and closely-spaced bars without confining reinforcement	195
Table 6.2 Statistical parameters of T/T_h using Eq. (6.6) for hooked bar specimens with widely- and closely-spaced bars with confining reinforcement used to develop descriptive equations Eq. (4.5) and (4.7)	198

Table 6.3 Statistical parameters of T/T_h ratio using Eq. (6.3) and (6.6) for hooked bar specimens used to develop descriptive equations Eq. (4.5) and (4.7)	198
Table 6.4 Statistical parameters of T/T_h ratio using Eq. (6.8) with applying $A_{th}/A_{hs} \leq 0.4$ for hooked bar specimens with widely- and closely-spaced bars with confining reinforcement used to develop descriptive equations Eq. (4.5) and (4.7)	199
Table 6.5 Modification factors for the proposed design equation for development of hooked bars	205
Table 6.6 Statistical parameters of test-to-calculated bar stress at failure $f_{su}/f_{s,calc}$ for hooked bar specimens without confining reinforcement, based on the proposed design equation, Eq. (6.17), and the full expression for ψ_r , Eq. (6.14).....	207
Table 6.7 Statistical parameters of test-to-calculated bar stress at failure $f_{su}/f_{s,calc}$ for hooked bar specimens without confining reinforcement, based on the proposed design equation, Eq. (6.17) and the simplified expressions for ψ_r , Eq. (6.15)	208
Table 6.8 Statistical parameters of test-to-calculated bar stress at failure $f_{su}/f_{s,calc}$ for hooked bar specimens with confining reinforcement, based on the proposed design equation, Eq. (6.17) and the full expression for ψ_r , Eq. (6.14)	208
Table 6.9 Statistical parameters of test-to-calculated bar stress at failure $f_{su}/f_{s,calc}$ for hooked bar specimens with confining reinforcement, based on the proposed design equation, Eq. (6.17) and the simplified expressions for ψ_r , Eq. (6.15)	209
Table 6.10 Statistical parameters of test-to-calculated bar stress at failure $f_{su}/f_{s,calc}$ for hooked bar specimens, without and with confining reinforcement, used to develop descriptive equations Eq. (4.5) and (4.7), based on the proposed design equation Eq. (6.17) and using the full expression for ψ_r , Eq. (6.14).....	210
Table 6.11 Statistical parameters of test-to-calculated bar stress at failure $f_{su}/f_{s,calc}$ for hooked bar specimens, without and with confining reinforcement, used to develop descriptive equations Eq. (4.5) and (4.7), based on the proposed design equation Eq. (6.17) and using the simplified expressions for ψ_r , Eq. (6.15)	211
Table 6.12 Comparison of hooked bar specimens tested by Marques and Jirsa (1975) versus the proposed design equation, Eq. (6.17) using full and simplified expressions for ψ_r	212
Table 6.13 Comparison of hooked bar specimens tested by Pinc et al. (1977) versus the proposed design equation, Eq. (6.17)	213

Table 6.14 Comparison of hooked bar specimens tested by Hamad et al. (1993) versus the proposed design equation, Eq. (6.17).....	213
Table 6.15 Comparison of hooked bar specimens tested by Ramirez and Russell (2008) versus the proposed design equation, Eq. (6.17).....	214
Table 6.16 Comparison of hooked bar specimens tested by Lee and Park (2010) versus the proposed design equation, Eq. (6.17).....	215
Table 6.17 Comparison of hooked bar specimens tested by Chun et al. (2017b) versus the proposed design equation, Eq. (6.17)	215
Table 6.18 Statistical parameters of $f_{su}/f_{s,calc}$ for hooked bar specimens tested outside University of Kansas, based on the proposed design equation Eq. (6.17) and using the full expression for ψ_r , Eq. (6.14)	216
Table 6.19 Statistical parameters of T/T_c ratio based on simplified descriptive equation, Eq. (6.20), for headed bar specimens with widely- and closely-spaced bars without parallel ties used to develop descriptive equations, Eq. (5.5) and (5.7)	219
Table 6.20 Statistical parameters of T/T_h ratio based on simplified descriptive equation, Eq. (6.23), for headed bar specimens with widely- and closely-spaced bars with parallel ties used to develop descriptive equations, Eq. (5.5) and (5.7)	221
Table 6.21 Statistical parameters of T/T_h ratio based on simplified descriptive equation, Eq. (6.20) and (6.23), for all headed bar specimens used to develop descriptive equations, Eq. (5.5) and (5.7)	223
Table 6.22 Modification factors for the proposed design equation for development of headed bars, Eq. (6.31)	228
Table 6.23 Statistical parameters of test-to-calculated bar stress at failure $f_{su}/f_{s,calc}$ based on the proposed design equation Eq. (6.32) and using the full expression for ψ_p , Eq. (6.29) for headed bar specimens without parallel tie used to develop descriptive equations, Eq. (5.5) and (5.7)	230
Table 6.24 Statistical parameters of test-to-calculated bar stress at failure $f_{su}/f_{s,calc}$ based on the proposed design equation Eq. (6.32) and using the full expression for ψ_p , Eq. (6.29) for headed bar specimens with parallel tie used to develop descriptive equations, Eq. (5.5) and (5.7)	230
Table 6.25 Statistical parameters of test-to-calculated bar stress at failure $f_{su}/f_{s,calc}$ based on the proposed design equation Eq. (6.32) and using the simplified expressions for ψ_p , Eq. (6.30) for	

headed bar specimens with parallel tie used to develop descriptive equations, Eq. (5.5) and (5.7)	231
Table 6.26 Statistical parameters of test-to-calculated bar stress at failure $f_{su}/f_{s,calc}$ based on the proposed design equation Eq. (6.32) and using the full expression for ψ_p , Eq. (6.29) for all headed bar specimens used to develop descriptive equations, Eq. (5.5) and (5.7)	231
Table 6.27 Statistical parameters of test-to-calculated bar stress at failure $f_{su}/f_{s,calc}$ based on the proposed design equation Eq. (6.32) and using the full expression for ψ_p , Eq. (6.30) for all headed bar specimens used to develop descriptive equations, Eq. (5.5) and (5.7)	232
Table 6.28 Comparison of beam-column joint test results by Bashandy (1996) versus the proposed design equation Eq. (6.32) (values converted from SI units)	233
Table 6.29 Comparison of headed bar specimens tested by Chun et al. (2017a) and Chun and Lee (2019) versus the proposed design equation, Eq. (6.32)	234
Table 6.30 Comparison of headed bar specimens tested by Sim and Chun (2022b) versus the proposed design equation, Eq. (6.32)	236
Table 6.31 Statistical parameters of $f_{su}/f_{s,calc}$ for all headed bar specimens tested outside University of Kansas (Bashandy 1996, Chun et al 2017a, Chun and Lee 2019, Sim and Chun 2022b) based on the proposed design equation Eq. (6.32), excluding specimens with shear failure and those with headed bars that yielded	237
Table B.1 Detailed properties and test results for No. 14 and No. 18 bar specimens tested in current study	274
Table B.2 Detailed properties and test results for hooked bar specimens having widely-spaced bars without confining reinforcement tested at the University of Kansas	278
Table B.3 Detailed properties and test results for hooked bar specimens having closely-spaced bars without confining reinforcement tested at the University of Kansas	287
Table B.4 Detailed properties and test results for hooked bar specimens having widely-spaced bars with confining reinforcement tested at the University of Kansas	290
Table B.5 Detailed properties and test results for hooked bar specimens having closely-spaced bars with confining reinforcement tested at the University of Kansas	300
Table B.6 Detailed properties and test results for hooked bar specimens with bars placed outside column longitudinal reinforcement (column core) tested at the University of Kansas	306

Table B.7 Detailed properties and test results for hooked bar specimens with effective beam depth to embedment ratio $d_{eff}/\ell_{eh} > 1.5$ tested at the University of Kansas	312
Table B.8 Detailed properties and test results for hooked bar specimens tested outside the University of Kansas	314
Table C.1 Detailed properties and test results for No. 14 and No. 18 bar specimens tested in current study	352
Table C.2 Detailed properties and test results for headed bar specimens having widely-spaced bars without parallel ties tested at the University of Kansas	360
Table C.3 Detailed properties and test results for headed bar specimens having closely-spaced bars without parallel ties tested at the University of Kansas	366
Table C.4 Detailed properties and test results for headed bar specimens having widely-spaced bars with parallel ties tested at the University of Kansas	372
Table C.5 Detailed properties and test results for headed bar specimens having closely-spaced bars with parallel ties tested at the University of Kansas	378
Table C.6 Detailed properties and test results for hooked bar specimens tested outside the University of Kansas	384

CHAPTER 1: INTRODUCTION

1.1 GENERAL

The bond between the reinforcing steel and concrete is a critical factor in reinforced concrete structures and must be sufficient so that forces can transfer between the two materials. Development length is defined as the “length of embedded reinforcement...required to develop the design strength of reinforcement at a critical section” (ACI 318-19) (such as the face of column in a beam-column joint connection). In some cases, such as in an external beam-column connection, it is possible that the member geometry does not allow for a straight deformed bar to fully develop its yield strength (that is, the required development length is longer than the column width). To address this issue, hooked and headed reinforcing bars are commonly used to mechanically anchor the bar within the connection. For both hooked and headed bars, a bearing force from the bent portion of the hook or from the head participates in transferring the force in the bar to the concrete, in addition to the force transferred along the straight portion of the bar, allowing for a shorter overall development length than can be achieved with a straight bar alone. The use of conventional hooked bars, however, can be problematic where steel congestion is a concern (for example, in a heavily reinforced beam-column joint). In such cases, headed bars can be used as an effective alternative.

The provisions for the development length of hooked and headed bars are provided in Sections 25.4.3 and 25.4.4, respectively, of the ACI 318-19 Building Code Requirements for Structural Concrete. Earlier editions of the ACI Code, including ACI 318-14, contained a number of restrictions applied to the use of hooked and headed bars, mainly due to limited test data and a limited range of material properties. For hooked bars, the yield strength was limited to 80,000 psi and the concrete strength was limited to 10,000 psi for use in calculating the development length. For headed bars, the steel yield strength was limited to 60,000 psi and concrete strength to just 6,000 psi. In addition, headed bars were required to be placed with a minimum clear spacing of $4d_b$ with a minimum cover of $2d_b$, where d_b is the nominal diameter of the bar.

The provisions in ACI 318-14 did not allow for the use of high-strength reinforcing steel and concrete, despite their expanding use in construction. High-strength steel helps reduce reinforcement congestion, and high-strength concrete yields smaller member sizes and increased usable floor area. A comprehensive study at the University of Kansas (Searle et al. 2014, Sperry et al. 2015a, 2015b, 2017a, 2017b, 2018, Yasso et al. 2017, Ajaam et al. 2017, 2018, Shao et al. 2018, 2019, 2020, 2021, 2022, 2023, 2024, 2025, 2026, 2027, 2028, 2029, 2030, 2031, 2032, 2033, 2034, 2035, 2036, 2037, 2038, 2039, 2040, 2041, 2042, 2043, 2044, 2045, 2046, 2047, 2048, 2049, 2050, 2051, 2052, 2053, 2054, 2055, 2056, 2057, 2058, 2059, 2060, 2061, 2062, 2063, 2064, 2065, 2066, 2067, 2068, 2069, 2070, 2071, 2072, 2073, 2074, 2075, 2076, 2077, 2078, 2079, 2080, 2081, 2082, 2083, 2084, 2085, 2086, 2087, 2088, 2089, 2090, 2091, 2092, 2093, 2094, 2095, 2096, 2097, 2098, 2099, 2100, 2101, 2102, 2103, 2104, 2105, 2106, 2107, 2108, 2109, 2110, 2111, 2112, 2113, 2114, 2115, 2116, 2117, 2118, 2119, 2120, 2121, 2122, 2123, 2124, 2125, 2126, 2127, 2128, 2129, 2130, 2131, 2132, 2133, 2134, 2135, 2136, 2137, 2138, 2139, 2140, 2141, 2142, 2143, 2144, 2145, 2146, 2147, 2148, 2149, 2150, 2151, 2152, 2153, 2154, 2155, 2156, 2157, 2158, 2159, 2160, 2161, 2162, 2163, 2164, 2165, 2166, 2167, 2168, 2169, 2170, 2171, 2172, 2173, 2174, 2175, 2176, 2177, 2178, 2179, 2180, 2181, 2182, 2183, 2184, 2185, 2186, 2187, 2188, 2189, 2190, 2191, 2192, 2193, 2194, 2195, 2196, 2197, 2198, 2199, 2200, 2201, 2202, 2203, 2204, 2205, 2206, 2207, 2208, 2209, 2210, 2211, 2212, 2213, 2214, 2215, 2216, 2217, 2218, 2219, 2220, 2221, 2222, 2223, 2224, 2225, 2226, 2227, 2228, 2229, 2230, 2231, 2232, 2233, 2234, 2235, 2236, 2237, 2238, 2239, 2240, 2241, 2242, 2243, 2244, 2245, 2246, 2247, 2248, 2249, 2250, 2251, 2252, 2253, 2254, 2255, 2256, 2257, 2258, 2259, 2260, 2261, 2262, 2263, 2264, 2265, 2266, 2267, 2268, 2269, 2270, 2271, 2272, 2273, 2274, 2275, 2276, 2277, 2278, 2279, 2280, 2281, 2282, 2283, 2284, 2285, 2286, 2287, 2288, 2289, 2290, 2291, 2292, 2293, 2294, 2295, 2296, 2297, 2298, 2299, 2300, 2301, 2302, 2303, 2304, 2305, 2306, 2307, 2308, 2309, 2310, 2311, 2312, 2313, 2314, 2315, 2316, 2317, 2318, 2319, 2320, 2321, 2322, 2323, 2324, 2325, 2326, 2327, 2328, 2329, 2330, 2331, 2332, 2333, 2334, 2335, 2336, 2337, 2338, 2339, 2340, 2341, 2342, 2343, 2344, 2345, 2346, 2347, 2348, 2349, 2350, 2351, 2352, 2353, 2354, 2355, 2356, 2357, 2358, 2359, 2360, 2361, 2362, 2363, 2364, 2365, 2366, 2367, 2368, 2369, 2370, 2371, 2372, 2373, 2374, 2375, 2376, 2377, 2378, 2379, 2380, 2381, 2382, 2383, 2384, 2385, 2386, 2387, 2388, 2389, 2390, 2391, 2392, 2393, 2394, 2395, 2396, 2397, 2398, 2399, 2400, 2401, 2402, 2403, 2404, 2405, 2406, 2407, 2408, 2409, 2410, 2411, 2412, 2413, 2414, 2415, 2416, 2417, 2418, 2419, 2420, 2421, 2422, 2423, 2424, 2425, 2426, 2427, 2428, 2429, 2430, 2431, 2432, 2433, 2434, 2435, 2436, 2437, 2438, 2439, 2440, 2441, 2442, 2443, 2444, 2445, 2446, 2447, 2448, 2449, 2450, 2451, 2452, 2453, 2454, 2455, 2456, 2457, 2458, 2459, 2460, 2461, 2462, 2463, 2464, 2465, 2466, 2467, 2468, 2469, 2470, 2471, 2472, 2473, 2474, 2475, 2476, 2477, 2478, 2479, 2480, 2481, 2482, 2483, 2484, 2485, 2486, 2487, 2488, 2489, 2490, 2491, 2492, 2493, 2494, 2495, 2496, 2497, 2498, 2499, 2500, 2501, 2502, 2503, 2504, 2505, 2506, 2507, 2508, 2509, 2510, 2511, 2512, 2513, 2514, 2515, 2516, 2517, 2518, 2519, 2520, 2521, 2522, 2523, 2524, 2525, 2526, 2527, 2528, 2529, 2530, 2531, 2532, 2533, 2534, 2535, 2536, 2537, 2538, 2539, 2540, 2541, 2542, 2543, 2544, 2545, 2546, 2547, 2548, 2549, 2550, 2551, 2552, 2553, 2554, 2555, 2556, 2557, 2558, 2559, 2560, 2561, 2562, 2563, 2564, 2565, 2566, 2567, 2568, 2569, 2570, 2571, 2572, 2573, 2574, 2575, 2576, 2577, 2578, 2579, 2580, 2581, 2582, 2583, 2584, 2585, 2586, 2587, 2588, 2589, 2590, 2591, 2592, 2593, 2594, 2595, 2596, 2597, 2598, 2599, 2600, 2601, 2602, 2603, 2604, 2605, 2606, 2607, 2608, 2609, 2610, 2611, 2612, 2613, 2614, 2615, 2616, 2617, 2618, 2619, 2620, 2621, 2622, 2623, 2624, 2625, 2626, 2627, 2628, 2629, 2630, 2631, 2632, 2633, 2634, 2635, 2636, 2637, 2638, 2639, 2640, 2641, 2642, 2643, 2644, 2645, 2646, 2647, 2648, 2649, 2650, 2651, 2652, 2653, 2654, 2655, 2656, 2657, 2658, 2659, 2660, 2661, 2662, 2663, 2664, 2665, 2666, 2667, 2668, 2669, 2670, 2671, 2672, 2673, 2674, 2675, 2676, 2677, 2678, 2679, 2680, 2681, 2682, 2683, 2684, 2685, 2686, 2687, 2688, 2689, 2690, 2691, 2692, 2693, 2694, 2695, 2696, 2697, 2698, 2699, 2700, 2701, 2702, 2703, 2704, 2705, 2706, 2707, 2708, 2709, 2710, 2711, 2712, 2713, 2714, 2715, 2716, 2717, 2718, 2719, 2720, 2721, 2722, 2723, 2724, 2725, 2726, 2727, 2728, 2729, 2730, 2731, 2732, 2733, 2734, 2735, 2736, 2737, 2738, 2739, 2740, 2741, 2742, 2743, 2744, 2745, 2746, 2747, 2748, 2749, 2750, 2751, 2752, 2753, 2754, 2755, 2756, 2757, 2758, 2759, 2760, 2761, 2762, 2763, 2764, 2765, 2766, 2767, 2768, 2769, 2770, 2771, 2772, 2773, 2774, 2775, 2776, 2777, 2778, 2779, 2780, 2781, 2782, 2783, 2784, 2785, 2786, 2787, 2788, 2789, 2790, 2791, 2792, 2793, 2794, 2795, 2796, 2797, 2798, 2799, 2800, 2801, 2802, 2803, 2804, 2805, 2806, 2807, 2808, 2809, 2810, 2811, 2812, 2813, 2814, 2815, 2816, 2817, 2818, 2819, 2820, 2821, 2822, 2823, 2824, 2825, 2826, 2827, 2828, 2829, 2830, 2831, 2832, 2833, 2834, 2835, 2836, 2837, 2838, 2839, 2840, 2841, 2842, 2843, 2844, 2845, 2846, 2847, 2848, 2849, 2850, 2851, 2852, 2853, 2854, 2855, 2856, 2857, 2858, 2859, 2860, 2861, 2862, 2863, 2864, 2865, 2866, 2867, 2868, 2869, 2870, 2871, 2872, 2873, 2874, 2875, 2876, 2877, 2878, 2879, 2880, 2881, 2882, 2883, 2884, 2885, 2886, 2887, 2888, 2889, 2890, 2891, 2892, 2893, 2894, 2895, 2896, 2897, 2898, 2899, 2900, 2901, 2902, 2903, 2904, 2905, 2906, 2907, 2908, 2909, 2910, 2911, 2912, 2913, 2914, 2915, 2916, 2917, 2918, 2919, 2920, 2921, 2922, 2923, 2924, 2925, 2926, 2927, 2928, 2929, 2930, 2931, 2932, 2933, 2934, 2935, 2936, 2937, 2938, 2939, 2940, 2941, 2942, 2943, 2944, 2945, 2946, 2947, 2948, 2949, 2950, 2951, 2952, 2953, 2954, 2955, 2956, 2957, 2958, 2959, 2960, 2961, 2962, 2963, 2964, 2965, 2966, 2967, 2968, 2969, 2970, 2971, 2972, 2973, 2974, 2975, 2976, 2977, 2978, 2979, 2980, 2981, 2982, 2983, 2984, 2985, 2986, 2987, 2988, 2989, 2990, 2991, 2992, 2993, 2994, 2995, 2996, 2997, 2998, 2999, 3000, 3001, 3002, 3003, 3004, 3005, 3006, 3007, 3008, 3009, 3010, 3011, 3012, 3013, 3014, 3015, 3016, 3017, 3018, 3019, 3020, 3021, 3022, 3023, 3024, 3025, 3026, 3027, 3028, 3029, 3030, 3031, 3032, 3033, 3034, 3035, 3036, 3037, 3038, 3039, 3040, 3041, 3042, 3043, 3044, 3045, 3046, 3047, 3048, 3049, 3050, 3051, 3052, 3053, 3054, 3055, 3056, 3057, 3058, 3059, 3060, 3061, 3062, 3063, 3064, 3065, 3066, 3067, 3068, 3069, 3070, 3071, 3072, 3073, 3074, 3075, 3076, 3077, 3078, 3079, 3080, 3081, 3082, 3083, 3084, 3085, 3086, 3087, 3088, 3089, 3090, 3091, 3092, 3093, 3094, 3095, 3096, 3097, 3098, 3099, 3100, 3101, 3102, 3103, 3104, 3105, 3106, 3107, 3108, 3109, 3110, 3111, 3112, 3113, 3114, 3115, 3116, 3117, 3118, 3119, 3120, 3121, 3122, 3123, 3124, 3125, 3126, 3127, 3128, 3129, 3130, 3131, 3132, 3133, 3134, 3135, 3136, 3137, 3138, 3139, 3140, 3141, 3142, 3143, 3144, 3145, 3146, 3147, 3148, 3149, 3150, 3151, 3152, 3153, 3154, 3155, 3156, 3157, 3158, 3159, 3160, 3161, 3162, 3163, 3164, 3165, 3166, 3167, 3168, 3169, 3170, 3171, 3172, 3173, 3174, 3175, 3176, 3177, 3178, 3179, 3180, 3181, 3182, 3183, 3184, 3185, 3186, 3187, 3188, 3189, 3190, 3191, 3192, 3193, 3194, 3195, 3196, 3197, 3198, 3199, 3200, 3201, 3202, 3203, 3204, 3205, 3206, 3207, 3208, 3209, 3210, 3211, 3212, 3213, 3214, 3215, 3216, 3217, 3218, 3219, 3220, 3221, 3222, 3223, 3224, 3225, 3226, 3227, 3228, 3229, 3230, 3231, 3232, 3233, 3234, 3235, 3236, 3237, 3238, 3239, 3240, 3241, 3242, 3243, 3244, 3245, 3246, 3247, 3248, 3249, 3250, 3251, 3252, 3253, 3254, 3255, 3256, 3257, 3258, 3259, 3260, 3261, 3262, 3263, 3264, 3265, 3266, 3267, 3268, 3269, 3270, 3271, 3272, 3273, 3274, 3275, 3276, 3277, 3278, 3279, 3280, 3281, 3282, 3283, 3284, 3285, 3286, 3287, 3288, 3289, 3290, 3291, 3292, 3293, 3294, 3295, 3296, 3297, 3298, 3299, 3300, 3301, 3302, 3303, 3304, 3305, 3306, 3307, 3308, 3309, 3310, 3311, 3312, 3313, 3314, 3315, 3316, 3317, 3318, 3319, 3320, 3321, 3322, 3323, 3324, 3325, 3326, 3327, 3328, 3329, 3330, 3331, 3332, 3333, 3334, 3335, 3336, 3337, 3338, 3339, 3340, 3341, 3342, 3343, 3344, 3345, 3346, 3347, 3348, 3349, 3350, 3351, 3352, 3353, 3354, 3355, 3356, 3357, 3358, 3359, 3360, 3361, 3362, 3363, 3364, 3365, 3366, 3367, 3368, 3369, 3370, 3371, 3372, 3373, 3374, 3375, 3376, 3377, 3378, 3379, 3380, 3381, 3382, 3383, 3384, 3385, 3386, 3387, 3388, 3389, 3390, 3391, 3392, 3393, 3394, 3395, 3396, 3397, 3398, 3399, 3400, 3401, 3402, 3403, 3404, 3405, 3406, 3407, 3408, 3409, 3410, 3411, 3412, 3413, 3414, 3415, 3416, 3417, 3418, 3419, 3420, 3421, 3422, 3423, 3424, 3425, 3426, 3427, 3428, 3429, 3430, 3431, 3432, 3433, 3434, 3435, 3436, 3437, 3438, 3439, 3440, 3441, 3442, 3443, 3444, 3445, 3446, 3447, 3448, 3449, 3450, 3451, 3452, 3453, 3454, 3455, 3456, 3457, 3458, 3459, 3460, 3461, 3462, 3463, 3464, 3465, 3466, 3467, 3468, 3469, 3470, 3471, 3472, 3473, 3474, 3475, 3476, 3477, 3478, 3479, 3480, 3481, 3482, 3483, 3484, 3485, 3486, 3487, 3488, 3489, 3490, 3491, 3492, 3493, 3494, 3495, 3496, 3497, 3498, 3499, 3500, 3501, 3502, 3503, 3504, 3505, 3506, 3507, 3508, 3509, 3510, 3511, 3512, 3513, 3514, 3515, 3516, 3517, 3518, 3519, 3520, 3521, 3522, 3523, 3524, 3525, 3526, 3527, 3528, 3529, 3530, 3531, 3532, 3533, 3534, 3535, 3536, 3537, 3538, 3539, 3540, 3541, 3542, 3543, 3544, 3545, 3546, 3547, 3548, 3549, 3550, 3551, 3552, 3553, 3554, 3555, 3556, 3557, 3558, 3559, 3560, 3561, 3562, 3563, 3564, 3565, 3566, 3567, 3568, 3569, 3570, 3571, 3572, 3573, 3574, 3575, 3576, 3577, 3578, 3579, 3580, 3581, 3582, 3583, 3584, 3585, 3586, 3587, 3588, 3589, 3590, 3591, 3592, 3593, 3594, 3595, 3596, 3597, 3598, 3599, 3600, 3601, 3602, 3603, 3604, 3605, 3606, 3607, 3608, 3609, 3610, 3611, 3612, 3613, 3614, 3615, 3616, 3617, 3618, 3619, 3620, 3621, 3622, 3623, 3624, 3625, 3626, 3627, 3628, 3629, 3630, 3631, 3632, 3633, 3634, 3635, 3636, 3637, 3638, 3639, 3640, 3641, 3642, 3643, 3644, 3645, 3646, 3647, 3648, 3649, 3650, 3651, 3652, 3653, 3654, 3655, 3656, 3657, 3658, 3659, 3660, 3661, 3662, 3663, 3664, 3665, 3666, 3667, 3668, 3669, 3670, 3671, 3672, 3673, 3674, 3675, 3676, 3677, 3678, 3679, 3680, 3681, 3682, 3683, 3684, 3685, 3686, 3687, 3688, 3689, 3690, 3691, 3692, 3693, 3694, 3695, 3696, 3697, 3698, 3699, 3700, 3701, 3702, 3703, 3704, 3705, 3706, 3707, 3708, 3709, 3710, 3711, 3712, 3713, 3714, 3715, 3716, 3717, 3718, 3719, 3720, 3721, 3722, 3723, 3724, 3725, 3726, 3727, 3728, 3729, 3730, 3731, 3732, 3733, 3734, 3735, 3736, 3737, 3738, 3739, 3740, 3741, 3742, 3743, 3744, 3745, 3746, 3747, 3748, 3749, 3750, 3751, 3752, 3753, 3754, 3755, 3756, 3757, 3758, 3759, 3760, 3761, 3762, 3763, 3764, 3765, 3766, 3767, 3768, 3769, 3770, 3771, 3772, 3773, 3774, 3775, 3776, 3777, 3778, 3779, 3780, 3781, 3782, 3783, 3784, 3785, 3786, 3787, 3788, 3789, 3790, 3791, 3792, 3793, 3794, 3795, 3796, 3797, 3798, 3799, 3800, 3801, 3802, 3803, 3804, 3805, 3806, 3807, 3808, 3809, 3810, 3811, 3812, 3813, 3814, 3815, 3816, 3817, 3818, 3819, 3820, 3821, 3822, 3823, 3824, 3825, 3826, 3827, 3828, 3829, 3830, 3831, 3832, 3833, 3834, 3835, 3836, 3837, 3838, 3839, 3840, 3841, 3842, 3843, 3844, 3845, 3846, 3847, 3848, 3849, 3850, 3851, 3852, 3853, 3854, 3855, 3856, 3857, 3858, 3859, 3860, 3861, 3862, 3863, 3864, 3865, 3866, 3867, 3868, 3869, 3870, 3871, 3872, 3873, 3874, 3875, 3876, 3877, 3878, 3879, 3880, 3881, 3882, 3883, 3884, 3885, 3886, 3887, 3888, 3889, 3890, 3891, 3892, 3893, 3894, 3895, 3896, 3897, 3898, 3899, 3900, 3901, 3902, 3903, 3904, 3905, 3906, 3907, 3908, 3909, 3910, 3911, 3912, 3913, 3914, 3915, 3916, 3917, 3918, 3919, 3920, 3921, 3922, 3923, 3924, 3925, 3926, 3927, 3928, 3929, 3930, 3931, 3932, 3933, 3934, 3935, 3936, 3937, 3938, 3939, 3940, 3941, 3942, 3943, 3944, 3945, 3946

2016, Ghimire et al. 2018, 2019a, 2019b) expanded the experimental database on hooked and headed bars in beam-column joints to provide a better understanding of their behavior and improve the Code provisions. The study included 338 simulated beam-column joint specimens with hooked bars and 202 specimens with headed bars tested to investigate the effect on anchorage strength of key parameters, including concrete compressive strength (3,960 to 16,510 psi), bar stress at failure (22,800 to 153,200 psi), bar size (No. 5, No. 8, and No. 11), number of bars (2, 3, 4, and 6 bars in one or two layers), bar spacing (1.7 to $11.8d_b$), embedment length (3.5 to 26.3 in.), and the amount of confining reinforcement (stirrups and ties for hooked bars and parallel ties for headed bars) in the joint region (none to No. 3 or No. 4 hoops or ties spaced at $3d_b$). Based on the test data, descriptive equations for anchorage strength of hooked and headed bars were developed that cover a wide range of material strengths and member properties. The descriptive equations were then simplified to propose new provisions for development length of hooked and headed bars that allow the safe use of high-strength reinforcing steel (up to 120,000 ksi) and concrete (up to 16,000 psi).

The findings at the University of Kansas became the basis for developing current Code provisions in ACI 318-19. Limitations, however, remain on the use of hooked and headed bars larger than No. 11 (that is, No. 14 and No. 18 bars), mainly due to a lack of experimental data. For both hooked and headed bars, the current provisions still limit concrete compressive strength to 10,000 psi for the purpose of calculating development length. For hooked bars, the Code gives no credit to confining reinforcement for hooked bars larger than No. 11, and for headed bars, bars larger than No. 11 are not permitted. These limitations were the motivation for the current study.

The research reported here is a continuation of the comprehensive study began at the University of Kansas on the anchorage of high-strength hooked and headed reinforcing bars. This study expands the available data on the anchorage strength of high-strength headed and hooked bars to include No. 14 and No. 18 bars, the largest sizes currently permitted in the ACI Building Code. These results are used as a basis for new design criteria.

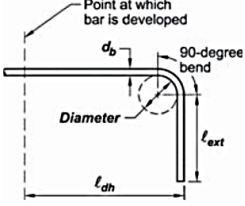
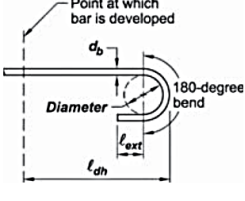
In this chapter, the background and relevant research work on the development of hooked and headed bars are provided, followed by a discussion of the current Code provisions, their development, and limitations. Finally, a summary of the objectives and scopes of this study is presented.

1.2 BACKGROUND AND PREVIOUS RESEARCH

1.2.1 Reinforcing Bars with Standard Hooks

When member dimensions do not allow for development of a straight bar, such as within an external beam-column joint, bars with a standard hook at their end (tail of the hook) can be used to provide anchorage to concrete. Standard hooks have 90° or 180° bends that meet the dimensional requirements specified in Table 25.3.1 of the ACI 318-19 Code, as shown in Table 1.1. The development length for hooked bars, ℓ_{dh} , is measured from back of the tail.

Table 1.1 Standard hook requirements (ACI 318-19)

Type of standard hook	Bar size	Minimum inside bend diameter, in.	Straight extension ^[1] ℓ_{ext} in.	Type of standard hook
90-degree hook	No. 3 through No. 8	$6d_b$	$12d_b$	
	No. 9 through No. 11	$8d_b$		
	No. 14 and No. 18	$10d_b$		
180-degree hook	No. 3 through No. 8	$6d_b$	Greater of $4d_b$ and 2.5 in.	
	No. 9 through No. 11	$8d_b$		
	No. 14 and No. 18	$10d_b$		

^[1]A standard hook for deformed bars in tension includes the specific inside bend diameter and straight extension length. It shall be permitted to use a longer straight extension at the end of a hook. A longer extension shall not be considered to increase the anchorage capacity of the hook.

Hooked bars provide anchorage force by engaging the concrete, as shown in Figure 1.1, with the anchorage strength governed, not ultimately by bond, but by the breakout or side-splitting strength of the concrete, as shown in Figure 1.2, which can be enhanced by confining reinforcement.

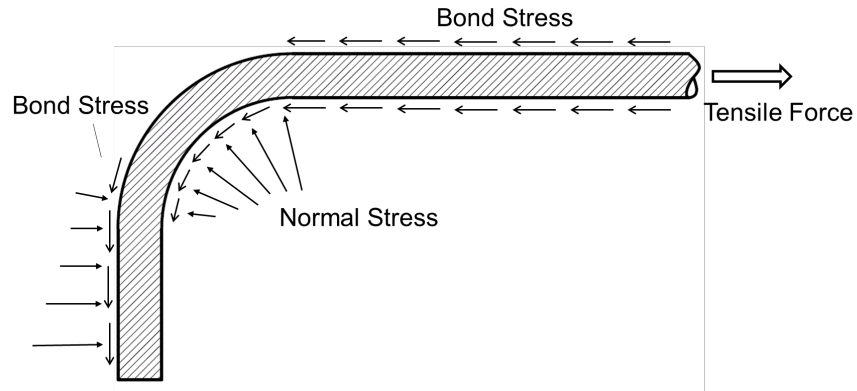


Figure 1.1. Anchorage mechanism of hooked bars (adapted from Marques and Jirsa 1975)

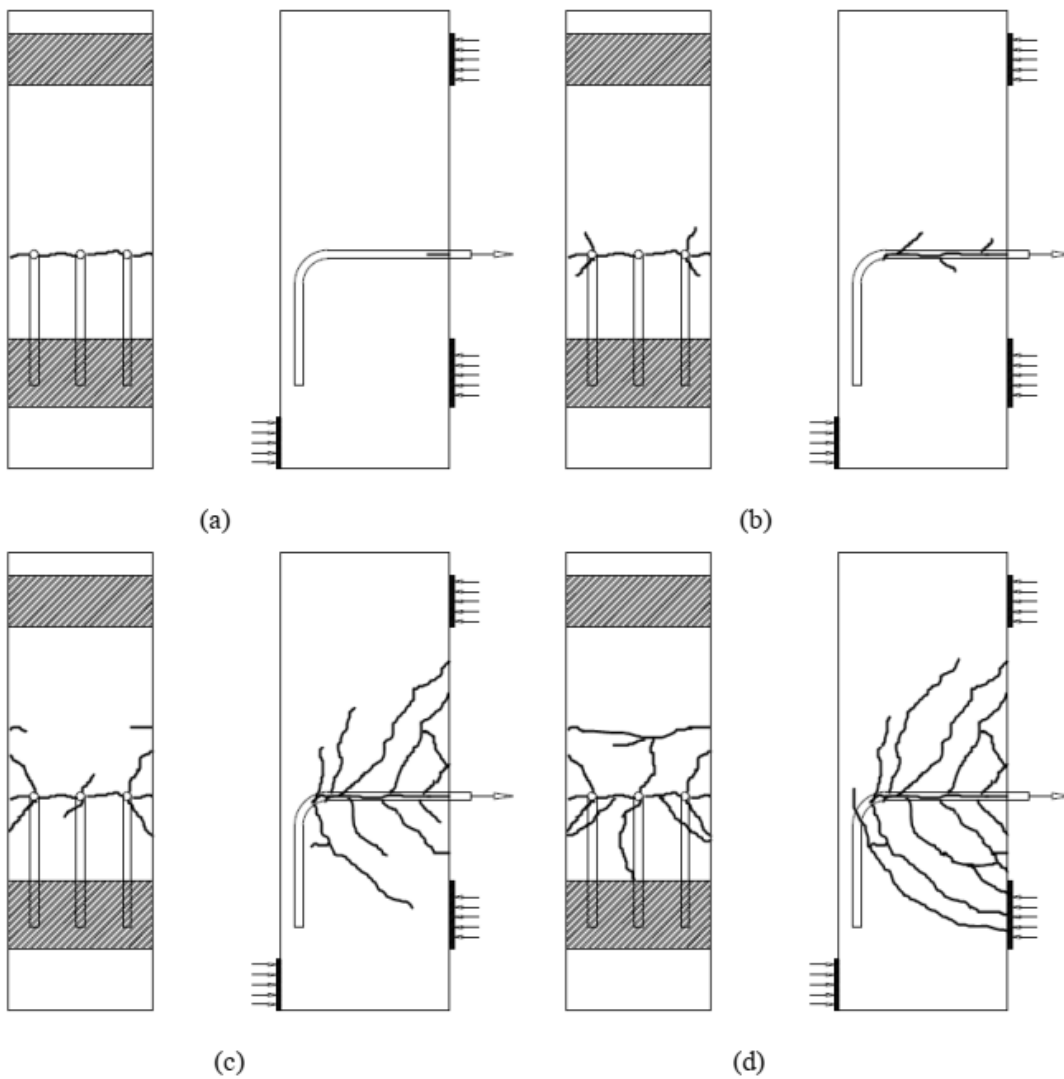


Figure 1.2 Crack progression observed in the beam-column joint specimens containing hooked bars (Sperry et al. 2015b, 2017a). Breakout failure is preceded by bond slip of the straight portion of the bars and cracking of the concrete

Marques and Jirsa (1975) studied No. 7 and No. 11 hooked bars anchored in simulated exterior beam-column joint with a width of 12 and 15 in. and a depth of 12 in. The study included twenty-two specimens with concrete compressive strengths of 3,600 to 5,100 psi, embedment lengths of 6.5 to 9.5 in. for No. 7 and 3 to 6 in. for No. 11 hooked bars, clear spacing between the two bars of 3.4 to 7.25 in., confining reinforcement in the joint region consisting of No. 3 ties spaced at 2.5 or 5 in., placement of hooked bars inside or outside of the column core), concrete side cover of 1.5 or 2.875 in., and an axial load of 135 to 450 kips. A schematic of the test specimens is shown in Figure 1.3. Marques and Jirsa (1975) found that increasing the embedment length increased the anchorage strength but that axial load variations and placement of hooked bars inside or outside of the column core had no noticeable effect on the anchorage strength.

As shown in Figure 1.3, the specimens had unconventional geometry and reinforcement layouts. All specimens were narrow, with a column width of 12 in. The side cover was almost 3 in. for the majority of specimens (Types 1, 2, 3, and 5), representing nearly half the specimen width. The hooked bars were placed outside column core, except in the Type 1 specimens. Also, in specimens with confining reinforcement, Types 3 and 5, there was a noticeable gap between the No. 3 bar tie legs and the column longitudinal reinforcement, uncommon in practice. The specimen proportions and location of applied forces along the height were also unrealistic, resulting in the joint carrying only 54% of the total force applied to the bars, significantly lower than would occur in a joint in a reinforced concrete frame structure, leading to unrealistically high anchorage strengths. These specimens are investigated in detail in Section 4.5. However, despite the unusual specimen geometry and reinforcement layouts, which were likely the result of the early nature of this research, the work by Marques and Jirsa (1975) paved the way for the many studies that followed.

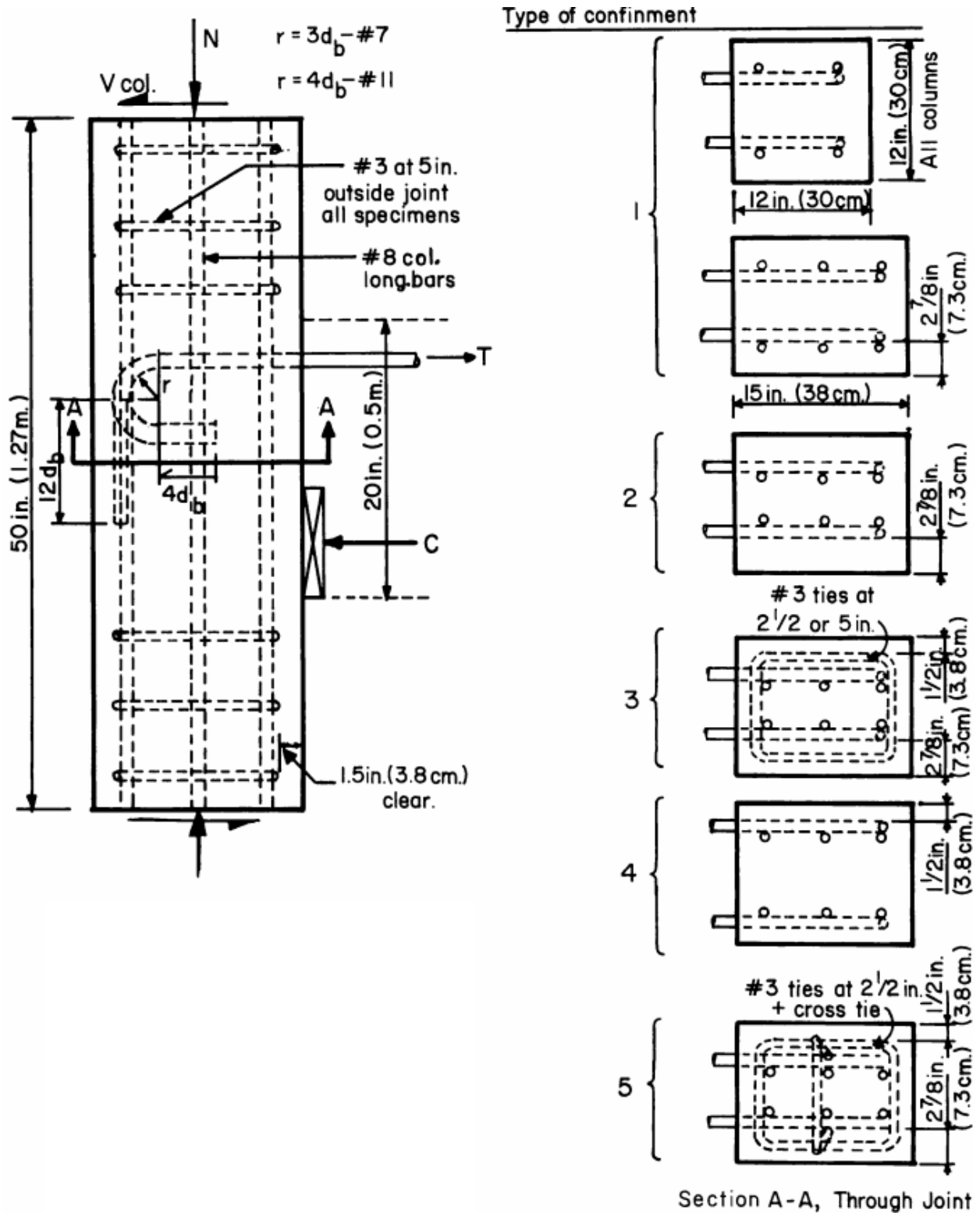


Figure 1.3 Schematic of test specimens used by Marques and Jirsa (1975); Type 1: Hooked bars inside column core without confining reinforcement, Type 2 and 4: Hooked bars outside column core without confining reinforcement, Type 3: Hooked bars outside column core with No. 3 ties, and Type 5: Hooked bars outside column core with No. 3 ties plus cross-tie

Pinc et al. (1977) tested 16 beam-column joint specimens, each with two hooked bars. No. 7, No. 9 and No. 11 hooked bars were used in normalweight and lightweight concrete. Concrete compressive strength ranged from 3,600 to 5,400 psi, clear bar spacing ranged from 3.4 to 4.0 in., and the side cover was $2\frac{7}{8}$ in. The specimens had no confining reinforcement in the joint region. A constant axial load (108 to 230 kips) was applied to specimens during the test. Pinc et al. concluded that embedment length was the key factors affecting the anchorage strength of hooked bars, and that the loss of side cover is the main factor governing the failure of hooked bars.

Joh et al. (1995) tested 19 beam-column specimens with 19 mm hooked bars; all but one contained four hooked bars. A single specimen contained eight hooked bars in two layers. Joh et al. investigated the effects of embedment length (nominally 5.2 to 13.0 in.), distance to the reaction representing the compression zone of the beam (nominally 9.0 to 16.9 in.), column depth (nominally 11.8 to 19.7 in.), spacing of the bars (1.9 to 2.6 in.), concrete side cover (2.54 to 14.5 in.), ratio of the confining reinforcement in the joint (0.2%, 0.4%, 0.8%), column axial stress (0 to 900 and 1887 psi, equal to 16.7% and 33.3% of the concrete compressive strength of the corresponding specimens), loading type (cyclic or monotonic), and concrete compressive strength (4,490 to 10,720 psi). Joh et al. found that applying a column axial stress equal to 16.7% (1/6) of concrete compressive strength increased the anchorage strength more than double (unlike Marques and Jirsa 1975), but increasing the axial stress from 16.7% (1/6) to 33.3% (1/3) of the concrete compressive strength had no effect on anchorage strength. They also found that anchorage strength increases proportionally with the addition of confining reinforcement, and that anchorage strength is proportional to the square root of the concrete compressive strength and the reciprocal of the sine of the compression strut angle (from the centroid of the compression zone of the beam to the bent portion of the hooked bar, as shown in Figure 1.4).

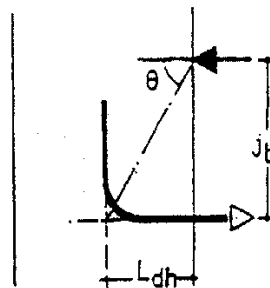


Figure 1.4 Strut angle as defined by Joh et al. (1995)

The work by Joh et al (1995) was continued by Joh and Shibata (1996), in which 13 beam-column specimens were tested. Each specimen had four 19-mm diameter hooked bars. The specimen parameters were concrete compressive strength (3,380 to 8,060 psi), center-to-center bar spacing (nominally 2.2 in.), side cover on the hooked bars (nominally 2.5 to 10.4 in.), and column axial stress (0 to 1,860 psi, equal to 0 to 33% of the concrete compressive strength of the corresponding specimens). The column ties were placed around the column longitudinal bars with a clear cover of 0.75 in. Joh and Shibata observed an increase in anchorage strength of hooked bars in specimens subjected to column axial stress compared to those with no axial stress. For pairs of specimens with similar concrete strengths and subjected to axial stress, however, increasing the axial stress beyond 8% of the corresponding concrete compressive strength (as opposed to 16.7% of the compressive strength in the previous research by Joh et al. 1995) did not have a noticeable effect on the anchorage strength. Anchorage strength also increased with increasing concrete side cover. However, when the side cover on the hooked bars was so large (10.4 in. versus 2.5 in.) that the breakout region ahead of the hooked bars (angle with respect to the longitudinal direction of the hooked bars of about 40°) did not reach the sides of the column, the effectiveness of the ties at the column boundaries decreased.

Twenty-one beam-column joint specimens were tested by Ramirez and Russell (2008). The specimens were cantilever columns with no axial load. The parameters included bar size (No. 6 or No. 11), confining reinforcement in the joint region (none to No. 3 ties spaced at $3d_b$), side cover (3.5 in.), back cover to the hook (0.75 to 2.5 in.), concrete compressive strength (8,910 to 16,500 psi), and embedment length (6.5 to 15.5 in.). They proposed increasing the modification factor 0.7 to 0.8 for No. 11 and smaller bars with a minimum side cover to the bar of 2.5 in. and cover to the back of the hook of 2 in. in ACI 318-05 and the AASHTO LRFD Bridge Specifications. Ramirez and Russell stated that the limit on concrete compressive strength could be increased to 15,000 psi in ACI 318-05 and the AASHTO LRFD Bridge Specifications if ties spaced at $3d_b$ are provided as confining reinforcement in the joint region.

To expand the available data to include a wide range of material properties, including high-strength concrete and reinforcing steel, a comprehensive study was initiated at the University of Kansas on the anchorage strength of standard hooked bars. The study included work by Searle et al. (2014), Sperry et al. (2015a, 2015b, 2017a, 2017b, 2018), Yasso et al. (2017), Ajaam et al. (2017, 2018). A total of 245 simulated beam-column joint specimens were tested in normalweight

concrete to investigate the effects of key parameters on the anchorage strength of hooked bars. The parameters included the number of hooked bars (2, 3, 4, or 6), arrangement of hooked bars (one or two layers), bar size (No. 5, No. 8, and No. 11), bar spacing (2 to $11.8d_b$ center-to-center), hook bend angle (90° or 180°), embedment length (3.5 to 26.3 in.), confining reinforcement in the joint region (none to nine No. 3 hoops spaced at no greater than $3d_b$), location of hooked bar within the column depth (hooks on the far side of the column or extending only to the middle of the column), placement of hooked bar inside or outside the column core (the area of concrete inside the column longitudinal reinforcement), bar stress at failure (22,800 to 141,600 psi), concrete compressive strength (4,300 to 16,510 psi), clear concrete side cover (1.5 to 4 in., with most values between 2.5 and 3.5 in.), cover to the tail of the hook (2 to 18 in.), and ratios of beam effective depth to embedment length (0.6 to 2.13).

A schematic of a specimen simulating an exterior beam-column joint with hooked bars placed inside the column core is shown in Figure 1.5. Tension and compression forces are applied using a self-reacting frame. The hooked bars represent the longitudinal reinforcement of a simulated beam, and the adjacent compression force represents the beam compression region.

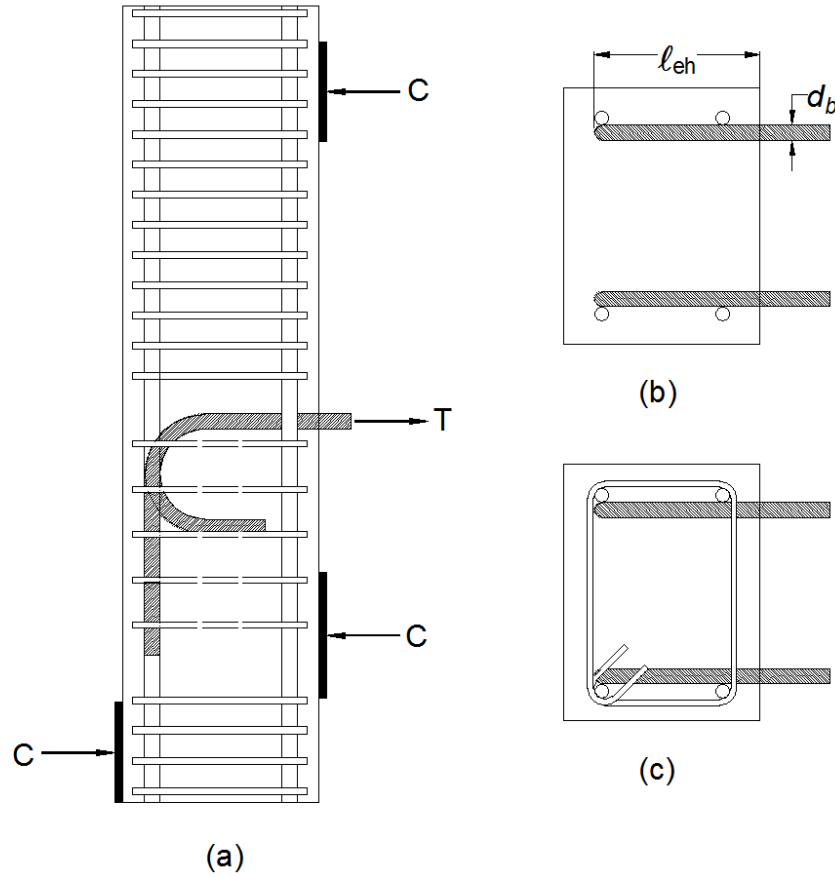


Figure 1.5 Schematic of specimens (a) side view (b) cross-section without confining reinforcement, and (c) cross-section with confining reinforcement, where ℓ_{eh} is the embedment length and d_b is bar diameter

The reaction frame to simulate the axial, tensile, and compression forces, shown in Figure 1.6, was a modified version of that used by Marques and Jirsa (1975). The beam compression zone was simulated using bearing member, and the upper compression and lower tension members prevented rotation of the specimen.

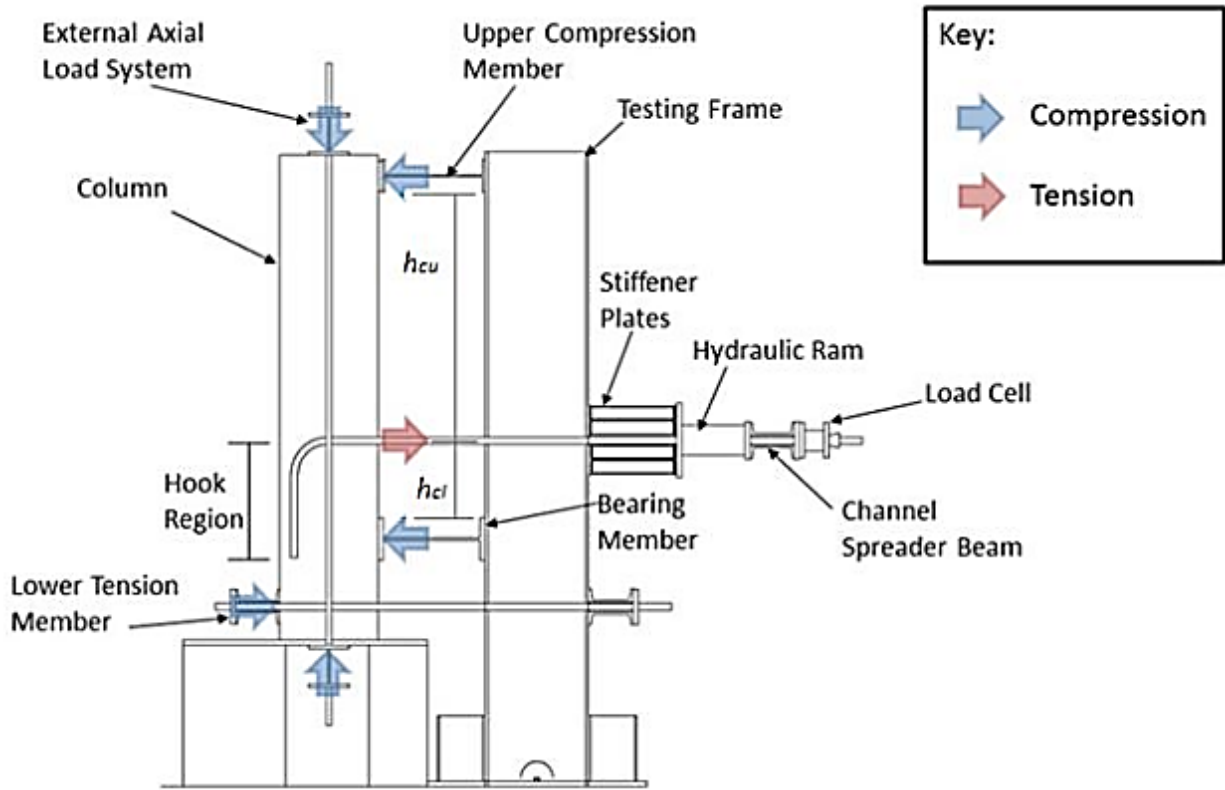


Figure 1.6 Schematic of the reaction frame (Sperry et al. 2015b)

Crack progression and the failure mechanism for the specimens is illustrated in Figure 1.2. The first cracks initiated from the hooked bars on the front face of the column due to slip of the straight portions of the bars and propagated horizontally on the column side face (Figure 1.2a). With an increase in load, the front face cracks continued to grow, radiating from the hooked bars. On the column side face, cracks continued to grow horizontally along the straight portion of the bars (Figure 1.2b). With more load, inclined cracks propagated on the column side face, in a cone-shaped manner, towards the bearing members (Figure 1.2c). These cracks further propagated and were widened near as the specimen got close to failure (Figure 1.2d).

Two primary failure modes were observed, namely concrete breakout and side splitting, as shown in Figure 1.7. Concrete breakout is characterized by a mass of concrete being pulled out along with the hooked bar from the front face of the specimen. Side splitting is marked by the side cover on the hooked bar separating from the specimen due to wedging action of the hook. In some specimens, a secondary failure mode, tail kickout, occurred along with other failure modes, marked by the concrete over being pushed off the back of the column by the tail of the hook, causing the

cover to spall and exposing the tail. Tail knockout occurred subsequent to the peak load and did not affect anchorage strength.



Figure 1.7 Primary failure modes observed in hooked bar specimens (Sperry et al. 2015b)

Based on the test results, descriptive equations were developed to characterize the anchorage strength of hooked bars, as shown in Eq. (1.1) and Eq. (1.2) for bars without and with confining reinforcement, respectively (Ajaam et al. 2017):

$$T_h = 294 f_{cm}^{0.295} \ell_{eh}^{1.0845} d_b^{0.47} \left(0.0974 \frac{s}{d_b} + 0.391 \right) \quad (1.1)$$

$$\left(0.0974 \frac{s}{d_b} + 0.391 \right) \leq 1.0$$

$$T_h = \left(294 f_{cm}^{0.295} \ell_{eh}^{1.0845} d_b^{0.47} + 55,050 \left(\frac{A_{th}}{n} \right)^{1.0175} d_b^{0.73} \right) \left(0.0516 \frac{s}{d_b} + 0.6572 \right) \quad (1.2)$$

$$\left(0.0516 \frac{s}{d_b} + 0.6572 \right) \leq 1.0$$

where T_h is the anchorage strength of hooked bars (lb); f_{cm} is the measured concrete compressive strength (psi); ℓ_{eh} is the embedment length of the hooked bar measured from the face of the column to the end of the hook (in.); d_b is the hooked bar diameter (in.); A_{hs} is the total area of the hooked bars (in.²); A_{th} is the effective confinement and defined as the area of confining reinforcement (in.²) within $8d_b$ from the top of the hooked bar for No. 8 bars and smaller or within $10d_b$ for No. 9 bars

or larger; n is the number of hooked bars in the joint; and s is the center-to-center spacing between hooked bars. The maximum effective value for A_{th}/A_{hs} is 0.2 when using the descriptive equations. [Note: The definition of A_{th} differs from that used in ACI 318-19.] The equations were used as the basis for the design provisions in ACI 318-19, allowing the use of high-strength concrete and reinforcing steel. The Code provisions for hooked bars in ACI 318-19 are discussed later in this chapter. The descriptive equations were also used in the current study as the basis for the design and evaluation of specimens with No. 14 and No. 18 hooked bars.

In addition to developing the descriptive equations and proposing new design provisions for ACI 318 Code, some of the key findings of the study at the University of Kansas were:

- Closely-spaced hooked bars (center-to-center spacing below $6d_b$) are weaker, individually, than widely-spaced hooked bars.
- Hooked bars with 90° and 180° bends have similar anchorage strengths.
- Confining reinforcement parallel and perpendicular to the bar increases the anchorage strength of hooked bars.
- Confining reinforcement contributes more to anchorage strength for closely-spaced bars than it does for widely-spaced bars.
- The provisions in ACI 318-14 did not accurately represent the anchorage strength of hooked bars in terms of the effect of bar size and the contributions of confining reinforcement and concrete compressive strength.
- The contribution of concrete compressive strength on the anchorage strength of hooked bars is best represented by a 0.295 power rather than by the square root of compressive strength (as used in ACI 318). For design purposes, compressive strength to the 0.25 power can be safely used.
- Specimens with a ratio of beam effective depth to the hooked bar embedment length (d_{eff}/ℓ_{eh}) greater than 1.5 had low anchorage strengths with respect to the descriptive equations, which were developed based on specimens with $d_{eff}/\ell_{eh} \leq 1.5$.
- Concrete breakout was the dominant failure mode, but side splitting tended to increase as the bar size increased.

1.2.2 Headed Reinforcing Bars

As discussed in the previous section, hooked bars can be used when straight bars cannot be fully developed. In some cases, such as a heavily reinforced region, however, hooked bars can cause congestion. When several and/or staggered hooked bars are required, the tail extension of the bars can cause steel congestion, which in turn can adversely affect the construction quality and structural performance of the member. An example of steel congestion in the presence of staggered hooked bars in an external beam-column joint is shown in Figure 1.8.

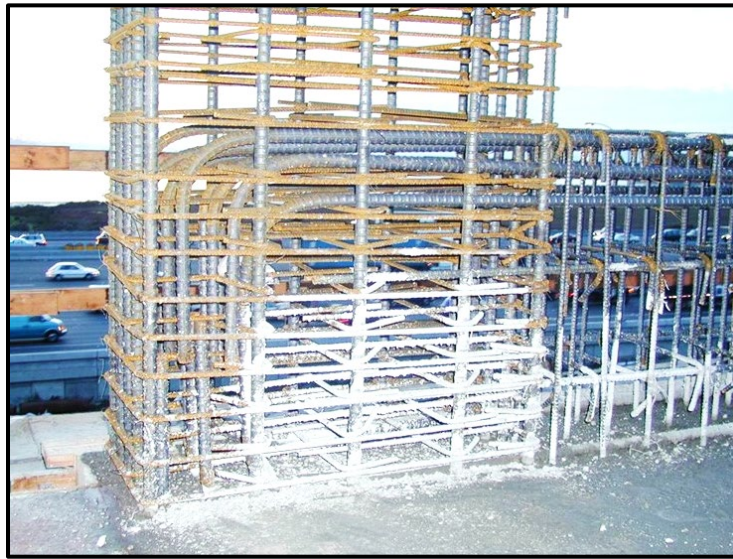


Figure 1.8 Steel congestion in an external beam-column joint caused by staggered hooked bars (<https://www.sefindia.org>)

A viable solution to the steel congestion problem is the use of headed reinforcing bars, which permit the tail extension of the hook to be eliminated. Instead, a head is forged or attached to one or both ends of the bar. The head can have a round, elliptical, or rectangular shape, and can vary in size, as shown in Figure 1.9.

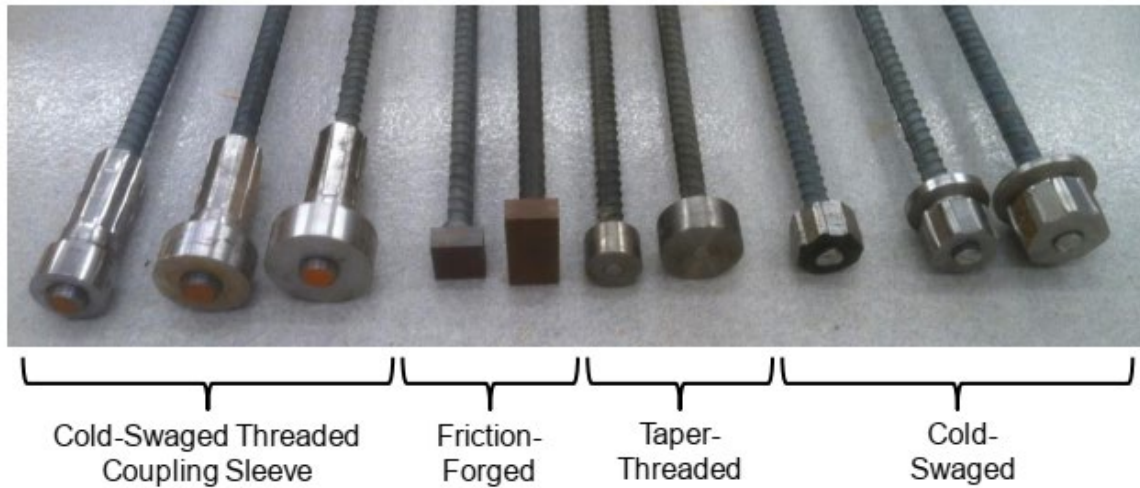


Figure 1.9 Different types of headed bars (Shao et al. 2016)

ACI 318 only permits the use of heads conforming to the Class HA requirements in ASTM A970. Based on these requirements, the net bearing area of the head, A_{brg} , must be at least four times the area of the bar, A_b . Net bearing area is defined as the gross area of the head minus the nominal area of the bar plus, in certain cases, any obstructions of the head induced by the manufacturing process. Prior to 2016, ASTM A970 required obstructions to have a width less than $1.5d_b$ (Figure 1.10). Shao et al. (2016) and Ghimire et al. (2018) found that some headed bars with obstructions exceeding the ASTM A970-16 dimensional limits provided adequate anchorage strength; as a result, the requirements were modified and updated in ASTM A970-17. The current requirements (ASTM A970-18) are shown in Figure 1.11.

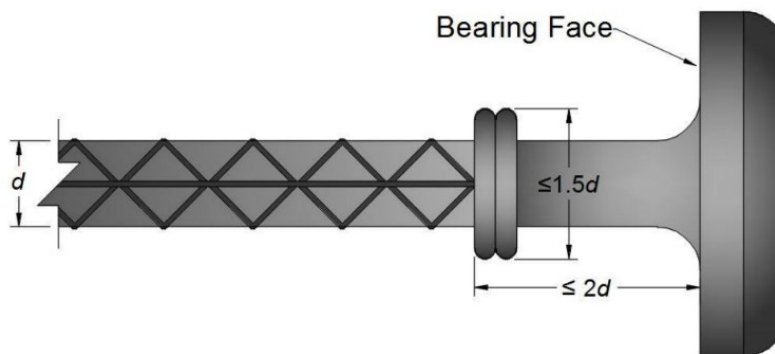


Figure 1.10 Previous limits on headed bar obstructions (ASTM A970/M970-16)

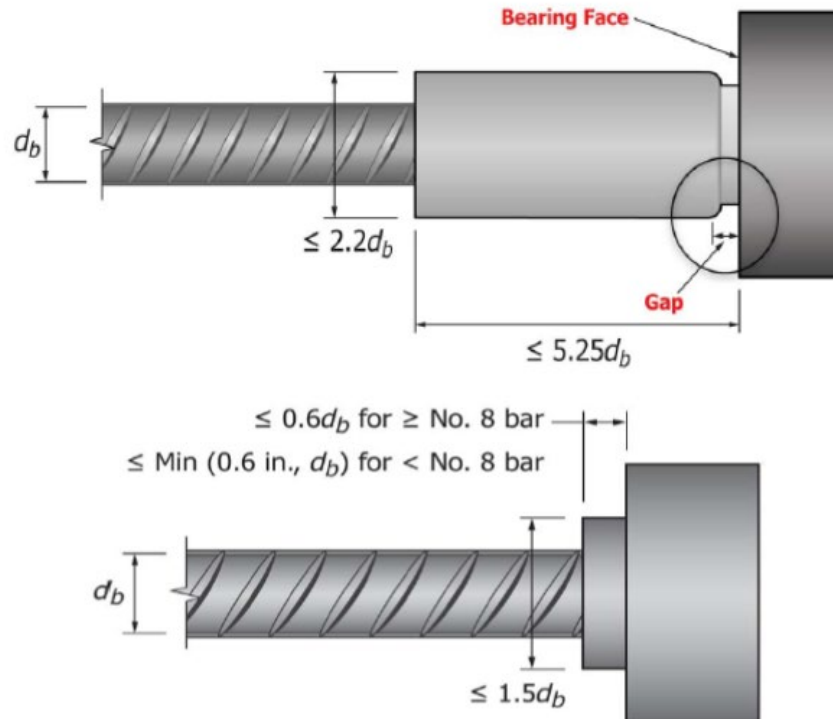


Figure 1.11 Current dimensional limits for obstructions or interruptions in headed bars (ASTM A970/M970-18)

Headed bars achieve anchorage by engaging the concrete through a combination of bond along the deformed bar length and the bearing of the head on concrete, as shown in Figure 1.12. Much like hooked bars, anchorage strength is governed by the breakout strength of the concrete, by mechanisms illustrated in Figure 1.13, which is enhanced by the presence of confining reinforcement. For headed bars, development length is measured from the face of the head, not the back of the head.

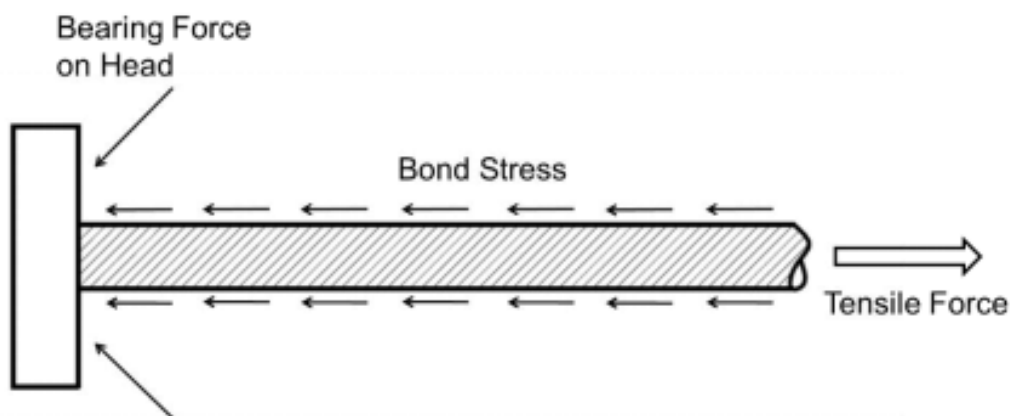


Figure 1.12 Anchorage and bond of headed bars (Shao et al. 2016)

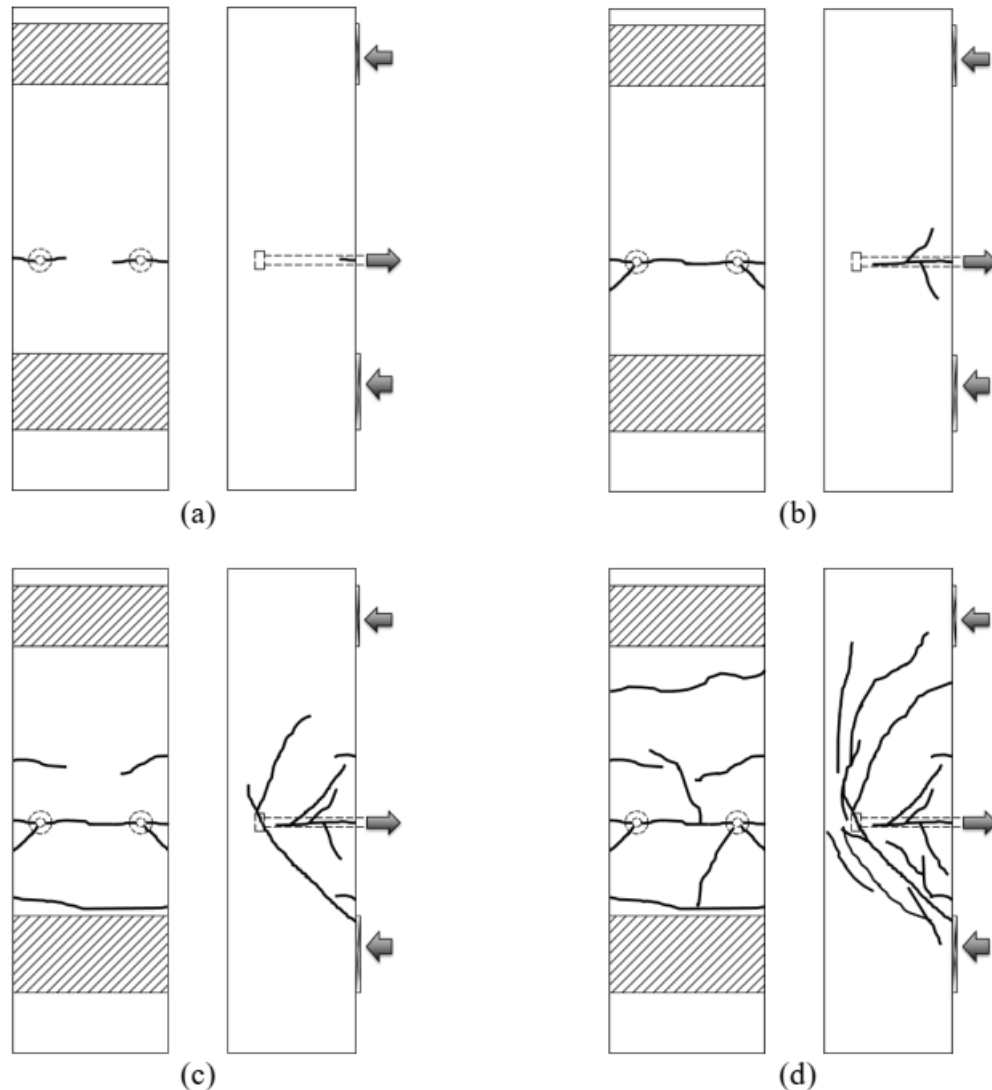


Figure 1.13 Crack progression observed in the beam-column joint specimens containing headed bars. Breakout failure is preceded by bond slip along the straight portion of the bars and cracking of the concrete (Shao et al. 2016, Ghimire et al. 2019a)

Previous studies on headed bars include tests on slab and column-like specimens, splices, compression-compression-tension (CCT) nodes, and beam-column joints under monotonic or cyclic loading. DeVries (1996), Bashandy (1996), and Wright and McCabe (1997) conducted beam-end tests, pullout tests, shallow- and deep-embedment tests, and simulated beam-column joint tests and proposed anchorage provisions. The first design provisions for headed bars were introduced in the 2008 edition of the ACI 318 Building Code, based primarily on the work by Thompson et al. (2005, 2006a, 2006b) in which CCT node tests and lap splice tests were conducted. Since the thrust of the current study is external beam-column joints under monotonic loading, the relevant literature is discussed next.

Bashandy (1996) tested thirty-two simulated beam-column joint specimens, each containing two headed bars, to investigate the effects of embedment length (8.5 to 17 in.), confining reinforcement in the joint region (26 specimens without confining reinforcement and 6 specimens with No. 3 ties spaced at 2 to 4 in.), bar size (No. 8 and No. 11), head size (2 to $7.1A_b$), concrete compressive strength (3,200 to 5,800 psi), and placement of headed bars (inside or outside the column core). The two main failure modes observed were side blowout (spalling of the concrete side cover, in 18 specimens) and along the diagonal cracks formed in the joint region (along the diagonal strut between the head and the top of the bearing plate simulating the beam compressive zone, in 14 specimens). Bashandy (1996) found that the anchorage strength of headed bars increased with increasing embedment length, confining reinforcement, head size, and concrete cover to bar, and that the bar size did not have a noticeable effect. Also, headed bars placed outside the column core had lower anchorage strength than those placed inside the column core.

Chun et al. (2009) tested 30 beam-column joint specimens, of which 24 had headed bars and 6 had hooked bars. Chun et al. investigated bar size (No. 8, No. 11, and No. 18) and embedment length (6.3 to $10.4d_b$ for No. 8 and No. 11 bars and 8.4 to $15.5d_b$ for No. 18 bars). Concrete compressive strength ranged from 3,510 to 3,640 psi. The specimens had a single headed or hooked bar with no confining reinforcement in the joint region. The heads used did not conform to Class HA requirements and had obstructions with a diameter of $1.5d_b$ and a length of $0.75d_b$, reducing the net bearing area of the head adjacent to the obstruction to 2.7 to $2.8A_b$. Concrete side cover to the bar was $2.5d_b$. It was observed that the models proposed by Bashandy (1996), DeVries (1996), and Thompson et al. (2006) for predicting the anchorage strength of headed bars based on failure modes did not provide an accurate prediction of the concrete contribution to anchorage strength. Chun et al. (2009) proposed a new model in which the anchorage strength of a headed bar was the sum of contributions from bond along the bar and head bearing. Chun et al. established the bond along the bar as a function of bar diameter, embedment length, and concrete compressive strength, and the bearing on head as a function of net bearing area, ratio of embedment length to column depth, and concrete compressive strength.

Kang et al. (2010) tested 12 beam-column joint specimens to investigate the effects of head size (large head with net bearing area of $4.5A_b$ and non-HA heads with net bearing area of 2.6 to $2.8A_b$), manufacturing process of the head (welding or threading), and loading condition (monotonic and reversed cyclic loading). The results showed that only the head size, among other

parameters, influenced the anchorage strength. Specimens with larger heads had a higher anchorage strength than those with smaller heads.

Chun et al. (2017a), Chun and Lee (2019), Sim and Chun (2022a, 2022b) tested a total of 53 simulated beam-column joint specimens to investigate the side-face blowout strength of headed bars. The headed bars used did not meet the Class HA requirements and had net bearing areas of 2.7 to $2.9A_b$. All specimens had double overlapping parallel ties in the joint region. The majority of specimens had a single layer of No. 7, No. 10, No. 14, or No. 18 headed bars. Ten specimens had two layers of No. 14 headed bars, with layers spaced at 1 or $2d_b$ on-center. All specimens had two bars per layer, and all bars were Gr. 80. Concrete compressive strength ranged from 5,450 to 16,680 psi. Bar stress at failure ranged from 43.1 to 93.4 ksi. Embedment length ranged from 6 to $20d_b$. Side cover to the bar ranged from 1 to $4d_b$. In these studies, the specimens were designed to force a side-face blowout failure. The schematic of the test setup and specimen proportions used in these studies are shown in Figure 1.14. Figure 1.14.a shows a side view of the specimen proportions as well as the cross section of specimens tested by Chun et al. (2017a) and Chun and Lee (2019), in which the compression reaction of the simulated beam was placed $2/3$ of the embedment length from the headed bars. Figure 1.14.b shows a side view of the specimen proportions used by Sim and Chun (2022b), in which the supports were placed farther from the bars (twice the embedment length, as opposed to one embedment length in the first two studies). A side view of the 10 specimens with two layers of headed bars tested by Sim and Chun (2022a) is shown in Figure 1.14.c, in which the compression reaction of the simulated beam was placed a distance equal to the embedment length (not $2/3$) from the bars, but the supports were placed closer to the bars ($2/3$ of the embedment length).

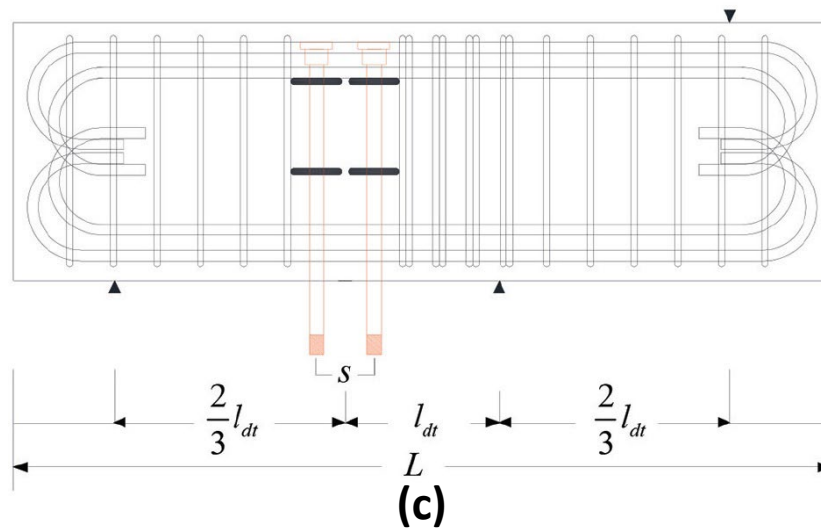
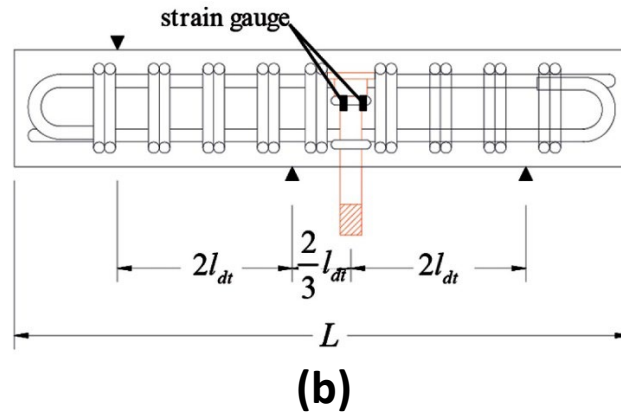
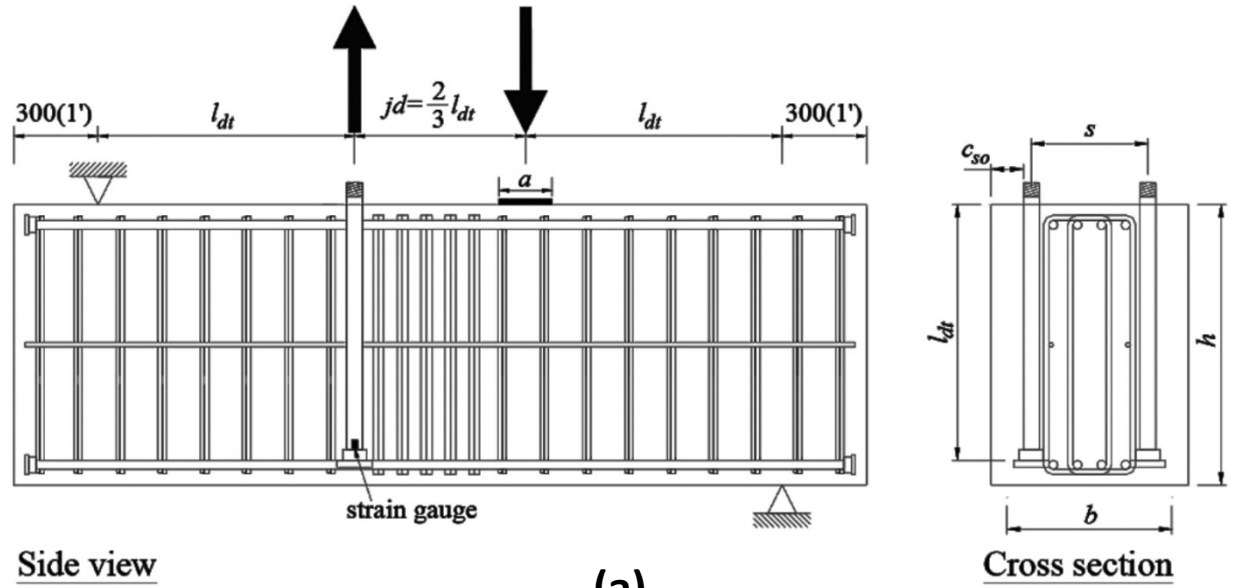


Figure 1.14 (a) Side view of specimen proportions used by Chun et al. (2017a) and Chun and Lee (2019); (b) Side view of the specimen proportions used by Sim and Chun (2022b); (c) Side view of the specimen proportions used by Sim and Chun (2022a)

Chun et al. (2017a), Chun and Lee (2019), Sim and Chun (2022a, 2022b) stated that the anchorage strength of headed bars depends on failure type and member geometry. The two components contributing to side-face blowout strength of headed bars, namely head bearing and bond along the bar, were evaluated. The head bearing contribution was based on the measured strain in the bar $1d_b$ from the bearing face of the head, and the bond contribution was calculated by deducting the head bearing contribution from the bar stress at failure. Initially, bond carried most of the load. As the load increased, the forces carried by both bond and head bearing increased, with head bearing carrying progressively more of the load – the majority at failure – with the load carried by bond dropping off. The researchers found that the bond contribution was linearly proportional to the development length for increases in ℓ_{dt}/d_b above 4.26 (negative intercept of -138 in Eq. (1.3)). The head bearing contribution was not affected by the development length. The side-face blowout strength of headed bars was enhanced with increasing side cover, embedment length, and hairpin-type transverse reinforcement. Simplified and detailed models were proposed for predicting the side-face blowout strength of headed bars, including the effects of side cover and transverse reinforcement. The detailed expression is provided in Eq. (1.3).

$$\begin{aligned}
 f_{dt,p} &= [523\psi_{brg} + (32.4\frac{\ell_{dt}}{d_b} - 138)\psi_b]\sqrt{f'_c} \\
 \psi_{brg} &= 0.7 + 0.3\frac{c_{so}}{d_b} + 0.325\frac{K_{tr}}{d_b} \\
 \psi_b &= 0.78 + 0.22\frac{c_{so}}{d_b} + 0.104\frac{K_{tr}}{d_b}
 \end{aligned} \tag{1.3}$$

where $f_{dt,p}$ is the side-face blowout strength of headed bars (psi), ℓ_{dt} is the embedment length (in.), d_b is the bar diameter (in.), f'_c is the concrete compressive strength (psi), ψ_{brg} is the head bearing factor, ψ_b is the bond factor, c_{so} is the side cover to the bar (in.), and K_{tr} is the transverse reinforcement index defined in Eq. (25.4.2.4b) of ACI 318-19 [$K_{tr} = 40A_{tr}/sn$ where A_{tr} is “total cross-sectional area of all transverse reinforcement within spacing s that crosses the potential plane of splitting through the reinforcement being developed, in.²”, s is the center-to-center spacing of transverse reinforcement, and n is the number of bars being developed.].

Sim and Chun (2022b) proposed a design equation for the development length of headed bars:

$$\frac{\ell_{dt,p}}{d_b} = \frac{f_y}{29\psi\sqrt{f'_c}} - 10 \quad (1.4)$$

$$\psi = 0.75 + 0.25\frac{c_{so}}{d_b} + 0.4\frac{K_{tr}}{d_b}$$

where $\ell_{dt,p}$ is the proposed development length (in.), and ψ is the modification factor for side cover and confining reinforcement. In these equations, K_{tr}/d_b cannot be greater than 0.7, $\ell_{dt,p}$ cannot be less than $6d_b$, f'_c cannot be greater than 17,400 psi, c_{so}/d_b cannot be less than 1.0 or greater than 3.0, and ψ cannot be greater than 1.5.

The work by Thompson et al. (2005, 2006a, 2006b), was used as a basis for the first design provisions for headed bars, in ACI 318-08. Due to the limited range of the material properties in those studies, however, the provisions were very conservative for headed bars such that in ACI 318-08 and ACI 318-14: the concrete compressive strength was limited to 6,000 psi for use in calculating development length and the specified steel yield strength was limited to 60,000 psi. Among other shortcomings, these limitations prevented application of the provisions to high-strength concrete and reinforcing steel. To address these limitations and to provide more experimental data to better understand the anchorage and development of headed bars, a comprehensive study was initiated at the University of Kansas, similar to the studies on the hooked bars (discussed in the previous section). A wide range of material properties (including high-strength concrete and reinforcing steel) and specimen configurations and their effects on the anchorage strength of headed bars were investigated.

A total of 233 specimens were tested by Shao et al. (2016), including 202 simulated exterior beam-column joint specimens, 10 CCT node specimens, 15 column-foundation joint specimens (each slab containing one to three headed bars for a total of 32 tests), and 6 splice specimens. The main variables investigated were bar size (No. 5, No. 8, and No. 11), number of headed bars (2, 3, or 4 per specimen), bar spacing (1.7 to $11.8d_b$ on-center), bar stress at failure (26,100 to 153,200 psi), head size (3.8 to $14.94d_b$), concrete compressive strength (3,960 to 16,030 psi), embedment length (4 to 6 in. for No. 5 bars, 6 to 14.5 in. for No. 8 bars, and 12 to 19.25 in. for No. 11 bars), and amount of confining reinforcement in the joint region (none to six No. 3 ties parallel to the headed bars spaced at $3d_b$). Some of the headed bars used had large obstructions (Figure 1.10) exceeding what were the dimensional limitations of Class HA heads in ASTM A970-16. Side cover to the bars themselves ranged from 2.5 to 4 in., with most specimens having a 2.5

in. side cover. A limited number of specimens had headed bars anchored in the middle of the column, but for the majority of the specimens, the headed bars were anchored at the far side of the column so that the back of the head touched the longitudinal reinforcement of the column.

The specimen design and configuration were very similar to those tested with hooked bars. A schematic of a typical simulated beam-column joint specimen is shown in Figure 1.15.

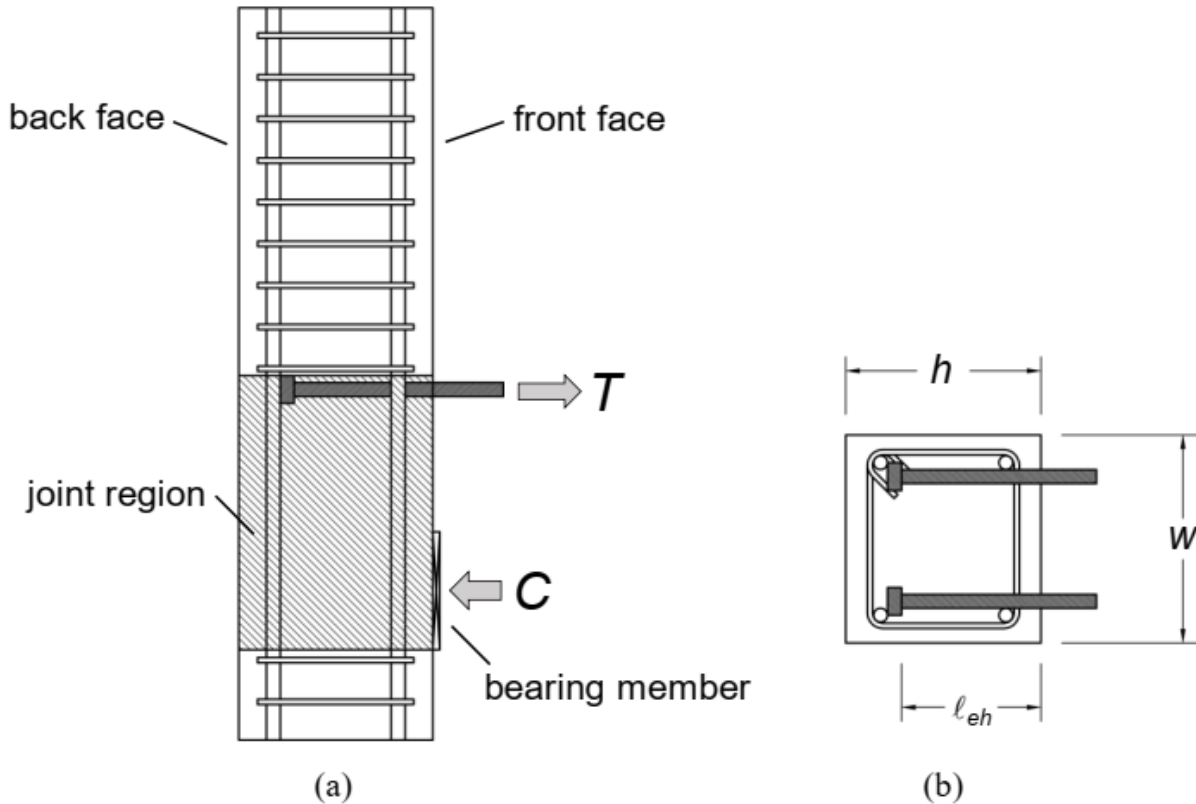


Figure 1.15 Schematic of headed bar specimens (a) side view (b) cross-section, where h and w are column height and width, respectively, and ℓ_{eh} is the embedment length (Shao et al. 2016)

The loading frame was the same as used by Sperry et al. (2015a, 2015b) and Ajaam et al. (2017) for testing simulated beam-column joint specimens containing hooked bars (Figure 1.6). Headed bars represented the top longitudinal reinforcement and the adjacent bearing member represented the compressive zone of the virtual beam, as shown in Figure 1.16. The tensile force applied to the bars and the compressive force by the bearing member acted as a couple, simulating the negative moment acting at a beam-column joint.

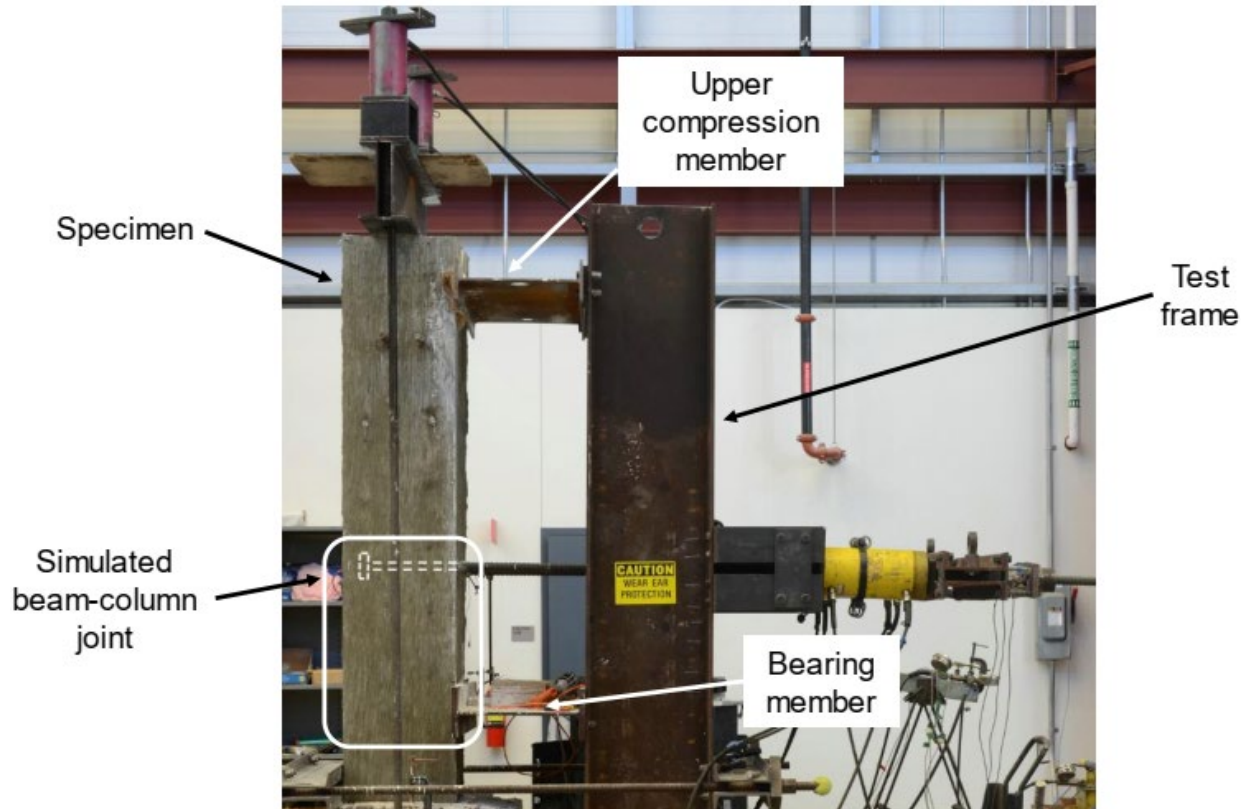


Figure 1.16 The loading frame and test setup of headed bar specimens (Shao et al. 2016)

The headed bar specimens exhibited cracking and failure mechanisms, as shown in Figure 1.13, that were similar to those of the hooked bar specimens (Figure 1.2). Cracking began with a horizontal crack on the front face of the column at the level of the headed bars and extending towards both sides (Figure 1.13a). With increasing load, the horizontal cracks started to connect, with new cracks radiating from the bars. On the sides, the horizontal crack grew along the length of the headed bars, while diagonal cracks started branching towards the upper compression and lower bearing members (Figure 1.13b). As the load continued to increase, more horizontal cracks appeared on the front face, while a large diagonal crack forming in the joint region between the head and the bearing member (Figure 1.13c). Near failure, the existing cracks got wider while new cracks continued to branch from the existing cracks in a cone-shaped form (Figure 1.13d).

Shao et al. (2016) observed two main failure modes, concrete breakout and side-face blowout. Concrete breakout occurred in the majority of specimens (149 out of 196) and was characterized by the separation of the concrete within the column in front of the head. As shown in Figure 1.17, two types of failure surface were observed, namely cone-shaped and back cover

spalling. About half of the specimens had a cone-shaped failure surface. No direct relationship was found between the shape of the failure surface and the anchorage strength of headed bars.

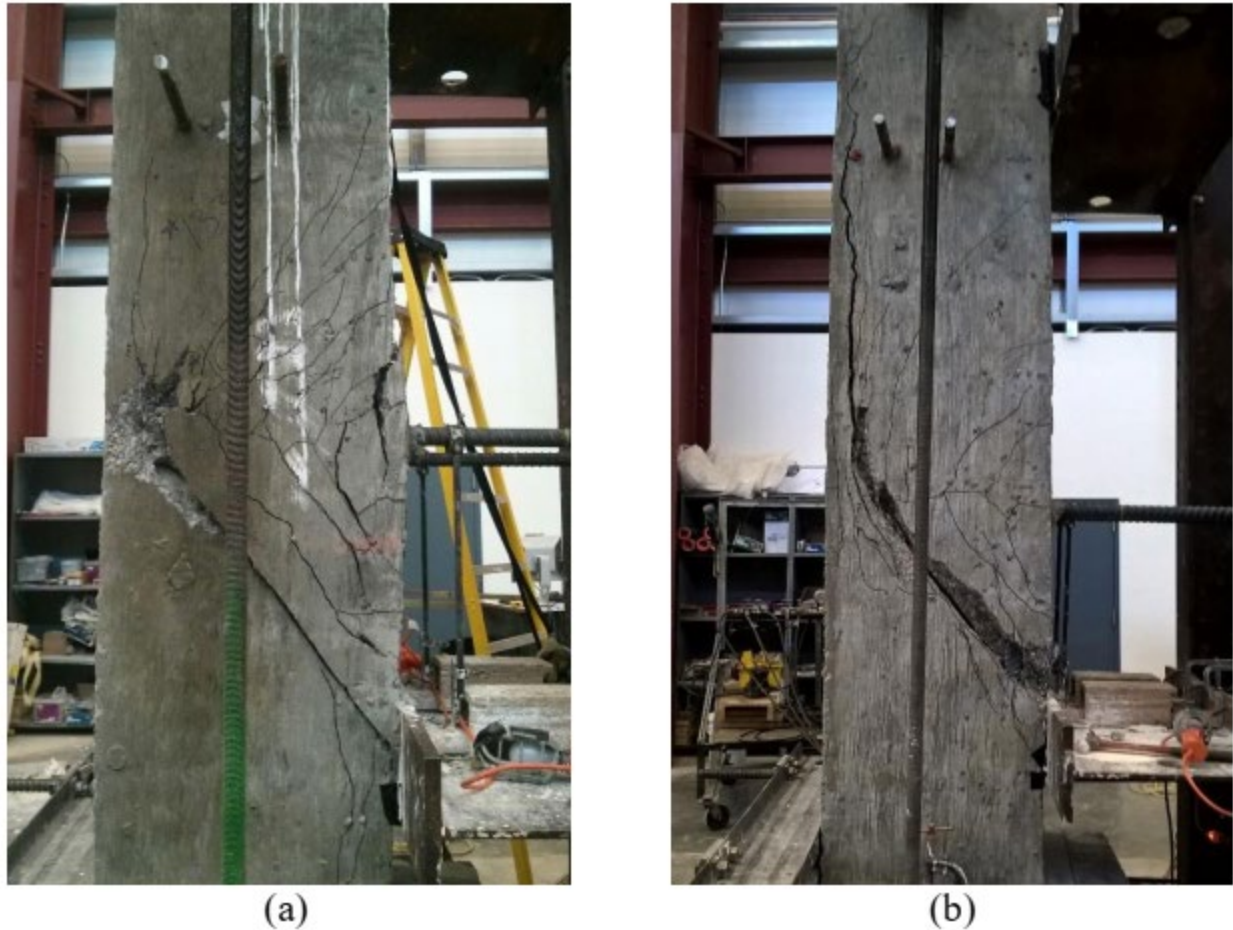


Figure 1.17 Concrete breakout (a) cone-shaped (b) back cover spalling (Shao et al. 2016)

Side-face blowout (in 47 out of 196 specimens) was characterized by local damage to the concrete around the head due to the head movement, resulting in spalling or separation of the concrete cover, sometimes in an explosive manner as shown in Figure 1.18.

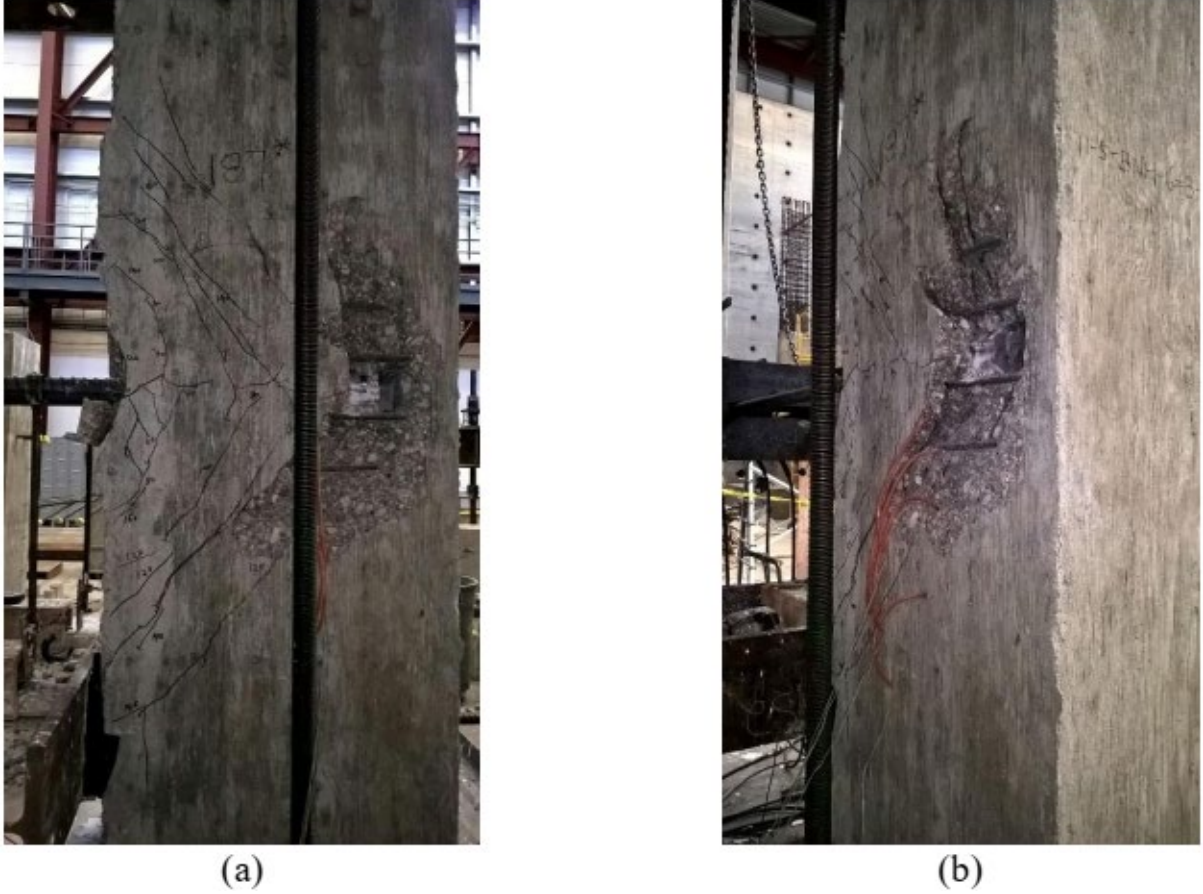


Figure 1.18 Side-face blowout (a) side view (b) back view (Shao et al. 2016)

As they were for hooked bars, descriptive equations were developed for headed bars based on a best fit of the experimental data (Shao et al. 2016, Ghimire et al. 2019b). The descriptive equations characterize the anchorage strength of headed bars as a function of concrete compressive strength, bar diameter and spacing, embedment length, and confining reinforcement in the joint region (parallel ties for headed bars). The equations for headed bars without and with confining reinforcement are shown in Eq. (1.5) and Eq. (1.6), respectively:

$$T_h = 781 f_{cm}^{0.24} \ell_{eh}^{1.03} d_b^{0.35} \left(0.0836 \frac{s}{d_b} + 0.344 \right) \left(0.0836 \frac{s}{d_b} + 0.344 \right) \leq 1.0 \quad (1.5)$$

$$T_h = \left(781 f_{cm}^{0.24} \ell_{eh}^{1.03} d_b^{0.35} + 48,800 \left(\frac{A_{th}}{n} \right) d_b^{0.88} \right) \left(0.0622 \frac{s}{d_b} + 0.5428 \right) \left(0.0622 \frac{s}{d_b} + 0.5428 \right) \leq 1.0 \quad \& \quad \frac{A_{th}}{n} \leq 0.3 A_b \quad (1.6)$$

where T_h is the anchorage strength of headed bars (lb); f_{cm} is the measured concrete compressive strength (psi); ℓ_{eh} is the embedment length of the headed bar measured from the face of the column to the bearing face of the head (in.); d_b is the headed bar diameter (in.); A_{hs} is the total area of the headed bars (in.²); A_{tt} is as the area of confining reinforcement (in.²) within $8d_b$ from the top of the headed bar for No. 8 bars and smaller or within $10d_b$ for No. 9 bars or larger (Figure 1.19); n is the number of headed bars in the joint; and s is the center-to-center spacing between headed bars. As shown in Eq. (1.6), Shao et al. (2016) showed that the maximum value of A_{tt}/n that contributes to T_h is $0.3A_b$. Equations (1.5) and (1.6) were used as the basis for the development length provisions in ACI 318-19, allowing the use of high-strength concrete and reinforcing steel. Equations (1.5) and (1.6) were also used as the basis for designing the specimens in this study.

Shao et al. (2016) also compared the descriptive equations with their test results and results from previous studies (exterior beam-column joints by Bashandy 1996 and Chun et al. 2009, CCT nodes by Thompson et al. 2006a, shallow embedment pullout tests by DeVries 1999, and lap splice tests by Thompson et al. 2006b and Chun 2015). The test-to-calculated ratio (T/T_h) for the specimens used in the comparison was generally conservative (> 1.0), but low anchorage strength was observed for the specimens tested by Chun et al. (2009) and Chun (2015), assumed to be due to Chun et al. (2009) and Chun (2015) using heads with large obstructions that resulted in net bearing areas of only 2.7 and $2.8A_b$. The descriptive equations, also were shown to be applicable to beam-column joints subjected to reversed cyclic loading (Ghimire et al. 2018). Shao et al. (2016) used Eq. (1.5) and (1.6) to develop design provisions for the development length of headed bars, that applied reinforcing steel with yield strengths up to 120,000 psi and concrete with compressive strengths up to 16,000 psi). The proposed design provisions will be discussed later in this chapter.

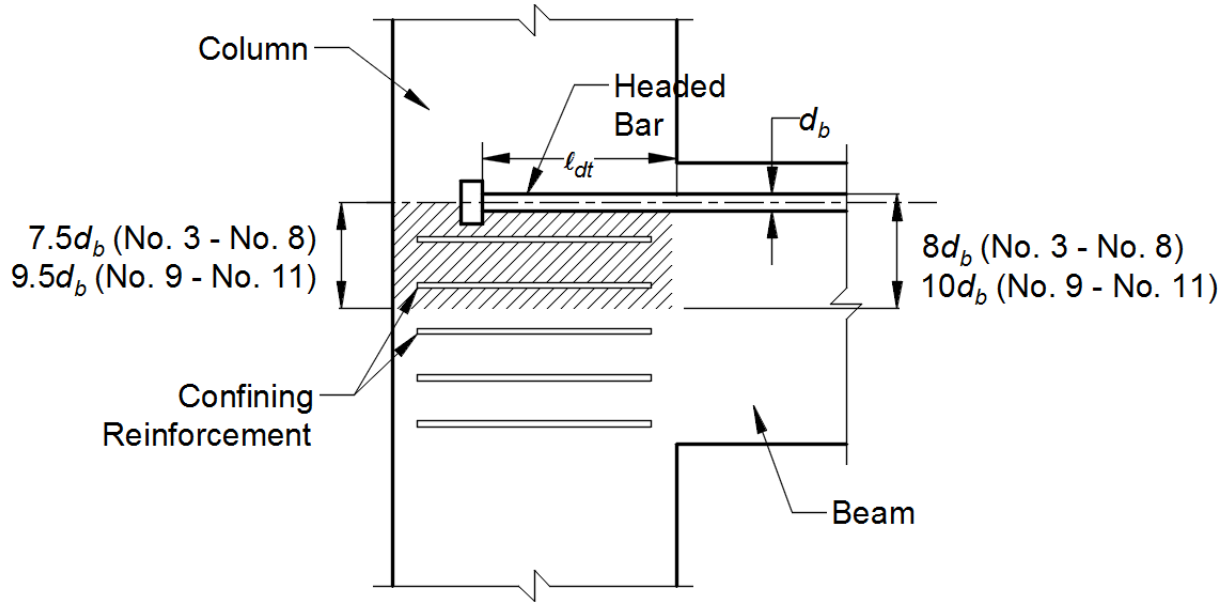


Figure 1.19 Confining reinforcement contributing to anchorage strength of headed bars anchored in beam-column joints (Shao et al. 2016, Ghimire et al. 2019)

In addition to developing descriptive equations and new design provisions, Shao et al. (2016) and Ghimire (2018, 2019a, 2018b) observed that:

- The development length provisions in ACI 318-14 became progressively less conservative as the bar size increased.
- The development length provisions in ACI 318-14 became progressively less conservative as the concrete compressive strength increased. The anchorage strength of headed bars increases with compressive strength to the 0.24 power, rather than the square root of the compressive strength as represented in ACI 318-14.
- Providing confining reinforcement parallel to the headed bars increases the anchorage strength in proportion to the amount of confining reinforcement per headed bar up to $0.3A_b$, as shown in Eq. (1.6).
- When center-to-center spacing of headed bars decreased below $8d_b$, anchorage strength decreased. “Widely-spaced” headed bars were defined as bars with center-to-center spacing was equal or greater than $8d_b$, and closely-spaced heads bars as bars with center-to-center spacing below $8d_b$.

- Headed bars with obstructions exceeding the limitations of HA heads in ASTM A970-16 and prior versions of the specification provided satisfactory anchorage strength, and the findings were incorporated in ASTM A970-17.
- Heads with bearing areas of 12.9 to $14.9A_b$ provided, on average, 17% and 7% more anchorage strength for No. 5 and No. 8 bars, respectively, than heads with smaller bearing areas between 3.8 and $9.5A_b$, but the increase in anchorage strength was not proportional to the bearing area.

Comparing the test results and findings of the studies on the anchorage of hooked and headed bars at the University of Kansas (Searle et al. 2014, Sperry et al. 2015a, 2015b, 2017a, 2017b, 2018, Yasso et al. 2017, Ajaam et al. 2017, 2018, Shao et al. 2016, Ghimire et al. 2018, 2019a, 2019b) provides the following valuable observations:

- Hooked and headed bars have a lot of similarities in terms of anchorage behavior
- For the same embedment length, headed bars provide a higher anchorage force than hooked bars.
- Closely-spaced hooked and headed bars are weaker, individually, than widely-spaced hooked and headed bars.
- Confining reinforcement parallel to the bar increases anchorage strength of hooked and headed bars.
- Confining reinforcement perpendicular to the bar increases anchorage strength of hooked but not headed bars.
- For both hooked and headed bars, confining reinforcement makes a bigger contribution for closely-spaced bars than for widely-spaced bars

1.3 CURRENT CODE PROVISIONS AND DESIGN GUIDELINES

In this section, the provisions in the ACI 318-14 for the development length of both hooked and headed bars are presented, followed by the proposed design provisions based on the studies at the University of Kansas (Sperry et al. 2015a, 2015b, 2017a, 2017b, 2018, Ajaam et al. 2017, 2018, Shao et al. 2016, Ghimire et al. 2018, 2019a, 2019b). Finally, the current Code provisions, in ACI 318-19, and their limitations are discussed.

1.3.1 Reinforcing Bars with Standard Hooks

The provisions for the development length of hooked bars in ACI 318-14 were based on 38 tests of simulated beam-column joints conducted in 1970s with concrete compressive strength ranging from 3.8 to 5.1 ksi and yield strengths of hooked bars of 64 or 68 ksi. Based on these limited experimental data, the following equation was given in ACI 318-14 and Codes dating back to 1983 to calculate the development length of deformed bars with standard hooks in tension (Eq. 1.7):

$$\ell_{dh} = \left(\frac{f_y \psi_e \psi_c \psi_r}{50 \lambda \sqrt{f'_c}} \right) d_b \quad (1.7)$$

where ℓ_{dh} is the embedment length of hooked bar (in.), f_y is the bar yield strength (psi), ψ_e is the coating factor, ψ_c is the concrete cover factor, ψ_r is the confining reinforcement factor, λ is the concrete density factor, f'_c is the concrete compressive strength (psi), and d_b is the bar diameter (in.). For lightweight concrete, $\lambda=0.75$, and for epoxy-coated bars, $\psi_e=1.2$; otherwise, these factors are equal to 1.0. For No. 11 and smaller hooks, $\psi_c=0.7$ if side cover is ≥ 2.5 in. and tail cover ≥ 2 in., $\psi_r=0.8$ if ties or stirrups are provided along or perpendicular the straight portion of the bar and spaced no greater than $3d_b$, as shown in Figure 1.20.

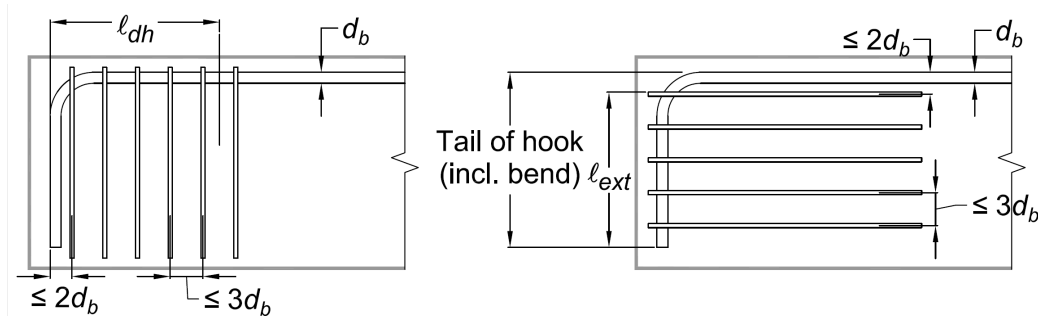


Figure 1.20 ACI 318-14 provisions for ties or stirrups placed perpendicular (left) or parallel (right) to the hooked bar being developed (ACI 318-14)

The ACI 318-14 provisions for hooked bars limited the concrete compressive strength to 10,000 psi and bar yield strength to 80,000 psi. At the University of Kansas, Sperry et al. (2015a, 2015b, 2017a, 2017b, 2018) compared test results from their study and earlier studies with the anchorage strength derived from ACI 318-14 provisions (Eq. 1.7). Specimens included in the analysis had two widely-spaced hooked bars. The yield strength f_y in Eq. 1.5 was replaced by bar stress, $f_{s,ACI}$, and f'_c was replaced by the measured compressive strength, f_{cm} . The equation was

then solved for $f_{s,ACI}$ to calculate the anchorage strength. Figure 1.21 shows the ratio of test-to-calculated stress $f_{su}/f_{s,ACI}$ versus f_{cm} for hooked bar specimens without confining reinforcement.

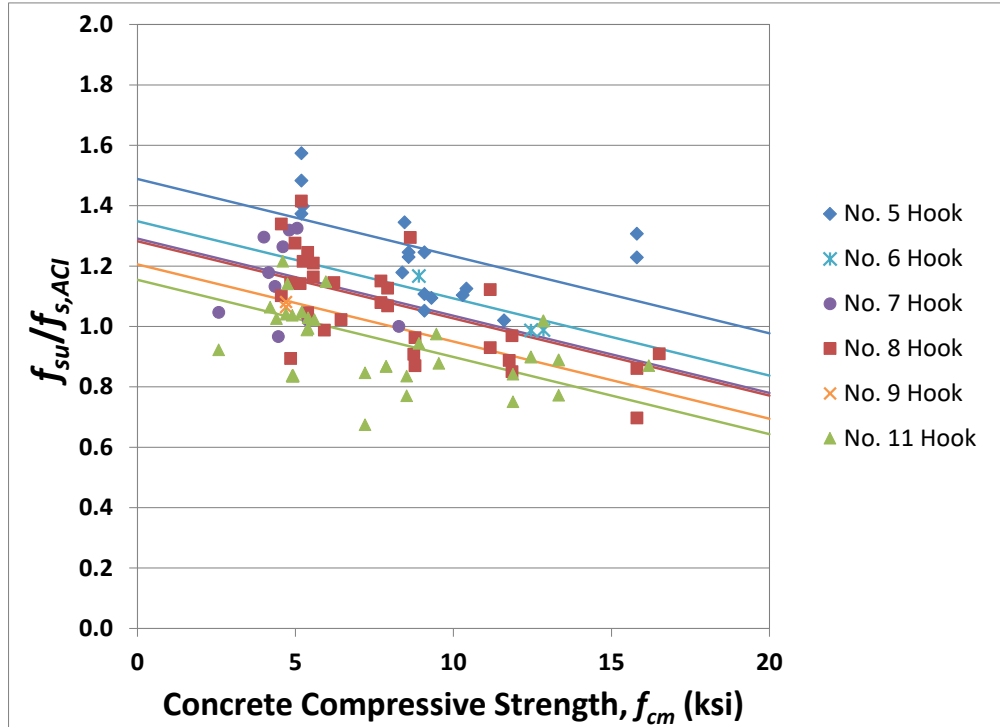


Figure 1.21 Ratio of test-to-calculated stress $f_{su}/f_{s,ACI}$ versus f_{cm} for hooked bars without confining reinforcement (Sperry et al. 2015b)

The trend lines in Figure 1.21 indicate that the test-to-calculated ratio $f_{su}/f_{s,ACI}$ decrease with increasing compressive strength and bar size. For No. 9 and No. 11 hooked bars, the ratio drops below 1.0 at approximately 8,000 and 6,000 psi, respectively. This observation showed that the ACI 318-14 provisions may be unconservative for No. 9 and larger bars in concrete with compressive strengths as low as 6,000 psi.

Figure 1.22 shows the same comparison for widely-spaced hooked bars with No. 3 ties in the joint region spaced at $3d_b$ or less. As shown in Figure 1.22, the $f_{su}/f_{s,ACI}$ ratio decreases as the bar size and compressive strength increase. For No. 8 and No. 11 hooked bars, the ratio drops below 1.0 at compressive strengths of about 11,000 and 5,000 psi, respectively, indicating unconservative designs produced by the ACI 318-14 provisions. Sperry et al. (2015b) concluded that the ACI 318-14 provisions overpredicted the effects of concrete compressive strength and confining reinforcement on the anchorage strength of hooked bars, and the anchorage strength of larger bars. Furthermore, the reduction factors applied to Eq. (1.7) for concrete cover and confining reinforcement, ψ_c and ψ_r , were found to be unconservative.

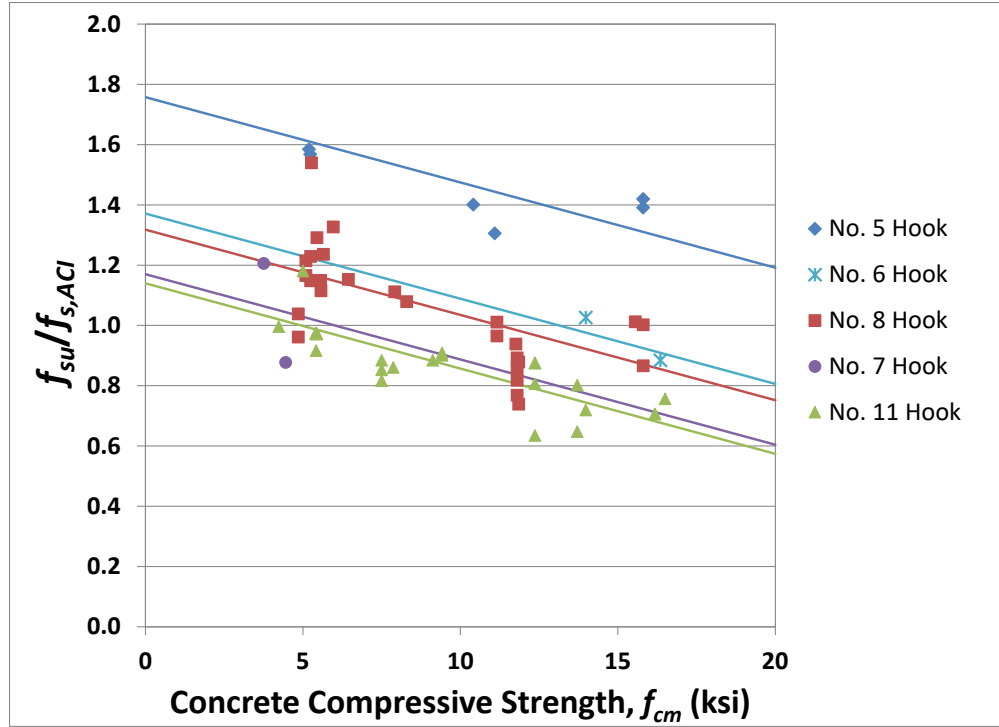


Figure 1.22 Ratio of test-to-calculated stress $f_{su}/f_{s,ACI}$ versus f_{cm} for hooked bars with No. 3 ties spaced at $3d_b$ in the joint region (Sperry et al. 2015b)

Based on these observations, the development length provisions for hooked bars in ACI 318-14 needed to be modified to more accurately reflect the effects of concrete compressive strength and bar size. To do so, Sperry et al. (2015b) and Ajaam et al. (2017) simplified the descriptive equations, Eq. (1.1) and (1.2) to propose a new design equation for the development length of hooked bars. For bars spaced at or greater than $6d_b$ (referred to as widely-spaced bars), the descriptive equations were converted to equations for development length (ℓ_{dh}), and were then accounted for closer bar spacing, confining reinforcement, and bar location within the member. Eq. (1.8) shows the proposed design equation:

$$\ell_{dh} = \left(\frac{f_y \psi_e \psi_{cs} \psi_o}{500 \lambda f_c'^{0.25}} \right) d_b^{1.5} \quad (1.8)$$

where ℓ_{dh} is the embedment length of hooked bar (in.), f_y is the bar yield stress (psi), ψ_e is the coating factor, ψ_{cs} is the confinement and spacing factor, ψ_o is the location factor, λ is the concrete density factor, f_c' is the concrete compressive strength, and d_b is the bar diameter (in.). The values of the modification factor for confining reinforcement and spacing, ψ_{cs} , are given in Table 1.2. The bar location factor, ψ_o , is 1.0 if hooked bars with a side cover to the bar of at least 2.5 in. terminate inside the column core, or in a member with a side cover to the bar of at least $6d_b$. In all

other cases, ψ_o is 1.25. The coating factor ψ_e (1.0 for uncoated bars and 1.2 epoxy-coated bars) and the concrete density factor λ (0.75 and 1.0 for lightweight and normalweight concrete, respectively) were retained from ACI 318-14.

Table 1.2 Values for the confinement and bar spacing factor, ψ_{cs} , as proposed by Ajaam et al. (2017) for hooked bars ^[1]

Confinement level	f_y (psi)	s	
		$2d_b$	$\geq 6d_b$
$A_{th}/A_{hs} \geq 0.2$ ^[2] or $A_{th}/A_{hs} \geq 0.4$ ^[3]	60,000	0.6	0.5
	120,000	0.66	0.55
None	all	1.0	0.6

^[1] Linear interpolation may be used for spacing or yield strengths not listed

^[2] Confining reinforcement parallel to straight portion of bar

^[3] Confining reinforcement perpendicular to straight portion of bar

Compared to the ACI 318-14 design equation (Eq. 1.7), the proposed equation incorporated a number of changes. The bar diameter d_b was raised to the 1.5 power rather than 1.0 and concrete compressive strength f'_c to the 0.25 power rather than $\sqrt{f'_c}$ for a more accurate representation of the effects of these two parameters. Also, the proposed equation was shown to provide conservative criteria for the development length of hooked bars for steel yield strengths up to 120,000 psi and concrete compressive strengths up to 16,000 psi, whereas ACI 318-14 limited these values to 80,000 psi and 10,000 psi, respectively.

The findings of the studies at the University of Kansas were used as a basis for developing the design provisions for hooked bars in the current edition of the ACI 318 Building Code, ACI 318-19 (Section 25.4.3). However, a modified version of the equation proposed by Ajaam et al. (2018) was adopted, because ACI Committee 318 did not want to incorporate a double interpolation for the confinement and bar spacing factor, as shown in Table 1.2, and did not want to represent the contribution of f'_c in the form of $f_c'^{0.25}$. Currently, Eq. (1.9) is used to calculate the development length of hooked bars in tension.

$$\ell_{dh} = \left(\frac{f_y \psi_e \psi_r \psi_o \psi_c}{55 \lambda \sqrt{f'_c}} \right) d_b^{1.5} \quad (1.9)$$

where ℓ_{dh} is the embedment length of hooked bar (in.), f_y is the bar yield strength (psi), ψ_e is the coating factor, ψ_r is the confining reinforcement factor, ψ_o is the location factor, ψ_c is the concrete strength factor, λ is the concrete density factor, f'_c is the concrete compressive strength, and d_b is the bar diameter (in.). Compared to the ACI 318-14 equation (Eq. 1.7), the bar diameter d_b is now raised to the 1.5 power in ACI 318-19 (as proposed by Ajaam et al. 2017 in Eq. (1.8)). The current Code equation is compared with the results obtained in this study in Chapter 4 and with newly proposed provisions for hooked bars in Chapter 6.

The modification factors for lightweight concrete, λ , and for epoxy-coated bars, ψ_e are 0.75 and 1.2, respectively. The other modification factors are given in Table 1.3.

Table 1.3 Modification factors for hooked bars as given in Table 25.4.3.2 of ACI 318-19

Modification Factor	Condition	Value
Confining reinforcement, ψ_r	$A_{th} \geq 0.4A_{hs}$ or $s^{[1]} \geq 6d_b^{[2]}$	1.0
	Other	1.6
Location, ψ_o	(1) Terminating inside column core with side cover normal to plane of hook ≥ 2.5 in., or (2) With side cover normal to plane of hook $\geq 6d_b$	1.0
	Other	1.25
Concrete strength, ψ_c	$f'_c < 6,000$ psi	$f'_c / 15,000 + 0.6$
	$f'_c \geq 6,000$ psi	1.0

[1] s is minimum center-to-center spacing of hooked bars

[2] d_b is nominal bar diameter

The bar location factor ψ_o is the same as proposed by Ajaam et al. (2017). In Table 1.3, A_{th} is the total cross-sectional area of ties or stirrups confining hooked bars within $15d_b$ of the centerline of the hooked bars and spaced no greater than $8d_b$, as defined in Figure 1.23, and A_{hs} is the total cross-sectional area of hooked bars developed at the critical section. In developing the Code (in both 318-14 and 318-19 editions), it was assumed that confining reinforcement would be uniformly distributed within the joint region. Based on this assumption, the choice was made to convert the maximum effective values based on confining reinforcement within $7.5d_b$ to $9.5d_b$ from the centerline of the hooked bars (as established by Ajaam et al 2017) to an approximate value within $15d_b$ (that is, $A_{th} = 0.4A_{hs}$, in place $0.2A_{hs}$). As shown in Table 1.3, the confining reinforcement factor ψ_r , which replaces the confining reinforcement and bar spacing factor, ψ_{cs} ,

is no longer variable, as proposed by Ajaam et al. (2017), but must be taken as 1.6 unless $A_{th} \geq 0.4A_{hs}$ or the center-to-center bar spacing $s \geq 6d_b$.

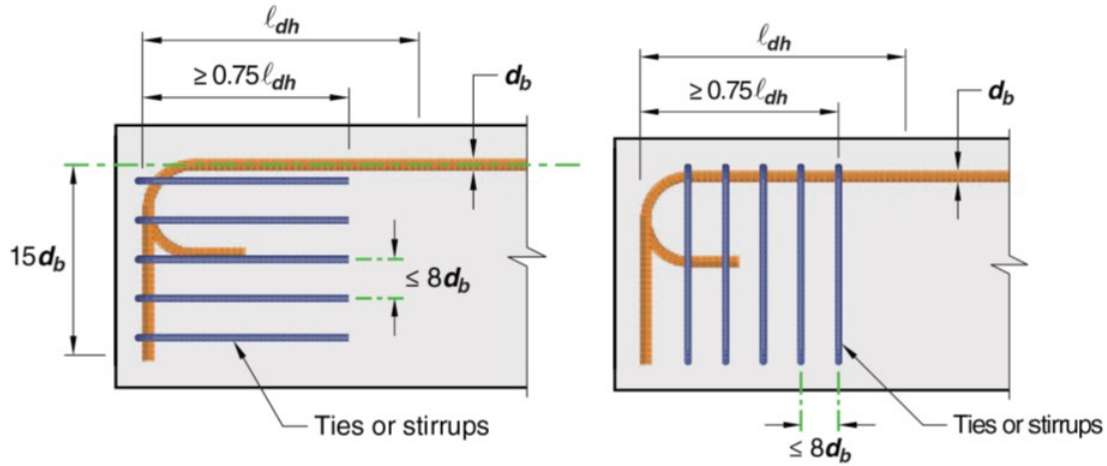


Figure 1.23 Confining reinforcement placed parallel (left) or perpendicular (right) to the hooked bar being developed as defined in ACI 318-19 (from ACI 318-19)

Although it was shown by the studies at the University of Kansas (Sperry et al. 2015b and Ajaam et al. 2017) that the effect of concrete compressive strength on the anchorage strength of hooked bars for design purposes is best represented by compressive strength to the 0.25 power (as reflected in their proposed design equation, Eq. (1.8), ACI Committee 318 chose to stay with the square root of compressive strength ($\sqrt{f'_c}$) in Eq. (1.9) during developing the 2019 edition of the Code. However, to prevent unreasonably long development lengths for the lower concrete strengths normally used in the practice (in the range of 4,000 to 6,000 psi), Eq. (1.9) was modified with the concrete strength factor, ψ_c , as defined in Table 1.2. The current Code equation becomes progressively less conservative as concrete strength increases above 6000 psi, up to 10,000 psi, at which point it begins to become more conservative as f'_c increases to 16,000 psi.

While improved, the Code provisions in ACI 318-19 still have limitations that need to be addressed. The maximum limit on concrete compressive strength is still 10,000 psi for use in calculating the development length, ℓ_{dh} , in Eq. (1.7), to prevent unconservative designs for higher-strength concretes (as discussed earlier, staying with $\sqrt{f'_c}$ in the current Code equation is already unconservative and the design becomes progressively more unconservative as the concrete strength increases to 10,000 psi). The binary choice of 1.6 and 1.0 for the confining reinforcement factor, ψ_r , limits the flexibility of the design; providing more detailed expressions would allow designers to take advantage of confining reinforcement $A_{th} < 0.4A_{hs}$ for bar spacing s less than $6d_b$.

Although there is no limit on the bar size, ACI 318-19 gives no credit to confining reinforcement for hooked bars larger than No. 11. That is, No. 14 and No. 18 hooked bars, even with confining reinforcement, are treated as if no confining reinforcement were present; thus, a ψ_r factor of 1.6 is applied as a penalty (increasing the required development length by 60%), unless the spacing $s > 6d_b$. This is mainly due to a lack of experimental data on No. 14 and No. 18 hooked bars, and one of the motivations for the current study.

1.3.2 Headed Reinforcing Bars

About 100 splice and CCT node tests were the basis for the provisions for the development of headed bars in ACI 318 Code before 2019. In these tests, the concrete compressive strength ranged from 3.5 to 5.5 ksi. The maximum yield strength of the headed bars used in the tests was 69 ksi. This very limited range of material properties and test specimens resulted in very conservative restrictions on the use of headed bars. Concrete compressive strength was limited to 6,000 psi, and the bar yield strength to 60,000 psi, impeding the use of high-strength concrete and reinforcing steel. ACI 318-14 provided the following equation to calculate the development length of headed bars:

$$\ell_{dt} = \left(\frac{0.016 f_y \psi_e}{\sqrt{f'_c}} \right) d_b \quad (1.10)$$

where ℓ_{dt} is the embedment length of headed bar (in.), f_y is the bar yield strength (psi), ψ_e is the coating factor (=1.2 for epoxy-coated reinforcement), f'_c is the concrete compressive strength (psi), and d_b is the bar diameter (in.). Unlike hooked bars, no modification factor was provided to account for confining reinforcement. The net bearing area of the head was required to be greater than or equal to 4 times the bar area ($A_{brg} \geq 4A_b$). The required concrete cover on the bar was $\geq 2d_b$ (same as for straight bars). The clear spacing between headed bars in both horizontal and vertical layers was required to be $\geq 4d_b$, not allowing the use of more closely spaced bars.

To evaluate the headed bar provisions in ACI 318-14, Shao et al. (2016) compared their beam-column joint test results with anchorage strengths based on Eq. (1.8). The bar stress at failure measured in the tests, f_{su} , was compared against the anchorage stress derived from Eq. (1.10), $f_{s,ACI}$. To do so, ℓ_{dt} was replaced with the measured embedment length, ℓ_{eh} , f'_c was replaced with the measured concrete compressive strength, f_{cm} , and f_y was replaced with $f_{s,ACI}$. Eq. (1.10) was then solved for $f_{s,ACI}$, and the test-to-calculated ratio, $f_{su}/f_{s,ACI}$, was used to perform the comparison. To

accurately evaluate the effect of f_{cm} raised to the 0.5 power, the upper limit of 6,000 psi on concrete compressive strength was not applied. Figure 1.24 shows the ratio of test-to-calculated stress $f_{su}/f_{s,ACI}$ versus f_{cm} for 46 specimens with two widely-spaced headed bars without confining reinforcement, and Figure 1.25 shows the same comparison for 35 specimens with two widely-spaced bars with No. 3 hoops spaced at $3d_b$ in the joint region.

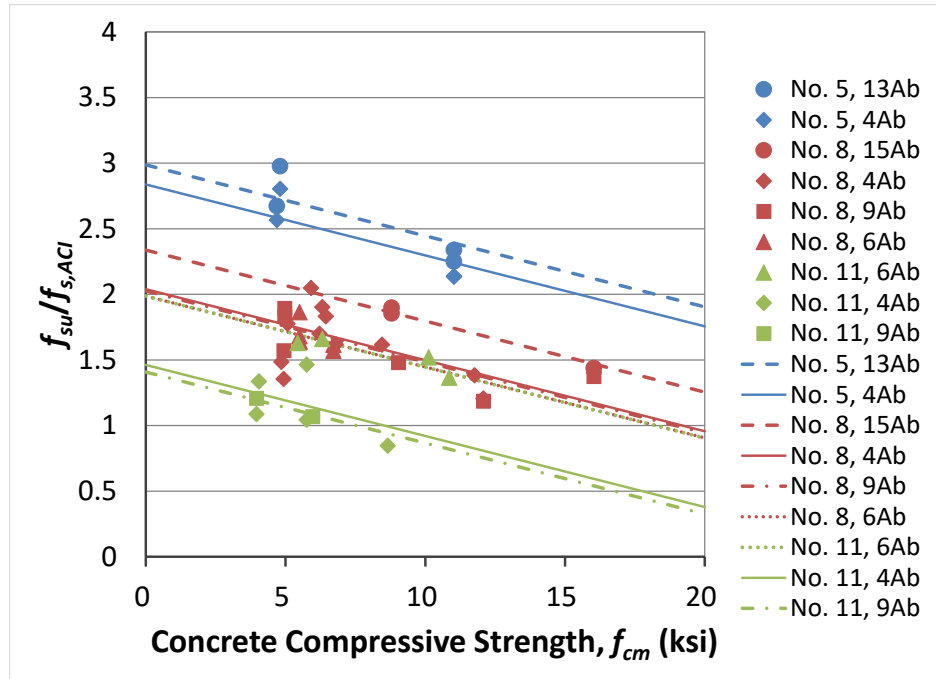


Figure 1.24 Ratio of test-to-calculated stress $f_{su}/f_{s,ACI}$ versus f_{cm} for two widely-spaced headed bars without confining reinforcement, where $f_{s,ACI}$ is based on ACI 318-14 (from Shao et al. 2016)

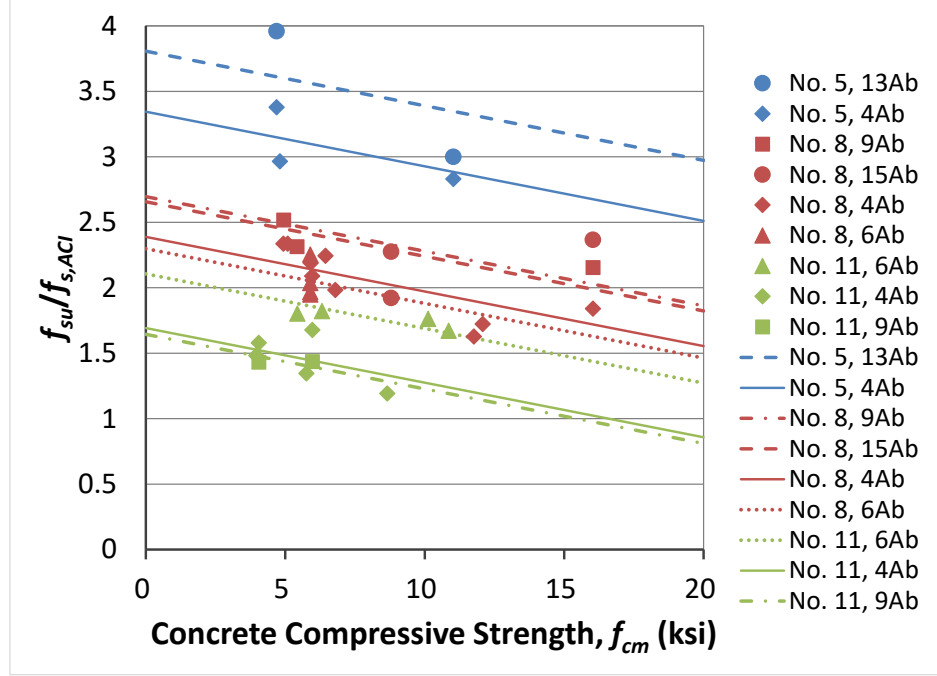


Figure 1.25 Ratio of test-to-calculated stress $f_{su}/f_{s,ACI}$ versus f_{cm} for two widely-spaced headed bars with No. 3 hoops spaced at $3d_b$, where $f_{s,ACI}$ is based on ACI 318-14 (Shao et al. 2016)

In both figures, 1.24 and 1.25, the trend lines have negative slopes, showing the overestimation of the effect of concrete compressive strength to the 0.5 power in the ACI equation. Comparing Figures 1.24 and 1.25 shows that the test-to-calculated ratio $f_{su}/f_{s,ACI}$ values for ACI 318-14 were higher for specimens with confining reinforcement, indicating an improvement in anchorage strength by providing confinement in the joint, a factor not accounted for in the ACI 318-14 provisions. The order of trend lines in both figures reveals that the 1914 Code became less conservative as the bar size increased. With these observations, Shao et al. (2016) concluded that the ACI 318-14 provisions need to be updated for headed bars to include a wider range of material properties and to account for factors such as confining reinforcement.

By converting the descriptive equations, Eq. (1.5) and (1.6), for widely-spaced headed bars (center-to-center spacing $\geq 8d_b$) without confining reinforcement to an equation for development length, ℓ_{dt} , Shao et al. (2016) proposed a new design expression. The expression incorporates the effects of close bar spacing (center-to-center spacing $< 8d_b$), confining reinforcement, and bar location within the member:

$$\ell_{dt} = \left(\frac{f_y \Psi_e \Psi_{cs} \Psi_o}{800 f_c^{0.25}} \right) d_b^{1.5} \quad (1.11)$$

where ℓ_{dt} is the embedment length of headed bar (in.), f_y is the bar yield stress (psi), ψ_e is the coating factor, ψ_{cs} is the confinement and spacing factor, ψ_o is the location factor, f'_c is the concrete compressive strength, and d_b is the bar diameter (in.).

Equation (1.11) is applicable for steel yield strengths up to 120,000 psi and concrete compressive strengths up to 16,000 psi. Equation (1.11) is similar to the proposed equation for hooked bars (Eq. 1.8) in form, with the exceptions of not having the concrete density factor, λ (since headed bars are not currently permitted to be used in lightweight concrete), and in the values of confinement and spacing factor, ψ_{cs} . Like Eq. (1.8), the bar diameter d_b is raised to the 1.5 power and the concrete compressive strength f'_c is raised to the 0.25 power. Table 1.4 gives the values for the confinement and bar spacing factor, ψ_{cs} .

Table 1.4 Values for the confinement and bar spacing factor, ψ_{cs} , as proposed by Shao et al. (2016) for headed bars

Confinement level	f_y (psi)	s	
		$2d_b$	$\geq 8d_b$
$A_{tt}/A_{hs} \geq 0.3$	$\leq 60,000$	0.6	0.4
	120,000	0.7	0.45
None	all	1.0	0.5

In Table 1.4, s is the center-to-center spacing of headed bars, A_{tt} is the effective amount of confining reinforcement in the joint region and is defined as the total cross-sectional area of all the ties parallel to the headed bars within $8d_b$ from the top of the headed bar for No. 8 bars and smaller or within $10d_b$ for No. 9 bars or larger, and A_{hs} is the total cross-sectional area of the headed bars being developed. The maximum limit of 0.3 on A_{tt}/A_{hs} is based on the observation during development of Eq. (1.6) that values of A_{tt}/n above $0.3A_b$ did not contribute to anchorage strength.

The bar location factor, ψ_o , is 1.25 unless the bars are located within the column core (the region inside column longitudinal reinforcement, as shown in Figure 1.26) with side cover ≥ 2.5 in., or in a wall with side cover $\geq 8d_b$, for either of which the factor is 1.0. The value of 1.25 was chosen based on the observations by Shao et al. (2016) that, in general, headed bars located outside the column core had an anchorage strength of about 80% of those within the column core. The value of 1.25 for ψ_o for headed bars matched the findings by Sperry et al. (2015b) for hooked bars.

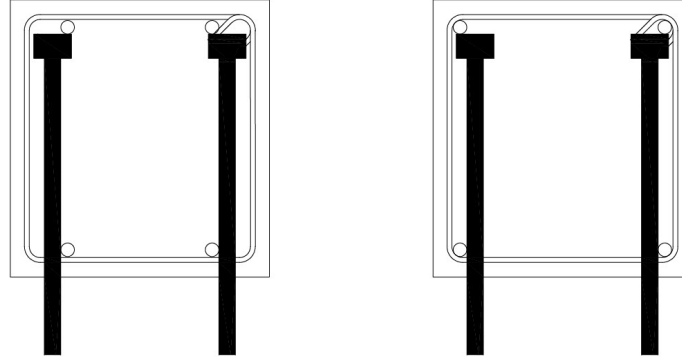


Figure 1.26 Bars located outside (left) or inside (right) of the column core

The expression for calculating the development length of headed bars proposed by Shao et al. (2016) was modified in the ACI 318-19 Code, including retention of $\sqrt{f'_c}$ to represent the contributing of concrete compressive strength rather than incorporating the proposed and more accurate $f_c'^{0.25}$, as shown in Eq. (1.12).

$$\ell_{dt} = \left(\frac{f_y \psi_e \psi_p \psi_o \psi_c}{75 \sqrt{f'_c}} \right) d_b^{1.5} \quad (1.12)$$

where ℓ_{dt} is the embedment length of headed bar (in.), f_y is the bar yield strength (psi), ψ_e is the coating factor, ψ_p is the parallel tie reinforcement factor, ψ_o is the location factor, ψ_c is the concrete strength factor, λ is the concrete density factor, f'_c is the concrete compressive strength, and d_b is the bar diameter (in.). Compared to the ACI 318-14 equation (Eq. 1.10), the current equation has changed significantly. The bar diameter is raised to the 1.5 power (same as for hooked bars), and three new modification factors (ψ_p , ψ_o , and ψ_c) are incorporated. The format of Eq. (1.12) is similar to the expression for development of hooked bars (Eq. 1.9), and the values for modification factors are also the same, as given in Table 1.5.

Table 1.5 Modification factors for headed bars as given in Table 25.4.4.3 of ACI 318-19

Modification Factor	Condition	Value
Parallel tie reinforcement, ψ_p	$A_{tt} \geq 0.3A_{hs}$ or $s^{[1]} \geq 6d_b^{[2]}$	1.0
	Other	1.6
Location, ψ_o	(1) Terminating inside column core with side cover ≥ 2.5 in., or (2) With side cover $\geq 6d_b$	1.0
	Other	1.25
Concrete strength, ψ_c	$f'_c < 6,000$ psi	$f'_c/15,000 + 0.6$
	$f'_c \geq 6,000$ psi	1.0

[1] s is minimum center-to-center spacing of hooked bars

[2] d_b is nominal bar diameter

In Table 1.5, A_{tt} is the total cross-sectional area of ties or stirrups parallel to headed bars within $8d_b$ from the centerline of the headed bars and spaced no greater than $8d_b$, as shown in Figure 1.27, and A_{hs} is the total cross-sectional area of headed bars being developed.

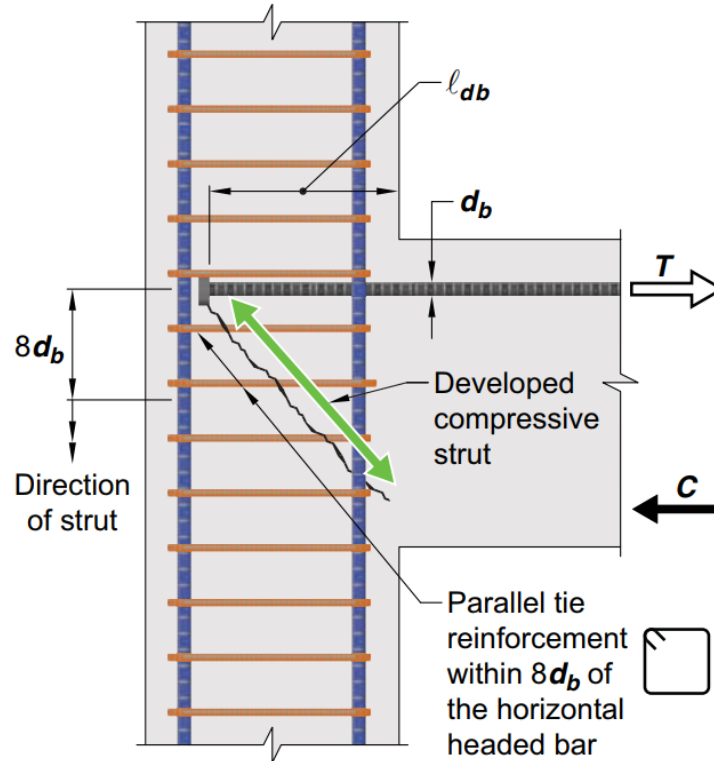


Figure 1.27 Parallel tie reinforcement that contribute to anchorage strength of headed bars as defined in ACI 318-19 (ACI 318-19)

Although the values for confining reinforcement factors for hooked and headed bars (ψ_r and ψ_p , respectively) are the same, the amount of confining reinforcement considered by the Code that contributes to anchorage strength are different. For hooked bars, it should be a minimum of

$0.4A_{hs}$ within $15d_b$ of the centerline of the bars (Figure 1.23), whereas for headed bars it is $0.3A_{hs}$ within $8d_b$ (Figure 1.27). The other difference between the hooked and headed bar equations is the constant multiplier; for hooked bars, it is $1/55=0.018$, whereas for headed bars it is $1/75=0.013$. This indicates that, if all other parameters are equal, headed bars require a shorter development length than hooked bars. The last difference is that, unlike hooked bars, the equation for headed bars does not have a concrete density factor, λ , to account for using lightweight concrete since only the use of normalweight concrete is permitted.

In addition to incorporating the three modification factors discussed above, ACI 318-19 has a few other improvements compared to the ACI 318-14 design provisions for headed bars. The upper limit of 60,000 psi on the bar yield strength is removed (ACI 318-19 currently allows up to 100,000 psi in general). The minimum required clear spacing between the bars has been reduced from $4d_b$ to $2d_b$. Similar to hooked bars, ACI 318-19 stayed with $\sqrt{f'_c}$ rather than incorporating the more accurate $f_c'^{0.25}$ as proposed by Shao et al. (2016), but includes the ψ_c factor to account for the effect of $f_c'^{0.25}$ for $f'_c < 6,000$ psi to prevent excessively long development lengths for lower compressive strengths, as discussed before. The minimum net bearing area of the head A_{brg} is $4A_b$, unchanged from ACI 318-14.

Despite the improvements, the headed bar development length provisions in ACI 318-19 have limitations. The maximum bar size allowed is No. 11 due to a lack of experimental data for larger bars (No. 14 and No. 18), a restriction that is one of the main motivations of the current study. The effect of confining reinforcement and bar spacing, simplified to a binary choice of 1.0 or 1.6 (similar to hooked bars), prevents designers from using values other than 1.6 (that is, shorter development lengths) in cases where the center-to-center bar spacing (s) is less than $6d_b$ and area of parallel ties (A_{tt}) is less than $0.3A_{hs}$. Also, although the concrete compressive strength factor ψ_c , is conservative for concrete compressive strengths below 6,000 psi, as will be shown in Chapter 6, it becomes progressively unconservative as the concrete strength increases from 6,000 to 10,000 psi and makes the development length equations for both hooked and headed bars slightly more complex. If the more accurate $f_c'^{0.25}$ could be used, a more uniform margin of safety would be provided for concrete strengths up to 16,000 psi and there would be no need for a concrete strength modification factor.

1.4 OBJECTIVE AND SCOPE

A comprehensive study has been underway at the University of Kansas since 2012 to investigate the anchorage and development of hooked and headed bars. To date, the study has included up to No. 11 and smaller bars anchored in members with a wide range of material and member properties, including high-strength reinforcing steel and concrete in beam-column joints, lap splices, bars with shallow embedments, and CCT node specimens (Searle et al. 2014, Sperry et al. 2015a, 2015b, 2017a, 2017b, 2018, Yasso et al. 2017, Ajaam et al. 2017, 2018, Shao et al. 2016, Ghimire et al. 2018, 2019a, 2019b). Descriptive equations to calculate the anchorage strength and design provisions for the development length, have been developed that apply to hooked and headed bars with yield strengths up to 120,000 psi and concrete compressive strengths up to 16,000 psi. The findings served as basis for the current design provisions, in ACI 318-19, for the development of hooked and headed bars. There are, however, a number of limitations in the Code provisions. For hooked bars, the provisions in ACI 318-19 give no credit to the contribution of confining reinforcement for hooked bars larger than No. 11. For headed bars, bars larger than No. 11 are not permitted. These limits are mainly due to a lack of experimental data on No. 14 and No. 18 bars. For both hooked and headed bars, $\sqrt{f'_c}$ does not provide an accurate representation of the contribution of concrete compressive strength to the anchorage strength.

The objective of this research is to continue the comprehensive study of the anchorage strength and development of headed reinforcing bars and to expand the available data to include the largest sizes currently permitted in the ACI Building Code, No. 14 and No. 18. The study also includes a limited number of specimens with No. 14 and No. 18 hooked bars to investigate the differences in performance between large hooked and headed bars in external beam-column joints. Test results are compared with anchorage strengths calculated using the descriptive equations developed based on No. 11 and smaller bars and those based on the development length and anchorage provisions in ACI 318-19. The findings are used as a basis for design criteria applicable to No. 14 and No. 18 bars, with the goal of addressing the current Code limitations on both hooked and headed bars.

Forty-two large-scale beam-column joint specimens containing No. 11, No. 14 and No. 18 headed and hooked bars are tested. Of the 42 specimens, 30 contain headed bars and 12 contain hooked bars. The effects of bar size, bar spacing, embedment length, confining transverse

reinforcement in the joint region, side cover, and concrete compressive strength on anchorage strength are investigated.

The 30 specimens containing headed bars include 2 with No. 11, 20 with No. 14, and 8 with No. 18 bars. Of the 20 specimens with No. 14 bars, 13 have two widely-spaced bars (center-to-center spacing $\geq 8d_b$), one has two closely-spaced bars (center-to-center spacing $< 8d_b$), and six have three closely-spaced bars. Of the eight specimens with No. 18 headed bars, four have two widely-spaced bars, two have two closely-spaced bars, and two have three closely-spaced bars. Concrete compressive strength ranges from 5,310 to 16,210 psi. Bar stresses at failure range from 54,900 to 148,300 psi. The center-to-center bar spacing range from $2.7d_b$ to $10.6d_b$. Headed bars from different manufacturers are used with net bearing areas of $4.2A_b$ to $4.4A_b$. The majority of specimens contain ties within the joint, with the total area of tie legs within $10d_b$ from the top of headed bars ranging from $0.178A_{hs}$ to $0.827A_{hs}$, where A_{hs} is the total area of the headed bars being developed. Most specimens have a side cover to the bar of 3.5 in. One No. 14 specimen and four No. 18 specimens have a side cover of 6.5 in.

Of the 12 specimens containing hooked bars, eight contain No. 14 and four contain No. 18 bars. The No. 14 bar specimens include six with two widely-spaced bars and two with three closely-spaced bars. All No. 18 bar specimens have two widely-spaced bars. Bar spacing ranges from $3.5d_b$ to $10.6d_b$. Specimens have concrete compressive strengths ranging from 6,390 to 15,770 psi, and bar stresses at failure range from 87,300 to 130,600 psi. Four No. 14 bar specimens have no confining reinforcement in the joint region. The remaining hooked bar specimens have ties in the joint region ranging from $0.178A_{hs}$ to $0.465A_{hs}$. All specimens have a side cover to the bar of 3.5 in.

CHAPTER 2: EXPERIMENTAL WORK

This chapter describes the details of the experimental work in this study, including the properties of the reinforcing steel (headed and hooked bars, column longitudinal reinforcement and ties) and concrete, specimen design and fabrication, testing apparatus (reaction frame, bearing plates, and load cells), and testing procedure. The testing program is summarized at the end of the chapter.

2.1 MATERIAL PROPERTIES

2.1.1 Hooked and Headed Bars

The hooked and headed bars used in this study were fabricated from No. 11, No. 14, and No. 18 high-strength ASTM A1035 steel. The hooked bars consisted of No. 14 and No. 18 bars with 90° standard hooks, as specified in Table 25.3.1 of the ACI 318-19 (Table 1.1). No. 11, No. 14, and No. 18 headed bars were supplied by three manufacturers. The heads were cold-swaged, taper-threaded, and cold-swaged with a threaded coupling sleeve, as shown in Figure 2.1.

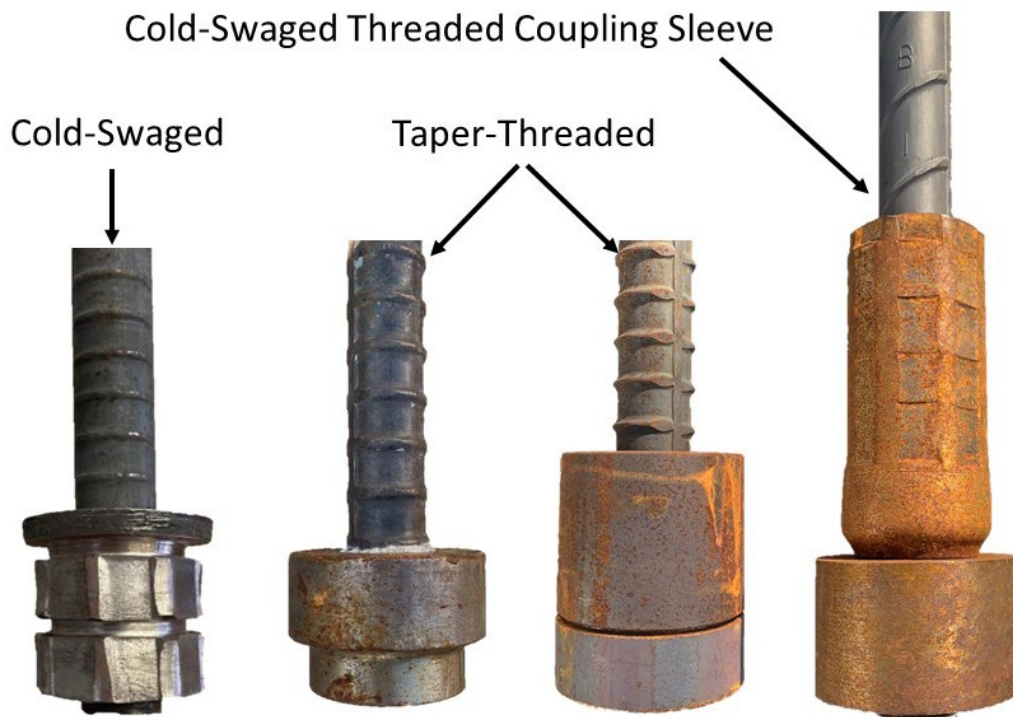





Figure 2.1 Different types of headed bars used in the study

Table 2.1 shows the dimensions of the heads used in this study. Each head has a designation consisting of a letter and a number, representing the head type and the net bearing area,

respectively. The obstruction on the No. 18 headed bar with coupling sleeve (Figure 2.1) was tapered to a smaller diameter adjacent to the head, and this diameter was used when calculating the net bearing area in accordance with ASTM A970-17.

Table 2.1 Dimensions of the headed bars

Head Type	Designation	Bar Size	d_1 (in.)	t_1 (in.)	d_2 (in.)	t_2 (in.)	A_{brg}^1
 Cold-Swaged	B4.2	No. 14	4.125	4.5	-	-	$4.2A_b^2$
 Taper-Threaded	L4.2	No. 14	3.875	2.5	-	-	$4.2A_b$
	H4.4	No. 18	5.25	6.25	-	-	$4.4A_b$
	L4.4	No. 18	5.25	3.25	-	-	$4.4A_b$
 Cold-Swaged Threaded Coupling Sleeve	O4.5	No. 11	3.75	2.125	2.25	6.75	$4.5A_b$
	O4.3	No. 18	6	3.75	3.75	10	$4.3A_b$

¹ Net bearing area

² Nominal area of the bar

2.1.2 Reinforcing Steel Properties

The hooked and headed bars were made of ASTM A1035 Gr. 120 reinforcing steel to ensure that the bars did not fracture prior to bond failure. In all specimens with No. 14 bars, Gr. 60 No. 11 reinforcing bars were used as column longitudinal reinforcement. Due to higher flexural demand in specimens with No. 18 bars, ASTM A615 Gr. 80 or A1035 No. 11 bars were used. For column shear reinforcement outside the joint region, ASTM A615 Gr. 60 No. 4 bars were used in all specimens. For confining reinforcement in the joint region, parallel ties made of ASTM A615 Gr. 60 No. 4 or No. 5 bars were used. Table 2.2 provides the physical properties of hooked and headed bars.

Table 2.2 Physical properties of reinforcing steel

Bar Size	Nominal diameter, d_b (in.)	Type	Yield strength (ksi)	Average rib spacing (in.)	Average rib height (in.)		Average gap width (in.)	Relative rib area ²
					A ¹ (in.)	B ² (in.)		
4 ⁶	0.5	Ties	72.7 ³	—	—	—	—	—
5 ⁶	0.625	Ties	66.7 ³	—	—	—	—	—
11 ⁶	1.41	Long. reinf.	79.6 ³	—	—	—	—	—
11 ⁶	1.41	Long. reinf.	80.4 ⁴	—	—	—	—	—
11 ⁶	1.41	Long. reinf.	120 ⁵	—	—	—	—	—
11	1.41	Head, O4.5	135 ⁵	0.838	0.097	0.092	0.394	0.099
14	1.693	Hook	127 ⁵	1.006	0.079	0.070	0.279	0.062
		Head, B4.2	127 ⁵	1.006	0.079	0.070	0.279	0.062
		Head, L4.2	127 ⁵	1.006	0.079	0.070	0.279	0.062
18	2.257	Hook	131 ⁵	1.449	0.121	0.117	0.312	0.074
		Head, H4.4	136 ⁵	1.502	0.144	0.130	0.316	0.078
		Head, L4.4	131 ⁵	1.449	0.121	0.117	0.312	0.074
		Head, O4.3	131 ⁵	1.449	0.121	0.117	0.312	0.074

¹ Per ASTM A615, A1035² Per ACI 408R- 3³ ASTM A615 Gr. 60⁴ ASTM A615 Gr. 80⁵ ASTM A1035 Gr. 120⁶ Rib area data not obtained

2.1.3 Concrete Properties

The specimens were cast with non-air-entrained ready-mix concrete with the mixture proportions given in Table 2.3. Different high-range polycarboxylate-based water reducers were used in the normal- and high-strength mixtures. The specific gravity (SG) for cementitious materials and the bulk saturated surface dry specific gravity BSG (SSD) for fine and coarse aggregates are also given in Table 2.3. The nominal maximum aggregate size was $\frac{3}{4}$ in. for all mixtures.

Table 2.3 Concrete mixture proportions

Material	Quantity (SSD)				SG or BSG (SSD)
	5,000 psi $w/c = 0.44$	12,000 psi $w/c = 0.26$	15,000 psi $w/cm = 0.21$	16,000 psi $w/cm = 0.21$	
Type I/II Cement, lb/yd ³	600	880	800	498	3.2
Type C Fly Ash, lb/yd ³	-	-	200	-	2.3
Slag Cement, lb/yd ³	-	-	-	373	2.9
Silica Fume lb/yd ³	-	-	-	25	2.2
Water, lb/yd ³	263	228	210	188	1.0
Kansas River Sand, lb/yd ³	1396	1517	1430	1214	2.63
Crushed Limestone, lb/yd ³	1735	-	-	-	2.59
Granite, lb/yd ³	-	1517	1430	1792	2.61
High-range Water Reducer (superplasticizer), oz (US)	40 ¹	44 ¹	147 ²	44 ¹ + 218 ³	-
Viscosity Modifier (VMAR), oz (US)	-	-	20	54	-
Set Retarder ⁴ , oz (US)	12	-	-	27	-

¹ ADVA® 140M² ADVA® Cast 575³ ADVA® Cast 600⁴ DARATARD®

2.2 TEST SPECIMENS

2.2.1 Specimen Design

The specimens represent exterior beam-column joints without casting the beam, similar to those used in previous studies beginning with the work of Marques and Jirsa (1975) and the studies at the University of Kansas by Searle et al. (2014), Sperry et al. (2015a, 2015b), Ajaam et al. (2017), Yasso et al. (2017), Shao et al. (2016). The top longitudinal reinforcement of the simulated beam is represented by the headed or hooked bars embedded in the column, and the compression region of the virtual beam is simulated by the bearing member below the test bars. Figures 2.2 and 2.3 show a schematic of the specimens with hooked and headed bars, respectively. As shown in the figures, a tensile force (T) was applied to hooked and headed bars during the test, and a compressive force (C) was applied through the bearing member below the test bars. The tensile and compressive forces, T and C , represent the forces at the face of the column due to the application of a negative bending moment by the beam.

The embedment length (ℓ_{eh} in Figures 2.2 and 2.3) was calculated based using the descriptive equations for hooked and headed bars, Eq. (1.1) and (1.2), and (1.3) and (1.4), respectively, to achieve a target bar stress so that the anchorage failure would occur prior to

fracture of the test bars. For hooked bars, the embedment length is the distance from the back of the hook to the front face of the column. For headed bars, the embedment length is defined as the distance from the bearing face of the head to the front face of the column. Because the bars were placed to provide the maximum embedment length, the depth of the column, h , equaled the sum of embedment length, head thickness, and cover to back of the head (3.5 in.) for headed bars, and the sum of embedment length and cover to the back of the hook (2 in.) for hooked bars. The column width, b , equaled the sum of out-to-out spacing of test bars and two times the side cover to the bar (3.5 in. for the majority of specimens).

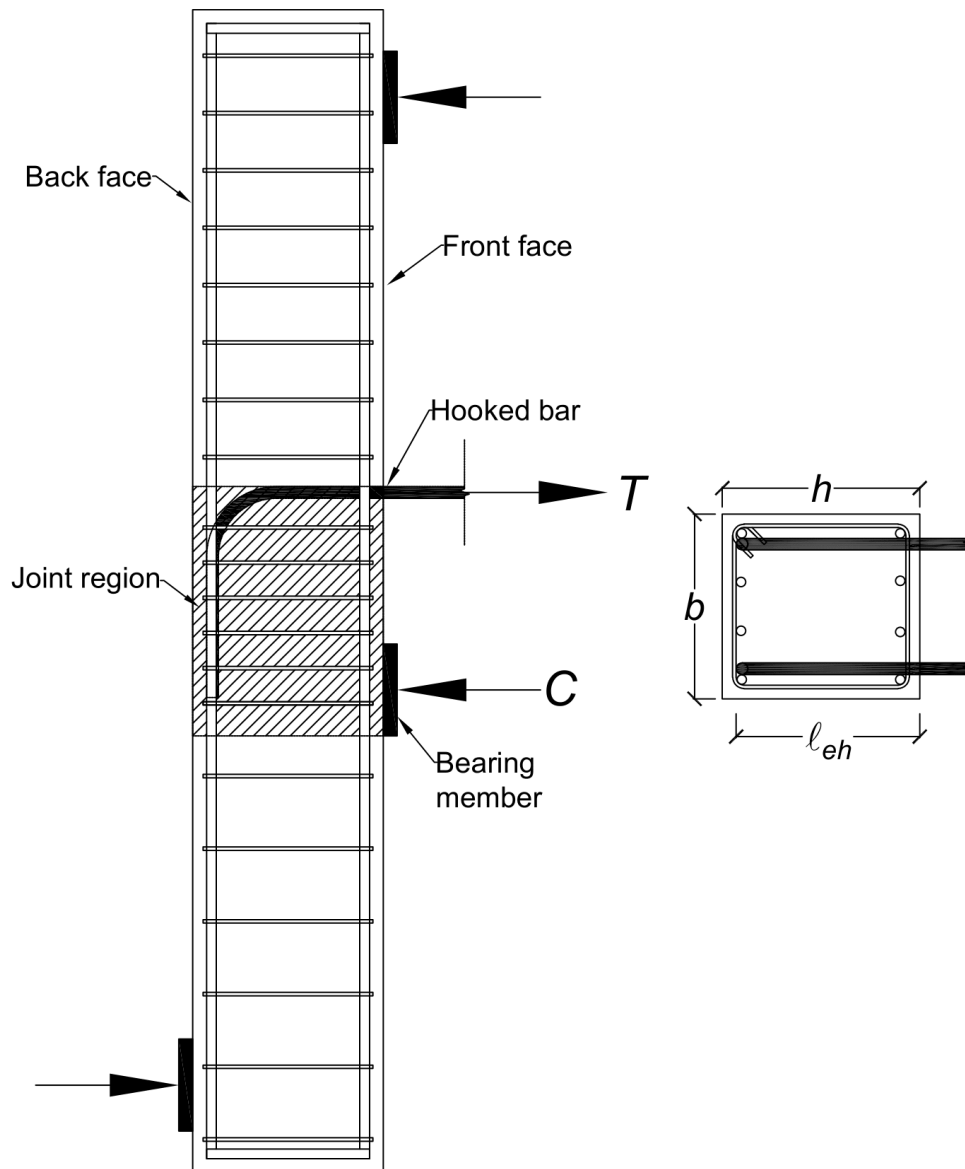


Figure 2.2 Schematic of the specimens with hooked bars, side view (left) and top view (right)

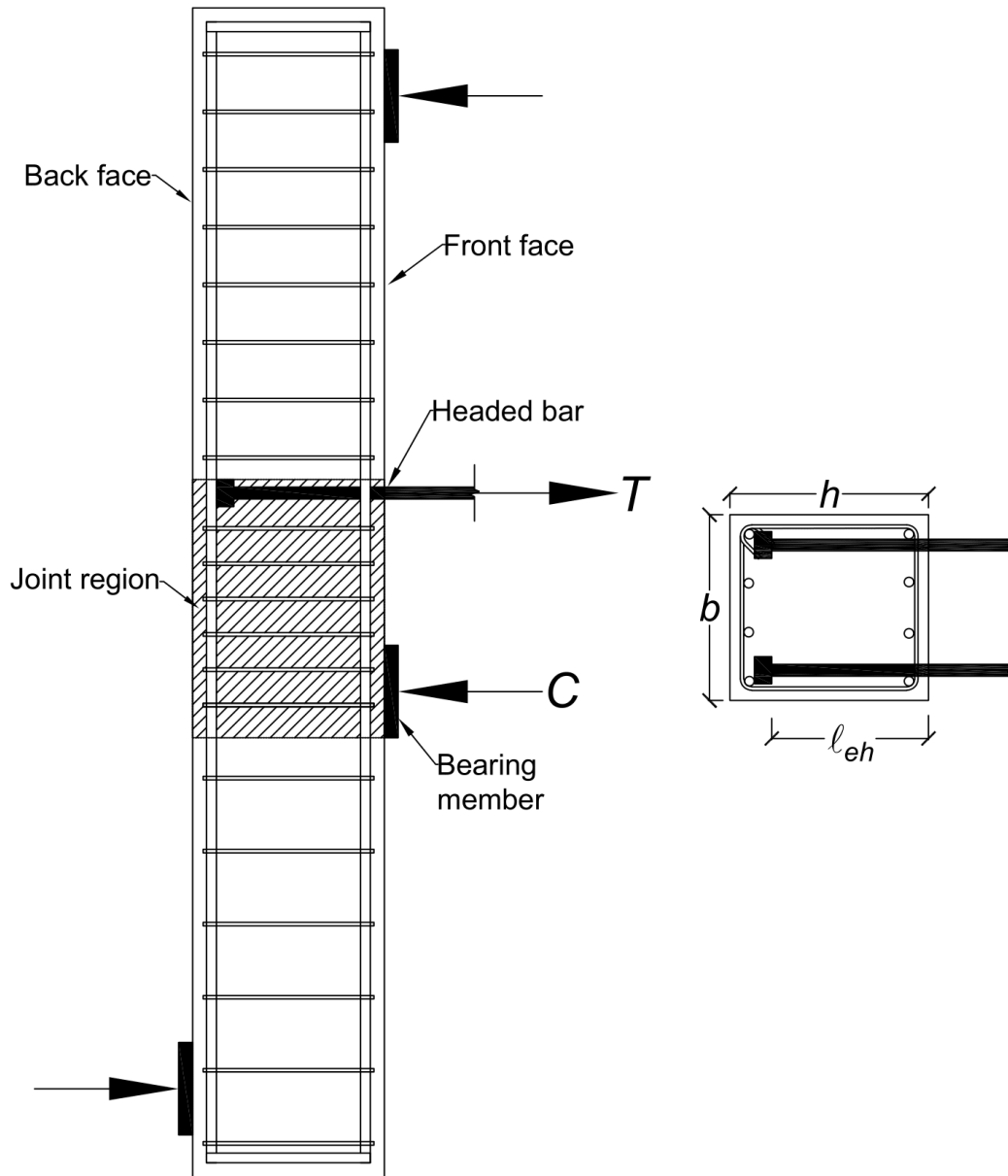


Figure 2.3 Schematic of the specimens with headed bars, side view (left) and top view (right)

The specimen simulated an exterior beam-column joint in a building located halfway between two inflection points. In most cases, load was applied so that the column moment demands above and below the joint were equal and the shear force within the joint region was 80% of the force applied to the hooked or headed bars. In other cases, the joint shear was reduced to about 69% of the force applied to the hooked or bars. Loading conditions are described in detail in Section 2.3.1. The specimens had the proportions shown in Figure 2.4. The dimension x_{mid} was 28.6 and 38.2 in. for specimens with No. 14 and No. 18 bars, respectively. The total height of the column, h_0 , was 14 ft and 18 ft for specimens with No. 14 and No. 18 bars, respectively.

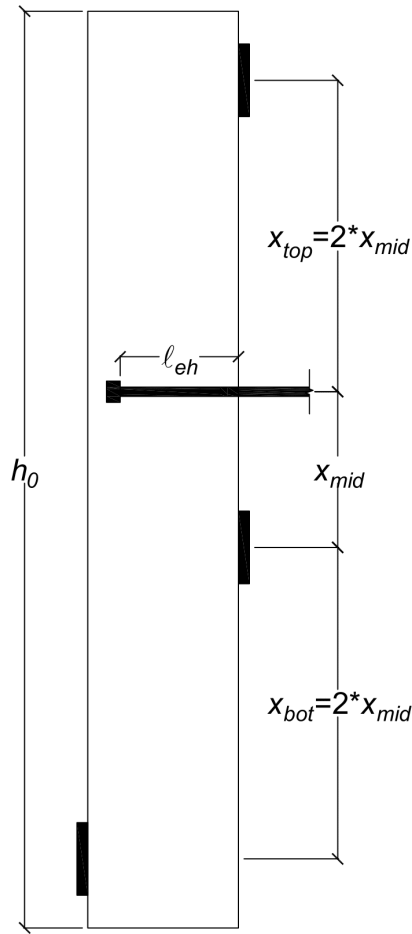


Figure 2.4 Dimensional proportions of the specimens; For specimens with No. 14 bar, $x_{mid} = 28.56$ in. and $h_0 = 14$ ft, and for specimens with No. 18 bar, $x_{mid} = 38.15$ in. and $h_0 = 18$ ft

The quantity of confining reinforcement in the form of ties parallel to the hooked or headed bars within the joint region (number, configuration, and spacing of ties) was one of the test parameters, as described in Section 2.2.2. Outside of the joint region, longitudinal and transverse reinforcement was designed to resist the flexural and shear demands on the column without yielding¹. The design was based on the assumption that all test bars reached the expected anchorage failure stress simultaneously. No axial force was applied because it has been shown to have a negligible effect on anchorage strength (Marquez and Jirsa, 1975, Sperry et al. 2015b).

¹ The contribution of concrete to shear, v_c , was taken as $2bd\sqrt{f'_c}$

2.2.2 Test Parameters

As discussed in Chapter 1, this study investigates the effects on anchorage strength of headed and hooked bars of bar size, number and spacing of bars, concrete compressive strength, embedment length, confining reinforcement within the joint region, and side cover to the bars, as follows:

Bar Size: No. 14 and No. 18 hooked bars; No. 11, No. 14 and No. 18 headed bars.

Number and spacing of bars: The majority of the specimens (32 out of 42) had two hooked or headed bars, and the remaining specimens contained three bars. Of the 32 specimens with two test bars, 29 specimens had widely-spaced bars (ranging from 8.0 to $10.6d_b$ on-center) and 3 specimens had closely-spaced bars ($5.3d_b$ to $7.1d_b$ on-center). All 10 specimens containing three bars had closely-spaced bars, with center-to-center spacing ranging from 2.7 to $3.5d_b$ on-center. Specimens with two widely-spaced bars had a center-to-center bar spacing of 18 in. Specimens with two closely-spaced bars had bars spaced at 12 in. on-center. Center-to-center spacing of bars in specimens with three closely-spaced bars was 6 in.

Concrete compressive strength: The concrete mix designs used (Table 2.3) had target compressive strengths of $5,000$, $12,000$, $15,000$, and $16,000$ psi. The measured concrete compressive strength (f_{cm}) ranged from $5,310$ to $16,210$ psi for the headed bar specimens and from $6,390$ to $15,770$ psi for the hooked bar specimens.

Embedment length: Nominal embedment lengths of 26.6 and 35.8 in. were used for the No. 14 hooked bars and 27.8 and 37.8 in. for the No. 18 hooked bars. A nominal embedment length of 18.5 in. was used for the No. 11 headed bars and ranged from 20.5 to 31.9 in. for the No. 14 headed bars and from 27.8 to 31.1 in. for the No. 18 headed bars.

Confining reinforcement within the joint region: The majority of specimens had confining reinforcement within the joint region in the form of No. 4 or No. 5 ties parallel to the hooked or headed bars. For the No. 14 hooked bar specimens, the ratio of confining reinforcement (total area of tie legs within $9.5d_b$ from the centerline of test bars, as shown in Figure 1.18) to the total cross-sectional area of the bars being developed, A_{th}/A_{hs} , ranged from 0 to 0.28 . For the No. 18 hooked bar specimens, A_{th}/A_{hs} ranged from 0.23 and 0.47 . For the No. 14 headed bar specimens, A_{th}/A_{hs} ranged from 0 to 0.83 . For the No. 18 headed bar specimens, ranged from 0.23 to 0.54 . Most of the No. 4 or No. 5 ties had two legs. Three specimens had double overlapping No. 5 ties (four legs, two internal legs and two external legs), as shown in Figure 2.5, to investigate the effect of having

middle legs within the joint. Three specimens had double No. 5 ties, which consisted of two single ties placed adjacent to each other (four external legs).

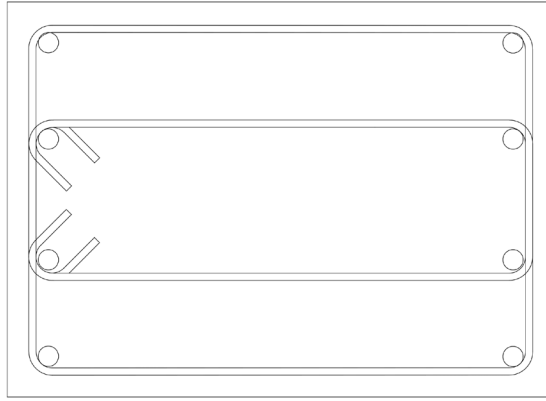


Figure 2.5 Double overlapping tie configuration

Side cover to the bars: Most specimens had side cover to the hooked or headed bars of 3.5 in. One No. 14 and four No. 18 headed bar specimens had a side cover of 6.5 in.

2.2.3 Specimen Designation

Each specimen has a designation denoting the design variables and parameters. For example, the designation shown in Figure 2.6 indicates a specimen containing two No. 14 headed bars with B4.9 heads (refer to Table 2.1) spaced at $10.6d_b$ on-center, cast in concrete with a nominal strength of 15 ksi concrete, and having a total of five No. 4 ties within the joint region. The headed bars were placed inside the column core, with a nominal side cover to the bar (c_{so}) and back cover to the head (c_{bc}) of 3.5 in., and a nominal embedment length (ℓ_{eh}) of 20.6 in. The confining reinforcement designation is removed from specimens without ties within the joint region. For the hooked bar specimens, the head type designation is removed, and the back cover is the cover to the back of the hook.

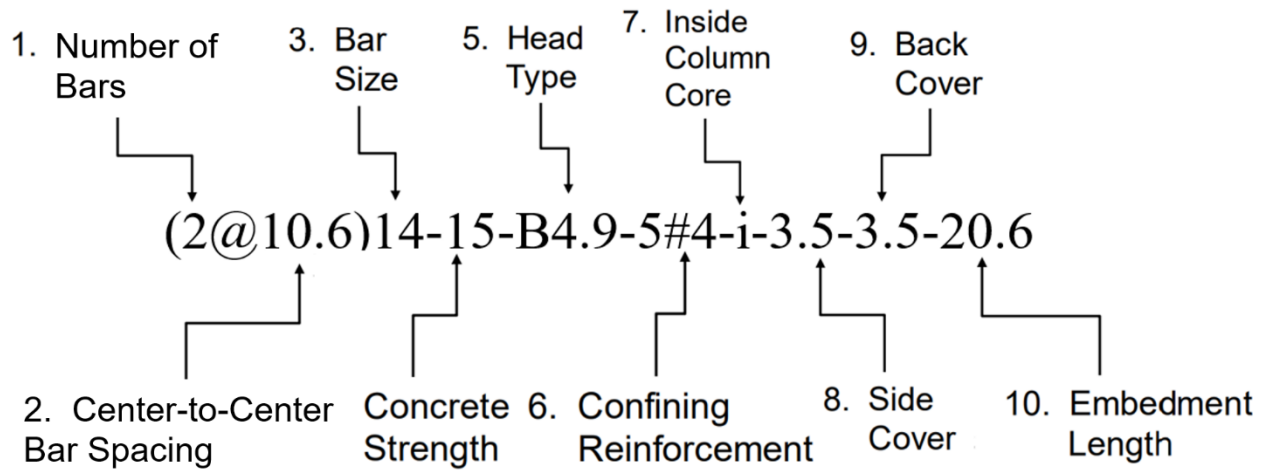


Figure 2.6 Example specimen designation

The cross-sectional dimensions of a typical headed bar specimen with variable callouts are shown in Figure 2.7.

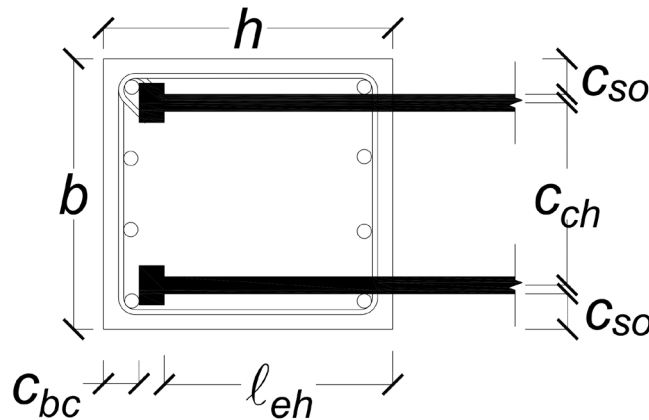


Figure 2.7 Cross-sectional dimensions and variable callouts of specimens

2.2.4 Specimen Fabrication

The formwork for the columns was fabricated using 2×4 dimension lumber and $\frac{3}{4}$ -in. plywood. The lower half of the formwork was braced with clamps consisting of 2×6 dimension lumber and all-thread rods to provide resistance against the lateral hydrostatic pressure of the fresh concrete during concrete placement. Reinforcement cages (steel cages) were built according to the specimen design, with No. 4 or No. 5 ties bent to the specified dimensions and tied to the No. 11 longitudinal reinforcing bars at the designated spacing. The clear cover to the No. 11 longitudinal bars was 2 in. in all specimens, maintained using 2-in. steel chairs that were tied to the reinforcement cages to maintain the side and back cover during casting. After the steel cages were

placed in the formwork, the headed or hooked bars were tied into the steel cage at the desired spacing and height in the column. The No. 14 bar specimens, with a height of 14 ft, were cast vertically, and large sawhorses were built and placed under the test bars to hold them level. The No. 18 bar specimens, with a height of 18 ft, were cast horizontally to ease concrete placement, and a wooden frame was built and bolted/screwed to the form to hold the test bars level vertically. Continuous bracing consisting of 2×6 lumber and all-thread rods was used to resist the lateral pressure of fresh concrete.

The vertical formwork for No. 14 bar specimens and the large sawhorses to hold the test bars is shown in Figure 2.8. The formwork bracing system used for No. 14 bar specimens is shown in Figure 2.9. The horizontal formwork for No. 18 bar specimens is shown in Figure 2.10. A typical reinforcement cage with steel chairs tied to the cage is shown in Figure 2.11. Cages with No. 14 headed and hooked bars tied to the vertical steel cage are shown in Figure 2.12. No. 18 headed and hooked bars tied to the horizontal steel cage are shown in Figure 2.13.



Figure 2.8 Vertical formwork for No. 14 bar specimens and sawhorses to hold the bars



Figure 2.9 Clamping system to brace the vertical forms for No. 14 bar specimens



Figure 2.10 Horizontal formwork for No. 18 bar specimens



Figure 2.11 A typical reinforcement cage (steel cage)



Figure 2.12 No. 14 hooked (left) and headed (right) bars tied to steel cages



Figure 2.13 No. 18 hooked (left) and headed (right) bars tied to steel cages

2.2.5 Specimen Instrumentation

In all specimens, strain gauges were installed on the first two ties above the joint region, some ties within the joint region, column longitudinal bars, and the headed or hooked bars to monitor the change in strain during the test. As shown in Figure 2.14, the strain gauges were attached to one headed or hooked bar and on the ties on one side of the specimen. In specimens with three test bars, strain gauges were attached to the middle bar in addition to one side bar. Two strain gauges were installed on the test bars. On headed bars, one gauge was placed 1.5 in. from the bearing face of the head (labeled T1) and the second gauge 1 in. from the column front face (labeled T2). On the hooked bars, one gauge was mounted just before the bend in the tail of the bar (labeled T1), and the second gauge 1 in. from the front face of the column (labeled T2). In all specimens, strain gauges were mounted on the first two ties above the joint region (labeled S1 and S2, with S2 being the closest to the test bar), and on the ties within the joint region, starting with S3. On the longitudinal column bars, one gauge was mounted on a corner bar (labeled L1) and the other gauge on an adjacent bar (labeled L2). Gauges L1 and L2 were installed at the location of headed or hooked bars along the length of the column bars.

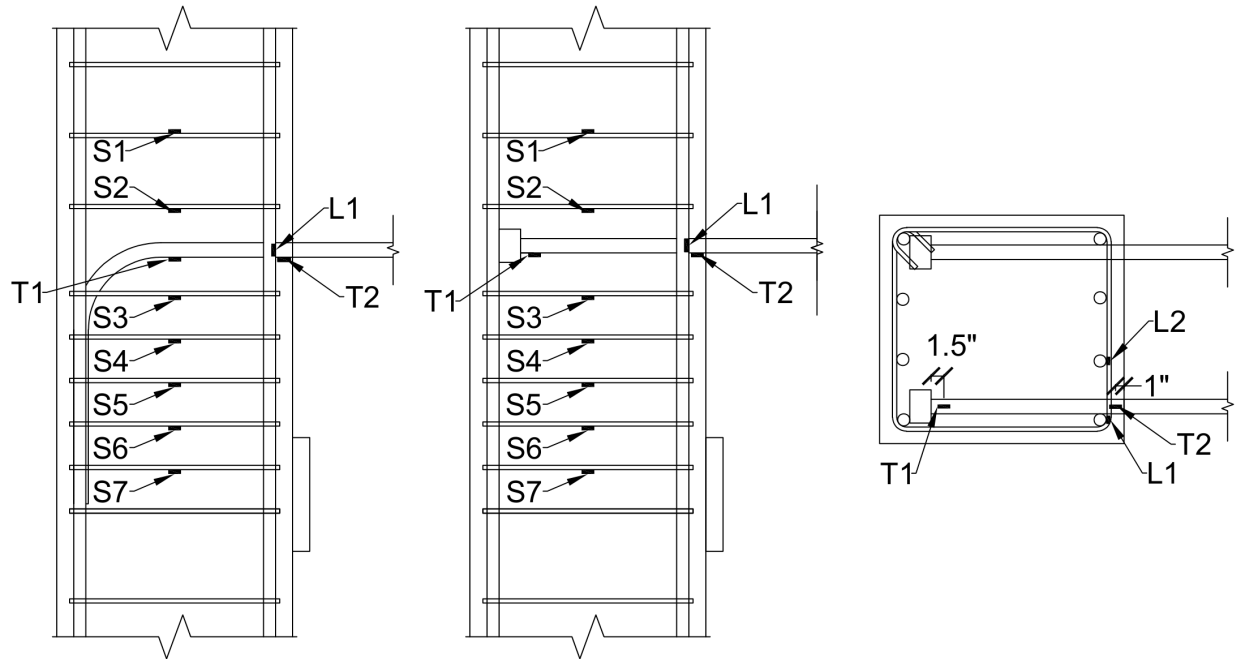


Figure 2.14 Side view (left and middle) and top view (right) of strain gauge locations

2.3 TESTING APPARATUS

2.3.1 Loading Conditions

The specimens were tested in the horizontal position. The forces applied to the specimens by the reaction frame (described in Section 2.3.2) during the test are shown in Figure 2.15. The upward force T was applied to the test bars using hydraulic jacks. The two downward compressive forces, C_1 and C_2 , were applied through bearing plates by bearing members of the reaction frame, and the upward compressive force C_3 was applied through a “lower tension member,” which consisted of two instrumented threaded rods – in some cases the force using a hydraulic jack and in some cases the force was due to the reaction induced in the rods, as explained next.

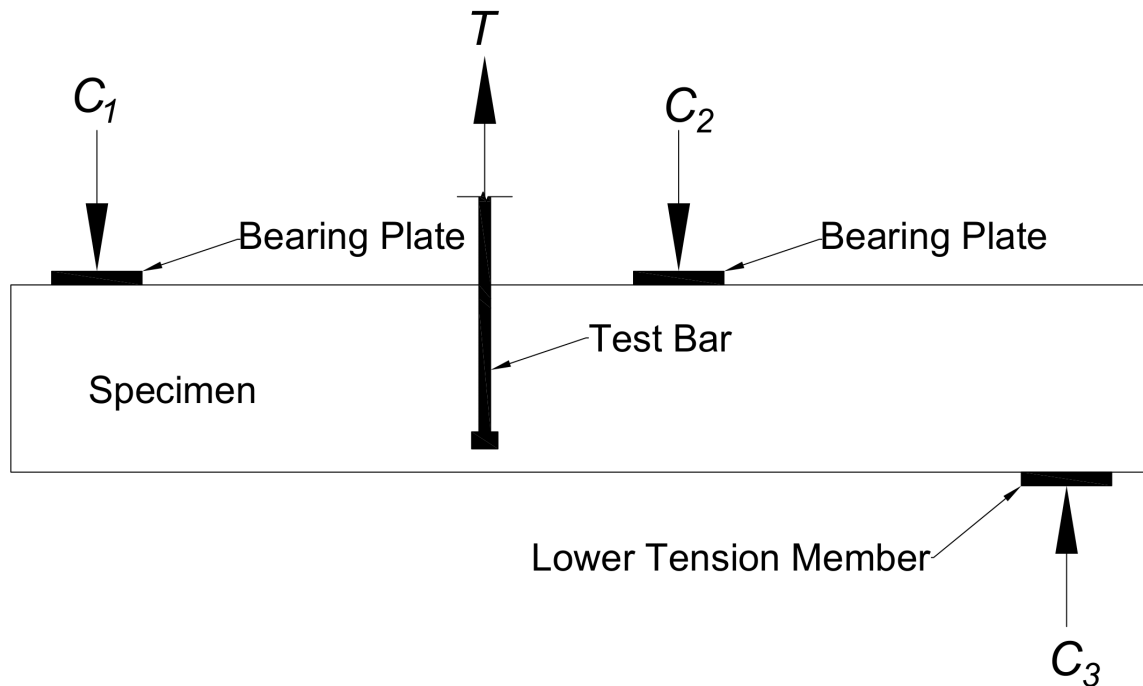


Figure 2.15 Forces applied to specimens by the reaction frame during the test

Two loading conditions were considered by testing the specimens with or without a hydraulic jack applying a load to the lower tension member:

Loading Condition A – Midheight between inflection points: In this loading condition, the specimen was tested with a hydraulic jack applying a load to the lower tension member equal to one-fifth the load applied to the hooked or headed bars, resulting in equal column moments above and below the joint and a shear force within the joint region was 80% of the force applied to the test bars. This loading condition simulates the forces in an exterior beam-column joint with the beam located at the midheight of the column between inflection points.

Loading Condition B – Anchorage only: In this loading condition, the specimen was tested without using a hydraulic jack to apply load to the lower tension member. In this case, the only load applied via the lower tension member, which was always in place and tightened, was due to the strain induced in the member due to deflection of the column as load was applied to the hooked or headed bars. Previous tests on No. 5, No. 8, and No. 11 hooked and headed bar specimens were based on this configuration (refer to Figures 1.5 and 1.14). Without the hydraulic jack applying load to the lower tension member, the force C_3 was approximately $0.04T$ (based on strain gage measurements), and the joint shear was reduced to about 69% of the force applied to the hooked or bars.

Table 2.4 summarizes the values of forces applied to the specimen for the two loading conditions. All 12 hooked bar specimens were tested under loading condition A. Of the 20 specimens containing No. 14 headed bars, nine were tested under loading condition A and 11 under loading condition B. Of the eight specimens with No. 18 headed bars, six were tested under loading condition A, and two under loading condition B.

Table 2.4 Values of forces applied to the specimens under the two loading conditions

Force	Loading Condition A ^[1]	Loading Condition B ^[2]
$C_1^{[3]}$	$0.2T$	$\approx 0.31T$
$C_2^{[3]}$	$T^{[6]}$	$\approx 0.73T$
$C_3^{[4]}$	$0.2T$	$\approx 0.04T$
$V_J^{[5]}$	$0.8T$	$\approx 0.69T$

^[1] Midheight between inflection points, test with the lower tension member

^[2] Anchorage only, test without hydraulic jack applying a load to lower tension member

^[3] Downward compressive forces applied by the bearing members

^[4] Upward compressive force applied by the lower tension member

^[5] Shear force in the joint region

^[6] Total force applied to the hooked or headed bars

2.3.2 Reaction Frame

The loading frame is a larger version of the system used by Shao et al. (2016) (Figure 1.14). The loading frame can apply loads up to 1620 kips and allows for a single row of two or three bars, as well as two rows of two or three bars, to be tested simultaneously. The frame can be modified to test specimens with No. 11, No. 14, or No. 18 bars. Side and end-elevation views of the reaction frame for No. 14 bar test setup are shown in Figure 2.16 and 2.17, respectively. The components of the test frame are described next.

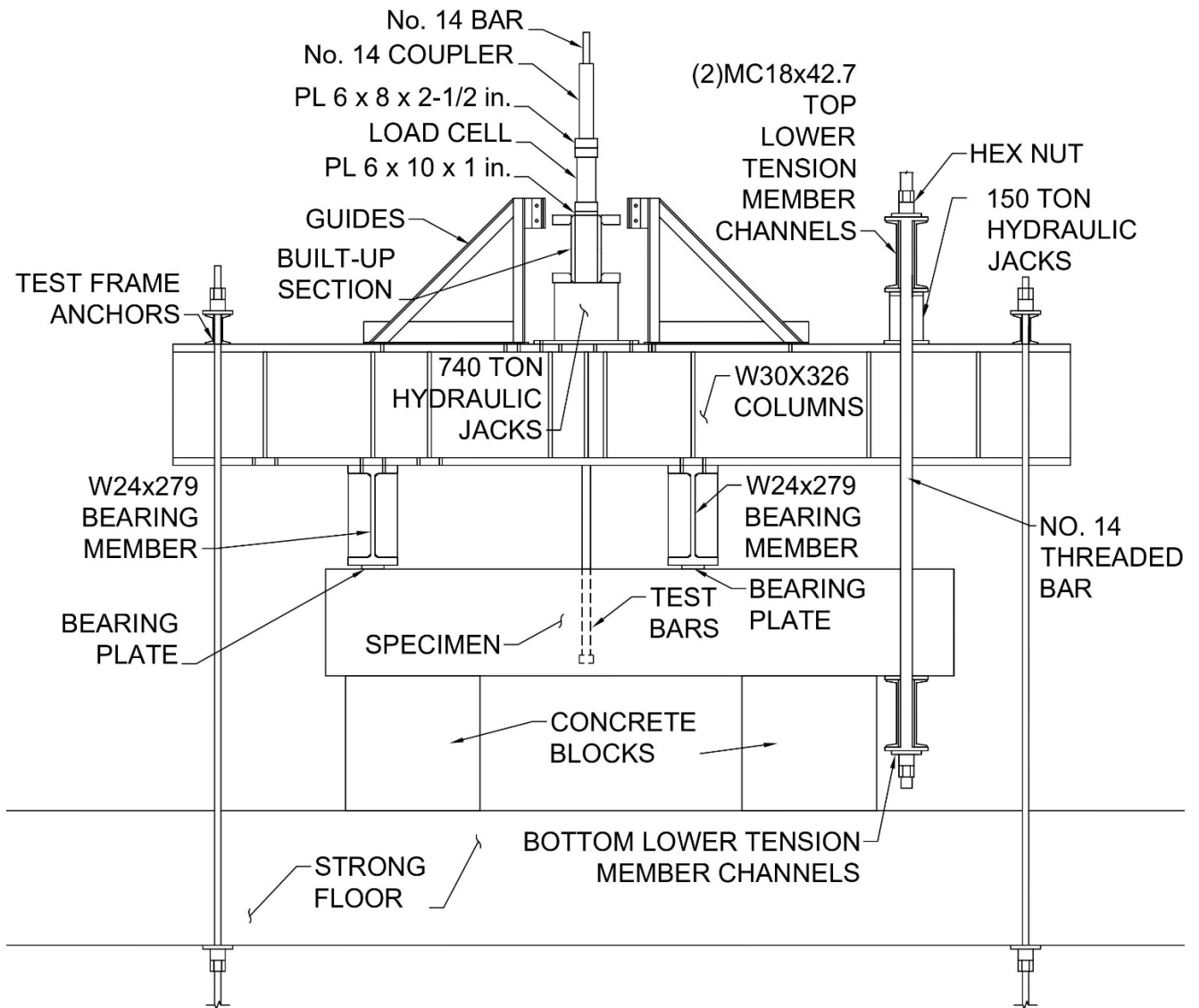


Figure 2.16 Side elevation of the reaction frame for the No. 14 bar setup

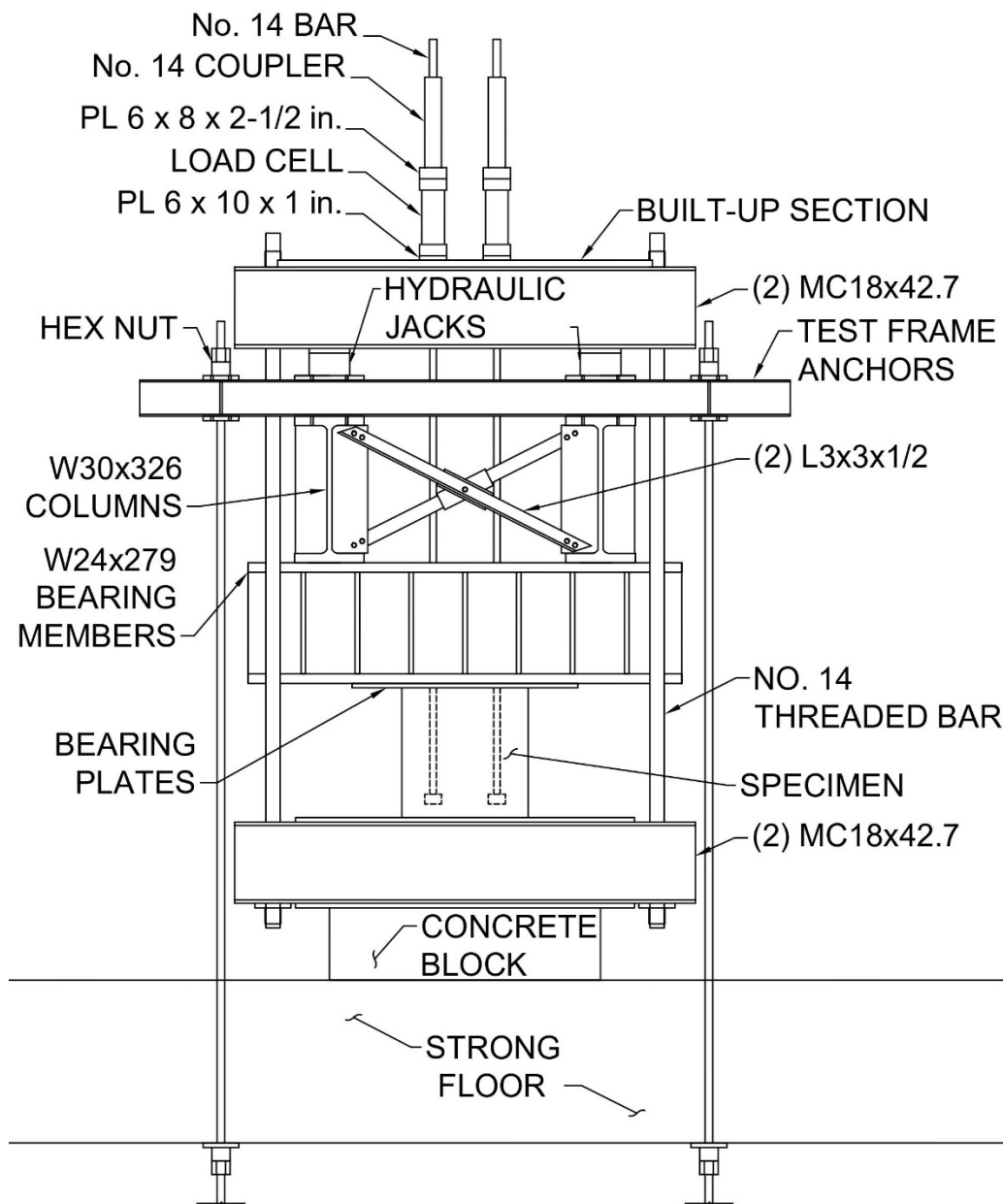


Figure 2.17 End-elevation of the reaction frame for the No. 14 bar setup

For the test, the specimens were placed horizontally on two $3 \times 3 \times 5$ ft concrete blocks with the hooked or headed bars oriented upward, as shown in Figure 2.18. The concrete blocks were cast with the 15,000-psi concrete and were placed so as to avoid applying any load near the tail of the hook. $6 \times 1 \times 36$ -in. steel plates were placed on the concrete blocks and leveled using hydrostone to provide a level surface to support the specimens.

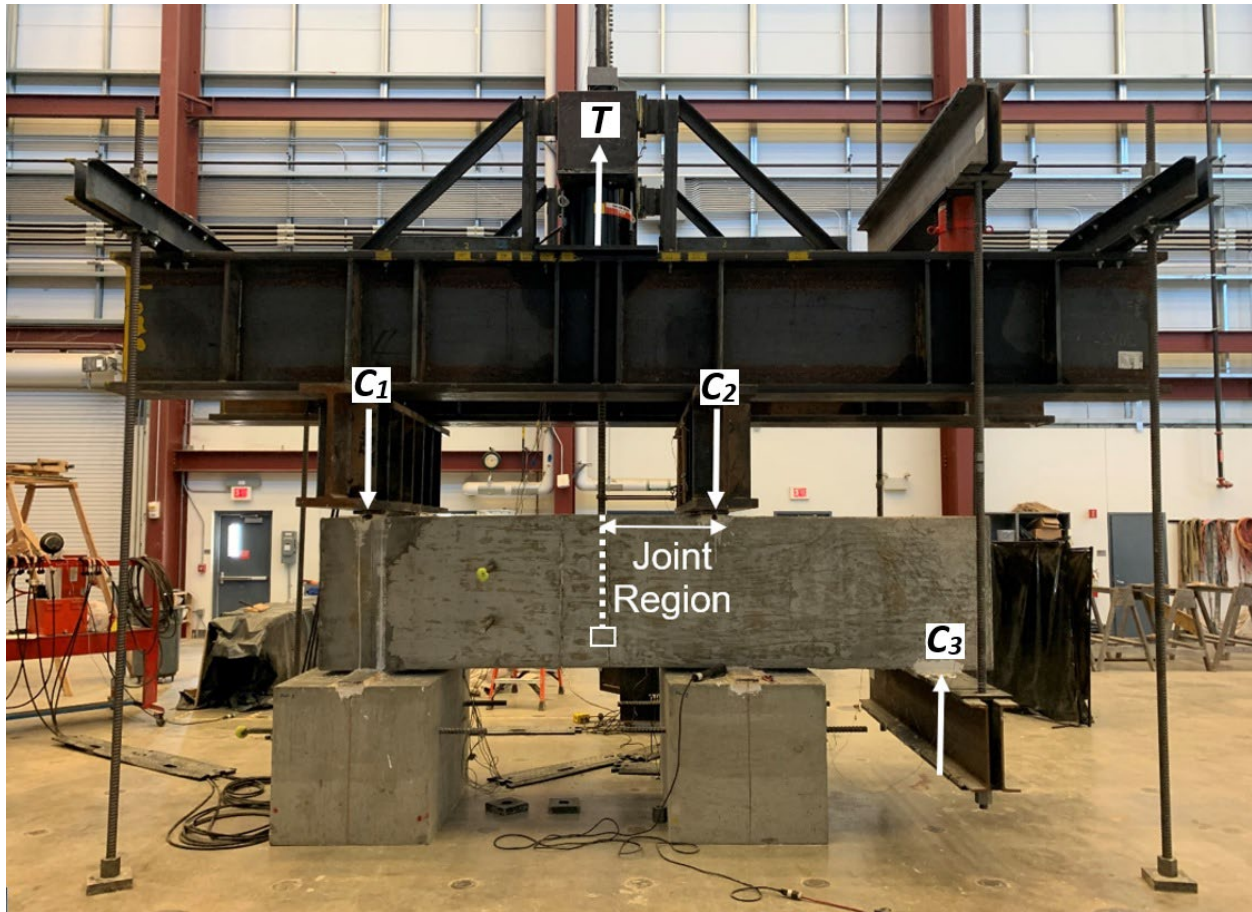


Figure 2.18 The reaction frame (No. 14 bar setup) and applied forces

The two downward compressive forces, C_1 and C_2 , shown in Figure 2.18, were applied by two $W24 \times 279$ bearing members as the load T was applied to the hooked or headed bars anchored in the column. The distances between the downward compressive forces and the hooked/headed bars are shown in Figure 2.4.

The upward compressive force C_3 shown in Figure 2.18 was applied through the lower tension member, using two 150-ton jacks when active (loading condition A, as described in Section 2.3.1). The 150-ton jacks were bolted to the top of each $W30 \times 326$ column. As shown in Figure 2.16, the lower tension member consisted of two sets of two $MC18 \times 42.7$ channels, the two 150-ton hydraulic jacks, and the two No. 14 threaded bar. As shown in Figures 2.16 and 2.18, one set of channels was placed on top of the two 150-ton jacks (across the jacks), and the other set of channels was placed in contact with the back face of the specimens. The No. 14 threaded rods connected the two sets of channels. Strain gauges were installed on these rods to track the force in the lower tension member during the test.

The force on the test bars, T , was applied by two 740-ton hydraulic jacks using an electric hydraulic pump. As shown in Figure 2.16, the jacks were bolted to horizontal W30×326 “columns,” and a built-up section was placed across the jacks, as shown in Figure 2.17. The W30 × 326 columns were bolted to the top of the bearing members, which have a center-to-center spacing of 60 in. that allows for all possible spacings of test bars. The built-up section consists of 1 and 2.5 in. steel plates welded together, and has rectangular openings spaced at 6 in. on-center for the test bars to pass through. The 6 in. spacing between the openings allows for testing specimens with two or three test bars spaced at 6, 12, or 18 in. on-center. As shown in Figure 2.16, two triangular-shaped bracing members were bolted on top of W30 × 326 columns to act as guides for positioning the built-up section prior to testing. The built-up section is shown in Figure 2.19.

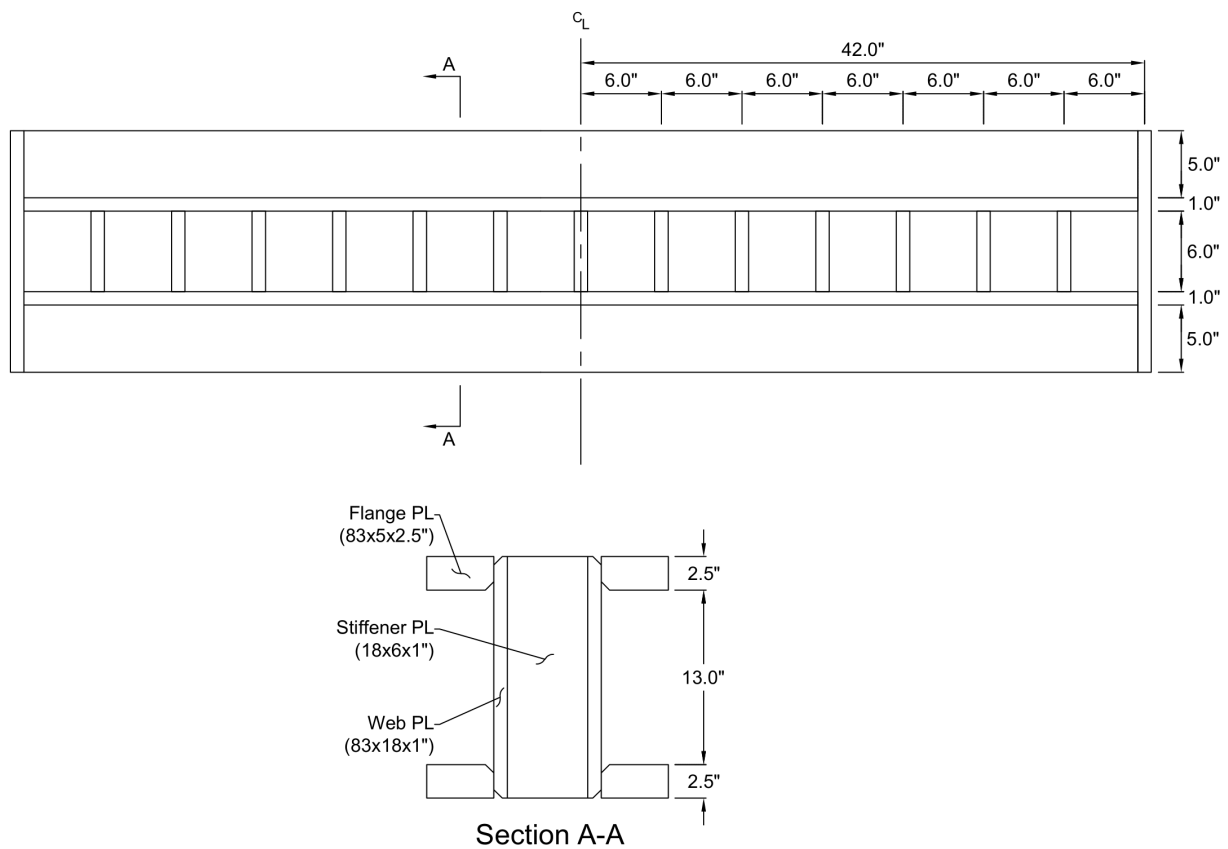


Figure 2.19 Plan view and cross-section of the built-up section

As shown in Figure 2.20 for No. 14 bars, the test bars passed through cylindrical load cells used to measure the applied force on each. A 1-in. thick washer plate was placed under each load cell to transfer the forces to the built-up section. The test bars were gripped at the top using mechanical reinforcing bar couplers. A 2.5-in. thick plate was placed between the couplers and the

load cells. As shown in Figures 2.16 and 2.18, the reaction frame was anchored to the strong floor at all four corners using test frame anchors consisting of C-channels and No. 14 threaded bars. The test frame anchors did not apply any force to the specimen during the test.

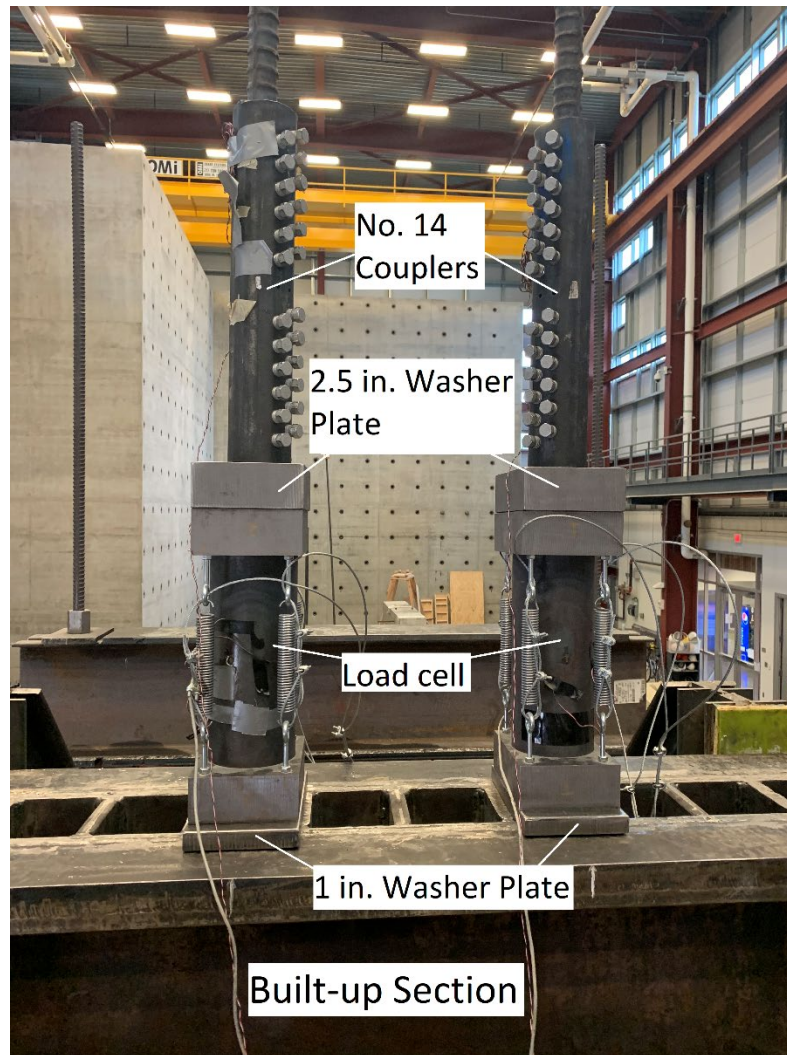


Figure 2.20 Load cells, washer plates, and couplers for No. 14 bar test setup

The test setup shown in Figures 2.16 and 2.18 was used in all No. 14 bar specimens and closely-spaced No. 18 bar specimens. For the widely-spaced No. 18 bar specimens (four specimens with headed bars and four with hooked bars), an alternative configuration was used in which hollow 434-ton jacks were used instead of the 740-ton jacks to apply the force directly to the bars. The alternative test setup is shown in Figure 2.21. In this case as shown in the figure, the built-up section was placed directly on top and across the two W30 \times 326 columns. No guides were used for the built-up section in this setup. New 1-in. thick washer plates were placed below and above the hollow jacks to transfer the forces to the built-up section and load cells, respectively. The

dimensions of the new washer plates were chosen to cover the entire area of the bottom of the jacks and the jack pistons at the top. The load cells and couplers in the original test setup were used. The alternative setup, shown in Figure 2.21, was used to test the two No. 11 headed bar specimens in which 150-ton jacks were used in place of the 434-ton jacks and collars with wedges were used instead of couplers as the gripping system.

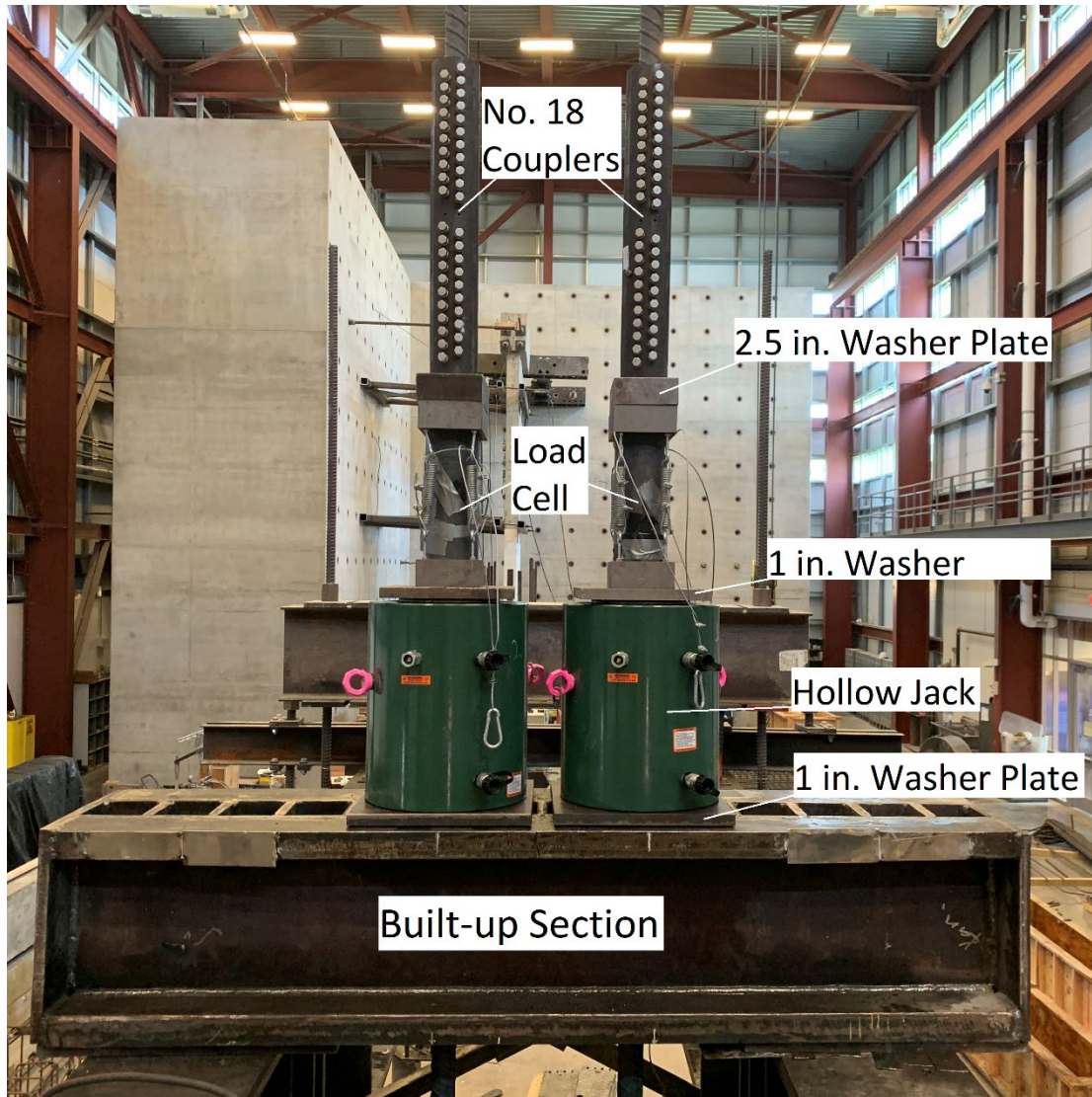


Figure 2.21 Alternative test setup used in widely-spaced No. 18 bar specimens

2.3.3 Bearing Plates

To represent the compression region a beam at the face of a column with depth of the neutral axis c , 1-in. thick by 48-in. long steel plates were placed between the specimen and each of the two W24 \times 279 bearing members, as shown in Figure 2.16. Plates with 6, 9, and 12 in.

widths were used when the calculated neutral axis depth was $c \leq 6$ in., $6 \text{ in.} < c \leq 9$ in., and $9 \text{ in.} < c \leq 12$ in., respectively. Based on the dimensional proportions for No. 14 or No. 18 bar setup, the locations of the bearing plates on the front face of the specimen were marked. The plates were then placed at those locations. Hydrostone was used between the plates and concrete surface to ensure plates are set in place level in both directions. The reaction frame is placed on the bearing plates.

2.3.4 Bar Displacement Measurement

The displacement of each test bar relative to the front face of the column was measured using linear variable differential transformers (LVDTs). The LVDTs, shown in Figure 2.22, were attached to 2×4 lumber. The lumber was then clamped to a stiffener on the lower bearing member between its flanges. A $3/8$ -in. solid square steel rod with a $1/8$ -in. thick plate bolted to one end and a steel tube welded to the other end was used. The LVDTs were in contact with the flat plate during the test. Two $3/4$ -in. nuts were welded to the tube so that the tube could be secured on the test bar by tightening the bolts against the bars. The LVDTs were connected to a data acquisition system (DAQ) during the test.



Figure 2.22 Setup for using the LVDTs

2.3.5 Load Cells

Five load cells were built and calibrated to measure the applied force on the test bars during the test. The same load cells were used for both No. 14 and No. 18 bars. The nominal capacity of load cells was 600 kips. The load cells consisted of a steel pipe with two 2.5-in. thick steel plates on top and bottom of the pipe, as shown in Figure 2.23. The pipe was connected to the plates using a spring and eye bolt at the corner of each plate. The 2.5-in. thick plates were dimensioned so that test bars could be spaced at 6 in. on-center without interfering with each other. Four 350-ohm strain gauges were installed on the pipe at midheight in a full bridge, with two gauges orienting parallel and two gauges perpendicular to the loading direction. The gauges were alternated at 90° intervals around the pipe.



Figure 2.23 Load cell for No. 14 and No. 18 bars

2.3.6 Testing Procedure

A more detailed, step-by-step procedure for placement of specimens and the reaction frame for testing is provided in the report by Blessent et al. (2020). In summary, the concrete blocks were placed in position with respect to holes in the strong floor. The location of the blocks depended on

the bar size, since they would be placed below the bearing members, as shown in Figures 2.16 and 2.18 (the location of bearing members was a function of bar size, Figure 2.4). The location of bearing plates and contact points with the concrete blocks were marked on the specimen, which was then lifted and placed on the blocks. Hydrostone was used between the specimen and the steel plates on the blocks. The bearing plates were then seated and leveled on the specimen using hydrostone. The reaction frame assembly, consisting of the two bearing members, two columns, guides, hydraulic jacks, lower tension member (excluding the bottom set of channels), and four corner anchors, was lifted and placed on top of the specimen, so the bearing members were centered and aligned on the bearing plates. After placement, the reaction frame was secured in place by tightening the corner anchor rods to the strong floor using a washer and nut above and below the strong floor. The nuts attaching the anchors to the reaction frame were then loosened slightly to avoid applying load to the specimen through them.

The LVDT bearing plate attachments were then placed on each test bar. The built-up section was then lifted and placed across the 740-ton jacks, with the test bars passing through the designated openings. The 1-in. washer plates, load cells, 2.5-in. washer plates, and the couplers were placed on each test bar. The screws on the couplers were then tightened using an impact wrench in accordance with the manufacturer guidelines. For the No. 18 bars, final tightening was performed using a torque meter to ensure that every screw had reached the target torque. The bottom set of channels of the lower tension member (Bottom Lower Tension Member Channels in Figure 2.16) was lifted using a forklift so that the No. 14 threaded bars passed through the designated holes on the channels. Before the bottom tension member was placed on the back face of the specimen, hydrostone was used between the concrete and steel surface to ensure a level contact area. A nut was then screwed onto each of the No. 14 threaded bars to lock the bottom tension member in place. Hydraulic lines were connected to all four jacks. The lines were labeled, and same lines were used for each jack throughout all tests for consistency and ease of a possible troubleshooting. The assemblies with the LVDTs were clamped in place, as described earlier. The strain gauges, load cells, and LVDTs were connected to the DAQ.

Initially, a trial load equal to 5% of the calculated failure load was applied to check if the system and the apparatus were functioning properly. Once verified, the specimen was loaded in increments, also equal to 5% of the calculated failure load. Cracks were marked and labeled at loads equal to 20, 40, 50, 60, and 70% of the calculated failure load. After marking the cracks at

70% of the estimated failure load, the specimen was covered with a tarp as a safety measure, and then loaded to failure. Photographs were taken each time after the cracks were marked, and after the failure.

2.3.7 Summary of Test Program

Forty-two simulated beam-column joint specimens with No. 11, No. 14 and No. 18 bars were tested, 12 with hooked bars and 30 with headed bars. For the hooked bars, concrete compressive strengths ranged from 6,390 to 15,770 psi and bar stress at failure ranged from 87,300 to 130,600 psi. For the headed bars, concrete compressive strengths ranged from 5,310 to 16,210 psi. and bar stresses at failure ranged from 54,900 to 148,300 psi. Table 2.5 presents the test program and the main test parameters. Table 2.6 gives a summary of the test program and number of specimens tested with each bar.

Table 2.5 Test program and the main parameters for No. 11, No. 14, and No. 18 bar specimens

ID ^[1]	Bar size	<i>n</i>	<i>c_{ch}</i> in.	<i>c_{ch}/d_b</i>	Bar spacing ^[2]	<i>f'_c</i> ksi	<i>ℓ_{eh}</i> in.	$\frac{A_{tl}/A_{hs}}{A_{th}/A_{hs}}$	<i>c_{so}</i> in.	L. C.
11-1	No. 11	2	14.1	10.0	Wide	16	18.5	0	3.5	B
11-2	No. 11	2	14.1	10.0	Wide	16	18.5	0.282	3.5	B
14-2	No. 14	2	18	10.6	Wide	15	20.5	0.267	3.5	A
14-3	No. 14	2	18	10.6	Wide	7	31.9	0	3.5	B
14-4	No. 14	2	18	10.6	Wide	7	31.9	0.267	3.5	A
14-15	No. 14	2	18	10.6	Wide	7	22.7	0	3.5	B
14-16	No. 14	2	18	10.6	Wide	7	22.7	0.178	3.5	A
14-16A ^[3]	No. 14	2	18	10.6	Wide	7	22.7	0.178	3.5	A
14-1A	No. 14	2	18	10.6	Wide	15	22.7	0	3.5	B
14-2A	No. 14	2	18	10.6	Wide	15	22.7	0.267	3.5	B
14-16B	No. 14	2	18	10.6	Wide	7	22.7	0.178	3.5	B
14-16C	No. 14	2	18	10.6	Wide	7	22.7	0.356	3.5	B
14-16D ^[4]	No. 14	2	18	10.6	Wide	7	22.7	0.827	3.5	A
14-16E ^[4]	No. 14	2	18	10.6	Wide	7	22.7	0.551	3.5	A
14-16F ^[5]	No. 14	2	18	10.6	Wide	7	22.7	0.551	3.5	A
14-17 ^{[5][6]}	No. 14	2	12	7.1	Close	7	22.7	0.551	6.5	A
14-5	No. 14	3	6	3.5	Close	7	22.7	0.178	3.5	B
14-6	No. 14	3	6	3.5	Close	7	22.7	0.276	3.5	B
14-7	No. 14	3	6	3.5	Close	7	31.9	0	3.5	B
14-8	No. 14	3	6	3.5	Close	7	31.9	0.276	3.5	B
14-9	No. 14	3	6	3.5	Close	12	22.7	0.276	3.5	B
14-10 ^[4]	No. 14	3	6	3.5	Close	7	22.7	0.551	3.5	A
H14-1	No. 14	2	18	10.6	Wide	15	26.6	0	3.5	A
H14-2	No. 14	2	18	10.6	Wide	15	26.6	0.267	3.5	A
H14-3	No. 14	2	18	10.6	Wide	7	35.8	0	3.5	A
H14-4	No. 14	2	18	10.6	Wide	7	35.8	0.267	3.5	A

H14-15	No. 14	2	18	10.6	Wide	7	26.6	0	3.5	A
H14-16	No. 14	2	18	10.6	Wide	7	26.6	0.178	3.5	A
H14-7	No. 14	3	6	3.5	Close	6	35.8	0	3.5	A
H14-8	No. 14	3	6	3.5	Close	6	35.8	0.276	3.5	A
18-1	No. 18	2	18	8.0	Wide	7	31.1	0.543	3.5	A
18-2	No. 18	2	18	8.0	Wide	15	27.8	0.543	3.5	A
18-3	No. 18	2	18	8.0	Wide	7	30.6	0.233	3.5	B
18-4	No. 18	2	18	8.0	Wide	7	30.6	0.465	3.5	B
18-5 ^[6]	No. 18	2	12	5.3	Close	7	30.9	0.543	6.5	A
18-6 ^[6]	No. 18	2	12	5.3	Close	15	27.8	0.543	6.5	A
18-7 ^[4] [6]	No. 18	3	6	2.7	Close	7	30.9	0.543	6.5	A
18-8 ^[5] [6]	No. 18	3	6	2.7	Close	7	27.8	0.543	6.5	A
H18-1	No. 18	2	18	8.0	Wide	16	28.6	0.233	3.5	A
H18-2	No. 18	2	18	8.0	Wide	16	28.6	0.465	3.5	A
H18-3	No. 18	2	18	8.0	Wide	7	37.8	0.233	3.5	A
H18-4	No. 18	2	18	8.0	Wide	7	37.8	0.465	3.5	A

- [1] Designations starting with “H” denote a hooked bar specimen
- [2] Widely-spaced bars: $c_{ch}/d_b \geq 8.0$ (6.0 for hooks), Closely-spaced bars: $c_{ch}/d_b < 8.0$ (6.0 for hooks)
- [3] Specimen had an additional No. 11 longitudinal bar on both sides, 2 in. from the bearing face on the head
- [4] Double overlapping No. 5 ties were used, refer to Figure 2.5
- [5] Double No. 5 ties were used
- [6] Specimen had an increased side cover of 6.5 in.
- n*** Number of bars
- c_{ch}*** Center-to-center bar spacing
- f'_c*** Target concrete compressive strength
- ℓ_{eh}*** Nominal embedment length
- A_{tt}*** Total area of tie legs within $9.5d_b$ from the centerline of headed bars
- A_{th}*** Total area of tie legs within $9.5d_b$ from the centerline of hooked bars
- A_{hs}*** Total area of headed or hooked bars being developed
- c_{so}*** Side cover to the headed or hooked bar
- L. C.** Loading condition, refer to Section 2.3.2

Table 2.6 Summary of the test program and number of specimens

Bar size	Confining reinforcement	Number of headed bar specimens		Number of hooked bar specimens	
		Two heads	Three heads	Two hooks	Three hooks
No. 11	Without	1	0	0	0
	With	1	0	0	0
No. 14	Without	3	1	3	1
	With	11	5	3	1
No. 18	Without	0	0	0	0
	With	6	2	4	0

CHAPTER 3: TEST RESULTS

In this chapter, the general behavior of the simulated beam-column joint specimens with No. 14 and No. 18 hooked bars and the No. 11, No. 14, and No. 18 headed bars is discussed. Cracking patterns, failure modes, and stress/strain development in test bars and parallel ties in the joint region as observed during the tests are presented. Anchorage strengths of the 42 specimens tested are tabulated at the end of the chapter. The effects on anchorage strength of key parameters, including bar size and spacing, concrete compressive strength, development length, confining reinforcement in the joint region, and side cover are discussed in Chapter 4 and 5.

3.1 CRACKING PATTERNS

3.1.1 Hooked Bars

Cracks propagated in patterns that were similar to those observed for No. 5 through No. 11 hooked bars by Sperry et al. (2015b, 2017a). Examples are shown in Figures 3.1 and 3.2. Cracking initiated on the front face of the specimen (top of the specimen as tested) adjacent to the hooked bars (Figure 3.1a) and propagated towards the sides of the specimens (Figure 3.2a). As the force in the hooked bar increased, cracks on the sides of the specimens grew along the straight portion of the bars and additional cracks branched towards the upper and lower bearing members (Figure 3.2b and 3.2c). On the front face, the cracks continued to extend, radiating from the hooked bars (Figure 3.1b). At higher loads, the cracks on the sides of the specimens continued to propagate and branch towards the bearing members, resulting in a cone-shaped pattern (Figure 3.2d). As shown in Figure 3.2d, diagonal cracks extended through the joint to the lower bearing member, while the inclined cracks outside the joint reached the upper bearing member. On the front face, the cracks that radiated from the hooked bars connected to each other and portions of concrete were pulled out resulting in local damage to the concrete near the surface (Figure 3.1c).

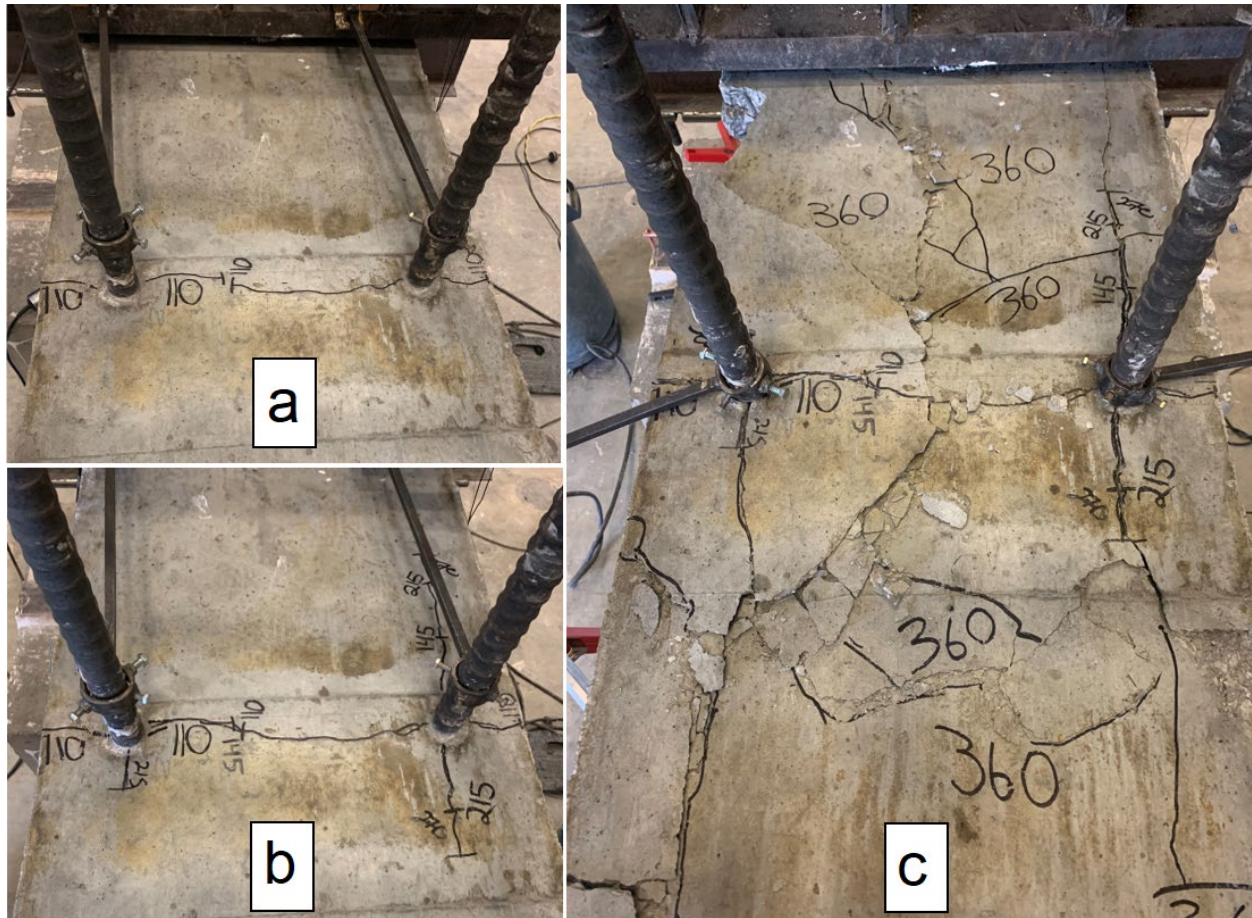


Figure 3.1 Example of cracking pattern in hooked bar specimens (front face, specimen H14-15): (a) Horizontal cracks likely initiating due to bar slip, (b) Cracks radiating from the hooked bars, and (c) Cracks radiated from the hooked bars connected to each other along with local concrete damage

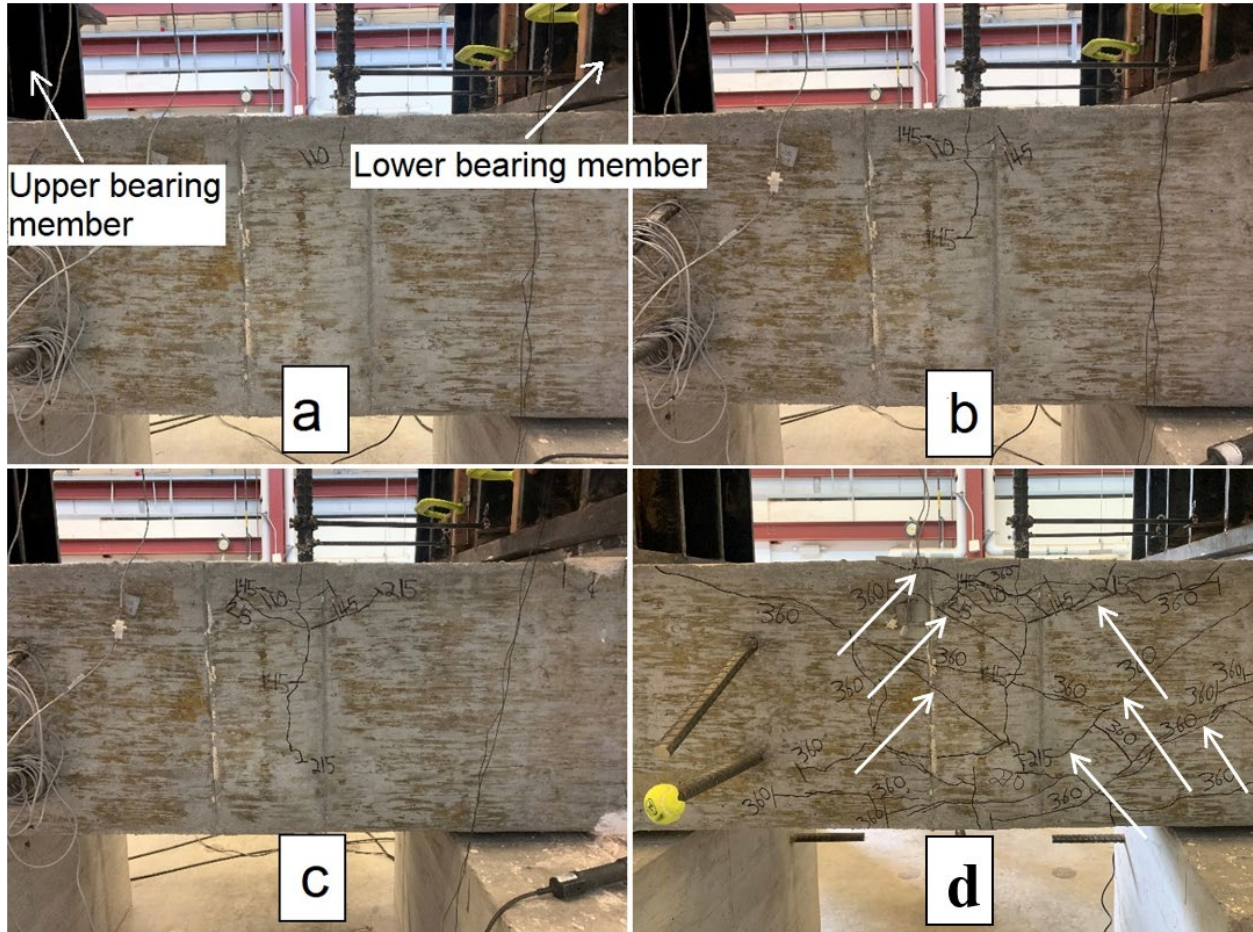


Figure 3.2 Example of cracking pattern in hooked bar specimens (side face, specimen H14-15): (a) Vertical crack likely initiating due to bar slip, (b) and (c) Cracks propagating and branching towards upper and lower bearing members, (d) Cone-shaped cracking pattern near failure (see arrows.)

3.1.2 Headed Bars

Headed bar specimens had cracking patterns similar to those observed for hooked bars. The side and top faces of specimen 18-3 are shown at the same load stages in Figures 3.3 and 3.4, illustrating the formation of cracks. Initially, a crack started to form on the front face adjacent to and between the headed bars (Figure 3.4a) and extended to the sides of the specimen, propagating along the bars (Figures 3.3a and 3.4a). This initial crack was likely due to the slip of the bars during the first stages of loading. As shown in Figure 3.4a, the cracks on the front face eventually radiated from the bars (Figure 3.4e) as the load increased. On the side faces, the crack in line with the bars continued to develop towards the head, while new cracks started to form, branching from this crack (Figure 3.3b). With an increase in load, a large diagonal crack appeared on the sides that extended

from the bearing face of the head to the edge of the nearest bearing member (compression region of the simulated beam) from one side of the joint to the other, as shown in Figure 3.3c. The formation of the first diagonal crack in the joint was often sudden and accompanied by a loud noise and a slight drop in the applied load. On the front face, more cracks parallel to the original crack between the bars formed across the column width above and below the level of headed bars (Figure 3.4b and 3.4c). Further increases in the load resulted in the formation of new diagonal cracks within the joint, and cracks branching towards upper and lower bearing members in a cone-shaped pattern (Figure 3.3d and 3.3e). The diagonal cracks in the joint usually extended parallel to the back face of the member towards the top of the column, passing close to the bearing face of the head (see dashed lines in Figures 3.3c-f). On the front face of the column, new cracks, primarily in the longitudinal direction, branched from the existing cracks that had formed across the column width, as shown in Figure 3.4d.

Near failure, the cracks grew wider, and the number of cone-shaped cracks on the sides branching towards bearing members increased (Figure 3.3f). The extension of diagonal cracks along the back face and towards the top of the column continued, and these cracks also extended diagonally towards the upper bearing member (bottom left corner of Figure 3.3f). On the front face of the specimen, the cracks branched further and connected to each other. The front face cracks extended towards the sides and connected to the cone-shaped cracks on both sides. The amount of cracking was mainly governed by the amount of confining reinforcement in the joint region, as specimens with parallel ties (or more parallel ties) generally underwent more deformation before failure and developed more cracks than specimens with no parallel ties or with a lower level of confinement, which failed in a more brittle fashion with fewer cracks at a lower force.

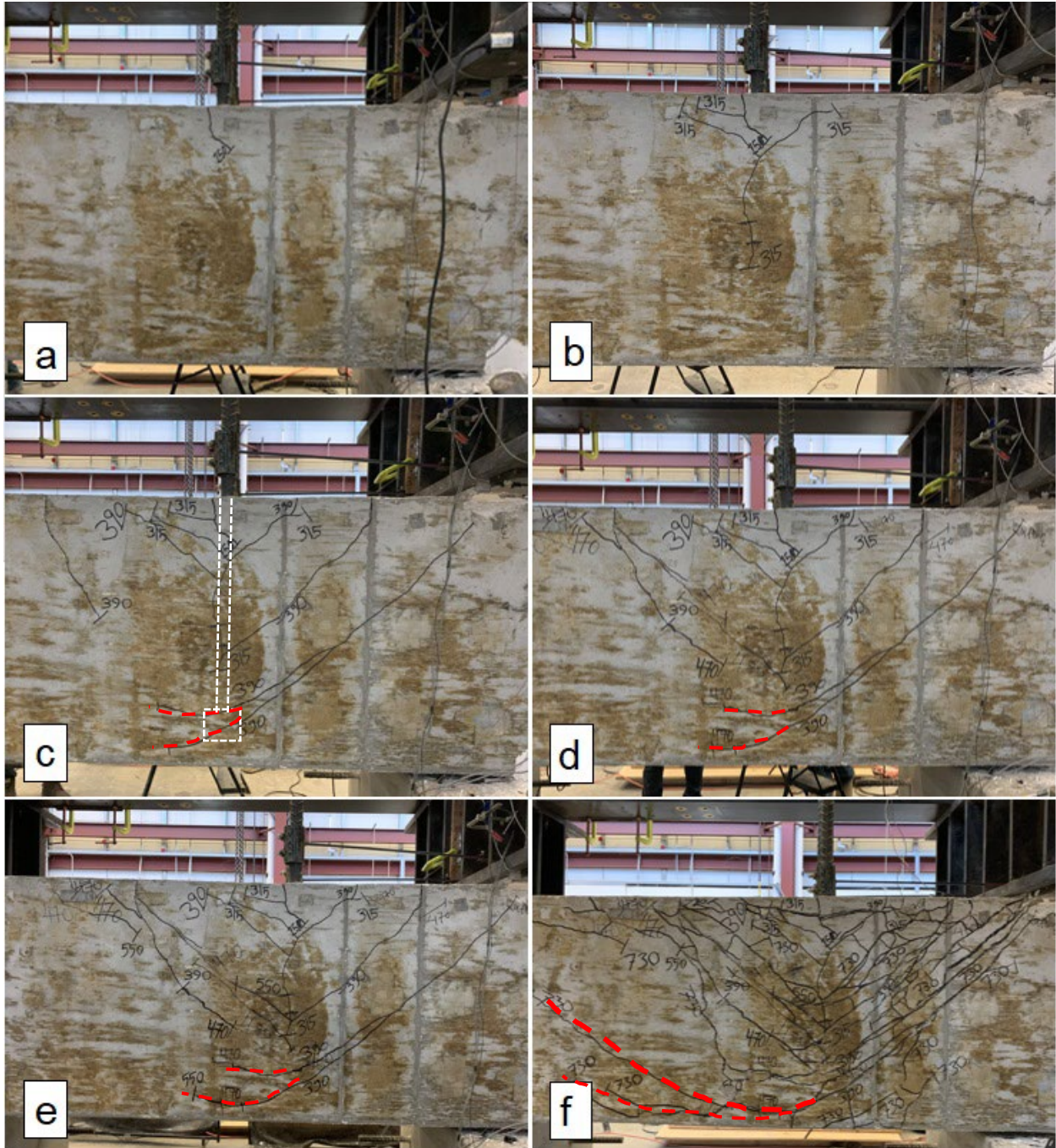


Figure 3.3 Example of cracking pattern in headed bar specimens (side face, specimen 18-3): (a) Vertical crack likely initiating due to bar slip, (b) Cracks branching towards bearing members, (c) First diagonal crack due to shear in joint, (d) and (e) Cracks propagating throughout the joint, (f) Cone-shaped cracking pattern after failure. (**Note:** Extension of diagonal cracks along the back face of the specimen towards the top of the column are marked by dashed lines.)

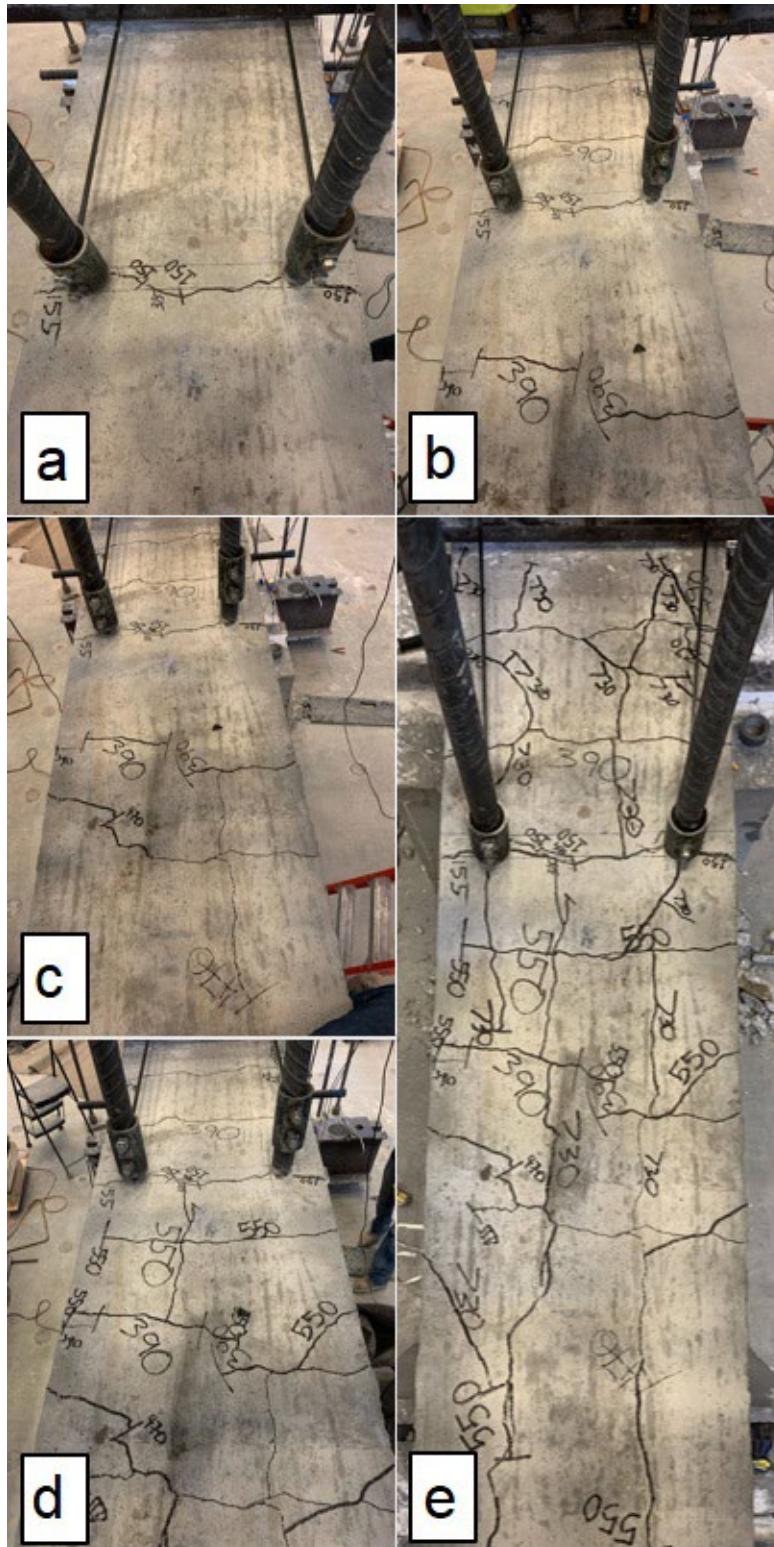


Figure 3.4 Example of cracking pattern in headed bar specimens (top face, specimen 18-3): (a) Crack between bars likely initiating due to bar slip, (b) Cracks branching towards bearing members, (c) First diagonal crack due to shear in joint, (d) and (e) Cracks propagating throughout the joint

3.2 FAILURE MODES

In this section, the different types of anchorage failure are discussed. For both hooked and headed bars, specimens showed two primary failure types, namely concrete breakout and side splitting. A few headed bar specimens failed in shear (not anchorage). In some specimens, a secondary failure mode was also observed.

3.2.1 Hooked Bars

As observed in previous research on No. 5 through No. 11 hooked bars (Sperry et al. 2015, Ajaam et al. 2017), two primary failure modes were observed in the specimens, concrete breakout and side splitting. A concrete breakout failure, accompanied by tail kickout, is shown in Figure 3.5. Concrete breakout, the only failure mode observed in seven out of the 12 specimens (four No. 14 bar and three No. 18 bar specimens), is characterized by a mass of concrete being pulled out along with the hooked bar from the front face of the specimen. As shown in Figure 3.5, the failure surface is cone-shaped, with spalling of concrete on the front face at failure. Side splitting is usually sudden and more explosive in nature than breakout failure and is marked by the side cover on the hooked bar separating from the column, as shown in Figure 3.6. Side splitting was observed as the only failure mode in three out of the 12 specimens (two No. 14 bar and one No. 18 bar specimen), while two specimens exhibited breakout on one hook and side splitting on the other.

The likelihood of a given failure mode depended on the amount of confinement in the joint. Three out of the four specimens without confining reinforcement in the joint region (all with No. 14 hooked bars) exhibited a breakout failure, while the other specimen without confining reinforcement had a breakout failure on one hook and a side-splitting failure on the other. Of the eight specimens with confining reinforcement, three (H14-4, H14-8, and H18-2) exhibited a side-splitting failure, four experienced a breakout failure, and one had a breakout failure on one hook and side-splitting failure on the other.

The effect of bar spacing on the failure mode was less clear. Of the two specimens with three closely-spaced bars, H14-7 (without confining reinforcement) exhibited a breakout failure, while the companion specimen H14-8 (with confining reinforcement) had a side-splitting failure. Of the ten specimens with widely spaced bars, six exhibited a breakout failure, two exhibited a side-splitting failure, and two (H14-2 and H14-3), experienced a breakout failure on one hook and side splitting on the other hook. In the latter case, it appeared that the bars acted independently



Figure 3.6 Side view of a side-splitting failure for hooked bars (H14-8)

3.2.2 Headed Bars

As observed for the hooked bar specimens, the two main anchorage failure types observed in headed bars were concrete breakout and side splitting, with the latter referred to as side-face blowout in some studies (Chun et al. 2017, Chun and Lee 2019, Sim and Chun 2022a, 2022b). The failure types generally matched those observed by Shao et al. (2016) and Ghimire et al. (2018) for No. 11 and smaller bars. Breakout or side-splitting failures were occasionally accompanied by a compression failure in the joint region along a line between the head and the lower bearing member. Four specimens (all with No. 14 bars) did not exhibit an anchorage failure. These specimens have been excluded from the analysis and are discussed later in this section.

The definitions of concrete breakout and side splitting for headed bars is similar to hooked bars. Breakout occurs when the concrete mass in front of the head separates from the front face of the column as the bar was being pulled out. Side splitting occurs when the movement of the head causes the concrete side cover around the head to spall and separate, usually blowing out in a sudden and explosive way, exposing the head.

Concrete breakout was the primary failure mode in six out of 20 No. 14 bar specimens and in two out of eight No. 18 specimens. Examples are shown in Figure 3.7. A cone-shaped failure

surface was observed in these specimens, characterized by diagonal cracks in the joint region extending beyond the joint, passing the location of the head and moving along the back face of the column in the form of splitting cracks (top and bottom images in Figure 3.7), or moving diagonally towards the upper bearing member (top image in Figure 3.7).

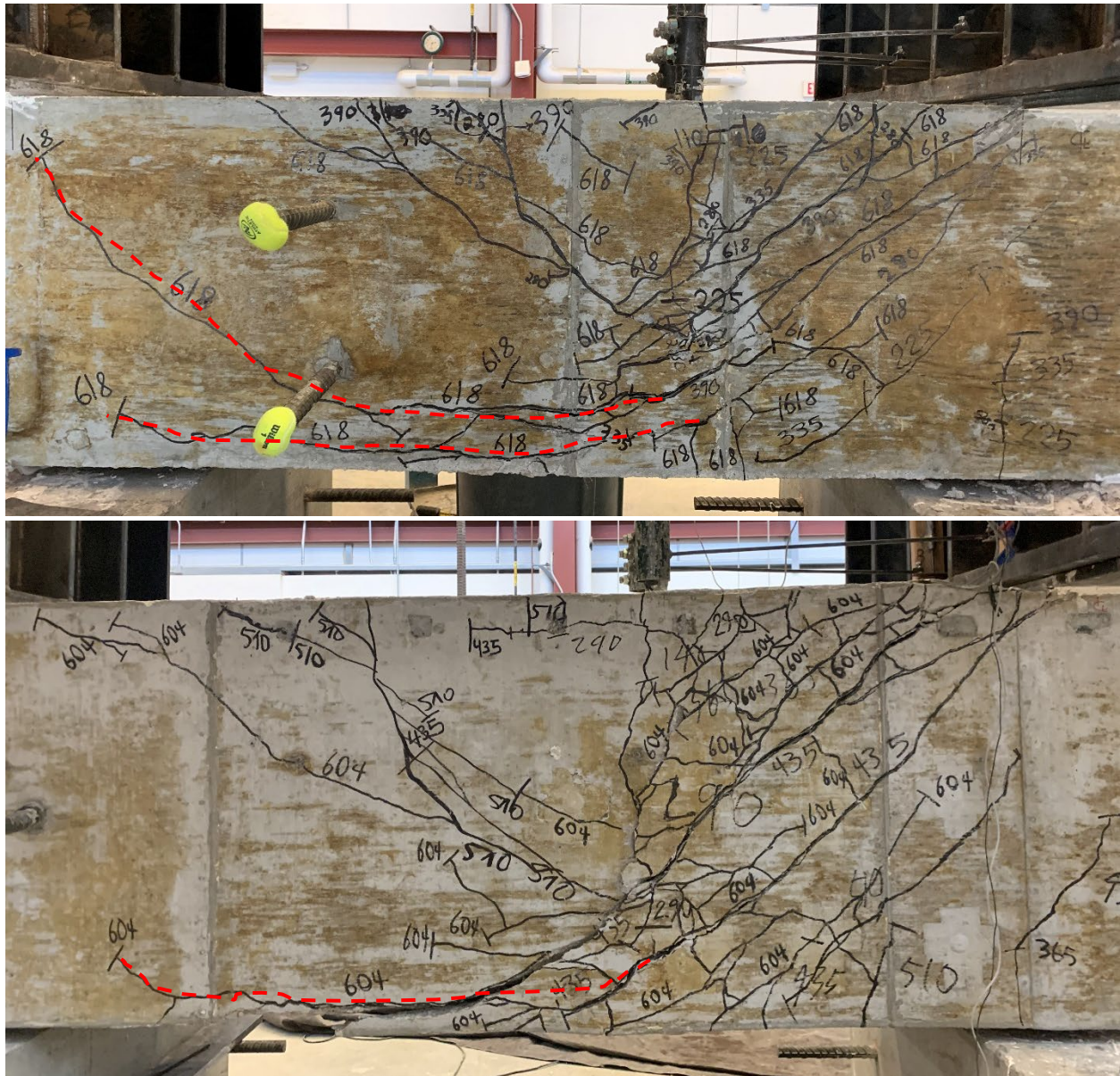


Figure 3.7 Primarily concrete breakout failure (top: specimen 14-10, bottom: specimen 18-5).
(Note: Dashed lines highlight the cracks extending beyond the joint and along the back face of the column or towards the upper bearing member)

In one No. 11 bar specimen, six out of the 20 No. 14 bar specimens, and three out of the eight No. 18 bar specimens, failure was primarily due to side splitting, as shown in Figure 3.8. In specimens failing primarily due to side splitting, the cracks extending beyond the head along the

back face of the column and diagonally towards the top of the column (highlighted by dashed lines in Figures 3.3 and 3.7) did not form, a key difference between side splitting and concrete breakout failures. A failure primarily involving side-splitting was more likely to occur in specimens with a higher number of parallel ties in the joint region.

In one No. 11 bar specimen, four out of 20 No. 14 bar specimens, and three out of eight No. 18 bar specimens, the failure mode was a combination of concrete breakout and side splitting, as shown in Figure 3.9.

In some specimens, breakout or side splitting occurred along with a compression failure within the joint (from the bearing face of the head to the bearing member representing the compression region of the simulated beam, as shown in Figure 1.27). A compression failure, which was often explosive, was observed in five out of 20 No. 14 bar specimens and in four out of eight No. 18 bar specimens, including four out of the six specimens cast with high-strength concrete ($> 12,000$ psi), and was more likely to occur in specimens with a higher level of confining reinforcement in the joint region. An example of concrete breakout accompanied by compressive strut failure is shown in Figure 3.10.



Figure 3.8 Primarily side-splitting failure (left: specimen 14-3, right: specimen 18-4)



Figure 3.9 Combination of concrete breakout and side splitting (specimen 14-15)



Figure 3.10 Concrete breakout accompanied by side splitting and compression failure of concrete between bearing face of the head and lower bearing member (specimen 14-16B)

As described earlier, four headed bar specimens did not exhibit an anchorage failure but, rather, failed at a relatively low load with a diagonal crack between bearing face of the head and lower bearing member that was reminiscent of what might occur due to a shear failure and is referred to here as a “shear-like” failure (Figure 3.11). Three out of the four specimens had relatively low levels of confining reinforcement (two specimens with A_{tf}/A_{hs} of 0.178, namely 14-16 and 14-16A, and one with A_{tf}/A_{hs} of 0.267, specimen 14-2) and were tested under loading condition A (joint shear equal to 80% of the force applied to bars). The fourth specimen with a

shear-like failure, specimen 14-1A, contained no confining reinforcement and was tested under loading condition B (joint shear ~69% of the force applied to bars).

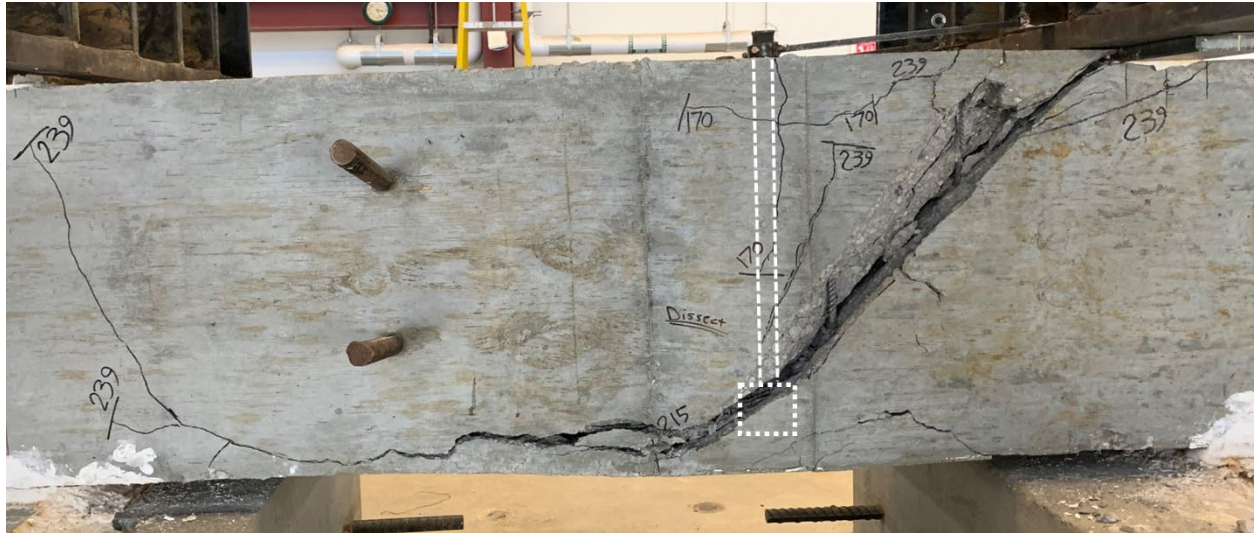


Figure 3.11 Shear-like failure in headed-bar specimen 14-16. (Note: The specimen shows no indication of a breakout or side-splitting failure.)

Shear-like failures occurred only in the headed bar specimens. The following characteristics were observed in these four specimens:

- The first diagonal crack in the joint region appeared at a force at or above 75% of the failure load with the specimen failing shortly after the formation of the crack.
- The diagonal crack extended beyond the joint, passing through the location of the head in the form of a splitting crack along the back face of the column.
- After formation of the diagonal crack, no more cone-shaped cracks, such as shown in Figures 3.2 and 3.3, formed.
- There was little to no damage on the front face of the columns around the headed bars.

The joint shear stress is worth analyzing for these four specimens. The shear force in the joint, V_J , depends on the loading condition, as discussed before. Under loading condition A, $V_J = 0.8T$, and under loading condition B, $V_J \approx 0.69T$. The joint shear stress is then V_J/bh , where b and h are column width and height, respectively. The joint shear stress is normalized with respect to $\sqrt{f_{cm}}$ for analysis. The values of $V_J/(bh\sqrt{f_{cm}})$ were 3.5, 3.5, 4.3, and 2.6 for specimens 14-2, 14-16, 14-16A, and 14-1A, respectively. These values are significantly lower than reflected in Table 15.4.2.3 of Chapter 15 in ACI 318-19 for a continuous column with a non-continuous beam that is not confined by transverse beams (which is the case in an external beam-column joint). For that

condition, Table 15.4.2.3 requires a nominal joint shear strength, V_n , to be $15bh\sqrt{f_{cm}}$, which is 3.5 to 5.7 times greater than obtained in the four specimens that exhibited a shear-like failure. This indicates that the shear-like failures were not strength-related and most likely the result of detailing issues. This point is further discussed in Section 5.5.1.

For two No. 14 headed bars specimens with widely-spaced bars (14-3 and 14-16D), one head failed first and loading continued until the failure of the second head. The load difference between the two bars was 26.2 and 29.1 kips, corresponding to a bar stress of 11.6 and 12.9 ksi, respectively. As in the similar hooked bar specimens, this difference in bar stress was less than 10% of the average bar stress at failure (8.6% and 10.0% in 14-3 and 14-16D, respectively). Although the widely-spaced bars failed independently, they were not treated as separate tests and the failure load was calculated as the average of the maximum load per bar. In all other specimens, the failure load is taken as the total peak load divided by the number of bars. The individual bar forces are reported in Appendix C2.

For specimens exhibiting an anchorage failure, no direct relationship was found between the type of failure and the anchorage strength. Tables 3.1 and 3.2 summarize the number of specimens for each failure type for, respectively, the hooked and headed bar specimens.

Table 3.1 Summary of hooked bar specimens with different failure types

Failure type	No. 14	No. 18	Total
CB ¹	4	3	7
SS ²	2	1	3
CB/SS ³	2	0	2
SF ⁴	0	0	0

¹ Primarily concrete breakout

² Primarily side splitting

³ Concrete breakout on one side and side splitting on the other side

⁴ Shear-like failure

Table 3.2 Summary of headed bar specimens with different failure types

Failure type	No. 11	No. 14	No. 18	Total
CB ¹	0	6	2	8
SS ²	1	6	3	10
CB+SS ³	1	4	3	8
SF ⁴	0	4	0	4

¹ Primarily concrete breakout

² Primarily side splitting

³ Combination of breakout and side splitting

⁴ Shear-like failure

3.3 STRAIN DEVELOPED IN REINFORCEMENT

In this section, the strain developed in the ties and the hooked and headed bars obtained from strain gauges during testing is discussed. As described in Section 2.2.5, strain gauges were mounted on the two parallel ties above the joint region (labeled S1 and S2) and on all ties within the joint region (labeled S3, S4, etc., in specimens with joint confining reinforcement). The gauges were installed at the center of each tie leg. Two strain gauges were mounted on one hooked or headed bar per specimen. On hooked bars, the first gauge was mounted just before the bend in the tail (labeled T1), and the second gauge 1 in. from the column front face (labeled T2). On headed bars, strain gauge T1 was mounted 1.5 in. from the bearing face of the head, and T2 was mounted 1 in. from the column front face. The strain gauge configuration is shown in Figure 2.14. Not all specimens provided good strain gauge readings due to damage to the gauges during concrete placement. The specimens selected for analysis in this section had all strain gauges working, providing good readings throughout the test.

3.3.1 Ties

In general, the strain development in the ties in specimens with confining reinforcement in the joint region was similar for hooked and headed bars. While the strain developed in each tie differed for each specimen, the overall load-strain curves showed similar patterns. The load-strain curves for the ties in hooked bar specimen H14-2 and headed bar specimen 14-6 are shown in Figure 3.12. Specimen H14-2 had two widely-spaced No. 14 hooked bars cast in high-strength concrete, with five No. 4 ties within the joint region. Specimen 14-6 had three closely-spaced headed bars cast in normal-strength concrete, with five No. 5 ties in the joint region.

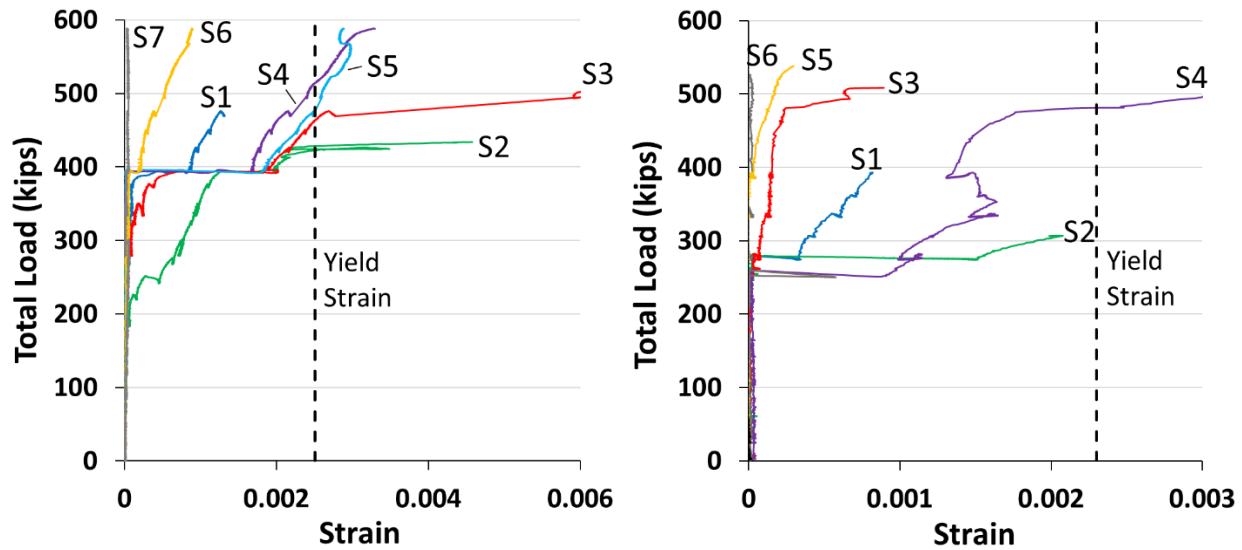


Figure 3.12 Examples of strain developed in parallel ties in hooked bar specimen H14-2 (left) and headed bar specimen 14-6 (right)

As shown in Figure 3.12, the strains developed in the ties for hooked and headed bar specimens were a function of their location. For hooked bar specimen H14-2, the ties just above and below the bars (S2 and S3, respectively) were the first ties to show a noticeable increase in strain. Up to about 200 kips, minimal strain developed in the ties. At a load close to 200 kips, S2 (the tie just above the hooked bars) started to show an increase in strain as the first diagonal crack appeared in the joint region. As the load increased to 350 kips, additional ties began to exhibit increases in strain as more diagonal cracks started to branch out from existing cracks above and below the joint. The increase in strain was generally more noticeable in ties closest to the hooked bars. The ties within the joint region (S3, S4, and S5) continued to undergo an increase in strain up to failure of the specimen. At a load of about 390 kips, a loud bang was heard. This marked the onset of a plateau in the load-strain curves of all ties, except for S7, the tie farthest from the hooked bars and closest to the bearing member at the base of the joint. While S6 (the second farthest tie from the bars) started to increase in strain at a load around 390 kips, S7 developed no significant strain during the test. The yield strength of the No. 4 ties was 72,700 psi, corresponding to a yield strain of 0.0025, as marked in Figure 3.12. In this specimen, four ties yielded, starting with S2 and followed by S3, S5, and S4. The peak load for specimen H14-2 was 587.8 kips. Figure 3.13 shows specimen H14-2 after failure along with the location of the ties and the corresponding strain gauges.

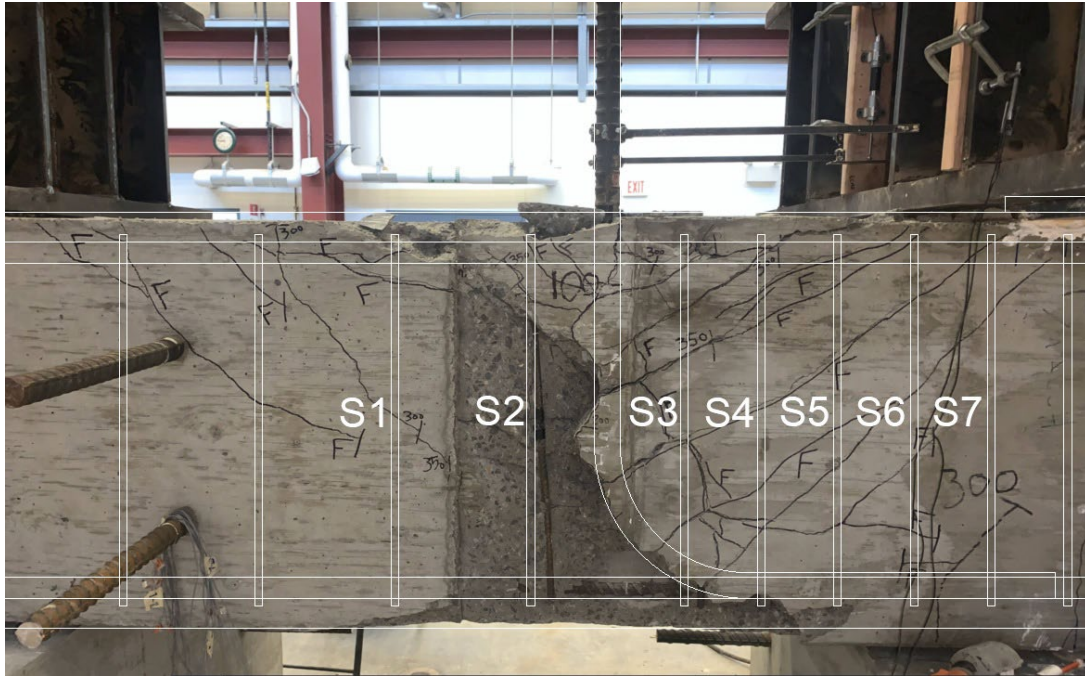


Figure 3.13 Specimens H14-2 at failure showing location of ties and strain gauges

As shown in Figure 3.12 for headed bar specimen 14-6, no strain development was observed up to a load of about 250 kips (only cracks in the plane of the headed bars, likely due to initial bar slip, had formed up to this point). At a load of about 255 kips, a loud pop was heard, coinciding with the formation of the first large diagonal crack in the joint, along with another diagonal crack above the joint. This was the onset of an increase in strain in all ties, except for the ties farthest from the headed bar, S5 and S6. At this point, the ties crossing the first diagonal cracks (S1, S2, S3, and S4, as shown in Figure 3.14 with the cracks marked at 280 kips) exhibited a sudden increase in strain, with S1, S2, and S4 almost immediately reaching a plateau in the load-strain curve. The noticeable increase in the strain in the ties arresting the first diagonal crack was observed in all specimens. The diagonal cracks passed close to the midheight of ties with strain gauges S2 and S4, which is likely the reason these gauges exhibited high strain. Strain gauge S2 indicated that the strain was close to yield at a load of 278 kips but provided no additional data at higher loads. S4 was the only tie in this specimen with an intact strain gage that yielded at a load close to failure. The tie just below the headed bars in the joint region, S3, did not have a plateau and continued showing a gradual increase in strain until a load of about 480 kips (failure load = 538.5 kips). Similar to hooked bar specimen H14-2, the ties farthest from the headed bars and closest to or in the compression region within the joint (S6 and S7) showed almost no strain development.



Figure 3.14 Parallel ties trapping the first diagonal cracks and their strain gauge labels in the headed bar specimen 14-6

These observations indicate that the ties closest to the hooked or headed bars were effective in arresting cracks and contributing to anchorage strength, as previously established by Sperry et al. (2015b) and Shao et al. (2016). In addition, by looking at the data for the specimens with strain gauges that provided readings throughout the test, the ties closest to the hooked or headed bars yielded in all cases (11 No. 14 headed bar specimens, all No. 18 headed bar specimens, 4 No. 14 hooked bar specimens, and 3 No. 18 hooked bar specimens). More specifically, the tie placed immediately below the bars (corresponding to strain gauge S3 in Figures 3.13 and 3.14) yielded in most cases, followed by the tie placed immediately above the bars (corresponding to strain gauge S2). In a few cases, ties corresponding to gauges S4 and S5 yielded as well. For the No. 18 bar specimens, it was generally observed that more ties yielded within the joint than for the No. 14 bar specimens, even those corresponding to strain gauges S6 and S7, indicating that larger bars are more likely to engage greater number of ties within the joint to arrest the large diagonal cracks.

3.3.2 Hooked Bars

As described in Section 2.2.5, two strain gauges were mounted on the hooked bars, T1 just before the bend in the tail of the bar and T2 at 1 in. from the front face of the column. The strain developed in hooked bars in the two locations generally followed a similar trend in all specimens. The load-strain behavior of hooked bars is plotted for specimens H14-2 and H14-15 in Figure 3.15.

The specimens had two widely-spaced No. 14 hooked bars. Specimen H14-2 had five No. 4 ties in the joint region, while H14-15 had none. It should be noted that, as shown in Figure 3.15, gauge T2 in specimen H14-15 stopped working at a load of about 150 kips. However, based on the similar trend observed in all specimens, it is fair to assume that the load-strain response of T2 followed the dashed line drawn.

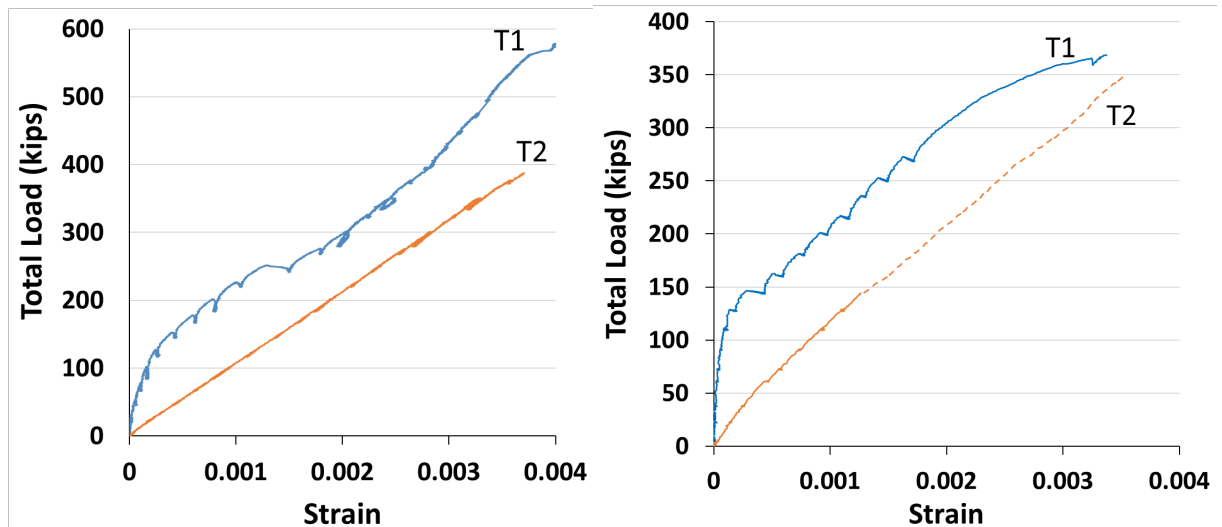


Figure 3.15 Strain developed in one hooked bar in specimens H14-2 (left) and H14-15 (right). (Note: T1 was mounted just before the bend in the tail, and T2 mounted 1 in. from the front face of the column)

As shown in Figure 3.15, the strain developed in the bar 1.5 in. from the column front face (T2) increased almost linearly during testing and was always higher than the strain at the bend (T1). The difference between the strains indirectly represents the force carried by bond along the straight portion of the bar. The strain at the bend increased slowly up to a load of about 100 kips for H14-2 and 150 kips for H14-15, corresponding to the first vertical cracks developing on the sides of the columns. The strain at the bend developed at a much faster rate as the load increased and once the cracks on the sides of the column reached the location of the bend. The strain at the bend continued to increase at a fast rate as the diagonal cracks appeared within the joint, indicating the increased contribution of the tail of the hook in carrying the load, holding the concrete in the joint together and providing anchorage. Due to increased damage on the front face of the column near failure, strain gauge T2 in specimen H14-2 failed at a load about 400 kips but gauge T1 remained functional until failure in both specimens.

3.3.3 Headed Bars

The strains developed in the headed bars (from gauges T1 and T2 as shown in Figure 2.14) are discussed in this section. Overall, the strain development in headed bars at both locations (1.5 in. from the bearing face of the head, T1, and 1 in. from the front face of the column, T2) followed a similar trend in all specimens regardless of bar size or confining reinforcement in the joint region. The load-strain curves for strain gauges T1 and T2 for specimens 14-16C and 18-8 are shown in Figure 3.16. Specimen 14-16C had two widely-spaced No. 14 bars with No. 4 ties in the joint region. Specimen 18-8 had three closely-spaced No. 18 bars with double overlapping No. 5 ties in the joint region.

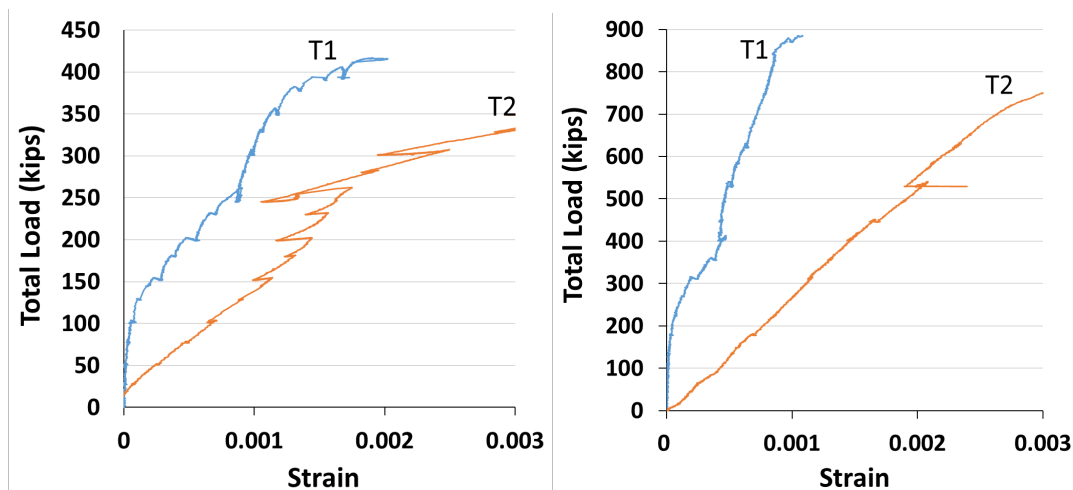


Figure 3.16 Strain developed in one headed bar in specimen 14-16C (left) and 18-8 (right) (Note: T1 was mounted 1.5 in. from the bearing face of the head, and T2 was mounted 1 in. from the column front face)

As shown in Figure 3.16, the strain in the bar 1 in. from the column front face (T2) started to increase almost as soon as the loading initiated and continued to develop throughout the test. At this point, a short crack started to form in the plane of the headed bars on the front face and extending on the sides of the column, likely due to initial bar slip. The strain in the bar 1.5 in. from the bearing face of the head (T1) remained near zero up to a load of about 100 kips in 14-16C and about 200 kips in 18-8. After the cracking initiated on the front face emanating from the bars, the strain near the head in both specimens increased at a faster rate as the vertical crack on the sides extended towards the location of the head. The first large diagonal cracks within and above the joint appeared at about 260 kips in specimen 14-16C and 400 kips in 18-8, accompanied by a small drop (~10 kips) in the load, as shown in Figure 3.16. After this point, the strain in the bar at both

locations continued to increase, at a slower rate near the head in both specimens and at a faster rate at the front face of the column in specimen 14-16C. The strain in the bar near the front face of the column always exceeded the strain near the head. The difference between the strain developed at the two locations provides an indication of the load transferred by the bond along the bar. This difference, however, is not a direct representation of load, since the bars were no longer on the linear portion of the stress-strain curve. The strain developed near the head increased much faster near failure, above 350 kips in 14-16C and 800 kips in 18-8, indicating the increased contribution of the head in carrying the applied force.

Looking at the available data for the headed bar specimens reveals that, at the initial stages of the loading (and in some cases up to about 50% of the failure load), the major portion of the applied force was carried by bond. As shown in Figure 3.16, the head would start to contribute in carrying the load after the initial cracking on the front face (Figure 3.4a) and continue to contribute, but would pick up load at a slower rate than it was by bond. The lower tensile stress near the head may have been due to the wedge of concrete forming on the head as the bar was being pulled out. If T1 had been mounted more than 1 in. from the head, a higher rate of increase in the strain may have resulted.

The difference observed between the contribution by bond and the head in carrying the forces in headed bar specimens seems to be a major distinction from the hooked bar specimens, comparing the plots in Figures 3.15 and 3.16. While both the hook and the head start to engage and provide anchorage after the start of cracking, the portion of the force carried by the hook increases with increasing load, while the portion of the load carried by bond remains nearly constant once cracking has occurred and may even drop off as the failure load is attained. In contrast, the contribution of the head increases at a slower rate than the contribution by bond up to failure based on the reading obtained for gauge locations used in this study.

3.4 ANCHORAGE STRENGTH

The anchorage strengths of the beam-column joint specimens measured in the tests are summarized in Tables 3.3 and 3.4 for the hooked and headed bars, respectively. The tables include the specimen ID (given in Table 2.5), specimen designation (described in Section 2.2.3), number of hooked or headed bars (n), center-to-center spacing between the bars in terms of bar diameter (c_{ch}/d_b), measured concrete compressive strength (f_{cm}), average measured embedment length ($\ell_{eh,avg}$), ratio of effective confining reinforcement in the joint region (A_{tt}/A_{hs} for headed bars or

A_{th}/A_{hs} for hooked bars; described in Figure 1.18), loading condition (discussed in Section 2.3.1), average peak load (T , total applied peak load divided by the number of bars), and failure mode (discussed in Section 3.2). Full details of the specimens are presented in Appendices B2 and C2. Analyses of the hooked and headed bar results are presented in Chapters 4 and 5, respectively.

Table 3.3 Summary of anchorage strength results for hooked bar specimens

ID ^[1]	Designation	n	c_{ch}/d_b	f_{cm} psi	$\ell_{eh,avg}$ in.	A_{th}/A_{hs}	L. C.	T kips	Failure Mode ^[2]
H14-1	(2@10.6)14-15-i-3.5-2-26.6	2	10.6	12,980	27.0	0	A	240.0	CB
H14-2 ^[3]	(2@10.6)14-15-5#4-i-3.5-2-26.6	2	10.6	13,010	24.8	0.267	A	293.9	CB/SS
H14-3 ^[3]	(2@10.6)14-15-i-3.5-2-35.8	2	10.6	8,100	36.7	0	A	279.1	CB/SS
H14-4	(2@10.6)14-15-5#4-i-3.5-2-35.8	2	10.6	7,570	34.9	0.267	A	268.5*	SS
H14-15	(2@10.6)14-7-i-3.5-2-26.6	2	10.6	6,980	26.5	0	A	196.5*	CB
H14-16	(2@10.6)14-7-3#4-i-3.5-2-26.6	2	10.6	6,810	25.9	0.178	A	235.3*	CB
H14-7	(3@3.5)14-6-i-3.5-2-35.8	3	3.5	6,390	36.4	0	A	250.8	CB
H14-8	(3@3.5)14-6-5#4-i-3.5-2-35.8	3	3.5	6,650	36.6	0.276	A	298.2	SS
H18-1	(2@8.0)18-16-6#5-i-3.5-2-26.6	2	8.0	15,310	28.5	0.233	A	358.2	CB
H18-2	(2@8.0)18-16-12#5-i-3.5-2-26.6	2	8.0	15,770	27.0	0.465	A	445	SS
H18-3	(2@8.0)18-7-6#5-i-3.5-2-35.8	2	8.0	7,560	36.5	0.233	A	371.4	CB
H18-4	(2@8.0)18-7-12#5-i-3.5-2-35.8	2	8.0	7,610	36.4	0.465	A	427.9*	CB

- n Number of bars
 c_{ch} Center-to-center bar spacing
 f_{cm} Measured concrete compressive strength
 $\ell_{eh,avg}$ Average measured embedment length
 A_{th} Total area of tie legs within $9.5d_b$ from the centerline of hooked bars larger than No' 8 – this differs from the definition in ACI 318-19
 A_{hs} Total area of headed or hooked bars being developed
L. C. Loading condition, refer to Section 2.3.2
 T Total applied peak load divided by the number of bars
^[1] The first number after “H” denotes the bar size
^[2] CB: Concrete breakout, SS: Side splitting
^[3] One bar had a breakout and the other bar had a side-splitting failure
* Bars failed independently, so T is the average of the maximum force on individual bar. Individual results in Appendix B2

Table 3.4 Summary of anchorage strength results for headed bar specimens

ID ^[1]	Designation	<i>n</i>	<i>c_{ch}/d_b</i>	<i>f_{cm}</i> psi	<i>ℓ_{eh,avg}</i> in.	<i>A_{th}/A_{hs}</i>	L. C.	<i>T</i> kips	Failure Mode ^[2]
11-1	(2@10)11-15-O4.5-i-3.5-3.5-18.25	2	10.0	16,210	18.5	0	B	163.0	CB+SS
11-2	(2@10)11-15-O4.5-7#3-i-3.5-3.5-18.25	2	10.0	15,850	18.5	0.282	B	221.0	SS
14-2	(2@10.6)14-15-B4.2-5#4-i-3.5-3.5-20.5	2	10.6	12,830	20.5	0.267	A	190.6	SF
14-3	(2@10.6)14-7-L4.2-i-3.5-3.5-31.9	2	10.6	8,510	31.8	0	B	303.0*	SS
14-4	(2@10.6)14-7-L4.2-5#4-i-3.5-3.5-31.9	2	10.6	7,700	32.0	0.267	A	333.6	SS
14-15	(2@10.6)14-7-L4.2-i-3.5-3.5-22.7	2	10.6	6,190	22.8	0	B	204.8	CB+SS
14-16	(2@10.6)14-7-L4.2-3#4-i-3.5-3.5-22.7	2	10.6	5,390	22.6	0.178	A	123.6	SF
14-16A ^[3]	(2@10.6)14-7-L4.2-3#4-i-3.5-3.5-22.7	2	10.6	8,350	22.4	0.178	A	186.0	SF
14-1A	(2@10.6)14-15-L4.2-i-3.5-3.5-22.7	2	10.6	12,030	22.4	0	B	160.0	SF
14-2A	(2@10.6)14-15-L4.2-5#4-i-3.5-3.5-22.7	2	10.6	13,750	23.0	0.267	B	248.1	CB
14-16B	(2@10.6)14-7-L4.2-3#4-i-3.5-3.5-22.7	2	10.6	7,500	22.1	0.178	B	191.7	CB+SS
14-16C	(2@10.6)14-7-L4.2-7#4-i-3.5-3.5-22.7	2	10.6	6,470	22.6	0.356	B	229.6	SS
14-16D ^[4]	(2@10.6)14-7-L4.2-10#5-i-3.5-3.5-22.7	2	10.6	6,900	22.9	0.827	A	289.8*	SS
14-16E ^[4]	(2@10.6)14-7-L4.2-6#5-i-3.5-3.5-22.7	2	10.6	6,170	22.4	0.551	A	218.6	SS
14-16F ^[5]	(2@10.6)14-7-L4.2-6#5-i-3.5-3.5-22.7	2	10.6	5,640	22.4	0.551	A	197.8	SS
14-17 ^{[5][6]}	(2@7.1)14-7-L4.2-6#5-i-6.5-3.5-22.7	2	7.1	6,540	22.4	0.551	A	206.7	CB
14-5	(3@3.5)14-7-L4.2-5#4-i-3.5-3.5-22.7	3	3.5	6,830	22.3	0.178	B	181.8	CB
14-6	(3@3.5)14-7-L4.2-5#5-i-3.5-3.5-22.7	3	3.5	6,890	22.4	0.276	B	179.5	CB
14-7	(3@3.5)14-7-L4.2-i-3.5-3.5-31.9	3	3.5	7,080	32.1	0	B	252.1	CB+SS
14-8	(3@3.5)14-7-L4.2-5#5-i-3.5-3.5-31.9	3	3.5	7,100	31.7	0.276	B	274.6	CB+SS
14-9	(3@3.5)14-12-L4.2-5#5-i-3.5-3.5-22.7	3	3.5	11,480	22.1	0.276	B	173.9	CB
14-10 ^[4]	(3@3.5)14-7-L4.2-10#5-i-3.5-3.5-22.7	3	3.5	6,820	22.3	0.551	A	206.6	CB
18-1	(2@8.0)18-7-L4.4-14#5-i-3.5-3.5-31.1	2	8.0	5,750	32.6	0.543	A	322.0	SS
18-2	(2@8.0)18-15-H4.4-14#5-i-3.5-3.5-27.8	2	8.0	11,770	28.4	0.543	A	406.6	CB+SS
18-3	(2@8.0)18-7-O4.3-6#5-i-3.5-3.5-30.6	2	8.0	6,540	30.9	0.233	B	366.5	CB
18-4	(2@8.0)18-7-O4.3-12#5-i-3.5-3.5-30.6	2	8.0	7,200	30.9	0.465	B	380.0	SS
18-5 ^[6]	(2@5.3)18-7-L4.4-14#5-i-6.5-3.5-31.1	2	5.3	5,310	32.5	0.543	A	300.8	CB
18-6 ^[6]	(2@5.3)18-15-H4.4-14#5-i-6.5-3.5-27.8	2	5.3	10,230	28.6	0.543	A	419.8	SS
18-7 ^{[4][6]}	(3@2.7)18-7-L4.4-20#5-i-6.5-3.5-31.1	3	2.7	5,890	32.1	0.543	A	252.1	CB+SS
18-8 ^{[5][6]}	(3@2.7)18-7-L4.4-20#5-i-6.5-3.5-31.1	3	2.7	6,380	32.3	0.543	A	295.3	CB+SS

n Number of bars

c_{ch} Center-to-center bar spacing

f_{cm} Measured concrete compressive strength

ℓ_{eh,avg} Average measured embedment length

A_{th} Total area of tie legs within 9.5*d_b* from the centerline of headed bars larger than No' 8 – this differs from the definition in ACI 318-19

A_{hs} Total area of headed or hooked bars being developed

L. C. Loading condition, refer to Section 2.3.2

T Total applied peak load divided by the number of bars

^[1] The first number in ID denotes the bar size.

^[2] CB: Primarily concrete breakout, SS: Primarily side splitting, CB+SS: Combination of breakout and side splitting

^[3] Specimen had an additional No. 11 longitudinal bar on both sides, 2 in. from the bearing face on the head

^[4] Double overlapping No. 5 ties were used, refer to Figure 2.5

^[5] Double No. 5 ties were used

^[6] Specimen had an increased side cover of 6.5 in.

* Bars failed independently, so *T* is the average of the maximum force on individual bar. Individual results in Appendix C2

CHAPTER 4: ANALYSIS AND DISCUSSION: HOOKED BARS

In this chapter, the test results of the hooked bar specimens are analyzed. First, the results are compared with stresses based on the provisions in ACI 318-19 to show the limitations of the current Code. The results are then compared with the forces obtained using the descriptive equations proposed by Ajaam et al. (2017, 2018), Eq. (1.1) and (1.2). New descriptive equations are then developed based on a database that includes the No. 14 and No. 18 bar test results from this study. Finally, the effects on anchorage strength of key parameters, such as confining reinforcement, bar size and spacing, and strut angle are discussed.

4.1 COMPARISON OF TEST RESULTS WITH ACI 318-19

The provisions in ACI 318-19 for the development of hooked bars are discussed in detail in Section 1.3.1. ACI 318-19 gives no credit to confining reinforcement or wide spacing for hooked bars larger than No. 11 and requires that a modification factor of $\psi_r = 1.6$ be applied for No. 14 and No. 18 bars (even if confining reinforcement is provided or the center-to-center spacing of the bars is $\geq 6d_b$) when calculating the development length using Eq. (1.7). To compare the test results with stresses corresponding to the Code equation, Eq. (1.7), yield strength f_y is replaced by bar stress, $f_{s,ACI}$, f'_c is replaced by the measured compressive strength, f_{cm} (with an upper limit of 10,000 psi), and development length ℓ_{dh} is replaced by the measured embedment length, ℓ_{eh} , and the equation is solved for $f_{s,ACI}$. To better evaluate the ACI 318-19 provisions for No. 14 and No. 18 bars, the ψ_r factor is taken as it is for No. 11 and smaller bars ($= 1.0$ if $s \geq 6d_b$ or $A_{th,ACI}/A_{hs}^2 \geq 0.4$), rather than applying 1.6 for all No. 14 and No. 18 bar specimens, which will result in very high $f_s/f_{s,ACI}$ values for the large bars.

$$f_{s,ACI} = \frac{55\lambda\sqrt{f_{cm}}\ell_{eh}}{\psi_e\psi_r\psi_o\psi_c d_b^{1.5}} \quad (4.1)$$

where ψ_e is the coating factor, ψ_r is the confining reinforcement factor, ψ_o is the location factor, ψ_c is the concrete strength factor, and λ is the concrete density factor as shown in Table 1.3.

Table 4.1 presents the measured bar stress at failure, f_s , and the ratio $f_s/f_{s,ACI}$ for the specimens in this study. The table also presents the values of bar forces T , T_h , and the ratio T/T_h ,

² A_{th} is defined differently in ACI 318-19 than in the descriptive equations. Code ($A_{th,ACI}$): total cross-sectional area of confining reinforcement within $15d_b$ from the centerline of hooked bars. Descriptive equations (A_{th}): within $8d_b$ for No. 9 and smaller bars and $10d_b$ for larger bars.

where T_h is based on the descriptive equations developed by Ajaam et al. (2017, 2018), as described in the next section, along with specimen ID and key parameters (number and spacing of bars, concrete compressive strength, embedment length, and confining reinforcement).

Table 4.1 Comparison of No. 14 and No. 18 hooked bar test results with descriptive equations by Ajaam et al. (2018), Eq. (1.1) and (1.2), also Eq. (4.2) and (4.3), and ACI 318-19. Eq. (4.1)

ID ^[1]	n	s/d_b	f_{cm} psi	$\ell_{eh,avg}$ in.	A_{th}/A_{hs}	$A_{th,ACI}/A_{hs}$	ψ_r	T kips	T_h kips	T/T_h	f_s ksi	$f_{s,ACI}$ ksi	$f_s/f_{s,ACI}$
H14-1	2	10.6	12,980	27.0	0	0	1.0	240.0	219.2	1.09	106.7	106.7	1.58
H14-2	2	10.6	13,010	24.8	0.267	0.356	1.0	293.9	248.2	1.18	130.6	130.6	2.11
H14-3	2	10.6	8,100	36.7	0	0	1.0	279.1	266.0	1.05	124.0	124.0	1.50
H14-4	2	10.6	7,570	34.9	0.267	0.356	1.0	268.5	295.1	0.91	119.3	119.3	1.57
H14-5	2	10.6	6,980	26.5	0	0	1.0	196.5	178.9	1.10	87.3	87.3	1.58
H14-6	2	10.6	6,810	25.9	0.178	0.267	1.0	235.3	204.9	1.15	104.6	104.6	1.96
H14-7	3	3.5	6,390	36.4	0	0	1.6	250.8	181.3	1.38	111.5	111.5	2.45
H14-8	3	3.5	6,650	36.6	0.276	0.367	1.6	298.2	252.0	1.18	132.5	132.5	2.85
H18-1	2	8.0	15,310	28.5	0.233	0.388	1.0	358.2	371.6	0.96	89.6	89.6	1.94
H18-2	2	8.0	15,770	27.0	0.465	0.620	1.0	445.0	452.4	0.98	111.3	111.3	2.54
H18-3	2	8.0	7,560	36.5	0.233	0.388	1.0	371.4	388.8	0.96	92.9	92.9	1.80
H18-4	2	8.0	7,610	36.4	0.465	0.620	1.0	427.9	482.7	0.89	107.0	107.0	2.08
									Max	1.38		Max	2.85
									Min	0.89		Min	1.50
									Mean	1.07		Mean	2.00
									CoV	0.132		CoV	0.228

n	Number of bars
s	Center-to-center spacing of bars
d_b	Nominal bar diameter
f_{cm}	Measured concrete compressive strength
$\ell_{eh,avg}$	Average measured embedment length
A_{th}	Total area of tie legs within $9.5d_b$ from the centerline of hooked bars
$A_{th,ACI}$	Total area of tie legs within $15d_b$ from the centerline of hooked bars
A_{hs}	Total area of hooked bars being developed
f_s	Bar stress at failure
T	Average force per bar at failure
T_h	Calculated failure load using descriptive equations (Ajaam et al. 2017, 2018), Eq. (1.1) and (1.2)
$f_{s,ACI}$	Bar stress calculated based on ACI 318-19 equation
^[1]	The first number after “H” denotes the bar size

Table 4.1 shows that ACI 318-19 provides very conservative estimates of anchorage strength for No. 14 and No. 18 hooked bars, with values of $f_s/f_{s,ACI}$ ranging from 1.50 to 2.85 with a mean of 2.00, demonstrating that ACI 318-19 requires unnecessarily long embedment lengths for No. 14 and No. 18 hooked bars. These high numbers are in spite of using $\psi_r = 1.0$ when $s/d_b \geq 6$ or $A_{th,ACI}/A_{hs} \geq 0.4$ (and not 1.6 for all specimens as required by ACI 318-19 for No. 14 and No. 18 hooked bars). A degree of the conservative nature reflected in these comparisons is expected

because, unlike the descriptive equation, the Code equation has an embedded strength reduction factor. The strength reduction factor alone, however, would result in $f_s/f_{s,ACI}$ values averaging near 1.25, not 2.00. Separate from the strength reduction factor, a key reason that the provisions in ACI 318-19 are conservative is that ψ_r does not account for the combined effects of widely-spaced bars and confining reinforcement, while the descriptive equation does. When widely-spaced bars are used and confining reinforcement is provided, the required development length can be safely reduced. As will be shown in Chapter 6, the proposed design provisions for hooked bars provide a modified ψ_r factor that varies as a function of s/d_b and A_{th}/A_{hs} , resulting in values < 1.0 when confining reinforcement is provided. Here, the use of $\psi_r = 1.0$ is due solely to bar spacing for specimens H14-2, H14-4, H18-1, and H18-3. All four specimens also contained confining reinforcement, which adds to anchorage strength that is not acknowledged by the current Code. Only for two of the specimens, H18-2 and H18-4, is $\psi_r = 1.0$ used due to confining reinforcement because $A_{th,ACI} \geq 0.4$. The highest values of $f_s/f_{s,ACI}$ are obtained for specimens H14-7 and H14-8, because neither has $s/d_b \geq 6$ or $A_{th,ACI}/A_{hs} \geq 0.4$, requiring that $\psi_r = 1.6$ under ACI 318-19. Both, however, have $s/d_b = 3.5$, and H18-4 has $A_{th,ACI} = 0.367$ ($A_{th,ACI} = 0.367$ for H18-3), which justify values of ψ_r below 1.6.

The ratio of bar stress measured in the tests to the bar stress calculated based on the ACI 318-19 equation, $f_s/f_{s,ACI}$, is plotted versus the concrete compressive strength (f_{cm}) in Figure 4.1. As shown in the figure, ACI 318-19 is unrealistically conservative, independent of concrete compressive strength. Clearly, improvements could be made in these provisions.

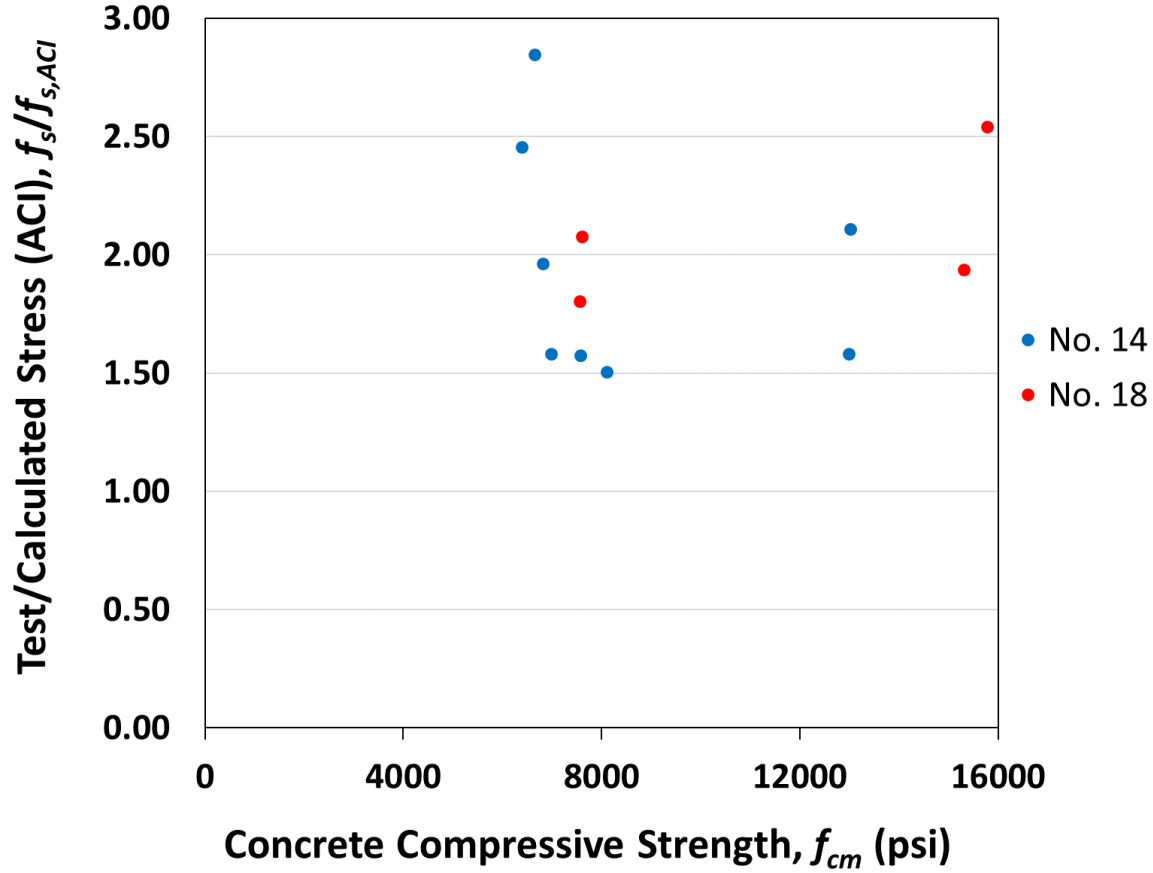


Figure 4.1 Ratio of test/calculated bar stress (ACI), $f_s/f_{s,ACI}$ versus concrete compressive strength f_{cm} for No. 14 and No. 18 hooked bar specimens (using values of ψ_r permitted for No. 11 and smaller bars, as shown in Table 4.1)

4.2 COMPARISON OF TEST RESULTS WITH DESCRIPTIVE EQUATIONS DEVELOPED BY AJAAM ET AL. (2017, 2018)

The descriptive equations to characterize the anchorage strength of hooked bars developed by Ajaam et al. (2017, 2018) based on test results for 245 beam-column joint specimens containing No. 5, No. 8, and No. 11 hooked bars without and with confining reinforcement are given in Eq. (1.1) and (1.2), respectively, and repeated here as Eq. (4.2) and (4.3).

$$T_h = 294 f_{cm}^{0.295} \ell_{eh}^{1.0845} d_b^{0.47} \left(0.0974 \frac{s}{d_b} + 0.391 \right) \quad (4.2)$$

where $\left(0.0974 \frac{s}{d_b} + 0.391 \right) \leq 1.0$.

$$T_h = \left(294 f_{cm}^{0.295} \ell_{eh}^{1.0845} d_b^{0.47} + 55,050 \left(\frac{A_{th}}{n} \right)^{1.0175} d_b^{0.73} \right) \left(0.0516 \frac{s}{d_b} + 0.6572 \right) \quad (4.3)$$

where $\left(0.0516 \frac{s}{d_b} + 0.6572 \right) \leq 1.0$.

and T_h is the anchorage strength of an individual hooked bar (lb); f_{cm} is the measured concrete compressive strength (psi); ℓ_{eh} is the embedment length of the hooked bar measured from the face of the column to the end of the hook (in.); d_b is the hooked bar diameter (in.); A_{hs} is the total area of the hooked bars (in.²); A_{th} is the effective confinement and defined as the area of confining reinforcement (in.²) within $8d_b$ from the top of the hooked bar for No. 8 bars and smaller or within $10d_b$ for No. 9 bars or larger; n is the number of hooked bars in the joint; and s is the center-to-center spacing between hooked bars. The specimens in this study were proportioned based on the descriptive equations.

To evaluate the applicability of Eq. (4.2) and (4.3) for No. 14 and No. 18 bars, the anchorage strengths measured in the tests, T (as reported in Table 3.4), are compared with the strengths calculated using the descriptive equations, T_h in Table 4.1. Table 4.2 summarizes the comparison of test results with Eq. (4.2) and (4.3), including the maximum, minimum, mean, standard deviation, and coefficient of variation. The specimens are categorized based on the presence of confining reinforcement in the joint region and bar size.

Table 4.2 Summary of test-to-calculated ratio for No. 14 and No. 18 hooked bars based on descriptive equations by Ajaam et al. (2017, 2018), Eq. (4.2) and (4.3)

	T/T_h				
	All	Without Confining Reinforcement	With Confining Reinforcement	No. 14	No. 18
No. of Specimens	12	4	8	8	4
Max	1.38	1.38	1.18	1.38	0.98
Min	0.89	1.05	0.89	0.91	0.89
Mean	1.07	1.16	1.03	1.13	0.95
STDEV	0.142	0.153	0.124	0.135	0.042
CoV	0.133	0.132	0.121	0.119	0.045

As shown in Table 4.2, the twelve hooked bar specimens had a mean test-to-calculated T/T_h ratio of 1.07 and a coefficient of variation of 0.133, with the values ranging from 0.89 to 1.38. The four specimens without confining reinforcement had a mean value of T/T_h of 1.16, higher than

the eight specimens with confining reinforcement with a mean value of T/T_h of 1.03. The mean value of T/T_h is 1.13 for the No. 14 bar specimens and 0.95 for the No. 18 bar specimens.

Student's t-test can be used to determine if the difference in the mean values is statistically significant. The type of t-test used in this study was homoscedastic (two-sample equal variance) with a two-tailed distribution. A threshold of 0.05 is used for the p value. Thus, if the p value is less than 0.05 the probability that the difference in to values occurred by chance is less than 5%. Values of p above 0.05 indicate the difference was not due to any meaningful difference in behavior.

Although the comparisons with Eq. (4.2) and (4.3) appear to be more conservative for the specimens without confining reinforcement than for the specimens with confining reinforcement (mean $T/T_h = 1.16$ and 1.03, respectively), $p = 0.144$, indicating that the difference in the mean values is not statistically significant. In terms of bar size, however, the difference in the mean values of T/T_h for the No. 14 and No. 18 bar specimens, 1.13 and 0.95, respectively, with $p = 0.026$.

4.3 NEW DESCRIPTIVE EQUATIONS

In this section, the descriptive equations developed for No. 11 and smaller hooked bars are updated by adding the No. 14 and 18 bar test results from this study to the database. Using the same procedure by Ajaam et al. (2017), an equation is first developed for specimens with widely-spaced bar (center-to-center spacing $\geq 6d_b$) without confining reinforcement using an iterative analysis resulting in $T/T_h = 1.00$. The effect of close bar spacing is then accounted for. The same procedure is then repeated for specimens with confining reinforcement. The database used by Ajaam et al. (2017, 2018) to develop the previous equations is used along with the results for the No. 14 and No. 18 bar specimens tested in this study. Eleven specimens with an effective beam depth to embedment length ratio (d_{eff}/ℓ_{eh} , as will be discussed in detail in Section 4.4.5) greater than 1.5 are removed from the analysis. Those include three No. 6 bar specimens by Ramirez and Russell (2008) and three No. 8 and five No. 11 bar specimens by Sperry et al. (2015b) and Ajaam (2017).

4.3.1 Widely-spaced Bars Without Confining Reinforcement

Developing a new descriptive equation starts with obtaining an expression for the 76 specimens with widely-spaced bars without confining reinforcement. The specimens include No. 7 hooked bars tested by Lee and Park (2010). The specimen details are presented in Table B.2 of

Section B3 (Specimens tested at the University of Kansas) and Table B.8 of Section B4 (Specimens tested in other studies) in Appendix B. The resulting expression is

$$T_c = 319 f_{cm}^{0.281} \ell_{eh}^{1.106} d_b^{0.430} \quad (4.4)$$

where T_c is the anchorage strength of hooked bars without confining reinforcement (lb), f_{cm} is concrete compressive strength on the day of test (psi), ℓ_{eh} is embedment length (in.), and d_b is bar diameter (in.). Compared with Eq. (4.2) developed by Ajaam et al. (2017, 2018), the constant has increased from 294 to 319, the power of f_{cm} has decreased from 0.295 to 0.281, the power of ℓ_{eh} has increased from 1.0845 to 1.106, and the power of d_b has decreased from 0.470 to 0.430. Figure 4.2 compares f_{cm} with T/T_c as a function of f_{cm} for the 76 specimens used to develop Eq. (4.4).

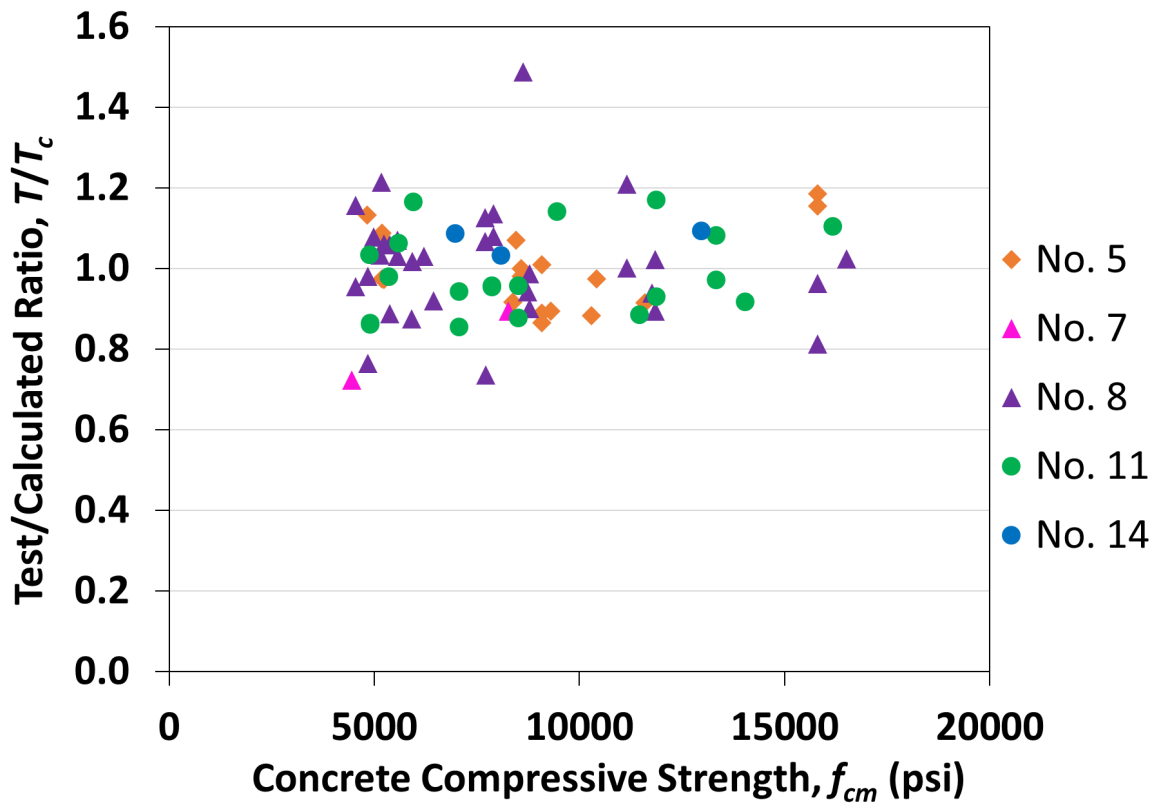


Figure 4.2 Ratio of test-to-calculated bar force at failure T/T_c versus concrete compressive strength for hooked bar specimens with widely-spaced bars (center-to-center spacing $\geq 6d_b$) without confining reinforcement

As shown in Figure 4.2, no noticeable trend is observed, indicating that the 0.281 power of f_{cm} captures the effect of concrete compressive strength. The statistical parameters for T/T_c are shown in Table 4.3, where T/T_c ranges from 0.72 to 1.49, with a mean of 1.00 and a coefficient of

variation of 0.122. Equation (4.4) is conservative for No. 14 bars with a mean of 1.07, but less so than Eq. (4.2) (mean = 1.13). At 0.81, the mean value of T/T_c are especially low for two No. 7 bar specimens tested by Lee and Park (2010).

Table 4.3 Statistical parameters of T/T_c ratio using Eq. (4.4) for hooked bar specimens with widely-spaced bars (center-to-center spacing $\geq 6d_b$) without confining reinforcement

Bar size	All	No. 5	No. 7	No. 8	No. 11	No. 14
No. of specimens	76	18	2	33	20	3
Max	1.49	1.19	0.89	1.49	1.17	1.09
Min	0.72	0.87	0.72	0.74	0.86	1.03
Mean	1.00	1.00	0.81	1.01	0.99	1.07
STDEV	0.122	0.099	0.120	0.141	0.103	0.027
CoV	0.122	0.099	0.149	0.139	0.105	0.025

4.3.2 Closely-spaced Bars Without Confining Reinforcement

For the 26 specimens with closely-spaced bars ($s/d_b < 6$, where s is the center-to-center spacing of hooked bars) without confining reinforcement, the values of T/T_c , with T_c based on Eq. (4.4), are plotted versus s/d_b in Figure 4.3. The specimens include two No. 7 bars by Hamad et al. (2003) and three No. 11 bars by Ramirez and Russell (2008). These specimens were tested as cantilevers, meaning the bottom of the columns were fixed and the only forces applied to specimens were tension on hooked bars and compression at the simulated beam. The specimens were retained for developing descriptive equations for consistency. Ajaam et al. (2017, 2018) also included six No. 7 bar specimens by Marques and Jirsa (1975), but those specimens are not used here due to their unrealistic geometry and proportions as well as yielding of the bars accompanied by relatively high bar slips, as discussed in detail in Section 4.5. The specimen details are presented in Table B.3 of Section B3 (Specimens tested at the University of Kansas) and Table B.8 of Section B4 (Specimens tested in other studies) in Appendix B.

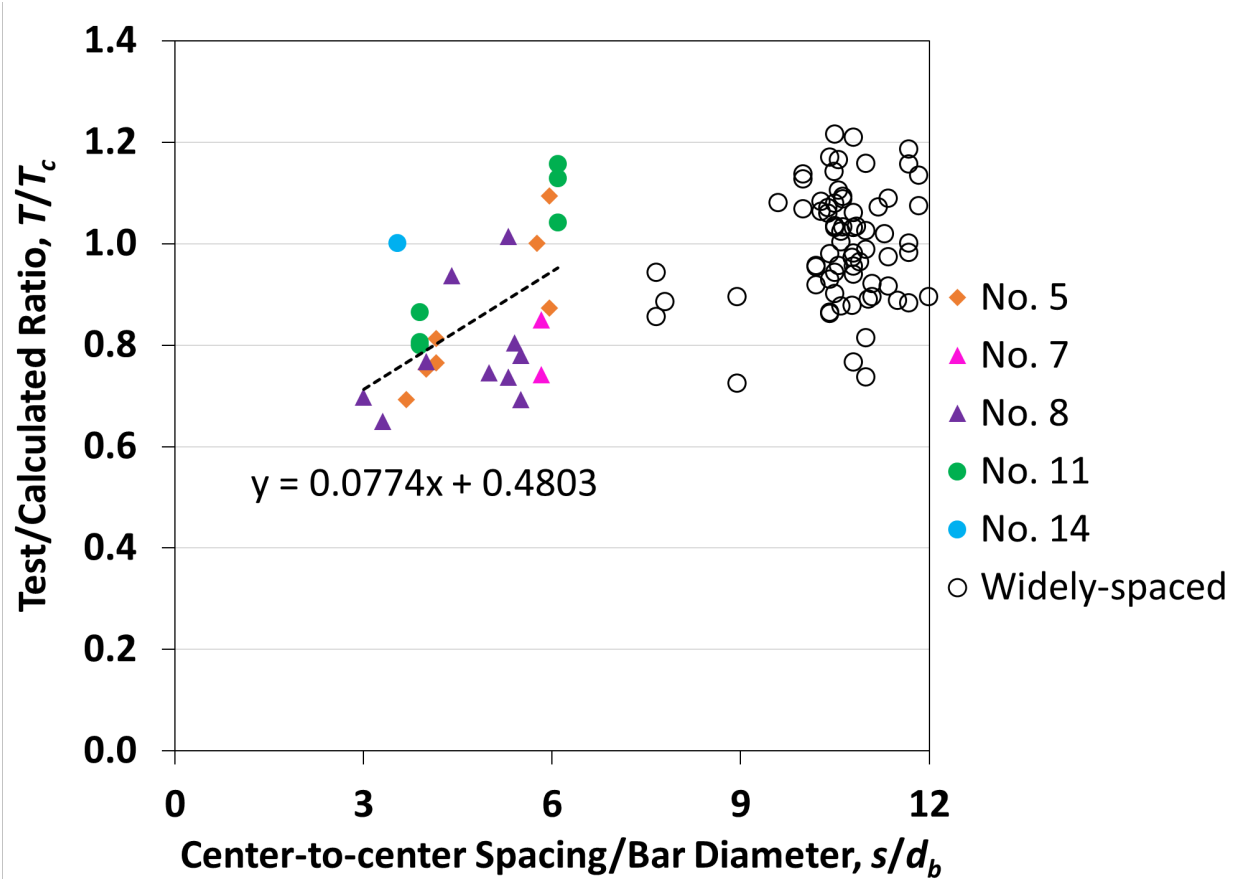


Figure 4.3 Test-to-calculated bar force at failure T/T_c versus ratio of center-to-center spacing to bar diameter s/d_b for widely- and closely-spaced hooked bars without confining reinforcement

As shown in Figure 4.3, the T/T_c ratio decreases with a decrease in s/d_b . T/T_c approaches 1.0 at $s/d_b = 6.0$. The linear trendline equation can be used as a multiplier to account for the effect of close bar spacing. When used in conjunction with Eq. (4.4), the equation for widely- and closely-spaced bars without confining reinforcement becomes

$$T_c = \left(319 f_{cm}^{0.281} \ell_{eh}^{1.106} d_b^{0.430} \right) \left(0.0774 \frac{s}{d_b} + 0.4803 \right) \quad (4.5)$$

where $\left(0.0774 \frac{s}{d_b} + 0.4803 \right) \leq 1.0$

It is worth noting that incorporating the effect of close bar spacing may actually be a convenient proxy for a bar group effect. For both hooked and headed bars, the majority of specimens with closely-spaced bars contain 3 or 4 bars, whereas all specimens with widely-spaced bars contain 2 bars. Therefore, what is considered to be the effect of close bar spacing on anchorage

strength, may be the effect of a greater total force on a member of fixed size. The center-to-center bar spacing, however, is a simple and safe proxy to take this effect into account.

The statistical parameters for the 26 specimens with closely-spaced bars and without confining reinforcement are shown in Table 4.4.

Table 4.4 Statistical parameters of T/T_c ratio using Eq. (4.5) for hooked bar specimens with closely-spaced ($s/d_b < 6d_b$) bars without confining reinforcement

Bar size	All	No. 5	No. 7	No. 8	No. 11	No. 14
No. of specimens	26	7	2	10	6	1
Max	1.33	1.16	0.91	1.14	1.22	1.33
Min	0.76	0.91	0.80	0.76	1.02	1.33
Mean	1.00	1.00	0.85	0.93	1.11	1.33
STDEV	0.141	0.092	0.083	0.126	0.079	0
CoV	0.141	0.092	0.097	0.135	0.071	0

As shown in Table 4.4 the T/T_c ratio ranged from 0.76 to 1.33 with a mean of 1.00 and a coefficient of variation of 0.141 for the specimens with closely-spaced bars and without confining reinforcement. The mean values range from 0.85 for No. 7 bars to 1.11 for No. 11 bars. T/T_c for the sole No. 14 bar is 1.33. T/T_c is plotted as a function of f_{cm} in Figure 4.4 for the 100 specimens without confining reinforcement. No visible trend is apparent, indicating that the effect of concrete compressive strength is adequately captured by Eq. (4.5). The statistical parameters of T/T_c ratio are presented in Table 4.5 for all specimens without confining reinforcement.

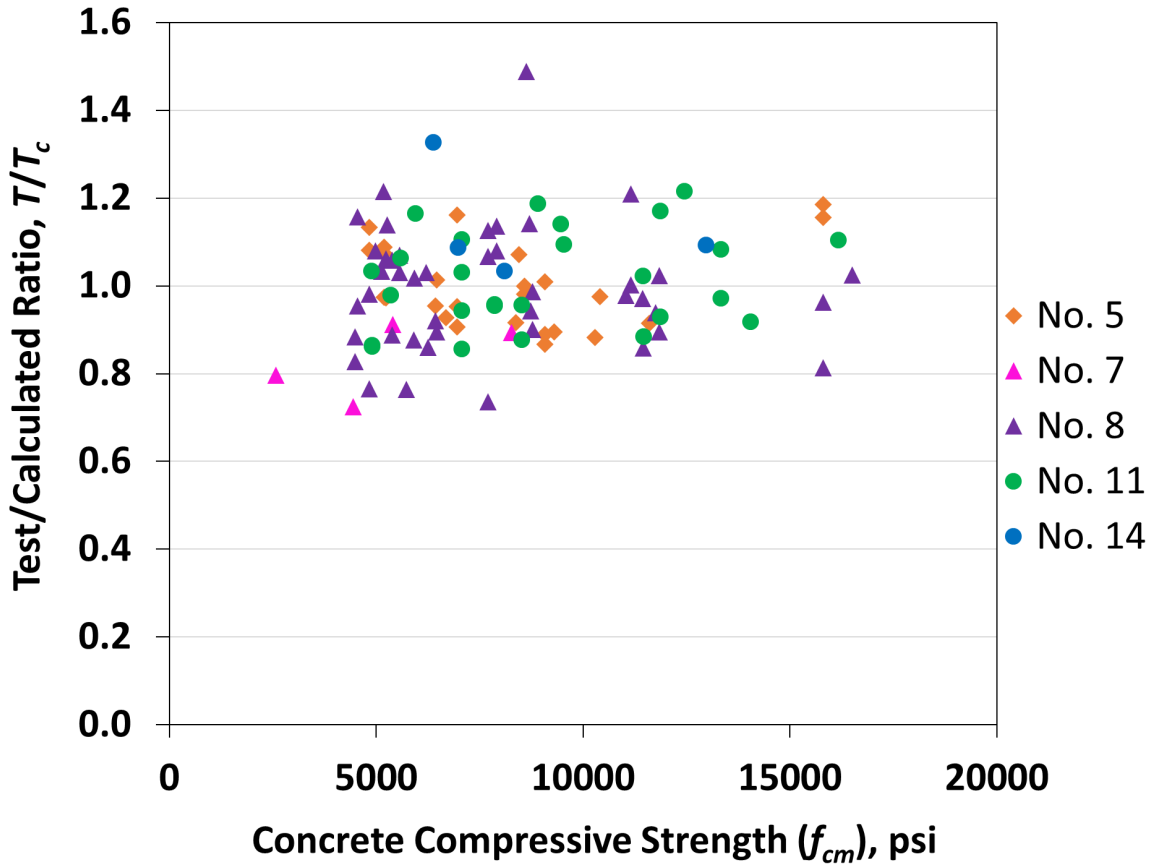


Figure 4.4 Ratio of test-to-calculated failure load T/T_c versus concrete compressive strength for hooked bar specimens having widely- and closely-spaced bars without confining reinforcement

Table 4.5 Statistical parameters of T/T_c ratio using Eq. (4.5) for hooked bar specimens with widely- and closely-spaced bars without confining reinforcement

Bar size	All	No. 5	No. 7	No. 8	No. 11	No. 14
No. of specimens	102	25	4	43	26	4
Max	1.49	1.19	0.89	1.49	1.22	1.33
Min	0.72	0.87	0.72	0.74	0.86	1.03
Mean	1.00	1.00	0.81	1.00	1.01	1.13
STDEV	0.128	0.095	0.120	0.141	0.110	0.131
CoV	0.128	0.095	0.149	0.142	0.109	0.115

As shown in Table 4.5, the 102 specimens without confining reinforcement had a mean T/T_c of 1.00, with individual values ranging from 0.72 to 1.49 with a coefficient of variation of 0.128. Based on bar size, the mean value of T/T_c ranges from 0.81 for the No. 7 bar specimens to 1.13 for the No. 14 bar specimens.

4.3.3 Widely-spaced Bars with Confining Reinforcement

The next step is developing an expression for the contribution of confining reinforcement. To begin, the same iterative analysis is performed for 54 specimens having widely-spaced bars with confining reinforcement (all tested at the University of Kansas as presented in detail in Table B.4 in Section B3 of Appendix B). The expression for the contribution of the confining steel, T_s , is added to the expression for the contribution of concrete, T_c , shown in Eq. (4.4), giving

$$T_h = T_c + T_s = 319 f_{cm}^{0.281} \ell_{eh}^{1.106} d_b^{0.430} + 54,568 \left(\frac{A_{th}}{n} \right) d_b^{0.693} \quad (4.6)$$

where A_{th} is total cross-sectional area (in.²) of tie legs within $8d_b$ from the top of the hooked bar for No. 8 bars and smaller or within $10d_b$ for No. 9 bars or larger, and n is the number of bars. Compared with the previous descriptive equation, Eq. (4.3), the constant in the T_s term has slightly decreased from 55,050 to 54,568, the power of A_{th}/n has decreased from 1.0175 to 1.0, and the power of d_b has decreased from 0.73 to 0.693. Figure 4.5 compares T/T_h calculated based on Eq. (4.6) with f_{cm} . As observed in the figure, Eq. (4.6) adequately captures the effect of concrete compressive strength, with no positive or negative trend in the data as a function of concrete compressive strength. Table 4.6 presents the statistical parameters of T/T_h for the specimens with widely-spaced bars and confining reinforcement.

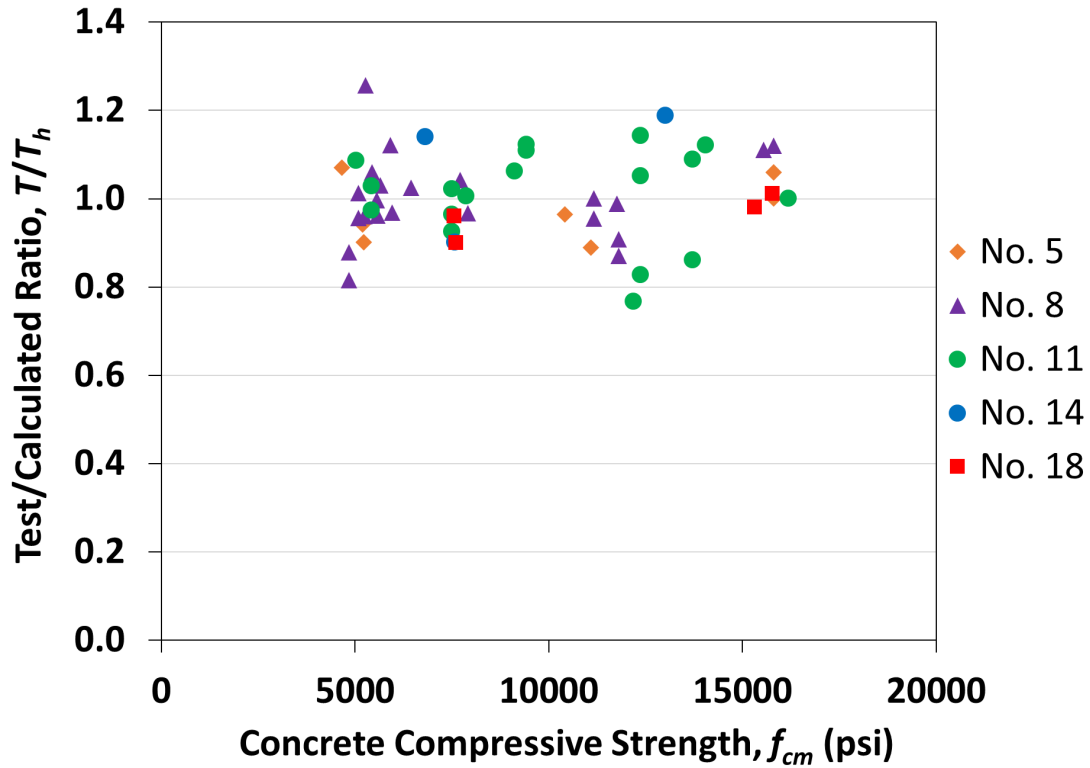


Figure 4.5 Ratio of test-to-calculated bar force at failure T/T_h versus concrete compressive strength for hooked bar specimens having widely-spaced ($s/d_b \geq 6d_b$) bars with confining reinforcement

Table 4.6 Statistical parameters of T/T_h ratio using Eq. (4.6) for hooked bar specimens with widely-spaced ($s/d_b \geq 6d_b$) bars with confining reinforcement

Bar size	All	No. 5	No. 8	No. 11	No. 14	No. 18
No. of specimens	54	7	22	18	3	4
Max	1.26	1.07	1.26	1.14	1.19	1.01
Min	0.77	0.89	0.82	0.77	0.90	0.90
Mean	1.00	0.98	1.00	1.01	1.08	0.96
STDEV	0.098	0.072	0.097	0.107	0.154	0.047
CoV	0.098	0.074	0.097	0.106	0.143	0.048

As shown in Table 4.6, T/T_h ranges from 0.77 to 1.26 with a mean of 1.00 and a coefficient of variation of 0.098. Based on bar size, the mean values of T/T_h range from a low of 0.96 for the No. 18 bar specimens to a high of 1.08 the No. 14 bar specimens.

4.3.4 Closely-spaced Bars with Confining Reinforcement

The last step in developing the new descriptive equations is to account for close bar spacing for specimens with confining reinforcement. The same approach used for specimens without confining reinforcement (Section 4.3.2) is followed. Figure 4.6 shows the plot of T/T_h versus s/d_b for 23 specimens having closely-spaced bars with confining reinforcement (all tested at the University of Kansas as presented in Table B.5 in Section B3 of Appendix B).

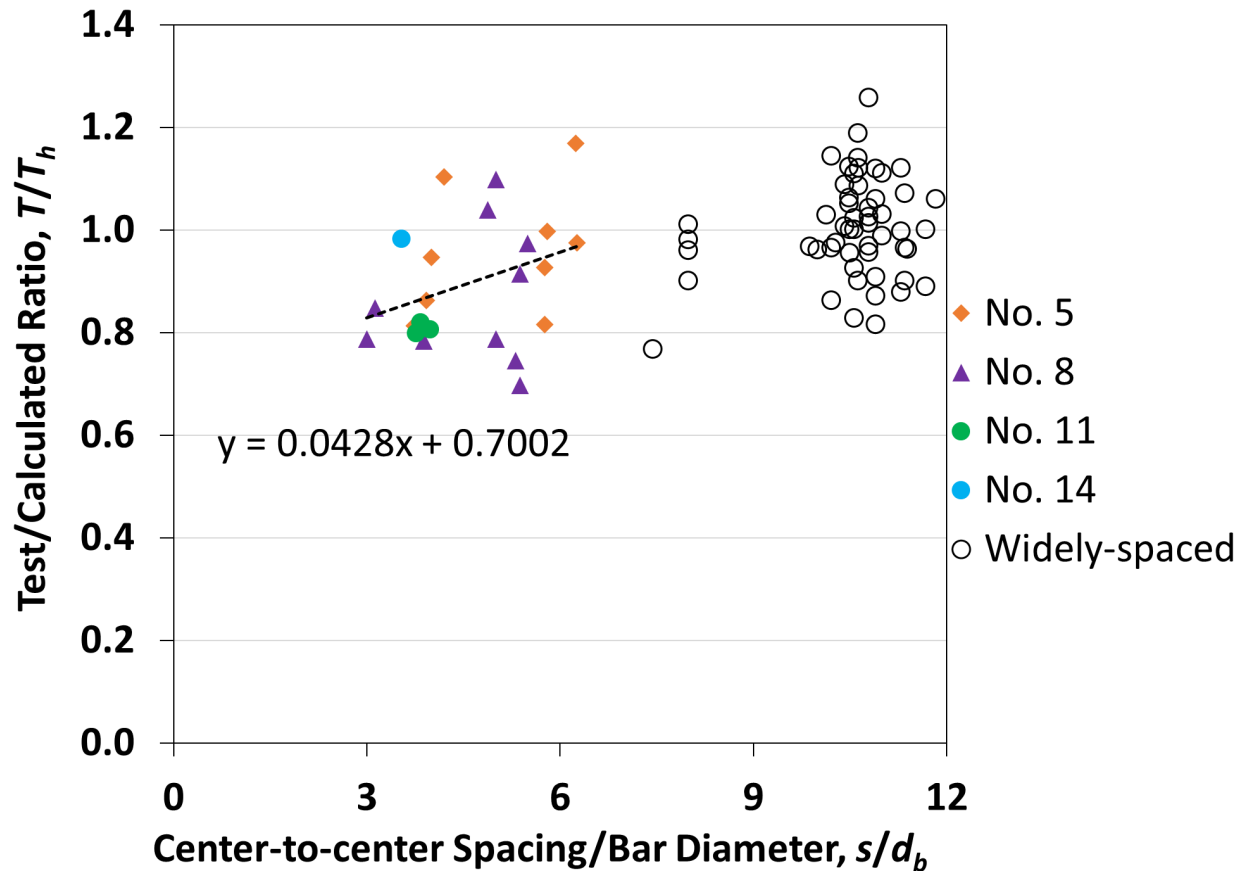


Figure 4.6 Test-to-calculated bar force T/T_h versus ratio of center-to-center spacing to bar diameter s/d_b for widely- and closely-spaced hooked bars with confining reinforcement

As shown in Figure 4.6, the correlation between anchorage strength and bar spacing is not strong for hooked bars with confining reinforcement and is less significant than it is for specimens without confining reinforcement, indicating the adverse effects of having closely-spaced bars are less detrimental when confining reinforcement is used. The linear trendline equation given in Figure 4.6 is multiplied by Eq. (4.6) to give the final equation for specimens with confining reinforcement having widely- and closely spaced bars:

$$T_h = \left(319 f_{cm}^{0.281} \ell_{eh}^{1.106} d_b^{0.430} + 54,568 \left(\frac{A_{th}}{n} \right) d_b^{0.693} \right) \left(0.0428 \frac{s}{d_b} + 0.7002 \right) \quad (4.7)$$

where $\left(0.0428 \frac{s}{d_b} + 0.7002 \right) \leq 1.0$

The statistical parameters for T/T_h using Eq. (4.7) for specimens with closely-spaced bars and confining reinforcement are shown in Table 4.7. T/T_h ranges from 0.75 to 1.25 with a mean of 1.00 and a coefficient of variation of 0.130. Based on bar size, the mean value of T/T_h ranges from a low of 0.93 for the No. 11 bar specimens to a high of 1.04 for the No. 5 bar specimens. T/T_h equals 1.15 for the single No. 14 bar specimen.

Table 4.7 Statistical parameters of T/T_h ratio using Eq. (4.7) for hooked bar specimens with closely-spaced bars with confining reinforcement

Bar size	All	No. 5	No. 8	No. 11	No. 14
No. of specimens	23	9	10	3	1
Max	1.25	1.25	1.20	0.95	1.15
Min	0.75	0.86	0.75	0.93	1.15
Mean	1.00	1.04	0.97	0.93	1.15
STDEV	0.130	0.124	0.143	0.012	0
CoV	0.130	0.119	0.148	0.013	0

Table 4.8 presents the statistical parameters of T/T_h for all specimens with confining reinforcement. T/T_h ratio ranges from 0.75 to 1.26, with a mean of 1.00 and a coefficient of variation of 0.107. Based on bar size, the mean value of T/T_h ranges from a low of 0.99 for the No. 8 to a high of 1.10 for No. 14 bar specimens.

Table 4.8 Statistical parameters of T/T_h ratio using Eq. (4.7) for hooked bar specimens with widely- and closely-spaced bars with confining reinforcement

Bar size	All	No. 5	No. 8	No. 11	No. 14	No. 18
No. of specimens	77	16	32	21	4	4
Max	1.26	1.25	1.26	1.14	1.19	1.01
Min	0.75	0.86	0.75	0.77	0.90	0.90
Mean	1.00	1.01	0.99	1.00	1.10	0.96
STDEV	0.107	0.107	0.112	0.102	0.131	0.047
CoV	0.107	0.106	0.113	0.102	0.120	0.048

Figure 4.7 compares T/T_h with the concrete compressive strength for the specimens with confining reinforcement. Similar to Figure 4.5, no noticeable trend can be detected. Thus, the descriptive equations developed in this study represent the effect of concrete strength for all of the specimens in the database.

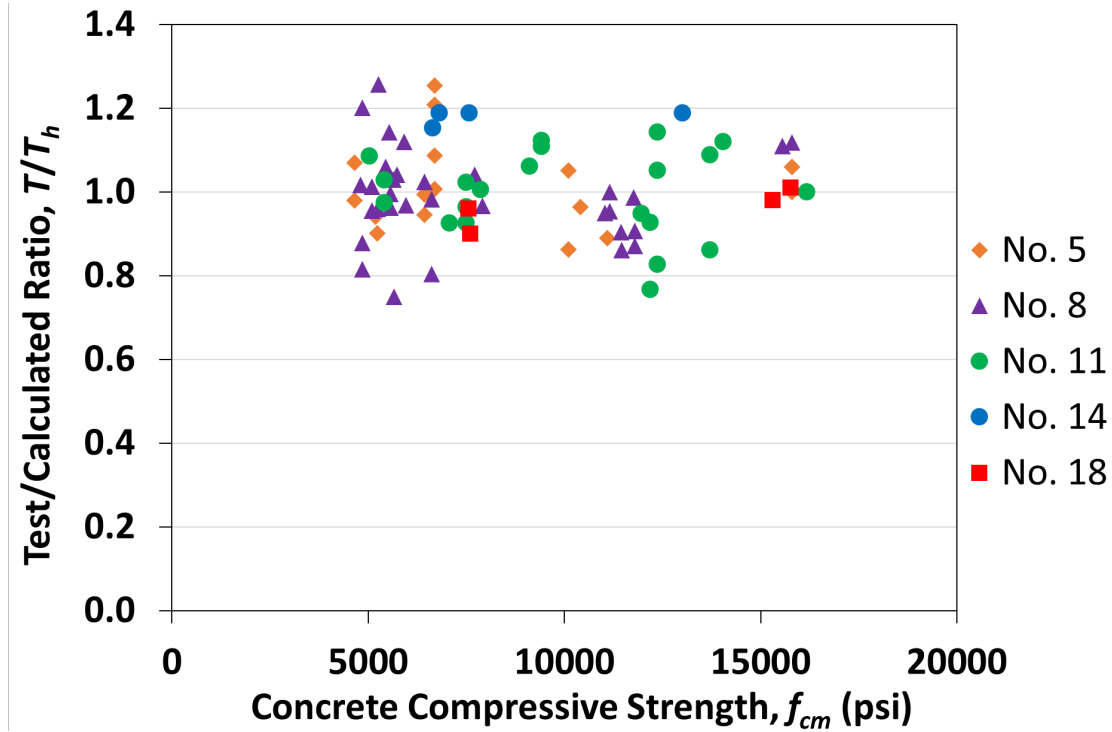


Figure 4.7 Ratio of test-to-calculated bar force at failure T/T_h versus concrete compressive strength for hooked bar specimens having widely- and closely-spaced bars with confining reinforcement

4.3.5 Summary

Table 4.9 presents the statistical parameters of T/T_h for all hooked bar specimens used to develop the descriptive equations.

Table 4.9 Statistical parameters of T/T_h ratio using Eq. (4.5) and (4.7) for all hooked bar specimens used to develop the descriptive equations

Bar size	All	No. 5	No. 7	No. 8	No. 11	No. 14	No. 18
No. of specimens	179	41	4	75	47	8	4
Max	1.49	1.25	0.89	1.49	1.22	1.33	1.01
Min	0.72	0.86	0.72	0.74	0.77	0.90	0.90
Mean	1.00	1.01	0.81	0.99	1.01	1.12	0.96
STDEV	0.117	0.099	0.098	0.129	0.106	0.123	0.047
CoV	0.117	0.099	0.122	0.130	0.105	0.110	0.048

As shown in Table 4.9, the test-to-calculated ratio T/T_h for all hooked bar specimens used to develop the new descriptive equations ranged from 0.72 to 1.49 with a mean of 1.00 and a coefficient of variation of 0.117. For No. 14 and No. 18 bars, the new equations provide improved coefficient of variation and mean compared with the equations developed previously for No. 11 and smaller bars by Ajaam et al. (2017, 2018), Eq. (4.2) and (4.3). Similar to Eqs. (4.2) and (4.3), the new equations are more conservative for No. 14 bars than No. 18 bars.

For the specimens in the database, the measured bar force at failure T is compared with the calculated failure load T_h in Figure 4.8. As shown in the figure, the best fit trendline for the specimens closely matches the dashed line representing $T = T_h$. The new descriptive equations are evaluated for No. 14 and No. 18 bars in Table 4.10.

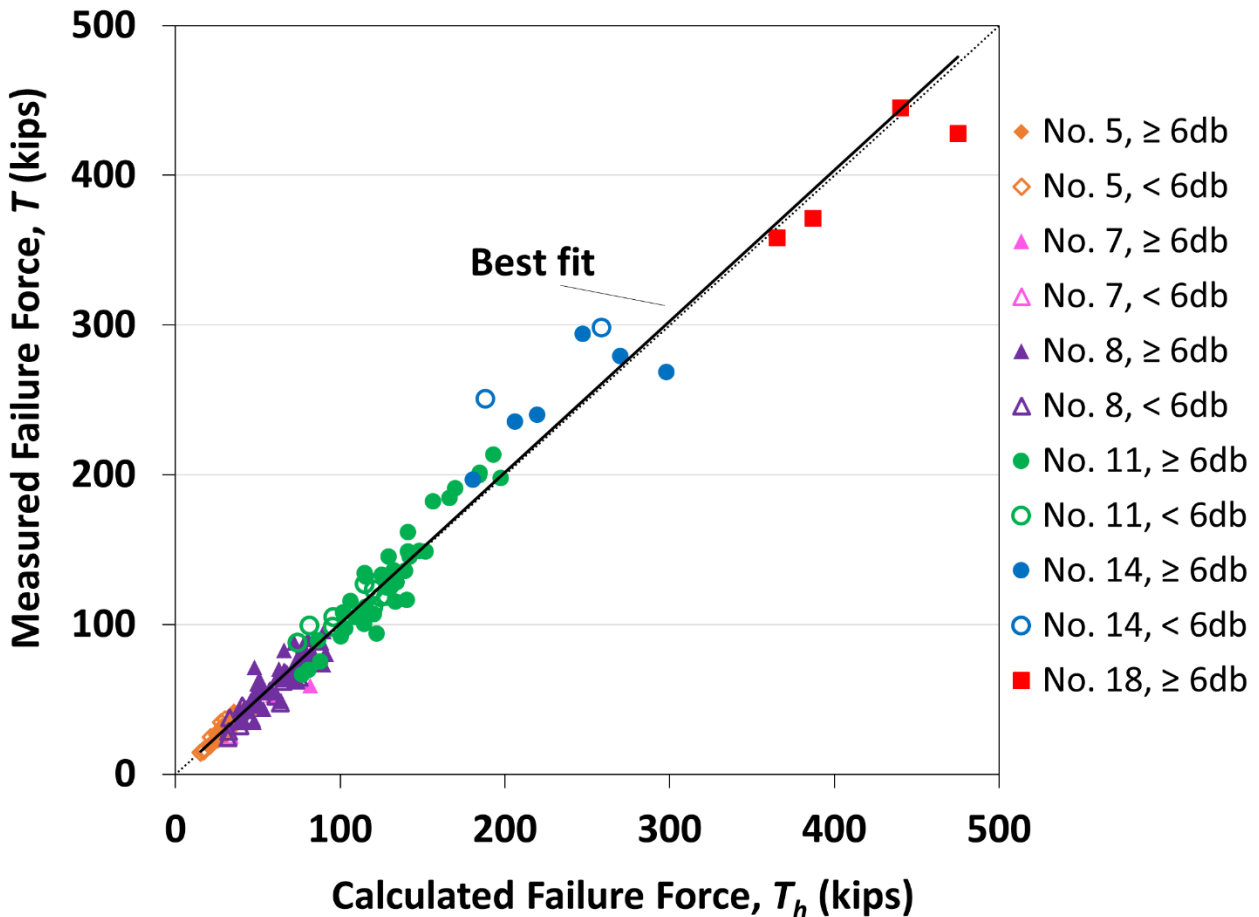


Figure 4.8 Measured versus calculated bar force at failure based on new descriptive equations for hooked bars, Eq. (4.5) and (4.7)

Table 4.10 Summary of test-to-calculated ratio T/T_h using Eq. (4.5) and (4.7) for No. 14 and No. 18 hooked bar specimens tested in this study

	T/T_h				
	All	Without Confining Reinforcement	With Confining Reinforcement	No. 14	No. 18
No. of Specimens	12	4	8	8	4
Max	1.33	1.33	1.19	1.33	1.01
Min	0.90	1.03	0.90	0.90	0.90
Mean	1.06	1.14	1.03	1.12	0.96
STDEV	0.127	0.133	0.116	0.124	0.047
CoV	0.119	0.117	0.112	0.111	0.048

As shown in Table 4.10, Eq. (4.5) and (4.7) are more conservative for No. 14 bars than No. 18 bars, with respective values of T/T_h of 1.12 and 0.96 for the No. 14 and No. 18 bar specimens, respectively, a difference that is statistically significant, with a p value of 0.042. Equations (4.5) and (4.7) give more conservative results, on average, for specimens without confining reinforcement than those with confining reinforcement, with respective mean T/T_h values of 1.14 and 1.03, similar to 1.16 and 1.03 obtained using Eq. (4.2) and (4.3). Overall, the new descriptive equations provide comparable results for No. 14 bars but are improved for No. 18 bars, compared with Eq. (4.2) and (4.3) developed for No. 11 and smaller bars. Compared with Eq. (4.2) and (4.3), the new equations have a lower overall coefficient of variation for No. 14 and No. 18 bar specimens (0.119 versus 0.133). Overall, Eq. (4.5) and (4.7) are appropriate for characterizing the anchorage strength of large hooked bars.

4.4 EVALUATING DESCRIPTIVE EQUATIONS

In this section, the descriptive equations are evaluated with respect to several key parameters, including bar location, confining reinforcement, bar spacing, strut angle, effective beam depth, and embedment length. In Section 4.5, the results for specimens not used to develop descriptive equations are investigated.

4.4.1 Bar Location

In accordance with Table 25.4.3.2 of ACI 318-19, the modification factor for bar location, ψ_o , is 1.0 for hooked bars terminating inside column longitudinal reinforcement (column core) with side cover normal to plane of hook ≥ 2.5 in., or with side cover normal to plane of hook $\geq 6d_b$. In all other cases, $\psi_o = 1.25$. These factors were adopted based on comparisons made by

Sperry et al. (2015b) and Ajaam et al. (2017, 2018) between 13 pairs of specimens with hooked bars placed outside versus inside the column core. The comparisons showed that specimens with hooked bars placed outside column core exhibited lower anchorage strength than the companion specimen with hooked bars inside the column core in 12 of 13 cases. $T_{\text{outside}}/T_{\text{inside}}$ ranged from 0.66 to 1.03 with an average of 0.85. The reduction in anchorage strength was then taken conservatively as 80% (therefore, $1/0.8 = 1.25$).

In this section, all of the specimens, not just paired specimens, tested by Sperry (2015b) and Ajaam et al. (2017) with hooked bars placed outside the column core are re-analyzed using the descriptive equations developed in this study, Eq. (4.5) and (4.7), to establish a more accurate bar location factor. Table 4.11 presents the key properties of these specimens along with their T/T_h ratio. Details of these specimens are presented in Table B.6 of Section B3 (specimens tested at the University of Kansas) of Appendix B.

Table 4.11 Test-to-calculated T/T_h ratio based on Eq. (4.5) and (4.7) for specimens with hooked bars placed outside column core (Ajaam et al. 2017)

Specimen ID	n	ℓ_{eh}	f_{cm}	d_b	s/d_b	A_{th}/A_{hs}	T	T_h	T/T_h
		in.	psi	in.			kips	kips	
5-5-90-0-o-1.5-2-5	2	5	4930	0.63	9.8	0	14.1	16.9	0.83
5-5-90-0-o-2.5-2-5	2	4.8	4930	0.63	9.2	0	19.3	16.2	1.19
5-5-90-0-o-1.5-2-6.5	2	6.2	5650	0.63	9.5	0	17.8	22.3	0.80
5-5-90-0-o-1.5-2-8	2	7.9	5650	0.63	9.5	0	22.8	29.2	0.78
5-5-90-0-o-2.5-2-8	2	9	5780	0.63	9.5	0	26.1	33.9	0.77
5-5-180-0-o-1.5-2-9.5	2	9.4	4420	0.63	9.2	0	29.5	33.0	0.89
5-5-180-0-o-2.5-2-9.5	2	9.5	4520	0.63	9.5	0	30.1	33.6	0.90
5-5-180-0-o-1.5-2-11.25	2	11.3	4520	0.63	9.5	0	32.4	40.8	0.80
5-5-180-2#3-o-2.5-2-9.5	2	9.2	4420	0.63	10.0	0.350	35.5	36.6	0.97
5-5-180-2#3-o-1.5-2-11.25	2	11.6	4420	0.63	10.0	0.350	43.1	46.0	0.94
5-5-180-2#3-o-1.5-2-9.5	2	8.8	4520	0.63	10.0	0.350	20.3	35.2	0.58
5-5-180-2#3-o-2.5-2-11.25	2	11.3	4520	0.63	10.0	0.350	42.3	45.1	0.94
5-5-90-5#3-o-1.5-2-5	2	5	5205	0.63	9.8	1.060	21.8	30.2	0.72
5-5-90-5#3-o-2.5-2-5	2	5.2	4930	0.63	10.0	1.060	22.5	30.7	0.73
5-5-90-5#3-o-1.5-2-8	2	7.9	5650	0.63	9.7	1.060	25.1	42.2	0.59
5-5-90-5#3-o-2.5-2-8	2	7.5	5650	0.63	9.8	1.060	24.9	40.6	0.61
5-5-90-5#3-o-1.5-2-6.5	2	6.5	5780	0.63	9.8	1.060	21.7	36.7	0.59
8-5-90-0-o-2.5-2-10a	2	10.4	5270	1	9.0	0	42.3	47.3	0.89
8-5-90-0-o-2.5-2-10b	2	9.8	5440	1	9.0	0	33.7	44.7	0.75
8-5-90-0-o-2.5-2-10c	2	10.6	5650	1	9.0	0	56.0	49.3	1.14
8-8-90-0-o-2.5-2-8	2	8.4	8740	1	8.0	0	33.0	43.1	0.77
8-8-90-0-o-3.5-2-8	2	7.8	8810	1	8.8	0	35.9	39.8	0.90
8-8-90-0-o-4-2-8	2	8.2	8630	1	8.8	0	37.5	41.8	0.90

8-5-90-5#3-o-2.5-2-10a	2	10.4	5270	1	9.1	0.420	54.3	65.4	0.83
8-5-90-5#3-o-2.5-2-10b	2	10.5	5440	1	9.1	0.420	65.6	66.4	0.99
8-5-90-5#3-o-2.5-2-10c	2	10.9	5650	1	9.1	0.420	57.7	69.0	0.84
8-8-90-5#3-o-2.5-2-8	2	8.5	8630	1	8.5	0.420	58.0	61.6	0.94
8-8-90-5#3-o-3.5-2-8	2	7.9	8810	1	8.7	0.420	55.0	58.5	0.94
8-8-90-5#3-o-4-2-8	2	8.3	8740	1	9.2	0.420	39.1	60.6	0.64
11-8-90-0-o-2.5-2-25	2	25.2	9460	1.41	8.6	0	174.7	172.2	1.01
11-8-90-0-o-2.5-2-17	2	16.6	9460	1.41	8.8	0	107.2	108.5	0.99
11-12-180-0-o-2.5-2-17	2	17.1	11800	1.41	8.5	0	83.5	119.3	0.70
11-12-90-0-o-2.5-2-17	2	16.9	11800	1.41	8.8	0	105.4	117.8	0.90
11-8-90-6#3-o-2.5-2-22	2	21.9	9120	1.41	8.5	0.210	170.2	168.6	1.01
11-8-90-6#3-o-2.5-2-16	2	16.2	9420	1.41	8.5	0.210	136.8	128.2	1.07
11-12-180-6#3-o-2.5-2-17	2	16.5	11800	1.41	8.5	0.210	113.1	137.4	0.82
11-12-90-6#3-o-2.5-2-17	2	16.4	11800	1.41	8.7	0.210	115.9	136.6	0.85
Mean									0.85
CoV									0.174

Based on the results shown in Table 4.11, the T/T_h ratio for the 37 specimens with hooked bars placed outside column core ranges from 0.58 to 1.19 with a mean of 0.85 and a coefficient of variation of 0.174. The average of 0.85 indicates that the bar location factor could be reduced to $1/0.85 = 1.17$. For simplification and for design purposes, a value of 1.15 is suggested.

Chun et al. (2017b) tested 26 specimens with No. 14 and No. 18 hooked bars, in which each specimen had two hooked bars placed outside column core. The specimens were designed to force a side-face blowout failure. All specimens had a high amount of confining reinforcement, with values of A_{th}/A_{hs} ranging from 0.44 to 0.88. In 20 of the specimens, the hooked bars were placed outside the confining ties, as shown in Figure 4.9.a, and were considered “unconfined” by Chun et al. (2017b). In the remaining 6 specimens, the confining ties were wrapped around the hooked bars, as shown in Figure 4.9.b; this configuration is the same as used by Sperry et al. (2015b) for hooked bars placed outside the column core, as shown in Figure 4.9.c.

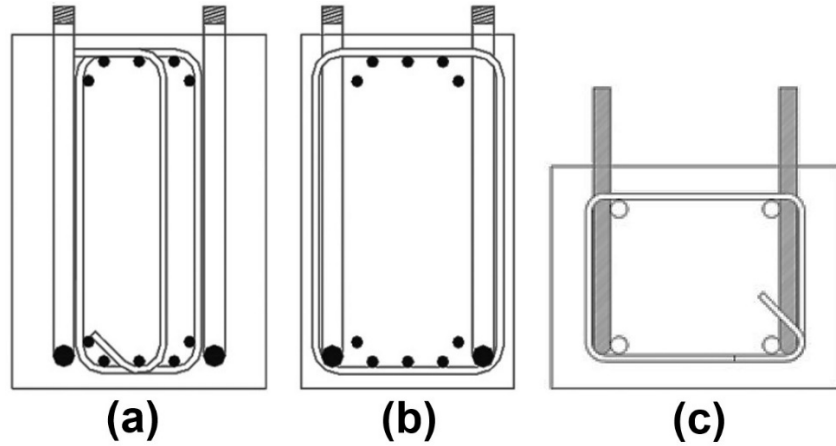


Figure 4.9 Confining reinforcement layouts in specimens with hooked bars placed outside the column core: (a) hooks outside the confining ties (Chun et al. 2017b), (b) hooks inside confining ties (Chun et al. 2017b), and (c) hooks inside confining ties (Sperry et al. 2015b)

Table 4.12 presents T/T_h based on Eq. (4.5) and (4.7) for the 26 specimens tested by Chun et al. (2017b). The specimens with hooks inside the confining ties are identified by Chun et al. as “confined” with a “C” at the end of the specimen ID. T/T_h is calculated for two cases. In the first case (second to last column), the confining reinforcement is counted as being effective and used to calculate T_h . In the second case (last column), the confining reinforcement is not counted for the specimens with hooks placed outside the confining ties (Figure 4.9a).

Table 4.12 Test-to-calculated ratio T/T_h based on Eq. (4.5) and (4.7) for specimens with No. 14 and No. 18 hooked bars placed outside column core by Chun et al. (2017b)

Specimen ID	n	ℓ_{eh}	f_{cm}	d_b	s/d_b	A_{th}/A_{hs}	T	T/T_h ^[2]	T/T_h ^[3]
		in.	psi	in.			kips		
D43-L10-C1-S42	2	16.9	6440	1.693	9.6	0.88	115.3	0.44	1.07
D43-L10-C1-S42-C ^[1]	2	16.9	6950	1.693	9.6	0.59	168.9	0.79	N/A
D43-L10-C1-S70	2	16.9	10010	1.693	9.6	0.88	123.2	0.44	1.01
D43-L10-C2-S42	2	16.9	7020	1.693	9.6	0.88	131.5	0.49	1.19
D43-L13-C1-S42	2	22.0	7020	1.693	9.6	0.88	144.9	0.48	0.98
D43-L13-C1-S42-C ^[1]	2	22.0	7020	1.693	9.6	0.59	170.7	0.68	N/A
D43-L13-C1-S70	2	22.0	10600	1.693	9.6	0.88	142.4	0.44	0.86
D43-L13-C2-S42	2	22.0	7020	1.693	9.6	0.88	154.5	0.51	1.05
D43-L16-C1-S42	2	27.1	7020	1.693	9.6	0.88	163.2	0.48	0.88
D43-L16-C1-S42-C ^[1]	2	27.1	7020	1.693	9.6	0.59	177.5	0.61	N/A
D43-L16-C1-S70	2	27.1	10010	1.693	9.6	0.88	172.7	0.48	0.84
D43-L16-C2-S42	2	27.1	7020	1.693	9.6	0.88	181.9	0.53	0.98
D43-L20-C1-S42	2	33.9	7020	1.693	9.6	0.88	172.0	0.44	0.72
D57-L10-C1-S42-a	2	22.6	5450	2.257	7.2	0.66	147.2	0.36	0.92
D57-L10-C1-S42-b	2	22.6	6150	2.257	7.2	0.66	150.4	0.36	0.91
D57-L10-C1-S42-C ^[1]	2	22.6	5450	2.257	7.2	0.44	223.2	0.68	N/A
D57-L10-C2-S42	2	22.6	5450	2.257	7.2	0.66	214.6	0.52	1.34

D57-L13-C1-S42-a	2	29.3	5450	2.257	7.2	0.66	236.4	0.51	1.11
D57-L13-C1-S42-b	2	29.3	6150	2.257	7.2	0.66	232.6	0.49	1.05
D57-L13-C1-S42-C ^[1]	2	29.3	5450	2.257	7.2	0.44	254.2	0.66	N/A
D57-L13-C2-S42	2	29.3	5450	2.257	7.2	0.66	273.4	0.59	1.28
D57-L16-C1-S42-a	2	36.1	5450	2.257	7.2	0.66	254.0	0.49	0.95
D57-L16-C1-S42-b	2	36.1	6150	2.257	7.2	0.66	284.0	0.53	1.02
D57-L16-C1-S42-C ^[1]	2	36.1	5450	2.257	7.2	0.44	279.6	0.64	N/A
D57-L16-C2-S42	2	36.1	6530	2.257	7.2	0.66	318.8	0.59	1.13
D57-L20-C1-S42	2	45.1	6530	2.257	7.2	0.66	328.4	0.53	0.91
							Max	0.79	1.34
							Min	0.36	0.61
							Mean	0.53	0.93
							CoV	0.192	0.210

^[1] Specimens with hooks placed inside the confining ties (Figure 4.9b)

^[2] Confining reinforcement counted towards anchorage strength

^[3] Confining reinforcement taken as not contributing to anchorage strength

As shown in Table 4.12, if the ties are taken as contributing to anchorage strength, T/T_h ranges from 0.36 to 0.89, with a mean of 0.53. The very low average indicates that confining reinforcement in specimens with hooks placed outside the confining ties (Figure 4.9.a) do not contribute to anchorage strength. If these specimens are treated as containing no confining reinforcement, the T/T_h ratio ranges from 0.61 to 1.34 with a mean of 0.93. Since the hooked bars were placed outside column core in all these specimens, a bar location factor of 1.17 should be applied, increasing the average T/T_h to 1.09, which is within the range of the coefficient of variation of the developed descriptive equations, Eq. (4.5) and (4.7).

For the six “confined” specimens (hooked bars inside confining ties, Figure 4.9.b), ties are counted towards anchorage strength and $A_{th}/A_{hs} = 0.4$ is used in calculating T_h , resulting in T/T_h ratio ranging from 0.72 to 0.92 with a mean of 0.79, after applying the bar location factor of 1.17. This indicates these specimens were weaker than similar specimens with respect to descriptive equations. For comparison, for the specimens by tested by Sperry et al. (2015b) and Ajaam et al. (2017) with a similar layout (shown in Figure 4.9c), T/T_h ranged from 0.68 to 1.25 with a mean of 0.96 after applying the bar location factor of 1.17. The lower T/T_h for specimens tested by Chun et al. (2017b) could be attributed to having a small concrete side cover, just $1d_b$ for No. 14 and No. 18 bars (to force a side-face blowout failure), whereas Ajaam et al. (2017) used 2.4 or $4d_b$ for No. 5 bars, 2.5 , 3.5 , or $4d_b$ for No. 8 bars, and $1.8d_b$ for No. 11 bars.

The justification for counting confining reinforcement towards anchorage strength when hooks are placed inside the confining ties (Figure 4.9.b and c) is that the tale of the hook is wrapped

by the column ties, thus mobilizing the outside longitudinal reinforcing bars when the hooked bars are being pulled out during the test. A direct design recommendation can be drawn from this observation; if the hooked bars are placed outside the column core and confining ties, the confining reinforcement should not be counted towards contributing to anchorage strength.

4.4.2 Confining Reinforcement

The effect of confining reinforcement on the anchorage strength of hooked bars is discussed in this section. Given the very limited number of specimens with No. 14 and No. 18 bars, earlier test results for No. 11 and smaller bars are also used in the analyses (Searle et al. 2014, Sperry et al. 2015a, 2015b, 2017a, 2017b, 2018, Yasso et al. 2017, Ajaam et al. 2017, 2018). The values of T/T_h based on new descriptive equations, Eq. (4.5) and (4.7), for specimens with confining reinforcement are compared with respect to A_{th}/A_{hs} in Figure 4.10. The details of these specimens are presented in Tables B.4 and B.5 of Section B3 in Appendix B.

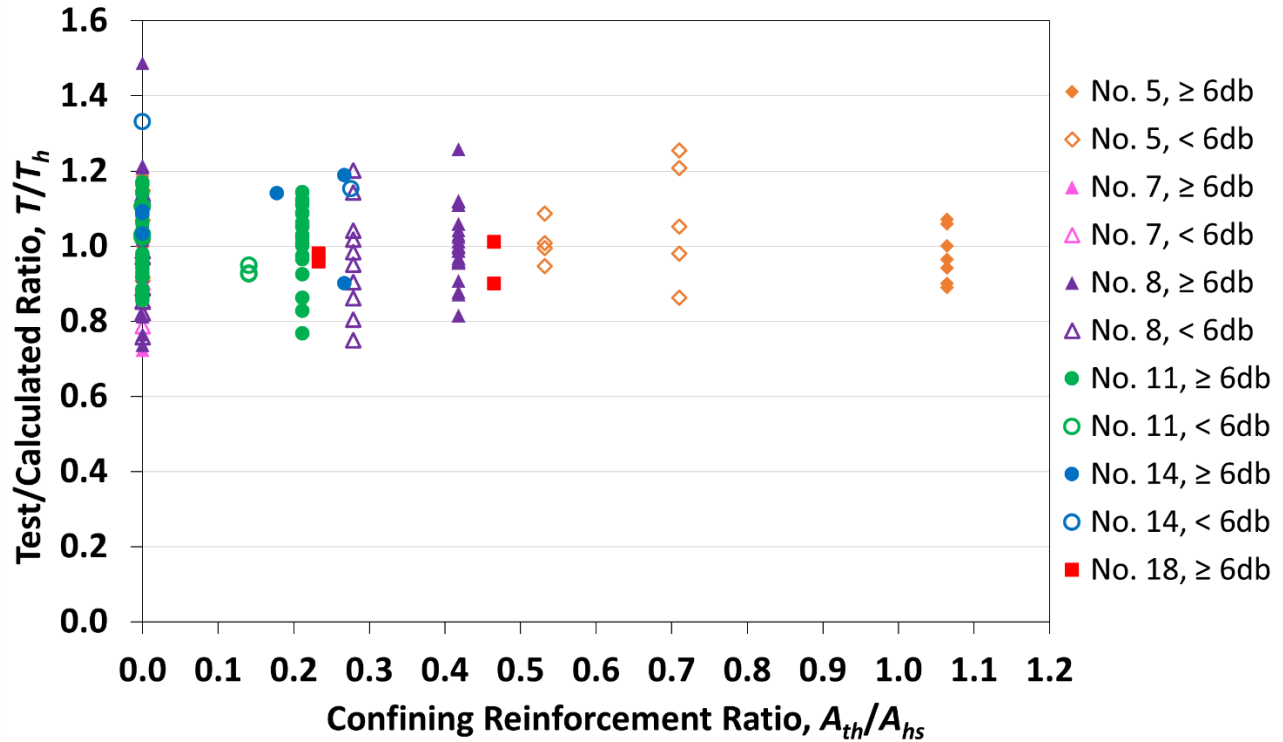


Figure 4.10 Test-to-calculated ratio T/T_h based on new descriptive equations, Eq. (4.5) and (4.7), for hooked bars versus confining reinforcement ratio A_{th}/A_{hs}

As shown in Figure 4.10, the A_{th}/A_{hs} ratio ranged from 0.14 to 1.06 for the specimens with confining reinforcement. The mean value of A_{th}/A_{hs} was 0.40 for all specimens. Values above 0.5 pertain solely to the No. 5 bars. No trend is evident, indicating the insensitivity of the descriptive

equations to the term A_{th}/n in Eq. (4.7). Since no bars larger than No. 8 had A_{th}/A_{hs} above 0.5, a cap on A_{th}/A_{hs} would be appropriate to consider for design purposes, as discussed in Chapter 6. Figure 4.10 also shows that, generally, the No. 14 and No. 18 bar specimens performed in a manner similar to the No. 11 and smaller bar specimens with comparable values of A_{th}/A_{hs} .

As discussed previously, the provisions in ACI 318-19 give no credit to confining reinforcement for hooked bars larger than No. 11, mainly due to a lack of test data on No. 14 and No. 18 bars. As shown in the test program for hooked bars (Table 2.5), the No. 14 and No. 18 hooked bar specimens were designed in pairs: one specimen without and the other specimen with confining reinforcement in the joint region, while keeping the dimensional properties, bar size, and bar spacing the same. The embedment lengths for each pair had close values (differing only within construction tolerances), with the exception of H14-1/H14-2, H14-3/H14-4, and H18-1/H18-2. Specimen H14-1 had a 2.2 in. longer embedment length than H14-2 (27.0 versus 24.8 in.), and specimen H14-3 had 1.8 in. longer embedment length than its companion H14-4 (36.7 versus 34.9 in.). Specimen H18-1 had a 1.5 in. longer embedment length than its companion H18-2 (28.5 in. versus 27.0 in.). The specimens in a pair were cast with the same concrete, but the measured concrete compressive strengths were slightly different due to different testing dates. Similarly, the No. 18 hooked bar specimens were also cast in pairs, with the second specimen in each pair having a higher quantity of confining reinforcement than the first.

Based on the results given in Table 4.1, providing confining reinforcement in the joint region contributes to the anchorage strength of No. 14 and No. 18 hooked bars. Comparing specimens without and with confining reinforcement in the joint region reveals that ties parallel to the straight portion of a hooked bar increase the anchorage strength for both widely-spaced ($s/d_b \geq 6$) and closely-spaced ($s/d_b < 6$) hooked bars. Figures 4.11 and 4.12 show bar charts displaying the anchorage strengths of the specimens in each pair of specimens for No. 14 and No. 18 hooked bars, respectively. The T/T_h ratios for each specimen are provided for comparison.

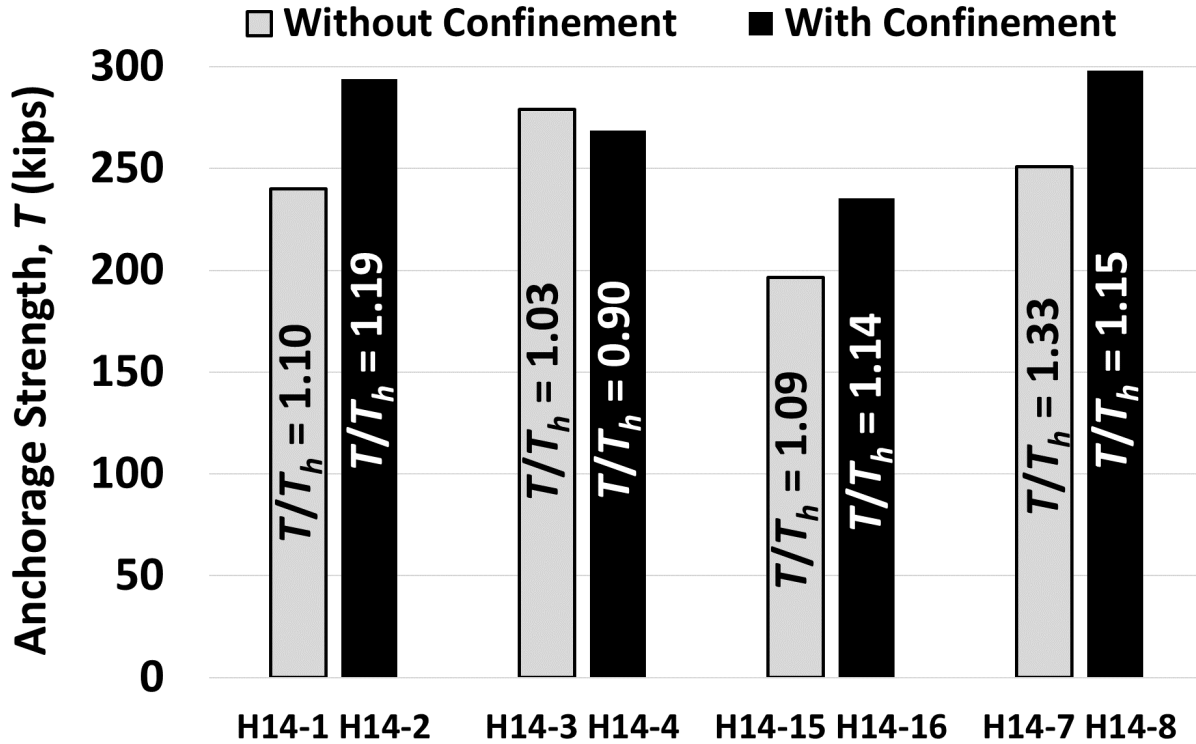


Figure 4.11 Comparing anchorage strength of No. 14 hooked bars for confining reinforcement. T/T_h ratios shown based on Eq. (4.5) and (4.7). Center-to-center spacing is $3.5d_b$ for specimens H14-7 and H14-8 (closely-spaced), and $10.6d_b$ for all other specimens (widely-spaced)

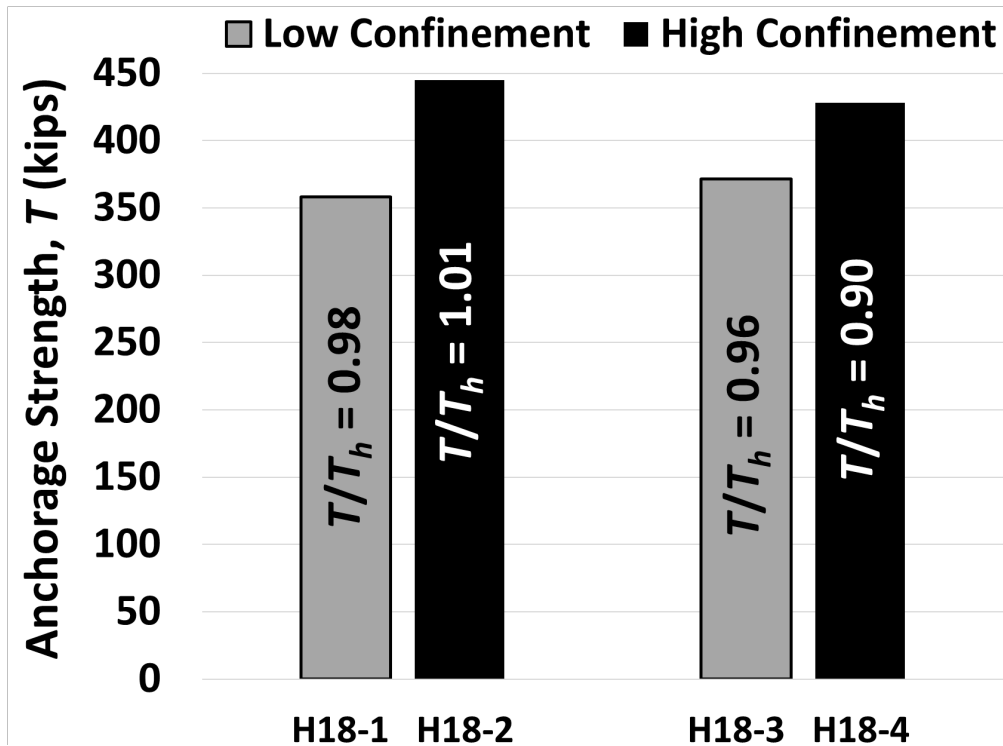


Figure 4.12 Comparing anchorage strength of No. 18 hooked bars for confining reinforcement. T/T_h ratios shown on top of each bar. Hooked bars have center-to-center spacing of $6d_b$.

As shown in Figures 4.11 and 4.12, the anchorage strength of the specimens with confining reinforcement or with the greater amount of confining reinforcement is higher than that of the companion specimen, with the exception of specimens H14-3 and H14-4, for which $T = 279.1$ kips and $T = 268.5$ kips, respectively. This might be attributed to the longer average embedment length in specimen H14-3 (36.7 in. compared with 34.9 in.) or to natural variability in test results. For the pair H14-1 and H14-2, the specimen with ties (H14-2) had a higher anchorage strength despite having a shorter average embedment length. Similarly, for the pair H18-1/H18-2, the specimen with a greater quantity of confining reinforcement (H18-2) had a higher anchorage strength than its companion despite having a shorter embedment length.

As discussed before, all hooked bar specimens were tested under loading condition A, in which the joint shear demand is equal to 80% of the load applied to the bars. All hooked bar specimens, even the four specimens without ties, carried the joint shear and exhibited an anchorage failure, whereas shear-like failures, as described in Section 3.2.2, were observed in headed bars under similar conditions, as will be discussed in Chapter 5. These observations reveal the distinct role of the tail of the hook in carrying the joint shear by preventing the inclined crack in the joint from propagating towards the back of the column.

Overall, the findings of this study indicate that the contribution by the ties in the joint region to the anchorage strength of hooked bars as large as No. 14 and No. 18 should be included in the ACI 318 Code.

4.4.3 Bar Spacing

As mentioned in Section 4.3.2, bar spacing is used as a useful proxy for a bar group effect on anchorage strength. In the database, bar spacing and number of bars are tied together, and it is not possible to separate the individual effects; therefore, the choice was made to continue using center-to-center bar spacing to represent the observed effect, done in previous studies, although the actual mechanism is not clear.

The relationship between spacing and the anchorage strength of hooked bars is discussed in Sections 4.3.2 and 4.3.4. The ratio of test-to-calculated failure load, T/T_h , is compared as a function of the center-to-center bar spacing normalized by bar diameter (s/d_b) in Figure 4.13.

As shown in Figure 4.13, no noticeable positive or negative trend can be observed for the data as a whole, indicating the match between the test results and the descriptive equation is not affected by s/d_b . It can also be observed that the results for No. 14 and No. 18 specimens fall within

the corresponding cluster of data points for both closely-spaced and widely spaced bars, suggesting that the relationship between bar spacing and anchorage strength as established for No. 11 and smaller bars is similar for larger bars. Of the specimens with closely-spaced bars, the highest T/T_h ratio belongs to the No. 14 bar specimen with three bars spaced at $3.5d_b$ on-center and no confining reinforcement (specimen H14-7).

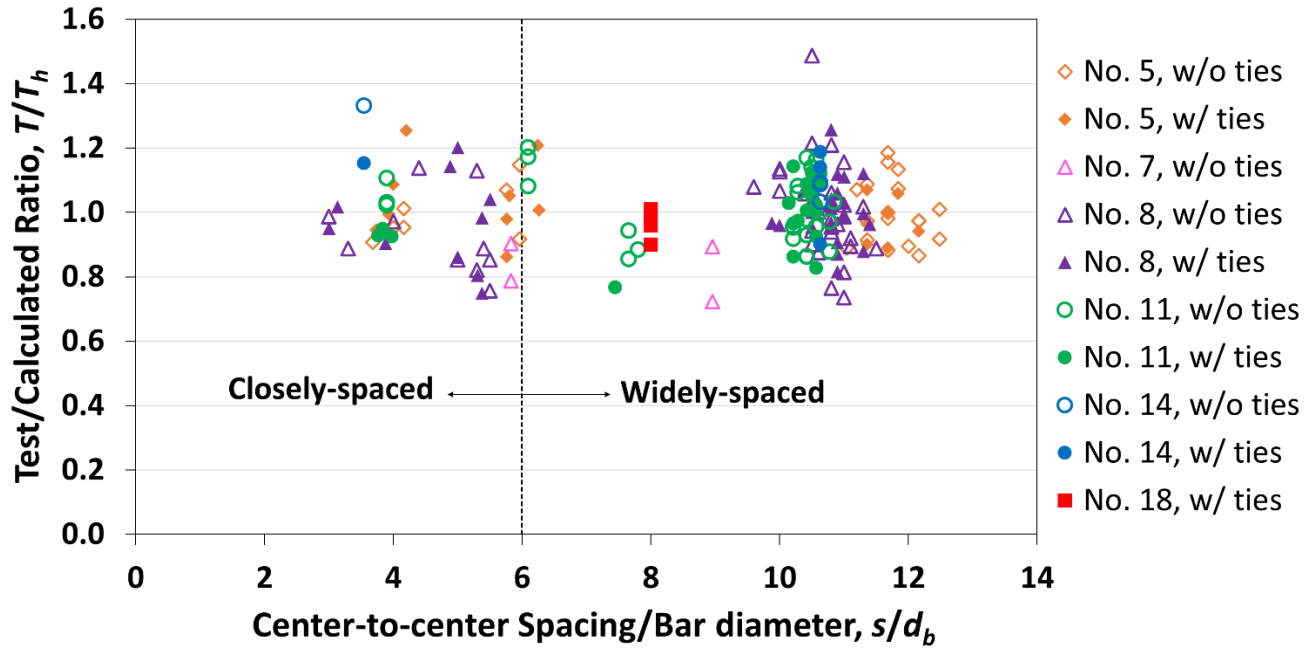


Figure 4.13 Test-to-calculated ratio T/T_h versus ratio of center-to-center spacing to bar diameter s/d_b based on Eq. (4.5) and (4.7), for hooked bar specimens used to develop the equations

4.4.4 Strut Angle

For hooked bars, the compression strut angle is defined as the angle from the centerline of the straight portion of the bar to an inclined line drawn between the intersection of the centerlines of the straight portion and tail of the hook and the center of the bearing plate simulating the compression zone of the imaginary beam, as shown in Figure 4.14. Among previous studies, Joh et al. (1993) and Coleman et al. (2023) investigated the influence of strut angle on anchorage strength. Joh et al. (1993) evaluated five specimens with the same column depth and proportions, but different embedment lengths, and observed that a decrease in strut angle θ resulted in an increase in anchorage strength. As shown in Figure 4.14, however, a decrease in θ will result from increasing the embedment length, which is, of course, expected to increase anchorage strength. This was also the case with the study by Coleman et al. (2023), as discussed later. A key point

often raised in a discussion of the effect of strut angle on anchorage strength of beam reinforcement in beam-column joints is the observed decrease in strength once the effective depth of a member exceeds $1.5\ell_{eh}$. This is discussed in Section 4.4.5. The results addressed in this section are for specimens in which the effective depth was less than or equal to $1.5\ell_{eh}$.

Any relationship between the strut angle and the test results for the specimens used in developing Eq. (4.5) and (4.7), including No. 14 and No. 18 bar specimens in this study (see Tables B.2 through B.5 in Section B3 in Appendix B) can be observed by comparing T/T_h versus θ for the specimens, as shown in Figure 4.15. The strut angle θ is calculated as the inverse tangent of the ratio x_{mid}/ℓ_{eh} , where x_{mid} is the distance from the center of the hooked bars to the center of the bearing plate representing the compression region of the simulated beam.

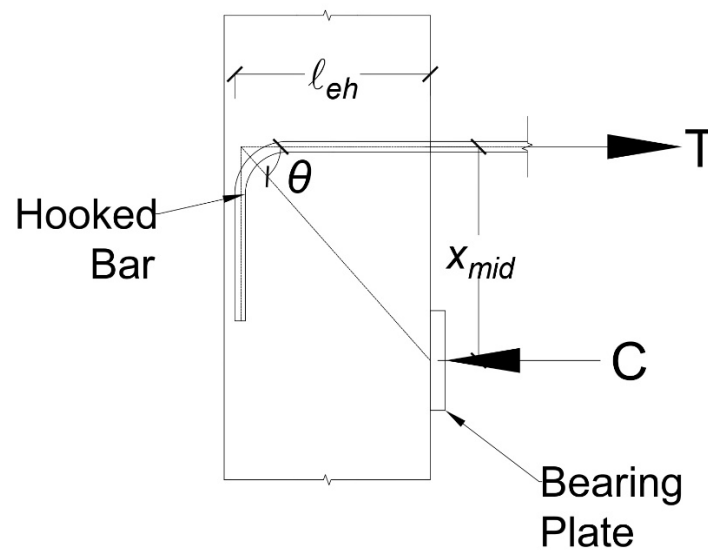


Figure 4.14 Definition of compression strut angle (θ) for hooked bars

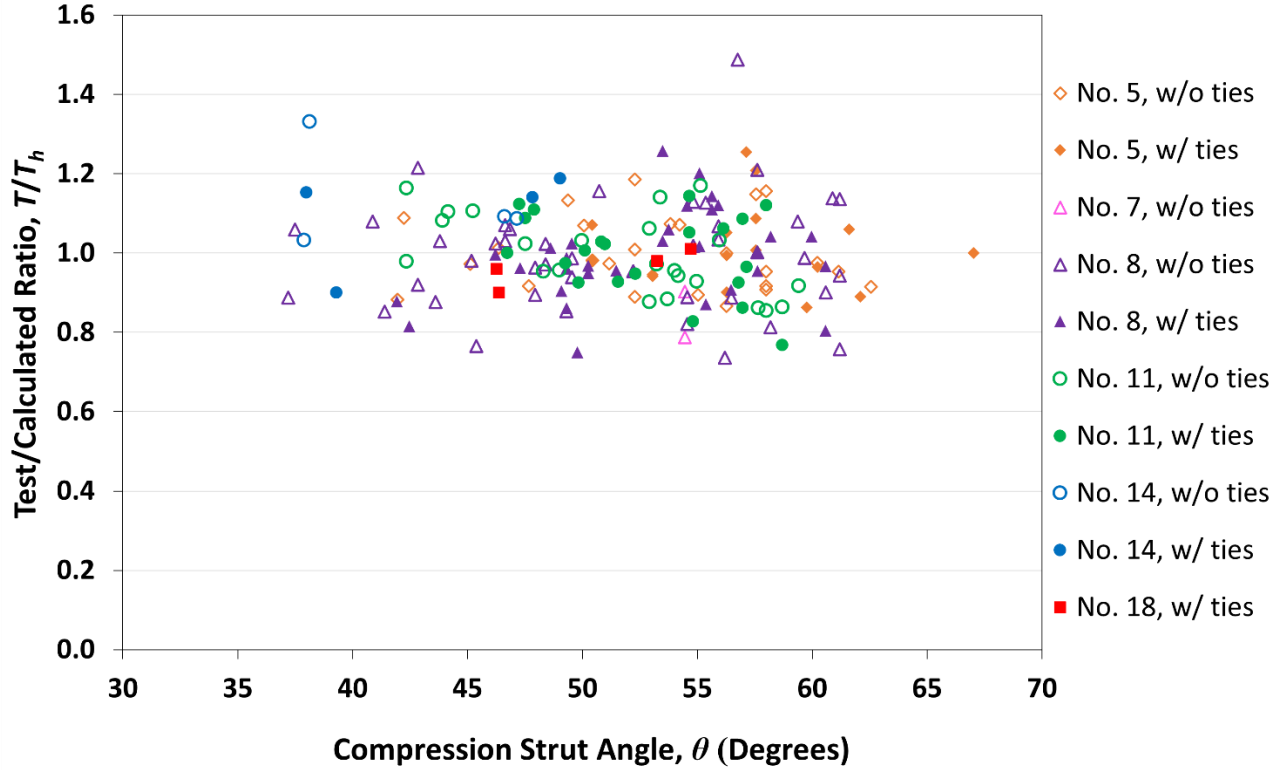


Figure 4.15 Test-to-calculated T/T_h ratio based on Eq. (4.5) and (4.7) versus compression strut angle θ for hooked bar specimens used to develop descriptive equations (not including specimens with $d_{eff}/\ell_{eh} > 1.5$)

As shown in Figure 4.15, there appears to be, at most, a weak negative trend, with T/T_h decreasing as the strut angle θ increases up to 60° , with a somewhat greater drop for the small number of specimens with $\theta > 60^\circ$, with 10 out of the 14 specimens in this range having $T/T_h < 1.0$. On the other hand, of the six specimens with a strut angle $\theta < 40^\circ$, four have $T/T_h > 1.0$, three of which are No. 14 bar specimens. The No. 14 and No. 18 bar specimens with $45^\circ < \theta < 55^\circ$ fall within the cloud of data points along with other bar sizes and do not exhibit a trend. Overall, Figure 4.15 indicates that descriptive equations are insensitive to strut angle.

The conclusion drawn here differs from that by Joh et al. (1993), as well as that in a recent study by Coleman et al. (2023), in which, like Joh et al., Coleman et al. also compared the strut angle θ with the bar stress at failure (f_{su}) normalized by concrete compressive strength (f_{cm}) to the 0.29 power, $f_{su} / f_{cm}^{0.29}$. The 0.29 power was chosen based on the descriptive equations developed by Sperry et al. (2015b). Coleman et al. (2023) observed a significant decrease in $f_{su} / f_{cm}^{0.29}$ with increase in θ and concluded that strut angle negatively affects the anchorage strength of hooked bars. Also, like Joh et al., however, Coleman et al. made a logical error, missing the point that the

increase in strut angle coincides with a decrease in the embedment length, as shown in Figure 4.16, where θ is plotted as a function of embedment length normalized by bar diameter, ℓ_{eh}/d_b , for specimens used to develop descriptive equations, Eq. (4.5) and (4.7). Bars of a given size are grouped together in the figure because each had a different value of x_{mid} .

Coleman et al. (2023) did make some comparisons for specimens with the same embedment length, but with increasing member depths, and made a similar observation. In that comparison, the reduction in anchorage strength with increasing strut angle only occurred for members with ratios of depth to embedment length over 1.5, a point that is discussed next in Section 4.4.5.

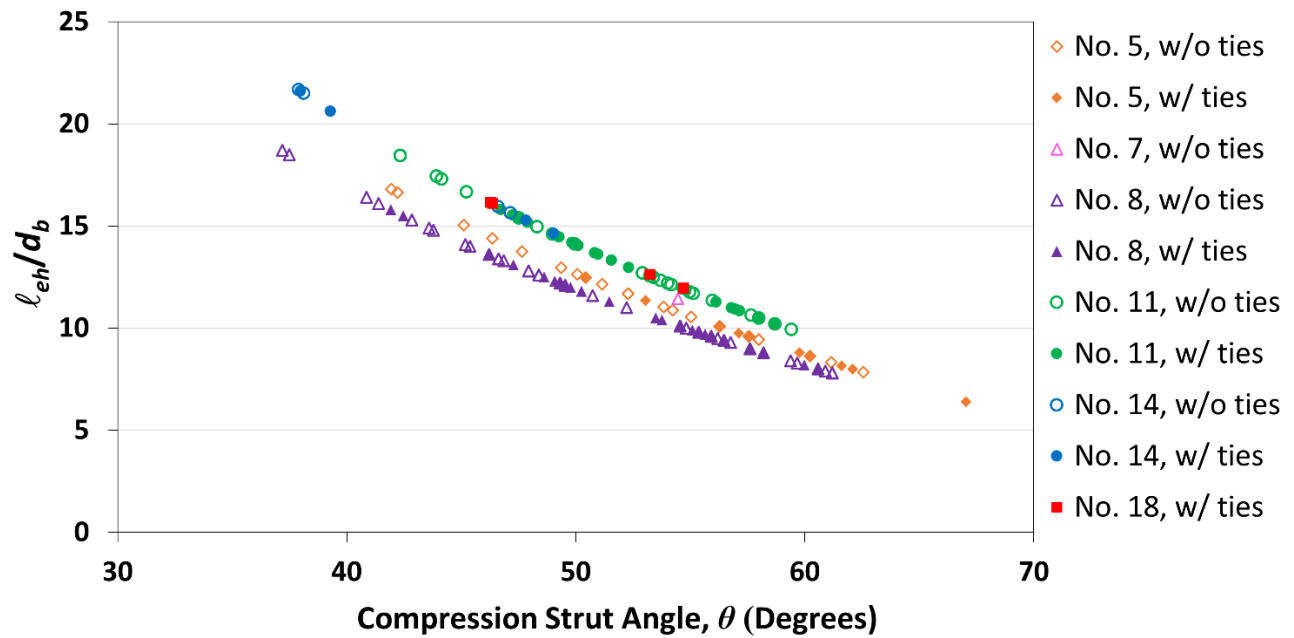


Figure 4.16 ℓ_{eh}/d_b versus compression strut angle θ for hooked bar specimens used to develop descriptive equations, Eq. (4.5) and (4.7)

4.4.5 Effective Beam Depth

The ratio of effective beam depth to embedment length, d_{eff}/ℓ_{eh} , is another parameter shown to affect the anchorage strength of hooked bars. For this analysis, the effective beam depth is defined in Figure 4.17 and is calculated as the sum of h_{cl} and c , where h_{cl} is the distance measured from the center of the hooked bars to the top edge of the bearing plate and c is the calculated neutral axis depth. c is calculated as a/β_1 , where a is the depth of equivalent rectangular compressive stress block and calculated as $nA_b f_s / 0.85 f_{cm} b$ per the flexural design procedure for reinforced concrete beams, $\beta_1 = 0.85 - 0.05((f_{cm} - 4000)/1000) \leq 0.65$ per Section 22.2.2.4.3 of ACI 318-19, and b is the

width of the specimen. Ajaam et al. (2017) showed that when $d_{eff}/\ell_{eh} > 1.5$ (deeper beam), specimens generally have a lower anchorage strength.

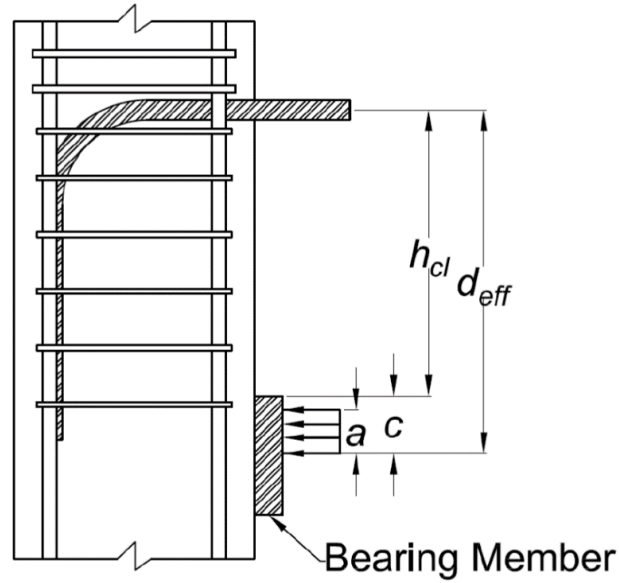


Figure 4.17 Effective beam depth d_{eff} for hooked bars (Ajaam et al. 2017)

Variations of T/T_h ratio with respect to d_{eff}/ℓ_{eh} for the hooked bar specimens used to develop descriptive equations, Eq. (4.5) and (4.7), are shown in Figure 4.18, plus specimens with $d_{eff}/\ell_{eh} > 1.5$ for comparison. Details of specimens with $d_{eff}/\ell_{eh} > 1.5$ are presented in Table B.7 in Section B3 of Appendix B.

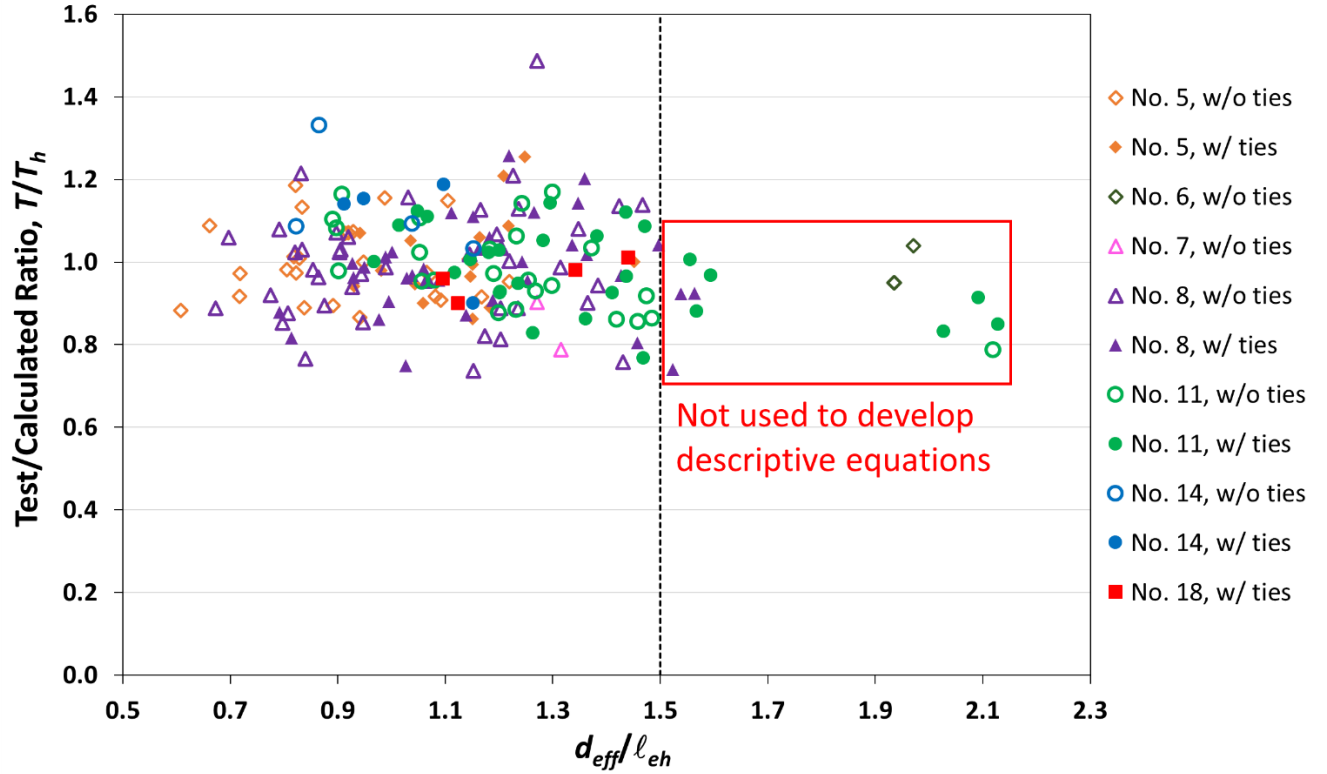


Figure 4.18 Test-to-calculated T/T_h ratio based on Eq. (4.5) and (4.7) versus effective beam depth to embedment length d_{eff}/ℓ_{eh} ratio for hooked bar specimens used to develop descriptive equations plus specimens with $d_{eff}/\ell_{eh} > 1.5$

As shown in Figure 4.18, all but two specimens with $d_{eff}/\ell_{eh} > 1.5$ have a T/T_h ratio < 1.0 . No noticeable positive or negative trend, however, is observed for the rest of the specimens, including those with No. 14 and No. 18 hooked bars, indicating that anchorage strength of hooked bars, as represented by those in the database, is not affected by the d_{eff}/ℓ_{eh} ratio when $d_{eff}/\ell_{eh} < 1.5$.

4.4.6 Embedment Length

Figure 4.19 compares T/T_h with the ℓ_{eh}/d_b ratio for the specimens used to develop descriptive equations. The figure shows that, generally, there is a no noticeable trend in T/T_h with increasing ℓ_{eh}/d_b . Of the specimens with the highest ℓ_{eh}/d_b ratio, four had No. 14 bars with $\ell_{eh}/d_b > 20$, three of which had $T/T_h > 1.0$.

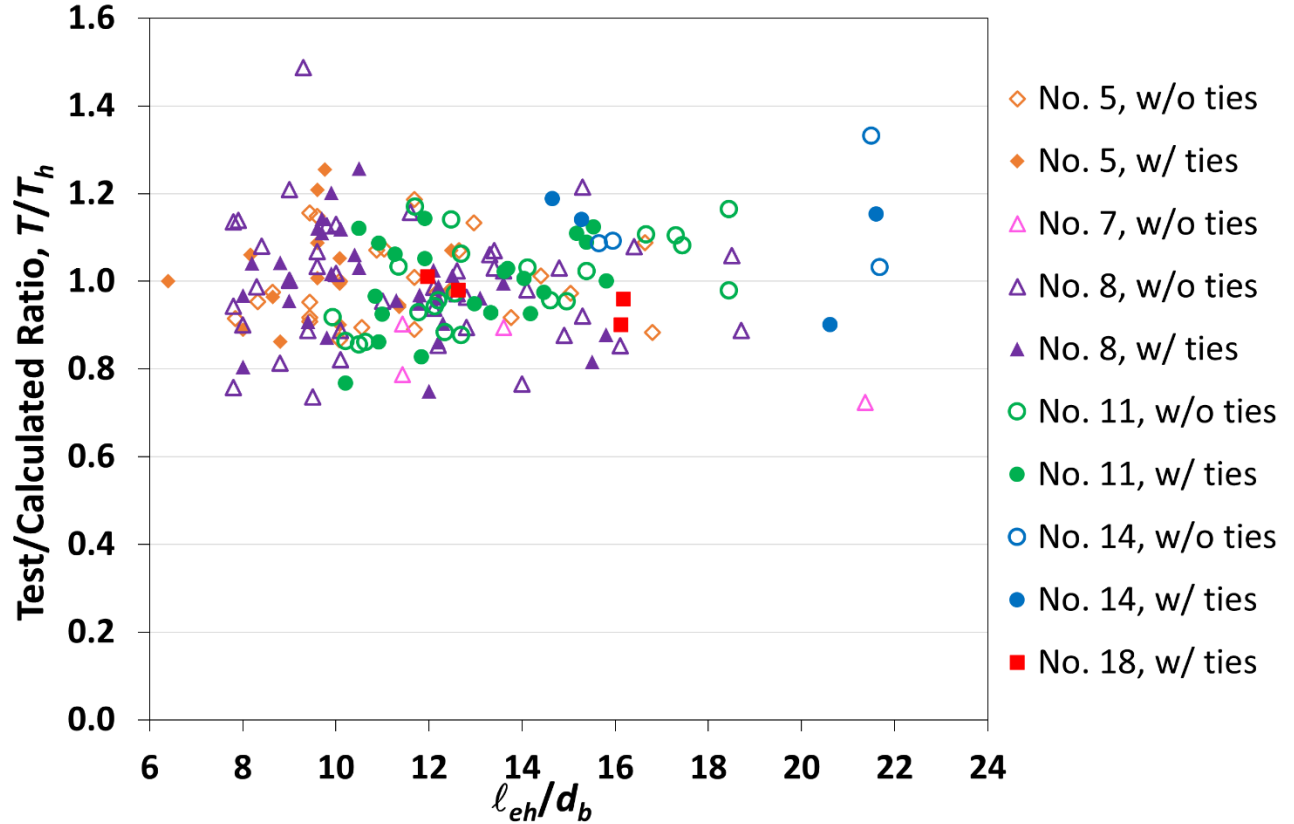


Figure 4.19 Test-to-calculated T/T_h ratio based on Eq. (4.5) and (4.7) versus embedment length to bar diameter ℓ_{eh}/d_b ratio for hooked bar specimens used to develop descriptive equations

4.5 SPECIMENS NOT USED TO DEVELOP DESCRIPTIVE EQUATIONS

In Section 4.3, Eq. (4.5) and (4.7) were developed to represent the anchorage strength of hooked bars by incorporating the results for No. 14 and No. 18 bar specimens in this study into the database used by Ajaam et al. (2017). The database included No. 11 bar and smaller hooked bar specimens tested at the University of Kansas (Searle et al. 2014, Sperry et al. 2015a, 2015b, 2017a, 2017b, 2018, Yasso et al. 2017, Ajaam et al. 2017, 2018) as well as two No. 7 bar specimens by Lee and Park (2010), two No. 7 bar specimens by Hamad et al. (1993), and three No. 11 bar specimens by Ramirez and Russell (2008). The details of these specimens are presented in Tables B.2 through B.5 in Section B3 (specimens tested at the University of Kansas) and Table B.8 in Section B4 (specimens tested in other studies) in Appendix B. As described in Section 4.3, three No. 6 bar specimens by Ramirez and Russell (2008) were originally included in the database but not used in this study because they had d_{eff}/ℓ_{eh} values > 1.5 . Those specimens are included in the analysis below.

In this section, the anchorage strengths based on the test results T for beam-column joint specimens tested in other studies and not used to develop descriptive equations are compared with those calculated using Eq. (4.5) and (4.7), T_h . The studies include those by Marques and Jirsa (1975), Pinc et al. (1977), Hamad et al. (1993), Ramirez and Russell (2008), and Lee and Park (2010). The specimens tested by Chun et al. (2017b) are covered in Section 4.4. The specimens tested by Marques and Jirsa (1975) (see Figure 1.3), discussed in detail later in this section, had narrow, short columns that reduced the force carried by the joint and an unrealistic reinforcement layout. The same is true of the specimens tested by Pinc et al. (1977). Some specimens tested by Hamad et al. (1993), Ramirez and Russell (2008), and Lee and Park (2010) were used by Ajaam et al. (2017) to develop the descriptive equations and were retained for that purpose in this study. The specimens tested by Hamad et al. (1993), Ramirez and Russell (2008), and Lee and Park (2010) that are discussed in this section were excluded for the same reasons they were excluded by Ajaam et al. (2017) when developing the descriptive equations: “because the number of the specimens was relatively small, 12 in total, and because of the inherent variability in the contribution of confining reinforcement to the anchorage strength of hooked bars as a result of the variations in test setup.” Table 4.13 shows a summary of these specimens, their key properties, and their T/T_h ratio based on Eq. (4.5) and (4.7). Full details of the specimens are presented in Table B.8 of Section B4 in Appendix B.

Table 4.13 Test-to-calculated T/T_h ratio based on Eq. (4.5) and (4.7) for specimens tested outside University of Kansas and not used to develop Eq. (4.5) and (4.7)

Study	Specimen ID	n	ℓ_{eh}	f_{cm}	d_b	s/d_b	A_{th}/A_{hs}	T	T_h	T/T_h
			in.	psi	in.			kips	kips	
Marques and Jirsa (1975)	J7-180-12-1-H	2	10.0	4350	0.875	6.1	0	36.6	38.8	0.94
	J7-180-15-1-H	2	13.0	4000	0.875	6.1	0	52.2	50.6	1.03
	J7-90-12-1-H	2	10.0	4150	0.875	6.1	0	37.2	38.3	0.97
	J7-90-15-1-H	2	13.0	4600	0.875	6.1	0	54.6	52.6	1.04
	J7-90-15-1-L	2	13.0	4800	0.875	6.1	0	58.2	53.3	1.09
	J7-90-15-1-M	2	13.0	5050	0.875	6.1	0	60.0	54.0	1.11
	J11-180-15-1-H	2	13.1	4400	1.41	3.4	0	70.2	50.1	1.40
	J11-90-12-1-H	2	10.1	4600	1.41	3.4	0	65.5	38.0	1.72
	J11-90-15-1-H	2	13.1	4900	1.41	3.4	0	74.9	50.6	1.48
	J11-90-15-1-L	2	13.1	4750	1.41	3.4	0	81.1	51.2	1.58
	J 7- 90 -15 -3a - H ^[1]	2	13.0	3750	0.875	6.1	0.367	58.8	53.8	1.09
	J 7- 90 -15 -3 - H ^[1]	2	13.0	4650	0.875	6.1	0.183	62.4	51.9	1.20
	J 11- 90 -15 -3a - L ^[1]	2	13.1	5000	1.41	3.4	0.282	107.6	72.5	1.48
	J 11- 90 -15 -3 - L ^[1]	2	13.1	4850	1.41	3.4	0.141	96.7	61.1	1.58

Pinc et al. (1977)	9-12	2	10.0	4700	1.13	4.5	0	47.0	36.6	1.28
	11-15	2	13.1	5400	1.41	3.4	0	78.0	47.6	1.64
	11-18	2	16.1	4700	1.41	3.4	0	90.5	57.5	1.57
Hamad et al. (1993)	11-90-U	2	13.0	2570	1.41	3.4	0	48.0	42.8	1.12
	11-90-U*	2	13.0	5400	1.41	3.4	0	75.0	52.7	1.42
	11-180-U-HS	2	13.0	7200	1.41	3.4	0	58.8	57.2	1.03
	11-90-U-HS	2	13.0	7200	1.41	3.4	0	73.8	57.2	1.29
	11-90-U-T6	2	13.0	3700	1.41	3.4	0.141	71.8	93.2	0.77
	7-180-U-T4	2	10.0	3900	0.88	6.1	0.183	34.6	32.2	1.08
	11-90-U-T4	2	13.0	4230	1.41	3.4	0.212	83.2	75.3	1.10
	7-90-U-SC ^[1]	2	10.0	4230	0.88	8.4	0	29.9	40.2	0.87
Ramirez and Russell (2008)	I-1 ^[2]	2	6.5	8910	0.75	12.3	0	30.0	28.8	1.04
	I-3 ^[2]	2	6.5	12460	0.75	12.3	0	30.0	31.7	0.95
	I-5 ^[2]	2	6.5	12850	0.75	12.3	0	30.5	31.9	0.95
	I-6	2	12.5	12850	1.41	6.1	0	114.0	86.4	1.32
	III-13	2	6.5	13980	0.75	12.3	0.500	41.3	42.6	0.97
	III-15	2	6.5	16350	0.75	12.3	0.500	38.5	44.0	0.87
	III-14	2	12.5	13980	1.41	6.1	0.212	105.0	111.3	0.94
	III-16	2	12.5	16500	1.41	6.1	0.212	120.0	115.5	1.04
Lee and Park (2010)	H3	2	15.0	4450	0.88	9.0	0.367	53.8	75.1	0.72
									Max	1.72
									Min	0.72
									Mean	1.18
									CoV	0.224

^[1] Hooked bars outside column core, bar location factor of 1.17 applied to T/T_h

^[2] Specimens had $d_{eff}/\ell_{eh} > 1.5$

The values of T/T_h for the specimens in Table 4.13 ranged from 0.72 to 1.72, with a mean of 1.18 and a coefficient of variation of 0.235. For the No. 7 and No. 11 bar specimens by Marques and Jirsa (1975), the mean T/T_h is 1.26. For the No. 9 and No. 11 bar specimens by Pinc et al. (1977), the mean T/T_h is 1.50. The mean T/T_h for the No. 7 and No. 11 bar specimens by Hamad et al. (1993) and No. 6 and No. 11 bar specimens by Ramirez and Russell (2008) are 1.12 and 0.98, respectively, both within the range of the coefficient of variation for Eq. (4.5) and (4.7), 12%.

The No. 7 bar specimens tested by Marques and Jirsa (1975) had a mean T/T_h value of 1.06. A careful look at the specimens tested by Marques and Jirsa (1975) reveals that, while the No. 7 bar specimens show a good match with the descriptive equations, the No. 11 bar specimens have

high T/T_h values with a mean of 1.54. The noticeable difference in the mean T/T_h values is despite the fact that the No. 7 bar specimens had the same specimen proportions and were tested in the same apparatus as the No. 11 bar specimens. For this reason, these specimens are investigated in more detail in terms of the test setup, specimen proportions, and applied forces.

The self-reacting system used to test specimens at the University of Kansas studies (Searle et al. 2014, Sperry et al. 2015a, 2015b, 2017a, 2017b, 2018, Yasso et al. 2017, Ajaam et al. 2017, 2018) was a modified version of the test apparatus used by Marques and Jirsa (1975). Both systems applied forces in a manner similar to loading condition B used in this study. The forces applied to specimens by the University of Kansas test setup and Marques and Jirsa (1975) are shown schematically in Figure 4.20.

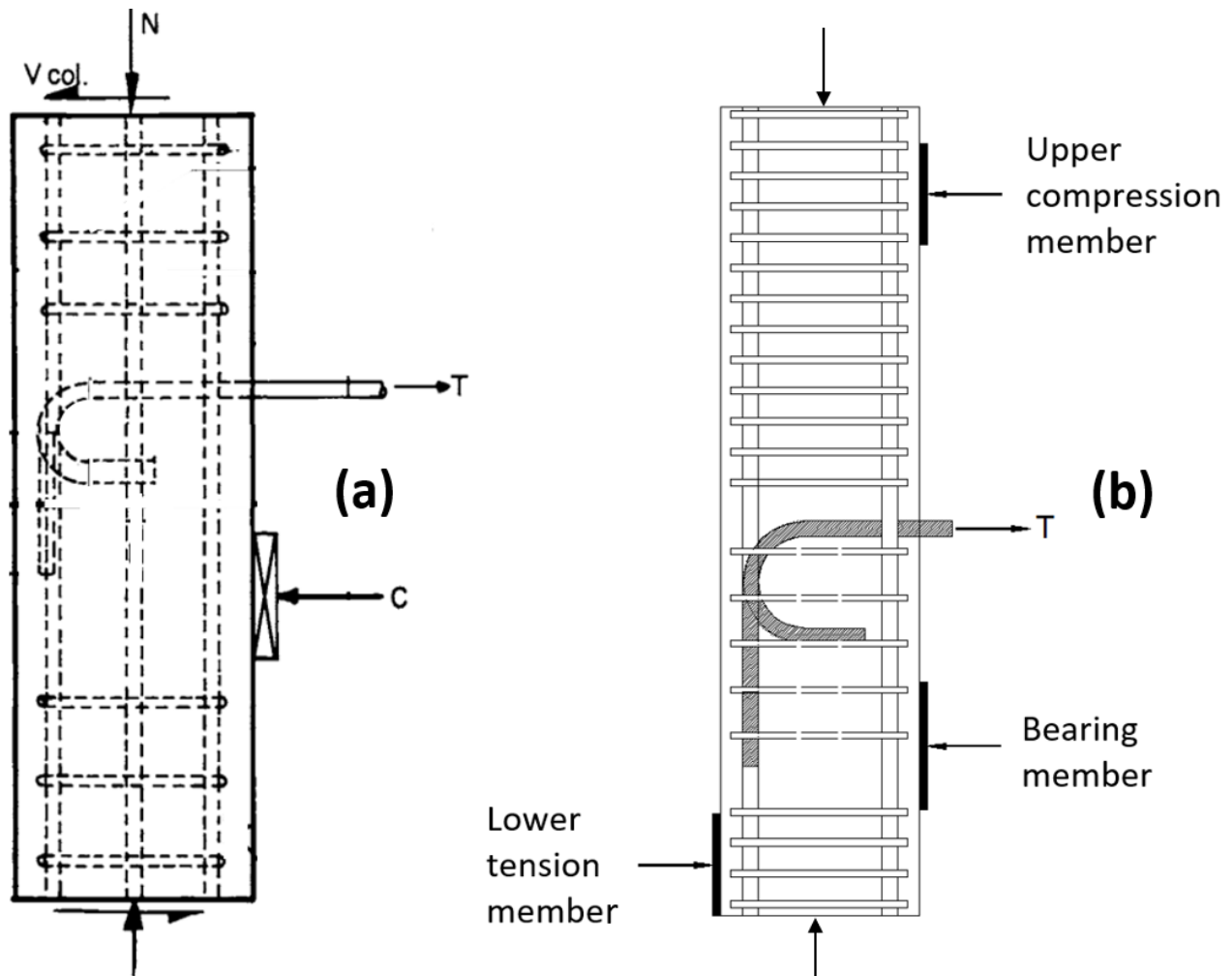


Figure 4.20 Schematic of the forces applied to specimens by (a) Marques and Jirsa (1975) and (b) University of Kansas studies (Searle et al. 2014, Sperry et al. 2015a, 2015b, 2017a, 2017b, 2018, Yasso et al. 2017, Ajaam et al. 2017, 2018) (**Note:** drawings are not to scale)

As shown in Figure 4.20, a bearing member was used to simulate the compression zone of the virtual beam in both studies. As shown on Figure 4.20b, two compressive reaction forces, one above and one below the joint region by the upper compression member and the lower tension member, respectively, counteracted the moment applied at the joint and prevented the specimen from rotating. In the schematic drawing provided by Marques and Jirsa (1975) and shown in Figure 4.20a, the two forces above and below the joint are represented by V_{col} . When describing the components of their test apparatus, however, Marques and Jirsa clearly state that “A horizontal reaction was provided at the top of the test column to balance the moment imposed by the simulated beam” but provide no information on how the force was applied at the bottom of the column, although the photo of the test setup shows something similar to a lower tension member with a tension rod at the bottom of the reaction frame. It is therefore fair to assume that the force at the bottom of the Marques and Jirsa (1975) specimens (below the joint) was provided solely by the stiffness of the test apparatus. For the tests in the University of Kansas studies, the compressive force at the bottom of the column was mobilized in the lower tension member (Peckover et al. 2013). In the latter case, that force was low due to the relative flexibility of tension tie used to provide that force (Searle et al. 2014, Sperry et al. 2015a, 2015b, 2017a, 2017b, 2018, Yasso et al. 2017, Ajaam et al. 2017, 2018). In this sense, the two test setups were similar.

The main difference between the approach taken by Marques and Jirsa and the studies at the University of Kansas, however, involves the specimen proportions. Marques and Jirsa (1975) used the same specimen proportions for No. 7 and No. 11 bar specimens, in which the distance from the center of the hooked bars to the center of the bearing member (x_{mid}) was 14.25 in. and the upper compression reaction was placed just $1.17x_{mid} = 16.75$ in. away from the hooked bars, as shown in Figure 4.21a. In addition to having the same proportions, the specimens also had the same geometry. All specimens were 12 in., had depths of 12 or 15 in., and had a height of 50 in. The specimen geometry and proportions used by Marques and Jirsa (1975) are not representative of those used in practice for reinforced concrete frames, although it was not unreasonable at the time for a study of the anchorage strength of hooked bars since the factors controlling the behavior of hooked bars were not known as well as they are now. The University of Kansas studies used specimens with more realistic proportions. The value of x_{mid} increased with the size of the hooked bar (9.5 in. for No. 5 bar, 14.25 in. for No. 8 bars, and 23.75 in. for No. 11 bars). Second, the upper compression member was placed farther away from the hooked bars than in Marques and Jirsa

(1975) specimens: $2.39x_{mid} = 22.75$ in. for No. 5 bars, $1.60x_{mid} = 22.75$ in. for No. 8 bars, and $2.22x_{mid} = 52.75$ in. for No. 11 bars. A total height of 54 in. was used for the No. 5 and No. 8 bar specimens and 96 in. for No. 11 bar specimens.

Figure 4.21 compares the specimen proportions and the resulting applied forces for the No. 11 bar specimens tested by Marques and Jirsa (1975) and at the University of Kansas (Searle et al. 2014, Sperry et al. 2015a, 2015b, 2017a, 2017b, 2018, Yasso et al. 2017, Ajaam et al. 2017, 2018). Because of its low value, the force in the lower tension member is neglected. As shown in the figure, a much higher portion of the total applied force T was shared with the upper region of the column in the No. 11 bar specimens by Marques and Jirsa (1975) ($0.46T$) than the University of Kansas specimens ($0.34T$). This means a much lower portion of T had to be carried within the joint in the Marques and Jirsa specimens than those tested at the University of Kansas ($0.54T$ versus $0.66T$)³. Thus, with the closer location of the upper compression member with respect to the hooked bars in the specimens tested by Marques and Jirsa specimens, the anchorage strength would be expected to be higher than if the geometry of the test specimens had been more realistic, such as that used in the specimens tested at the University of Kansas. This explains the higher strength of the No. 11 bar Marques and Jirsa specimens with respect to Eq. (4.5) and (4.7).

³ $0.695T$ and $0.60T$ for No. 5 and No 8 bar specimens, respectively, tested at the University of Kansas

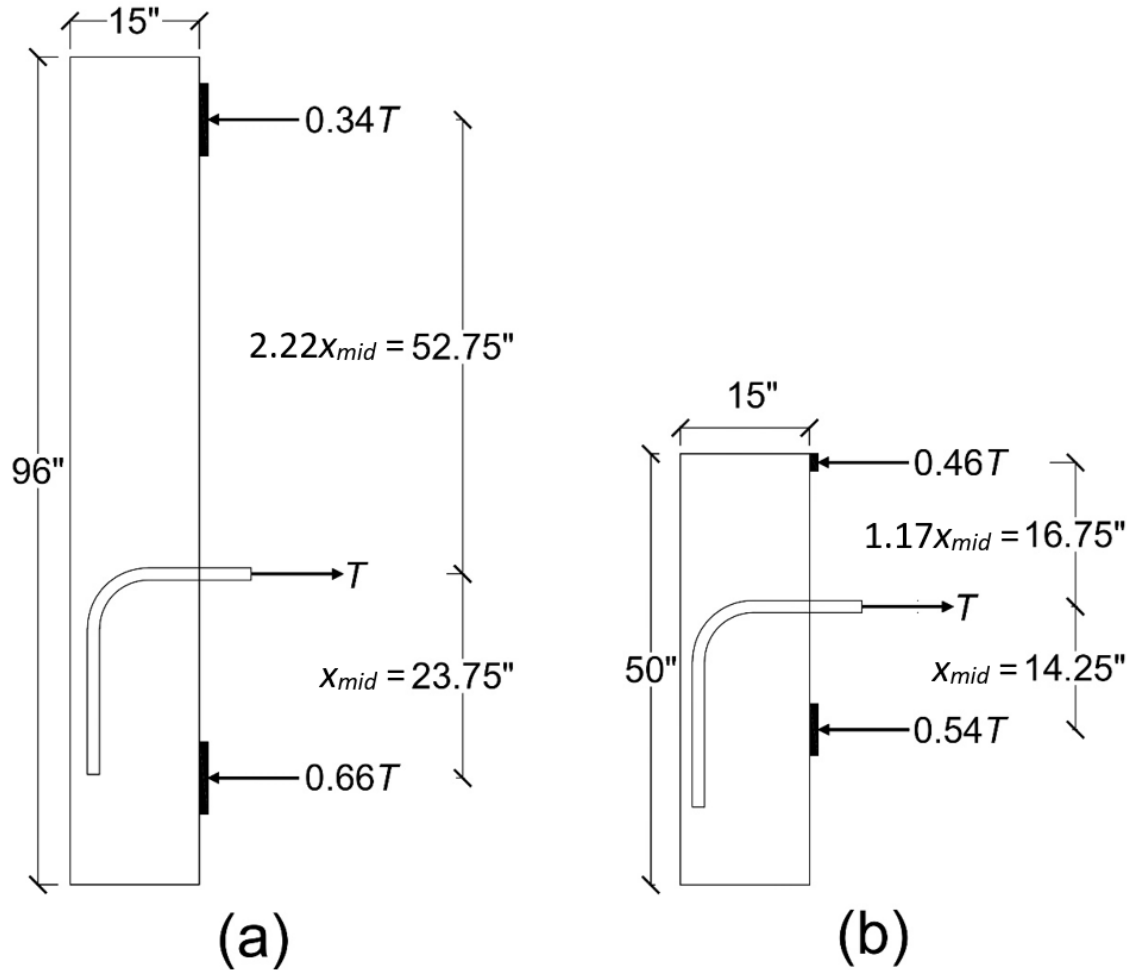


Figure 4.21 No. 11 hooked bar specimen proportions and applied forces: (a) University of Kansas (Searle et al. 2014, Sperry et al. 2015a, 2015b, 2017a, 2017b, 2018, Yasso et al. 2017, Ajaam et al. 2017, 2018), and (b) Marques and Jirsa (1975) (**Note:** T is the total applied force, and the force in the lower tension member is neglected)

The reasons for the higher strengths of the No. 11 bar specimens by Marques and Jirsa (1975) with respect to Eq. (4.5) and (4.7) also applies for the specimens tested by Pinc et al. (1977), as they used the same specimen proportions, with the exception that Pinc et al. used column depths between 12 and 24 in.

The question then arises as to why the No. 7 bar specimens tested by Marques and Jirsa (1975) had a mean T/T_h of just 1.05, despite having the same specimen proportions as the No. 11 bar specimens. The answer is found by looking at the bar stresses and approximate slip at failure reported for these specimens, as shown in Table 4.14.

Table 4.14 Bar stresses and slip at failure for No. 7 and No. 11 hooked bar specimens by Marques and Jirsa (1975) along with T/T_h based on descriptive equations, Eq. (4.5) and (4.7)

Specimen ID	Bar size	Slip	f_{su}	T	T_h	T/T_h
		in.	ksi	kips	kips	
J7-180-12-1-H	No. 7	0.07	61.0	36.6	38.8	0.94
J7-180-15-1-H	No. 7	0.15	87.0	52.2	50.6	1.03
J7-90-12-1-H	No. 7	0.08	62.0	37.2	38.3	0.97
J7-90-15-1-H	No. 7	0.15	91.0	54.6	52.6	1.04
J7-90-15-1-L	No. 7	0.21	97.0	58.2	53.3	1.09
J7-90-15-1-M	No. 7	0.18	100.0	60.0	54.0	1.11
J 7- 90 -15 -3a - H ^[1]	No. 7	0.22	98.0	58.8	50.1	1.40
J 7- 90 -15 -3 - H ^[1]	No. 7	0.21	104.0	62.4	38.0	1.72
J11-180-15-1-H	No. 11	0.05	45.0	70.2	50.6	1.48
J11-90-12-1-H	No. 11	0.04	42.0	65.5	51.2	1.58
J11-90-15-1-H	No. 11	0.06	48.0	74.9	53.8	1.09
J11-90-15-1-L	No. 11	0.06	52.0	81.1	51.9	1.20
J 11- 90 -15 -3a - L ^[1]	No. 11	0.06	69.0	107.6	72.5	1.48
J 11- 90 -15 -3 - L ^[1]	No. 11	0.09	62.0	96.7	61.1	1.58

^[1] Hooked bars outside column core, bar location factor of 1.17 applied to T/T_h

For the No. 11 bar specimens, the bar stress at failure ranged from 42 to 69 ksi with a mean of 53 ksi. The bars were Grade 60 and, although the actual yield stress is not reported by Marques and Jirsa (1975), it can be assumed to be about 69 ksi (Bournonville et al. 2004). This means that only one of the No. 11 bar specimens had bars that yielded (or were close to yield), while the other specimens had bar stresses at failure much below the yield stress. For the No. 7 bar specimens, however, the bar stresses ranged from 61 to 104 ksi, with a mean of 87.5 ksi, meaning that is likely that all but two of the No. 7 bar specimens had hooked bars that yielded prior to failure. This observation is further reinforced by the values of bar slip at failure. For the No. 7 bar specimens, slip ranged from 0.07 to 0.22 in., with a mean of 0.16 in., while for the No. 11 bar specimens, slip ranged from just 0.04 to 0.09, with a mean of 0.06 in. The prime mode of failure of the Marques and Jirsa specimens was side splitting, which would have been enhanced by the high slip of the No. 7 bars. The combined yielding and high slip are the likely reason for the lower values of T/T_h for the No. 7 bar specimens than for the No. 11 bar specimens.

CHAPTER 5: ANALYSIS AND DISCUSSION: HEADED BARS

In this chapter, the test results of the headed bar specimens are analyzed. The results are compared with stresses at anchorage failure based on the provisions in ACI 318-19 to evaluate the suitability of current Code provisions to large headed bars. The results are then compared with the forces at anchorage failure based on the descriptive equations proposed by Shao et al. (2016) and Ghimire et al. (2018, 2019a), Eq. (1.5) and (1.6). New descriptive equations developed to better represent the behavior of the larger bars are then presented and compared with the test database. After that, the effects on anchorage strength of key parameters, such as loading condition, contribution of parallel ties, bar size and spacing, bar placement within the cross-section, compression strut angle, and bar location are discussed.

5.1 COMPARISON OF TEST RESULTS WITH ACI 318-19

The provisions in ACI 318-19 for the development of headed bars are discussed in detail in Section 1.3.2. Under those provisions, No. 14 and No. 18 headed bars are not allowed, mainly due to a lack of experimental data. For No. 11 bars and smaller, the Code provides a binary choice of 1.0 or 1.6 for the parallel tie reinforcement modification factor, ψ_p . ψ_p equal to 1.0 can be applied only if $A_{t,ACI} \geq 0.3A_{hs}$ or $s \geq 6d_b$, where $A_{t,ACI}$ is the total cross-sectional area of ties or stirrups parallel to headed bars within $8d_b$ from the centerline of the headed bars and spaced no greater than $8d_b$ (as shown in Figure 1.26), A_{hs} is the total cross-sectional area of headed bars being developed, and s is the minimum center-to-center spacing of the headed bars. In all other cases, ψ_p is 1.6. To compare the test results with stresses corresponding to the Code equation, Eq. (1.10), yield strength f_y is replaced by bar stress, $f_{s,ACI}$, f'_c is replaced by the measured compressive strength, f_{cm} (with an upper limit of 10,000 psi), and the development length ℓ_{dh} is replaced by the measured embedment length, ℓ_{eh} . The equation is then solved for $f_{s,ACI}$:

$$f_{s,ACI} = \frac{75\sqrt{f_{cm}}\ell_{eh}}{\psi_e\psi_p\psi_o\psi_c d_b^{1.5}} \quad (5.1)$$

Using Eq. (5.1) and the modification factors for No. 11 and smaller bars, the ratios of bar stress measured in the tests to the bar stress calculated based on the Code equation, $f_s/f_{s,ACI}$, are presented in Table 5.1 and plotted versus the concrete compressive strength (f_{cm}) for the No. 14 and No. 18 headed bars in Figure 5.1. The four specimens that failed in shear (14-1A, 14-2, 14-16, 14-16A) are not included in the figure.

Table 5.1 Comparison of No. 14 and No. 18 headed bar test results with descriptive equations by Shao et al. (2016), Eq. (1.5) and (1.6), also (5.2) and (5.3), and ACI 318-19

ID ^[1]	<i>n</i>	<i>s/d_b</i>	<i>f_{cm}</i> psi	<i>ℓ_{eh,avg}</i> in.	<i>A_{tt}/A_{hs}</i>	<i>A_{tt,ACI}/A_{hs}</i>	L. C.	<i>T</i> kips	<i>T_h</i> kips	<i>T/T_h</i> ^[2]	<i>f_s</i> ksi	<i>f_{s,ACI}</i> ksi	<i>f_s/f_{s,ACI}</i>
11-1	2	10.0	16,210	18.5	0	0	B	163.0	182.5	0.89	104.5	69.8	1.26
11-2	2	10.0	15,850	18.5	0.282	0.212	B	221.0	210.6	1.05	141.7	99.9	1.71
14-2*	2	10.6	12,830	20.5	0.267	0.178	A	190.6	250.6	0.76	84.7	95.6	1.21
14-3	2	10.6	8,510	31.8	0	0.000	B	303.0	290.6	1.04	134.7	61.1	1.35
14-4	2	10.6	7,700	32.0	0.267	0.178	A	333.6	332.1	1.00	148.3	58.9	1.55
14-15	2	10.6	6,190	22.8	0	0.000	B	204.8	191.1	1.07	91.0	69.7	1.49
14-16*	2	10.6	5,390	22.6	0.178	0.089	A	123.6	213.9	0.58	54.9	76.4	0.93
14-16A ^{*[3]}	2	10.6	8,350	22.4	0.178	0.089	A	186.0	233.0	0.80	82.7	78.3	1.19
14-1A*	2	10.6	12,030	22.4	0	0.000	B	160.0	220.1	0.73	71.1	65.2	0.93
14-2A	2	10.6	13,750	23.0	0.267	0.178	B	248.1	280.1	0.89	110.3	61.8	1.41
14-16B	2	10.6	7,500	22.1	0.178	0.089	B	191.7	225.1	0.85	85.2	64.7	1.31
14-16C	2	10.6	6,470	22.6	0.356	0.267	B	208.4	243.5	0.86	92.6	59.8	1.50
14-16D ^[4]	2	10.6	6,900	22.9	0.827	0.827	A	289.8	249.2	1.16	128.8	58.0	1.99
14-16E ^[4]	2	10.6	6,170	22.4	0.551	0.276	A	218.6	239.7	0.91	97.2	61.7	1.62
14-16F ^[5]	2	10.6	5,640	22.4	0.551	0.276	A	197.8	233.6	0.85	87.9	39.2	1.50
14-17 ^{[5][6]}	2	7.1	6,540	22.4	0.551	0.276	A	206.7	238.4	0.87	91.9	39.6	1.49
14-5	3	3.5	6,830	22.3	0.178	0.119	B	181.8	169.6	1.07	80.8	57.5	2.06
14-6	3	3.5	6,890	22.4	0.276	0.184	B	179.5	183.9	0.98	79.8	56.8	2.01
14-7	3	3.5	7,080	32.1	0	0.000	B	252.1	179.9	1.40	112.0	47.1	1.95
14-8	3	3.5	7,100	31.7	0.276	0.184	B	274.6	248.2	1.11	122.0	62.6	2.15
14-9	3	3.5	11,480	22.1	0.276	0.184	B	173.9	200.7	0.87	77.3	55.5	1.64
14-10 ^[4]	3	3.5	6,820	22.3	0.551	0.551	A	206.6	185.6	1.11	91.8	62.9	1.47
18-1	2	8.0	5,750	32.6	0.543	0.465	A	322.0	419.7	0.77	80.5	55.3	1.45
18-2	2	8.0	11,770	28.4	0.543	0.465	A	406.6	429.5	0.95	101.7	58.0	1.62
18-3	2	8.0	6,540	30.9	0.233	0.155	B	366.5	386.2	0.95	91.6	54.9	1.66
18-4	2	8.0	7,200	30.9	0.465	0.388	B	380.0	419.4	0.91	95.0	63.3	1.64
18-5 ^[6]	2	5.3	5,310	32.5	0.543	0.465	A	300.8	361.1	0.83	75.2	54.9	1.37
18-6 ^[6]	2	5.3	10,230	28.6	0.543	0.465	A	419.8	368.0	1.14	105.0	57.1	1.66
18-7 ^{[4][6]}	3	2.7	5,890	32.1	0.543	0.413	A	252.1	295.2	0.85	63.0	82.9	1.15
18-8 ^{[5][6]}	3	2.7	6,380	32.3	0.543	0.413	A	295.3	301.0	0.98	73.8	82.9	1.29

- n* Number of bars
s/d_b Center-to-center spacing of bars normalized by nominal bar diameter
f_{cm} Measured concrete compressive strength
ℓ_{eh,avg} Average measured embedment length
A_{tt} Total area of tie legs within 9.5*d_b* from the centerline of headed bars (as defined in descriptive equation)
A_{tt,ACI} Total area of tie legs within 8.5*d_b* from the centerline of headed bars (as defined by ACI 318-19)
A_{hs} Total area of headed bars being developed
L. C. Loading condition, as defined in Section 2.3.2
f_s Bar stress at failure
f_{s,ACI} Bar stress calculated based on ACI 318-19 equation (Eq. 5.1)
T Average force per bar at failure
T_h Anchorage strength of headed bars calculated using descriptive equations by Shao et al. (2016)
^[1] The first number in ID denotes the bar size
^[2] Maximum effective value for *A_{tt}/A_{hs}* of 0.3 applied for calculating *T_h*
^[3] Specimen had an additional No. 11 longitudinal bar on both sides, 2 in. from the bearing face of the head
^[4] Double overlapping No. 5 ties were used, refer to Figure 2.5

- [5] Double No. 5 ties were used
 [6] Specimen had a side cover of 6.5 in.
 * Specimen exhibited a shear-like failure (not anchorage)

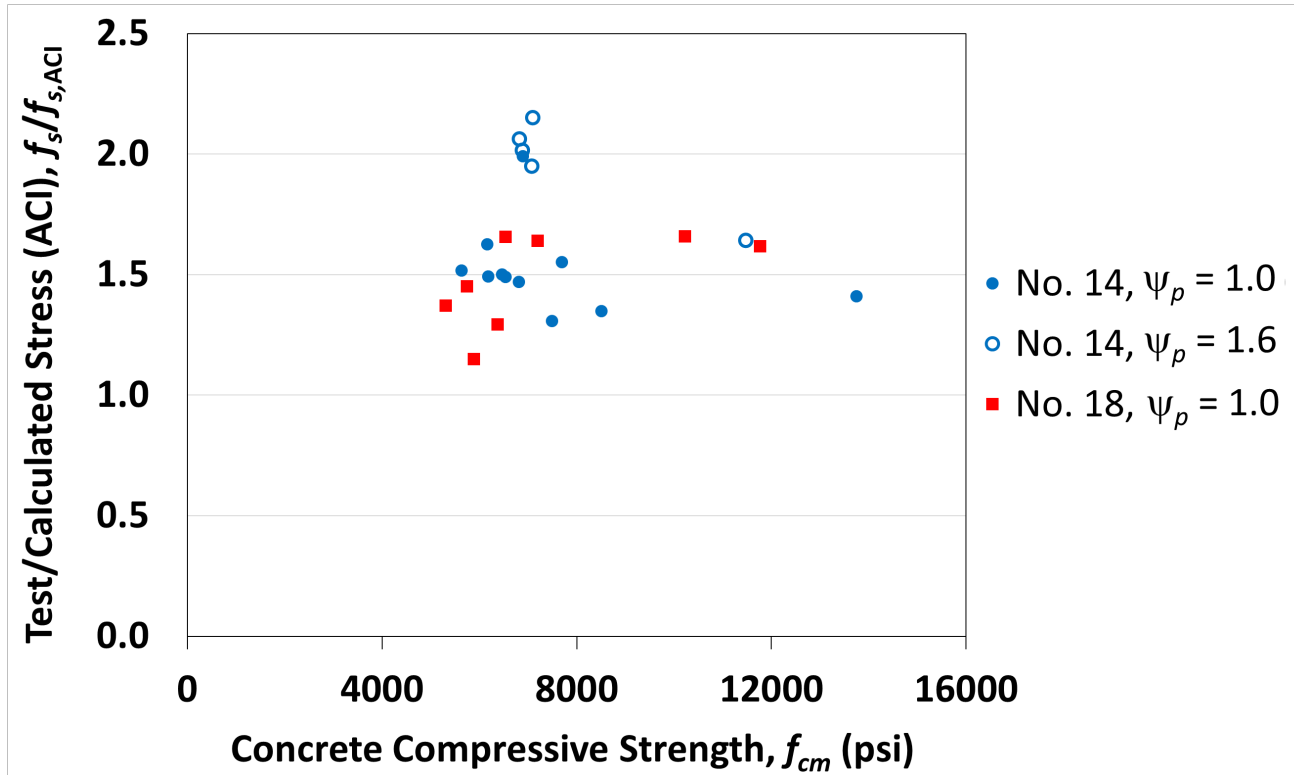


Figure 5.1 Ratio of test/calculated bar stress $f_s/f_{s,ACI}$ applying the ACI 318-19 provisions to No. 14 and No. 18 headed bar specimens versus concrete compressive strength f_{cm} , excluding specimens that failed in shear

As shown in Table 5.1, $f_s/f_{s,ACI}$ for the four specimens that failed in shear ranged from 0.93 to 1.21 with an average of 1.07. For the rest of the specimens, the $f_s/f_{s,ACI}$ ratio ranged from 1.15 to 2.15, with an average of 1.59, as shown in Figure 5.1. This indicates that the current ACI equation would be very conservative if applied to No. 14 and No. 18 bars. There are several reasons for this conservatism. First, relative to descriptive equation the Code equation has an embedded strength reduction factor that results in $f_s/f_{s,ACI}$ values greater than T/T_h . This is reflected in the minimum $f_s/f_{s,ACI}$ value being 1.15 among specimens with an anchorage failure. Second, the current Code does not allow the ψ_p modification factor to be less than 1.0, whereas it would be appropriate to use in cases where bars are widely-spaced ($s \geq 6d_b$ based on Code and $\geq 8d_b$ based on descriptive equations) and parallel ties are provided, as will be shown when presenting the proposed design equation in Chapter 6. Despite applying $\psi_p = 1.0$ when $s \geq 6d_b$, $f_s/f_{s,ACI}$ for the specimens with widely-spaced bars ranges from 1.26 to 1.99, with an average of 1.53, indicating an

overconservative estimation by the current Code provisions, even for specimens with bars spaced as wide as $10.6d_b$ with parallel ties, which could permit a shorter development length. Third, for specimens for which ACI 318-19 requires that $\psi_p = 1.6$ to be applied, the Code is unnecessarily conservative, resulting in values of $f_s/f_{s,ACI}$ ranging from 1.64 to 2.15, with an average of 1.96. Four out of five specimens with $\psi_p = 1.6$ had parallel ties in the joint region (with $A_{tt,ACI}/A_{hs}$ values of 0.119 and 0.184), and as will be discussed in Section 5.5.2, providing parallel ties improves the anchorage strength even when $A_{tt,ACI} < 0.3A_{hs}$, a fact not recognized in ACI 318-19.

Overall, these observations show that the current Code provisions will have limitations that would cause an inaccurate representation of the effects of bar spacing and parallel tie reinforcement if extended to No. 14 and No. 18 headed bars. A modified approach is needed to provide alternative expressions for ψ_p , permitting the use of shorter development lengths (that is, ψ_p other than 1.6) under conditions where $s < 6d_b$ and $A_{tt,ACI} < 0.3A_{hs}$, and permitting ψ_p values < 1.0 when bars are widely-spaced and parallel ties are provided. These points are addressed in developing the design equation proposed in Chapter 6.

5.2 COMPARISON OF TEST RESULTS WITH DESCRIPTIVE EQUATIONS DEVELOPED BASED ON TESTS OF NO. 5 THROUGH NO. 11 HEADED BARS

In this section, the test results are compared with the descriptive equations developed by Shao et al. (2016) and Ghimire et al. (2018, 2019a, 2019b). As described in Section 1.2.2, the equations characterize the anchorage strength of headed bars based on 202 tests of simulated beam-column joint specimens with No. 5, No. 8, and No. 11 headed bars tested under a loading condition similar to that of loading condition B in this study. The descriptive equations are given below for headed bars without and with confining reinforcement in the joint region as Eq. (5.2) and (5.3), respectively:

$$T_h = 781 f_{cm}^{0.24} \ell_{eh}^{1.03} d_b^{0.35} \left(0.0836 \frac{s}{d_b} + 0.344 \right) \quad (5.2)$$

where $\left(0.0836 \frac{s}{d_b} + 0.344 \right) \leq 1.0$.

$$T_h = \left(781 f_{cm}^{0.24} \ell_{eh}^{1.03} d_b^{0.35} + 48,800 \frac{A_{tt}}{n} d_b^{0.88} \right) \left(0.0622 \frac{s}{d_b} + 0.5428 \right) \quad (5.3)$$

where $\left(0.0622 \frac{s}{d_b} + 0.5428\right) \leq 1.0$ and $A_{tt} \leq 0.3A_{hs}$, T_h is the anchorage strength of an individual headed bar (lb); f_{cm} is the measured concrete compressive strength (psi); ℓ_{eh} is the embedment length of the headed bar measured from the face of the column to the bearing face of the head (in.); d_b is the headed bar diameter (in.); A_{tt} is the area of confining reinforcement (in.²) within $8d_b$ from the top of the headed bar for No. 8 bars and smaller or within $10d_b$ for No. 9 bars or larger (Figure 1.18); A_{hs} is the total area of the headed bars (in.²) in a joint; n is the number of headed bars in the joint; and s is the center-to-center spacing between headed bars. The maximum value of A_{tt} in Eq. (5.3) is $0.3A_{hs}$ (Shao et al. 2016, Ghimire et al. 2018, 2019a, 2019b).

The specimens in this study were designed based on Eq. (5.2) and (5.3). To evaluate the applicability of the equations for the tests of No. 14 and No. 18 bars in this study, the anchorage strengths measured in the tests, T (reported in Table 3.4), are compared with the calculated strengths based on the descriptive equations, T_h . Table 5.1 presents the values of T , T_h , and the ratio of T/T_h for all specimens, along with specimen ID and key parameters (number and spacing of bars, concrete compressive strength, embedment length, confining reinforcement in the joint region, and loading condition).

Based on Table 5.1, the test-to-calculated ratio T/T_h varied among specimens with different properties. Among the No. 14 bar specimens with confining reinforcement, specimens 14-16B and 14-16F had the lowest T/T_h ratio (0.85). Specimen 14-16D with the highest amount of confining reinforcement ($A_{tt}/A_{hs} = 0.83$) had the highest T/T_h ratio (1.16). The test-to-calculated ratio T/T_h is below 1.0 for all but one No. 18 bar specimen. The specimens that failed in shear had the lowest T/T_h ratios, ranging from 0.58 to 0.80, with 14-16 with the lowest T/T_h ratio (0.58) among all specimens.

The test results can be compared with the descriptive equations based on specimen properties, including bar size, parallel ties, and loading condition. In the following comparisons, the four specimens exhibiting a shear-like failure (see Section 3.2.2) are excluded from analysis.

Table 5.2 summarizes the T/T_h values based on bar size and parallel ties for the No. 14 and No. 18 bar specimens, regardless of loading condition and excluding the specimens with a shear-like failure.

As shown in Table 5.2, the values of T/T_h range from 0.77 to 1.40, with a mean of 0.98 and a coefficient of variation of 0.147. The three specimens without parallel ties (all No. 14 bars) have

a mean T/T_h ratio of 1.17, while those with parallel ties have a mean T/T_h ratio of 0.95, a statistically significant difference with a p value of 0.01. Based on bar size, the mean T/T_h is 1.00 for the No. 14 bar specimens and 0.92 for the No. 18 bar specimens (0.92), but the difference is not statistically significant ($p = 0.20$).

Table 5.2 Summary of test-to-calculated ratio T/T_h for No. 14 and No. 18 headed bars based on bar size and parallel ties with T_h based on Eq. (5.2) or (5.3), excluding specimens that failed in shear

	T/T_h				
	All	All - Without Parallel Ties	All - With Parallel Ties	All No. 14	All No. 18
No. of Specimens	24	3	21	16	8
Max	1.40	1.40	1.16	1.40	1.14
Min	0.77	1.04	0.77	0.85	0.77
Mean	0.98	1.17	0.95	1.00	0.92
STDEV	0.143	0.199	0.114	0.152	0.113
CoV	0.147	0.170	0.120	0.151	0.123

Table 5.3 summarizes the T/T_h values for the No. 14 and No. 18 headed bar specimens tested under loading condition A (joint shear equal to 80% of the applied load), excluding those with a shear-like failure. All specimens had parallel ties within the joint.

Table 5.3 Summary of test-to-calculated ratio T/T_h for No. 14 and No. 18 headed bars tested under loading condition A (all with parallel ties) with T_h based on Eq. (5.3), excluding specimens that failed in shear

	T/T_h – Loading Condition A		
	All	No. 14	No. 18
No. of Specimens	12	6	6
Max	1.16	1.16	1.14
Min	0.77	0.85	0.77
Mean	0.95	0.98	0.92
STDEV	0.131	0.132	0.133
CoV	0.137	0.134	0.145

As shown in Table 5.3, the headed bar specimens tested under loading condition A have test-to-calculated T/T_h ratios ranging from 0.77 to 1.16 with a mean of 0.95 and a coefficient of variation of 0.137. Under this loading condition, the mean T/T_h for No. 14 bars (0.98) is higher than that of No. 18 bars (0.92), but the difference is not statistically significant ($p = 0.42$).

Specimens with parallel ties and tested under loading condition B can be compared based on bar size, as shown in Table 5.4.

Table 5.4 Summary of test-to-calculated ratio T/T_h for No. 14 and No. 18 headed bars with parallel ties and tested under loading condition B with T_h based on Eq. (5.3)

	$T/T_h^{[1]}$ – Loading Condition B – with Parallel Ties		
	All	No. 14	No. 18
No. of Specimens	9	7	2
Max	1.11	1.11	0.95
Min	0.85	0.85	0.91
Mean	0.94	0.95	0.93
STDEV	0.094	0.107	0.030
COV	0.099	0.113	0.033

As shown in Table 5.4, the headed bar specimens with parallel ties and tested under loading condition B had T/T_h ratios ranging from 0.85 to 1.11, with a mean of 0.94 and a coefficient of variation of 0.099. Comparing based on bar size, the No. 14 bar specimens had a mean T/T_h of 0.95, slightly higher than that of No. 18 bars (0.93). This small difference is not statistically significant ($p = 0.83$).

The similarities in the mean values of T/T_h for the specimens with parallel ties tested under loading conditions A and B (0.95 and 0.94) indicate that in cases where confining reinforcement within a joint is adequate to prevent a shear-like failure, the differences in the two loading conditions did not affect anchorage strength.

The average force per bar at failure, T , for all No. 14 and No. 18 headed bar specimens (excluding those that failed in shear) is compared with that calculated using descriptive equations, T_h , in Figure 5.2.

As shown in Figure 5.2, the best fit trendline on all specimens starts slightly above $T = T_h$ for lower values of T and becomes less conservative as T increases, suggesting that it would be worthwhile to update the descriptive equations to more accurately represent the anchorage strength of headed bars larger than No. 11.

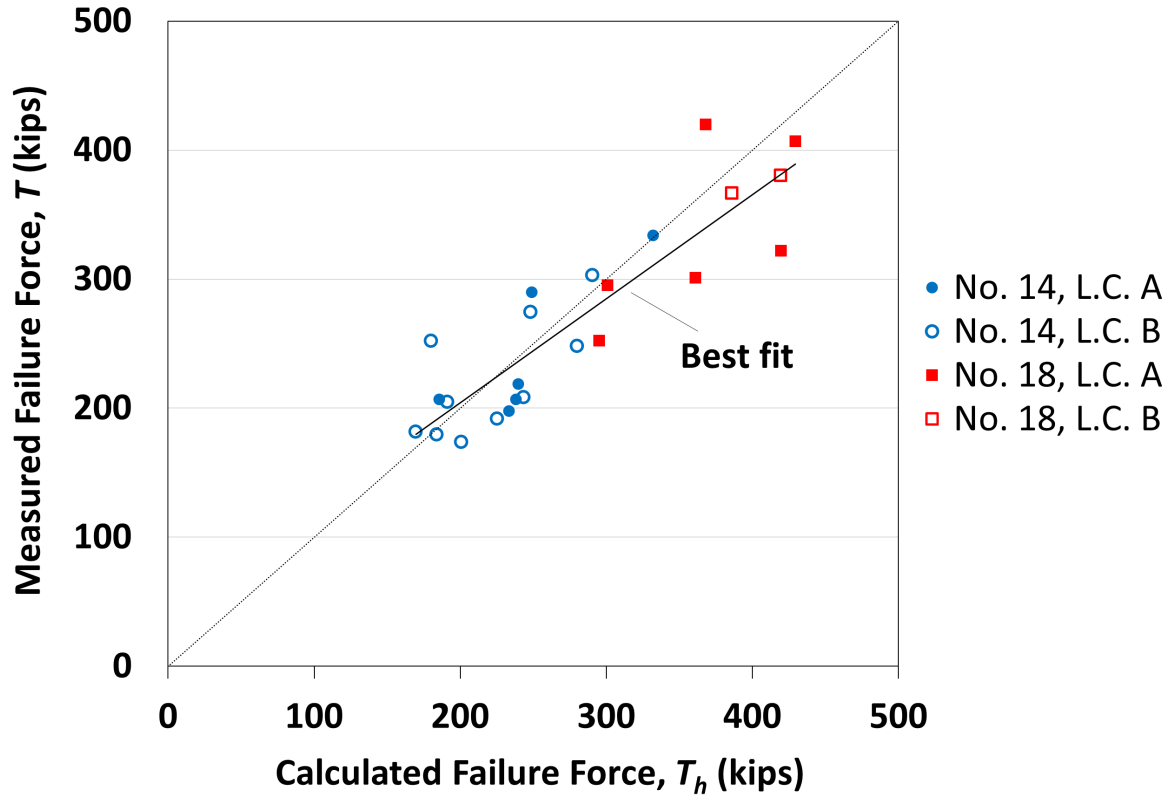


Figure 5.2 Test versus calculated force per bar at failure for No. 14 and No. 18 headed bar specimens based on descriptive equations by Shao et. al (2016)

5.3 NEW DESCRIPTIVE EQUATIONS

New descriptive equations were developed following the iterative analyses procedure used by Shao et al. (2016) for headed bars and Ajaam et al. (2017) for hooked bars. In summary, a base equation is first developed for specimens with widely-spaced bars without parallel ties. Using the same equation, an expression to account for close bar spacing is developed using specimens with closely-spaced bars without parallel ties. Next, the same base equation is used for specimens with widely-spaced bars with parallel ties to develop an expression representing the contribution of the parallel ties. Finally, the equation for widely-spaced bars with parallel tie is applied to specimens with closely-spaced bars and parallel ties to develop an expression for closely spaced bars. The new descriptive equations have the same format as Eq. (5.2) and (5.3). The iterative analysis is based on forcing the average T/T_h to be 1.00, in which T is the measured and T_h is the calculated failure load. The database used for analyses includes No. 5, No. 8, and No. 11 bar specimens tested by Shao et al. (2016) and the specimens tested in this study, excluding those that failed in shear.

5.3.1 Widely-spaced Bars Without Parallel Ties

The best-fit equation obtained using the iterative analysis for the 33 specimens with widely-spaced bars (center-to center bar spacing $\geq 8d_b$) without parallel ties is

$$T_c = 1296 f_{cm}^{0.207} \ell_{eh}^{0.941} d_b^{0.498} \quad (5.4)$$

where T_c is the anchorage strength of headed bars without parallel ties (lb), f_{cm} is concrete compressive strength (psi), ℓ_{eh} is embedment length (in.), and d_b is bar diameter (in.). Compared with Eq. (5.2), the constant increased from 768 to 1296, the power of f_{cm} decreased from 0.24 to 0.207, the power of ℓ_{eh} decreased from 1.03 to 0.941, and the power of d_b increased from 0.35 to 0.498. The T/T_c ratio is compared with f_{cm} in Figure 5.3.

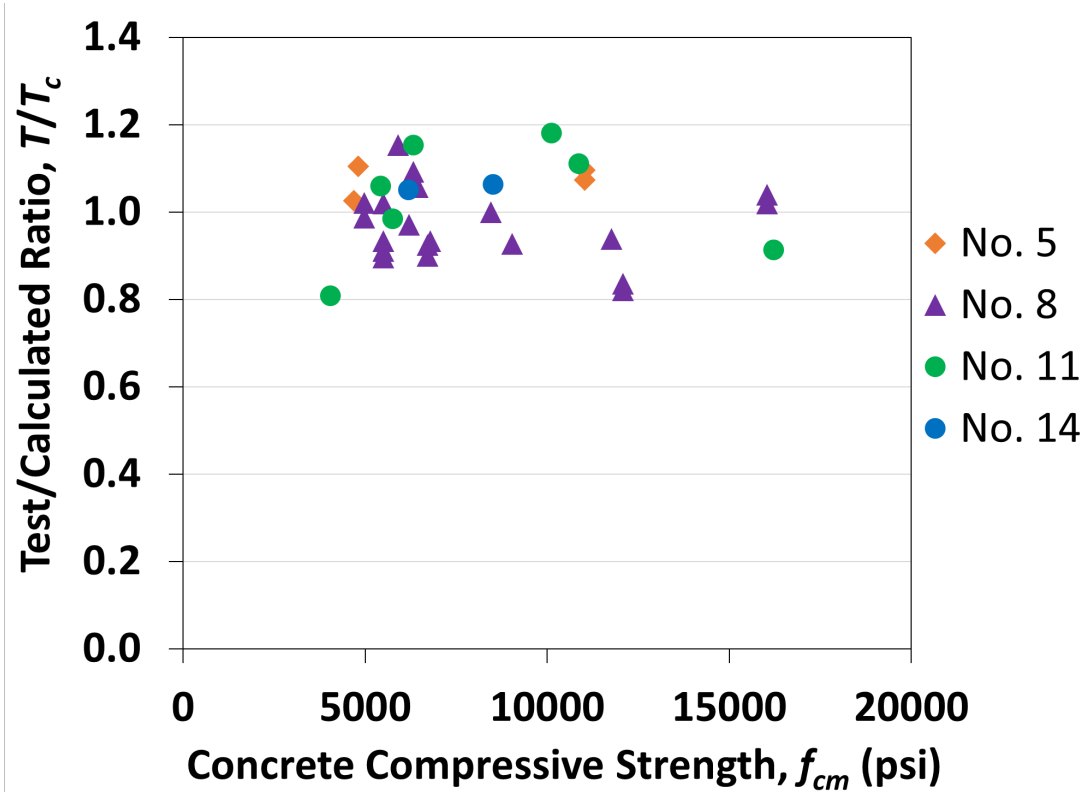


Figure 5.3 Ratio of test-to-calculated bar force at failure T/T_c , with T_c based on Eq. (5.4), versus concrete compressive strength for headed bar specimens with widely-spaced bars without parallel ties

As shown in Figure 5.3, there is no noticeable trend in T/T_c as function of f_{cm} indicating that the 0.207 power provides an adequate representation of the effect of concrete compressive strength on anchorage strength. Also, the distribution the of T/T_c values indicates no noticeable bias towards bar size. The statistical parameters for the 33 specimens are presented in Table 5.5.

Table 5.5 Statistical parameters for T/T_c ratio for headed bar specimens with widely-spaced bars without parallel ties with T_c based on Eq. (5.4)

Bar size	All	No. 5	No. 8	No. 11	No. 14	No. 18
No. of specimens	33	4	20	7	2	0
Max	1.18	1.10	1.15	1.18	1.06	-
Min	0.81	1.03	0.82	0.81	1.05	-
Mean	1.00	1.07	0.97	1.03	1.06	-
STDEV	0.095	0.035	0.083	0.135	0.007	-
CoV	0.095	0.033	0.086	0.131	0.006	-

As shown in Table 5.5, the T/T_c ratio ranges from 0.81 to 1.18 with a mean of 1.00 and a coefficient of variation of 0.095 for the 33 headed bar specimens with widely-spaced bars and no parallel ties.

5.3.2 Closely-spaced Bars Without Parallel Ties

As discussed in Sections 4.3.2 and 4.4.3, center-to-center bar spacing is used as a proxy to represent the effects on anchorage strength for members with more than two widely spaced bars. Using Eq. (5.4), the effect of close bar spacing (center-to-center spacing $< 8d_b$) can be determined. To do so, the T/T_c is calculated for the 35 specimens with closely-spaced bars and no parallel ties. T/T_c versus s/d_b for these specimens is shown in Figure 5.4.

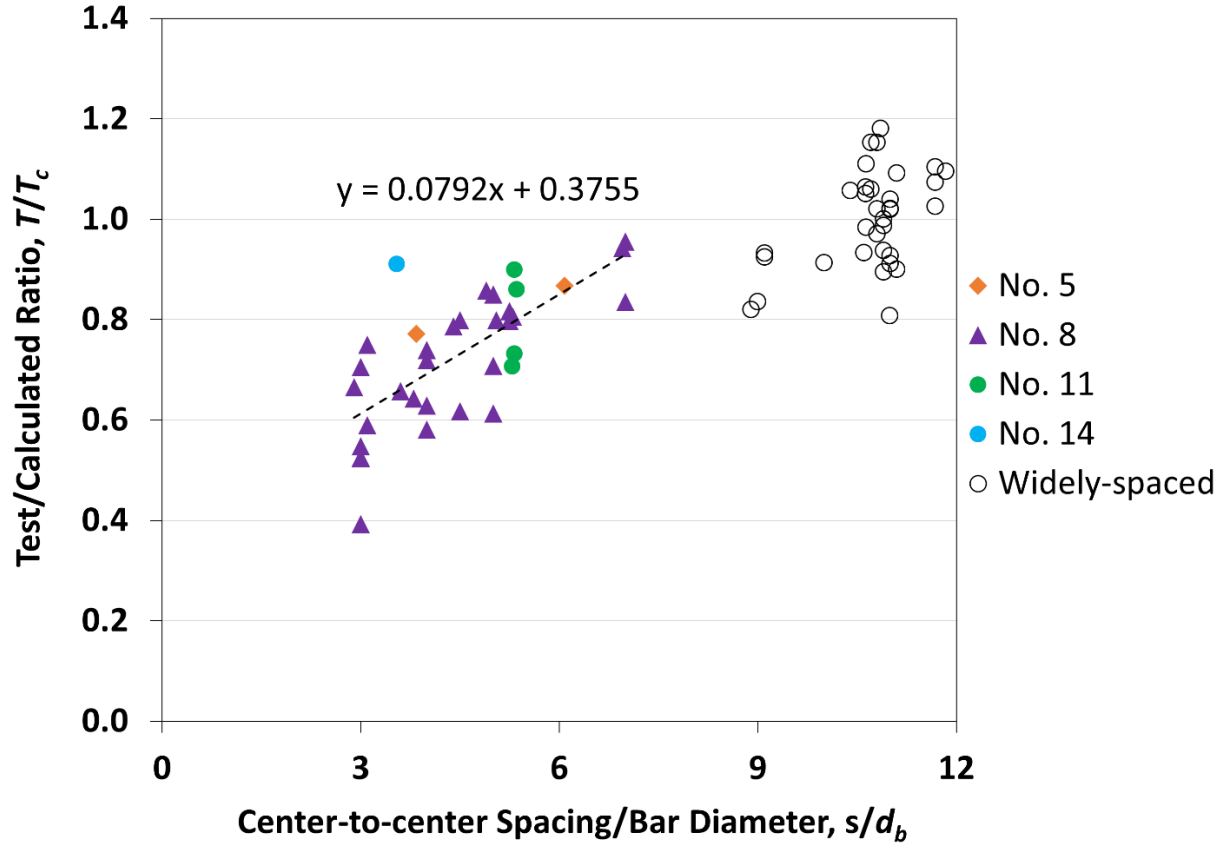


Figure 5.4 Test-to-calculated bar force at failure T/T_c versus ratio of center-to-center spacing to bar diameter s/d_b for widely- and closely-spaced headed bars without parallel ties with T_c based on Eq. (5.4)

As shown the figure, the T/T_c ratio (and therefore anchorage strength) decreases with a decrease in bar spacing. To account for the effect of bar spacing, the linear trendline equation shown in Figure 5.4 is combined with Eq. (5.4) to give

$$T_c = \left(1296 f_{cm}^{0.207} \ell_{eh}^{0.941} d_b^{0.498} \right) \left(0.0792 \frac{s}{d_b} + 0.3755 \right) \quad (5.5)$$

where $\left(0.0792 \frac{s}{d_b} + 0.3755 \right) \leq 1.0$, and s is the center-to-center spacing of the bars (in.). The statistical parameters for T/T_c for the 35 specimens with closely-spaced bars and no parallel ties are given in Table 5.6.

Table 5.6 Statistical parameters of T/T_c ratio for headed bar specimens with closely-spaced bars without parallel ties with T_c based on Eq. (5.5)

Bar size	All	No. 5	No. 8	No. 11	No. 14	No. 18
No. of specimens	35	2	28	4	1	0
Max	1.39	1.14	1.21	1.15	1.39	-
Min	0.64	1.01	0.64	0.89	1.39	-
Mean	1.00	1.07	0.98	1.01	1.39	-
STDEV	0.136	0.087	0.125	0.111	0	-
CoV	0.136	0.081	0.127	0.109	0	-

As shown in the table for the specimens with closely-spaced headed bars and no parallel ties, the T/T_c ratio ranges from 0.64 to 1.39, with a mean value of 1.00 and a coefficient of variation of 0.136. For all headed bar specimens without parallel ties, T/T_c is compared with the concrete compressive strength in Figure 5.5. The statistical parameters for T/T_c for the specimens without parallel ties are given in Table 5.7.

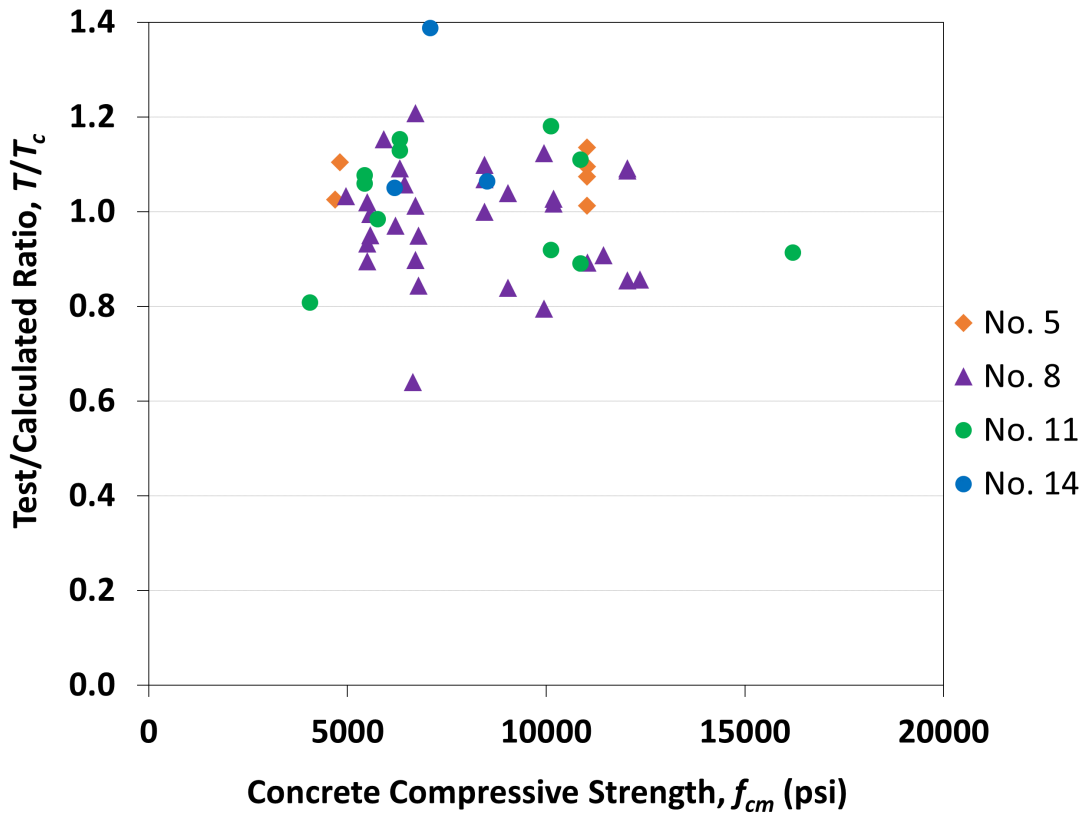


Figure 5.5 Ratio of test-to-calculated bar force at failure T/T_c , based on Eq. (5.5), versus concrete compressive strength for headed bar specimens with widely- and closely-spaced bars without parallel ties

As shown in Table 5.6 and Figure 5.5, the single specimen with three closely-spaced No. 14 bars, 14-7, had the highest T/T_h ratio of 1.39. If the close-bar spacing term in Eq. (5.5) is not applied, however, the T/T_c ratio is 0.91. This observation indicates that bar spacing might not be the controlling factor here, but as mentioned earlier, it can be safely used as a convenient representation of the effect of multiple bars anchored in a member.

Table 5.7 Statistical parameters of T/T_c , with T_c based on Eq. (5.5), for headed bar specimens with widely- and closely-spaced bars without parallel ties

Bar size	All	No. 5	No. 8	No. 11	No. 14	No. 18
No. of specimens	68	6	48	11	3	0
Max	1.39	1.14	1.21	1.18	1.39	-
Min	0.64	1.01	0.64	0.81	1.05	-
Mean	1.00	1.07	0.98	1.02	1.17	-
STDEV	0.119	0.048	0.109	0.124	0.191	-
CoV	0.119	0.044	0.111	0.121	0.164	-

As shown in Table 5.7, the 68 specimens without parallel ties have a T/T_c ratio ranging from 0.64 to 1.39 with a mean value of 1.00 and a coefficient of variation of 0.119.

5.3.3 Widely-Spaced Bars with Parallel Ties

The procedure to develop Eq. (5.4) was used for 55 specimens with widely-spaced bars with parallel ties to obtain an expression representing the contribution of ties to anchorage strength (T_s), assuming that Eq. (5.4) represents the contribution of concrete (T_c). In developing an expression for T_s , it is assumed that an effective area of parallel ties, A_{tt} contribute to anchorage strength. The definition of A_{tt} is retained from the previous research (Shao et al. 2016), that is, the total area of tie legs within $8d_b$ from the top of the headed bars for No. 3 through No. 8 bars and $10d_b$ for No. 11 and larger bars.

As stated earlier, Shao et al. (2016) limited A_{tt} to $0.3A_{hs}$, where A_{hs} is the total area of headed bars. The limit was chosen based on the range of A_{tt}/A_{hs} values tested (0.07 to 1.07, with an average of 0.3). If the No. 14 and No. 18 specimens are included, the average of A_{tt}/A_{hs} values increases to 0.33. If only the No. 14 and No. 18 bar specimens are considered, the average value of A_{tt}/A_{hs} is 0.42. Therefore, to better permit the effect of A_{tt}/A_{hs} to be evaluated for larger bars, the limit for A_{tt}

was chosen as $0.4A_{hs}$ for this study. As shown in the next few pages, the new limit provides a good match between calculated and measured failure loads.

For the 55 specimens with widely-spaced bars with parallel ties, the following equation is obtained using iterative analysis:

$$T_h = T_c + T_s = 1296 f_{cm}^{0.207} \ell_{eh}^{0.941} d_b^{0.498} + 49,402 \left(\frac{A_{tt}}{n} \right) d_b^{0.11} \text{ and } A_{tt} \leq 0.4A_{hs} \quad (5.6)$$

where n is the number of headed bars.

The noticeable difference between Eq. (5.6) and the equation developed by Shao et al. (2016), Eq. (5.3), is the reduction in the power of d_b in the expression for T_s from 0.88 to 0.11. This indicates a much lower effect of bar size on the contribution of parallel ties than previously obtained. The other difference is a very slight increase in the constant from 48,800 to 49,402.

The ratio T/T_h is compared with the concrete compressive strength for the 55 specimens used to develop Eq. (5.6) in Figure 5.6.

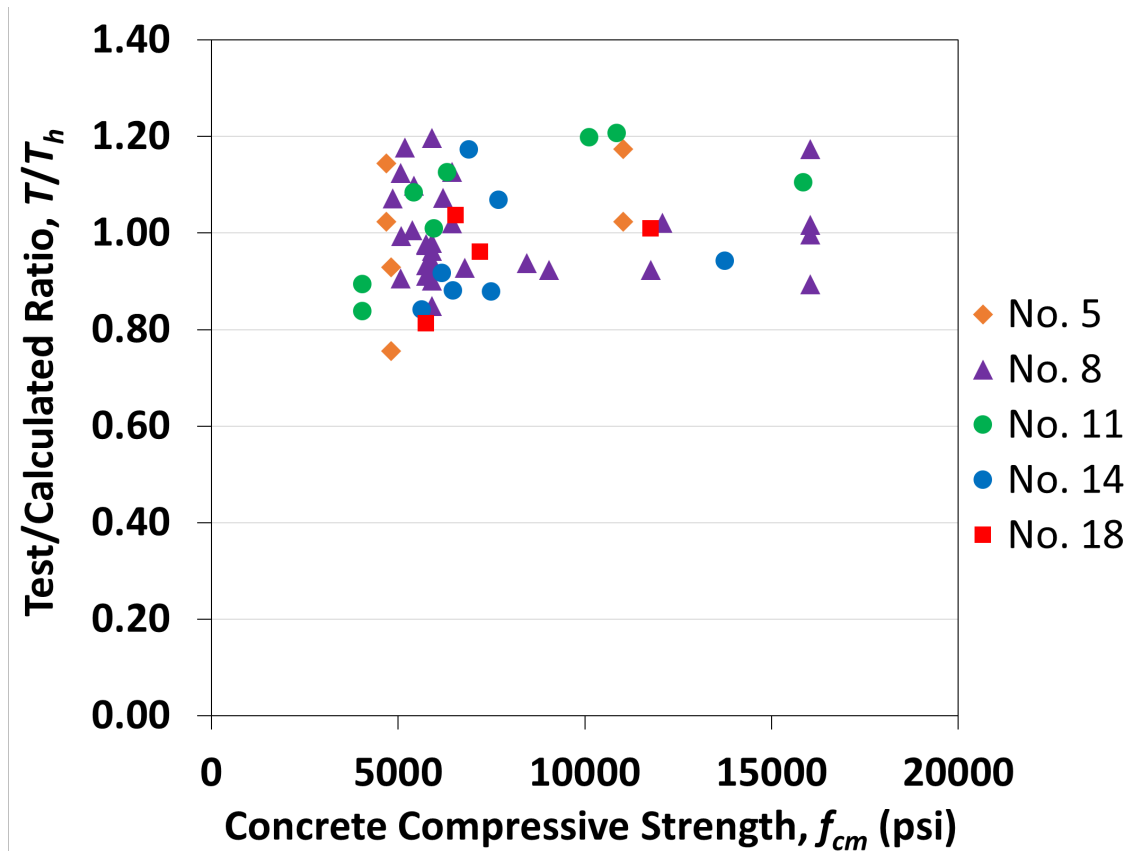


Figure 5.6 Ratio of test-to-calculated bar force at failure T/T_h versus concrete compressive strength for headed bar specimens with widely-spaced bars with parallel ties with T_h based on Eq. (5.6)

As shown in Figure 5.6, the data points show, perhaps, a slight positive trend, indicating a slight underestimation of the effect of concrete compressive strength by Eq. (5.6). The statistical parameters for T/T_h values for the specimens with widely-spaced bars and parallel ties are shown in Table 5.8. In this case, T/T_h ranges from 0.76 to 1.21, with an average of 1.00 and a coefficient of variation of 0.109.

Table 5.8 Statistical parameters of T/T_h ratio for headed bar specimens with widely-spaced bars with parallel ties with T_h based on Eq. (5.6)

Bar size	All	No. 5	No. 8	No. 11	No. 14	No. 18
No. of specimens	55	6	30	8	7	4
Max	1.21	1.17	1.20	1.21	1.17	1.04
Min	0.76	0.76	0.85	0.84	0.84	0.81
Mean	1.00	1.01	1.00	1.06	0.96	0.95
STDEV	0.109	0.153	0.093	0.135	0.111	0.086
CoV	0.109	0.151	0.093	0.127	0.116	0.091

5.3.4 Closely-Spaced Bars with Parallel Ties

As for the specimens without parallel ties, an expression to account for close bar spacing can be developed for specimens with parallel ties. To this end, T_h was calculated for 41 specimens with closely-spaced bars and parallel ties using Eq. (5.6), and the ratio T/T_h is plotted versus s/d_b in Figure 5.7.

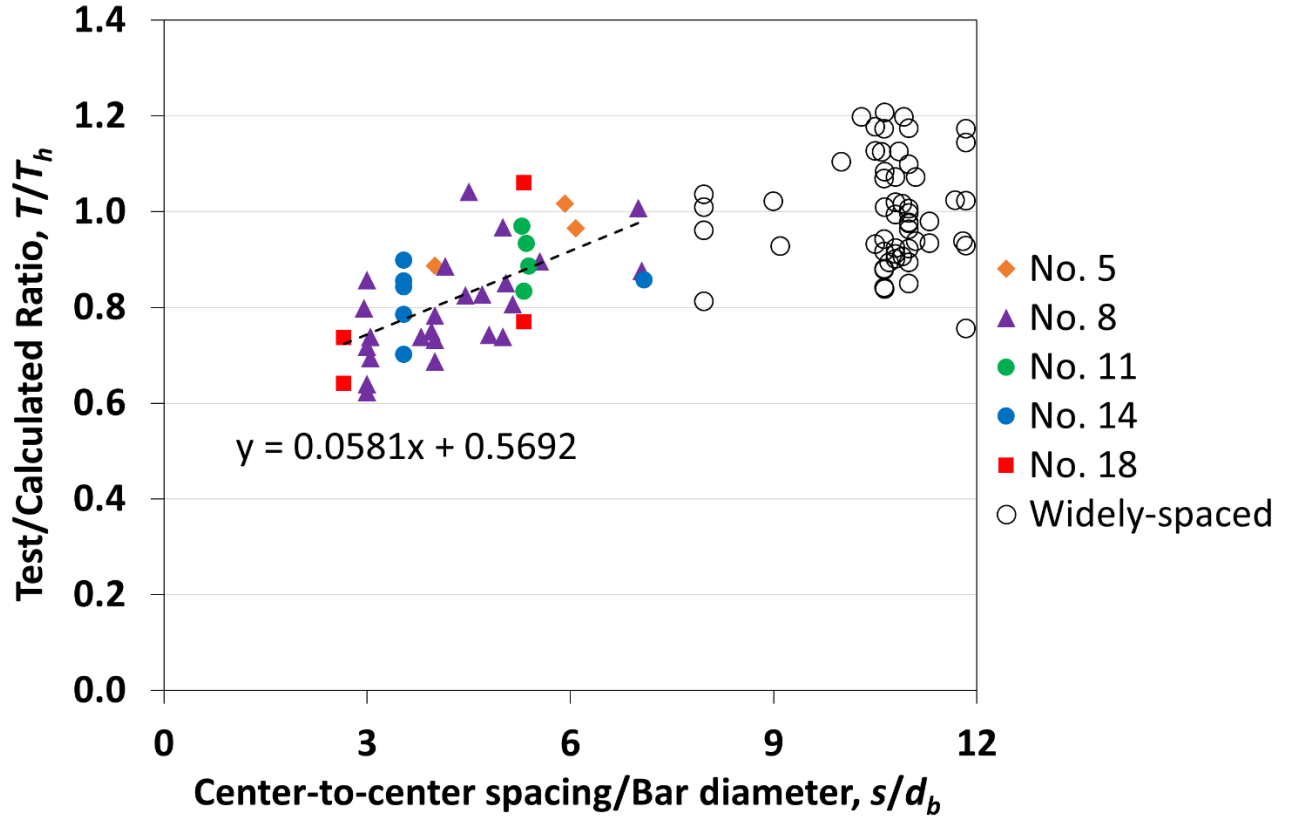


Figure 5.7 Test-to-calculated bar force at failure T/T_h versus ratio of center-to-center spacing to bar diameter s/d_b for widely- and closely-spaced headed bars with parallel ties with T_h based on Eq. (5.6)

As shown in Figure 5.7, and similar to specimens without parallel ties, the T/T_h ratio decreases as the spacing between bars decreases. Eq. (5.7) is multiplied by the equation given by the trendline to give

$$T_h = \left(1296 f_{cm}^{0.207} \ell_{eh}^{0.941} d_b^{0.498} + 49,402 \left(\frac{A_t}{n} \right) d_b^{0.11} \right) \left(0.0581 \frac{c_{ch}}{d_b} + 0.5692 \right) \quad (5.7)$$

where $\left(0.0581 \frac{c_{ch}}{d_b} + 0.5692 \right) \leq 1.0$ and $A_t \leq 0.4 A_{hs}$. Table 5.9 shows the statistical parameters of T/T_h ratio for 41 specimens with closely-spaced bars with parallel ties.

Table 5.9 Statistical parameters of T/T_h ratio for headed bar specimens with closely-spaced bars with parallel ties with T_h based on Eq. (5.7)

Bar size	All	No. 5	No. 8	No. 11	No. 14	No. 18
No. of specimens	41	3	24	4	6	4
Max	1.25	1.11	1.25	1.11	1.16	1.21
Min	0.84	1.05	0.84	0.95	0.87	0.88
Mean	1.00	1.09	0.98	1.03	1.02	1.00
STDEV	0.104	0.037	0.104	0.068	0.114	0.155
CoV	0.104	0.034	0.106	0.066	0.112	0.155

As shown in Table 5.9, the headed bar specimens with closely-spaced bars and parallel ties the T/T_h ratios ranges from 0.84 to 1.25, with an average of 1.00 and coefficient of variation of 0.104. Using Eq. (5.7), the ratio of T/T_h for specimens with widely- and closely-spaced bars with parallel ties are plotted versus concrete compressive strength in Figure 5.8.

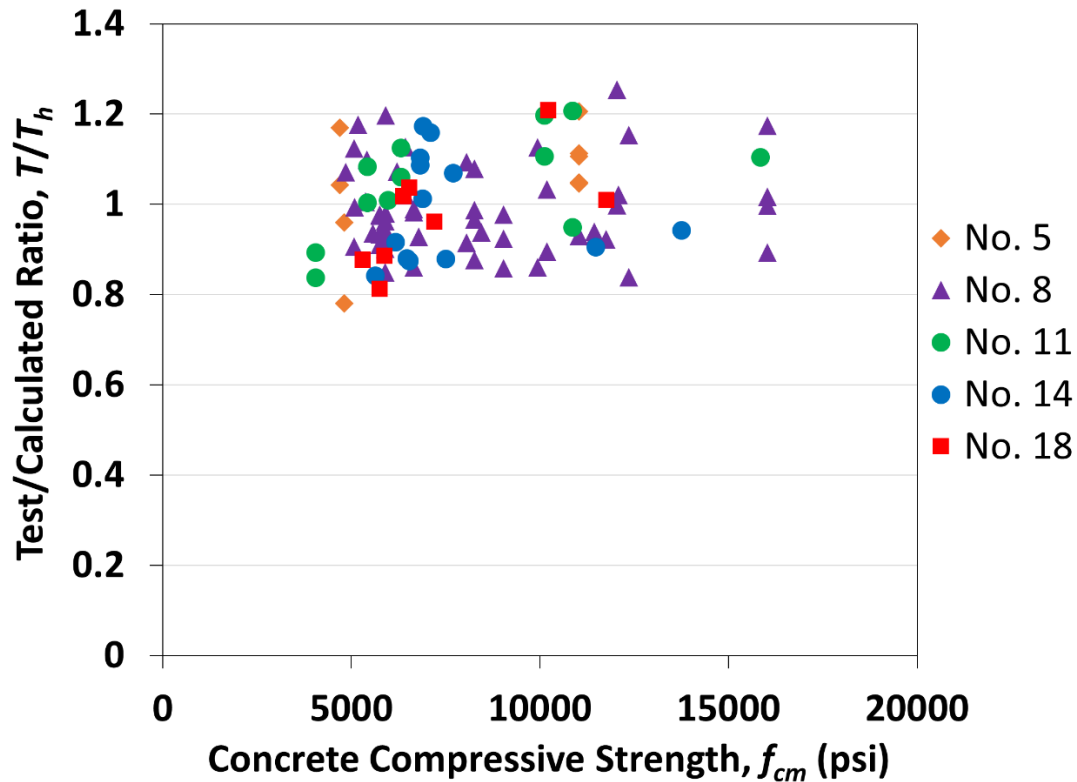


Figure 5.8 Ratio of test-to-calculated bar force at failure T/T_h versus concrete compressive strength for headed bar specimens with widely- and closely-spaced bars with parallel ties with T_h based on Eq. (5.7)

As shown in Figure 5.8, no trend is apparent with respect to concrete compressive strength. The statistical parameters of T/T_h are shown for all specimens with parallel ties in Table 5.10. As shown in table, T/T_h for specimens with parallel ties in the joint region range from 0.76 to 1.25 with an average of 1.00 and a coefficient of variation of 0.108.

Table 5.10 Statistical parameters of T/T_h ratio for headed bar specimens with widely- and closely-spaced bars with parallel ties with T_h based on Eq. (5.7)

Bar size	All	No. 5	No. 8	No. 11	No. 14	No. 18
No. of specimens	96	9	54	12	13	8
Max	1.25	1.17	1.25	1.21	1.17	1.21
Min	0.76	0.76	0.84	0.84	0.84	0.81
Mean	1.00	1.04	0.99	1.05	0.99	0.98
STDEV	0.108	0.128	0.097	0.114	0.117	0.123
CoV	0.108	0.124	0.098	0.109	0.119	0.126

5.3.5 Summary

Table 5.11 presents the statistical parameters of T/T_h for all headed bar specimens used to develop Eq. (5.5) and (5.7). As shown in the table, T/T_h averages of 1.00, with a coefficient of variation of 0.112. T/T_h values based on Eq. (5.5) and (5.7) for the No. 14 and No. 18 bar specimens tested in this study are summarized in Table 5.12 and further evaluated in the Section 5.4. The measured bar force at failure T is compared with the calculated failure load T_h based on Eq. (5.5) and (5.7) for the No. 14 and No. 18 bar specimens tested in this study in Figure 5.9. The best-fit line closely matches the $T = T_h$ dashed line. These comparisons indicate that Eq. (5.5) and (5.7), along with the new upper limit on A_{tt} of $0.4A_{hs}$, provide very good estimates of the anchorage strength of headed bars.

Table 5.11 Statistical parameters of T/T_h ratio for all headed bar specimens with T_h based on Eq. (5.5) or (5.7)

Bar size	All	No. 5	No. 8	No. 11	No. 14	No. 18
No. of specimens	164	15	102	23	16	8
Max	1.39	1.17	1.25	1.21	1.39	1.21
Min	0.64	0.76	0.64	0.81	0.84	0.81
Mean	1.00	1.05	0.98	1.03	1.02	0.98
STDEV	0.112	0.103	0.103	0.117	0.145	0.123
CoV	0.112	0.098	0.104	0.113	0.142	0.126

Table 5.12 Summary of T/T_h values for No. 14 and No. 18 headed bars specimens tested in this study based on the developed descriptive equations, Eq. (5.5) and (5.7)

ID	n	s/d_b	Bar spacing	f_{cm} psi	$\ell_{eh,avg}$ in.	A_{tt}/A_{hs}	L. C.	T kips	T_h kips	T/T_h
14-2*	2	10.6	Wide	12,830	20.5	0.267	A	190.6	237.6	0.80
14-3	2	10.6	Wide	8,510	31.8	0	B	303.0	284.8	1.06
14-4	2	10.6	Wide	7,700	32.0	0.267	A	333.6	312.1	1.07
14-15	2	10.6	Wide	6,190	22.8	0	B	204.8	194.9	1.05
14-16*	2	10.6	Wide	5,390	22.6	0.178	A	123.6	208.8	0.59
14-16A*	2	10.6	Wide	8,350	22.4	0.178	A	186.0	225.0	0.83
14-1A*	2	10.6	Wide	12,030	22.4	0	B	160.0	184.7	0.87
14-2A	2	10.6	Wide	13,750	23.0	0.267	B	248.1	263.3	0.94
14-16B	2	10.6	Wide	7,500	22.1	0.178	B	191.7	218.2	0.88
14-16C	2	10.6	Wide	6,470	22.6	0.356	B	208.4	236.7	0.88
14-16D	2	10.6	Wide	6,900	22.9	0.827	A	289.8	247.1	1.17
14-16E	2	10.6	Wide	6,170	22.4	0.551	A	218.6	238.5	0.92
14-16F	2	10.6	Wide	5,640	22.4	0.551	A	197.8	235.0	0.84
14-17	2	7.1	Close	6,540	22.4	0.551	A	206.7	236.5	0.87
14-5	3	3.5	Close	6,830	22.3	0.178	B	181.8	167.2	1.09
14-6	3	3.5	Close	6,890	22.4	0.276	B	179.5	177.3	1.01
14-7	3	3.5	Close	7,080	32.1	0	B	252.1	181.6	1.39
14-8	3	3.5	Close	7,100	31.7	0.276	B	274.6	237.0	1.16
14-9	3	3.5	Close	11,480	22.1	0.276	B	173.9	192.2	0.90
14-10	3	3.5	Close	6,820	22.3	0.551	A	206.6	187.2	1.10
18-1	2	8.0	Wide	5,750	32.6	0.543	A	322.0	396.3	0.81
18-2	2	8.0	Wide	11,770	28.4	0.543	A	406.6	402.9	1.01
18-3	2	8.0	Wide	6,540	30.9	0.233	B	366.5	353.7	1.04
18-4	2	8.0	Wide	7,200	30.9	0.465	B	380.0	395.3	0.96
18-5	2	5.3	Close	5,310	32.5	0.543	A	300.8	343.1	0.88
18-6	2	5.3	Close	10,230	28.6	0.543	A	419.8	347.5	1.21
18-7	3	2.7	Close	5,890	32.1	0.543	A	252.1	284.8	0.89
18-8	3	2.7	Close	6,380	32.3	0.543	A	295.3	290.2	1.02

* Specimens failed in shear (not anchorage)

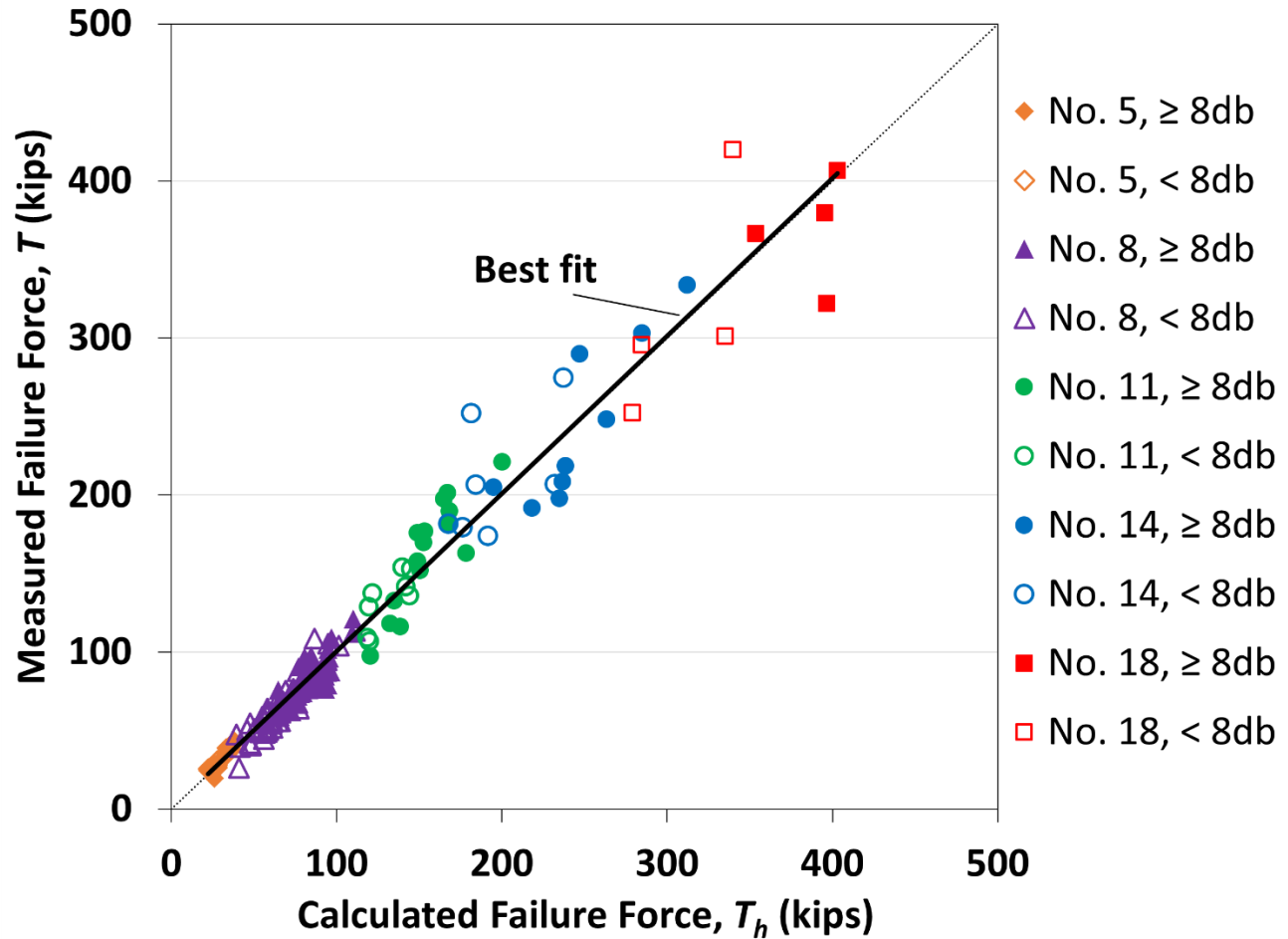


Figure 5.9 Measured versus calculated bar force at failure using new descriptive equations for all headed bar specimens, excluding those with a shear-like failure, with the calculated bar force, T_h , based on Eq. (5.5) or (5.7)

5.4 EVALUATING NEW DESCRIPTIVE EQUATIONS FOR NO. 14 AND NO. 18 BARS

In this section, the new descriptive equations, Eq. (5.5) and (5.7), are evaluated in more detail for the No. 14 and No. 18 bar specimens in this study. Table 5.13 summarizes the T/T_h values based on bar size and the presence of parallel ties for the No. 14 and No. 18 bar specimens, regardless of loading condition and excluding the specimens that failed in shear.

Table 5.13 Summary of test-to-calculated ratio T/T_h for No. 14 and No. 18 headed bars based on bar size and parallel ties, with T_h based on Eq. (5.5) or (5.7), excluding specimens that failed in shear

	T/T_h				
	All	All - Without Parallel Ties	All - With Parallel Ties	All No. 14	All No. 18
No. of Specimens	24	3	21	16	8
Max	1.39	1.39	1.21	1.39	1.21
Min	0.81	1.05	0.81	0.84	0.81
Mean	1.01	1.17	0.98	1.02	0.98
STDEV	0.137	0.191	0.117	0.145	0.123
CoV	0.136	0.164	0.119	0.142	0.126

As shown in Table 5.13, the T/T_h ratio, with T_h based on Eq. (5.5) or (5.7), has improved for No. 14 and No. 18 bar specimens, compared with the values based on the equations developed for No. 11 and smaller headed bars (given in Table 5.2). Most noticeably, the average T/T_h is now 0.98 for No. 18 bars compared with 0.92 based on Eq. (5.2) and (5.3). For all specimens with parallel ties, the new equations result in an average T/T_h of 0.98, compared with 0.95 based on Eq. (5.2) and (5.3). An overall improvement in the coefficient of variation is also observed. With Eq. (5.5) or (5.7), T/T_h for No. 14 and No. 18 bar specimens ranges from 0.81 to 1.39, with an average of 1.01 and a coefficient of variation of 0.136 (0.147 based on Eq. (5.2) and (5.3)).

Table 5.14 presents the new T/T_h values for No. 14 and No. 18 headed bar specimens with parallel ties and tested under loading condition A (joint shear equal to 80% of the applied load), excluding those with a shear-like failure.

Table 5.14 Summary of test-to-calculated ratio T/T_h for No. 14 and No. 18 headed bars tested under loading condition A (all with parallel ties) with T_h based on Eq. (5.7), excluding specimens that failed in shear

	T/T_h – Loading Condition A		
	All	No. 14	No. 18
No. of Specimens	12	6	6
Max	1.21	1.17	1.21
Min	0.81	0.84	0.81
Mean	0.98	1.00	0.97
STDEV	0.134	0.136	0.142
CoV	0.136	0.137	0.147

As shown in Table 5.14, T/T_h for the specimens with parallel ties and tested under loading condition A ranges from 0.81 to 1.21 with an average of 0.98 and a coefficient of variation of 0.136. These numbers show improvements compared with Eq. (5.3) (Table 5.3), most noticeably for No. 18 bars where the average T/T_h is now 0.97 compared with 0.92. The overall average is also improved, being 0.98 compared with 0.95 based on Eq. (5.3).

A similar summary is shown in Table 5.15 for specimens with parallel ties and tested under loading condition B.

Table 5.15 Summary of test-to-calculated ratio T/T_h for No. 14 and No. 18 headed bars with parallel ties and tested under loading condition B with T_h based on Eq. (5.7)

	T/T_h ^[1] – Loading Condition B – with Parallel Ties		
	All	No. 14	No. 18
No. of Specimens	9	7	2
Max	1.16	1.16	1.04
Min	0.88	0.88	0.96
Mean	0.98	0.98	1.00
STDEV	0.097	0.109	0.053
CoV	0.098	0.111	0.053

As shown in Table 5.15, T/T_h for the specimens with parallel ties and tested under loading condition B ranges from 0.88 to 1.16 with an average of 0.98 and a coefficient of variation of 0.098. A noticeable improvement in the average and coefficients of variation is, again, observed, compared with the values based on previous equations given in Table 5.4. The overall average increased from 0.94 to 0.98 for No. 14 bars and most noticeably from 0.93 to 1.00 for No. 18 bars.

Tables 5.14 and 5.15 show that the match of the test results provided by Eq. (5.7) is not affected by the loading condition, with the average T/T_h value of 0.98 for both cases.

The average force per bar at failure, T , for all No. 14 and No. 18 headed bar specimens (excluding those that failed in shear) is compared with that calculated using Eq. (5.5) or (5.7), T_h , in Figure 5.10. As shown in the figure, the best fit line is slightly above the dashed line representing $T = T_h$ for lower bar forces, indicating a slight overestimation of anchorage strength by Eq. (5.5) or (5.7), similar to what was observed based on Eq. (5.2) and (5.3) and shown in Figure 5.2. For higher bar forces, however, the best fit is slightly below the dashed line representing $T = T_h$, but much less so than observed in Figure 5.2 for Eq. (5.2) and (5.3). Overall, and compared with the

plot in Figure 5.2, Eq. (5.5) and (5.7) provide a more accurate representation of anchorage strength of the larger headed bars.

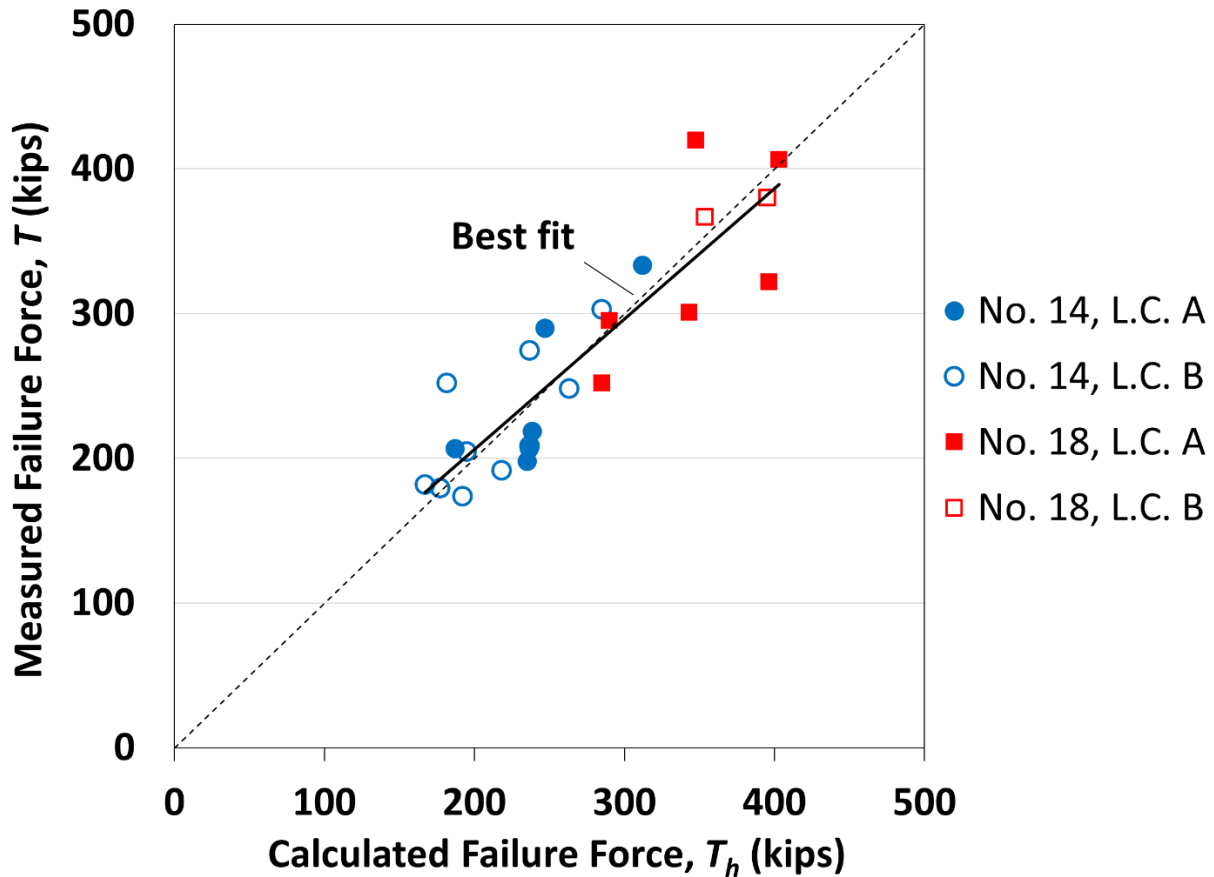


Figure 5.10 Measured versus calculated bar force at failure using new descriptive equations for No. 14 and No. 18 headed bar specimens, excluding those with a shear-like failure, with the calculated bar force, T_h , based on Eq. (5.5) or (5.7)

Values of T/T_h based on Eq. (5.5) and (5.7) are compared as a function of concrete compressive strength f_{cm} for the No. 14 and No. 18 headed bar specimens tested in this study, excluding those that failed in shear, in Figure 5.11. As shown in the figure, no noticeable trend is observed, indicating that the effect of concrete compressive strength on the anchorage strength of No. 14 and No. 18 headed bars is adequately captured by Eq. (5.5) and (5.7).

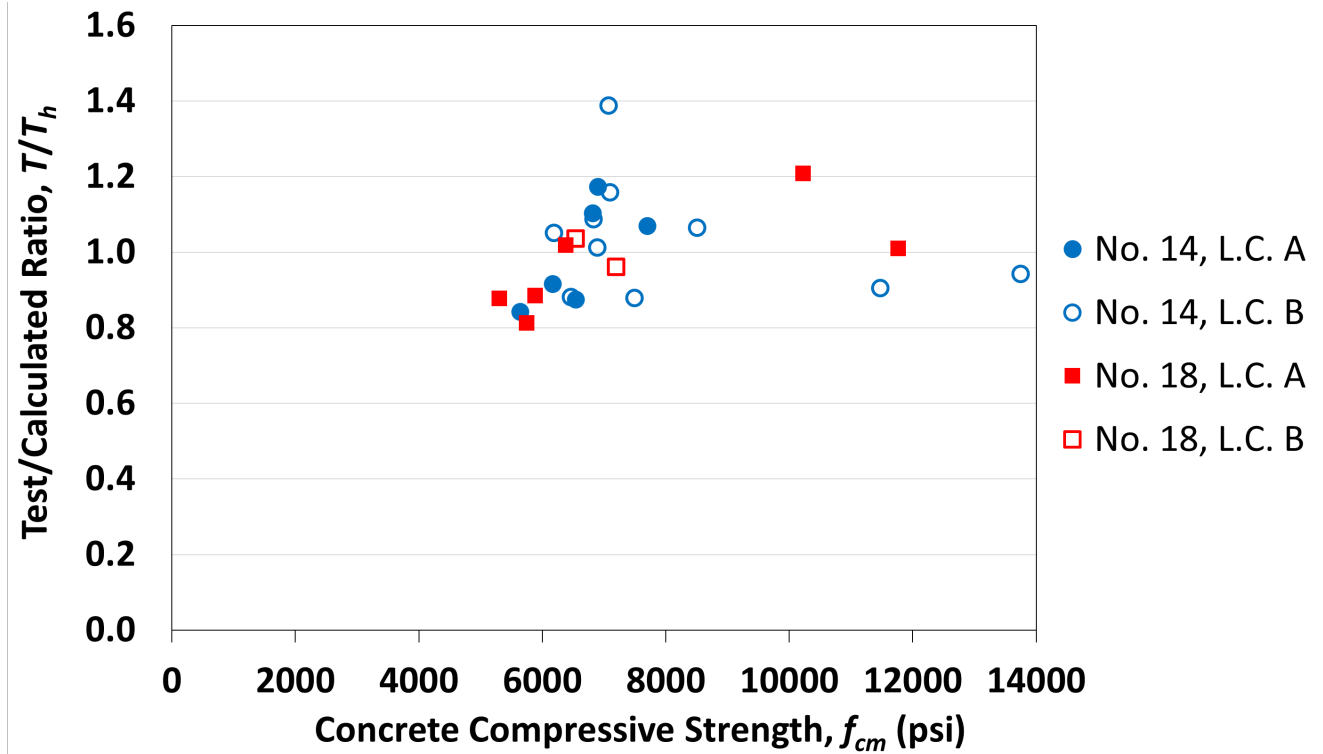


Figure 5.11 Ratio of test/calculated ratio T/T_h versus concrete compressive strength f_{cm} for No. 14 and No. 18 headed bar specimens, with the calculated bar force, T_h , based on Eq. (5.5) or (5.7)

Figure 5.12 shows T/T_h as a function of A_{tl}/A_{hs} for the No. 14 and No. 18 specimens, excluding those that failed in shear.

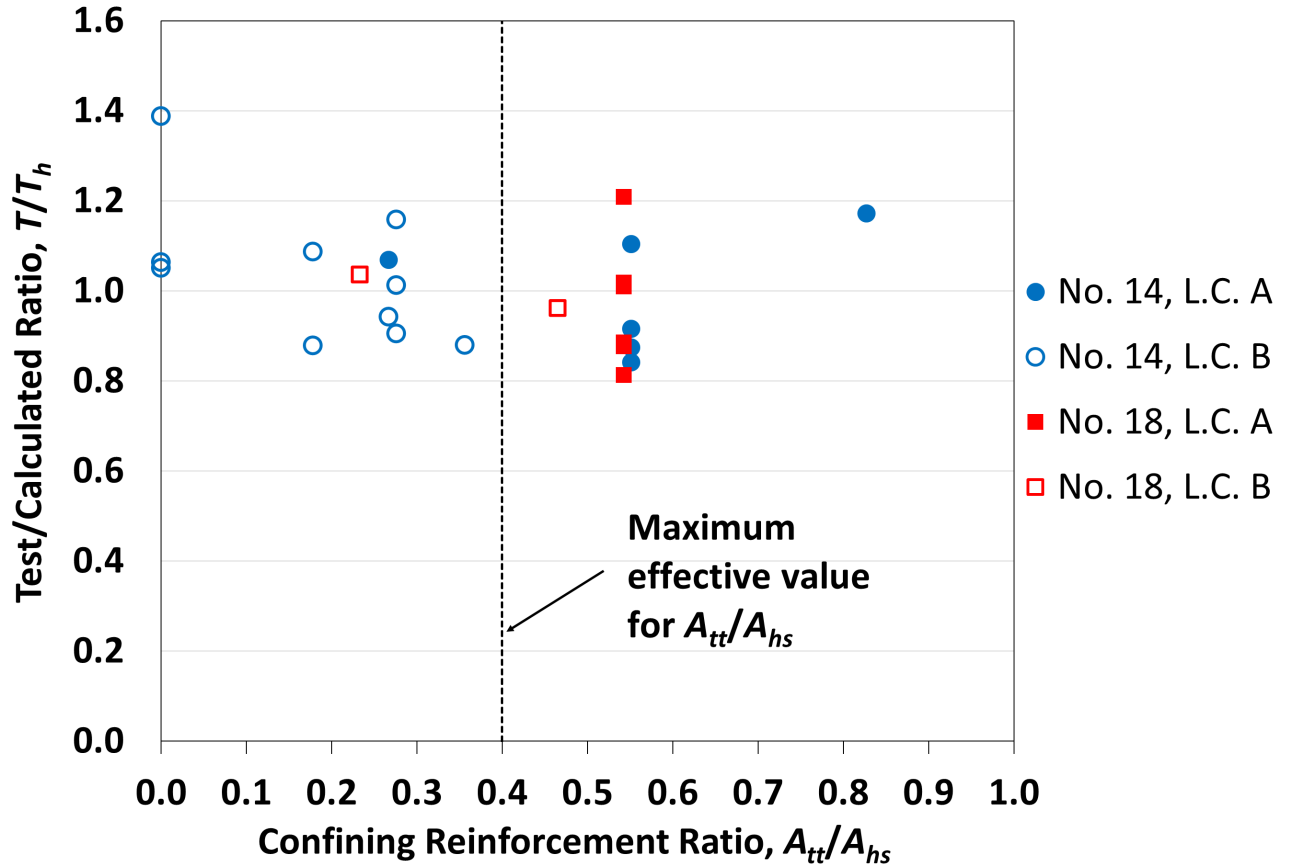


Figure 5.12 Ratio of test/calculated ratio T/T_h versus parallel tie reinforcement ratio A_{tt}/A_{hs} for No. 14 and No. 18 headed bar specimens, with the calculated bar force, T_h , based on Eq. (5.5) or (5.7)

As discussed in Section 5.3.3, the maximum effective limit for A_{tt}/A_{hs} was previously established as 0.3 (Shao et al. 2016, Ghimire et al. 2018, Ghimire et al. 2019a, 2019b). When applied with Eq. (5.7), it is increased to 0.4. A 0.4 limit on A_{tt}/A_{hs} means that values above 0.4 were not found to contribute to anchorage strength of headed bars. Figure 5.12 shows that T/T_h is largely independent of A_{tt}/A_{hs} with the upper limit of 0.4 in place for No. 14 and No. 18 headed bars.

A comparison between the test-to-calculated ratio T/T_h and the center-to-center bar spacing s normalized by bar diameter (d_b) is shown in Figure 5.13 for No. 14 and No. 18 headed bars. As shown in the figure, T/T_h for both loading conditions is largely independent of s/d_b .

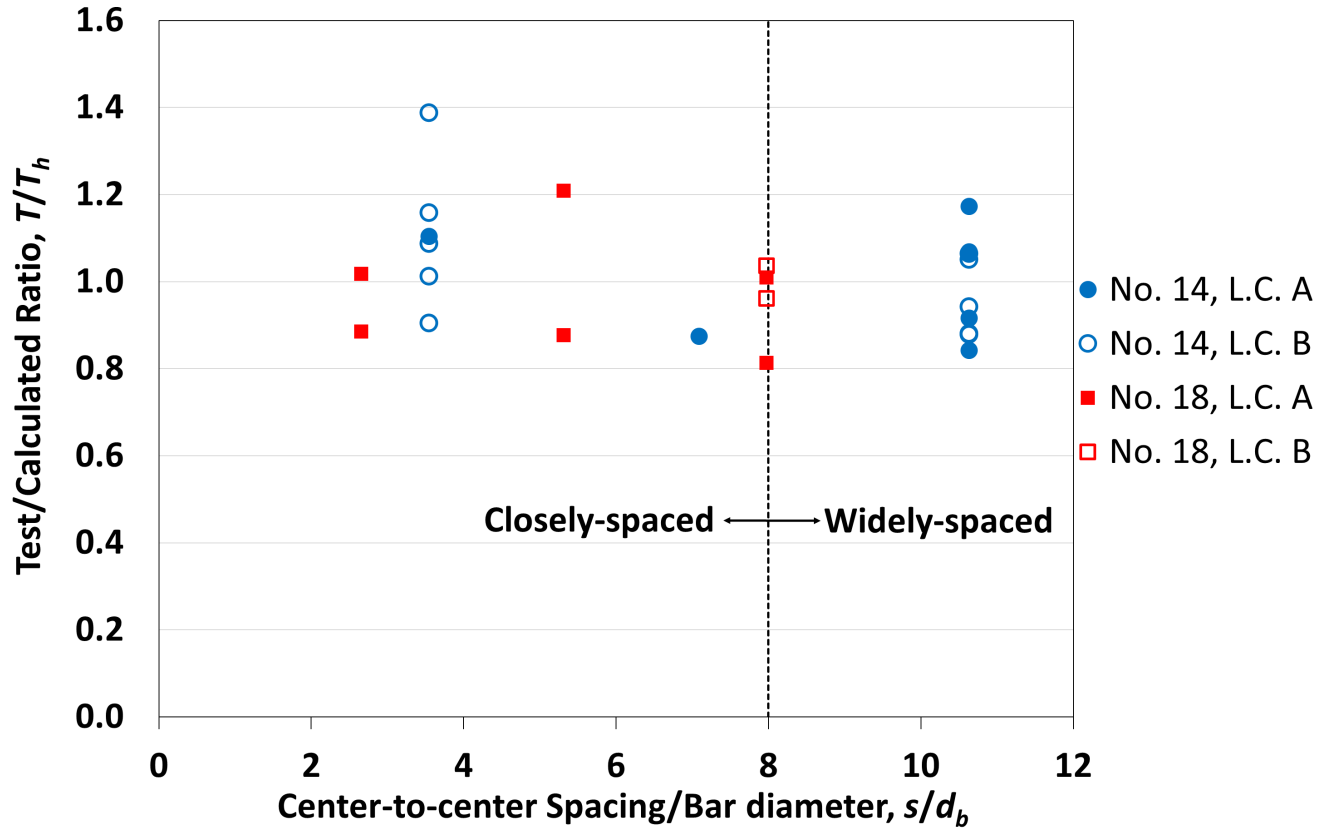


Figure 5.13 Ratio of test/calculated ratio T/T_h versus ratio of center-to-center spacing to bar diameter s/d_b for No. 14 and No. 18 headed bar specimens, with the calculated bar force, T_h , based on Eq. (5.5) or (5.7)

5.5 EFFECT OF TEST PARAMETERS

In this section, the effects of key test parameters in this study are discussed, including: loading condition, confining reinforcement, bar size and spacing, side cover, and strut angle.

5.5.1 Loading Condition

As described in Section 2.3.1, two loading conditions were considered:

Loading Condition A – Beam located at column midheight between inflection points: In this loading condition, the column moment demands above and below the joint were equal, and the shear force within the joint region equals 80% of the force applied to the test bars. This loading condition simulates an exterior beam-column joint with the beam located at the midheight of the column.

Loading Condition B – Anchorage only: In this loading condition, the joint shear is equal to ~69% of applied force to the test bars.

The 11% difference in joint shear within the joint region between loading conditions A and B and the moment reversal present in loading condition A, appears to play a major role in the type of failure and anchorage strength of headed bars for joints without a minimum quantity of shear reinforcement parallel to the headed bars within the joint, as will be discussed in this section.

The first headed bar specimen tested under loading condition A was 14-2, which had two widely-spaced No. 14 bars (18 in. on-center or $10.6d_b$) cast with high-strength (15 ksi) concrete. The specimen had five No. 4 parallel ties in the joint region, three of which were within $9.5d_b$ of the centerline of the headed bars, resulting in an A_{tt}/A_{hs} ratio (based on the descriptive equations) of 0.267. The specimen exhibited a shear-like failure, as described in Section 3.2.2, and had a test-to-calculated ratio of just 0.76 based on Eq. (5.2) and (5.3), the descriptive equations developed by Shao et al. (2016) and Ghimire et al. (2018, 2019b), and 0.80 based on Eq. (5.5) and (5.7), the equations developed in this study. The next specimen exhibiting a shear-like failure under loading condition A was 14-16, with the same dimensions as 14-2 but cast with normal-strength concrete and with an A_{tt}/A_{hs} ratio of 0.178. Specimen 14-16 is shown in Figure 5.14a following failure. Figure 5.14b shows the specimen after dissection, in which the diagonal shear crack can be seen crossing the bearing face of the head towards the back of the column along the bottom face, extending through the width of the column. Specimen 14-16 had the lowest T/T_h ratio, 0.59, based on Eq. (5.7), among the specimens tested in this study.

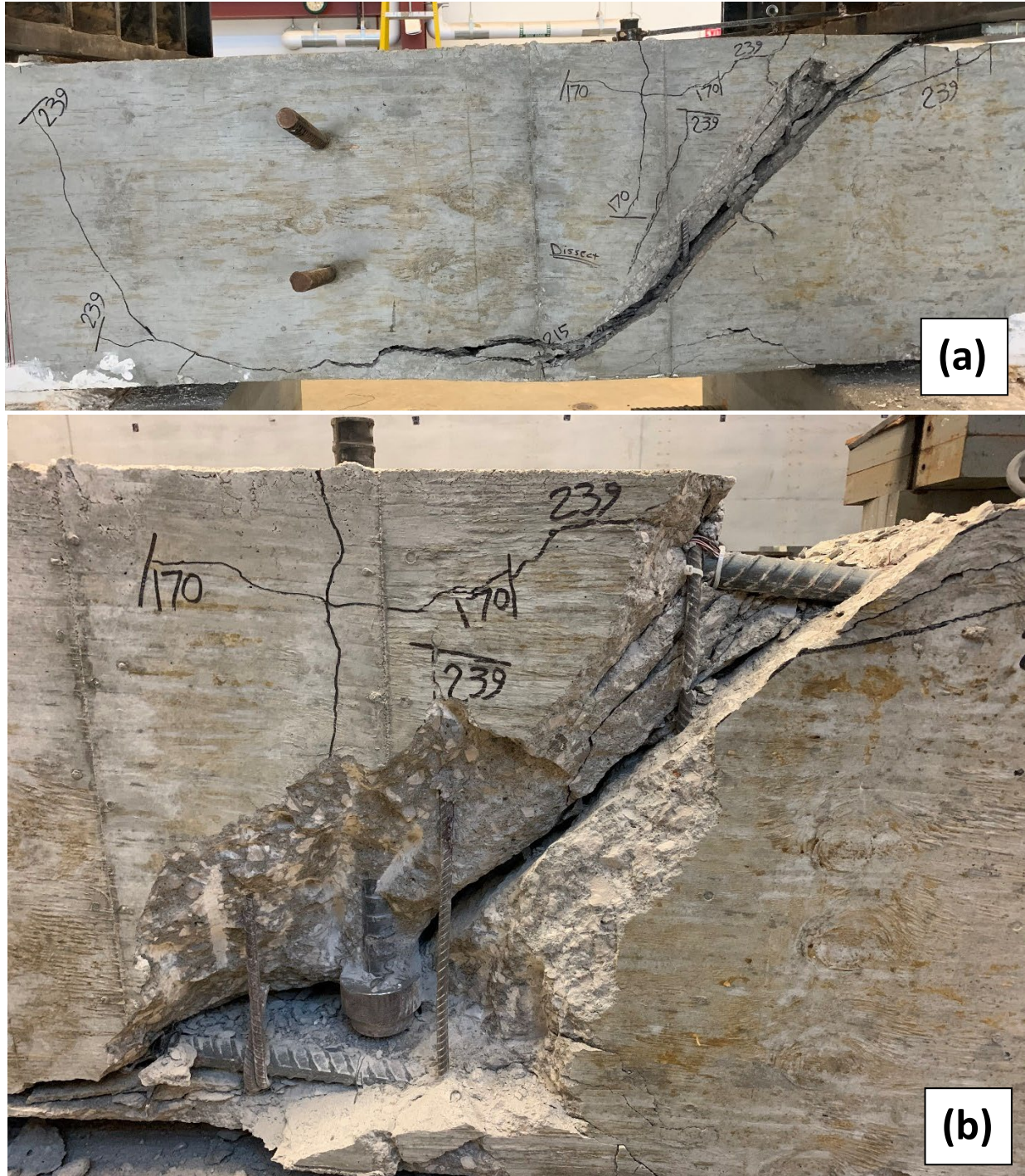


Figure 5.14 Shear-like failure observed in specimen 14-16 ($A_{tl}/A_{hs} = 0.178$) tested under loading condition A: (a) after failure and (b) after dissection

Because of the shear-like failures of specimens 14-2 and 14-16 under loading condition A, specimen 14-15, which had the same dimensions, number and spacing of headed and column bars and concrete strength as specimen 14-16, but without parallel ties, was tested under loading

condition B to reduce the shear demand in the joint region, remove the moment reversal, and promote an anchorage failure. Specimen 14-15 failed in anchorage with concrete breakout, as shown in Figure 5.15, with a test-to-calculated ratio T/T_h of 1.05 based on Eq. (5.5), illustrating the role of the loading condition on the anchorage strength of headed bars in a beam-column joint. At the time, the exact effect was not yet clear.



Figure 5.15 Anchorage failure observed in specimen 14-15 ($A_{tr}/A_{hs} = 0$) tested under loading condition B

Specimen 14-16 was then duplicated by a specimen designated as 14-16A with a modification to the longitudinal reinforcement. One additional No. 11 longitudinal bar was added on each side of the column, 2 in. from the bearing face of the headed bars, to help distribute the tensile force in the headed bars along the longitudinal bars, which serve as ties in the strut and tie model used to represent the member. The additional No. 11 bars are shown in Figure 5.16.



Figure 5.16 Additional No. 11 longitudinal bars in specimen 14-16A

Specimen 14-16A was tested under loading condition A. The specimen, however, again failed in shear, as did specimen 14-16, although the test-to-calculated ratio T/T_h increased from 0.59 to 0.83 based on Eq. (5.7). Specimen 14-16A following failure is shown in Figure 5.17.



Figure 5.17 Shear-like failure observed in specimen 14-16A ($A_{tt}/A_{hs} = 0.178$) tested under loading condition A

The final specimen in the study to exhibit a shear-like failure was 14-1A. It had two widely-spaced ($10.6d_b$ center-to-center) headed bars in high-strength concrete. The specimen had no parallel ties in the joint region and was tested under loading condition B to promote an anchorage failure. The specimen, however, failed in shear (shown in Figure 5.18) with a test-to-calculated ratio T/T_h of 0.87 based on Eq. (5.5).

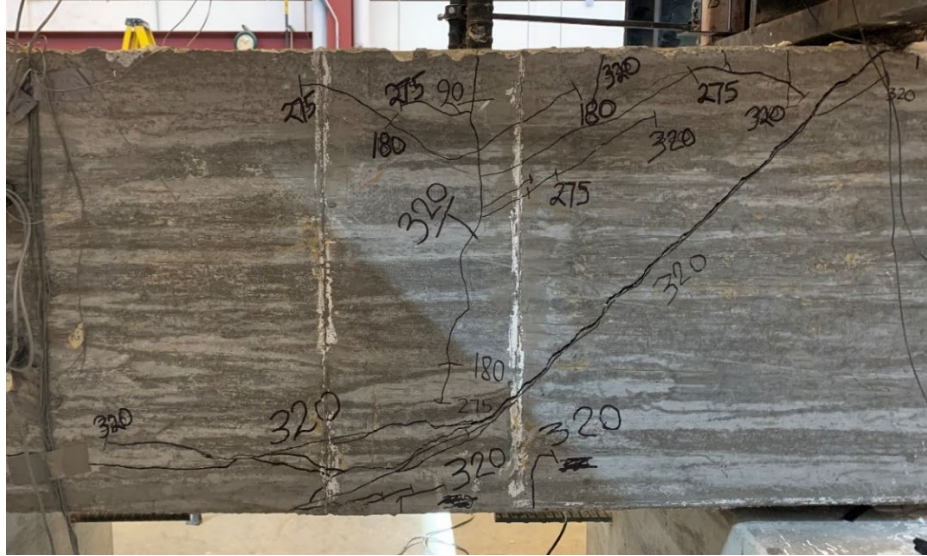


Figure 5.18 Shear-like failure observed in specimen 14-1A ($A_{tt}/A_{hs} = 0$) tested under loading condition B

The companion specimen to 14-1A, designated as 14-2A, had properties similar to 14-1A, but with parallel ties in the joint region (A_{tt}/A_{hs} of 0.267). This specimen was also tested under loading condition B. The specimen failed in anchorage as shown in Figure 5.19, with an average test-to-calculated ratio T/T_h of 0.94 based on Eq. (5.7). Comparing the failure modes of specimens 14-1A and 14-2A revealed that the joint region must contain parallel ties to provide adequate shear strength when using large-diameter headed bars to preclude a shear-like failure.



Figure 5.19 Anchorage failure observed in specimen 14-2A ($A_{tt}/A_{hs} = 0.267$) tested under loading condition B



Figure 5.21 Anchorage failure observed in specimen 14-16C ($A_{tt}/A_{hs} = 0.356$) tested under loading condition B

To gain an improved understanding of the role of shear reinforcement within a beam-column joint on the anchorage strength of headed bars, another specimen with the same dimensions as 14-16 (designated as 14-16D) was tested under loading condition A. Using five double overlapping No. 5 ties, the number and spacing of ties were designed to carry the full shear within the joint (that is, treating the concrete contribution V_c as 0). The first tie was placed 2.5 in. from the center of the headed bar, with the balance placed 5 in. on center. Three of the five overlapping ties were located within $10d_b$ from the center of the bar, resulting in A_{tt}/A_{hs} of 0.827, the highest value used in this study. The double overlapping ties are shown in Figure 5.22. Specimen 14-16D failed in anchorage, as shown in Figure 5.23, with a T/T_h of 1.17 based on Eq. (5.7) with the $0.4A_{hs}$ limit on A_{tt} .

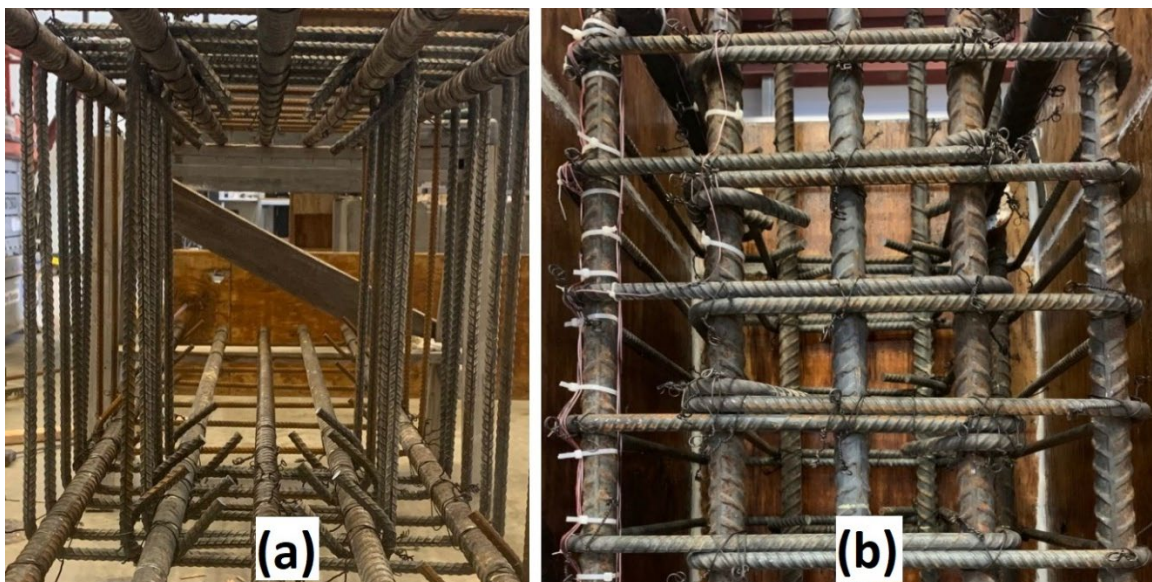


Figure 5.22 Double overlapping No. 5 ties in specimen 14-16D; (a) top view, (b) front view



Figure 5.23 Anchorage failure observed in specimen 14-16D ($A_{tt}/A_{hs} = 0.827$) tested under loading condition A (after removal of loose concrete)

Because specimen 14-16D was designed so that the entire joint shear would be carried by the ties within the joint, one question to be answered was whether less shear reinforcement proved to be adequate. To address this question, specimen 14-16E with two double overlapping No. 5 ties within $10d_b$ (8 legs total, $A_{tt}/A_{hs} = 0.551$) was tested under loading condition A. The specimen failed in anchorage, as shown in Figure 5.24, similar to 14-16D (Figure 5.23). T/T_h was 0.92 based on Eq. (5.7) applying the maximum effective value for A_{tt}/A_{hs} of 0.4. For comparison, using the

actual values of A_{tt}/A_{hs} of 0.827 for specimen 14-16D and 0.551 in specimen 14-16E result in respective values of T/T_h of 0.97 and 0.85.



Figure 5.24 Anchorage failure observed in specimen 14-16E ($A_{tt}/A_{hs} = 0.551$)

Based on the performance of specimens 14-16D and 14-16E, it is clear that, at least for larger headed bars, transverse reinforcement is needed within the joint to prevent a shear-like failure within an exterior beam-column joint with the beam located at the midheight of the column – loading simulated by loading condition A. In this study, the majority of No. 14 and No. 18 bar specimens with parallel ties that were tested under loading condition A and failed in anchorage (14-16E, 14-16F, 14-17, 14-10, 18-1, 18-2, 18-5, 18-6, 18-7, and 18-8) had A_{tt}/A_{hs} of 0.54 or 0.55 (14-16D had $A_{tt}/A_{hs} = 0.827$). These specimens included both widely- and closely-spaced bars and cast in both normal- and high-strength concrete. Since the ties in these specimens, with a wide range of properties, were effective in preventing a shear-like failure, it can be concluded that the minimum area of parallel ties (A_{tt}) needed for larger bars to address the joint shear demand is $0.5A_{hs}$. The single exception is specimen 14-4 with $A_{tt}/A_{hs} = 0.267$, the only specimen to fail in anchorage under loading condition A with $A_{tt}/A_{hs} < 0.5$. The only tests of beam-column joints containing No. 11 and smaller headed bars that failed in anchorage when loaded in a manner similar to condition A are those by Bashandy (1996) who tested 15 specimens, as discussed in more detail later in Section 5.6. All but one of the specimens had A_{tt}/A_{hs} values > 0.7 , with the majority having values as high as 1.0 or 2.0. Therefore, more study is warranted to investigate if parallel ties $< 0.5A_{hs}$ would be adequate to prevent a shear-like failure under loading condition A.

The 0.4 limit on the effective value of A_{tt}/A_{hs} , however, indicates that providing ties (A_{tt}) above $0.4A_{hs}$ does not add to the anchorage strength of headed bars. Thus, the addition of parallel ties to limit shear-like failures appears to be separate from their contribution to the anchorage strength of headed bars.

5.5.2 Parallel tie Reinforcement

Here, pairs of specimens with and without parallel ties are compared to investigate the effectiveness of ties when $A_{tt,ACI} < 0.3A_{hs}$, a case where the current Code gives no credit to parallel ties while the descriptive equations does. The contribution of middle legs (in specimens with double overlapping ties, as shown in Figure 5.22) is also investigated.

First, pairs of specimens are investigated in which one had parallel ties and the other did not. Figure 5.25 compares the anchorage strength of four pairs of specimens, 11-1 and 11-2, 14-3 and 14-4, 14-1A and 14-2A, and 14-7 and 14-8, where the first specimen in each pair did not contain parallel ties, while the second one did. All specimens with parallel ties had $A_{tt,ACI} < 0.3A_{hs}$.

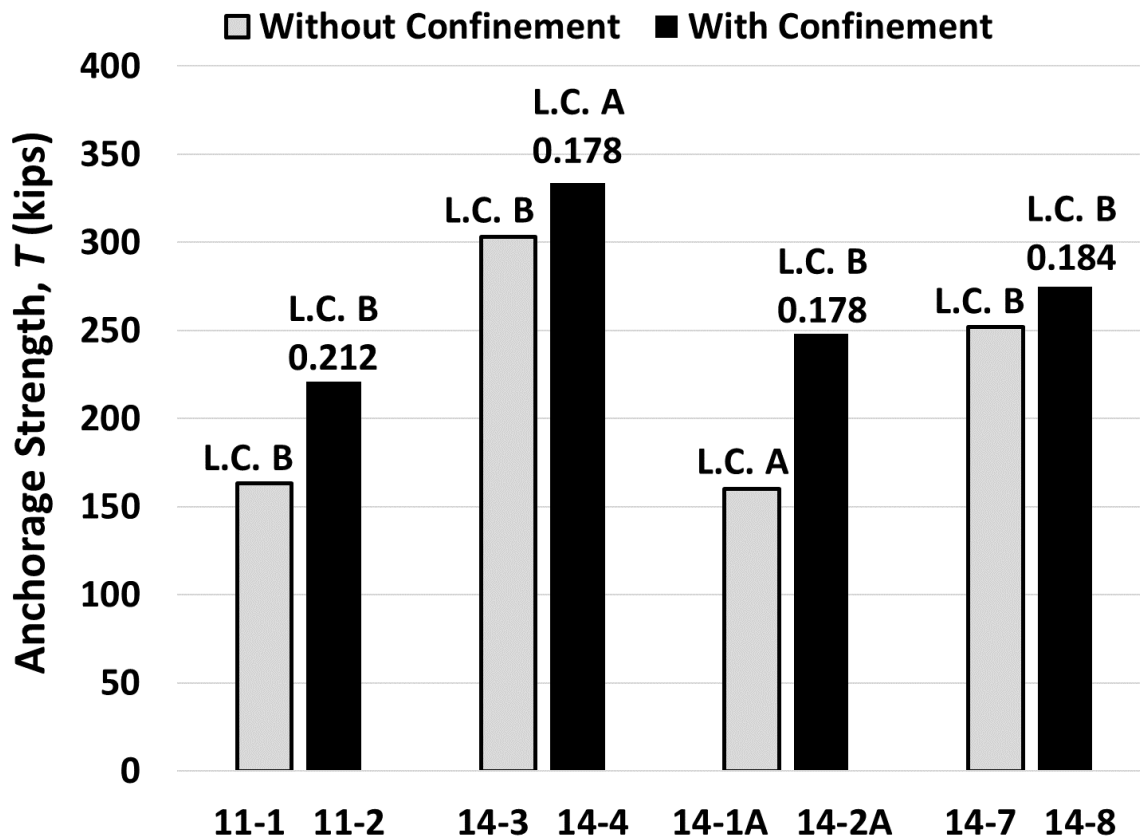


Figure 5.25 Comparing anchorage strength of headed bars with and without parallel ties (Note: L.C. = Loading Condition, and the number below L.C. denotes $A_{tt,ACI}/A_{hs}$)

As shown in Figure 5.25, providing ties in the joint region, even as low as $A_{tt,ACI}/A_{hs} = 0.178$, increased the anchorage strength in each case. These observations show that, as observed in earlier tests (Shao et al. 2016, Ghimire et al. 2018, 2019a, 2019b), and as would be predicted based on Eq. (5.7), providing ties within the joint region improves the anchorage strength of headed bars even when $A_{tt,ACI} < 0.3A_{hs}$, whereas the current Code does not allow taking advantage of such cases.

The contribution of middle legs to anchorage strength has also been investigated. To this end, two pairs of specimens are compared, namely 14-16E and 14-16F, and 18-7 and 18-8. Both specimens in each pair had the same size and spacing of ties and, therefore, the same A_{tt}/A_{hs} ratio. The only difference was that double overlapping ties were used (two external legs and two middle legs) in specimen 14-16E (similar to 14-16D, as shown in Figure 5.22) and specimen 18-8, while double ties (all four legs near the exterior) were used in specimen 14-16F (as shown in Figure 5.26) and specimen 18-7.

Specimens 14-16E and 14-16F had $A_{tt}/A_{hs} = 0.56$, were tested under loading condition A, and failed in anchorage as shown in Figure 5.27. The T/T_h ratios were 0.92 and 0.84 based on Eq. (5.7) for specimens 14-16E and 14-16F, respectively, meaning the specimen with middle legs had a 9.5% higher value of T/T_h .

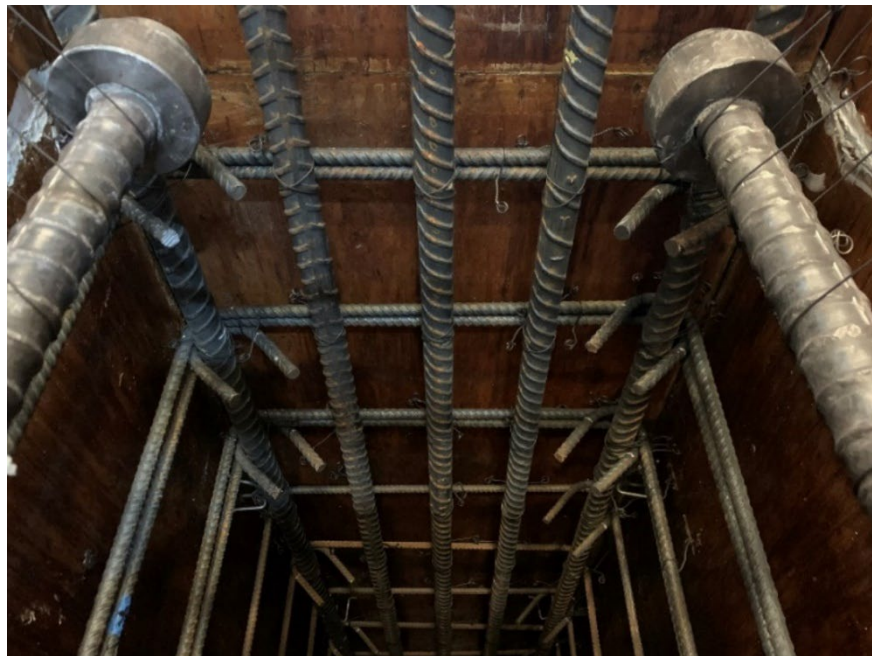


Figure 5.26 Double No. 5 ties used in specimen 14-16F

higher than that of specimen 18-7 (with external ties only), 0.89. The concrete compressive strength of specimen 18-8 was 490 psi higher than that of specimen 18-7, but based on descriptive equations, this difference should be responsible for only about 2% of the increase in anchorage strength. Therefore, the improvement in anchorage strength can be mainly attributed to the middle legs in specimen 18-8. These observations suggest that interior legs of parallel ties in the joint region contribute to anchorage strength of headed bars at least as well as exterior legs and that middle legs might be more effective in some cases.

5.5.3 Bar Spacing

Figure 5.28 presents comparisons between the anchorage strength of specimens based on bar spacing. The concrete compressive strength and A_{tl}/A_{hs} ratio were similar for each pair of specimens shown in the figure. Overall, anchorage strength for No. 14 and No. 18 headed bars correlates with bar spacing as observed for No. 11 and smaller bars, that is, individually, closely-spaced bars are weaker (lower anchorage strength) than widely-spaced bars. In general, the reduced area of the breakout surface in specimens with more closely-spaced bars can explain the differences in anchorage strength.

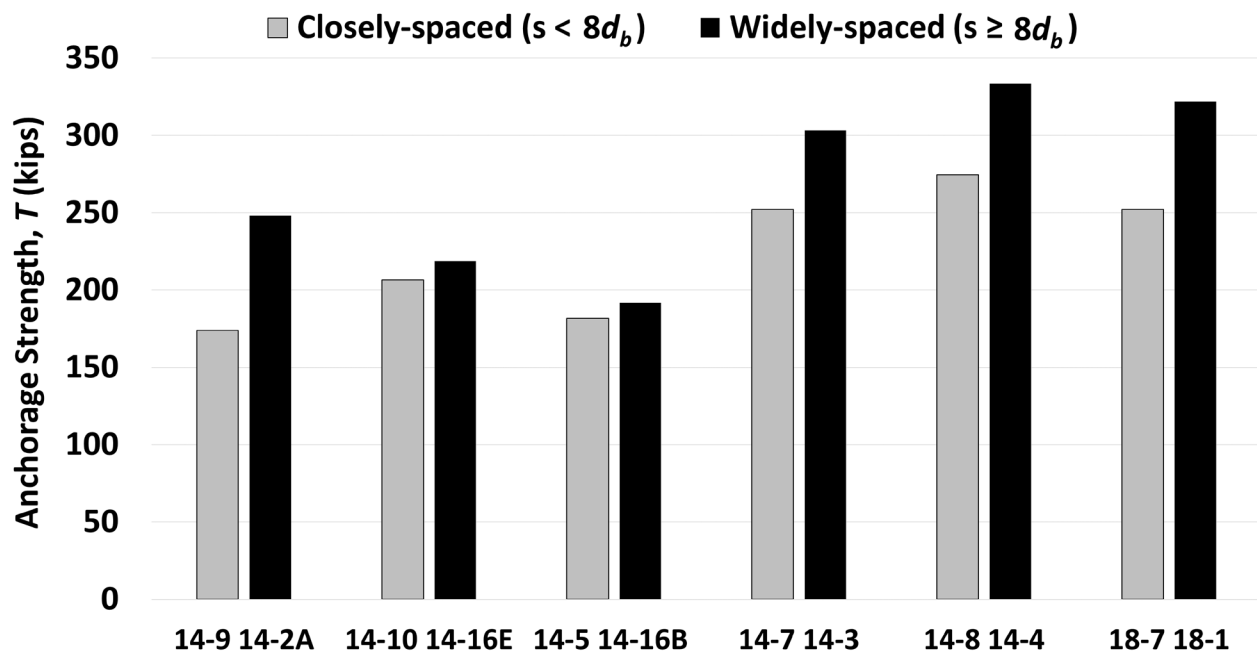


Figure 5.28 Comparing the anchorage strength (average force per bar at failure) of No. 14 and No. 18 headed bars based on bar spacing

5.5.4 Placement of Bars Within the Cross-section

The effect of placement of bars within the cross-section on the anchorage strength of headed bars is discussed in this section. The majority of specimens had a side cover to the bar of 3.5 in., similar to those tested by Shao et al. (2016). The low values of T/T_h for specimens 14-16E and 14-16F, 0.92 and 0.84, respectively, based on Eq. (5.5) and (5.7), combined with the side-splitting failure mode observed for both specimens, raised a question about the role of side cover in the anchorage strength. Both specimens had two widely-spaced headed bars, A_{th}/A_{hs} of 0.551 and were tested under loading condition A. A third specimen, 14-17, was designed with the same properties and cross-sectional dimensions as specimen 14-16F, but with the two headed bars spaced at 12 in., which increased the side cover to the bar from 3.5 in. to 6.5 in and the side cover to the head from 2.4 in. to 5.4 in. while reducing the center-to center spacing from $10.6d_b$ to $7.1d_b$.

The combination of increased side cover and closer bar spacing seemed to have only a minimal effect on the anchorage strength, as the average test-to-calculated ratio T/T_h was 0.87, close to the value of 0.84 for 14-16F. Specimen 14-17, however, failed by concrete breakout, as shown in Figure 5.29, rather than the side splitting observed in specimens 14-16E and 14-16F (Figure 5.27).



Figure 5.29 Concrete breakout observed in specimen 14-17 ($A_t/A_{hs} = 0.551$) with increased side cover to the bar and decreased bar spacing

The next comparison can be made between No. 18 bar specimens 18-1 and 18-5. The specimens had similar concrete strength, embedment length, and A_{tt}/A_{hs} (0.543) but different side cover to the bar and bar spacing. Specimen 18-1 had two bars spaced at 18 in. on-center ($8.0d_b$)

with a side cover to the bar of 3.5 in., while specimen 18-5 had two bars spaced at 12 in. on-center (5.3*d_b*), increasing the side cover to 6.5 in. The cover to the head was increased from 2.1 in. in specimen 18-1 to 5.1 in. in specimen 18-5. Both specimens were tested under loading condition A. The anchorage strength of specimen 18-1 ($T = 322.0$ kips) was 7% higher than that of specimen 18-5 ($T = 300.8$ kips), of which about 2% can be attributed to higher concrete compressive strength in 18-1 (5,750 versus 5,310 psi). T/T_h equals 0.81 and 0.88 for specimens 18-1 and 18-5, respectively. Similar to the previous comparison, however, increasing the side cover altered the failure mode from primarily side splitting (18-1) to primarily concrete breakout (18-5), as shown in Figure 5.30.

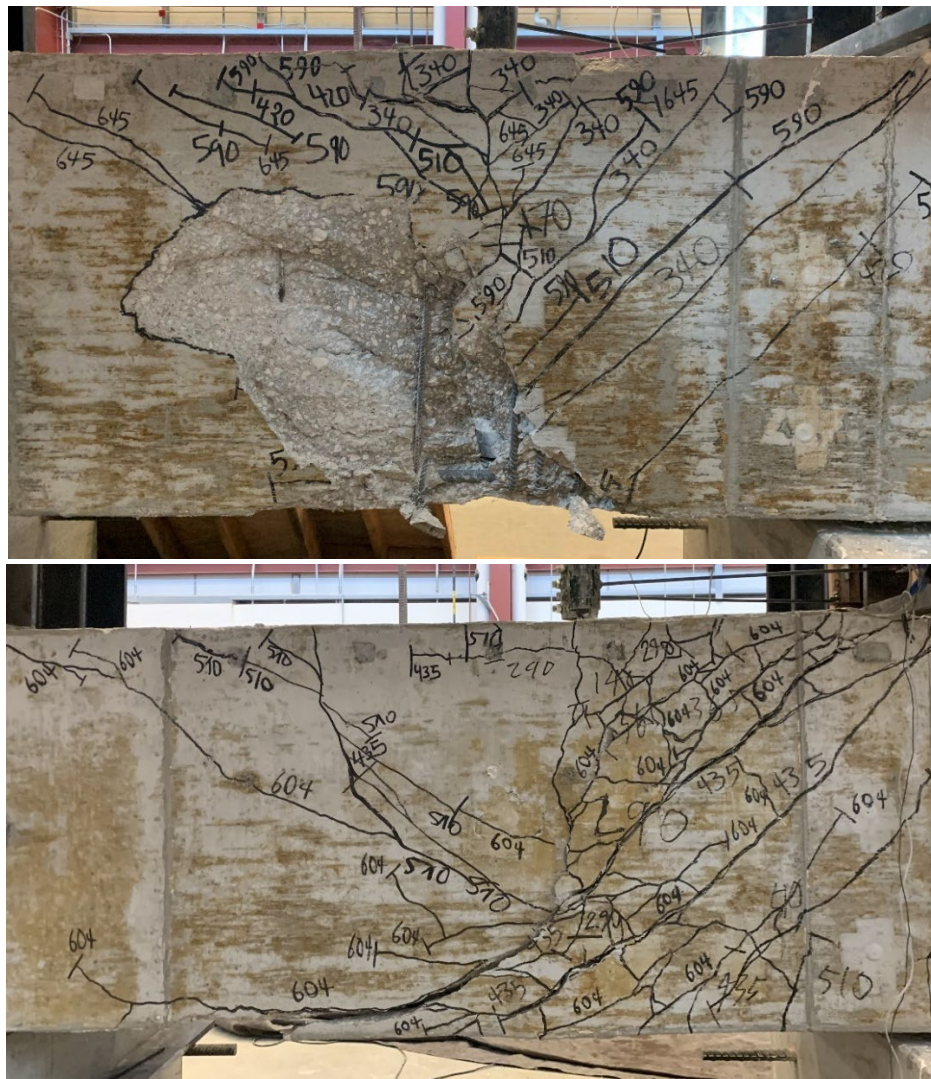


Figure 5.30 Comparing failure modes of specimen 18-1 with 3.5 in. side cover to the bar (top, side splitting) with specimen 18-5 with 6.5 in. side cover to the bar (bottom, concrete breakout), both with $A_{tr}/A_{hs} = 0.543$

The last pair of specimens to compare are 18-2 and 18-6. Both specimens contained high-strength concrete. The specimens had the same A_{tl}/A_{hs} (0.543) and were tested under loading condition A. The side cover to the bar and head in specimens 18-2 (3.5 and 2.1 in.) and 18-6 (6.5 and 5.1 in.) were the same as those in specimens 18-1 and 18-5, respectively. The anchorage strength of the specimen with increased side cover, 18-6 ($T = 419.8$ kips), was slightly higher (3.2%) than that of specimen 18-2 ($T = 406.6$ kips), despite having a lower concrete compressive strength (10,230 versus 11,770 psi). T/T_h was 1.01 and 1.21 for 18-2 and 18-6, respectively. The higher value of T/T_h for specimen 18-6 is due to the lower value of s/d_b compared with that of specimen 18-2, leading to a lower value of T_h . Figure 5.31 shows that the failure mode in specimen 18-2 was a combination of concrete breakout and side splitting, while that of specimen 18-6 appears to be side splitting (unlike previous specimens with increased side cover, 14-17 and 18-5) combined with an inclined crack through the column thickness.



Figure 5.31 Comparing failure modes of specimen 18-2 with 3.5 in. side cover to the bar (top) with specimen 18-6 with 6.5 in. side cover to the bar (bottom), both with $A_{tl}/A_{hs} = 0.543$

Overall, these observations indicate that the combined effects of increasing side cover to the bar (and thus, concrete cover to head) and decreasing bar spacing for joint with the same width did not have a major effect on the anchorage strength of No. 14 and No. 18 headed bars, but can change the failure type from side splitting to concrete breakout.

5.5.5 Compression Strut Angle

The compression strut angle is defined as the angle from the centerline of the headed bar to a line drawn between the centroid of the bearing face of the head and the center of the bearing plate simulating the compression zone of the imaginary beam, as shown in Figure 5.32. Based on the figure, the compression strut angle θ can be calculated as the inverse tangent (arctan) of x_{mid}/ℓ_{eh} . The effect of compression strut angle on the anchorage strength of hooked bars was discussed in Section 4.7, and its effect on the anchorage strength of headed bars is evaluated in this section.

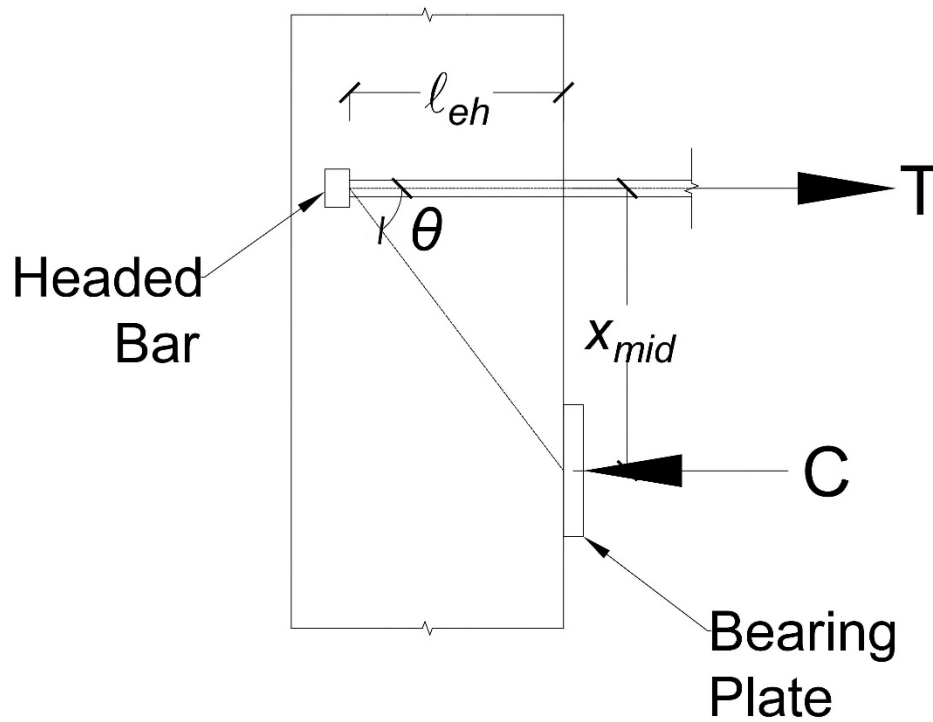


Figure 5.32 Compression strut angle (θ) for headed bars (x_{mid} is 28.56 and 38.15 in. for No. 14 and No. 18 bars, respectively, and ℓ_{eh} is the embedment length)

The values of T/T_h , with T_h based on Eq. (5.5) and (5.7), are plotted as a function of the strut angle θ for the No. 11 headed bar specimens tested by Shao et al. (2016) and Ghimire et al. (2018) and those tested in this study in Figure 5.33. Specimens with $d_{eff}/\ell_{eh} > 1.5$ are excluded from the figure, where d_{eff} is described in Section 2.3.3 and below.

As shown in Figure 5.33, no noticeable trend can be observed between T/T_h and θ with the exception of one of the specimens with the lowest (flattest) compression strut angles ($< 45^\circ$) that had a T/T_h ratio of 1.39. The rest of the specimens had values of T/T_h between 0.81 and 1.21. The insensitivity of the descriptive equations to strut angle for specimens with $d_{eff}/\ell_{eh} < 1.5$ matches the observation for hooked bars presented previously in Section 4.7 and Figure 4.15.

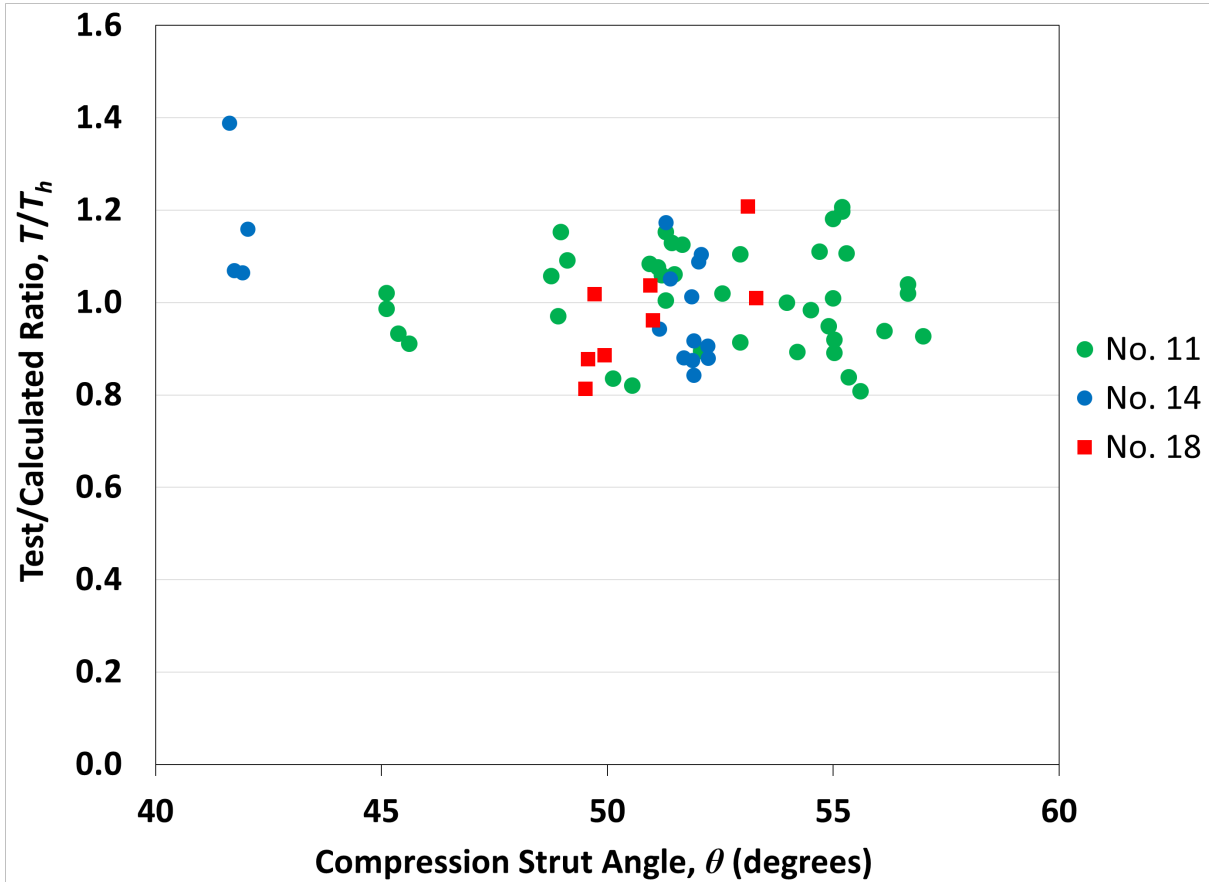


Figure 5.33 Comparison of strut angle θ versus test-to-calculated ratio T/T_h based on Eq. (5.5) and (5.7) for large (No. 11, No. 14, and No. 18) headed bars for specimens with $d_{eff}/\ell_{eh} < 1.5$

5.5.6 Effective Beam Depth

Another parameter closely related to the strut angle is ratio of the effective depth of the simulated beam to embedment length, d_{eff}/ℓ_{eh} . The approach used by Shao et al. (2016) to calculate d_{eff} is adopted here. The neutral axis of the beam is assumed to be represented by the top edge of the bearing plate, and the extreme compression fiber is assumed to be some distance c below that point. c is calculated as a/β_1 , where a is the depth of equivalent rectangular compressive stress block and calculated as $nA_b f_s / 0.85 f_{cm} b$ per flexural design procedure for reinforced concrete

beams, $\beta_1 = 0.85 - 0.05((f_{cm} - 4000)/1000) \leq 0.65$ per Section 22.2.2.4.3 of ACI 318-19, and b is the width of the specimen. The effective depth of the beam, d_{eff} , is then calculated as the sum of h_{cl} and c as shown in Figure 5.34, where h_{cl} is the distance from the center of headed bars to the top edge of the bearing plate. Bearing plates with three different widths, 6, 9, and 12 in., were used. As described in Section 2.3.3, if the calculated value of c was < 6 in., the 6 in. plate was used. If $6 \text{ in.} < c \leq 9 \text{ in.}$, the 9 in. plate was used, and, for calculated value of $c > 9 \text{ in.}$, the 12 in. plate was used.

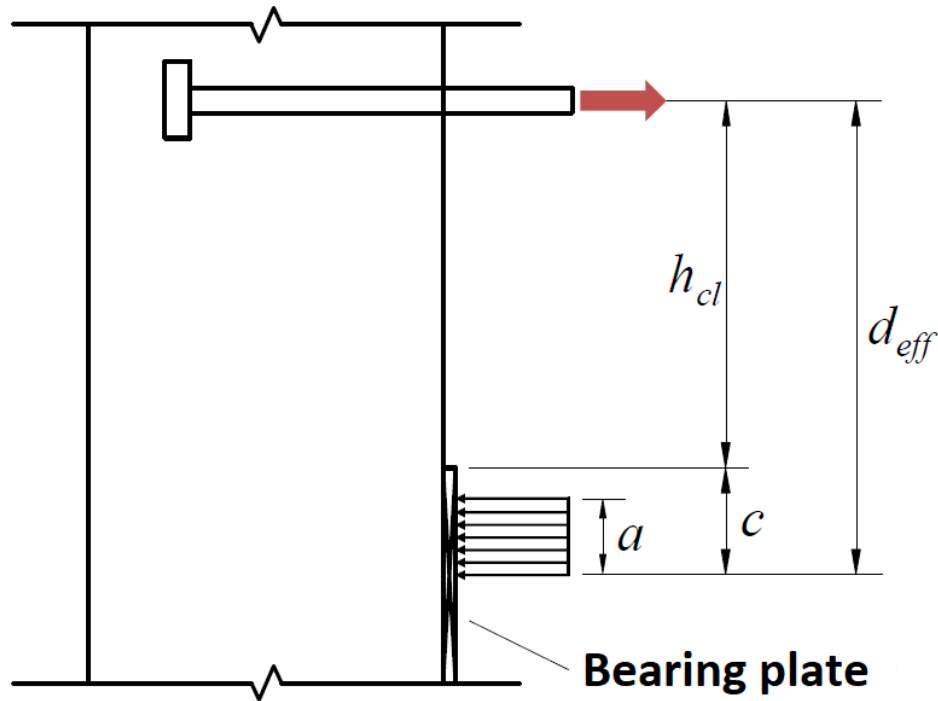


Figure 5.34 Effective beam depth d_{eff} for headed bars (Shao et al. 2016)

As established by Shao et al. (2016), specimens with $d_{eff}/\ell_{eh} > 1.5$ (that is, a deeper beam) generally have lower test-to-calculated T/T_h ratios and anchorage strengths than those with $d_{eff}/\ell_{eh} \leq 1.5$, which were used to develop descriptive equations. This point was considered in this study, with the specimens designed so that d_{eff}/ℓ_{eh} was below 1.5 to prevent possible lower anchorage strengths. As suggested in the commentary section of ACI 318-19, beam-column joints for which $d_{eff}/\ell_{eh} > 1.5$ should be provided with transverse reinforcement in the form of hoops or ties to “establish a load path in accordance with strut-and-tie modeling principles” (enable a strut-and-tie mechanism).

For the specimens shown in the previous plot (Figure 5.33), T/T_h is plotted as a function of the ratio of d_{eff}/ℓ_{eh} in Figure 5.35 below. As shown in the figure, no noticeable trend can be seen for T/T_h as function of d_{eff}/ℓ_{eh} for values of d_{eff}/ℓ_{eh} between 0.92 and 1.42 for No. 11 and larger bars. This observation is similar to that for hooked bars in Section 4.8.

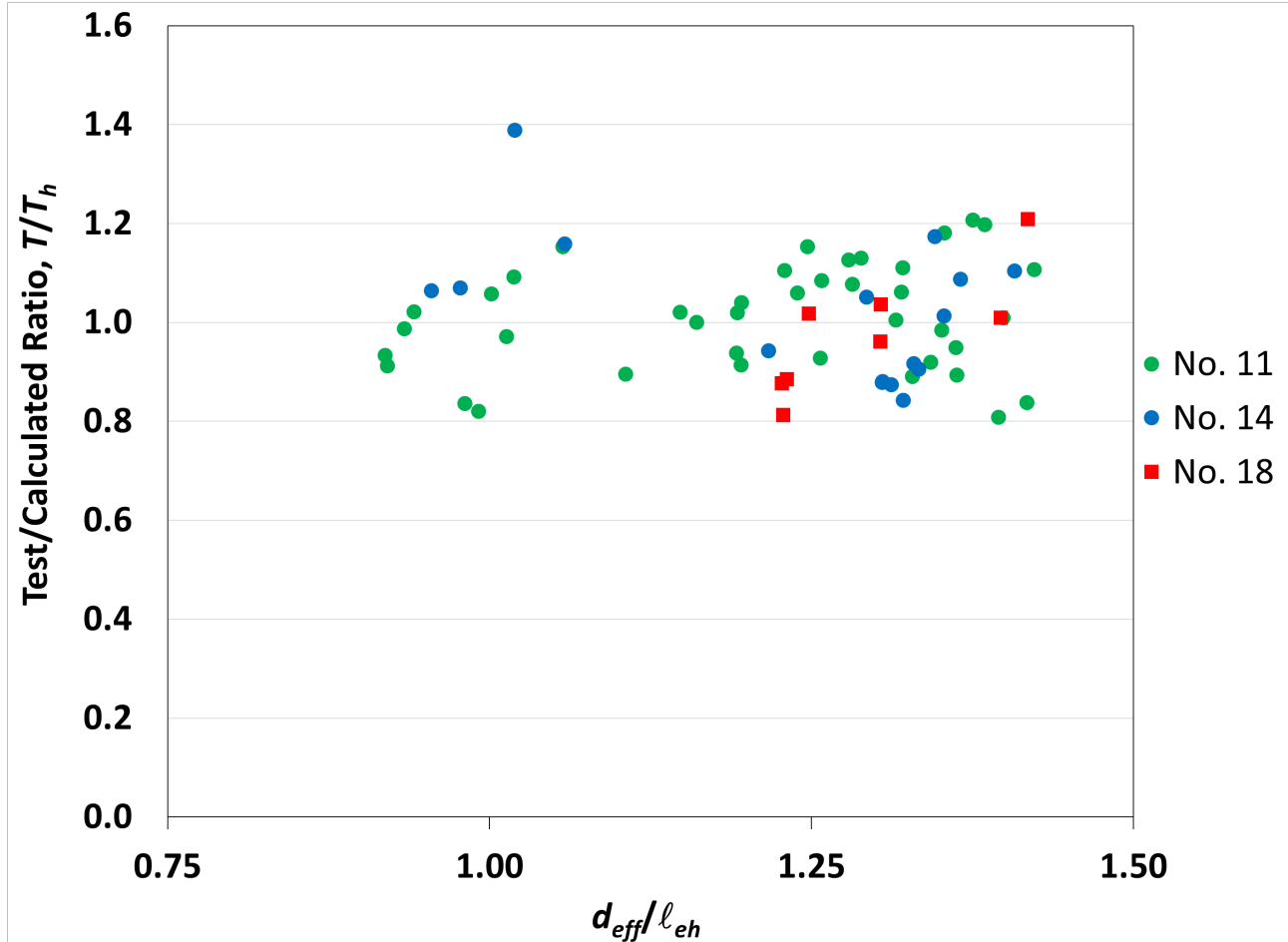


Figure 5.35 Comparison of d_{eff}/ℓ_{eh} versus test-to-calculated ratio T/T_h based on Eq. (5.5) and (5.7) for large (No. 11, No. 14, and No. 18) headed bars

5.5.7 Embedment Length

Figure 5.36 compares the values of T/T_h as a function of the ratio of embedment length to bar diameter ℓ_{eh}/d_b for the No. 11, No. 14, and No. 18 headed bar specimens used to develop Eq. (5.5) and (5.7). The majority of the specimens had ℓ_{eh}/d_b values ranging from 9.4 to 14.4. Four No. 14 bar specimens had the highest ℓ_{eh}/d_b values of 18.7-18.9, all of which had $T/T_h > 1.0$. As shown in the figure, no significant trend in T/T_h can be observed as ℓ_{eh}/d_b increases, indicating that the

accuracy of the descriptive equations developed in this study, Eq. (5.5) and (5.7), is generally not sensitive to the value of ℓ_{eh}/d_b .

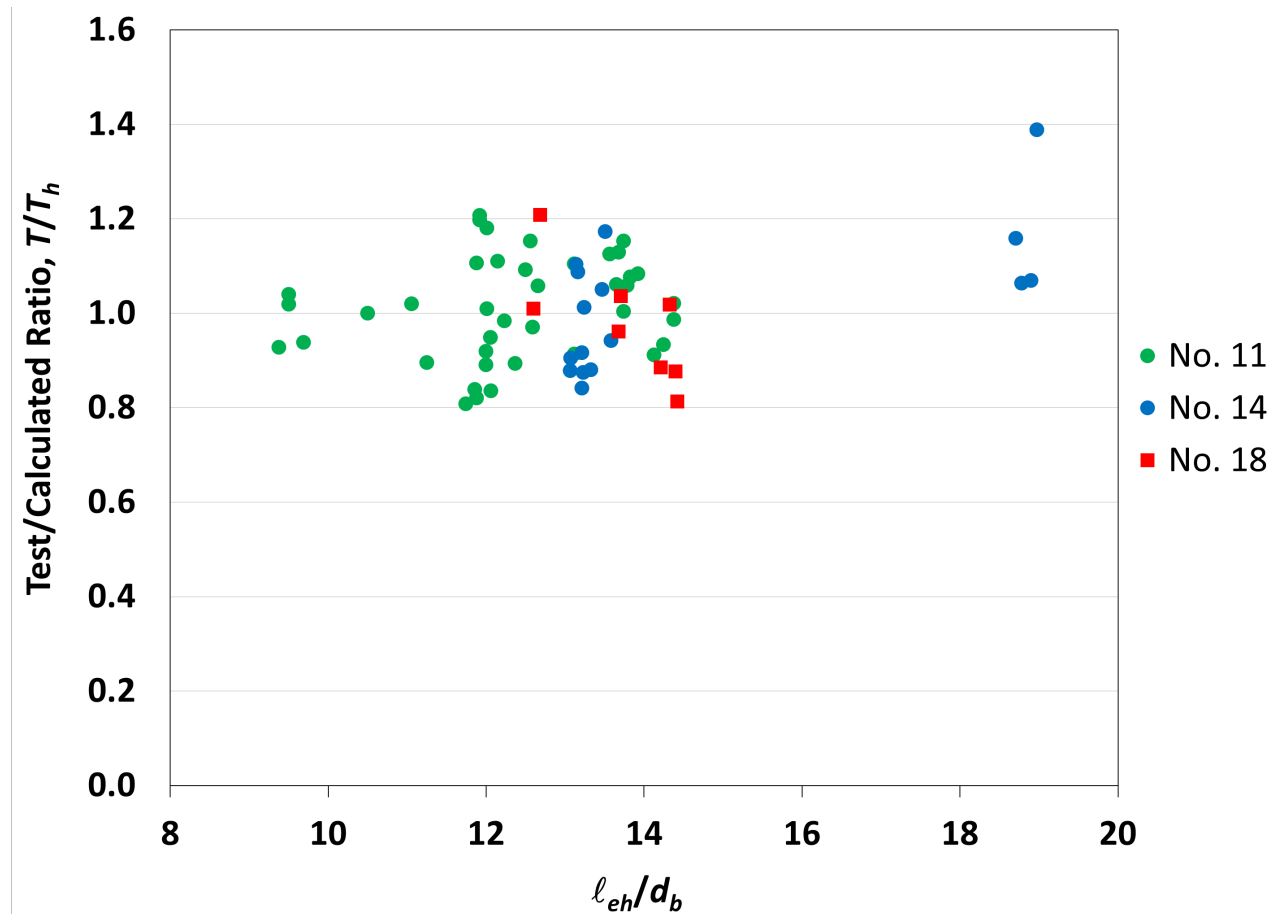


Figure 5.36 Comparison of ℓ_{eh}/d_b versus test-to-calculated ratio T/T_h for based on Eq. (5.5) and (5.7) for large (No. 11, No. 14, and No. 18) headed bars

5.5.8 Bar Location

The headed bar specimens tested at the University of Kansas, including this study, contained headed bars placed inside the column core (the area confined by the column longitudinal reinforcement, as shown in Figure 1.26). Sperry et al. (2015b) tested a limited number of hooked bar specimens with the hooked bars placed outside the column core and observed, generally, lower anchorage strengths (taken conservatively as 80%) compared with specimens with hooked bars placed inside the column core. For design purposes, Sperry et al. (2015b) suggested a bar location factor of 1.25 (1/0.8) to be applied to bars placed outside the column core, which was also adopted by Shao et al. (2016) for headed bars and eventually by the current ACI 318-19 provisions for both

hooked and headed bars. However, as the re-analysis of the hooked bar specimens in Section 4.4 showed, the bar location factor can be reasonably reduced to 1.17 (1.15 for design purposes).

To investigate the influence of bar location for headed bars and to verify the applicability of a reduced bar location factor of 1.17, specimens tested by Chun et al. (2017a) and Sim and Chun (2022a, 2022b) are used. As discussed in Section 1.2.2, these specimens were designed to force a side-blowout failure. The headed bars were placed outside the column core in all specimens. Each specimen had two headed bars in a single layer, except for those tested by Sim and Chun (2022a) where each specimen had four headed bars in two layers. The center-to-center spacing between the layers were used as s to calculate T_h for those specimens. The specimens were heavily reinforced in the joint region using double overlapping No. 5 ties providing A_{tt}/A_{hs} values between 1.01 and 1.37. The 0.4 cap on A_{tt}/A_{hs} , therefore, is applied to all specimens. The tests involve No. 14 and No. 18 (Chun et al. 2017a), No. 14 (Sim and Chun 2022a), and No. 7 and No. 10 (Sim and Chun 2022b) headed bars. The specimens were tested in a manner similar to loading condition B in this study, but with different specimen proportions, as discussed below.

In the majority of these specimens, the headed bars were placed outside the ties in addition to being placed outside the column core, as shown in Figure 5.37a, and were considered by the authors as “unconfined.” This configuration is similar to that used by Chun et al. (2017b) for No. 14 and No. 18 hooked bars, as shown in Figure 4.9a. As established in Section 4.4 for hooked bars, when bars are placed outside the column core and the confining reinforcement, ties should not be considered contributing to anchorage strength. Similarly, for the headed bar specimens in which the bars are outside the column core and parallel ties as in Figure 5.37a, A_{tt}/A_{hs} is taken as zero. In the rest of the specimens, the headed bars were wrapped by ties or hairpin transverse reinforcement, as shown in Figure 5.37b and 5.37c, respectively. For those specimens, the parallel ties were counted towards the anchorage strength. For eight specimens, the test was stopped after the headed bars yielded; those results are not considered in this analysis.

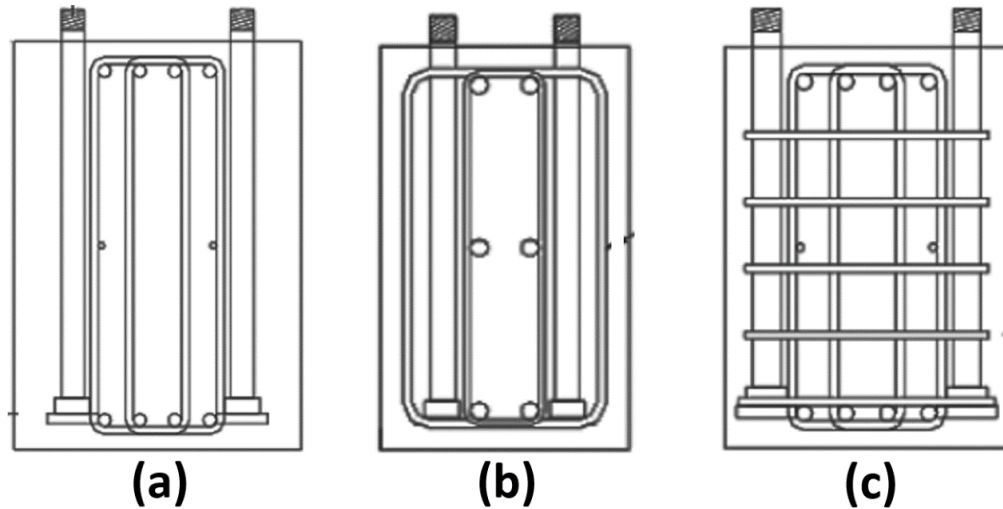


Figure 5.37 Parallel tie layouts in specimens with headed bars placed outside the column core tested by Chun et al. (2017) and Sim and Chun (2022a, 2022b): **(a)** heads outside parallel ties (“unconfined”), **(b)** heads inside parallel ties (“confined”), and **(c)** heads outside parallel ties but “confined” by hairpin transverse reinforcement

Table 5.15 summarizes the specimen details, including values of T/T_h based on two approaches. In approach one, parallel ties are counted for all specimens and no bar location factor is applied. In the second approach, parallel ties are not counted for specimens with bars outside the ties and a bar location factor of 1.17 is applied to all specimens.

Table 5.16 Details and test-to-calculated T/T_h ratios of the specimens tested by Chun et al. (2017) and Sim and Chun (2022a, 2022b) with headed bars outside column core

ID ^[1]	n	$\ell_{eh,avg}$ in.	f_{cm} psi	d_b in.	s/d_b	A_{tt}/A_{hs} ^[2]	T kips	T/T_h ^[3]	T/T_h ^[4]
D43-L7-C1-S42	2	11.9	6950	1.693	9.6	0.4	102.0	0.66	1.11
D43-L7-C1-S42-HP0.5	2	11.9	6950	1.693	9.6	0.4	136.0	0.88	1.03
D43-L7-C1-S70	2	11.9	9890	1.693	9.6	0.4	163.6	1.00	1.65
D43-L10-C1-S42	2	16.9	7570	1.693	9.6	0.4	142.7	0.71	1.09
D43-L10-C1-S42-HP0.5	2	16.9	7570	1.693	9.6	0.4	161.0	0.80	0.94
D43-L10-C1-S70	2	16.9	11,770	1.693	9.6	0.4	193.4	0.90	1.34
D43-L13-C1-S42	2	22.0	6640	1.693	5	0.4	155.0	0.76	1.23
D43-L13-C2-S42	2	22.0	6420	1.693	5	0.4	176.2	0.86	1.41
D43-L13-C1-S42-T1.5	2	22.0	5870	1.693	5	0.4	152.8	0.76	0.89
D43-L13-C2-S42-T1.5*	2	22.0	6060	1.693	5	0.4	210.2	1.04	1.22
D43-L16-C1-S42	2	27.1	6640	1.693	5	0.4	186.8	0.78	1.22
D43-L16-C2-S42*	2	27.1	6640	1.693	5	0.4	198.0	0.82	1.29
D43-L16-C1-S42-T1.5	2	27.1	6060	1.693	5	0.4	138.4	0.58	0.68
D43-L16-C2-S42-T1.5*	2	27.1	6420	1.693	5	0.4	205.0	0.86	1.00
D57-L7-C1-S42	2	15.8	7450	2.257	7.2	0.4	193.8	0.78	1.45
D57-L7-C1-S42-HP0.5	2	15.8	7450	2.257	7.2	0.4	246.0	0.99	1.16
D57-L7-C1-S70	2	15.8	11,150	2.257	7.2	0.4	230.0	0.87	1.58
D57-L10-C1-S42	2	22.6	7450	2.257	7.2	0.4	212.8	0.68	1.14

D57-L10-C1-S42-HP0.5	2	22.6	7450	2.257	7.2	0.4	274.2	0.87	1.02
D57-L10-C1-S70	2	22.6	11,150	2.257	7.2	0.4	258.0	0.77	1.27
D57-L13-C1-S42	2	29.3	5870	2.257	7.2	0.4	254.8	0.70	1.12
D57-L13-C1-S42-HP0.5*	2	29.3	5870	2.257	7.2	0.4	340.0	0.93	1.09
D57-L13-C1-S42-HP1.0a*	2	29.3	5870	2.257	7.2	0.4	340.0	0.93	1.09
D57-L13-C1-S42-HP1.0b*	2	29.3	5870	2.257	7.2	0.4	341.2	0.94	1.10
D57-L13-C2-S42	2	29.3	5870	2.257	7.2	0.4	319.2	0.88	1.40
D57-L16-C1-S42	2	36.1	6060	2.257	7.2	0.4	296.0	0.69	1.06
D57-L16-C2-S42*	2	36.1	6060	2.257	7.2	0.4	341.2	0.80	1.22
D43-L13-C1-42	4	22.0	6260	1.693	1**	0.4	88.9	0.60	1.21
D43-L13-C2-42	4	22.0	6260	1.693	2**	0.4	103.4	0.64	1.20
D43-L13-C2-70	4	22.0	12590	1.693	2**	0.4	143.2	0.79	1.44
D43-L13-C2-42-C	4	22.0	6260	1.693	2**	0.4	145.6	0.90	1.05
D43-L16-C1-42	4	27.1	6850	1.693	1**	0.4	114.6	0.65	1.26
D43-L16-C2-42	4	27.1	6850	1.693	2**	0.4	134.1	0.70	1.26
D43-L16-C2-70	4	27.1	11450	1.693	2**	0.4	156.2	0.74	1.31
D43-L16-C2-42-C*	4	27.1	6850	1.693	2**	0.4	164.3	0.85	1.00
D43-L20-C1-42	4	33.9	6260	1.693	1**	0.4	123.1	0.59	1.12
D43-L20-C2-42	4	33.9	6260	1.693	2**	0.4	135.6	0.60	1.05
D22-L6-C1	2	5.3	12020	0.875	13.5	0.4	41.4	0.79	1.20
D22-L6-C1.5	2	5.3	12020	0.875	13.5	0.4	33.7	0.65	0.98
D22-L6-C1-TR	2	5.3	12020	0.875	13.5	0.4	47.9	0.92	1.07
D22-L9-C1	2	7.9	12020	0.875	13.5	0.4	44.0	0.62	0.87
D32-L6-C1	2	7.6	12020	1.27	9.3	0.4	104.7	1.10	1.77
D32-L6-C1.5	2	7.6	12020	1.27	9.3	0.4	102.9	1.08	1.74
D32-L6-C1-TR	2	7.6	12020	1.27	9.3	0.4	91.3	0.96	1.13
D32-L9-C1	2	11.4	12020	1.27	9.3	0.4	92.6	0.73	1.07
D22-L6-C1	2	5.3	16680	0.875	13.5	0.4	38.7	0.70	1.05
D22-L6-C1.5	2	5.3	16680	0.875	13.5	0.4	31.5	0.57	0.85
D22-L6-C1-TR	2	5.3	16680	0.875	13.5	0.4	39.0	0.71	0.83
D22-L9-C1	2	7.9	16680	0.875	13.5	0.4	35.9	0.48	0.66
D32-L6-C1	2	7.6	16680	1.27	9.3	0.4	108.1	1.08	1.71
D32-L6-C1.5	2	7.6	16680	1.27	9.3	0.4	108.5	1.09	1.72
D32-L6-C1-TR	2	7.6	16680	1.27	9.3	0.4	101.5	1.02	1.19
D32-L9-C1	2	11.4	16680	1.27	9.3	0.4	103.2	0.77	1.12
							Mean:	0.79	1.19
							CoV:	0.199	0.223

- n Number of headed bars
 $\ell_{eh,avg}$ Measured embedment length
 f_{cm} Measured concrete compressive strength
 d_b Nominal diameter of the headed bar
 s Center-to-center spacing of the bars
 A_{tt} Total area of parallel ties within 8 or $10d_b$ from the top of the headed bar
 A_{hs} Total area of headed bars
 T Measured failure load
 T_h Calculated failure load based on descriptive equations, Eq. (5.5) or (5.7)
^[1] HP, C, and TR at the end of the designations denote a “confined” specimen per Figure 5.37b and 5.37c
^[2] Cap of 0.4 applied to all specimens
^[3] Parallel ties counted for all specimens and no bar location factor applied
^[4] Parallel ties not counted for specimens with bars outside the ties, and bar location factor of 1.17 applied
* Headed bars yielded; specimens not included in calculation of Mean and CoV of T/T_h

**

Center-to-center spacing between the two layers of headed bars was taken as s

As shown in Table 5.15, for the 45 specimens tested by Chun et al. (2017) and Sim and Chun (2022a, 2022b) in which headed bars did not yield, if the parallel ties are counted as contributing and no bar location being applied, T/T_h ranges from 0.48 to 1.10, with an average of 0.79 and coefficient of variation of 0.199. If the parallel ties are not counted towards anchorage strength for specimens with headed bars outside of the ties (“unconfined” per Figure 5.37a) and a bar location of 1.17 applied to all specimens, T/T_h ranges from 0.66 to 1.77, with an average of 1.19 and a coefficient of variation of 0.223. The average T/T_h of 1.19 is beyond the range of the coefficient of variation of descriptive equations (11.2%), indicating a generally conservative estimation of anchorage strength for these specimens for reasons discussed next.

This overall conservatism can be attributed to the specimen proportions used by Chun et al. (2017a) and Sim and Chun (2022a), shown in Figure 1.14. As shown in the figure, in specimens tested by Chun et al. (2017a), the distance from the center of the headed bar to the center of the bearing plate in the joint representing the compression region of the beam, x_{mid} , was $2/3$ of ℓ_{dt} , while the compressive reaction force above the joint was placed $1.0\ell_{dt}$ ($= 1.5x_{mid}$) from the center of the headed bars. For the specimens tested by Sim and Chun (2022a), x_{mid} equaled ℓ_{dt} and the compressive reaction force above the joint was placed $2/3\ell_{dt}$ ($= 0.67x_{mid}$) from the center of the headed bars. These specimen proportions resulted in forces within the joint of $0.6T$ and $0.4T$, respectively, in the specimens tested by Chun et al. (2017) and Sim and Chun (2022a). The geometry of their test specimens was clearly dissimilar to what would be expected in reinforced concrete frame structures. By way of comparison, the forces within the joints for the specimens tested in this study were $\sim 0.69T$ under loading condition B and $0.80T$ under loading condition A, both of which had realistic specimen geometries. The values of $0.6T$ and $0.4T$ indicate that lower forces were carried in the joint for these specimens compared with the specimens used to develop the descriptive equations in this study and by Shao et al. (2016) and Ghimire et al. (2018, 2019a, 2019b). It also means that a higher portion of the total applied force T was shared with the upper compression reaction. This is similar to the hooked bar specimens tested by Marques and Jirsa (1975) and Pinc et al. (1977) where in the force in the joint was just $0.54T$ (Figure 4.21b) and the resulting strength of the specimens was high compared to that calculated using the descriptive equations, as discussed in Section 4.9. Relatively high average T/T_h ratios are, thus, expected for headed bar specimens tested by Chun et al. (2017a) and Sim and Chun (2022a, 2022b).

Overall, the analysis presented in this Section indicates that applying a bar location factor of 1.17 (1.15 for design purposes) for headed bars placed outside the column core provides adequately safe results.

5.6 BEAM-COLUMN JOINT SPECIMENS NOT USED TO DEVELOP DESCRIPTIVE EQUATIONS

The descriptive equations in this study, Eq. (5.5) and (5.7), were developed based on No. 11 bar and smaller specimens tested by Shao et al. (2016) and No. 11 and larger bar specimens tested in this study, all at the University of Kansas. This section evaluates application of Eq. (5.5) and (5.7) to test results for beam-column joint specimens in other studies. The specimens include those by Bashandy (1996), Chun et al. (2009), Chun et al. (2017a), and Sim and Chun (2022a, 2022b). These four studies were described in Section 1.2.2. The study by Chun et al. (2009) is excluded because the specimens had a single headed bar, and, as discussed by Shao et al. (2016), the descriptive equations were developed based on the results from specimens with at least two headed bars and may not apply to single-bar specimens. As shown by Shao et al. (2016), most single-bar specimens tested by Chun et al. (2009) exhibited very low T/T_h values based on descriptive equations Eq. (5.2) and (5.3). The specimens tested by Chun et al. (2017a) and Sim and Chun (2022a, 2022b) were covered in the previous section. The specimens tested by Bashandy (1996) are therefore investigated here in more detail.

Bashandy (1996) tested 32 specimens, each containing two No. 8 or No. 11 headed bars, with and without parallel tie reinforcement. Specimens with parallel ties had A_{tt}/A_{hs} ratios ranging from 0.212 up to 2.025, with the majority having very high A_{tt}/A_{hs} (> 0.75). Also, all but two specimens had closely-spaced bars, with values of s/d_b of 4.6 or 5.0. The specimens were narrow, with a column width of 12 in., and depths of 12 or 15 in. Similar to the current study, two loading conditions were considered, comparable to loading conditions A and B (as defined in Section 2.3.1). In the first loading condition (comparable to loading condition A and is identified here as A'), the joint shear was almost the same as loading condition A (79.5% versus 80% of the total force applied to the headed bars for loading condition A). In the second loading condition (comparable to loading condition B and identified here as B'), the joint shear was ~66% of the force applied to the headed bars (comparable to ~69% in loading condition B in this study). Although the loading conditions used by Bashandy (1996) were similar to those in this study, the specimen proportions were different. As shown in Figure 5.38, the distance from the center of the

headed bars to the compression reaction above the joint, x_{top} , was almost the same in both studies – $2x_{mid}$ and $1.96x_{mid}$ for this study and Bashandy (1996), respectively. However, the compressive forces acting at the bottom of the specimen (equivalent to the force C_3 by the lower tension member in Figure 2.15) were placed closer to the joint region in Bashandy’s specimens than in this study. For Bashandy (1996), the distance from the center of the compression zone of the simulated beam to the compressive force at the bottom of the specimen, x_{bot} , was $1.18x_{mid}$, compared with $2x_{mid}$ in this study. As shown in Figure 5.38, despite the difference in x_{bot} , the shear force in the joint was still $0.8T$ in loading condition A’ (similar to loading condition A) since the force applied at the bottom of the specimen was chosen by Bashandy (1996) to equal $0.33T$.

Of the 32 specimens tested by Bashandy (1996), 19 were tested using loading condition A’ and 13 were tested using loading condition B’. Eleven of the specimens tested by Bashandy failed in shear, rather than anchorage and, hence, were not used by Bashandy in his analyses. Those specimens are also excluded from the comparisons provided here, as are three specimens in which the headed bars were anchored behind the column longitudinal bars leaving 18 specimens.

Bashandy (1996) used three different reinforcement configurations, shown schematically in Figure 5.39. In the first layout (specimens T10, T12, and T13), the headed bars were located outside the column core and the parallel ties (Figure 5.39a), similar to the layout used by Chun et al. (2017a) and shown in Figure 5.37a. The one distinction between the two is that, in Bashandy’s tests, the headed bars were in contact with column longitudinal bars and the parallel ties overlap with the headed bars, whereas in Chun et al.’s layout, the external legs of the ties were placed between the headed bars and column longitudinal bars. The headed bars had a side cover of 1.5 in. (equal to $1.1d_b$ for T10 and $1.5d_b$ for T12 and T13). For these three specimens, a bar location factor ψ_o of 1.17 is applied when calculating T/T_h using Eq. (5.5) and (5.7). In addition, as discussed in Sections 4.4 and 5.5.8, the ties are not taken as contributing to anchorage strength (that is, A_{ti}/A_{hs} should be taken as 0) when bars are placed outside the column core and confining ties. In the second layout, (specimens T14 and T25), the headed bars were placed inside the column core and parallel ties were wrapped around the column longitudinal bars (Figure 5.39b). For the rest of the specimens, both the headed bars and the parallel ties were placed inside the column longitudinal bars (Figure 5.39c). A side cover to the headed bars of 3 in. ($2.13d_b$ or $3d_b$) was used for the specimens shown in Figures 5.39b and c. The reinforcement layouts shown in Figure 5.39a and c are not common in practice, and along with the narrow column width, are not indicative of

reinforced concrete frames. For these reasons, the specimens tested by Bashandy (1996) were not used in developing the descriptive equations.

Table 5.17 presents the key specimen parameters along with the T/T_h ratios based on Eq. (5.5) and (5.7) for the 18 specimens considered for analysis.

Table 5.17 Test-to-calculated ratio T/T_h based on Eq. (5.5) and (5.7) for beam-column joint specimens tested by Bashandy (1996) (values converted from SI units)

Specimen ID	n	ℓ_{eh}	f_{cm}	d_b	s/d_b	A_{tl}/A_{hs}^*	L. C.	T	T_h	T/T_h
		in.	psi	in.				kips	kips	
T9	2	11.0	5000	1.41	3.3	0.641	B'	76.4	89.6	0.85
T10**	2	12.5	5000	1.41	5.4	0.596	B'	60.9	77.8	0.92
T12**	2	9.8	5110	1	8.0	0.557	B'	40.0	65.1	0.72
T13**	2	12.8	5560	1	8.0	0.785	A'	61.4	85.1	0.84
T14	2	11.0	5400	1.41	3.3	0.212	A'	93.5	79.1	1.18
T16	2	14.0	5740	1.41	3.3	1.026	A'	95.8	108.5	0.88
T20	2	8.2	5110	1.41	3.3	1.026	A'	78.5	74.1	1.06
T21	2	8.3	5110	1	5.0	2.025	A'	49.0	61.4	0.80
T22	2	8.3	5110	1	5.0	2.025	A'	41.1	61.4	0.67
T23	2	11.2	4820	1.41	3.3	1.026	A'	68.8	90.1	0.76
T24	2	11.2	4690	1.41	3.3	1.026	A'	80.3	89.8	0.89
T25	2	11.0	4690	1.41	3.3	1.962	A'	95.8	88.7	1.08
T26	2	17.0	4550	1.41	3.3	1.026	A'	111.3	120.6	0.92
T27	2	8.0	4550	1.41	3.3	1.026	A'	44.5	71.8	0.62
T28	2	11.2	4830	1.41	3.3	1.026	A'	97.1	90.2	1.08
T29	2	11.0	4830	1.41	3.3	1.026	A'	86.6	89.1	0.97
T30	2	11.3	3210	1	5.0	2.025	A'	62.7	71.6	0.88
T32	2	8.0	4830	1	5.0	2.025	A'	48.6	59.4	0.82
									Mean:	0.89
									CoV:	0.168

* Cap of 0.4 applied to all specimens, except T10, T12, T13 (refer to next footnote)

** Headed bars were outside column core and side cover was 1.5 in. (half of other specimens), so bar location factor of 1.17 applied. Also, headed bars were outside parallel ties, therefore ties were not counted towards anchorage strength ($A_{tl}/A_{hs} = 0$)

As shown in Table 5.17, T/T_h for the 18 specimens ranges from 0.62 to 1.18, with a mean of 0.89 and a coefficient of variation of 0.168. For the 15 specimens tested under loading condition A', T/T_h ranges from 0.62 to 1.18 with a mean of 0.90 and a coefficient of variation of 0.175. The mean values are within the range of the coefficients of variation of Eq. (5.5) and (5.7), 11.8%. The mean values of 0.89 or 0.90, however, indicate these specimens are relatively weak with respect to values calculated using the descriptive equations and thus, the majority of other specimens subjected to similar loading.

The low mean values of T/T_h also would seem to support the use of a limit on A_{tt}/A_{hs} , in this case 0.4, since 17 out of the 18 specimens had A_{tt}/A_{hs} values > 0.55 and 13 had values of 1.0 or 2.0. Clearly, all of parallel ties provided did not contribute to anchorage strength. Without applying the 0.4 limit on A_{tt}/A_{hs} (that is, assuming all ties contributed to anchorage strength), the mean T/T_h would drop to 0.65.

The last observation is that specimens T14 and T25, the only two specimens that, realistically, contained parallel ties wrapped around both the headed bars and column longitudinal reinforcement (Figure 5.39b), had the highest T/T_h values (1.18 and 1.08, respectively), suggesting that Eq. (5.5) and (5.7) are applicable to beam-column joints, as used in conventional practice.

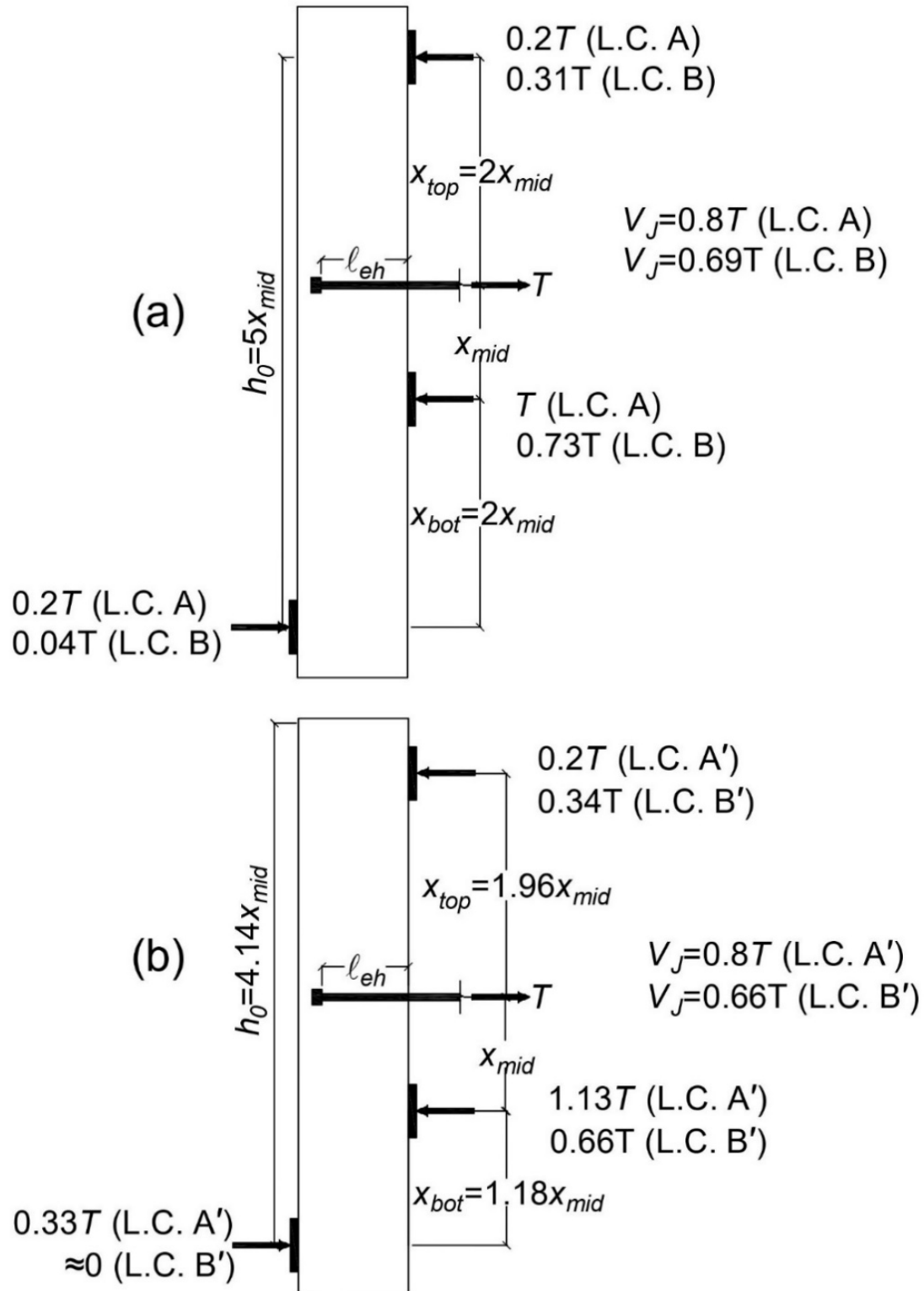


Figure 5.38 Specimen proportions and applied forces: (a) current study; (b) Bashandy 1996
(Note: the bottom drawing is not to scale, L.C. = Loading condition, V_J = Joint Shear)

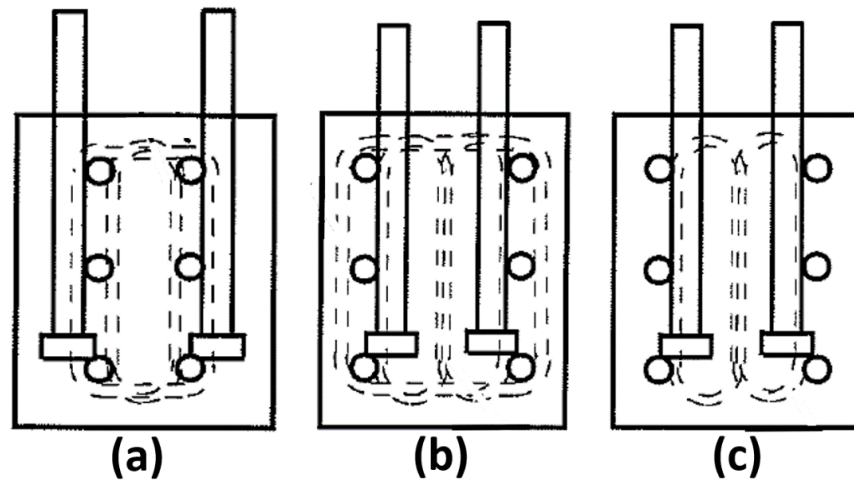


Figure 5.39 Schematic of the reinforcement layouts used by Bashandy (1996): (a) Headed bars outside the column core and parallel ties (specimens T10, T12, and T13); (b) Headed bars inside the column core and parallel ties (specimens T14 and T25); and (c) Headed bars inside column core but ties were not wrapped around column longitudinal bars (rest of the specimens)

CHAPTER 6: DESIGN APPROACH

In the previous chapters, the test results for hooked and headed bar beam-column joints containing No. 11, No. 14, and No. 18 bars were presented and discussed. Previous descriptive equations to characterize anchorage strength developed for No. 11 and smaller bars were evaluated for No. 14 and No. 18 bars. New descriptive equations were then developed to represent the anchorage strength of bars as large as No. 18. In this chapter, new design provisions are proposed for hooked and headed bars, including new equations to calculate development length. The proposed design equations are based on simplified versions of the new descriptive equations, Eq. (4.5) and (4.7) for hooked and Eq. (5.5) and Eq. (5.7) for headed bars to include the effects of bar spacing and confining/parallel tie reinforcement. The procedure is discussed in the next sections, and the proposed design equations are evaluated for the hooked and headed bar beam-column joint database.

6.1 HOOKED BARS

6.1.1 Simplified Descriptive Equations

Simplifying the descriptive equations is accomplished by rounding the powers of different variables (such as f_{cm} and d_b) to numbers suitable for a design equation and finding new constants so that the mean test-to-calculated ratio T/T_h is 1.0. The procedure used by Ajaam et al. (2017) is followed to simplify the descriptive equations, which starts with the base equation for widely-spaced (center-to-center spacing $\geq 6d_b$) hooked bars without confining reinforcement, as shown in Eq. (4.4) and repeated here.

$$T_c = 319 f_{cm}^{0.281} \ell_{eh}^{1.106} d_b^{0.430} \quad (6.1)$$

where T_c is the anchorage strength of hooked bars without confining reinforcement (lb), f_{cm} is concrete compressive strength (psi), ℓ_{eh} is embedment length (in.), and d_b is bar diameter (in.). Rounding the powers of f_{cm} , ℓ_{eh} , and d_b to 0.25, 1.0, and 0.5, respectively, a new constant is then found using the same iterative analysis used to derive Eq. (6.1).

$$T_c = 551 f_{cm}^{0.25} \ell_{eh} d_b^{0.5} \quad (6.2)$$

A new expression for the effect of close bar spacing is found by plotting center-to-center spacing/ d_b versus T/T_c using Eq. (6.2), as shown in Figure 6.1.

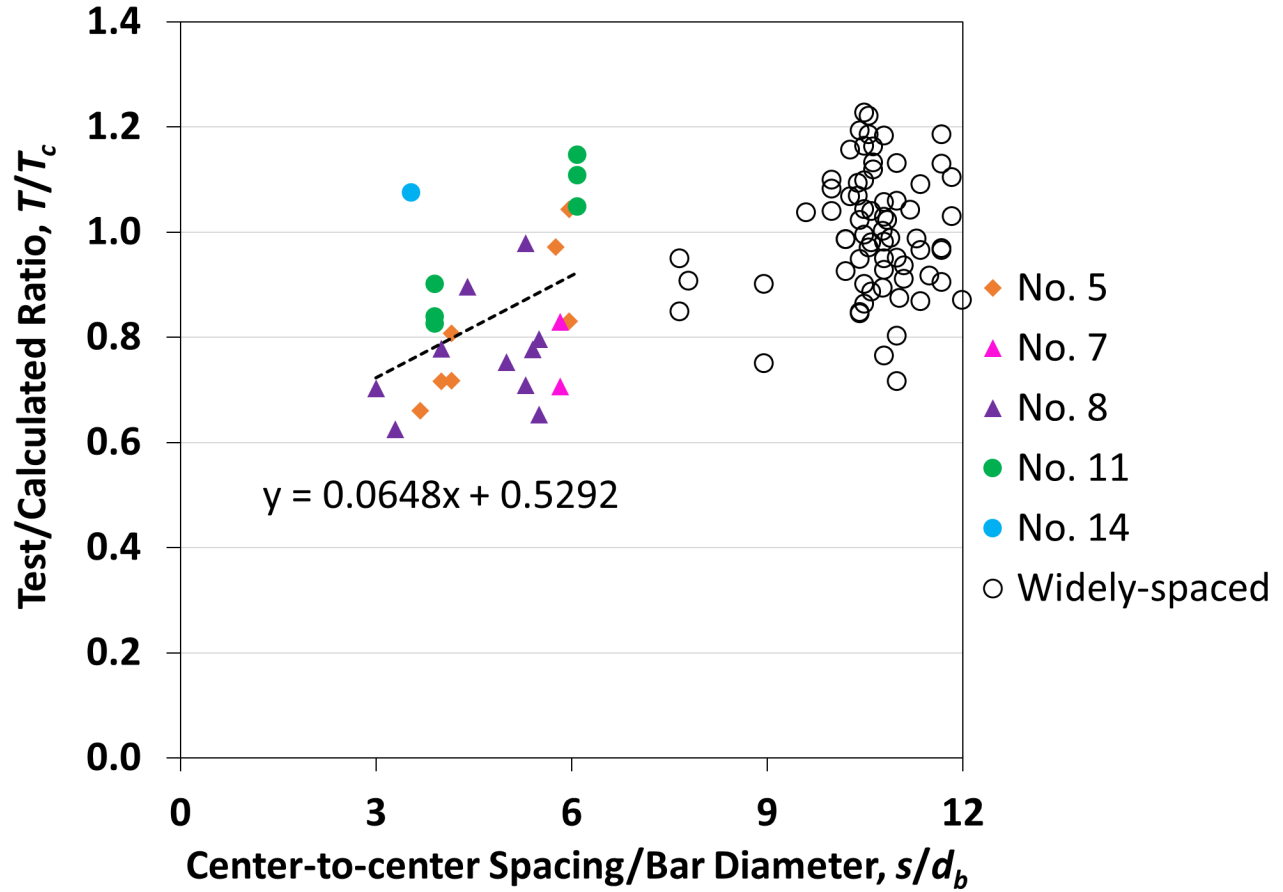


Figure 6.1 Test-to-calculated bar force at failure T/T_c based on simplified Eq. (6.2) versus ratio of center-to-center spacing to bar diameter s/d_b for widely- and closely-spaced hooked bars without confining reinforcement used to develop descriptive equations, Eq. (4.5) and (4.7)

Using the trendline equation given in Figure 6.1, the simplified descriptive equation for widely- and closely-spaced hooked bars without confining reinforcement becomes:

$$T_c = \left(551 f_{cm}^{0.25} \ell_{eh} d_b^{0.5} \right) \left(0.0648 \frac{s}{d_b} + 0.5292 \right) \quad (6.3)$$

where $\left(0.0648 \frac{s}{d_b} + 0.5292 \right) \leq 1.0$.

The plot of T/T_c based on Eq. (6.3) versus concrete compressive strength is shown in Figure 6.2, where no noticeable trend can be seen in T/T_c as a function of f_{cm} . The statistical parameters of T/T_c for specimens without confining reinforcement are given in Table 6.1.

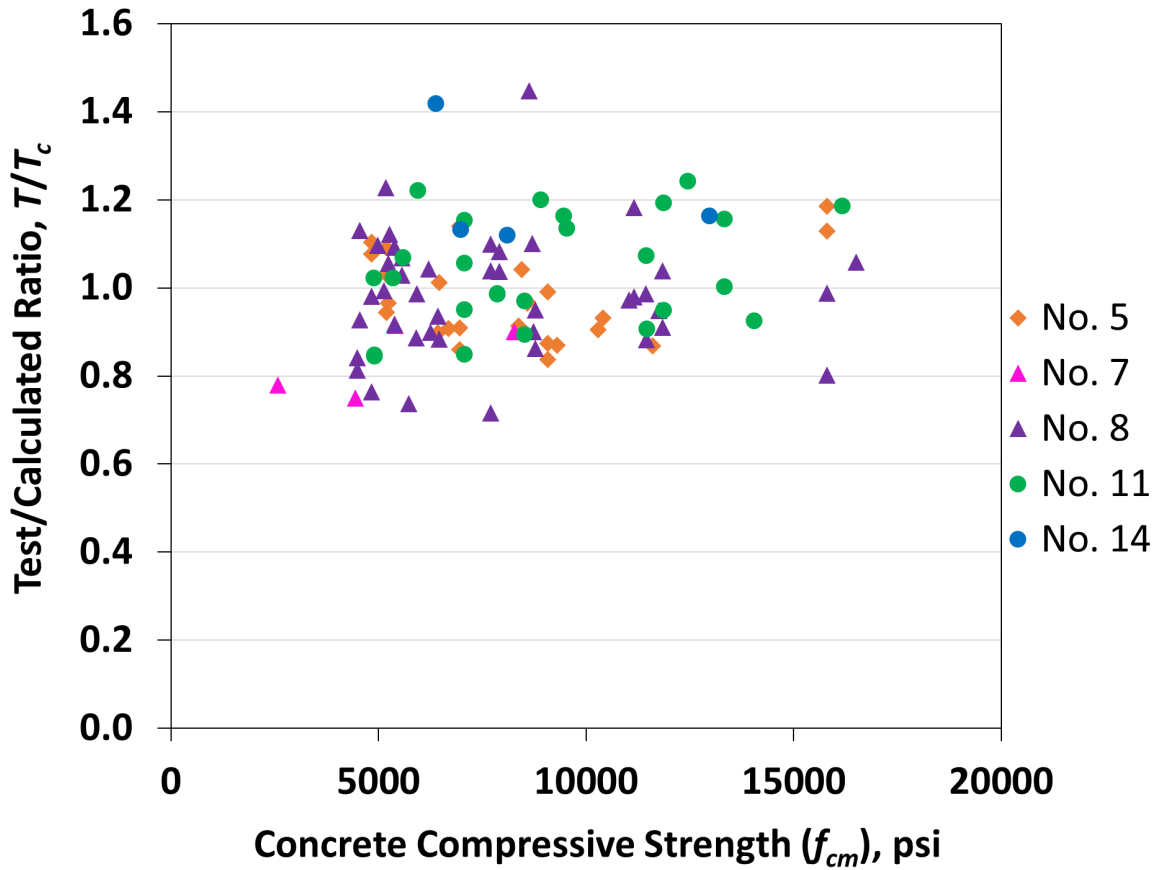


Figure 6.2 Ratio of test-to-calculated bar force at failure T/T_c based on simplified descriptive equation Eq. (6.3) versus concrete compressive strength f_{cm} for hooked bar specimens with widely- and closely-spaced bars without confining reinforcement used to develop descriptive equations, Eq. (4.5) and (4.7)

Table 6.1 Statistical parameters of T/T_c ratio using Eq. (6.3) for hooked bar specimens with widely- and closely-spaced bars without confining reinforcement

Bar size	All	No. 5	No. 7	No. 8	No. 11	No. 14
No. of specimens	102	25	4	43	26	4
Max	1.45	1.18	0.90	1.45	1.24	1.42
Min	0.72	0.84	0.75	0.72	0.84	1.12
Mean	1.00	0.98	0.83	0.99	1.04	1.21
STDEV	0.135	0.099	0.106	0.137	0.125	0.141
CoV	0.135	0.102	0.129	0.139	0.120	0.117

As shown in Table 6.1, T/T_c ranges from 0.72 to 1.45, with a mean of 1.00 and a coefficient of variation of 0.135. The lowest mean is for No. 7 bars (0.83) and the highest is for No. 14 bars

(1.21). The next step involves developing a simplified the equation for specimens with confining reinforcement. The original equation (4.6) is

$$T_h = T_c + T_s = 319f_{cm}^{0.281}\ell_{eh}^{1.106}d_b^{0.430} + 54,568\left(\frac{A_{th}}{n}\right)d_b^{0.693} \quad (6.4)$$

where A_{th} is the total cross-sectional area (in.²) of tie legs within $8d_b$ from the top of the hooked bar for No. 8 bars and smaller or within $10d_b$ for No. 9 bars or larger, and n is the number of hooked bars. The power of d_b in the steel contribution term, T_s , is rounded to 0.75 and the simplified equation becomes

$$T_h = 551f_{cm}^{0.25}\ell_{eh}d_b^{0.5} + 54,067\left(\frac{A_{th}}{n}\right)d_b^{0.75} \quad (6.5)$$

Figure 6.3 shows the plot of T/T_h using Eq. (6.5) versus ratio of bar spacing to bar diameter s/d_b .

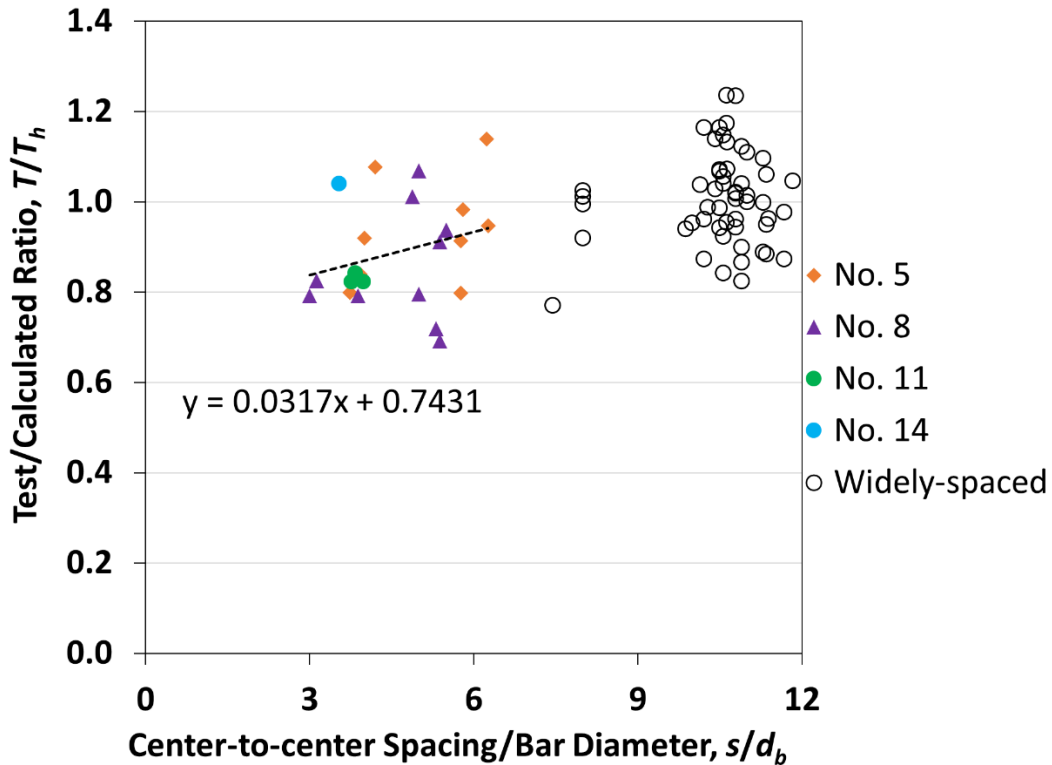


Figure 6.3 Test-to-calculated bar force at failure T/T_h based on simplified Eq. (6.5) versus ratio of center-to-center spacing to bar diameter s/d_b for widely- and closely-spaced hooked bars with confining reinforcement used to develop descriptive equations, Eq. (4.5) and (4.7)

The trendline equation given in Figure 6.3 is used as the expression to account for close bar spacing, giving a simplified descriptive equation for bars with confining reinforcement.

$$T_h = \left(551 f_{cm}^{0.25} \ell_{eh} d_b^{0.5} + 54,067 \left(\frac{A_{th}}{n} \right) d_b^{0.75} \right) \left(0.0317 \frac{s}{d_b} + 0.7431 \right) \quad (6.6)$$

where $\left(0.0317 \frac{s}{d_b} + 0.7431 \right) \leq 1.0$.

Figure 6.4 shows the variation of T/T_h using Eq. (6.6) with concrete compressive strength.

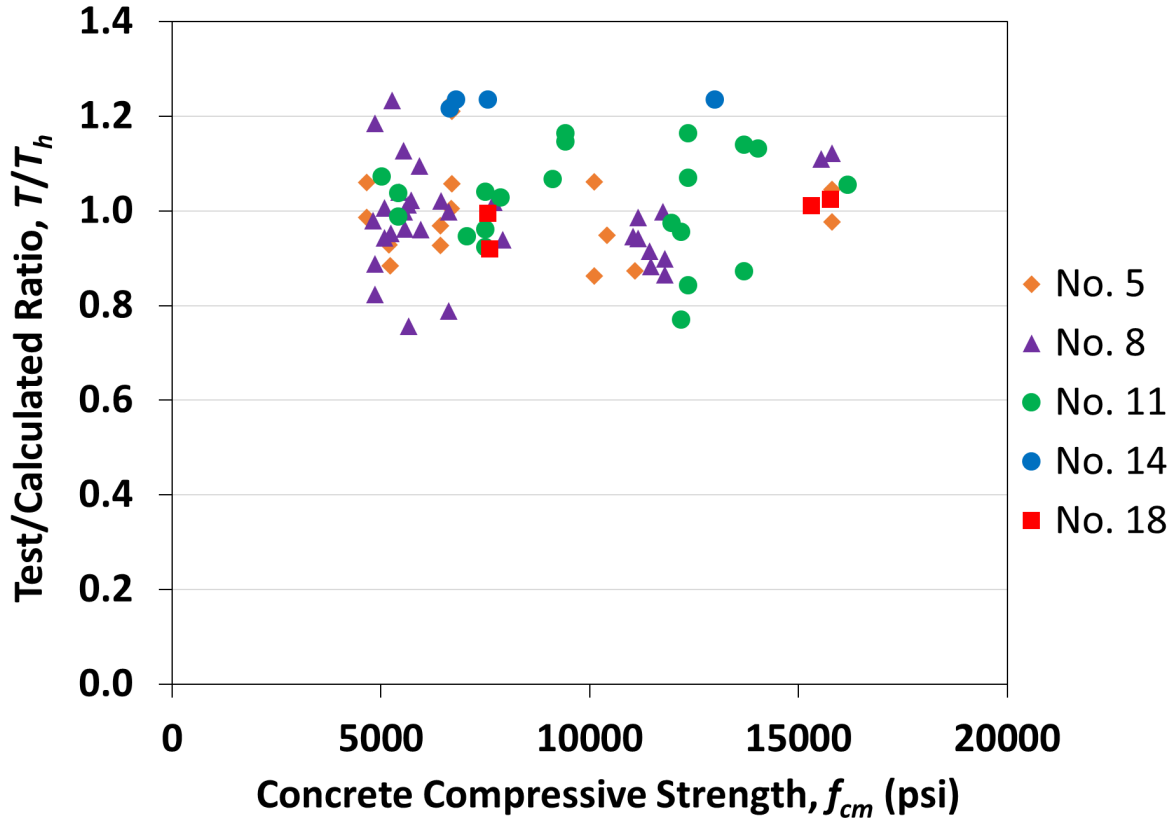


Figure 6.4 Ratio of test-to-calculated bar force T/T_c based on simplified Eq. (6.6) versus concrete compressive strength for hooked bars with widely- and closely-spaced bars with confining reinforcement used to develop descriptive equations, Eq. (4.5) and (4.6)

As shown in Figure 6.4, Eq. (6.6) captures the effect of concrete compressive strength, as no trend is visible on the data points as a function of concrete compressive strength. Table 6.2 presents the statistical parameters for specimens with confining reinforcement. As shown in the table, the specimens with confining reinforcement had a mean T/T_h of 1.00 and a coefficient of variation of 0.110. The statistical parameters of T/T_h are given in Table 6.3 for the hooked bar specimens used to develop the simplified descriptive equations.

Table 6.2 Statistical parameters of T/T_h using Eq. (6.6) for hooked bar specimens with widely- and closely-spaced bars with confining reinforcement used to develop descriptive equations Eq. (4.5) and (4.7)

Bar size	All	No. 5	No. 8	No. 11	No. 14	No. 18
No. of specimens	77	16	32	21	4	4
Max	1.23	1.23	1.23	1.16	1.23	1.02
Min	0.76	0.86	0.76	0.77	0.95	0.92
Mean	1.00	1.00	0.98	1.02	1.14	0.99
STDEV	0.110	0.107	0.106	0.108	0.130	0.047
CoV	0.110	0.107	0.108	0.107	0.113	0.047

Table 6.3 Statistical parameters of T/T_h ratio using Eq. (6.3) and (6.6) for hooked bar specimens used to develop descriptive equations Eq. (4.5) and (4.7)

Bar size	All	No. 5	No. 7	No. 8	No. 11	No. 14	No. 18
No. of specimens	179	41	4	75	47	8	4
Max	1.45	1.23	0.90	1.45	1.24	1.42	1.02
Min	0.72	0.84	0.75	0.72	0.77	0.95	0.92
Mean	1.00	0.99	0.83	0.98	1.03	1.18	0.99
STDEV	0.125	0.102	0.087	0.124	0.117	0.130	0.047
CoV	0.124	0.103	0.105	0.126	0.114	0.110	0.047

As shown in Table 6.3, the simplified equations for hooked bars result in values of T/T_h that range from 0.72 to 1.45, with a mean of 1.00 and a coefficient of variation of 0.124. The next step, converting the simplified descriptive equations to a design equation for the development length of hooked bars, is described in the next section.

6.1.2 Design Equation for Development Length

To derive a design equation for development length, the simplified descriptive equation for widely-spaced hooked bars without confining reinforcement, Eq. (6.2), is considered. In Eq. (6.2), T_c is replaced by $A_b f_y$, with $A_b = \pi d_b^2/4$. The equation is then solved for ℓ_{eh} to become:

$$\ell_{eh} = 0.0014 \frac{f_s \Psi_{cr}}{f_{cm}^{0.25}} d_b^{1.5} \quad (6.9)$$

where $\psi_{cr} = 1 - \frac{54,067}{f_s} \frac{A_{th}}{A_{hs}} d_b^{0.75}$ and is the modification factor for the contribution of confining reinforcement on the anchorage strength, f_s is the bar stress at failure (psi), A_{th} is the total area of tie legs within $8d_b$ from the top of the hooked bars for No. 3 through No. 8 bars and $10d_b$ for No. 11 and larger bars (in.²), A_{hs} is the total area of hooked bars (in.²), d_b is the bar diameter (in.), and f_{cm} is the measured concrete compressive strength (psi). For design, embedment length ℓ_{eh} is replaced by development length ℓ_{dt} , bar stress at failure f_s by yield strength f_y , and measured concrete strength f_{cm} by target compressive strength f'_c , resulting in

$$\ell_{dt} = 0.0014 \frac{f_y \psi_{cr}}{f_{cm}^{0.25}} d_b^{1.5} \quad (6.10)$$

where $\psi_{cr} = 1 - \frac{54,067}{f_y} \frac{A_{th}}{A_{hs}} d_b^{0.75}$, as defined earlier. Since ψ_{cr} decreases with increasing A_{th}/A_{hs} , an upper limit should be selected for A_{th}/A_{hs} . As discussed in Section 4.4 following Figure 4.9, the A_{th}/A_{hs} ratio ranges from 0.14 to 1.06 in specimens with confining reinforcement, with a mean of 0.40 among all specimens. All specimens had $A_{th}/A_{hs} \leq 0.40$, except for No. 5 bar specimens and two No. 18 bar specimens. Therefore, an upper limit of 0.4 on A_{th}/A_{hs} is selected. To evaluate this upper limit, the statistical parameters for T/T_h based on Eq. (6.8) with applying the 0.4 limit of A_{th}/A_{hs} is presented in Table 6.4.

Table 6.4 Statistical parameters of T/T_h ratio using Eq. (6.8) with applying $A_{th}/A_{hs} \leq 0.4$ for hooked bar specimens with widely- and closely-spaced bars with confining reinforcement used to develop descriptive equations Eq. (4.5) and (4.7)

Bar size	All	No. 5	No. 8	No. 11	No. 14	No. 18
No. of specimens	77	16	32	21	4	4
Max	1.39	1.39	1.25	1.16	1.23	1.09
Min	0.76	0.97	0.76	0.77	0.95	0.97
Mean	1.04	1.17	0.99	1.02	1.14	1.02
STDEV	0.133	0.134	0.108	0.108	0.130	0.050
CoV	0.127	0.115	0.109	0.107	0.113	0.049

Comparing the results shown in Table 6.4 with those in Table 6.3 shows that applying the 0.4 upper limit on A_{th}/A_{hs} had the greatest effect on the No. 5 bar specimens, as expected, increasing

the mean T/T_h for those specimens from 1.00 to 1.17. For No. 18 bar specimens, the mean T/T_h increased slightly from 0.99 to 1.02.

As described in Section 4.1, A_{th} is defined differently in the ACI 318 Code than in the descriptive equations. In the Code, A_{th} is the total area of confining reinforcement within $15d_b$ from the centerline of hooked bars. The notation designated in Section 4.1, Table 4.1 for A_{th} within $15d_b$, $A_{th,ACI}$, is used in the following sections. The 0.4 limit on $A_{th,ACI}$ is retained from ACI 318-19.

6.1.2.1 Modification Factor for Confining Reinforcement and Bar Spacing

As described in Section 1.3.1 and as shown in Table 1.3, the current provisions in ACI 318-19 for hooked bars do not provide flexibility for designers because the factor ψ_r , which is based on confining reinforcement and bar spacing, is limited to a binary choice between 1.0 (if specific requirements for confining reinforcement or bars spacing are met) and 1.6 (all other cases). Modifying the provisions for ψ_r to allow the use of a function or functions of $A_{th,ACI}/A_{hs}$ and s/d_b to account for confining reinforcement and spacing of the hooked bars in cases other than those that meet the specific conditions included in ACI 318-19 would provide designers with more avenues for calculating ψ_r and ultimately allow the use of shorter development lengths.

As a first step, a single expression can be developed for ψ_r based on the combined effects of bar spacing and confining reinforcement. The linear trendline equations for T/T_h versus s/d_b in Figures 6.1 and 6.3 based on the simplified descriptive equations for hooked bar specimens without and with confining reinforcement, respectively are used to start. For $s/d_b = 2$, T/T_h is 0.66 and 0.81 for hooked bars without and with confining reinforcement, respectively, which can be conservatively taken as 0.60 and 0.75, and for simplicity, T/T_h is taken as 1 for $s/d_b = 6$. Using the value of 0.60, a linear equation for hooked bars without confining reinforcement becomes

$$\psi_{r1} = 2 - \frac{1}{6} \frac{s}{d_b} \quad (6.11)$$

For bars with confining reinforcement, the resulting linear equation is multiplied by the expression for the effect of confining reinforcement, ψ_{cr} , given following Eq. (6.10), to give

$$\psi_{r2} = \left(\frac{3}{2} - \frac{1}{12} \frac{s}{d_b} \right) \left(1 - \frac{54,067}{f_y} \frac{A_{th,ACI}}{A_{hs}} d_b^{0.75} \right) \quad (6.12)$$

which is a best-fit for all values of $A_{th,ACI}/A_{hs}$ for specimens with confining reinforcement. To find a single expression for ψ_r , the expressions developed above, ψ_{r1} and ψ_{r2} , need to be combined. To

do so, a bilinear interpolation analysis can be performed to find the constants A, B, C, and D in an expression of the general form

$$\psi_r = A + B \frac{A_{th,ACI}}{A_{hs}} + C \frac{s}{d_b} + D \frac{A_{th,ACI}}{A_{hs}} \frac{s}{d_b} \quad (6.13)$$

which would be form obtained if the two terms in Eq. (6.12) are multiplied. To perform the bilinear interpolation analysis, values for ψ_r need to be generated. Each value of ψ_r is called an observation. For the case of $A_{th,ACI}/A_{hs} = 0$, Eq. (6.11) is used, producing five observations for integer values of s/d_b from 2 to 6 in Eq. (6.11).

For $A_{th,ACI}/A_{hs} \neq 0$, Eq. (6.12) is used. Using five values for s/d_b (2, 3, 4, 5, 6), four values for $A_{th,ACI}/A_{hs}$ (0.1, 0.2, 0.3, and 0.4), three values for f_y (60,000, 80,000, 100,000 psi), and five values for d_b (0.625, 1, 1.41, 1.693, 2.257 corresponding respectively to No. 5, No. 8, No. 11, No. 14, No. 18), generates 300 observations (values of ψ_r) using Eq. (6.12).

Since five values for s/d_b and four values for $A_{th,ACI}/A_{hs}$ are used, there are 20 combinations of $(\frac{A_{th,ACI}}{A_{hs}}, \frac{s}{d_b}, \frac{A_{th,ACI}}{A_{hs}} \frac{s}{d_b})$. For each combination of s/d_b and $A_{th,ACI}/A_{hs}$, there are 15 different values of ψ_r based on the integer values of f_y and d_b . These 15 different ψ_r values are averaged for each combination of $(\frac{A_{th,ACI}}{A_{hs}}, \frac{s}{d_b}, \frac{A_{th,ACI}}{A_{hs}} \frac{s}{d_b})$ to give a single value of ψ_r .

The four constants in Eq. (6.13) can be found by performing an Ordinary Least Squares (OLS) regression analysis (in this case, using the “Data Analysis” tool in Excel) on the final 25 observations (5 generated using Eq. (6.11) for specimens without confining reinforcement and 20 using Eq. (6.13) for specimens with confining reinforcement). The OLS method minimizes the sum of the squares of the residuals. A residual is the difference between the values of the dependent variable, in this case the ψ_r values obtained using Eq. (6.11) and (6.12), and corresponding values based on Eq. (6.13). Since 25 observations were used, there are 25 residual values used to establish the four constants. The values obtained for A, B, C, and D from this analysis are 1.8, -2.34, -0.13, and 0.24, respectively. The constants A and C are changed to 2 and -0.167 (-1/6), respectively, to match Eq. (6.1). The constants B and D were rounded to -2.5 and 0.25, respectively. The final expression for ψ_r then is:

$$\begin{aligned}\psi_r &= 2 - 2.5 \frac{A_{th,ACI}}{A_{hs}} - \frac{1}{6} \frac{s}{d_b} + \frac{1}{4} \frac{A_{th,ACI}}{A_{hs}} \frac{s}{d_b} \\ &\geq 0.9 \text{ for No. 11 and smaller bars and} \\ &\geq 0.7 \text{ for No. 14 and No. 18 bars}\end{aligned}\tag{6.14}$$

where $2 \leq \frac{s}{d_b} \leq 6$ and $\frac{A_{th,ACI}}{A_{hs}} \leq 0.4$. The cap of 0.4 on $A_{th,ACI}/A_{hs}$ is retained from ACI 318-19 since values higher than 0.4 do not result in increased anchorage strength and would, thus, result in an unconservative designs, as explained below.

Although ψ_r varies from 0.86 to 1.67 for $s/d_b = 2$ and from 0.6 to 1.0 for $s/d_b = 6$, depending on the amount of confining reinforcement, Eq. (6.14) contains limits on the minimum values of ψ_r of 0.9 for No. 11 and smaller hooked bars and 0.7 for No. 14 and No. 18 hooked bars to avoid very high calculated anchorage strengths with respect to the test results and to ensure that no more than 5% of all specimens have a test-to-calculated ratio less than 1.0 when used in a design expression for development length (discussed in Section 6.1.2.4). ψ_r is permitted to be as low as 0.7 for No. 14 and No. 18 bars since, as shown in Eq. (4.7), the effect of confining reinforcement increases as the hooked bar size increases. The effect is less significant for smaller bars, but is high enough that it is worth taking advantage of for the larger bars.

The approach used to find ψ_r is similar to that used by Ajaam et al. (2017) to develop a modification factor for confining reinforcement and bar spacing. Instead of using bilinear interpolation to find a single expression for ψ_r , Ajaam et al. (2017) provided six values for ψ_r for two confinement levels, none and $A_{th}/A_{hs} > 0.2$; two bar spacings, $s = 2d_b$ and $s > 6d_b$; and two values of f_y , 60,000 and 120,000 psi, as shown in Table 1.2; allowing linear interpolation to obtain intermediate values.

Because ACI Committee 318 has chosen not to adopt an expression similar to Eq. (6.14) in the past, a conservative simplification of the ψ_r expression is worthy of consideration that consists of two terms each for No. 11 and smaller bars and for No. 14 and No. 18 bars: one expressed as a function of s/d_b for $A_{th,ACI}/A_{hs} = 0$ and one expressed as a function of $A_{th,ACI}/A_{hs}$ for $s/d_b = 2$. Using $s/d_b = 2$ in Eq. (6.14) gives $\psi_r = 5/3 - 2A_{th,ACI}/A_{hs}$. For simplicity, $5/3$ is rounded to 1.6. To take advantage of the increasing effect of confining reinforcement on anchorage strength with increasing hooked bar size the expression is changed to $\psi_r = 5/3 - 3A_{th,ACI}/A_{hs}$ for No. 14 and

No. 18 bars. Also, the minimum value for ψ_r for No. 14 and No. 18 bars is increased from 0.7 to 0.8 to avoid high calculated anchorage strengths. The final form of simplified expressions is

$$\begin{aligned}\psi_r &= \min \left\{ 2 - \frac{1}{6} \frac{s}{d_b}, 1.6 - 2 \frac{A_{th,ACI}}{A_{hs}} \right\} \geq 0.9 \text{ for No. 11 and smaller} \\ \psi_r &= \min \left\{ 2 - \frac{1}{6} \frac{s}{d_b}, 1.6 - 3 \frac{A_{th,ACI}}{A_{hs}} \right\} \geq 0.8 \text{ for No. 14 and No. 18}\end{aligned}\tag{6.15}$$

As shown in Section 4.4.1, if the hooked bars are placed outside the column core and confining ties, the confining reinforcement should not be counted towards contributing to anchorage strength, meaning $A_{th,ACI}/A_{hs}$ should equal 0 when calculating ψ_r .

6.1.2.2 Modification Factor for Bar Coating and Concrete Density

The values currently provided for the modification factors for coated bars and lightweight concrete, ψ_e and λ , are retained. Per Table 25.4.3.2 of ACI 318-19, for epoxy-coated or zinc and epoxy dual-coated bars, $\psi_e = 1.2$, and for uncoated or zinc-coated bars, $\psi_e = 1.0$. $\lambda = 0.75$ is applied when using lightweight concrete and $\lambda = 0.1.0$ when using normalweight concrete.

6.1.2.3 Modification Factor for Bar Location

The provisions in ACI 318-19 include a bar location factor $\psi_o = 1.0$ for hooked bars terminating inside the column core with a side cover to the bar of at least 2.5 in., or terminating in supporting members with a side cover of at least $6d_b$, and $\psi_o = 1.25$ for other cases. The value 1.25 is based on the observations by Sperry et al. (2015a) and Ajaam et al. (2017) that, in general, specimens with hooked bars placed outside the column core had a lower anchorage strength than those with bars inside column core. Therefore, conservatively, a strength modification factor of 0.8 was suggested, and later retained by Shao et al. (2016) for headed bars ($1/0.8 = 1.25$).

The re-analysis of the specimens with hooked bars placed outside column core in Section 4.4.1 has shown, however, that a bar location factor of 1.17 would be more appropriate based on the mean test-to-calculated T/T_h ratio of 0.85 for those specimens based on descriptive equations. For design purposes, a bar location factor of 1.15 is suggested.

6.1.2.4 Strength-Reduction Factor and Final Design Equation

Now that all the modification factors are in hand, a strength-reduction factor, ϕ , needs to be incorporated into Eq. (6.10) to limit the probability of failure, as shown in Eq. (6.16).

$$\ell_{dh} = \frac{0.0014}{\phi} \frac{f_y \psi_e \psi_r \psi_o}{f_c^{0.25}} d_b^{1.5} \quad (6.16)$$

The criterion for selecting the value for ϕ is that 5% or less of beam-column test specimens have a test-to-calculated ratio of below 1.0. Using $\phi = 0.79$ results in 4.0% of the specimens used to develop the descriptive equations having a test-to-calculated ratio of below 1.0. Imbedding $\phi = 0.79$ within the design equation (as is traditionally applied in ACI 318) and using $0.0014/0.79 = 1/570$, the design equation for development of hooked bars is

$$\ell_{dh} = \frac{f_y \psi_e \psi_r \psi_o}{570 \lambda f_c^{0.25}} d_b^{1.5} \quad (6.17)$$

Eq. (6.17) is similar in format to that proposed by Ajaam et al. (2018). Equation (6.17) has advantages compared with the equation in Section 25.4.3.1 of ACI 318-19. First, the expressions developed for confining reinforcement and bar spacing factor, ψ_r , provides design flexibility compared to the limited choice between 1.0 and 1.6 in ACI 318-19. Second, using $f_c^{0.25}$ provides a better representation of the contribution of concrete compressive strength and eliminates the need for a concrete strength modification factor (ψ_c in Table 25.4.3.2 of ACI 318-19), and, thus, simplifies the design process. Third, the bar location factor ψ_o is reduced from 1.25 to 1.15. These advantages can result in shorter development lengths. In addition, given the range of concrete compressive strength (up to 16,200 psi) and bar stress at failure (up to 144,000 psi) available in the database used to develop Eq. (6.17), the proposed design equation is applicable to bars for specified yield strengths up to 120,000 psi and concrete strengths up to 16,000 psi.

A summary of the modification factors incorporated into Eq. (6.17) is given in Table 6.5.

Table 6.5 Modification factors for the proposed design equation for development of hooked bars

Modification Factor	Condition	Value ^{[1][2][3][4]}
Concrete Density, λ	Lightweight concrete	0.75
	Normalweight concrete	1.0
Epoxy coating, ψ_e	Epoxy- or zinc and epoxy dual-coated bars	1.2
	Uncoated or zinc-coated (galvanized) bars	1.0
Confining reinforcement and bar spacing, ψ_r ^{[5][6]}	For No. 11 and smaller bars	$2 - 2.5 \frac{A_{th,ACI}}{A_{hs}} - \frac{1}{6} \frac{s}{d_b} + \frac{1}{4} \frac{A_{th,ACI}}{A_{hs}} \frac{s}{d_b} \geq 0.9$ <p style="text-align: center;">or, smaller of</p> $\left\{ 2 - \frac{1}{6} \frac{s}{d_b} \text{ and } 1.6 - 2 \frac{A_{th,ACI}}{A_{hs}} \right\} \geq 0.9$
	For No. 14 and No. 18 bars	$2 - 2.5 \frac{A_{th,ACI}}{A_{hs}} - \frac{1}{6} \frac{s}{d_b} + \frac{1}{4} \frac{A_{th,ACI}}{A_{hs}} \frac{s}{d_b} \geq 0.7$ <p style="text-align: center;">or, smaller of</p> $\left\{ 2 - \frac{1}{6} \frac{s}{d_b} \text{ and } 1.6 - 3 \frac{A_{th,ACI}}{A_{hs}} \right\} \geq 0.8$
Bar location, ψ_o	(1) Bars terminating inside column core with a minimum side cover to bar of 2.5 in., or (2) Bars terminating in supporting members with a side cover of at least $6d_b$	1.0
	Other	1.15

^[1] $A_{th,ACI}$: Total cross-sectional area of tie legs within $15d_b$ from the centerline of the hooked bars, in.²

^[2] A_{hs} : Total cross-sectional area of the hooked bars being developed, in.²

^[3] s : Minimum center-to-center spacing of hooked bars, in.

^[4] d_b : Nominal diameter of hooked bar, in.

^[5] When calculating ψ_r , $A_{th,ACI}/A_{hs}$ shall not exceed 0.4 and s/d_b shall not exceed 6

^[6] When bars are placed outside both the column core and the confining ties, $A_{th,ACI}/A_{hs} = 0$ when calculating ψ_r

6.1.3 Evaluating Proposed Design Equation

In this section, the proposed design equation for development length of hooked bars, Eq. (6.17), is compared with the results in the beam-column joint database. The database includes the beam-column joint tests at the University of Kansas by Searle et al. (2014), Sperry et al. (2015a, 2015b, 2017a, 2017b, 2018), Yasso et al. (2017), Ajaam et al. (2017, 2018), plus tests available in the literature including those by Marques and Jirsa (1975), Pinc et al (1977), Hamad et al. (1993), Ramirez and Russell (2008), Lee and Park (2010), and Chun et al. (2017b). Details of the University of Kansas specimens are provided in Tables B2 through B5 in Section B3 of Appendix B, and the other specimens are presented in Table B8 in Section B4.

For the comparison, the bar stress at failure measured in the test, f_{su} , is compared with the bar stress calculated based on Eq. (6.17), $f_{s,calc}$. To find $f_{s,calc}$, Eq. (6.17) is solved for yield strength, f_y , which is replaced by $f_{s,calc}$, specified concrete compressive strength f'_c is replaced by the measured concrete strength f_{cm} , and development length ℓ_{dh} is replaced by measured embedment length ℓ_{eh} . The resulting equation is

$$f_{s,calc} = \frac{570\lambda\ell_{eh}f_{cm}^{0.25}}{\psi_e\psi_r\psi_o d_b^{1.5}} \quad (6.18)$$

6.1.3.1 University of Kansas Database

The design equation is first compared with the tests results in the database available in Ajaam et al. (2017, 2018), presented in detail in Tables B2 to B5 in Section B3 of Appendix B. The database, with a total of 251 specimens, is an extended version of the one with 185 specimens used to develop the descriptive equations, Eq. (4.5) and (4.7). The database includes No. 5, No. 8, and No. 11 hooked bar specimens tested at the University of Kansas by Searle et al. (2014), Sperry et al. (2015a, 2015b, 2017a, 2017b, 2018), Yasso et al. (2017), Ajaam et al. (2017, 2018), No. 14 and No. 18 bars tested in this study, plus three No. 6 and three No. 11 bar specimens by Ramirez and Russell (2008), two No. 7 bar specimens by Lee and Park (2010), six No. 7 bar specimens by Marques and Jirsa (1975), and two No. 7 bar specimens by Hamad et al. (1993).

The statistical parameters of $f_{s,calc}/f_{su}$ using the full expression for ψ_r , Eq. (6.14), are presented for specimens without confining reinforcement in Table 6.6.

Table 6.6 Statistical parameters of test-to-calculated bar stress at failure $f_{su}/f_{s,calc}$ for hooked bar specimens without confining reinforcement, based on the proposed design equation, Eq. (6.17), and the full expression for ψ_r , Eq. (6.14)

	All	$s \geq 6d_b$					$2d_b \leq s < 6d_b$				
		No. 5	No. 7	No. 8	No. 11	No. 14	No. 5	No. 7	No. 8	No. 11	No. 14
Number of specimens	108	18	2	33	20	3	7	8	10	6	1
Max	1.87	1.44	1.12	1.77	1.50	1.43	1.29	1.32	1.39	1.50	1.87
Min	0.87	1.02	0.94	0.88	1.04	1.38	1.01	0.91	0.87	1.29	1.87
Mean	1.23	1.19	1.03	1.23	1.24	1.40	1.17	1.16	1.14	1.39	1.87
STDEV	0.167	0.121	0.132	0.168	0.149	0.022	0.097	0.138	0.172	0.068	0.0
CoV	0.136	0.102	0.129	0.136	0.120	0.016	0.082	0.120	0.151	0.049	0.0
No. with $f_{su}/f_{s,calc} < 1.0$	7	0	1	3	0	0	0	1	2	0	0

As shown in Table 6.6, $f_{s,calc}/f_{su}$ using the full expression for ψ_r for hooked bar specimens without confining reinforcement ranges from 0.87 to 1.87 with a mean of 1.23 and a coefficient of variation of 0.136. The design equation is least conservative for the two No. 7 bar specimens with widely-spaced bars (Lee and Park 2010), and most conservative for the single No. 14 bar test specimen with closely-spaced bars, which appears to be an outlier, with a $f_{su}/f_{s,calc} = 1.87$. This specimen was tested only to be compared to its companion specimen with confining reinforcement. Otherwise, using multiple closely-spaced No. 14 hooked bars without confining reinforcement in practice is highly unlikely.

The statistical parameters of $f_{s,calc}/f_{su}$ using the simplified expressions for ψ_r , Eq. (6.15), are presented for specimens without confining reinforcement in Table 6.7.

Table 6.7 Statistical parameters of test-to-calculated bar stress at failure $f_{su}/f_{s,calc}$ for hooked bar specimens without confining reinforcement, based on the proposed design equation, Eq. (6.17) and the simplified expressions for ψ_r , Eq. (6.15)

	All	$s \geq 6d_b$					$2d_b \leq s < 6d_b$				
		No. 5	No. 7	No. 8	No. 11	No. 14	No. 5	No. 7	No. 8	No. 11	No. 14
Number of specimens	108	18	2	33	20	3	7	8	10	6	1
Max	1.87	1.44	1.12	1.77	1.50	1.43	1.29	1.32	1.39	1.50	1.87
Min	0.87	1.02	0.94	0.88	1.04	1.38	1.01	0.91	0.87	1.29	1.87
Mean	1.23	1.19	1.03	1.23	1.24	1.40	1.17	1.16	1.14	1.39	1.87
STDEV	0.167	0.121	0.132	0.168	0.149	0.022	0.097	0.138	0.172	0.068	0
CoV	0.136	0.102	0.129	0.136	0.120	0.016	0.082	0.120	0.151	0.049	0
No. with $f_{su}/f_{s,calc} < 1.0$	7	0	1	3	0	0	0	1	2	0	0

As shown in Table 6.7, the results obtained using the simplified expressions for ψ_r are identical to those obtained using the full expression for ψ_r (Table 6.6).

The statistical parameters of $f_{s,calc}/f_{su}$ using the full expression for ψ_r , Eq. (6.14), are presented for specimens with confining reinforcement in Table 6.8. As shown in the table, the hooked bar specimens with confining reinforcement had values of $f_{s,calc}/f_{su}$ ranging from 0.89 to 1.85, with a mean of 1.29 and a coefficient of variation of 0.147. The specimens with widely-spaced bars have higher mean values.

Table 6.8 Statistical parameters of test-to-calculated bar stress at failure $f_{su}/f_{s,calc}$ for hooked bar specimens with confining reinforcement, based on the proposed design equation, Eq. (6.17) and the full expression for ψ_r , Eq. (6.14)

	All	$s \geq 6d_b$					$2d_b \leq s < 6d_b$			
		No. 5	No. 8	No. 11	No. 14	No. 18	No. 5	No. 8	No. 11	No. 14
Number of specimens	143	24	49	26	3	4	11	20	5	1
Max	1.85	1.76	1.85	1.55	1.33	1.52	1.69	1.48	1.33	1.27
Min	0.89	1.03	1.08	1.05	0.99	1.13	0.91	0.89	1.04	1.27
Mean	1.29	1.37	1.34	1.32	1.20	1.28	1.26	1.14	1.16	1.27
STDEV	0.190	0.227	0.157	0.146	0.180	0.177	0.242	0.179	0.145	0
COV	0.147	0.166	0.117	0.110	0.151	0.138	0.192	0.156	0.125	0
No. with $f_{su}/f_{s,calc} < 1.0$	6	0	0	0	1	0	2	3	0	0

The statistical parameters of $f_{s,calc}/f_{su}$ using the simplified expressions for ψ_r , Eq. (6.15), are presented for specimens with confining reinforcement in Table 6.9. Using the simplified expressions for ψ_r results in values of $f_{s,calc}/f_{su}$ ranging from 0.91 to 1.85, matching the range for the full expression for ψ_r , a higher overall mean value of $f_{s,calc}/f_{su}$, 1.35 versus 1.29, and a lower coefficient of variation, 0.134. As a result of using simplified expressions, No. 8 through No. 18 bar specimens with $s \geq 6d_b$ have noticeably higher mean values of $f_{s,calc}/f_{su}$.

Table 6.9 Statistical parameters of test-to-calculated bar stress at failure $f_{su}/f_{s,calc}$ for hooked bar specimens with confining reinforcement, based on the proposed design equation, Eq. (6.17) and the simplified expressions for ψ_r , Eq. (6.15)

	All	$s \geq 6d_b$					$2d_b \leq s < 6d_b$			
		No. 5	No. 8	No. 11	No. 14	No. 18	No. 5	No. 8	No. 11	No. 14
Number of specimens	143	24	49	26	3	4	11	20	5	1
Max	1.85	1.76	1.85	1.55	1.52	1.74	1.69	1.56	1.48	1.24
Min	0.91	1.03	1.09	1.05	1.13	1.29	0.91	0.92	1.18	1.24
Mean	1.35	1.37	1.41	1.36	1.34	1.47	1.26	1.23	1.30	1.24
STDEV	0.181	0.227	0.144	0.126	0.198	0.203	0.242	0.178	0.158	0.0
COV	0.134	0.166	0.102	0.093	0.147	0.138	0.192	0.144	0.121	0.0
No. with $f_{su}/f_{s,calc} < 1.0$	3	0	0	0	0	0	2	1	0	0

The statistical parameters of $f_{su}/f_{s,calc}$ using the full expression for ψ_r are presented in Table 6.10 for the hooked bar specimens, without and with confining reinforcement, used to develop descriptive equations Eq. (4.5) and (4.7).

Table 6.10 Statistical parameters of test-to-calculated bar stress at failure $f_{su}/f_{s,calc}$ for hooked bar specimens, without and with confining reinforcement, used to develop descriptive equations Eq. (4.5) and (4.7), based on the proposed design equation Eq. (6.17) and using the full expression for ψ_r , Eq. (6.14)

Bar size	All	No. 5	No. 7	No. 8	No. 11	No. 14	No. 18
No. of specimens	251	60	10	112	57	8	4
Max	1.87	1.76	1.32	1.85	1.55	1.87	1.52
Min	0.87	0.91	0.91	0.87	1.04	0.99	1.13
Mean	1.26	1.27	1.13	1.25	1.29	1.36	1.28
STDEV	0.184	0.205	0.140	0.183	0.151	0.244	0.177
COV	0.145	0.161	0.124	0.146	0.118	0.179	0.138
No. with $f_{su}/f_{s,calc} < 1.0$	13	2	2	8	0	1	0

As shown in Table 6.10, for the 251 hooked bar specimens for comparison, $f_{su}/f_{s,calc}$ based on the proposed design equation and using the full expression for ψ_r ranges from 0.87 to 1.87 with a mean of 1.26 and a coefficient of variation of 0.145. The mean $f_{su}/f_{s,calc}$ is the highest for No. 14 bars, in part due to the two specimens with closely-spaced bars as mentioned previously. A total of 13 specimens (5.2% of all specimens) had $f_{su}/f_{s,calc} < 1.0$.

A similar table can be presented for the case of using the simplified expressions for ψ_r , as shown below. As shown in Table 6.11, the simplified expressions for ψ_r result in a higher overall mean (1.30 versus 1.27), the same coefficient of variation, and a higher overall mean for No. 14 and No. 18 bars (1.42 and 1.47 versus 1.36 and 1.28, respectively). Ten specimens (4.0 % of all specimens) have $f_{su}/f_{s,calc} < 1.0$.

Table 6.11 Statistical parameters of test-to-calculated bar stress at failure $f_{su}/f_{s,calc}$ for hooked bar specimens, without and with confining reinforcement, used to develop descriptive equations Eq. (4.5) and (4.7), based on the proposed design equation Eq. (6.17) and using the simplified expressions for ψ_r , Eq. (6.15)

Bar size	All	No. 5	No. 7	No. 8	No. 11	No. 14	No. 18
No. of specimens	251	60	10	112	57	8	4
Max	1.76	1.32	1.85	1.55	1.87	1.74	1.76
Min	0.91	0.91	0.87	1.04	1.13	1.29	0.91
Mean	1.27	1.13	1.30	1.32	1.42	1.47	1.27
STDEV	0.205	0.140	0.186	0.143	0.217	0.203	0.205
COV	0.161	0.124	0.143	0.108	0.153	0.138	0.161
No. with $f_{su}/f_{s,calc} < 1.0$	10	2	2	6	0	0	0

6.1.3.2 Marques and Jirsa (1975)

Table 6.12 presents the comparisons of the No. 7 and No. 11 specimens tested by Marques and Jirsa (1975) with the proposed design equation.

As shown in Table 6.12, $f_{su}/f_{s,calc}$ for the specimens tested by Marques and Jirsa (1975) using the full expression for ψ_r ranges from 1.09 to 2.12, with a mean of 1.54 and a coefficient of variation of 0.227. Using the simplified expressions for ψ_r results in comparable values for $f_{su}/f_{s,calc}$, with a slightly higher mean of 1.56. The relatively higher overall mean obtained here is mainly due to the No. 11 bar specimens, which also had high T/T_h ratios based on descriptive equation. As discussed in Section 4.5, the specimens carried a much lower portion of the total applied force within the joint due to the close spacing between the upper compression member and the hooked bars, resulting in higher anchorage strength than if the geometry of the test specimens had been more realistic, such as the specimens tested at the University of Kansas. If only the No. 7 bars are considered, the mean is 1.27 using both full and simplified expressions for ψ_r , which is consistent with the values reported for the University of Kansas database. Although the specimen geometry was the same as that of the No. 11 bar specimens, the No. 7 bar specimens did not have high anchorage strengths or T/T_h ratios, likely due to bars yielding and high bar slip prior to failure, as explained in Section 4.5.

Table 6.12 Comparison of hooked bar specimens tested by Marques and Jirsa (1975) versus the proposed design equation, Eq. (6.17) using full and simplified expressions for ψ_r

Specimen ID	n	ℓ_{eh} in.	f_{cm} psi	d_b in.	s/d_b	$\frac{A_{th,ACI}}{A_{hs}}$	$\psi_r^{[1]}$	$\psi_r^{[2]}$	f_{su} ksi	$f_{su}/f_{s,calc}^{[1]}$	$f_{su}/f_{s,calc}^{[2]}$
J7-180-12-1-H	2	10.0	4350	0.88	6.1	0	1.00	1.00	61.0	1.09	1.09
J7-180-15-1-H	2	13.0	4000	0.88	6.1	0	1.00	1.00	87.0	1.22	1.22
J7-90-12-1-H	2	10.0	4150	0.88	6.1	0	1.00	1.00	62.0	1.12	1.12
J7-90-15-1-H	2	13.0	4600	0.88	6.1	0	1.00	1.00	91.0	1.23	1.23
J7-90-15-1-L	2	13.0	4800	0.88	6.1	0	1.00	1.00	97.0	1.30	1.30
J7-90-15-1-M	2	13.0	5050	0.88	6.1	0	1.00	1.00	100.0	1.32	1.32
J11-180-15-1-H	2	13.1	4400	1.41	3.4	0	1.43	1.43	45.0	1.77	1.77
J11-90-12-1-H	2	10.1	4600	1.41	3.4	0	1.43	1.43	42.0	2.12	2.12
J11-90-15-1-H	2	13.1	4900	1.41	3.4	0	1.43	1.43	48.0	1.84	1.84
J11-90-15-1-L	2	13.1	4750	1.41	3.4	0	1.43	1.43	52.0	2.01	2.01
J7-90-15-3a-H	2	13.0	3750	0.875	6.1	0.917	0.90	0.90	98.0	1.43	1.43
J7-90-1-3-H	2	13.0	4650	0.875	6.1	0.367	0.90	0.90	104.0	1.44	1.44
J11-90-15-3a-L	2	13.1	5000	1.41	3.4	0.564	0.90	0.90	69.0	1.90	1.90
J11-90-15-3-L	2	13.1	4850	1.41	3.4	0.282	0.90	1.04	62.0	1.72	1.98
									Mean	1.54	1.56
									CoV	0.227	0.235

^[1] Using the full expression for ψ_r , Eq. (6.14)

^[2] Using the simplified expressions for ψ_r , Eq. (6.15)

6.1.3.3 Pinc et al. (1977)

Table 6.13 presents the comparisons of the three No. 9 and No. 11 specimens tested by Pinc et al. (1977) with the proposed design equation.

As shown for the tests by Marques and Jirsa (1975) in Table 6.12, the proposed design equation provides very conservative results for the specimens tested by Pinc et al. (1977), with a mean $f_{su}/f_{s,calc}$ ratio of 1.73 using both full and simplified expressions for ψ_r . These specimens also had high T/T_h ratios based on descriptive equations, similar to and for the same reason as No. 11 bar specimens by Marques and Jirsa (1975), as discussed in the previous section and Section 4.5.

Table 6.13 Comparison of hooked bar specimens tested by Pinc et al. (1977) versus the proposed design equation, Eq. (6.17)

Specimen ID	n	ℓ_{eh}	f_{cm}	d_b	s/d_b	$\frac{A_{th,ACI}}{A_{hs}}$	$\psi_r^{[1]}$	$\psi_r^{[2]}$	f_{su}	$f_{su}/f_{s,calc}^{[1]}$	$f_{su}/f_{s,calc}^{[2]}$
		in.	psi	in.					ksi		
9-12	2	10.0	4700	1.130	4.5	0	1.24	1.24	47.0	1.49	1.49
11-15	2	13.1	5400	1.41	3.4	0	1.43	1.43	50.0	1.87	1.87
11-18	2	16.1	4700	1.41	3.4	0	1.43	1.43	58.0	1.83	1.83
									Mean	1.73	1.73
									CoV	0.122	0.122

^[1] Using the full expression for ψ_r , Eq. (6.14)

^[2] Using the simplified expressions for ψ_r , Eq. (6.15)

6.1.3.4 Hamad et al. (1993)

Hamad et al. (1993) tested both coated and uncoated hooked bars specimens. Table 6.14 presents the comparisons with the proposed design equation for four No. 7 and four No. 11 specimens with uncoated bars tested by Hamad et al. (1993).

Table 6.14 Comparison of hooked bar specimens tested by Hamad et al. (1993) versus the proposed design equation, Eq. (6.17)

Specimen ID	n	ℓ_{eh}	f_{cm}	d_b	s/d_b	$\frac{A_{th,ACI}}{A_{hs}}$	$\psi_r^{[1]}$	$\psi_r^{[2]}$	f_{su}	$f_{su}/f_{s,calc}^{[1]}$	$f_{su}/f_{s,calc}^{[2]}$
		in.	psi	in.					ksi		
7-90-U	2	10.0	2570	0.88	6.1	0	1.00	1.00	43.3	0.88	0.88
7-90-U*	2	10.0	5400	0.88	6.1	0	1.00	1.00	61.2	1.03	1.03
11-90-U	2	13.0	2570	1.41	3.4	0	1.43	1.30	30.8	1.40	1.27
11-90-U*	2	13.0	5400	1.41	3.4	0	1.43	1.30	48.1	1.81	1.65
11-180-U-HS	2	13.0	7200	1.41	3.4	0	1.43	1.30	37.7	1.32	1.20
11-90-U-HS	2	13.0	7200	1.41	3.4	0	1.43	1.30	47.3	1.66	1.51
11-90-U-T6	2	13.0	3700	1.41	3.4	0.212	1.00	1.09	46.0	1.34	1.45
7-180-U-T4	2	10.0	3900	0.88	6.1	0.550	0.90	0.90	57.7	0.95	0.95
11-90-U-T4	2	13.0	4230	1.41	3.4	0.353	0.90	0.95	53.3	1.34	1.42
7-90-U-SC ^[3]	2	10.0	4230	0.88	8.4	0	1.00	1.00	49.9	1.03	1.03
									Mean	1.26	1.30
									CoV	0.241	0.245

^[1] Using the full expression for ψ_r , Eq. (6.14)

^[2] Using the simplified expressions for ψ_r , Eq. (6.15)

^[3] Hooked bars outside column core, bar location ψ_r of 1.15 applied

As shown in Table 6.14, $f_{su}/f_{s,calc}$ ratio for these specimens ranges from 0.88 to 1.81, with a mean of 1.26 and a coefficient of variation of 0.241 using the full expression for ψ_r , and higher mean (1.30) using the simplified expressions. The mean values are consistent with those reported for the University of Kansas database.

6.1.3.5 Ramirez and Russell (2008)

Table 6.15 presents the comparisons of the No. 6 and No. 11 specimens tested by Ramirez and Russell (2008) with the proposed design equation.

Table 6.15 Comparison of hooked bar specimens tested by Ramirez and Russell (2008) versus the proposed design equation, Eq. (6.17)

Specimen ID	n	ℓ_{eh}	f_{cm}	d_b	s/d_b	$\frac{A_{th,ACI}}{A_{hs}}$	$\psi_r^{[1]}$	$\psi_r^{[2]}$	f_{su}	$f_{su}/f_{s,calc}^{[1]}$	$f_{su}/f_{s,calc}^{[2]}$
		in.	psi	in.					ksi		
I-1	2	6.5	8910	0.75	12.3	0	1.00	1.00	68.2	1.23	1.23
I-3	2	6.5	12460	0.75	12.3	0	1.00	1.00	68.2	1.13	1.13
I-5	2	6.5	12850	0.75	12.3	0	1.00	1.00	69.3	1.14	1.14
I-2	2	12.5	8910	1.41	6.1	0	1.00	1.00	56.4	1.36	1.36
I-2'	2	15.5	9540	1.41	6.1	0	1.00	1.00	67.3	1.29	1.29
I-4	2	12.5	12460	1.41	6.1	0	1.00	1.00	63.5	1.41	1.41
I-6	2	12.5	12850	1.41	6.1	0	1.00	1.00	73.1	1.61	1.61
III-13	2	6.5	13980	0.75	12.3	1.000	0.90	0.90	93.9	1.36	1.36
III-15	2	6.5	16350	0.75	12.3	1.000	0.90	0.90	87.5	1.22	1.22
III-14	2	12.5	13980	1.41	6.1	0.282	0.90	1.00	67.3	1.31	1.45
III-16	2	12.5	16500	1.41	6.1	0.282	0.90	1.00	76.9	1.44	1.59
									Mean	1.32	1.35
									CoV	0.107	0.122

^[1] Using the full expression for ψ_r , Eq. (6.14)

^[2] Using the simplified expressions for ψ_r , Eq. (6.15)

As shown in Table 6.15, for the 11 specimens tested by Ramirez and Russell (2008), the $f_{su}/f_{s,calc}$ ratio ranges from 1.13 and 1.61 with a mean of 1.32 and a coefficient of variation of 0.107 using the full expression for ψ_r , and a slightly higher mean and coefficient of variation using the simplified expressions (1.35 and 0.122, respectively). These numbers are similar to the mean and coefficient of variation values reported for the University of Kansas database in Section 6.1.3.1.

6.1.3.6 Lee and Park (2010)

Table 6.16 presents the comparisons of the three No. 7 specimens tested by Lee and Park (2010) with the proposed design equation. As shown in the table, the three specimens tested by Lee and Park (2010) had a mean $f_{su}/f_{s,calc}$ ratio of 1.00 using both the full and simplified expressions for ψ_r , the lowest among all studies reported.

Table 6.16 Comparison of hooked bar specimens tested by Lee and Park (2010) versus the proposed design equation, Eq. (6.17)

Specimen ID	n	ℓ_{eh}	f_{cm}	d_b	s/d_b	$\frac{A_{th,ACI}}{A_{hs}}$	$\psi_r^{[1]}$	$\psi_r^{[2]}$	f_{su}	$f_{su}/f_{s,calc}^{[1]}$	$f_{su}/f_{s,calc}^{[2]}$
		in.	psi	in.					ksi		
H1	2	18.7	4450	0.88	9.0	0	1.00	1.00	98.7	0.94	0.93
H2	2	11.9	8270	0.88	9.0	0	1.00	1.00	88.0	1.12	1.12
H3	2	15.0	4450	0.88	9.0	0.733	0.90	0.90	89.6	0.95	0.95
									Mean	1.00	1.00
									CoV	0.121	0.102

^[1] Using the full expression for ψ_r , Eq. (6.14)

^[2] Using the simplified expressions for ψ_r , Eq. (6.15)

6.1.3.7 Chun et al. (2017b)

Table 6.17 presents the comparisons with the proposed design equation for the 26 No. 14 and No. 18 bar specimens tested by Chun et al. (2017). As discussed in Chapter 1, these specimens were designed to force a side-blowout failure. The hooked bars were placed outside the column core in all these specimens, therefore $\psi_o = 1.15$ applies. Also, the majority of specimens had a unconventional reinforcement layout with the hooked bars outside the confining ties, as described in Section 4.4.1 and Figure 4.9a. Therefore, although all specimens had $A_{th}/A_{hs} > 0.6$, ties are not counted for the specimens with hooks outside the ties.

Table 6.17 Comparison of hooked bar specimens tested by Chun et al. (2017b) versus the proposed design equation, Eq. (6.17)

Specimen ID ^[1]	n	ℓ_{eh}	f_{cm}	d_b	s/d_b	$\frac{A_{th,ACI}}{A_{hs}}$	$\psi_r^{[2]}$	$\psi_r^{[3]}$	f_{su}	$f_{su}/f_{s,calc}^{[2]}$	$f_{su}/f_{s,calc}^{[3]}$
		in.	psi	in.					ksi		
D43-L10-C1-S42*	2	16.9	6440	1.693	9.6	0	1.00	1.00	51.3	1.50	1.50
D43-L10-C1-S42-C**	2	16.9	6950	1.693	9.6	1.173	0.70	0.80	75.1	1.51	1.73
D43-L10-C1-S70*	2	16.9	10010	1.693	9.6	0	1.00	1.00	54.8	1.44	1.44
D43-L10-C2-S42*	2	16.9	7020	1.693	9.6	0	1.00	1.00	58.5	1.68	1.68
D43-L13-C1-S42*	2	22.0	7020	1.693	9.6	0	1.00	1.00	64.4	1.42	1.42
D43-L13-C1-S42-C**	2	22.0	7020	1.693	9.6	0.978	0.70	0.80	75.9	1.17	1.34
D43-L13-C1-S70*	2	22.0	10600	1.693	9.6	0	1.00	1.00	63.3	1.26	1.26
D43-L13-C2-S42*	2	22.0	7020	1.693	9.6	0	1.00	1.00	68.7	1.51	1.51
D43-L16-C1-S42*	2	27.1	7020	1.693	9.6	0	1.00	1.00	72.6	1.30	1.30
D43-L16-C1-S42-C**	2	27.1	7020	1.693	9.6	0.978	0.70	0.80	78.9	0.99	1.13
D43-L16-C1-S70*	2	27.1	10010	1.693	9.6	0	1.00	1.00	76.8	1.26	1.26
D43-L16-C2-S42*	2	27.1	7020	1.693	9.6	0	1.00	1.00	80.9	1.45	1.45
D43-L20-C1-S42*	2	33.9	7020	1.693	9.6	0	1.00	1.00	76.5	1.10	1.10
D57-L10-C1-S42-a*	2	22.6	5450	2.257	7.2	0	1.00	1.00	36.8	1.30	1.30
D57-L10-C1-S42-b*	2	22.6	6150	2.257	7.2	0	1.00	1.00	37.6	1.29	1.29
D57-L10-C1-S42-C**	2	22.6	5450	2.257	7.2	0.660	0.70	0.80	55.8	1.38	1.57

D57-L10-C2-S42*	2	22.6	5450	2.257	7.2	0	1.00	1.00	53.7	1.89	1.89
D57-L13-C1-S42-a*	2	29.3	5450	2.257	7.2	0	1.00	1.00	59.1	1.60	1.60
D57-L13-C1-S42-b*	2	29.3	6150	2.257	7.2	0	1.00	1.00	58.2	1.53	1.53
D57-L13-C1-S42-C**	2	29.3	5450	2.257	7.2	0.660	0.70	0.80	63.6	1.21	1.38
D57-L13-C2-S42*	2	29.3	5450	2.257	7.2	0	1.00	1.00	68.4	1.85	1.85
D57-L16-C1-S42-a	2	36.1	5450	2.257	7.2	0	1.00	1.00	63.5	1.40	1.40
D57-L16-C1-S42-b*	2	36.1	6150	2.257	7.2	0	1.00	1.00	71.0	1.52	1.52
D57-L16-C1-S42-C**	2	36.1	5450	2.257	7.2	0.660	0.70	0.80	69.9	1.08	1.23
D57-L16-C2-S42*	2	36.1	6530	2.257	7.2	0	1.00	1.00	79.7	1.68	1.68
D57-L20-C1-S42*	2	45.1	6530	2.257	7.2	0	1.00	1.00	82.1	1.38	1.38
									Mean	1.41	1.45
									CoV	0.158	0.141

* Specimens with hooks placed outside the confining ties (Figure 4.9.a), ties not counted towards ψ_r ($A_{th}/A_{hs} = 0$)

** Specimens with hooks placed inside the confining ties (Figure 4.9.b), ties counted towards ψ_r

^[1] Bar location factor ψ_o of 1.15 applied to all specimens

^[2] Using the full expression for ψ_r , Eq. (6.14)

^[3] Using the simplified expressions for ψ_r , Eq. (6.15)

As shown in Table 6.17, the $f_{su}/f_{s,calc}$ ratio using both the full expressions for ψ_r ranges from 0.99 to 1.89 with a mean of 1.41 and a coefficient of variation of 0.158 for the No. 14 and No. 18 bar specimens tested by Chun et al. (2017b). A higher mean of 1.45 is obtained using the simplified expression for ψ_r . These values are similar to the mean values obtained for No. 14 and No. 18 bar specimens tested in this study (1.42 and 1.47, respectively, as given in Table 6.11).

A summary of the statistical parameters of $f_{su}/f_{s,calc}$ ratio for specimens tested outside the University of Kansas using the full expression for ψ_r is presented in Table 6.18.

Table 6.18 Statistical parameters of $f_{su}/f_{s,calc}$ for hooked bar specimens tested outside University of Kansas, based on the proposed design equation Eq. (6.17) and using the full expression for ψ_r , Eq. (6.14)

Bar size	All	No. 6	No. 7	No. 9	No. 11	No. 14	No. 18
No. of specimens	71	5	17	1	22	13	13
Max	2.12	1.36	1.44	1.49	2.12	1.68	1.89
Min	0.88	1.13	0.88	1.49	1.20	0.99	1.08
Mean	1.39	1.22	1.16	1.49	1.59	1.35	1.47
STDEV	0.275	0.093	0.180	N/A	0.273	0.194	0.242
COV	0.198	0.076	0.155	N/A	0.172	0.143	0.164
No. with $f_{su}/f_{s,calc} < 1.0$	4	0	3	0	0	1	0

As shown in Table 6.18, for the 70 hooked bar specimens tested outside the University of Kansas, $f_{su}/f_{s,calc}$ using the full expression for ψ_r ranges from 0.88 to 2.12 with a mean of 1.40 and a coefficient of variation of 0.195. Using the simplified expressions for ψ_r give similar results, with a slightly higher overall mean and lower coefficient of variation (1.42 and 0.195, respectively), and a higher mean No. 11 through No. 18 bar specimens (1.63, 1.39, and 1.51 for No. 11, No. 14, and No. 18 bar specimens, respectively). The proposed design equation performs adequately, in line with the values previously reported for comparisons with the University of Kansas database. The exception, the mean of 1.60 for the No. 11 bar specimens, which is due to the specimens tested by Marques and Jirsa (1975) and Pinc et al. (1977). As discussed before, those specimens had relatively high anchorage strength because of the use of specimens with a geometry not representing that in reinforced concrete frame structures for which a reduced load was carried within the joint, resulting in a higher anchorage strength.

6.2 HEADED BARS

6.2.1 Simplified Descriptive Equations

To simplify the descriptive equations, the approach used by Sperry et al. (2015b) for hooked bars and Shao et al. (2016) for headed bars is followed. The specimens used are the same as those used to develop the descriptive equations, Eq. (5.5) and (5.7), presented in detail in Tables C2 to C5 in Section C3 of Appendix C. The process starts with the descriptive equation for widely-spaced headed bars (center-to-center spacing $\geq 8d_b$) without parallel ties, Eq. (5.4), and repeated here.

$$T_c = 1296 f_{cm}^{0.207} \ell_{eh}^{0.941} d_b^{0.498} \quad (6.18)$$

where T_c is the anchorage strength of headed bars without parallel ties (lb), f_{cm} is concrete compressive strength (psi), ℓ_{eh} is embedment length (in.), and d_b is bar diameter (in.). To simplify the equation, the powers of f_{cm} , ℓ_{eh} , and d_b is increased to 0.25, 1.0, and 0.5, respectively. Then, using the same iterative analysis described in Section 5.3, a new constant is found so that the mean test-to-calculated ratio T/T_c equals 1.0, giving

$$T_c = 764 f_{cm}^{0.25} \ell_{eh} d_b^{0.5} \quad (6.19)$$

To account for the effect of close bar spacing (center-to-center spacing $< 8d_b$), the procedure used in Section 5.3.2 is followed and the values of T/T_c are plotted versus s/d_b , as shown in Figure 6.5, with T_c being calculated based on Eq. (6.19).

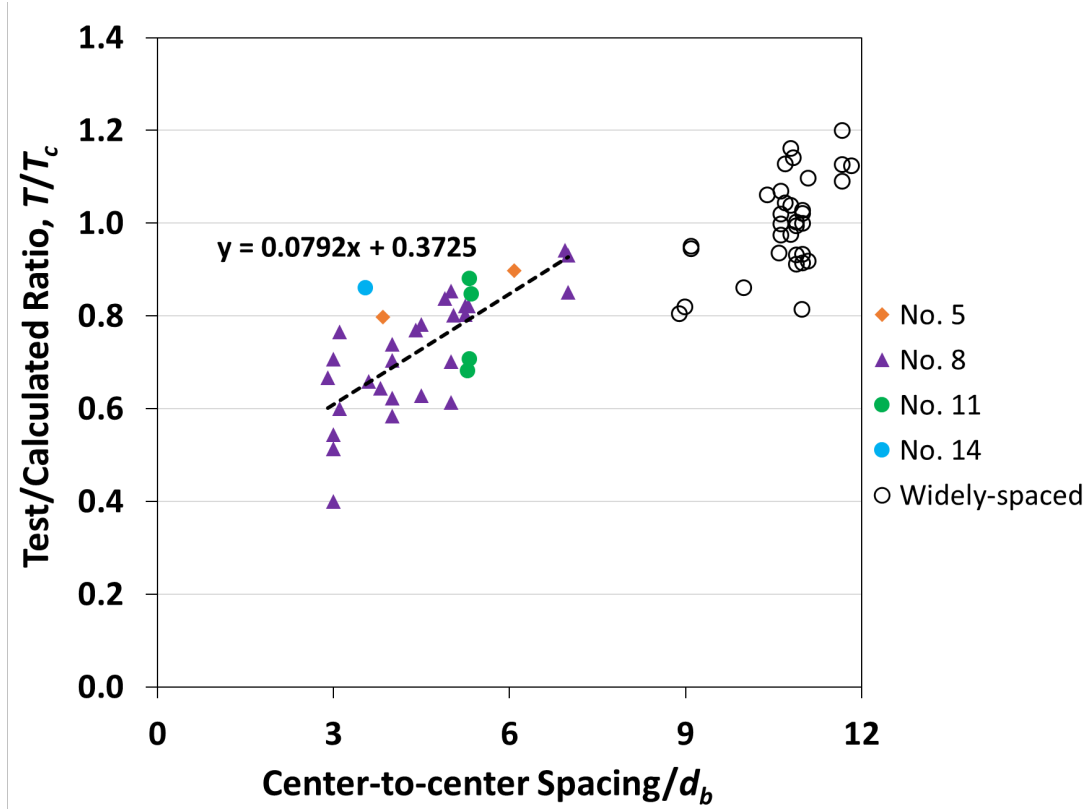


Figure 6.5 Test-to-calculated bar force at failure T/T_c based on Eq. (6.19) versus ratio of center-to-center spacing to bar diameter s/d_b for widely- and closely-spaced headed bars without parallel ties

Using the linear trendline equation shown in Figure 6.5, the simplified descriptive equation for widely- and closely-spaced headed bars without parallel ties becomes

$$T_h = \left(764 f_{cm}^{0.25} \ell_{eh} d_b^{0.5} \right) \left(0.0792 \frac{s}{d_b} + 0.3725 \right) \quad (6.20)$$

where $\left(0.0792 \frac{s}{d_b} + 0.3725 \right) \leq 1.0$, s is the center-to-center spacing of the bars (in.). The statistical parameters of T/T_c for all specimens without parallel ties are given in Table 6.19.

Table 6.19 Statistical parameters of T/T_c ratio based on simplified descriptive equation, Eq. (6.20), for headed bar specimens with widely- and closely-spaced bars without parallel ties used to develop descriptive equations, Eq. (5.5) and (5.7)

Bar size	All	No. 5	No. 8	No. 11	No. 14	No. 18
No. of specimens	68	6	48	11	3	0
Max	1.32	1.20	1.24	1.14	1.32	-
Min	0.66	1.05	0.66	0.81	1.00	-
Mean	1.00	1.13	0.98	1.00	1.11	-
STDEV	0.118	0.055	0.109	0.120	0.179	-
CoV	0.118	0.048	0.112	0.121	0.161	-

As shown in Table 6.19, the mean value of T/T_c for headed bar specimens without parallel ties using simplified descriptive equations is 1.00, with a coefficient of variation of 0.118. The T/T_c ratios are compared as a function of concrete compressive strength in Figure 6.6.

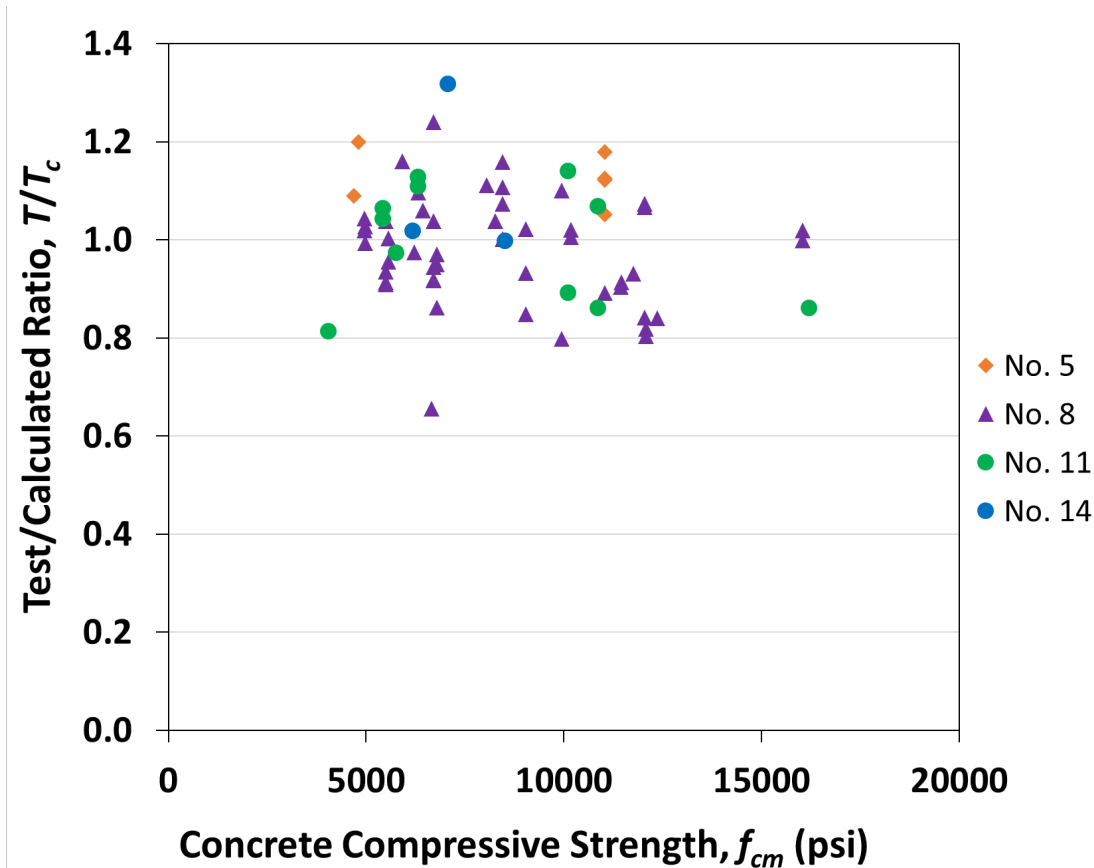


Figure 6.6 Ratio of test-to-calculated bar force at failure T/T_c based on simplified descriptive equation, Eq. (6.20), versus concrete compressive strength f_{cm} for headed bar specimens with widely- and closely-spaced bars without parallel ties used to develop descriptive equations, Eq. (5.5) and (5.7)

As shown in Figure 6.6, T/T_c decreases slightly as the concrete compressive strength increases, due to the small overestimation of the effect of concrete strength by the 0.25 power used in Eq. (6.20) compared with 0.207 in the original descriptive equation, Eq. (6.18).

The original descriptive equation for specimens with parallel ties is given below:

$$T_h = T_c + T_s = 1296 f_{cm}^{0.207} \ell_{eh}^{0.941} d_b^{0.498} + 49,402 \left(\frac{A_t}{n} \right) d_b^{0.11} \quad (6.21)$$

where A_t is the total area of tie legs within $8d_b$ from the top of the headed bars for No. 3 through No. 8 bars and $10d_b$ for No. 11 and larger bars, and n is the number of bars. The first term in Eq. (6.21), T_c , is already simplified and given in Eq. (6.19). Using Eq. (6.19), the second term in Eq. (6.21), T_s , can be simplified by changing the power of d_b to 0.1 and finding a new constant to replace 49,402 so that the mean T/T_h in specimens with widely-spaced bars with parallel ties is 1.0. The resulting equation is given below in Eq. (6.22).

$$T_h = 764 f_{cm}^{0.25} \ell_{eh} d_b^{0.5} + 41,150 \left(\frac{A_t}{n} \right) d_b^{0.1} \quad (6.22)$$

Using Eq. (6.22), T/T_h versus s/d_b for specimens with parallel ties with both widely- and closely-spaced bars and parallel ties is shown in Figure 6.7.

To account for the effect of close bar spacing, the linear trendline equation shown in Figure 6.8 is multiplied by Eq. (6.22) to give Eq. (6.23):

$$T_h = \left(764 f_{cm}^{0.25} \ell_{eh} d_b^{0.5} + 41,150 \left(\frac{A_t}{n} \right) d_b^{0.1} \right) \left(0.0559 \frac{s}{d_b} + 0.5743 \right) \quad (6.23)$$

where $\left(0.0559 \frac{s}{d_b} + 0.5743 \right) \leq 1.0$.

The statistical parameters of T/T_h for all specimens with parallel ties are given in Table 6.20.

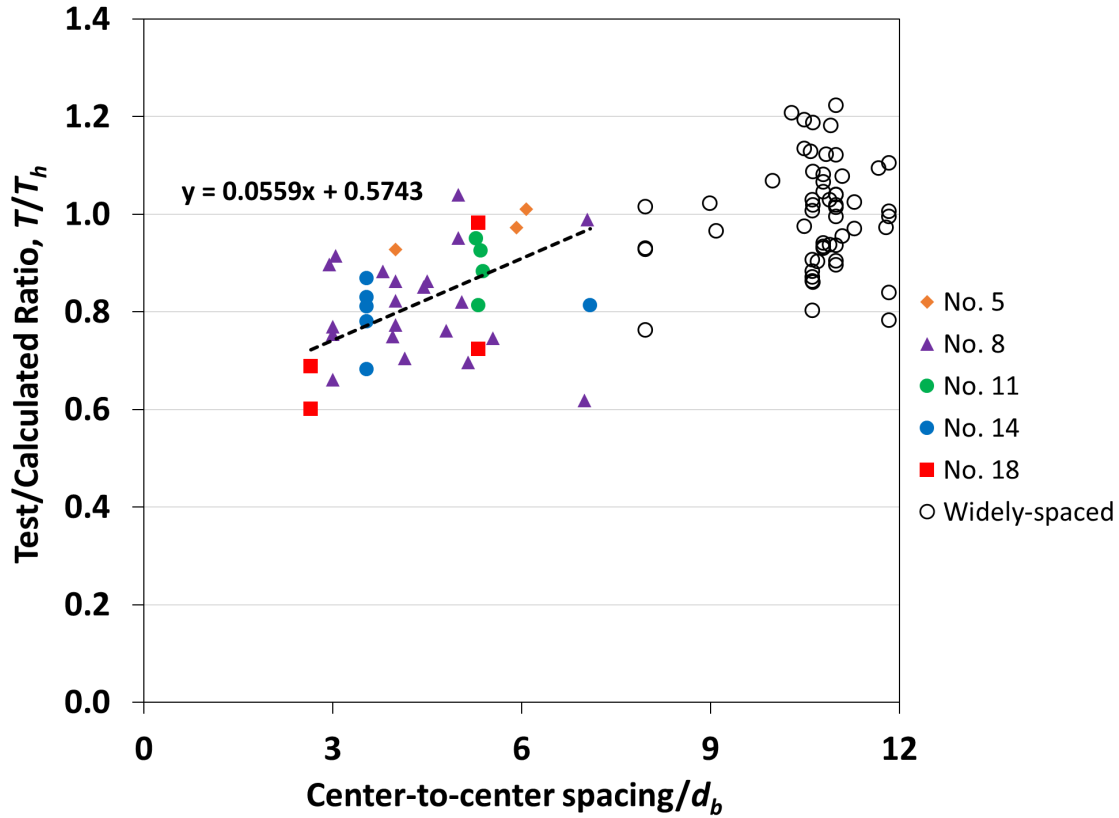


Figure 6.7 Test-to-calculated bar force at failure T/T_c based on Eq. (6.22) versus ratio of center-to-center spacing to bar diameter s/d_b for widely- and closely-spaced headed bars with parallel ties used to develop descriptive equations, Eq. (5.5) and (5.7)

Table 6.20 Statistical parameters of T/T_h ratio based on simplified descriptive equation, Eq. (6.23), for headed bar specimens with widely- and closely-spaced bars with parallel ties used to develop descriptive equations, Eq. (5.5) and (5.7)

Bar size	All	No. 5	No. 8	No. 11	No. 14	No. 18
No. of specimens	96	9	54	12	13	8
Max	1.26	1.16	1.26	1.19	1.12	1.13
Min	0.76	0.78	0.83	0.86	0.80	0.76
Mean	1.00	1.02	1.01	1.04	0.95	0.92
STDEV	0.106	0.129	0.095	0.104	0.103	0.116
CoV	0.106	0.127	0.094	0.099	0.109	0.126

As shown in Table 6.20, the test-to-calculated ratio T/T_h using the simplified descriptive equations for specimens with parallel ties ranges from 0.76 to 1.26, with a mean value of 1.00 and a coefficient of variation of 0.106. The variation of T/T_h using Eq. (6.23) versus concrete compressive strength can be evaluated, as plotted in Figure 6.8.

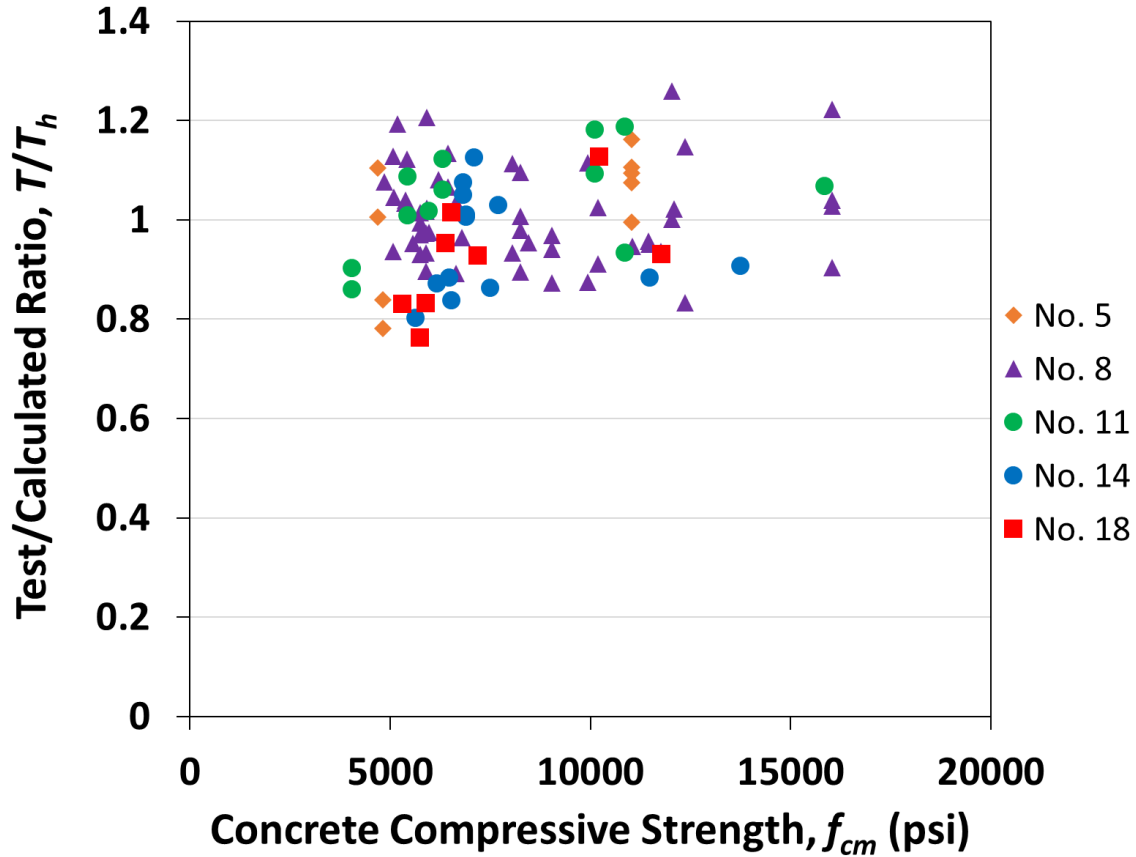


Figure 6.8 Ratio of test-to-calculated bar force at failure T/T_c based on simplified descriptive equation, Eq. (6.23), versus concrete compressive strength f_{cm} for headed bar specimens with widely- and closely-spaced bars with parallel ties used to develop descriptive equations, Eq. (5.5) and (5.7)

Figure 6.8 shows a very slight positive trend of T/T_c with respect to concrete compressive strength, but overall the 0.25 power for f_{cm} in Eq. (6.6) adequately captures the effect of concrete compressive strength.

In summary, the simplified descriptive equations are presented in Eq. (6.20) and (6.23) for headed bar specimens without and with parallel ties, respectively. For all 164 headed bar specimens, the statistical parameters of T/T_h using Eq. (6.20) and (6.23) are tabulated in Table 6.21.

Table 6.21 Statistical parameters of T/T_h ratio based on simplified descriptive equation, Eq. (6.20) and (6.23), for all headed bar specimens used to develop descriptive equations, Eq. (5.5) and (5.7)

Bar size	All	No. 5	No. 8	No. 11	No. 14	No. 18
No. of specimens	164	15	102	23	16	8
Max	1.32	1.20	1.26	1.19	1.32	1.13
Min	0.66	0.78	0.66	0.81	0.80	0.76
Mean	1.00	1.06	1.00	1.02	0.98	0.92
STDEV	0.111	0.117	0.103	0.112	0.131	0.116
CoV	0.111	0.110	0.103	0.110	0.133	0.126

As presented in Table 6.21, the simplified descriptive equations result in a mean value of T/T_h of 1.00 for all headed bar specimens, with a coefficient of variation of 0.111. For the No. 18 bar specimens, the mean dropped to 0.92 in simplified equations, similar to the mean obtained using the descriptive equations by Shao et al. (2016). The procedure for converting the simplified equations to a design equation for development length is discussed next.

6.2.2 Design Equation for Development Length

The simplified descriptive equations developed in the previous section can be used to derive a design expression for development length. To start, the equation for widely-spaced bars without parallel ties, Eq. (6.19), is solved for embedment length, ℓ_{eh} and T_h is replaced by $A_b f_s = \pi f_s d_b^2 / 4$. The resulting expression is

$$\ell_{eh} = 0.001 \frac{f_s \psi_{pr}}{f_{cm}^{0.25}} d_b^{1.5} \quad (6.24)$$

where $\psi_{pr} = 1 - \frac{41,150}{f_s} \frac{A_{tt}}{A_{hs}} d_b^{0.1}$ is the modification factor for the contribution of parallel tie reinforcement on the anchorage strength, f_s is the bar stress at failure (psi), A_{tt} is the total area of tie legs within $8d_b$ from the top of the headed bars for No. 3 through No. 8 bars and $10d_b$ for No. 11 and larger bars (in.²), A_{hs} is the total area of headed bars (in.²), d_b is the bar diameter (in.), and f_{cm} is the measured concrete compressive strength (psi).

To be used for design, Eq. (6.24) is modified by replacing embedment length ℓ_{eh} by development length ℓ_{dt} , bar stress at failure f_s by yield strength f_y , and measured concrete strength f_{cm} by the specified compressive strength f'_c . The resulting equation is:

$$\ell_{dt} = 0.001 \frac{f_y \psi_{pr}}{f_c^{0.25}} d_b^{1.5} \quad (6.25)$$

where $\psi_{pr} = 1 - \frac{41,150}{f_y} \frac{A_{tt}}{A_{hs}} d_b^{0.1}$ accounts for the effect of parallel ties. As discussed in Section 5.3.3, an upper limit of 0.4 on A_{tt}/A_{hs} was chosen when developing the new descriptive equations for headed bars and was shown to provide reasonable calculated failure loads. Therefore, the same upper limit is retained and used here for the proposed design equation.

6.2.2.1 Modification Factor for Parallel Tie Reinforcement and Bar Spacing

In this section, an expression is developed to account for the contribution of parallel tie reinforcement and the effect of bar spacing. As discussed in Chapter 1, as for hooked bars, the design provisions for headed bars in ACI 318-19 limit the flexibility in design by providing a binary choice between 1.0 and 1.6 for the parallel tie reinforcement factor, ψ_p . If $A_{tt}/A_{hs} \geq 0.3$ or $s \geq 6d_b$ per ACI 318-19 Table 25.4.4.3 are met, ψ_p is 1.0, otherwise, it jumps to 1.6. This means that designers cannot take advantage of the intermediate values of A_{tt}/A_{hs} and s/d_b . Developing an alternative expression for ψ_p that varies as a function of A_{tt}/A_{hs} and s/d_b will result in shorter development lengths in cases where one of the two requirements on parallel ties or headed bar are not satisfied.

The effect of bar spacing can be accounted for using descriptive equations for headed bars without and with parallel ties. For headed bars without parallel ties, the linear trendline equation in Figure 6.5 reveals that for $s/d_b = 2$, the T/T_h is 0.53 which, conservatively, can be taken as 0.5. Similarly, for specimens with parallel ties and as shown in Figure 6.7, T/T_h is 0.69 for $s/d_b = 2$, where T_h is the strength for widely-space bars, which is taken conservatively as 0.6. Taking T/T_h as 1.0 when $s/d_b = 8$ for both cases and using linear interpolation, the effects of bar spacing and parallel ties for headed bars without and with parallel tie reinforcement can be expressed, respectively as

$$\psi_{p1} = \left(\frac{7}{3} - \frac{1}{6} \frac{s}{d_b} \right) \quad (6.26)$$

$$\psi_{p2} = \left(\frac{17}{9} - \frac{1}{9} \frac{s}{d_b} \right) \left(1 - \frac{41,150}{f_y} \frac{A_{tt}}{A_{hs}} d_b^{0.1} \right) \quad (6.27)$$

For headed bars with parallel ties, the bar spacing expression is multiplied by the parallel tie expression, ψ_{pr} , given in Eq. (6.10). To simplify design, and as used for hooked bars, a single expression for ψ_p as a function of A_{tt}/A_{hs} and s/d_b is needed. The general form of the expression is

$$\psi_p = A + B \frac{A_{tt}}{A_{hs}} + C \frac{s}{d_b} + D \frac{A_{tt}}{A_{hs}} \frac{s}{d_b} \quad (6.28)$$

To find the constants A, B, C, and D, a bilinear interpolation needs to be conducted. The procedure is the same as what used to develop an expression for confining reinforcement and bar spacing factor for hooked bars, ψ_r , as described in detail in Section 6.2.1. The only difference is the range of values used for s/d_b , which is 3 to 8 here for headed bars, rather than 2 to 6. The lower bound for s/d_b was chosen to be 3, the minimum value currently permitted in ACI 318-19. The coefficients A, B, and C and the intercept D are found through performing regression analysis using the “Data Analysis” tool in Excel. The resulting expression for ψ_p is

$$\begin{aligned} \psi_p &= 2 - 2.5 \frac{A_{tt}}{A_{hs}} - \frac{1}{8} \frac{s}{d_b} + \frac{1}{6} \frac{A_{tt}}{A_{hs}} \frac{s}{d_b} \\ &\geq 0.85 \text{ for No. 11 and smaller bars and} \\ &\geq 0.95 \text{ for No. 14 and No. 18 bars} \end{aligned} \quad (6.29)$$

where $3 \leq \frac{s}{d_b} \leq 8$ and $\frac{A_{tt}}{A_{hs}} \leq 0.4$. The values of ψ_p obtained using Eq. (6.29) are limited to 0.85 for No. 11 and smaller and 0.95 for No. 14 and No. 18 bars to avoid overprediction of anchorage strength and to ensure that no more than 5% of specimens have a test-to-calculated ratio < 1.0 . The expression for ψ_p has the same form as the expression for ψ_r for hooked bars, but with a difference in constants and the limit for No. 14 and No. 18 bars. For hooked bars, the limit was chosen as 0.7, whereas here the limit is 0.95. For $s/d_b = 3$, ψ_p varies from 0.85 or 0.95 to 1.625 depending on the ratio of the area of the parallel ties to the area of the headed bars A_{tt}/A_{hs} . Similarly, when bars are widely-spaced ($s/d_b \geq 8.0$), ψ_p ranges from 0.85 or 0.95 to 1.0.

Alternatively, and since an expression in a form similar to Eq. (6.29) has not been considered simple enough by ACI Committee 318, a conservative simplification of the ψ_p expression is worthy of consideration that consists of two terms based Eq. (6.15) for the cases of $A_{tt}/A_{hs} = 0$ and $s/d_b = 3$, respectively.

$$\psi_p = \min \left\{ 2 - \frac{1}{8} \frac{s}{d_b}, 1.6 - 2 \frac{A_{tt}}{A_{hs}} \right\}$$

$$\geq 0.85 \text{ for No. 11 and smaller bars and}$$

$$\geq 0.95 \text{ for No. 14 and No. 18 bars} \quad (6.30)$$

Although A_{tt} cannot exceed $0.4A_{hs}$ when calculating ψ_p using either the full or simplified expression, as demonstrated in Section 5.5.1, No. 14 and No. 18 headed bars need at least $0.5A_{hs}$ to address the joint shear demand and prevent a shear failure in cases in beam-column joints. Also, as established in Section 5.5.8, when headed bars are placed outside the column core and the parallel ties, ties should not be counted as contributing to anchorage strength. In such cases, $A_{th}/A_{hs} = 0$ when calculating ψ_p .

6.2.2.2 Modification Factor for Bar Coating

For the modification factor for coated bars, ψ_e , given in Table 25.4.4.3 of ACI 318-19 are retained. For epoxy-coated or zinc and epoxy dual-coated bars, $\psi_e = 1.2$. For uncoated or zinc-coated bars, $\psi_e = 1.0$.

6.2.2.3 Modification Factor for Bar Location

In Table 25.4.4.3 of ACI 318-19, for headed bars terminating inside the column core with a side cover to the bar of at least 2.5 in., or terminating in supporting members with a side cover of at least $6d_b$, $\psi_o = 1.0$. In all other cases, $\psi_o = 1.25$. The value of 1.25 is based on the observations by Sperry et al. (2015a) that, in general, specimens with hooked bars placed outside the column core had a lower anchorage strength than those with bars inside column core. Therefore, conservatively, a strength modification factor of 0.8 was suggested, and later retained by Shao et al. (2016) for headed bars ($1/0.8 = 1.25$).

However, as the re-analysis of the hooked bar specimens in Section 4.4.1 and later analysis of the headed bar specimens tested by Chun et al. (2017a) and Sim and Chun (2022a, 2022b) in Section 5.5.8 reveal, the bar location factor can safely be reduced to 1.15 for headed as well as bars. Therefore, the value of 1.15 is used here as well.

6.2.2.4 Strength-Reduction Factor

Incorporating the three modification factors, ψ_e , ψ_p , and ψ_o , to represent the effects of bar coating, parallel tie reinforcement and bar spacing, and bar location into Eq. (6.10), along with strength-reduction factor ϕ gives

$$\ell_{dt} = \frac{0.001}{\phi} \frac{f_y \psi_e \psi_p \psi_o}{f_c'^{0.25}} d_b^{1.5} \quad (6.30)$$

In this study, the value of ϕ is selected so that 5% or less of all beam-column test specimens used to develop the descriptive equations, Eq. (5.5) and (5.7), have a test-to-calculated ratio of below 1.0. An analysis of the data using Eq. (6.30) shows that a value of $\phi = 0.78$ results in 3.05% of the specimens having a test-to-calculated ratio < 1.0 . For developing reinforcement, the strength-reduction factor has, by tradition, been incorporated in the expression for ℓ_{dt} . Doing so for Eq. (6.30) and recognizing that $0.001/0.78 = 1/780$ gives

$$\ell_{dt} = \frac{f_y \psi_e \psi_p \psi_o}{780 f_c'^{0.25}} d_b^{1.5} \quad (6.31)$$

The format of Eq. (6.31) is similar to those previously proposed at the University of Kansas (Shao et al. 2016, Ghimire et al. 2018, Ghimire et al. 2019b). Compared with the design equation in Section 25.4.4.2 of ACI 318-19, Eq. (6.31) provides more flexibility for designers as the binary choice of 1.0 and 1.6 for the parallel tie and bar spacing factor, ψ_p , is replaced by an expression that varies as a function of A_{tt}/A_{hs} and s/d_b . Also, with the proposed equation, the modification factor for concrete strength (ψ_c in ACI 318-19) is no longer needed, as $f_c'^{0.25}$ provides a good representation of the contribution of concrete compressive strength to anchorage of headed bars and is applicable up to 16,000 psi, as later discussed further in Section 6.3.1. Finally, given the range of bar stresses at failure (up to 150,000 psi) available in the database used to develop Eq. (6.31), the proposed design equation can be applied to high-strength headed bars with specified yield strengths up to 120,000 psi. Table 6.22 summarizes the modification factors and their values incorporated in the proposed design equation.

Table 6.22 Modification factors for the proposed design equation for development of headed bars, Eq. (6.31)

Modification Factor	Condition	Value ^{[1][2][3][4]}
Epoxy coating, ψ_e	Epoxy- or zinc and epoxy dual-coated bars	1.2
	Uncoated or zinc-coated (galvanized) bars	1.0
Parallel tie reinforcement and bar spacing, ψ_p ^{[5][6]}	For No. 11 and smaller bars	$2 - 2.5 \frac{A_{tt}}{A_{hs}} - \frac{1}{8} \frac{s}{d_b} + \frac{1}{6} \frac{A_{tt}}{A_{hs}} \frac{s}{d_b} \geq 0.85$ <p>or, smaller of</p> $\left\{ 2 - \frac{1}{8} \frac{s}{d_b}, 1.6 - 2 \frac{A_{tt}}{A_{hs}} \right\} \geq 0.85$
	For No. 14 and No. 18 bars ^[7]	$2 - 2.5 \frac{A_{tt}}{A_{hs}} - \frac{1}{8} \frac{s}{d_b} + \frac{1}{6} \frac{A_{tt}}{A_{hs}} \frac{s}{d_b} \geq 0.95$ <p>or, smaller of</p> $\left\{ 2 - \frac{1}{8} \frac{s}{d_b}, 1.6 - 2 \frac{A_{tt}}{A_{hs}} \right\} \geq 0.95$
Bar location, ψ_o	(1) Bars terminating inside column core with a minimum side cover to bar of 2.5 in., or (2) Bars terminating in supporting members with a side cover of at least $6d_b$	1.0
	Other	1.15

^[1] A_{tt} : Total cross-sectional area of tie legs within $8d_b$ from the top of the headed bars for No. 3 through No. 8 bars and $10d_b$ for No. 11 and larger bars, in.²

^[2] A_{hs} : Total cross-sectional area of the headed bars being developed, in.²

^[3] s : Minimum center-to-center spacing of headed bars, in.

^[4] d_b : Nominal diameter of headed bar, in.

^[5] When calculating ψ_p , A_{tt}/A_{hs} shall not exceed 0.4 and s/d_b shall not exceed 8

^[6] When bars are placed outside both the column core and the parallel ties, $A_{tt}/A_{hs} = 0$ when calculating ψ_p

^[7] Larger bars need at least $A_{tt} = 0.5A_{hs}$ to address the joint shear demand and prevent a shear failure

6.2.3 Evaluating Proposed Design Equation

In this section, the proposed design equation for the development length of headed bars, Eq. (6.31), is compared with the results in the beam-column joint database. The database includes

the beam-column joint tests at the University of Kansas by Shao et al. (2016), plus tests available in literature including Bashandy (1996) at the University of Texas at Austin and Chun et al. (2017), Chun and Lee (2019), and Sim and Chun (2022a, 2022b) at South Korea. For the comparison, the bar stress at failure measured in the test, f_{su} , is compared with the bar stress calculated based on Eq. (6.16), $f_{s,calc}$. To find $f_{s,calc}$, Eq. (6.16) is solved for yield strength, f_y , which is replaced by $f_{s,calc}$, specified concrete compressive strength f'_c is replaced by the measured concrete strength f_{cm} , and development length ℓ_{dt} is replaced by measured embedment length ℓ_{eh} . The resulting equation is

$$f_{s,calc} = \frac{780 \ell_{eh} f_{cm}^{0.25}}{\psi_e \psi_p \psi_o d_b^{1.5}} \quad (6.32)$$

6.2.3.1 University of Kansas Database

In this section, the stresses calculated based on the proposed design equation, Eq. (6.32), are compared with the results for specimens tested at the University of Kansas, including No. 5, No. 8, and No. 11 headed bars tested by Shao et al. (2016) and the specimens with No. 11, No. 14, and No. 18 bars from the current study. The specimen details are presented in Tables C2 to C5 in Section C3 of Appendix C.

Table 6.23 presents the statistical parameters of $f_{su}/f_{s,calc}$ ratio based on the proposed design provisions for specimens without parallel ties, using the full expression for ψ_p . The same results are obtained if the simplified expressions for ψ_p is used since for $A_{tt}/A_{hs} = 0$, both the full and simplified expressions are governed solely by s/d_b . As shown in the table, for specimens without parallel tie reinforcement, the test-to-calculated $f_{su}/f_{s,calc}$ ranges from 0.81 to 1.67, with a mean of 1.26 and a coefficient of variation of 0.121. For No. 5 bars, the proposed equation is more conservative than for No. 8 and larger bars. The single specimen with three closely-spaced No. 14 bars has a noticeably higher $f_{su}/f_{s,calc}$ ratio of 1.67 than the other specimens, and is likely an outlier, similar to its companion specimen with hooked bars.

Table 6.23 Statistical parameters of test-to-calculated bar stress at failure $f_{su}/f_{s,calc}$ based on the proposed design equation Eq. (6.32) and using the full expression for ψ_p , Eq. (6.29) for headed bar specimens without parallel tie used to develop descriptive equations, Eq. (5.5) and (5.7)

	All	$s \geq 8d_b$					$3d_b \leq s < 8d_b$				
		No. 5	No. 8	No. 11	No. 14	No. 18	No. 5	No. 8	No. 11	No. 14	No. 18
Number of specimens	68	4	20	7	2	0	2	28	4	1	0
Max	1.67	1.48	1.44	1.42	1.27	-	1.50	1.53	1.47	1.67	-
Min	0.81	1.35	1.00	1.02	1.25	-	1.38	0.81	1.14	1.67	-
Mean	1.26	1.40	1.20	1.25	1.26	-	1.44	1.26	1.30	1.67	-
STDEV	0.153	0.057	0.106	0.159	0.013	-	0.086	0.164	0.163	0	-
CoV	0.121	0.041	0.088	0.127	0.010	-	0.060	0.131	0.126	0	-
No. with $f_{su}/f_{s,calc} < 1.0$	2	0	1	0	0	0	0	1	0	0	0

Table 6.24 presents the statistical parameters of $f_{su}/f_{s,calc}$ for specimens with parallel tie reinforcement using the full expression for ψ_p .

Table 6.24 Statistical parameters of test-to-calculated bar stress at failure $f_{su}/f_{s,calc}$ based on the proposed design equation Eq. (6.32) and using the full expression for ψ_p , Eq. (6.29) for headed bar specimens with parallel tie used to develop descriptive equations, Eq. (5.5) and (5.7)

	All	$s \geq 8d_b$					$3d_b \leq s < 8d_b$				
		No. 5	No. 8	No. 11	No. 14	No. 18	No. 5	No. 8	No. 11	No. 14	No. 18
Number of specimens	96	6	30	8	7	4	3	24	4	6	4
Max	1.66	1.56	1.65	1.37	1.66	1.42	1.44	1.52	1.40	1.37	1.51
Min	0.93	1.08	1.02	1.02	1.11	1.17	1.21	0.99	1.19	0.98	0.93
Mean	1.26	1.36	1.28	1.23	1.29	1.33	1.32	1.22	1.31	1.19	1.15
STDEV	0.162	0.170	0.174	0.129	0.164	0.094	0.116	0.157	0.090	0.128	0.249
COV	0.128	0.125	0.136	0.105	0.127	0.071	0.088	0.129	0.069	0.107	0.216
No. with $f_{su}/f_{s,calc} < 1.0$	3	0	0	0	0	0	0	1	0	1	1

As shown in Table 6.24, for specimens with parallel ties, $f_{su}/f_{s,calc}$ ranges from 0.93 to 1.66, with a mean of 1.26 and a coefficient of variation of 0.128. The mean obtained here is the same as that for specimens without parallel ties, indicating a consistent margin of safety provided by the proposed design equation. The design equation is the most conservative for widely spaced No. 5

bars and the least conservative for closely spaced ($3d_b \leq s < 8d_b$) No. 18 bars. A similar table is presented for the case of using the simplified expressions for ψ_p , as shown below.

Table 6.25 Statistical parameters of test-to-calculated bar stress at failure $f_{su}/f_{s,calc}$ based on the proposed design equation Eq. (6.32) and using the simplified expressions for ψ_p , Eq. (6.30) for headed bar specimens with parallel tie used to develop descriptive equations, Eq. (5.5) and (5.7)

	All	$s \geq 8d_b$					$3d_b \leq s < 8d_b$				
		No. 5	No. 8	No. 11	No. 14	No. 18	No. 5	No. 8	No. 11	No. 14	No. 18
Number of specimens	96	6	30	8	7	4	3	24	4	6	4
Max	1.67	1.56	1.65	1.62	1.66	1.44	1.53	1.67	1.66	1.40	1.51
Min	0.93	1.13	1.16	1.17	1.17	1.17	1.30	0.97	1.42	1.00	0.93
Mean	1.33	1.39	1.33	1.43	1.32	1.35	1.45	1.30	1.56	1.21	1.15
STDEV	0.170	0.152	0.133	0.170	0.154	0.105	0.130	0.181	0.105	0.131	0.249
COV	0.127	0.109	0.101	0.119	0.117	0.078	0.089	0.139	0.067	0.108	0.216
No. with $f_{su}/f_{s,calc} < 1.0$	3	0	0	0	0	0	0	1	0	1	1

As shown in Table 6.25 and as expected, using the simplified expressions for ψ_p results in a higher mean for $f_{su}/f_{s,calc}$ (1.33 compared to 1.26 using the full expression for ψ_p), more noticeable for No. 11 and smaller bars.

The statistical parameters of $f_{su}/f_{s,calc}$ using the full expression for ψ_p are presented in Table 6.26 for all headed bar specimens tested at the University of Kansas.

Table 6.26 Statistical parameters of test-to-calculated bar stress at failure $f_{su}/f_{s,calc}$ based on the proposed design equation Eq. (6.32) and using the full expression for ψ_p , Eq. (6.29) for all headed bar specimens used to develop descriptive equations, Eq. (5.5) and (5.7)

Bar size	All	No. 5	No. 8	No. 11	No. 14	No. 18
No. of specimens	164	15	102	23	16	8
Max	1.67	1.56	1.65	1.47	1.67	1.51
Min	0.81	1.08	0.81	1.02	0.98	0.93
Mean	1.26	1.37	1.24	1.26	1.27	1.24
STDEV	0.158	0.122	0.156	0.134	0.178	0.203
COV	0.125	0.089	0.126	0.106	0.139	0.163
No. with $f_{su}/f_{s,calc} < 1.0$	5	0	3	0	1	1

For all 164 headed bar specimens in the University of Kansas database (Section C3 in Appendix C), the test-to-calculated ratio $f_{su}/f_{s,calc}$ based on the proposed design equation using the full expression for ψ_p ranges from 0.81 to 1.67, with a mean of 1.26 and a coefficient of variation of 0.125. Only five specimens (3.05% of all specimens) had $f_{su}/f_{s,calc} < 1.0$. A similar table is shown below for the case of using the simplified expressions for ψ_p .

Table 6.27 Statistical parameters of test-to-calculated bar stress at failure $f_{su}/f_{s,calc}$ based on the proposed design equation Eq. (6.32) and using the full expression for ψ_p , Eq. (6.30) for all headed bar specimens used to develop descriptive equations, Eq. (5.5) and (5.7)

Bar size	All	No. 5	No. 8	No. 11	No. 14	No. 18
No. of specimens	164	15	102	23	16	8
Max	1.67	1.56	1.67	1.66	1.67	1.51
Min	0.81	1.13	0.81	1.02	1.00	0.93
Mean	1.30	1.41	1.28	1.38	1.29	1.25
STDEV	0.166	0.112	0.155	0.186	0.173	0.211
COV	0.127	0.080	0.121	0.135	0.134	0.168
No. with $f_{su}/f_{s,calc} < 1.0$	5	0	3	0	1	1

As shown in Table 6.27, using the simplified expressions for ψ_p results in a higher mean $f_{su}/f_{s,calc}$ ratio than when the full expression for ψ_p is used (1.31 versus 1.26), more noticeably for No. 5 and No. 11 bars than for the other bar sizes.

6.2.3.2 Bashandy (1996)

To further evaluate the proposed design provisions, results from the beam-column joint specimens tested in other studies available in literature can be compared against Eq. (6.32). In Section 1.2.2, beam-column specimens tested by Bashandy (1996), Chun et al. (2009), and Chun et al. (2017a), Chun and Lee (2019), Sim and Chun (2022a, 2022b) were presented. The study by Chun et al. (2009) is excluded because the specimens had a single headed bar, as previously described in Section 5.6. The specimens tested by Sim and Chun (2022a) are also excluded because the specimens had two layers of headed bars with s/d_b of either 1 or 2, which is less than 3 and therefore the proposed design equation is not applicable.

The specimens tested by Bashandy (1996) are described in Section 5.6. Table 6.28 presents the key specimen parameters along with the bar stresses at failure f_{su} and the bar stresses based on Eq. (6.32), $f_{s,calc}$. As shown in the table, the values of $f_{su}/f_{s,calc}$ for the 18 specimens shown ranges

from 0.79 to 1.64, with a mean of 1.05 and a coefficient of variation of 0.199 using the full expression for ψ_p . The results are almost the same using the simplified expressions for ψ_p . As discussed in Section 5.6, the majority of these specimens used unconventional reinforcement layouts in which parallel ties did not enclose the headed bars (Figure 5.39a and c) and were relatively weak with respect to values calculated using the descriptive equations, as reflected also here in the relatively low mean values of $f_{su}/f_{s,calc}$ of 1.05 shown in Table 6.28.

Table 6.28 Comparison of beam-column joint test results by Bashandy (1996) versus the proposed design equation Eq. (6.32) (values converted from SI units)

Specimen ID	n	ℓ_{eh} in.	f_{cm} psi	d_b in.	s/d_b	A_{tr}/A_{hs}^*	$\psi_p^{[1]}$	$\psi_p^{[2]}$	L. C.	f_{su} ksi	$f_{su}/f_{s,calc}^{[1]}$	$f_{su}/f_{s,calc}^{[2]}$
T9	2	11.0	5000	1.41	3.3	0.641	0.85	0.85	B'	49.0	0.96	0.96
T10**	2	12.5	5000	1.41	5.4	0.596	1.33	1.33	B'	39.1	1.21	1.21
T12**	2	9.8	5110	1	8.0	0.557	1.00	1.00	B'	50.7	0.90	0.90
T13**	2	12.8	5560	1	8.0	0.785	1.00	1.00	A'	77.7	1.03	1.03
T14	2	11.0	5400	1.41	3.3	0.212	1.18	1.20	A'	59.9	1.60	1.64
T16	2	14.0	5740	1.41	3.3	1.026	0.85	0.85	A'	61.4	0.92	0.92
T20	2	8.2	5110	1.41	3.3	1.026	0.85	0.85	A'	50.3	1.32	1.32
T21	2	8.3	5110	1	5.0	2.025	0.85	0.85	A'	62.0	0.96	0.96
T22	2	8.3	5110	1	5.0	2.025	0.85	0.85	A'	52.1	0.81	0.81
T23	2	11.2	4820	1.41	3.3	1.026	0.85	0.85	A'	44.1	0.86	0.86
T24	2	11.2	4690	1.41	3.3	1.026	0.85	0.85	A'	51.4	1.01	1.01
T25	2	11.0	4690	1.41	3.3	1.962	0.85	0.85	A'	61.4	1.23	1.23
T26	2	17.0	4550	1.41	3.3	1.026	0.85	0.85	A'	71.3	0.93	0.93
T27	2	8.0	4550	1.41	3.3	1.026	0.85	0.85	A'	28.5	0.79	0.79
T28	2	11.2	4830	1.41	3.3	1.026	0.85	0.85	A'	62.3	1.21	1.21
T29	2	11.0	4830	1.41	3.3	1.026	0.85	0.85	A'	55.5	1.10	1.10
T30	2	11.3	3210	1	5.0	2.025	0.85	0.85	A'	79.4	1.02	1.02
T32	2	8.0	4830	1	5.0	2.025	0.85	0.85	A'	61.5	1.00	1.00
Mean											1.05	1.05
CoV											0.194	0.199

^[1] Using the full expression for ψ_p , Eq. (6.29)

^[2] Using the simplified expressions for ψ_p , Eq. (6.30)

* Cap of 0.4 applied to all specimens, except T10, T12, T13 (refer to next footnote)

** Headed bars were outside column core and side cover was 1.5 in. (half of other specimens), so bar location factor of 1.15 applied. Also, headed bars were outside parallel ties (Figure 5.39.a), therefore ties were not counted towards ψ_p ($A_{tr}/A_{hs} = 0$)

6.2.3.3 Chun et al. (2017a) and Chun and Lee (2019)

Table 6.29 presents the comparisons with the proposed design equation for the 27 No. 14 and No. 18 bar specimens tested by Chun et al. (2017a) and Chun and Lee (2019). As described in Section 5.5.8, these specimens were designed to force a side-blowout failure. The headed bars

were placed outside the column core; therefore, $\psi_o = 1.15$ applies. All specimens had $A_{th}/A_{hs} > 0.4$, but the majority had headed bars were placed outside the parallel ties, as described in Section 5.5.8 and shown in Figure 5.37a. For those specimens, the ties are not used when calculating ψ_p . In seven specimens, headed bars yielded. Those specimens are reported in Table 6.29 but excluded from the analysis. For this and the following study in Section 6.2.3.4, the same results are obtained using full or simplified expressions for ψ_p since all specimens have A_{th}/A_{hs} values of either 0 or 0.4, therefore the expressions are either only a function of s/d_b , or a cap of 0.85 or 0.95 applies.

Table 6.29 Comparison of headed bar specimens tested by Chun et al. (2017a) and Chun and Lee (2019) versus the proposed design equation, Eq. (6.32)

Specimen ID ^{[1][2]}	<i>n</i>	ℓ_{eh}	f_{cm}	d_b	<i>s/d_b</i>	A_{th}/A_{hs} ^[3]	ψ_p ^[4]	f_{su}	$f_{su}/f_{s,calc}$ ^[4]
		in.	psi	in.				ksi	
D43-L7-C1-S42	2	11.9	6950	1.693	9.6	0.4	1.00	45.4	1.36
D43-L7-C1-S42-HP0.5	2	11.9	6950	1.693	9.6	0.4	0.95	60.5	1.72
D43-L7-C1-S70	2	11.9	9890	1.693	9.6	0.4	1.00	72.7	2.00
D43-L10-C1-S42	2	16.9	7570	1.693	9.6	0.4	1.00	63.4	1.30
D43-L10-C1-S42-HP0.5	2	16.9	7570	1.693	9.6	0.4	0.95	71.6	1.40
gD43-L10-C1-S70	2	16.9	11770	1.693	9.6	0.4	1.00	86.0	1.58
D43-L13-C1-S42	2	22.0	6640	1.693	5.0	0.4	1.38	68.9	1.55
D43-L13-C2-S42	2	22.0	6420	1.693	5.0	0.4	1.38	78.3	1.77
D43-L13-C1-S42-T1.5	2	22.0	5870	1.693	5.0	0.4	0.95	67.9	1.09
D43-L13-C2-S42-T1.5*	2	22.0	6060	1.693	5.0	0.4	0.95	93.4	1.48
D43-L16-C1-S42	2	27.1	6640	1.693	5.0	0.4	1.38	83.0	1.52
D43-L16-C2-S42*	2	27.1	6640	1.693	5.0	0.4	1.38	88.0	1.61
D43-L16-C1-S42-T1.5	2	27.1	6060	1.693	5.0	0.4	0.95	61.5	0.79
D43-L16-C2-S42-T1.5*	2	27.1	6420	1.693	5.0	0.4	0.95	91.1	1.16
D57-L7-C1-S42	2	15.8	7450	2.257	7.2	0.4	1.10	48.5	1.82
D57-L7-C1-S42-HP0.5	2	15.8	7450	2.257	7.2	0.4	0.95	61.5	1.99
D57-L7-C1-S70	2	15.8	11150	2.257	7.2	0.4	1.10	57.5	1.95
D57-L10-C1-S42	2	22.6	7,450	2.257	7.2	0.4	1.10	53.2	1.40
D57-L10-C1-S42-HP0.5	2	22.6	7450	2.257	7.2	0.4	0.95	68.6	1.55
D57-L10-C1-S70	2	22.6	11150	2.257	7.2	0.4	1.10	64.5	1.53
D57-L13-C1-S42	2	29.3	5,870	2.257	7.2	0.4	1.10	63.7	1.36
D57-L13-C1-S42-HP0.5*	2	29.3	5870	2.257	7.2	0.4	0.95	85.0	1.57
D57-L13-C1-S42-HP1.0a*	2	29.3	5870	2.257	7.2	0.4	0.95	85.0	1.57
D57-L13-C1-S42-HP1.0b*	2	29.3	5870	2.257	7.2	0.4	0.95	85.3	1.58
D57-L13-C2-S42	2	29.3	5870	2.257	7.2	0.4	1.10	79.8	1.71
D57-L16-C1-S42	2	36.1	6060	2.257	7.2	0.4	1.10	74.0	1.28
D57-L16-C2-S42*	2	36.1	6060	2.257	7.2	0.4	1.10	85.3	1.47
								Mean	1.53
								CoV	0.199

^[1] HP and C at the end of the designations denote a “confined” specimen per Figure 5.37b and 5.37c, thus parallel ties counted towards ψ_p . For all other specimens (Figure 5.37a), $A_{th}/A_{hs} = 0$ when calculating ψ_p .

^[2] Bar location factor $\psi_o = 1.15$ applied to all specimens

^[3] Cap of 0.4 applied to all specimens

^[4] Using both the full and simplified expressions for ψ_p , Eq. (6.29) and (6.30)

* Headed bars yielded, specimens excluded from the analysis

As shown in Table 6.29, for the 20 specimens tested by Chun et al. (2017) and Chun and Lee (2019) for which the headed bars did not yield, $f_{su}/f_{s,calc}$ ranges from 0.79 to 2.00, with a mean of 1.53 and a coefficient of variation of 0.199 using both full and simplified expressions for ψ_p . As discussed in Section 5.5.8, these specimens also had a relatively high mean value of T/T_h based on descriptive equations, Eq. (5.5) and (5.7). The high values of T/T_h were primarily due to the specimen proportions, which results in relatively low force within the joint, similar to the No. 11 hooked bars tested by Marques and Jirsa (1975) and Pinc et al. (1977), as described in Section 4.5. The geometry of these specimens is dissimilar to what would be expected in reinforced concrete frame structures.

6.2.3.4 Sim and Chun (2022b)

Table 6.30 presents the comparisons of the 16 No. 7 and No. 10 specimens tested by Sim and Chun (2022b) with the proposed design equation. These specimens were also designed to force a side-blowout failure. The headed bars were placed outside the column core in all these specimens; therefore $\psi_o = 1.15$. Also, all specimens had $A_{th}/A_{hs} > 0.4$. The parallel ties are counted towards ψ_p only for specimens where ties were wrapped around the headed bars (Figure 5.37b), as discussed in Section 5.5.8.

As shown in Table 6.30 for the specimens tested by Sim and Chun (2022b), $f_{su}/f_{s,calc}$ ranges from 0.81 to 2.18, with a mean of 1.50 and a coefficient of variation of 0.287. The relatively high mean is similar to the one obtained for Chun et al. (2017a), mainly due to using unconventional specimen proportions and geometry that results in a relatively low force carried by the joint.

Table 6.30 Comparison of headed bar specimens tested by Sim and Chun (2022b) versus the proposed design equation, Eq. (6.32)

Specimen ID ^{[1][2]}	<i>n</i>	ℓ_{eh}	f_{cm}	d_b	<i>s/d_b</i>	A_{th}/A_{hs} ^[3]	ψ_p ^[4]	f_{su}	$f_{su}/f_{s,calc}$ ^[4]
		in.	psi	in.				ksi	
D22-L6-C1	2	5.3	12020	0.875	13.5	0.4	1.00	69.0	1.51
D22-L6-C1.5	2	5.3	12020	0.875	13.5	0.4	1.00	56.2	1.23
D22-L6-C1-TR	2	5.3	12020	0.875	13.5	0.4	0.85	79.8	1.49
D22-L9-C1	2	7.9	12020	0.875	13.5	0.4	1.00	73.4	1.07
D32-L6-C1	2	7.6	12020	1.27	9.3	0.4	1.00	82.5	2.18
D32-L6-C1.5	2	7.6	12020	1.27	9.3	0.4	1.00	81.0	2.14
D32-L6-C1-TR	2	7.6	12020	1.27	9.3	0.4	0.85	71.9	1.62
D32-L9-C1	2	11.4	12020	1.27	9.3	0.4	1.00	73.0	1.29
D22-L6-C1	2	5.3	16680	0.875	13.5	0.4	1.00	64.5	1.31
D22-L6-C1.5	2	5.3	16680	0.875	13.5	0.4	1.00	52.4	1.06
D22-L6-C1-TR	2	5.3	16680	0.875	13.5	0.4	0.85	65.0	1.12
D22-L9-C1	2	7.9	16680	0.875	13.5	0.4	1.00	59.8	0.81
D32-L6-C1	2	7.6	16680	1.27	9.3	0.4	1.00	85.1	2.07
D32-L6-C1.5	2	7.6	16680	1.27	9.3	0.4	1.00	85.4	2.08
D32-L6-C1-TR	2	7.6	16680	1.27	9.3	0.4	0.85	79.9	1.66
D32-L9-C1	2	11.4	16680	1.27	9.3	0.4	1.00	81.3	1.32
								Mean	1.50
								CoV	0.287

^[1] TR at the end of the designations denote a “confined” specimen per Figure 5.37b and 5.37c, therefore parallel ties counted towards ψ_p . For all other specimens (Figure 5.37a), $A_{th}/A_{hs} = 0$ when calculating ψ_p .

^[2] Bar location factor $\psi_o = 1.15$ applied to all specimens

^[3] Cap of 0.4 applied to all specimens

^[4] Using both the full and simplified expressions for ψ_p , Eq. (6.29) and (6.30)

* Headed bars yielded, specimens excluded from the analysis

A summary of the statistical parameters of $f_{su}/f_{s,calc}$ for the specimens described in this chapter that were tested outside the University of Kansas is presented in Table 6.32. As shown in the table, for the 54 specimens tested outside the University of Kansas, $f_{su}/f_{s,calc}$ ranges from 0.79 to 2.18 with a mean of 1.36 and a coefficient of variation of 0.283. Almost the same results are obtained using the simplified expressions for ψ_p (very slightly higher overall coefficient of variation of 0.284, and slightly higher coefficient of variation of 0.216 for No. 11 bar specimens). The relatively high mean values obtained for No. 10, No. 14, and No. 18 bars are due mainly to the specimen proportions and geometry used by Chun et al. (2017a) and Sim and Chun (2022b) that results in lower forces in the joint and do not represent usual reinforced concrete structures. The relatively low mean values seen for No. 8 and No. 11 bars (responsible for 8 out of 10 specimens with $f_{su}/f_{s,calc} < 1.0$) are primarily due to the unconventional reinforcement layouts used by Bashandy (1996) that results in low anchorage strengths.

Table 6.31 Statistical parameters of $f_{su}/f_{s,calc}$ for all headed bar specimens tested outside University of Kansas (Bashandy 1996, Chun et al 2017a, Chun and Lee 2019, Sim and Chun 2022b) based on the proposed design equation Eq. (6.32), excluding specimens with shear failure and those with headed bars that yielded

Bar size	All ^[1]	No. 7	No. 8	No. 10	No. 11	No. 14	No. 18
No. of specimens	54	8	6	8	12	11	9
Max	2.18	1.51	1.03	2.18	1.60	2.00	1.99
Min	0.79	0.81	0.81	1.29	0.79	0.79	1.28
Mean	1.36	1.20	0.95	1.79	1.10	1.46	1.62
STDEV	0.386	0.237	0.086	0.371	0.231	0.332	0.259
COV	0.283	0.197	0.090	0.207	0.211	0.227	0.160
No. with $f_{su}/f_{s,calc} < 1.0$	10	1	3	0	5	1	0

^[1] Using the full expression for ψ_p , Eq. (6.29)

6.3 COMPARISONS WITH ACI 318-19

In this section, the proposed design provisions for hooked and headed bars are compared with the provisions in ACI 318-19.

6.3.1 Concrete Compressive Strength

As discussed in Section 1.3.1, ACI Committee 318 chose to stay with the square root of compressive strength $\sqrt{f'_c}$ for both hooked and headed bar design equations when finalizing the 2019 edition of the Code, rather than incorporating the more accurate $f_c'^{0.25}$ as originally proposed (Sperry et al. 2015b, Ajaam 2017, Shao et al. 2016, and Ghimire et al. 2018). To account for the difference between the square root and the quarter power, a concrete strength factor ($\psi_c = f'_c/15,000 + 0.6$) was included in the development length expressions for values of $f'_c \leq 6,000$ psi, with the principle goal of preventing excessively long development lengths for lower compressive strength concretes, while limiting the potential for low anchorage strengths at higher compressive strengths. The original proposal included an upper compressive strength of 16,000 psi for application of the design equations. As adopted, the equations in ACI 318-19 have an upper limit of $f'_c = 10,000$ psi, corresponding to the maximum permitted value on $\sqrt{f'_c}$ of 100 psi.

As a result of the original proposal modifications, the development length provisions for hooked and headed bars provide a decreased margin of safety for concretes with compressive

strengths near 10,000 psi; they are, also, slightly more complex than necessary due to the addition of the concrete strength factor ψ_c . This decreased margin of safety can be illustrated by comparing the ACI 318-19 provisions with the best-fit expression upon which the provisions are based. The expression for development length in ACI 318-19 is:

$$\ell_{dt} = \left(\frac{f_y \psi_e \psi_p \psi_o \psi_c}{75 \sqrt{f'_c}} \right) d_b^{1.5} \quad (6.33)$$

where $\sqrt{f'_c}$ may not exceed 100 psi.

For uncoated, headed bars in a beam-column joint with side cover to bar ≥ 2.5 in., and center-to-center bar spacing $s \geq 6d_b$ or $A_{tt}/A_{hs} \geq 0.3$, $\psi_e = \psi_p = \psi_o = 1.0$. Now, replacing f_y with $f_{s,calc}$, f'_c with f_{cm} , and ℓ_{dt} with ℓ_{eh} , and solving for the bar stress gives:

$$f_{s,calc} = \frac{75 \ell_{eh} \sqrt{f'_c}}{\psi_c d_b^{1.5}} \quad (6.34)$$

where $\psi_c = f'_c/15,000 + 0.6$. Under the same conditions for bar spacing and parallel ties, the proposed design equation gives $\psi_p = 1.25$ for No. 11 and smaller bars.

The experimentally-based descriptive expression for the headed bar stress at failure $f_{s,Descriptive}$ for these conditions with $s = 6d_b$ and $A_{tt}/A_{hs} = 0$ based on Eq. (5.5) is

$$f_{s,Descriptive} = \frac{1650 \ell_{eh}^{0.941} f_{cm}^{0.207}}{d_b^{1.502}} \quad (6.35)$$

where ℓ_{eh} is the embedded length of the headed bar and f_{cm} is the actual concrete compressive strength. The mean and coefficient of variation for the descriptive equation are, respectively, 1.00, and 0.112. Equation (6.35) is valid up to 16,000 psi. Figure 6.9 shows the ratio $f_{s,Descriptive}/f_{s,calc}$ for No. 8 bars for a given ℓ_{eh} of 15 in. as a function of concrete compressive strength for both the proposed and ACI 318-19 design equations, Eq. (6.32) and (6.34), respectively.

As shown in Figure 6.9, the ratio $f_{s,Descriptive}/f_{s,calc}$ based on the ACI 318-19 equation, Eq. (6.34), reaches a peak of approximately 1.25 for concrete with a compressive strength of 6,000 psi and then drops to a low point of approximately 1.07 at a compressive strength of 10,000 psi, corresponding to the upper limit for $\sqrt{f'_c}$ of 100 psi. Because $\sqrt{f'_c}$ for use in design is limited to a maximum of 100, the ratio $f_{s,Descriptive}/f_{s,calc}$ increases as the compressive strength increases above 10,000 psi to 1.18 at 16,000 psi. Similar variations in safety margin occur for hooked bars. Figure

6.9 also shows $f_{s,Descriptive}/f_{s,calc}$ as a function of f'_c for the proposed expression, Eq. (6.32) with $s = 6d_b$ and $A_{tt}/A_{hs} = 0$, indicating that the proposed equation provides a more uniform margin of safety.

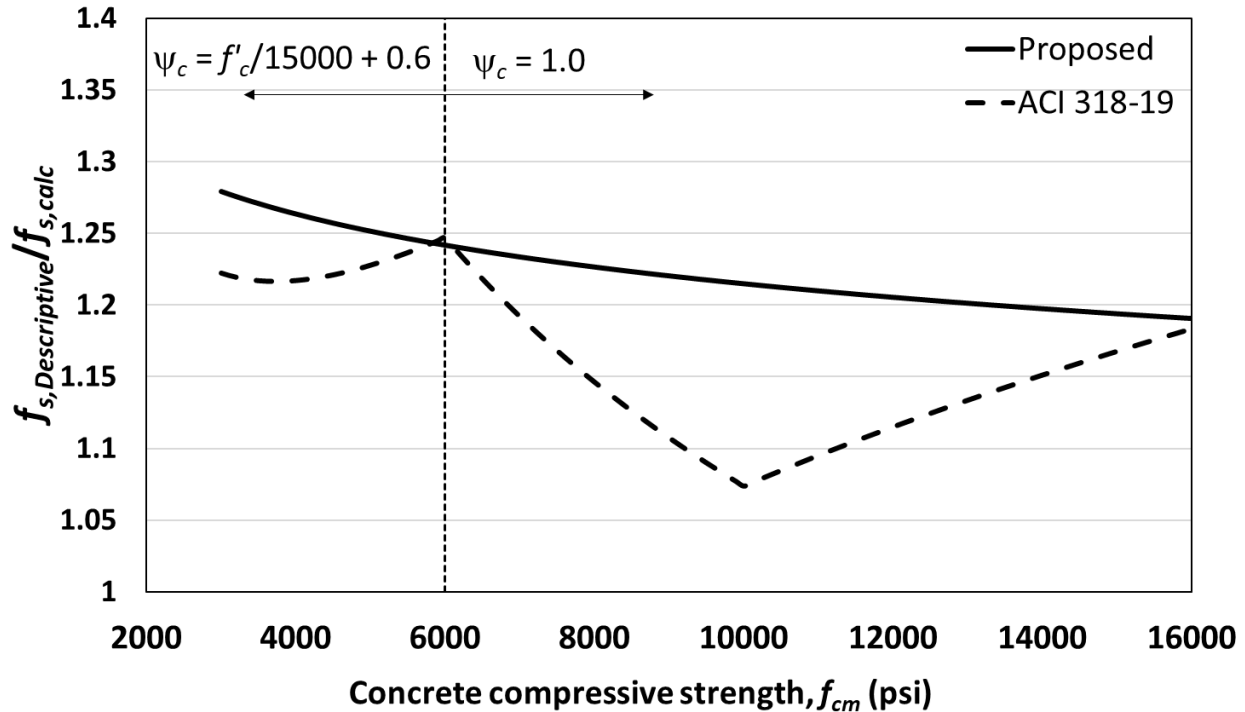


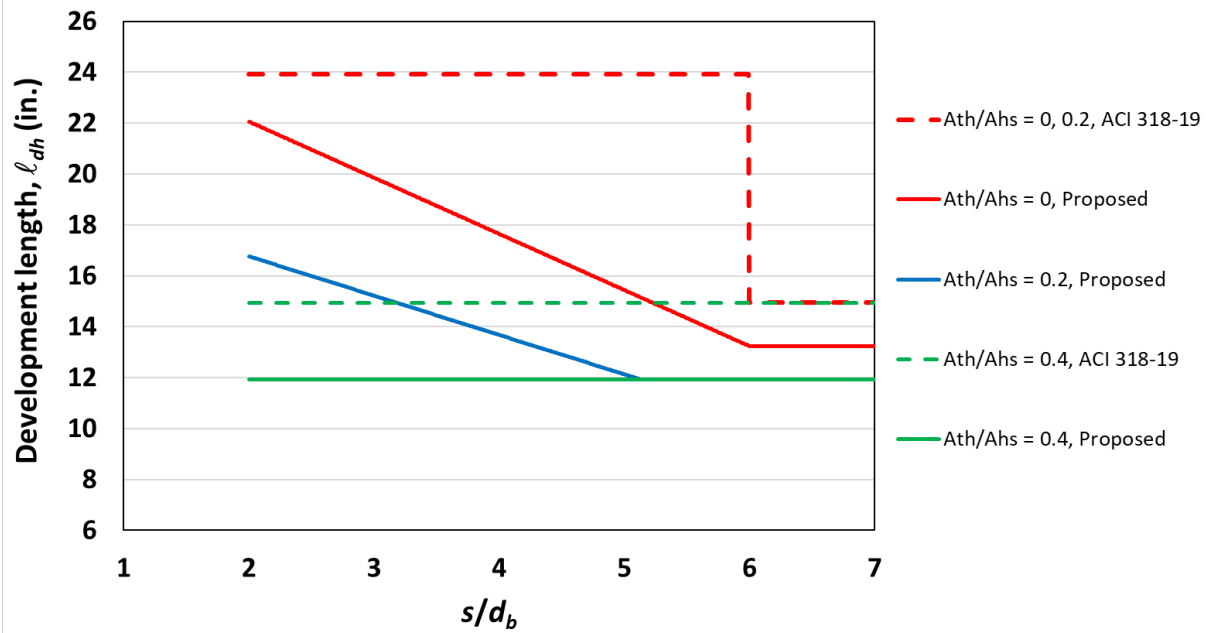
Figure 6.9 Ratio $f_{s,Descriptive}/f_{s,calc}$ versus concrete compressive strength f_{cm} for No. 8 bars headed bars with $s = 6d_b$ and $A_{tt}/A_{hs} = 0$ for ACI 318-19 and proposed design provisions

6.3.2 Required Development Length

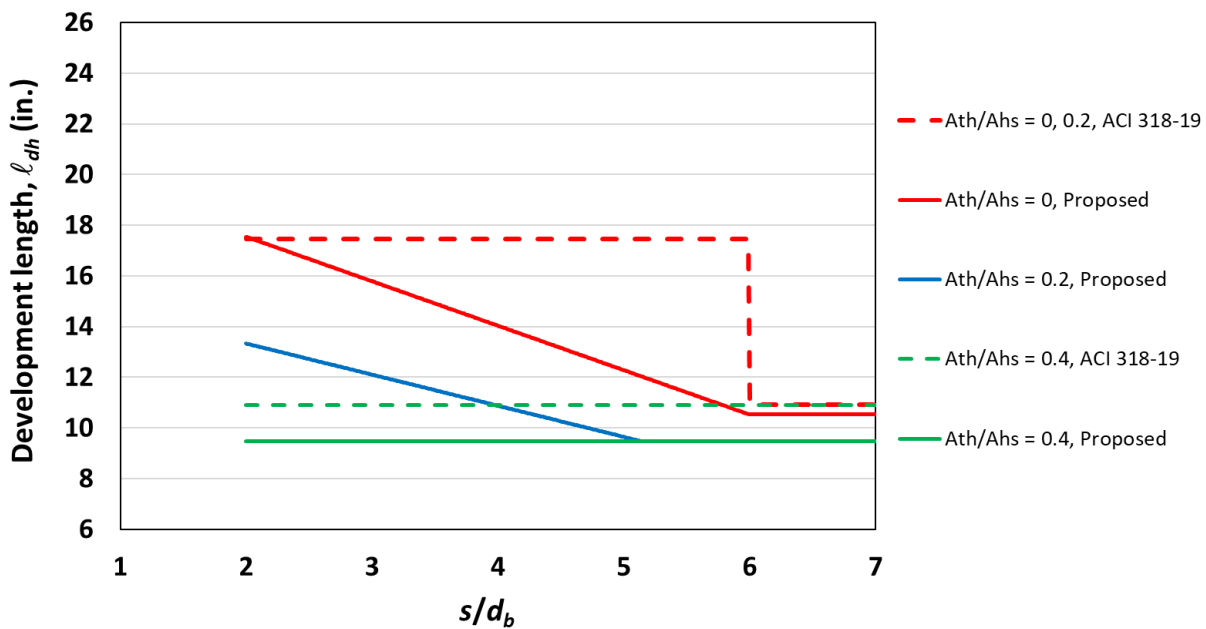
The effects of the provisions for ψ_r and ψ_p in ACI 318-19 are illustrated in Figures 6.10 and 6.11 for hooked bars, and 6.12, and 6.13 for headed bars, which show the required development lengths for No. 8 bars in beam-column joints with at least 2.5 in. of side cover on the exterior bars in normalweight concrete. The figures also show the required development lengths based on the proposed provisions, using the full (Figures 6.10 and 6.12) and simplified (Figures 6.11 and 6.13) expressions for ψ_r and ψ_p .

As discussed before, ACI 318-19 adopted a binary choice, 1.0 or 1.6, on the confining reinforcement and parallel-tie reinforcement factors, ψ_r and ψ_p , in place of factors that vary as a function of bar spacing and the level of confinement. The factor 1.0 is applied only if the confining reinforcement equals or exceeds a specific value ($A_{th,ACI} \geq 0.4A_{hs}$ and $A_{tt} \geq 0.3A_{hs}$ for hooked and headed bars, respectively) or the center-to-center spacing between the bars, s , exceeds $6d_b$.

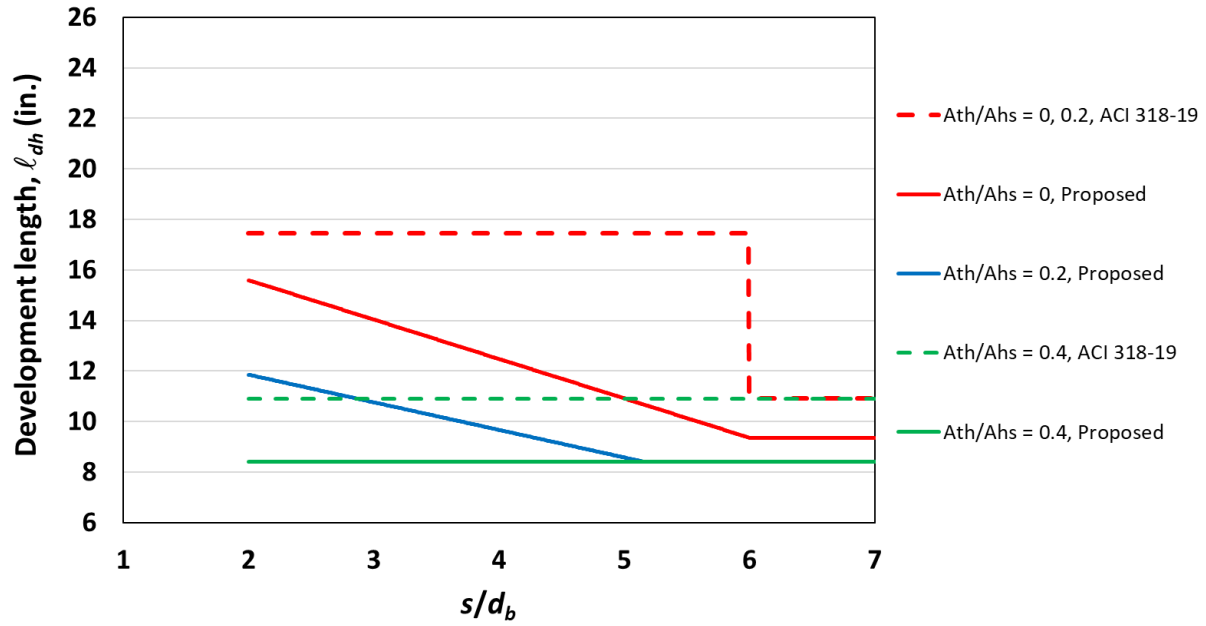
Intermediate values of ψ_r or ψ_p in cases where the spacing and confining reinforcement do not meet one of the requirements are not permitted by ACI 318-19, resulting in higher values of ℓ_{dh} and ℓ_{dt} than needed to develop f_y . Intermediate values of ψ_r and ψ_p are permitted by the proposed expressions, as given respectively in Eqs. (6.14) or (6.15) for hooked and (6.29) or (6.30) for headed bars.



(a)

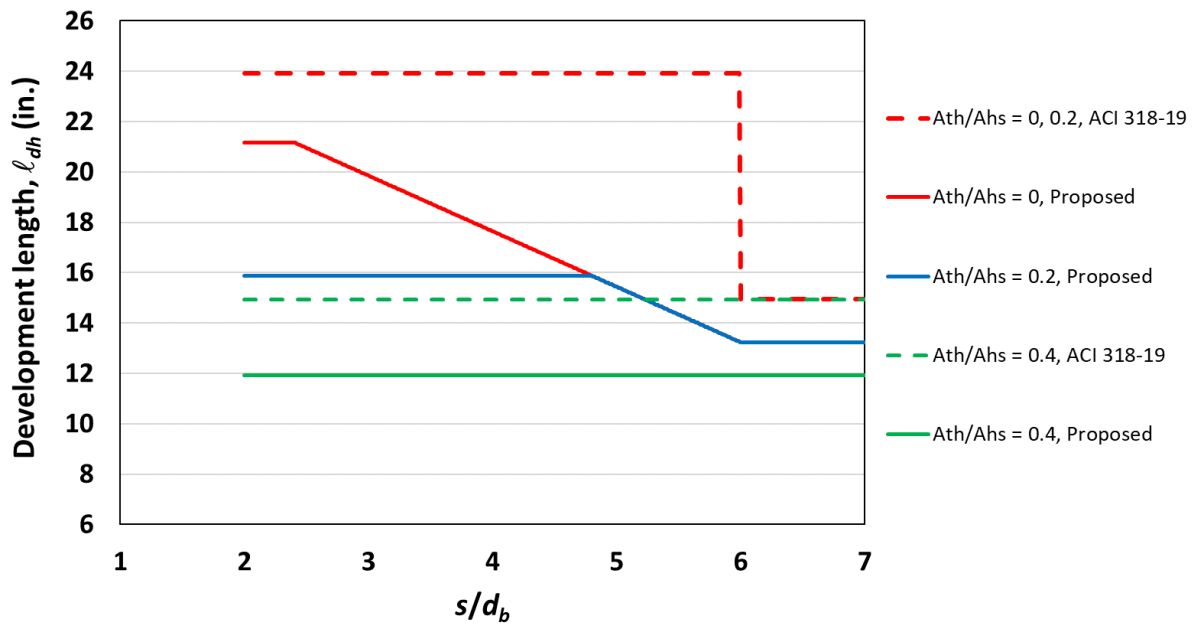


(b)

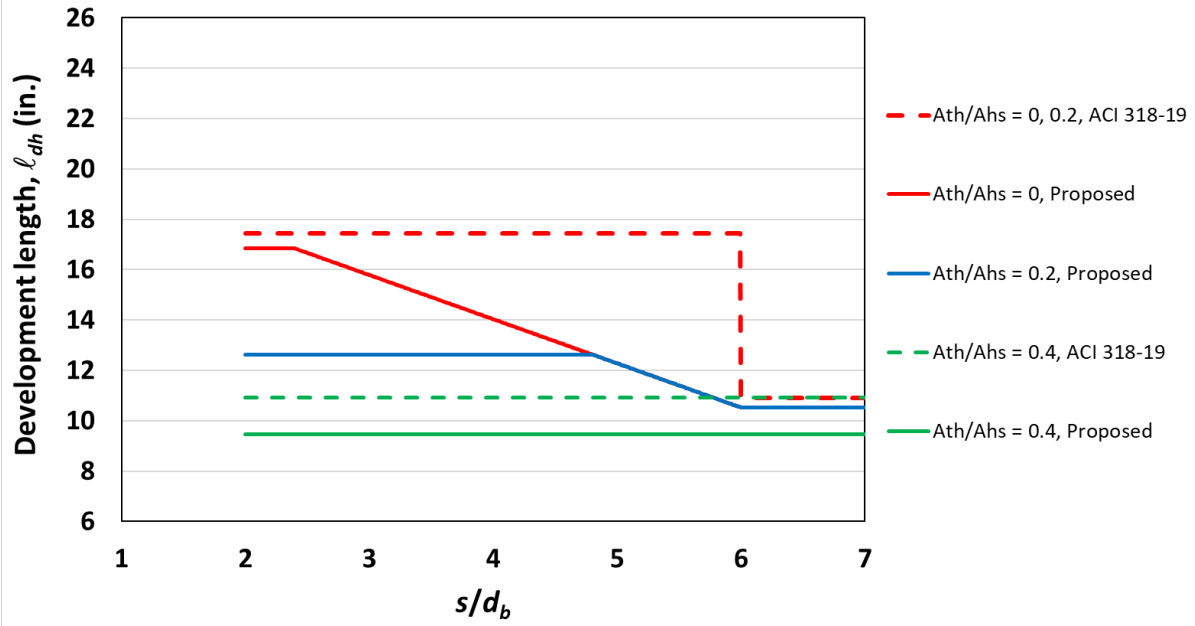


(c)

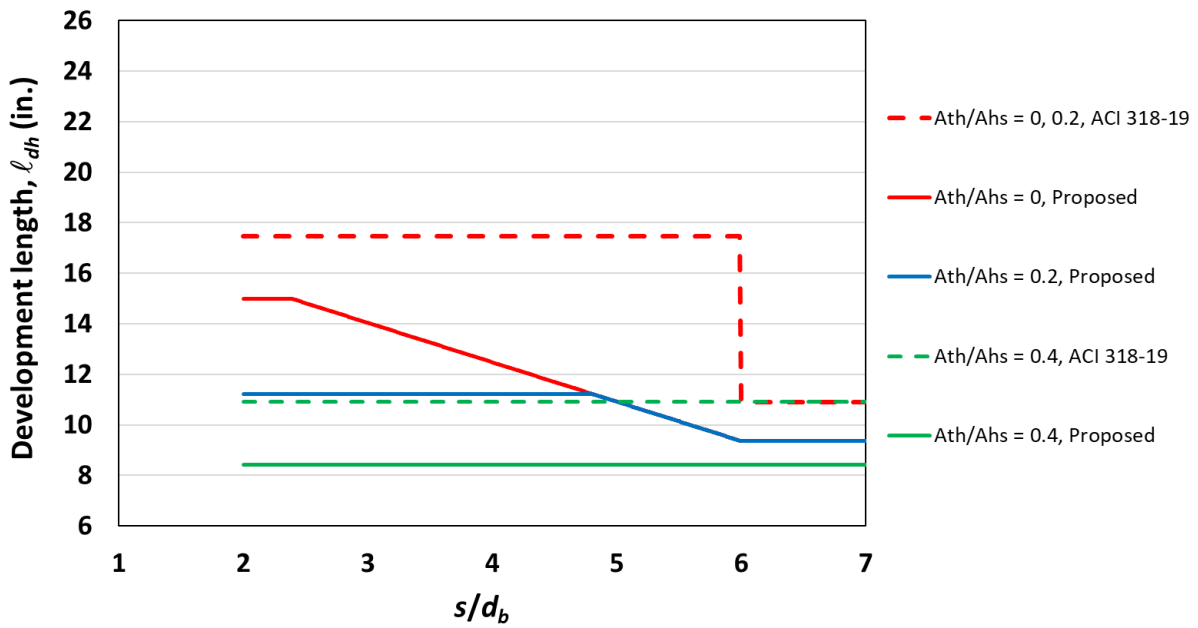
Figure 6.10 Required development lengths of No. 8 hooked bars for $f'_c =$ (a) 4000 psi, (b) 10,000 psi, and (c) 16,000 psi as a function of s/d_b and A_{th}/A_{hs} based on based on ACI 318-19 and the proposed provisions using the full expression for ψ_r , Eq. (6.14)



(a)

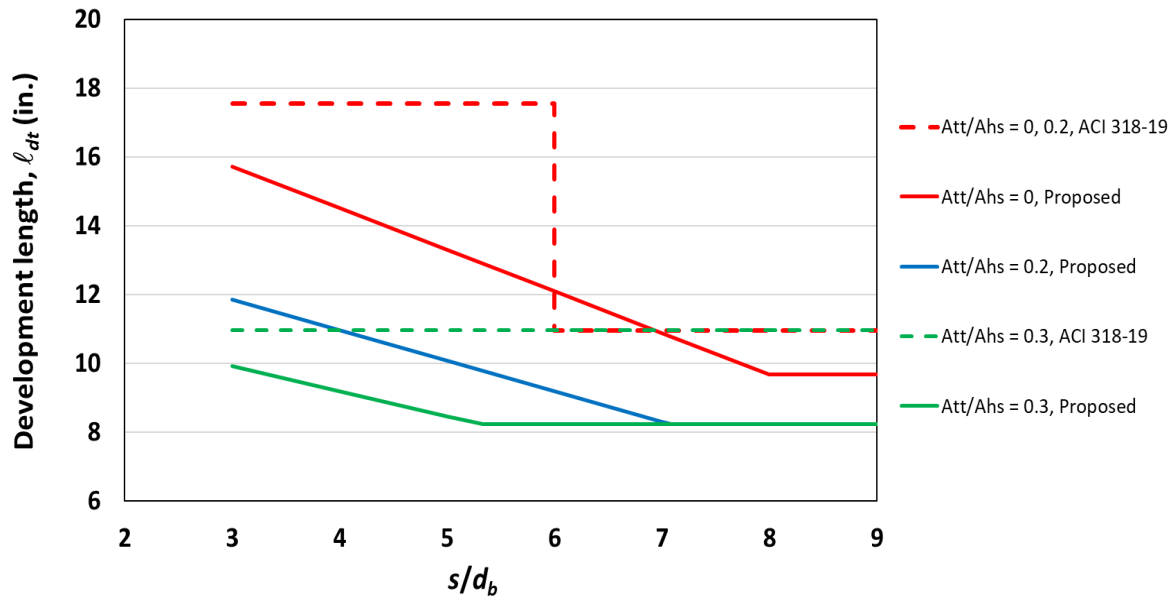


(b)

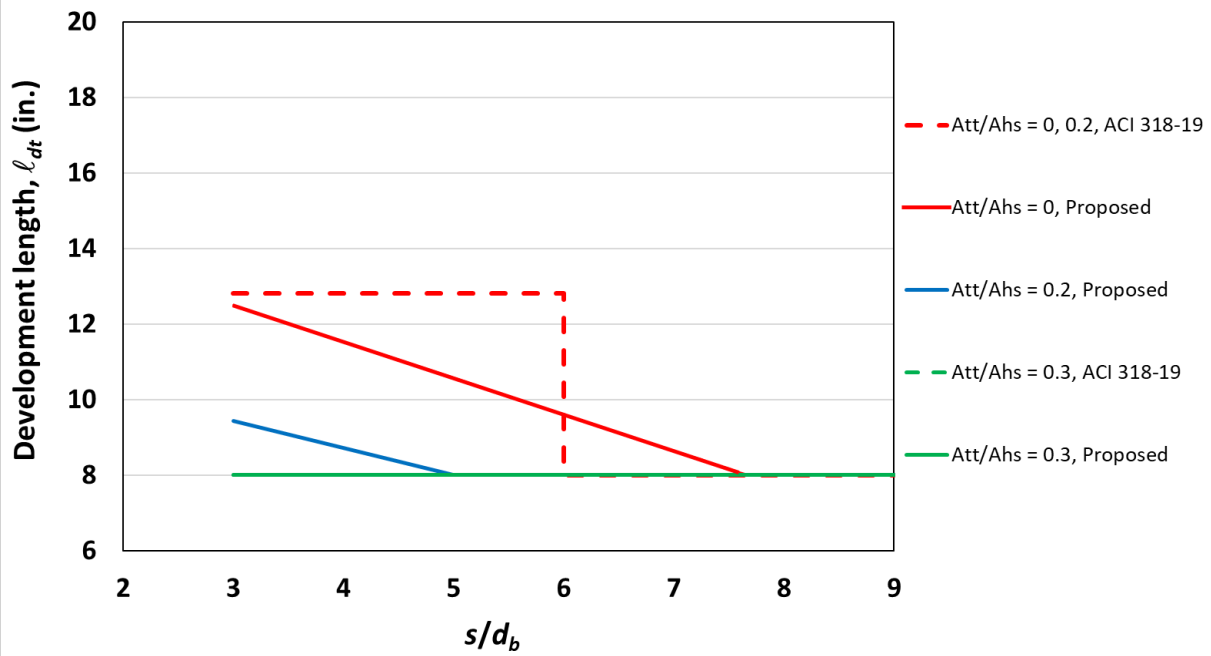


(c)

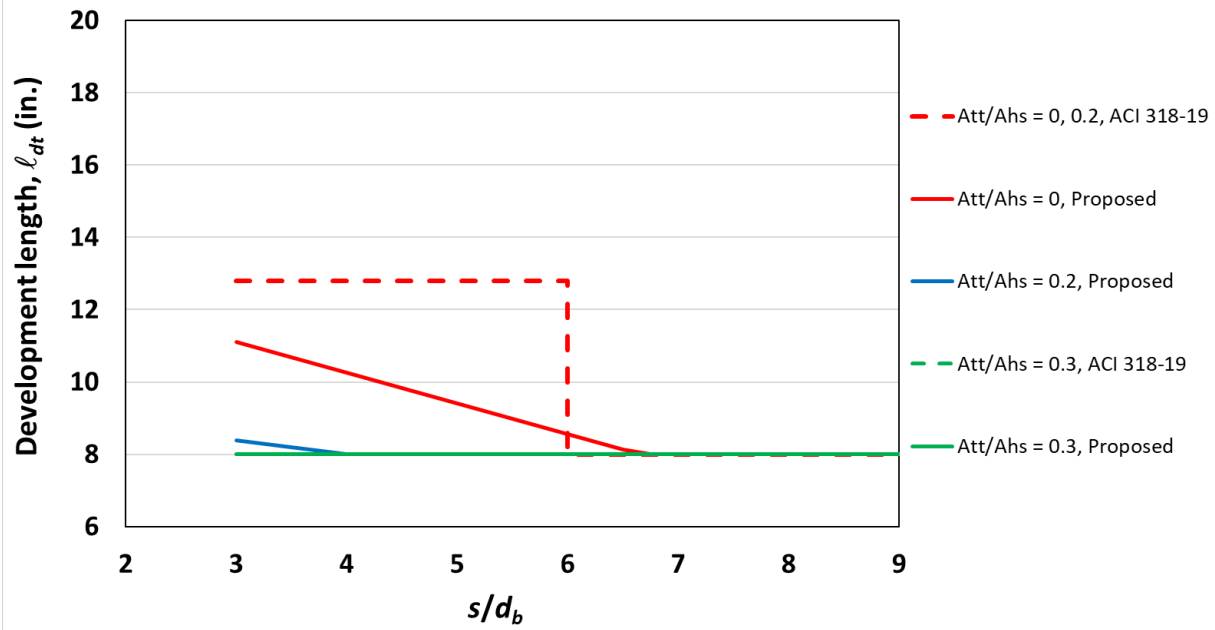
Figure 6.11 Required development lengths of No. 8 hooked bars for $f'_c =$ (a) 4000 psi, (b) 10,000 psi, and (c) 16,000 psi as a function of s/d_b and A_{th}/A_{hs} based on ACI 318-19 and the proposed provisions using the simplified expressions for ψ_r , Eq. (6.15)



(a)

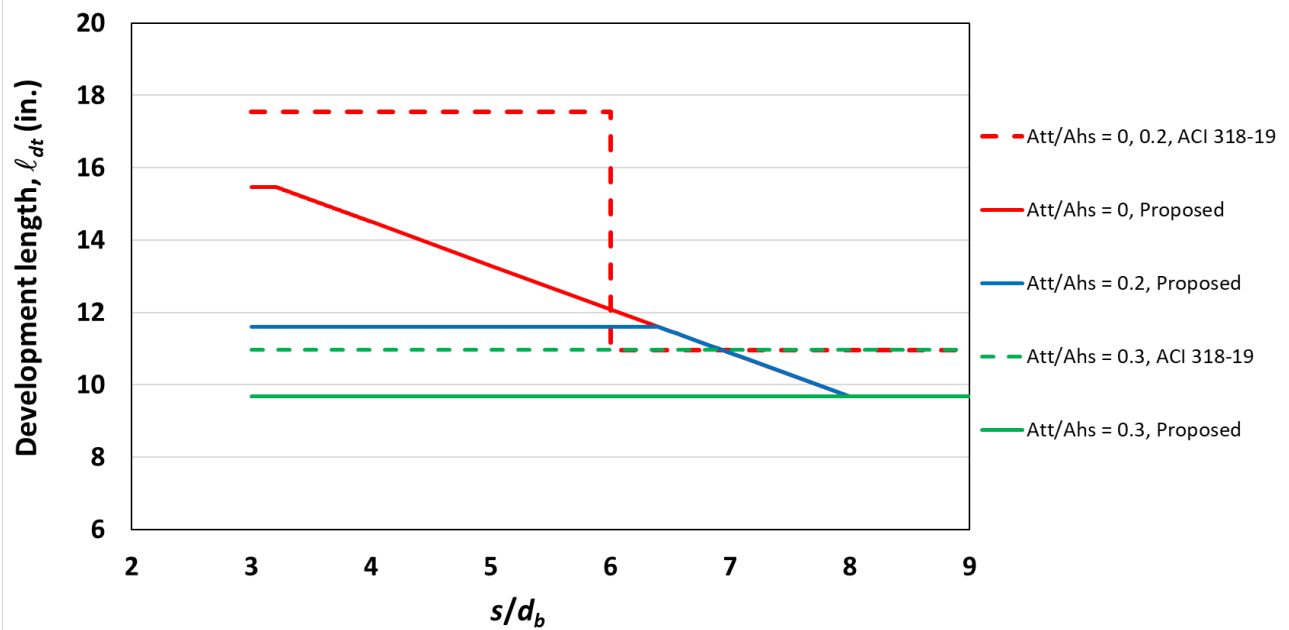


(b)

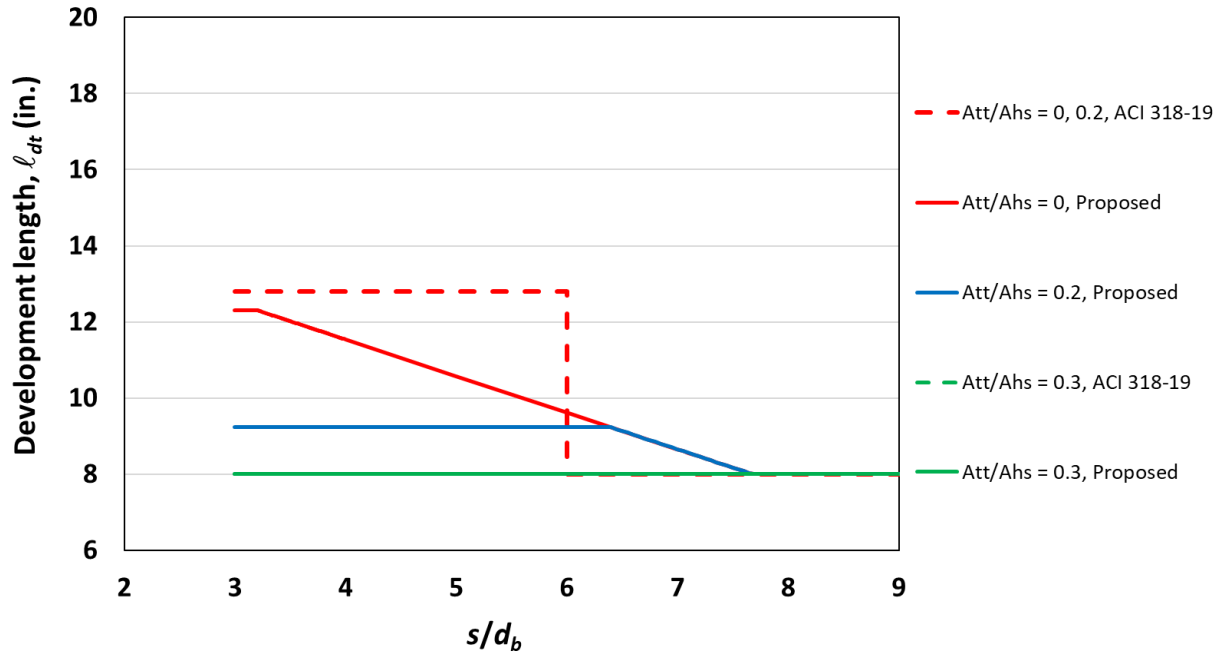


(c)

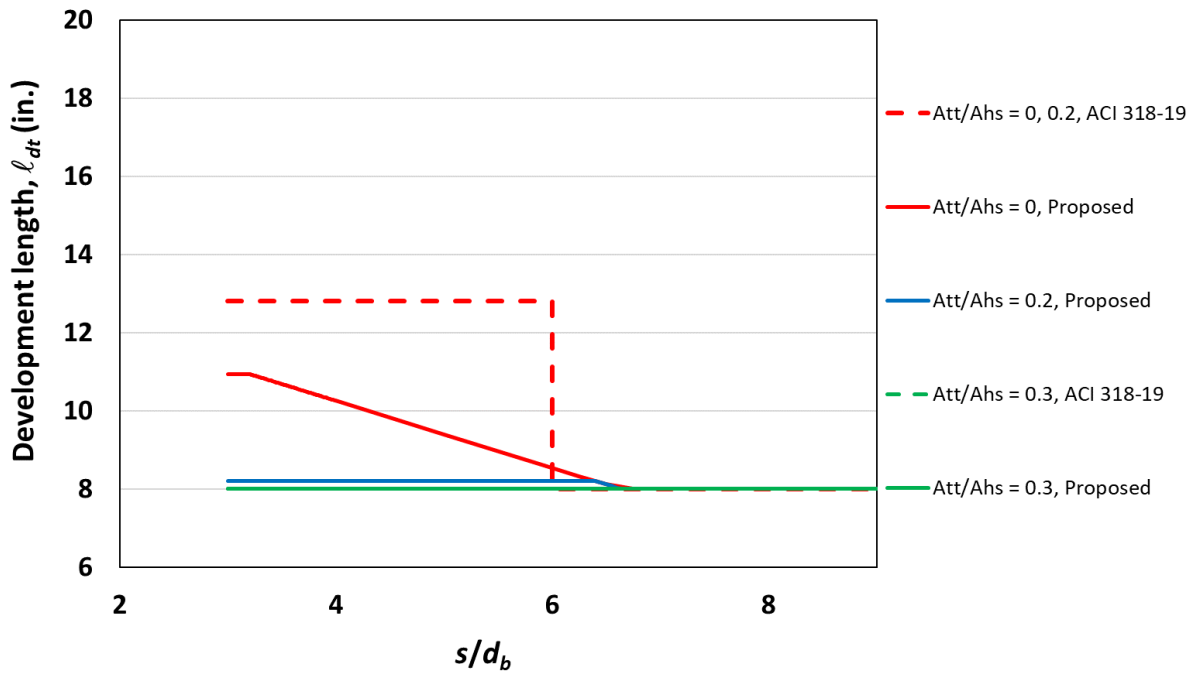
Figure 6.12 Required development lengths of No. 8 headed bars for $f'_c =$ (a) 4000 psi, (b) 10,000 psi, and (c) 16,000 psi as a function of s/d_b and A_{tt}/A_{hs} based on ACI 318-19 and the proposed provisions using the full expression for ψ_p , Eq. (6.29)



(a)



(b)



(c)

Figure 6.13 Required development lengths of No. 8 headed bars for $f'_c =$ (a) 4000 psi, (b) 10,000 psi, and (c) 16,000 psi as a function of s/d_b and A_{tt}/A_{hs} based on ACI 318-19 and the proposed provisions using the simplified expressions for ψ_p , Eq. (6.30)

As shown in Figures 6.10 to 6.13, for both hooked and headed bars, the proposed provisions result in shorter development lengths than those required by ACI 318-19 for most values of A_{th}/A_{hs} or A_{tl}/A_{hs} and s/d_b , for both the full and simplified expressions for ψ_r and ψ_p . The differences between the development lengths based on the proposed provisions and those based on ACI 318-19 are greatest for lower concrete compressive strengths and in cases where ACI 318-19 gives no credit for intermediate values of A_{th}/A_{hs} or A_{tl}/A_{hs} and s/d_b , a prime example being the case where $A_{th}/A_{hs} = 0.2$ and $s/d_b < 6$ for hooked bars, as shown Figures 6.10a and 6.11a.

CHAPTER 7: SUMMARY, CONCLUSIONS, AND FUTURE WORK

7.1 SUMMARY

This research continues a series of studies of the anchorage and development of high-strength reinforcing bars with standard hooks and heads (Searle et al. 2014, Sperry et al. 2015a, 2015b, 2017a, 2017b, 2018, Yasso et al. 2017, Ajaam et al. 2017, 2018, Shao et al. 2016, Ghimire et al. 2018, 2019a, 2019b) to expand the available data to include bars larger than No. 11 (No. 14 and No. 18). Forty-two large-scale simulated beam-column joint specimens containing No. 11, No. 14 and No. 18 hooked and headed bars were tested. Of the 42 specimens, 12 contained hooked bars and 30 contained headed bars. The effects of bar size, bar spacing, bar location, embedment length, confining transverse reinforcement in the joint region, placement of bars within the cross-section, concrete compressive strength, compression strut angle, and effective beam depth on anchorage strength were investigated.

Two loading conditions were used. In loading condition A, the joint shear was 80% of the total applied force to the bars, simulating the forces in an exterior beam-column joint with the beam located at the midheight of the column. The joint shear was reduced to ~69% of the total applied force in loading condition B. Loading condition A also had a moment reversal within the joint (with equal and opposite column moments acting on opposing joint faces), whereas loading condition B did not. All hooked bar specimens and 15 headed bar specimens were tested under loading condition A, while the other 15 headed bar specimens tested using loading condition B.

Of the 12 specimens containing hooked bars, eight contained No. 14 and four contained No. 18 bars. The No. 14 bar specimens included six with two widely-spaced bars (center-to-center spacing $s \geq 6d_b$) and two with three closely-spaced bars ($s < 6d_b$), where d_b = hooked or headed bar diameter. All four No. 18 bar specimens had two widely-spaced bars. Bar spacing ranged from $3.5d_b$ to $10.6d_b$. The hooked bar specimens had concrete compressive strengths ranging from 6,390 to 15,770 psi and bar stresses at failure ranging from 87,300 to 130,600 psi. Four No. 14 bar specimens had no confining reinforcement in the joint region. The remaining hooked bar specimens had ties in the joint region A_{th} ranging from $0.178A_{hs}$ to $0.465A_{hs}$, where A_{th} is the total cross-sectional area of tie legs within $8d_b$ from the top of the hooked bar for No. 8 bars and smaller or within $10d_b$ for No. 9 bars or larger, and A_{hs} is the total area of the hooked bars being developed. All specimens had a side cover to the bar of 3.5 in.

The 30 specimens containing headed bars included two with No. 11, 20 with No. 14, and eight with No. 18 bars. Of the 20 specimens with No. 14 bars, 13 had two widely-spaced (center-to-center spacing $\geq 8d_b$) bars, one had two closely-spaced bars (center-to-center spacing $< 8d_b$), and six had three closely-spaced bars. Of the eight specimens with No. 18 headed bars, four had two widely-spaced bars, two had two closely-spaced bars, and two had three closely-spaced bars. Concrete compressive strength ranged from 5,310 to 16,210 psi, and bar stresses at failure ranged from 54,900 to 148,300 psi. The center-to-center bar spacing ranged from $2.7d_b$ to $10.6d_b$. Headed bars from different manufacturers were used with net bearing areas between 4.2 and 4.4 times the bars area. The majority of the specimens contained parallel ties within the joint, with the total area of tie legs within $10d_b$ from the top of headed bars ranging from $0.178A_{hs}$ to $0.827A_{hs}$, where A_{ti} is the total cross-sectional area of tie legs within $8d_b$ from the top of the headed bar for No. 8 bars and smaller or within $10d_b$ for No. 9 bars or larger, and A_{hs} is the total area of the headed bars being developed. Most specimens had a side cover to the bar of 3.5 in. One No. 14 specimen and four No. 18 specimens had a side cover of 6.5 in.

Test results are compared with the current provisions for the development length of hooked and headed bars in Chapter 25 of ACI 318-19 Building Code. Descriptive equations to characterize anchorage strength of hooked and headed bars developed previously for No. 11 and smaller bars are evaluated. New descriptive equations are developed to more accurately represent the anchorage strength for bars as large as No. 18. The equations are compared with the test results available in the literature. New design provisions for development length are developed for hooked and headed bars and evaluated with respect to test results and the provisions of ACI 318-19.

7.2 CONCLUSIONS

The following conclusions are based on the observations and analyses described in this report:

1. ACI 318-19 is unnecessarily conservative for No. 14 and No. 18 hooked and headed bars, independent of concrete compressive strength.
2. The bar location factor ψ_o of 1.25 in ACI 318-19, applied to hooked and headed bars terminating inside column longitudinal reinforcement (column core) with side cover < 2.5 in. or bars with side cover $< 6d_b$, can be safely reduced to 1.15 for design.

3. For both hooked and headed bars, confining reinforcement does not contribute to anchorage strength when bars are placed outside both the column core and the confining reinforcement.
4. The descriptive equations for hooked and headed bars developed in this study accurately account for concrete compressive strength, confining reinforcement, and bar spacing. The ability of the equations to accurately represent anchorage strength is insensitive to variations in compression strut angle and effective beam depth in cases where the ratio of effective beam depth to embedment length < 1.5 .
5. Specimens with widely-spaced No. 14 and 18 bars had higher anchorage strengths than those with closely-spaced bars in most but not all cases similar to the observations for No. 11 and smaller bars.
6. Although not reflected in the current Code provisions, providing confining reinforcement in the joint region, even when $A_{th,ACI}^4 < 0.4A_{hs}$, contributes to anchorage strength of No. 14 and No. 18 hooked bars.
7. Under loading condition A, all hooked bar specimens, even the four specimens without confining reinforcement, carried the joint shear and exhibited an anchorage failure, whereas shear-like failures were observed in some headed bar specimens under similar conditions. These observations reveal the distinct role of the tail of the hook in resisting the propagation of joint shear cracks to the back of the joint, thereby allowing the joints with hooked bars to carry more shear.
8. The contribution of confining reinforcement to anchorage strength increases with hooked bar size. The contribution is high enough for No. 14 and No. 18 hooked bars as to warrant special treatment in design.
9. Compared with the descriptive equations developed for No. 11 headed bars and smaller, the power of headed bar diameter, d_b , in the expression for contribution of parallel ties (T_s) is reduced from 0.88 to 0.11 in the new equations, indicating a much lower effect of bar size on the contribution of parallel ties than previously obtained.
10. Loading condition and joint shear demand play a major role for headed bars. The difference in joint shear between 0.80 and 0.69 times the force in the headed bar under loading conditions A and B, respectively, combined with differences in the column

⁴ Total area of tie legs within $15d_b$ from the centerline of hooked bars, based on ACI 318-19.

moment distributions, are key factors in the type of failure and anchorage strength of headed bars for joints without a minimum quantity of shear reinforcement parallel within the joint.

11. The minimum area of parallel ties (A_{tt}) needed for larger bars to address the joint shear demand is $0.5A_{hs}$. More study is warranted to investigate if parallel ties providing values below $0.5A_{hs}$ would be adequate to prevent a shear-like failure under loading condition A.
12. For headed bars, the upper limit on A_{tt}/A_{hs} is increased to 0.4 for both the descriptive equations and design purposes. The limit was previously 0.3 based on No. 11 and smaller bar tests.
13. The upper limit of 0.4 on A_{tt}/A_{hs} indicates that providing ties (A_{tt}) above $0.4A_{hs}$ does not add to the anchorage strength of headed bars. Thus, the contribution of parallel ties to joint shear strength appears to be separate from their contribution to the anchorage strength.
14. Providing parallel ties within the joint region improves the anchorage strength of headed bars even when $A_{tt,ACI}^5 < 0.3A_{hs}$ (not reflected in ACI 318-19).
15. The interior legs of parallel ties within joints contribute to the anchorage strength of headed bars at least as well as exterior legs.
16. Increasing side cover to the bar (and thus, concrete cover to head) did not have a major effect on the anchorage strength of No. 14 and No. 18 headed bars, but changed the failure type from side splitting to concrete breakout.
17. The proposed design equations for hooked and headed bars are applicable to concrete with compressive strengths up to 16,000 psi, steel with yield strengths up to 120,000 psi, and bars up to No. 18.
18. Similar to earlier findings established for No. 11 and smaller hooked and headed bars, the effect on anchorage strength of concrete compressive strength is best represented by the 0.25 power for design purposes.
19. The proposed modification factors for confining reinforcement (expressed as A_{th}/A_{hs} or A_{tt}/A_{hs}) and bar spacing (expressed as s/d_b), in the form of a single expression or simplified expressions that address the effects of confining reinforcement and bar

⁵ Total area of tie legs within $8d_b$ from the centerline of headed bars, based on ACI 318-19.

spacing independently, provide more flexibility for designers, enabling them with more avenues to take advantage of a range of values for A_{th}/A_{hs} or A_{tl}/A_{hs} and s/d_b and ultimately use a shorter development length as they would using the current provisions.

7.3 FUTURE WORK

This study included only a limited number of specimens with No. 14 and No. 18 hooked bars under loading condition A. For example, no specimens had closely-spaced No. 18 hooked bars or more than a single layer of No. 14 or No. 18 bars. Expanding the scope of the test parameters would provide a better understanding of the anchorage strength of large bars. It would, also, be worthwhile to test No. 11 and smaller hooked bar specimens under loading condition A since, other than the tests on No. 14 and No. 18 bars in this study, no data are available on hooked bars under monotonic loading in a configuration matching that found in most beam-column joints.

More study is needed of headed bars in beam-column joints under loading condition A with different bar sizes and quantities of parallel ties to establish the minimum area of parallel ties needed to address the joint shear demand and prevent a shear-like failure. In addition, the effects of concrete side cover to the bar for larger headed bars can be further investigated by testing specimens with the same bar spacing but different side cover. Both the current Code and the proposed design provisions only permit anchoring headed bars in normalweight concrete because no tests have been performed on headed bars in lightweight concrete. Therefore, tests using different size headed bars cast in lightweight concrete are recommended.

For both hooked and headed bars, it is not clear if bar spacing is the best parameter to address the effects on anchorage strength of groups of closely-spaced bars. A broader range of specimen configurations would be useful to answer this question.

REFERENCES

ACI Committee 318, 2014. “Building Code Requirements for Structural Concrete (ACI 318-14) and Commentary,” (ACI 318R-14), American Concrete Institute, Farmington Hills, Michigan, 520 pp.

ACI Committee 318, 2019. “Building Code Requirements for Structural Concrete (ACI 318-19) and Commentary,” (ACI 318R-19), American Concrete Institute, Farmington Hills, Michigan, 625 pp.

Ajaam, A., Yasso, S., Darwin, D., O'Reilly, M., and Sperry, J., 2018. “Anchorage Strength of Closely-Spaced Hooked Bars,” *ACI Structural Journal*, Vol. 115, No. 4, July-Aug., pp. 1143-1152.

Ajaam, A., Darwin, D., and O'Reilly, M., 2017. “Anchorage Strength of Reinforcing Bars with Standard Hooks,” *SM Report* No. 125, University of Kansas Center for Research, Inc., Lawrence, KS, Apr., 372 pp.

ASTM A970, 2016. “Standard Specification for Headed Steel Bars for Concrete Reinforcement,” (ASTM A970/A970M-16), ASTM International, West Conshohocken, Pennsylvania, 9 pp.

ASTM A970, 2018. “Standard Specification for Headed Steel Bars for Concrete Reinforcement,” (ASTM A970/A970M-18), ASTM International, West Conshohocken, Pennsylvania, 10 pp.

Bashandy, T. R., 1996. “Application of Headed Bars in Concrete Members,” *PhD dissertation*, University of Texas at Austin, Dec., 303 pp.

Blessent, M., Darwin, D., Lepage, A., Lequesne, R.D., and O'Reilly, M., 2020. “Anchorage of Large High-Strength Reinforcing Bars with Standard Hooks and Heads: Initial Tests,” *SL Report* 20-3, University of Kansas Center for Research, Inc., Lawrence, KS, Feb., 40 pp.

Bournonville, M., Dahnke, J., and Darwin, D., 2004. “Statistical Analysis of the Mechanical Properties and Weight of Reinforcing Bars,” *SL Report* 04-1, The University of Kansas Center for Research, Inc., Lawrence, Kansas, Dec., 194 pp.

Chun, S.-C., 2015, “Lap Splice Tests Using High-Strength Headed Bars of 550 MPa (80 ksi) Yield Strength,” *ACI Structural Journal*, Vol. 112, No. 6, Nov.-Dec., pp. 679-688.

Chun, S.-C., B.-S. Lee. 2019. “Components of Side-Face Blowout Strengths of Headed Bars in Exterior Beam-Column Joints.” *ACI Structural Journal*. Vol. 116, No. 3, Mar., pp 159–170.

Chun, S.-C., Choi C.-S., and Jung H.-S., 2017a. “Side-face blowout failure of large-diameter high-strength headed bars in beam–column joints.” *ACI Structural Journal*. Vol. 114, No. 1, Jan.-Feb., pp 161–172.

Chun, S.-C., Bae M.-S., and Lee B.-S., 2017b. “Side-Face Blowout Strength of 43 and 57 mm (No. 14 and No. 18) Hooked Bars in Beam-Column Joints.” *ACI Structural Journal*. Vol. 114, No. 5, Sep.-Oct., pp 1227–1238.

Chun, S.-C., Oh, B., Lee, S.-H., and Naito, C. J., 2009. “Anchorage Strength and Behavior of Headed Bars in Exterior Beam-Column Joints,” *ACI Structural Journal*, Vol. 120, No. 3, May, pp. 579-590.

Coleman, Z., Jacques, E., and Roberts-Wollmann, C., 2023. “Effect of Beam Depth on Anchorage Strength of Hooked and Headed Bars” *ACI Structural Journal*, Vol. 106, No. 5, Sep.-Oct., pp. 197-206.

DeVries, R. A., 1996. “Anchorage of Headed Reinforcement in Concrete,” *PhD dissertation*, University of Texas at Austin, Dec., 294 pp.

Ghimire, K. P., Shao, Y., Darwin, D., and O’Reilly, M., 2019a. “Conventional and High-Strength Headed Bars – Part 1: Anchorage Tests,” *ACI Structural Journal*, Vol. 116, No. 4, May, pp. 255-264.

Ghimire, K. P., Shao, Y., Darwin, D., and O’Reilly, M., 2019b. “Conventional and High-Strength Headed Bars – Part 2: Data Analysis,” *ACI Structural Journal*, Vol. 116, No. 4, May, pp. 265-272.

Ghimire, K., Darwin, D., and O’Reilly, M., 2018. “Anchorage of Headed Reinforcing Bars in Concrete,” *SM Report* No. 127, University of Kansas Center for Research, Inc., Lawrence, KS, Jan., 278 pp.

Hamad, B. S.; Jirsa, J. O.; and de Paolo, N. I., 1993. “Anchorage Strength of Epoxy-Coated Hooked Bars,” *ACI Structural Journal*, V. 90, No. 2, Mar.-Apr., pp. 210-217.

Joh, O., Goto, Y., and Shibata, T. 1995. “Anchorage of Beam Bars with 90-Degree Bend in Reinforced Concrete Beam-Column Joints,” *ACI Special Publication*, Vol. 157, Oct., pp. 97-116.

Joh, O. and Shibata, T. 1996. "Anchorage of Beam Bars with 90-Degree Bend in Reinforced Concrete Beam-Column Joints," *Eleventh World Conference Earthquake Engineering*, No. 1196, Elsevier Science Ltd., 8 pp.

Kang, T. H.-K., Ha, S.-S., and Choi, D.-U., 2010. "Bar Pullout Tests and Seismic Tests of Small-Headed Bars in Beam-Column Joints," *ACI Structural Journal*, Vol. 107, No. 1, Jan.-Feb., pp. 32-42.

Lee, J., and Park, H., 2010. "Bending - Applicability Study of Ultra-Bar (SD 600) and Ultra-Bar for Rebar Stirrups and Ties (SD 500 and 600) for Compression Rebar," [Translated from Korean] Korea Concrete Institute, Aug., 504 pp.

Marques, J. L., and Jirsa, J. O., 1975. "A Study of Hooked Bar Anchorages in Beam-Column Joints," *ACI Journal, Proceedings* Vol. 72, No. 5, May-Jun., pp. 198-209.

Nazzal, L. A., Darwin, D., and O'Reilly, M., 2023. "Anchorage of High-Strength Reinforcing Bars in Concrete," *SM Report No. 150*, University of Kansas Center for Research, Inc., Lawrence, KS, Jan., 300 pp.

Peckover, J. and Darwin, D., 2013. "Anchorage of High-Strength Reinforcing Bars with Standard Hooks: Initial Tests," *SL Report 13-1*, The University of Kansas Center for Research, Inc., Lawrence, Kansas, Jan., 55 pp.

Pinc, R. L., Watkins, M. D., and Jirsa, J. O., 1977. "The Strength of Hooked Bar Anchorages in Beam-Column Joints," *CESRL Report No. 77-3*, Department of Civil Engineering-Structures Research Laboratory, University of Texas, Austin, Texas, 67 pp.

Ramirez, J. and Russell, B. 2008. "Transfer, Development, and Splice Length for Standard/Reinforcement in High-strength Concrete," Washington, D.C.: Transportation Research Board, National Research Council, pp. 99-120.

Searle, N., DeRubeis, M., Darwin, D., Matamoros, A. B., O'Reilly, M., and Feldman, L., 2014. "Anchorage of High-Strength Reinforcing Bars with Standard Hooks - Initial Tests," *SM Report No. 108*, University of Kansas Center for Research, Inc., Lawrence, KS, Feb., 120 pp.

Shao, Y., Darwin, D., O'Reilly, M., Lequesne, R.D., Ghimire, K., Hano, Muna, 2016. "Anchorage of Conventional and High-Strength Headed Reinforcing Bars," *SM Report No. 117*, University of Kansas Center for Research, Inc., Lawrence, KS, Aug., 234 pp.

Sim, H.-J., and Chun, S.-C. 2022a. “Side-Face Blowout Strength of Two-Layer Headed Bars Embedded in Exterior Beam-Column Joints.” *ACI Structural Journal*. Vol. 119, No. 2, Mar., pp 221–231.

Sim, H.-J., and Chun, S.-C. 2022b. “Side-Face Blowout Failure of Headed Bars in High-Strength Concrete.” *ACI Structural Journal*. Vol. 119, No. 5, Sep., pp 221–231.

Sperry, J., Darwin, D., O'Reilly, M., Lequesne, R. D., Yasso, S., Matamoros, A., Feldman, L. R., and Lepage, A., 2017b. “Conventional and High-Strength Hooked Bars - Part 2: Data Analysis,” *ACI Structural Journal*, Vol. 114, No. 1, Jan.-Feb., pp. 267-314.

Sperry, J., Al-Yasso, S., Searle, N., DeRubeis, M., Darwin, D., O'Reilly, M., Matamoros, A. B., Feldman, L., Lepage, A., Lequesne, R., and Ajaam, A., 2015a. “Anchorage of High-Strength Reinforcing Bars with Standard Hooks,” *SM Report No. 111*, University of Kansas Center for Research, Inc., Lawrence, KS, June, 266 pp.

Sperry, J., Darwin, D., O'Reilly, M., Lepage, A., Lequesne, R., Matamoros, A., Feldman, L., Yasso, S., Searle, N., DeRubeis, M., and Ajaam, A., 2018. “Conventional and High-Strength Hooked Bars: Detailing Effects,” *ACI Structural Journal*, Vol. 115, No. 1, Jan.-Feb., pp. 247-257.

Sperry, J., Darwin, D., O'Reilly, M., and Lequesne, R., 2015b. “Anchorage Strength of Conventional and High-Strength Hooked Bars in Concrete,” *SM Report No. 115*, University of Kansas Center for Research, Inc., Lawrence, KS, Dec., 281 pp.

Sperry, J., Yasso, S., Searle, N., DeRubies, M., Darwin, D., O'Reilly, M., Matamoros, A., Feldman, L.R., Lepage, A., Lequesne, R.D., and Ajaam, A., 2017a. “Conventional and High-Strength Hooked Bars - Part 1: Anchorage Tests,” *ACI Structural Journal*, Vol. 114, No. 1, Jan.-Feb., pp. 255-342.

Thompson, M. K., Jirsa, J. O., and Breen, J. E., 2006a. “CCT Nodes Anchored by Headed Bars-Part 2: Capacity of Nodes,” *ACI Structural Journal*, Vol. 103, No. 1, Jan.-Feb., pp. 65-73.

Thompson, M. K., Ledesma, A., Jirsa, J. O., and Breen, J. E., 2006b. “Lap Splices Anchored by Headed Bars,” *ACI Structural Journal*, Vol. 103, No. 2, Mar.-Apr., pp. 271-279.

Thompson, M. K., Ziehl, M. J., Jirsa, J. O., and Breen, J. E., 2005. “CCT Nodes Anchored by Headed Bars-Part 1: Behavior of Nodes,” *ACI Structural Journal*, Vol. 102, No. 6, Nov.-Dec., pp. 808-815.

Wright, J. L., and McCabe, S. L., 1997. “The Development Length and Anchorage Behavior of Headed Reinforcing Bars,” *SM Report* No. 44, University of Kansas Center for Research, Inc., Lawrence, Kansas, Sep., 147 pp.

Yasso, S., Darwin, D., and O'Reilly, M., 2017. “Anchorage Strength of Standard Hooked Bars in Simulated Exterior Beam-Column Joints,” *SM Report* No. 124, University of Kansas Center for Research, Inc., Lawrence, KS, Apr., 330 pp.

Yasso, S., Darwin, D., and O'Reilly, M. O., 2021 “Effects of Concrete Tail Cover and Tail Kickout on Anchorage Strength of 90-Degree Hooks,” *ACI Structural Journal*, Vol. 118, No. 6, Nov., pp. 227-236.

APPENDIX A: NOTATION

a	Depth of equivalent rectangular compressive stress block, in.
A_b	Cross-sectional area of an individual hooked or headed bar, in. ²
A_{brg}	Net bearing area of the head calculated as the gross head area minus maximum area of the obstruction adjacent to the head; net bearing area of the head calculated as gross head area minus bar area if no obstruction is present or the obstruction, in. ²
A_{hs}	Total cross-sectional area of hooked or headed bars being developed (nA_b), in. ²
A_{tp}	Cross-sectional area of a single leg of parallel ties within the joint region for headed bars, in. ²
A_{tr}	Cross-sectional area of a single leg of confining reinforcement within the joint region for hooked bars, in. ²
A_{th}	Total cross-sectional area of effective confining reinforcement ($n_{tl}A_{tr}$) for hooked bars being developed within $8d_b$ from top of the hooked bars for No. 3 through No. 8 bars or within $10d_b$ for No. 9 bars and larger, in. ²
$A_{th,ACI}$	Total cross-sectional area of effective confining reinforcement for hooked bars being developed within $15d_b$ from centerline of hooked bars, per ACI 318-19, in. ²
A_{tt}	Total cross-sectional area of effective parallel ties ($n_{tl}A_{tp}$) for headed bars being developed within $8d_b$ from top of the headed bars for No. 3 through No. 8 bars or within $10d_b$ for No. 9 bars and larger, in. ²
$A_{tt,ACI}$	Total cross-sectional area of effective parallel ties for headed bars being developed within $8d_b$ from centerline of headed bars, per ACI 318-19, in. ²
b	Width of column, in.
b_{BP}	Width of the bearing plate, in.
c	Depth of neutral axis from the extreme compression fiber, in.
c_{bc}	Clear cover from the back of the head to the back of the column, in.
c_{bh}	Clear cover from the back of the hook to the back of the column, in.
c_o	Clear side cover to the head, in.
c_{so}	Clear side cover to the hooked or headed bar, in.
d	Distance from the centroid of the tension bar to the extreme compression fiber of the beam, in.
d_b	Nominal diameter of bar, in.
d_{eff}	Effective depth of the simulated beam, in.
d_{to}	Nominal diameter of ties outside the joint region, in.
d_{tp}	Nominal diameter of parallel ties within the joint region for headed bars, in.
d_{tr}	Nominal diameter of confining reinforcement within the joint region for hooked bars, in.
f'_c	Specified or target concrete compressive strength, psi
f_{cm}	Measured concrete compressive strength, psi

f_s, f_{su}	Stress in the hooked or headed bar at failure, ksi
$f_{s,ACI}$	Calculated stress in the hooked or headed bar per ACI 318-19, ksi
$f_{s,max}$	Maximum stress in individual hooked or headed bar, ksi
$f_{s,calc}$	Calculated stress in the hooked or headed bar, ksi
f_y	Measured yield strength of the hooked or headed bar, ksi
h	Depth of column, in.
h_o	Total height of column, in.
h_{cl}	Distance between the center of hooked or headed bar to the top of the bearing plate or bearing member in the joint region, in.
K_{tr}	Confining reinforcement index per ACI 318-19
ℓ_{dh}	Development length in tension of deformed bar or deformed wire with a standard hook, measured from outside end of hook, point of tangency, toward critical section, in.
ℓ_{dt}	Development length in tension of headed deformed bar, measured from the critical section to the bearing face of the head, in.
ℓ_{eh}	Embedment length measured from the bearing face of the head to the front face of the specimen for headed bars and embedment length of a standard hook measured from the outside of the hook to the front face of the specimen for hooked bars, in.
$\ell_{eh,avg}$	Average embedment length of hooked or headed bars, in.
n	Number of hooked or headed bars loaded simultaneously in tension, in.
n_{tl}	Number of tie legs within $10d_b$ from top of hooked or headed bars
n_{tp}	Number of parallel ties (single, double overlapping, or double) within $10d_b$ from top of headed bars
n_{tr}	Number of single confining reinforcement ties within $10d_b$ from top of hooked bars
N_{tp}	Number of parallel ties (single, double overlapping, or double) within the joint region for headed bars
N_{tr}	Number of single confining reinforcement ties within the joint region for hooked bars
s	Center-to-center spacing of hooked or headed bars (previously c_{ch}), in.
T	Average load on a hooked or headed bar at failure, pounds, kips
T_c	Anchorage strength of a hooked or headed bar without confining reinforcement ties; contribution of concrete to anchorage strength of a hooked or headed bar, pounds, kips
T_h	Anchorage strength of a hooked or headed bar using descriptive equations, pounds, kips
T_{ind}	Peak load on individual hooked or headed bar at failure, kips
T_{max}	Maximum load on individual hooked or headed bar, kips
T_s	Contribution of steel confining reinforcement ties to anchorage strength of a hooked or headed bar, pounds, kips
T_{total}	Sum of loads on hooked or headed bars at failure, kips
V_J	Shear force in the joint, kips
w/c	Water-to-cement ratio by weight

x_{bot}	Height measured from the center of the test bar to the center of the lower tension member, in.
x_{mid}	Height measured from the center of the test bar to the center of the bearing member in the joint, in.
x_{top}	Height measured from the center of the test bar to the center of the upper bearing member, in.
β_1	Factor relating depth of equivalent rectangular compressive stress block to neutral axis depth
Δ_{ind}	Measured displacement of individual hooked or headed bar at failure, relative to the front face of the column, in.
Δ_{max}	Maximum displacement of individual hooked or headed bar relative to the front face of the column, in.
ϕ	Strength-reduction factor
ψ_c	Factor used to modify development length based on concrete compressive strength
ψ_{cr}	Factor used to modify development length based on confining reinforcement for hooked bars
ψ_e	Factor used to modify development length based on reinforcement coating
ψ_o	Factor used to modify development length based on bar location within member
ψ_p	Factor used to modify development length based on parallel ties and bar spacing for headed bars
ψ_{p1}	Factor used to modify development length based on bar spacing for headed bars without parallel ties
ψ_{p2}	Factor used to modify development length based on bar spacing and parallel ties for headed bars with parallel ties
ψ_{pr}	Factor used to modify development length based on parallel ties for headed bars
ψ_r	Factor used to modify development length based on confining reinforcement and bar spacing for hooked bars
ψ_{r1}	Factor used to modify development length based on bar spacing for hooked bars without confining reinforcement
ψ_{r2}	Factor used to modify development length based on bar spacing and confining reinforcement for hooked bars with confining reinforcement
θ	Compression strut angle, degrees
λ	Modification factor to reflect the reduced mechanical properties of lightweight concrete relative to normalweight concrete of the same compressive strength

Acronym list

ACI	American Concrete Institute
ASTM	American Society of Testing and Materials - International
BSG	Bulk Specific Gravity (Oven Dry)
BSG (SSD)	Bulk Specific Gravity (Saturated Surface Dry)
CCT	Compression-Compression-Tension
CoV	Coefficient of Variation
HA	Class of head satisfying head dimension requirements detailed in ASTM A970
L. C.	Loading Condition as described in Section 2.3.1
MAX	Maximum
MIN	Minimum
SG	Specific Gravity
SN	Specimen Number
SSD	Saturated Surface Dry
STDEV	Standard Deviation

Failure Types

CB	Concrete breakout
SS	Side splitting
SF	Shear failure

APPENDIX B: HOOKED BAR BEAM-COLUMN JOINT SPECIMENS

Appendix B presents the details of the hooked bar specimens. Appendix B1 presents specimen drawings and reinforcement layouts for No. 14 and No. 18 bars tested in this study. Appendix B2 presents detailed properties and test results for the No. 14 and No. 18 bar specimens of this study. Appendix B3 presents specimens tested at the University of Kansas, including those used to develop descriptive equations, Eq. (4.5) and (4.7). The specimens include No. 5, No. 8, and No. 11 bar specimens by Searle et al. (2014), Sperry et al. (2015a, 2015b, 2017a, 2017b, 2018), Yasso et al. (2017), Ajaam et al. (2017, 2018), and No. 14 and No. 18 bars tested in this study. Appendix B4 presents the specimens tested outside the University of Kansas, a few of which were used to develop descriptive equations, including those by Marques and Jirsa (1975), Pinc et al (1977), Hamad et al. (1993), Ramirez and Russel (2008), Lee and Park (2010), and Chun et al. (2017b). In each section, specimens not used to develop descriptive equations are identified.

B.1 DRAWINGS AND REINFORCEMENT LAYOUTS FOR NO. 14 AND NO. 18 BAR SPECIMENS TESTED IN CURRENT STUDY

This section presents elevation and cross-sectional drawings of the No. 14 and No. 18 bar specimens tested in this study, showing the details of the reinforcement layouts. In the cross-sectional drawings, confining reinforcement is omitted for clarity.

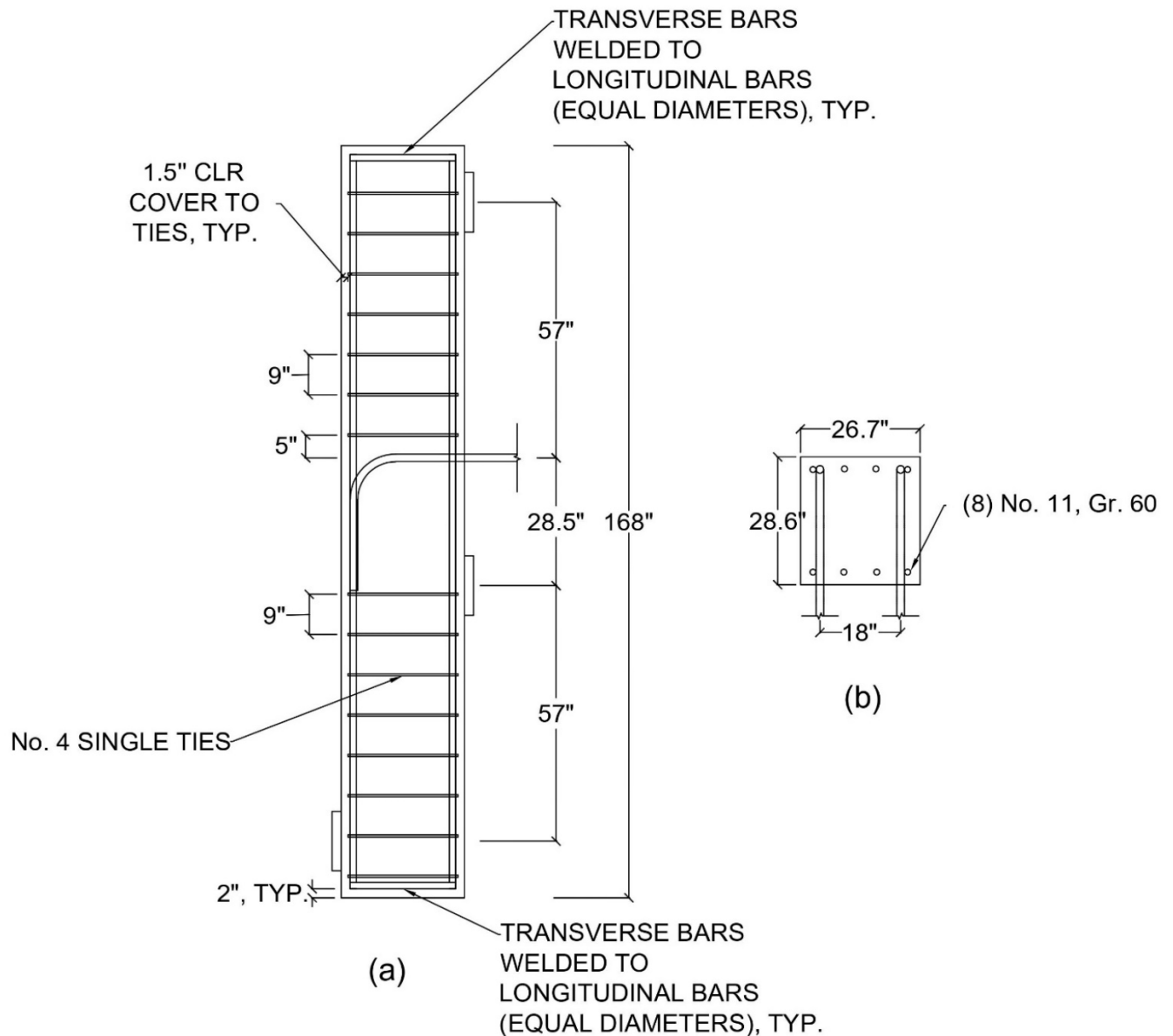


Figure B.1 Details of reinforcement layout for No. 14 hooked bar specimen H14-1: (a) elevation, (b) cross-section

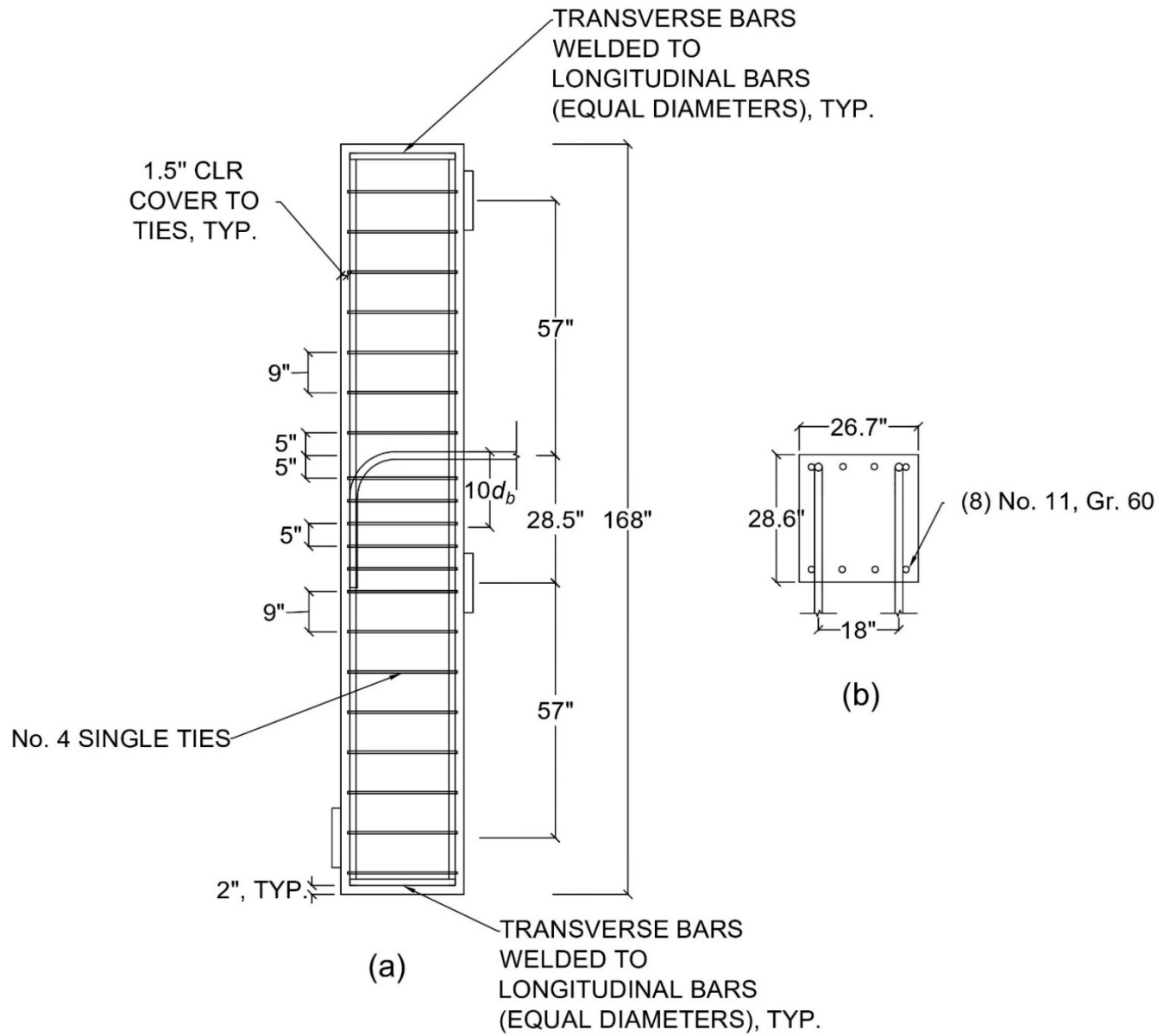


Figure B.2 Details of reinforcement layout for No. 14 hooked bar specimen H14-2: (a) elevation, (b) cross-section

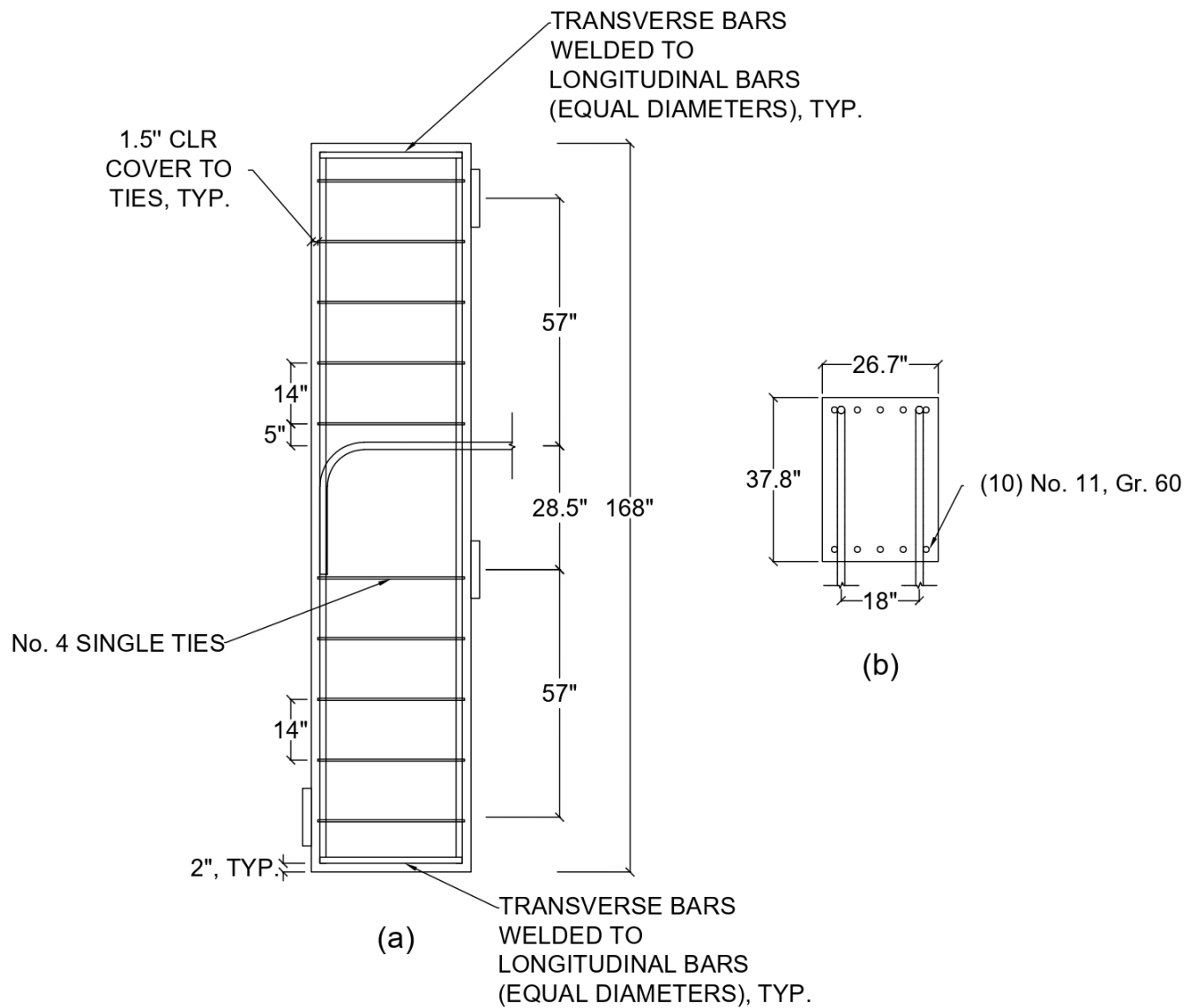


Figure B.3 Details of reinforcement layout for No. 14 hooked bar specimen H14-3: (a) elevation, (b) cross-section

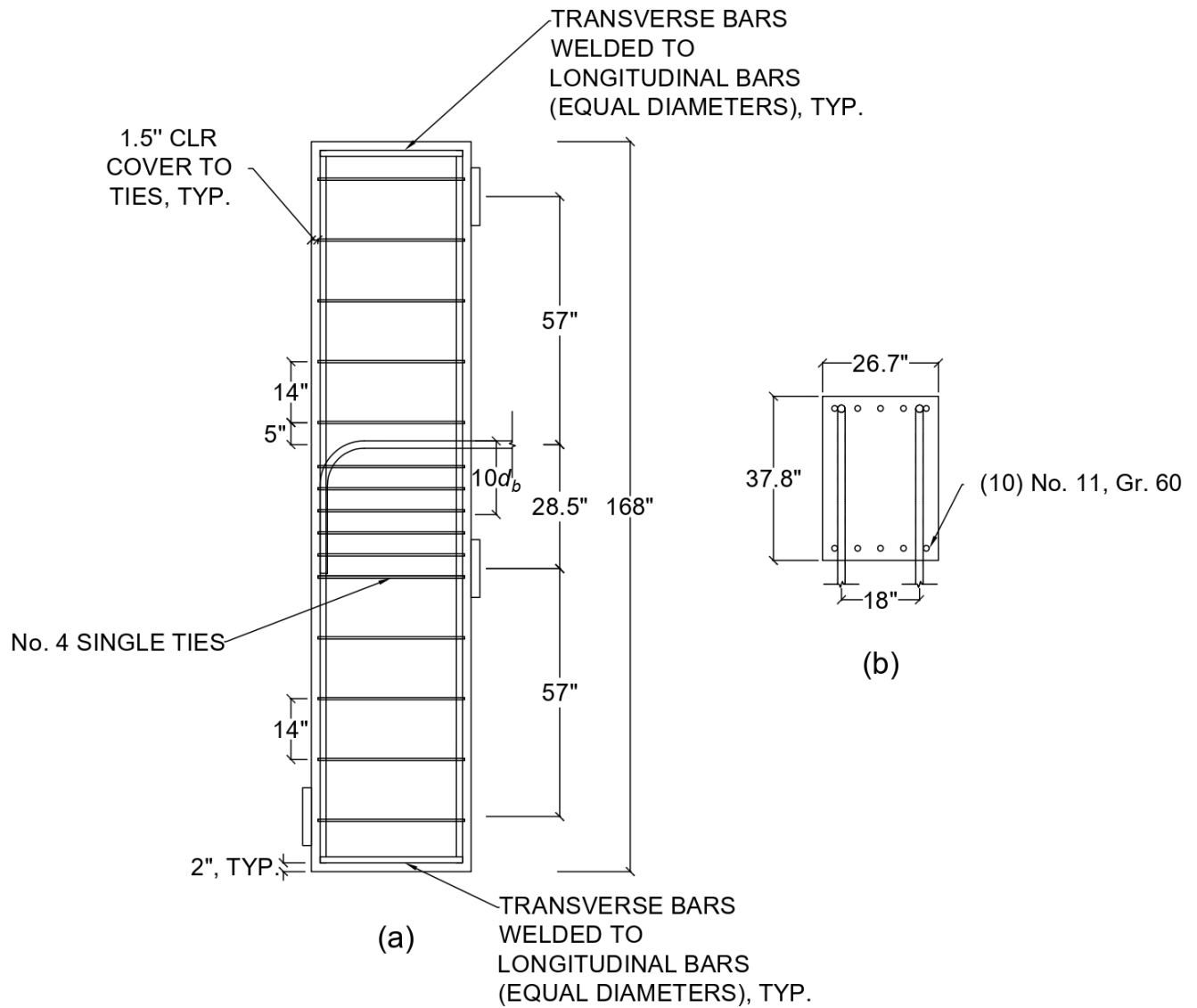


Figure B.4 Details of reinforcement layout for No. 14 hooked bar specimen H14-3: (a) elevation, (b) cross-section

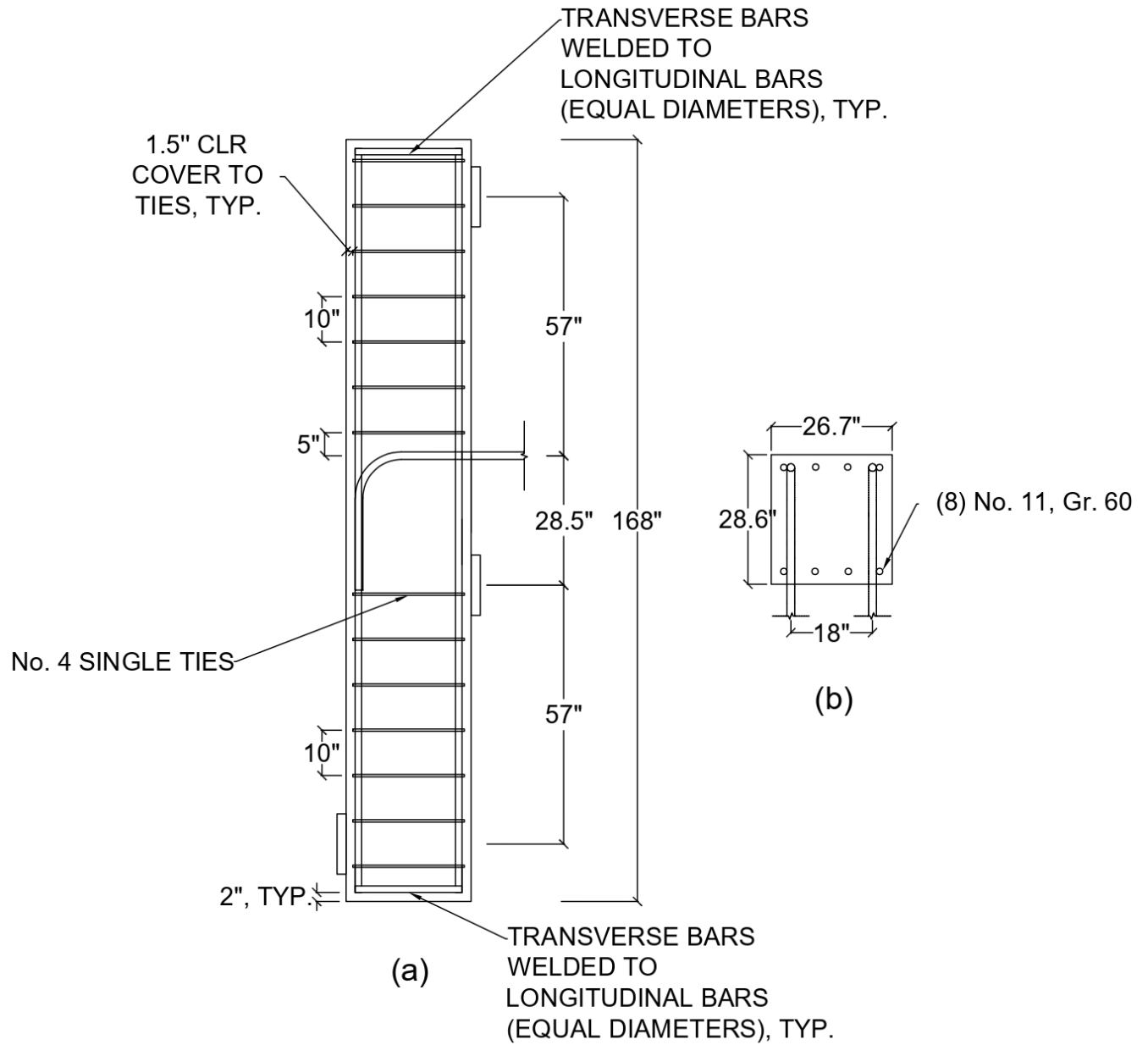


Figure B.5 Details of reinforcement layout for No. 14 hooked bar specimen H14-15: (a) elevation, (b) cross-section

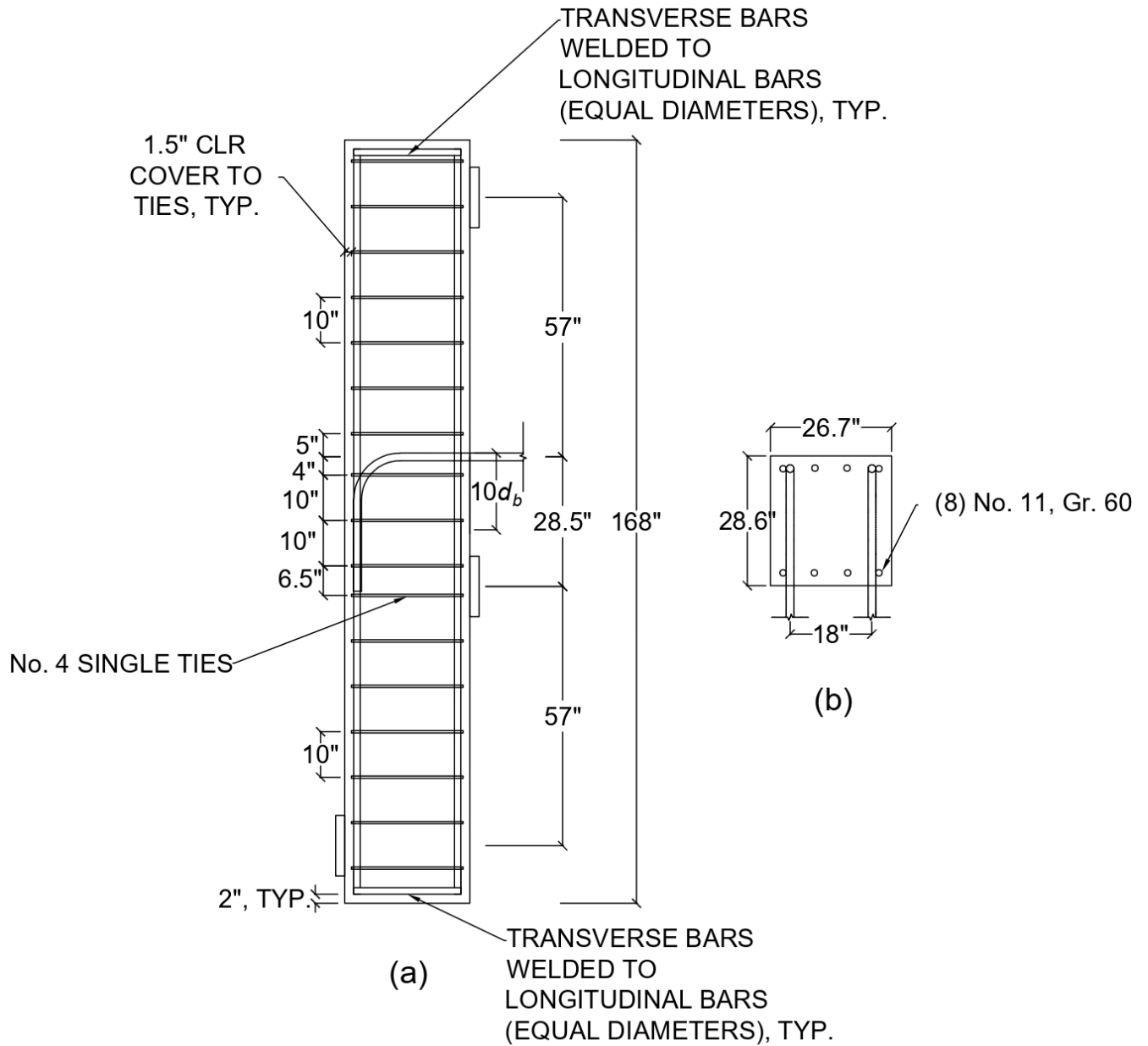


Figure B.6 Details of reinforcement layout for No. 14 hooked bar specimen H14-16: (a) elevation, (b) cross-section

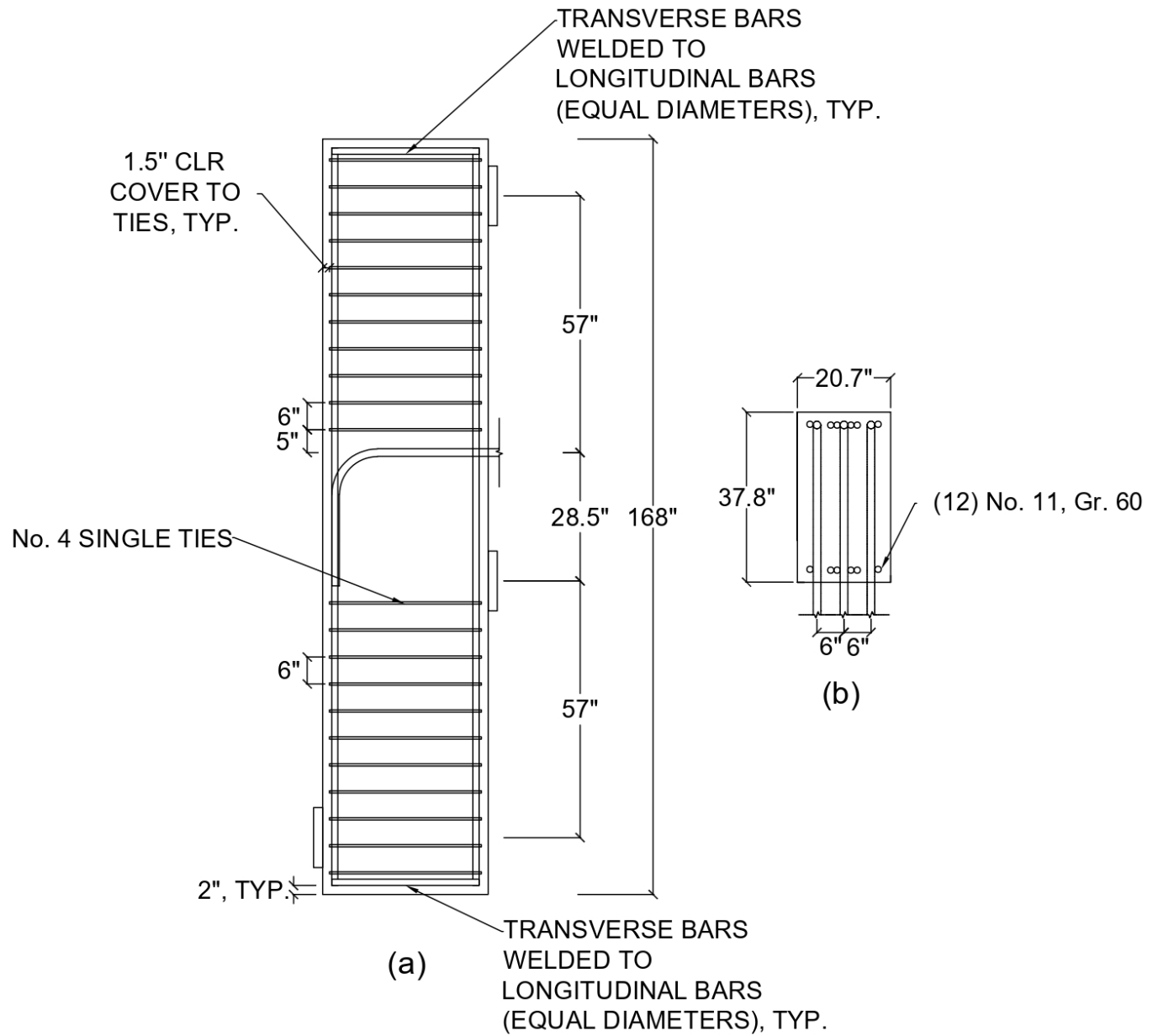


Figure B.7 Details of reinforcement layout for No. 14 hooked bar specimen H14-7: (a) elevation, (b) cross-section

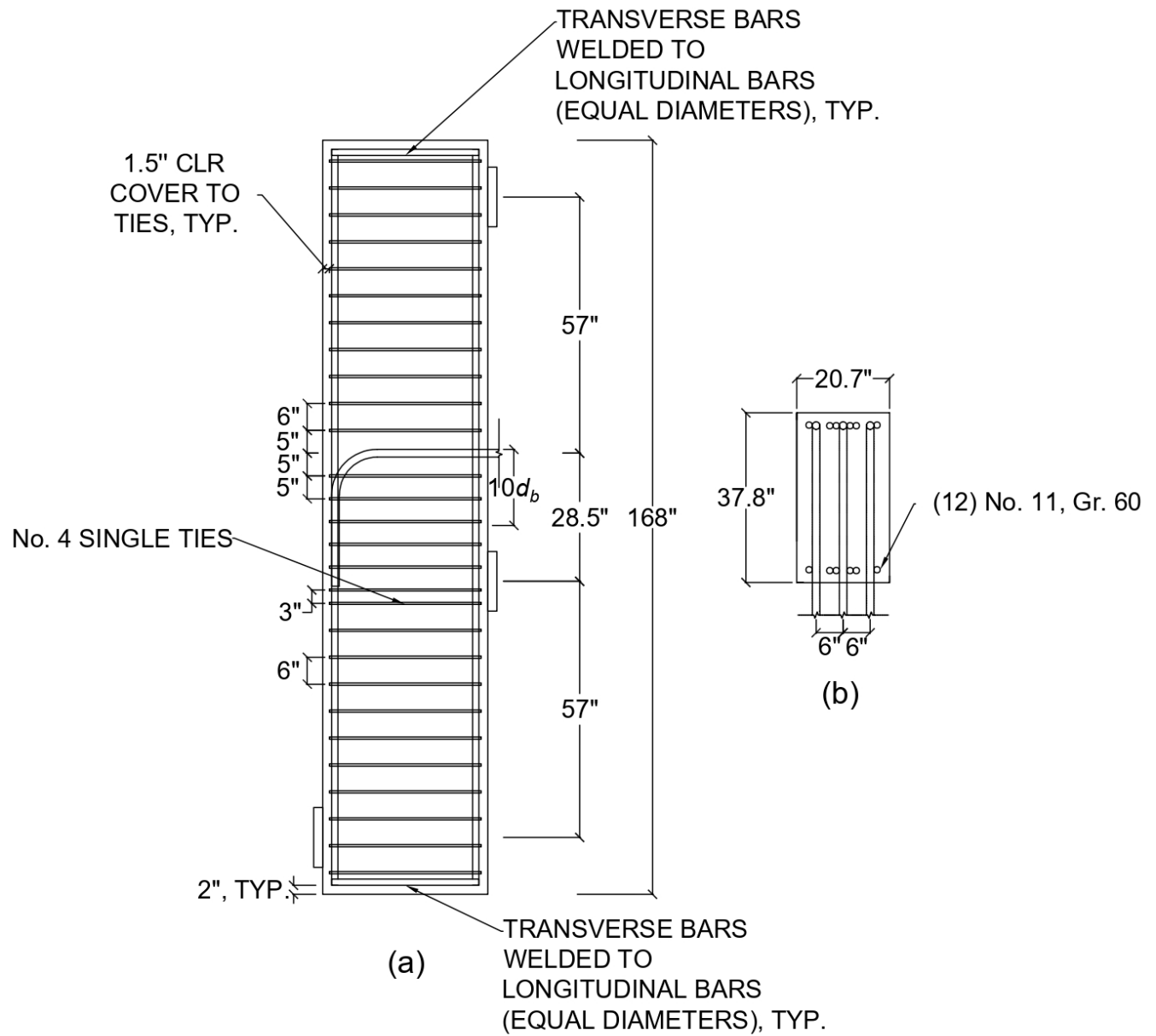


Figure B.8 Details of reinforcement layout for No. 14 hooked bar specimen H14-8: (a) elevation, (b) cross-section

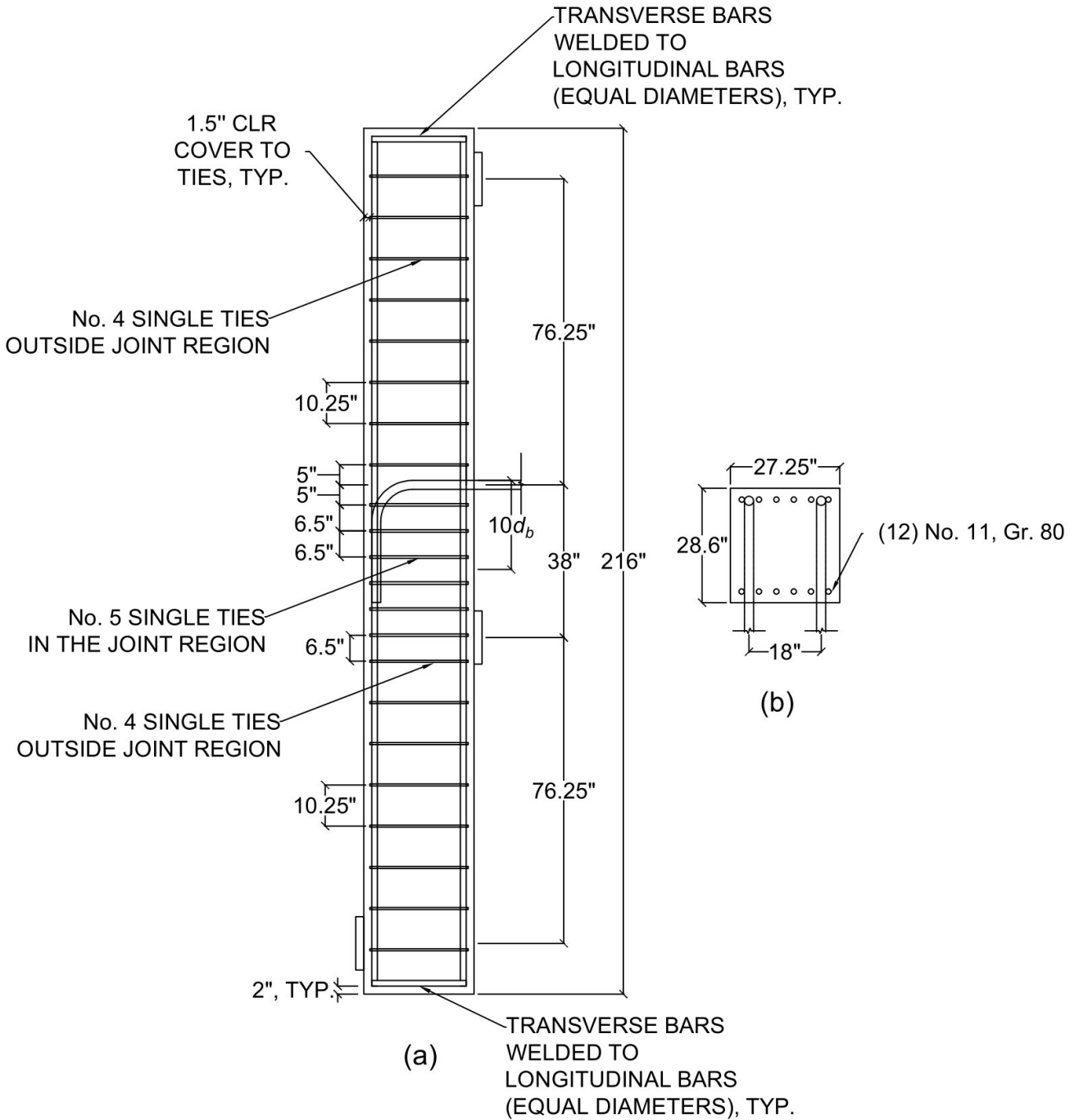


Figure B.9 Details of reinforcement layout for No. 18 hooked bar specimen H18-1: (a) elevation, (b) cross-section

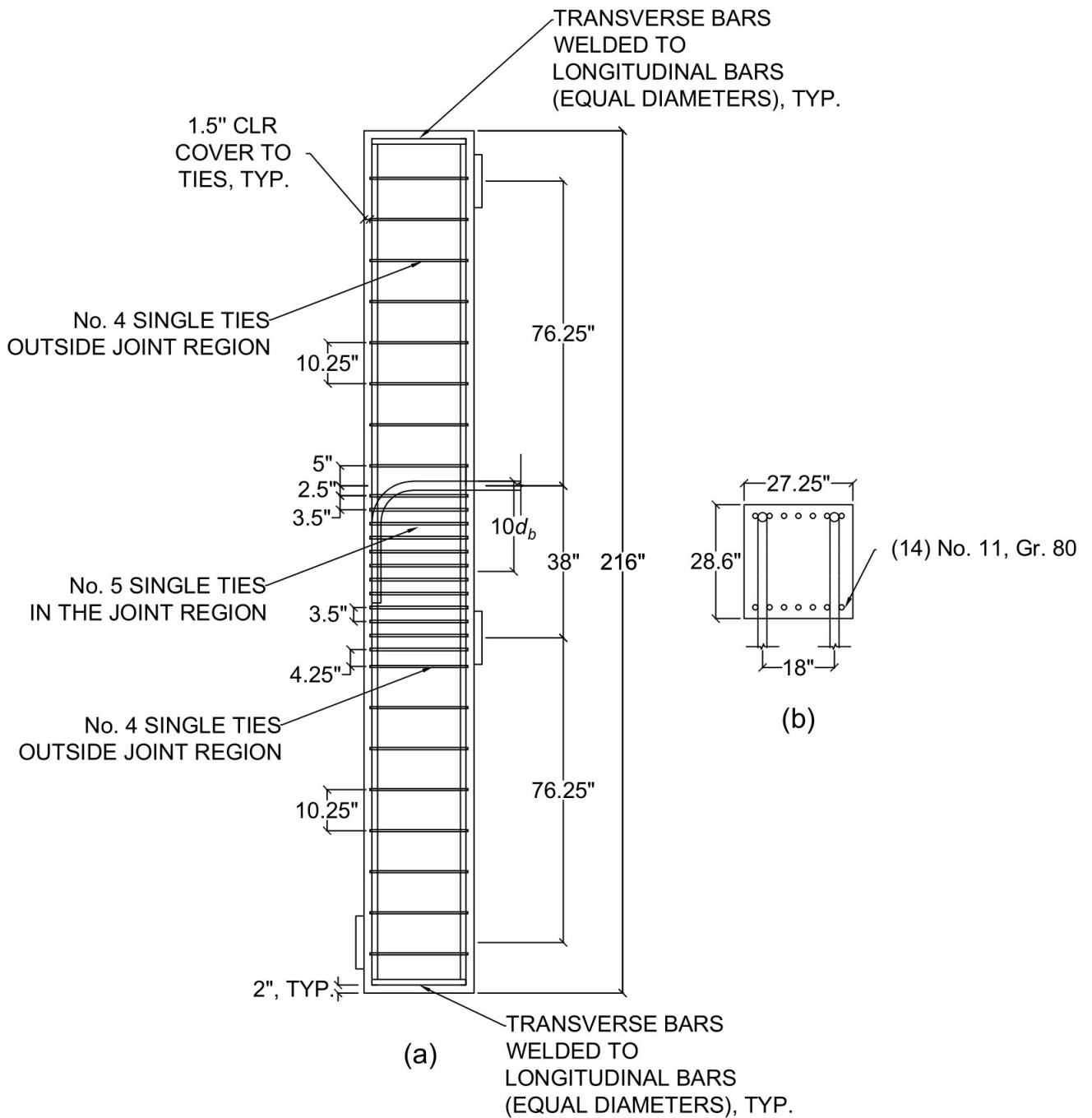


Figure B.10 Details of reinforcement layout for No. 18 hooked bar specimen H18-2: (a) elevation, (b) cross-section

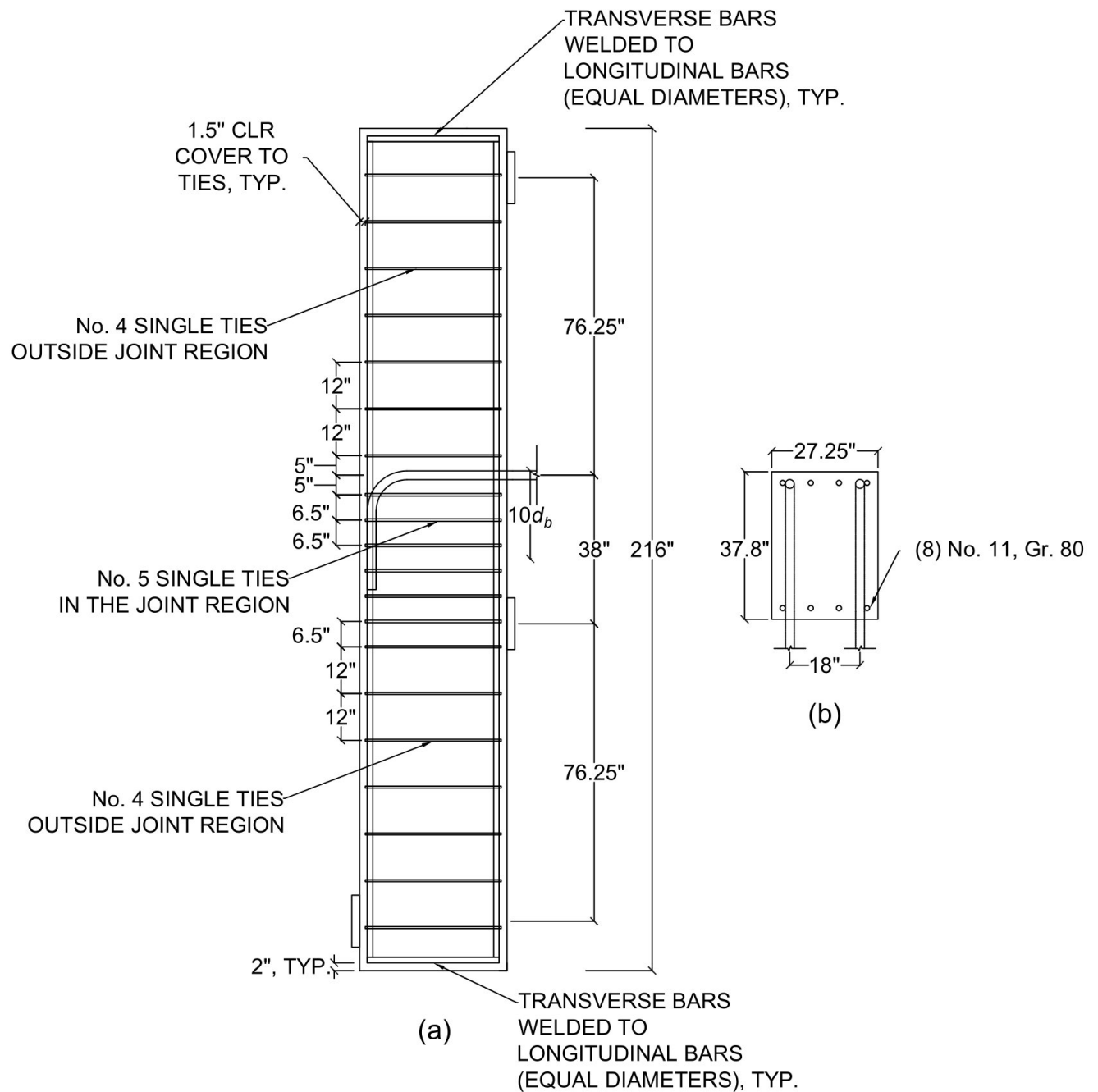


Figure B.11 Details of reinforcement layout for No. 18 hooked bar specimen H18-3: (a) elevation, (b) cross-section

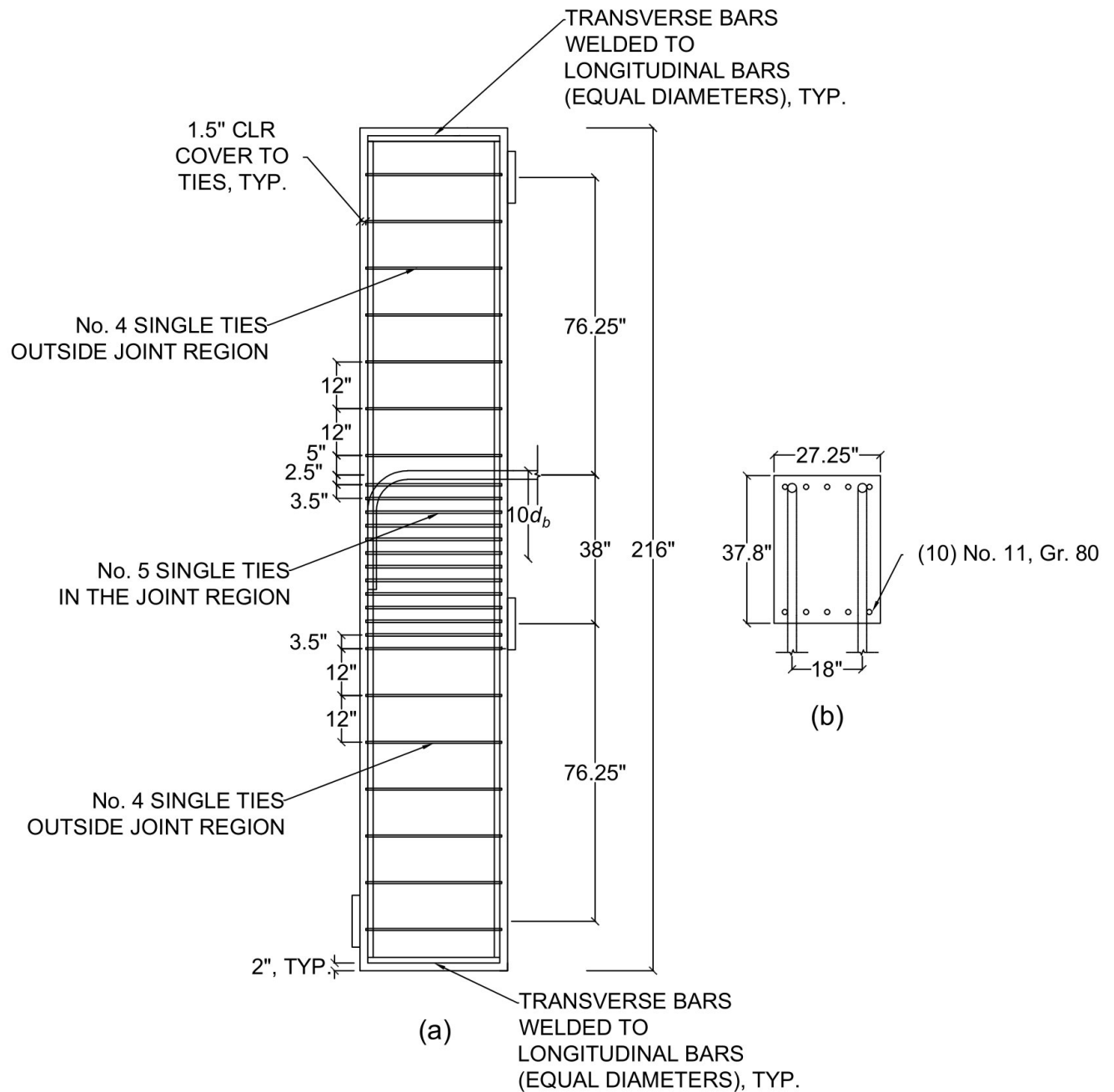


Figure B.12 Details of reinforcement layout for No. 18 hooked bar specimen H18-4: (a) elevation, (b) cross-section

B.2 DETAILED PROPERTIES AND TEST RESULTS FOR NO. 14 AND NO. 18 BAR SPECIMENS TESTED IN CURRENT STUDY

Table B.1 Detailed properties and test results for No. 14 and No. 18 bar specimens tested in current study

ID	Designation	<i>n</i>	Hook	ℓ_{eh}	$\ell_{eh,avg}$	f_{cm}	Age	d_b	A_b
				in.	in.	psi	Days	in.	in. ²
H14-1	(2@10.6)14-15-i-3.5-2-26.6	2	A	27.3	27.0	12,980	77	1.693	2.25
			B	26.8					
H14-2	(2@10.6)14-15-5#4-i-3.5-2-26.6	2	A	24.5	24.8	13,010	88	1.693	2.25
			B	25.0					
H14-3	(2@10.6)14-15-i-3.5-2-35.8	2	A	36.8	36.7	8,100	49	1.693	2.25
			B	36.6					
H14-4	(2@10.6)14-15-5#4-i-3.5-2-35.8	2	A	34.9	34.9	7,570	53	1.693	2.25
			B	35.0					
H14-15	(2@10.6)14-7-i-3.5-2-26.6	2	A	26.5	26.5	6,980	38	1.693	2.25
			B	26.3					
H14-16	(2@10.6)14-7-3#4-i-3.5-2-26.6	2	A	26.0	25.9	6,810	44	1.693	2.25
			B	25.8					
H14-7	(3@3.5)14-6-i-3.5-2-35.8	3	A	36.5	36.4	6,390	27	1.693	2.25
			B	36.5					
			C	36.3					
H14-8	(3@3.5)14-6-5#4-i-3.5-2-35.8	3	A	36.3	36.6	6,650	33	1.693	2.25
			B	37.5					
			C	36.0					
H18-1	(2@8.0)18-16-6#5-i-3.5-2-26.6	2	A	28.5	28.5	15,310	41	2.257	4.00
			B	28.5					
H18-2	(2@8.0)18-16-12#5-i-3.5-2-26.6	2	A	28.5	27.0	15,770	46	2.257	4.00
			B	25.5					
H18-3	(2@8.0)18-7-6#5-i-3.5-2-35.8	2	A	36.5	36.5	7,560	85	2.257	4.00
			B	36.5					
H18-4	(2@8.0)18-7-12#5-i-3.5-2-35.8	2	A	36.4	36.4	7,610	113	2.257	4.00
			B	36.4					

Table B.1 Cont. Detailed properties and test results for No. 14 and No. 18 bar specimens tested in current study

ID	b	h	h_{cl}	b_{BP}	d_{eff}	d_{eff}/ℓ_{eh}	θ	c_{so}	c_{bh}	s	s/d_b	Bar spacing
	in.	in.	in.	in.	in.		°	in.	in.	in.		
H14-1	26.7	28.6	25.5	6	28.05	1.04	46.6	3.5	2.0	18	10.6	Wide
H14-2	26.7	28.6	25.5	6	28.60	1.15	49.0	3.5	2.0	18	10.6	Wide
H14-3	26.7	37.8	25.5	6	30.21	0.82	37.9	3.5	2.0	18	10.6	Wide
H14-4	26.7	37.8	25.5	6	30.19	0.87	39.3	3.5	2.0	18	10.6	Wide
H14-15	26.7	28.6	25.5	6	29.08	1.10	47.1	3.5	2.0	18	10.6	Wide
H14-16	26.7	28.6	25.5	6	29.83	1.15	47.8	3.5	2.0	18	10.6	Wide
H14-7	20.7	37.8	24.0	9	33.20	0.91	38.1	3.5	2.0	6	3.5	Close
H14-8	20.7	37.8	24.0	9	34.70	0.95	37.9	3.5	2.0	6	3.5	Close
H18-1	27.25	28.6	35.2	6	38.26	1.34	53.2	3.5	2.0	18	8.0	Wide
H18-2	27.25	28.6	35.2	6	38.90	1.44	54.7	3.5	2.0	18	8.0	Wide
H18-3	27.25	37.8	33.7	9	39.96	1.09	46.3	3.5	2.0	18	8.0	Wide
H18-4	27.25	37.8	33.7	9	40.90	1.12	46.3	3.5	2.0	18	8.0	Wide

Table B.1 Cont. Detailed properties and test results for No. 14 and No. 18 bar specimens tested in current study

ID	d_{to}	N_{tr}	n_{tr}	n_d	d_{tr}	A_{tr}	A_{th}	A_{hs}	A_{tr}/A_{hs}	L. C.
	in.				in.	in. ²	in. ²	in. ²		
H14-1	0.5	0	0	0	0.5	0.2	0	4.50	0	A
H14-2	0.5	5	3	6	0.5	0.2	1.2	4.50	0.267	A
H14-3	0.5	0	0	0	0	0	0	4.50	0	A
H14-4	0.5	5	3	6	0.5	0.2	1.2	4.50	0.267	A
H14-15	0.5	0	0	0	0	0	0	4.50	0	A
H14-16	0.5	3	2	4	0.5	0.2	0.8	4.50	0.178	A
H14-7	0.5	0	0	0	0	0	0	6.75	0	A
H14-8	0.5	5	3	6	0.625	0.31	1.86	6.75	0.276	A
H18-1	0.5	6	3	6	0.625	0.31	1.86	8.00	0.233	A
H18-2	0.5	12	6	12	0.625	0.31	3.72	8.00	0.465	A
H18-3	0.5	6	3	6	0.625	0.31	1.86	8.00	0.233	A
H18-4	0.5	12	6	12	0.625	0.31	3.72	8.00	0.465	A

Table B.1 Cont. Detailed properties and test results for No. 14 and No. 18 bar specimens tested in current study

ID	Δ_{max}	Δ_{ind}	T_{max}	$f_{s,max}$	T_{ind}	T_{total}	T	f_{su}	Failure Type
	in.	in.	kips	ksi	kips	kips	kips	ksi	
H14-1	0.52	0.27	250.1	111.2	244.2	480.0	240.0	106.7	CB
	1.53	0.02	236.3	105.0	235.8				
H14-2	0.41	0.41	296.4	131.8	296.1	587.8	293.9	130.6	CB/SS
	0.02	0.02	292.2	129.9	291.8				
H14-3	0.11	0.02	289.1	128.5	280	558.2	279.1	124.0	CB/SS
	1.39	0.26	278.8	123.9	278.3				
H14-4*	0.72	0.13	259.7	115.4	259.3	537.0	268.5	119.3	SS
	0.95	0.02	277.7	123.4	246.2				
H14-15*	0.66	0.08	206.0	91.6	181.7	393.0	196.5	87.3	CB
	0.15	0.15	187.1	83.1	186.8				
H14-16*	0.18	0.08	229.5	102.0	229.4	470.6	235.3	104.6	CB
	1.36	0.07	241.0	107.1	203				
H14-7	0.97	0.07	251.7	111.9	251.7	752.4	250.8	111.5	CB
	0.14	0.00	250.4	111.3	250.4				
	1.17	0.28	250.3	111.2	250.3				
H14-8	1.72	0.31	314.6	139.8	297.1	894.6	298.2	132.5	SS
	0.48	0.28	329.5	146.4	301.1				
	1.60	0.12	296.7	131.9	296.4				
H18-1	0.32	0.11	357.6	89.4	356.8	716.4	358.2	89.6	CB
	1.26	0.24	375.9	94.0	359.5				
H18-2	1.61	0.22	444.9	111.2	444.6	890.0	445.0	111.3	SS
	0.67	0.37	445.3	111.3	445.3				
H18-3	0.47	0.35	370.5	92.6	370.5	742.8	371.4	92.9	CB
	0.80	0.36	372.4	93.1	372.4				
H18-4*	0.41	0.37	437.7	109.4	417.2	855.8	427.9	107.0	CB
	0.46	0.18	418.6	104.7	418.1				

* Bars failed independently, so T is the average of the maximum force on individual bar

B.3 SPECIMENS TESTED AT THE UNIVERSITY OF KANSAS

This section presents the specimens tested at the University of Kansas, including No. 5, No. 8, and No. 11 bar specimens tested by Searle et al. (2014), Sperry et al. (2015a, 2015b, 2017a, 2017b, 2018), Yasso et al. (2017), Ajaam et al. (2017, 2018), and No. 14 and No. 18 bar specimens tested in this study. Specimens are tabulated in six categories: widely-spaced bars without confining reinforcement (Table B2), closely-spaced bars without confining reinforcement (Table B3), widely-spaced bars with confining reinforcement (Table B4), closely-spaced bars with confining reinforcement (Table B5), specimens with bars outside column core (Table B6), and specimens with $d_{eff}/\ell_{eh} > 1.5$ (Table B7). In each category, specimens not used to develop descriptive equations, Eq. (4.5) and (4.7), are identified, if any.

Table B.2 Detailed properties and test results for hooked bar specimens having widely-spaced bars without confining reinforcement tested at the University of Kansas

SN	ID	b	h	$\ell_{eh,avg}$	f_{cm}	d_b	A_b	s	s/db
		in.	in.	in.	psi	in.	in. ²	in.	
1	5-5-90-0-i-2.5-2-8	13.0	10.1	8.1	4830	0.625	0.31	7.4	11.8
2	5-5-90-0-i-2.5-2-10	12.7	11.4	9.4	5230	0.625	0.31	7.1	11.4
3	5-5-90-0-i-2.5-2-7	13.0	8.9	6.9	5190	0.625	0.31	7.4	11.8
4	5-8-90-0-i-2.5-2-6	12.6	8.8	6.8	8450	0.625	0.31	7.0	11.2
5	5-8-90-0-i-2.5-2-6(1)	13.2	8.3	6.3	9080	0.625	0.31	7.6	12.2
6	5-8-90-0-i-2.5-2-8	12.9	9.8	7.8	8580	0.625	0.31	7.3	11.7
7	5-12-90-0-i-2.5-2-10	12.9	12.5	10.5	10290	0.625	0.31	7.3	11.7
8	5-12-90-0-i-2.5-2-5	12.7	6.9	4.9	11600	0.625	0.31	7.1	11.4
9	5-15-90-0-i-2.5-2-5.5	12.9	7.9	5.9	15800	0.625	0.31	7.3	11.7
10	5-15-90-0-i-2.5-2-7.5	12.9	9.3	7.3	15800	0.625	0.31	7.3	11.7
11	5-5-90-0-i-3.5-2-10	14.7	12.4	10.4	5190	0.625	0.31	7.1	11.4
12	5-5-90-0-i-3.5-2-7	15.2	9.6	7.6	5190	0.625	0.31	7.6	12.2
13	5-8-90-0-i-3.5-2-6	14.9	8.3	6.3	8580	0.625	0.31	7.3	11.7
14	5-8-90-0-i-3.5-2-6(1)	15.1	8.6	6.6	9300	0.625	0.31	7.5	12.0
15	5-8-90-0-i-3.5-2-8	15.4	10.6	8.6	8380	0.625	0.31	7.8	12.5
16	5-12-90-0-i-3.5-2-5	15.2	7.4	5.4	10410	0.625	0.31	7.6	12.2
17	5-8-180-0-i-2.5-2-7	12.5	9.3	7.3	9080	0.625	0.31	6.9	11.0
18	5-8-180-0-i-3.5-2-7	15.4	9.3	7.3	9080	0.625	0.31	7.8	12.5

Table B.2 Cont. Detailed properties and test results for hooked bar specimens having widely-spaced bars without confining reinforcement tested at the University of Kansas

SN	n	A_{th}	A_{hs}	A_{th}/A_{hs}	h_{cl}	x_{mid}	d_{eff}	d_{eff}/ℓ_{eh}	θ
		in. ²	in. ²		in.	in.	in.		°
1	2	0	0.62	0	5.25	9.44	6.75	0.83	49.4
2	2	0	0.62	0	5.25	9.44	6.76	0.72	45.1
3	2	0	0.62	0	5.25	9.44	6.41	0.93	53.8
4	2	0	0.62	0	5.25	9.44	6.25	0.92	54.2
5	2	0	0.62	0	5.25	9.44	5.93	0.94	56.3
6	2	0	0.62	0	5.25	9.44	6.28	0.81	50.4
7	2	0	0.62	0	5.25	9.44	6.38	0.61	41.9
8	2	0	0.62	0	5.25	9.44	5.72	1.17	62.6
9	2	0	0.62	0	5.25	9.44	5.83	0.99	58.0
10	2	0	0.62	0	5.25	9.44	6.00	0.82	52.3
11	2	0	0.62	0	5.25	9.44	6.88	0.66	42.2
12	2	0	0.62	0	5.25	9.44	6.25	0.82	51.2
13	2	0	0.62	0	5.25	9.44	5.97	0.95	56.3
14	2	0	0.62	0	5.25	9.44	5.88	0.89	55.0
15	2	0	0.62	0	5.25	9.44	6.17	0.72	47.7
16	2	0	0.62	0	5.25	9.44	5.76	1.07	60.2
17	2	0	0.62	0	5.25	9.44	6.11	0.84	52.3
18	2	0	0.62	0	5.25	9.44	6.04	0.83	52.3

Table B.2 Cont. Detailed properties and test results for hooked bar specimens having widely-spaced bars without confining reinforcement tested at the University of Kansas

SN	T	T_h ^[1]	T/T_h	f_{su}	$f_{su}/f_{s,calc}$ ^[2]	$f_{su}/f_{s,calc}$ ^[3]
	lb	lb		ksi		
1	32448	28627	1.13	104.7	1.34	1.34
2	33583	34515	0.97	108.3	1.17	1.17
3	26265	24463	1.07	84.7	1.25	1.25
4	29570	27604	1.07	95.4	1.27	1.27
5	22425	25885	0.87	72.3	1.02	1.02
6	31673	32267	0.98	102.2	1.18	1.18
7	41657	47180	0.88	134.4	1.10	1.10
8	19220	20998	0.92	62.0	1.06	1.06
9	32511	28126	1.16	104.9	1.37	1.37
10	42221	35598	1.19	136.2	1.44	1.44
11	41927	38517	1.09	135.2	1.33	1.33
12	26516	27223	0.97	85.5	1.15	1.15
13	25475	25476	1.00	82.2	1.17	1.17
14	24541	27436	0.89	79.2	1.06	1.06
15	32745	35710	0.92	105.6	1.11	1.11
16	22121	22680	0.98	71.4	1.13	1.13
17	27108	30467	0.89	87.4	1.06	1.06
18	30754	30467	1.01	99.2	1.21	1.21

^[1] Based on descriptive equations, Eq. (4.5) and (4.7)

^[2] Based on design equation, Eq. (6.18), using full expression for ψ_r , Eq. (6.14)

^[3] Based on design equation, Eq. (6.18), using simplified expression for ψ_r , Eq. (6.15)

Table B.2 Cont. Detailed properties and test results for hooked bar specimens having widely-spaced bars without confining reinforcement tested at the University of Kansas

SN	ID	b	h	$\ell_{eh,avg}$	f_{cm}	d_b	A_b	s	s/d_b
		in.	in.	in.	psi	in.	in. ²	in.	
19	8-5-90-0-i-2.5-2-16	16.5	18.4	16.4	4980	1	0.79	10.5	10.5
20	8-5-90-0-i-2.5-2-9.5	16.5	11.6	9.6	5140	1	0.79	10.5	10.5
21	8-5-90-0-i-2.5-2-12.5	16.8	15.3	13.3	5240	1	0.79	10.8	10.8
22	8-5-90-0-i-2.5-2-18	17.5	20.7	18.7	5380	1	0.79	11.5	11.5
23	8-5-90-0-i-2.5-2-13	16.8	15.4	13.4	5560	1	0.79	10.8	10.8
24	8-5-90-0-i-2.5-2-15(1)	16.6	16.9	14.9	5910	1	0.79	10.6	10.6
25	8-5-90-0-i-2.5-2-15	16.5	16.8	14.8	6210	1	0.79	10.5	10.5
26	8-5-90-0-i-2.5-2-10	17.3	12.0	10.0	5920	1	0.79	11.3	11.3
27	8-8-90-0-i-2.5-2-8	15.6	10.4	8.4	7910	1	0.79	9.6	9.6
28	8-8-90-0-i-2.5-2-10	16.0	11.6	9.6	7700	1	0.79	10.0	10.0
29	8-8-90-0-i-2.5-2-8(1)	16.5	10.0	8.0	8780	1	0.79	10.5	10.5
30	8-8-90-0-i-2.5-2-9	17.0	11.5	9.5	7710	1	0.79	11.0	11.0
31	8-12-90-0-i-2.5-2-9	16.6	11.0	9.0	11160	1	0.79	10.6	10.6
32	8-12-90-0-i-2.5-2-12.5	17.1	14.8	12.8	11850	1	0.79	11.1	11.1
33	8-12-90-0-i-2.5-2-12	16.8	14.1	12.1	11760	1	0.79	10.8	10.8
34	8-15-90-0-i-2.5-2-8.5	17.0	10.8	8.8	15800	1	0.79	11.0	11.0
35	8-15-90-0-i-2.5-2-13	16.9	14.8	12.8	15800	1	0.79	10.9	10.9
36	8-5-90-0-i-3.5-2-18	18.4	20.5	18.5	5380	1	0.79	10.4	10.4
37	8-5-90-0-i-3.5-2-13	18.4	15.4	13.4	5560	1	0.79	10.4	10.4
38	8-5-90-0-i-3.5-2-15(2)	18.5	17.3	15.3	5180	1	0.79	10.5	10.5
39	8-5-90-0-i-3.5-2-15(1)	19.1	17.3	15.3	6440	1	0.79	11.1	11.1
40	8-8-90-0-i-3.5-2-8(1)	18.0	9.8	7.8	7910	1	0.79	10.0	10.0
41	8-8-90-0-i-3.5-2-10	18.0	11.8	9.8	7700	1	0.79	10.0	10.0
42	8-8-90-0-i-3.5-2-8(2)	19.0	10.3	8.3	8780	1	0.79	11.0	11.0
43	8-12-90-0-i-3.5-2-9	18.8	11.0	9.0	11160	1	0.79	10.8	10.8
44	8-8-90-0-i-4-2-8	19.5	9.8	7.8	8740	1	0.79	10.5	10.5
45	8-5-180-0-i-2.5-2-11	16.8	13.0	11.0	4550	1	0.79	10.8	10.8
46	8-5-180-0-i-2.5-2-14	16.8	16.0	14.0	4840	1	0.79	10.8	10.8

Table B.2 Cont. Detailed properties and test results for hooked bar specimens having widely-spaced bars without confining reinforcement tested at the University of Kansas

SN	n	A_{th}	A_{hs}	A_{th}/A_{hs}	h_{cl}	x_{mid}	d_{eff}	d_{eff}/ℓ_{eh}	θ
		in. ²	in. ²		in.	in.	in.		°
19	2	0	1.58	0	10.00	14.19	12.98	0.79	40.9
20	2	0	1.58	0	10.00	14.19	11.56	1.20	55.9
21	2	0	1.58	0	10.00	14.19	12.23	0.92	46.8
22	2	0	1.58	0	10.00	14.19	12.59	0.67	37.2
23	2	0	1.58	0	10.00	14.19	12.14	0.91	46.6
24	2	0	1.58	0	10.00	14.19	12.03	0.81	43.6
25	2	0	1.58	0	10.00	14.19	12.34	0.83	43.8
26	2	0	1.58	0	10.00	14.19	11.45	1.15	54.8
27	2	0	1.58	0	10.00	14.19	11.32	1.35	59.4
28	2	0	1.58	0	10.00	14.19	11.48	1.20	55.9
29	2	0	1.58	0	10.00	14.19	10.92	1.37	60.6
30	2	0	1.58	0	10.00	14.19	10.95	1.15	56.2
31	2	0	1.58	0	10.00	14.19	10.98	1.22	57.6
32	2	0	1.58	0	10.00	14.19	11.2	0.87	47.9
33	2	0	1.58	0	10.00	14.19	11.21	0.93	49.5
34	2	0	1.58	0	10.00	14.19	10.59	1.20	58.2
35	2	0	1.58	0	10.00	14.19	11.06	0.86	47.9
36	2	0	1.58	0	10.00	14.19	12.9	0.70	37.5
37	2	0	1.58	0	10.00	14.19	12.03	0.90	46.6
38	2	0	1.58	0	10.00	14.19	12.72	0.83	42.8
39	2	0	1.58	0	10.00	14.19	11.86	0.77	42.8
40	2	0	1.58	0	10.00	14.19	11.11	1.42	61.2
41	2	0	1.58	0	10.00	14.19	11.42	1.17	55.4
42	2	0	1.58	0	10.00	14.19	10.91	1.31	59.7
43	2	0	1.58	0	10.00	14.19	11.04	1.23	57.6
44	2	0	1.58	0	10.00	14.19	10.8	1.38	61.2
45	2	0	1.58	0	10.00	14.19	11.73	1.07	52.2
46	2	0	1.58	0	10.00	14.19	11.76	0.84	45.4

Table B.2 Cont. Detailed properties and test results for hooked bar specimens having widely-spaced bars without confining reinforcement tested at the University of Kansas

SN	T	T_h ^[1]	T/T_h	f_{su}	$f_{su}/f_{s,calc}$ ^[2]	$f_{su}/f_{s,calc}$ ^[3]
	lb	lb		ksi		
19	83239	77119	1.08	105.4	1.34	1.34
20	44485	43023	1.03	56.3	1.22	1.22
21	65819	62044	1.06	83.3	1.29	1.29
22	80881	91128	0.89	102.4	1.12	1.12
23	65539	63611	1.03	83.0	1.26	1.26
24	63767	72772	0.88	80.7	1.08	1.08
25	75478	73243	1.03	95.5	1.28	1.28
26	47681	46834	1.02	60.4	1.21	1.21
27	45243	41893	1.08	57.3	1.27	1.27
28	51455	48197	1.07	65.1	1.27	1.27
29	36821	40872	0.90	46.6	1.06	1.06
30	35100	47659	0.74	44.4	0.88	0.88
31	49923	49807	1.00	63.2	1.20	1.20
32	66937	74791	0.89	84.7	1.11	1.11
33	65879	70129	0.94	83.4	1.16	1.16
34	43575	53569	0.81	55.2	0.98	0.98
35	78120	81087	0.96	98.9	1.21	1.21
36	95372	90050	1.06	120.7	1.34	1.34
37	68099	63611	1.07	86.2	1.31	1.31
38	87709	72211	1.21	111.0	1.50	1.50
39	70651	76766	0.92	89.4	1.14	1.14
40	43845	38595	1.14	55.5	1.32	1.32
41	55567	49309	1.13	70.3	1.34	1.34
42	42034	42571	0.99	53.2	1.16	1.16
43	60238	49807	1.21	76.3	1.45	1.45
44	37431	39692	0.94	47.4	1.10	1.10
45	46143	48332	0.95	58.4	1.13	1.13
46	49152	64218	0.77	62.2	0.93	0.93

^[1] Based on descriptive equations, Eq. (4.5) and (4.7)

^[2] Based on design equation, Eq. (6.18), using full expression for ψ_r , Eq. (6.14)

^[3] Based on design equation, Eq. (6.18), using simplified expression for ψ_r , Eq. (6.15)

Table B.2 Cont. Detailed properties and test results for hooked bar specimens having widely-spaced bars without confining reinforcement tested at the University of Kansas

SN	ID	b	h	$\ell_{eh,avg}$	f_{cm}	d_b	A_b	s	s/d_b
		in.	in.	in.	psi	in.	in. ²	in.	
47	8-8-180-0-i-2.5-2-11.5	16.5	11.3	9.3	8630	1	0.79	10.5	10.5
48	8-12-180-0-i-2.5-2-12.5	16.6	14.6	12.6	11850	1	0.79	10.6	10.6
49	8-5-180-0-i-3.5-2-11	19.0	13.6	11.6	4550	1	0.79	11.0	11.0
50	8-5-180-0-i-3.5-2-14	18.8	16.1	14.1	4840	1	0.79	10.8	10.8
51	8-15-180-0-i-2.5-2-13.5	17.0	15.6	13.6	16510	1	0.79	11.0	11.0
52	11-5-90-0-i-2.5-2-14	21.1	16.4	14.4	4910	1.41	1.56	14.7	10.4
53	11-5-90-0-i-2.5-2-26	21.1	28.0	26.0	5360	1.41	1.56	14.7	10.4
54	11-5-90-0-i-2.5-2-16	21.7	18.0	16.0	4890	1.41	1.56	15.3	10.9
55	(2@7.5) 11-8-90-0-i-2.5-2-15	17.2	16.8	14.8	7070	1.41	1.56	10.8	7.7
56	(2@7.5) 11-8-90-0-i-2.5-2-18	17.2	19.1	17.1	7070	1.41	1.56	10.8	7.7
57	11-8-90-0-i-2.5-2-17	21.2	19.6	17.6	9460	1.41	1.56	14.8	10.5
58	11-8-90-0-i-2.5-2-21	20.8	22.6	20.6	7870	1.41	1.56	14.4	10.2
59	11-8-90-0-i-2.5-2-17	21.3	19.2	17.2	8520	1.41	1.56	14.9	10.6
60	(2@7.5) 11-12-90-0-i-2.5-2-17	17.4	19.4	17.4	11476	1.41	1.56	11.0	7.8
61	11-12-90-0-i-2.5-2-17	21.1	18.5	16.5	11880	1.41	1.56	14.7	10.4
62	11-12-90-0-i-2.5-2-17.5	21.6	19.7	17.7	13330	1.41	1.56	15.2	10.8
63	11-12-90-0-i-2.5-2-25	20.9	26.6	24.6	13330	1.41	1.56	14.5	10.3
64	11-15-90-0-i-2.5-2-24	21.3	26.4	24.4	16180	1.41	1.56	14.9	10.6
65	11-15-90-0-i-2.5-2-15	20.8	16.0	14.0	14050	1.41	1.56	14.4	10.2
66	11-5-90-0-i-3.5-2-17	22.9	19.9	17.9	5600	1.41	1.56	14.5	10.3
67	11-5-90-0-i-3.5-2-14	23.1	17.0	15.0	4910	1.41	1.56	14.7	10.4
68	11-5-90-0-i-3.5-2-26	23.3	28.0	26.0	5960	1.41	1.56	14.9	10.6
69	11-8-180-0-i-2.5-2-21	20.8	23.1	21.1	7870	1.41	1.56	14.4	10.2
70	11-8-180-0-i-2.5-2-17	21.6	19.9	17.9	8520	1.41	1.56	15.2	10.8
71	11-12-180-0-i-2.5-2-17	21.1	18.6	16.6	11880	1.41	1.56	14.7	10.4
72	H14-1	26.7	28.6	27.0	12980	1.693	2.25	18.0	10.6
73	H14-3	26.7	37.8	36.7	8100	1.693	2.25	18.0	10.6
74	H14-15	26.7	28.6	26.5	6980	1.693	2.25	18.0	10.6

Table B.2 Cont. Detailed properties and test results for hooked bar specimens having widely-spaced bars without confining reinforcement tested at the University of Kansas

SN	n	A_{th}	A_{hs}	A_{th}/A_{hs}	h_{cl}	x_{mid}	d_{eff}	d_{eff}/ℓ_{eh}	θ
		in. ²	in. ²		in.	in.	in.		°
47	2	0	1.58	0	10.00	14.19	11.82	1.27	56.8
48	2	0	1.58	0	10.00	14.19	11.38	0.90	48.4
49	2	0	1.58	0	10.00	14.19	11.96	1.03	50.7
50	2	0	1.58	0	10.00	14.19	12.03	0.85	45.2
51	2	0	1.58	0	10.00	14.19	11.16	0.82	46.2
52	2	0	3.12	0	19.50	23.69	21.38	1.48	58.7
53	2	0	3.12	0	19.50	23.69	23.45	0.90	42.3
54	2	0	3.12	0	19.50	23.69	21.96	1.37	56.0
55	2	0	3.12	0	19.50	23.69	21.59	1.46	58.0
56	2	0	3.12	0	19.50	23.69	22.2	1.30	54.2
57	2	0	3.12	0	19.50	23.69	21.88	1.24	53.4
58	2	0	3.12	0	19.50	23.69	22.24	1.08	49.0
59	2	0	3.12	0	19.50	23.69	21.59	1.26	54.0
60	2	0	3.12	0	19.50	23.69	21.43	1.23	53.7
61	2	0	3.12	0	19.50	23.69	21.44	1.30	55.1
62	2	0	3.12	0	19.50	23.69	21.07	1.19	53.2
63	2	0	3.12	0	19.50	23.69	22.09	0.90	43.9
64	2	0	3.12	0	19.50	23.69	21.74	0.89	44.2
65	2	0	3.12	0	19.50	23.69	20.64	1.47	59.4
66	2	0	3.12	0	19.50	23.69	22.08	1.23	52.9
67	2	0	3.12	0	19.50	23.69	21.29	1.42	57.7
68	2	0	3.12	0	19.50	23.69	23.6	0.91	42.3
69	2	0	3.12	0	19.50	23.69	22.3	1.06	48.3
70	2	0	3.12	0	19.50	23.69	21.47	1.20	52.9
71	2	0	3.12	0	19.50	23.69	21.05	1.27	55.0
72	2	0	4.5	0	25.5	28.54	28.05	1.04	46.6
73	2	0	4.5	0	25.5	28.54	30.21	0.82	37.9
74	2	0	4.5	0	25.5	28.54	29.08	1.10	47.1

Table B.2 Cont. Detailed properties and test results for hooked bar specimens having widely-spaced bars without confining reinforcement tested at the University of Kansas

SN	T	T_h ^[1]	T/T_h	f_{su}	$f_{su}/f_{s,calc}$ ^[2]	$f_{su}/f_{s,calc}$ ^[3]
	lb	lb		ksi		
47	71484	48048	1.49	90.5	1.77	1.77
48	75208	73500	1.02	95.2	1.27	1.27
49	59292	51257	1.16	75.1	1.38	1.38
50	63504	64725	0.98	80.4	1.20	1.20
51	89916	87790	1.02	113.8	1.30	1.30
52	66590	77100	0.86	42.7	1.04	1.04
53	148727	151937	0.98	95.3	1.26	1.26
54	89396	86533	1.03	57.3	1.26	1.26
55	75313	88045	0.86	48.3	1.04	1.04
56	97379	103303	0.94	62.4	1.17	1.17
57	132055	115743	1.14	84.7	1.43	1.43
58	125126	130818	0.96	80.2	1.21	1.21
59	104779	109566	0.96	67.2	1.19	1.19
60	106718	120663	0.88	68.4	1.12	1.12
61	134371	114888	1.17	86.1	1.47	1.47
62	124622	128251	0.97	79.9	1.23	1.23
63	199743	184601	1.08	128.0	1.42	1.42
64	213265	193176	1.10	136.7	1.46	1.46
65	92168	100415	0.92	59.1	1.14	1.14
66	108122	101775	1.06	69.3	1.31	1.31
67	69514	80662	0.86	44.6	1.04	1.04
68	182254	156535	1.16	116.8	1.50	1.50
69	128123	134336	0.95	82.1	1.21	1.21
70	100453	114510	0.88	64.4	1.10	1.10
71	107461	115659	0.93	68.9	1.17	1.17
72	240000	219708	1.09	106.7	1.43	1.43
73	279100	270268	1.03	124.0	1.38	1.38
74	196500	180788	1.09	87.3	1.39	1.39

^[1] Based on descriptive equations, Eq. (4.5) and (4.7)

^[2] Based on design equation, Eq. (6.18), using full expression for ψ_r , Eq. (6.14)

^[3] Based on design equation, Eq. (6.18), using simplified expression for ψ_r , Eq. (6.15)

Table B.3 Detailed properties and test results for hooked bar specimens having closely-spaced bars without confining reinforcement tested at the University of Kansas

SN	ID	<i>b</i>	<i>h</i>	$\ell_{eh,avg}$	f_{cm}	d_b	A_b	<i>s</i>	<i>s/d_b</i>
		in.	in.	in.	psi	in.	in. ²	in.	
75	(3) 5-5-90-0-i-2.5-2-8	12.8	9.9	7.9	4830	0.625	0.31	3.6	5.8
76	(4@4) 5-5-90-0-i-2.5-2-6	13.4	7.2	5.2	6430	0.625	0.31	2.6	4.2
77	(4@4) 5-5-90-0-i-2.5-2-10	13.4	11.0	9.0	6470	0.625	0.31	2.6	4.2
78	(4@4) 5-8-90-0-i-2.5-2-6	12.5	7.9	5.9	6950	0.625	0.31	2.3	3.7
79	(3@4) 5-8-90-0-i-2.5-2-6	10.6	7.9	5.9	6950	0.625	0.31	2.5	4.0
80	(4@6) 5-8-90-0-i-2.5-2-6	17.0	7.9	5.9	6693	0.625	0.31	3.8	6.1
81	(3@6) 5-8-90-0-i-2.5-2-6	13.2	8.0	6.0	6950	0.625	0.31	3.8	6.1
82	(3@5.5) 8-5-90-0-i-2.5-2-16	17.0	18.1	16.1	6255	1	0.79	5.5	5.5
83	(3@5.5) 8-5-90-0-i-2.5-2-10	16.8	11.4	9.4	6461	1	0.79	5.4	5.4
84	(3@5.5) 8-5-90-0-i-2.5-2-8	17.0	9.8	7.8	5730	1	0.79	5.5	5.5
85	(3@3) 8-5-90-0-i-2.5-2-10	12.6	12.1	10.1	4490	1	0.79	3.3	3.3
86	(3@5) 8-5-90-0-i-2.5-2-10	16.6	12.1	10.1	4490	1	0.79	5.3	5.3
87	(3@5.5) 8-8-90-0-i-2.5-2-8	14.8	9.9	7.9	8700	1	0.79	4.4	4.4
88	(3@3) 8-12-90-0-i-2.5-2-12	12.0	14.1	12.1	11040	1	0.79	3.0	3.0
89	(3@4) 8-12-90-0-i-2.5-2-12	14.0	14.6	12.6	11440	1	0.79	4.0	4.0
90	(3@5) 8-12-90-0-i-2.5-2-12	16.0	14.2	12.2	11460	1	0.79	5.0	5.0
91	(3@5) 8-5-180-0-i-2.5-2-10	16.6	12.0	10.0	5260	1	0.79	5.3	5.3
92	(3@3.75) 11-8-90-0-i-2.5-2-20	17.4	21.9	19.9	7070	1.41	1.56	5.5	3.9
93	(3@3.75) 11-8-90-0-i-2.5-2-24	17.4	25.5	23.5	7070	1.41	1.56	5.5	3.9
94	(3@3.75) 11-12-90-0-i-2.5-2-22	17.4	23.7	21.7	11460	1.41	1.56	5.5	3.9
95	H14-7	20.7	37.8	36.4	6390	1.693	2.25	6.0	3.5

Table B.3 Cont. Detailed properties and test results for hooked bar specimens having closely-spaced bars without confining reinforcement tested at the University of Kansas

SN	n	A_{th}	A_{hs}	A_{th}/A_{hs}	h_{cl}	x_{mid}	d_{eff}	d_{eff}/ℓ_{eh}	θ
		in. ²	in. ²		in.	in.	in.		°
75	3	0	0.93	0	5.25	9.44	7.21	0.91	50.1
76	4	0	1.24	0	5.25	9.44	6.34	1.22	61.1
77	4	0	1.24	0	5.25	9.44	7.37	0.82	46.4
78	4	0	1.24	0	5.25	9.44	6.44	1.09	58.0
79	3	0	0.93	0	5.25	9.44	6.39	1.08	58.0
80	4	0	1.24	0	5.25	9.44	6.36	1.08	58.0
81	3	0	0.93	0	5.25	9.44	6.61	1.10	57.6
82	3	0	2.37	0	10.00	14.19	12.83	0.80	41.4
83	3	0	2.37	0	10.00	14.19	11.61	1.24	56.5
84	3	0	2.37	0	10.00	14.19	11.16	1.43	61.2
85	3	0	2.37	0	10.00	14.19	12.15	1.20	54.6
86	3	0	2.37	0	10.00	14.19	11.85	1.17	54.6
87	3	0	2.37	0	10.00	14.19	11.59	1.47	60.9
88	3	0	2.37	0	10.00	14.19	11.97	0.99	49.5
89	3	0	2.37	0	10.00	14.19	11.89	0.94	48.4
90	3	0	2.37	0	10.00	14.19	11.55	0.95	49.3
91	3	0	2.37	0	10.00	14.19	12.36	1.24	54.8
92	3	0	4.68	0	19.50	23.69	23.55	1.18	50.0
93	3	0	4.68	0	19.50	23.69	24.73	1.05	45.2
94	3	0	4.68	0	19.50	23.69	22.85	1.05	47.5
95	3	0	6.75	0	24.00	28.54	33.20	0.91	38.1

Table B.3 Cont. Detailed properties and test results for hooked bar specimens having closely-spaced bars without confining reinforcement tested at the University of Kansas

SN	T	T_h ^[1]	T/T_h	f_{su}	$f_{su}/f_{s,calc}$ ^[2]	$f_{su}/f_{s,calc}$ ^[3]
	lb	lb		ksi		
75	27869	25789	1.08	89.9	1.23	1.23
76	14542	15243	0.95	46.9	1.14	1.14
77	28402	28016	1.01	91.6	1.29	1.29
78	15479	17086	0.91	49.9	1.11	1.11
79	16805	17639	0.95	54.2	1.16	1.16
80	19303	21008	0.92	62.3	1.01	1.01
81	24886	21633	1.15	80.3	1.27	1.27
82	62798	72985	0.86	79.5	1.06	1.06
83	36054	40262	0.90	45.6	1.05	1.05
84	24411	31939	0.76	30.9	0.87	0.87
85	28480	32234	0.88	36.1	1.11	1.11
86	32300	39016	0.83	40.9	0.97	0.97
87	37670	33002	1.14	47.7	1.39	1.39
88	48039	49088	0.98	60.8	1.29	1.29
89	55822	57486	0.97	70.7	1.27	1.27
90	52352	60935	0.86	66.3	1.07	1.07
91	45930	40344	1.14	58.1	1.34	1.34
92	98488	95566	1.03	63.1	1.37	1.37
93	126976	114868	1.11	81.4	1.50	1.50
94	123180	120461	1.02	79.0	1.39	1.39
95	250800	189076	1.33	111.5	1.87	1.87

^[1] Based on descriptive equations, Eq. (4.5) and (4.7)

^[2] Based on design equation, Eq. (6.18), using full expression for ψ_r , Eq. (6.14)

^[3] Based on design equation, Eq. (6.18), using simplified expression for ψ_r , Eq. (6.15)

Table B.4 Detailed properties and test results for hooked bar specimens having widely-spaced bars with confining reinforcement tested at the University of Kansas

SN	ID	<i>b</i>	<i>h</i>	$\ell_{eh,avg}$	f_{cm}	d_b	A_b	<i>s</i>	<i>s/d_b</i>
		in.	in.	in.	psi	in.	in. ²	in.	
96	5-5-90-5#3-i-2.5-2-8	12.7	9.8	7.8	4660	0.625	0.31	7.1	11.4
97	5-5-90-5#3-i-2.5-2-7	12.7	8.3	6.3	5230	0.625	0.31	7.1	11.4
98	5-12-90-5#3-i-2.5-2-5	12.7	7.4	5.4	10410	0.625	0.31	7.1	11.4
99	5-15-90-5#3-i-2.5-2-4	12.9	6.0	4.0	15800	0.625	0.31	7.3	11.7
100	5-15-90-5#3-i-2.5-2-5	13.0	7.1	5.1	15800	0.625	0.31	7.4	11.8
101	5-5-90-5#3-i-3.5-2-7	13.2	9.1	7.1	5190	0.625	0.31	7.6	12.2
102	5-12-90-5#3-i-3.5-2-5	12.9	7.0	5.0	11090	0.625	0.31	7.3	11.7
103*	5-5-90-2#3-i-2.5-2-8	12.9	9.8	7.8	5860	0.625	0.31	7.3	11.7
104*	5-5-90-2#3-i-2.5-2-6	12.9	7.9	5.9	5800	0.625	0.31	7.3	11.7
105*	5-8-90-2#3-i-2.5-2-6	12.4	8.0	6.0	8580	0.625	0.31	6.8	10.9
106*	5-8-90-2#3-i-2.5-2-8	12.7	10.4	8.4	8380	0.625	0.31	7.1	11.4
107*	5-12-90-2#3-i-2.5-2-5	12.7	7.8	5.8	11090	0.625	0.31	7.1	11.4
108*	5-15-90-2#3-i-2.5-2-6	12.9	8.4	6.4	15800	0.625	0.31	7.3	11.7
109*	5-15-90-2#3-i-2.5-2-4	13.0	5.8	3.8	15800	0.625	0.31	7.4	11.8
110*	5-5-90-2#3-i-3.5-2-6	14.7	7.9	5.9	5230	0.625	0.31	7.1	11.4
111*	5-5-90-2#3-i-3.5-2-8	15.0	9.7	7.7	5190	0.625	0.31	7.4	11.8
112*	5-8-90-2#3-i-3.5-2-6	14.6	8.3	6.3	8580	0.625	0.31	7.0	11.2
113*	5-8-90-2#3-i-3.5-2-8	14.9	9.1	7.1	8710	0.625	0.31	7.3	11.7
114*	5-12-90-2#3-i-3.5-2-5	14.9	7.4	5.4	10410	0.625	0.31	7.3	11.7
115*	5-5-180-2#3-i-2.5-2-8	13.1	10.0	8.0	5670	0.625	0.31	7.5	12.0
116*	5-5-180-2#3-i-2.5-2-6	12.9	7.6	5.6	5860	0.625	0.31	7.3	11.7
117*	5-8-180-2#3-i-2.5-2-7	12.6	9.1	7.1	9080	0.625	0.31	7.0	11.2
118*	5-8-180-2#3-i-3.5-2-7	15.2	8.8	6.8	9080	0.625	0.31	7.6	12.2
119*	(3@10) 5-5-90-2#3-i-2.5-2-7	18.4	9.0	7.0	5950	0.625	0.31	6.4	10.2
120	8-5-90-5#3-i-2.5-2-10b	16.9	12.4	10.4	5440	1	0.79	10.9	10.9
121	8-5-90-5#3-i-2.5-2-10c	17.0	12.5	10.5	5650	1	0.79	11	11.0
122	8-5-90-5#3-i-2.5-2-15	16.9	17.5	15.5	4850	1	0.79	10.9	10.9
123	8-5-90-5#3-i-2.5-2-13	17.3	15.6	13.6	5560	1	0.79	11.3	11.3
124	8-5-90-5#3-i-2.5-2-12(1)	16.8	13.3	11.3	5090	1	0.79	10.8	10.8
125	8-5-90-5#3-i-2.5-2-12	16.8	13.8	11.8	5960	1	0.79	10.8	10.8
126	8-5-90-5#3-i-2.5-2-12(2)	16.0	14.2	12.2	5240	1	0.79	10	10.0
127	8-5-90-5#3-i-2.5-2-10a	16.8	12.5	10.5	5270	1	0.79	10.8	10.8
128	8-5-90-5#3-i-2.5-2-10	17.3	11.6	9.6	5920	1	0.79	11.3	11.3
129	8-8-90-5#3-i-2.5-2-9	16.8	10.8	8.8	7710	1	0.79	10.8	10.8

* Specimens not used to develop descriptive equations, Eq. (4.5) and (4.7)

Table B.4 Cont. Detailed properties and test results for hooked bar specimens having widely-spaced bars with confining reinforcement tested at the University of Kansas

SN	n	A_{th}	A_{hs}	A_{th}/A_{hs}	$A_{th,ACI}/A_{hs}$	h_{cl}	x_{mid}	d_{eff}	d_{eff}/ℓ_{eh}	θ
		in. ²	in. ²			in.	in.	in.		°
96	2	0.66	0.62	1.065	1.774	5.25	9.44	7.34	0.94	50.4
97	2	0.66	0.62	1.065	1.774	5.25	9.44	6.67	1.06	56.3
98	2	0.66	0.62	1.065	1.774	5.25	9.44	6.19	1.15	60.2
99	2	0.66	0.62	1.065	1.774	5.25	9.44	5.81	1.45	67.0
100	2	0.66	0.62	1.065	1.774	5.25	9.44	5.94	1.16	61.6
101	2	0.66	0.62	1.065	1.774	5.25	9.44	6.81	0.96	53.0
102	2	0.66	0.62	1.065	1.774	5.25	9.44	6.02	1.20	62.1
103*	2	0.22	0.62	0.355	0.710	5.25	9.44	6.77	0.87	50.4
104*	2	0.22	0.62	0.355	0.710	5.25	9.44	6.47	1.10	58.0
105*	2	0.22	0.62	0.355	0.710	5.25	9.44	6.29	1.05	57.6
106*	2	0.22	0.62	0.355	0.710	5.25	9.44	6.61	0.79	48.3
107*	2	0.22	0.62	0.355	0.710	5.25	9.44	5.87	1.01	58.4
108*	2	0.22	0.62	0.355	0.710	5.25	9.44	6.01	0.94	55.9
109*	2	0.22	0.62	0.355	0.710	5.25	9.44	5.58	1.47	68.1
110*	2	0.22	0.62	0.355	0.710	5.25	9.44	6.07	1.03	58.0
111*	2	0.22	0.62	0.355	0.710	5.25	9.44	6.95	0.90	50.8
112*	2	0.22	0.62	0.355	0.710	5.25	9.44	6.12	0.97	56.3
113*	2	0.22	0.62	0.355	0.710	5.25	9.44	6.05	0.85	53.0
114*	2	0.22	0.62	0.355	0.710	5.25	9.44	5.91	1.09	60.2
115*	2	0.22	0.62	0.355	0.710	5.25	9.44	6.66	0.83	49.7
116*	2	0.22	0.62	0.355	0.710	5.25	9.44	6.35	1.13	59.3
117*	2	0.22	0.62	0.355	0.710	5.25	9.44	6.17	0.87	53.0
118*	2	0.22	0.62	0.355	0.710	5.25	9.44	6.06	0.89	54.2
119*	3	0.22	0.93	0.237	0.473	5.25	9.44	6.59	0.94	53.4
120	2	0.66	1.58	0.418	0.696	10.00	14.19	12.29	1.18	53.8
121	2	0.66	1.58	0.418	0.696	10.00	14.19	12.20	1.16	53.5
122	2	0.66	1.58	0.418	0.696	10.00	14.19	12.61	0.81	42.5
123	2	0.66	1.58	0.418	0.696	10.00	14.19	12.61	0.93	46.2
124	2	0.66	1.58	0.418	0.696	10.00	14.19	12.30	1.09	51.5
125	2	0.66	1.58	0.418	0.696	10.00	14.19	12.25	1.04	50.2
126	2	0.66	1.58	0.418	0.696	10.00	14.19	12.55	1.03	49.3
127	2	0.66	1.58	0.418	0.696	10.00	14.19	12.80	1.22	53.5
128	2	0.66	1.58	0.418	0.696	10.00	14.19	12.14	1.26	55.9
129	2	0.66	1.58	0.418	0.696	10.00	14.19	11.76	1.34	58.2

* Specimens not used to develop descriptive equations, Eq. (4.5) and (4.7)

Table B.4 Cont. Detailed properties and test results for hooked bar specimens having widely-spaced bars with confining reinforcement tested at the University of Kansas

SN	T	$T_h^{[1]}$	T/T_h	f_{su}	$f_{su}/f_{s,calc}^{[2]}$	$f_{su}/f_{s,calc}^{[3]}$
	lb	lb		ksi		
96	43030	40185	1.07	138.8	1.68	1.68
97	31696	35172	0.90	102.2	1.49	1.49
98	34420	35684	0.96	111.0	1.59	1.59
99	31318	31300	1.00	101.0	1.76	1.76
100	39156	36942	1.06	126.3	1.72	1.72
101	36025	38252	0.94	116.2	1.50	1.50
102	30441	34207	0.89	98.2	1.49	1.49
103*	37154	33323	1.11	119.9	1.37	1.37
104*	29444	25559	1.15	95.0	1.44	1.44
105*	30638	28472	1.08	98.8	1.34	1.34
106*	40168	39127	1.03	129.6	1.26	1.26
107*	24348	29321	0.83	78.5	1.03	1.03
108*	42638	35110	1.21	137.5	1.50	1.50
109*	18667	21621	0.86	60.2	1.10	1.10
110*	21093	24951	0.85	68.0	1.06	1.06
111*	44665	31954	1.40	144.1	1.72	1.72
112*	30035	29811	1.01	96.9	1.25	1.25
113*	28656	33536	0.85	92.4	1.05	1.05
114*	28364	27015	1.05	91.5	1.31	1.31
115*	34078	33872	1.01	109.9	1.24	1.24
116*	26728	24426	1.09	86.2	1.37	1.37
117*	29230	33880	0.86	94.3	1.06	1.06
118*	30931	32502	0.95	99.8	1.17	1.17
119*	31296	28718	1.09	101.0	1.28	1.28
120	69715	65770	1.06	88.2	1.56	1.56
121	68837	66795	1.03	87.1	1.51	1.51
122	73377	89921	0.82	92.9	1.13	1.13
123	82376	82669	1.00	104.3	1.40	1.40
124	66363	69394	0.96	84.0	1.39	1.39
125	72000	74359	0.97	91.1	1.39	1.39
126	71470	74399	0.96	90.5	1.38	1.38
127	82800	65849	1.26	104.8	1.85	1.85
128	70356	62773	1.12	89.1	1.67	1.67
129	64397	61797	1.04	81.5	1.56	1.56

* Specimens not used to develop descriptive equations, Eq. (4.5) and (4.7)

[1] Based on descriptive equations, Eq. (4.5) and (4.7)

[2] Based on design equation, Eq. (6.18), using full expression for ψ_r , Eq. (6.14)

[3] Based on design equation, Eq. (6.18), using simplified expression for ψ_r , Eq. (6.15)

Table B.4 Cont. Detailed properties and test results for hooked bar specimens having widely-spaced bars with confining reinforcement tested at the University of Kansas

SN	ID	<i>b</i>	<i>h</i>	$\ell_{eh,avg}$	f_{cm}	d_b	A_b	<i>s</i>	<i>s/d_b</i>
		in.	in.	in.	psi	in.	in. ²	in.	
130	8-12-90-5#3-i-2.5-2-9	16.5	11.0	9	11160	1	0.79	10.5	10.5
131	8-12-90-5#3-i-3.5-2-9	18.5	11.0	9	11160	1	0.79	10.5	10.5
132	8-12-90-5#3-i-2.5-2-10	16.9	11.4	9.4	11800	1	0.79	10.9	10.9
133	8-12-90-5#3-i-2.5-2-12	17.0	14.2	12.2	11760	1	0.79	11	11.0
134	8-15-90-5#3-i-2.5-2-10	16.9	12.1	10.1	15800	1	0.79	10.9	10.9
135	8-5-90-5#3-i-3.5-2-15	19.3	17.8	15.8	4850	1	0.79	11.3	11.3
136	8-5-90-5#3-i-3.5-2-13	19.4	15.1	13.1	5570	1	0.79	11.4	11.4
137	8-5-90-5#3-i-3.5-2-12(1)	18.8	14.5	12.5	5090	1	0.79	10.8	10.8
138	8-5-90-5#3-i-3.5-2-12	18.8	14.1	12.1	6440	1	0.79	10.8	10.8
139	8-12-180-5#3-i-2.5-2-10	16.9	11.8	9.8	11800	1	0.79	10.9	10.9
140	8-15-180-5#3-i-2.5-2-9.5	17.0	11.7	9.7	15550	1	0.79	11	11.0
141	8-8-90-5#3-i-3.5-2-8	17.9	10.0	8	7910	1	0.79	9.88	9.9
142*	8-5-90-2#3-i-2.5-2-16	16.5	17.4	15.4	4810	1	0.79	10.5	10.5
143*	8-5-90-2#3-i-2.5-2-9.5	17.0	11.1	9.1	5140	1	0.79	11	11.0
144*	8-5-90-2#3-i-2.5-2-12.5	16.5	14.0	12	5240	1	0.79	10.5	10.5
145*	8-5-90-2#3-i-2.5-2-8.5	16.1	11.3	9.3	5240	1	0.79	10.1	10.1
146*	8-5-90-2#3-i-2.5-2-14	16.3	15.8	13.8	5450	1	0.79	10.3	10.3
147*	8-5-90-2#3-i-2.5-2-10	17.3	12.1	10.1	5920	1	0.79	11.3	11.3
148*	8-8-90-2#3-i-2.5-2-8	16.0	10.3	8.3	7700	1	0.79	10	10.0
149*	8-8-90-2#3-i-2.5-2-10	15.5	11.7	9.7	8990	1	0.79	9.5	9.5
150*	8-12-90-2#3-i-2.5-2-9	16.5	11.0	9	11160	1	0.79	10.5	10.5
151*	8-12-90-2#3-i-2.5-2-11	16.5	12.9	10.9	12010	1	0.79	10.5	10.5
152*	8-15-90-2#3-i-2.5-2-11	17.0	13.0	11	15800	1	0.79	11	11.0
153*	8-5-90-2#3-i-3.5-2-17	17.1	19.3	17.3	5570	1	0.79	11.1	11.1
154*	8-5-90-2#3-i-3.5-2-13	19.3	15.6	13.6	5560	1	0.79	11.3	11.3
155*	8-8-90-2#3-i-3.5-2-8	17.5	10.1	8.1	8290	1	0.79	9.5	9.5
156*	8-8-90-2#3-i-3.5-2-10	17.5	10.8	8.8	8990	1	0.79	9.5	9.5
157*	8-12-90-2#3-i-3.5-2-9	18.6	11.0	9	11160	1	0.79	10.6	10.6
158*	8-5-180-2#3-i-2.5-2-11	16.5	12.6	10.6	4550	1	0.79	10.5	10.5
159*	8-5-180-2#3-i-2.5-2-14	16.8	15.8	13.8	4870	1	0.79	10.8	10.8
160*	8-8-180-2#3-i-2.5-2-11.5	17.0	12.4	10.4	8810	1	0.79	11	11.0
161*	8-12-180-2#3-i-2.5-2-11	16.6	12.8	10.8	12010	1	0.79	10.6	10.6
162*	8-5-180-2#3-i-3.5-2-11	18.8	12.4	10.4	4300	1	0.79	10.8	10.8
163*	8-5-180-2#3-i-3.5-2-14	18.8	15.6	13.6	4870	1	0.79	10.8	10.8

* Specimens not used to develop descriptive equations, Eq. (4.5) and (4.7)

Table B.4 Cont. Detailed properties and test results for hooked bar specimens having widely-spaced bars with confining reinforcement tested at the University of Kansas

SN	n	A_{th}	A_{hs}	A_{th}/A_{hs}	$A_{th,ACI}/A_{hs}$	h_{cl}	x_{mid}	d_{eff}	d_{eff}/ℓ_{eh}	θ
		in. ²	in. ²			in.	in.	in.		°
130	2	0.66	1.58	0.418	0.696	10	14.19	11.27	1.25	57.6
131	2	0.66	1.58	0.418	0.696	10	14.19	11.19	1.24	57.6
132	2	0.66	1.58	0.418	0.696	10	14.19	11.17	1.19	56.5
133	2	0.66	1.58	0.418	0.696	10	14.19	11.59	0.95	49.3
134	2	0.66	1.58	0.418	0.696	10	14.19	11.22	1.11	54.6
135	2	0.66	1.58	0.418	0.696	10	14.19	12.50	0.79	41.9
136	2	0.66	1.58	0.418	0.696	10	14.19	12.18	0.93	47.3
137	2	0.66	1.58	0.418	0.696	10	14.19	12.36	0.99	48.6
138	2	0.66	1.58	0.418	0.696	10	14.19	12.11	1.00	49.5
139	2	0.66	1.58	0.418	0.696	10	14.19	11.16	1.14	55.4
140	2	0.66	1.58	0.418	0.696	10	14.19	11.18	1.15	55.6
141	2	0.66	1.58	0.418	0.696	10	14.19	11.42	1.43	60.6
142*	2	0.66	1.58	0.418	0.278	10	14.19	12.92	0.84	42.7
143*	2	0.66	1.58	0.418	0.278	10	14.19	11.82	1.30	57.3
144*	2	0.22	1.58	0.139	0.278	10	14.19	12.49	1.04	49.8
145*	2	0.22	1.58	0.139	0.278	10	14.19	11.79	1.27	56.8
146*	2	0.22	1.58	0.139	0.278	10	14.19	12.62	0.91	45.8
147*	2	0.22	1.58	0.139	0.278	10	14.19	11.71	1.16	54.6
148*	2	0.22	1.58	0.139	0.278	10	14.19	11.37	1.37	59.7
149*	2	0.22	1.58	0.139	0.278	10	14.19	11.59	1.19	55.6
150*	2	0.22	1.58	0.139	0.278	10	14.19	11.20	1.24	57.6
151*	2	0.22	1.58	0.139	0.278	10	14.19	11.25	1.03	52.5
152*	2	0.22	1.58	0.139	0.278	10	14.19	11.12	1.01	52.2
153*	2	0.22	1.58	0.139	0.278	10	14.19	12.88	0.74	39.4
154*	2	0.22	1.58	0.139	0.278	10	14.19	12.28	0.90	46.2
155*	2	0.22	1.58	0.139	0.278	10	14.19	11.22	1.38	60.3
156*	2	0.22	1.58	0.139	0.278	10	14.19	11.24	1.28	58.2
157*	2	0.22	1.58	0.139	0.278	10	14.19	10.87	1.21	57.6
158*	2	0.22	1.58	0.139	0.278	10	14.19	12.30	1.16	53.2
159*	2	0.22	1.58	0.139	0.278	10	14.19	12.72	0.92	45.8
160*	2	0.22	1.58	0.139	0.278	10	14.19	11.41	1.10	53.8
161*	2	0.22	1.58	0.139	0.278	10	14.19	11.17	1.03	52.7
162*	2	0.22	1.58	0.139	0.278	10	14.19	11.95	1.15	53.8
163*	2	0.22	1.58	0.139	0.278	10	14.19	12.02	0.88	46.2

* Specimens not used to develop descriptive equations, Eq. (4.5) and (4.7)

Table B.4 Cont. Detailed properties and test results for hooked bar specimens having widely-spaced bars with confining reinforcement tested at the University of Kansas

SN	T	T_h ^[1]	T/T_h	f_{su}	$f_{su}/f_{s,calc}$ ^[2]	$f_{su}/f_{s,calc}$ ^[3]
	lb	lb		ksi		
130	64753	67814	0.95	82.0	1.40	1.40
131	67830	67814	1.00	85.9	1.47	1.47
132	64530	71094	0.91	81.7	1.32	1.32
133	87711	88778	0.99	111.0	1.38	1.38
134	90003	80398	1.12	113.9	1.59	1.59
135	80341	91463	0.88	101.7	1.22	1.22
136	77069	80076	0.96	97.6	1.36	1.36
137	76431	75465	1.01	96.7	1.45	1.45
138	79150	77221	1.02	100.2	1.46	1.46
139	64107	73599	0.87	81.1	1.25	1.25
140	85951	77403	1.11	108.8	1.59	1.59
141	55810	57699	0.97	70.6	1.48	1.48
142*	79629	89242	0.89	100.8	1.24	1.38
143*	53621	58558	0.92	67.9	1.39	1.55
144*	72067	61372	1.17	91.2	1.41	1.57
145*	50561	47766	1.06	64.0	1.28	1.42
146*	76964	71349	1.08	97.4	1.30	1.44
147*	56203	53354	1.05	71.1	1.27	1.41
148*	47876	47032	1.02	60.6	1.23	1.37
149*	61024	56923	1.07	77.2	1.29	1.43
150*	61013	55809	1.09	77.2	1.32	1.46
151*	68683	68849	1.00	86.9	1.20	1.34
152*	83320	74572	1.12	105.5	1.35	1.50
153*	89914	90432	0.99	113.8	1.20	1.34
154*	80360	70664	1.14	101.7	1.37	1.52
155*	48773	46777	1.04	61.7	1.26	1.40
156*	53885	51723	1.04	68.2	1.26	1.40
157*	49777	55809	0.89	63.0	1.08	1.19
158*	60235	52394	1.15	76.2	1.38	1.54
159*	76279	69316	1.10	96.6	1.32	1.47
160*	58171	60693	0.96	73.6	1.15	1.28
161*	64655	68211	0.95	81.8	1.14	1.27
162*	55869	50711	1.10	70.7	1.33	1.47
163*	63467	68301	0.93	80.3	1.12	1.24

* Specimens not used to develop descriptive equations, Eq. (4.5) and (4.7)

^[1] Based on descriptive equations, Eq. (4.5) and (4.7)

^[2] Based on design equation, Eq. (6.18), using full expression for ψ_r , Eq. (6.14)

^[3] Based on design equation, Eq. (6.18), using simplified expression for ψ_r , Eq. (6.15)

Table B.4 Cont. Detailed properties and test results for hooked bar specimens having widely-spaced bars with confining reinforcement tested at the University of Kansas

SN	ID	<i>b</i>	<i>h</i>	$\ell_{eh,avg}$	f_{cm}	d_b	A_b	<i>s</i>	<i>s/d_b</i>
		in.	in.	in.	psi	in.	in. ²	in.	
164*	8-15-180-2#3-i-2.5-2-11	16.8	13.1	11.1	15550	1	0.79	10.8	10.8
165*	8-12-90-5#3vr-i-2.5-2-10	16.8	12.2	10.2	11800	1	0.79	10.8	10.8
166*	8-12-90-4#3vr-i-2.5-2-10	16.0	12.4	10.4	11850	1	0.79	10	10.0
167*	8-12-180-5#3vr-i-2.5-2-10	16.8	12.8	10.8	11800	1	0.79	10.8	10.8
168*	8-12-180-4#3vr-i-2.5-2-10	16.8	12.3	10.3	11850	1	0.79	10.8	10.8
169	11-5-90-6#3-i-2.5-2-20	20.7	21.3	19.3	5420	1.41	1.56	14.3	10.1
170	11-5-90-6#3-i-2.5-2-16	21.4	17.4	15.4	5030	1.41	1.56	15	10.6
171	11-8-90-6#3-i-2.5-2-16	21.2	17.9	15.9	9120	1.41	1.56	14.8	10.5
172	11-8-90-6#3-i-2.5-2-22	21.3	23.4	21.4	9420	1.41	1.56	14.9	10.6
173	11-8-90-6#3-i-2.5-2-22	21.2	23.9	21.9	9420	1.41	1.56	14.8	10.5
174	11-8-90-6#3-i-2.5-2-15	21.3	17.5	15.5	7500	1.41	1.56	14.9	10.6
175	11-8-90-6#3-i-2.5-2-19	21.3	21.2	19.2	7500	1.41	1.56	14.9	10.6
176	11-12-90-6#3-i-2.5-2-17	20.8	18.8	16.8	12370	1.41	1.56	14.4	10.2
177	11-12-90-6#3-i-2.5-2-16	20.8	17.4	15.4	13710	1.41	1.56	14.4	10.2
178	11-12-90-6#3-i-2.5-2-22	21.1	23.7	21.7	13710	1.41	1.56	14.7	10.4
179	11-15-90-6#3-i-2.5-2-22	21.3	24.3	22.3	16180	1.41	1.56	14.9	10.6
180	11-15-90-6#3-i-2.5-2-15	21.4	16.8	14.8	14045	1.41	1.56	15	10.6
181	11-5-90-6#3-i-3.5-2-20	22.9	22.4	20.4	5420	1.41	1.56	14.5	10.3
182	11-8-180-6#3-i-2.5-2-15	20.8	17.3	15.3	7500	1.41	1.56	14.4	10.2
183	11-8-180-6#3-i-2.5-2-19	21.1	21.8	19.8	7870	1.41	1.56	14.7	10.4
184	(2@7.5) 11-12-180-6#3-i-2.5-2-14	16.9	16.4	14.4	12190	1.41	1.56	10.5	7.4
185	11-12-180-6#3-i-2.5-2-17	21.3	18.7	16.7	12370	1.41	1.56	14.9	10.6
186	11-12-180-6#3-i-2.5-2-17	21.2	18.8	16.8	12370	1.41	1.56	14.8	10.5
187*	11-5-90-2#3-i-2.5-2-17	21.2	19.6	17.6	5600	1.41	1.56	14.8	10.5
188*	(2@7.5) 11-8-90-2#3-i-2.5-2-17a	17.2	18.4	16.4	7070	1.41	1.56	10.8	7.7
189*	(2@7.5) 11-12-90-2#3-i-2.5-2-16a	16.9	17.3	15.3	11850	1.41	1.56	10.5	7.4
190*	11-12-90-2#3-i-2.5-2-17.5	21.1	19.8	17.8	13710	1.41	1.56	14.7	10.4
191*	11-15-90-2#3-i-2.5-2-23	20.8	25.5	23.5	16180	1.41	1.56	14.4	10.2
192*	11-15-90-2#3-i-2.5-2-15	21.4	16.1	14.1	14045	1.41	1.56	15	10.6
193*	11-5-90-2#3-i-3.5-2-17	23.2	19.6	17.6	7070	1.41	1.56	14.8	10.5
194*	(2@7.5) 11-8-90-6#3-i-2.5-2-15a	17.2	16.0	14	7070	1.41	1.56	10.8	7.7

* Specimens not used to develop descriptive equations, Eq. (4.5) and (4.7)

Table B.4 Cont. Detailed properties and test results for hooked bar specimens having widely-spaced bars with confining reinforcement tested at the University of Kansas

SN	n	A_{th}	A_{hs}	A_{th}/A_{hs}	$A_{th,ACI}/A_{hs}$	h_{cl}	x_{mid}	d_{eff}	d_{eff}/ℓ_{eh}	θ
		in. ²	in. ²			in.	in.	in.		°
164*	2	0.22	1.58	0.139	0.278	10	14.19	11.09	1.00	52.0
165*	2	0.66	1.58	0.418	0.696	10	14.19	11.10	1.09	54.3
166*	2	0.66	1.58	0.418	0.557	10	14.19	11.13	1.07	53.8
167*	2	0.22	1.58	0.139	0.696	10	14.19	11.24	1.04	52.7
168*	2	0.22	1.58	0.139	0.557	10	14.19	11.26	1.09	54.0
169	2	0.66	3.12	0.212	0.423	19.5	23.69	23.17	1.20	50.8
170	2	0.66	3.12	0.212	0.423	19.5	23.69	22.66	1.47	57.0
171	2	0.66	3.12	0.212	0.423	19.5	23.69	21.99	1.38	56.1
172	2	0.66	3.12	0.212	0.423	19.5	23.69	22.83	1.07	47.9
173	2	0.66	3.12	0.212	0.423	19.5	23.69	22.96	1.05	47.2
174	2	0.66	3.12	0.212	0.423	19.5	23.69	21.86	1.41	56.8
175	2	0.66	3.12	0.212	0.423	19.5	23.69	22.67	1.18	51.0
176	2	0.66	3.12	0.212	0.423	19.5	23.69	21.77	1.30	54.7
177	2	0.66	3.12	0.212	0.423	19.5	23.69	20.96	1.36	57.0
178	2	0.66	3.12	0.212	0.423	19.5	23.69	22.02	1.01	47.5
179	2	0.66	3.12	0.212	0.423	19.5	23.69	21.58	0.97	46.7
180	2	0.66	3.12	0.212	0.423	19.5	23.69	21.25	1.44	58.0
181	2	0.66	3.12	0.212	0.423	19.5	23.69	22.80	1.12	49.3
182	2	0.66	3.12	0.212	0.423	19.5	23.69	21.99	1.44	57.1
183	2	0.66	3.12	0.212	0.423	19.5	23.69	22.71	1.15	50.1
184	2	0.66	3.12	0.212	0.423	19.5	23.69	21.15	1.47	58.7
185	2	0.66	3.12	0.212	0.423	19.5	23.69	21.10	1.26	54.8
186	2	0.66	3.12	0.212	0.423	19.5	23.69	21.55	1.28	54.7
187*	2	0.22	3.12	0.071	0.141	19.5	23.69	22.09	1.26	53.4
188*	2	0.22	3.12	0.071	0.141	19.5	23.69	22.44	1.37	55.3
189*	2	0.22	3.12	0.071	0.141	19.5	23.69	21.46	1.40	57.1
190*	2	0.22	3.12	0.071	0.141	19.5	23.69	21.13	1.19	53.1
191*	2	0.22	3.12	0.071	0.141	19.5	23.69	21.75	0.93	45.2
192*	2	0.22	3.12	0.071	0.141	19.5	23.69	20.89	1.48	59.2
193*	2	0.22	3.12	0.071	0.141	19.5	23.69	21.76	1.24	53.4
194*	2	0.66	3.12	0.212	0.423	19.5	23.69	22.45	1.60	59.4

* Specimens not used to develop descriptive equations, Eq. (4.5) and (4.7)

Table B.4 Cont. Detailed properties and test results for hooked bar specimens having widely-spaced bars with confining reinforcement tested at the University of Kansas

SN	T	T_h ^[1]	T/T_h	f_{su}	$f_{su}/f_{s,calc}$ ^[2]	$f_{su}/f_{s,calc}$ ^[3]
	lb	lb		ksi		
164*	78922	74953	1.05	99.9	1.27	1.41
165*	60219	76115	0.79	76.2	1.13	1.13
166*	59241	77448	0.76	75.0	1.09	1.09
167*	67780	67904	1.00	85.8	1.20	1.20
168*	69188	64811	1.07	87.6	1.29	1.29
169	136272	132453	1.03	87.4	1.39	1.39
170	115623	106456	1.09	74.1	1.51	1.51
171	132986	125227	1.06	85.2	1.45	1.45
172	184569	166365	1.11	118.3	1.48	1.48
173	191042	170080	1.12	122.5	1.50	1.50
174	108312	117059	0.93	69.4	1.27	1.27
175	145430	142238	1.02	93.2	1.38	1.38
176	161648	141386	1.14	103.6	1.55	1.55
177	115197	133663	0.86	73.8	1.17	1.17
178	201189	184800	1.09	129.0	1.45	1.45
179	197809	197713	1.00	126.8	1.33	1.33
180	145267	129618	1.12	93.1	1.53	1.53
181	135821	139385	0.97	87.1	1.31	1.31
182	111678	115715	0.97	71.6	1.33	1.33
183	149000	148055	1.01	95.5	1.35	1.35
184	93955	122388	0.77	60.2	1.05	1.05
185	116371	140606	0.83	74.6	1.12	1.12
186	148678	141386	1.05	95.3	1.42	1.42
187*	100695	107505	0.94	64.5	1.12	1.25
188*	106031	106250	1.00	68.0	1.19	1.33
189*	108718	113221	0.96	69.7	1.15	1.28
190*	130389	137692	0.95	83.6	1.15	1.27
191*	209575	192923	1.09	134.3	1.34	1.49
192*	115189	108814	1.06	73.8	1.27	1.41
193*	109644	114265	0.96	70.3	1.15	1.28
194*	106190	105641	1.01	68.1	1.40	1.40

* Specimens not used to develop descriptive equations, Eq. (4.5) and (4.7)

^[1] Based on descriptive equations, Eq. (4.5) and (4.7)

^[2] Based on design equation, Eq. (6.18), using full expression for ψ_r , Eq. (6.14)

^[3] Based on design equation, Eq. (6.18), using simplified expression for ψ_r , Eq. (6.15)

Table B.4 Cont. Detailed properties and test results for hooked bar specimens having widely-spaced bars with confining reinforcement tested at the University of Kansas

SN	ID	b	h	$\ell_{eh,avg}$	f_{cm}	d_b	A_b	s	s/d_b
		in.	in.	in.	psi	in.	in. ²	in.	
195	H14-2	26.7	28.6	24.8	13010	1.693	2.25	18	10.6
196	H14-4	26.7	37.8	34.9	7570	1.693	2.25	18	10.6
197	H14-16	26.7	28.6	25.9	6810	1.693	2.25	18	10.6
198	H18-1	27.25	28.6	28.5	15310	2.25	4	18	8.0
199	H18-2	27.25	28.6	27.0	15770	2.25	4	18	8.0
200	H18-3	27.25	37.8	36.5	7560	2.25	4	18	8.0
201	H18-4	27.25	37.8	36.4	7610	2.25	4	18	8.0

Table B.4 Cont. Detailed properties and test results for hooked bar specimens having widely-spaced bars with confining reinforcement tested at the University of Kansas

SN	n	A_{th}	A_{hs}	A_{th}/A_{hs}	$A_{th,ACI}/A_{hs}$	h_{cl}	x_{mid}	d_{eff}	d_{eff}/ℓ_{eh}	θ
		in. ²	in. ²			in.	in.	in.		°
195	2	1.20	4.5	0.267	0.356	25.5	28.54	28.60	1.15	49.0
196	2	1.20	4.5	0.267	0.356	25.5	28.54	30.19	0.87	39.3
197	2	0.80	4.5	0.178	0.267	25.5	28.54	29.83	1.15	47.8
198	2	1.86	8	0.233	0.388	35.15	38.15	38.26	1.34	53.2
199	2	3.72	8	0.465	0.620	35.15	38.15	38.90	1.44	54.7
200	2	1.86	8	0.233	0.388	33.65	38.15	39.96	1.09	46.3
201	2	3.72	8	0.465	0.620	33.65	38.15	40.90	1.12	46.4

Table B.4 Cont. Detailed properties and test results for hooked bar specimens having widely-spaced bars with confining reinforcement tested at the University of Kansas

SN	T	T_h ^[1]	T/T_h	f_{su}	$f_{su}/f_{s,calc}$ ^[2]	$f_{su}/f_{s,calc}$ ^[3]
	lb	lb		ksi		
195	293900	247326	1.19	130.6	1.33	1.52
196	268500	298033	0.90	119.3	0.99	1.13
197	235300	206333	1.14	104.6	1.26	1.38
198	358200	365269	0.98	89.6	1.17	1.34
199	445000	440211	1.01	111.3	1.52	1.74
200	371400	386914	0.96	92.9	1.13	1.29
201	427900	475138	0.90	107.0	1.31	1.49

^[1] Based on descriptive equations, Eq. (4.5) and (4.7)

^[2] Based on design equation, Eq. (6.18), using full expression for ψ_r , Eq. (6.14)

^[3] Based on design equation, Eq. (6.18), using simplified expression for ψ_r , Eq. (6.15)

Table B.5 Detailed properties and test results for hooked bar specimens having closely-spaced bars with confining reinforcement tested at the University of Kansas

SN	ID	<i>b</i>	<i>h</i>	$\ell_{eh,avg}$	f_{cm}	d_b	A_b	<i>s</i>	<i>s/d_b</i>
		in.	in.	in.	psi	in.	in. ²	in.	
202	(3@6) 5-8-90-5#3-i-2.5-2-6.25	12.8	7.5	5.5	10110	0.625	0.31	3.6	5.8
203	(3@4) 5-8-90-5#3-i-2.5-2-6	10.9	8.1	6.1	6700	0.625	0.31	2.6	4.2
204	(3@6) 5-8-90-5#3-i-2.5-2-6	13.4	8.0	6.0	6700	0.625	0.31	3.9	6.2
205	(3) 5-5-90-5#3-i-2.5-2-8	12.8	9.8	7.8	4660	0.625	0.31	3.6	5.8
206	(4@4) 5-5-90-5#3-i-2.5-2-7	12.6	9.1	7.1	6430	0.625	0.31	2.3	3.7
207	(4@4) 5-5-90-5#3-i-2.5-2-6	13.0	8.3	6.3	6430	0.625	0.31	2.5	3.9
208	(4@4) 5-8-90-5#3-i-2.5-2-6	13.1	8.0	6.0	6700	0.625	0.31	2.5	4.0
209	(4@6) 5-8-90-5#3-i-2.5-2-6	17.4	8.0	6.0	6690	0.625	0.31	3.9	6.3
210	(3@6) 5-8-90-5#3-i-3.5-2-6.25	12.9	8.3	6.3	10110	0.625	0.31	3.6	5.8
211*	(4@4) 5-5-90-2#3-i-2.5-2-6	13.1	8.3	6.3	6430	0.625	0.31	2.5	4.0
212*	(4@4) 5-5-90-2#3-i-2.5-2-8	13.1	10.0	8.0	6430	0.625	0.31	2.5	4.0
213	(3@5.5) 8-5-90-5#3-i-2.5-2-8	16.6	10.0	8	6620	1	0.79	5.3	5.3
214	(3@5.5) 8-5-90-5#3-i-2.5-2-12	16.8	14.2	12.2	6620	1	0.79	5.4	5.4
215	(3@5.5) 8-5-90-5#3-i-2.5-2-12(1)	16.8	14.0	12	5660	1	0.79	5.4	5.4
216	(3@5.5) 8-5-90-5#3-i-2.5-2-8(2)	17.0	10.2	8.2	5730	1	0.79	5.5	5.5
217	(3@3) 8-5-90-5#3-i-2.5-2-10	12.3	11.9	9.9	4810	1	0.79	3.1	3.1
218	(3@5) 8-5-90-5#3-i-2.5-2-10	16.0	11.9	9.9	4850	1	0.79	5.0	5.0
219	(3@3) 8-12-90-5#3-i-2.5-2-12	12.0	13.8	11.8	11040	1	0.79	3.0	3.0
220	(3@4) 8-12-90-5#3-i-2.5-2-12	13.8	14.3	12.3	11440	1	0.79	3.9	3.9

* Specimens not used to develop descriptive equations, Eq. (4.5) and (4.7)

Table B.5 Cont. Detailed properties and test results for hooked bar specimens having closely-spaced bars with confining reinforcement tested at the University of Kansas

SN	<i>n</i>	A_{th}	A_{hs}	A_{th}/A_{hs}	$A_{th,ACI}/A_{hs}$	h_{cl}	x_{mid}	d_{eff}	d_{eff}/ℓ_{eh}	θ
		in. ²	in. ²			in.	in.	in.		°
202	3	0.66	0.93	0.710	1.183	5.25	9.44	6.33	1.15	59.8
203	3	0.66	0.93	0.710	1.183	5.25	9.44	7.61	1.25	57.1
204	3	0.66	0.93	0.710	1.183	5.25	9.44	7.25	1.21	57.6
205	3	0.66	0.93	0.710	1.183	5.25	9.44	7.65	0.98	50.4
206	4	0.66	1.24	0.532	0.887	5.25	9.44	7.41	1.04	53.0
207	4	0.66	1.24	0.532	0.887	5.25	9.44	7.25	1.15	56.3
208	4	0.66	1.24	0.532	0.887	5.25	9.44	7.31	1.22	57.6
209	4	0.66	1.24	0.532	0.887	5.25	9.44	6.85	1.14	57.6
210	3	0.66	0.93	0.710	1.183	5.25	9.44	6.72	1.07	56.3
211*	4	0.22	1.24	0.177	0.355	5.25	9.44	6.89	1.09	56.3
212*	4	0.22	1.24	0.177	0.355	5.25	9.44	7.24	0.91	49.7
213	3	0.66	2.37	0.278	0.464	10	14.19	11.66	1.46	60.6
214	3	0.66	2.37	0.278	0.464	10	14.19	12.92	1.06	49.3
215	3	0.66	2.37	0.278	0.464	10	14.19	12.32	1.03	49.8
216	3	0.66	2.37	0.278	0.464	10	14.19	12.28	1.50	60.0
217	3	0.66	2.37	0.278	0.464	10	14.19	13.50	1.36	55.1
218	3	0.66	2.37	0.278	0.464	10	14.19	13.45	1.36	55.1
219	3	0.66	2.37	0.278	0.464	10	14.19	12.55	1.06	50.2
220	3	0.66	2.37	0.278	0.464	10	14.19	12.24	1.00	49.1

* Specimens not used to develop descriptive equations, Eq. (4.5) and (4.7)

Table B.5 Cont. Detailed properties and test results for hooked bar specimens having closely-spaced bars with confining reinforcement tested at the University of Kansas

SN	T	T_h ^[1]	T/T_h	f_{su}	$f_{su}/f_{s,calc}$ ^[2]	$f_{su}/f_{s,calc}$ ^[3]
	lb	lb		ksi		
202	25830	29941	0.86	83.3	1.18	1.18
203	34889	27808	1.25	112.5	1.59	1.59
204	36448	30166	1.21	117.6	1.69	1.69
205	33260	33941	0.98	107.3	1.30	1.30
206	27114	28656	0.95	87.5	1.07	1.07
207	25898	26045	0.99	83.5	1.16	1.16
208	27493	25287	1.09	88.7	1.27	1.27
209	28300	28090	1.01	91.3	1.31	1.31
210	35268	33525	1.05	113.8	1.41	1.41
211*	21405	22360	0.96	69.0	0.95	0.95
212*	26017	28553	0.91	83.9	0.91	0.91
213	37126	46151	0.80	47.0	1.03	1.03
214	66094	67203	0.98	83.7	1.20	1.20
215	47851	63818	0.75	60.6	0.92	0.92
216	47994	46091	1.04	60.8	1.34	1.34
217	47276	46460	1.02	59.8	1.15	1.15
218	61305	51010	1.20	77.6	1.48	1.48
219	62206	65470	0.95	78.7	1.03	1.03
220	64940	71784	0.90	82.2	1.02	1.02

* Specimens not used to develop descriptive equations, Eq. (4.5) and (4.7)

^[1] Based on descriptive equations, Eq. (4.5) and (4.7)

^[2] Based on design equation, Eq. (6.18), using full expression for ψ_r , Eq. (6.14)

^[3] Based on design equation, Eq. (6.18), using simplified expression for ψ_r , Eq. (6.15)

Table B.5 Cont. Detailed properties and test results for hooked bar specimens having closely-spaced bars with confining reinforcement tested at the University of Kansas

SN	ID	<i>b</i>	<i>h</i>	$\ell_{eh,avg}$	f_{cm}	d_b	A_b	<i>s</i>	<i>s/d_b</i>
		in.	in.	in.	psi	in.	in. ²	in.	
221	(3@5) 8-12-90-5#3-i-2.5-2-12	16.0	14.2	12.2	11460	1	0.79	5.0	5.0
222	(3@5) 8-5-180-5#3-i-2.5-2-10	15.8	11.7	9.7	5540	1	0.79	4.9	4.9
223*	(2@3) 8-5-90-2#3-i-2.5-2-10	9.3	12.3	10.3	4760	1	0.79	3.3	3.3
224*	(2@5) 8-5-90-2#3-i-2.5-2-10	10.9	11.8	9.8	4760	1	0.79	4.9	4.9
225*	(2@3) 8-5-90-5#3-i-2.5-2-10	9.0	12.3	10.3	4805	1	0.79	3	3.0
226*	(2@5) 8-5-90-5#3-i-2.5-2-10	11.3	11.7	9.7	4805	1	0.79	5.3	5.3
227*	(3@5.5) 8-5-90-2#3-i-2.5-2-14	17.0	16.4	14.4	6460	1	0.79	5.5	5.5
228*	(3@5.5) 8-5-90-2#3-i-2.5-2-8.5	16.6	11.1	9.1	6460	1	0.79	5.3	5.3
229*	(3@5.5) 8-5-90-2#3-i-2.5-2-14(1)	16.6	16.9	14.9	5450	1	0.79	5.3	5.3
230*	(3@5.5) 8-5-90-2#3-i-2.5-2-8.5(1)	16.6	10.2	8.2	5450	1	0.79	5.3	5.3
231*	(3@5) 8-5-90-2#3-i-2.5-2-10	15.8	12.5	10.5	4760	1	0.79	4.9	4.9
232*	(3@5) 8-5-180-2#3-i-2.5-2-10	16.4	11.7	9.7	5400	1	0.79	5.2	5.2
233	(3@3.75) 11-8-90-6#3-i-2.5-2-21	17.6	22.0	20	7070	1.41	1.56	5.6	4.0
234	(3@3.75) 11-12-90-6#3-i-2.5-2-19	17.2	20.3	18.3	11960	1.41	1.56	5.4	3.8
235	(3@3.75) 11-12-180-6#3-i-2.5-2-19	17.0	20.8	18.8	12190	1.41	1.56	5.3	3.8
236*	(3@3.75) 11-8-90-2#3-i-2.5-2-23	17.4	24.0	22	7070	1.41	1.56	5.5	3.9
237*	(3@3.75) 11-12-90-2#3-i-2.5-2-21	17.4	23.0	21	11850	1.41	1.56	5.5	3.9
238	H14-8	20.7	37.8	36.6	6650	1.693	2.25	6	3.5

* Specimens not used to develop descriptive equations, Eq. (4.5) and (4.7)

Table B.5 Cont. Detailed properties and test results for hooked bar specimens having closely-spaced bars with confining reinforcement tested at the University of Kansas

SN	n	A_{th}	A_{hs}	A_{th}/A_{hs}	$A_{th,ACI}/A_{hs}$	h_{cl}	x_{mid}	d_{eff}	d_{eff}/ℓ_{eh}	θ
		in. ²	in. ²			in.	in.	in.		°
221	3	0.66	2.37	0.278	0.464	10	14.19	11.92	0.98	49.3
222	3	0.66	2.37	0.278	0.464	10	14.19	13.07	1.35	55.6
223*	2	0.22	1.58	0.139	0.278	10	14.19	13.06	1.27	54.0
224*	2	0.44	1.58	0.278	0.278	10	14.19	12.71	1.30	55.4
225*	2	0.66	1.58	0.418	0.696	10	14.19	13.89	1.35	54.0
226*	2	0.66	1.58	0.418	0.696	10	14.19	12.99	1.34	55.6
227*	3	0.22	2.37	0.093	0.186	10	14.19	12.53	0.87	44.6
228*	3	0.22	2.37	0.093	0.186	10	14.19	11.85	1.30	57.3
229*	3	0.22	2.37	0.093	0.186	10	14.19	13.28	0.89	43.6
230*	3	0.22	2.37	0.093	0.186	10	14.19	11.62	1.42	60.0
231*	3	0.22	2.37	0.093	0.186	10	14.19	12.58	1.20	53.5
232*	3	0.22	2.37	0.093	0.186	10	14.19	12.63	1.30	55.6
233	3	0.66	4.68	0.141	0.282	19.5	23.69	24.02	1.20	49.8
234	3	0.66	4.68	0.141	0.282	19.5	23.69	22.62	1.24	52.3
235	3	0.66	4.68	0.141	0.282	19.5	23.69	22.61	1.20	51.6
236*	3	0.22	4.68	0.047	0.094	19.5	23.69	24.30	1.10	47.1
237*	3	0.22	4.68	0.047	0.094	19.5	23.69	22.86	1.09	48.4
238	3	1.86	6.75	0.276	0.367	24.0	28.54	34.70	0.95	38.0

* Specimens not used to develop descriptive equations, Eq. (4.5) and (4.7)

Table B.5 Cont. Detailed properties and test results for hooked bar specimens having closely-spaced bars with confining reinforcement tested at the University of Kansas

SN	T	T_h ^[1]	T/T_h	f_{su}	$f_{su}/f_{s,calc}$ ^[2]	$f_{su}/f_{s,calc}$ ^[3]
	lb	lb		ksi		
221	64761	75205	0.86	82.0	1.03	1.03
222	58669	51317	1.14	74.3	1.40	1.40
223*	46810	43348	1.08	59.3	1.20	1.27
224*	48515	50120	0.97	61.4	1.19	1.38
225*	57922	52734	1.10	73.3	1.35	1.35
226*	55960	56281	0.99	70.8	1.38	1.38
227*	57261	70966	0.81	72.5	0.89	1.07
228*	40885	43795	0.93	51.8	1.00	1.24
229*	65336	69653	0.94	82.7	1.02	1.27
230*	32368	37767	0.86	41.0	0.92	1.14
231*	44668	45946	0.97	56.5	1.08	1.35
232*	51501	44411	1.16	65.2	1.25	1.56
233	111288	120200	0.93	71.3	1.04	1.18
234	118300	124742	0.95	75.8	1.08	1.21
235	119045	128284	0.93	76.3	1.06	1.18
236*	119045	122782	0.97	74.7	1.31	1.47
237*	119045	134402	0.89	81.9	1.33	1.48
238	298200	258627	1.15	132.5	1.27	1.24

* Specimens not used to develop descriptive equations, Eq. (4.5) and (4.7)

^[2] Based on design equation, Eq. (6.18), using full expression for ψ_r , Eq. (6.14)

^[3] Based on design equation, Eq. (6.18), using simplified expression for ψ_r , Eq. (6.15)

Table B.6 Detailed properties and test results for hooked bar specimens with bars placed outside column longitudinal reinforcement (column core) tested at the University of Kansas

SN*	ID	<i>b</i>	<i>h</i>	$\ell_{eh,avg}$	f_{cm}	d_b	A_b	<i>s</i>	<i>s/d_b</i>
		in.	in.	in.	psi	in.	in. ²	in.	
239	5-5-90-0-o-1.5-2-5	9.8	7.0	5.0	4930	0.63	0.31	6.2	9.8
240	5-5-90-0-o-2.5-2-5	11.4	6.8	4.8	4930	0.63	0.31	5.8	9.2
241	5-5-90-0-o-1.5-2-6.5	9.6	8.2	6.2	5650	0.63	0.31	6.0	9.5
242	5-5-90-0-o-1.5-2-8	9.6	9.9	7.9	5650	0.63	0.31	6.0	9.5
243	5-5-90-0-o-2.5-2-8	11.6	11.0	9.0	5780	0.63	0.31	6.0	9.5
244	5-5-180-0-o-1.5-2-9.5	9.4	11.4	9.4	4420	0.63	0.31	5.8	9.2
245	5-5-180-0-o-2.5-2-9.5	11.6	11.5	9.5	4520	0.63	0.31	6.0	9.5
246	5-5-180-0-o-1.5-2-11.25	9.6	13.3	11.3	4520	0.63	0.31	6.0	9.5
247	5-5-180-2#3-o-2.5-2-9.5	11.9	11.2	9.2	4420	0.63	0.31	6.3	10.0
248	5-5-180-2#3-o-1.5-2-11.25	9.9	13.6	11.6	4420	0.63	0.31	6.3	10.0
249	5-5-180-2#3-o-1.5-2-9.5	9.9	10.8	8.8	4520	0.63	0.31	6.3	10.0
250	5-5-180-2#3-o-2.5-2-11.25	11.9	13.3	11.3	4520	0.63	0.31	6.3	10.0
251	5-5-90-5#3-o-1.5-2-5	9.8	7.0	5.0	5205	0.63	0.31	6.2	9.8
252	5-5-90-5#3-o-2.5-2-5	11.9	7.2	5.2	4930	0.63	0.31	6.3	10.0
253	5-5-90-5#3-o-1.5-2-8	9.7	9.9	7.9	5650	0.63	0.31	6.1	9.7
254	5-5-90-5#3-o-2.5-2-8	11.8	9.5	7.5	5650	0.63	0.31	6.2	9.8
255	5-5-90-5#3-o-1.5-2-6.5	9.8	8.5	6.5	5780	0.63	0.31	6.2	9.8

* No specimen used in developing descriptive equations, Eq. (4.5) and (4.7)

Table B.6 Cont. Detailed properties and test results for hooked bar specimens with bars placed outside column longitudinal reinforcement (column core) tested at the University of Kansas

SN*	<i>n</i>	A_{th}	A_{hs}	A_{th}/A_{hs}	$A_{th,ACI}/A_{hs}$	h_{cl}	x_{mid}	d_{eff}	d_{eff}/ℓ_{eh}	θ
		in. ²	in. ²			in.	in.	in.		°
239	2	0	0.62	0	0	5.25	9.44	6.10	1.22	62.1
240	2	0	0.62	0	0	5.25	9.44	6.25	1.30	63.0
241	2	0	0.62	0	0	5.25	9.44	6.25	1.01	56.7
242	2	0	0.62	0	0	5.25	9.44	6.54	0.83	50.1
243	2	0	0.62	0	0	5.25	9.44	6.45	0.72	46.4
244	2	0	0.62	0	0	5.25	9.44	7.26	0.77	45.1
245	2	0	0.62	0	0	5.25	9.44	6.89	0.72	44.8
246	2	0	0.62	0	0	5.25	9.44	7.38	0.65	39.9
247	2	0.22	0.62	0.350	0.583	5.25	9.44	7.16	0.78	45.7
248	2	0.22	0.62	0.350	0.583	5.25	9.44	8.04	0.69	39.1
249	2	0.22	0.62	0.350	0.583	5.25	9.44	6.54	0.74	47.0
250	2	0.22	0.62	0.350	0.583	5.25	9.44	7.49	0.66	39.9
251	2	0.66	0.62	1.060	1.767	5.25	9.44	6.52	1.30	62.1
252	2	0.66	0.62	1.060	1.767	5.25	9.44	6.37	1.23	61.1
253	2	0.66	0.62	1.060	1.767	5.25	9.44	6.65	0.84	50.1
254	2	0.66	0.62	1.060	1.767	5.25	9.44	6.39	0.85	51.5
255	2	0.66	0.62	1.060	1.767	5.25	9.44	6.43	0.99	55.4

* No specimen used in developing descriptive equations, Eq. (4.5) and (4.7)

Table B.6 Cont. Detailed properties and test results for hooked bar specimens with bars placed outside column longitudinal reinforcement (column core) tested at the University of Kansas

SN*	<i>T</i>	<i>T_h</i> ^[1]	<i>T/T_h</i> ^[2]	<i>f_{su}</i>	<i>f_{su}/f_{s,calc}</i> ^[3]	<i>f_{su}/f_{s,calc}</i> ^[4]
	lb	lb		ksi		
239	14100	16942	0.97	45.5	1.10	1.10
240	19300	16194	1.39	62.3	1.56	1.56
241	17800	22333	0.93	57.4	1.08	1.08
242	22800	29200	0.91	73.5	1.08	1.08
243	26100	33947	0.90	84.2	1.08	1.08
244	29500	33034	1.04	95.2	1.25	1.25
245	30100	33634	1.05	97.1	1.26	1.26
246	32400	40752	0.93	104.5	1.14	1.14
247	35500	36556	1.14	114.5	1.39	1.39
248	43100	45987	1.10	139.0	1.33	1.33
249	20300	35202	0.67	65.5	0.82	0.82
250	42300	45051	1.10	136.5	1.34	1.34
251	21800	30222	0.84	70.3	1.50	1.50
252	22500	30713	0.86	72.6	1.51	1.51
253	25100	42221	0.70	81.0	1.07	1.07
254	24900	40589	0.72	80.3	1.12	1.12
255	21700	36703	0.69	70.0	1.12	1.12

* No specimen used in developing descriptive equations, Eq. (4.5) and (4.7)

[1] Based on descriptive equations, Eq. (4.5) and (4.7)

[2] Bar location factor of 1.17 applied

[3] Based on design equation, Eq. (6.18), using full expression for ψ_r , Eq. (6.14)

[4] Based on design equation, Eq. (6.18), using simplified expression for ψ_r , Eq. (6.15)

Table B.6 Cont. Detailed properties and test results for hooked bar specimens with bars placed outside column longitudinal reinforcement (column core) tested at the University of Kansas

SN*	ID	<i>b</i>	<i>h</i>	$\ell_{eh,avg}$	f_{cm}	d_b	A_b	<i>s</i>	<i>s/d_b</i>
		in.	in.	in.	psi	in.	in. ²	in.	
256	8-5-90-0-o-2.5-2-10a	15.0	12.4	10.4	5270	1	0.79	9.0	9.0
257	8-5-90-0-o-2.5-2-10b	15.0	11.8	9.8	5440	1	0.79	9.0	9.0
258	8-5-90-0-o-2.5-2-10c	15.0	12.6	10.6	5650	1	0.79	9.0	9.0
259	8-8-90-0-o-2.5-2-8	14.0	10.4	8.4	8740	1	0.79	8.0	8.0
260	8-8-90-0-o-3.5-2-8	16.8	9.8	7.8	8810	1	0.79	8.8	8.8
261	8-8-90-0-o-4-2-8	17.8	10.2	8.2	8630	1	0.79	8.8	8.8
262	8-5-90-5#3-o-2.5-2-10a	15.1	12.4	10.4	5270	1	0.79	9.1	9.1
263	8-5-90-5#3-o-2.5-2-10b	15.1	12.5	10.5	5440	1	0.79	9.1	9.1
264	8-5-90-5#3-o-2.5-2-10c	15.1	12.9	10.9	5650	1	0.79	9.1	9.1
265	8-8-90-5#3-o-2.5-2-8	14.5	10.5	8.5	8630	1	0.79	8.5	8.5
266	8-8-90-5#3-o-3.5-2-8	16.7	9.9	7.9	8810	1	0.79	8.7	8.7
267	8-8-90-5#3-o-4-2-8	18.2	10.3	8.3	8740	1	0.79	9.2	9.2
268	11-8-90-0-o-2.5-2-25	18.5	27.2	25.2	9460	1.41	1.56	12.1	8.6
269	11-8-90-0-o-2.5-2-17	18.8	18.6	16.6	9460	1.41	1.56	12.4	8.8
270	11-12-180-0-o-2.5-2-17	18.4	19.1	17.1	11800	1.41	1.56	12.0	8.5
271	11-12-90-0-o-2.5-2-17	18.8	18.9	16.9	11800	1.41	1.56	12.4	8.8
272	11-8-90-6#3-o-2.5-2-22	18.4	23.9	21.9	9120	1.41	1.56	12.0	8.5
273	11-8-90-6#3-o-2.5-2-16	18.4	18.2	16.2	9420	1.41	1.56	12.0	8.5
274	11-12-180-6#3-o-2.5-2-17	18.4	18.5	16.5	11800	1.41	1.56	12.0	8.5
275	11-12-90-6#3-o-2.5-2-17	18.7	18.4	16.4	11800	1.41	1.56	12.3	8.7

* No specimen used in developing descriptive equations, Eq. (4.5) and (4.7)

Table B.6 Cont. Detailed properties and test results for hooked bar specimens with bars placed outside column longitudinal reinforcement (column core) tested at the University of Kansas

SN*	<i>n</i>	A_{th}	A_{hs}	A_{th}/A_{hs}	$A_{th,ACI}/A_{hs}$	h_{cl}	x_{mid}	d_{eff}	d_{eff}/ℓ_{eh}	θ
		in. ²	in. ²			in.	in.	in.		°
256	2	0	1.58	0	0	10.00	14.19	11.60	1.12	53.8
257	2	0	1.58	0	0	10.00	14.19	11.25	1.15	55.4
258	2	0	1.58	0	0	10.00	14.19	12.03	1.13	53.2
259	2	0	1.58	0	0	10.00	14.19	10.98	1.31	59.4
260	2	0	1.58	0	0	10.00	14.19	10.88	1.39	61.2
261	2	0	1.58	0	0	10.00	14.19	10.88	1.33	60.0
262	2	0.66	1.58	0.420	0.700	10.00	14.19	12.04	1.16	53.8
263	2	0.66	1.58	0.420	0.700	10.00	14.19	12.42	1.18	53.5
264	2	0.66	1.58	0.420	0.700	10.00	14.19	12.07	1.11	52.5
265	2	0.66	1.58	0.420	0.700	10.00	14.19	11.68	1.37	59.1
266	2	0.66	1.58	0.420	0.700	10.00	14.19	11.35	1.44	60.9
267	2	0.66	1.58	0.420	0.700	10.00	14.19	10.89	1.31	59.7
268	2	0	3.12	0	0	19.50	23.69	23.11	0.92	43.2
269	2	0	3.12	0	0	19.50	23.69	21.68	1.31	55.0
270	2	0	3.12	0	0	19.50	23.69	20.89	1.22	54.2
271	2	0	3.12	0	0	19.50	23.69	21.22	1.26	54.5
272	2	0.66	3.12	0.210	0.350	19.50	23.69	23.17	1.06	47.2
273	2	0.66	3.12	0.210	0.350	19.50	23.69	22.36	1.38	55.6
274	2	0.66	3.12	0.210	0.350	19.50	23.69	21.39	1.30	55.1
275	2	0.66	3.12	0.210	0.350	19.50	23.69	21.40	1.31	55.3

* No specimen used in developing descriptive equations, Eq. (4.5) and (4.7)

Table B.6 Cont. Detailed properties and test results for hooked bar specimens with bars placed outside column longitudinal reinforcement (column core) tested at the University of Kansas

SN [*]	<i>T</i>	<i>T_h</i> ^[1]	<i>T/T_h</i> ^[2]	<i>f_{su}</i>	<i>f_{su}/f_{s,calc}</i> ^[3]	<i>f_{su}/f_{s,calc}</i> ^[4]
	lb	lb		ksi		
256	42300	47338	1.05	53.5	1.22	1.22
257	33700	44723	0.88	42.7	1.02	1.02
258	56000	49301	1.33	70.9	1.56	1.56
259	33000	43084	0.90	41.8	1.04	1.04
260	35900	39781	1.06	45.4	1.21	1.21
261	37500	41801	1.05	47.5	1.21	1.21
262	54300	65444	0.97	68.7	1.41	1.41
263	65600	66376	1.16	83.0	1.67	1.67
264	57700	68953	0.98	73.0	1.40	1.40
265	58000	61602	1.10	73.4	1.63	1.63
266	55000	58452	1.10	69.6	1.65	1.65
267	39100	60622	0.75	49.5	1.12	1.12
268	174700	172174	1.19	112.0	1.52	1.52
269	107200	108489	1.16	68.7	1.42	1.42
270	83500	119293	0.82	53.5	1.01	1.01
271	105400	117750	1.05	67.6	1.30	1.30
272	170200	168581	1.18	109.1	1.55	1.55
273	136800	128155	1.25	87.7	1.67	1.67
274	113100	137350	0.96	72.5	1.28	1.28
275	115900	136582	0.99	74.3	1.32	1.32

* No specimen used in developing descriptive equations, Eq. (4.5) and (4.7)

[1] Based on descriptive equations, Eq. (4.5) and (4.7)

[2] Bar location factor of 1.17 applied

[3] Based on design equation, Eq. (6.18), using full expression for ψ_r , Eq. (6.14)

[4] Based on design equation, Eq. (6.18), using simplified expression for ψ_r , Eq. (6.15)

Table B.7 Detailed properties and test results for hooked bar specimens with effective beam depth to embedment ratio $d_{eff}/\ell_{eh} > 1.5$ tested at the University of Kansas

SN*	ID	b	h	$\ell_{eh,avg}$	f_{cm}	d_b	A_b	s	s/d_b
		in.	in.	in.	psi	in.	in. ²	in.	
276	8-5-90-5#3-i-2.5-2-8	16.0	9.6	7.6	5240	1	0.79	10	10.0
277	8-8-90-5#3-i-2.5-2-8	15.5	9.3	7.3	8290	1	0.79	9.5	9.5
278	(3@5.5) 8-5-90-5#3-i-2.5-2-8(1)	16.2	9.6	7.6	5660	1	0.79	5.1	5.1
279	11-15-90-0-i-2.5-2-10	20.9	11.5	9.5	14050	1.41	1.56	15.0	10.6
280	11-5-90-2#3-i-2.5-2-14	21.1	15.6	13.6	4910	1.41	1.56	14.7	10.4
281	11-15-90-2#3-i-2.5-2-10	21.2	12.0	10.0	14045	1.41	1.56	14.8	10.5
282	11-5-90-2#3-i-3.5-2-14	23.1	15.9	13.9	4910	1.41	1.56	14.7	10.4
283	(2@7.5) 11-12-90-6#3-i-2.5-2-14a	16.9	15.6	13.6	11960	1.41	1.56	10.5	7.4
284	11-15-90-6#3-i-2.5-2-10a	21.2	11.8	9.8	14045	1.41	1.56	14.8	10.5
285	11-15-90-6#3-i-2.5-2-10b	20.8	11.6	9.6	14050	1.41	1.56	14.4	10.2

* No specimen used in developing descriptive equations, Eq. (4.5) and (4.7)

Table B.7 Cont. Detailed properties and test results for hooked bar specimens with effective beam depth to embedment ratio $d_{eff}/\ell_{eh} > 1.5$ tested at the University of Kansas

SN*	n	A_{th}	A_{hs}	A_{th}/A_{hs}	$A_{th,ACI}/A_{hs}$	h_{cl}	x_{mid}	d_{eff}	d_{eff}/ℓ_{eh}	θ
		in. ²	in. ²			in.	in.	in.		°
276	2	0.66	1.58	0.418	0.696	10.00	14.19	11.69	1.54	61.8
277	2	0.66	1.58	0.418	0.696	10.00	14.19	11.42	1.56	62.8
278	3	0.66	2.37	0.278	0.464	10.00	14.19	11.57	1.52	61.8
279	2	0	3.12	0	0	19.5	23.69	20.13	2.12	68.1
280	2	0.22	3.12	0.071	0.118	19.5	23.69	21.68	1.59	60.1
281	2	0.22	3.12	0.071	0.118	19.5	23.69	20.28	2.03	67.1
282	2	0.22	3.12	0.071	0.118	19.5	23.69	21.62	1.56	59.6
283	2	0.66	3.12	0.212	0.353	19.5	23.69	21.33	1.57	60.1
284	2	0.66	3.12	0.212	0.353	19.5	23.69	20.50	2.09	67.5
285	2	0.66	3.12	0.212	0.353	19.5	23.69	20.44	2.13	67.9

* No specimen used in developing descriptive equations, Eq. (4.5) and (4.7)

Table B.7 Cont. Detailed properties and test results for hooked bar specimens with effective beam depth to embedment ratio $d_{eff}/\ell_{eh} > 1.5$ tested at the University of Kansas

SN [*]	<i>T</i>	<i>T_h</i> ^[1]	<i>T/T_h</i>	<i>f_{su}</i>	<i>f_{su}/f_{s,calc}</i> ^[2]	<i>f_{su}/f_{s,calc}</i> ^[3]
	lb	lb		ksi		
276	47478	51412	0.92	60.1	1.47	1.47
277	50266	54351	0.92	63.6	1.44	1.44
278	31369	42379	0.74	39.7	0.95	0.95
279	51481	65385	0.79	33.0	0.94	0.94
280	77422	79990	0.97	49.6	1.15	1.28
281	63940	76811	0.83	41.0	1.00	1.11
282	82275	81759	1.01	52.7	1.20	1.33
283	102038	115789	0.88	65.4	1.22	1.22
284	82681	90512	0.91	53.0	1.31	1.31
285	75579	88993	0.85	48.4	1.23	1.23

* No specimen used in developing descriptive equations, Eq. (4.5) and (4.7)

[1] Based on descriptive equations, Eq. (4.5) and (4.7)

[2] Based on design equation, Eq. (6.18), using full expression for ψ_r , Eq. (6.14)

[3] Based on design equation, Eq. (6.18), using simplified expression for ψ_r , Eq. (6.15)

B.4 SPECIMENS TESTED IN OTHER STUDIES

This section presents the specimens tested outside the University of Kansas, including those by Marques and Jirsa (1975), Pinc et al (1977), Hamad et al. (1993), Ramirez and Russel (2008), Lee and Park (2010), and Chun et al. (2017b), as tabulated in Table B.8. A few of these specimens were used in developing the descriptive equations, Eq. (4.5) and (4.7), which are identified here.

Table B.8 Detailed properties and test results for hooked bar specimens tested outside the University of Kansas

Study	SN	ID	b	h	$\ell_{eh,avg}$	f_{cm}	d_b	A_b	s	s/d_b
			in.	in.	in.	psi	in.	in. ²	in.	
Marques and Jirsa (1975)	286	J7-180-12-1-H	12.0	12.0	10.0	4350	0.875	0.6	5.3	6.1
	287	J7-180-15-1-H	12.0	15.0	13.0	4000	0.875	0.6	5.3	6.1
	288	J7-90-12-1-H	12.0	12.0	10.0	4150	0.875	0.6	5.3	6.1
	289	J7-90-15-1-H	12.0	15.0	13.0	4600	0.875	0.6	5.3	6.1
	290	J7-90-15-1-L	12.0	15.0	13.0	4800	0.875	0.6	5.3	6.1
	291	J7-90-15-1-M	12.0	15.0	13.0	5050	0.875	0.6	5.3	6.1
	292	J11-180-15-1-H	12.0	15.0	13.1	4400	1.41	1.56	4.8	3.4
	293	J11-90-12-1-H	12.0	12.0	10.1	4600	1.41	1.56	4.8	3.4
	294	J11-90-15-1-H	12.0	15.0	13.1	4900	1.41	1.56	4.8	3.4
	295	J11-90-15-1-L	12.0	15.0	13.1	4750	1.41	1.56	4.8	3.4
	296	J7-90-15-3a-H	12.0	15.0	13.0	3750	0.875	0.6	5.3	6.1
	297	J7-90-15-3-H	12.0	15.0	13.0	4650	0.875	0.6	5.3	6.1
	298	J11-90-15 -3a-L	12.0	15.0	13.1	5000	1.41	1.56	4.8	3.4
	299	J11-90-15-3-L	12.0	15.0	13.1	4850	1.41	1.56	4.8	3.4
Pinc et al. (1977)	300	9-12	12.0	12.0	10.0	4700	1.13	1	5.1	4.5
	301	11-15	12.0	15.0	13.1	5400	1.41	1.56	4.8	3.4
	302	11-18	12.0	18.0	16.1	4700	1.41	1.56	4.8	3.4

Table B.8 Cont. Detailed properties and test results for hooked bar specimens tested outside the University of Kansas

Study	SN	n	A_{th}	A_{hs}	A_{th}/A_{hs}	$A_{th,ACI}/A_{hs}$	h_{cl}	x_{mid}	d_{eff}	d_{eff}/ℓ_{eh}	θ
			in. ²	in. ²			in.	in.	in.		°
Marques and Jirsa (1975)	286	2	0	1.20	0	0	11.25	14.25	13.48	1.35	55.4
	287	2	0	1.20	0	0	11.25	14.25	14.51	1.12	48.1
	288	2	0	1.20	0	0	11.25	14.25	13.59	1.36	55.4
	289	2	0	1.20	0	0	11.25	14.25	14.34	1.10	48.1
	290	2	0	1.20	0	0	11.25	14.25	14.44	1.11	48.1
	29	2	0	1.20	0	0	11.25	14.25	14.42	1.11	48.1
	292	2	0	3.12	0	0	11.25	14.25	15.02	1.15	47.4
	293	2	0	3.12	0	0	11.25	14.25	14.66	1.45	54.7
	294	2	0	3.12	0	0	11.25	14.25	14.97	1.14	47.4
	295	2	0	3.12	0	0	11.25	14.25	15.37	1.17	47.4
	296	2	0.44	1.20	0.367	0.917	11.25	14.25	14.81	1.14	47.6
	297	2	0.22	1.20	0.183	0.367	11.25	14.25	14.47	1.11	47.6
	298	2	0.88	3.12	0.282	0.564	11.25	14.25	16.53	1.26	47.4
	299	2	0.44	3.12	0.141	0.282	11.25	14.25	16.09	1.23	47.4
Pinc et al. (1977)	300	2	0	2.00	0	0	11.25	14.25	13.66	1.37	54.9
	301	2	0	3.12	0	0	11.25	14.25	14.88	1.14	47.4
	302	2	0	3.12	0	0	11.25	14.25	15.88	0.99	41.5

Table B.8 Cont. Detailed properties and test results for hooked bar specimens tested outside the University of Kansas

Study	SN	T	T_h ^[1]	T/T_h	f_{su}	$f_{su}/f_{s,calc}$ ^[2]	$f_{su}/f_{s,calc}$ ^[3]
		lb	lb		ksi		
Marques and Jirsa (1975)	286	36600	39236	0.93	61.0	1.08	1.08
	287	52200	51230	1.02	87.0	1.21	1.21
	288	37200	38721	0.96	62.0	1.11	1.11
	289	54600	53281	1.02	91.0	1.22	1.22
	290	58200	53922	1.08	97.0	1.29	1.29
	291	60000	54697	1.10	100.0	1.31	1.31
	292	70200	49787	1.41	45.0	1.78	1.78
	293	65520	37873	1.73	42.0	2.13	2.13
	294	74880	50255	1.49	48.0	1.84	1.84
	295	81120	51019	1.59	52.0	2.01	2.01
	296	58800	53945	1.09	98.0	1.24	1.24
	297	62400	52000	1.20	104.0	1.25	1.25
	298	107640	72730	1.48	69.0	1.66	1.66
	299	96720	61215	1.58	62.0	1.61	1.73
Pinc et al. (1977)	300	47000	36719	1.28	47.0	1.50	1.50
	301	78000	46988	1.66	50.0	1.87	1.87
	302	90480	56906	1.59	58.0	1.83	1.83

^[1] Based on descriptive equations, Eq. (4.5) and (4.7)

^[2] Based on design equation, Eq. (6.18), using the full expression for ψ_r , Eq. (6.14)

^[3] Based on design equation, Eq. (6.18), using the simplified expression for ψ_r , Eq. (6.15)

Table B.8 Cont. Detailed properties and test results for hooked bar specimens tested outside the University of Kansas

Study	SN	ID	b	h	$\ell_{eh,avg}$	f_{cm}	d_b	A_b	s	s/d_b
			in.	in.	in.	psi	in.	in. ²	in.	
Hamad et al. (1993)	303*	7-90-U	12.0	12.0	10	2570	0.875	0.6	5.3	6.1
	304*	7-90-U'	12.0	12.0	10	5400	0.875	0.6	5.3	6.1
	305	11-90-U	12.0	15.0	13	2570	1.41	1.56	4.8	3.4
	306	11-90-U'	12.0	15.0	13	5400	1.41	1.56	4.8	3.4
	307	11-180-U-HS	12.0	15.0	13	7200	1.41	1.56	4.8	3.4
	308	11-90-U-HS	12.0	15.0	13	7200	1.41	1.56	4.8	3.4
	309	11-90-U-T6	12.0	15.0	13	3700	1.41	1.56	4.8	3.4
	310	7-180-U-T4	12.0	12.0	10	3900	0.875	0.6	5.3	6.1
	311	11-90-U-T4	12.0	15.0	13	4230	1.41	1.56	4.8	3.4
	312	7-90-U-SC**	12.0	12.0	10	4230	0.875	0.6	7.4	8.4
Ramirez and Russel (2008)	313	I-1	15.0	9.0	6.5	8910	0.75	0.44	9.2	12.3
	314	I-3	15.0	9.0	6.5	12460	0.75	0.44	9.2	12.3
	315	I-5	15.0	9.0	6.5	12850	0.75	0.44	9.2	12.3
	316*	I-2	15.0	15.0	12.5	8910	1.41	1.56	8.6	6.1
	317*	I-2'	15.0	18.0	15.5	9540	1.41	1.56	8.6	6.1
	318*	I-4	15.0	15.0	12.5	12460	1.41	1.56	8.6	6.1
	319	I-6	15.0	15.0	12.5	12850	1.41	1.56	8.6	6.1
	320	III-13	15.0	9.0	6.5	13980	0.75	0.44	9.2	12.3
	321	III-15	15.0	9.0	6.5	16350	0.75	0.44	9.2	12.3
	322	III-14	15.0	15.0	12.5	13980	1.41	1.56	8.6	6.1
	323	III-16	15.0	15.0	12.5	16500	1.41	1.56	8.6	6.1
Lee and Park (2010)	324*	H1	14.6	20.7	18.7	4450	0.875	0.6	7.9	9.0
	325*	H2	14.6	13.9	11.9	8270	0.875	0.6	7.9	9.0
	326	H3	14.6	17.0	15.0	4450	0.875	0.6	7.9	9.0

* Specimens used in developing descriptive equations, Eq. (4.5) and (4.7)

** Bars outside column core

Table B.8 Cont. Detailed properties and test results for hooked bar specimens tested outside the University of Kansas

Study	SN	n	A_{th}	A_{hs}	A_{th}/A_{hs}	$A_{th,ACI}/A_{hs}$	h_{cl}	x_{mid}	d_{eff}	d_{eff}/ℓ_{eh}	θ
			in. ²	in. ²			in.	in.	in.		°
Hamad et al. (1993)	303*	2	0	1.20	0	0	12.00	15.00	14.15	1.42	56.3
	304*	2	0	1.20	0	0	12.00	15.00	13.71	1.37	56.3
	305	2	0	3.12	0	0	12.00	15.00	15.98	1.23	49.1
	306	2	0	3.12	0	0	12.00	15.00	15.49	1.19	49.1
	307	2	0	3.12	0	0	12.00	15.00	14.32	1.10	49.1
	308	2	0	3.12	0	0	12.00	15.00	14.91	1.15	49.1
	309	2	0.44	3.12	0.141	0.141	12.00	15.00	16.40	1.26	49.1
	310	2	0.22	1.20	0.183	0.183	12.00	15.00	14.04	1.40	56.3
	311	2	0.66	3.12	0.212	0.212	12.00	15.00	16.60	1.28	49.1
	312	2	0	1.20	0	0	12.00	15.00	13.66	1.37	56.3
Ramirez and Russel (2008)	313	2	0	0.88	0	0	12.00	15.00	12.81	1.97	66.6
	314	2	0	0.88	0	0	12.00	15.00	12.58	1.94	66.6
	315	2	0	0.88	0	0	12.00	15.00	12.57	1.93	66.6
	316*	2	0	3.12	0	0	12.00	15.00	14.38	1.15	50.2
	317*	2	0	3.12	0	0	12.00	15.00	14.66	0.95	44.1
	318*	2	0	3.12	0	0	12.00	15.00	13.92	1.11	50.2
	319	2	0	3.12	0	0	12.00	15.00	14.14	1.13	50.2
	320	2	0.44	0.88	0.5	0.5	12.00	15.00	12.71	1.96	66.6
	321	2	0.44	0.88	0.5	0.5	12.00	15.00	12.57	1.93	66.6
	322	2	0.66	3.12	0.212	0.212	12.00	15.00	13.81	1.10	50.2
	323	2	0.66	3.12	0.212	0.212	12.00	15.00	13.75	1.10	50.2
Lee and Park (2010)	324*	2	0	1.2	0	0	**	**			
	325*	2	0	1.2	0	0	**	**			
	326	2	0.44	1.2	0.367	0.367	**	**			

* Specimens used in developing descriptive equations, Eq. (4.5) and (4.7)

** Information not provided

Table B.8 Cont. Detailed properties and test results for hooked bar specimens tested outside the University of Kansas

Study	SN	T	T_h ^[1]	T/T_h	f_{su}	$f_{su}/f_{s,calc}$ ^[2]	$f_{su}/f_{s,calc}$ ^[3]
		lb	lb		ksi		
Hamad et al. (1993)	303*	25980	32994	0.79	43.3	0.87	0.87
	304*	36720	40662	0.90	61.2	1.03	1.03
	305	48048	42520	1.13	30.8	1.40	1.40
	306	75036	52473	1.43	48.1	1.82	1.82
	307	58812	57099	1.03	37.7	1.33	1.33
	308	73788	56760	1.30	47.3	1.66	1.66
	309	71760	92000	0.78	46.0	1.44	1.57
	310	34620	32056	1.08	57.7	0.94	0.94
	311	83148	74239	1.12	53.3	1.34	1.34
	312	29940	40237	0.87**	49.9	1.02	1.02
Ramirez and Russel (2008)	313	30008	28854	1.04	68.2	1.23	1.23
	314	30008	31587	0.95	68.2	1.13	1.13
	315	30492	32097	0.95	69.3	1.14	1.14
	316*	87984	75072	1.17	56.4	1.36	1.36
	317*	104988	97097	1.08	67.3	1.29	1.29
	318*	99060	82471	1.20	63.5	1.41	1.41
	319	114036	86391	1.32	73.1	1.61	1.61
	320	41316	42159	0.98	93.9	1.36	1.36
	321	38500	43750	0.88	87.5	1.22	1.22
	322	104988	110514	0.95	67.3	1.31	1.45
	323	119964	114251	1.05	76.9	1.43	1.59
Lee and Park (2010)	324*	59220	81795	0.72	98.7	0.93	0.93
	325*	52800	59034	0.89	88.0	1.11	1.11
	326	53760	74667	0.72	89.6	0.95	0.95

* Specimens used in developing descriptive equations, Eq. (4.5) and (4.7)

** Bar location factor of 1.17 applied

[1] Based on descriptive equations, Eq. (4.5) and (4.7)

[2] Based on design equation, Eq. (6.18), using the simplified expression for ψ_r , Eq. (6.14)

[3] Based on design equation, Eq. (6.18), using the simplified expression for ψ_r , Eq. (6.15)

Table B.8 Cont. Detailed properties and test results for hooked bar specimens tested outside the University of Kansas

Study	SN	ID	b	h	$\ell_{eh,avg}$	f_{cm}	d_b	A_b	s	s/d_b
			in.	in.	in.	psi	in.	in. ²	in.	
Chun et al. (2017b)*	327	D43-L10-C1-S42	21.1	18.9	16.9	6440	1.693	2.25	16.3	9.6
	328	D43-L10-C1-S42-C	21.1	18.9	16.9	6950	1.693	2.25	16.3	9.6
	329	D43-L10-C1-S70	21.1	18.9	16.9	10010	1.693	2.25	16.3	9.6
	330	D43-L10-C2-S42	24.5	18.9	16.9	7020	1.693	2.25	16.3	9.6
	331	D43-L13-C1-S42	21.1	24.0	22	7020	1.693	2.25	16.3	9.6
	332	D43-L13-C1-S42-C	21.1	24.0	22	7020	1.693	2.25	16.3	9.6
	333	D43-L13-C1-S70	21.1	24.0	22	10600	1.693	2.25	16.3	9.6
	334	D43-L13-C2-S42	24.5	24.0	22	7020	1.693	2.25	16.3	9.6
	335	D43-L16-C1-S42	21.1	29.1	27.1	7020	1.693	2.25	16.3	9.6
	336	D43-L16-C1-S42-C	21.1	29.1	27.1	7020	1.693	2.25	16.3	9.6
	337	D43-L16-C1-S70	21.1	29.1	27.1	10010	1.693	2.25	16.3	9.6
	338	D43-L16-C2-S42	24.5	29.1	27.1	7020	1.693	2.25	16.3	9.6
	339	D43-L20-C1-S42	21.1	36.5	33.9	7020	1.693	2.25	16.3	9.6
	340	D57-L10-C1-S42-a	22.2	24.4	22.6	5450	2.257	4	16.3	7.2
	341	D57-L10-C1-S42-b	22.2	24.4	22.6	6150	2.257	4	16.3	7.2
	342	D57-L10-C1-S42-C	22.2	24.4	22.6	5450	2.257	4	16.3	7.2
	343	D57-L10-C2-S42	26.7	24.4	22.6	5450	2.257	4	16.3	7.2
	344	D57-L13-C1-S42-a	22.2	31.5	29.3	5450	2.257	4	16.3	7.2
	345	D57-L13-C1-S42-b	22.2	31.5	29.3	6150	2.257	4	16.3	7.2
	346	D57-L13-C1-S42-C	22.2	31.5	29.3	5450	2.257	4	16.3	7.2
	347	D57-L13-C2-S42	26.7	31.5	29.3	5450	2.257	4	16.3	7.2
	348	D57-L16-C1-S42-a	22.2	38.3	36.1	5450	2.257	4	16.3	7.2
	349	D57-L16-C1-S42-b	22.2	38.3	36.1	6150	2.257	4	16.3	7.2
	350	D57-L16-C1-S42-C	22.2	38.3	36.1	5450	2.257	4	16.3	7.2
	351	D57-L16-C2-S42	26.7	38.3	36.1	6530	2.257	4	16.3	7.2
	352	D57-L20-C1-S42	22.2	47.2	45.1	6530	2.257	4	16.3	7.2

* Bars outside column core in all specimens. Bars outside confining ties in specimens without “-C” at the end of their designation, therefore $A_{th}/A_{hs} = 0$ when calculating ψ_r .

Table B.8 Cont. Detailed properties and test results for hooked bar specimens tested outside the University of Kansas

Study	SN	n	A_{th}	A_{hs}	A_{th}/A_{hs}	$A_{th,ACI}/A_{hs}$	h_{cl}	x_{mid}	d_{eff}	d_{eff}/ℓ_{eh}	θ
			in. ²	in. ²			in.	in.	in.		°
Chun et al. (2017b)	327	2	3.96	4.5	0.88	0.196	8.74	11.3	11.48	0.68	33.7
	328	2	2.66	4.5	0.59	1.173	8.74	11.3	12.60	0.75	33.7
	329	2	3.96	4.5	0.88	0.196	8.74	11.3	10.85	0.64	33.7
	330	2	3.96	4.5	0.88	0.196	8.74	11.3	11.31	0.67	33.7
	331	2	3.96	4.5	0.88	0.196	11.82	14.7	15.12	0.69	33.7
	332	2	2.66	4.5	0.59	0.978	11.82	14.7	15.70	0.71	33.7
	333	2	3.96	4.5	0.88	0.196	12.12	14.7	14.43	0.66	33.7
	334	2	3.96	4.5	0.88	0.196	11.82	14.7	14.85	0.68	33.7
	335	2	3.96	4.5	0.88	0.196	14.71	18.1	18.42	0.68	33.7
	336	2	2.66	4.5	0.59	0.978	14.71	18.1	18.74	0.69	33.7
	337	2	3.96	4.5	0.88	0.196	15.21	18.1	18.17	0.67	33.7
	338	2	3.96	4.5	0.88	0.196	14.71	18.1	18.27	0.67	33.7
	339	2	3.96	4.5	0.88	0.196	18.82	22.6	22.74	0.67	33.7
	340	2	5.28	8	0.66	0.083	11.30	15.1	14.97	0.66	33.7
	341	2	5.28	8	0.66	0.083	11.30	15.1	14.78	0.65	33.7
	342	2	3.52	8	0.44	0.660	11.30	15.1	16.87	0.75	33.7
	343	2	5.28	8	0.66	0.083	11.70	15.1	16.16	0.71	33.7
	344	2	5.28	8	0.66	0.083	15.36	19.5	21.27	0.73	33.7
	345	2	5.28	8	0.66	0.083	15.36	19.5	20.76	0.71	33.7
	346	2	3.52	8	0.44	0.660	15.36	19.5	21.72	0.74	33.7
	347	2	5.28	8	0.66	0.083	15.36	19.5	21.04	0.72	33.7
	348	2	5.28	8	0.66	0.083	19.37	24.1	25.72	0.71	33.7
	349	2	5.28	8	0.66	0.083	19.37	24.1	25.96	0.72	33.7
	350	2	3.52	8	0.44	0.660	19.37	24.1	26.36	0.73	33.7
	351	2	5.28	8	0.66	0.083	19.37	24.1	25.31	0.70	33.7
	352	2	5.28	8	0.66	0.083	24.79	30.1	32.15	0.71	33.7

Table B.8 Cont. Detailed properties and test results for hooked bar specimens tested outside the University of Kansas

Study	SN	T	T_h ^[1]	T/T_h	f_{su}	$f_{su}/f_{s,calc}$ ^[2]	$f_{su}/f_{s,calc}$ ^[3]
		lb	lb		ksi		
Chun et al. (2017b)	327	115425	92200	1.25	51.3	1.51	1.51
	328	168975	182814	0.92	75.1	1.51	1.73
	329	123300	104341	1.18	54.8	1.44	1.44
	330	131625	94538	1.39	58.5	1.68	1.68
	331	144900	126374	1.15	64.4	1.42	1.42
	332	170775	214649	0.80	75.9	1.17	1.34
	333	142425	141547	1.01	63.3	1.26	1.26
	334	154575	125824	1.23	68.7	1.52	1.52
	335	163350	158654	1.03	72.6	1.30	1.30
	336	177525	248739	0.71	78.9	0.99	1.13
	337	172800	175824	0.98	76.8	1.26	1.26
	338	182025	158752	1.15	80.9	1.45	1.45
	339	172125	204327	0.84	76.5	1.10	1.10
	340	147200	136752	1.08	36.8	1.30	1.30
	341	150400	141260	1.06	37.6	1.29	1.29
	342	223200	280543	0.80	55.8	1.38	1.57
	343	214800	137007	1.57	53.7	1.89	1.89
	344	236400	182028	1.30	59.1	1.61	1.61
	345	232800	189499	1.23	58.2	1.53	1.53
	346	254400	329448	0.77	63.6	1.21	1.38
	347	273600	182692	1.50	68.4	1.86	1.86
	348	254000	228520	1.11	63.5	1.40	1.40
	349	284000	237976	1.19	71.0	1.52	1.52
	350	279600	373397	0.75	69.9	1.08	1.23
	351	318800	241132	1.32	79.7	1.68	1.68
	352	328400	308444	1.06	82.1	1.39	1.39

^[1] Based on descriptive equations, Eq. (4.5) and (4.7)

^[2] Based on design equation, Eq. (6.18), using the simplified expression for ψ_r , Eq. (6.14)

^[3] Based on design equation, Eq. (6.18), using the simplified expression for ψ_r , Eq. (6.15)

APPENDIX C: HEADED BAR BEAM-COLUMN JOINT SPECIMENS

Appendix C presents the details of the headed bar specimens. Appendix C1 presents specimen drawings and reinforcement layouts for No. 14 and No. 18 bars tested in this study. Appendix C2 presents detailed properties and test results for the No. 14 and No. 18 bar specimens of this study. Appendix C3 presents specimens tested at the University of Kansas used to develop descriptive equations, Eq. (5.5) and (5.7), including No. 5, No. 8, and No. 11 bar specimens by Shao et al. (2016), and No. 14 and No. 18 bars tested in this study. Appendix C4 presents the specimens tested outside the University of Kansas, including those by Bashandy (1996), Chun et al. (2017a), and Sim and Chun (2022a, 2022b), none of which were used to develop descriptive equations.

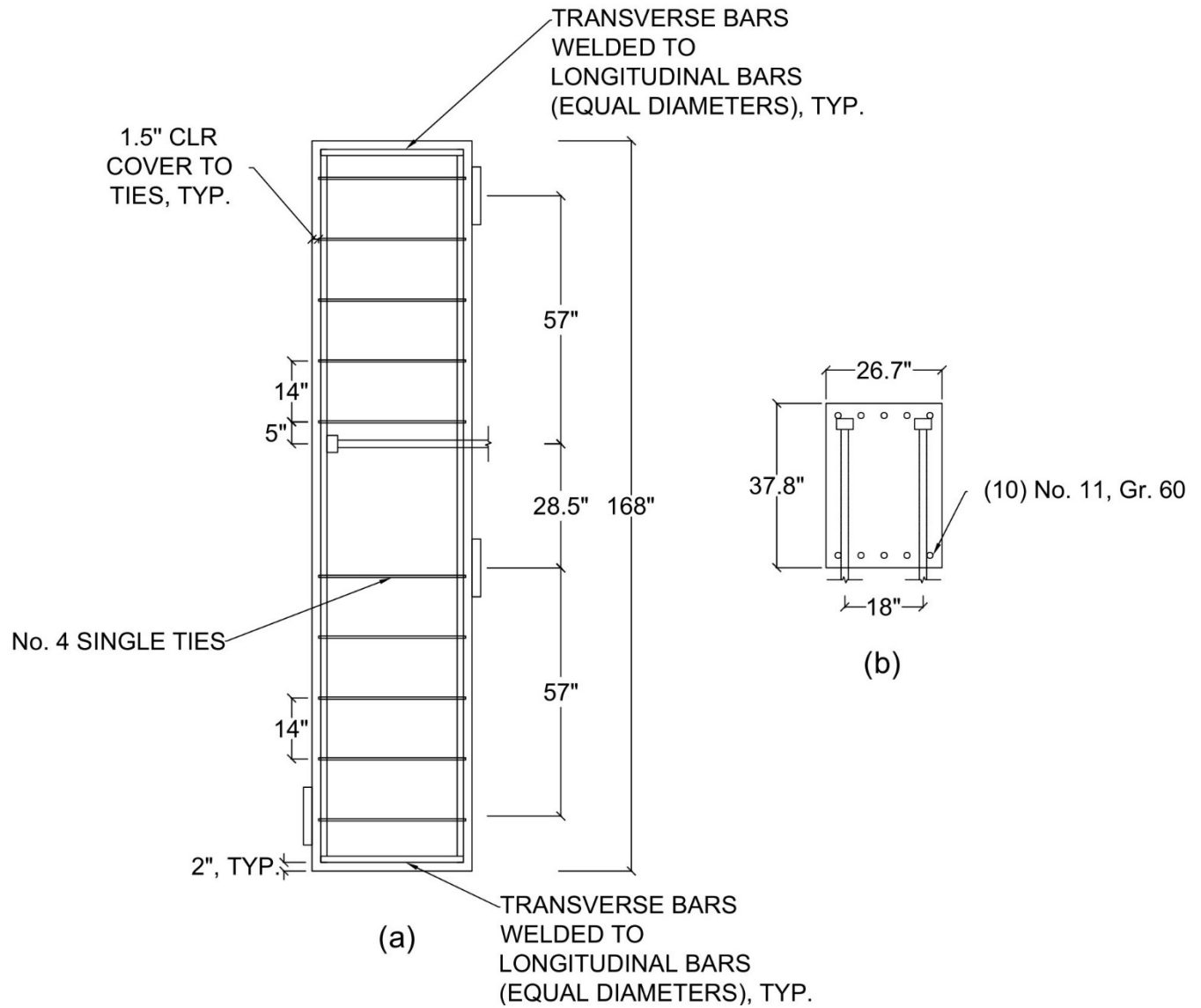


Figure C.2 Details of reinforcement layout for No. 14 headed bar specimen 14-3: (a) elevation, (b) cross-section

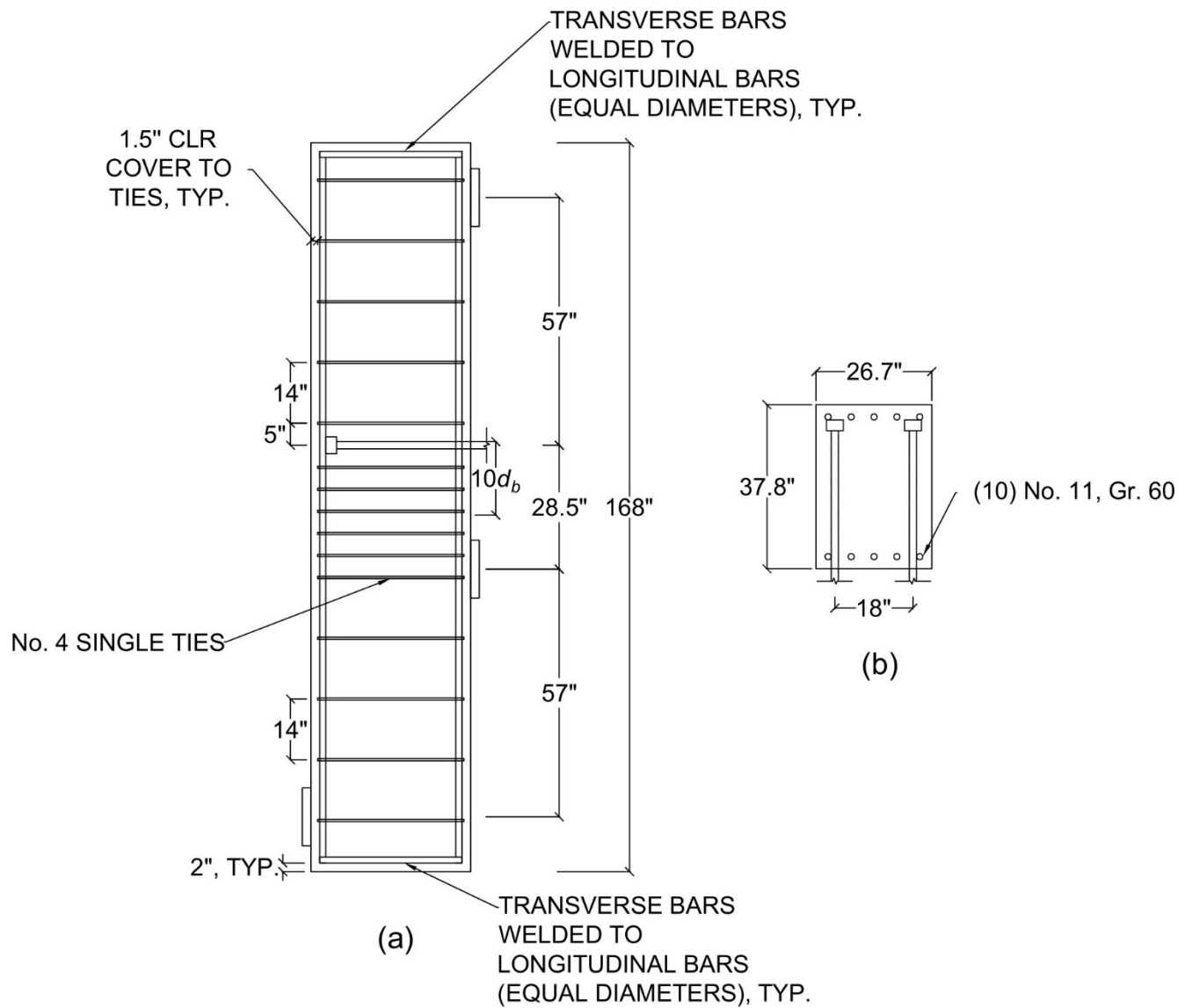


Figure C.3 Details of reinforcement layout for No. 14 headed bar specimen 14-4: (a) elevation, (b) cross-section

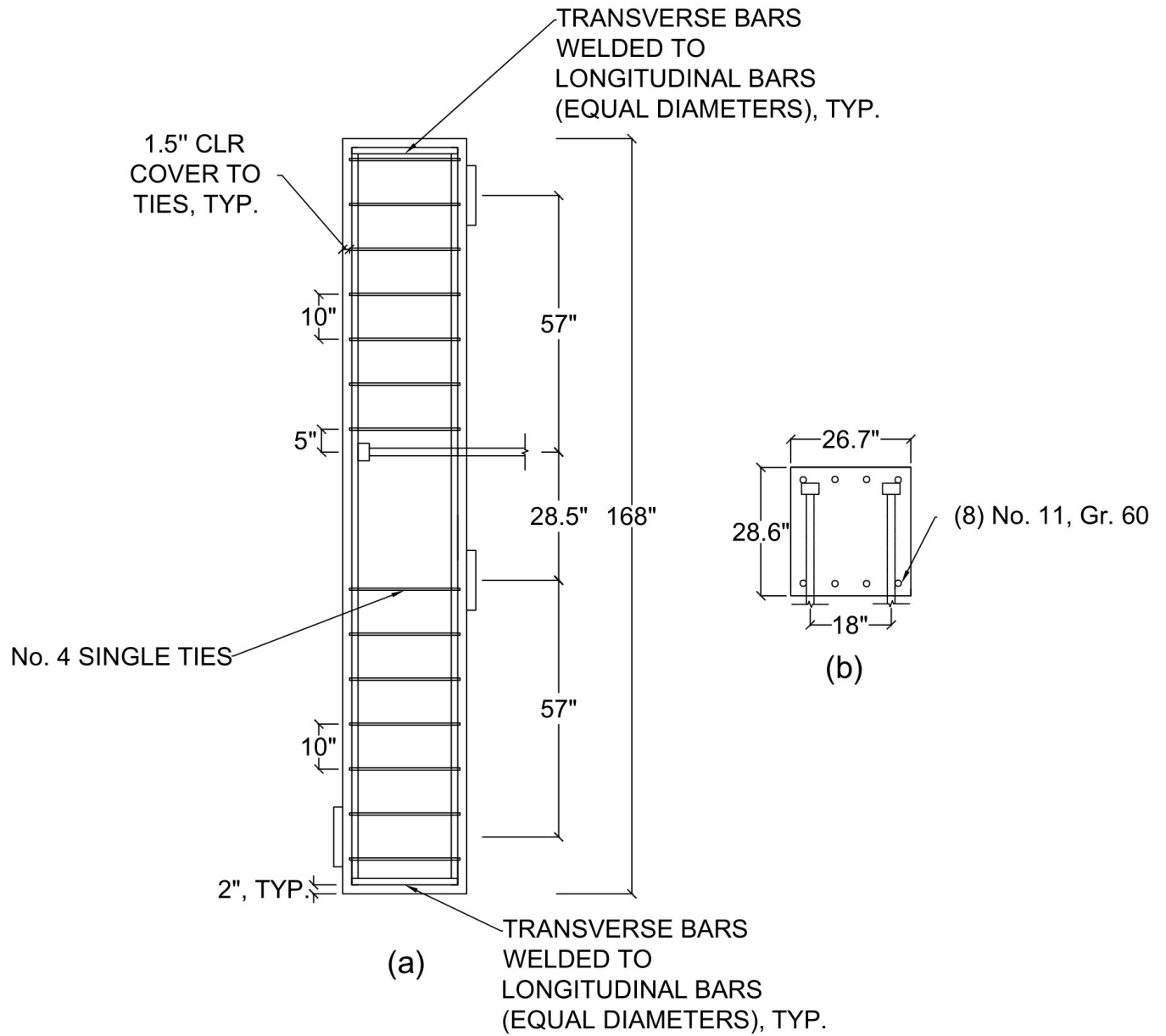


Figure C.4 Details of reinforcement layout for No. 14 headed bar specimen 14-15: (a) elevation, (b) cross-section

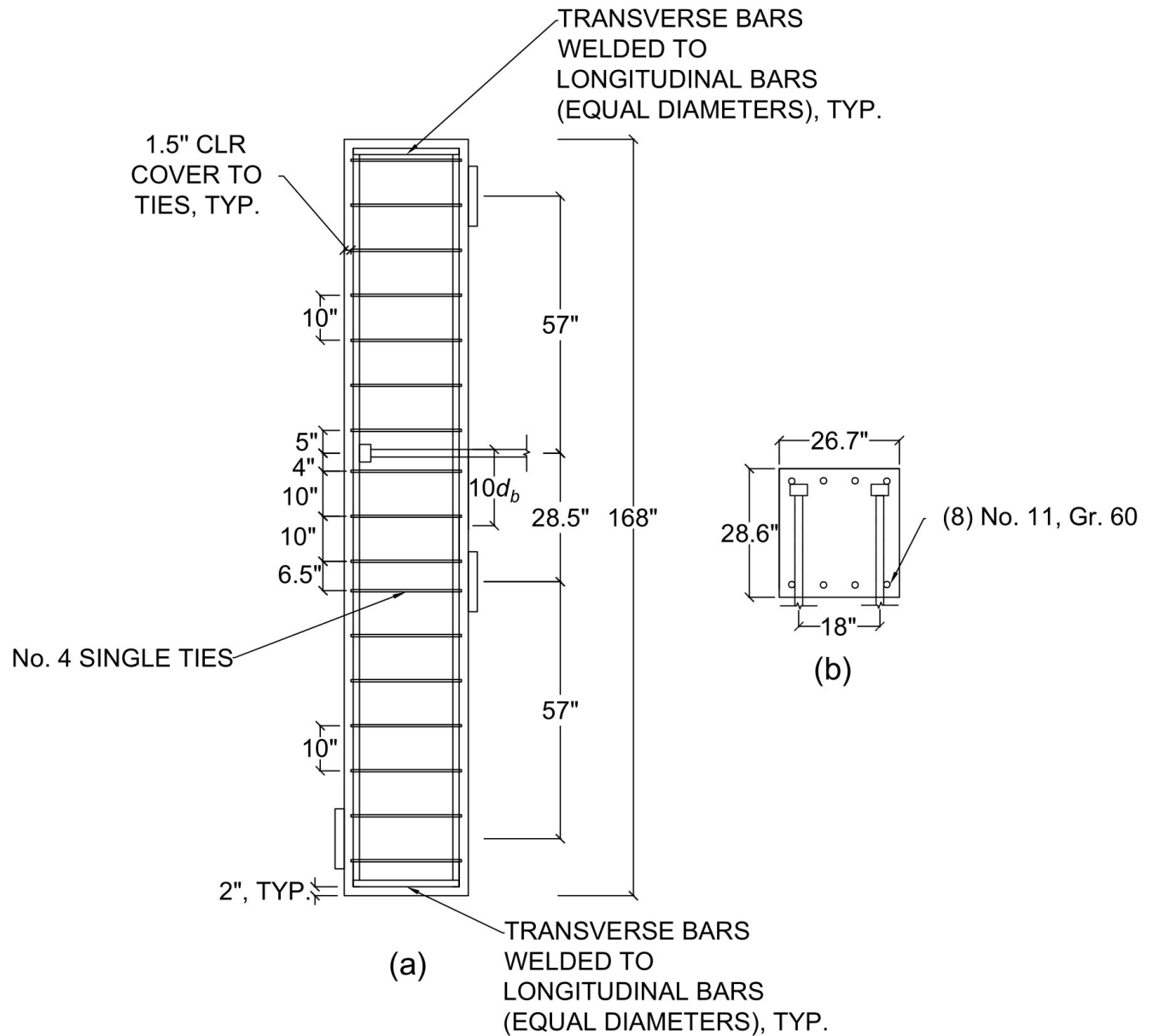


Figure C.5 Details of reinforcement layout for No. 14 headed bar specimen 14-16: (a) elevation, (b) cross-section

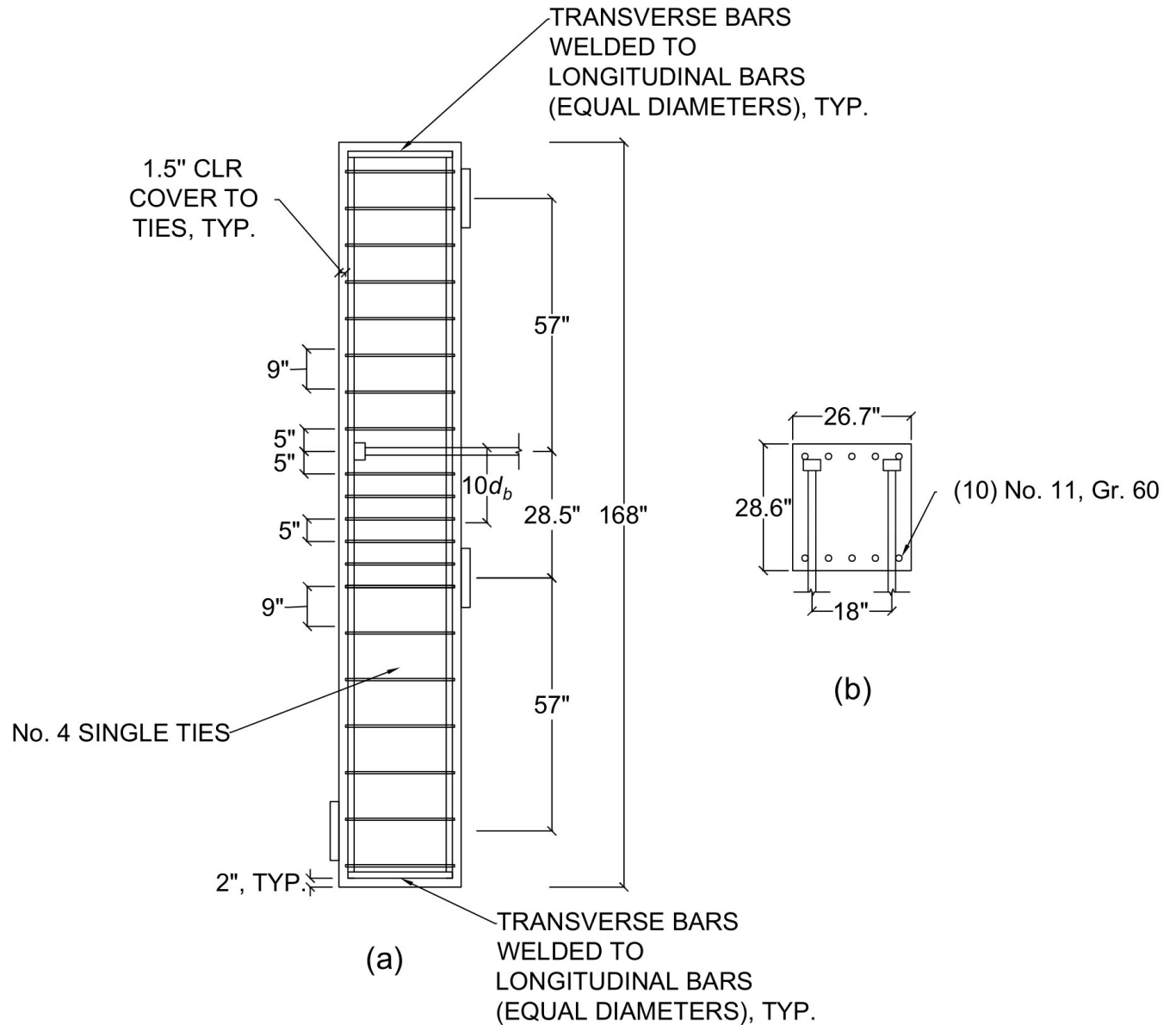


Figure C.8 Details of reinforcement layout for No. 14 headed bar specimen 14-2A: (a) elevation, (b) cross-section

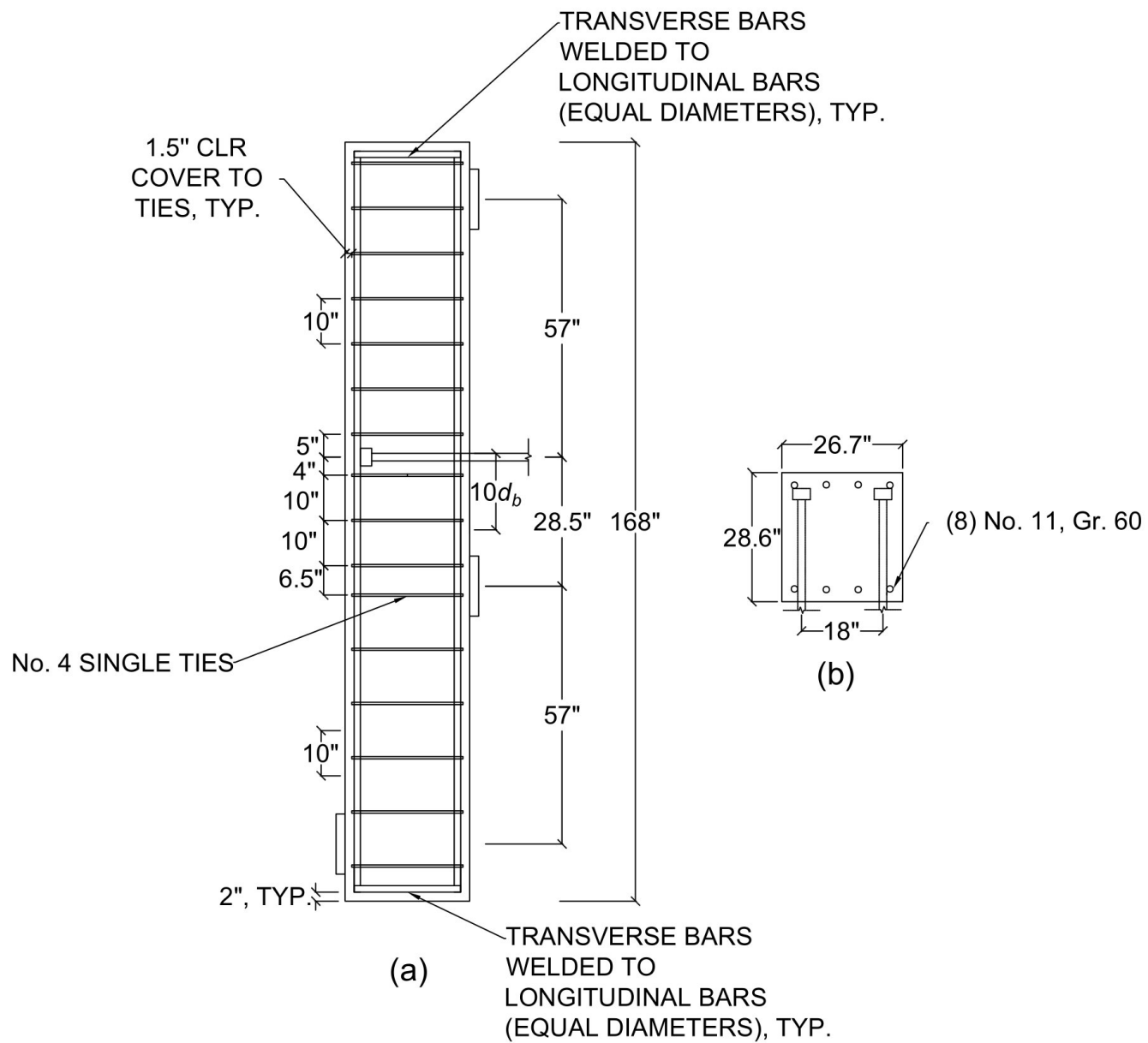


Figure C.9 Details of reinforcement layout for No. 14 headed bar specimen 14-16B: (a) elevation, (b) cross-section

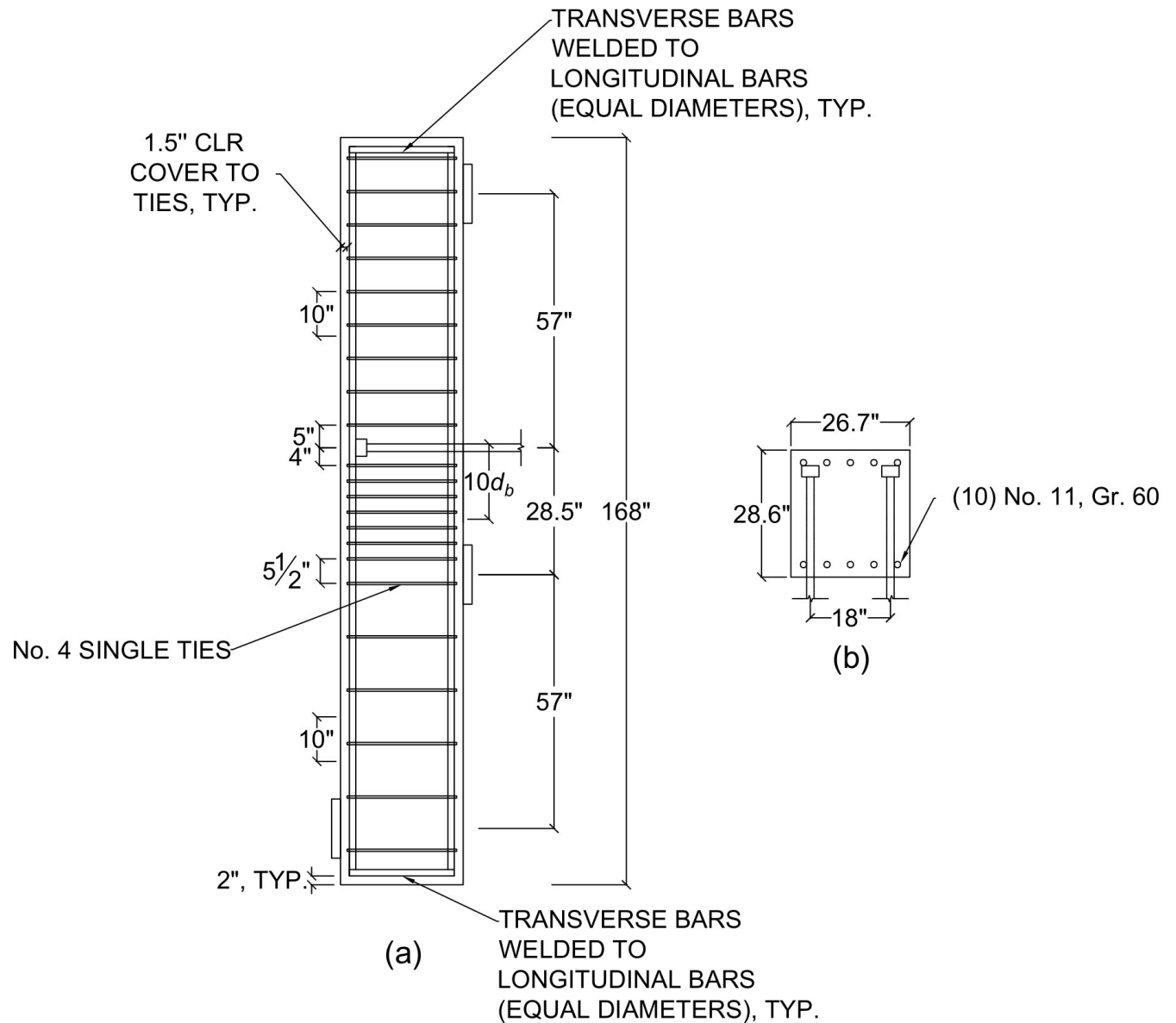


Figure C.10 Details of reinforcement layout for No. 14 headed bar specimen 14-16C: (a) elevation, (b) cross-section

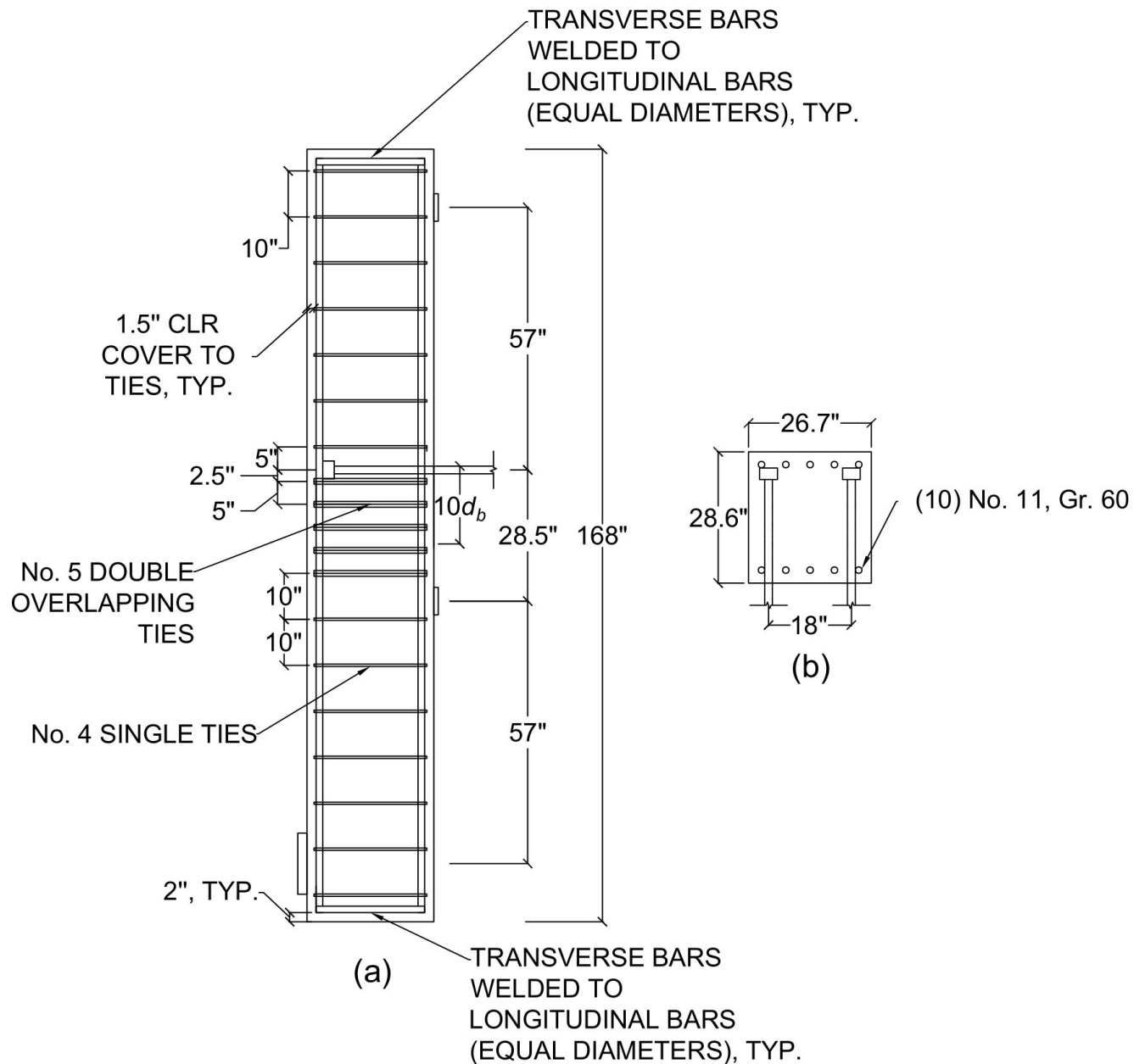


Figure C.11 Details of reinforcement layout for No. 14 headed bar specimen 14-16D: (a) elevation, (b) cross-section

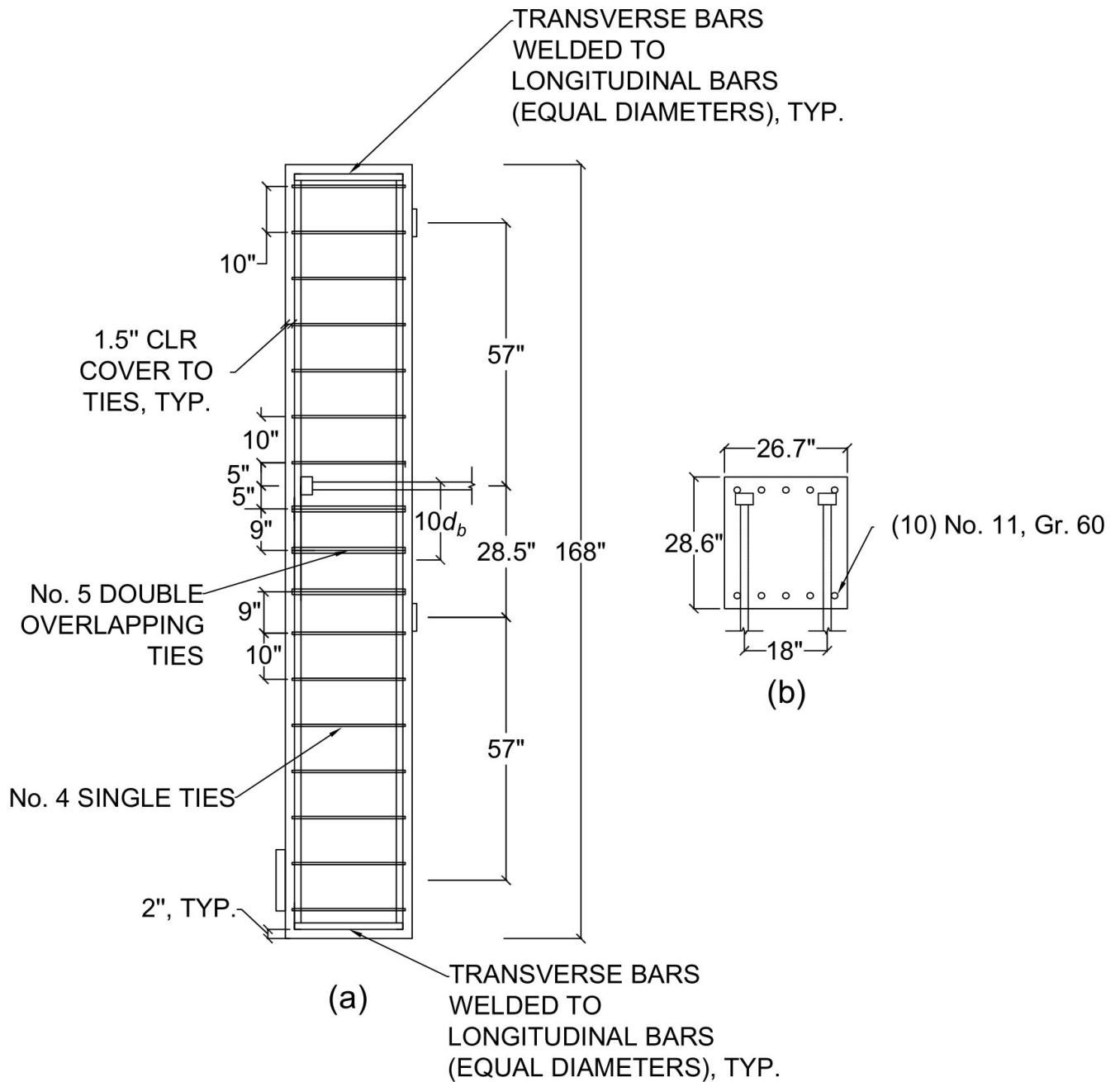


Figure C.12 Details of reinforcement layout for No. 14 headed bar specimen 14-16E: (a) elevation, (b) cross-section

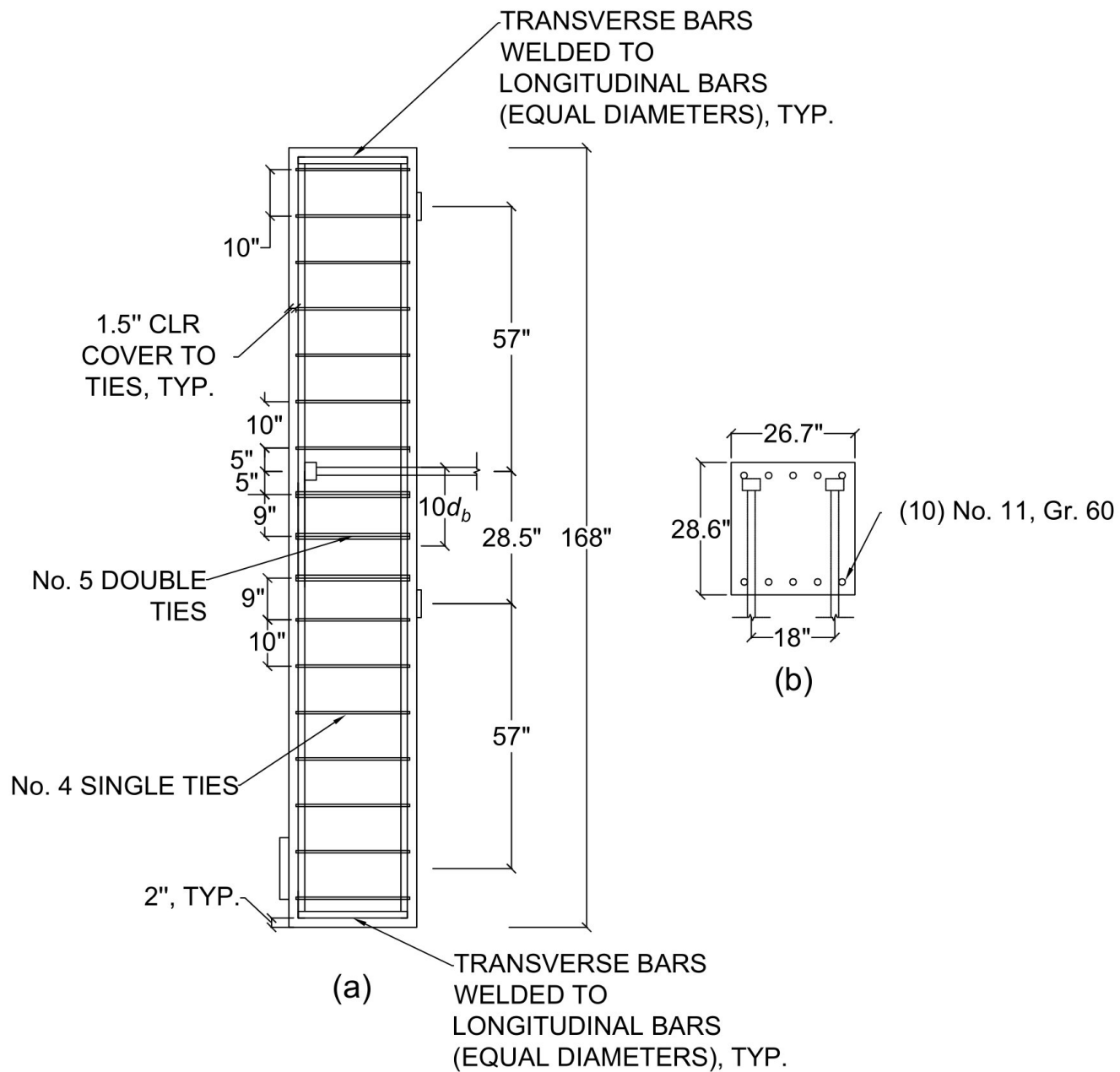


Figure C.13 Details of reinforcement layout for No. 14 headed bar specimen 14-16F: (a) elevation, (b) cross-section

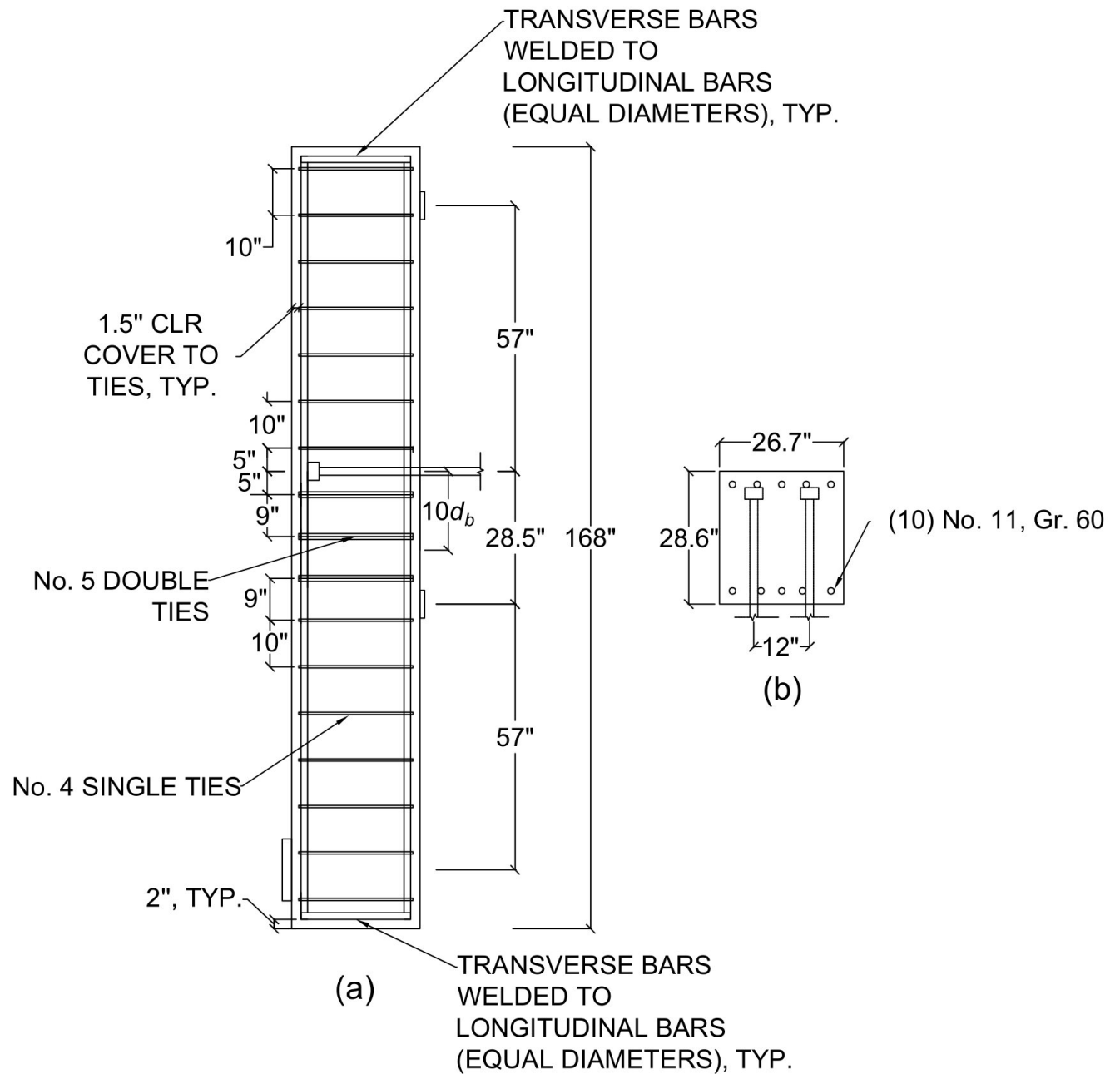


Figure C.14 Details of reinforcement layout for No. 14 headed bar specimen 14-17: (a) elevation, (b) cross-section

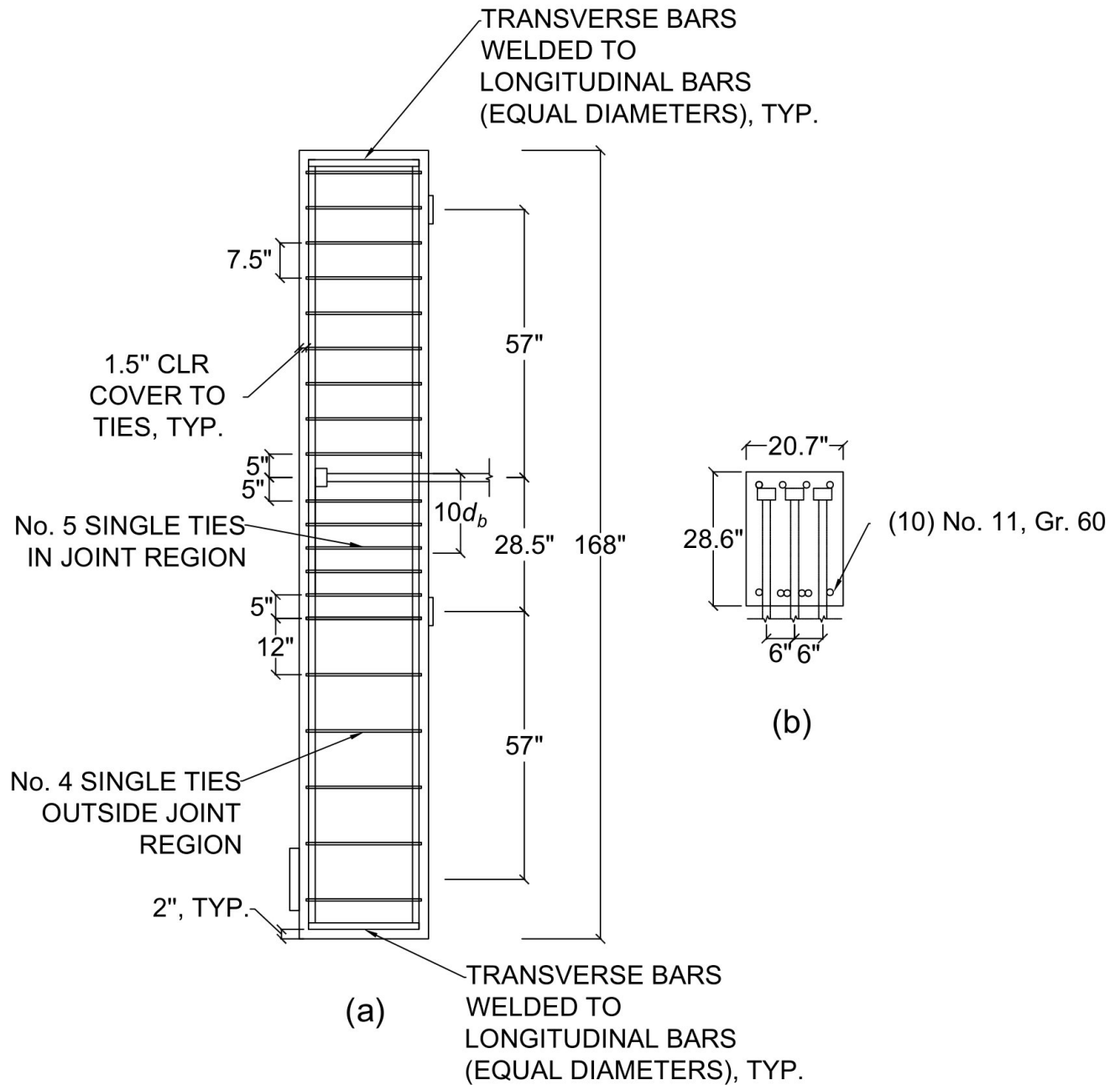


Figure C.16 Details of reinforcement layout for No. 14 headed bar specimen 14-6: (a) elevation, (b) cross-section

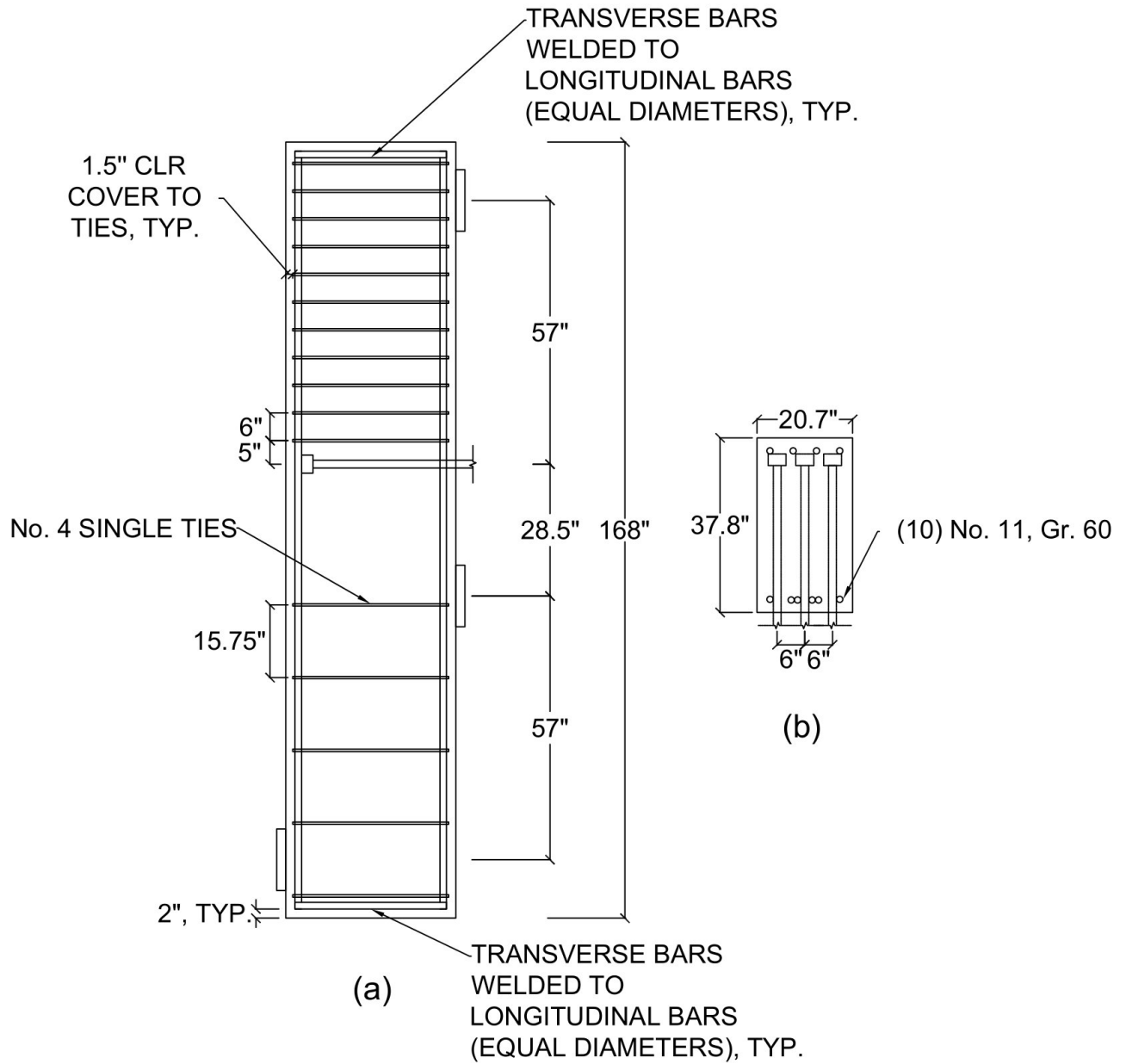


Figure C.17 Details of reinforcement layout for No. 14 headed bar specimen 14-7: (a) elevation, (b) cross-section

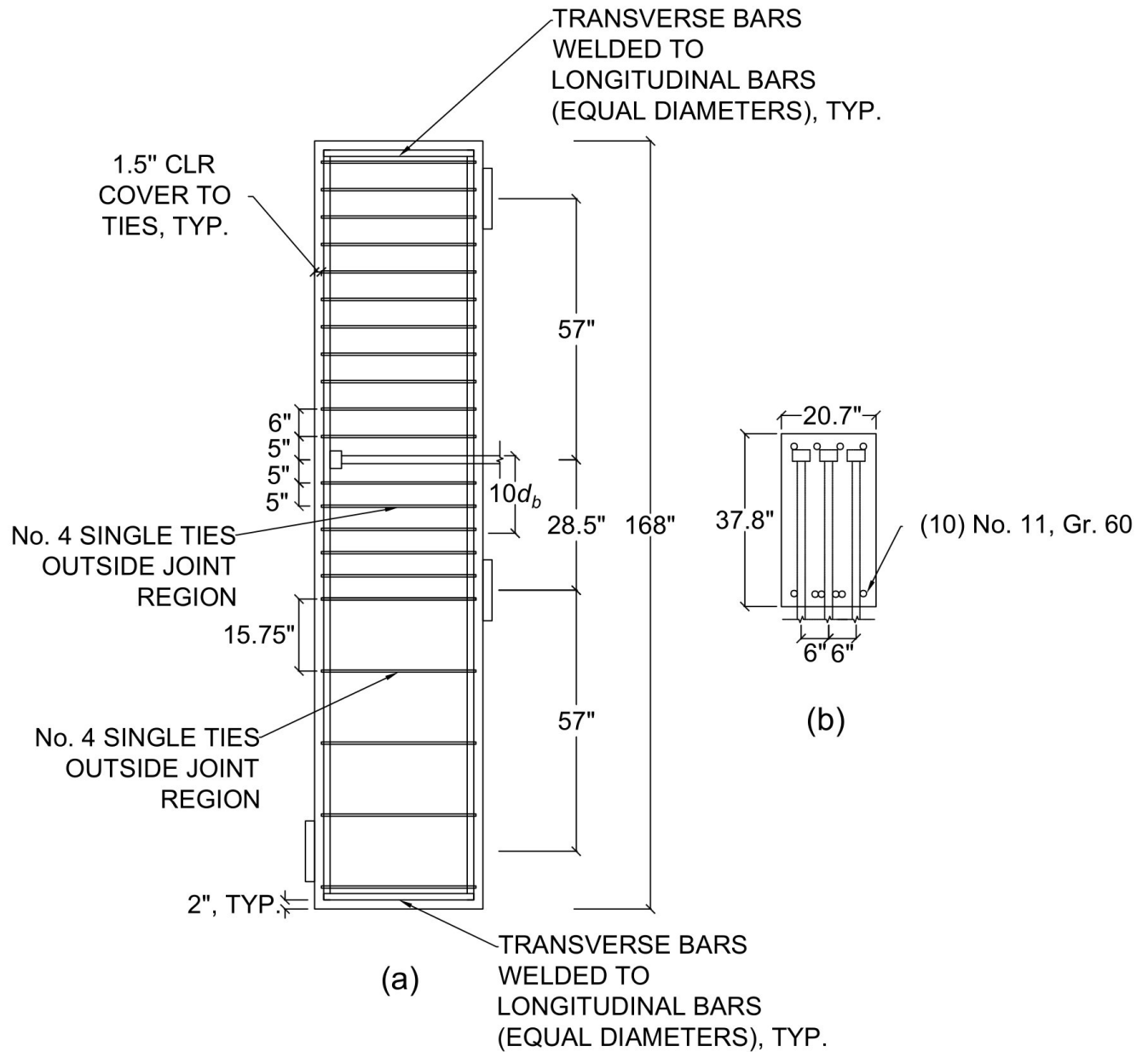


Figure C.18 Details of reinforcement layout for No. 14 headed bar specimen 14-8: (a) elevation, (b) cross-section

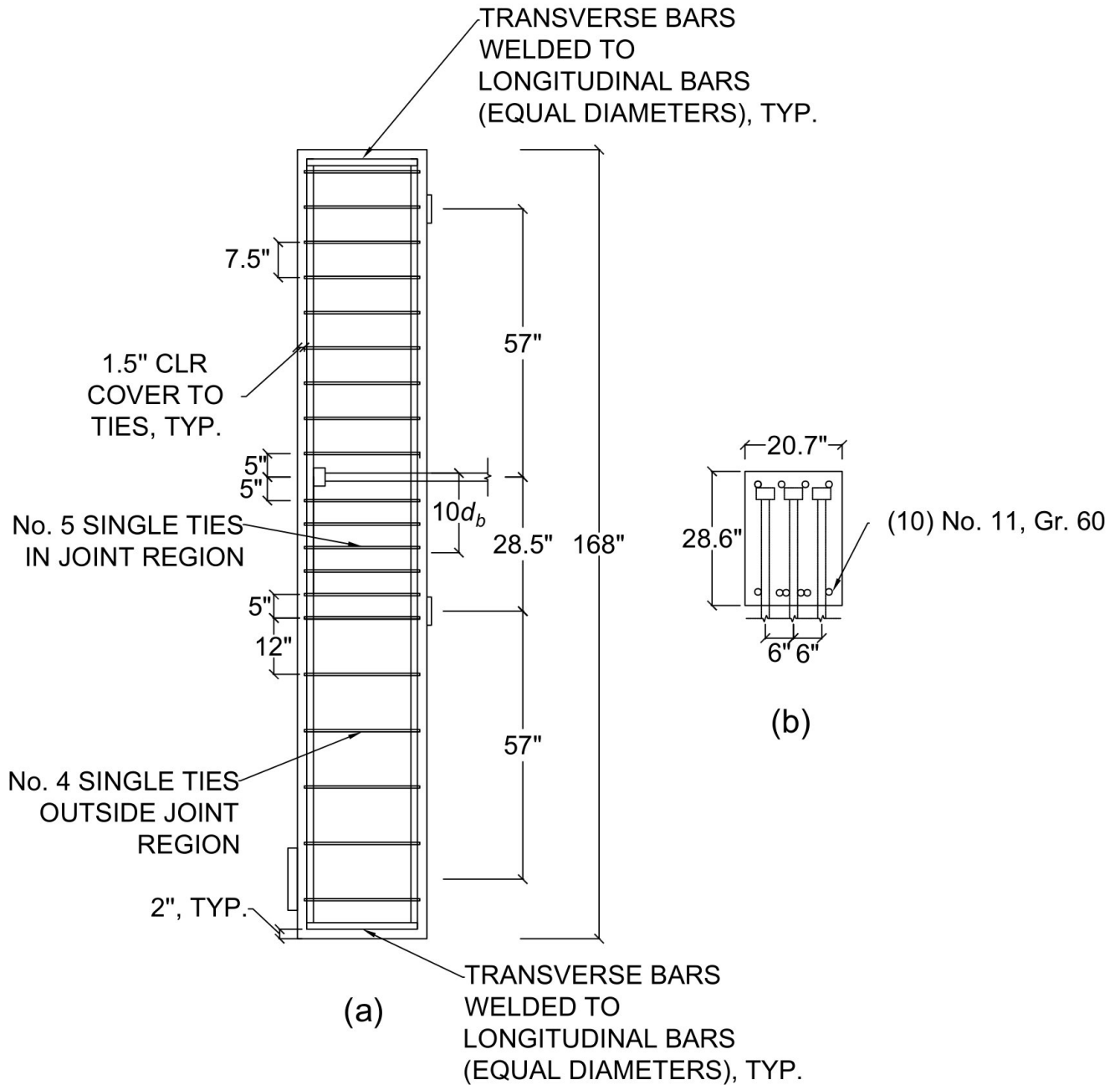


Figure C.19 Details of reinforcement layout for No. 14 headed bar specimen 14-9: (a) elevation, (b) cross-section

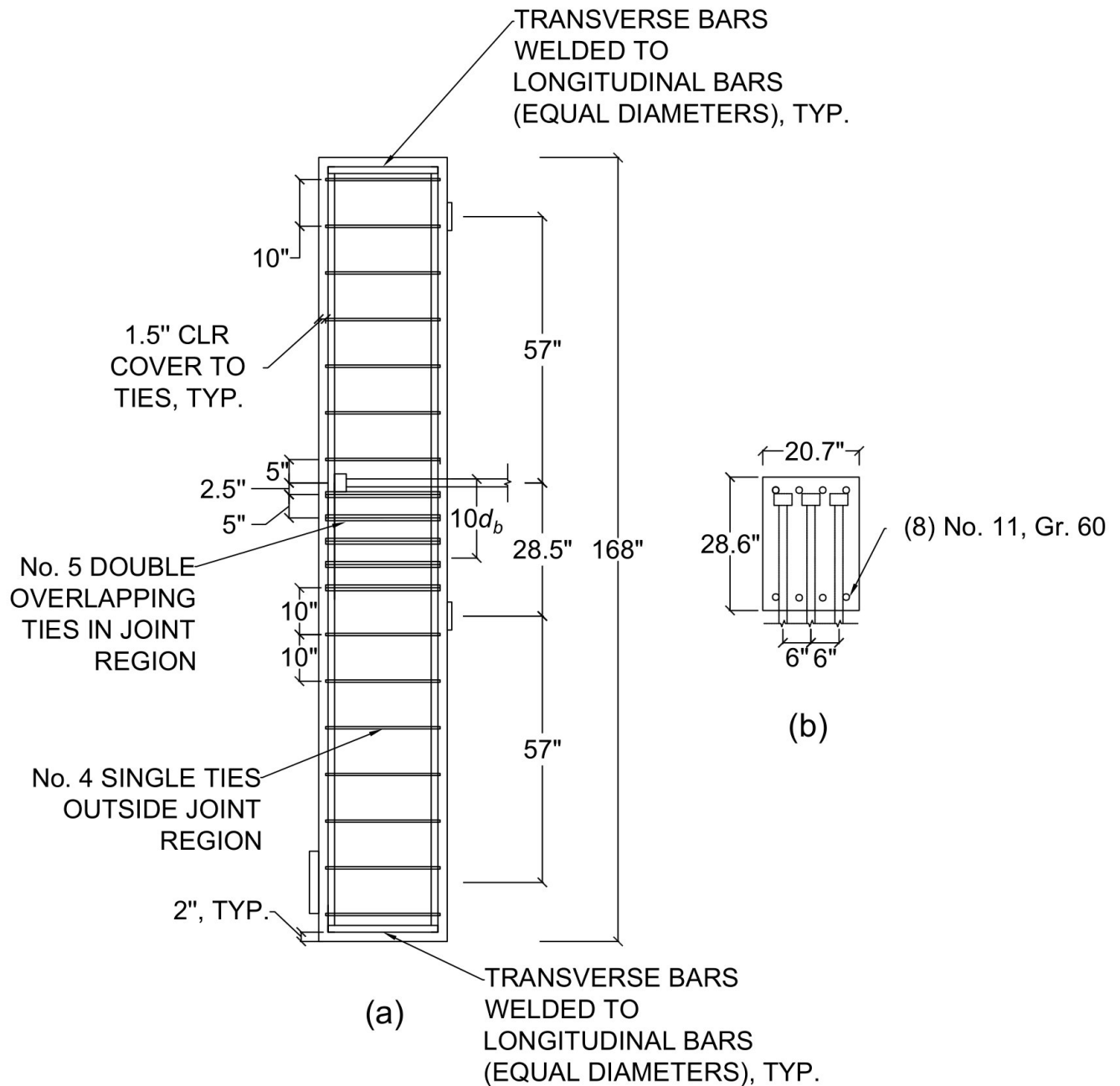


Figure C.20 Details of reinforcement layout for No. 14 headed bar specimen 14-10: (a) elevation, (b) cross-section

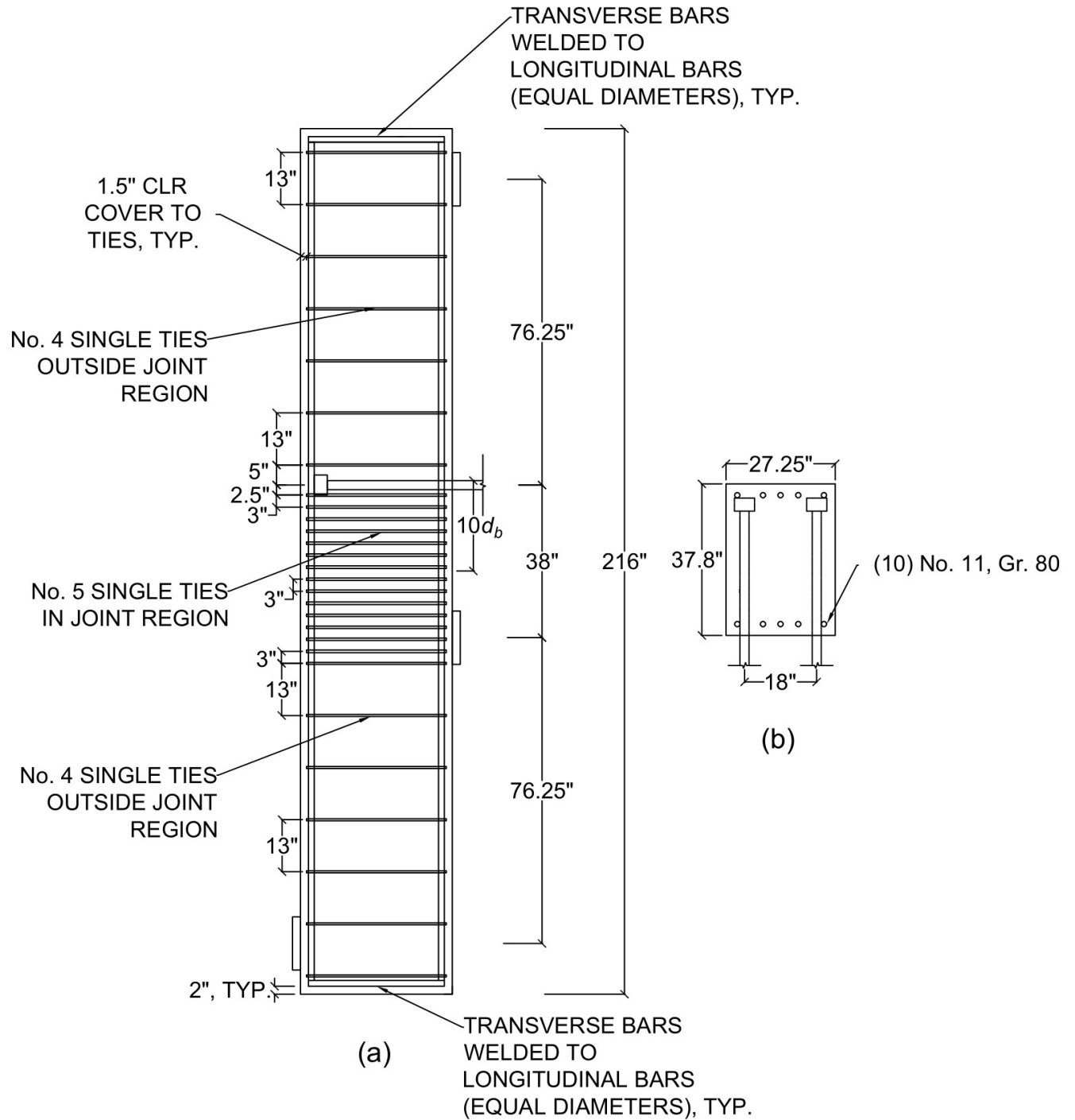


Figure C.21 Details of reinforcement layout for No. 18 headed bar specimen 18-1: (a) elevation, (b) cross-section

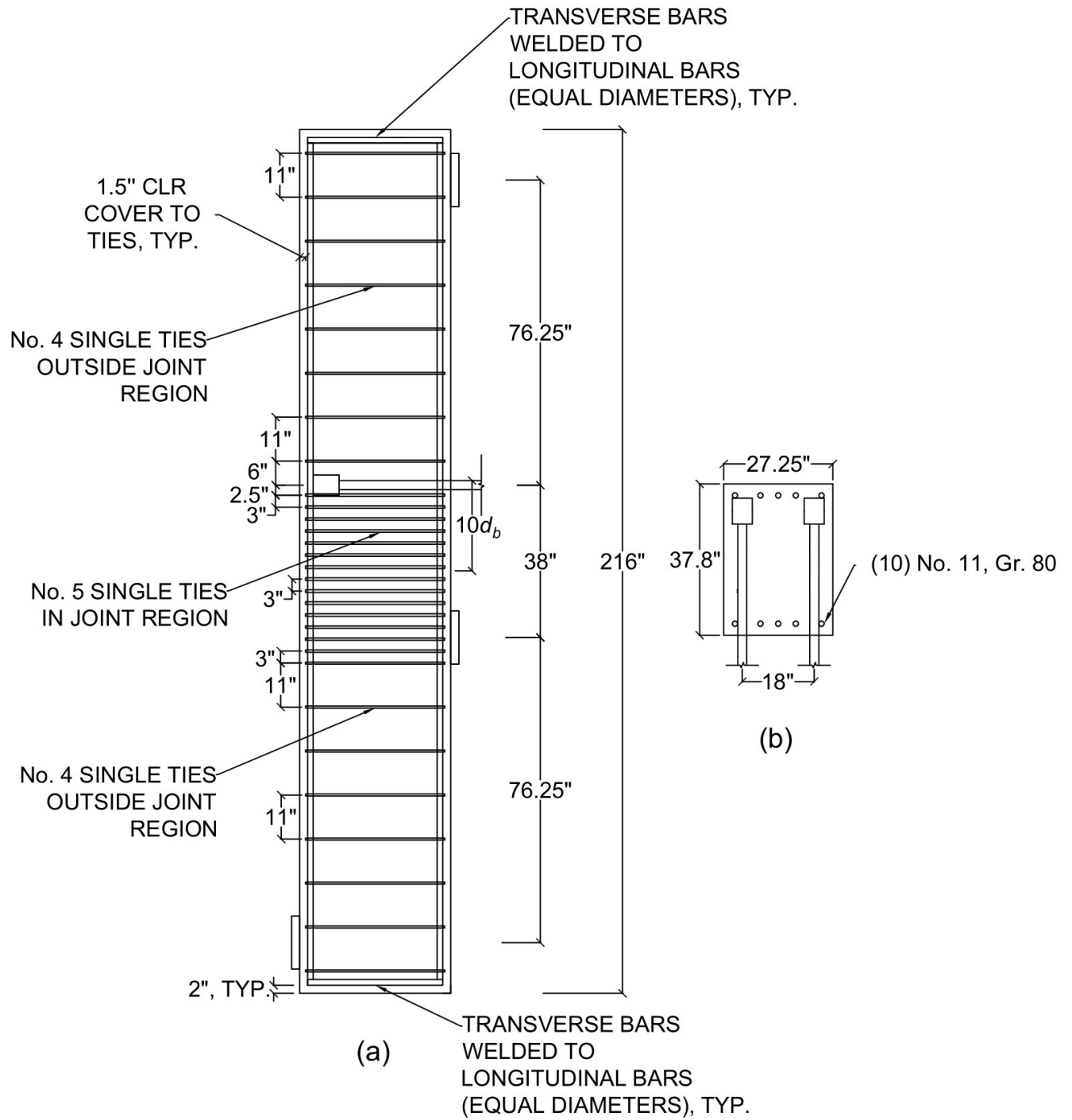


Figure C.22 Details of reinforcement layout for No. 18 headed bar specimen 18-2: (a) elevation, (b) cross-section

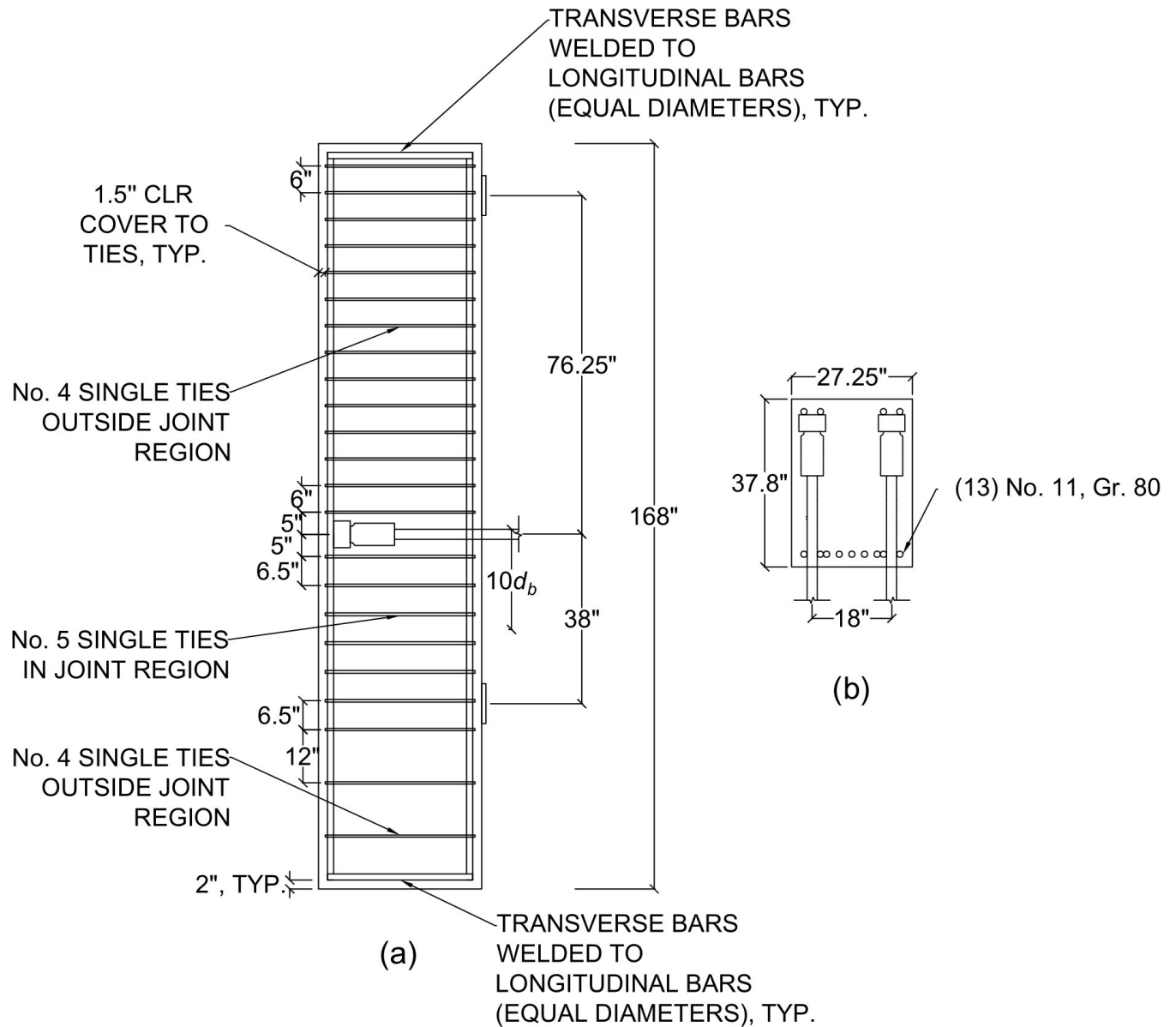


Figure C.23 Details of reinforcement layout for No. 18 headed bar specimen 18-3: (a) elevation, (b) cross-section

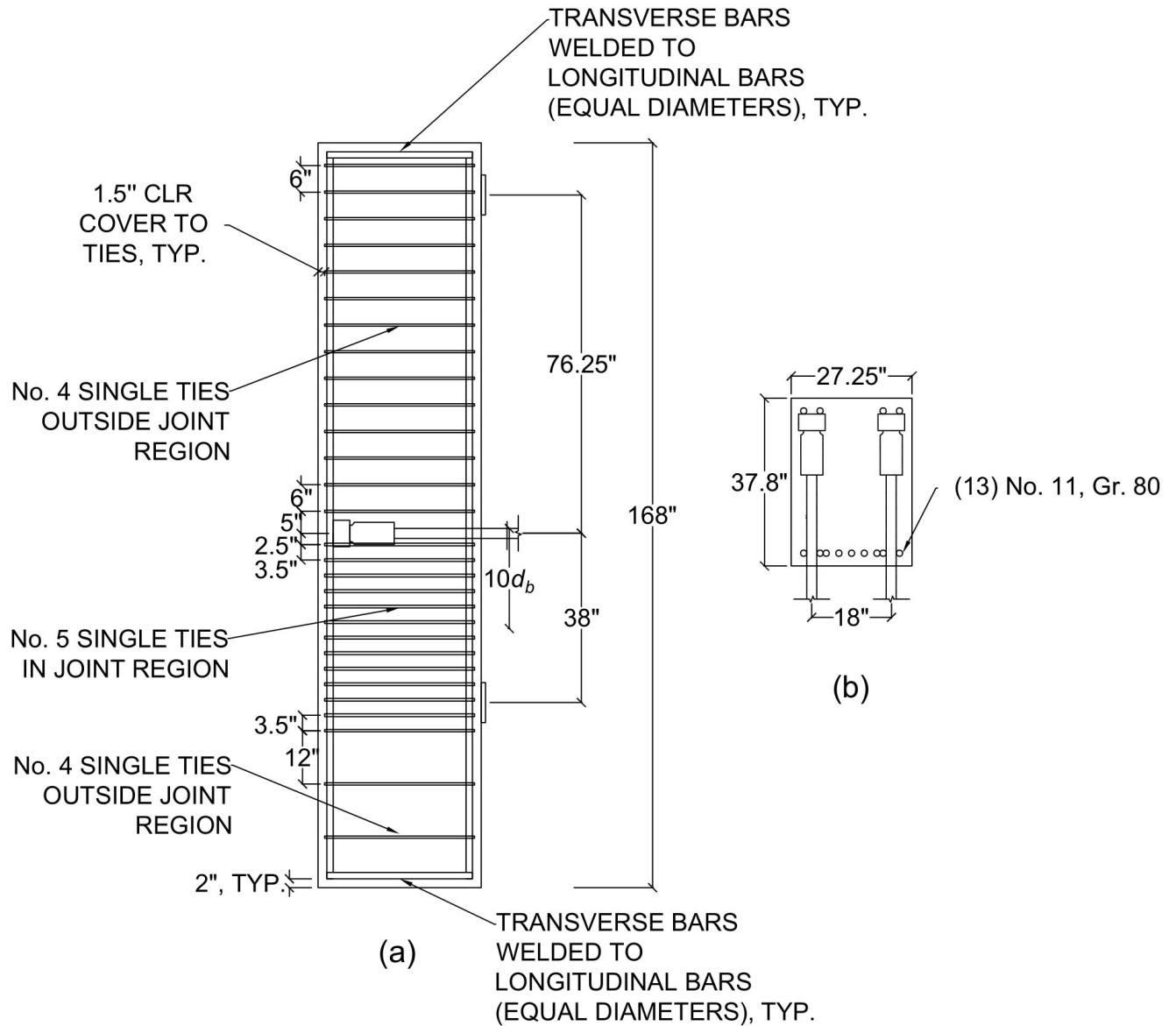


Figure C.24 Details of reinforcement layout for No. 18 headed bar specimen 18-4: (a) elevation, (b) cross-section

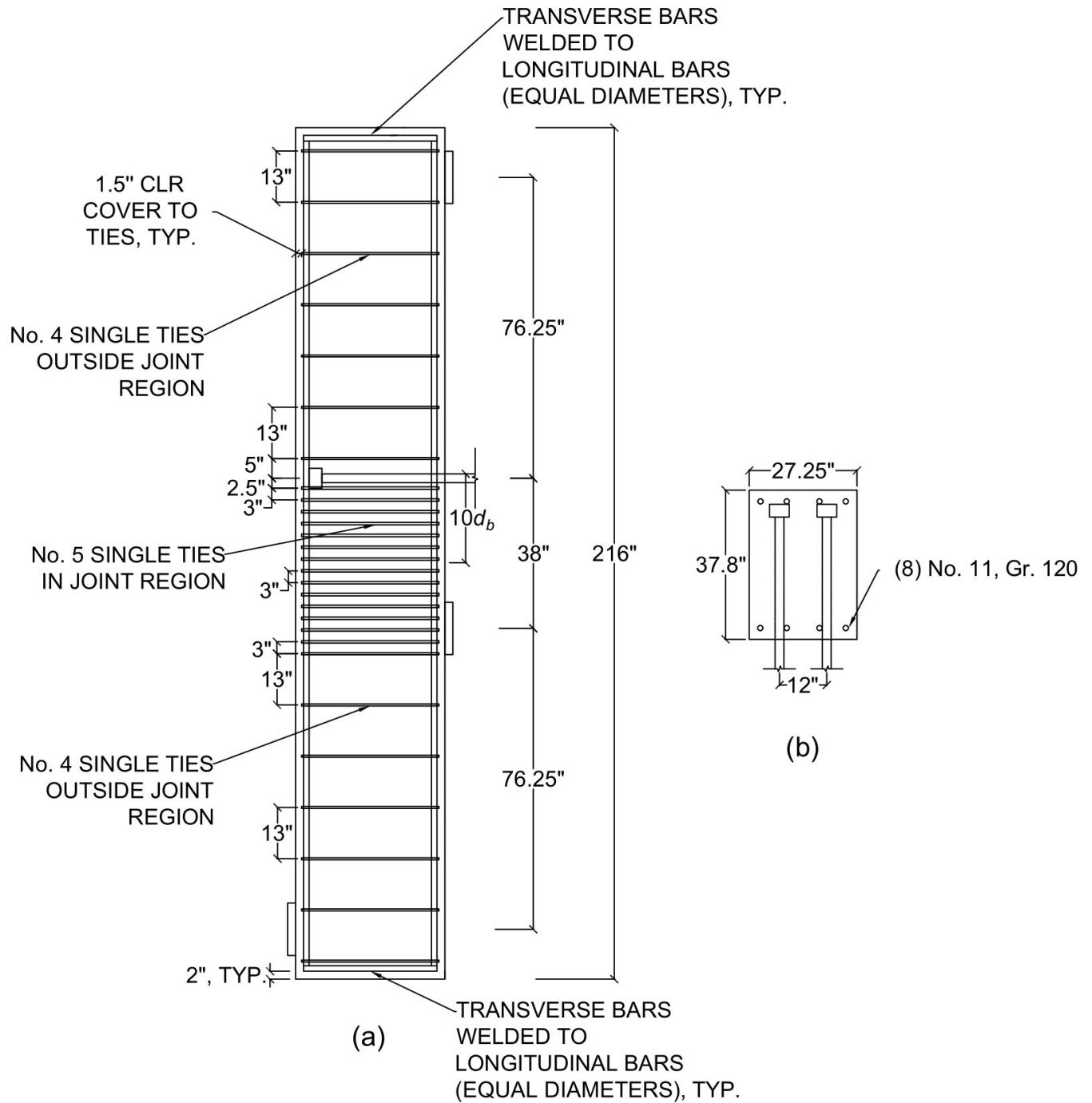


Figure C.25 Details of reinforcement layout for No. 18 headed bar specimen 18-5: (a) elevation, (b) cross-section

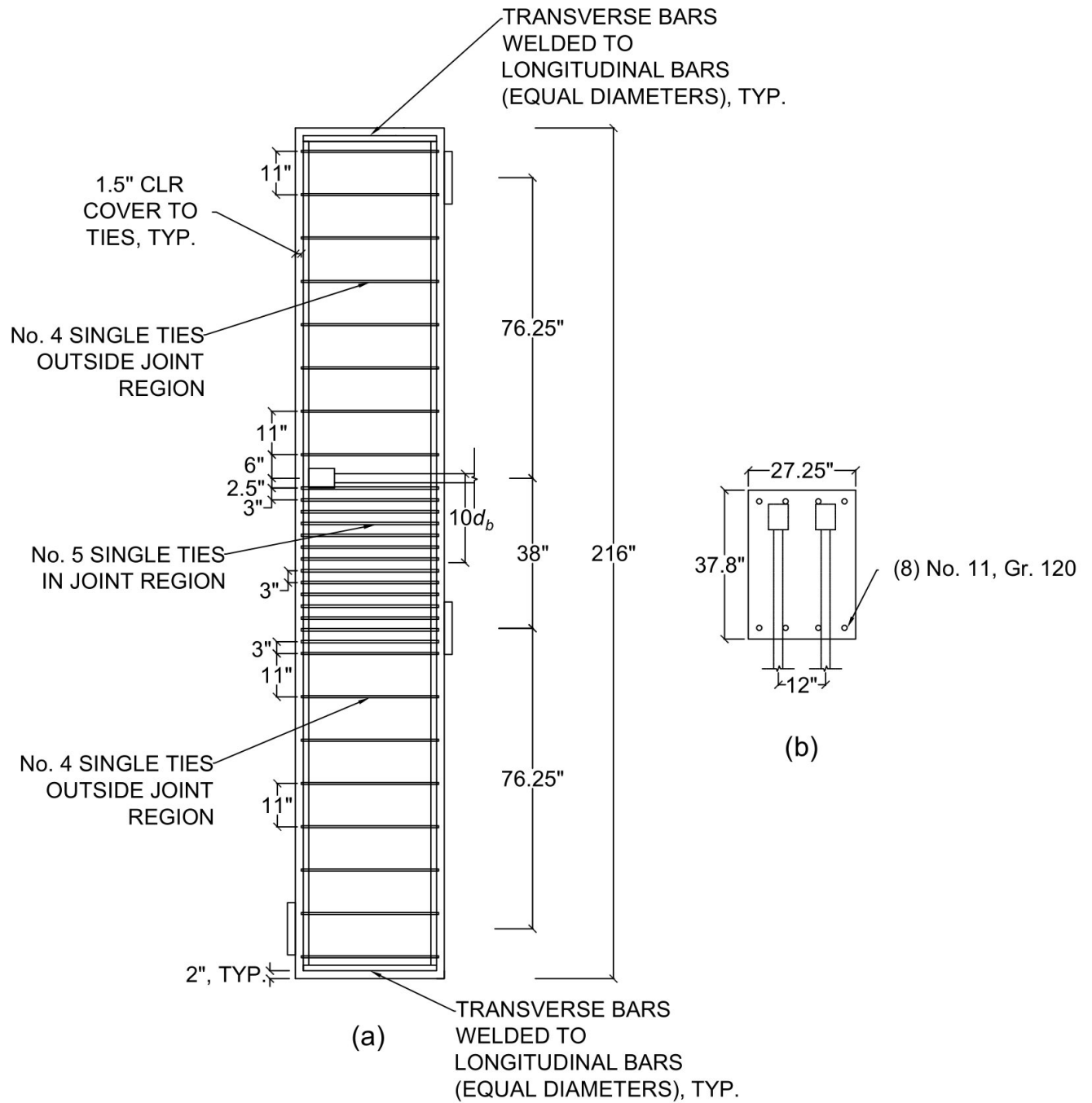


Figure C.26 Details of reinforcement layout for No. 18 headed bar specimen 18-6: (a) elevation, (b) cross-section

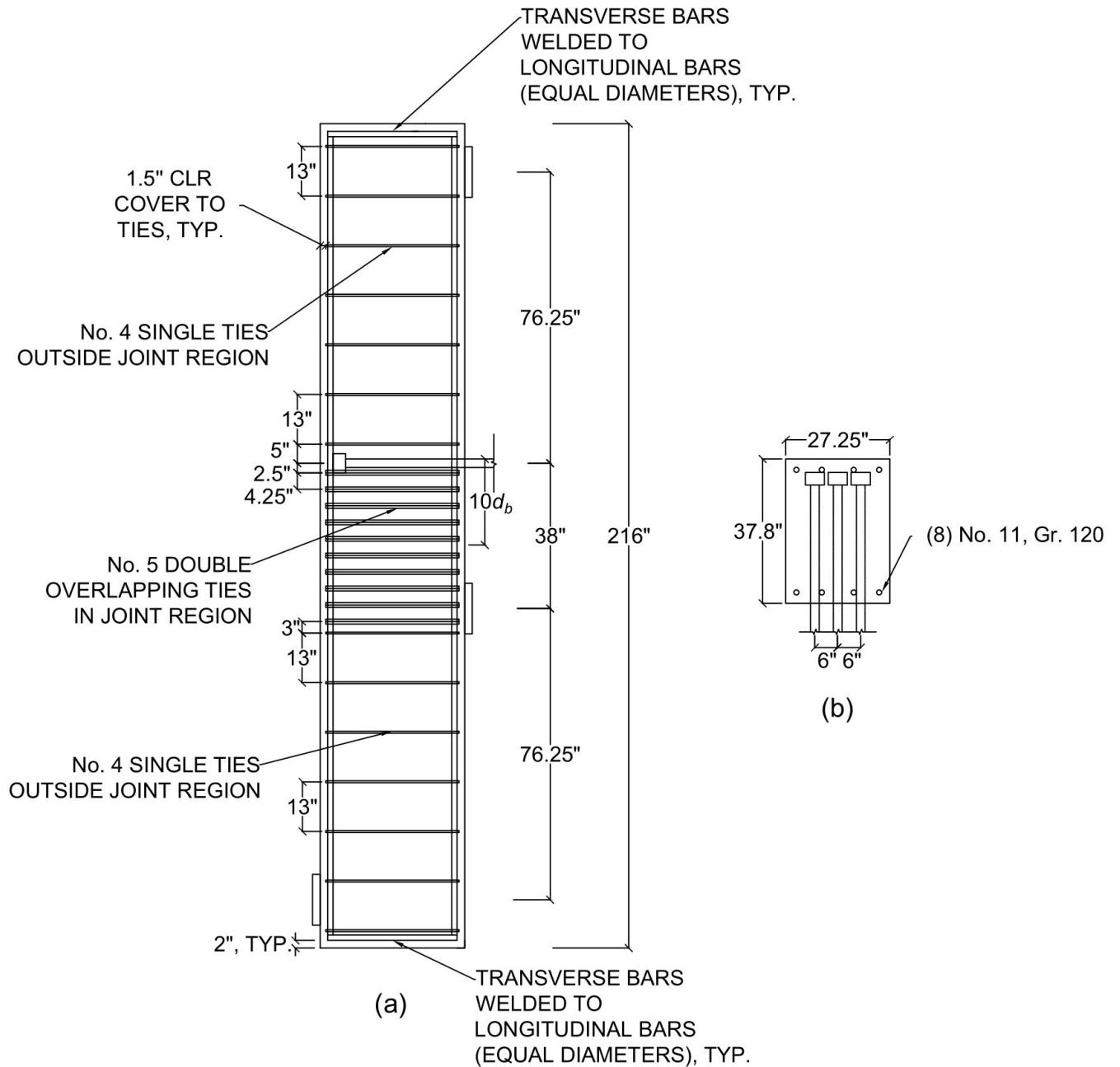


Figure C.27 Details of reinforcement layout for No. 18 headed bar specimen 18-7: (a) elevation, (b) cross-section

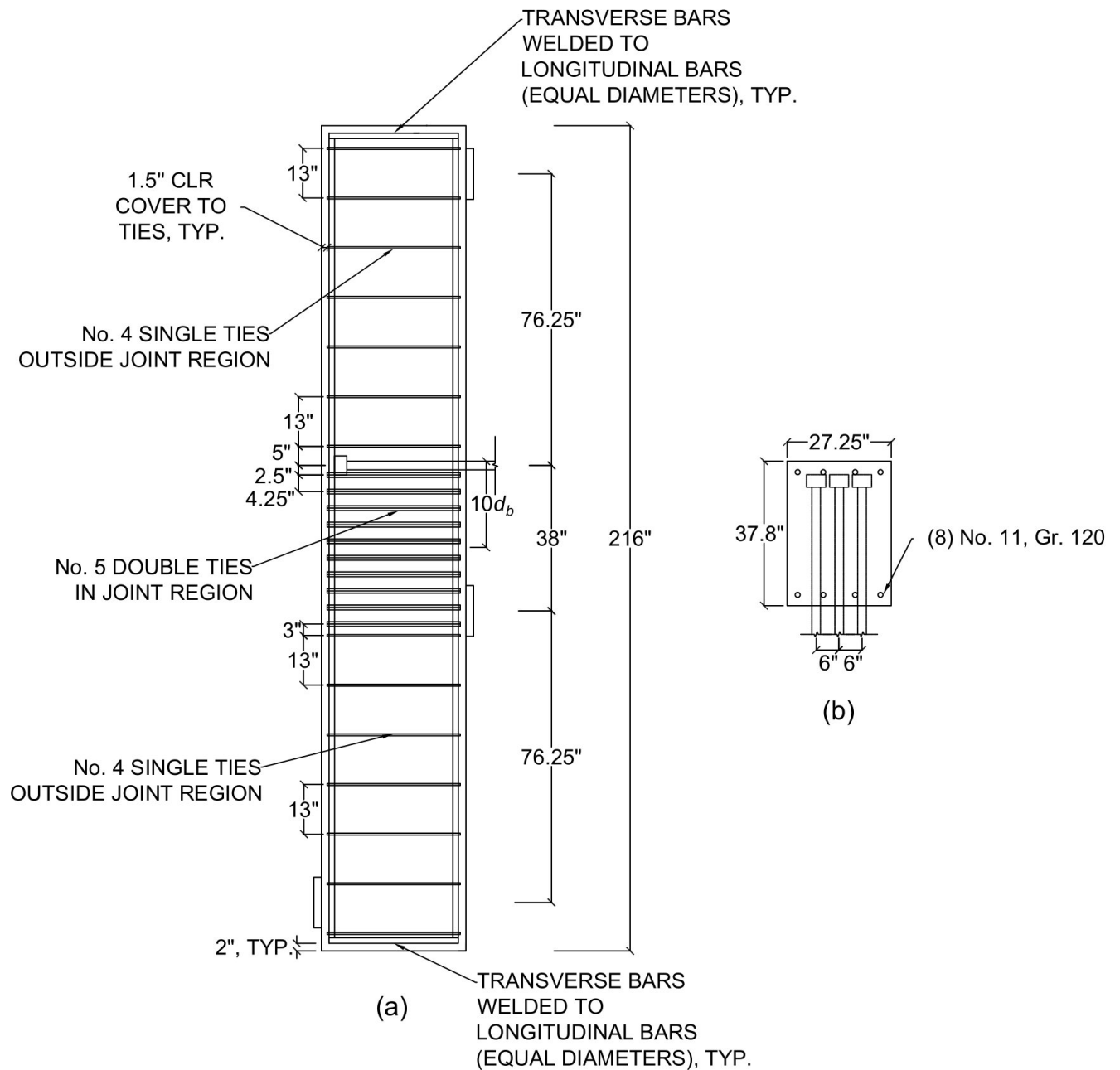


Figure C.28 Details of reinforcement layout for No. 18 headed bar specimen 18-8: (a) elevation, (b) cross-section

C.2 DETAILED PROPERTIES AND TEST RESULTS FOR NO. 14 AND NO. 18 BAR SPECIMENS TESTED IN CURRENT STUDY

Table C.1 Detailed properties and test results for No. 14 and No. 18 bar specimens tested in current study

ID	Designation	n	Head	ℓ_{eh}	$\ell_{eh,avg}$	f_{cm}	Age	d_b	A_b	A_{brg}
				in.	in.	psi	Days	in.	in. ²	
11-1	(2@10)11-15-O4.5-i- 3.5-3.5-18.25	2	A	18.5	18.5	16,210	265	1.41	1.56	4.5
			B	18.5						
11-2	(2@10)11-15-O4.5-7#3-i- 3.5-3.5-18.25	2	A	18.5	18.5	15,850	275	1.41	1.56	4.5
			B	18.5						
14-2	(2@10.6)14-15-B4.2-5#4-i-3.5-3.5-20.5	2	A	20.5	20.5	12,830	69	1.693	2.25	4.2
			B	20.5						
14-3	(2@10.6)14-7-L4.2-i-3.5-3.5-31.9	2	A	32.1	31.8	8,510	170	1.693	2.25	4.2
			B	31.4						
14-4	(2@10.6)14-7-L4.2-5#4-i-3.5-3.5-31.9	2	A	32.0	32.0	7,700	16	1.693	2.25	4.2
			B	32.0						
14-15	(2@10.6)14-7-L4.2-i-3.5-3.5-22.7	2	A	22.6	22.8	6,190	21	1.693	2.25	4.2
			B	23.1						
14-16	(2@10.6)14-7-L4.2-3#4-i-3.5-3.5-22.7	2	A	23.1	22.6	5,390	8	1.693	2.25	4.2
			B	22.0						
14-16A	(2@10.6)14-7-L4.2-3#4-i-3.5-3.5-22.7	2	A	22.6	22.4	8,350	14	1.693	2.25	4.2
			B	22.3						
14-1A	(2@10.6)14-15-L4.2-i-3.5-3.5-22.7	2	A	22.3	22.4	12,030	122	1.693	2.25	4.2
			B	22.6						
14-2A	(2@10.6)14-15-L4.2-5#4-i-3.5-3.5-22.7	2	A	23.1	23.0	13,750	136	1.693	2.25	4.2
			B	22.9						
14-16B	(2@10.6)14-7-L4.2-3#4-i-3.5-3.5-22.7	2	A	22.5	22.1	7,500	28	1.693	2.25	4.2
			B	21.8						
14-16C	(2@10.6)14-7-L4.2-7#4-i-3.5-3.5-22.7	2	A	22.8	22.6	6,470	7	1.693	2.25	4.2
			B	22.4						
14-16D	(2@10.6)14-7-L4.2-10#5-i-3.5-3.5-22.7	2	A	22.8	22.9	6,900	32	1.693	2.25	4.2
			B	23.0						
14-16E	(2@10.6)14-7-L4.2-6#5-i-3.5-3.5-22.7	2	A	22.3	22.4	6,170	16	1.693	2.25	4.2
			B	22.5						
14-16F	(2@10.6)14-7-L4.2-6#5-i-3.5-3.5-22.7	2	A	22.1	22.1	5,640	8	1.693	2.25	4.2
			B	22.1						
14-17	(2@7.1)14-7-L4.2-6#5-i-6.5-3.5-22.7	2	A	22.5	22.4	6,540	16	1.693	2.25	4.2
			B	22.3						

Table C.1 Cont. Detailed properties and test results for No. 14 and No. 18 bar specimens tested in current study

ID	b	h	h_{cl}	b_{BP}	d_{eff}	d_{eff}/ℓ_{eh}	c_{so}	c_o	c_{bc}	s	s/d_b	Bar spacing
	in.	in.	in.	in.	in.		in.	in.	in.	in.		
11-1	22.5	24.5	20.5	6	22.12	1.20	3.5	2.3	3.5	14.1	10.0	Wide
11-2	22.5	24.5	20.5	6	22.74	1.23	3.5	2.3	3.5	14.1	10.0	Wide
14-2	26.7	28.6	25.5	6	27.55	1.34	3.5	2.4	3.5	18	10.6	Wide
14-3	26.7	37.8	25.5	6	30.37	0.95	3.5	2.4	3.5	18	10.6	Wide
14-4	26.7	37.8	25.5	6	31.28	0.98	3.5	2.4	3.5	18	10.6	Wide
14-15	26.7	28.6	25.5	6	29.48	1.29	3.5	2.4	3.5	18	10.6	Wide
14-16	26.7	28.6	25.5	6	28.13	1.24	3.5	2.4	3.5	18	10.6	Wide
14-16A	26.7	28.6	25.5	6	28.56	1.28	3.5	2.4	3.5	18	10.6	Wide
14-1A	26.7	28.6	25.5	6	27.34	1.22	3.5	2.4	3.5	18	10.6	Wide
14-2A	26.7	28.6	25.5	6	27.99	1.22	3.5	2.4	3.5	18	10.6	Wide
14-16B	26.7	28.6	25.5	6	28.88	1.31	3.5	2.4	3.5	18	10.6	Wide
14-16C	26.7	28.6	25.5	6	29.45	1.30	3.5	2.4	3.5	18	10.6	Wide
14-16D	26.7	28.6	25.5	6	30.79	1.34	3.5	2.4	3.5	18	10.6	Wide
14-16E	26.7	28.6	25.5	6	29.75	1.33	3.5	2.4	3.5	18	10.6	Wide
14-16F	26.7	28.6	25.5	6	29.56	1.34	3.5	2.4	3.5	18	10.6	Wide
14-17	26.7	28.6	25.5	6	29.39	1.31	6.5	5.4	3.5	12	7.1	Close

Table C.1 Cont. Detailed properties and test results for No. 14 and No. 18 bar specimens tested in current study

ID	d_{to}	N_p	n_p	n_u	d_p	A_p	A_{tt}	A_{hs}	A_{tt}/A_{hs}	L. C.
	in.				in.	in. ²	in. ²	in. ²		
11-1	0.38	0	0	0	0	0	0	3.12	0	B
11-2	0.38	7	4	8	0.375	0.11	0.88	3.12	0.282	B
14-2	0.5	5	3	6	0.5	0.2	1.2	4.50	0.267	A
14-3	0.5	0	0	0	0	0	0	4.50	0	B
14-4	0.5	5	3	6	0.5	0.2	1.2	4.50	0.267	A
14-15	0.5	0	0	0	0	0	0	4.50	0	B
14-16	0.5	3	2	4	0.5	0.2	0.8	4.50	0.178	A
14-16A	0.5	3	2	4	0.5	0.2	0.8	4.50	0.178	A
14-1A	0.5	0	0	0	0	0	0	4.50	0	B
14-2A	0.5	5	3	6	0.5	0.2	1.2	4.50	0.267	B
14-16B	0.5	3	2	4	0.5	0.2	0.8	4.50	0.178	B
14-16C	0.5	7	4	8	0.5	0.2	1.6	4.50	0.356	B
14-16D	0.5	5	3	12	0.625	0.31	3.72	4.50	0.827	A
14-16E	0.5	5	2	8	0.625	0.31	2.48	4.50	0.551	A
14-16F	0.5	3	2	8	0.625	0.31	2.48	4.50	0.551	A
14-17	0.5	3	2	8	0.625	0.31	2.48	4.50	0.551	A

Table C.1 Cont. Detailed properties and test results for No. 14 and No. 18 bar specimens tested in current study

ID	Δ_{max}	Δ_{ind}	T_{max}	$f_{s,max}$	T_{ind}	T_{total}	T	f_s	Failure Type
	in.	in.	kips	ksi	kips	kips	kips	ksi	
11-1	2.22	0.84	165.2	105.91	165.1	326.0	163.0	104.5	CB+SS
	1.02	0.76	160.2	102.71	160.2				
11-2	0.61	0.26	229.7	147.23	229.7	442.0	221.0	141.7	SS
	2.35	0.30	212.8	136.4	212.8				
14-2	1.48	0.25	194	86.2	193.5	381.2	190.6	84.7	SF
	1.48	0.21	188.1	83.6	187.8				
14-3*	-	0.26	289.9	128.8	289.5	606.0	303.0	134.7	SS
	0.90	0.24	316.1	140.5	273.5				
14-4	0.17	0.08	331.1	147.2	328.5	667.2	333.6	148.3	SS
	0.33	0.14	339.1	150.7	339.1				
14-15	1.07	0.52	217.2	96.5	217.2	409.6	204.8	91.0	CB+SS
	1.39	0.26	192.4	85.5	192.4				
14-16	1.2	0.08	127.8	56.8	127.8	247.2	123.6	54.9	SF
	1.3	0.05	119.4	53.1	119.4				
14-16A	0.71	0.26	190.8	84.8	190.8	372.0	186.0	82.7	SF
	0.70	0.15	181.5	80.7	181.1				
14-1A	0.15	0.04	159.2	70.7	159.0	320.0	160.0	71.1	SF
	0.72	0.42	163.5	72.6	163.5				
14-2A	0.41	0.36	258.2	114.8	258.1	496.2	248.1	110.3	CB
	0.63	0.20	238.0	105.8	237.8				
14-16B	1.91	1.60	201.1	89.4	200.9	383.4	191.7	85.2	CB+SS
	0.96	0.67	182.4	81.1	182.4				
14-16C	0.26	0.11	192.1	85.4	191.1	416.9	208.4	92.6	SS
	0.51	0.41	225.8	100.4	225.7				
14-16D*	0.67	0.25	304.4	135.3	273.5	579.6	289.8	128.8	SS
	0.21	0.18	275.3	122.4	275.1				
14-16E	1.28	0.21	219	97.3	219.0	437.2	218.6	97.2	SS
	1.10	0.05	227.4	101.1	218.2				
14-16F	0.93	0.13	198.09	88.0	198.1	395.6	197.8	87.9	SS
	1.20	0.14	197.5	87.8	197.5				
14-17	0.81	0.19	203.5	90.5	203.5	413.4	206.7	91.9	CB
	0.90	0.25	210.1	93.4	209.9				

* Bars failed independently, so T is the average of the maximum force on individual bar

Table C.1 Cont. Detailed properties and test results for No. 14 and No. 18 bar specimens tested in current study

ID	Designation	<i>n</i>	Head	ℓ_{eh}	$\ell_{eh,avg}$	f_{cm}	Age	d_b	A_b	A_{brg}
				in.	in.	psi	Days	in.	in. ²	
14-5	(3@3.5)14-7-L4.2-5#4-i-3.5-3.5-22.7	3	A	22.3	22.3	6,830	31	1.693	2.25	4.2
			B	22.3						
			C	22.4						
14-6	(3@3.5)14-7-L4.2-5#5-i-3.5-3.5-22.7	3	A	22.3	22.4	6,890	51	1.693	2.25	4.2
			B	22.5						
			C	22.5						
14-7	(3@3.5)14-7-L4.2-i-3.5-3.5-31.9	3	A	32.0	32.1	7,080	102	1.693	2.25	4.2
			B	32.1						
			C	32.3						
14-8	(3@3.5)14-7-L4.2-5#5-i-3.5-3.5-31.9	3	A	31.6	31.7	7,100	109	1.693	2.25	4.2
			B	31.8						
			C	31.6						
14-9	(3@3.5)14-12-L4.2-5#5-i-3.5-3.5-22.7	3	A	22.3	22.1	11,480	38	1.693	2.25	4.2
			B	22.0						
			C	22.1						
14-10	(3@3.5)14-7-L4.2-10#5-i-3.5-3.5-22.7	3	A	22.3	22.3	6,820	42	1.693	2.25	4.2
			B	22.1						
			C	22.4						
18-1	(2@8.0)18-7-L4.4-14#5-i-3.5-3.5-31.1	2	A	32.5	32.6	5,750	20	2.257	4.00	4.4
			B	32.6						
18-2	(2@8.0)18-15-H4.4-14#5-i-3.5-3.5-27.8	2	A	28.3	28.4	11,770	45	2.257	4.00	4.4
			B	28.6						
18-3	(2@8.0)18-7-O4.3-6#5-i-3.5-3.5-30.6	2	A	31.1	30.9	6,540	8	2.257	4.00	4.3
			B	30.8						
18-4	(2@8.0)18-7-O4.3-12#5-i-3.5-3.5-30.6	2	A	30.8	30.9	7,200	15	2.257	4.00	4.3
			B	31.0						
18-5	(2@5.3)18-7-L4.4-14#5-i-6.5-3.5-31.1	2	A	32.0	32.5	5,310	23	2.257	4.00	4.4
			B	33.0						
18-6	(2@5.3)18-15-H4.4-14#5-i-6.5-3.5-27.8	2	A	28.6	28.6	10,230	53	2.257	4.00	4.4
			B	28.6						
18-7	(3@2.7)18-7-L4.4-20#5-i-6.5-3.5-31.1	3	A	32.0	32.1	5,890	20	2.257	4.00	4.4
			B	32.0						
			C	32.3						
18-8	(3@2.7)18-7-L4.4-20#5-i-6.5-3.5-31.1	3	A	32.3	32.3	6,380	27	2.257	4.00	4.4
			B	32.0						
			C	32.8						

Table C.1 Cont. Detailed properties and test results for No. 14 and No. 18 bar specimens tested in current study

ID	b	h	h_{cl}	b_{BP}	d_{eff}	d_{eff}/ℓ_{eh}	c_{so}	c_o	c_{bc}	s	s/d_b	Bar spacing
	in.	in.	in.	in.	in.		in.	in.	in.	in.		
14-5	20.7	28.6	24.0	9	30.45	1.37	3.5	2.4	3.5	6	3.5	Close
14-6	20.7	28.6	24.0	9	30.34	1.35	3.5	2.4	3.5	6	3.5	Close
14-7	20.7	37.8	24.0	9	32.76	1.02	3.5	2.4	3.5	6	3.5	Close
14-8	20.7	37.8	24.0	9	33.53	1.06	3.5	2.4	3.5	6	3.5	Close
14-9	20.7	28.6	25.5	6	29.51	1.34	3.5	2.4	3.5	6	3.5	Close
14-10	20.7	28.6	24.0	9	31.33	1.40	3.5	2.4	3.5	6	3.5	Close
18-1	27.3	37.8	33.7	9	39.99	1.23	3.5	2.1	3.5	18	8.0	Wide
18-2	27.3	37.8	35.2	6	39.74	1.40	3.5	2.1	3.5	18	8.0	Wide
18-3	27.3	37.8	33.7	9	40.34	1.31	3.5	1.7	3.5	18	8.0	Wide
18-4	27.3	37.8	33.7	9	40.25	1.30	3.5	1.7	3.5	18	8.0	Wide
18-5	27.3	37.8	33.7	9	39.88	1.23	6.5	5.1	3.5	12	5.3	Close
18-6	27.3	37.8	35.2	6	40.60	1.42	6.5	5.1	3.5	12	5.3	Close
18-7	27.3	37.8	32.2	12	39.49	1.23	6.5	5.1	3.5	6	2.7	Close
18-8	27.3	37.8	32.2	12	40.35	1.25	6.5	5.1	3.5	6	2.7	Close

Table C.1 Cont. Detailed properties and test results for No. 14 and No. 18 bar specimens tested in current study

ID	d_{to}	N_{tp}	n_{tp}	n_{tt}	d_{tp}	A_{tp}	A_{tt}	A_{hs}	A_{tt}/A_{hs}	L. C.
	in.				in.	in. ²	in. ²	in. ²		
14-5	0.5	5	3	6	0.5	0.2	1.2	6.75	0.178	B
14-6	0.5	5	3	6	0.625	0.31	1.86	6.75	0.276	B
14-7	0.5	0	0	0	0	0	0	6.75	0	B
14-8	0.5	5	3	6	0.625	0.31	1.86	6.75	0.276	B
14-9	0.5	5	3	6	0.625	0.31	1.86	6.75	0.276	B
14-10	0.5	5	3	12	0.625	0.31	3.72	6.75	0.551	A
18-1	0.5	14	7	14	0.625	0.31	4.34	8.00	0.543	A
18-2	0.5	14	7	14	0.625	0.31	4.34	8.00	0.543	A
18-3	0.5	6	3	6	0.625	0.31	1.86	8.00	0.233	B
18-4	0.5	12	6	12	0.625	0.31	3.72	8.00	0.465	B
18-5	0.5	14	7	14	0.625	0.31	4.34	8.00	0.543	A
18-6	0.5	14	7	14	0.625	0.31	4.34	8.00	0.543	A
18-7	0.5	10	5	20	0.625	0.31	6.2	12.00	0.517	A
18-8	0.5	10	5	20	0.625	0.31	6.2	12.00	0.517	A

Table C.1 Cont. Detailed properties and test results for No. 14 and No. 18 bar specimens tested in current study

ID	Δ_{max}	Δ_{ind}	T_{max}	$f_{s,max}$	T_{ind}	T_{total}	T	f_s	Failure Type
	in.	in.	kips	ksi	kips	kips	kips	ksi	
14-5	0.71	0.11	188.0	83.6	188.0	545.4	181.8	80.8	CB
	1.01	0.24	174.5	77.5	174.5				
	0.92	0.08	182.9	81.3	182.9				
14-6	0.66	0.06	179.7	79.9	179.5	538.5	179.5	79.8	CB
	0.78	0.25	176.3	78.4	176.3				
	0.73	0.20	182.7	81.2	182.6				
14-7	1.22	0.11	254.7	113.2	254.7	756.3	252.1	112.0	CB+SS
	2.03	0.27	248.8	110.6	248.6				
	1.73	0.28	253.2	112.5	253.2				
14-8	0.64	0.10	279.1	124.1	279.1	823.8	274.6	122.0	CB+SS
	0.57	0.13	266.0	118.2	266.0				
	0.34	0.02	278.7	123.9	278.7				
14-9	0.94	0.32	178.8	79.4	178.8	521.7	173.9	77.3	CB
	0.87	0.40	165.5	73.6	165.4				
	1.00	0.45	177.8	79.0	177.4				
14-10	0.60	0.26	208.1	92.5	207.9	619.8	206.6	91.8	CB
	0.81	0.30	205.3	91.3	205.3				
	0.73	0.28	206.4	91.7	206.4				
18-1	0.90	0.24	366.7	91.7	323.8	644.0	322.0	80.5	SS
	0.74	0.31	320.1	80.0	320.1				
18-2	2.74	1.35	406.3	101.6	404.7	813.2	406.6	101.7	CB+SS
	1.86	1.38	408.5	102.1	408.5				
18-3	1.07	0.34	366.0	91.5	364.8	733.0	366.5	91.6	CB
	1.07	0.34	368.3	92.1	368.3				
18-4	0.99	0.13	382.1	95.5	382.1	760.0	380.0	95.0	SS
	1.08	0.04	378.4	94.6	378.0				
18-5	1.20	0.98	300.5	75.1	300.5	601.6	300.8	75.2	CB
	1.16	0.02	301.1	75.3	301.1				
18-6	1.64	1.33	418.4	104.6	418.4	839.6	419.8	105.0	SS
	1.73	1.41	421.3	105.3	421.3				
18-7	0.49	0.13	256.4	64.1	256.2	756.3	252.1	63.0	CB+SS
	0.54	0.30	241.6	60.4	241.6				
	0.46	0.20	258.5	64.6	258.5				
18-8	2.32	0.48	291.7	72.9	291.7	885.9	295.3	73.8	CB+SS
	1.98	0.28	303.6	75.9	303.6				
	2.07	0.23	290.8	72.7	290.5				

C.3 SPECIMENS TESTED AT THE UNIVERSITY OF KANSAS

This section presents the specimens tested at the University of Kansas, including No. 5, No. 8, and No. 11 bar specimens tested by Shao et al. (2016), and No. 14 and No. 18 bar specimens tested in this study. Specimens are tabulated in four categories: widely-spaced bars without parallel ties (Table C2), closely-spaced bars without parallel ties (Table C3), widely-spaced bars with parallel ties (Table C4), and closely-spaced bars with parallel ties (Table C5). In each category, specimens not used to develop descriptive equations, Eq. (5.5) and (5.7), are identified, if any.

Table C.2 Detailed properties and test results for headed bar specimens having widely-spaced bars without parallel ties tested at the University of Kansas

SN	ID	b	h	$\ell_{eh,avg}$	f_{cm}	d_b	A_b	s	s/d_b
		in.	in.	in.	psi	in.	in. ²	in.	
1	5-5-F4.0-0-i-2.5-5-4	12.9	9.6	4.1	4810	0.625	0.31	7.3	11.7
2	5-5-F4.0-0-i-2.5-3-6	14.9	9.5	6.0	4690	0.625	0.31	7.3	11.7
3	5-12-F4.0-0-i-2.5-5-4	12.9	9.6	4.1	11030	0.625	0.31	7.3	11.7
4	5-12-F4.0-0-i-2.5-3-6	15.0	9.5	6.0	11030	0.625	0.31	7.4	11.8
5	8-5g-T4.0-0-i-2.5-3-12.5	16.8	17.1	12.6	5910	1	0.79	10.8	10.8
6	8-5g-T4.0-0-i-3.5-3-12.5	17.1	17.0	12.5	6320	1	0.79	11.1	11.1
7	8-5-T4.0-0-i-2.5-3-12.5	16.8	17.1	12.6	6210	1	0.79	10.8	10.8
8	8-5-T4.0-0-i-3.5-3-12.5	16.4	17.2	12.7	6440	1	0.79	10.4	10.4
9	8-8-F4.1-0-i-2.5-3-10.5	16.9	14.5	10.5	8450	1	0.79	10.9	10.9
10	8-12-F4.1-0-i-2.5-3-10	16.9	13.7	9.7	11760	1	0.79	10.9	10.9
11	8-5-S6.5-0-i-2.5-3-11.25	16.8	15.8	11.1	5500	1	0.79	10.8	10.8
12	8-5-S6.5-0-i-2.5-3-14.25	16.6	19.0	14.3	5500	1	0.79	10.6	10.6
13	8-5-O4.5-0-i-2.5-3-11.25	16.9	19.5	11.3	5500	1	0.79	10.9	10.9
14	8-5-O4.5-0-i-2.5-3-14.25	17.0	22.4	14.1	5500	1	0.79	11.0	11.0
15	8-5-T9.5-0-i-2.5-3-14.5	16.9	18.9	14.4	4970	1	0.79	10.9	10.9
16	8-5-O9.1-0-i-2.5-3-14.5	17.0	22.6	14.4	4970	1	0.79	11.0	11.0
17	8-15-T4.0-0-i-2.5-4.5-9.5	17.0	15.5	9.5	16030	1	0.79	11.0	11.0

Table C.2 Cont. Detailed properties and test results for headed bar specimens having widely-spaced bars without parallel ties tested at the University of Kansas

SN	n	A_t	A_{hs}	A_t/A_{hs}	h_{cl}	x_{mid}	d_{eff}	d_{eff}/ℓ_{eh}	θ
		in. ²	in. ²		in.	in.	in.		°
1	2	0	0.62	0	5.25	9.44	6.40	1.58	66.7
2	2	0	0.62	0	5.25	9.44	6.60	1.10	57.6
3	2	0	0.62	0	5.25	9.44	5.97	1.47	66.7
4	2	0	0.62	0	5.25	9.44	6.16	1.03	57.6
5	2	0	1.58	0	10.0	14.19	13.07	1.04	48.5
6	2	0	1.58	0	10.0	14.19	12.77	1.02	48.6
7	2	0	1.58	0	10.0	14.19	12.54	1.00	48.4
8	2	0	1.58	0	10.0	14.19	12.81	1.01	48.3
9	2	0	1.58	0	10.0	14.19	11.95	1.14	53.5
10	2	0	1.58	0	10.0	14.19	11.31	1.17	55.7
11	2	0	1.58	0	10.0	14.19	12.48	1.13	52.1
12	2	0	1.58	0	10.0	14.19	12.92	0.91	44.9
13	2	0	1.58	0	10.0	14.19	12.20	1.08	51.6
14	2	0	1.58	0	10.0	14.19	12.76	0.90	45.1
15	2	0	1.58	0	10.0	14.19	13.20	0.92	44.6
16	2	0	1.58	0	10.0	14.19	13.29	0.92	44.6
17	2	0	1.58	0	10.0	14.19	11.11	1.17	56.2

Table C.2 Cont. Detailed properties and test results for headed bar specimens having widely-spaced bars without parallel ties tested at the University of Kansas

SN	T	$T_h^{[1]}$	T/T_h	f_{su}	$f_{su}/f_{s,calc}^{[2]}$	$f_{su}/f_{s,calc}^{[3]}$
	lb	lb		ksi		
1	24500	22194	1.10	79.0	1.48	1.48
2	32700	31887	1.03	105.5	1.35	1.35
3	28300	26355	1.07	91.3	1.39	1.39
4	41700	38065	1.10	134.5	1.39	1.39
5	97700	84758	1.15	123.7	1.44	1.44
6	93400	85541	1.09	118.2	1.36	1.36
7	83300	85808	0.97	105.4	1.21	1.21
8	91900	86910	1.06	116.3	1.32	1.32
9	77100	77095	1.00	97.6	1.24	1.24
10	71800	76548	0.94	90.9	1.15	1.15
11	75555	74071	1.02	95.6	1.29	1.29
12	87720	94024	0.93	111.0	1.16	1.16
13	67390	75268	0.90	85.3	1.13	1.13
14	85000	93279	0.91	107.6	1.13	1.13
15	91650	92862	0.99	116.0	1.23	1.23
16	94800	92862	1.02	120.0	1.27	1.27
17	83300	80113	1.04	105.4	1.26	1.26

^[1] Based on descriptive equations, Eq. (5.5) and (5.7)

^[2] Based on proposed design equation, Eq. (6.32), using full expression for ψ_p , Eq. (6.29)

^[3] Based on proposed design equation, Eq. (6.32), using simplified expression for ψ_p , Eq. (6.30)

Table C.2 Cont. Detailed properties and test results for headed bar specimens having widely-spaced bars without parallel ties tested at the University of Kansas

SN	ID	<i>b</i>	<i>h</i>	$\ell_{eh,avg}$	f_{cm}	d_b	A_b	<i>s</i>	<i>s/d_b</i>
		in.	in.	in.	psi	in.	in. ²	in.	
18	8-15-S9.5-0-i-2.5-3-9.5	17.0	15.3	9.5	16030	1	0.79	11.0	11.0
19	8-8-T9.5-0-i-2.5-3-9.5	17.0	13.9	9.4	9040	1	0.79	11.0	11.0
20	(2@9)8-12-F4.1-0-i-2.5-3-12	15.0	16.1	12.1	12080	1	0.79	9.0	9.0
21	(2@9)8-12-F9.1-0-i-2.5-3-12	14.9	15.9	11.9	12080	1	0.79	8.9	8.9
22	8-8-O4.5-0-i-2.5-3-9.5	17.1	17.4	9.2	6710	1	0.79	11.1	11.1
23	(2@9)8-8-O4.5-0-i-2.5-3-9.5	15.1	17.3	9.0	6710	1	0.79	9.1	9.1
24	(2@9)8-8-T4.0-0-i-2.5-3-9.5	15.1	13.9	9.4	6790	1	0.79	9.1	9.1
25	11-5a-F3.8-0-i-2.5-3-17	21.9	20.9	16.6	4050	1.41	1.56	15.5	11.0
26	11-5-F3.8-0-i-2.5-3-17	21.4	21.6	17.3	5760	1.41	1.56	15.0	10.6
27	11-12-O4.5-0-i-2.5-3-16.75	21.4	26.9	17.1	10860	1.41	1.56	15.0	10.6
28	11-12-S5.5-0-i-2.5-3-16.75	21.7	22.7	16.9	10120	1.41	1.56	15.3	10.9
29	11-5-O4.5-0-i-2.5-3-19.25	21.5	29.2	19.4	5430	1.41	1.56	15.1	10.7
30	11-5-S5.5-0-i-2.5-3-19.25	21.5	25.1	19.4	6320	1.41	1.56	15.1	10.7
31	11-1	22.5	24.5	18.5	16210	1.41	1.56	14.1	10.0
32	14-3	26.7	37.8	31.8	8510	1.693	2.25	18.0	10.6
33	14-15	26.7	28.6	22.8	6190	1.693	2.25	18.0	10.6
34	14-1A*	26.7	28.6	22.4	12030	1.693	2.25	18.0	10.6

* Specimen failed in shear, not used to develop descriptive equations, Eq. (5.5) and (5.7)

Table C.2 Cont. Detailed properties and test results for headed bar specimens having widely-spaced bars without parallel ties tested at the University of Kansas

SN	n	A_t	A_{hs}	A_t/A_{hs}	h_{cl}	x_{mid}	d_{eff}	d_{eff}/ℓ_{eh}	θ
		in. ²	in. ²		in.	in.	in.		°
18	2	0	1.58	0	10.0	14.19	11.08	1.17	56.2
19	2	0	1.58	0	10.0	14.19	11.54	1.23	56.5
20	2	0	1.58	0	10.0	14.19	11.58	0.96	49.6
21	2	0	1.58	0	10.0	14.19	11.54	0.97	50.1
22	2	0	1.58	0	10.0	14.19	11.67	1.27	57.1
23	2	0	1.58	0	10.0	14.19	11.91	1.32	57.6
24	2	0	1.58	0	10.0	14.19	12.00	1.28	56.5
25	2	0	3.12	0	19.5	23.69	22.55	1.36	55.0
26	2	0	3.12	0	19.5	23.69	22.82	1.32	53.9
27	2	0	3.12	0	19.5	23.69	22.14	1.29	54.1
28	2	0	3.12	0	19.5	23.69	22.40	1.32	54.4
29	2	0	3.12	0	19.5	23.69	23.59	1.21	50.6
30	2	0	3.12	0	19.5	23.69	23.67	1.22	50.7
31	2	0	3.12	0	20.5	23.50	22.12	1.20	51.8
32	2	0	4.5	0	25.5	28.54	30.33	0.95	41.9
33	2	0	4.5	0	25.5	28.54	29.44	1.29	51.4
34	2	0	4.5	0	25.5	28.54	27.30	1.22	51.9

Table C.2 Cont. Detailed properties and test results for headed bar specimens having widely-spaced bars without parallel ties tested at the University of Kansas

SN	T	$T_h^{[1]}$	T/T_h	f_{su}	$f_{su}/f_{s,calc}^{[2]}$	$f_{su}/f_{s,calc}^{[3]}$
	lb	lb		ksi		
18	81650	80113	1.02	103.4	1.24	1.24
19	65200	70305	0.93	82.5	1.16	1.16
20	79050	94579	0.84	100.1	1.01	1.01
21	76500	93249	0.82	96.8	1.00	1.00
22	58350	64836	0.90	73.9	1.14	1.14
23	58800	63573	0.92	74.4	1.17	1.17
24	61800	66259	0.93	78.2	1.18	1.18
25	97500	120635	0.81	62.5	1.02	1.02
26	132700	134846	0.98	85.1	1.22	1.22
27	169600	152764	1.11	108.7	1.33	1.33
28	175900	148975	1.18	112.8	1.42	1.42
29	157900	149070	1.06	101.2	1.30	1.30
30	176800	153383	1.15	113.3	1.41	1.41
31	163000	178441	0.91	104.5	1.07	1.07
32	303000	284810	1.06	134.7	1.25	1.25
33	204800	194950	1.05	91.0	1.27	1.27
34	160000	220013	0.73	71.1	0.86	0.86

^[1] Based on descriptive equations, Eq. (5.5) and (5.7)

^[2] Based on proposed design equation, Eq. (6.32), using full expression for ψ_p , Eq. (6.29)

^[3] Based on proposed design equation, Eq. (6.32), using simplified expression for ψ_p , Eq. (6.30)

Table C.3 Detailed properties and test results for headed bar specimens having closely-spaced bars without parallel ties tested at the University of Kansas

SN	ID	<i>b</i>	<i>h</i>	$\ell_{eh,avg}$	f_{cm}	d_b	A_b	<i>s</i>	<i>s/d_b</i>
		in.	in.	in.	psi	in.	in. ²	in.	
35	(3@5.9)5-12-F4.0-0-i-2.5-4-5	13.2	9.5	5.0	11030	0.625	0.31	3.8	6.1
36	(4@3.9)5-12-F4.0-0-i-2.5-4-5	12.8	9.7	5.2	11030	0.625	0.31	2.4	3.8
37	(3@3)8-8-F4.1-0-i-2.5-3-10.5	12.0	14.6	10.6	8450	1	0.79	3.0	3.0
38	(3@3)8-8-F4.1-0-i-2.5-3-10.5-HP	11.8	14.3	10.3	8450	1	0.79	2.9	2.9
39	(3@4)8-8-F4.1-0-i-2.5-3-10.5	14.0	14.8	10.8	8450	1	0.79	4.0	4.0
40	(3@5)8-8-F4.1-0-i-2.5-3-10.5	16.0	14.4	10.4	8050	1	0.79	5.0	5.0
41	(3@5)8-8-F4.1-0-i-2.5-3-10.5-HP	16.1	14.3	10.3	8260	1	0.79	5.1	5.1
42	(3@3)8-12-F4.1-0-i-2.5-3-10	12.0	13.9	9.9	11040	1	0.79	3.0	3.0
43	(3@4)8-12-F4.1-0-i-2.5-3-10	14.0	13.9	9.9	11440	1	0.79	4.0	4.0
44	(3@5)8-12-F4.1-0-i-2.5-3-10	16.0	13.9	9.9	11460	1	0.79	5.0	5.0
45	(3@5.5)8-5-T9.5-0-i-2.5-3-14.5	16.5	18.8	14.3	4960	1	0.79	5.3	5.3
46	(3@5.5)8-5-O9.1-0-i-2.5-3-14.5	16.5	22.6	14.4	4960	1	0.79	5.3	5.3
47	(4@3.7)8-5-T9.5-0-i-2.5-3-14.5	17.4	18.8	14.3	5570	1	0.79	3.8	3.8
48	(4@3.7)8-5-O9.1-0-i-2.5-3-14.5	16.8	22.3	14.1	5570	1	0.79	3.6	3.6
49	(3@4)8-8-T9.5-0-i-2.5-3-9.5	14.0	13.8	9.3	9040	1	0.79	4.0	4.0
50	(3@5)8-8-T9.5-0-i-2.5-3-9.5	16.0	14.0	9.5	9940	1	0.79	5.0	5.0

Table C.3 Cont. Detailed properties and test results for headed bar specimens having closely-spaced bars without parallel ties tested at the University of Kansas

SN	n	A_{tt}	A_{hs}	A_{tt}/A_{hs}	h_{cl}	x_{mid}	d_{eff}	d_{eff}/ℓ_{eh}	θ
		in. ²	in. ²		in.	in.	in.		°
35	3	0	0.93	0	5.25	9.44	6.29	1.25	61.9
36	4	0	1.24	0	5.25	9.44	6.56	1.26	61.2
37	3	0	2.37	0	10.0	14.19	12.93	1.22	53.3
38	3	0	2.37	0	10.0	14.19	12.75	1.23	53.9
39	3	0	2.37	0	10.0	14.19	12.69	1.17	52.6
40	3	0	2.37	0	10.0	14.19	12.70	1.23	53.9
41	3	0	2.37	0	10.0	14.19	12.45	1.21	54.2
42	3	0	2.37	0	10.0	14.19	11.73	1.18	55.1
43	3	0	2.37	0	10.0	14.19	11.66	1.18	55.0
44	3	0	2.37	0	10.0	14.19	11.63	1.17	55.0
45	3	0	2.37	0	10.0	14.19	13.95	0.98	44.9
46	3	0	2.37	0	10.0	14.19	14.07	0.98	44.7
47	4	0	3.16	0	10.0	14.19	13.83	0.97	44.8
48	4	0	3.16	0	10.0	14.19	13.99	1.00	45.3
49	3	0	2.37	0	10.0	14.19	11.73	1.27	56.9
50	3	0	2.37	0	10.0	14.19	11.52	1.21	56.2

Table C.3 Cont. Detailed properties and test results for headed bar specimens having closely-spaced bars without parallel ties tested at the University of Kansas

SN	T	$T_h^{[1]}$	T/T_h	f_{su}	$f_{su}/f_{s,calc}^{[2]}$	$f_{su}/f_{s,calc}^{[3]}$
	lb	lb		ksi		
35	28033	27686	1.01	90.4	1.38	1.38
36	25633	22569	1.14	82.7	1.50	1.50
37	54800	47606	1.15	69.4	1.42	1.40
38	50500	45945	1.10	63.9	1.35	1.32
39	58700	54950	1.07	74.3	1.38	1.38
40	64000	58092	1.10	81.0	1.46	1.46
41	59900	58169	1.03	75.8	1.36	1.36
42	42200	47266	0.89	53.4	1.10	1.08
43	48900	53869	0.91	61.9	1.16	1.16
44	55100	60053	0.92	69.7	1.20	1.20
45	73400	72826	1.01	92.9	1.34	1.34
46	75700	73307	1.03	95.8	1.37	1.37
47	60800	63981	0.95	77.0	1.22	1.22
48	61225	61495	1.00	77.5	1.27	1.27
49	40300	48037	0.84	51.0	1.09	1.09
50	44500	55983	0.79	56.3	1.05	1.05

^[1] Based on descriptive equations, Eq. (5.5) and (5.7)

^[2] Based on proposed design equation, Eq. (6.32), using full expression for ψ_p , Eq. (6.29)

^[3] Based on proposed design equation, Eq. (6.32), using simplified expression for ψ_p , Eq. (6.30)

Table C.3 Cont. Detailed properties and test results for headed bar specimens having closely-spaced bars without parallel ties tested at the University of Kansas

SN	ID	b	h	$\ell_{eh,avg}$	f_{cm}	d_b	A_b	s	s/d_b
		in.	in.	in.	psi	in.	in. ²	in.	
51	(3@7)8-8-T9.5-0-i-2.5-3-9.5	19.9	14.0	9.5	10180	1	0.79	7.0	7.0
52	(3@4)8-8-T9.5-0-i-2.5-3-14.5	14.0	19.1	14.6	9040	1	0.79	4.0	4.0
53	(3@5)8-8-T9.5-0-i-2.5-3-14.5	15.8	19.1	14.6	9940	1	0.79	4.9	4.9
54	(3@7)8-8-T9.5-0-i-2.5-3-14.5	20.0	19.0	14.5	10180	1	0.79	7.0	7.0
55	(3@4.5)8-12-F4.1-0-i-2.5-3-12	14.8	16.2	12.2	12040	1	0.79	4.4	4.4
56	(3@4.5)8-12-F9.1-0-i-2.5-3-12	15.0	16.0	12.0	12040	1	0.79	4.5	4.5
57	(4@3)8-12-F4.1-0-i-2.5-3-12	15.0	16.0	12.0	12040	1	0.79	3.0	3.0
58	(4@3)8-12-F9.1-0-i-2.5-3-12	15.0	16.2	12.2	12360	1	0.79	3.0	3.0
59	(2@7)8-8-O4.5-0-i-2.5-3-9.5	13.0	17.5	9.3	6710	1	0.79	7.0	7.0
60	(2@5)8-8-O4.5-0-i-2.5-3-9.5	11.3	17.3	9.0	6710	1	0.79	5.3	5.3
61	(2@3)8-8-O4.5-0-i-2.5-3-9.5	9.1	17.3	9.0	6710	1	0.79	3.1	3.1
62	(3@4.5)8-8-T4.0-0-i-2.5-3-9.5	15.0	13.8	9.3	6790	1	0.79	4.5	4.5
63	(4@3)8-8-T4.0-0-i-2.5-3-9.5	15.0	14.0	9.5	6650	1	0.79	3.0	3.0
64	(3@3)8-8-T4.0-0-i-2.5-3-9.5	12.2	14.0	9.5	6790	1	0.79	3.1	3.1
65	(3@5.35)11-12-O4.5-0-i-2.5-3-16.75	21.3	26.7	16.9	10860	1.41	1.56	7.5	5.3
66	(3@5.35)11-12-S5.5-0-i-2.5-3-16.75	21.4	22.7	16.9	10120	1.41	1.56	7.5	5.3
67	(3@5.35)11-5-O4.5-0-i-2.5-3-19.25	21.5	29.3	19.5	5430	1.41	1.56	7.6	5.4
68	(3@5.35)11-5-S5.5-0-i-2.5-3-19.25	21.4	25.0	19.3	6320	1.41	1.56	7.5	5.3
69	14-7	20.7	37.8	32.1	7080	1.693	2.25	6.0	3.5

Table C.3 Cont. Detailed properties and test results for headed bar specimens having closely-spaced bars without parallel ties tested at the University of Kansas

SN	n	A_t	A_{hs}	A_t/A_{hs}	h_{cl}	x_{mid}	d_{eff}	d_{eff}/ℓ_{eh}	θ
		in. ²	in. ²		in.	in.	in.		°
51	3	0	2.37	0	10.0	14.19	11.84	1.25	56.2
52	3	0	2.37	0	10.0	14.19	13.29	0.91	44.2
53	3	0	2.37	0	10.0	14.19	13.22	0.91	44.2
54	3	0	2.37	0	10.0	14.19	12.77	0.88	44.3
55	3	0	2.37	0	10.0	14.19	12.29	1.01	49.3
56	3	0	2.37	0	10.0	14.19	12.27	1.02	49.7
57	4	0	3.16	0	10.0	14.19	11.98	1.00	49.8
58	4	0	3.16	0	10.0	14.19	11.97	0.98	49.4
59	2	0	1.58	0	10.0	14.19	12.06	1.30	56.9
60	2	0	1.58	0	10.0	14.19	12.22	1.36	57.6
61	2	0	1.58	0	10.0	14.19	12.57	1.40	57.6
62	3	0	2.37	0	10.0	14.19	11.99	1.28	56.7
63	4	0	3.16	0	10.0	14.19	11.72	1.24	56.3
64	3	0	2.37	0	10.0	14.19	12.36	1.31	56.3
65	3	0	4.68	0	19.5	23.69	22.01	1.30	54.5
66	3	0	4.68	0	19.5	23.69	22.23	1.31	54.5
67	3	0	4.68	0	19.5	23.69	24.50	1.26	50.5
68	3	0	4.68	0	19.5	23.69	24.38	1.26	50.8
69	3	0	6.75	0	24.0	28.54	32.73	1.02	41.6

Table C.3 Cont. Detailed properties and test results for headed bar specimens having closely-spaced bars without parallel ties tested at the University of Kansas

SN	T	$T_h^{[1]}$	T/T_h	f_{su}	$f_{su}/f_{s,calc}^{[2]}$	$f_{su}/f_{s,calc}^{[3]}$
	lb	lb		ksi		
51	68700	67522	1.02	87.0	1.32	1.32
52	76600	73720	1.04	97.0	1.31	1.31
53	93200	82924	1.12	118.0	1.44	1.44
54	104000	101224	1.03	131.6	1.30	1.30
55	75233	69227	1.09	95.2	1.38	1.38
56	75400	69067	1.09	95.4	1.39	1.39
57	49300	57675	0.85	62.4	1.03	1.02
58	50325	58762	0.86	63.7	1.03	1.02
59	54500	60661	0.90	69.0	1.19	1.19
60	51200	50557	1.01	64.8	1.36	1.36
61	47700	39480	1.21	60.4	1.53	1.52
62	40700	48252	0.84	51.5	1.12	1.12
63	26150	40814	0.64	33.1	0.81	0.79
64	39367	41479	0.95	49.8	1.20	1.19
65	106800	119889	0.89	68.5	1.14	1.14
66	109000	118568	0.92	69.9	1.18	1.18
67	128700	119541	1.08	82.5	1.41	1.41
68	137400	121678	1.13	88.1	1.47	1.47
69	252100	181632	1.39	112.0	1.67	1.67

^[1] Based on descriptive equations, Eq. (5.5) and (5.7)

^[2] Based on proposed design equation, Eq. (6.32), using full expression for ψ_p , Eq. (6.29)

^[3] Based on proposed design equation, Eq. (6.32), using simplified expression for ψ_p , Eq. (6.30)

Table C.4 Detailed properties and test results for headed bar specimens having widely-spaced bars with parallel ties tested at the University of Kansas

SN	ID	<i>b</i>	<i>h</i>	$\ell_{eh,avg}$	f_{cm}	d_b	A_b	<i>s</i>	<i>s/d_b</i>
		in.	in.	in.	psi	in.	in. ²	in.	
70	5-5-F4.0-2#3-i-2.5-5-4	13.0	9.3	3.8	4810	0.625	0.31	7.4	11.8
71	5-5-F4.0-5#3-i-2.5-5-4	13.0	9.7	4.2	4810	0.625	0.31	7.4	11.8
72	5-5-F4.0-2#3-i-2.5-3-6	13.0	9.5	6.0	4690	0.625	0.31	7.4	11.8
73	5-5-F4.0-5#3-i-2.5-3-6	13.0	9.6	6.1	4690	0.625	0.31	7.4	11.8
74	5-12-F4.0-2#3-i-2.5-5-4	12.9	9.6	4.1	11030	0.625	0.31	7.3	11.7
75	5-12-F4.0-5#3-i-2.5-5-4	13.0	9.7	4.2	11030	0.625	0.31	7.4	11.8
76	8-5-T4.0-4#3-i-3-3-12.5	17.9	16.9	12.4	5070	1	0.79	10.9	10.9
77	8-5-T4.0-4#3-i-4-3-12.5	20.0	16.6	12.1	5380	1	0.79	11.0	11.0
78	8-5-T4.0-4#4-i-3-3-12.5	17.6	16.9	12.4	5070	1	0.79	10.6	10.6
79	8-5-T4.0-4#4-i-4-3-12.5	20.1	16.7	12.2	4850	1	0.79	11.1	11.1
80	8-5g-T4.0-5#3-i-2.5-3-9.5	16.8	14.1	9.6	5090	1	0.79	10.8	10.8
81	8-5g-T4.0-5#3-i-3.5-3-9.5	19.3	14.1	9.6	5910	1	0.79	11.3	11.3
82	8-5g-T4.0-4#4-i-2.5-3-9.5	16.5	13.7	9.2	5180	1	0.79	10.5	10.5
83	8-5g-T4.0-4#4-i-3.5-3-9.5	16.3	14.0	9.5	5910	1	0.79	10.3	10.3
84	8-5-T4.0-5#3-i-2.5-3-9.5	16.5	13.8	9.3	5960	1	0.79	10.5	10.5
85	8-5-T4.0-5#3-i-3.5-3-9.5	18.8	13.6	9.1	6440	1	0.79	10.8	10.8
86	8-5-T4.0-4#4-i-2.5-3-9.5	16.5	13.8	9.3	6440	1	0.79	10.5	10.5
87	8-5-T4.0-4#4-i-3.5-3-9.5	18.8	13.8	9.3	6210	1	0.79	10.8	10.8
88	8-8-F4.1-2#3-i-2.5-3-10	17.1	13.9	9.9	8450	1	0.79	11.1	11.1
89	8-12-F4.1-5#3-i-2.5-3-10	17.0	14.0	10.0	11760	1	0.79	11.0	11.0
90	8-5-S6.5-2#3-i-2.5-3-9.25	17.3	13.9	9.1	5750	1	0.79	11.3	11.3
91	8-5-S6.5-2#3-i-2.5-3-12.25	17.0	17.1	12.3	5750	1	0.79	11.0	11.0
92	8-5-O4.5-2#3-i-2.5-3-9.25	17.0	17.6	9.4	5750	1	0.79	11.0	11.0
93	8-5-O4.5-2#3-i-2.5-3-12.25	16.8	20.3	12.0	5750	1	0.79	10.8	10.8
94	8-5-S6.5-5#3-i-2.5-3-8.25	17.0	13.1	8.3	5900	1	0.79	11.0	11.0
95	8-5-S6.5-5#3-i-2.5-3-11.25	17.8	15.7	10.9	5900	1	0.79	11.8	11.8
96	8-5-O4.5-5#3-i-2.5-3-8.25	17.0	16.3	8.0	5900	1	0.79	11.0	11.0
97	8-5-O4.5-5#3-i-2.5-3-11.25	16.8	19.4	11.1	5900	1	0.79	10.8	10.8
98	8-5-T9.5-5#3-i-2.5-3-14.5	17.0	18.9	14.4	5420	1	0.79	11.0	11.0

Table C.4 Cont. Detailed properties and test results for headed bar specimens having widely-spaced bars with parallel ties tested at the University of Kansas

SN	n	A_t	A_{hs}	A_t/A_{hs}	h_{cl}	x_{mid}	d_{eff}	d_{eff}/ℓ_{eh}	θ
		in. ²	in. ²		in.	in.	in.		°
70	2	0.22	0.62	0.355	5.25	9.44	6.16	1.62	68.0
71	2	0.66	0.62	1.065	5.25	9.44	6.48	1.56	66.2
72	2	0.22	0.62	0.355	5.25	9.44	7.04	1.17	57.6
73	2	0.66	0.62	1.065	5.25	9.44	7.30	1.21	57.3
74	2	0.22	0.62	0.355	5.25	9.44	6.08	1.47	66.4
75	2	0.66	0.62	1.065	5.25	9.44	6.23	1.48	65.9
76	2	0.66	1.58	0.418	10.0	14.19	12.85	1.04	48.9
77	2	0.66	1.58	0.418	10.0	14.19	12.69	1.05	49.6
78	2	0.8	1.58	0.506	10.0	14.19	13.61	1.09	48.8
79	2	0.8	1.58	0.506	10.0	14.19	13.03	1.07	49.3
80	2	0.66	1.58	0.418	10.0	14.19	12.72	1.33	56.0
81	2	0.66	1.58	0.418	10.0	14.19	12.17	1.27	56.0
82	2	0.8	1.58	0.506	10.0	14.19	13.16	1.43	57.1
83	2	0.8	1.58	0.506	10.0	14.19	13.13	1.38	56.2
84	2	0.66	1.58	0.418	10.0	14.19	12.36	1.33	56.7
85	2	0.66	1.58	0.418	10.0	14.19	12.15	1.34	57.4
86	2	0.8	1.58	0.506	10.0	14.19	12.75	1.38	56.9
87	2	0.8	1.58	0.506	10.0	14.19	12.33	1.33	56.9
88	2	0.22	1.58	0.139	10.0	14.19	11.84	1.20	55.1
89	2	0.66	1.58	0.418	10.0	14.19	11.58	1.16	54.8
90	2	0.22	1.58	0.139	10.0	14.19	11.97	1.31	57.2
91	2	0.22	1.58	0.139	10.0	14.19	12.71	1.03	49.1
92	2	0.22	1.58	0.139	10.0	14.19	12.14	1.29	56.5
93	2	0.22	1.58	0.139	10.0	14.19	12.51	1.04	49.8
94	2	0.66	1.58	0.418	10.0	14.19	11.93	1.44	59.6
95	2	0.66	1.58	0.418	10.0	14.19	12.51	1.14	52.4
96	2	0.66	1.58	0.418	10.0	14.19	12.12	1.52	60.6
97	2	0.66	1.58	0.418	10.0	14.19	12.59	1.13	51.9
98	2	0.66	1.58	0.418	10.0	14.19	13.97	0.97	44.6

Table C.4 Cont. Detailed properties and test results for headed bar specimens having widely-spaced bars with parallel ties tested at the University of Kansas

SN	T	$T_h^{[1]}$	T/T_h	f_{su}	$f_{su}/f_{s,calc}^{[2]}$	$f_{su}/f_{s,calc}^{[3]}$
	lb	lb		ksi		
70	19700	26065	0.76	63.5	1.08	1.13
71	26500	28524	0.93	85.5	1.33	1.33
72	37900	37047	1.02	122.3	1.33	1.39
73	43500	38004	1.14	140.3	1.51	1.51
74	32700	31943	1.02	105.5	1.34	1.41
75	38900	33148	1.17	125.5	1.56	1.56
76	87509	96598	0.91	110.8	1.16	1.16
77	96172	95603	1.01	121.7	1.28	1.28
78	109032	96967	1.12	138.0	1.43	1.43
79	101480	94697	1.07	128.5	1.38	1.38
80	78700	79159	0.99	99.6	1.34	1.34
81	79500	81155	0.98	100.6	1.31	1.31
82	90700	77064	1.18	114.8	1.60	1.60
83	96700	80768	1.20	122.4	1.60	1.60
84	74200	79652	0.93	93.9	1.25	1.25
85	80600	79041	1.02	102.0	1.37	1.37
86	90500	80293	1.13	114.6	1.51	1.51
87	85600	79807	1.07	108.4	1.44	1.44
88	73400	78237	0.94	92.9	1.07	1.26
89	87200	94462	0.92	110.4	1.16	1.16
90	63350	67844	0.93	80.2	1.10	1.29
91	85960	88117	0.98	108.8	1.11	1.30
92	67910	69451	0.98	86.0	1.15	1.35
93	78510	86156	0.91	99.4	1.04	1.22
94	62040	73036	0.85	78.5	1.18	1.18
95	84480	89999	0.94	106.9	1.22	1.22
96	68390	71017	0.96	86.6	1.35	1.35
97	82230	91214	0.90	104.1	1.16	1.16
98	121000	110155	1.10	153.2	1.35	1.35

^[1] Based on descriptive equations, Eq. (5.5) and (5.7)

^[2] Based on proposed design equation, Eq. (6.32), using full expression for ψ_p , Eq. (6.29)

^[3] Based on proposed design equation, Eq. (6.32), using simplified expression for ψ_p , Eq. (6.30)

Table C.4 Cont. Detailed properties and test results for headed bar specimens having widely-spaced bars with parallel ties tested at the University of Kansas

SN	ID	<i>b</i>	<i>h</i>	$\ell_{eh,avg}$	<i>f_{cm}</i>	<i>d_b</i>	<i>A_b</i>	<i>s</i>	<i>s/d_b</i>
		in.	in.	in.	psi	in.	in. ²	in.	
99	8-15-T4.0-2#3-i-2.5-4.5-7	17.0	13.1	7.1	16030	1	0.79	11.0	11.0
100	8-15-S9.5-2#3-i-2.5-3-7	16.9	12.8	7.1	16030	1	0.79	10.9	10.9
101	8-15-T4.0-5#3-i-2.5-4.5-5.5	17.0	11.5	5.5	16030	1	0.79	11.0	11.0
102	8-15-S9.5-5#3-i-2.5-3-5.5	17.0	11.4	5.6	16030	1	0.79	11.0	11.0
103	8-8-T9.5-2#3-i-2.5-3-9.5	16.8	13.7	9.2	9040	1	0.79	10.8	10.8
104	(2@9)8-12-F4.1-5#3-i-2.5-3-12	15.0	16.0	12.0	12080	1	0.79	9.0	9.0
105	(2@9)8-8-T4.0-5#3-i-2.5-3-9.5	15.1	14.0	9.5	6790	1	0.79	9.1	9.1
106	11-5a-F3.8-2#3-i-2.5-3-17	21.5	21.8	17.4	4050	1.41	1.56	15.1	10.7
107	11-5a-F3.8-6#3-i-2.5-3-17	21.4	21.1	16.7	4050	1.41	1.56	15.0	10.6
108	11-5-F3.8-6#3-i-2.5-3-17	21.4	21.3	16.9	5970	1.41	1.56	15.0	10.6
109	11-12-O4.5-6#3-i-2.5-3-16.75	21.4	26.6	16.8	10860	1.41	1.56	15.0	10.6
110	11-12-S5.5-6#3-i-2.5-3-16.75	21.8	22.6	16.8	10120	1.41	1.56	15.4	10.9
111	11-5-O4.5-6#3-i-2.5-3-19.25	21.4	29.4	19.6	5430	1.41	1.56	15.0	10.6
112	11-5-S5.5-6#3-i-2.5-3-19.25	21.7	24.9	19.1	6320	1.41	1.56	15.3	10.9
113	11-2	22.5	24.5	18.5	15850	1.41	1.56	14.1	10.0
114	14-4	26.7	37.8	32.0	7700	1.693	2.25	18.0	10.6
115	14-2A	26.7	28.6	23.0	13750	1.693	2.25	18.0	10.6
116	14-16B	26.7	28.6	22.1	7500	1.693	2.25	18.0	10.6
117	14-16C	26.7	28.6	22.6	6470	1.693	2.25	18.0	10.6
118	14-16D	26.7	28.6	22.9	6900	1.693	2.25	18.0	10.6
119	14-16E	26.7	28.6	22.4	6170	1.693	2.25	18.0	10.6
120	14-16F	26.7	28.6	22.4	5640	1.693	2.25	18.0	10.6
121	14-2*	26.7	28.6	20.5	12830	1.693	2.25	18.0	10.6
122	14-16*	26.7	28.6	22.6	5390	1.693	2.25	18.0	10.6
123	14-16A*	26.7	28.6	22.4	8350	1.693	2.25	18.0	10.6
124	18-1	27.3	37.8	32.6	5750	2.257	4	18.0	8.0
125	18-2	27.3	37.8	28.4	11770	2.257	4	18.0	8.0
126	18-3	27.3	37.8	30.9	6540	2.257	4	18.0	8.0
127	18-4	27.3	37.8	30.9	7200	2.257	4	18.0	8.0

* Specimen failed in shear, not used to develop descriptive equations, Eq. (5.5) and (5.7)

Table C.4 Cont. Detailed properties and test results for headed bar specimens having widely-spaced bars with parallel ties tested at the University of Kansas

SN	n	A_t	A_{hs}	A_t/A_{hs}	h_{cl}	x_{mid}	d_{eff}	d_{eff}/ℓ_{eh}	θ
		in. ²	in. ²		in.	in.	in.		°
99	2	0.22	1.58	0.139	10.0	14.19	10.78	1.53	63.5
100	2	0.22	1.58	0.139	10.0	14.19	10.90	1.54	63.5
101	2	0.66	1.58	0.418	10.0	14.19	10.84	1.97	68.8
102	2	0.66	1.58	0.418	10.0	14.19	11.01	1.96	68.4
103	2	0.22	1.58	0.139	10.0	14.19	11.64	1.27	57.1
104	2	0.66	1.58	0.418	10.0	14.19	12.24	1.02	49.8
105	2	0.66	1.58	0.418	10.0	14.19	12.48	1.31	56.2
106	2	0.22	3.12	0.071	19.5	23.69	23.27	1.33	53.6
107	2	0.66	3.12	0.212	19.5	23.69	23.22	1.39	54.8
108	2	0.66	3.12	0.212	19.5	23.69	23.22	1.37	54.4
109	2	0.66	3.12	0.212	19.5	23.69	22.64	1.35	54.6
110	2	0.66	3.12	0.212	19.5	23.69	22.74	1.35	54.6
111	2	0.66	3.12	0.212	19.5	23.69	24.22	1.23	50.4
112	2	0.66	3.12	0.212	19.5	23.69	23.93	1.25	51.1
113	2	0.88	3.12	0.282	20.5	23.50	22.74	1.23	51.8
114	2	1.2	4.5	0.267	25.5	28.54	31.24	0.98	41.7
115	2	1.2	4.5	0.267	25.5	28.54	27.95	1.22	51.1
116	2	0.8	4.5	0.178	25.5	28.54	28.84	1.30	52.2
117	2	1.6	4.5	0.356	25.5	28.54	29.41	1.30	51.7
118	2	3.72	4.5	0.827	25.5	28.54	30.75	1.34	51.3
119	2	2.48	4.5	0.551	25.5	28.54	29.71	1.33	51.9
120	2	2.48	4.5	0.551	25.5	28.54	29.52	1.32	51.9
121	2	1.24	4.5	0.276	25.5	28.54	27.51	1.34	54.3
122	2	0.8	4.5	0.178	25.5	28.54	28.09	1.24	51.6
123	2	0.8	4.5	0.178	25.5	28.54	28.52	1.27	51.9
124	2	4.34	8	0.543	33.7	38.15	40.04	1.23	49.5
125	2	4.34	8	0.543	35.2	38.15	39.79	1.40	53.3
126	2	1.86	8	0.233	33.7	38.15	40.39	1.31	51.0
127	2	3.72	8	0.465	33.7	38.15	40.30	1.31	51.0

Table C.4 Cont. Detailed properties and test results for headed bar specimens having widely-spaced bars with parallel ties tested at the University of Kansas

SN	T	$T_h^{[1]}$	T/T_h	f_{su}	$f_{su}/f_{s,calc}^{[2]}$	$f_{su}/f_{s,calc}^{[3]}$
	lb	lb		ksi		
99	59000	66018	0.89	74.7	1.02	1.21
100	67100	66018	1.02	84.9	1.17	1.37
101	63300	63505	1.00	80.1	1.41	1.41
102	75800	64570	1.17	95.9	1.65	1.65
103	68700	74398	0.92	87.0	1.06	1.24
104	111900	109525	1.02	141.6	1.23	1.23
105	76700	82668	0.93	97.1	1.23	1.23
106	118200	132304	0.89	75.8	1.07	1.17
107	116200	138665	0.84	74.5	1.02	1.20
108	151900	150483	1.01	97.4	1.19	1.40
109	201500	167009	1.21	129.2	1.37	1.62
110	197400	164831	1.20	126.5	1.37	1.61
111	181400	167374	1.08	116.3	1.26	1.48
112	189600	168453	1.13	121.5	1.30	1.53
113	221100	200186	1.10	141.7	1.25	1.47
114	333600	312075	1.07	148.3	1.33	1.40
115	248100	263338	0.94	110.3	1.19	1.25
116	191700	218167	0.88	85.2	1.11	1.17
117	208400	236732	0.88	92.6	1.23	1.23
118	289800	247121	1.17	128.8	1.66	1.66
119	218600	238520	0.92	97.2	1.31	1.31
120	197800	234993	0.84	87.9	1.22	1.22
121	190600	237632	0.80	84.7	1.04	1.10
122	123600	208846	0.59	54.9	0.76	0.80
123	186000	224958	0.83	82.7	1.04	1.09
124	322000	396331	0.81	80.5	1.17	1.17
125	406600	402909	1.01	101.7	1.42	1.42
126	366500	353676	1.04	91.6	1.36	1.44
127	380000	395312	0.96	95.0	1.38	1.38

^[1] Based on descriptive equations, Eq. (5.5) and (5.7)

^[2] Based on proposed design equation, Eq. (6.32), using full expression for ψ_p , Eq. (6.29)

^[3] Based on proposed design equation, Eq. (6.32), using simplified expression for ψ_p , Eq. (6.30)

Table C.5 Detailed properties and test results for headed bar specimens having closely-spaced bars with parallel ties tested at the University of Kansas

SN	ID	b	h	$\ell_{eh,avg}$	f_{cm}	d_b	A_b	s	s/d_b
		in.	in.	in.	psi	in.	in. ²	in.	
128	(3@5.9)5-12-F4.0-2#3-i-2.5-4-5	13.2	9.7	5.2	11030	0.625	0.31	3.8	6.1
129	(3@5.9)5-12-F4.0-5#3-i-2.5-4-5	13.0	9.5	5.0	11030	0.625	0.31	3.7	5.9
130	(4@3.9)5-12-F4.0-2#3-i-2.5-4-5	13.1	9.5	5.0	11030	0.625	0.31	2.5	4.0
131	(3@3)8-8-F4.1-2#3-i-2.5-3-10	11.9	14.1	10.1	8260	1	0.79	3.0	3.0
132	(3@3)8-8-F4.1-2#3-i-2.5-3-10-HP	12.0	14.3	10.3	8260	1	0.79	3.0	3.0
133	(3@4)8-8-F4.1-2#3-i-2.5-3-10	14.0	13.9	9.9	8050	1	0.79	4.0	4.0
134	(3@4)8-8-F4.1-2#3-i-2.5-3-10-HP	14.3	14.3	10.3	8050	1	0.79	4.2	4.2
135	(3@5)8-8-F4.1-2#3-i-2.5-3-10.5	15.6	13.8	9.8	8260	1	0.79	4.8	4.8
136	(3@5)8-8-F4.1-2#3-i-2.5-3-10.5-HP	16.1	14.0	10.0	8260	1	0.79	5.1	5.1
137	(3@3)8-12-F4.1-5#3-i-2.5-3-10	12.1	14.0	10.0	11040	1	0.79	3.1	3.1
138	(3@4)8-12-F4.1-5#3-i-2.5-3-10	13.9	13.8	9.8	11440	1	0.79	4.0	4.0
139	(3@5)8-12-F4.1-5#3-i-2.5-3-10	16.3	13.6	9.6	11460	1	0.79	5.2	5.2
140	(3@5.5)8-5-T9.5-5#3-i-2.5-3-14.5	17.1	18.9	14.4	5370	1	0.79	5.6	5.6
141	(4@3.7)8-5-T9.5-5#3-i-2.5-3-14.5	17.4	19.0	14.5	5570	1	0.79	3.8	3.8
142	(3@4)8-8-T9.5-2#3-i-2.5-3-9.5	14.0	14.1	9.6	9040	1	0.79	4.0	4.0
143	(3@5)8-8-T9.5-2#3-i-2.5-3-9.5	16.0	13.9	9.4	9940	1	0.79	5.0	5.0
144	(3@7)8-8-T9.5-2#3-i-2.5-3-9.5	20.1	14.1	9.6	10180	1	0.79	7.1	7.1
145	(3@4)8-8-T9.5-2#3-i-2.5-3-14.5	14.0	18.9	14.4	9040	1	0.79	4.0	4.0
146	(3@5)8-8-T9.5-2#3-i-2.5-3-14.5	16.0	18.6	14.1	9940	1	0.79	5.0	5.0
147	(3@7)8-8-T9.5-2#3-i-2.5-3-14.5	20.0	19.0	14.5	10180	1	0.79	7.0	7.0

Table C.5 Cont. Detailed properties and test results for headed bar specimens having closely-spaced bars with parallel ties tested at the University of Kansas

SN	n	A_t	A_{hs}	A_t/A_{hs}	h_{cl}	x_{mid}	d_{eff}	d_{eff}/ℓ_{eh}	θ
		in. ²	in. ²		in.	in.	in.		°
128	3	0.22	0.93	0.237	5.25	9.44	6.56	1.27	61.4
129	3	0.66	0.93	0.710	5.25	9.44	6.71	1.34	62.0
130	4	0.22	1.24	0.177	5.25	9.44	6.80	1.35	61.9
131	3	0.22	2.37	0.093	10.0	14.19	13.42	1.33	54.6
132	3	0.22	2.37	0.093	10.0	14.19	13.11	1.27	54.0
133	3	0.22	2.37	0.093	10.0	14.19	12.67	1.28	55.1
134	3	0.22	2.37	0.093	10.0	14.19	13.29	1.29	53.9
135	3	0.22	2.37	0.093	10.0	14.19	12.36	1.26	55.4
136	3	0.22	2.37	0.093	10.0	14.19	12.67	1.27	54.8
137	3	0.66	2.37	0.278	10.0	14.19	12.50	1.25	54.8
138	3	0.66	2.37	0.278	10.0	14.19	12.24	1.25	55.4
139	3	0.66	2.37	0.278	10.0	14.19	12.03	1.25	55.9
140	3	0.66	2.37	0.278	10.0	14.19	14.65	1.02	44.5
141	4	0.66	3.16	0.209	10.0	14.19	14.84	1.02	44.4
142	3	0.22	2.37	0.093	10.0	14.19	12.22	1.28	56.0
143	3	0.22	2.37	0.093	10.0	14.19	11.91	1.26	56.4
144	3	0.22	2.37	0.093	10.0	14.19	11.79	1.23	56.0
145	3	0.22	2.37	0.093	10.0	14.19	13.66	0.95	44.5
146	3	0.22	2.37	0.093	10.0	14.19	13.59	0.97	45.2
147	3	0.22	2.37	0.093	10.0	14.19	13.02	0.90	44.3

Table C.5 Cont. Detailed properties and test results for headed bar specimens having closely-spaced bars with parallel ties tested at the University of Kansas

SN	T	$T_h^{[1]}$	T/T_h	f_{su}	$f_{su}/f_{s,calc}^{[2]}$	$f_{su}/f_{s,calc}^{[3]}$
	lb	lb		ksi		
128	35133	33584	1.05	113.3	1.21	1.53
129	38633	34700	1.11	124.6	1.30	1.30
130	30900	27915	1.11	99.7	1.44	1.53
131	61900	57369	1.08	78.4	1.51	1.48
132	56700	58670	0.97	71.8	1.35	1.33
133	55500	60679	0.91	70.3	1.28	1.36
134	69800	63840	1.09	88.4	1.52	1.64
135	56100	63998	0.88	71.0	1.21	1.37
136	65500	66344	0.99	82.9	1.35	1.53
137	61600	66202	0.93	78.0	1.04	1.02
138	65700	69943	0.94	83.2	1.05	1.10
139	69700	74981	0.93	88.2	1.02	1.19
140	94600	94050	1.01	119.7	1.08	1.30
141	76867	82141	0.94	97.3	1.13	1.18
142	51800	60391	0.86	65.6	1.20	1.27
143	55900	65003	0.86	70.8	1.18	1.33
144	67600	75489	0.90	85.6	1.14	1.28
145	85400	87381	0.98	108.1	1.31	1.39
146	105200	93460	1.13	133.2	1.48	1.67
147	113400	109767	1.03	143.5	1.26	1.42

^[1] Based on descriptive equations, Eq. (5.5) and (5.7)

^[2] Based on proposed design equation, Eq. (6.32), using full expression for ψ_p , Eq. (6.29)

^[3] Based on proposed design equation, Eq. (6.32), using simplified expression for ψ_p , Eq. (6.30)

Table C.5 Cont. Detailed properties and test results for headed bar specimens having closely-spaced bars with parallel ties tested at the University of Kansas

SN	ID	b	h	$\ell_{eh,avg}$	f_{cm}	d_b	A_b	s	s/d_b
		in.	in.	in.	psi	in.	in. ²	in.	
148	(3@4.5)8-12-F4.1-5#3-i-2.5-3-12	14.9	16.2	12.2	12040	1	0.79	4.5	4.5
149	(3@4.5)8-12-F9.1-5#3-i-2.5-3-12	15.0	15.9	11.9	12040	1	0.79	4.5	4.5
150	(4@3)8-12-F4.1-5#3-i-2.5-3-12	15.0	16.0	12.0	12360	1	0.79	3.0	3.0
151	(4@3)8-12-F9.1-5#3-i-2.5-3-12	15.0	16.0	12.0	12360	1	0.79	3.0	3.0
152	(3@4.5)8-8-T4.0-5#3-i-2.5-3-9.5	15.4	13.7	9.2	6650	1	0.79	4.7	4.7
153	(4@3)8-8-T4.0-5#3-i-2.5-3-9.5	15.0	14.2	9.7	6650	1	0.79	3.0	3.0
154	(3@3)8-8-T4.0-5#3-i-2.5-3-9.5	12.1	13.8	9.3	6650	1	0.79	3.1	3.1
155	(3@5.35)11-12-O4.5-6#3-i-2.5-3-16.75	21.4	26.8	17.0	10860	1.41	1.56	7.5	5.3
156	(3@5.35)11-12-S5.5-6#3-i-2.5-3-16.75	21.3	22.5	16.8	10120	1.41	1.56	7.5	5.3
157	(3@5.35)11-5-O4.5-6#3-i-2.5-3-19.25	21.6	29.1	19.4	5430	1.41	1.56	7.6	5.4
158	(3@5.35)11-5-S5.5-6#3-i-2.5-3-19.25	21.5	25.0	19.3	6320	1.41	1.56	7.6	5.4
159	14-17	26.7	28.6	22.4	6540	1.693	2.25	12.0	7.1
160	14-5	20.7	28.6	22.3	6830	1.693	2.25	6.0	3.5
161	14-6	20.7	28.6	22.4	6890	1.693	2.25	6.0	3.5
162	14-8	20.7	37.8	31.7	7100	1.693	2.25	6.0	3.5
163	14-9	20.7	28.6	22.1	11480	1.693	2.25	6.0	3.5
164	14-10	20.7	28.6	22.3	6820	1.693	2.25	6.0	3.5
165	18-5	27.3	37.8	32.5	5310	2.257	4	12.0	5.3
166	18-6	27.3	37.8	28.6	10230	2.257	4	12.0	5.3
167	18-7	27.3	37.8	32.1	5890	2.257	4	6.0	2.7
168	18-8	27.3	37.8	32.3	6380	2.257	4	6.0	2.7

Table C.5 Cont. Detailed properties and test results for headed bar specimens having closely-spaced bars with parallel ties tested at the University of Kansas

SN	n	A_t	A_{hs}	A_t/A_{hs}	h_{cl}	x_{mid}	d_{eff}	d_{eff}/ℓ_{eh}	θ
		in. ²	in. ²		in.	in.	in.		°
148	3	0.66	2.37	0.278	10.0	14.19	12.65	1.04	49.4
149	3	0.66	2.37	0.278	10.0	14.19	13.26	1.11	50.0
150	4	0.66	3.16	0.209	10.0	14.19	12.51	1.04	49.7
151	4	0.66	3.16	0.209	10.0	14.19	13.43	1.12	49.9
152	3	0.66	2.37	0.278	10.0	14.19	13.00	1.42	57.1
153	4	0.66	3.16	0.209	10.0	14.19	13.20	1.37	55.7
154	3	0.66	2.37	0.278	10.0	14.19	13.46	1.44	56.7
155	3	0.66	4.68	0.141	19.5	23.69	22.67	1.33	54.3
156	3	0.66	4.68	0.141	19.5	23.69	23.37	1.40	54.7
157	3	0.66	4.68	0.141	19.5	23.69	24.97	1.29	50.7
158	3	0.66	4.68	0.141	19.5	23.69	24.91	1.29	50.9
159	2	2.48	4.5	0.551	25.5	28.54	29.35	1.31	51.9
160	3	1.20	6.75	0.178	24.0	28.54	30.41	1.36	52.0
161	3	1.86	6.75	0.276	24.0	28.54	30.30	1.35	51.8
162	3	1.86	6.75	0.276	24.0	28.54	33.49	1.06	42.0
163	3	1.86	6.75	0.276	25.5	28.54	29.47	1.33	52.2
164	3	3.72	6.75	0.551	24.0	28.54	31.29	1.41	52.1
165	2	4.344	8	0.543	33.7	38.15	39.88	1.23	49.6
166	2	4.344	8	0.543	35.2	38.15	40.60	1.42	53.1
167	3	6.516	12	0.543	32.2	38.15	7.34	0.23	49.9
168	3	6.516	12	0.543	32.2	38.15	8.20	0.25	49.7

Table C.5 Cont. Detailed properties and test results for headed bar specimens having closely-spaced bars with parallel ties tested at the University of Kansas

SN	T	T_h ^[1]	T/T_h	f_{su}	$f_{su}/f_{s,calc}$ ^[2]	$f_{su}/f_{s,calc}$ ^[3]
	lb	lb		ksi		
148	87700	87901	1.00	111.0	1.07	1.16
149	108567	86555	1.25	137.4	1.34	1.47
150	64175	76549	0.84	81.2	0.99	0.97
151	87800	76107	1.15	111.1	1.37	1.34
152	62467	63550	0.98	79.1	1.14	1.28
153	48600	56489	0.86	61.5	1.09	1.07
154	56533	57108	0.99	71.6	1.16	1.14
155	135800	143119	0.95	87.1	1.19	1.42
156	153800	139041	1.11	98.6	1.40	1.66
157	141700	141112	1.00	90.8	1.29	1.54
158	152900	144108	1.06	98.0	1.35	1.62
159	206700	236469	0.87	91.9	1.22	1.22
160	181800	167221	1.09	80.8	1.37	1.40
161	179500	177273	1.01	79.8	1.14	1.16
162	274600	237013	1.16	122.0	1.22	1.24
163	173900	192173	0.90	77.3	0.98	1.00
164	206600	187191	1.10	91.8	1.22	1.22
165	300800	343107	0.88	75.2	1.12	1.12
166	419800	347541	1.21	105.0	1.51	1.51
167	252100	284797	0.89	63.0	0.93	0.93
168	295300	290162	1.02	73.8	1.06	1.06

^[1] Based on descriptive equations, Eq. (5.5) and (5.7)

^[2] Based on proposed design equation, Eq. (6.32), using full expression for ψ_p , Eq. (6.29)

^[3] Based on proposed design equation, Eq. (6.32), using simplified expression for ψ_p , Eq. (6.30)

C.4 SPECIMENS TESTED IN OTHER STUDIES

This section presents the specimens tested outside the University of Kansas, including those by Bashandy (1996), Chun et al. (2017a), and Sim and Chun (2022a, 2022b), as tabulated in Table C.6. None of these specimens were used in developing descriptive equations, Eq. (5.5) and (5.7).

Table C.6 Detailed properties and test results for hooked bar specimens tested outside the University of Kansas

Study	SN	ID	b	h	$\ell_{eh,avg}$	f_{cm}	d_b	A_b	s	s/d_b
			in.	in.	in.	psi	in.	in. ²	in.	
Bashandy (1996)	169	T9	15.0	12.0	11.0	5000	1.41	1.56	4.7	3.3
	170	T10**	15.0	12.0	12.5	5000	1.41	1.56	7.6	5.4
	171	T12**	12.0	12.0	9.8	5110	1	0.79	8.0	8.0
	172	T13**	15.0	12.0	12.8	5560	1	0.79	8.0	8.0
	173	T14	15.0	12.0	11.0	5400	1.41	1.56	4.7	3.3
	174	T16	18.0	12.0	14.0	5740	1.41	1.56	4.7	3.3
	175	T20	12.0	12.0	8.2	5110	1.41	1.56	4.7	3.3
	176	T21	12.0	12.0	8.3	5110	1	0.79	5.0	5.0
	177	T22	12.0	12.0	8.3	5110	1	0.79	5.0	5.0
	178	T23	15.0	12.0	11.2	4820	1.41	1.56	4.7	3.3
	179	T24	15.0	12.0	11.2	4690	1.41	1.56	4.7	3.3
	180	T25	15.0	12.0	11.0	4690	1.41	1.56	4.7	3.3
	181	T26	21.0	12.0	17.0	4550	1.41	1.56	4.7	3.3
	182	T27	12.0	12.0	8.0	4550	1.41	1.56	4.7	3.3
	183	T28	15.0	12.0	11.2	4830	1.41	1.56	4.7	3.3
	184	T29	15.0	12.0	11.0	4830	1.41	1.56	4.7	3.3
	185	T30	15.0	12.0	11.3	3210	1	0.79	5.0	5.0
	186	T32	12.0	12.0	8.0	4830	1	0.79	5.0	5.0

** Specimens with bars outside column core and parallel ties, therefore $Att/Ahs = 0$ when calculating ψ_p

Table C.6 Cont. Detailed properties and test results for hooked bar specimens tested outside the University of Kansas

SN	n	A_t	A_{hs}	A_t/A_{hs}	h_{cl}	x_{mid}	d_{eff}	d_{eff}/ℓ_{eh}	θ
		in. ²	in. ²		in.	in.	in.		°
169	2	2.00	3.12	0.641	11.0	14.0	14.02	1.27	51.9
170	2	1.86	3.12	0.596	11.0	14.0	13.41	1.07	48.3
171	2	0.88	1.58	0.557	11.0	14.0	12.95	1.32	55.0
172	2	1.24	1.58	0.785	11.0	14.0	13.27	1.04	47.6
173	2	0.66	3.12	0.212	11.0	14.0	14.51	1.32	51.9
174	2	3.20	3.12	1.026	11.0	14.0	13.88	0.99	45.0
175	2	3.20	3.12	1.026	11.0	14.0	14.81	1.81	59.7
176	2	3.20	1.58	2.025	11.0	14.0	13.39	1.61	59.4
177	2	3.20	1.58	2.025	11.0	14.0	13.01	1.57	59.4
178	2	3.20	3.12	1.026	11.0	14.0	13.79	1.23	51.4
179	2	3.20	3.12	1.026	11.0	14.0	14.32	1.28	51.4
180	2	6.12	3.12	1.962	11.0	14.0	14.95	1.36	51.9
181	2	3.20	3.12	1.026	11.0	14.0	14.36	0.84	39.5
182	2	3.20	3.12	1.026	11.0	14.0	13.35	1.67	60.3
183	2	3.20	3.12	1.026	11.0	14.0	14.92	1.33	51.4
184	2	3.20	3.12	1.026	11.0	14.0	14.50	1.32	51.9
185	2	3.20	1.58	2.025	11.0	14.0	14.47	1.28	51.1
186	2	3.20	1.58	2.025	11.0	14.0	13.46	1.68	60.3

Table C.6 Cont. Detailed properties and test results for hooked bar specimens tested outside the University of Kansas

SN	T	$T_h^{[1]}$	T/T_h	f_{su}	$f_{su}/f_{s,calc}^{[2]}$	$f_{su}/f_{s,calc}^{[3]}$
	lb	lb		ksi		
169	76400	89600	0.85	49.0	0.97	0.97
170	60900	77800	0.92	39.0	1.21	1.21
171	40000	65100	0.72	50.6	0.90	0.90
172	61400	85100	0.84	77.7	1.04	1.04
173	93500	79100	1.18	59.9	1.60	1.60
174	95800	108500	0.88	61.4	0.92	0.92
175	78500	74100	1.06	50.3	1.32	1.32
176	49000	61400	0.8	62.0	0.96	0.96
177	41100	61400	0.67	52.0	0.81	0.81
178	68800	90100	0.76	44.1	0.86	0.86
179	80300	89800	0.89	51.5	1.01	1.01
180	95800	88700	1.08	61.4	1.23	1.23
181	111300	120600	0.92	71.3	0.93	0.93
182	44500	71800	0.62	28.5	0.79	0.79
183	97100	90200	1.08	62.2	1.22	1.22
184	86600	89100	0.97	55.5	1.10	1.10
185	62700	71600	0.88	79.4	1.02	1.02
186	48600	59400	0.82	61.5	1.01	1.01

^[1] Based on descriptive equations, Eq. (5.5) and (5.7)

^[2] Based on proposed design equation, Eq. (6.32), using full expression for ψ_p , Eq. (6.29)

^[3] Based on proposed design equation, Eq. (6.32), using simplified expression for ψ_p , Eq. (6.30)

Table C.6 Cont. Detailed properties and test results for hooked bar specimens tested outside the University of Kansas

Study	SN	ID ^{[1][2][3]}	<i>b</i>	<i>h</i>	$\ell_{eh,avg}$	f_{cm}	d_b	A_b	<i>s</i>	<i>s/d_b</i>
			in.	in.	in.	psi	in.	in. ²	in.	
Chun et al. (2017a)	187	D43-L7-C1-S42	21.3	14.8	11.9	6950	1.693	2.25	16.3	9.6
	188	D43-L7-C1-S42-HP0.5	21.3	14.8	11.9	6950	1.693	2.25	16.3	9.6
	189	D43-L7-C1-S70	21.3	14.8	11.9	9890	1.693	2.25	16.3	9.6
	190	D43-L10-C1-S42	21.3	19.8	16.9	7570	1.693	2.25	16.3	9.6
	191	D43-L10-C1-S42- HP0.5	21.3	19.8	16.9	7570	1.693	2.25	16.3	9.6
	192	D43-L10-C1-S70	21.3	19.8	16.9	11,770	1.693	2.25	16.3	9.6
	193	D43-L13-C1-S42	13.5	24.9	22	6640	1.693	2.25	8.5	5
	194	D43-L13-C2-S42	16.9	24.9	22	6420	1.693	2.25	8.5	5
	195	D43-L13-C1-S42-T1.5	13.5	24.9	22	5870	1.693	2.25	8.5	5
	196	D43-L13-C2-S42-T1.5*	16.9	24.9	22	6060	1.693	2.25	8.5	5
	197	D43-L16-C1-S42	13.5	30.0	27.1	6640	1.693	2.25	8.5	5
	198	D43-L16-C2-S42*	16.9	30.0	27.1	6640	1.693	2.25	8.5	5
	199	D43-L16-C1-S42-T1.5	13.5	30.0	27.1	6060	1.693	2.25	8.5	5
	200	D43-L16-C2-S42-T1.5*	16.9	30.0	27.1	6420	1.693	2.25	8.5	5
	201	D57-L7-C1-S42	23.0	18.9	15.8	7450	2.257	4	16.3	7.2
	202	D57-L7-C1-S42-HP0.5	23.0	18.9	15.8	7450	2.257	4	16.3	7.2
	203	D57-L7-C1-S70	23.0	18.9	15.8	11,150	2.257	4	16.3	7.2
	204	D57-L10-C1-S42	23.0	25.7	22.6	7450	2.257	4	16.3	7.2
	205	D57-L10-C1-S42-HP0.5	23.0	25.7	22.6	7450	2.257	4	16.3	7.2
	206	D57-L10-C1-S70	23.0	25.7	22.6	11,150	2.257	4	16.3	7.2
	207	D57-L13-C1-S42	23.0	32.4	29.3	5870	2.257	4	16.3	7.2
	208	D57-L13-C1-S42-HP0.5*	23.0	32.4	29.3	5870	2.257	4	16.3	7.2
	209	D57-L13-C1-S42-HP1.0a*	23.0	32.4	29.3	5870	2.257	4	16.3	7.2
	210	D57-L13-C1-S42-HP1.0b*	23.0	32.4	29.3	5870	2.257	4	16.3	7.2
	211	D57-L13-C2-S42	27.5	32.4	29.3	5870	2.257	4	16.3	7.2
	212	D57-L16-C1-S42	23.0	39.2	36.1	6060	2.257	4	16.3	7.2
	213	D57-L16-C2-S42*	27.5	39.2	36.1	6060	2.257	4	16.3	7.2

^[1] No specimen used in developing descriptive equations, Eq. (5.5) and 95.7)

^[2] Bars outside column core in all specimens

^[3] HP and T at the end of the designations denote a "confined" specimen. In all other cases, bars are outside parallel ties, therefore $A_{tr}/A_{hs} = 0$ when calculating ψ_p .

* Bars yielded

Table C.6 Cont. Detailed properties and test results for hooked bar specimens tested outside the University of Kansas

SN	n	A_{tt}	A_{hs}	A_{tt}/A_{hs}^*	h_{cl}	x_{mid}	d_{eff}	d_{eff}/ℓ_{eh}	θ
		in. ²	in. ²		in.	in.	in.		°
187	2	1.8	4.5	0.4	5.5	7.9	7.79	0.65	33.7
188	2	1.8	4.5	0.4	5.5	7.9	8.56	0.72	33.7
189	2	1.8	4.5	0.4	5.5	7.9	8.29	0.70	33.7
190	2	1.8	4.5	0.4	8.8	11.3	11.91	0.70	33.7
191	2	1.8	4.5	0.4	8.8	11.3	12.31	0.73	33.7
192	2	1.8	4.5	0.4	8.8	11.3	11.61	0.69	33.7
193	2	1.8	4.5	0.4	10.7	14.7	16.36	0.74	33.7
194	2	1.8	4.5	0.4	10.7	14.7	15.95	0.72	33.7
195	2	1.8	4.5	0.4	10.7	14.7	16.69	0.76	33.7
196	2	1.8	4.5	0.4	10.7	14.7	17.17	0.78	33.7
197	2	1.8	4.5	0.4	14.1	18.1	20.92	0.77	33.7
198	2	1.8	4.5	0.4	14.1	18.1	19.89	0.73	33.7
199	2	1.8	4.5	0.4	14.1	18.1	19.43	0.72	33.7
200	2	1.8	4.5	0.4	14.1	18.1	20.20	0.75	33.7
201	2	3.2	8	0.4	6.9	10.5	10.81	0.68	33.7
202	2	3.2	8	0.4	6.9	10.5	11.86	0.75	33.7
203	2	3.2	8	0.4	6.9	10.5	10.13	0.64	33.7
204	2	3.2	8	0.4	11.4	15.1	15.73	0.70	33.7
205	2	3.2	8	0.4	11.4	15.1	16.97	0.75	33.7
206	2	3.2	8	0.4	11.4	15.1	15.06	0.67	33.7
207	2	3.2	8	0.4	14.8	19.5	20.70	0.71	33.7
208	2	3.2	8	0.4	14.8	19.5	22.66	0.77	33.7
209	2	3.2	8	0.4	14.8	19.5	22.66	0.77	33.7
210	2	3.2	8	0.4	14.8	19.5	22.69	0.77	33.7
211	2	3.2	8	0.4	14.8	19.5	20.98	0.72	33.7
212	2	3.2	8	0.4	19.4	24.1	26.05	0.72	33.7
213	2	3.2	8	0.4	19.4	24.1	25.81	0.71	33.7

* Cap of 0.4 applied to all specimens

Table C.6 Cont. Detailed properties and test results for hooked bar specimens tested outside the University of Kansas

SN	T	$T_h^{[1]}$	T/T_h	f_{su}	$f_{su}/f_{s,calc}^{[2]}$	$f_{su}/f_{s,calc}^{[3]}$
	lb	lb		ksi		
187	102000	91892	1.11	45.3	1.36	1.36
188	136000	132039	1.03	60.4	1.72	1.72
189	163600	99152	1.65	72.7	1.99	1.99
190	142700	130917	1.09	63.4	1.31	1.31
191	161000	171277	0.94	71.6	1.40	1.40
192	193400	144328	1.34	86.0	1.59	1.59
193	155000	126016	1.23	68.9	1.55	1.55
194	176200	124965	1.41	78.3	1.78	1.78
195	152800	171685	0.89	67.9	1.09	1.09
196	210200	172295	1.22	93.4	1.48	1.48
197	186800	153115	1.22	83.0	1.52	1.52
198	198000	153488	1.29	88.0	1.61	1.61
199	138400	203529	0.68	61.5	0.79	0.79
200	205000	205000	1.00	91.1	1.16	1.16
201	193800	133655	1.45	48.5	1.82	1.82
202	246000	212069	1.16	61.5	1.99	1.99
203	230000	145570	1.58	57.5	1.95	1.95
204	212800	186667	1.14	53.2	1.39	1.39
205	274200	268824	1.02	68.6	1.55	1.55
206	258000	203150	1.27	64.5	1.53	1.53
207	254800	227500	1.12	63.7	1.37	1.37
208	340000	311927	1.09	85.0	1.57	1.57
209	340000	311927	1.09	85.0	1.57	1.57
210	341200	310182	1.10	85.3	1.58	1.58
211	319200	228000	1.40	79.8	1.71	1.71
212	296000	279245	1.06	74.0	1.28	1.28
213	341200	279672	1.22	85.3	1.47	1.47

^[1] Based on descriptive equations, Eq. (5.5) and (5.7)

^[2] Based on proposed design equation, Eq. (6.32), using full expression for ψ_p , Eq. (6.29)

^[3] Based on proposed design equation, Eq. (6.32), using simplified expression for ψ_p , Eq. (6.30)

Table C.6 Cont. Detailed properties and test results for hooked bar specimens tested outside the University of Kansas

Study	SN	ID ^{[1][2][3]}	<i>b</i>	<i>h</i>	$\ell_{eh,avg}$	f_{cm}	d_b	A_b	<i>s</i>	s/d_b^{**}
			in.	in.	in.	psi	in.	in. ²	in.	
Sim and Chun (2022a)	214	D43-L13-C1-42	21.4	25.2	22.0	6260	1.693	2.25	1.7	1
	215	D43-L13-C2-42	24.8	25.2	22.0	6260	1.693	2.25	3.4	2
	216	D43-L13-C2-70	24.8	25.2	22.0	12590	1.693	2.25	3.4	2
	217	D43-L13-C2-42-C	24.8	25.2	22.0	6260	1.693	2.25	3.4	2
	218	D43-L16-C1-42	21.4	30.2	27.1	6850	1.693	2.25	1.7	1
	219	D43-L16-C2-42	24.8	30.2	27.1	6850	1.693	2.25	3.4	2
	220	D43-L16-C2-70	24.8	30.2	27.1	11450	1.693	2.25	3.4	2
	221	D43-L16-C2-42-C*	24.8	30.2	27.1	6850	1.693	2.25	3.4	2
	222	D43-L20-C1-42	21.4	37.0	33.9	6260	1.693	2.25	1.7	1
	223	D43-L20-C2-42	24.8	37.0	33.9	6260	1.693	2.25	3.4	2
Sim and Chun (2022b)	224	D22-L6-C1	14.4	6.9	5.3	12020	0.875	0.6	11.8	13.5
	225	D22-L6-C1.5	15.3	6.9	5.3	12020	0.875	0.6	11.8	13.5
	226	D22-L6-C1-TR	14.4	6.9	5.3	12020	0.875	0.6	11.8	13.5
	227	D22-L9-C1	14.4	9.5	7.9	12020	0.875	0.6	11.8	13.5
	228	D32-L6-C1	15.6	10.1	7.6	12020	1.27	1.27	11.8	9.3
	229	D32-L6-C1.5	16.9	10.1	7.6	12020	1.27	1.27	11.8	9.3
	230	D32-L6-C1-TR	15.6	10.1	7.6	12020	1.27	1.27	11.8	9.3
	231	D32-L9-C1	15.6	13.9	11.4	12020	1.27	1.27	11.8	9.3
	232	D22-L6-C1	14.4	6.9	5.3	16680	0.875	0.6	11.8	13.5
	233	D22-L6-C1.5	15.3	6.9	5.3	16680	0.875	0.6	11.8	13.5
	234	D22-L6-C1-TR	14.4	6.9	5.3	16680	0.875	0.6	11.8	13.5
	235	D22-L9-C1	14.4	9.5	7.9	16680	0.875	0.6	11.8	13.5
	236	D32-L6-C1	15.6	10.1	7.6	16680	1.27	1.27	11.8	9.3
	237	D32-L6-C1.5	16.9	10.1	7.6	16680	1.27	1.27	11.8	9.3
	238	D32-L6-C1-TR	15.6	10.1	7.6	16680	1.27	1.27	11.8	9.3
	239	D32-L9-C1	15.6	13.9	11.4	16680	1.27	1.27	11.8	9.3

^[1] No specimen used in developing descriptive equations, Eq. (5.5) and 95.7)

^[2] Bars outside column core in all specimens

^[3] C and TR at the end of the designations denote a "confined" specimen. In all other cases, bars are outside parallel ties, therefore $A_{tl}/A_{hs} = 0$ when calculating ψ_p .

* Bars yielded

** Center-to-center spacing between the two layers of headed bars was taken as *s* for Sim and Chun (2022a)

Table C.6 Cont. Detailed properties and test results for hooked bar specimens tested outside the University of Kansas

SN	<i>n</i>	A_{tt}	A_{hs}	A_{tt}/A_{hs}^*	h_{cl}	x_{mid}	d_{eff}	d_{eff}/ℓ_{eh}	θ
		in. ²	in. ²		in.	in.	in.		°
214	4	3.6	9	0.4	**	22.0	**	**	45.0
215	4	3.6	9	0.4	**	22.0	**	**	45.0
216	4	3.6	9	0.4	**	22.0	**	**	45.0
217	4	3.6	9	0.4	**	22.0	**	**	45.0
218	4	3.6	9	0.4	**	27.1	**	**	45.0
219	4	3.6	9	0.4	**	27.1	**	**	45.0
220	4	3.6	9	0.4	**	27.1	**	**	45.0
221	4	3.6	9	0.4	**	27.1	**	**	45.0
222	4	3.6	9	0.4	**	33.9	**	**	45.0
223	4	3.6	9	0.4	**	33.9	**	**	45.0
224	2	0.48	1.2	0.4	**	3.5	**	**	33.7
225	2	0.48	1.2	0.4	**	3.5	**	**	33.7
226	2	0.48	1.2	0.4	**	3.5	**	**	33.7
227	2	0.48	1.2	0.4	**	5.3	**	**	33.7
228	2	1.016	2.54	0.4	**	5.1	**	**	33.7
229	2	1.016	2.54	0.4	**	5.1	**	**	33.7
230	2	1.016	2.54	0.4	**	5.1	**	**	33.7
231	2	1.016	2.54	0.4	**	7.6	**	**	33.7
232	2	0.48	1.2	0.4	**	3.5	**	**	33.7
233	2	0.48	1.2	0.4	**	3.5	**	**	33.7
234	2	0.48	1.2	0.4	**	3.5	**	**	33.7
235	2	0.48	1.2	0.4	**	5.3	**	**	33.7
236	2	1.016	2.54	0.4	**	5.1	**	**	33.7
237	2	1.016	2.54	0.4	**	5.1	**	**	33.7
238	2	1.016	2.54	0.4	**	5.1	**	**	33.7
239	2	1.016	2.54	0.4	**	7.6	**	**	33.7

* Cap of 0.4 applied to all specimens

** Information not provided

Table C.6 Cont. Detailed properties and test results for hooked bar specimens tested outside the University of Kansas

SN	T	$T_h^{[1]}$	T/T_h	f_{su}	$f_{su}/f_{s,calc}^{[2]}$	$f_{su}/f_{s,calc}^{[3]}$
	lb	lb		ksi		
214*	88900	73471	1.21	39.5	N/A	N/A
215*	103400	86167	1.20	46.0	N/A	N/A
216*	143200	99444	1.44	63.6	N/A	N/A
217*	145600	138667	1.05	64.7	N/A	N/A
218*	114600	90952	1.26	50.9	N/A	N/A
219*	134100	106429	1.26	59.6	N/A	N/A
220*	156200	119237	1.31	69.4	N/A	N/A
221*	164300	164300	1.00	73.0	N/A	N/A
222*	123100	109911	1.12	54.7	N/A	N/A
223*	135600	129143	1.05	60.3	N/A	N/A
224	41400	34500	1.20	69.0	1.50	1.50
225	33700	34388	0.98	56.2	1.22	1.22
226	47900	44766	1.07	79.8	1.48	1.48
227	44000	50575	0.87	73.3	1.07	1.07
228	104700	59153	1.77	82.4	2.19	2.19
229	102900	59138	1.74	81.0	2.15	2.15
230	91300	80796	1.13	71.9	1.62	1.62
231	92600	86542	1.07	72.9	1.29	1.29
232	38700	36857	1.05	64.5	1.29	1.29
233	31500	37059	0.85	52.5	1.05	1.05
234	39000	46988	0.83	65.0	1.11	1.11
235	35900	54394	0.66	59.8	0.80	0.80
236	108100	63216	1.71	85.1	2.08	2.08
237	108500	63081	1.72	85.4	2.09	2.09
238	101500	85294	1.19	79.9	1.66	1.66
239	103200	92143	1.12	81.3	1.32	1.32

^[1] Based on descriptive equations, Eq. (5.5) and (5.7)

^[2] Based on proposed design equation, Eq. (6.32), using full expression for ψ_p , Eq. (6.29)

^[3] Based on proposed design equation, Eq. (6.32), using simplified expression for ψ_p , Eq. (6.30)

* Proposed design provisions do not apply since $s < 3d_b$

ANCHORAGE OF HIGH-STRENGTH REINFORCING BARS IN CONCRETE

By
Luay Ali Nazzal
David Darwin
Matthew O'Reilly

A Report on Research Sponsored by



**CHARLES PANKOW
FOUNDATION**

Charles Pankow Foundation Research Grant Agreement #05-18, D16
ACI Foundation, BarSplice Products,
Headed Reinforcement Corporation, nVENT Lenton,
CRSI Education and Research Foundation,
Precast/Prestressed Concrete Institute,
Commercial Metals Company, Nucor Corporation

Structural Engineering and Engineering Materials
SM Report No. 150
January 2023



THE UNIVERSITY OF KANSAS CENTER FOR RESEARCH, INC.
2385 Irving Hill Road, Lawrence, Kansas 66045-7563

ANCHORAGE OF HIGH-STRENGTH REINFORCING BARS IN CONCRETE

By
Luay Ali Nazzal
David Darwin
Matt O'Reilly

A Report on Research Sponsored by



Charles Pankow Foundation Research Grant Agreement #05-18, D16

**ACI Foundation, BarSplice Products,
Headed Reinforcement Corporation, nVENT Lenton,
CRSI Education and Research Foundation,
Precast/Prestressed Concrete Institute,
Commercial Metals Company, Nucor Corporation**

Structural Engineering and Engineering Materials

SM Report No. 150

THE UNIVERSITY OF KANSAS CENTER FOR RESEARCH, INC.

LAWRENCE, KANSAS

January 2023

ABSTRACT

Hooked and headed reinforcing bars are commonly used as a means of shortening development length of reinforcing bars, but a limited amount of previous research has resulted in restrictions on their use in practice. This study included two phases: In the first phase, 31 tests of simulated column-foundation joints were conducted to investigate the anchorage strength and behavior of large and high-strength headed bars as functions of the distance between the anchored headed bar and the compression reaction, number of headed bars tested simultaneously (1 or 2), size of the headed bars (No. 11 or No. 14), center-to-center spacing between headed bars loaded simultaneously (3.2 or $8.2d_b$), amount of confining reinforcement within the joint region (zero to six No. 4 closed stirrups), and concrete compressive strength (5,060 to 14,470 psi). The embedment length of the headed bars ranged from $12\frac{5}{8}$ to 14 in., and the stresses in the headed bars at failure ranged from 41,800 to 144,400 psi. The test results are compared with anchorage strengths based on the descriptive equations for headed bars developed at the University of Kansas, ACI 318-19 Code provisions, and proposed Code provisions. Recommended changes to Chapters 17 and 25 of ACI 318-19 are presented. In the second phase of the study, descriptive equations for beam-column joints tested under monotonic loading are investigated their applicability to predict the anchorage strength of hooked bars anchored in members subjected to reversed cyclic loading. Comparisons are made with test results from 24 studies of 146 exterior beam-column joint specimens subjected to reversed cyclic loading in which the beam bars are anchored by hooks. Key variables include embedment lengths of the hooked bars (6 to 21 in.), concrete compressive strength (3,140 to 13,700 psi), center-to-center spacing between the hooked bars (1.75 to 6.5 in.), bar size (No. 3 to No. 9), and confining reinforcement within the joint region parallel to the straight portion of the hooked bars (none to nine hoops spaced at 1.25 to 6.0 in.). The yield strength of the hooked bars ranged from 42,900 to 103,000 psi. Proposed changes to Chapters 18 of ACI 318-19 are presented.

The results of the experimental study show that the anchorage strength of headed bars anchored in column-foundation joints is improved by parallel tie reinforcement located on all sides of the headed bars, a contribution that is not included in the provisions of ACI 318-19. Similar to observations for beam-column joints, the anchorage strength of headed bars anchored in simulated

column-foundation joints decreases as the center-to-center spacing decreases below $8d_b$. The descriptive equations developed based on tests of beam-column joints are suitable for predicting the anchorage strength of headed bars anchored in column-foundation joints. Chapter 17 of ACI 318-19 does not accurately predict the anchorage strength of headed bars tested when parallel tie/anchor reinforcement is used and should be modified to combine the contributions of concrete strength and parallel tie reinforcement. The descriptive equations developed for beam-column joints apply to column-foundation joints and could serve as a basis for the anchorage provisions in Chapter 17 of ACI 318. The provisions in Chapter 25 of ACI 318-19 should be updated to include the effect of parallel tie reinforcement in connections other than beam-column joints. The descriptive equations for the anchorage strength of hooked bars in beam-column joints tested under monotonic loading are suitable for predicting the anchorage strength of hooked bars anchored in members subjected to reversed cyclic loading. The ACI Code provisions for the development length of hooked bars in tension in beam-column joints in special moment frames (Section 18.8.5.1 of ACI 318-19), derived from the development length provisions for non-seismic loading in earlier Codes, permit development lengths that are shorter needed for gravity load by Chapter 25. Changes in Chapter 18 of ACI 318-19 are proposed that require the use of the provisions in Chapter 25 to establish the minimum development length for hooked bars anchored in joints for frames subjected to seismic loading.

Keywords: anchorage, beam-column joint, column-foundation joint, development length, headed bar, high-strength concrete, high-strength steel, hooked bar, reversed cyclic loading

ACKNOWLEDGEMENTS

This report is based on a thesis presented by Luay Ali Nazzal in partial fulfillment of the requirements for the Ph.D. degree from the University of Kansas. Support for the study was provided by the Charles Pankow Foundation under Research Grant Agreement #05-18, the ACI Foundation, BarSplice Products, Headed Reinforcement Corporation, nVENT Lenton, the CRSI Education and Research Foundation, the Precast/Prestressed Concrete Institute, Commercial Metals Company, and Nucor Corporation.

Additional support was provided by Dayton Superior, Midwest Concrete Materials, and Grace Construction Products. Thanks are due to Jack Moehle, Amy Trygstad, Javeed Munshi, and Andrew Taylor who served on the advisory panel.

TABLE OF CONTENTS

ABSTRACT.....	i
ACKNOWLEDGEMENTS	iii
LIST OF FIGURES	ix
LIST OF TABLES	xv
CHAPTER 1: INTRODUCTION.....	1
1.1 GENERAL.....	1
1.2 HOOKED AND HEADED REINFORCING BARS	4
1.2.1 Hooked reinforcing bars	4
1.2.2 Headed reinforcing bars	5
1.3 PREVIOUS WORK.....	6
1.3.1 Early studies on hooked and headed bars	6
1.3.1.1 Hooked bars	6
1.3.1.2 Headed studs and bars.....	10
1.3.2 Simulated beam-column joints with hooked bars subjected to monotonic loading.....	11
1.3.3 Beam-column joints with hooked bars subjected to reversed cyclic loading	20
1.3.4 Simulated beam-column joints with headed bars subjected to monotonic loading	21
1.3.5 Headed bars in slab specimens	27
1.4 CONCRETE CAPACITY DESIGN METHOD.....	30
1.5 UNIVERSITY OF KANSAS - SIMULATED COLUMN-FOUNDATION JOINTS.....	36
1.6 UNIVERSITY OF CALIFORNIA, BERKELEY – STEEL COLUMN-CONCRETE FOUNDATION JOINTS	39
1.7 CODE PROVISIONS	43
1.7.1 Anchorage provisions	43
1.7.2 Design provisions for hooked and headed bars	46
1.7.3 Design provisions for hooked bars in earthquake resistant structures	48
1.8 OBJECTIVE AND SCOPE	49

CHAPTER 2: EXPERIMENTAL WORK.....	52
2.1 MATERIAL PROPERTIES	52
2.1.1 Concrete Properties.....	52
2.1.2 Steel Properties	53
2.2 SLAB SPECIMEN DESIGN.....	54
2.3 TEST PARAMETERS.....	66
2.4 SPECIMEN DESIGNATION.....	67
2.5 SPECIMEN FABRICATION.....	68
2.6 TEST PROCEDURE	69
2.7 SPECIMEN INSTRUMENTATION.....	72
CHAPTER 3: TEST RESULTS AND ANALYSIS OF SIMULATED COLUMN- FOUNDATION JOINT SPECIMENS TESTED IN THE CURRENT AND PREVIOUS STUDIES AND COMPARISON BETWEEN THE PROPOSED EQUATIONS AND ACI 318-19 CODE PROVISIONS.....	74
3.1 TESTS OF HEADED BARS ANCHORED IN SIMULATED COLUMN-FOUNDATION JOINT SPECIMENS WITH SHALLOW EMBEDMENT	74
3.1.1 Failure and Failure Modes	81
3.1.2 Effect of Strut Angle.....	90
3.1.3 Effect of Concrete Compressive Strength.....	93
3.1.4 Effect of Grouped Anchors and Headed Bar Spacing	97
3.1.5 Effect of Parallel Tie Reinforcement	101
3.1.6 Examination of Value of Effective Parallel Tie Reinforcement A_{tt} used in Descriptive Equation, Eq. (1.8).....	115
3.2 ANALYSIS OF TEST RESULTS FROM OTHER STUDIES AND COMPARISONS WITH THE CURRENT STUDY	117
3.2.1 Headed Bars Tested in Slab Specimens.....	122
3.2.1.1 Analysis Based on Descriptive Equations, ACI 318-19 Code Provisions, and Proposed Version of Code Provisions	128
3.2.1.2 Comparison Between the Descriptive Equations, ACI 318-19 Code Provisions, and Proposed Code Provisions	140
3.3 RECOMMENDED CHANGES TO CHAPTERS 17 AND 25 OF ACI 318-19	144

3.3.1 Proposed Changes in Chapter 25 of ACI 318-19.....	145
CHAPTER 4: ANALYSIS OF BEAM-COLUMN JOINT SPECIMENS WITH BEAM BARS ANCHORED WITH HOOKS SUBJECTED TO REVERSED CYCLIC LOADING	151
4.1 INTRODUCTION	151
4.2 ANALYSIS BASED ON PROPOSED DESCRIPTIVE AND DESIGN EQUATIONS..	151
4.2.1 Descriptive Equations and Design Provisions Proposed by Ajaam et al. (2017)	151
4.2.2 Exterior Beam-Column Joints.....	154
4.2.2.1 Specimens with $d/\ell_{eh} \leq 1.5$ and $\ell_{eh}/\ell_{ehy} < 1.0$	169
4.2.2.2 Specimens with $d/\ell_{eh} \leq 1.5$ and $\ell_{eh}/\ell_{ehy} \geq 1.0$	171
4.2.2.3 Specimens with $d/\ell_{eh} > 1.5$	174
4.2.2.4 Applicability of Descriptive Equations to Predict Anchorage Strength of Hooked Bars Anchored in Members Subjected to Reversed Cyclic Loading.....	185
4.3 GUIDELINES AND RECOMMENDATIONS FOR CHAPTER 18 OF ACI 318-19	198
4.3.1 Comparison Between the Development Lengths of Hooked Bars Required for Seismic and Non-Seismic (Gravity) Loading (Chapter 18 vs. 25 of ACI 318-19)	198
4.3.2 Proposed Changes in Chapter 18 of ACI 318-19.....	200
CHAPTER 5: SUMMARY AND CONCLUSIONS	202
5.1 SUMMARY	202
5.2 CONCLUSION.....	203
5.3 FUTURE WORK.....	205
REFERENCES.....	206
APPENDIX A: NOTATION.....	213
APPENDIX B: DETAILS OF SLAB SPECIMENS TESTED IN THE CURRENT STUDY	217
B.1 STRESS-STRAIN CURVES FOR HEADED BARS	217
B.2 SCHEMATICS OF SLAB SPECIMENS	219
B.3 TEST RESULTS AND SPECIMENS CONSTRUCTED AND TESTED IN THE CURRENT STUDY	223

APPENDIX C: TEST RESULTS AND SPECIMENS FROM OTHER STUDIES INCLUDED IN THE CURRENT STUDY	229
C.1 SLAB SPECIMENS TESTED BY DEVRIES ET AL. (1999) AND CHOI ET AL. (2002)	229
C.2 SLAB SPECIMENS TESTED AT THE UNIVERSITY OF KANSAS	233
C.3 SLAB SPECIMENS TESTED AT THE UNIVERSITY OF CALIFORNIA, BERKELEY	236
C.4 EXTERIOR BEAM-COLUMN JOINT SPECIMENS	237
APPENDIX D: SUMMARY OF STUDIES ON BEAM-COLUMN JOINT SPECIMENS TESTED UNDER REVERSED CYCLIC LOADING	279

LIST OF FIGURES

Figure 1.1 Force transfer on a hooked bar (Minor and Jirsa 1975)	4
Figure 1.2 Standard hook details (ACI 318-11).....	5
Figure 1.3 Force transfer on a headed bar (Bashandy 1996)	5
Figure 1.4 Maximum dimensions of obstructions or interruptions for headed bars (ASTM A970/A970M-17)	6
Figure 1.5 Small concrete blocks (a) specimen for 90° hooked bars, (b) specimen for 180° hooked bars (Hribar and Vasko 1969).....	7
Figure 1.6 Loading apparatus (Hribar and Vasko 1969)	8
Figure 1.7 Test specimen (Minor and Jirsa 1975)	9
Figure 1.8 Details of push-out specimens (Viest 1956).....	10
Figure 1.9 Test specimen (Marques and Jirsa 1975)	12
Figure 1.10 Specimen and test setup (Hamad et al. 1993).....	14
Figure 1.11 Test setup (Ramirez and Russell 2008)	15
Figure 1.12 Test setup (Sperry et al. 2015a).....	16
Figure 1.13 Test Setup (Bashandy 1996).....	22
Figure 1.14 Test setup (Chun et al. 2009).....	24
Figure 1.15 Failure modes: (a) concrete breakout, (b) and (c) joint shear failure (Chun et al. 2009)	24
Figure 1.16 Test Frame (Shao et al. 2016).....	25
Figure 1.17 Test setup (DeVries et al. 1999)	28
Figure 1.18 Headed reinforcing bars (a) unbonded and (b) bonded embedment length (DeVries et al. 1999)	28
Figure 1.19 Transverse reinforcement configuration (DeVries et al. 1999).....	28
Figure 1.20 Slab specimens (Choi et al. 2002)	30
Figure 1.21 CCD idealized concrete cone for an individual anchor (Fuchs et al. 1995).....	31

Figure 1.22 Projected area of an individual anchor according to the CCD method (Fuchs et al. 1995)	32
Figure 1.23 Calculation of the projected area, A_N , according to the CCD method (Fuchs et al. 1995)	34
Figure 1.24 Test setup (Nilforoush et al. 2017)	35
Figure 1.25 Test setup of the first group (a) front view, (b) side view (Ghimire et al. 2018)	37
Figure 1.26 Test setup of the final group (a) front view, (b) side view (Ghimire et al. 2018)	38
Figure 1.27 Steel-column-to-concrete-foundation joint specimen M01 (Worsfold et al. 2022) .	40
Figure 1.28 Steel-column-to-concrete-foundation joint specimen M02 (Worsfold et al. 2022) .	41
Figure 1.29 Plan view of specimen M02 (Worsfold et al. 2022).....	41
Figure 1.30 Idealized cone geometry shown in elevation and observed cone geometry intersecting top surface in plan view for specimen M01 (Worsfold et al. 2022).....	42
Figure 1.31 Cross section and plan view highlighting crack patterns and breakout cone geometry for Specimen M02 (Worsfold et al. 2022)	43
Figure 1.32 Calculation of A_{Nco} for a single anchor (ACI 318-19).....	45
Figure 1.33 Calculation of A_{Nc} for a single anchor and group of anchors (ACI 318-19)	46
Figure 1.34 Strut angle between anchored headed bar and nearest support reaction	51
Figure 2.1 Headed bars (a) No. 11 S5.5 bar (b) No. 11 S9.2 bar (c) No. 14 B4.2 headed bar	54
Figure 2.2 Location of headed bars and reinforcement for Slab 1 (a) side view, (b) end view...	58
Figure 2.3 Location of headed bars and reinforcement for Slab 2 (a) side view, (b) end view...	59
Figure 2.4 Location of headed bars and reinforcement for Slab 3 (a) side view, (b) end view...	60
Figure 2.5 Location of headed bars and reinforcement for Slab 4 (a) side view, (b) end view...	61
Figure 2.6 Location of headed bars and reinforcement for Slab 5 (a) side view, (b) end view...	62
Figure 2.7 Location of headed bars and reinforcement for Slabs 6,7, and 10 (a) side view, (b) end view	63
Figure 2.8 Location of headed bars and reinforcement for Slabs 8, 9, and 11 (a) side view, (b) end view	64

Figure 2.9 Location of headed bars and reinforcement for Slabs 12 and 14 (a) side view, (b) end view	65
Figure 2.10 Location of headed bars and reinforcement for Slabs 13 and 15 (a) side view, (b) end view	66
Figure 2.11 Example specimen designation	68
Figure 2.12 Slab specimen formwork	69
Figure 2.13 Test frame – first configuration	70
Figure 2.14 Test frame – second configuration	71
Figure 2.15 LVDTs clamped to the top flange of the spreader beams	72
Figure 2.16 LVDT plates attached to test bars.....	72
Figure 2.17 Location of the strain gauges on parallel ties	73
Figure 3.1 Concrete surface failure (crack propagation top and side views).....	84
Figure 3.2 Concrete cone-shaped breakout failure (a) schematic drawing (b) Slab Specimen 5 (test 2, 11-5-S5.5-6#6-2#4-12.75) after removal of breakout region	85
Figure 3.3 Concrete breakout failure. Slab Specimen 5 (test 1, 11-5-S5.5-6#6-2#4-12.75) with both support reactions just outside anticipated failure region (test had one headed bar with parallel tie reinforcement on both sides of headed bar).....	86
Figure 3.4 Concrete breakout failure of Slab Specimen 6 (test 1, (2@8.2)11-5-S5.5-7#11-0-12.75) with one of the support reactions placed within anticipated failure region (test had two headed bars without parallel tie reinforcement) (a) concrete surface failure (b) cone-shaped failure after removal of breakout region	87
Figure 3.5 Concrete breakout failure of Slab Specimen 8 (test 1, (2@8.2)11-5-S9.2-7#11-3#4-12.75) with one of the support reactions placed within anticipated failure region (test had two headed bars with parallel tie reinforcement only on one side of headed bars) (a) concrete surface failure (b) cone-shaped failure after removal of breakout region	88
Figure 3.6 Concrete breakout failure of Slab Specimen 8 (test 2, (2@8.2)11-5-S9.2-7#11-6#4-12.75) with one of the support reactions placed within anticipated failure region (test had two headed bars with parallel tie reinforcement on both sides of headed bars) (a) concrete surface failure (b) cone-shaped failure after removal of breakout region	89

Figure 3.7 Concrete breakout failure of Slab Specimen 3 (11-5-S5.5-6#11-0-12.75) with both support reactions placed far away from anticipated failure region (test had one headed bars without parallel tie reinforcement).....	90
Figure 3.8 Strut angle between anchored headed bar and nearest support reaction (Krishna et al. 2018)	91
Figure 3.9 Bar force at failure normalized with respect to a concrete compressive strength of 5,000 psi, and an embedment length of 12.75 in., T_N , versus the ratio h_{cl}/ℓ_{eh} (defined in Figure 3.8). Tests with No. 8 headed bars are from Ghimire et al. (2018), and tests with No. 11 headed bars are from the current study	92
Figure 3.10 Normalized bar force at failure T_N [using Eq. (3.2)] versus concrete compressive strength f_{cm} for specimens presented in Table 3.3.....	95
Figure 3.11 Ratio of test-to-calculated failure load T/T_h versus concrete compressive strength f_{cm} for all the current study tests that contained two headed bars load simultaneously with the presence of the parallel tie reinforcement within the joint region presented in Table 3.1.....	96
Figure 3.12 Bar force at failure normalized with respect to a concrete compressive strength of 5,000 psi and an embedment length of 12.75 in. T_N versus the number of headed bars being developed in tests (a) with individual and closely spaced headed bars loaded simultaneously (b) with individual and widely spaced headed bars loaded simultaneously. Results for individual bars are the same in figures (a) and (b).....	99
Figure 3.13 Bar force at failure normalized with respect to a concrete compressive strength of 5,000 psi and an embedment length of 12.75 in. T_N versus center-to-center spacing between headed bars with respect to the bar diameter (d_b)	100
Figure 3.14 Parallel tie reinforcement for Slab Specimen 5 (11-5-S5.5-6#6-2#4-12.75) (a) front view, (b) side view, (c) load versus strain curves for Test 1, (d) load versus strain curves for Test 2, (e) load versus strain curves for Test 3	104
Figure 3.15 Average load per headed bar versus strain in parallel tie reinforcement for Slab Specimen 8 (a) location of the parallel tie reinforcement and the strain gauge locations (b) load versus strain curves for hoops in test included hoops only on one side of the bars Group A [(2@8.2)11-5-S9.2-7#11-3#4-12.75] (c) load versus strain curves for hoops in the test included hoops on both sides of the bars Group B [(2@8.2)11-5-S9.2-7#11-6#4-12.75]	106
Figure 3.16 Average load per headed bar versus strain in parallel tie reinforcement for Slab Specimen 9 (a) load versus strain curves for hoops in test included hoops only on one side of the bars Group A [(2@8.2)11-5-S9.2-7#11-3#4-12.75] (b) load versus strain curves for hoops in the test included hoops on both sides of the bars Group B [(2@8.2)11-5-S9.2-7#11-6#4-12.75] ...	110

Figure 3.17 Normalized bar force at failure T_N [using Eq. (3.1)] versus normalized parallel tie reinforcement A_{tl}/A_{hs} , within a $10d_b$ radial distance from the centerline of the headed bars, for specimens with and without parallel tie reinforcement	113
Figure 3.18 Headed reinforcing bars (a) unbonded and (b) bonded embedment length (DeVries et al. 1999)	123
Figure 3.19 Slab specimens (Choi et al. 2002)	124
Figure 3.20 Steel-column-to-concrete-foundation joint specimen M01 (Worsfold et al. 2022)	126
Figure 3.21 Steel-column-to-concrete-foundation joint specimen M02 (Worsfold et al. 2022)	127
Figure 3.22 Plan view of specimen M02 (Worsfold et al. 2022).....	127
Figure 3.23 Measured force at failure T versus anchorage strength T_h calculated using Eq. (3.3) and (3.4) for slab specimens tested by DeVries et al. (1999), Choi et al. (2002), Ghimire et al. (2018), Worsfold et al. (2022), and in the current study; a reduction factor of 0.8 is applied to T_h for headed bars with concrete cover less than $8d_b$	130
Figure 3.24 Measured force at failure T versus the anchorage strength T_{anc} calculated using Eq. (3.6), incorporating the modification factor ψ_{mean} , for slab specimens tested by DeVries et al. (1999), Choi et al. (2002), Ghimire et al. (2018), Worsfold et al. (2022), and in the current study	133
Figure 3.25 Measured force at failure T versus the anchorage strength $T_{ACI 318}$ calculated using Eq. (3.11) for slab specimens tested by DeVries et al. (1999), Choi et al. (2002), Ghimire et al. (2018), Worsfold et al. (2022), and in the current study.....	136
Figure 3.26 Measured force at failure T versus the anchorage strength T_{calc} calculated using Eq. (3.14) for slab specimens tested by DeVries et al. (1999), Choi et al. (2002), Ghimire et al. (2018), Worsfold et al. (2022), and in the current study.....	139
Figure 3.27 Average values of T/T_h , T/T_{anc} , $T/T_{ACI 318}$, and T/T_{calc} for tests involving two headed bars without and with parallel tie reinforcement, Slab Specimens 6, 7 and 10 [(2@8.2)11-5-S5.5-7#11-0-12.75], Slab Specimens 12 and 14 [(2@6.8)14-5-B4.2-7#11-0-12.75], Slab Specimens 8, 9 and 11 [(2@8.2)11-5-S9.2-7#11-6#4-12.75], and Slab Specimens 13 and 15 [(2@6.8)14-5-B4.2-7#11-6#4-12.75].....	142
Figure 4.1 Effective confining reinforcement for hooked bars within the joint region of beam-column joints suggested by Ajaam et al. (2017).....	152
Figure 4.2 M_{peak}/M_n versus ℓ_{eh}/ℓ_{ehy} for specimens with $d/\ell_{eh} \leq 1.5$ and $V_p/V_n \leq 1.0$. M_{peak}/M_n is the ratio of peak moment to nominal flexural strength, and ℓ_{eh}/ℓ_{ehy} is the ratio of embedment length	

to the embedment length required to yield the hooked bar calculated using the descriptive equations developed by Ajaam et al. (2017), Eq. (4.1) and (4.2)	168
Figure 4.3 M_{peak}/M_n versus ℓ_{eh}/ℓ_{ehy} for specimens with $d/\ell_{eh} \leq 1.5$ and $V_p/V_n > 1.0$. M_{peak}/M_n is the ratio of peak moment to nominal flexural strength, and ℓ_{eh}/ℓ_{ehy} is the ratio of embedment length to the embedment length required to yield the hooked bar calculated using the descriptive equations developed by Ajaam et al. (2017), Eq. (4.1) and (4.2)	169
Figure 4.4 V_p/V_n versus ℓ_{eh}/ℓ_{ehy} for specimens with $d/\ell_{eh} \leq 1.5$. V_p/V_n is the ratio of peak joint shear to nominal joint shear strength, and ℓ_{eh}/ℓ_{ehy} is the ratio of embedment length to the embedment length required to yield the hooked bar calculated using the descriptive equations developed by Ajaam et al. (2017), Eq. (4.1) and (4.2)	173
Figure 4.5 M_{peak}/M_n versus V_p/V_n for specimens with $d/\ell_{eh} \leq 1.5$ and $\ell_{eh}/\ell_{ehy} \geq 1.0$. M_{peak}/M_n is the ratio of peak moment to nominal flexural strength, and V_p/V_n is the ratio of peak joint shear to nominal joint shear strength.....	174
Figure 4.6 Ratio of test-to-calculated bar force at failure T/T_h versus ratio of effective beam depth to embedment length d/ℓ_{eh} for specimens without confining reinforcement [T_h is calculated using Eq. (4.1)] (Ajaam et al. 2017)	175
Figure 4.7 Ratio of test-to-calculated bar force at failure T/T_h versus ratio of effective beam depth to embedment length d/ℓ_{eh} for specimens with confining reinforcement [T_h is calculated using Eq. (4.2)] (Ajaam et al. 2017)	176
Figure 4.8 Load transfer within the beam-column joint based on the strut-and-tie mechanism (column longitudinal reinforcement and beam compression reinforcement are not shown for clarity)	180
Figure 4.9 M_{peak}/M_n versus ℓ_{eh}/ℓ_{ehy} for specimens with $d/\ell_{eh} > 1.5$. M_{peak}/M_n is the ratio of peak moment to nominal flexural strength, and ℓ_{eh}/ℓ_{ehy} is the ratio of embedment length to the embedment length required to yield the hooked bar calculated using the descriptive equations developed by Ajaam et al. (2017), Eq. (4.1) and (4.2)	184
Figure 4.10 M_{peak}/M_n versus ℓ_{eh}/ℓ_{ehy} for beam-column joint specimens with $\ell_{eh}/\ell_{ehy} \geq 1.0$. The value of M_{peak}/M_n for one specimen is projected on the line $\ell_{eh}/\ell_{ehy} = 1.0$ line by extending a line parallel to the trend line for specimens with $\ell_{eh}/\ell_{ehy} \geq 1.0$	192
Figure 4.11 Estimated hooked bar force at failure T'_{mod} versus hooked bar force T_h [based on the descriptive equations, Eq. (4.1) and (4.2)] for specimens with $d/\ell_{eh} \leq 1.5$, $V_p/V_n \leq 1.0$, and $\ell_{eh}/\ell_{ehy} \geq 1.0$	197

LIST OF TABLES

Table 1.1 Modification factor ψ_{cs} for confining reinforcement and spacing	19
Table 1.2 Modification factor ψ_{cs} for confining reinforcement and spacing	26
Table 2.1 Concrete mixture proportions	53
Table 2.2 Properties of headed bars and parallel tie reinforcement	53
Table 2.3 Head dimensions	54
Table 2.4 Detail of slab specimens	55
Table 2.4 Cont. Detail of slab specimens	56
Table 3.1 Summary of key parameters of slab specimens	76
Table 3.1 Cont. Summary of key parameters of slab specimens	76
Table 3.1 Cont. Summary of key parameters of slab specimens.....	77
Table 3.1 Cont. Summary of key parameters of slab specimens.....	78
Table 3.2 Summary of key parameters of slab specimens (Ghimire et al. 2018)	79
Table 3.2 Cont. Summary of key parameters of slab specimens (Ghimire et al. 2018).....	80
Table 3.3 Test results for specimens containing No. 11 and No. 14 headed bars tested with different concrete strength	94
Table 3.4 Statistical parameters of T/T_h values for tests containing two headed bars with parallel tie reinforcement within the joint region	96
Table 3.5 Test results for specimens containing individual and two closely-spaced or widely-spaced grouped headed bars.....	98
Table 3.6 Test results for specimens containing No. 11 and No. 14 headed bars with and without parallel tie reinforcement	112
Table 3.6 Cont. Test results for specimens containing No. 11 and No. 14 headed bars with and without parallel tie reinforcement	113
Table 3.7 Effective parallel tie reinforcement (A_{tt}) and T/T_h values for tests containing two headed bars loaded simultaneously with parallel tie reinforcement within the joint region, the cap $0.3A_b$ is not applied to the descriptive equation (Eq. 1.8).....	116

Table 3.8 Effective parallel tie reinforcement (A_{tt}) and T/T_h values for tests containing two headed bars loaded simultaneously with parallel tie reinforcement within the joint region, the cap $0.3A_b$ is applied to the descriptive equation (Eq. 1.8).....	117
Table 3.9 Test results for headed bars anchored in slab specimens tested by DeVries et al. (1999), Choi et al. (2002), and Worsfold et al. (2022) and comparisons with anchorage provisions of Chapter 17 of ACI 318-19 [Eq. (3.9)], descriptive equations [Eq. (3.3) and (3.4)], design provisions of Chapter 25 of ACI 318-19 [Eq. (3.11)], and proposed Code provisions [Eq. (3.14)], (a reduction factor of 0.8 is applied to T_h as appropriate).....	129
Table 3.10 Statistical parameters of T/T_h values for slab specimens tested by DeVries et al. (1999), Choi et al. (2002), Ghimire et al. (2018), Worsfold et al. (2022), and in the current study	132
Table 3.11 Statistical parameters of T/T_{anc} values for slab specimens for which T_{anc} is governed by concrete breakout tested by DeVries et al. (1999), Choi et al. (2002), Ghimire et al. (2018), Worsfold et al. (2022), and in the current study	135
Table 3.12 Statistical parameters of $T/T_{ACI 318}$ values for slab specimens tested by DeVries et al. (1999), Choi et al. (2002), Ghimire et al. (2018), Worsfold et al. (2022), and in the current study	138
Table 3.13 Statistical parameters of T/T_{calc} values for slab specimens tested by DeVries et al. (1999), Choi et al. (2002), Ghimire et al. (2018), Worsfold et al. (2022), and in the current study	140
Table 4.1 Modification factor ψ_{cs} for confining reinforcement, expressed as ratio of area of confining reinforcement, A_{th} , to area of hooked bars, A_{hs} , and center-to center bar spacing, $c_{ch}^{[1]}$	154
Table 4.2 Detail of exterior beam-column joint specimens tested under reversed cyclic loading	156
Table 4.2 Cont. Detail of exterior beam-column joint specimens tested under reversed cyclic loading.....	157
Table 4.2 Cont. Detail of exterior beam-column joint specimens tested under reversed cyclic loading.....	158
Table 4.2 Cont. Detail of exterior beam-column joint specimens tested under reversed cyclic loading.....	159
Table 4.2 Cont. Detail of exterior beam-column joint specimens tested under reversed cyclic loading.....	160

Table 4.2 Cont. Detail of exterior beam-column joint specimens tested under reversed cyclic loading.....	161
Table 4.2 Cont. Detail of exterior beam-column joint specimens tested under reversed cyclic loading.....	162
Table 4.2 Cont. Detail of exterior beam-column joint specimens tested under reversed cyclic loading.....	163
Table 4.2 Cont. Detail of exterior beam-column joint specimens tested under reversed cyclic loading.....	164
Table 4.2 Cont. Detail of exterior beam-column joint specimens tested under reversed cyclic loading.....	165
Table 4.3 Detail of exterior beam-column joint specimens tested under reversed cyclic loading with $d/\ell_{eh} > 1.5$	178
Table 4.3 Cont. Detail of exterior beam-column joint specimens tested under reversed cyclic loading with $d/\ell_{eh} > 1.5$	179
Table 4.4 Test parameters for exterior beam-column joint specimens containing hooked bars with $d/\ell_{eh} > 1.5$ and tested under reversed cyclic loading	181
Table 4.4 Cont. Test parameters for exterior beam-column joint specimens containing hooked bars with $d/\ell_{eh} > 1.5$ and tested under reversed cyclic loading.....	183
Table 4.5 Detail of exterior beam-column joint specimens tested under reversed cyclic loading with $d/\ell_{eh} \leq 1.5$ and $V_p/V_n \leq 1.0$ used in this evaluation and comparisons with descriptive equations, Eq. (4.1) and (4.2).....	186
Table 4.5 Cont. Detail of exterior beam-column joint specimens tested under reversed cyclic loading with $d/\ell_{eh} \leq 1.5$ and $V_p/V_n \leq 1.0$ used in this evaluation and comparisons with descriptive equations, Eq. (4.1) and (4.2).....	187
Table 4.5 Cont. Detail of exterior beam-column joint specimens tested under reversed cyclic loading with $d/\ell_{eh} \leq 1.5$ and $V_p/V_n \leq 1.0$ used in this evaluation and comparisons with descriptive equations, Eq. (4.1) and (4.2).....	188
Table 4.6 Statistical parameters for test-to-calculated ratio in beam-column joint specimens with $\ell_{eh}/\ell_{ehy} < 1.0$ tested under reversed cyclic loading and in beam-column joint specimens tested under monotonic loading and used by Ajaam et al. (2017) to develop the descriptive equations, Eq. (4.1) and (4.2).....	190

Table 4.7 Statistical parameters for T'_{mod}/T_h in beam-column joint specimens with $\ell_{eh}/\ell_{ehy} \geq 1.0$ tested under reversed cyclic loading	193
Table 4.8 Detail of exterior beam-column joint specimens tested under reversed cyclic loading with $d/\ell_{eh} \leq 1.5$, $V_p/V_n \leq 1.0$, and $\ell_{eh}/\ell_{ehy} \geq 1.0$ used in this evaluation and comparisons with descriptive equations, Eq. (4.1) and (4.2)	194
Table 4.8 Cont. Detail of exterior beam-column joint specimens tested under reversed cyclic loading with $d/\ell_{eh} \leq 1.5$, $V_p/V_n \leq 1.0$, and $\ell_{eh}/\ell_{ehy} \geq 1.0$ used in this evaluation and comparisons with descriptive equations, Eq. (4.1) and (4.2)	195
Table 4.8 Cont. Detail of exterior beam-column joint specimens tested under reversed cyclic loading with $d/\ell_{eh} \leq 1.5$, $V_p/V_n \leq 1.0$, and $\ell_{eh}/\ell_{ehy} \geq 1.0$ used in this evaluation and comparisons with descriptive equations, Eq. (4.1) and (4.2)	196

CHAPTER 1: INTRODUCTION

1.1 GENERAL

In reinforced concrete structures, the reinforcing steel and the surrounding concrete must be sufficiently bonded to each other to transfer internal stresses, allowing the structure to behave as a composite and resist external forces. When smooth bar reinforcement was used, the mechanism of the bond involved only adhesion and friction between the reinforcing steel and the surrounding concrete. For deformed bar reinforcement, an additional (and principal) bond mechanism results from physical interlocking between the reinforcing steel and the surrounding concrete, along with the frictional and adhesive forces.

Reinforcing steel must be embedded in the concrete for a certain length to fully develop the required stress, usually the yield strength, at critical sections where stresses in reinforcement are maximum. In cases such as external beam-column joints, however, the length required for a bar to develop its yield strength may be greater than the column dimensions. In such cases, hooks or heads can provide the required anchorage strength with a much shorter embedment length than is possible with straight reinforcing bars. The required embedment length is referred to as the development length in the ACI Building Code (ACI Committee 318 2019). Sections 25.4.3.1 and 25.4.4.2 of ACI 318-19 Building Code Requirements for Structural Concrete contain equations to calculate the development length of hooked and headed deformed bars in tension.

Prior to ACI 318-19, the development length provisions for hooked and headed bars were based on studies of limited scope. As a result, significant limitations were placed on the application of hooked and headed bars, such as limiting the yield strength of the bar to 60,000 psi for headed bars and 80,000 psi for hooked bars and limiting the concrete compressive strength to 6,000 psi for headed bars and 10,000 psi for hooked bars. Higher-strength materials (reinforcing steel with yield strengths up to 120,000 psi and concrete strengths above 16,000 psi), however, are now available for use in reinforced concrete construction. To gain a better understanding of the behavior of hooked and headed bars and to allow the use of higher strength materials, researchers at the University of Kansas (KU) initiated a comprehensive study to investigate the anchorage strength of both methods of anchorage for bars in tension (Sperry et al. 2015a,b, 2017a,b, 2018, Ajaam et al. 2017, 2018, Yasso et al. 2017, 2021, Shao et al. 2016, Ghimire et al. 2018, 2019a,b) that

included a range in values of concrete cover, bar spacing, and embedment length, and high-strength materials. Based on these studies, the development length provisions in ACI 318 were updated in 2019. In spite of this comprehensive effort, however, a number of key questions remain. Two of those questions are specifically addressed in this study.

Headed reinforcing bars serve as a viable alternative to hooked bars for anchorage in concrete due to their ability to reduce congestion and development length. Very limited research, however, has been performed on the behavior of headed bars anchored in members other than beam-column joints, with none available regarding the effect of parallel reinforcement (stirrups or hoops oriented parallel to the headed bars). As a result, Section R25.4.4.5 of ACI 318-19 prohibits consideration of parallel reinforcement in the anchorage strength in members other than beam-column joints. Shao et al. (2016) and Ghimire et al. (2018, 2019a,b) have shown that the presence of parallel tie reinforcement (the term used for parallel reinforcement when used with headed bars) within the joint region increases the anchorage strength of headed bars. Taking full advantage of headed reinforcing bars requires a better understanding of the behavior of headed reinforcing bars in a wider range of member configurations, including, but not limited to, column-foundations joints.

The design provisions for calculating the development lengths of hooked and headed bars, ℓ_{dh} and ℓ_{dt} , respectively, are presented in Sections 25.4.3 and 25.4.4 of ACI 318-19 (described in greater detail in Section 1.6.2). In ACI 318-19, ℓ_{dh} and ℓ_{dt} are functions of the specified yield strength of the bar (f_y), the square root of concrete compressive strength (f'_c), bar diameter (d_b) to the power of 1.5, bar location (inside or outside of a column core) and spacing, quantity of confining reinforcement for hooks and parallel tie reinforcement for heads, and if used, epoxy coating on the bar and lightweight concrete.

The design provisions in Section 25.4.4.2 of ACI 318-19 for calculating the development length of headed bars can be used if the headed bars satisfy specific requirements, described in Section 25.4.4.1 of ACI 318-19. For cases where the development length of headed bars cannot be designed in accordance with 25.4.4.2 and for cases where concrete breakout (a mass of concrete being pulled out of the specimen along with the headed bar, forming a cone-shaped failure surface) is expected, use of the anchorage provisions in Chapter 17 of ACI 318-19 should be considered.

Current ACI anchorage provisions, particularly for concrete breakout strength, given in Section 17.6.2.1 of ACI 318-19 and described in Section 1.6.1 of this report, were developed for headed studs and headed anchor bolts that are generally smooth. Therefore, the effect of deformations on reinforcing bars, which contribute significantly to bond in straight reinforcing bars, are not considered. Moreover, Section 17.6.2.1 of ACI 318-19 does not take into account the effect of the parallel tie reinforcement on anchorage capacity. Because the ACI anchorage provisions may be overly conservative when applied to headed reinforcing bars, it is important to evaluate the accuracy of those provisions for predicting the anchorage strength in parallel with consideration of the development length provisions in the Code.

The current Code design provisions (ACI 318 Building Code and ACI 349 Code Requirements for Nuclear Safety-Related Concrete Structures) for the development length of hooked bars in tension under reversed cyclic loading (Section 18.8.5.1 of ACI 318-19) were derived directly from the development length provisions for non-seismic (monotonic) loading (Section 25.4.3.1) that existed in ACI 318 Building Codes prior to 2019. Even though the development length provisions (Section 25.4.3.1) were updated in ACI 318-19 due to the comprehensive study conducted at KU using specimens tested under monotonic loading (Sperry et al. 2015a,b, 2017a,b, 2018, Ajaam et al. 2017, 2018, Yasso et al. 2017), the code design provisions for the development length of hooked bars in tension under cyclic loading did not change. This has resulted in provisions that permit hooked bar development lengths designed under the provisions of Chapter 18 to be *shorter* than those required for gravity load by Chapter 25. This rather strange situation justifies an evaluation of the current code provisions in Section 18.8.5.1 and the appropriateness of applying the development length requirements of 25.4.3 to the design of hooked bars subjected to reversed cyclic loading. Such an evaluation has already been performed for beam-column joints under reversed cyclic loading in which the beam bars are anchored with heads (Ghimire et al. 2018, 2021), resulting in a modification of Section 18.8.5.2 of ACI 318-19 to require that the development length of headed bars in such cases satisfy the requirements of Section 25.4.4 of Chapter 25 of the Code.

This study addresses two areas: The first focuses on an experimental investigation of the anchorage strength of headed bars anchored in members other than beam-column joints, such as

column-foundation joints, using larger bar sizes (No. 11 and No. 14) and high-strength materials, both with and without parallel tie reinforcement. The second involves the analysis of test data for exterior beam-column joints subjected to reversed cyclic loading in which the beam bars are anchored with hooks. The goal of this second area is to determine the applicability of the development length provisions for hooked bars in tension to hooked bars under reversed cyclic loading.

This chapter introduces previous research relevant to the current study, provides a detailed explanation of the code anchorage provisions, and describes the objective and the scope of the research effort.

1.2 HOOKED AND HEADED REINFORCING BARS

1.2.1 Hooked reinforcing bars

Hooked reinforcing bars provide anchorage strength by a combination of the direct bearing of the hook on the concrete and the bond along the straight portion of the bars. The force transfer on a hooked bar is shown in Figure 1.1.

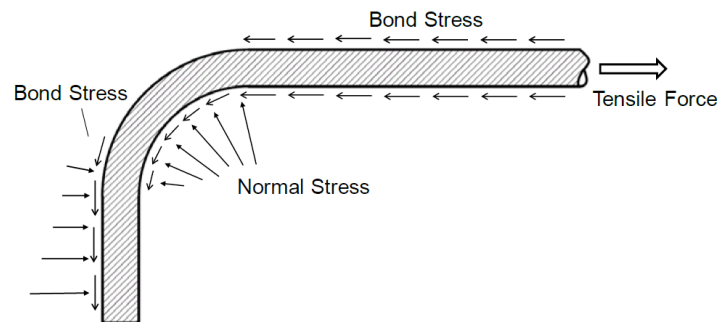


Figure 1.1 Force transfer on a hooked bar (Minor and Jirsa 1975)

Hooked bars are referred to as “standard hooks” if the geometry of the hooked bars meets the requirement specified in ACI 318-19 Section 25.3.1. Figure 1.2 shows the details of standard hooks with 90° and 180° bend angles.

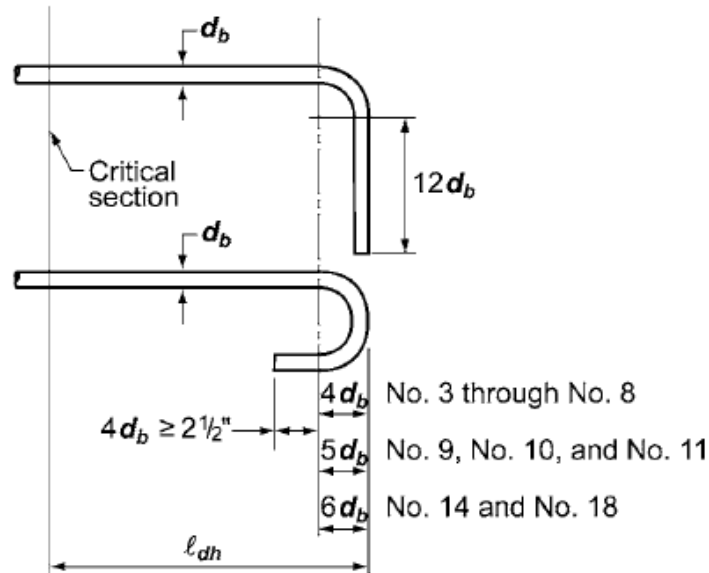


Figure 1.2 Standard hook details (ACI 318-11)

1.2.2 Headed reinforcing bars

A headed reinforcing bar is a type of deformed bar with a round, elliptical, or rectangular shape attached to one or both ends (ASTM A970). Headed reinforcing bars provide anchorage strength by a combination of direct bearing of the head on the concrete and the bond along the straight portion of the bars. The force transfer on a headed bar is shown in Figure 1.3.

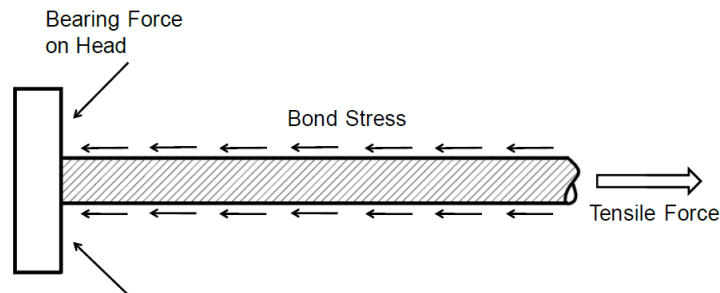


Figure 1.3 Force transfer on a headed bar (Bashandy 1996)

Headed reinforcing bars do not have a bend or tail extension length as with hooked reinforcing bars, so they have the ability to reduce congestion and ease construction. Heads may vary in size, shape, and manufacturing process, but only those comply with the Class HA requirements in ASTM A970 are allowed for use in reinforced concrete structures by ACI 318-19. According to Annex A1.2.1 of ASTM A970/A970M – 17, Class HA headed bars must develop the minimum specified tensile strength of the reinforcing bars. According to Annex A1.1.1.3 of

ASTM A970/A970M – 17, the net bearing area of a head (A_{brg}) shall be equal to or greater than four times the nominal cross-sectional area of the bar ($4A_b$). The net bearing area of a head (A_{brg}) is the gross area of the head minus the nominal area of the deformed reinforcing bar (A_b).

In addition to the head size, the obstructions or interruptions produced from the manufacturing process also must comply with certain dimensional requirements in order for the headed bars to meet Class HA requirements. According to Annex A1 of ASTM A970/A970M – 17, the maximum dimensions of the obstructions or interruptions is shown in Figure 1.4. Headed bars not meeting the requirements of Class HA heads may be used in concrete structures if tests showing the adequacy of these devices are approved by the building official.

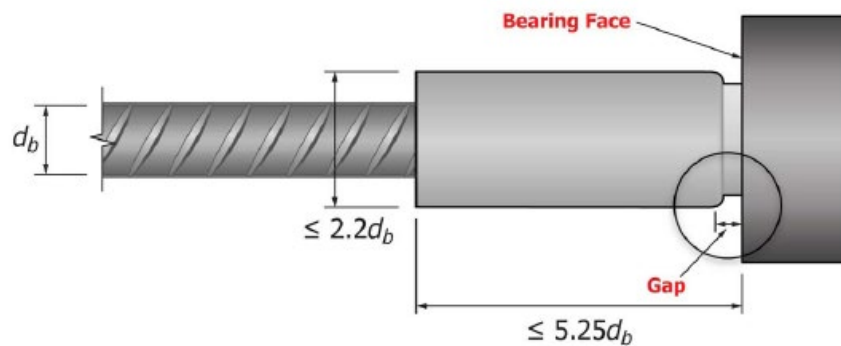


Figure 1.4 Maximum dimensions of obstructions or interruptions for headed bars (ASTM A970/A970M-17)

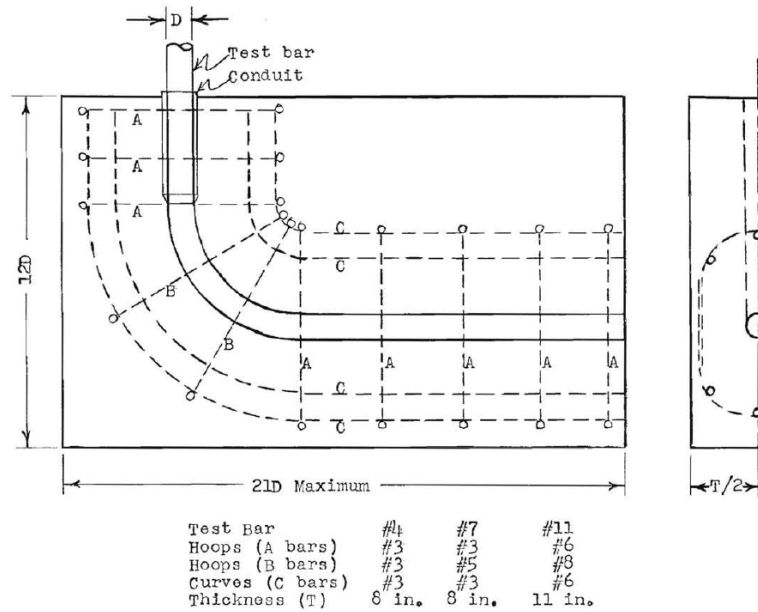
1.3 PREVIOUS WORK

1.3.1 Early studies on hooked and headed bars

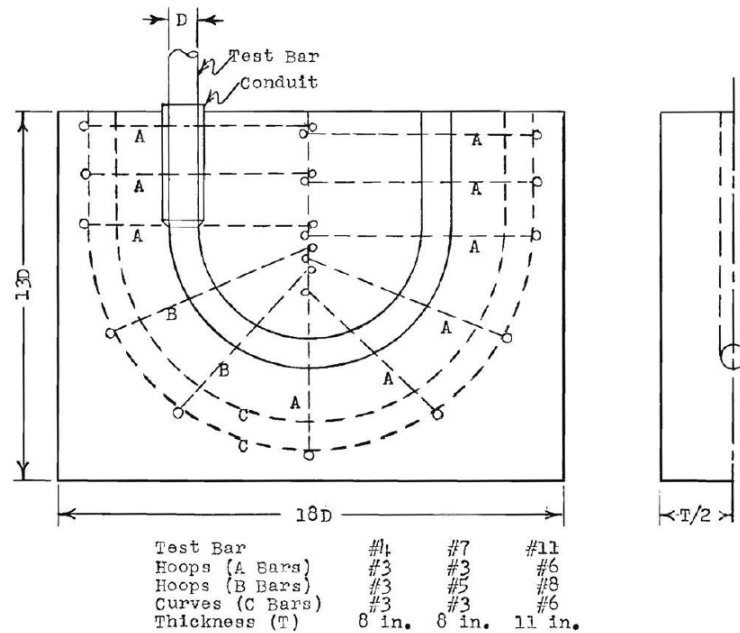
1.3.1.1 Hooked bars

Hribar and Vasko (1969) conducted 96 pull-out tests on straight and hooked bars to evaluate the end anchorage of the test bars. Three test series were performed in the study. The first series included 35 test bars, of which 18 were embedded individually, and the remaining 17 were embedded in a $16 \times 16 \times 5$ ft concrete block. In the second series, 44 test bars were embedded in a $16 \times 16 \times 5.5$ ft concrete block, and the third series included 17 bars embedded in a $10 \times 12 \times 5$ ft concrete block. Test bars embedded in large concrete blocks were embedded far apart (center-to-center 2 to 4 ft) so that a test failure of one bar did not interfere with the failure of the others. The main variables included in the study were the bar size (No. 4, No. 7, and No. 11), type of hook

(straight, 90° bend angle hooked bars, and 180° bend angle), and bend diameter (5 to $12d_b$). The smaller concrete blocks were heavily reinforced, as shown in Figure 1.5, to prevent splitting, while the larger concrete blocks were unreinforced. Concrete compressive strengths ranged from 3,700 to 4,750 psi. The loading apparatus is shown in Figure 1.6.



(a)



(b)

Figure 1.5 Small concrete blocks (a) specimen for 90° hooked bars, (b) specimen for 180° hooked bars (Hribar and Vasko 1969)

As shown in Figure 1.5, the dimensions of the specimens are given in bar diameters. Therefore, the size of the small concrete blocks varied with the size of the test bar. The dashed lines shown in Figure 1.5 represent supplementary steel reinforcement. A thin-wall conduit was used to debond the straight portion of the bar preceding the hook, as shown in Figure 1.5.

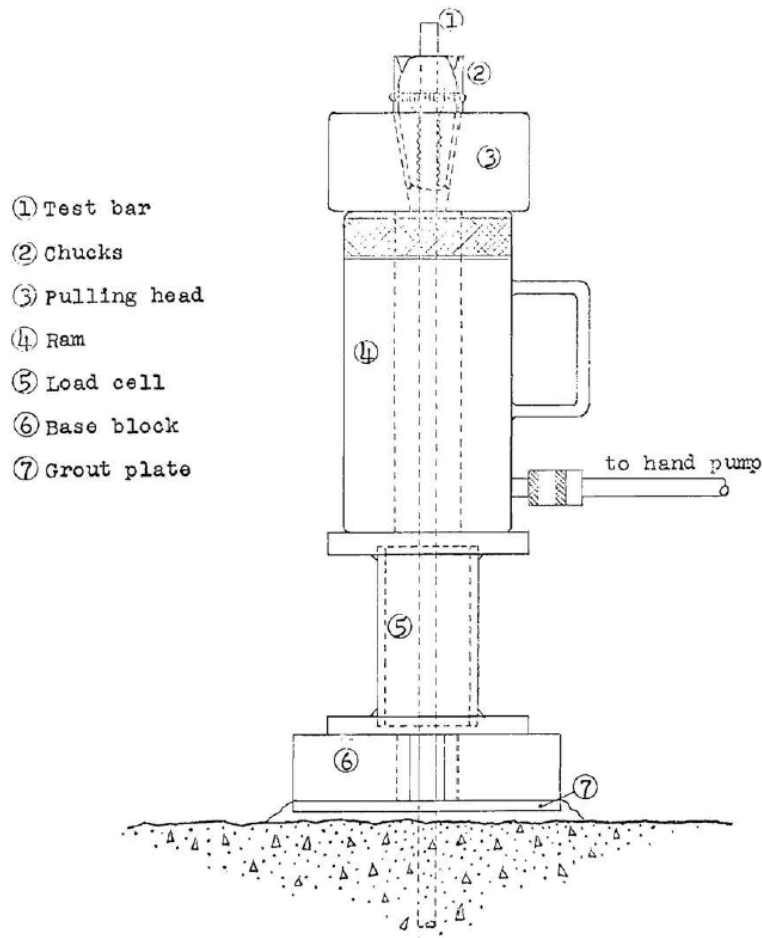


Figure 1.6 Loading apparatus (Hribar and Vasko 1969)

Hribar and Vasko found that the anchorage capacity of the test bars increased as the bend angle increased for an equivalent embedment length. Hribar and Vasko observed that the anchorage capacity of the test bars and the average bond stress at a given displacement increased with the square root of the concrete compressive strength (f'_c). Hribar and Vasko also found that the bar failure load increased as the embedment length and the bar diameter increased.

Minor and Jirsa (1975) conducted pullout tests on 80 deformed straight and hooked bars embedded in concrete blocks to examine some of the parameters that affect the anchorage capacity

of bent deformed reinforcing bars. The dimensions of the concrete block were chosen to be large enough to provide adequate cover for the hooked bars and to prevent the concrete block from splitting. Each concrete block contained one test bar without confining reinforcement. For specimens with a hooked bar, the straight portion of the bars was covered with a loose-fitting plastic tube so that bond was provided only by the hooked portion and the tail extension, as shown in Figure 1.7. The main variables included in the study were the bonded length measured from the beginning of the bend (1.6 to 8.5 in.), the bend angle (0° to 180° in 45° increments), the inside radius of bend (1.15 to $4.6d_b$), and bar diameter (No. 5, No. 7, and No. 9). The average concrete compressive strengths were 4,500, 5,500, and 3,300 psi for specimens containing No. 5, No. 7, and No. 9 test bars, respectively.

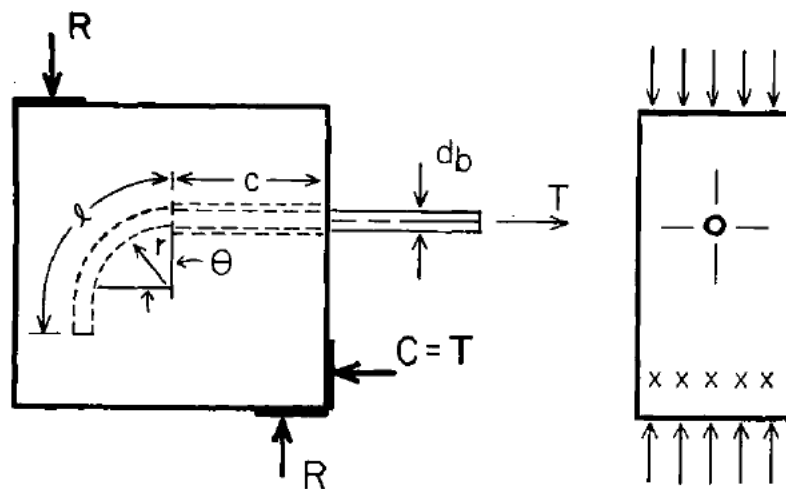


Figure 1.7 Test specimen (Minor and Jirsa 1975)

Minor and Jirsa observed that for test bars with both bent and straight sections (tail extension), most of the slip occurred in the bent portion of the bars. They also found that there was little difference in strength between the straight and bent bars for an equal bonded length, which is the length of the bar in contact with the concrete (see ℓ in Figure 1.7). It is important to note that the bonded length as defined by Minor and Jirsa is different than the development length defined by ACI 318 and ACI 408. Minor and Jirsa found that for equal bonded length to bar diameter ratios, bar slip increased as the bend angle increased and as the ratio of bend radius to bar diameter decreased. Therefore, they stated that in joint details where hooked or bent bars are required,

hooked bars with 90° bend angles were preferable to those with 180° bend angles, and the bend radius should be as large as practical to reduce the slip of the hooked bar.

1.3.1.2 Headed studs and bars

Viest (1956) tested 12 push-out specimens to study the behavior and the load-carrying capacity of stud shear connectors (headed steel studs). Each specimen (Figure 1.8) consisted of two rectangular concrete slabs ($30 \times 24 \times 7$ in.) connected to a wide flange steel beam by four or eight headed steel studs, which were welded to the steel beam. Viest found that headed steel studs could be used as shear connectors in composite concrete and steel construction. He proposed empirical equations for calculating the shear capacity of the stud shear connectors.

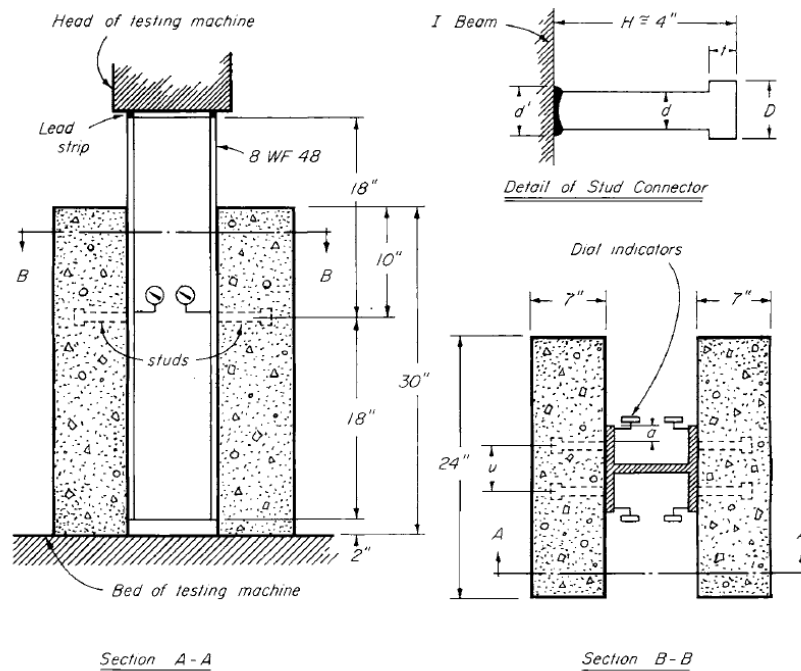


Figure 1.8 Details of push-out specimens (Viest 1956)

McMackin et al. (1973) tested 60 headed steel anchor studs embedded in twelve concrete blocks to study their behavior and strength under a variety of loading conditions. They conducted pure tension loading tests on 22 anchor studs, pure shear loading tests on 12 anchor studs, and combined shear and tension loading tests on the remaining 26 anchor studs. The main variables involved in this study were the type of concrete (normalweight or lightweight), anchor stud length (4 to 8 in.), angle of loading (0°, 30°, and 60°), and free edge distance, distance from the center of

the anchor to the edge of the concrete block, (2 to 12 in.). McMackin et al. concluded that an edge distance of at least 4 in. was required to develop the capacity of anchors with 7 in. embedment lengths loaded in pure tension.

Stoker et al. (1974) conducted pullout tests on 19 concrete blocks with 1-in. thick steel plates attached to the end of No. 11, No. 14, or No. 18 test bars to evaluate their anchorage strength. The 1-in. thick steel plates were 5 in. square, 6 in. square, and 7.5 in. square for the No. 11, No. 14, and No. 18 bars, respectively. The net bearing areas (gross area of the plate minus the nominal area of the test bar, A_b) were $15A_b$ for No. 11 and No. 14 test bars and $13A_b$ for No. 18 test bars. Stoker et al. found that an anchorage device consisting of a 1-in. thick steel plate attached to the bar allowed for the use of shorter embedment lengths than required for straight bars.

1.3.2 Simulated beam-column joints with hooked bars subjected to monotonic loading

Marques and Jirsa (1975) tested 22 exterior beam-column joint specimens to investigate the anchorage strength of hooked bars. The main variables were column axial load (135 to 540 kips), concrete side cover (1.5 to 2.875 in.), location of the hooked bars (inside or outside the column core, the region of the column cross-section confined by the column longitudinal reinforcement), and confining reinforcement within the joint (none or No. 3 hoops spaced at 2.5 or 5 in.). The tests were performed using either No. 7 or No. 11 hooked bars with 90° or 180° bends. Each specimen contained two hooked bars. The nominal concrete compressive strength was 4,500 psi. Figure 1.9 shows the type of test specimen used in this study. Marques and Jirsa found that the effect of the column axial load on the anchorage strength of hooked bars was negligible. They observed that the specimens with 90° hooked bars showed similar behavior to those with 180° hooked bars. They also found that the location of the hooked bars, inside or outside the column core, had very little influence on the anchorage strength of hooked bars. All of the specimens with hooked bars outside the column core, however, had confining reinforcement. Marques and Jirsa found that the effect of closely spaced confining reinforcement within the joints was higher in the case of large anchored hooked bars and that the reduction of the concrete side cover from 2.875 in. to 1.5 in. reduced anchorage strength.

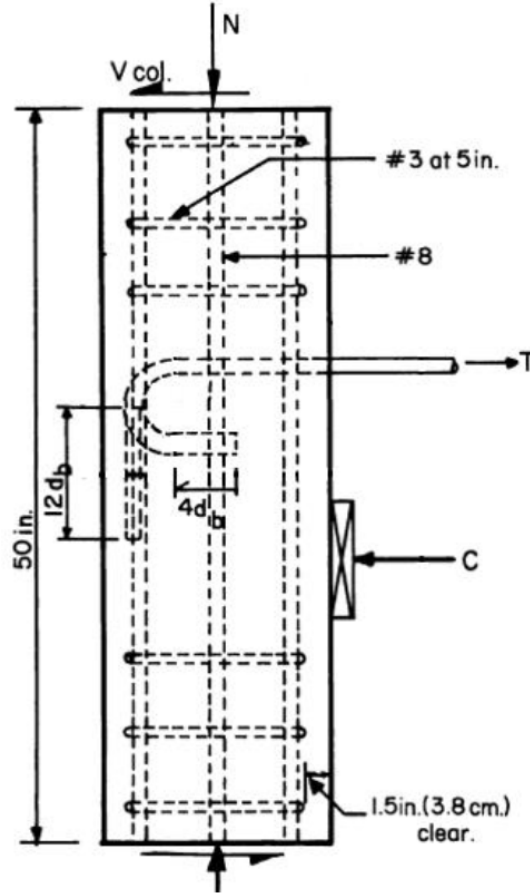


Figure 1.9 Test specimen (Marques and Jirsa 1975)

Based on the test results, Marques and Jirsa developed a design equation to calculate the anchorage strength of standard hooked bars:

$$f_h = 700(1 - 0.3d_b)\psi\sqrt{f'_c} \leq f_y \quad (1.1)$$

where f_h is the tensile stress of a hooked bar (psi); d_b is the hooked bar diameter (in.); f'_c is the concrete compressive strength (psi). ψ is equal to 1.4 if the hooked bar is No. 11 or smaller, the lead straight embedment length (the length of the straight portion of the hooked bar between the hook and the column face) is at least the greater of $4d_b$ or 4 in., the concrete side cover to the hooked bar is at least 2.5 in., and the concrete cover on the tail extension is at least 2 in; ψ equals 1.8 if there is confining reinforcement spaced at $3d_b$ or less within the joint region and the joint meets the requirements for $\psi = 1.4$.

Soroushian et al. (1988) tested seven exterior beam-column joint specimens to determine the anchorage strength and behavior of hooked bars. The main variables were hooked bar diameter

(No. 6, No. 8, and No. 10), confining reinforcement within the joint region (No. 3 hoops spaced at 3 in. or 4 in., and No. 4 hoops spaced at 3 in.), and concrete compressive strength (3,780 to 6,050 psi). Each specimen contained two 90° hooked bars; the straight embedment lengths were covered with a plastic tube to eliminate the bond of the straight portion of the bar. No axial load was applied to the specimens in this study. Soroushian et al. found that the anchorage strength (force at failure) of hooked bars increased as bar diameter increased and as the confining reinforcement within the joint region increased. Soroushian et al. also found that within the range of test variables, concrete compressive strength did not significantly affect the anchorage strength of hooked bars.

Hamad et al. (1993) tested 25 simulated exterior beam-column joint specimens to determine anchorage characteristics of uncoated and epoxy-coated hooked bars. The test setup (Figure 1.10) was similar to that used by Marques and Jirsa (1975) but without horizontal support at the top and no axial load applied to the concrete columns. Each specimen contained two hooked bars. The main variables were bar size (No. 7 and No. 11), hooked bar geometry (90° and 180° bend angles), concrete compressive strength (2,570 to 7,200 psi), concrete side cover (1.75 to 3 in.), confining reinforcement within the joint (none, No. 3 hoops spaced at 4 in. or 6 in.), and hooked bar surface condition (uncoated or epoxy-coated hooked bar).

Hamad et al. found that No. 11 hooked bars (coated and uncoated) showed more slip than No. 7 hooked bars at a given stress level. They also found that the anchorage capacity of hooked bars increased as the concrete compressive strength increased, and using the square root of concrete compressive strength was appropriate for modeling the effect of concrete strength on bond strength. The anchorage capacity of hooked bars increased as the confining reinforcement within the joint region increased. At load levels prior to failure, hooked bars with 90° bend angles were stiffer than hooked bars with 180° bend angles. Hamad et al. observed that the anchorage strength of hooked bars decreased about 8% when the concrete side cover was reduced from 3 to 1.75 in. Specimens with epoxy-coated hooked bars consistently showed lower anchorage strength than specimens with uncoated hooked bars. Hamad et al. recommended a 20 percent increase in the basic development length of an uncoated hooked bar for epoxy-coated hooked bars.

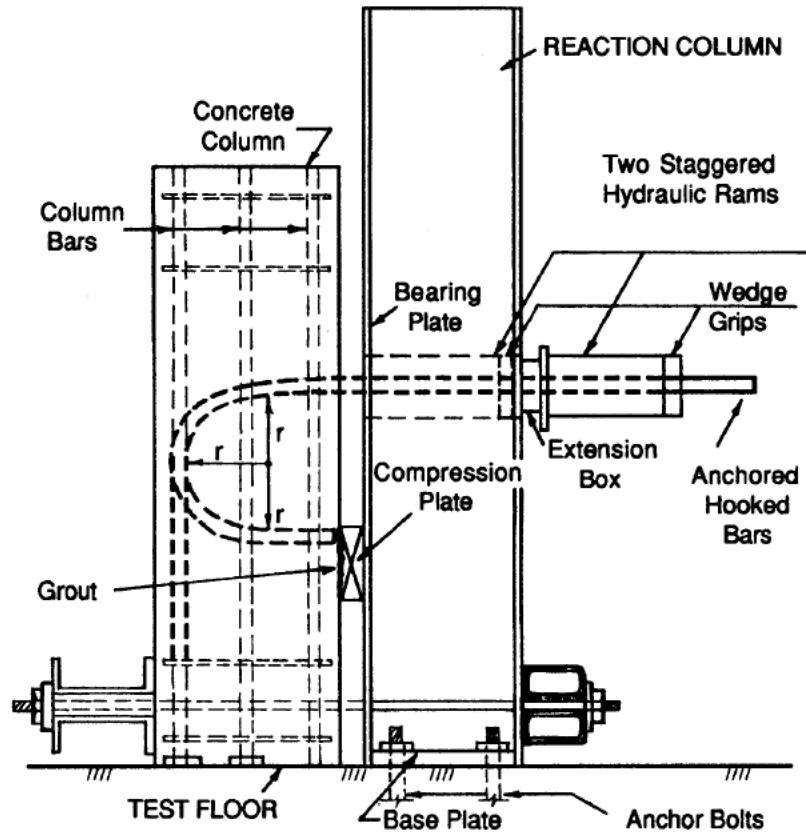


Figure 1.10 Specimen and test setup (Hamad et al. 1993)

Ramirez and Russell (2008) tested 21 exterior beam-column joint specimens to evaluate the anchorage strength of uncoated and epoxy-coated hooked bars anchored in high-strength concrete specimens. The main variables were bar size (No. 6 and No. 11), concrete compressive strength (8,910 to 16,500 psi), confining reinforcement within the joint region (none and ties spaced at $3d_b$), and tail cover (0.75 to 2.5 in.). Each specimen contained two 90° bend angle hooked bars. The test setup (Figure 1.11) was similar to that used by Marques and Jirsa (1975) and Hamad et al. 1993, except that the columns had no horizontal support at the top. No axial load was applied to these specimens.

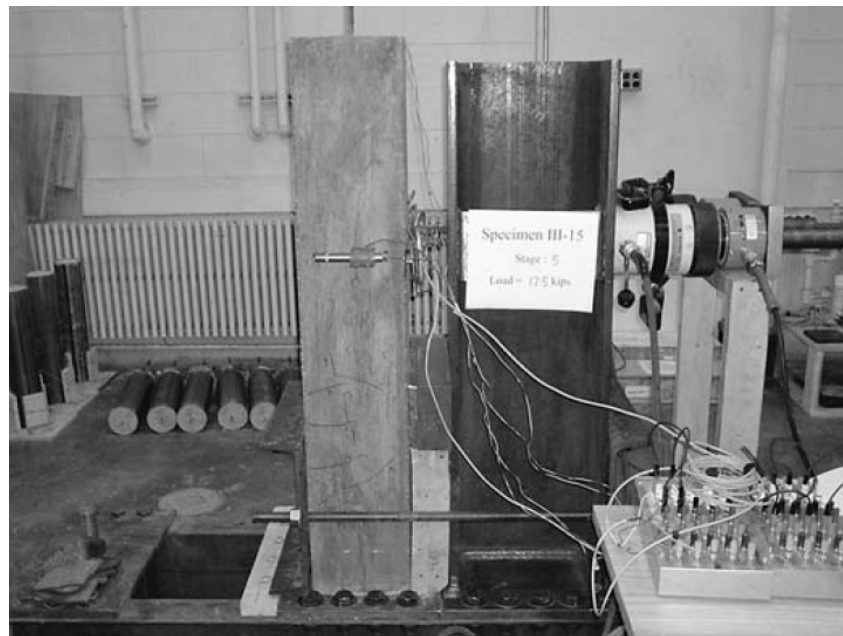
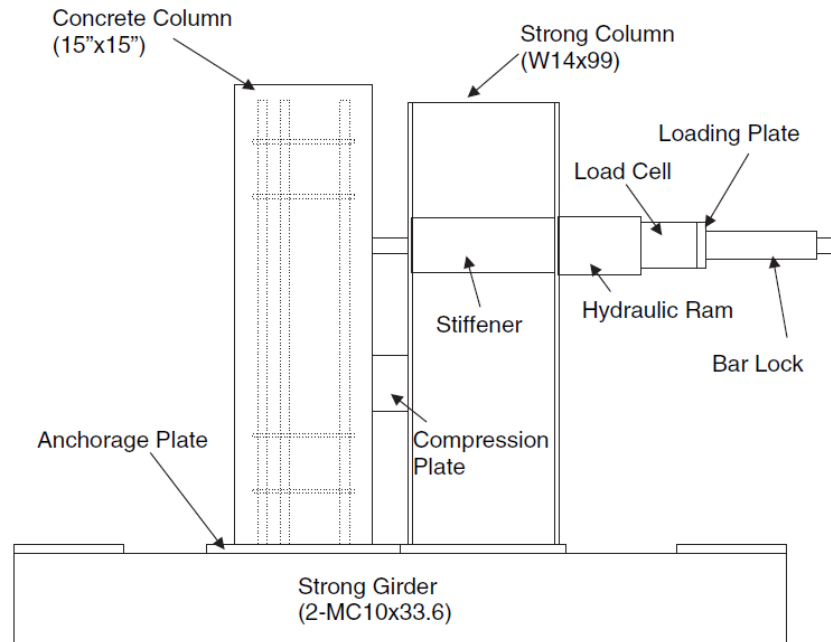


Figure 1.11 Test setup (Ramirez and Russell 2008)

Ramirez and Russell found that specimens with epoxy-coated hooked bar had lower anchorage strength than specimens with uncoated hooked bars. The presence of confining reinforcement within the joint region increased the anchorage strength of both coated and uncoated hooked bars. Ramirez and Russell concluded that the limit on the concrete compressive strength in the ACI 318-05 provisions for the anchorage of standard hooked bars could be extended up to

15,000 psi. However, they also recommended that minimum confining reinforcement spaced at $3d_b$ should be provided in high-strength concrete. Ramirez and Russell proposed that the minimum tail concrete cover of 2.5 in. be reduced to d_b if confining reinforcement is provided.

Sperry et al. (2015a, 2015b, 2017a, 2017b, 2018) tested 337 simulated exterior beam-column joint specimens to investigate the factors that affect the anchorage strength of hooked bars and to develop design guidelines for the development length of hooked bars. The main variables were the number of hooked bars in a specimen (2, 3, or 4), concrete compressive strength (4,300 to 16,510 psi), hooked bar stress at failure (22,800 to 141,600 psi), test bar size (No. 5, No. 8, and No. 11), concrete side cover (1.5 to 4 in.), confining reinforcement within the joint region (none, two No. 3 hoops, or No. 3 hoops spaced at $3d_b$), center-to-center spacing between the test bars (3 to $11d_b$), hook bend angle (90° or 180°), location of hooked bars (inside or outside the column core), and embedment length. Of the 337 beam-column joint specimens, 276 specimens contained two hooked bars, and 61 specimens included three or four hooked bars. The test setup was a modified version of the test setup used by Marques and Jirsa (1975).

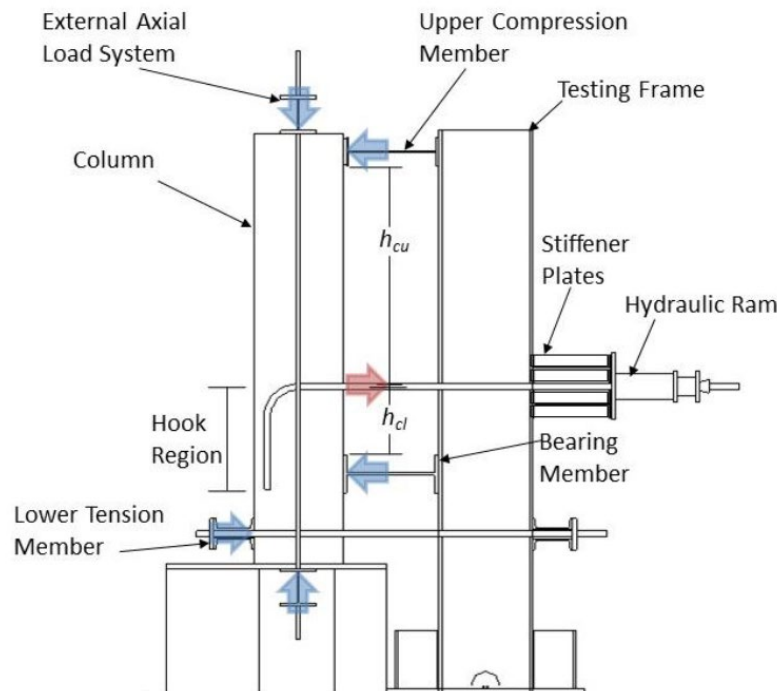


Figure 1.12 Test setup (Sperry et al. 2015a)

Sperry et al. found that the concrete contribution to the anchorage strength of hooked bars can be represented by the concrete compressive strength to the 0.29 power, instead of the square root of concrete compressive strength used in the ACI 318 provisions. Sperry et al. further found that for a given embedment length, the anchorage strength of hooked bars, expressed as a force, increases as the test bar diameter increases. The anchorage strength of hooked bars with a 90° bend was similar to that of hooks with a 180° bend. There was no effect on anchorage strength when the concrete side cover was increased from 2.5 to 3.5 in. Based on the test results, Sperry et al. (2015 a,b) developed descriptive equations, Eqs. (1.2) and (1.3), to characterize the anchorage strength of hooked bars in beam-column joints without and with confining reinforcement, respectively.

$$T_c = 332 f_{cm}^{0.29} \ell_{eh}^{1.06} d_b^{0.54} \quad (1.2)$$

$$T_h = 332 f_{cm}^{0.29} \ell_{eh}^{1.06} d_b^{0.54} + 54,250 \left(\frac{N A_{tr}}{n} \right)^{1.06} d_b^{0.59} \quad (1.3)$$

where T_c is the anchorage strength of a hooked bar without confining reinforcement (lb); T_h is the anchorage strength of a hooked bar with confining reinforcement (lb); f_{cm} is the measured concrete compressive strength (psi); ℓ_{eh} is the embedment length of hooked bar (in.); d_b is the diameter of the hooked bar (in.); N is the number of legs of effective confining reinforcement parallel to the hooked bars being developed; A_{tr} is the area of a single leg of the confining reinforcement (in²); n is the number of hooked bars. Sperry et al. (2015b) found that only confining reinforcement placed within $8d_b$ of the straight portion of the hooked bar for No. 3 through No. 8 test bars or within $10d_b$ of the straight portion of the hooked bar for No. 9 through No. 11 test bars was effective in beam-column joints.

Ajaam et al. (2017, 2018) tested 67 simulated beam-column joint specimens to expand the understanding of the behavior of hooked bars and to develop design guidelines allowing for the use of high-strength materials with special emphasis on the effects of spacing between hooked bars. The main variables were bar size (No. 5, No. 8, and No. 11), hook bend angle (90° and 180°), embedment length (5.5 to 23.5 in.), confining reinforcement within the joint region (none to nine No. 3 hoops), maximum stress in the hooked bar (22,800 to 138,800 psi), concrete compressive strength (4,490 to 14,050 psi), center-to-center spacing between the hooked bars (2 to $11.8d_b$), number of hooked bars in a specimen (2 to 6 bars), and one layer or two layers of test bars in a

specimen. The test frame was the same as that used by Sperry et al. (2015a, 2015b). Ajaam et al. analyzed their results, along with 214 test results from previous studies, and found that the contribution of concrete compressive strength to the anchorage strength of hooked bars can be represented by the concrete compressive strength to the 0.295 power, and that the anchorage strength of hooked bars increases as the amount of confining reinforcement within the joint region increases and is lower for individual closely-spaced (less than or equal to $6d_b$) hooked bars than it is for individual widely-spaced bars. Specimens with a ratio of beam effective depth to embedment length (d/ℓ_{eh}) greater than 1.5 exhibited lower anchorage strengths than those with a (d/ℓ_{eh}) ratio of less than 1.5. Based on the results of this and previous studies, Ajaam et al. developed descriptive equations, Eq. (1.4) and (1.5), to characterize the anchorage strength of hooked bars in beam-column joints for concrete compressive strengths up to 16,000 psi and hooked bar stresses up to 120,000 psi, respectively, without and with confining reinforcement:

$$T_c = \left(294 f_{cm}^{0.295} \ell_{eh}^{1.0845} d_b^{0.47} \right) \left(0.0974 \frac{c_{ch}}{d_b} + 0.3911 \right) \quad (1.4)$$

$$\text{with } \left(0.0974 \frac{c_{ch}}{d_b} + 0.3911 \right) \leq 1.0$$

$$T_h = \left(294 f_{cm}^{0.295} \ell_{eh}^{1.0845} d_b^{0.47} + 55050 \left(\frac{A_{th}}{n} \right)^{1.0175} d_b^{0.73} \right) \left(0.0516 \frac{c_{ch}}{d_b} + 0.6572 \right) \quad (1.5)$$

$$\text{with } \left(0.0516 \frac{c_{ch}}{d_b} + 0.6572 \right) \leq 1.0$$

where T_c is the anchorage strength of a hooked bar without confining reinforcement (lb); T_h is the anchorage strength of a hooked bar with confining reinforcement (lb); f_{cm} is the measured concrete compressive strength (psi); ℓ_{eh} is the embedment length of hooked bar (in.); d_b is the diameter of the hooked bar (in.); c_{ch} is the center-to-center spacing between hooked bars (in.); A_{th} is the total cross-sectional area of all parallel confining reinforcement located within $8d_b$ of the top or bottom of the test bars for No. 3 through No. 8 hooked bars or within $10d_b$ for No. 9 through No. 11 hooked bars (in.²); and n is the number of hooked bars.

Based on their study, Ajaam et al. (2017) recommended design provisions for hooked bars, with ℓ_{dh} (incorporating a strength reduction, ϕ , factor of 0.81) based on the bar diameter d_b to the 1.5 power and the concrete compressive strength f'_c to the 0.25 power.

$$\ell_{dh} = 0.003 \frac{f_y \Psi_e \Psi_{cs} \Psi_o}{\lambda f_c^{0.25}} d_b^{1.5} \quad (1.6)$$

where Ψ_e is the epoxy coating factor, equal to 1.2 for epoxy-coated or zinc and epoxy dual-coated reinforcement and 1.0 for uncoated or zinc-coated (galvanized) reinforcement; Ψ_o equals 1.0 for hooked bars terminating inside a column core with clear side cover to the bar ≥ 2.5 in., or terminating in a supporting member with side cover to the bar $\geq 6d_b$; in other cases, Ψ_o is taken as 1.25. Ψ_{cs} is confining reinforcement and spacing factor, calculated using Table 1.1.

Table 1.1 Modification factor Ψ_{cs} for confining reinforcement and spacing ^[1]

Confinement level	f_y	C_{ch}	
		$2d_b$	$\geq 6d_b$
$\frac{A_{th}}{A_{hs}} \geq 0.2$ ^[2] or $\frac{A_{th}}{A_{hs}} \geq 0.4$ ^[3]	60,000	0.6	0.5
	120,000	0.66	0.55
No confining reinforcement	all	1.0	0.6

^[1] Ψ_{cs} may be linearly interpolated for spacing or yield strengths not listed

^[2] Confining reinforcement parallel to straight portion of bar

^[3] Confining reinforcement perpendicular to straight portion of bar

Yasso et al. (2017, 2021) examined a subset of 195 specimens from those reported by Sperry et al. (2015a, 2015b) to investigate the effects of concrete tail cover and tail kickout on the anchorage strength of 90-degree hooked bars. The main variables were concrete tail cover (0.75 to 3.625 in.), concrete compressive strength (4,490 to 16,180 psi), hooked bar stresses at failure (33,000 to 141,000 psi), test bar size (No. 5, No. 8, and No. 11), confining reinforcement within the joint region (none to six No. 3 hoops), and location of hooked bars (inside or outside the column core). All specimens contained two hooked bars. Of the 195 beam-column joint specimens, 167 had hooked bars placed inside the column core, 113 with confining reinforcement within the joint region and 54 without. Twenty-eight specimens had the hooked bars placed outside the column core, 14 with confining reinforcement within the joint region and 14 without. Yasso et al. observed that tail kickout occurred for approximately 7% of the specimens used in the analysis and was only observed in conjunction with other failure modes, with the likelihood of tail kickout increasing as

confining reinforcement within the joint region decreased, as the hooked bar size increased, and for hooked bars placed outside the column core. The anchorage strength of hooked bars was not affected by hook tail covers as low as 0.75 in. or by tail kickout at failure.

1.3.3 Beam-column joints with hooked bars subjected to reversed cyclic loading

This study includes an analysis of the results of 146 exterior beam-column joint specimens containing hooked bars tested under reversed cyclic loading by Hanson and Connor (1967), Hanson (1971), Megget (1974), Uzumeri (1977), Lee et al. (1977), Scribner (1978), Paulay and Scarpas (1981), Ehsani and Wight (1982), Kanada et al. (1984), Zerbe and Durrani (1985), Ehsani et al. (1987), Ehsani and Alameddine (1991), Kaku and Asakusa (1991), Tsonos et al. (1992), Pantelides et al. (2002), Chutarat and Aboutaha (2003), Hwang et al. (2005), Lee and Ko (2007), Chun et al. (2007), Tsonos (2007), Kang et al. (2010), Chun and Shin (2014), Hwang et al. (2014), and Choi and Bae (2019). A summary of these studies is presented in this section, and complete details are presented in Appendix D.

The main variables used in these studies were embedment length (6 to 21 in.), concrete compressive strength (3,140 to 13,700 psi), center-to-center spacing between the hooked bars (1.75 to 6.5 in.), bar size (No. 3 to No. 9), and confining reinforcement within the joint region. In addition, Hanson (1971), Uzumeri (1977), and Zerbe and Durrani (1985) studied the effect of transverse beams (beams perpendicular to the test beam at the joint) and slabs on the performance of beam-column joints. Of the 146 beam-column joint specimens, 3 contained transverse beams and slabs, and 6 had only transverse beams. The yield strength of the hooked bars ranged from 42,900 to 103,000 psi. Concrete side cover ranged from 0.7 to 8.6 in. Deformed confining reinforcement within the joint region, parallel to the straight portion of the hooked bars, ranged from none to 8 hoops, and the area of a single leg of a hoop ranged from 0.078 to 0.31 in.², with the exception of two studies (Kaku and Asakusa 1991, Tsonos 2007), which used plain round steel bars as confining reinforcement within the joint region with an area of a single leg ranging from 0.011 to 0.044 in.². Of the 146 specimens, 14 had no confining reinforcement within the joint region. Column axial compressive load applied during the test ranged from zero to $0.25A_gf'_c$, where A_g is the column cross-sectional area (in.²) and f'_c is the nominal concrete compressive

strength (psi). Of the 146 specimens, 11 specimens had $M_R \leq 1.2$, and 135 specimens had $M_R \geq 1.2$, where M_R is a ratio of the flexural strength of the column to the flexural strength of the beam. In accordance with Section 4.4.2 of ACI 352R-02 for connections that are subjected to reversed cyclic loading, the flexural strength of the column should be at least 20 percent greater than the flexural strength of the beam to produce flexural hinging in the beams rather than in the columns. Therefore, only specimens with $M_R \geq 1.2$ were used in this analysis.

The test results showed that 120 out of the 135 beam-column joint specimens with $M_R \geq 1.2$ performed satisfactorily under reversed cyclic loading, attaining a peak moment 1 to 45% greater than the nominal flexural strength of the beam anchored at the joint using hooked bars. Of the 120 specimens, 108 exhibited less than a 20% reduction in peak load at 3.5% drift, indicating a satisfactory level of performance, and the remaining specimens exhibited less than a 20% reduction in peak load at a drift less than 3.5% (1.1 to 3.0%). The peak moment of the remaining 15 specimens was less than the nominal flexural strength. A detailed description of the performance of these specimens is presented in Appendix D.

1.3.4 Simulated beam-column joints with headed bars subjected to monotonic loading

Bashandy (1996) tested 32 simulated exterior beam-column joint specimens to evaluate the effects of head size (ranging from 2 to $7.1A_b$), head aspect ratio and orientation (the ratio between the vertical and horizontal dimensions of the head based on orientation relative to the concrete surface), anchored bar size (No. 8 and No. 11), embedment length (8.5 to 17 in.), side cover to the headed bar (1.5 and 3 in.), and confining reinforcement within the joint region (no ties or No. 3 ties spaced at 2 in. or 4 in.) on the anchorage strength of headed bars. The column width was 12 in., while the depth depended on the embedment length of the headed bars. Each specimen contained two headed bars with a spacing that depended on the concrete side cover. The concrete compressive strength ranged from 3,200 to 5,800 psi. Figure 1.13 shows the test setup used by Bashandy.

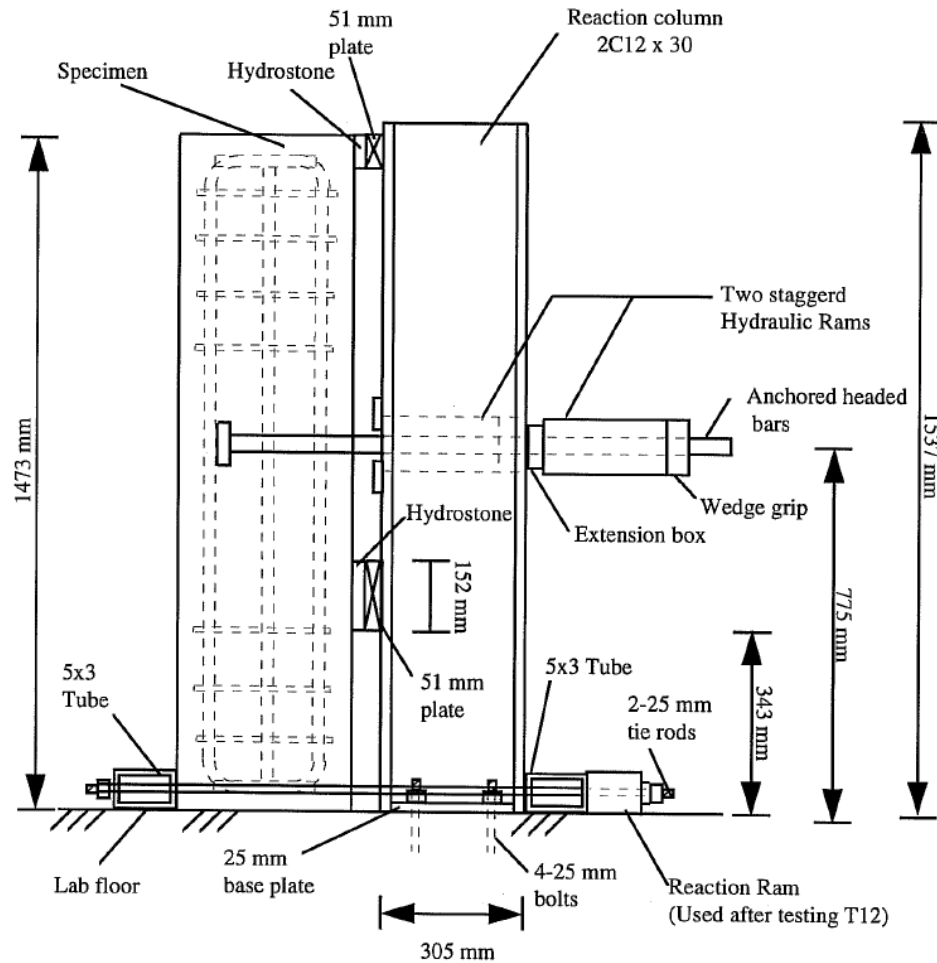


Figure 1.13 Test Setup (Bashandy 1996)

Bashandy divided the test specimens into two major groups depending on the mode of failure. Eighteen specimens failed in a mode referred to as side blowout, characterized by spalling of concrete side cover. This failure mode was a function of embedment length, head dimensions, confining reinforcement, and concrete side cover. The remaining fourteen specimens failed in shear. This failure mode was a function of the embedment depth and shear reinforcement. Bashandy found that the anchorage capacity of the headed bars increased as embedment length, head size, and confining reinforcement within the joint region increased. The effects of aspect ratio, head orientation, and bar diameter on the anchorage capacity of headed bars were insignificant.

Chun et al. (2009) tested 30 exterior beam-column joint specimens to measure the anchorage strength of hooked and headed bars. The main variables were the anchorage configuration (headed bar or 90-degree hooked bar), bar size (No. 8, No. 11, or No. 18), and

embedment length (6.3 to 35.7 in.). The specimens were tested in a horizontal position, as shown in Figure 1.14. No axial load was applied to the columns during the test. Each specimen contained a single hooked or headed bar without confining reinforcement in the joint region. The column depth was fixed for each bar size, and the ratio of the embedment length to column depth was 0.5, 0.7, and 0.9 for No. 8, No. 11, and No. 18 bars, respectively. Two types of failure, concrete breakout and joint shear, were observed in this study. In a concrete breakout failure, diagonal cracks radiating from both sides of the head and a concrete cone was formed and pulled out with the bar, as shown in Figure 1.15a. In a joint shear failure, a diagonal crack formed within the joint and extended to the other column side, as shown in Figures 1.15b and c. Chun et al. compared the test results of headed bar specimens with the models proposed by Thompson et al. (2006), Bashandy (1996), and DeVries (1996). Chun et al. found that the existing models were not suitable for predicting the contribution of the concrete to the anchorage strength of a single headed bar. Therefore, based on the experimental results of this study, Chun et al. developed a new model to predict the anchorage strength of headed bars in exterior beam-column joints. Chun et al. concluded that the anchorage strength of a headed bar results from a combination of bearing on the head and bond along the bar. Chun et al. also found that the anchorage strength of headed bars increased as the embedment length increased.

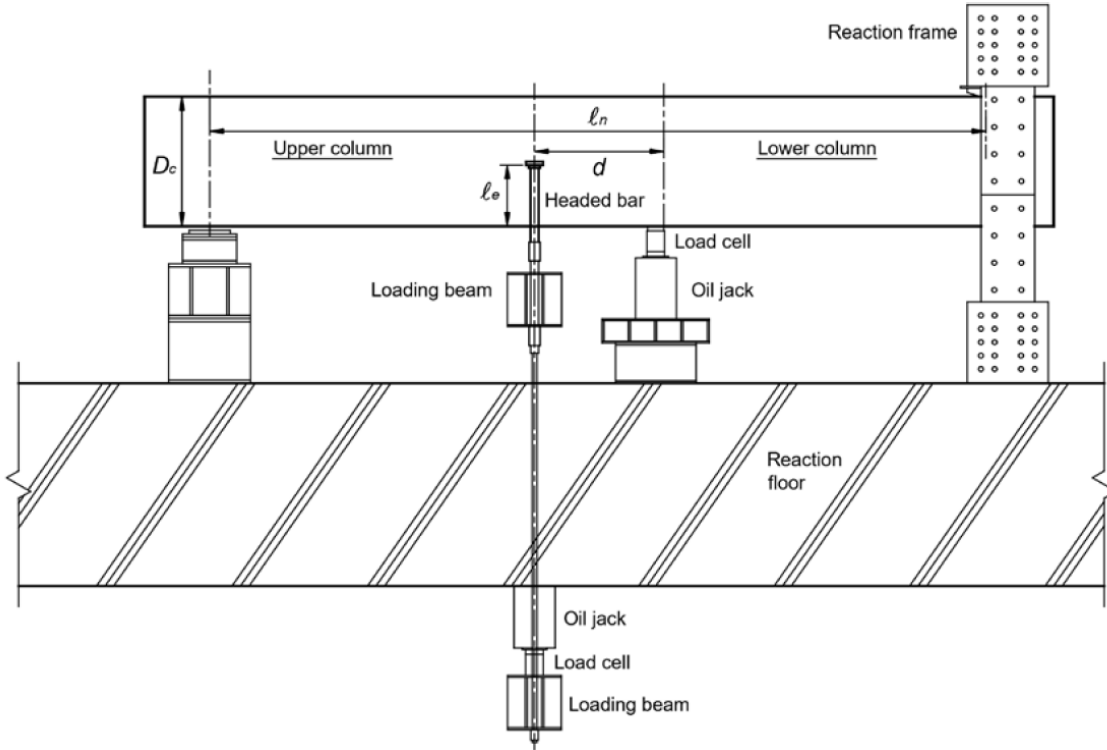


Figure 1.14 Test setup (Chun et al. 2009)

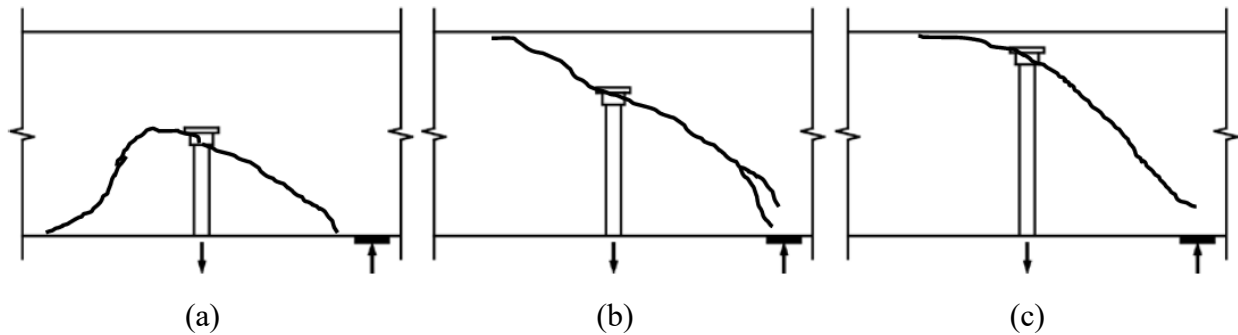


Figure 1.15 Failure modes: (a) concrete breakout, (b) and (c) joint shear failure (Chun et al. 2009)

Shao et al. (2016) and Ghimire et al. (2019a, 2019b) tested 202 simulated exterior beam-column joint specimens to investigate the anchorage strength of headed bars. The main variables were embedment length (4 to 19.25 in.), confining reinforcement within the joint region (no confining reinforcement, two No. 3 hoops, or No. 3 hoops spaced at $3d_b$, where d_b is the bar diameter), concrete compressive strength (3,960 to 16,030 psi), bar size (No. 5, No. 8, and No. 11), head size (the net bearing area from 3.8 to $14.9A_b$, where A_b is bar area), test bar stresses at failure (26,100 to 153,200 psi), number of test bars in a specimen (2, 3, or 4 bars), center-to-center spacing between the test bars (3 to $11.8d_b$), and concrete side cover to the test bar (2.5 to 4 in.).

The test frame (Figure 1.16) was the same as that used by Sperry et al. (2015a, 2015b) and Ajaam et al. (2017).

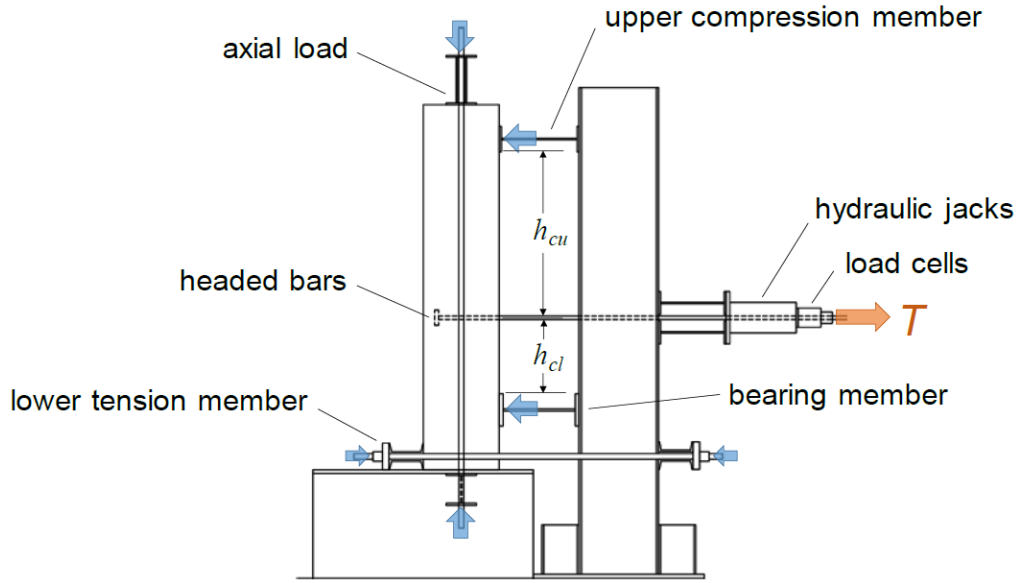


Figure 1.16 Test Frame (Shao et al. 2016)

Shao et al. (2016) and Ghimire et al. (2019 a, 2019b) found that the contribution of concrete to the anchorage strength of a headed bar is more accurately represented by the compressive strength of the concrete to the 0.24 power, instead of the square root of the compressive strength, as used in ACI 318. Shao et al. (2016) and Ghimire et al. (2019a, 2019b) observed that the anchorage strength of headed bars increased as the confining reinforcement parallel to the bars increased and that the strength increase was proportional to the amount of confining reinforcement per headed bar. They also found that the headed bars with bearing areas between 12.9 and $14.9A_b$ provided higher anchorage strengths than those with bearing areas between 3.8 and $9.5A_b$. Based on the results of the study, Shao et al. developed descriptive equations for concrete compressive strengths up to 16,000 psi and headed bar stresses up to 120,000 psi for headed bars without and with confining reinforcement shown, respectively, in Eq. (1.7) and (1.8).

$$T_c = \left(781 f_{cm}^{0.24} \ell_{eh}^{1.03} d_b^{0.35} \right) \left(0.0836 \frac{s}{d_b} + 0.3444 \right) \quad (1.7)$$

with $0.0836 \frac{s}{d_b} + 0.3444 \leq 1.0$, and

$$T_h = \left(781 f_{cm}^{0.24} \ell_{eh}^{1.03} d_b^{0.35} + 48,800 \frac{A_{tr}}{n} d_b^{0.88} \right) \left(0.0622 \frac{s}{d_b} + 0.5428 \right) \quad (1.8)$$

with $0.0622 \frac{s}{d_b} + 0.5428 \leq 1.0$ and $\frac{A_{tr}}{n} \leq 0.3 A_b$

where T_c is the anchorage strength of a headed bar without confining reinforcement (lb); T_h is the anchorage strength of a headed bar with confining reinforcement (lb); f_{cm} is the measured concrete compressive strength (psi); ℓ_{eh} is the embedment length (in.); d_b is the diameter of the headed bar (in.); s is the center-to-center spacing between the bars (in.); A_{tr} is the total cross-sectional area of effective confining reinforcement (NA_{tr}) parallel to the headed bars being developed (in.²); N is the number of legs of effective confining reinforcement parallel to the headed bars being developed; A_{tr} is the area of a single leg of the confining reinforcement (in.²); n is the number of headed bars in tension; A_b is the area of the headed bar (in.²).

Based on their study, Shao et al. (2016) recommended design provisions for headed bars, with ℓ_{dt} (incorporating a strength reduction, ϕ , factor of 0.833) based on the bar diameter d_b to the 1.5 power and the concrete compressive strength f'_c to the 0.25 power.

$$\ell_{dt} = \left(0.0024 \frac{f_y \psi_e \psi_{cs} \psi_o}{f_c'^{0.25}} \right) d_b^{1.5} \quad (1.9)$$

where ψ_e is the epoxy coating factor, equal to 1.2 for epoxy-coated or zinc and epoxy dual-coated reinforcement and 1.0 for uncoated or zinc-coated (galvanized) reinforcement; ψ_o equals 1.0 for headed bars terminating inside a column core with clear side cover to the bar ≥ 2.5 in., or terminating in a supporting member with side cover to the bar $\geq 8d_b$; in other cases, ψ_o is taken as 1.25. ψ_{cs} is confining reinforcement and spacing factor, calculated using Table 1.2.

Table 1.2 Modification factor ψ_{cs} for confining reinforcement and spacing ^[1]

Confinement level	f_y	s	
		$2d_b$	$\geq 8d_b$
$\frac{A_{tr}}{A_{hs}} \geq 0.3$	$\leq 60,000$	0.6	0.4
	120,000	0.7	0.45
No confining reinforcement	all	1.0	0.5

^[1] ψ_{cs} is permitted to be linearly interpolated for values of A_{tr}/A_{hs} between 0 and 0.3 and for spacing s or yield strength of headed bar f_y intermediate to those in the table

1.3.5 Headed bars in slab specimens

DeVries et al. (1999) tested three concrete slab specimens containing three to 11 headed reinforcing bars each (for a total of 18 test bars) embedded in concrete slabs to investigate the effects of several variables on the anchorage capacity and behavior of headed bars. The slabs (Figure 1.17) had dimensions of $5 \times 9 \times 1.75$ ft. The test bars were spaced at a center-to-center distance of at least three times the embedment length of the headed bars to avoid an overlap of the anticipated failure region. The bars were tested individually in tension until failure. The main variables were embedment length (1.375 to 9 in.), bonded length (length along the deformed bar in contact with concrete as shown in Figure 1.18, ranging from 0 to 9 in.), concrete cover to the bar (1.6 to 17.6 in.), bar size (No. 6, No. 8, and No. 11), head size (net bearing area 4.7 to $7.4A_b$), head aspect ratio (the ratio of the largest to the smallest dimension of the head, ranging from 1 to 2), concrete compressive strength (3,920 to 12,040 psi), and transverse reinforcement (of the 18 tests, four had two No. 3 bars as transverse reinforcement perpendicular to the headed bar, distributed evenly along the embedment length, as shown in Figure 1.19, and the other 14 had none). The nominal yield strength of the headed bars was 72,000 psi. Fourteen of the headed bars were unbonded along the embedment length using a PVC pipe, as shown in Figure 1.18a. Four headed bars with embedment lengths equal to 9 in. were bonded, as shown in Figure 1.18b. During the test, the bearing reactions (support plates) were placed at least two times the embedment length away from the headed bars, outside the anticipated failure region, as shown in Figure 1.17, to limit the effect of the bearing reaction on the anchorage strength of the bars.

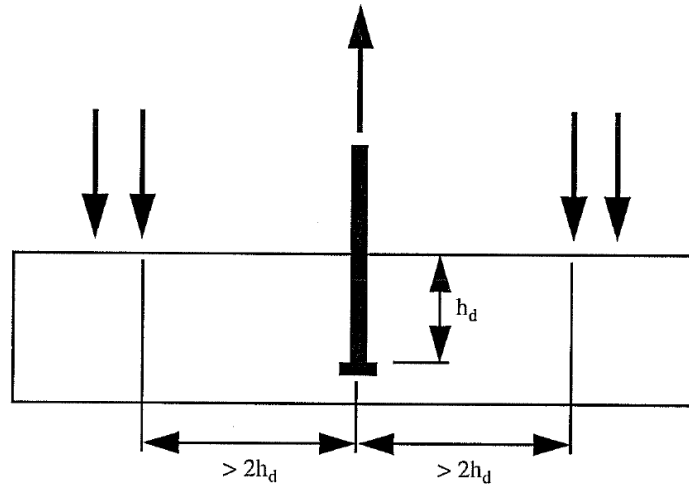


Figure 1.17 Test setup (DeVries et al. 1999)

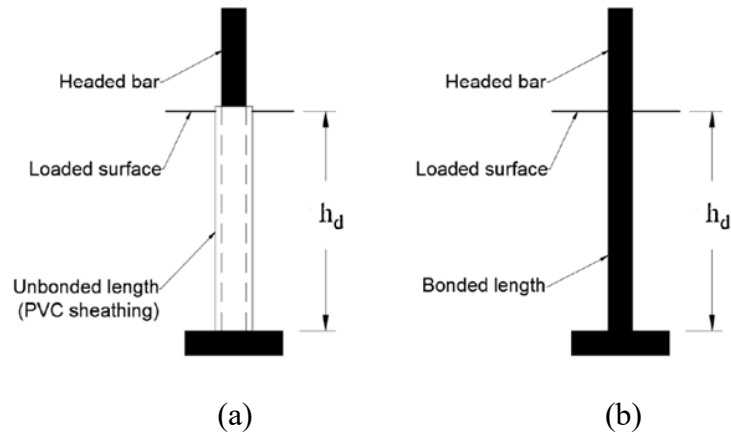


Figure 1.18 Headed reinforcing bars (a) unbonded and (b) bonded embedment length (DeVries et al. 1999)

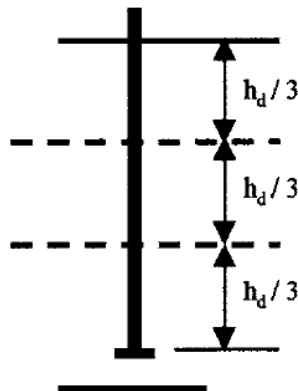


Figure 1.19 Transverse reinforcement configuration (DeVries et al. 1999)

DeVries et al. observed two types of failure – concrete breakout and fracture of the test bar. The three bars that fractured before a concrete breakout occurred were excluded from their analysis. Concrete breakout failures were sudden, and the load carried by the test bar dropped to zero instantly; no cracking was observed before failure – even for the bonded specimens. DeVries et al. observed that the size of the pullout cone (concrete breaking out with headed bar) increased as the edge distance, head size, and embedment length increased. DeVries et al. found that the anchorage strength of headed bars increased and the slip of the head prior to failure decreased as the embedment length and the edge distance were increased. They also found that transverse reinforcement placed perpendicular to the headed bar did not affect the anchorage strength of the headed bar. Lastly, they observed that the anchorage strength of headed bars was not affected by changing the aspect ratio of the head.

Choi et al. (2002) conducted 16 tests on headed bars anchored in slabs (Figure 1.20) to investigate the anchorage strength and behavior of headed bars. The main variables were concrete compressive strength (3,930 to 5,270 psi), bar size (No. 5 to No. 9), embedment length (4.4 to 13.7 in.), and concrete cover to the bar (1.6 to 35 in.). Two test configurations were used for slab specimens. In the first configuration, the headed bar was anchored in the middle of the concrete slab so that the concrete breakout failure region was not affected by the test support reactions. In this configuration, the distance measured from the surface of the headed bar to the edge of the slab was greater than two times the embedment length of the bar, as shown in Figure 1.20. In the second configuration, the headed bar was anchored close to the slab boundaries to study the effect of edge distance on the anchorage strength of headed bars. In this configuration, the concrete cover to the bar ranged from 1.6 to 4.9 in. Headed bars anchored in slab specimens were tested one at a time. Choi et al. (2002) found that the anchorage strength of headed bars decreased as the edge distance decreased.

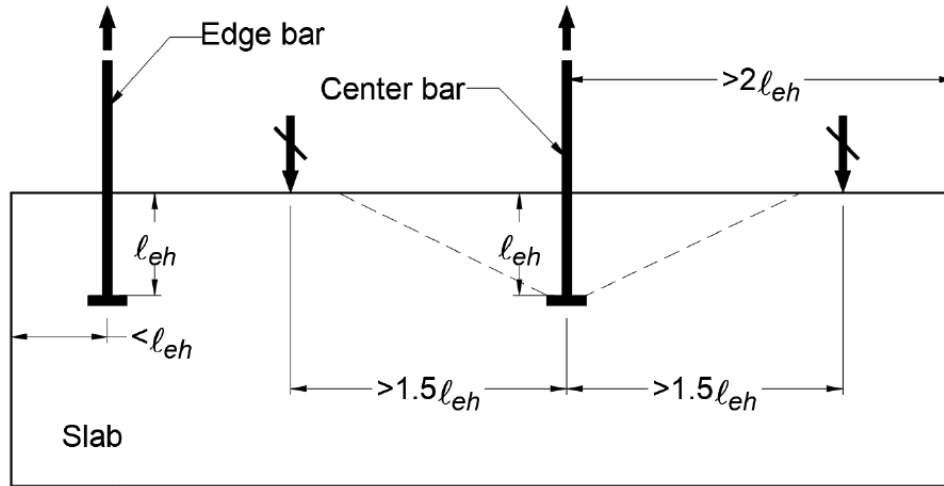


Figure 1.20 Slab specimens (Choi et al. 2002)

1.4 CONCRETE CAPACITY DESIGN METHOD

Fuchs et al. (1995) presented a new method, Concrete Capacity Design (CCD), to predict the concrete failure load of anchor bolts and headed studs embedded in uncracked concrete. The CCD method is the basis for the equations in Sections 17.6.2.1 through 17.6.2.4 of ACI 318-19, calculating the concrete breakout strength of a single anchor or an anchor group. The main variables included the use of single anchors away from and close to the edge of the concrete, anchor groups, and tension loading. The CCD method is an adapted version of the so-called Kappa Method (K-method), which was developed at the University of Stuttgart (Eligehausen et al. 1987), with an assumed breakout failure surface angle of approximately 35 degrees. The CCD method is based on a physical model in which the tension force on an anchor bolt or headed stud is resisted by the stress distributed in the concrete over a failure area. Fuchs et al. assumed that the concrete failure surface of an individual anchor is a pyramid with a base length equal to three times the embedment length and a height equal to the embedment length, as shown in Figure 1.21.

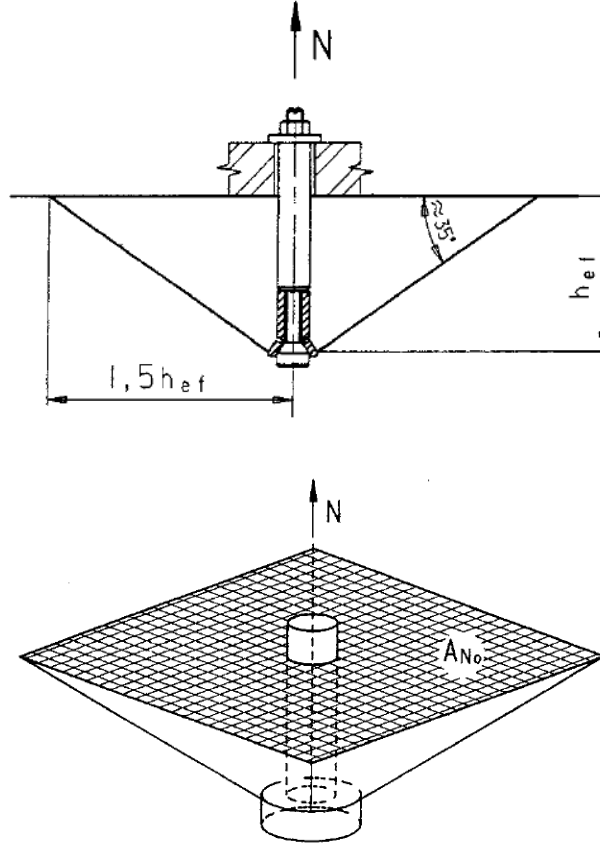


Figure 1.21 CCD idealized concrete cone for an individual anchor (Fuchs et al. 1995)

The concrete cone failure load of a single anchor bolt or headed stud in uncracked concrete unaffected by close spacing of adjacent anchors or edge influences can be represented by a best fit equation:

$$N_{no} = k_{nc} \cdot \sqrt{f'_c} \cdot h_{ef}^{1.5} \quad (1.10)$$

where N_{no} is the concrete cone failure load of a single anchor (lb), k_{nc} is a calibration factor equal to 40 for cast-in headed studs and headed anchor bolts in uncracked concrete, f'_c is the concrete compressive strength (psi), and h_{ef} is the embedment length (in.).

When an anchor bolt is placed close to an edge or corner, the concrete failure area is less than the area assumed for Eq. (1.10), and the anchor's resulting failure load is also reduced. This scenario is also true for anchor groups spaced so closely that the concrete breakout cones overlap. To take into account the reduction in the concrete failure area, N_{no} [Eq. (1.10)] is multiplied by the ratio of the available concrete failure area and the concrete failure area for an individual anchor placed away from an edge and a modification factor Ψ_1 , as shown in Eq. (1.11).

$$N_n = \frac{A_N}{A_{No}} \cdot \psi_1 \cdot N_{no} \quad (1.11)$$

where A_N is the actual projected area at the concrete surface (in.²); A_{No} is the assumed projected area of an individual anchor uninfluenced by edge effects (Figure 1.22), equal to $9h_{ef}^2$; ψ_1 is a modification factor for edge effects for single or anchor groups, equal to 1.0 if the smallest side cover distance is at least $1.5h_{ef}$; otherwise, ψ_1 is equal to $0.7 + 0.3(c_1 / 1.5h_{ef})$, where c_1 is the smallest distance between the center of an anchor and the edge of the concrete (in.).

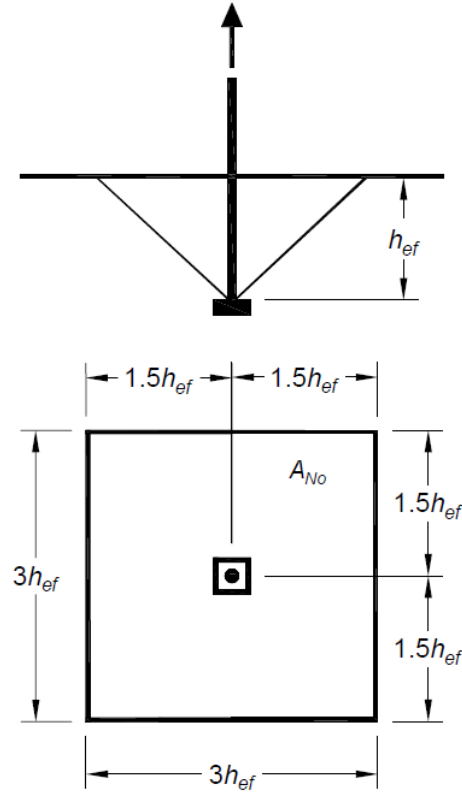
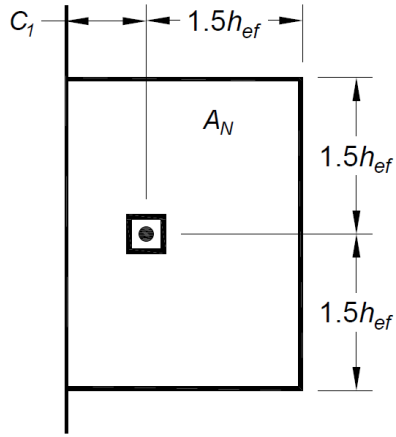


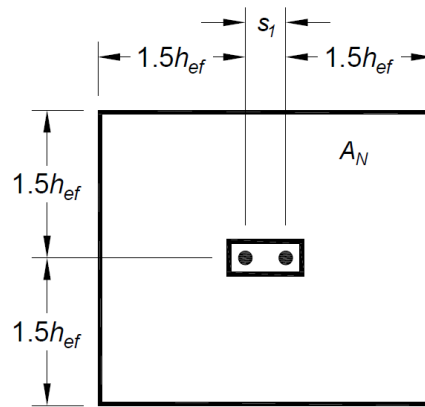
Figure 1.22 Projected area of an individual anchor according to the CCD method (Fuchs et al. 1995)

Fuchs et al. proposed examples for calculating the projected areas, A_N , in accordance with the CCD method shown in Figure 1.23.



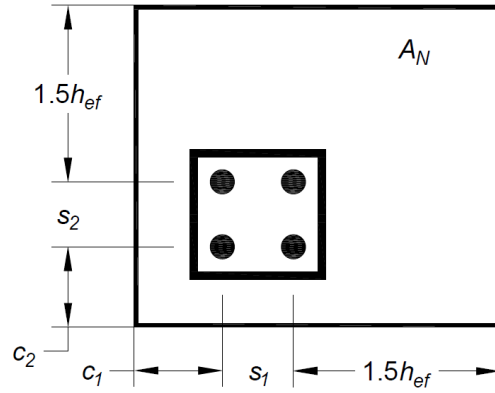
$$A_N = (c_1 + 1.5h_{ef}) \times (2 \times 1.5h_{ef})$$

$$c_1 < 1.5h_{ef}$$



$$A_N = (2 \times 1.5h_{ef} + s_1) \times (2 \times 1.5h_{ef})$$

$$s_1 < 3h_{ef}$$



$$A_N = (c_1 + s_1 + 1.5h_{ef}) \times (c_2 + s_2 + 1.5h_{ef})$$

$$c_1, c_2 < 1.5h_{ef}$$

$$s_1, s_2 < 3h_{ef}$$

Figure 1.23 Calculation of the projected area, A_N , according to the CCD method (Fuchs et al. 1995)

Fuchs et al. developed Eq. (1.11) based on the assumption that the anchor groups are loaded concentrically in tension. However, if the anchor group is loaded eccentrically in tension, the applied resultant tensile load is not shared equally by the anchors. Fuchs et al. added another modification factor to Eq. (1.11) to consider the eccentricity of the applied resultant tensile load, as shown in Eq. (1.12).

$$N_n = \frac{A_N}{A_{No}} \cdot \psi_1 \cdot \psi_2 \cdot N_{no} \quad (1.12)$$

where ψ_2 is a modification factor for anchor groups loaded eccentrically in tension, equal to $\frac{1}{1 + 2e'_N / (3h_{ef})} \leq 1$, where e'_N is the distance between the resultant tensile load on a group of anchors loaded in tension and the centroid of the group of anchors loaded in tension (in.).

The CCD method does not take into account the effect of the parallel tie reinforcement on the concrete failure load of the anchor bolts. The CCD method also applies to expansion anchors embedded in plain concrete, as well as anchor bolts and headed studs.

Nilforoush et al. (2017) tested 19 single cast-in-place headed anchors in plain and steel fiber-reinforced normal- and high-strength concrete specimens to investigate anchorage capacity

and behavior of headed anchors and to evaluate the Concrete Capacity Design (CCD) method. The main variables were concrete compressive strength, use of steel fibers, and concrete member thickness. The concrete slabs had plan dimensions of 51×51 in. and depths ranging from 13 to 26 in. The yield strength of the anchors was 130 ksi, and concrete compressive strengths ranged from 5,650 to 11,890 psi. Each specimen contained a single anchor placed at the center of the slab with an embedment length of 8.5 in. The test setup used is shown in Figure 1.24.

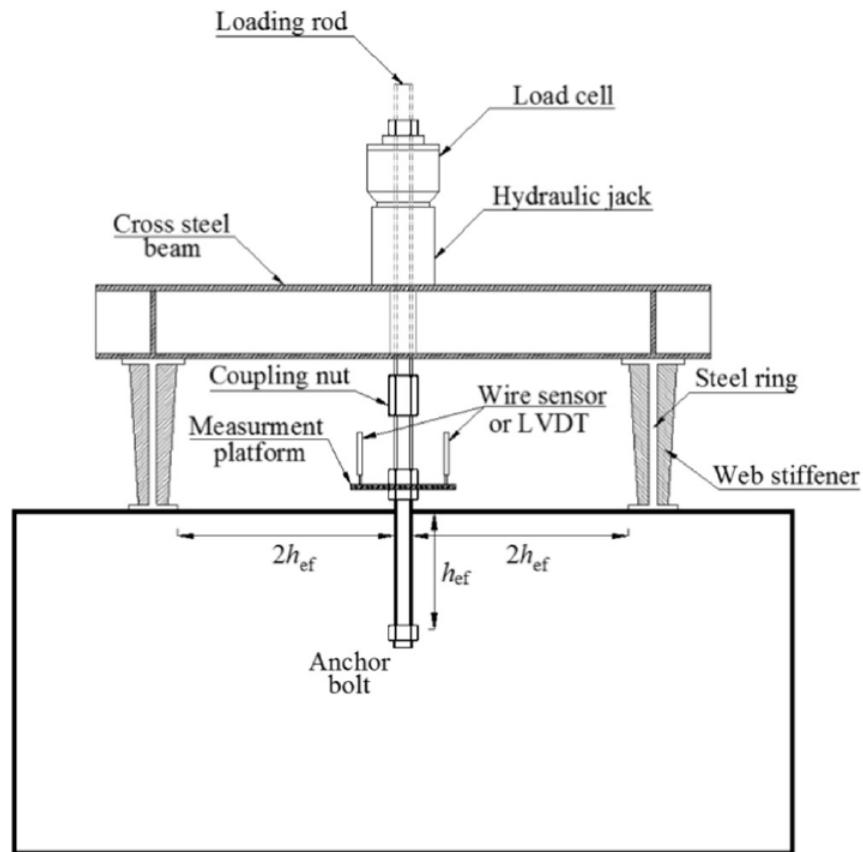


Figure 1.24 Test setup (Nilforoush et al. 2017)

Nilforoush et al. found that the capacity of the headed anchors increased as the concrete member thickness and concrete compressive strength increased. They also found that the anchorage capacity of headed anchors significantly increased when steel fibers were used in the concrete mixture. Nilforoush et al. concluded that the CCD method underestimates the anchorage capacity of headed anchors in steel-fiber reinforced concrete.

1.5 UNIVERSITY OF KANSAS - SIMULATED COLUMN-FOUNDATION JOINTS

Ghimire et al. (2018) tested 32 headed bars anchored in simulated column-foundation joints (represented by headed bars anchored in slab specimens) to study the anchorage capacity and behavior of headed bars in tension. The test bars were embedded in a concrete slab simulating column foundation reinforcement, as shown in Figures 1.26 and 1.27. The main variables were the head size (net bearing area 4 to 15 times the bar area), embedment length (6 to 8.5 in.) ℓ_{eh} , reinforcement in a plane perpendicular to the test bars, and concrete compressive strength (4,200 to 8,620 psi). Stresses in the headed bars at failure ranged from 49,500 to 117,000 psi. The concrete slab specimens contained 2 or 3 test bars, which were tested one at a time. The slab specimens were tested in two groups, each with a different test configuration; the first group had one of the support plates located close to the test bar, while the other support plate was located far away from the test bar, as shown in Figure 1.25. This test configuration was intended to simulate loading conditions of a column subjected to an overturning moment, with the reaction support plate nearest to the test bar representing the compression zone of the column and the test bar representing anchored tension reinforcement. The other reaction support plate was placed far away from the test bar to avoid interference with the concrete breakout failure surface. In the second group, both support plates were located outside the anticipated failure region, as shown in Figure 1.26. The anticipated failure region was equal to $1.5\ell_{eh}$ from the center of the headed bar according to Section 17.6.2.1 of ACI 318-19.

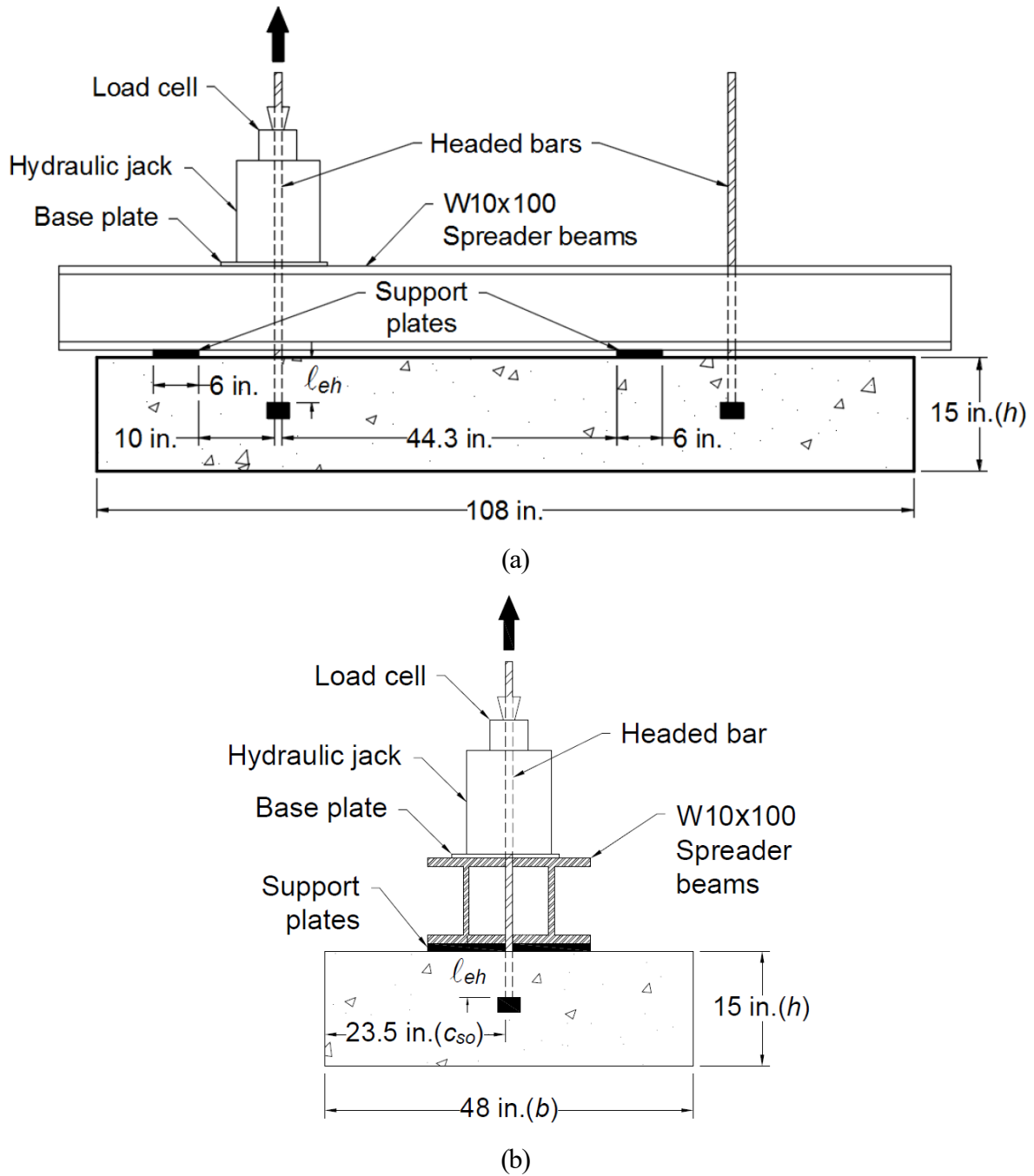


Figure 1.25 Test setup of the first group (a) front view, (b) side view (Ghimire et al. 2018)

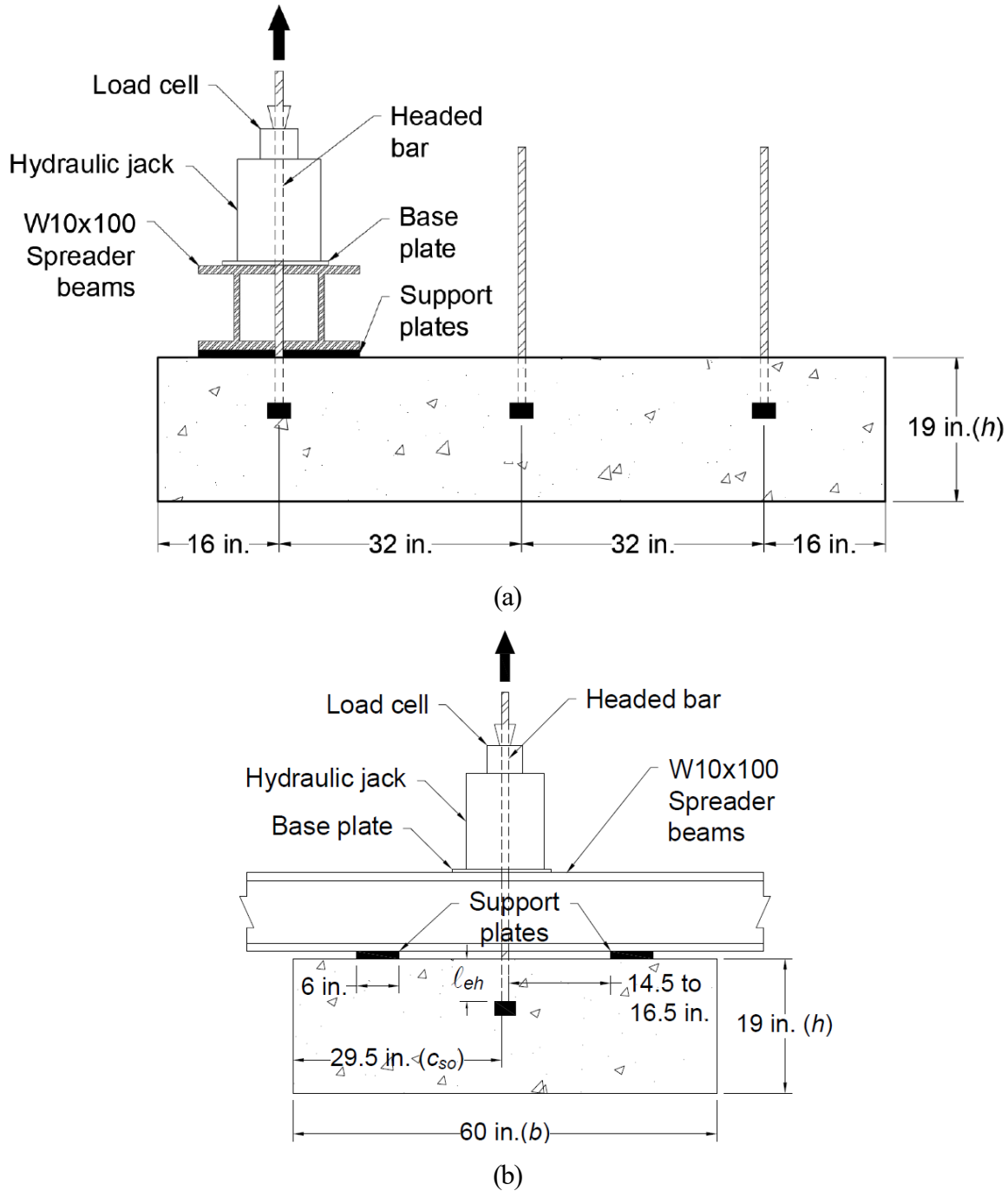


Figure 1.26 Test setup of the final group (a) front view, (b) side view (Ghimire et al. 2018)

All specimens tested by Ghimire et al. exhibited breakout failure (a cone shape of concrete pulled out of the slab along with the test bar). Like Choi et al. (2002), Ghimire et al. found that the presence of reinforcement perpendicular to headed bars did not increase the anchorage strength of headed bars. They also found that increasing the net bearing area of the head from 4 to $9.5A_b$ did not increase the anchorage strength of headed bars; however, the anchorage strength of headed

bars increased about 15% for heads with a net bearing area ranging from 13 to $15A_b$. Ghimire et al. observed that the anchorage strength of headed bars increased about 37% as the concrete compressive strength increased from 4,200 to 8,600 psi.

1.6 UNIVERSITY OF CALIFORNIA, BERKELEY – STEEL COLUMN-CONCRETE FOUNDATION JOINTS

Worsfold et al. (2022) tested two steel-column-to-concrete-foundation joints located away from foundation edges under reversed cyclic loading with and without parallel tie reinforcement in the foundation to study the failure mechanisms and design requirements. As depicted in Figures (1.27) and (1.28), the test specimens consisted of a steel column (W12x106 ASTM A992 Grade 50) connected to a foundation slab by cast-in-place anchor bolts. The column was subjected to reversed cyclic lateral loads with no axial load other than column self-weight. Four 1.5 in. diameter anchor bolts with heavy hex nuts as heads in the first specimen M01 and with steel plate washers in the second specimen M02, as shown in Figures (1.27) and (1.28), respectively, were cast into the 18 in. thick foundation on each side of the column with an effective embedment length from the top of the slab to the bearing surface equal to 14.3 in. The head net bearing areas A_{brg} in specimens M01 and M02 were $1.5A_b$ and $5.5A_b$, respectively. The concrete compressive strengths were 3700 and 3930 psi on test day in specimens M01 and M02, respectively. The nominal yield strength of the anchor bolts was 105,000 psi. Specimen M01 had five perpendicular No. 4 hoops in the joint region, as shown in Figure (1.27), whereas specimen M02 contained No.4 parallel tie reinforcement shaped as 180-degree hooks on the top and heads on the bottom, as shown in Figure (1.28). The parallel tie reinforcement in specimen M02 extended two rows farther on the west side than on the east side of the slab (Figure 1.29), with no hoops placed around the anchors. A load cell was placed on each anchor bolt to measure the anchorage strength.

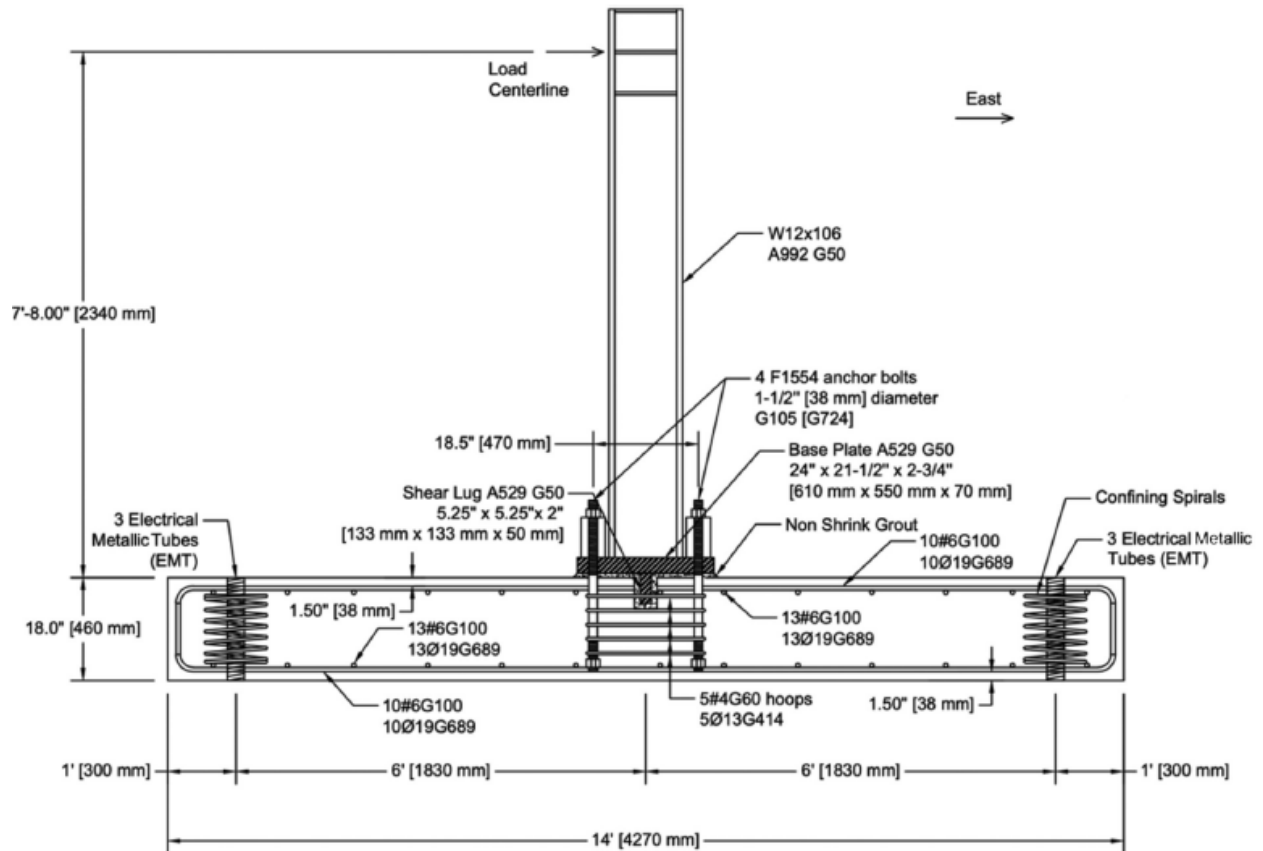


Figure 1.27 Steel-column-to-concrete-foundation joint specimen M01 (Worsfold et al. 2022)

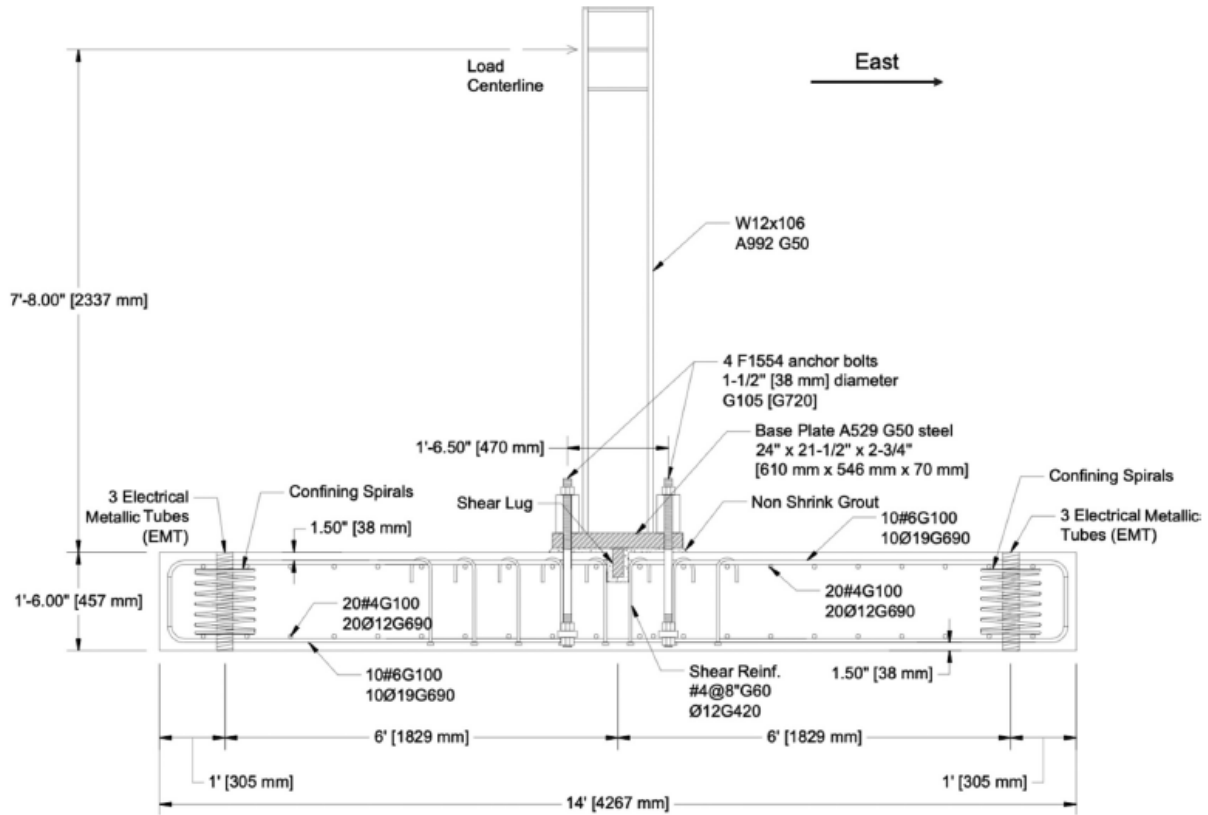


Figure 1.28 Steel-column-to-concrete-foundation joint specimen M02 (Worsfold et al. 2022)

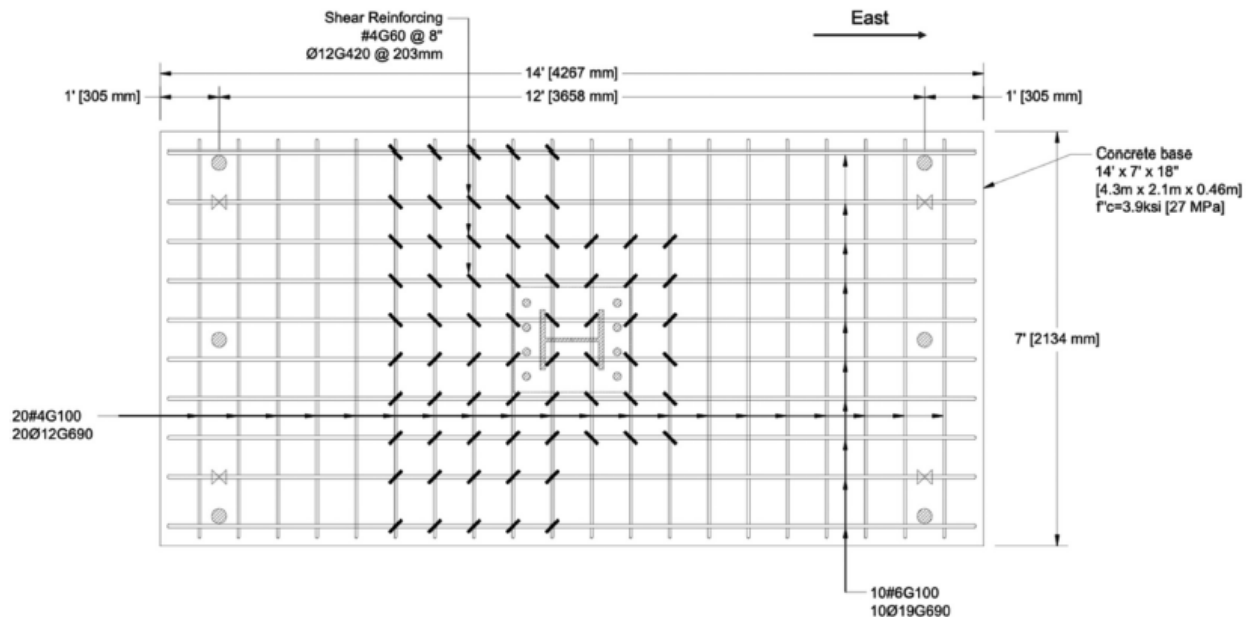


Figure 1.29 Plan view of specimen M02 (Worsfold et al. 2022)

Both specimens M01 and M02 tested by Worsfold et al. exhibited breakout failure (a cone shape of concrete pulled out of the slab along with the anchor bolts). Based on the surface cracks,

Worsfold et al. observed that the breakout failure cones were asymmetric with a steeper slope toward the interior of the joint, as shown in Figures (1.30) and (1.31) for specimens M01 and M02, respectively. Like Choi et al. (2002) and Ghimire et al. (2018), Worsfold et al. found, based on the strain gauge data, that the perpendicular No. 4 hoops in the joint region of specimen M01 were not effective in increasing the anchorage strength of anchor bolts. Worsfold et al. discovered that adding parallel tie reinforcement to Specimen M02 increased the breakout force by 72% and displacement capacity by a factor of three on average compared to Specimen M01. Worsfold et al. suggested that ACI 318 should consider including provisions that combine concrete strength and shear reinforcement (parallel tie reinforcement) for the concrete breakout failure mode.

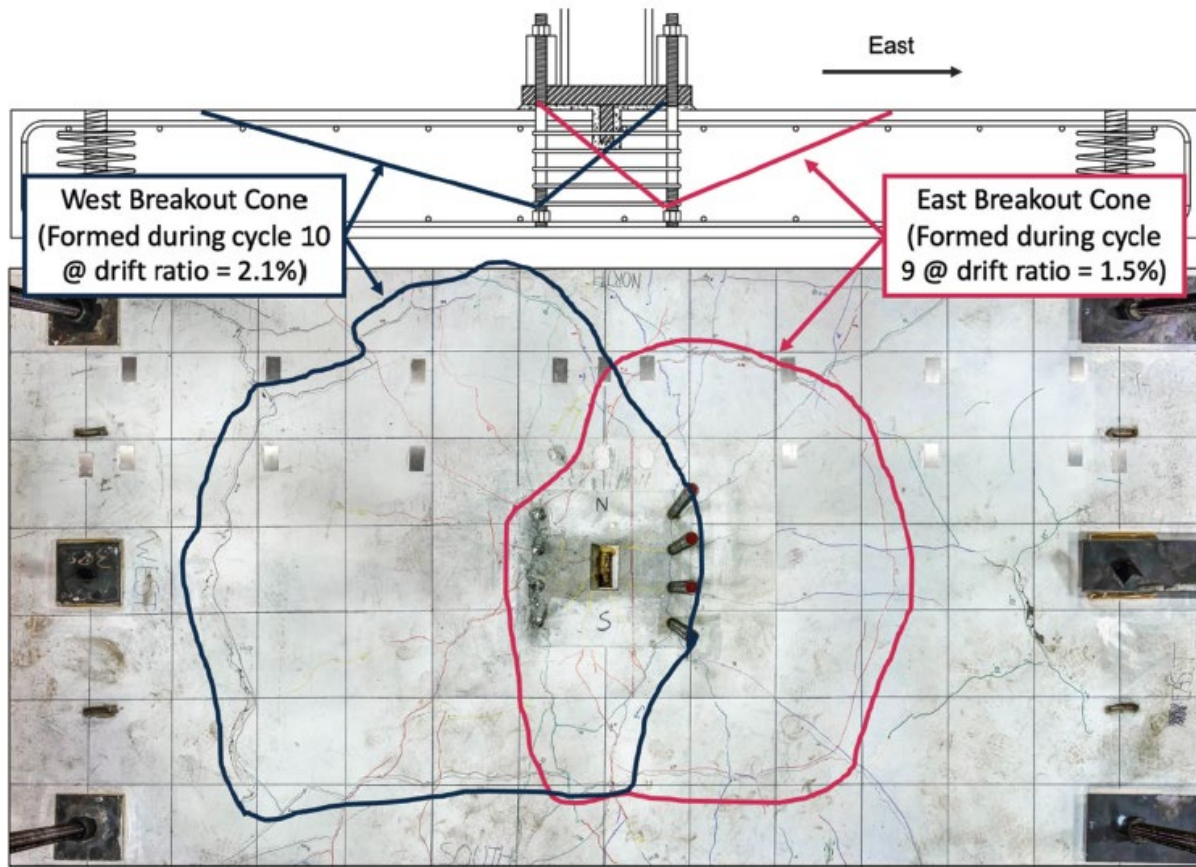


Figure 1.30 Idealized cone geometry shown in elevation and observed cone geometry intersecting top surface in plan view for specimen M01 (Worsfold et al. 2022)



Figure 1.31 Cross section and plan view highlighting crack patterns and breakout cone geometry for Specimen M02 (Worsfold et al. 2022)

1.7 CODE PROVISIONS

1.7.1 Anchorage provisions

The provisions for calculating the concrete breakout strength of the anchors first appeared in ACI 318-02 Appendix D, with no significant changes through the current ACI 318-19 provisions. These provisions are based on the CCD method. In accordance with Section 17.6.2.1 of ACI 318-19, the nominal concrete breakout strength of a single anchor (N_{cb}) or group of anchors (N_{cbg}) in tension is given by Eq. (1.13) and (1.14).

$$N_{cb} = \frac{A_{Nc}}{A_{Nco}} \psi_{ed,N} \psi_{c,N} \psi_{cp,N} N_b \quad (1.13)$$

$$N_{cbg} = \frac{A_{Nc}}{A_{Nco}} \psi_{ec,N} \psi_{ed,N} \psi_{c,N} \psi_{cp,N} N_b \quad (1.14)$$

where A_{Nco} is the projected concrete failure area of a single anchor with an edge distance of at least $1.5h_{ef}$ and is equal to $9h_{ef}^2$ (in.²), as shown in Figure 1.32, where h_{ef} is the embedment length of

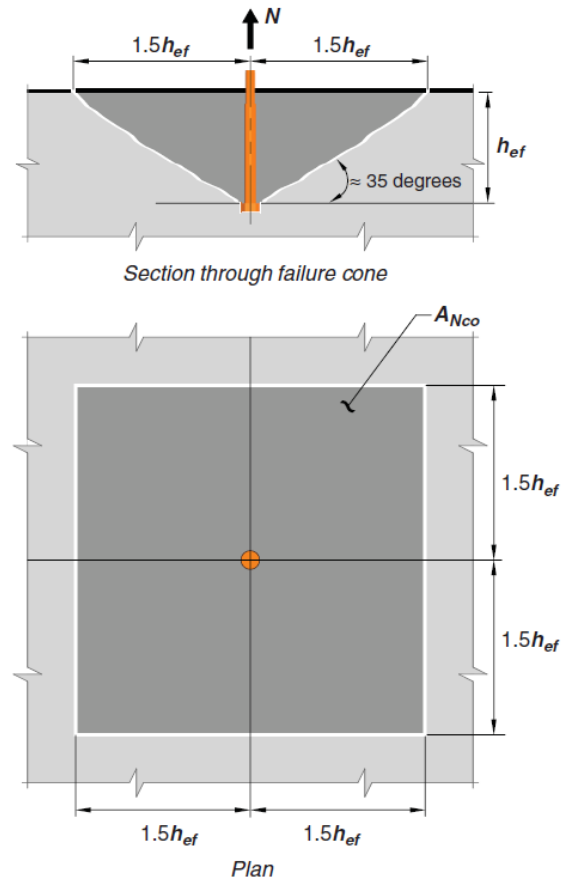
headed bars (in.); A_{Nc} is the projected concrete failure area of a single anchor or group of anchors (in.²), as shown in Figure 1.33; N_b is the basic concrete breakout strength of a single anchor loaded in tension, calculated as

$$N_b = k_c \cdot \lambda_a \cdot \sqrt{f'_c} \cdot h_{ef}^{1.5} \quad (1.15)$$

where k_c is a calibration factor equal to 24 for cast-in anchors in cracked concrete based on the 5 percent fractile; λ_a is a modification factor for lightweight concrete equal to 1.0λ for cast-in and undercut anchors and 0.8λ for expansion, screw, and adhesive anchors, λ is equal to 0.75 for lightweight concrete and 1.0 for normalweight concrete; f'_c is the concrete compressive strength (limited to a maximum 10,000 psi). $\Psi_{ec,N}$ is a modification factor for a group of anchors loaded

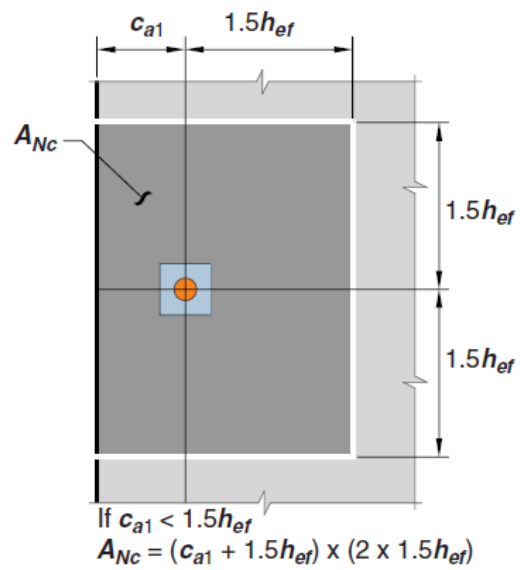
eccentrically in tension, equal to $\frac{1}{1 + e'_N / (1.5h_{ef})} \leq 1$, where e'_N is the distance between resultant

tensile load on a group of anchors loaded in tension and the centroid of the group of anchors loaded in tension (in.). $\Psi_{ed,N}$ is a modification factor for edge effects for a single anchor or group of anchors loaded in tension, equal to 1.0 if the smallest side concrete cover distance from the center of an anchor is at least $1.5h_{ef}$; otherwise, $\Psi_{ed,N}$ is equal to $0.7 + 0.3(c_{a,min} / 1.5h_{ef})$, where $c_{a,min}$ is the minimum distance from the center of an anchor to the edge of concrete (in.). $\Psi_{c,N}$ is a modification factor for the influence of cracking in anchor regions at service load levels, equal to 1.25 if anchors are located in a region of a concrete member where analysis indicates no cracking at service load levels; otherwise, $\Psi_{c,N}$ is equal to 1.0. $\Psi_{cp,N}$ is a modification factor for post-installed anchors, and is equal to 1.0 for cast-in anchors.



$$A_{Nco} = (2 \times 1.5h_{ef}) \times (2 \times 1.5h_{ef}) = 9h_{ef}^2$$

Figure 1.32 Calculation of A_{Nco} for a single anchor (ACI 318-19)



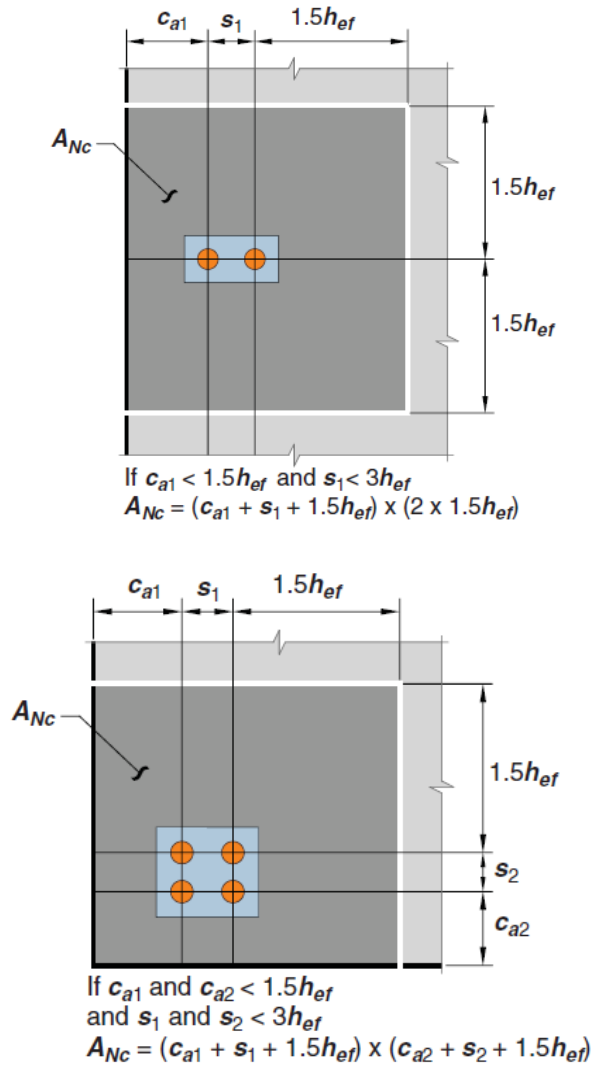


Figure 1.33 Calculation of A_{Nc} for a single anchor and group of anchors (ACI 318-19)

Anchorage provisions in Section 17.6.2.1 of ACI 318 do not take into account the effect of the parallel tie reinforcement on the concrete breakout strength of the anchor(s). Moreover, the anchorage provisions in Chapter 17 of ACI 318 are based on the CCD method, which was developed for anchor bolt types such as studs, bolts, and expansion anchors embedded in plain concrete. Anchor bolts are generally smooth, and thus the CCD method does not take into account contributions of deformed reinforcing bars on anchorage strength.

1.7.2 Design provisions for hooked and headed bars

The equations in ACI 318-19 for calculating the development lengths of hooked and headed bars are presented in Sections 25.4.3 and 25.4.4 and shown in Eq. (1.16) and (1.17),

respectively. The development lengths are functions of the yield strength of the bar (f_y); the square root of concrete compressive strength (f'_c), not to exceed maximum of 10,000 psi for use in the equation; and the bar diameter (d_b) to the power of 1.5.

$$\ell_{dh} = \left(\frac{f_y \Psi_e \Psi_r \Psi_o \Psi_c}{55 \lambda \sqrt{f'_c}} \right) d_b^{1.5} \quad (1.16)$$

$$\ell_{dt} = \left(\frac{f_y \Psi_e \Psi_p \Psi_o \Psi_c}{75 \sqrt{f'_c}} \right) d_b^{1.5} \quad (1.17)$$

where ℓ_{dh} is the development length of a hooked bar in tension (in.); ℓ_{dt} is the development length of a headed bar in tension (in.); Ψ_e is a factor based on the presence or absence of a coating on the bars, equal to 1.2 for epoxy-coated or zinc and epoxy dual-coated reinforcement and 1.0 for uncoated or zinc-coated (galvanized) reinforcement; Ψ_r is a confining reinforcement factor equal to 1.0 for No. 11 and smaller hooked bars spaced at a center-to-center distance not less than $6d_b$ and for hooked bars with A_{th}/A_{hs} not less than 0.4, where A_{th} is the total cross-sectional area of ties or stirrups confining hooked bars (in.²) and A_{hs} is the total cross-sectional area of hooked bars being developed at a critical section (in.²); otherwise, Ψ_r is equal to 1.6; Ψ_o is the bar location factor equal to 1.0 for No. 11 and smaller hooked or headed bars anchored within a column core with side cover not less than 2.5 in. or in other members with side cover not less than $6d_b$; otherwise, Ψ_o is equal to 1.25; Ψ_c is the concrete strength factor equal to $f'_c/15,000 + 0.6$ if f'_c is less than 6000 psi and equal to 1.0 if f'_c is greater than or equal to 6000 psi; Ψ_p is the parallel tie reinforcement factor equal to 1.0 for No. 11 and smaller headed bars spaced at a center-to-center distance not less than $6d_b$ and with A_{tt}/A_{hs} not less than 0.3, where A_{tt} is the total cross-sectional area of ties or stirrups acting as parallel tie reinforcement (in.²) and A_{hs} is the total cross-sectional area of headed bars being developed at a critical section (in.²); otherwise, Ψ_p is equal to 1.6; λ is a lightweight concrete factor equal to 0.75 for lightweight concrete and 1.0 for normalweight concrete. The modification factors in Eq. (1.16) and (1.17) are defined in Table 25.4.3.2 and Table 25.4.4.3 of ACI 318-19, respectively.

The development lengths, ℓ_{dh} and ℓ_{dt} , may not be less than either $8d_b$ or 6 in.

The design provisions in Section 25.4.4.2 of ACI 318-19 for headed bars can be used if the headed bars satisfy specific requirements, described in Section 25.4.4.1 of ACI 318-19.

The key differences in the ACI 318-19 provisions and those proposed by Ajaam et al. (2017) and Shao et al. (2016) for hooked and headed bars, respectively, are:

1. Use of the $\sqrt{f'_c}$ combined with ψ_c in ACI 318-19 in place of $f_c'^{0.25}$ to represent the role of concrete strength.
2. An effective upper limit on f'_c of 10,000 psi in ACI 318-19, rather than an upper limit of 16,000 psi.
3. Use of the step functions ψ_r and ψ_p in ACI 318-19 to represent the effect of anchored bar spacing and confining reinforcement or parallel ties (in the case of headed bars) in place of the variable values permitted for ψ_{cs} .

1.7.3 Design provisions for hooked bars in earthquake resistant structures

The current code design provisions (ACI 318 Building Code and ACI 349 Code Requirements for Nuclear Safety-Related Concrete Structures) for the development length of hooked bars in tension under reversed cyclic loading in earthquake resistant structures (Section 18.8.5.1 of ACI 318-19) were derived directly from the development length provisions for non-seismic loading (Section 25.4.3.1) that existed in ACI 318 Building Codes before 2019. These provisions were based on studies of limited scope conducted in the 1970s (Marques and Jirsa 1975, 1977, Pinc et al. 1977) that included reinforcing steel with yield strengths of 64,000 and 68,000 psi and concrete compressive strengths between 3,750 and 5,100 psi. However, high-strength materials (reinforcing steel with yield strengths up to 120,000 psi and concrete strengths up to 16,000 psi) are now in use. The development length provisions for monotonic loading (Section 25.4.3.1) were modified in the 2019 Code based on the comprehensive study conducted at KU of high-strength hooked bars anchored in beam-column joints tested under monotonic loading (Sperry et al. 2015a,b, 2017a,b, 2018, Ajaam et al. 2017, 2018, Yasso et al. 2017). However, the code design provisions for the development length of hooked bars in tension under cyclic loading did not change in the new ACI Building Code. Therefore, it is important to evaluate the current code provisions for monotonic loading to determine if they can be applied under cyclic loading.

The design provisions for the development of standard hooked bars for beam-column joints under reversed cyclic loading first appeared in the ACI 318-83 Building Code, with no changes in the current ACI 318-19 provisions. In accordance with Section 18.8.5.1 of ACI 318-19, the development length of a standard hooked bar in tension, ℓ_{dh} , for No. 11 and smaller bars embedded in beam-column joints under reversed cyclic loading is given in Eq. (1.18), with ℓ_{dh} should not be less than the maximum of $8d_b$ and 6 in. for normalweight concrete and $10d_b$ and 7.5 in. for lightweight concrete.

$$\ell_{dh} = \frac{f_y d_b}{65\lambda\sqrt{f'_c}} \quad (1.18)$$

where f_y is the specified yield strength of the hooked bar (psi); d_b is the hooked bar diameter (in.); λ is the lightweight modification factor, equal to 0.75 for lightweight concrete and 1.0 for normalweight concrete; f'_c is the concrete compressive strength (psi).

1.8 OBJECTIVE AND SCOPE

In 2013, the University of Kansas started a comprehensive study of the anchorage strength of hooked and headed bars, primarily in exterior beam-column joints. Sperry et al. (2015a,b, 2017a,b, 2018), Ajaam et al. (2017, 2018), Yasso et al. (2017, 2021), Shao et al. (2016), and Ghimire et al. (2018, 2019a,b) developed descriptive equations, presented in Sections 1.3.2 and 1.3.4, and proposed design equations to allow for the use of hooked and headed reinforcing bars with yield strengths up to 120,000 psi and concrete compressive strengths up to 16,000 psi. These equations were developed based on the results of testing 394 simulated beam-column joint specimens using hooked bars and 202 simulated beam-column joint specimens using headed bars. It is worth noting that the proposed design equations were modified in the process of development the provisions in ACI 318-19. The current study is an extension of the earlier comprehensive research program.

The objectives of this study are as follows:

First, expand KU's study on the behavior of large, high-strength headed bars anchored in members other than beam-column joints, such as column-foundation joints;

Second, use data from previous studies and from the current study to evaluate the accuracy of the anchorage provisions in Chapter 17 of ACI 318-19 for predicting the anchorage strength of headed bars; third, use data from the current study to evaluate the applicability of the equations developed by Shao et al. (2016) for predicting the anchorage strength of headed bars anchored in members other than beam-column joints, such as column-foundation joints; and

Third, use and analyze test results of 146 exterior beam-column joint specimens subjected to reversed cyclic loading tested by researchers from outside of KU [Hanson and Connor (1967), Hanson (1971), Megget (1974), Uzumeri (1977), Lee et al. (1977), Scribner (1978), Paulay and Scarpas (1981), Ehsani and Wight (1982), Kanada et al. (1984), Zerbe and Durrani (1985), Ehsani et al. (1987), Ehsani and Alameddine (1991), Kaku and Asakusa (1991), Tsonos et al. (1992), Pantelides et al. (2002), Chutarat and Aboutaha (2003), Hwang et al. (2005), Lee and Ko (2007), Chun et al. (2007), Tsonos (2007), Kang et al. (2010), Chun and Shin (2014), Hwang et al. (2014), and Choi and Bae (2019)] to investigate the applicability of the descriptive equations developed at KU for beam-column joints tested under monotonic loading to predict the anchorage strength of hooked bars anchored in members subjected to reversed cyclic loading.

This study includes two phases:

The first phase involves 31 tests of simulated column-foundation joints to investigate the anchorage strength and behavior of large and high-strength headed bars. The work involved 15 specimens, each with one to three simulated column-foundation joints. The main variables were strut angle between the anchored headed bar and the nearest support reaction (Figure 1.34), number of headed bars tested simultaneously (1 or 2), size of the headed bars (No. 11 or No. 14), spacing between headed bars loaded simultaneously (3.2 or $8.2d_b$), amount of parallel tie reinforcement within the joint region (zero to six No. 4 closed stirrups), and concrete compressive strength (5,060 to 14,470 psi). The embedment length of the headed bars ranged from 12.625 to 14 in. The stresses in the headed bars at failure ranged from 41,800 to 144,400 psi. The net bearing area of the headed bars ranged from 4.2 to $9.2A_b$. This study also includes an evaluation of tests on headed bars tested in simulated column-foundation joints by DeVries et al. (1999), Choi et al. (2002), and Ghimire et al. (2018), and on anchor bolts tested in steel column-concrete foundation joints by Worsfold et al. (2022), described earlier in this chapter. The test results of this study and other studies are

compared with anchorage strengths based on the anchorage provisions in Section 17.6.2 of ACI 318-19 with a strength reduction, ϕ , factor equal to 1.0, and the descriptive equations for headed bars developed by Shao et al. (2016).

The second phase of the study involves the analysis of the test results of 146 exterior beam-column joint specimens subjected to reversed cyclic loading. The summary of these tests is presented in Section 1.2.4. The data from these tests are analyzed using the equations developed by Ajaam et al. (2017) to investigate their applicability to calculate the anchorage strength of hooked bars anchored in beam-column joints subjected to reversed cyclic loading. This analysis is used, in turn, to propose a change in Section 18.8.5.1 of ACI 318 to require the use of Section 25.4.3 of ACI 318 to establish the minimum development length ℓ_{dh} for hooked bars anchored in joints for frames subjected to seismic loading.

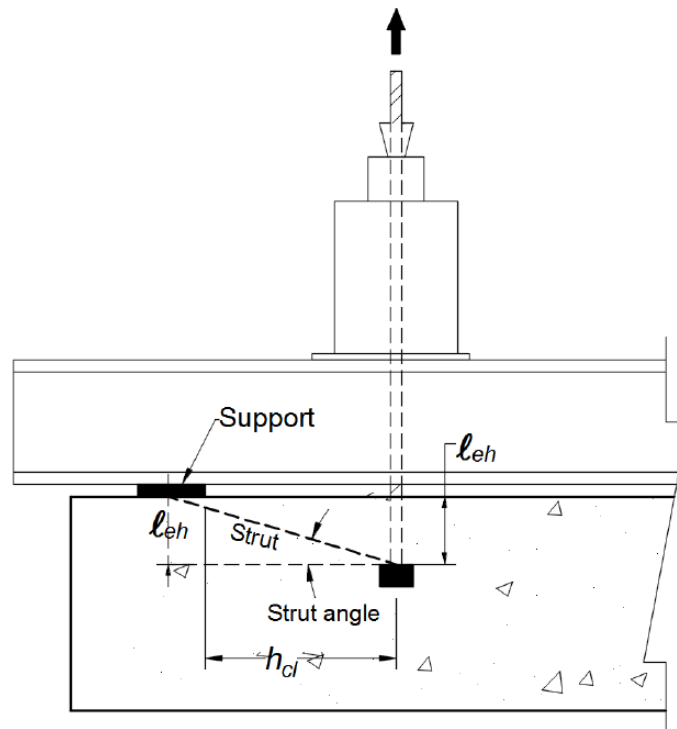


Figure 1.34 Strut angle between anchored headed bar and nearest support reaction

CHAPTER 2: EXPERIMENTAL WORK

Thirty-one tests were performed on headed reinforcing bars in slab specimens to investigate the anchorage strength and behavior of No. 11 and No. 14 headed bars used as column longitudinal reinforcing bars in column-foundation joints. The details of the slab specimens, including material properties, specimen design, test parameters, specimen designations, specimen fabrication and test procedures, and specimen instrumentation, are presented in this chapter.

2.1 MATERIAL PROPERTIES

2.1.1 Concrete Properties

Non-air entrained ready-mix concrete with nominal compressive strengths of 5,000 and 15,000 psi was used in this study. Type I/II portland cement and Kansas River sand were used for both 5,000 and 15,000 psi concrete mixtures. In the 5,000 psi concrete mixture, a mid-to-high-range polycarboxylate-based water reducer (ADVA 140 or ADVA 195) was used as the water reducing agent, while in the 15,000 psi concrete mixture, a high-range polycarboxylate-based water reducer (ADVA 575) was used as the water reducing agent. Crushed limestone with a maximum aggregate size of $\frac{3}{4}$ in. was used in the 5,000 psi concrete mixture, while crushed granite with a maximum aggregate size of $\frac{3}{4}$ in. was used in the 15,000 psi concrete mixture. Class C fly ash and a viscosity modifier (V-MAR) were also used in the 15,000 psi concrete mixtures to increase the workability, strength, and viscosity of the concrete. The mixture proportions of the concrete are given in Table 2.1.

Table 2.1 Concrete mixture proportions

Material	Quantity (SSD)	
	5,000 psi w/cm ^[1] = 0.44	15,000 psi w/cm = 0.21
Type I/II Cement (lb/yd ³)	600	800
Water (lb/yd ³)	263	210
Fly Ash Type C (lb/yd ³)	-	200
Crushed Limestone (lb/yd ³)	1735	-
Granite (lb/yd ³)	-	1430
Kansas River Sand (lb/yd ³)	1396	1430
Mid-to-High Range Water Reducer, ADVA 140 or 195 (oz.) (US)	40	-
High Range Water Reducer, ADVA 575 (oz.) (US)	-	147
Viscosity Modifier (V-MAR) (oz.) (US)	-	20

^[1] w/cm = Water-to-cementitious material ratio

2.1.2 Steel Properties

The No. 11 and No. 14 headed bars used in this study were fabricated from ASTM A1035 Grade 120 steel to ensure that anchorage failure was not governed by the tensile strength of the headed bars. The No. 6 and No. 11 flexural reinforcement placed perpendicular to the headed bars and the No. 4 parallel tie reinforcement were all made of ASTM A615 Grade 60 steel. The properties of the headed bars and parallel tie reinforcement are shown in Table 2.2. Head types used in this study are shown in Figure 2.1, and the head dimensions are given in Table 2.3.

Table 2.2 Properties of headed bars and parallel tie reinforcement

Bar Size	Head Designation	Yield Strength (ksi)	Nominal Diameter (in.)	Average Rib Spacing (in.)	Average Rib Height (in.)		Average Gap Width (in.)	Relative Rib Area ^[2]
					A ^[1]	B ^[2]		
11	S5.5, S9.2	135	1.41	0.917	0.092	0.087	0.424	0.086
14	B4.2	127	1.69	0.992	0.085	0.078	0.523	0.070
4	-	63	0.50	0.350	0.026	0.025	0.220	0.062

^[1] Per ASTM A615, A706; ^[2] Per ACI 408-3

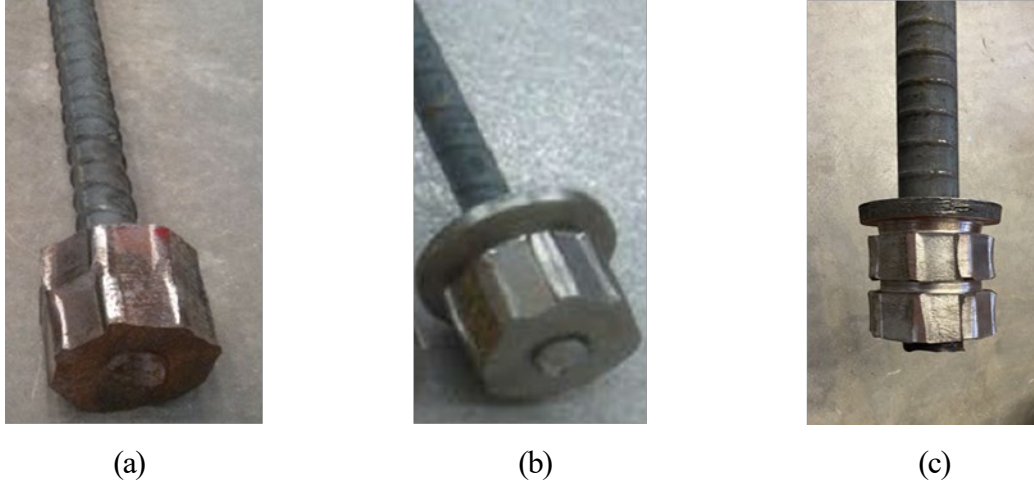

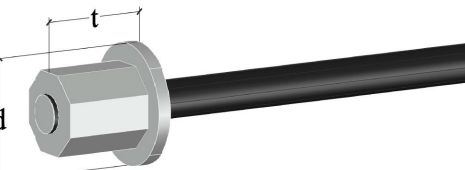



Figure 2.1 Headed bars (a) No. 11 S5.5 bar (b) No. 11 S9.2 bar (c) No. 14 B4.2 headed bar

Table 2.3 Head dimensions

Headed bars	Designation	Bar Size	d (in.)	t (in.)	Net Bearing Area ^[1]
	S5.5 ^[2]	No. 11	3.5	2.75	$5.5A_b$
	S9.2	No. 11	4.5	3.75	$9.2A_b$
	B4.2	No. 14	3.875	4.375	$4.2A_b$

^[1] Net bearing area calculated as gross head area minus bar area

^[2] Octagonal-shape head

2.2 SLAB SPECIMEN DESIGN

Fifteen slab specimens were designed to simulate column-foundation joints: A total of 31 tests, summarized in Table 2.4, were conducted on headed bars anchored with a nominal embedment length $\ell_{eh} = 12\frac{3}{4}$ in. to study the effects of support location (distance between the headed bars and the compression reaction), the number of headed bars (group effects), the spacing between headed bars in a group, bar size (No. 11 and No. 14), the quantity of parallel tie

reinforcement (stirrups or ties placed parallel to the headed bars), and the concrete compressive strength on the anchorage strength of headed bars. The specimens are shown in Figures 2.2 through 2.10.

Table 2.4 Detail of slab specimens ^[1]

Specimens ^[2]			ℓ_{eh} (in.)	f_{cm} (psi)	A_{tt} (in. ²)	$\frac{h_{cl}}{\ell_{eh}}$	$\frac{A_{brg}}{A_b}$	$\frac{A_{tt}}{A_{hs}}$
SN	Description	Head						
1	11-5-S5.5-6#6-0-12.75	A	13.375	5060	0.0	1.85	5.5	0.00
	11-5-S5.5-6#6-0-12.75	B	13.125		0.0	1.88	5.5	0.00
	11-5-S5.5-6#6-0-12.75	C	13.375		0.0	1.85	5.5	0.00
2	11-5-S5.5-10#6-0-12.75	A	13.375	5490	0.0	1.47	5.5	0.00
	11-5-S5.5-10#6-0-12.75	B	12.75		0.0	1.55	5.5	0.00
3	11-5-S5.5-6#11-0-12.75 ^[3]	A	13.625	5740	0.0	5.24	5.5	0.00
4	(2@3.2)11-5-S5.5-6#11-0-12.75	A1	13.50	5550	0.0	1.46	5.5	0.00
		A2	13.50		0.0	1.46	5.5	0.00
	(2@3.2)11-5-S5.5-6#11-0-12.75	B1	13.375	6190	0.0	1.47	5.5	0.00
		B2	13.375		0.0	1.47	5.5	0.00
5	11-5-S5.5-6#6-2#4-12.75	A	13.00	5810	0.8	1.90	5.5	0.51
	11-5-S5.5-6#6-2#4-12.75	B	12.875		0.8	1.92	5.5	0.51
	11-5-S5.5-6#6-2#4-12.75	C	13.125		0.8	1.88	5.5	0.51
6	(2@8.2)11-5-S5.5-7#11-0-12.75	A1	13.50	5370	0.0	1.46	5.5	0.00
		A2	13.50		0.0	1.46	5.5	0.00
	(2@8.2)11-5-S5.5-7#11-0-12.75	B1	14.0625		0.0	1.40	5.5	0.00
		B2	14.0625		0.0	1.40	5.5	0.00
7	(2@8.2)11-5-S5.5-7#11-0-12.75	A1	13.25	5110	0.0	1.49	5.5	0.00
		A2	13.25		0.0	1.49	5.5	0.00
	(2@8.2)11-5-S5.5-7#11-0-12.75	B1	13.3125		0.0	1.48	5.5	0.00
		B2	13.3125		0.0	1.48	5.5	0.00
8	(2@8.2)11-5-S9.2-7#11-3#4-12.75	A1	13.125	7950	0.8	1.50	9.2	0.26
		A2	13.125		0.8	1.50	9.2	0.26
	(2@8.2)11-5-S9.2-7#11-6#4-12.75	B1	13.00		1.6	1.52	9.2	0.51
		B2	13.00		1.6	1.52	9.2	0.51
9	(2@8.2)11-5-S9.2-7#11-3#4-12.75	A1	13.25	7680	0.8	1.49	9.2	0.26
		A2	13.25		0.8	1.49	9.2	0.26
	(2@8.2)11-5-S9.2-7#11-6#4-12.75	B1	13.375		1.6	1.47	9.2	0.51
		B2	13.375		1.6	1.47	9.2	0.51

^[1] SN = specimen number; ℓ_{eh} = measured embedment length; f_{cm} = measured concrete compressive strength; A_{tt} = total cross-sectional area of effective confining reinforcement parallel to the headed bars being developed; h_{cl} = distance between the center of headed bar to the inner face of the nearest support plate; A_{brg} = net bearing area of the head (Table 2.3); A_b = area of the headed bar; A_{hs} = total cross-sectional area of headed bars being developed (nA_b), where n is the number of headed bars being developed.

^[2] Multiple headed bars in a single specimen tested individually are denoted by letters A, B, and C, and grouped headed bars tested simultaneously are denoted with a number after a common letter (A1, A2).

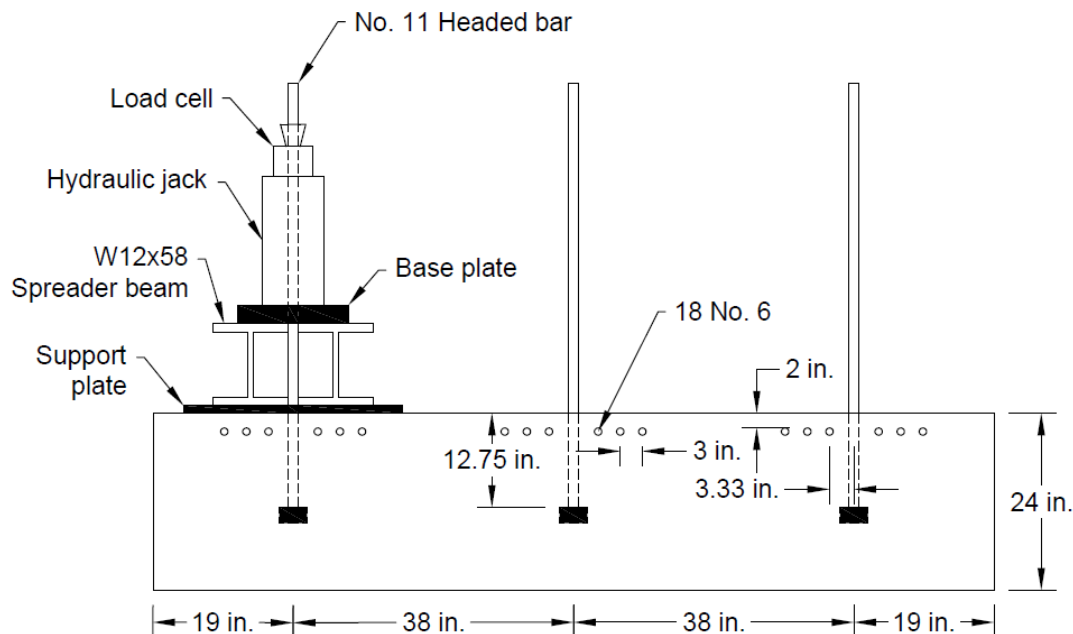
^[3] Specimen contained a single centrally placed headed bar.

Table 2.4 Cont. Detail of slab specimens

Specimens			ℓ_{eh} (in.)	f_{cm} (psi)	A_{tt} (in. ²)	$\frac{h_{cl}}{\ell_{eh}}$	$\frac{A_{brg}}{A_b}$	$\frac{A_{tt}}{A_{hs}}$
SN	Description	Head						
10	(2@8.2)11-15-S9.2-7#11-0-12.75	A1	12.6875	14470	0.0	1.55	9.2	0.00
		A2	12.6875		0.0	1.55	9.2	0.00
	(2@8.2)11-15-S9.2-7#11-0-12.75	B1	12.75		0.0	1.55	9.2	0.00
		B2	12.75		0.0	1.55	9.2	0.00
11	(2@8.2)11-15-S9.2-7#11-3#4-12.75	A1	12.75	14140	0.8	1.55	9.2	0.26
		A2	12.75		0.8	1.55	9.2	0.26
	(2@8.2)11-15-S9.2-7#11-6#4-12.75	B1	12.625	14080	1.6	1.56	9.2	0.51
		B2	12.625		1.6	1.56	9.2	0.51
12	(2@6.8)14-5-B4.2-7#11-0-12.75	A1	13.00	6040	0.0	1.53	4.2	0.00
		A2	13.00		0.0	1.53	4.2	0.00
	(2@6.8)14-5-B4.2-7#11-0-12.75	B1	13.125	6180	0.0	1.51	4.2	0.00
		B2	13.125		0.0	1.51	4.2	0.00
13	(2@6.8)14-5-B4.2-7#11-3#4-12.75	A1	13.00	5440	0.8	1.53	4.2	0.18
		A2	13.00		0.8	1.53	4.2	0.18
	(2@6.8)14-5-B4.2-7#11-6#4-12.75	B1	12.75	5480	1.6	1.56	4.2	0.36
		B2	12.75		1.6	1.56	4.2	0.36
14	(2@6.8)14-15-B4.2-7#11-0-12.75	A1	13.125	14030	0.0	1.51	4.2	0.00
		A2	13.125		0.0	1.51	4.2	0.00
	(2@6.8)14-15-B4.2-7#11-0-12.75	B1	13.125	14050	0.0	1.51	4.2	0.00
		B2	13.125		0.0	1.51	4.2	0.00
15	(2@6.8)14-15-B4.2-7#11-3#4-12.75	A1	13.375	13190	0.8	1.48	4.2	0.18
		A2	13.375		0.8	1.48	4.2	0.18
	(2@6.8)14-15-B4.2-7#11-6#4-12.75	B1	12.875	13020	1.6	1.54	4.2	0.36
		B2	12.875		1.6	1.54	4.2	0.36

The slab specimens were designed as simply-supported beams (neglecting self-weight) to resist bending and shear at the maximum expected failure stress on the anchored bars. Of the 15 slab specimens, four contained one, two, or three headed bars, which were loaded one at a time, as shown in Figures 2.2 through 2.4, and eleven contained two groups of two headed bars loaded simultaneously, as shown in Figures 2.5 through 2.10. The individual or groups of headed bars were embedded sufficiently far apart so that an anchorage failure in one test did not interfere with the anchorage failure of the other test or tests in the slab. The width of the slabs was chosen so that it was greater than the diameter of the anticipated concrete breakout failure region, which is equal to $3\ell_{eh}$ according to Section 17.6.2.1 of ACI 318-19, where ℓ_{eh} is the embedment length of the headed bars. The depth of the slab specimens was sufficient to provide flexural and shear strength;

the specimens included flexural reinforcement in the vicinity of the head, as shown in Figures 2.2 through 2.10; Ghimire et al. (2018) showed that the presence of reinforcement perpendicular to headed bars does not affect anchorage strength. In the test of Slabs 1 and 5, both support reactions were placed just outside the anticipated failure region; the clear distance between the support reactions and the headed bar was 24 in., as shown in Figures 2.2 and 2.6. In the test of Slab 3, both support reactions were located far away from the anticipated failure region, as shown in Figure 2.4, to avoid interference with the concrete breakout failure surface. In the tests of the remaining slabs, the test headed bars involved a shallow compressive strut on one side of the bars, indicative of loading conditions of a column or wall subjected to an overturning moment; the clear distance between the nearest support reaction representing the compression zone of the column and the headed bars representing anchored tension reinforcement was 19 in.; the clear distance between the other support reaction, which was placed far away from the anticipated failure region to avoid interference with the concrete breakout failure surface, and the headed bars was 83 in., as shown in Figure 2.3. Six slab specimens contained parallel tie reinforcement; in one specimen, the parallel ties were located on both sides of the headed bars, as shown in Figure 2.6, and in the remaining specimens, one pair of headed bars had parallel ties on both sides of the headed bars, and the other pair had parallel ties only on one side, as shown in Figures 2.8 and 2.10.



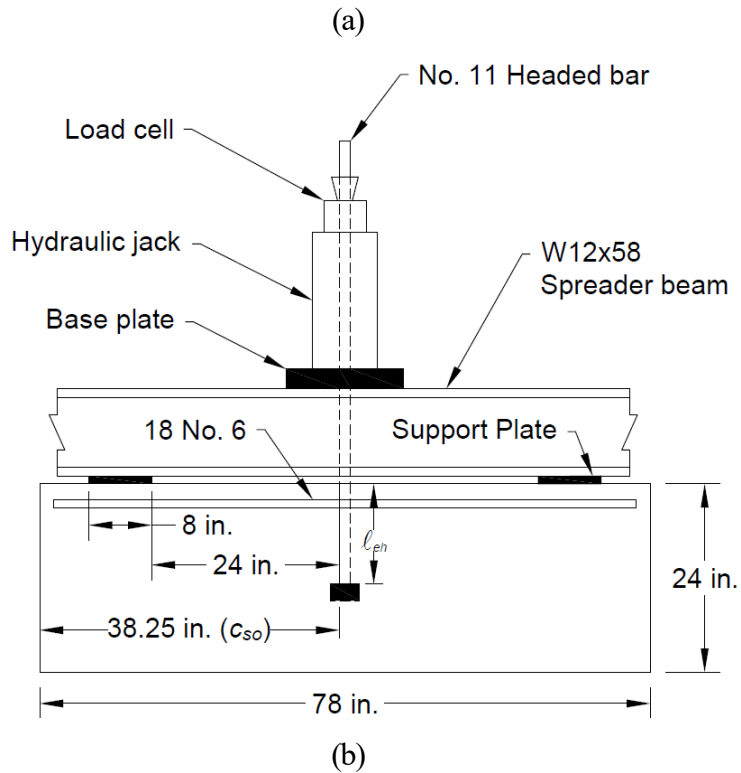
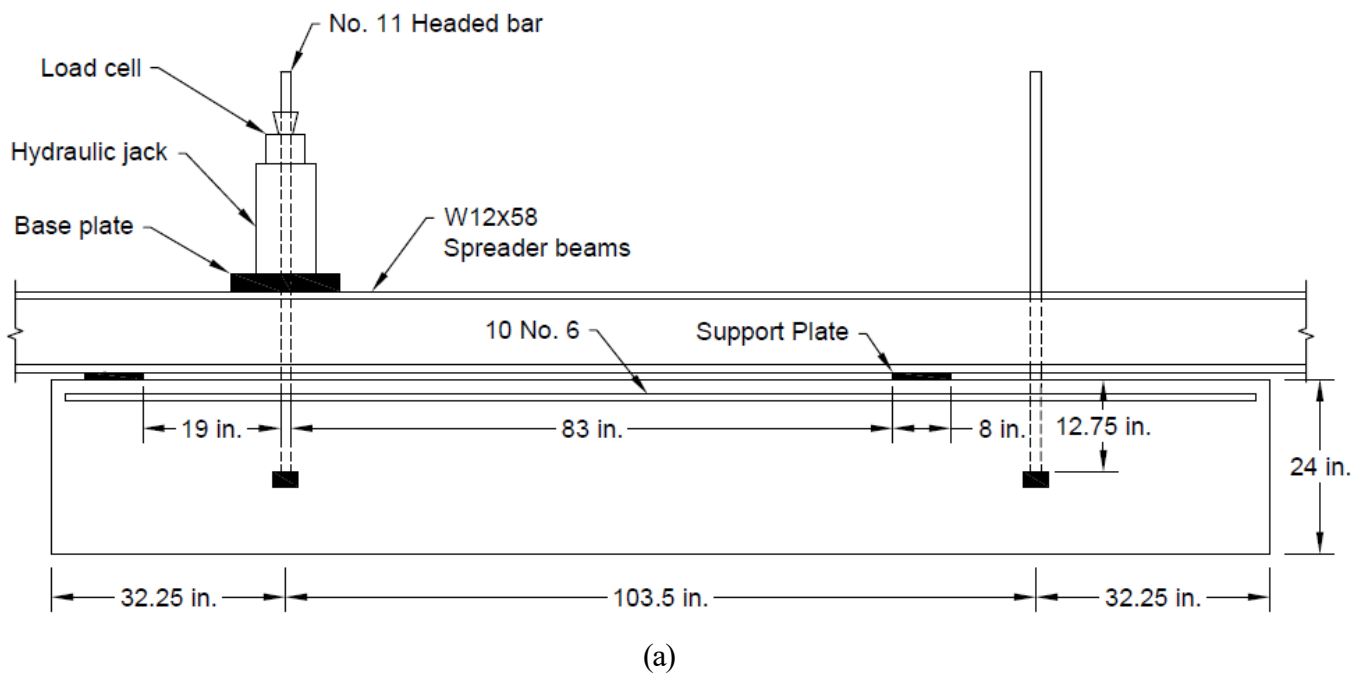
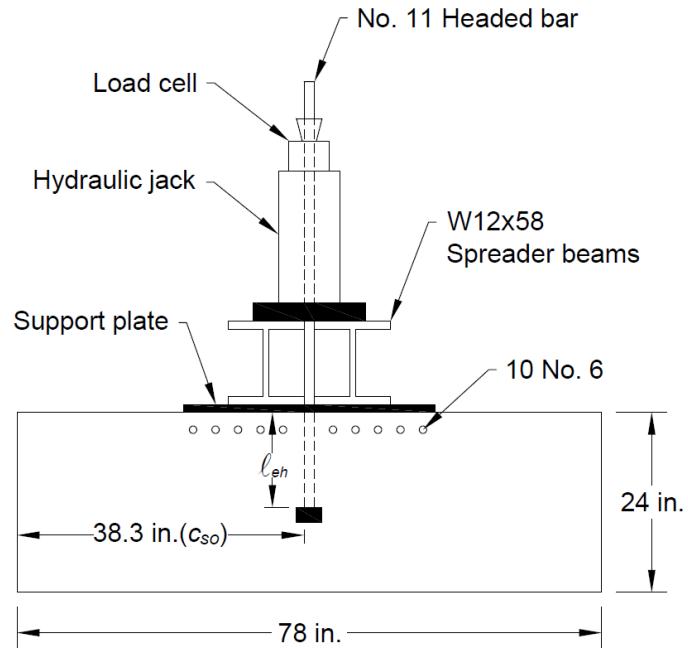


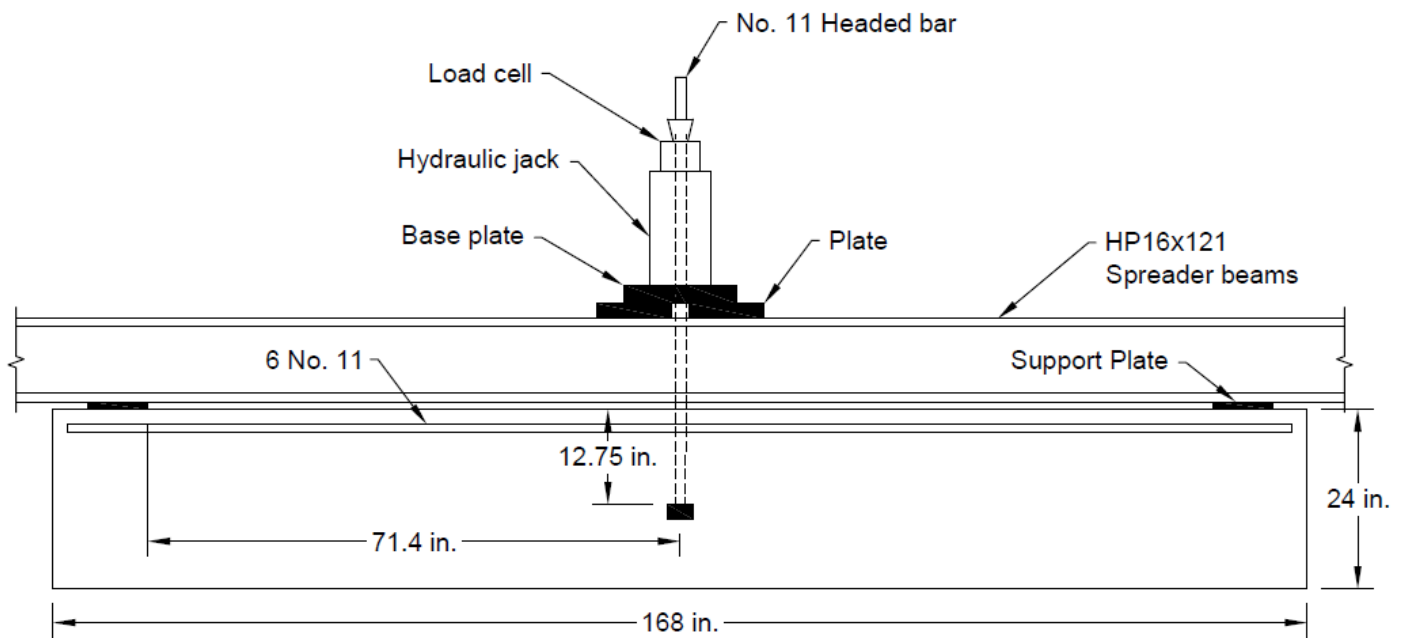
Figure 2.2 Location of headed bars and reinforcement for Slab 1 (a) side view, (b) end view



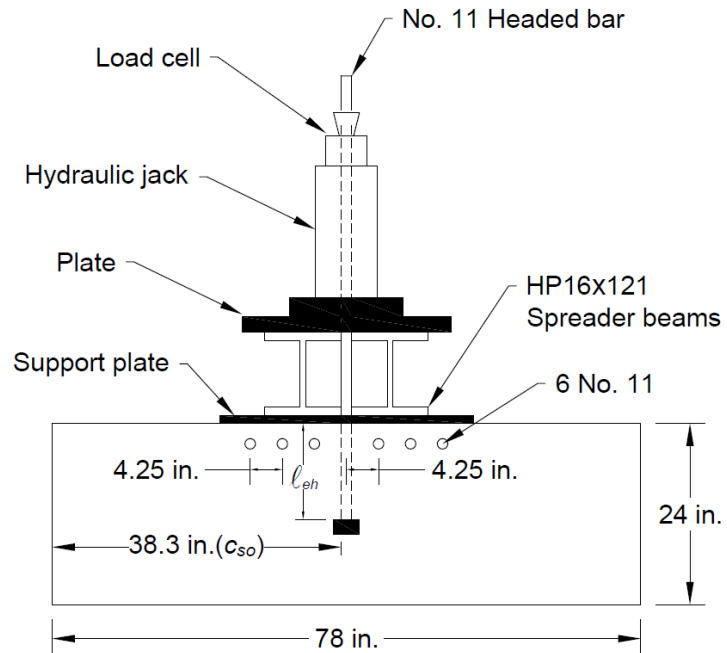


(b)

Figure 2.3 Location of headed bars and reinforcement for Slab 2 (a) side view, (b) end view

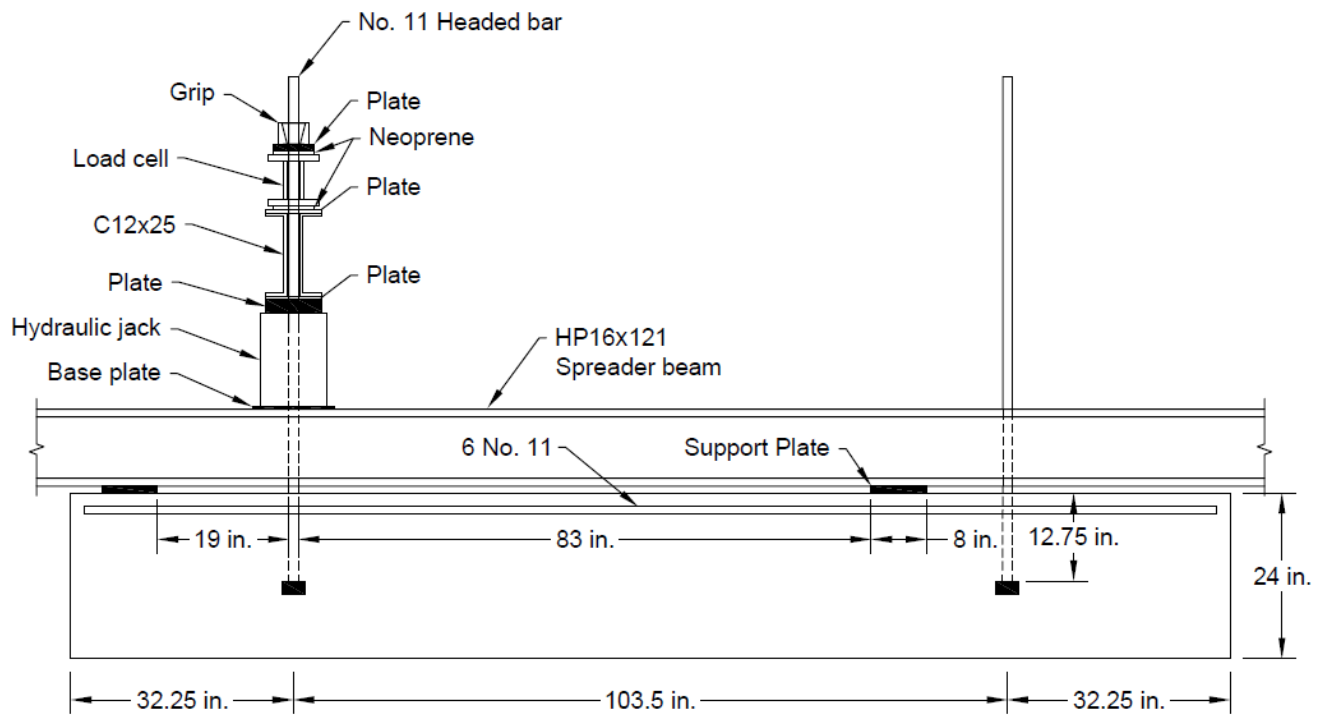


(a)

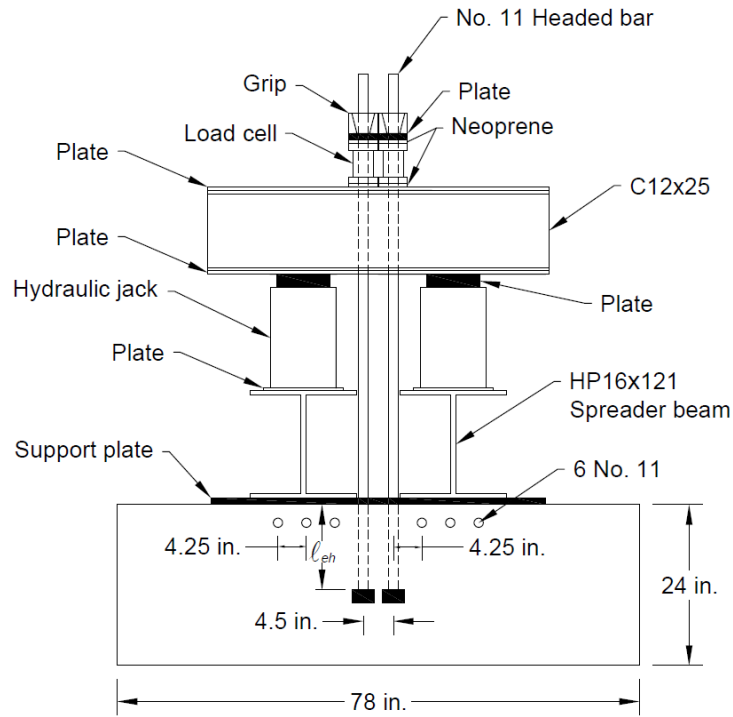


(b)

Figure 2.4 Location of headed bars and reinforcement for Slab 3 (a) side view, (b) end view

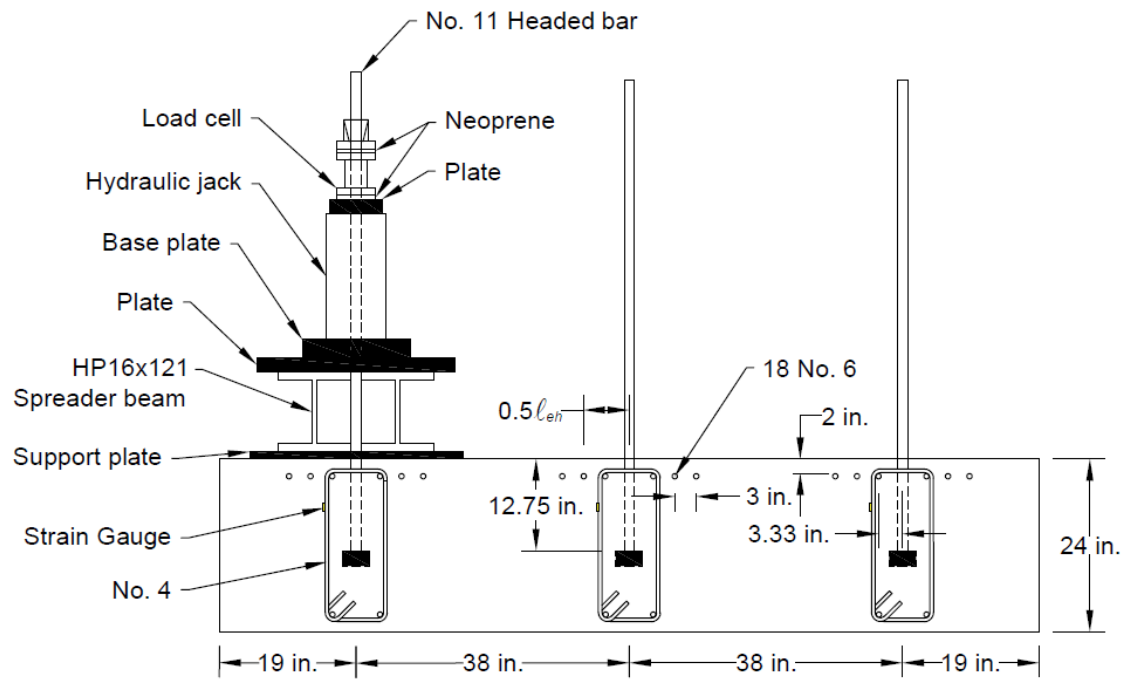


(a)

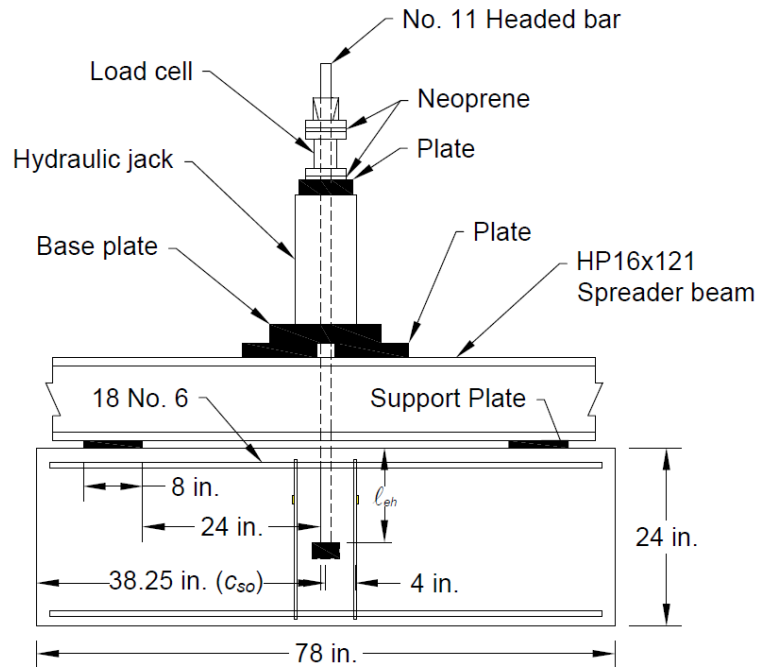


(b)

Figure 2.5 Location of headed bars and reinforcement for Slab 4 (a) side view, (b) end view

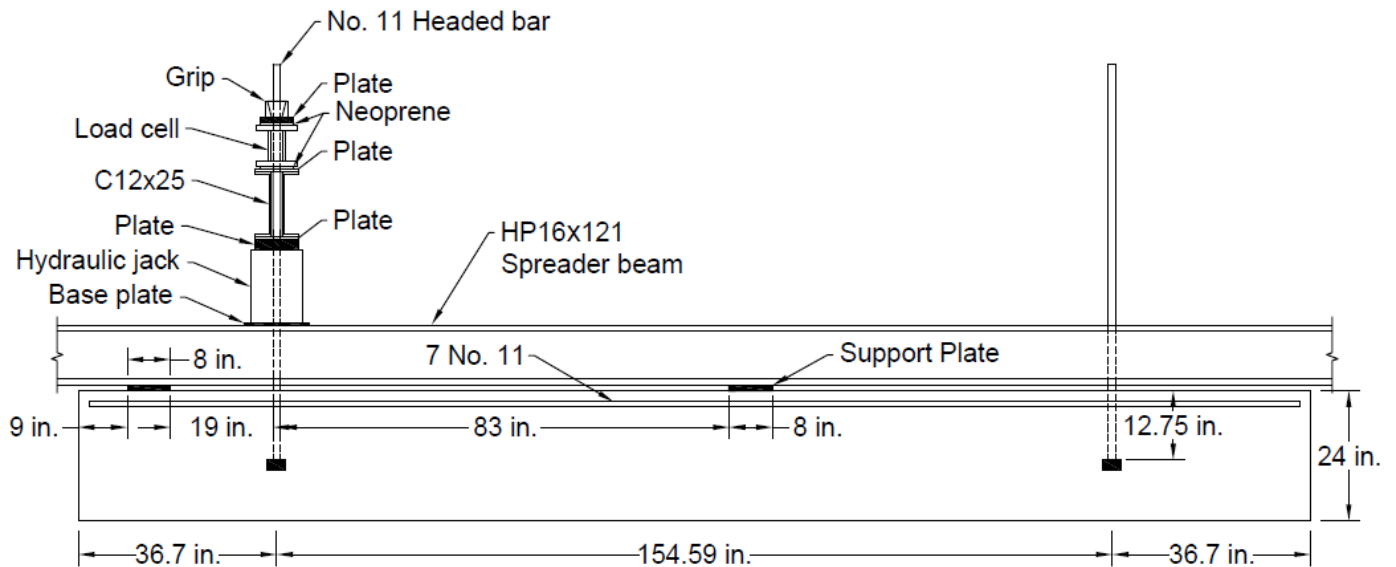


(a)

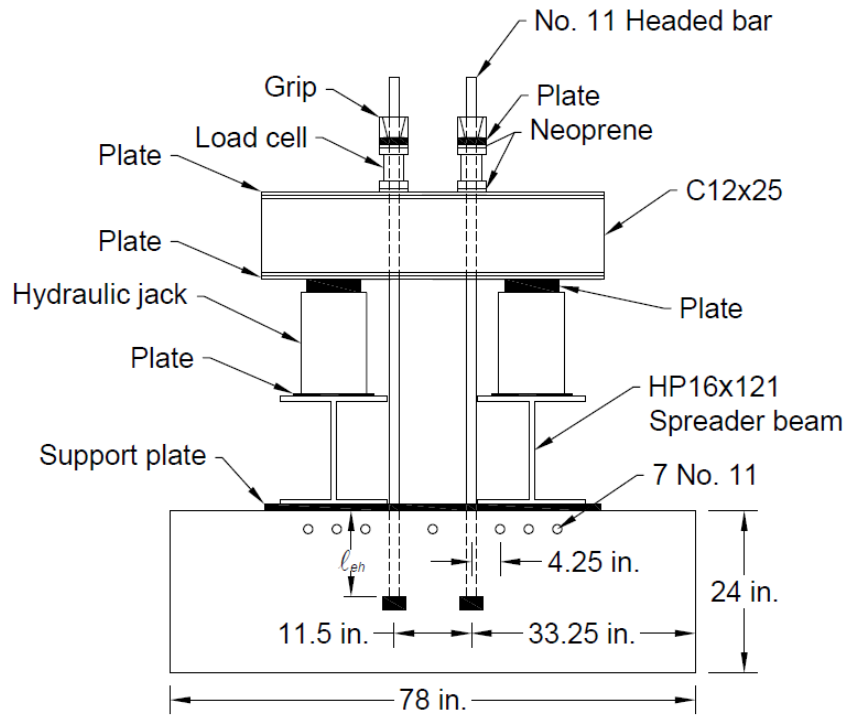


(b)

Figure 2.6 Location of headed bars and reinforcement for Slab 5 (a) side view, (b) end view

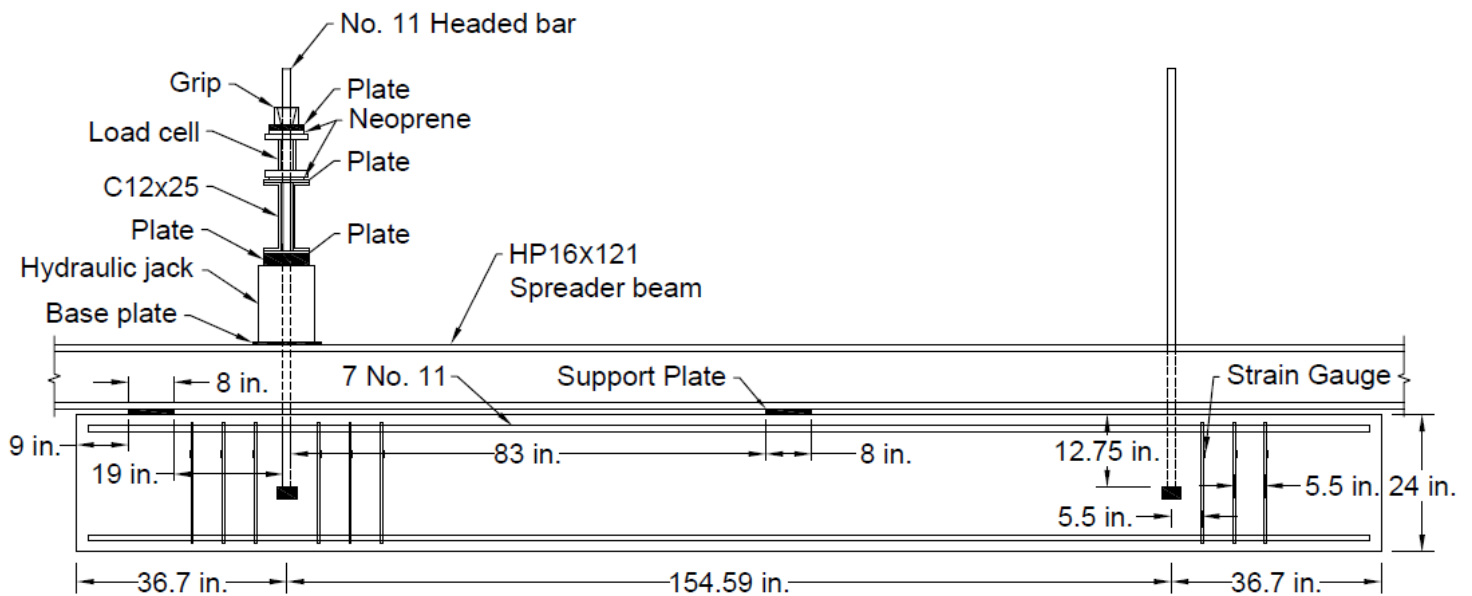


(a)

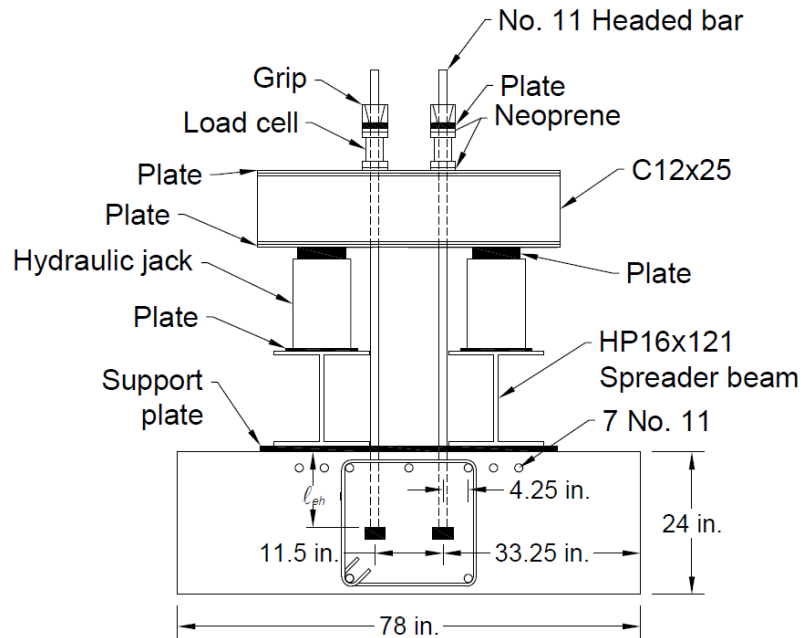


(b)

Figure 2.7 Location of headed bars and reinforcement for Slabs 6,7, and 10 (a) side view, (b) end view

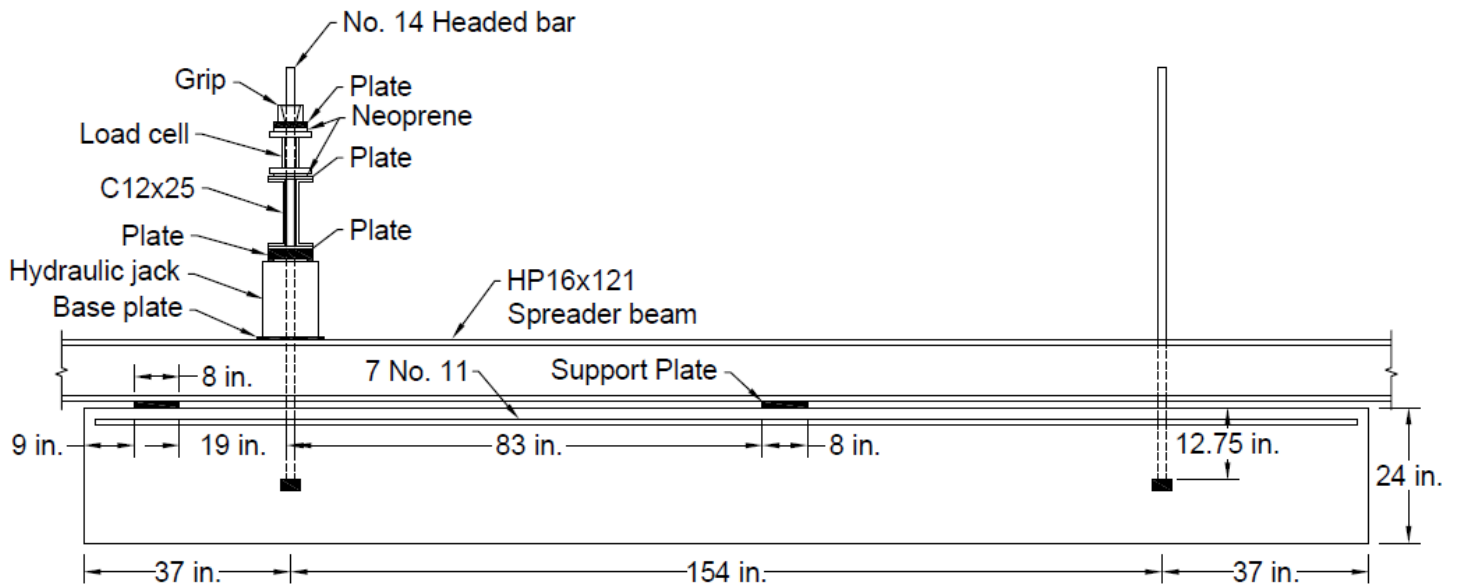


(a)

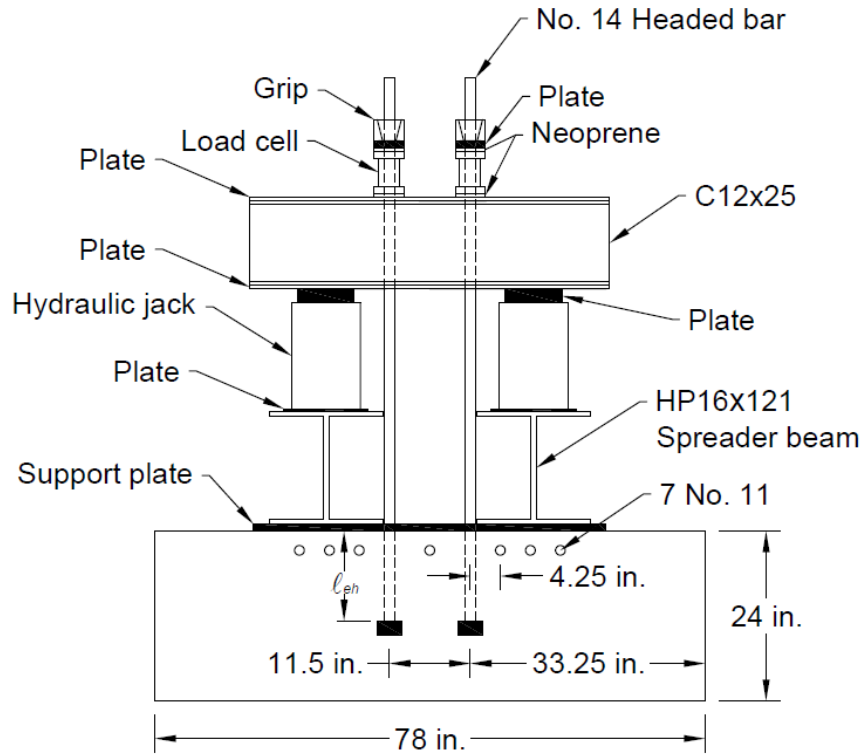


(b)

Figure 2.8 Location of headed bars and reinforcement for Slabs 8, 9, and 11 (a) side view, (b) end view

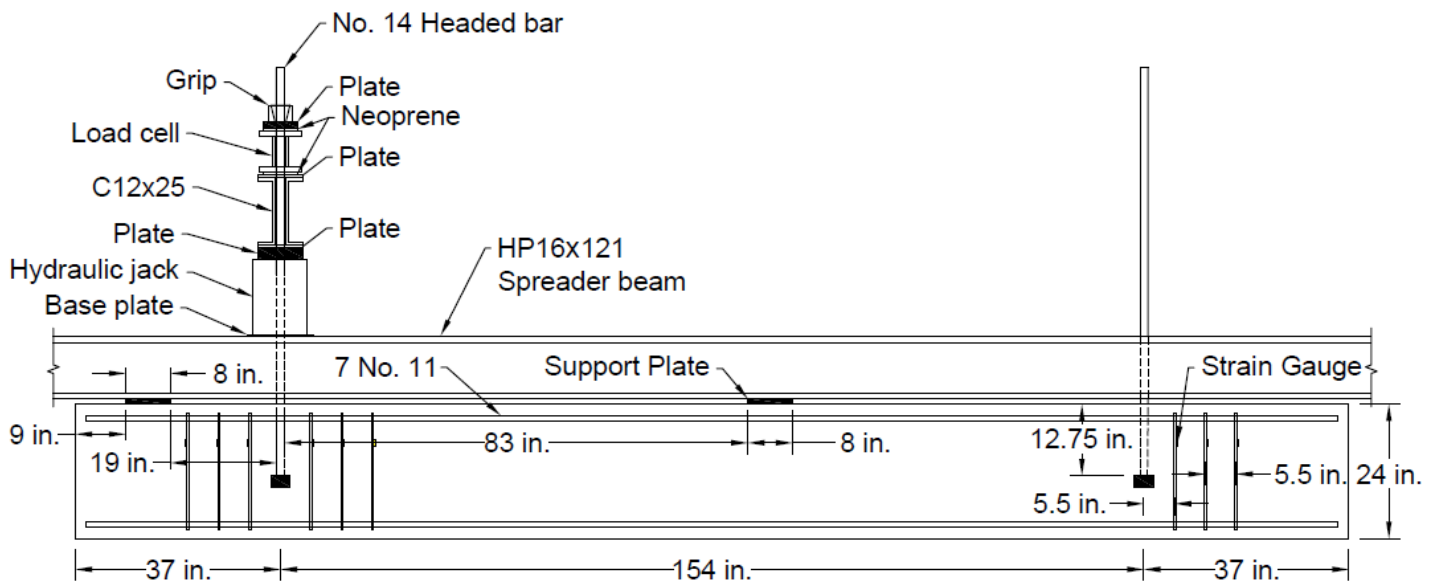


(a)

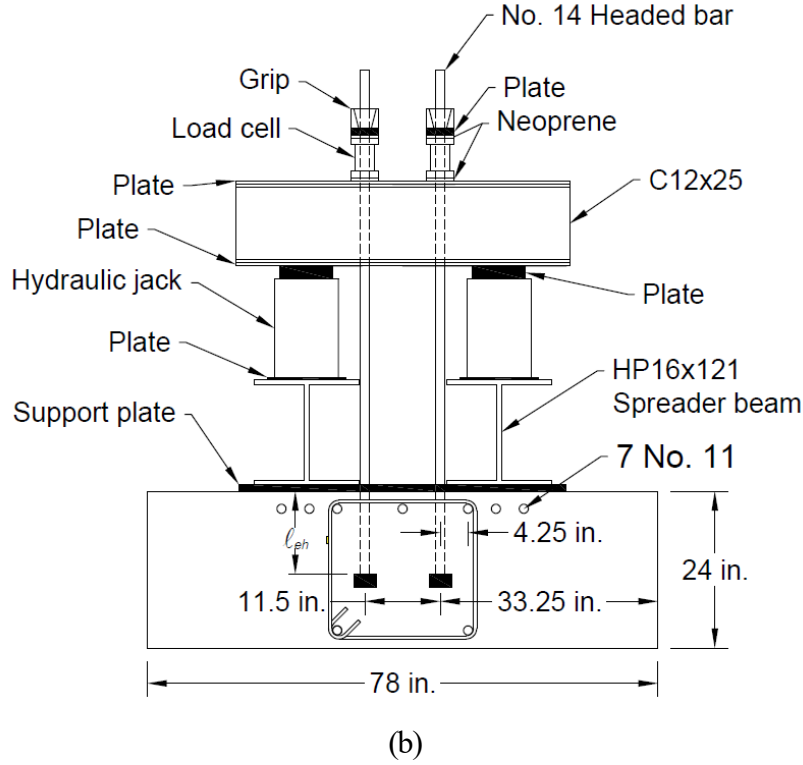


(b)

Figure 2.9 Location of headed bars and reinforcement for Slabs 12 and 14 (a) side view, (b) end view



(a)



(b)
Figure 2.10 Location of headed bars and reinforcement for Slabs 13 and 15 (a) side view, (b) end view

2.3 TEST PARAMETERS

The test parameters in this study were bar size, concrete compressive strength, number of headed bars, the spacing between the headed bars, embedment length, support reaction placement, and parallel tie reinforcement. The ranges of these variables are described below:

Bar size: Two headed bar sizes were used – No. 11 and No. 14. The net bearing areas A_{brg} of the headed bars were $5.5A_b$ and $9.2A_b$ for No. 11 headed bars and $4.2A_b$ for No. 14 headed bars, where A_b is the bar area. Shao et al. (2016) and Ghimire et al. (2018) found that the anchorage strength of headed bars was not sensitive to bearing area for bars with net bearing areas A_{brg} between $3.8A_b$ and $9.5A_b$.

Concrete compressive strength: The target concrete compressive strengths were 5,000 and 15,000 psi. Measured concrete compressive strengths ranged from 5,060 to 14,470 psi. Concrete mixture proportions are given in Section 2.1.1.

Number and spacing of headed bars: Of the 31 tests, nine tests contained one headed bar, and twenty-two tests included two headed bars loaded simultaneously. For the tests with two headed bars, the nominal center-to-center spacing between the bars was either $3.2d_b$ or $8.2d_b$ (where d_b is the bar diameter). The spacing between the bars ($3.2d_b$ and $8.2d_b$) is considered closely and widely spaced, respectively, according to Shao et al. (2016).

Embedment length: Nominal embedment length was $12^{3/4}$ in., and measured embedment lengths ranged from $12^{5/8}$ to $14^{1/16}$ in.

Support reaction placement: The distance from the center of the headed bar to the center of the closest support reaction plate ranged from $23^{3/4}$ to $75^{3/8}$ in.

Parallel tie reinforcement: Parallel tie reinforcement within the joint region ranged from no parallel tie reinforcement to 6 No. 4 hoops, each with two legs. Of the 31 tests, 18 had no parallel tie reinforcement, three had two No. 4 hoops placed on both sides of the headed bar, spaced at $3d_b$ from the center of the headed bar; five had three No. 4 hoops placed only on one side of the headed bars, spaced at $4d_b$ from the center of the headed bar (with one hoop placed outside $10d_b$), and five had six No. 4 hoops placed on both sides of the bars, spaced at $4d_b$ from the center of the headed bar (with two hoops located outside $10d_b$). Details of the three levels of parallel tie reinforcement are shown in Figures 2.6 and 2.8.

2.4 SPECIMEN DESIGNATION

The test variables are denoted in the specimen designation. An example is shown in Figure 2.11. In this example, the first term $[(2@8.2)11]$ indicates that the test had two No. 11 headed bars spaced at 8.2 times the bar diameter (center-to-center); the second term (5) is the nominal concrete compressive strength (ksi); the third term (S9.2) represents the head type (refer to Table 2.3); the fourth term (7#11) denotes the amount of flexural reinforcement placed perpendicular to the headed bars; the fifth term (6#4) represents the number and size of the parallel tie used within the joint region (six hoops, with three on each side of the headed bars); and the final term ($12^{3/4}$) represents the nominal value of the embedment length (in.).

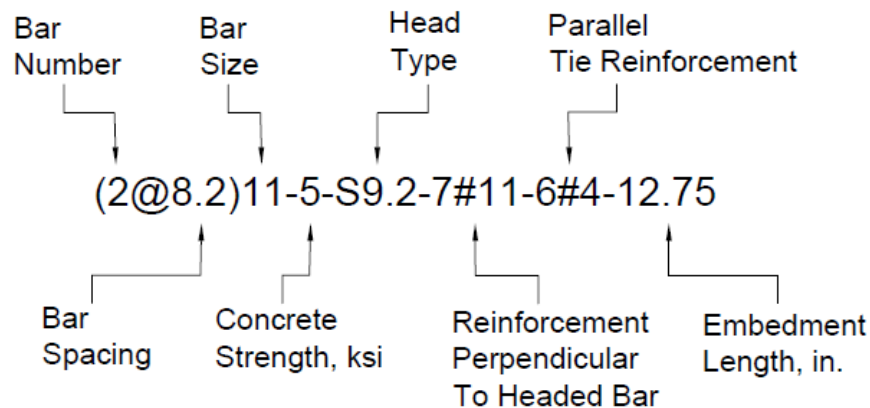


Figure 2.11 Example specimen designation

2.5 SPECIMEN FABRICATION

Formwork of the slab specimens was constructed using $\frac{3}{4}$ -in. thick plywood and 2×4 dimension lumber, as shown in Figure 2.12. The reinforcing steel and headed bars were then placed in the formwork with the support provided for headed bars from the bottom by chairs made of wood and from the top with a wooden truss to hold the headed bar(s) upright until the concrete had set. The specimens were cast in two layers, and each layer was consolidated using a spud vibrator. In accordance with ASTM C172, during casting, two samples of fresh concrete were obtained from the middle portion of the batch and combined to measure slump, temperature, and unit weight. Concrete cylinders (4×8 in. and 6×12 in.) were prepared in accordance with ASTM C31 and stored with the specimens until they were tested. The 4×8 in. concrete cylinders were used to track of concrete compressive strength gain, and the 6×12 in. concrete cylinders were used to measure the concrete compressive strength on the day of testing. For 5,000 psi concrete, the test specimens were wet-cured with saturated burlap and plastic sheeting until the concrete compressive strength reached 3,000 psi; the formwork was then removed, and the specimens were allowed to dry until they reached the desired strength before testing. For high-strength concrete (15,000 psi concrete), the specimens were continuously wet-cured after removing the formwork at a strength of 3,000 psi to allow the concrete to continue to gain strength. When the concrete reached the desired strength, the burlap and the plastic sheeting were removed and the specimens were prepared for testing.



Figure 2.12 Slab specimen formwork

2.6 TEST PROCEDURE

The test frame systems were a modified version of the test system used by Ghimire et al. (2018). Two test frame configurations were used in this study. The first configuration was used for tests with a single headed bar, while the second configuration was used for tests with two bars. In the first configuration (Figures 2.2 to 2.4 and Figure 2.13), two $1 \times 8 \times 50$ in. support reaction plates were first placed on the slab using high-strength gypsum cement paste (Hydrostone) between the concrete and the plates to ensure uniform contact. Two W12 \times 58 spreader beams were then placed on the support plates on either side of the anchored headed bar(s) to transfer loads from the hydraulic cylinder to the reaction support plates, as shown in Figures 2.2 to 2.4. A $15 \times 15 \times 2.5$ in. steel plate with a center hole (lower steel plate in Figure 2.13) was placed on the two spreader beams with the test bar passing through the hole in the plate. A 150-ton capacity hydraulic cylinder was then placed on the steel plate. A $6 \times 6 \times 1$ in. steel plate with a center hole (middle steel plate in Figure 2.13) was placed on the hydraulic cylinder. Then, a load cell with a $6 \times 6 \times 1$

in. steel plate (upper steel plate in Figure 2.13) was installed. The headed bar was locked in place using a collar and wedges.

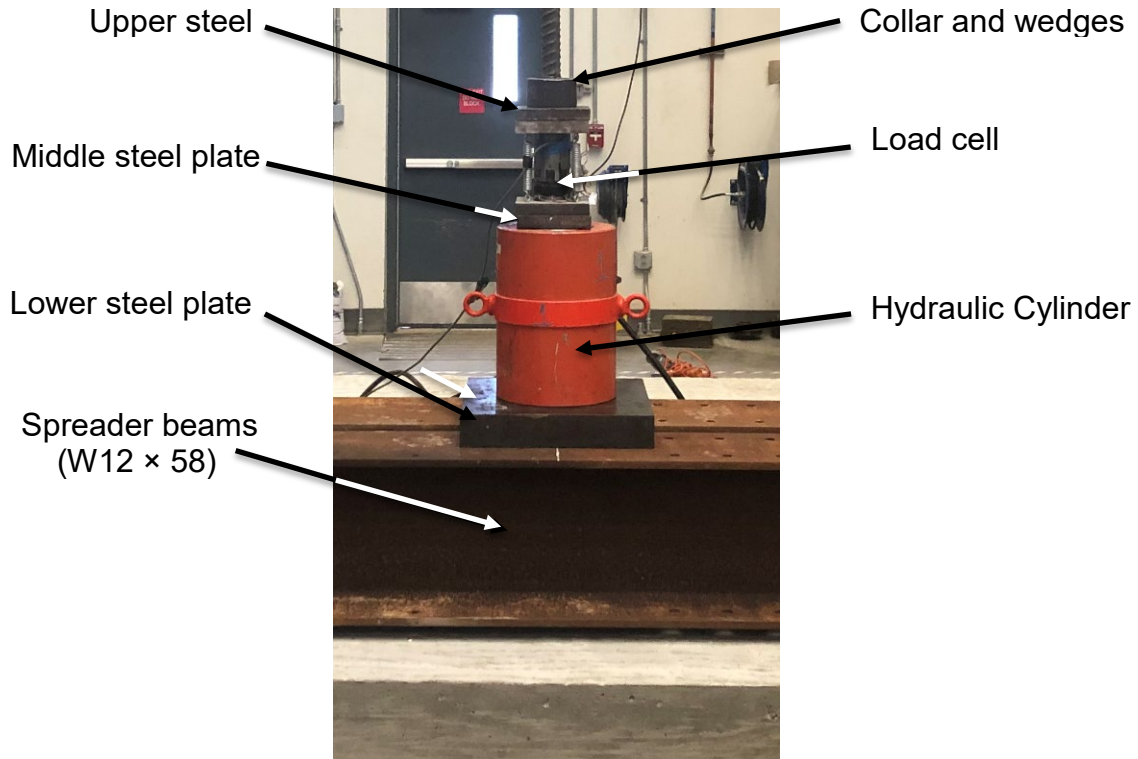


Figure 2.13 Test frame – first configuration

The second configuration (Figures 2.5 to 2.10 and Figure 2.14) was assembled with two $1 \times 8 \times 50$ in. support reaction plates placed on the slab using gypsum cement paste between the concrete and the plates to ensure uniform contact. Two HP16 \times 121 spreader beams were then placed on the support plates on either side of the headed bars to transfer loads from the hydraulic cylinders to the reaction support plates, as shown in Figures 2.5 to 2.10. Two 150-ton hydraulic cylinders were then placed on the spreader beams. An $8 \times 8 \times 2$ in. steel plate was placed on each hydraulic cylinder (the steel plate between the built-up section and the hydraulic cylinder in Figure 2.14). A built-up section, which consists of two steel channels (C12 \times 25) and two 1 in. thick steel plates welded on top and bottom of the steel channels, was then placed on top of the plates and hydraulic cylinders; the built-up section has holes on the top and the bottom plates that allow the test headed bars to pass through. Load cells, with $8 \times 8 \times 2$ in. steel plates (upper and lower steel

plates in Figure 2.14) and neoprene pads above and below each load cell, were placed on each test bar. The test bars were locked in place using collars and wedges. The complete test frame set up for this configuration is shown in Figure 2.14.



Figure 2.14 Test frame – second configuration

During testing, tensile load was applied monotonically to the headed bar(s) at intervals of 10 kips or 20 kips, depending on the anticipated failure load. Loading was paused after each interval to allow cracks to be marked. When the applied tensile load reached about 80% of the expected failure load, the specimen was loaded continuously until failure. The tensile load applied to each headed bar was measured using a load cell. After failure, cracks were marked, and photos were taken. The test frame was then disassembled, and the specimen dissected to examine internal cracks.

2.7 SPECIMEN INSTRUMENTATION

In addition to using the load cells to measure the applied tensile loads, LVDTs (linear variable differential transformers) and strain gauges were used in slab specimens that contained parallel tie reinforcement. LVDTs were used in specimens 8 through 15 to measure the slip of the headed bars. The LVDTs were clamped to the top flange of the spreader beams, as shown in Figure 2.15. A flat $\frac{1}{8}$ -in. thick plate welded to a steel ring was attached to each test bar and tightened in place using bolts to give the LVDTs a point of contact during the test, as shown in Figure 2.16.



Figure 2.15 LVDTs clamped to the top flange of the spreader beams



Figure 2.16 LVDT plates attached to test bars

Strain gauges were used on the parallel ties of slab specimens to measure the change in strain in the tie reinforcement at varying distances from the headed bar(s). One strain gauge was attached to a single leg of each hoop in the top quarter of the leg, as shown in Figure 2.17.

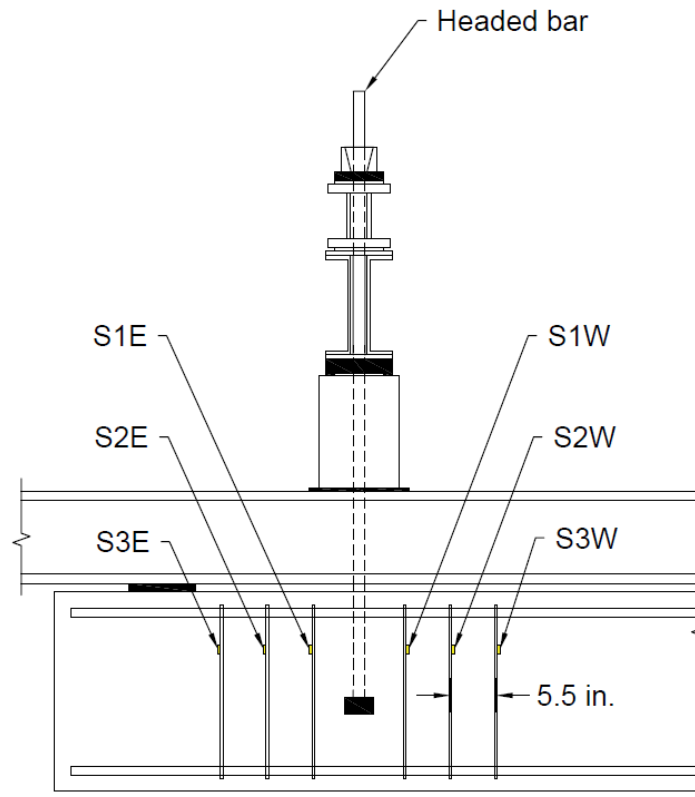


Figure 2.17 Location of the strain gauges on parallel ties

CHAPTER 3: TEST RESULTS AND ANALYSIS OF SIMULATED COLUMN-FOUNDATION JOINT SPECIMENS TESTED IN THE CURRENT AND PREVIOUS STUDIES AND COMPARISON BETWEEN THE PROPOSED EQUATIONS AND ACI 318-19 CODE PROVISIONS

In this chapter, the test results for the simulated column-foundation joint specimens using headed bars are presented. Failure mode, effects of test parameters on the anchorage strength of headed bars, and an analysis of test results from other studies and comparisons with the current study are presented. A comparison between descriptive equations developed by Shao et al. (2016) and the ACI 318-19 Code provisions is conducted. Finally, this chapter ends with recommended changes to Chapters 17 and 25 of ACI 318-19.

Student's t-test, is used throughout the chapter to determine if differences between two sets of data for a particular test parameter (such as the difference in failure load for test bars anchored in slab specimens with different concrete compressive strengths) are statistically significant. In the current study, a significance level of $\alpha = 0.05$ is used as the threshold, which means that there is at most a 5% probability that the difference between the two sets of data is due to random variation and not a difference in behavior. Smaller values of α indicate a greater probability of statistical significance.

3.1 TESTS OF HEADED BARS ANCHORED IN SIMULATED COLUMN-FOUNDATION JOINT SPECIMENS WITH SHALLOW EMBEDMENT

Headed bars, representing column longitudinal reinforcing bars, anchored in slab specimens were tested to investigate the anchorage strength and behavior of headed bars in column-foundation joints with the columns subjected to bending. Fifteen slab specimens, described in detail in Chapter 2, were tested to study the effects of support location, grouping of headed bars, spacing between the bars, bar size, parallel tie reinforcement, and concrete compressive strength on the anchorage strength of headed bars. Of the fifteen slab specimens, 11 contained two groups of two headed bars with the two bars in a group loaded simultaneously, two specimens had three headed bars loaded individually, one specimen contained two headed bars, each loaded individually, and one specimen had only one headed bar anchored in the center of the slab, for a total of 31 tests. The individual and grouped headed bars were embedded sufficiently far apart so that the anchorage failure of one headed bar or group did not interfere with anchorage

of the others. Of the 31 tests, 13 had parallel tie reinforcement within the joint region, while the remaining 18 had none. In the tests with parallel tie reinforcement, three tests included one No. 11 headed bar with one No. 4 bar hoop on both sides of the headed bar spaced at $2.8d_b$ (4 in.) from the centerline of the headed bar, as shown in Figure 2.6; three tests included two No. 11 headed bars loaded simultaneously with three No. 4 bar hoops placed on one side of the headed bars and spaced at $3.9d_b$ (5.5 in.), as shown in Figure 2.8; three tests involved two No. 11 headed bars loaded simultaneously with three No. 4 bar hoops placed on both sides of the headed bars and spaced at $3.9d_b$ (5.5 in.), as shown in Figure 2.8; two tests included two No. 14 headed bars loaded simultaneously with three No. 4 bar hoops placed on one side of the headed bars and spaced at $3.2d_b$ (5.5 in.), as shown in Figure 2.10; and two tests involved two No. 14 headed bars loaded simultaneously with three No. 4 bar hoops placed on both sides of the headed bars and spaced at $3.2d_b$ (5.5 in.), as shown in Figure 2.10. Embedment lengths ranged from $12\frac{5}{8}$ to 14 in., and parallel tie reinforcement within the joint region ranged between zero and six No. 4 stirrups, in the latter case with three on both sides of the headed bar. Concrete compressive strengths ranged from 5,060 to 14,470 psi, and stresses in the headed bars at failure ranged from 41,800 to 144,400 psi. The net bearing area of the headed bars ranged from 4.2 to $9.2A_b$.

A summary of 31 tests performed on the fifteen slab specimens, including the measured embedment length ℓ_{eh} , the measured concrete compressive strength f_{cm} , the total cross-sectional area of effective confining reinforcement parallel to the headed bars being developed A_{tt} (see Section 3.1.5), the distance between the center of the headed bars and the inner face of the nearest support reaction h_{cl} divided by the measured embedment length ℓ_{eh} , the net bearing area of the head A_{brg} divided by the headed bar area A_b , the ratio A_{tt}/A_{hs} (A_{hs} is the total cross-sectional area of headed bars being developed), the peak load on the headed bar at failure T_{peak} , the total peak load applied on the specimen T_{total} , the average peak load (total peak load applied on the specimen divided by the number of headed bars being developed) T , the anchorage strength calculated based on anchorage provisions in Chapter 17 of ACI 318-19 T_{anc} , the anchorage strength of a headed bar calculated based on descriptive equations (Shao et al. 2016) T_h , and the anchorage strength calculated based on Chapter 25 of ACI 318-19 $T_{ACI\ 318}$, is provided in Table 3.1, with the full details in Table B.1 of Appendix B. In addition to these specimens, the results of 32 tests conducted

on simulated column-foundation joints and reported by Ghimire et al. 2018 are shown in Table 3.2, with the full details in Table C.2 of Appendix C.

Table 3.1 Summary of key parameters of slab specimens^[1]

Specimens ^[2]			ℓ_{eh} (in.)	f_{cm} (psi)	A_{tr} (in. ²)	$\frac{h_{cl}}{\ell_{eh}}$	$\frac{A_{brg}}{A_b}$	$\frac{A_{tr}}{A_{hs}}$	T_{peak} (kips)	T_{total} (kips)	T (kips)
SN	Description	Group/ Head									
1	11-5-S5.5-6#6-0-12.75	A	13.38	5060	0.0	1.85	5.5	0.0	147.1	-	147.1
	11-5-S5.5-6#6-0-12.75	B	13.13		0.0	1.88	5.5	0.0	137.8	-	137.8
	11-5-S5.5-6#6-0-12.75	C	13.38		0.0	1.85	5.5	0.0	136.3	-	136.3
2	11-5-S5.5-10#6-0-12.75	A	13.38	5490	0.0	1.47	5.5	0.0	161.0	-	161.0
	11-5-S5.5-10#6-0-12.75	B	12.75		0.0	1.55	5.5	0.0	143.7	-	143.7
3	11-5-S5.5-6#11-0-12.75 ^[3]	A	13.63	5740	0.0	5.24	5.5	0.0	119.2	-	119.2
4	(2@3.2)11-5-S5.5-6#11-0-12.75	A1	13.50	5550	0.0	1.46	5.5	0.0	84.6	180.5	90.3
		A2	13.50		0.0	1.46	5.5	0.0	95.9		
	(2@3.2)11-5-S5.5-6#11-0-12.75	B1	13.38	6190	0.0	1.47	5.5	0.0	65.3	154.3	77.2
		B2	13.38		0.0	1.47	5.5	0.0	89.0		
5	11-5-S5.5-6#6-2#4-12.75	A	13.00	5810	0.8	1.90	5.5	0.51	203.7	-	203.7
	11-5-S5.5-6#6-2#4-12.75	B	12.88		0.8	1.92	5.5	0.51	220.9	-	220.9
	11-5-S5.5-6#6-2#4-12.75	C	13.13		0.8	1.88	5.5	0.51	225.2	-	225.2
6	(2@8.2)11-5-S5.5-7#11-0-12.75	A1	13.50	5370	0.0	1.46	5.5	0.0	91.3	199.0	99.5
		A2	13.50		0.0	1.46	5.5	0.0	107.7		
	(2@8.2)11-5-S5.5-7#11-0-12.75	B1	14.06		0.0	1.40	5.5	0.0	89.8	213.0	106.5
		B2	14.06		0.0	1.40	5.5	0.0	123.2		
7	(2@8.2)11-5-S5.5-7#11-0-12.75	A1	13.25	5110	0.0	1.49	5.5	0.0	84.7	176.2	88.1
		A2	13.25		0.0	1.49	5.5	0.0	91.5		
	(2@8.2)11-5-S5.5-7#11-0-12.75	B1	13.31		0.0	1.48	5.5	0.0	93.7	175.3	87.7
		B2	13.31		0.0	1.48	5.5	0.0	81.6		
8	(2@8.2)11-5-S9.2-7#11-3#4-12.75	A1	13.13	7950	0.8	1.50	9.2	0.26	130.4	267.0	133.5
		A2	13.13		0.8	1.50	9.2	0.26	136.5		
	(2@8.2)11-5-S9.2-7#11-6#4-12.75	B1	13.00		1.6	1.52	9.2	0.51	190.4	370.0	185.0
		B2	13.00		1.6	1.52	9.2	0.51	179.6		

^[1] SN = specimen number; ℓ_{eh} = measured embedment length; f_{cm} = measured concrete compressive strength; A_{tr} = total cross-sectional area of effective confining reinforcement (NA_{tr}) parallel to the headed bars being developed (in.²), N = total number of legs of effective confining reinforcement parallel to the headed bars being developed, A_{tr} = area of a single leg of confining reinforcement (in.²); h_{cl} = distance between the center of headed bar to the inner face of the nearest support plate; A_{brg} = net bearing area of the head (Table 2.3); A_b = area of the headed bar; A_{hs} = total cross-sectional area of headed bars being developed (nA_b), where n is the number of headed bars being developed; T_{peak} = peak load on the headed bar at failure; T_{total} = total peak load applied on the specimen; T = average peak load (total peak load applied on the specimen divided by the number of headed bars being developed)

^[2] Multiple headed bars in a single specimen loaded individually are denoted by letters A, B, and C, and grouped headed bars loaded simultaneously are denoted with a number after a common letter (A1, A2)

^[3] Specimen contained a single centrally placed headed bar

Table 3.1 Cont. Summary of key parameters of slab specimens^[1]

Specimens			T_{anc}	T_h	$T_{ACI\ 318}$	T_{calc}	$\frac{T}{T_{anc}}$	$\frac{T}{T_h}$	$\frac{T}{T_{ACI\ 318}}$	$\frac{T}{T_{calc}}$
SN	Description	Group/ Head	(kips)	(kips)	(kips)	(kips)				
1	11-5-S5.5-6#6-0-12.75	A	142.3	98.6	70.9	84.1	1.03	1.49	2.07	1.75
	11-5-S5.5-6#6-0-12.75	B	137.9	96.7	69.6	82.5	1.00	1.42	1.98	1.67
	11-5-S5.5-6#6-0-12.75	C	142.3	98.6	70.9	84.1	0.96	1.38	1.92	1.62
2	11-5-S5.5-10#6-0-12.75	A	148.3	100.6	71.7	85.8	1.09	1.60	2.25	1.88
	11-5-S5.5-10#6-0-12.75	B	136.9	95.7	68.3	81.8	1.05	1.50	2.10	1.76
3	11-5-S5.5-6#11-0-12.75	A	156.4	103.6	73.4	88.4	0.76	1.15	1.62	1.35
4	(2@3.2)11-5-S5.5-6#11-0-12.75	A1	84.1	62.3	45.3	48.3	1.07	1.45	1.99	1.87
		A2								
	(2@3.2)11-5-S5.5-6#11-0-12.75	B1	87.5	63.3	46.0	49.1	0.88	1.22	1.68	1.57
		B2								
5	11-5-S5.5-6#6-2#4-12.75	A	145.5	129.9	70.1	105.8	1.40	1.57	2.90	1.93
	11-5-S5.5-6#6-2#4-12.75	B	143.1	128.9	69.5	104.7	1.54	1.71	3.18	2.11
	11-5-S5.5-6#6-2#4-12.75	C	147.8	130.9	70.8	106.8	1.52	1.72	3.18	2.11
6	(2@8.2)11-5-S5.5-6#11-0-12.75	A1	95.6	101.0	72.2	86.1	1.04	0.99	1.38	1.16
		A2								
	(2@8.2)11-5-S5.5-6#11-0-12.75	B1	101.4	105.3	75.2	89.7	1.05	1.01	1.42	1.19
		B2								
7	(2@8.2)11-5-S5.5-6#11-0-12.75	A1	90.8	97.9	70.4	83.5	0.97	0.90	1.25	1.06
		A2								
	(2@8.2)11-5-S5.5-6#11-0-12.75	B1	91.4	98.4	70.7	83.9	0.96	0.89	1.24	1.04
		B2								
8	(2@8.2)11-5-S9.2-7#11-3#4-12.75	A1	111.7	134.2	81.8	111.4	1.19	0.99	1.63	1.20
		A2								
	(2@8.2)11-5-S9.2-7#11-6#4-12.75	B1	110.2	137.6	81.0	114.4	1.68	1.34	2.28	1.62
		B2								

^[1] SN = specimen number; T = average peak load (total peak load applied on the specimen divided by the number of headed bars being developed); T_{anc} = anchorage strength calculated based on anchorage provisions in Chapter 17 of ACI 318-19 divided by the number of headed bars being developed (in all cases concrete breakout failure governed the anchorage strength); T_h = anchorage strength of a headed bar calculated based on descriptive equations (Shao et al. 2016); $T_{ACI\ 318}$ = anchorage strength calculated based on Chapter 25 of ACI 318-19; T_{calc} = anchorage strength calculated based on the proposed Code provisions

Table 3.1 Cont. Summary of key parameters of slab specimens

Specimens			ℓ_{eh} (in.)	f_{cm} (psi)	A_{tt} (in. ²)	$\frac{h_{cl}}{\ell_{eh}}$	$\frac{A_{brg}}{A_b}$	$\frac{A_{tt}}{A_{hs}}$	T_{peak} (kips)	T_{total} (kips)	T (kips)
SN	Description	Group/ Head									
9	(2@8.2)11-5-S9.2- 7#11-3#4-12.75	A1	13.25	7680	0.8	1.49	9.2	0.26	138.6	281.3	140.7
		A2	13.25		0.8	1.49	9.2	0.26	142.7		
	(2@8.2)11-5-S9.2- 7#11-6#4-12.75	B1	13.38		1.6	1.47	9.2	0.51	179.3	354.2	177.1
		B2	13.38		1.6	1.47	9.2	0.51	174.9		
10	(2@8.2)11-15-S9.2- 7#11-0-12.75	A1	12.69	14470	0.0	1.55	9.2	0.00	124.3	249.6	124.8
		A2	12.69		0.0	1.55	9.2	0.00	125.3		
	(2@8.2)11-15-S9.2- 7#11-0-12.75	B1	12.75		0.0	1.55	9.2	0.00	134.5	261.9	131.0
		B2	12.75		0.0	1.55	9.2	0.00	127.4		
11	(2@8.2)11-15-S9.2- 7#11-3#4-12.75	A1	12.75	14140	0.8	1.55	9.2	0.26	156.6	314.5	157.3
		A2	12.75		0.8	1.55	9.2	0.26	157.9		
	(2@8.2)11-15-S9.2- 7#11-6#4-12.75	B1	12.63	14080	1.6	1.56	9.2	0.51	168.4	335.5	167.8
		B2	12.63		1.6	1.56	9.2	0.51	167.1		
12	(2@6.8)14-5-B4.2- 7#11-0-12.75	A1	13.00	6040	0.0	1.53	4.2	0.00	121.5	239.0	119.5
		A2	13.00		0.0	1.53	4.2	0.00	117.5		
	(2@6.8)14-5-B4.2- 7#11-0-12.75	B1	13.13	6180	0.0	1.51	4.2	0.00	129.1	259.0	129.5
		B2	13.13		0.0	1.51	4.2	0.00	129.9		
13	(2@6.8)14-5-B4.2- 7#11-3#4-12.75	A1	13.00	5440	1.2	1.53	4.2	0.27	139.0	274.6	137.3
		A2	13.00		1.2	1.53	4.2	0.27	135.6		
	(2@6.8)14-5-B4.2- 7#11-6#4-12.75	B1	12.75	5480	2.4	1.56	4.2	0.53	164.0	319.8	159.9
		B2	12.75		2.4	1.56	4.2	0.53	155.8		
14	(2@6.8)14-15-B4.2- 7#11-0-12.75	A1	13.13	14030	0.0	1.51	4.2	0.00	171.2	346.0	173.0
		A2	13.13		0.0	1.51	4.2	0.00	174.8		
	(2@6.8)14-15-B4.2- 7#11-0-12.75	B1	13.13	14050	0.0	1.51	4.2	0.00	160.5	323.8	161.9
		B2	13.13		0.0	1.51	4.2	0.00	163.3		
15	(2@6.8)14-15-B4.2- 7#11-3#4-12.75	A1	13.38	13190	1.2	1.48	4.2	0.27	182.6	370.1	185.1
		A2	13.38		1.2	1.48	4.2	0.27	187.5		
	(2@6.8)14-15-B4.2- 7#11-6#4-12.75	B1	12.88	13020	2.4	1.54	4.2	0.53	195.0	388.8	194.4
		B2	12.88		2.4	1.54	4.2	0.53	193.8		

Table 3.1 Cont. Summary of key parameters of slab specimens

Specimens			T_{anc}	T_h	$T_{ACI\ 318}$	T_{calc}	$\frac{T}{T_{anc}}$	$\frac{T}{T_h}$	$\frac{T}{T_{ACI\ 318}}$	$\frac{T}{T_{calc}}$
SN	Description	Group/ Head	(kips)	(kips)	(kips)	(kips)				
9	(2@8.2)11-5-S9.2-7#11-3#4-12.75	A1	111.3	134.4	81.1	111.5	1.26	1.05	1.73	1.26
		A2								
	(2@8.2)11-5-S9.2-7#11-6#4-12.75	B1	112.8	139.9	81.9	116.7	1.57	1.27	2.16	1.52
		B2								
10	(2@8.2)11-15-S9.2-7#11-0-12.75	A1	143.5	120.2	106.7	103.7	0.87	1.04	1.17	1.20
		A2								
	(2@8.2)11-15-S9.2-7#11-0-12.75	B1	144.5	120.8	107.2	104.2	0.91	1.08	1.22	1.26
		B2								
11	(2@8.2)11-15-S9.2-7#11-3#4-12.75	A1	142.9	146.5	105.9	125.0	1.10	1.07	1.48	1.26
		A2								
	(2@8.2)11-15-S9.2-7#11-6#4-12.75	B1	140.6	149.7	104.7	128.1	1.19	1.12	1.60	1.31
		B2								
12	(2@6.8)14-5-B4.2-7#11-0-12.75	A1	96.0	97.2	77.4	77.9	1.24	1.23	1.54	1.53
		A2								
	(2@6.8)14-5-B4.2-7#11-0-12.75	B1	98.5	98.7	79.0	79.1	1.32	1.31	1.64	1.64
		B2								
13	(2@6.8)14-5-B4.2-7#11-3#4-12.75	A1	91.1	145.2	76.3	99.6	1.51	0.95	1.80	1.38
		A2								
	(2@6.8)14-5-B4.2-7#11-6#4-12.75	B1	88.9	149.0	74.9	101.8	1.80	1.07	2.13	1.57
		B2								
14	(2@6.8)14-15-B4.2-7#11-0-12.75	A1	148.4	120.1	119.1	97.1	1.17	1.44	1.45	1.78
		A2								
	(2@6.8)14-15-B4.2-7#11-0-12.75	B1	148.5	120.2	119.2	97.2	1.09	1.35	1.36	1.67
		B2								
15	(2@6.8)14-15-B4.2-7#11-3#4-12.75	A1	147.8	172.6	117.7	127.8	1.25	1.07	1.57	1.45
		A2								
	(2@6.8)14-15-B4.2-7#11-6#4-12.75	B1	139.0	172.9	112.5	127.6	1.40	1.12	1.73	1.52
		B2								

Table 3.2 Summary of key parameters of slab specimens (Ghimire et al. 2018) ^[1]

Specimens			ℓ_{eh}	f_{cm}	h_{cl}	$\frac{h_{cl}}{\ell_{eh}}$	$\frac{A_{brg}}{A_b}$	$\frac{A_{st}}{A_b}$ [2]	T
SN	Description	Group/ Head	(in.)	(psi)	(in.)				(kips)
1	8-5-T9.5-8#5-6 [3]	A	8.00	7040	10.5	1.31	9.5	1.29	65.6
	8-5-T9.5-8#5-6 [3]	B	8.25		10.5	1.27	9.5	1.29	67.8
2	8-5-T4.0-8#5-6	A	8.50	7040	10.5	1.24	4	0.00	61.8
	8-5-T4.0-8#5-6	B	7.50		10.5	1.40	4	0.00	56.3
3	8-5-F4.1-8#5-6 [3]	A	7.44	5220	10.5	1.41	4.1	1.29	68.9
	8-5-F4.1-8#5-6 [3]	B	7.38		10.5	1.42	4.1	1.29	64.4
4	8-5-F9.1-8#5-6 [3]	A	7.13	5220	10.5	1.47	9.1	1.29	69.9
	8-5-F9.1-8#5-6 [3]	B	7.00		10.5	1.50	9.1	1.29	54.9
5	8-5-F4.1-2#8-6	A	6.00	7390	10.5	1.75	4.1	0.00	64.4
	8-5-F9.1-2#8-6	B	6.00		10.5	1.75	9.1	0.00	65.0
6	8-5-T4.0-2#8-6	A	6.06	7390	10.5	1.73	4	0.00	60.5
	8-5-T9.5-2#8-6	B	6.13		10.5	1.71	9.5	0.00	57.7
7	8-8-O12.9-6#5-6	A	6.25	8620	9.8	1.57	13	0.00	79.0
	8-8-O9.1-6#5-6	B	6.25		10.5	1.68	9.1	0.00	70.9
8	8-8-S6.5-6#5-6	A	6.38	8620	10	1.57	6.5	0.00	73.0
	8-8-O4.5-6#5-6	B	6.50		10.8	1.66	4.5	0.00	74.0
9	8-5-S14.9-6#5-6	A	6.50	4200	10.3	1.58	15	0.00	61.8
	8-5-S6.5-6#5-6	B	6.50		10	1.54	6.5	0.00	49.2
10	8-5-O12.9-6#5-6	A	6.63	4200	10	1.51	13	0.00	52.4
	8-5-O4.5-6#5-6	B	6.50		10.1	1.55	4.5	0.00	50.1
11	8-5-S9.5-6#5-6	A	6.50	4200	10.3	1.58	9.5	0.00	48.9
	8-5-S9.5-6#5-6	B	6.38		10.1	1.58	9.5	0.00	54.5
12	8-5-F4.1-6#5-6 [4]	-	8.44	4200	47.3	5.60	4.1	0.00	39.1
13	8-5-F4.1-0-6	A	6.50	5180	15	2.31	4.1	0.00	50.5
	8-5-F4.1-0-6	B	6.25		17	2.72	4.1	0.00	48.9
	8-5-F4.1-2#5-6	C	6.75		17	2.52	4.1	0.78	61.5
14	8-5-F4.1-4#5-6	A	6.00	5180	16.8	2.80	4.1	1.57	53.4
	8-5-F4.1-4#5-6	B	6.13		17	2.77	4.1	1.57	52.4
	8-5-F4.1-4#5-6	C	6.75	5460	17	2.52	4.1	1.57	53.5
15	8-5-F4.1-6#5-6	A	6.25	5460	17	2.72	4.1	2.35	47.3
	8-5-F4.1-6#5-6	B	6.63		16.8	2.53	4.1	2.35	55.9
	8-5-F4.1-6#5-6	C	6.88		17	2.47	4.1	2.35	52.6

[1] All tests had individual headed bar; T = peak load on the headed bar at failure

[2] A_{st} = area of reinforcement in a plane perpendicular to the headed bar within a $1.5\ell_{eh}$ radial distance from the center of the bar (in.²)

[3] In addition to 8 No. 5 bars as reinforcement perpendicular to the headed bar, specimens contained No. 4 bars spaced at 12 in. in a direction perpendicular to the No. 5 bars

[4] Specimen contained a single centrally placed headed bar

Table 3.2 Cont. Summary of key parameters of slab specimens (Ghimire et al. 2018)

Specimens			T_{anc}	T_h	T_{ACI318}	T_{calc}	$\frac{T}{T_{anc}}$	$\frac{T}{T_h}$	$\frac{T}{T_{ACI318}}$	$\frac{T}{T_{calc}}$
SN	Description	Group/ Head	(kips)	(kips)	(kips)	(kips)				
1	8-5-T9.5-8#5-6	A	75.6	55.8	39.8	46.3	0.87	1.18	1.65	1.42
	8-5-T9.5-8#5-6	B	79.2	57.5	41.0	47.8	0.86	1.18	1.65	1.42
2	8-5-T4.0-8#5-6	A	82.8	59.3	42.3	49.2	0.75	1.04	1.46	1.26
	8-5-T4.0-8#5-6	B	68.6	52.2	37.3	43.4	0.82	1.08	1.51	1.30
3	8-5-F4.1-8#5-6	A	58.4	48.2	33.6	40.0	1.18	1.43	2.05	1.72
	8-5-F4.1-8#5-6	B	57.7	47.8	33.3	39.6	1.12	1.35	1.93	1.62
4	8-5-F9.1-8#5-6	A	54.8	46.1	32.2	38.3	1.28	1.52	2.17	1.82
	8-5-F9.1-8#5-6	B	53.3	45.2	31.6	37.6	1.03	1.21	1.74	1.46
5	8-5-F4.1-2#8-6	A	50.3	41.9	30.6	35.2	1.28	1.54	2.11	1.83
	8-5-F9.1-2#8-6	B	50.3	41.9	30.6	35.2	1.29	1.55	2.13	1.85
6	8-5-T4.0-2#8-6	A	51.1	42.4	30.9	35.5	1.18	1.43	1.96	1.70
	8-5-T9.5-2#8-6	B	52.0	42.9	31.2	35.9	1.11	1.35	1.85	1.61
7	8-8-O12.9-6#5-6	A	57.8	45.4	34.4	38.1	1.37	1.74	2.30	2.08
	8-8-O9.1-6#5-6	B	57.8	45.4	34.4	38.1	1.23	1.56	2.06	1.86
8	8-8-S6.5-6#5-6	A	59.6	46.4	35.1	38.9	1.23	1.57	2.08	1.88
	8-8-O4.5-6#5-6	B	61.3	47.3	35.8	39.6	1.21	1.57	2.07	1.87
9	8-5-S14.9-6#5-6	A	42.8	39.8	28.4	33.1	1.44	1.55	2.18	1.87
	8-5-S6.5-6#5-6	B	42.8	39.8	28.4	33.1	1.15	1.24	1.73	1.49
10	8-5-O12.9-6#5-6	A	44.1	40.6	28.9	33.7	1.19	1.29	1.81	1.55
	8-5-O4.5-6#5-6	B	42.8	39.8	28.4	33.1	1.17	1.26	1.77	1.51
11	8-5-S9.5-6#5-6	A	42.8	39.8	28.4	33.1	1.14	1.23	1.72	1.48
	8-5-S9.5-6#5-6	B	41.6	39.0	27.8	32.5	1.31	1.40	1.96	1.68
12	8-5-F4.1-6#5-6	-	63.3	52.0	36.8	42.9	0.62	0.75	1.06	0.91
13	8-5-F4.1-0-6	A	47.5	41.8	29.3	34.9	1.06	1.21	1.72	1.45
	8-5-F4.1-0-6	B	44.8	40.2	28.2	33.5	1.09	1.22	1.73	1.46
	8-5-F4.1-2#5-6	C	50.3	43.5	30.4	36.2	1.22	1.41	2.02	1.70
14	8-5-F4.1-4#5-6	A	42.1	38.5	27.1	32.2	1.27	1.39	1.97	1.66
	8-5-F4.1-4#5-6	B	43.5	39.4	27.7	32.9	1.20	1.33	1.89	1.59
	8-5-F4.1-4#5-6	C	51.6	44.0	30.7	36.7	1.04	1.22	1.75	1.46
15	8-5-F4.1-6#5-6	A	46.0	40.7	28.4	34.0	1.03	1.16	1.67	1.39
	8-5-F4.1-6#5-6	B	50.2	43.2	30.1	36.0	1.11	1.29	1.86	1.55
	8-5-F4.1-6#5-6	C	53.1	44.9	31.2	37.4	0.99	1.17	1.68	1.41

3.1.1 Failure and Failure Modes

The anchorage failures observed during the tests are described in this section. Anchorage failure is defined as the failure of the concrete around the test bar(s) accompanied by the loss of load carrying capacity of the bars. Figure 3.1 depicts the typical concrete surface failure and crack progression observed on the top and sides of the specimens. Although the quantity and shape of

cracking varied between specimens, overall crack propagation followed similar patterns. Cracking almost always started with a horizontal crack on the top face of the specimen at the level of the headed bars, extending slightly on both sides of the bars, as shown in Figure 3.1a. This cracking pattern is similar to that found in reinforced concrete beams with bond failures for straight bar reinforcement, and it is most likely caused by slip of the straight portion of the bar. As the load increased, the horizontal cracks on both sides of the bars connected and extended toward the sides of the specimen, accompanied by radial cracks extending from the bars, as shown in Figure 3.1b. As the load further increased, the horizontal and the radial cracks continued to grow toward the sides of the specimen and the test frame support reactions. In the meantime, vertical and diagonal cracks branching from the horizontal and the radial cracks towards the sides of the specimen and the test frame support reactions. At this level, as shown in Figure 3.1c, the cracks on the top face of the specimen had reached the nearest test frame support reaction, which served as the compression region of the virtual column in a column-foundation joint; at this point, no cracks had formed on the sides of the specimen. Near failure, new cracks branching from the existing cracks on the top face of the specimen extended along with the horizontal and radial cracks toward the sides of the specimen and the test frame support reactions. Cracks around the headed bars grew toward the farthest test frame support reaction and the sides of the specimen, forming diagonal cracks on the side face of the specimen extending from the headed bar toward the nearest and farthest test frame support reactions, as shown in Figure 3.1d. The presence of parallel tie reinforcement within the joint region was found to have a direct correlation with the amount of cracking: specimens that contained parallel tie reinforcement, in general, exhibited a greater amount of cracking prior to failure than those that did not contain parallel tie reinforcement. All specimens exhibited a concrete breakout failure, as defined by Section R17.5.1.2 of ACI 318-19. Concrete breakout failures are characterized by a mass of concrete being pulled out of the slab along with the headed bar, forming a cone-shaped failure surface, as shown in Figure 3.2. The cone-shaped pattern region formed during concrete breakout suggests that the head attached to the test bar provides the primary anchorage after slip has occurred along the straight portion of the headed bar. The specific failure pattern was dependent on the location of the test frame support reactions, as shown in Figures 3.3 through 3.7. Figure 3.3 shows the failure pattern of specimens

that have both of the test frame support reactions placed at a clear distance of 24 in. from the headed bar to the inner face of the support reaction plate, just outside the anticipated failure region; this test included one headed bar with parallel tie reinforcement on both sides of the headed bar (Figure 2.6). Figures 3.4 through 3.6 show the failure patterns of specimens that have one of the test frame support reactions placed at a clear distance of 19 in. from the headed bar to the inner face of the support reaction plate (within the anticipated failure region) and the other support reaction placed at a clear distance of 83 in. from the headed bar to the inner face of the support reaction plate (outside the anticipated failure region); a configuration representing the compression zone of a column anchored in a foundation subjected to an overturning moment. Figure 3.4 shows the failure pattern of slab specimens containing two headed bars loaded simultaneously without parallel tie reinforcement, while Figures 3.5 and 3.6 show the failure patterns of slab specimens containing two headed bars loaded simultaneously with parallel tie reinforcement only on one side and on both sides of the headed bars, respectively. Figure 3.7 shows the failure pattern of the slab specimen containing only one headed bar anchored at the middle of the slab without parallel tie reinforcement, with both of the test frame support reactions located at a clear distance of 74 in. from the headed bar to the inner face of the support reaction plate, outside of the anticipated failure region to avoid interference with the concrete breakout failure surface. The effect of the test frame support reactions on the anchorage strength of headed bar(s) is described in Section 3.1.2.

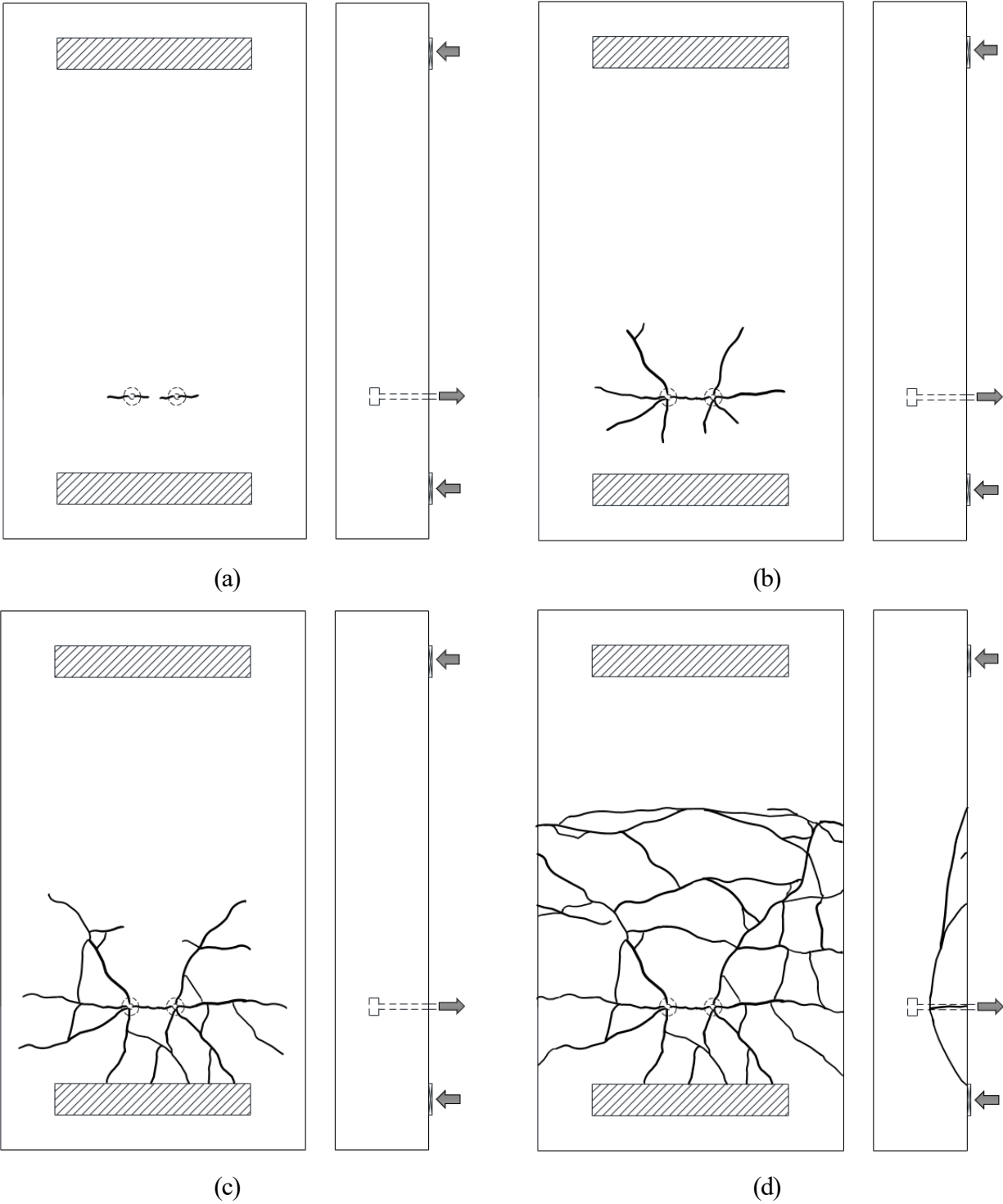
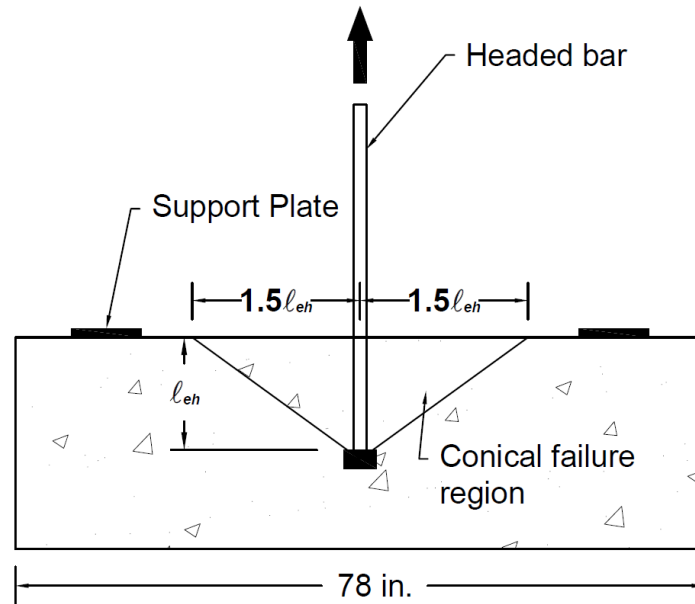
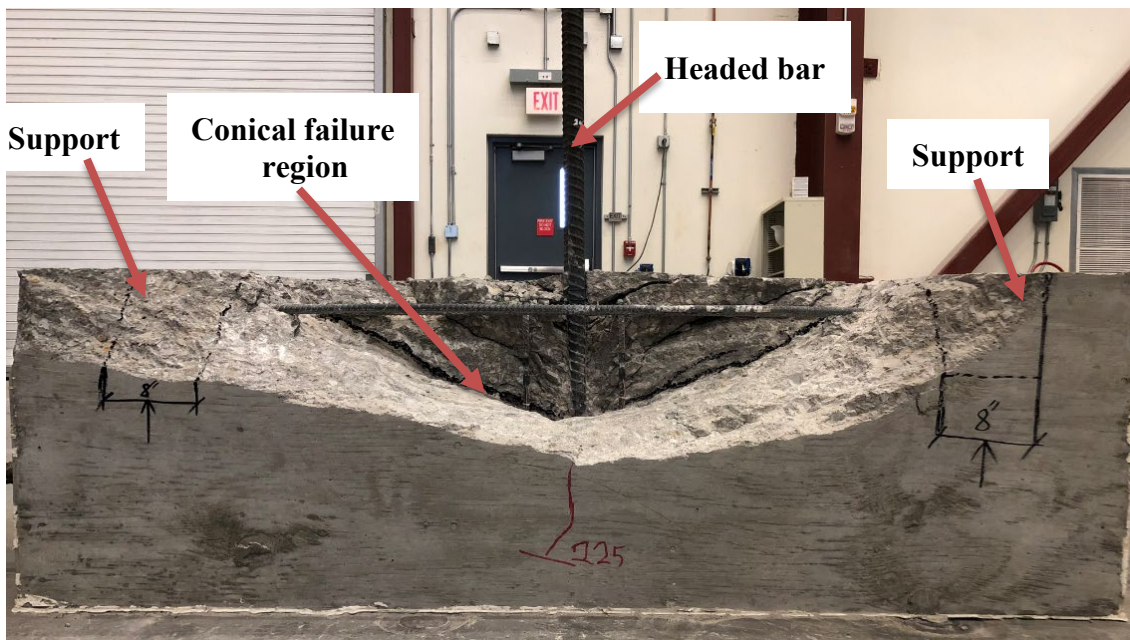


Figure 3.1 Concrete surface failure (crack propagation top and side views)



(a)



(b)

Figure 3.2 Concrete cone-shaped breakout failure (a) schematic drawing (b) Slab Specimen 5 (test 2, 11-5-S5.5-6#6-2#4-12.75) after removal of breakout region

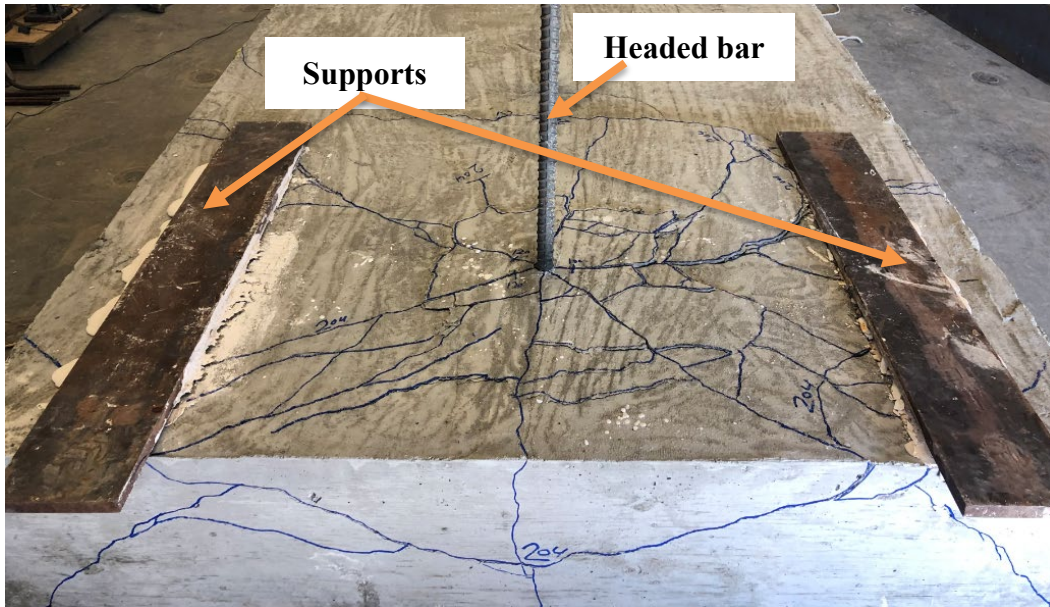
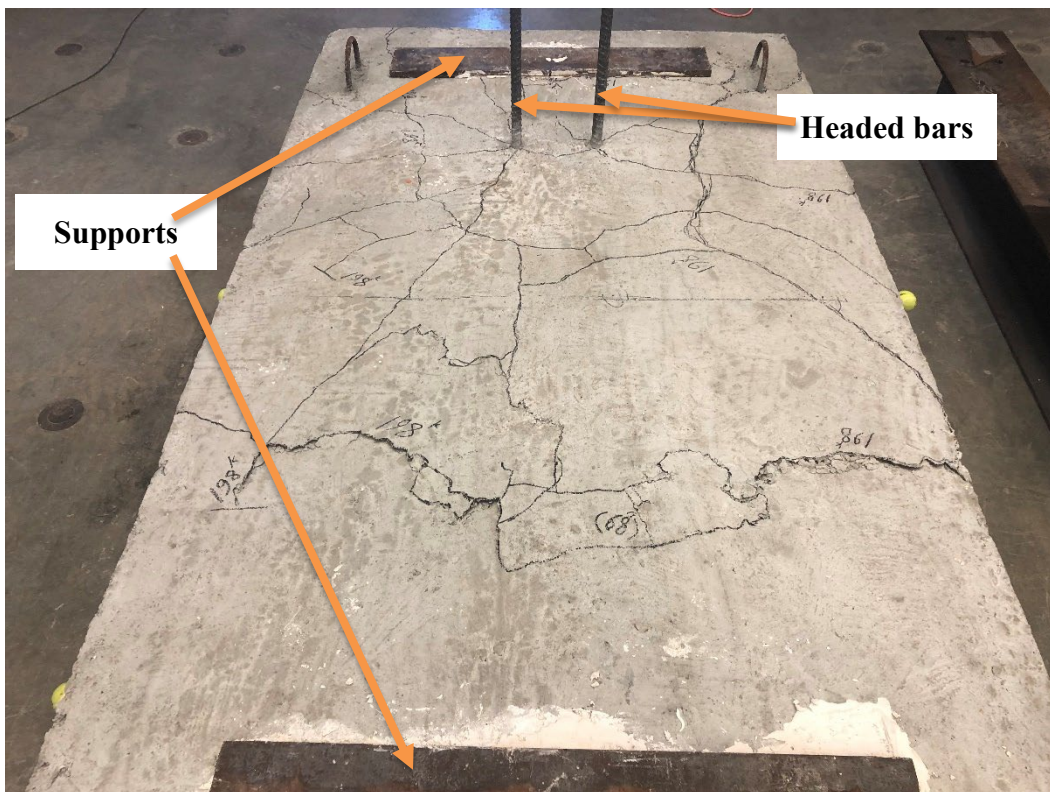
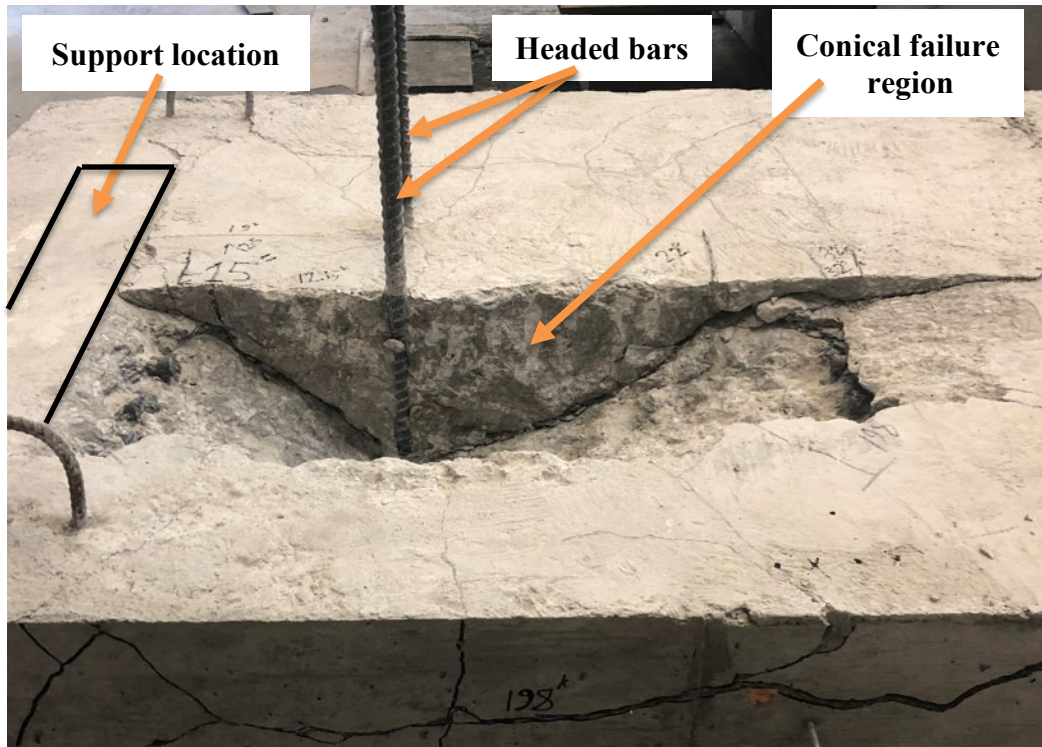


Figure 3.3 Concrete breakout failure. Slab Specimen 5 (test 1, 11-5-S5.5-6#6-2#4-12.75) with both support reactions just outside anticipated failure region (test had one headed bar with parallel tie reinforcement on both sides of headed bar)

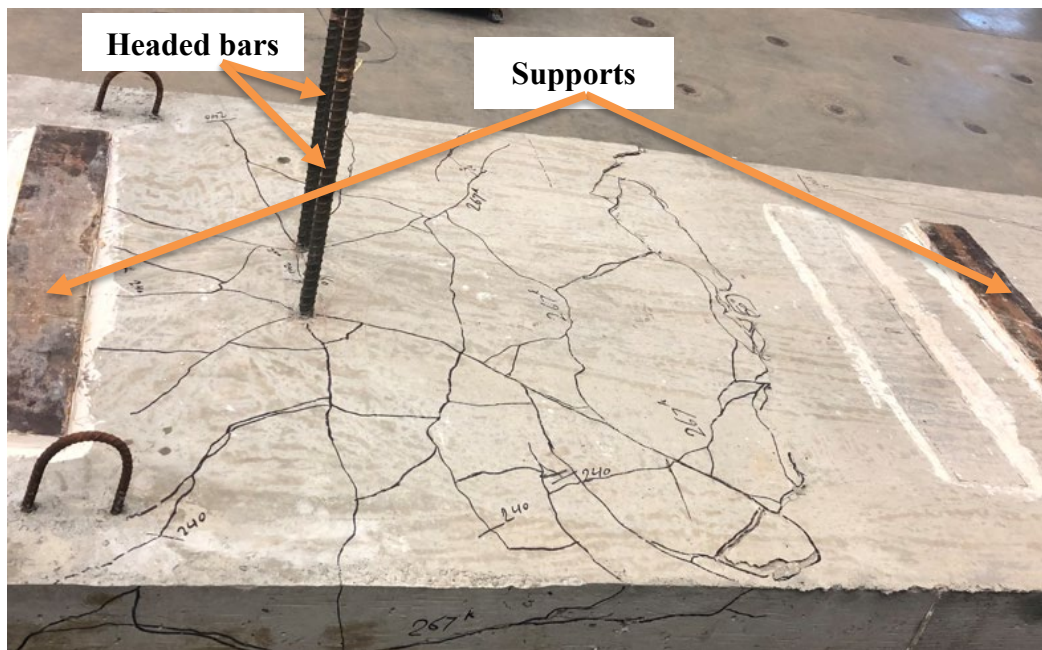


(a)

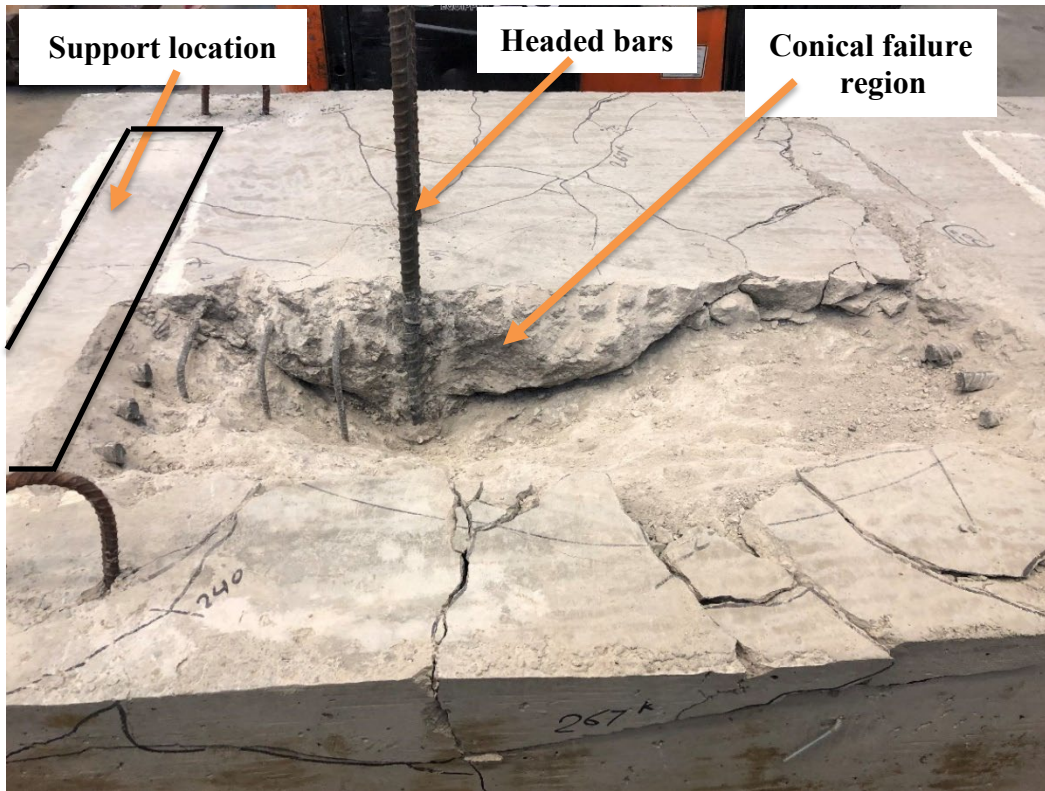


(b)

Figure 3.4 Concrete breakout failure of Slab Specimen 6 (test 1, (2@8.2)11-5-S5.5-7#11-0-12.75) with one of the support reactions placed within anticipated failure region (test had two headed bars without parallel tie reinforcement) (a) concrete surface failure (b) cone-shaped failure after removal of breakout region

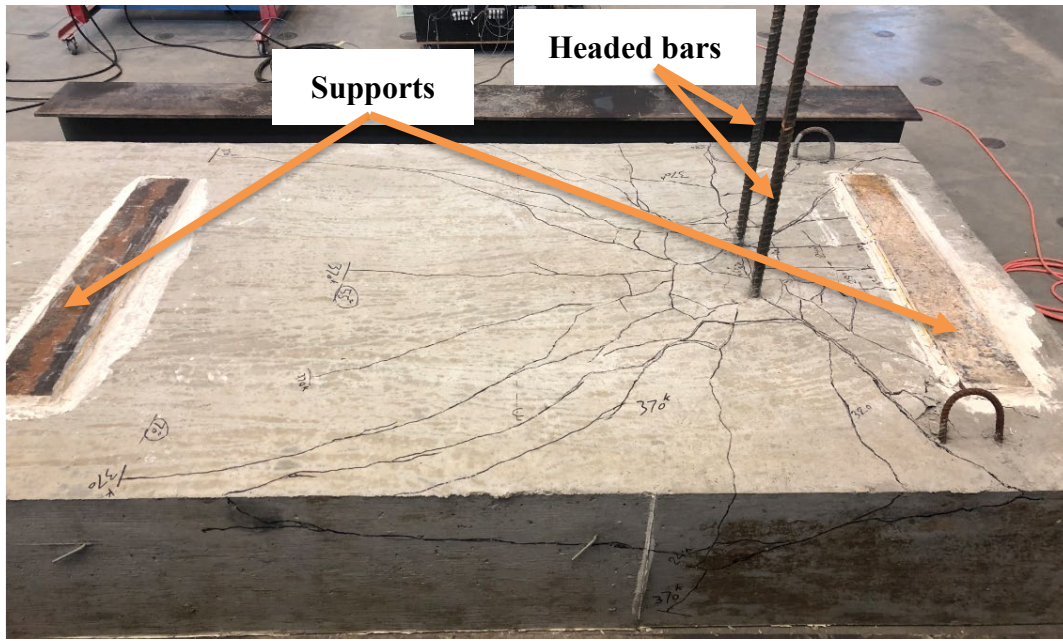


(a)

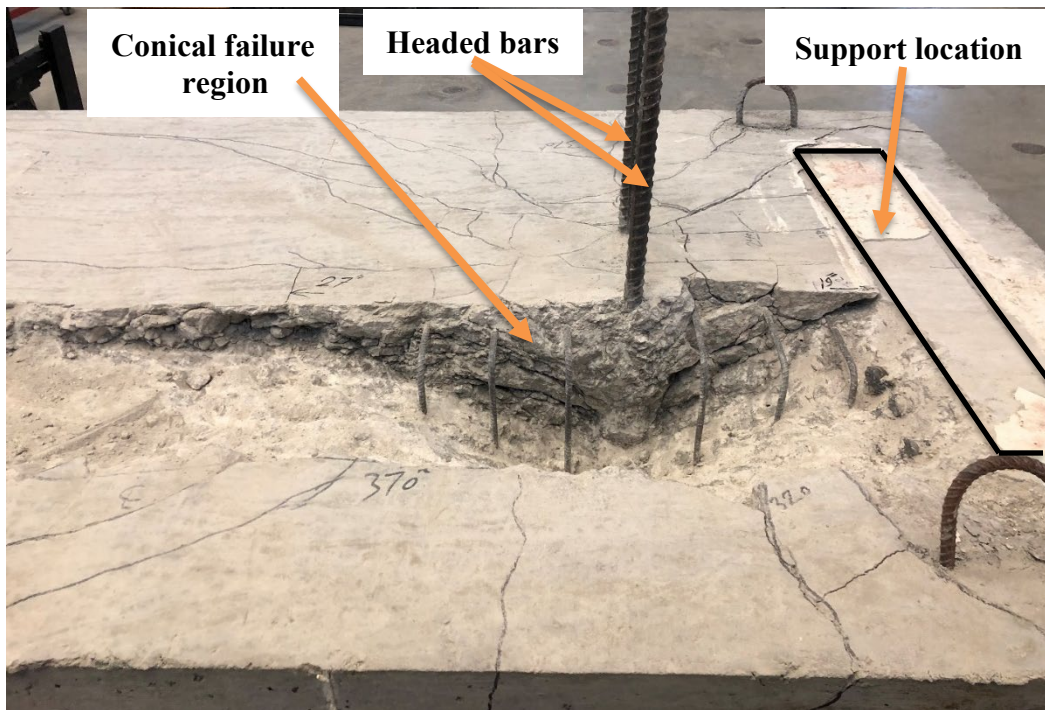


(b)

Figure 3.5 Concrete breakout failure of Slab Specimen 8 (test 1, (2@8.2)11-5-S9.2-7#11-3#4-12.75) with one of the support reactions placed within anticipated failure region (test had two headed bars with parallel tie reinforcement only on one side of headed bars) (a) concrete surface failure (b) cone-shaped failure after removal of breakout region



(a)



(b)

Figure 3.6 Concrete breakout failure of Slab Specimen 8 (test 2, (2@8.2)11-5-S9.2-7#11-6#4-12.75) with one of the support reactions placed within anticipated failure region (test had two headed bars with parallel tie reinforcement on both sides of headed bars) (a) concrete surface failure (b) cone-shaped failure after removal of breakout region

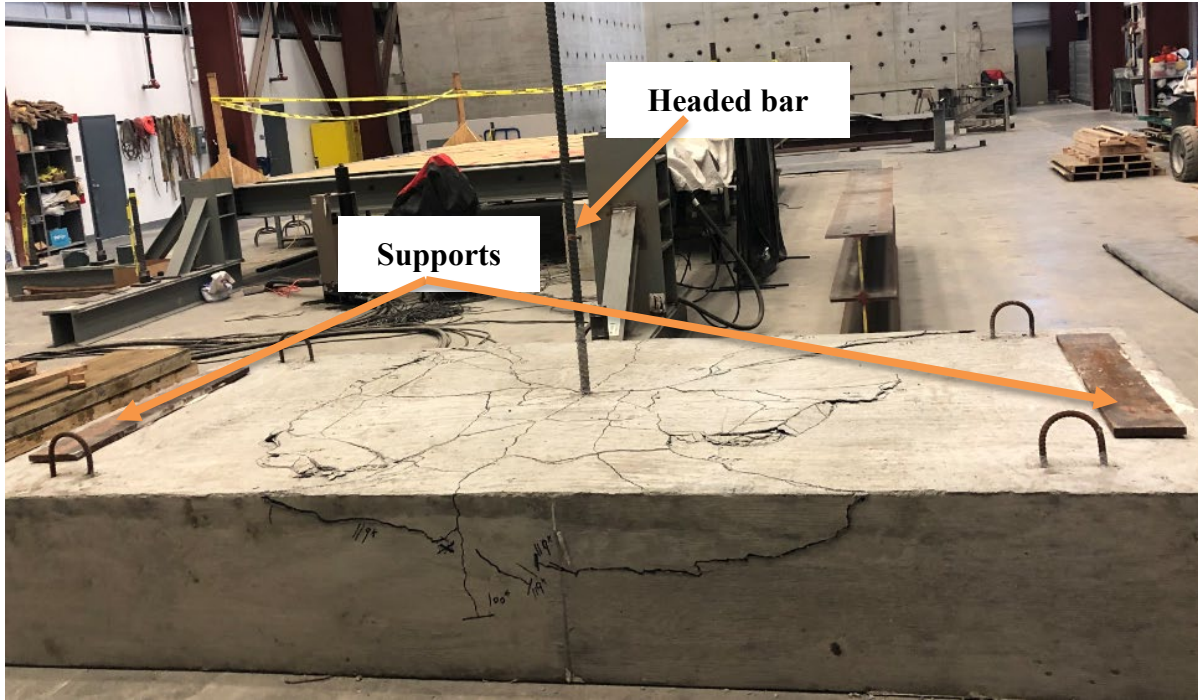


Figure 3.7 Concrete breakout failure of Slab Specimen 3 (11-5-S5.5-6#11-0-12.75) with both support reactions placed far away from anticipated failure region (test had one headed bars without parallel tie reinforcement)

3.1.2 Effect of Strut Angle

The anchorage strength of headed bars is affected by the strut angle (Figure 3.8) between the head and the compressive reaction (Eligehausen et al. 2006b). In general, the flatter the strut angle, the lower the anchorage strength. Shao et al. (2016) found that headed bars in beam-column joints exhibited low anchorage strengths when the ratio of the effective depth of the beam d to the embedment length ℓ_{eh} increased above 1.5, equivalent to a strut angle of 35 degrees. Shao et al.'s (2016) observations match the recommendations in Commentary Section R25.4.4.2 of ACI 318-19, which states that “anchorage strengths will be generally higher if the anchorage length is equal to or greater than $d/1.5$.” To determine if this behavior is observable in column-foundation joints as well, the effect of the strut angle on the anchorage strength of headed bars was investigated. The anchorage strength of headed bars in the slab specimens is plotted versus the ratio h_{cl}/ℓ_{eh} in Figure 3.9, where h_{cl} is the horizontal distance from the center of the headed bar to the face of the nearest support reaction plate, as shown in Figure 3.8. The effect of the strut angle on the anchorage

strength of headed bars was examined using the test results of Slab Specimens 1, 2, and 3 (Table 3.1) and the results from the tests conducted by Ghimire et al. (2018) (Table 3.2).

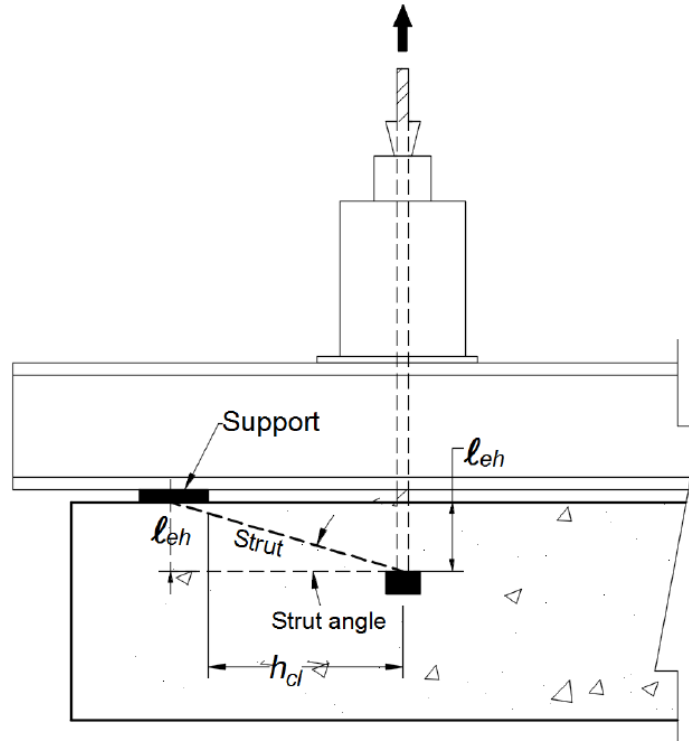


Figure 3.8 Strut angle between anchored headed bar and nearest support reaction (Krishna et al. 2018)

Shao et al. (2016) observed from tests of exterior beam-column joints that headed bars with a net bearing area, A_{brg} , ranging from 3.8 to $9.5A_b$ had similar anchorage strengths; in contrast, A_{brg} greater than $9.5A_b$ ($A_{brg} = 13$ to $15A_b$) tended to increase the anchorage strength of headed bars by about 15%. Therefore, only tests with A_{brg} less than or equal to $9.5A_b$ are included in Figure 3.9. Specimens included in Figure 3.9 have different concrete compressive strengths and embedment lengths. Thus, the peak load on the headed bar at failure (T) is normalized with respect to a concrete compressive strength of 5,000 psi and an embedment length of 12.75 in. using Eq. (3.1). The powers of 0.24 and 1.03 in Eq. (3.1) are those for f_{cm} and ℓ_{eh} , respectively, in the descriptive equations developed by Shao et al. (2016), Eq. (1.7) and (1.8).

$$T_N = T \left(\frac{5000 \text{ psi}}{f_{cm}} \right)^{0.24} \left(\frac{12.75 \text{ in.}}{\ell_{eh}} \right)^{1.03} \quad (3.1)$$

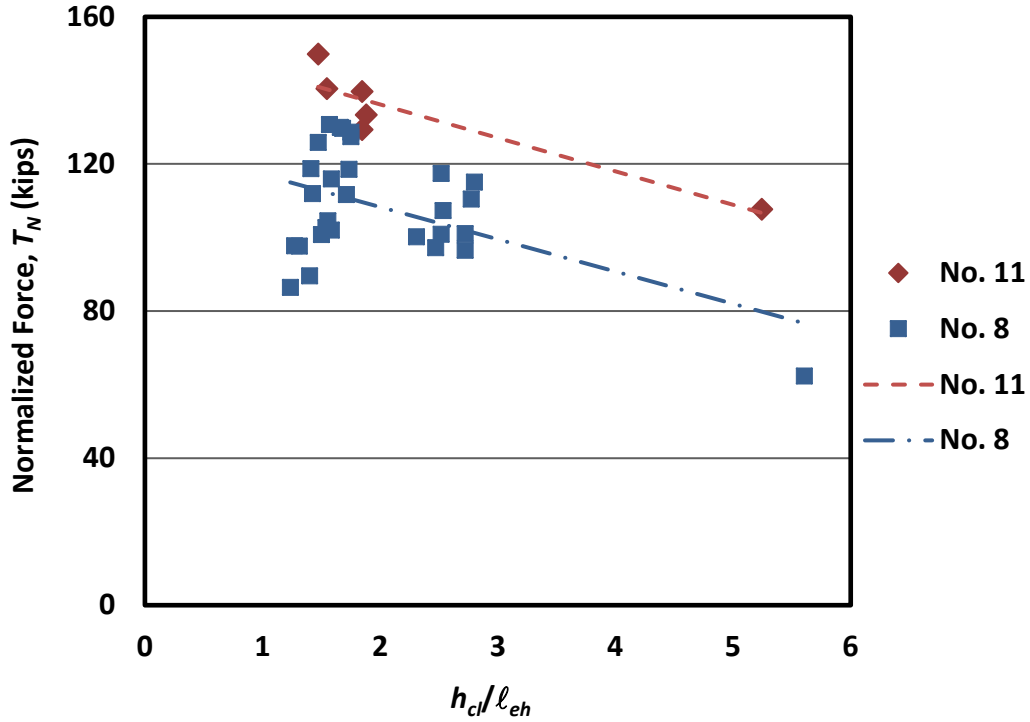


Figure 3.9 Bar force at failure normalized with respect to a concrete compressive strength of 5,000 psi, and an embedment length of 12.75 in., T_N , versus the ratio h_{cl}/ℓ_{eh} (defined in Figure 3.8). Tests with No. 8 headed bars are from Ghimire et al. (2018), and tests with No. 11 headed bars are from the current study

As shown in Figure 3.9, the specimens containing No. 11 headed bars showed a slight drop in anchorage strength T_N as the ratio h_{cl}/ℓ_{eh} increased from 1.47 to 1.88 and a much greater drop as the ratio h_{cl}/ℓ_{eh} increased to 5.24. This observation matches that of Ghimire et al. (2018) for specimens containing No. 8 headed bars. Ghimire et al. (2018) concluded that the anchorage strength of headed bars did not significantly change as the value of the ratio h_{cl}/ℓ_{eh} increased from 1.24 to 2.79, while T_N decreased when the ratio h_{cl}/ℓ_{eh} increased to 5.6, as shown in Figure 3.9. In light of the plot shown in Figure 3.9, it may be appropriate to observe Ghimire et al. also had a slight drop in T_N as the ratio h_{cl}/ℓ_{eh} increased from 1.24 to 2.79. The anchorage strength of specimens with a ratio h_{cl}/ℓ_{eh} of 5.24 and 5.6 are only about 80% and 60% of the average anchorage strength of the other specimens, respectively. Since there is only one specimen with a ratio h_{cl}/ℓ_{eh} of 5.24 and 5.6 for tests with No. 11 and No. 8 headed bars, respectively, the statistical significance of these differences cannot be evaluated. The ratios of h_{cl}/ℓ_{eh} of these specimens, however, are

much higher than the maximum ratio of 1.5 suggested in Commentary Section R25.4.4.2 of ACI 318-19, which explains the reduction of the anchorage strength of the headed bars.

3.1.3 Effect of Concrete Compressive Strength

The effect of concrete compressive strength on the anchorage strength of headed bars anchored in a simulated column-foundation joint is presented in this section. Ten tests were conducted on headed bars anchored in slab specimens to investigate the effect of concrete compressive strength on the anchorage strength. Only specimens with $A_{brg} \leq 9.5A_b$ are included in this evaluation. Of the ten tests, six included two No. 11 headed bars spaced at $8.2d_b$ (widely-spaced) and loaded simultaneously, and four involved two No. 14 headed bars spaced at $6.8d_b$ (closely-spaced) and loaded simultaneously. “Widely-spaced” and “closely-spaced” are defined in accordance with Shao et al. (2016) for beam-column joint specimens as bars with a center-to-center bar spacing greater than or equal to $8d_b$ and with a center-to-center bar spacing less than $8d_b$, respectively. The concrete compressive strength ranged from 5,110 to 14,470 psi. The test results for the specimens used in this analysis are presented in Table 3.3. Since the embedment length of headed bars varied, the average peak load on the headed bar at failure (total peak load applied on the specimen divided by the number of headed bars loaded simultaneously) is normalized with respect to an embedment length of 12.75 in. using Eq. (3.2).

$$T_N = T \left(\frac{12.75 \text{ in.}}{\ell_{eh}} \right)^{1.03} \quad (3.2)$$

where T is the average peak load on the headed bar at failure (kips), and ℓ_{eh} is the measured embedment length of the headed bar (in.). The power 1.03 in Eq. (3.2) is that for ℓ_{eh} in the descriptive equations developed by Shao et al. (2016), Eq. (1.7) and (1.8).

The slab specimen properties, including the measured embedment length ℓ_{eh} , the measured concrete compressive strength f_{cm} , the distance between the center of the headed bars and the inner face of the nearest support reaction h_{cl} , the ratio h_{cl}/ℓ_{eh} , the net bearing area of the head A_{brg} divided by the headed bar area A_b , the average peak load on the headed bar at failure T , and the normalized average peak load on the headed bar at failure T_N , are presented in Table 3.3. T_N is plotted versus the concrete compressive strength in Figure 3.10.

Table 3.3 Test results for specimens containing No. 11 and No. 14 headed bars tested with different concrete strength

Specimens			ℓ_{eh}	f_{cm}	h_{cl}	$\frac{h_{cl}}{\ell_{eh}}$	$\frac{A_{brg}}{A_b}$	$T^{[1]}$	$T_N^{[2]}$
SN	Description	Head	(in.)	(psi)	(in.)			(kips)	(kip)
6	(2@8.2)11-5-S5.5-7#11-0-12.75	A1	13.50	5370	19.7	1.46	5.5	99.5	93.8
		A2	13.50		19.7	1.46	5.5		
	(2@8.2)11-5-S5.5-7#11-0-12.75	B1	14.06		19.7	1.40	5.5	106.5	96.4
		B2	14.06		19.7	1.40	5.5		
7	(2@8.2)11-5-S5.5-7#11-0-12.75	A1	13.25	5110	19.7	1.49	5.5	88.1	84.7
		A2	13.25		19.7	1.49	5.5		
	(2@8.2)11-5-S5.5-7#11-0-12.75	B1	13.31		19.7	1.48	5.5	87.7	83.8
		B2	13.31		19.7	1.48	5.5		
10	(2@8.2)11-15-S9.2-7#11-0-12.75	A1	12.69	14470	19.7	1.55	9.2	124.8	125.4
		A2	12.68		19.7	1.55	9.2		
	(2@8.2)11-15-S9.2-7#11-0-12.75	B1	12.75		19.7	1.55	9.2	131.0	131.0
		B2	12.75		19.7	1.55	9.2		
12	(2@6.8)14-5-B4.2-7#11-0-12.75	A1	13.00	6040	19.8	1.53	4.2	119.5	117.1
		A2	13.00		19.8	1.53	4.2		
	(2@6.8)14-5-B4.2-7#11-0-12.75	B1	13.13	6180	19.8	1.51	4.2	129.5	125.7
		B2	13.13		19.8	1.51	4.2		
14	(2@6.8)14-15-B4.2-7#11-0-12.75	A1	13.13	14030	19.8	1.51	4.2	173.0	167.9
		A2	13.13		19.8	1.51	4.2		
	(2@6.8)14-15-B4.2-7#11-0-12.75	B1	13.13	14050	19.8	1.51	4.2	161.9	157.1
		B2	13.13		19.8	1.51	4.2		

^[1] Average peak load (total peak load applied on the specimen divided by the number of headed bars being developed)

^[2] Normalized force on the headed bar at failure using Eq. (3.2)

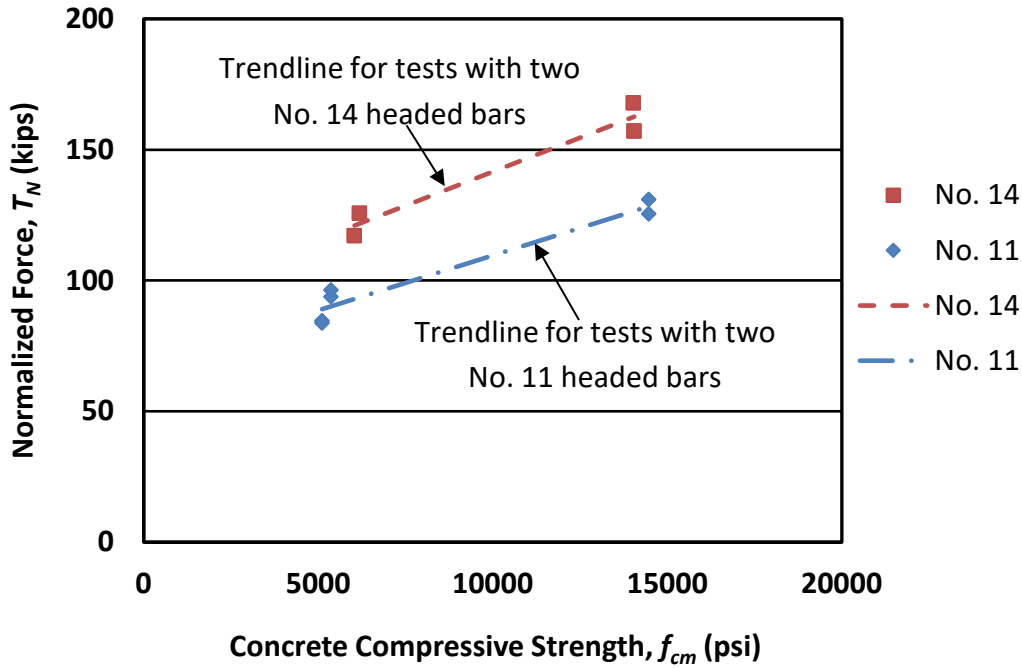


Figure 3.10 Normalized bar force at failure T_N [using Eq. (3.2)] versus concrete compressive strength f_{cm} for specimens presented in Table 3.3.

Figure 3.10 shows that, on average, the anchorage strength of No. 11 headed bars increased about 42% (from 90 to 128 kips) as the concrete compressive strength increased from 5,240 to 14,470 psi, while the anchorage strength of No. 14 headed bars increased about 34% (from 122 to 163 kips) as the concrete compressive strength increased from 6,110 to 14,040 psi. Student's t-test shows that these differences are statistically significant, with $p = 0.0016$ for No. 11 headed bars and $p = 0.0269$ for No. 14 headed bars.

Figure 3.11 compares the ratio T/T_h to the concrete compressive strength f_{cm} for all tests that contained two headed bars load simultaneously with parallel tie reinforcement within the joint region from the current study. T is the average peak load on the headed bar at failure, and T_h is the calculated anchorage strength based on the descriptive equations developed by Shao et al. (2016), Eq. (1.7) and (1.8).

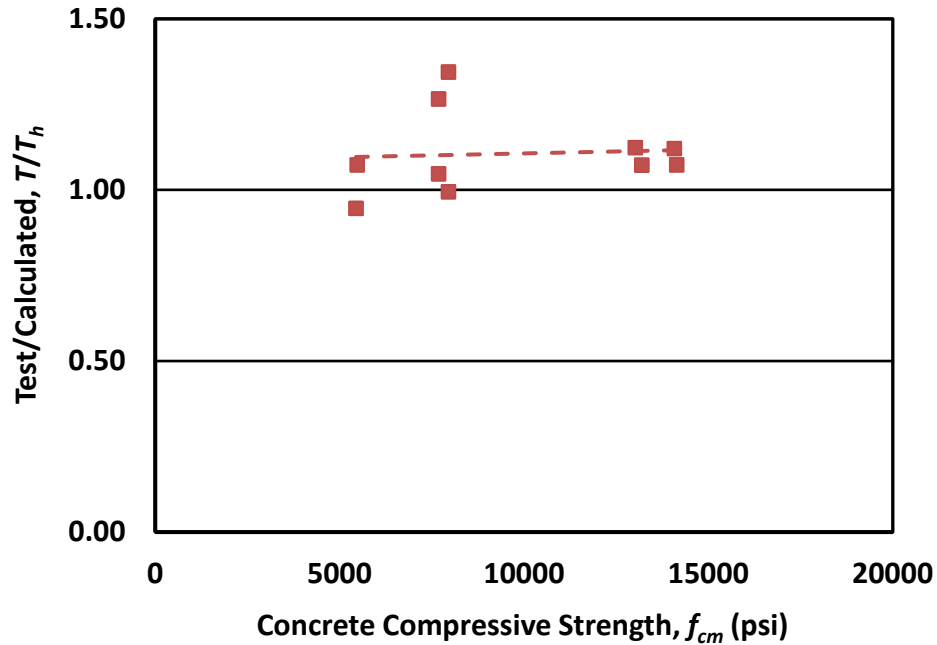


Figure 3.11 Ratio of test-to-calculated failure load T/T_h versus concrete compressive strength f_{cm} for all the current study tests that contained two headed bars load simultaneously with the presence of the parallel tie reinforcement within the joint region presented in Table 3.1.

The trend line in Figure 3.11 is almost horizontal, indicating that the effect of concrete compressive strength is accurately captured by the 0.24 power in the descriptive equation, Eq.(1.8). The values of T/T_h range from 0.95 to 1.34, with a coefficient of variation of 0.105. The maximum, minimum, mean, standard deviation (STD), and coefficients of variation (COV) of T/T_h for the results shown in Figure 3.11 are presented in Table 3.4.

Table 3.4 Statistical parameters of T/T_h values for tests containing two headed bars with parallel tie reinforcement within the joint region

Number of tests	All (10)	No. 11 (6)	No. 14 (4)
Max	1.34	1.34	1.12
Min	0.95	0.99	0.95
Mean	1.11	1.14	1.05
STD	0.116	0.130	0.070
COV	0.105	0.114	0.067

3.1.4 Effect of Grouped Anchors and Headed Bar Spacing

The effects of grouped anchors–headed bars placed closely or widely and loaded simultaneously–and headed bar spacing on the anchorage strength of a headed bar embedded in simulated column–foundation joints are discussed in this section. Thirteen tests were conducted on individual and grouped headed bars anchored in slab specimens to investigate the effect of grouped anchors and the spacing between the headed bars on the anchorage strength (Table 3.5). Of the thirteen tests, five included only one headed bar, two included two headed bars loaded simultaneously with a center-to-center spacing of $3.2d_b$ (closely-spaced), and six included two headed bars with a center-to-center spacing of $8.2d_b$ (widely-spaced). The slab specimen properties, including the measured embedment length ℓ_{eh} , the measured concrete compressive strength f_{cm} , the distance between the center of the headed bars and the inner face of the nearest support reaction h_{cl} , the ratio h_{cl}/ℓ_{eh} , the net bearing area of the head A_{brg} divided by the headed bar area A_b , the average peak load T (total peak load applied on the specimen divided by the number of headed bars loaded simultaneously), and the normalized anchorage strength of headed bars T_N , which is calculated using Eq. (3.1), are presented in Table 3.5.

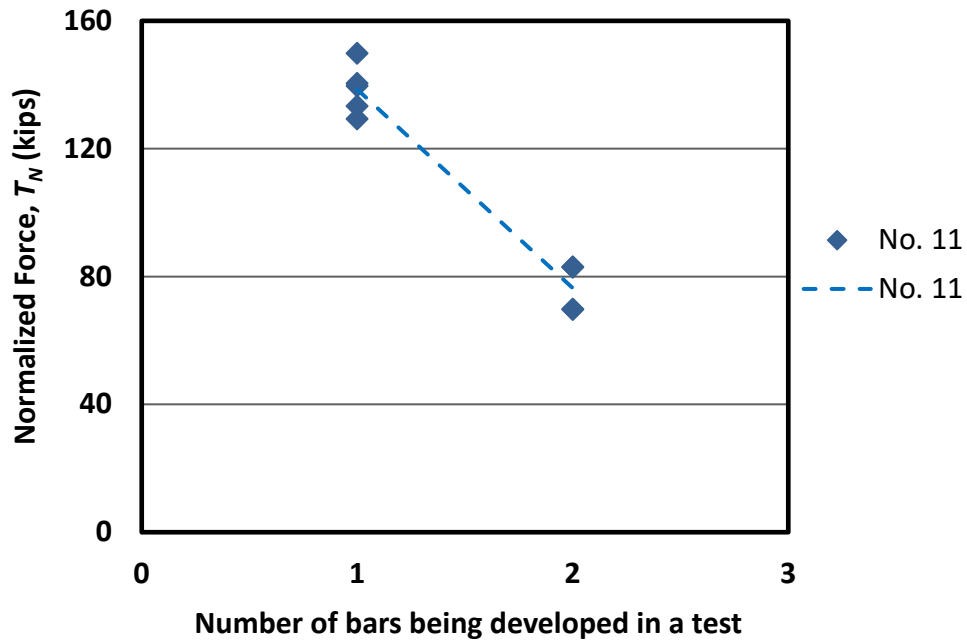
For comparison between the anchorage strength of headed bars tested individually and in a group of headed bars loaded simultaneously, the anchorage strength of headed bars in the slab specimens, normalized with respect to the concrete compressive strength f_{cm} and the embedment length of the headed bar ℓ_{eh} using Eq. (3.1), is plotted versus the number of headed bars being developed in a test in Figures 3.12a (closely-spaced bars) and 3.12b (widely-spaced bars). Since Ghimire et al. (2018) found that the anchorage strength of headed bars did not significantly change with the presence of reinforcement oriented perpendicular to the headed bars, Figures 3.12a and 3.12b include specimens with reinforcement placed perpendicular to the headed bars. The figures include specimens containing headed bars with a net bearing area of the head (A_{brg}) ranging from 3.8 to $9.5A_b$ based on the observation by Shao et al. (2016) that headed bars with bearing area A_{brg} between 3.8 to $9.5A_b$ had similar anchorage strengths. The figures include specimens with h_{cl}/ℓ_{eh} 1.24 to 2.79 based on the observation, discussed in relation to Fig 3.9 showing results presented by Ghimire et al. (2018), that there was drop in T_N as h_{cl}/ℓ_{eh} increased from 1.24 to 2.79, but that the drop was small.

Table 3.5 Test results for specimens containing individual and two closely-spaced or widely-spaced grouped headed bars

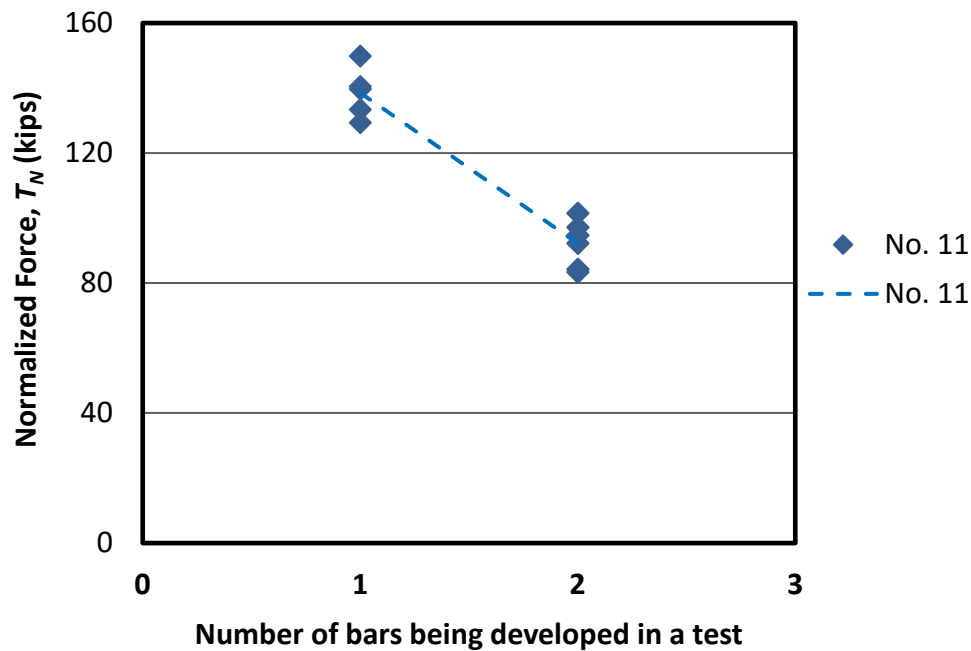
Specimens			ℓ_{eh}	f_{cm}	h_{cl}	$\frac{h_{cl}}{\ell_{eh}}$	$\frac{A_{brg}}{A_b}$	$T^{[1]}$	$T_N^{[2]}$
SN	Description	Head	(in.)	(psi)	(in.)			(kips)	(kips)
1	11-5-S5.5-6#6-0-12.75	A	13.38	5060	24.7	1.85	5.5	147.1	139.7
	11-5-S5.5-6#6-0-12.75	B	13.13		24.7	1.88	5.5	137.8	133.4
	11-5-S5.5-6#6-0-12.75	C	13.38		24.7	1.85	5.5	136.3	129.3
2	11-5-S5.5-10#6-0-12.75	A	13.38	5490	19.7	1.47	5.5	161.0	149.9
	11-5-S5.5-10#6-0-12.75	B	12.75		19.7	1.55	5.5	143.7	140.5
4	(2@3.2)11-5-S5.5-6#11-0-12.75	A1	13.50	5550	19.7	1.46	5.5	90.3	82.9
		A2	13.50		19.7	1.46	5.5		
	(2@3.2)11-5-S5.5-6#11-0-12.75	B1	13.38	6190	19.7	1.47	5.5	77.2	69.7
		B2	13.38		19.7	1.47	5.5		
6	(2@8.2)11-5-S5.5-7#11-0-12.75	A1	13.50	5370	19.7	1.46	5.5	99.5	92.2
		A2	13.50		19.7	1.46	5.5		
	(2@8.2)11-5-S5.5-7#11-0-12.75	B1	14.06		19.7	1.40	5.5	106.5	94.7
		B2	14.06		19.7	1.40	5.5		
7	(2@8.2)11-5-S5.5-7#11-0-12.75	A1	13.25	5110	19.7	1.49	5.5	88.1	84.2
		A2	13.25		19.7	1.49	5.5		
	(2@8.2)11-5-S5.5-7#11-0-12.75	B1	13.31		19.7	1.48	5.5	87.7	83.4
		B2	13.31		19.7	1.48	5.5		
10	(2@8.2)11-15-S9.2-7#11-0-12.75	A1	12.69	14470	19.7	1.55	9.2	124.8	97.2
		A2	12.69		19.7	1.55	9.2		
	(2@8.2)11-15-S9.2-7#11-0-12.75	B1	12.75		19.7	1.55	9.2	131.0	101.5
		B2	12.75		19.7	1.55	9.2		

^[1] Average peak load (total peak load applied on the specimen divided by the number of headed bars being developed)

^[2] Normalized force on the headed bar at failure using Eq. (3.1)



(a)



(b)

Figure 3.12 Bar force at failure normalized with respect to a concrete compressive strength of 5,000 psi and an embedment length of 12.75 in. T_N versus the number of headed bars being developed in tests (a) with individual and closely spaced headed bars loaded simultaneously (b) with individual and widely spaced headed bars loaded simultaneously. Results for individual bars are the same in figures (a) and (b)

Based on the test results shown in Figures 3.12a and 3.12b for these tests of No. 11 bars, the average anchorage strength of headed bars loaded individually was 139 kips, compared to values of 76 and 92 kips for two headed bars loaded simultaneously when closely and widely spaced, respectively. In these cases, on average, loading two closely or widely spaced headed bars simultaneously resulted in an anchorage strength of about 55% and 66%, respectively, of the anchorage strength of headed bars tested individually. Student's t-test indicates that these differences are statistically significant, with $p = 0.0003$ and 0.000003 , respectively. The reduction in the anchorage strength of grouped headed bars is likely due to the limited amount of concrete available between the bars to resist the applied forces.

Figure 3.13 compares the normalized anchorage strengths of two headed bars as a function of the center-to-center spacing divided by the bar diameter d_b for headed bars with a net bearing area of the head A_{brg} ranging from 3.8 to $9.5A_b$ and specimens with ratios h_{cl}/ℓ_{eh} ranging from 1.24 to 2.79.

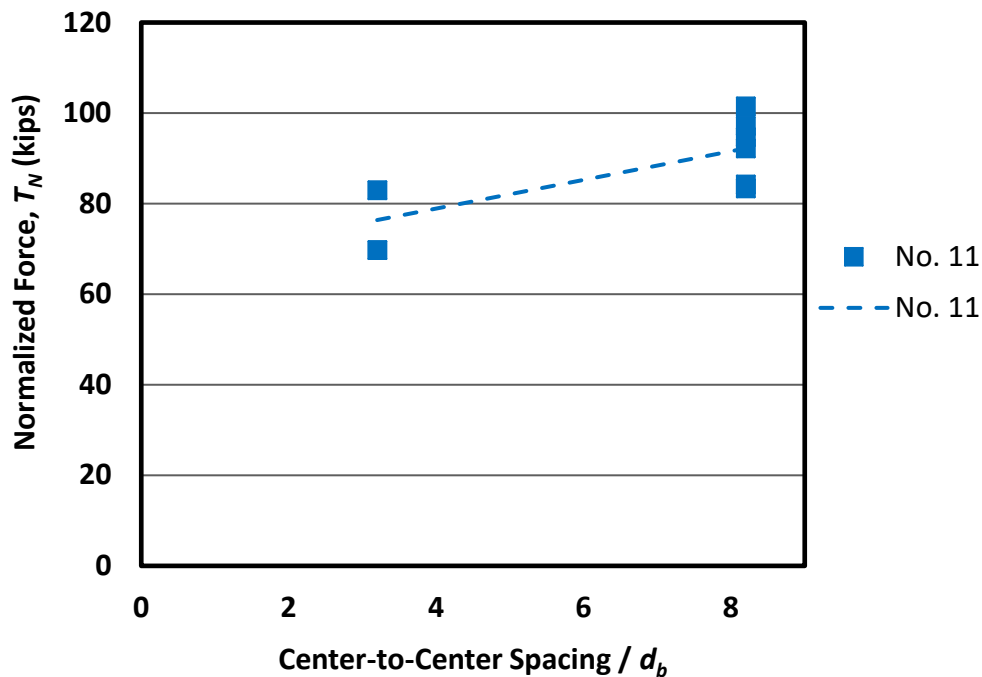


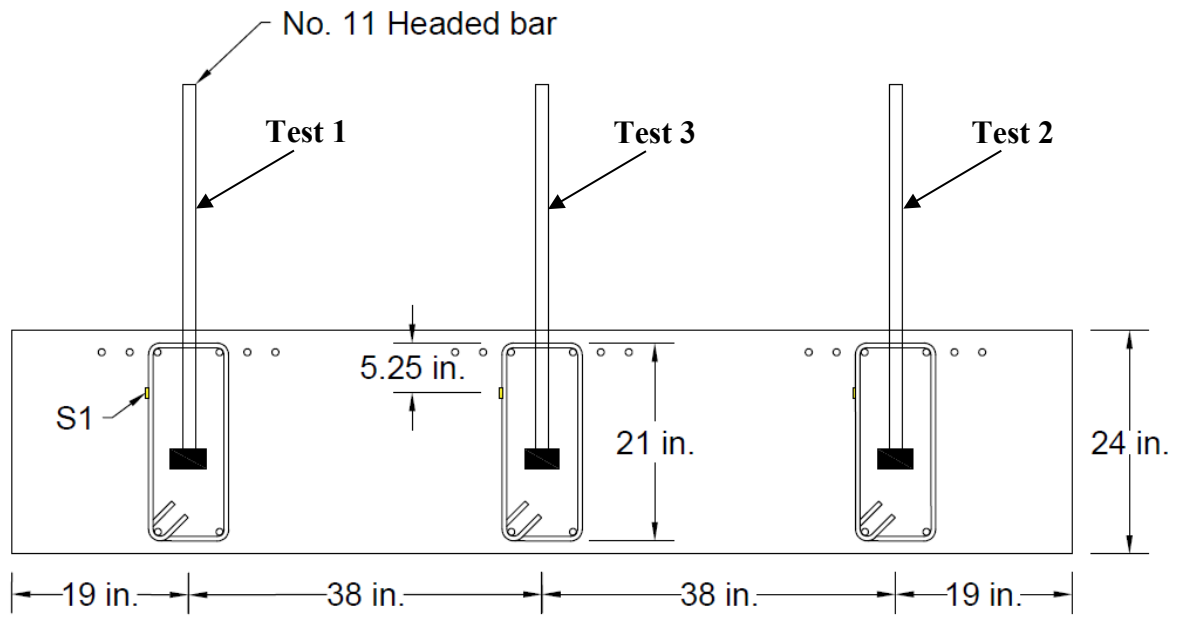
Figure 3.13 Bar force at failure normalized with respect to a concrete compressive strength of 5,000 psi and an embedment length of 12.75 in. T_N versus center-to-center spacing between headed bars with respect to the bar diameter (d_b)

For these tests, the average anchorage strength of headed bars with a center-to-center spacing of $3.2d_b$ is 76.4 kips, while the average anchorage strength of headed bars with a center-to-center spacing of $8.2d_b$ is 92.2 kips, a 21% increase. This difference is statistically significant, with $p = 0.043$. This observation indicates that headed bar spacing has an effect on anchorage strength that the ACI 318-19 Chapter 17 anchorage provisions do not account for. This observation matches the findings by Shao et al. (2016) for beam-column joints who observed that the anchorage strength of headed bars decreases with center-to-center as the center-to-center spacing decreases below $8d_b$.

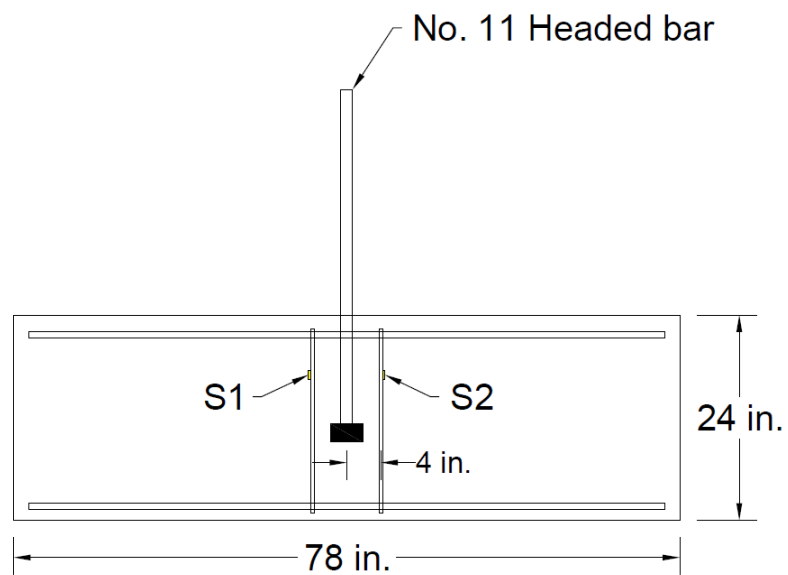
3.1.5 Effect of Parallel Tie Reinforcement

The contribution of parallel tie reinforcement—ties or hoops placed parallel to the headed bars within the joint region—to the anchorage strength of headed bars is discussed in this section. In beam-column joints, Sperry et al. (2015b) and Shao et al. (2016) found that only hoops within $8d_b$ of the top of the hooked or headed bars for No. 3 through No. 8 bars or within $10d_b$ for No. 9 through No. 11 bars were effective in increasing the anchorage strength of hooked or headed bars. To investigate the contribution of parallel tie reinforcement to the anchorage strength of headed bars anchored in simulated column-foundation joints, 26 tests were conducted on headed bars anchored in specimens with and without parallel tie reinforcement within the joint region.

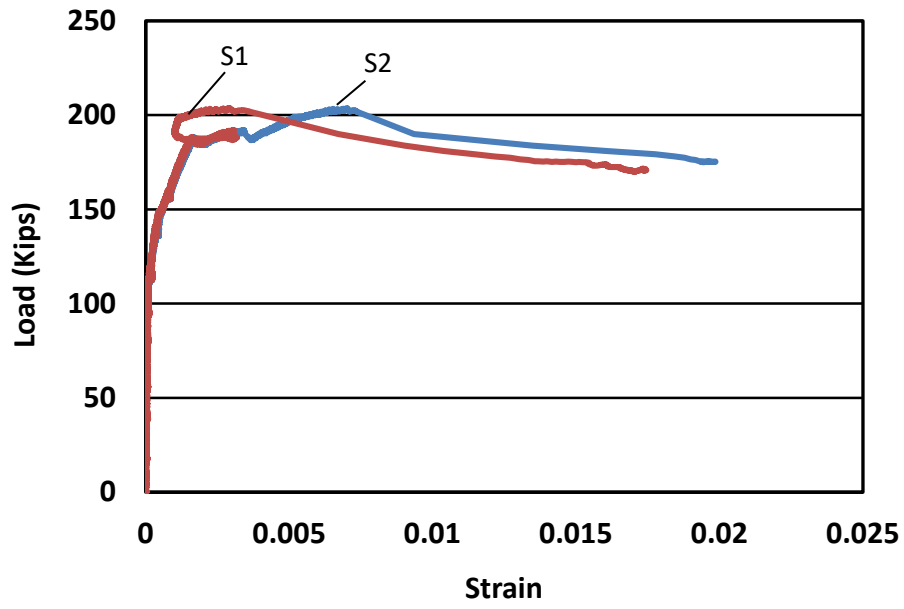
To support this investigation, described in Section 2.7, strain gages were used to measure the strain in parallel tie reinforcement (in the form of hoops) at different distances from the headed bars. One strain gauge was mounted to each hoop mounted in the top quarter of the leg, oriented parallel to the headed bars, as shown in Figures 3.14a and b for Slab Specimen 5 (11-5-S5.5-6#6-2#4-12.75), which contained three headed bars loaded individually and had No. 4 bar hoops placed within the joint region on both sides of the headed bars. Figures 3.14c, d, and e show the load-strain curves for the parallel ties in each of the three tests. A summary of the key parameters of Slab Specimen 5 is presented in Table 3.1. As shown in Figure 3.14b, one No. 4 bar hoop was placed on both sides of the headed bar spaced at $2.8d_b$ (4 in.) from the centerline of the headed bar.



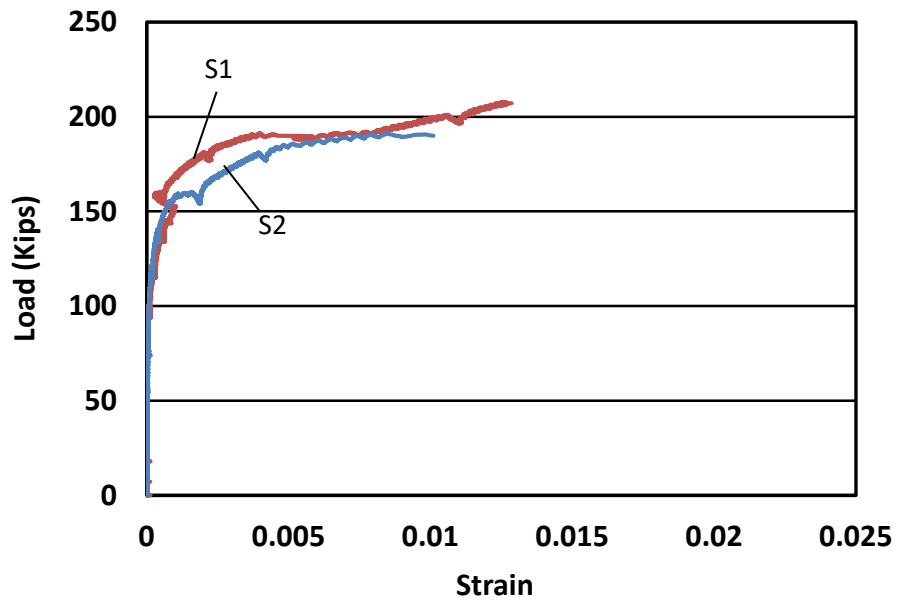
(a)



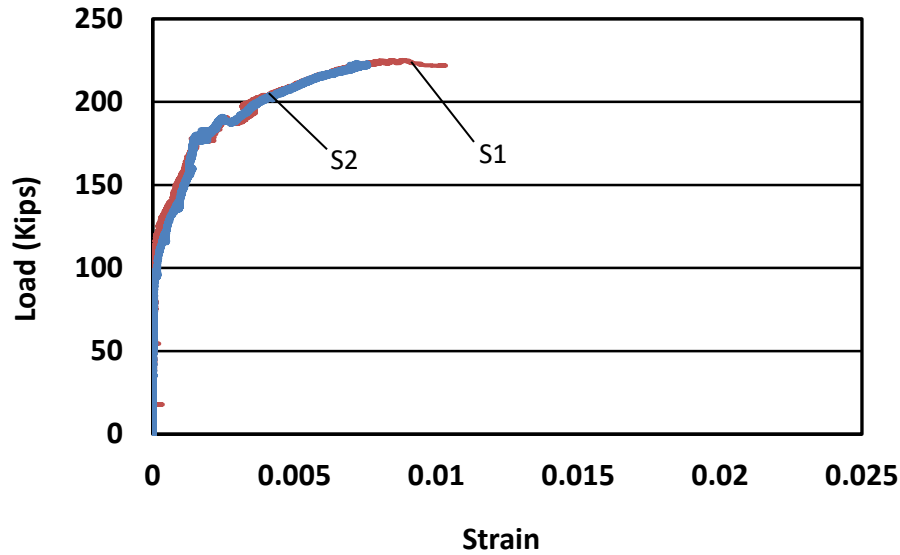
(b)



(c)



(d)



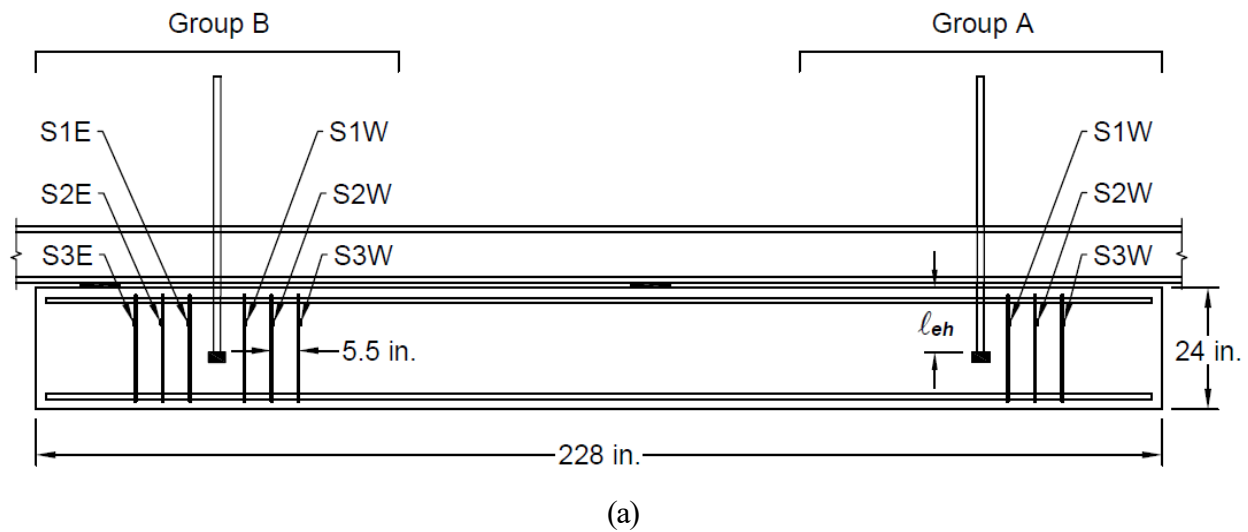
(e)

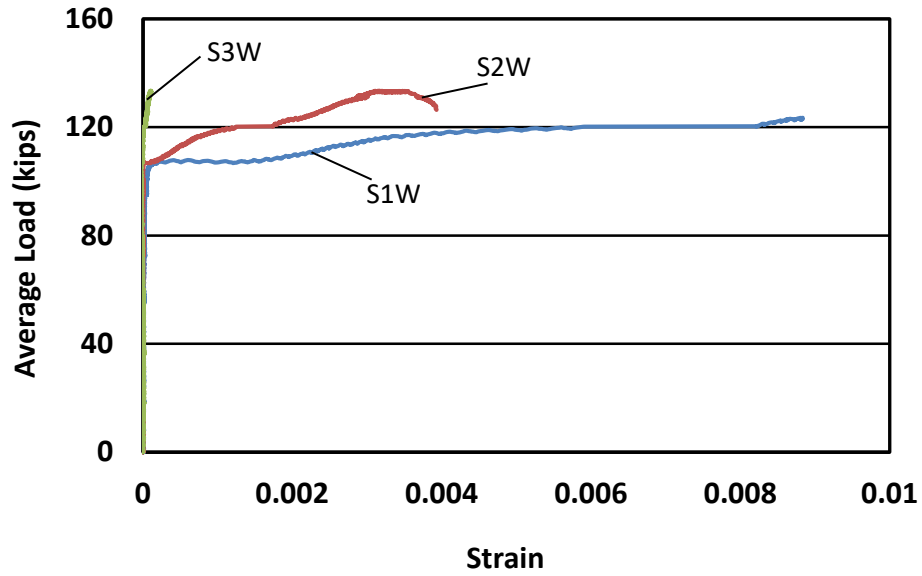
Figure 3.14 Parallel tie reinforcement for Slab Specimen 5 (11-5-S5.5-6#6-2#4-12.75) (a) front view, (b) side view, (c) load versus strain curves for Test 1, (d) load versus strain curves for Test 2, (e) load versus strain curves for Test 3

Figure 3.14c shows the load-strain curves for Test 1 of Slab Specimen 5 (11-5-S5.5-6#6-2#4-12.75). As shown in the figure, the strain in both hoops (S1 and S2) began to increase once the load reached about 120 kips (59% of the peak load) when the first crack in the concrete appeared. The strain in the hoops increased slowly at loads above 120 kips. S1 and S2 reached a strain of 0.001 at about 170 kips (83% of the peak load), and increased more rapidly at loads above 170 kips, reaching 0.003 and 0.006 for S1 and S2, respectively, at the peak load, indicating that both hoops yielded. The load-strain curve for Test 2 of Slab Specimen 5 (11-5-S5.5-6#6-2#4-12.75) is shown in Figure 3.14d. The strain in hoops began to increase at an applied load of about 110 kips (49% of the peak load) when the first crack in the concrete formed. The strain in the hoops increased slowly at loads below 150 kips (67% of the peak load), increasing more rapidly above 150 kips, reaching a strain of 0.01 for both S1 and S2 at the peak load, indicating that both hoops yielded. Figure 3.14e shows the load-strain curve for Test 3. The strain in the hoops started to increase at an applied load of 120 kips (54% of the peak load) when the first crack in the concrete formed. The strain increase for S1 and S2 continued with the applied load and reached as much as 0.007 at the peak load, again indicating that both hoops had yielded. Overall, the strain in the hoops

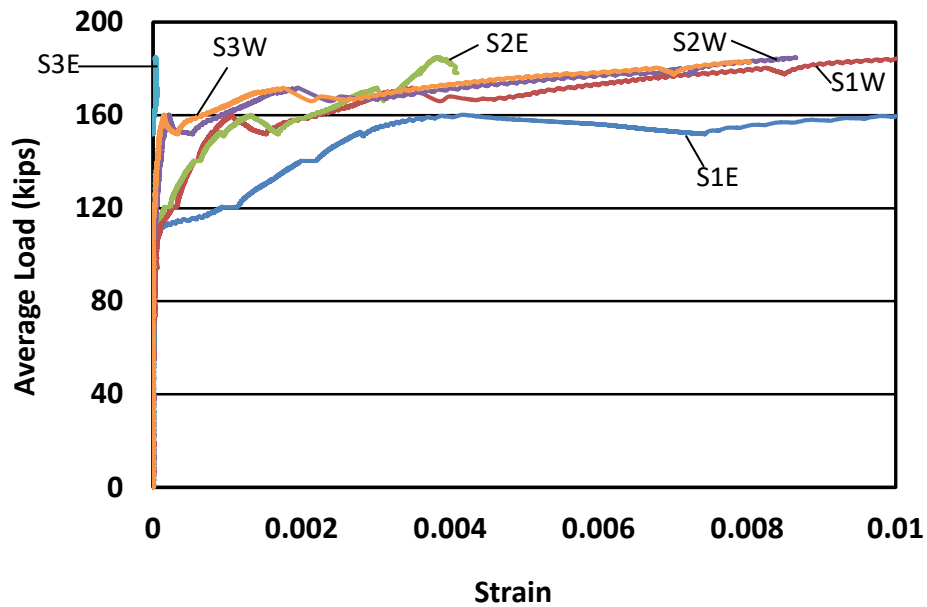
in these tests, located at a distance equal to $2.8d_b$ from the centerline of the headed bar, began to increase once the first crack formed in the concrete and exceeded the yield point before the peak load was reached.

Figure 3.15 shows the strain gauge locations and the load-strain curves for Slab Specimen 8. This specimen contained two groups of two headed bars loaded simultaneously with parallel tie reinforcement (hoops) in the joint region. Group A [(2@8.2)11-5-S9.2-7#11-3#4-12.75] contained three No. 4 bar hoops on one side of the headed bars spaced at $3.9d_b$ (5.5 in.) and Group B [(2@8.2)11-5-S9.2-7#11-6#4-12.75] included three No. 4 bar hoops on two sides of the headed bars spaced at $3.9d_b$ (5.5 in.), as shown in Figure 3.15a. The key parameters of Slab Specimen 8 are presented in Table 3.1. The strain gauge locations are shown in Figure 3.15a. Figures 3.15b and 3.14c show the average load (total load applied during the test divided by the number of headed bars being developed) versus the strain in the hoops used in Group A [(2@8.2)11-5-S9.2-7#11-3#4-12.75] and Group B [(2@8.2)11-5-S9.2-7#11-6#4-12.75], respectively.





(b)



(c)

Figure 3.15 Average load per headed bar versus strain in parallel tie reinforcement for Slab Specimen 8 (a) location of the parallel tie reinforcement and the strain gauge locations (b) load versus strain curves for hoops in test included hoops only on one side of the bars Group A [(2@8.2)11-5-S9.2-7#11-3#4-12.75] (c) load versus strain curves for hoops in the test included hoops on both sides of the bars Group B [(2@8.2)11-5-S9.2-7#11-6#4-12.75]

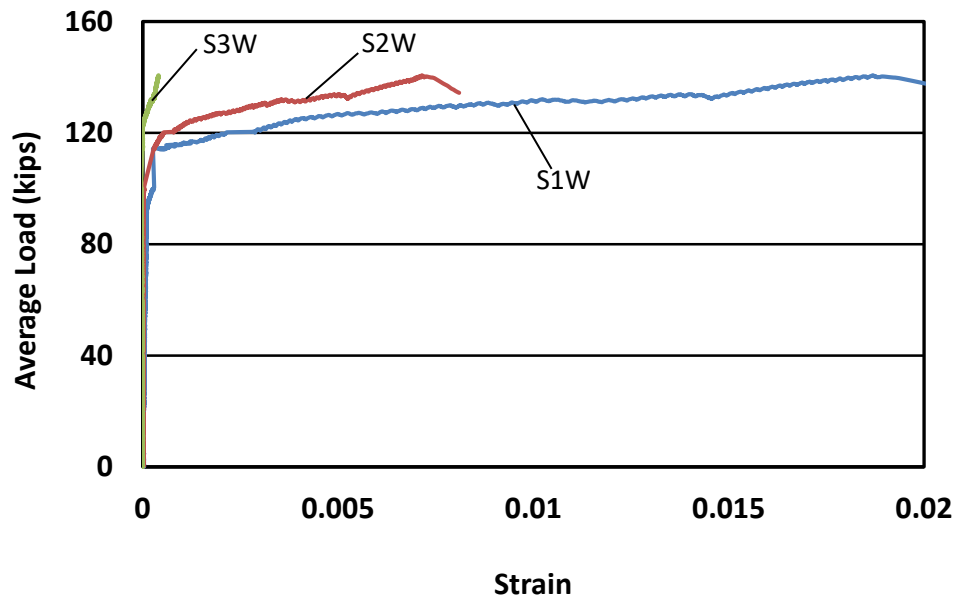
Figure 3.15b shows the hoop load-strain curves for the test conducted on the Group A headed bars anchored in Slab Specimen 8 [(2@8.2)11-5-S9.2-7#11-3#4-12.75], which had two No. 11 headed bars loaded simultaneously with three No. 4 bar hoops placed on one side of the headed bars between the nearest support reaction and the headed bars and spaced at $3.9d_b$ (5.5 in.), as shown in Figure 3.15a. The hoop closest to the headed bars (S1W), $3.9d_b$ (5.5 in.) from the centerline of the headed bars, showed an increase in the strain at lower loads than the hoops placed further from the headed bars (S2W and S3W), as shown in the figure. The strain in hoop S1W began to increase at an applied load of about 106 kips (80% of the average peak load) and exceeded the yield strain at a load of about 111 kips (83% of the average peak load), while the strain in the hoop S2W, located $7.8d_b$ (11 in.) from the centerline of the headed bars, started to increase at 82% of the average peak load and exceeded the yield strain at 98% of the peak load. Hoop S3W, located close to the nearest support reaction and $11.7d_b$ (16.5 in.) from the centerline of the headed bars, exhibited minimal strain throughout the test, reaching a strain of just 0.0001 at the peak load, demonstrating, as shown for beam-column joints tests (Sperry et al. (2015b) and Shao et al. (2016)), that the effectiveness of hoops is directly related to their location from the headed bars and the angle of the concrete crack, as shown in Figure 3.5b; the flatter the concrete crack, the greater the chance that the crack will intercept a hoop.

Figure 3.15c shows the hoop load-strain curves for the test conducted on the Group B headed bars in Slab Specimen 8 [(2@8.2)11-5-S9.2-7#11-6#4-12.75]. This test included two No. 11 headed bars loaded simultaneously with No. 4 bar hoops placed on both sides of the headed bars and spaced at $3.9d_b$ (5.5 in.). As shown in Figure 3.15c, the load-strain curves for the hoops differ depending on the location of hoops from the headed bars. Hoops S1E, S2E, and S3E were located at $3.9d_b$ (5.5 in.), $7.8d_b$ (11 in.), and $11.7d_b$ (16.5 in.), respectively, from the centerline of the headed bars, while hoops S1W, S2W, and S3W were located on the other side of the headed bars at $3.9d_b$ (5.5 in.), $7.8d_b$ (11 in.), and $11.7d_b$ (16.5 in.), respectively, from the centerline of the headed bars. The hoops close to the headed bars (S1E, S1W, S2E, and S2W) showed increases in the strain at lower loads than the hoops placed further from the headed bars (S3W and S3E). Hoop S1E, the closest to the headed bars in the region between anchored headed bars and the nearest support reaction, exhibited an increase in strain at an applied load of about 110 kips (59% of the

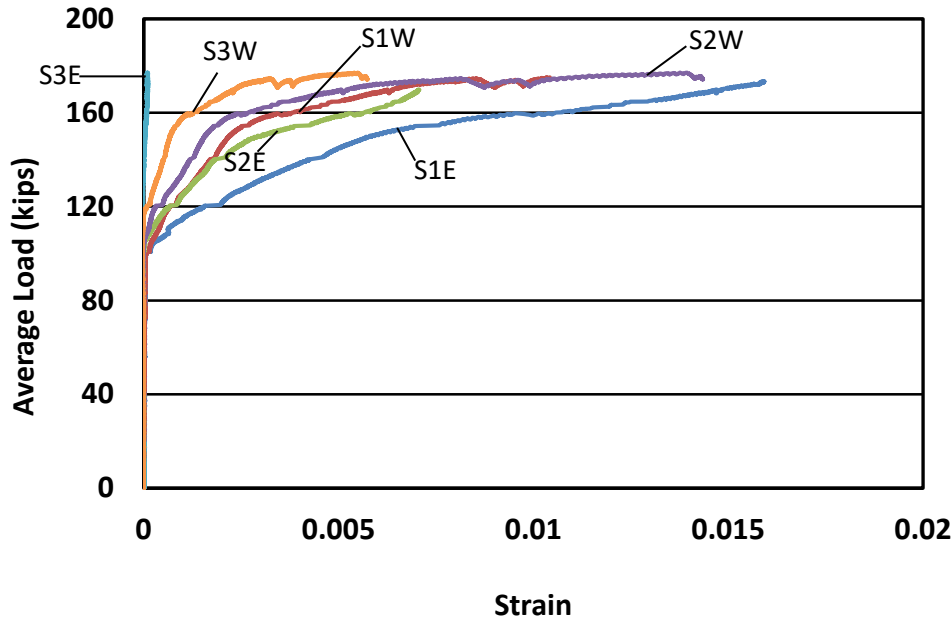
average peak load), with a steady increase in strain up to 0.004 (beyond the yield strain) at an applied load of about 160 kips (86% of the average peak load) and reached a strain of 0.01 at the peak load. The strain in hoops S1W and S2E began to increase at an applied load of about 117 kips (63% of the average peak load), and both hoops reached a strain value of 0.001 at a load of 160 kips (86% of the average peak load). The strain increase for S1W and S2E continued with the applied load, and reached strains of 0.01 and 0.004, respectively, at the peak load, indicating that both hoops had yielded. The strain in hoops S2W and S3W started to increase at an applied load of about 140 kips (76% of the average peak load) and reached a value of 0.0008 at an applied load of about 160 kips (86% of the average peak load). The strain in hoops S2W and S3W continued increasing with applied load and reached a strain of 0.006 at the peak load, indicating that both hoops (S2W and S3W) yielded. Hoop S3E, located close to the nearest support reaction, exhibited minimal strain throughout the test, reaching a strain of just 0.00004 at the peak load. These observations indicate that hoops placed close to the headed bars are more effective in improving the anchorage strength of headed bars than those located further from the bars. Moreover, in this test conducted, two of the three hoops located between the headed bars and the nearest support reaction yielded, while all three hoops located on the other side of the headed bars between the headed bars and the furthest support reaction yielded. These results support the observation for the Group A test that the effectiveness of hoops is directly related to their distance from the headed bars *and* the angle of the concrete failure cracks. The effect of concrete crack angle on the effectiveness of hoops is shown in Figure 3.6b.

Figure 3.16 shows the load-strain curves for Slab Specimen 9. This specimen contained two groups of two headed bars loaded simultaneously with the presence of No. 4 bar hoops in the joint region. Group A [(2@8.2)11-5-S9.2-7#11-3#4-12.75] contained three No. 4 bar hoops spaced at $3.9d_b$ (5.5 in.) on one side of the headed bars while Group B [(2@8.2)11-5-S9.2-7#11-6#4-12.75] contained three No. 4 bar hoops spaced at $3.9d_b$ (5.5 in.) on both sides of the headed bars. The location of the hoops and the strain gauges are the same as shown in Figure 3.15a for Slab Specimen 8. The key parameters of Slab Specimen 9 are presented in Table 3.1. Figures 3.16a and 3.16b show the average load versus strain in hoops used in Group A [(2@8.2)11-5-S9.2-7#11-3#4-12.75] and Group B [(2@8.2)11-5-S9.2-7#11-6#4-12.75], respectively.

Figure 3.16a shows the load-strain curves for the test conducted on the first group of headed bars anchored in Slab Specimen 9 Group A [(2@8.2)11-5-S9.2-7#11-3#4-12.75]. This test contained two No. 11 headed bars loaded simultaneously with three No. 4 bar hoops spaced at $3.9d_b$ (5.5 in.) on one side of the headed bars between the nearest support reaction and the headed bars, as shown in Figure 3.15a for Slab Specimen 8. The strain in hoop S1W, located $3.9d_b$ (5.5 in.) from the centerline of the headed bars, began to increase at an applied load of about 92 kips (66% of the average peak load) and exceeded the yield strain at a load of 120 kips (86% of the average peak load), while the strain in hoop S2W, located $7.8d_b$ (11 in.) from the centerline of the headed bars, started to increase at a load of about 114 kips (81% of the average peak load) and passed the yield strain at a load of about 130 kips (93% of the average peak load). Hoop S3W, located close to the nearest support reaction and $11.7d_b$ (16.5 in.) from the centerline of the headed bars, exhibited minimal strain throughout the test, reaching a strain of just 0.0003 at the peak load. These findings again support the earlier observations that the effectiveness of hoops depends on where they are placed with respect to headed bars and the direction of concrete cracks, as illustrated in figure 3.5b.



(a)



(b)

Figure 3.16 Average load per headed bar versus strain in parallel tie reinforcement for Slab Specimen 9 (a) load versus strain curves for hoops in test included hoops only on one side of the bars Group A [(2@8.2)11-5-S9.2-7#11-3#4-12.75] (b) load versus strain curves for hoops in the test included hoops on both sides of the bars Group B [(2@8.2)11-5-S9.2-7#11-6#4-12.75]

Figure 3.16b shows the load-strain curves for the test conducted on the second group of headed bars anchored in Slab Specimen 9 [(2@8.2)11-5-S9.2-7#11-6#4-12.75]. This test contained two No. 11 headed bars loaded simultaneously with three No. 4 bar hoops spaced at $3.9d_b$ (5.5 in.) and placed on both sides of the headed bars. As shown in Figure 3.16b, the load-strain curves for the hoops are a function of the hoop locations from the headed bars. The strain in hoop S1W, located $3.9d_b$ (5.5 in.) from the centerline of the headed bars, exhibited an increase at a load of 100 kips (56% of the average peak load) and passed the yield strain at a load of 152 kips (86% of the average peak load), while hoop S2W, located $7.8d_b$ (11 in.) from the centerline of the headed bars, showed an increase in strain at a load of 110 kips and exceeded the yield strain at a load of 160 kips (91% of the average peak load). The strain in hoop S3W, located $11.7d_b$ (16.5 in.) from the centerline of the headed bars, began to increase at a load of 120 kips (68% of the average peak load) and reached the yield strain at 170 kips (96% of the peak load). The strain in hoop S1E, located $3.9d_b$ (5.5 in.) from the centerline of the headed bars, began to increase at a load of 100 kips (56% of the average peak load) and passed the yield strain at a load of 125 kips (70% of the

average peak load), while hoop S2E, located $7.8d_b$ (11 in.) from the centerline of the headed bars, exhibited an increase in strain at a load of 107 kips (60% of the average peak load) and exceeded the yield strain at a load of 144 kips (81% of the average peak load). Hoop S3E, the furthest from the headed bars at $11.7d_b$ (16.5 in.) from the centerline of the headed bars and located close to the nearest support reaction, exhibited minimal strain increase throughout the test, reaching a strain of just 0.0001 at the peak load. Once again, these findings suggest that the effectiveness of hoops is directly proportional to their distance from the headed bars and the angle of the concrete cracks. The illustration in Figure 3.6b supports these conclusions.

A summary of test results of the 26 tests with No. 11 and No. 14 headed bars is given in Table 3.1 and repeated in Table 3.6. The specimen properties, including the measured embedment length ℓ_{eh} , the measured concrete compressive strength f_{cm} , h_{cl} , the ratio h_{cl}/ℓ_{eh} , the net bearing area of the head A_{brg} divided by the headed bar area A_b , the average peak load T (the total peak load applied on the specimen divided by the number of headed bars loaded simultaneously), and the normalized anchorage strength of headed bars T_N , which is calculated using Eq. (3.1), are presented in Table 3.6. Based on the strain gauge results, the hoops located within the region of $8d_b$ from the centerline of the headed bars experienced a significant increase in strain at failure. In contrast, the hoops located outside this region ($8d_b$) on the side of the headed bars between the nearest support reaction and the headed bars did not yield, but on the other side, between the furthest support reaction and the headed bars, they did yield because the concrete crack has a flatter angle and thus intercepted the hoop, as described in Section 3.1.1. For comparison, the normalized anchorage strengths of headed bars at failure T_N based on Eq. (3.1) are plotted versus A_{tt}/A_{hs} in Figure 3.17, where A_{tt} is the total cross-sectional area of parallel tie reinforcement within a $10d_b$ radial distance from the centerline of the headed bars (in.²) and A_{hs} is the total cross-sectional area of the headed bars being developed (in.²). As described earlier, these specimens had $A_{brg} \leq 9.5A_b$ and h_{cl}/ℓ_{eh} ranging from 1.46 to 1.92. As described in Section 2.2, the slab specimens contained flexural reinforcement in the vicinity of the head.

Table 3.6 Test results for specimens containing No. 11 and No. 14 headed bars with and without parallel tie reinforcement

Specimens			ℓ_{eh}	f_{cm}	h_{cl}	$\frac{h_{cl}}{\ell_{eh}}$	$\frac{A_{brg}}{A_b}$	$\frac{A_{tt}}{A_{hs}}$	$T^{[1]}$	$T_N^{[2]}$
SN	Description	Head	(in.)	(psi)	(in.)				(kips)	(kip)
1	11-5-S5.5-6#6-0-12.75	A	13.38	5060	24.70	1.85	5.5	0.00	147.1	139.7
	11-5-S5.5-6#6-0-12.75	B	13.13		24.70	1.88	5.5	0.00	137.8	133.4
	11-5-S5.5-6#6-0-12.75	C	13.38		24.70	1.85	5.5	0.00	136.3	129.3
5	11-5-S5.5-6#6-2#4-12.75	A	13.00	5810	24.70	1.90	5.5	0.51	203.7	192.6
	11-5-S5.5-6#6-2#4-12.75	B	12.88		24.70	1.92	5.5	0.51	220.9	210.9
	11-5-S5.5-6#6-2#4-12.75	C	13.13		24.70	1.88	5.5	0.51	225.2	210.8
6	(2@8.2)11-5-S5.5-7#11-0-12.75	A1	13.50	5370	19.70	1.46	5.5	0.00	99.5	92.2
		A2	13.50		19.70	1.46	5.5	0.00		
	(2@8.2)11-5-S5.5-7#11-0-12.75	B1	14.06		19.70	1.40	5.5	0.00	106.5	94.7
		B2	14.06		19.70	1.40	5.5	0.00		
7	(2@8.2)11-5-S5.5-7#11-0-12.75	A1	13.25	5110	19.70	1.49	5.5	0.00	88.1	84.2
		A2	13.25		19.70	1.49	5.5	0.00		
	(2@8.2)11-5-S5.5-7#11-0-12.75	B1	13.31		19.70	1.48	5.5	0.00	87.7	83.4
		B2	13.31		19.70	1.48	5.5	0.00		
8	(2@8.2)11-5-S9.2-7#11-3#4-12.75	A1	13.13	7950	19.70	1.50	9.2	0.26	133.5	115.9
		A2	13.13		19.70	1.50	9.2	0.26		
	(2@8.2)11-5-S9.2-7#11-6#4-12.75	B1	13.00		19.70	1.52	9.2	0.51	185.0	162.2
		B2	13.00		19.70	1.52	9.2	0.51		
9	(2@8.2)11-5-S9.2-7#11-3#4-12.75	A1	13.25	7680	19.70	1.49	9.2	0.26	140.7	121.9
		A2	13.25		19.70	1.49	9.2	0.26		
	(2@8.2)11-5-S9.2-7#11-6#4-12.75	B1	13.38		19.70	1.47	9.2	0.51	177.1	152.1
		B2	13.38		19.70	1.47	9.2	0.51		
10	(2@8.2)11-15-S9.2-7#11-0-12.75	A1	12.69	14470	19.70	1.55	9.2	0.00	124.8	97.2
		A2	12.69		19.70	1.55	9.2	0.00		
	(2@8.2)11-15-S9.2-7#11-0-12.75	B1	12.75		19.70	1.55	9.2	0.00	131.0	101.5
		B2	12.75		19.70	1.55	9.2	0.00		
11	(2@8.2)11-15-S9.2-7#11-3#4-12.75	A1	12.75	14140	19.70	1.55	9.2	0.26	157.3	122.5
		A2	12.75		19.70	1.55	9.2	0.26		
	(2@8.2)11-15-S9.2-7#11-6#4-12.75	B1	12.63	14080	19.70	1.56	9.2	0.51	167.8	132.2
		B2	12.63		19.70	1.56	9.2	0.51		
12	(2@6.8)14-5-B4.2-7#11-0-12.75	A1	13.00	6040	19.85	1.53	4.2	0.00	119.5	111.9
		A2	13.00		19.85	1.53	4.2	0.00		
	(2@6.8)14-5-B4.2-7#11-0-12.75	B1	13.13	6180	19.85	1.51	4.2	0.00	129.5	119.5
		B2	13.13		19.85	1.51	4.2	0.00		

^[1] Average peak load (total peak load applied on the specimen divided by the number of headed bars being developed)

^[2] Normalized force on the headed bar at failure using Eq. (3.1)

Table 3.6 Cont. Test results for specimens containing No. 11 and No. 14 headed bars with and without parallel tie reinforcement

Specimens			ℓ_{eh}	f_{cm}	h_{cl}	$\frac{h_{cl}}{\ell_{eh}}$	$\frac{A_{brg}}{A_b}$	$\frac{A_{tt}}{A_{hs}}$	$T^{[1]}$	$T_N^{[2]}$
SN	Description	Head	(in.)	(psi)	(in.)				(kips)	(kip)
13	(2@6.8)14-5-B4.2-7#11-3#4-12.75	A1	13.00	5440	19.85	1.53	4.2	0.27	137.3	131.9
		A2	13.00		19.85	1.53	4.2	0.27		
	(2@6.8)14-5-B4.2-7#11-6#4-12.75	B1	12.75	5480	19.85	1.56	4.2	0.53	160.0	156.4
		B2	12.75		19.85	1.56	4.2	0.53		
14	(2@6.8)14-15-B4.2-7#11-0-12.75	A1	13.13	14030	19.85	1.51	4.2	0.00	173.0	131.1
		A2	13.13		19.85	1.51	4.2	0.00		
	(2@6.8)14-15-B4.2-7#11-0-12.75	B1	13.13	14050	19.85	1.51	4.2	0.00	161.9	122.6
		B2	13.13		19.85	1.51	4.2	0.00		
15	(2@6.8)14-15-B4.2-7#11-3#4-12.75	A1	13.38	13190	19.85	1.48	4.2	0.27	185.1	139.6
		A2	13.38		19.85	1.48	4.2	0.27		
	(2@6.8)14-15-B4.2-7#11-6#4-12.75	B1	12.88	13020	19.85	1.54	4.2	0.53	194.4	153.0
		B2	12.88		19.85	1.54	4.2	0.53		

^[1] Average peak load (total peak load applied on the specimen divided by the number of headed bars being developed)

^[2] Normalized force on the headed bar at failure using Eq. (3.1)

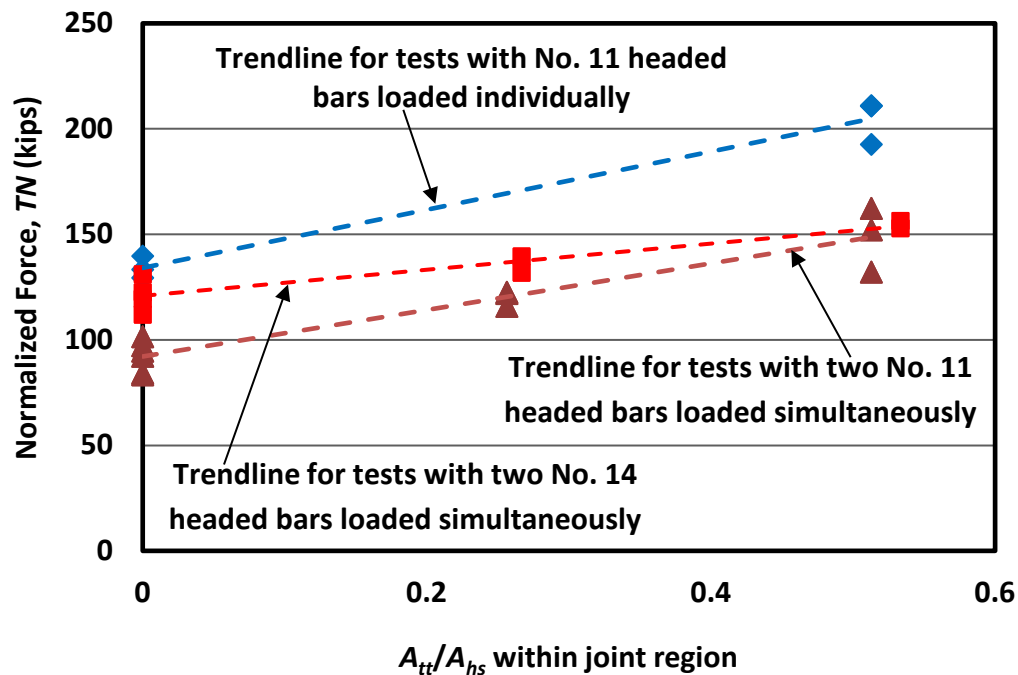


Figure 3.17 Normalized bar force at failure T_N [using Eq. (3.1)] versus normalized parallel tie reinforcement A_{tt}/A_{hs} , within a $10d_b$ radial distance from the centerline of the headed bars, for specimens with and without parallel tie reinforcement

As shown in Figure 3.17, the presence of parallel tie reinforcement within the joint region increases the anchorage strength of headed bars. The average anchorage strength for No. 11 headed bars loaded individually without parallel tie reinforcement in the form of hoops within the joint region is 134 kips, while the average strength for similar specimens with parallel tie reinforcement located on both sides of the headed bars $2.8d_b$ (4 in.) from the centerline of the headed bars with $A_{tt}/A_{hs} = 0.51$ is 205 kips (53% greater). Student's t-test shows that this difference in anchorage strength is statistically significant, with $p = 0.0005$. The average anchorage strength for two widely-spaced ($8.2d_b$) No. 11 headed bars loaded simultaneously without parallel tie reinforcement within the joint region is 92 kips, while the average strength for similar specimens with parallel tie reinforcement on both sides of the headed bars and spaced at $3.9d_b$ (5.5 in.) with $A_{tt}/A_{hs} = 0.51$ is 148 kips (61% greater). Student's t-test also shows that this difference is statistically significant, with $p = 0.0001$. The average strength for tests that included two widely-spaced ($8.2d_b$) No. 11 headed bars loaded simultaneously with parallel tie reinforcement placed only on one side of the headed bars and spaced at $3.9d_b$ (5.5 in.) with $A_{tt}/A_{hs} = 0.26$ is 120 kips (about 30% greater than those that did not include parallel tie reinforcement ($p = 0.0005$) and about 23% less than those that contained parallel tie reinforcement on both sides of the headed bars ($p = 0.034$)).

The average anchorage strength for two No. 14 headed bars spaced at $6.8d_b$ and loaded simultaneously without parallel tie reinforcement within the joint region is 121 kips, while the average strength for similar specimens with parallel tie reinforcement on both sides of the headed bars and spaced at $3.2d_b$ (5.5 in.) with $A_{tt}/A_{hs} = 0.53$ is 155 kips (28% greater). Student's t-test shows that this difference is statistically significant, with $p = 0.005$. The average strength for tests that included two No. 14 headed bars spaced at $6.8d_b$ and loaded simultaneously with parallel tie reinforcement placed only on one side of the headed bars and spaced at $3.2d_b$ (5.5 in.) with $A_{tt}/A_{hs} = 0.27$ is 136 kips (about 12% greater than those that did not include parallel tie reinforcement ($p = 0.086$) and about 14% less than those that contained parallel tie reinforcement on both sides of the headed bars ($p = 0.046$)). These observations indicate that the parallel tie reinforcement within column-foundation joint is effective in improving the anchorage strength of headed bars—behavior that is not accounted for in ACI 318-19. Moreover, these results show that parallel tie reinforcement increases the anchorage strength of widely-spaced bars. This observation matches

the findings by Shao et al. (2016) for beam-column joints, who observed that even for widely-spaced headed bars, the addition of parallel tie reinforcement increases the anchorage strength. The contribution of parallel tie reinforcement to the anchorage strength of widely-spaced bars is not taken into account by the development length provisions of the ACI 318-19 Code.

3.1.6 Examination of Value of Effective Parallel Tie Reinforcement A_{tt} used in Descriptive Equation, Eq. (1.8)

As mentioned earlier, Sperry et al. (2015b) and Shao et al. (2016) found that confining reinforcement within $8d_b$ of the top of the hooked or headed bars for No. 3 through No. 8 bars or within $10d_b$ for No. 9 through No. 11 bars were effective in increasing the anchorage strength of hooked or headed bars in beam-column joints. Shao et al. (2016) found that, based on their analysis, the total area of the effective parallel tie reinforcement per headed bar A_{tt}/n in the descriptive equation (Eq. 1.8) must be less than or equal to $0.3A_b$, where A_{tt} is the total area of the effective parallel tie reinforcement in the joint region, n is the number of headed bars being developed and A_b is the area of the headed bar. Shao et al. (2016) concluded that the values above $0.3A_b$ did not contribute to the anchorage strength of headed bars in beam-column joints. The value of A_{tt}/n versus the $0.3A_b$ for column-foundation joint specimens is explained next.

For the specimens with two widely-spaced No. 11 headed bars with parallel tie reinforcement only on one side of the headed bars, A_{tt}/n within $10d_b$ equals 0.40 in.^2 (area of four legs of No. 4 ties), which is less than the value of $0.3A_b$ (0.47 in.^2). For tests conducted on similar specimens but with parallel tie reinforcement on both sides of the headed bars, A_{tt}/n within $10d_b$ has an area of 0.80 in.^2 (area of eight No. 4 ties), which is greater than the $0.3A_b$. The ratio of the measured anchorage strength T to that calculated using the descriptive equation (Eq. 1.8) T_h ranges from 0.98 to 1.16 when the cap of $0.3A_b$ is not applied and from 0.99 to 1.34 when the cap is applied, as shown in Tables 3.7 and 3.8, respectively. For tests of the specimens with No. 14 headed bars with parallel tie reinforcement only on one side of the headed bars, the value of A_{tt}/n for the hoops within $10d_b$ equals 0.60 in.^2 (area of six legs of No. 4 ties), which is less than $0.3A_b$ (0.68 in.^2). However, for similar specimens with parallel tie reinforcement on both sides of the headed bars, A_{tt}/n within $10d_b$ has an area of 1.2 in.^2 (area of twelve No. 4 ties), which is greater

than the value of $0.3A_b$. The ratio of the measured anchorage strength T to that calculated using the descriptive equation (Eq. 1.8) T_h ranges from 0.85 to 1.07 when the cap of $0.3A_b$ is not applied and from 0.95 to 1.12 when the cap is applied, as shown in Tables 3.7 and 3.8, respectively.

Table 3.7 Effective parallel tie reinforcement (A_{tt}) and T/T_h values for tests containing two headed bars loaded simultaneously with parallel tie reinforcement within the joint region, the cap $0.3A_b$ is not applied to the descriptive equation (Eq. 1.8)

Specimens			$N_{legs}^{[1]}$	$N_{layers}^{[2]}$	A_{tt} (in. ²)	$\frac{A_{tt}}{n}$	$0.3A_b$ (in. ²)	$T^{[3]}$ (kips)	T_h (kips)	$\frac{T}{T_h}$
SN	Description	Head								
8	(2@8.2)11-5-S9.2-7#11-3#4-12.75	A1	2	2	0.80	0.40	0.47	133.5	134.2	0.99
		A2								
	(2@8.2)11-5-S9.2-7#11-6#4-12.75	B1	2	4	1.60	0.80	0.47	185.0	159.6	1.16
		B2								
9	(2@8.2)11-5-S9.2-7#11-3#4-12.75	A1	2	2	0.80	0.40	0.47	140.7	134.4	1.05
		A2								
	(2@8.2)11-5-S9.2-7#11-6#4-12.75	B1	2	4	1.60	0.80	0.47	177.1	161.8	1.09
		B2								
11	(2@8.2)11-15-S9.2-7#11-3#4-12.75	A1	2	2	0.80	0.40	0.47	157.3	146.5	1.07
		A2								
	(2@8.2)11-15-S9.2-7#11-6#4-12.75	B1	2	4	1.60	0.80	0.47	167.8	171.6	0.98
		B2								
13	(2@6.8)14-5-B4.2-7#11-3#4-12.75	A1	2	3	1.20	0.60	0.68	137.3	145.2	0.95
		A2								
	(2@6.8)14-5-B4.2-7#11-6#4-12.75	B1	2	6	2.40	1.20	0.68	160.0	188.3	0.85
		B2								
15	(2@6.8)14-15-B4.2-7#11-3#4-12.75	A1	2	3	1.20	0.60	0.68	185.1	172.6	1.07
		A2								
	(2@6.8)14-15-B4.2-7#11-6#4-12.75	B1	2	6	2.40	1.20	0.68	194.4	212.2	0.92
		B2								

^[1] Number of legs in one layer

^[2] Number of layers included in the calculation of A_{tt}

^[3] T = average peak load (total peak load applied on the specimen divided by the number of headed bars being developed)

Table 3.8 Effective parallel tie reinforcement (A_{tt}) and T/T_h values for tests containing two headed bars loaded simultaneously with parallel tie reinforcement within the joint region, the cap $0.3A_b$ is applied to the descriptive equation (Eq. 1.8)

Specimens			$N_{legs}^{[1]}$	$N_{layers}^{[2]}$	A_{tt} (in. ²)	$\frac{A_{tt}}{n}$	$0.3A_b$ (in. ²)	$T^{[3]}$ (kips)	T_h (kips)	$\frac{T}{T_h}$
SN	Description	Head								
8	(2@8.2)11-5-S9.2-7#11-3#4-12.75	A1	2	2	0.80	0.40	0.47	133.5	134.2	0.99
		A2								
	(2@8.2)11-5-S9.2-7#11-6#4-12.75	B1	2	4	1.60	0.80	0.47	185.0	137.6	1.34
		B2								
9	(2@8.2)11-5-S9.2-7#11-3#4-12.75	A1	2	2	0.80	0.40	0.47	140.7	134.4	1.05
		A2								
	(2@8.2)11-5-S9.2-7#11-6#4-12.75	B1	2	4	1.60	0.80	0.47	177.1	139.9	1.27
		B2								
11	(2@8.2)11-15-S9.2-7#11-3#4-12.75	A1	2	2	0.80	0.40	0.47	157.3	146.5	1.07
		A2								
	(2@8.2)11-15-S9.2-7#11-6#4-12.75	B1	2	4	1.60	0.80	0.47	167.8	149.7	1.12
		B2								
13	(2@6.8)14-5-B4.2-7#11-3#4-12.75	A1	2	3	1.20	0.60	0.68	137.3	145.2	0.95
		A2								
	(2@6.8)14-5-B4.2-7#11-6#4-12.75	B1	2	6	2.40	1.20	0.68	160.0	149.0	1.07
		B2								
15	(2@6.8)14-15-B4.2-7#11-3#4-12.75	A1	2	3	1.20	0.60	0.68	185.1	172.6	1.07
		A2								
	(2@6.8)14-15-B4.2-7#11-6#4-12.75	B1	2	6	2.40	1.20	0.68	194.4	172.9	1.12
		B2								

^[1] Number of legs in one layer

^[2] Number of layers included in the calculation of A_{tt}

^[3] T = average peak load (total peak load applied on the specimen divided by the number of headed bars being developed)

3.2 ANALYSIS OF TEST RESULTS FROM OTHER STUDIES AND COMPARISONS WITH THE CURRENT STUDY

The descriptive equations developed by Shao et al. (2016) are based on beam-column joint specimens. In this section, test results from current and previous studies are compared with the anchorage strengths predicted by the descriptive equations developed by Shao et al. (2016) to evaluate their applicability to predict the anchorage strength of headed bars anchored in members other than beam-column joints. The test results are also compared with the anchorage strengths predicted by the ACI code provisions in Chapter 17 and Chapter 25 of ACI 318-19 and proposed Code provisions to evaluate their accuracy for predicting the anchorage strength of headed bars

anchored in members other than beam-column joints. Equations (3.3) and (3.4) are the descriptive equations developed by Shao et al. (2016) for the anchorage of headed bars without and with confining reinforcement, respectively. The descriptive equations were developed as a best fit of the test results with an *average* ratio of test-to-calculated failure load equal to 1.0.

$$T_h = \left(781 f_{cm}^{0.24} \ell_{eh}^{1.03} d_b^{0.35} \right) \left(0.0836 \frac{s}{d_b} + 0.3444 \right) \quad (3.3)$$

with $0.0836 \frac{s}{d_b} + 0.3444 \leq 1.0$, and

$$T_h = \left(781 f_{cm}^{0.24} \ell_{eh}^{1.03} d_b^{0.35} + 48,800 \frac{A_{tr}}{n} d_b^{0.88} \right) \left(0.0622 \frac{s}{d_b} + 0.5428 \right) \quad (3.4)$$

with $0.0622 \frac{s}{d_b} + 0.5428 \leq 1.0$ and $\frac{A_{tr}}{n} \leq 0.3 A_b$

where T_h is the anchorage strength of a headed bar (lb); f_{cm} is the measured concrete compressive strength (psi); ℓ_{eh} is the embedment length (in.); d_b is the diameter of the headed bar (in.); s is the center-to-center spacing between the bars (in.); A_{tr} is the total cross-sectional area of effective confining reinforcement (NA_{tr}) parallel to the headed bars being developed (in.²); N is the number of legs of the effective confining reinforcement parallel to the headed bars being developed; A_{tr} is the area of a single leg of the confining reinforcement (in.²); n is the number of headed bars in tension; A_b is the nominal area of the headed bar (in.²).

A modification factor of 0.8 is applied to the anchorage strength T_h for headed bars terminating outside a column core (a region of column cross-section confined by the column longitudinal reinforcement) with side cover to the bar < 2.5 in., or terminating in a member other than beam-column joints with side cover to the bar $< 8d_b$.

The test results are also compared with the anchorage strengths predicted by the anchorage provisions in Chapter 17 of ACI 318-19. The anchorage provisions for different failure modes, such as concrete breakout strength (Section 17.6.2 of ACI 318-19) and the anchorage strength provided by anchor reinforcement (Section 17.5.2.1 of ACI 318-19), are presented below. Anchor reinforcement is defined in accordance with Section 17.5.2.1 of ACI 318-19 as stirrups, ties, or hairpins parallel to the headed bars and placed within $0.5\ell_{eh}$ from the centerline of the headed bars.

According to Section 17.6.2.1 of ACI 318-19, the nominal concrete breakout strength of a

single anchor (N_{cb}) or group of anchors (N_{cbg}) in tension is given by Eq. (3.5) and (3.6), respectively. The nominal concrete breakout strength equations are based on the 5% fractile of the test results used to develop the breakout equations. Therefore, the anchorage strength calculated based on the concrete breakout strength equations must be converted to a mean value to have a fair comparison with other design equations. A modification factor (ψ_{mean}) of 1.33 can be applied to the concrete breakout strength equations in ACI 318-19 to convert the 5% fractile value to a mean value. The 1.33 modification factor is calculated using Eq. (3.7), which is based on the standard normal distribution n -value = -1.645 for a 5% fractile (ACI 318-19) and the coefficient of variation (COV = 0.15) of the data used to develop the concrete breakout equations (Fuchs et al. 1995).

$$N_{cb} = \frac{A_{Nc}}{A_{Nco}} \psi_{ed,N} \psi_{c,N} \psi_{cp,N} N_b \quad (3.5)$$

$$N_{cbg} = \frac{A_{Nc}}{A_{Nco}} \psi_{ec,N} \psi_{ed,N} \psi_{c,N} \psi_{cp,N} N_b \quad (3.6)$$

$$\psi_{mean} = \frac{1}{1 + n \cdot COV} \quad (3.7)$$

where A_{Nc} is the projected concrete failure area of a single anchor or group of anchors (in.²); A_{Nco} is the projected concrete failure area of a single anchor with an edge distance of at least $1.5\ell_{eh}$ and is equal to $9\ell_{eh}^2$ (in.²), where ℓ_{eh} is the embedment length of headed anchors (in.); N_b is the basic concrete breakout strength of a single anchor loaded in tension, calculated as $N_b = k_c \cdot \lambda_a \cdot \sqrt{f'_c} \cdot \ell_{eh}^{1.5}$ if the embedment length of the headed bar $\ell_{eh} < 11$ in. and as $N_b = 16 \cdot \lambda_a \cdot \sqrt{f'_c} \cdot \ell_{eh}^{5/3}$ if $11 \text{ in.} \leq \ell_{eh} \leq 25 \text{ in.}$, where k_c is a calibration factor equal to 24 for cast-in anchors in cracked concrete; λ_a is a modification factor for lightweight concrete equal to 1.0λ for cast-in and undercut anchors and 0.8λ for expansion, screw, and adhesive anchors, λ is equal to 0.75 for lightweight concrete and 1.0 for normalweight concrete; f'_c is the concrete compressive strength (limited to 10,000 psi). $\psi_{ec,N}$ is a modification factor for a group of anchors loaded eccentrically in tension equal to $1/[1 + e'_N/(1.5\ell_{eh})] \leq 1$, where e'_N is the distance between resultant tensile load on a group of anchors loaded in tension and the centroid of the group of anchors loaded in tension (in.). $\psi_{ed,N}$ is a modification factor for edge effects for a single anchor or group of anchors loaded in tension equal to 1.0 if the smallest side concrete cover distance from the center

of an anchor is at least $1.5\ell_{eh}$; otherwise, $\psi_{ed,N}$ is equal to $0.7 + 0.3(c_{a,\min}/1.5\ell_{eh})$, where $c_{a,\min}$ is the minimum distance from the center of an anchor to the edge of concrete (in.). $\psi_{c,N}$ is a modification factor for the influence of cracking in anchor regions at service load levels, equal to 1.25 if anchors are located in a region of a concrete member where analysis indicates no cracking at service load levels; otherwise, $\psi_{c,N}$ is equal to 1.0. $\psi_{cp,N}$ is a modification factor for post-installed anchors and is equal to 1.0 for cast-in anchors.

The nominal anchorage strength of headed bars provided by anchor reinforcement N_{arg} (Section 17.5.2.1 of ACI 318-19) is given by Eq. (3.8).

$$N_{arg} = NA_{tr}f_y \quad (3.8)$$

where N is the total number of legs of anchor reinforcement parallel to the headed bars within a $0.5\ell_{eh}$ radial distance from the centerline of the headed bars; A_{tr} is the area of a single leg of the anchor reinforcement (in.²); f_y is the yield strength of the anchor reinforcement (psi).

The nominal anchorage strength of a headed bar in tension T_{anc} , governed by anchor reinforcement N_{arg} or concrete breakout N_{cbg} (incorporating the modification factor ψ_{mean}), is calculated using Eq. (3.9).

$$T_{anc} = \max\left(\frac{N_{cbg}}{n}, \frac{N_{arg}}{n}\right) \quad (3.9)$$

where n is the number of headed bars tested simultaneously in tension.

The test results are also compared with the anchorage strength of headed bars predicted by the design provisions in Chapter 25 of ACI 318-19 Section 25.4.4. The design provision is shown in Eq. (3.10).

$$\ell_{dt} = \left(\frac{f_y \psi_e \psi_p \psi_o \psi_c}{75\sqrt{f'_c}}\right) d_b^{1.5} \quad (3.10)$$

where ℓ_{dt} is the development length of a headed bar in tension (in.) not less than either $8d_b$ or 6 in.; ψ_e is a factor based on the presence or absence of a coating on the bars, equal to 1.2 for epoxy-coated or zinc and epoxy dual-coated reinforcement and 1.0 for uncoated or zinc-coated (galvanized) reinforcement; ψ_o is the bar location factor equal to 1.0 for No. 11 and smaller headed bars anchored within a column core with side cover not less than 2.5 in. or in other members with

side cover not less than $6d_b$; otherwise, ψ_o is equal to 1.25; ψ_c is the concrete strength factor equal to $f'_c/15,000 + 0.6$ if f'_c is less than 6000 psi and equal to 1.0 if f'_c is greater than or equal to 6000 psi; ψ_p is the parallel tie reinforcement factor equal to 1.0 for No. 11 and smaller headed bars spaced at a center-to-center distance not less than $6d_b$ or with A_{tt}/A_{hs} not less than 0.3, where A_{tt} is the total cross-sectional area of ties or stirrups acting as parallel tie reinforcement (in.²) and A_{hs} is the total cross-sectional area of headed bars being developed at a critical section (in.²); otherwise, ψ_p is equal to 1.6. It is worth noting that the value of ψ_p for column-foundation joint specimens is taken as 1.0 in this analysis only when the center-to-center spacing between headed bars $\geq 6d_b$ because parallel tie reinforcement, A_{tt} , is not considered for members other than beam-column joints, as mentioned in Section 25.4.4.5 of ACI 318-19. The modification factors in Eq. (3.10) are defined in Table 25.4.4.3 of ACI 318-19.

The design provisions in Chapter 25 of ACI 318-19 are a modified version of the descriptive equations, Eq. (3.3) and (3.4), with a strength reduction factor, ϕ , of 0.83 built-in, the square root of concrete compressive strength f'_c and ψ_c (defined above) rather than f_{cm} to the 0.24 power as in the descriptive equations, and use the modification factor ψ_p equal to 1 or 1.6 (intermediate values are not permitted) to represent the effect of anchored bar spacing and parallel ties instead of factors that varied as a function of bar spacing and the level of parallel tie reinforcement. Therefore, the anchorage strength calculated based on this design provision is expected to be conservative.

Equation (3.10) is solved for anchorage strength $T_{ACI\ 318}$ and replacing ℓ_{dt} and f'_c with ℓ_{eh} and f_{cm} , respectively, as shown in Eq. (3.11).

$$T_{ACI\ 318} = \left(\frac{75\sqrt{f_{cm}}\ell_{eh}}{\psi_e\psi_p\psi_o\psi_c d_b^{1.5}} \right) A_b \quad (3.11)$$

The test results are also compared with the anchorage strength of headed bars calculated using a proposed version of the design provisions based on a smoothed version of the descriptive equations that incorporates the effects headed bar spacing and parallel ties. The expression for development length in the proposed provisions is shown in Eq. (3.12). This expression is a modified version of the descriptive equations, Eq. (3.3) and (3.4), with a built-in strength reduction

factor, ϕ , of 0.83. Thus, the anchorage strength calculated based on Eq. (3.12) is expected to be conservative.

$$\ell_{dt} = \left(\frac{f_y \psi_e \psi_p \psi_o}{600 f_c'^{0.25}} \right) d_b^{1.5} \quad (3.12)$$

where ℓ_{dt} is the development length of a headed bar in tension (in.) not less than either $8d_b$ or 6 in.; ψ_e is a factor based on the presence or absence of a coating on the bars, equal to 1.2 for epoxy-coated or zinc and epoxy dual-coated reinforcement and 1.0 for uncoated or zinc-coated (galvanized) reinforcement; ψ_o is the bar location factor equal to 1.0 for headed bars anchored within a column core with side cover not less than 2.5 in. or in other members with side cover not less than $6d_b$; otherwise, ψ_o is equal to 1.25; ψ_p is the parallel tie reinforcement factor calculated using Eq. (3.13).

$$\psi_p = \frac{1}{4} \left(7 - 10 \frac{A_{tt}}{A_{hs}} - 0.5 \frac{s}{d_b} + \frac{A_{tt}}{A_{hs}} \frac{s}{d_b} \right) \quad (3.13)$$

where A_{tt} is the total cross-sectional area of ties or stirrups acting as parallel tie reinforcement (in.²), A_{hs} is the total cross-sectional area of headed bars being developed at a critical section (in.²), s is the minimum center-to-center spacing of headed bars, d_b is the nominal diameter of headed bars, A_{tt}/A_{hs} shall not exceed 0.3, and s/d_b shall not exceed 8 when calculating ψ_p .

Equation (3.12) is solved for anchorage strength T_{calc} and replacing ℓ_{dt} and f_c' with ℓ_{eh} and f_{cm} , respectively, as shown in Eq. (3.14).

$$T_{calc} = \left(\frac{600 f_{cm}^{0.25} \ell_{eh}}{\psi_e \psi_p \psi_o d_b^{1.5}} \right) A_b \quad (3.14)$$

3.2.1 Headed Bars Tested in Slab Specimens

DeVries et al. (1999) tested 18 headed bars with net bearing areas A_{brg} ranging from 4.7 to $7.4A_b$ in three concrete slab specimens with embedment lengths ranging from 1.375 to 9 in. The concrete compressive strength ranged from 3,920 to 12,040 psi, and the nominal yield strength of the headed bars was 72,000 psi. The headed bars anchored in slabs were spaced at a center-to-

center distance of at least three times the embedment length of the headed bars to avoid an overlap of the anticipated failure region. Of the 18 headed bars, eight bars were anchored at the center of the slab with a clear cover to the bars not less than two times the embedment length of the headed bars, five bars were anchored at the edge of the slab with a clear cover of 1.6 in. on one side and 17.6 in. on the adjacent side, and five bars were anchored at the corner of the slab with a clear cover of 1.6 in. on both side faces. These headed bars were tested individually in tension. During the tests, the support reaction plates were placed away from the headed bars at a distance equal to at least two times the embedment length with the goal of preventing the support reactions from influencing the anchorage strength. Of the 18 headed bars, 14 were unbonded along the total embedment length using a PVC pipe, as shown in Figure 3.18a, and four, all with an embedment length equal to 9 in., were bonded, as shown in Figure 3.18b. Results of the tests with unbonded headed bars are not included in the analysis because the behavior of unbonded bars is expected to be different from that of fully bonded bars. The center-to-center spacing between the headed bars s required in the descriptive equations [Eq. (3.3) and (3.4)] to calculate anchorage strength of headed bars is taken as twice of the minimum concrete cover to the center of the headed bar.

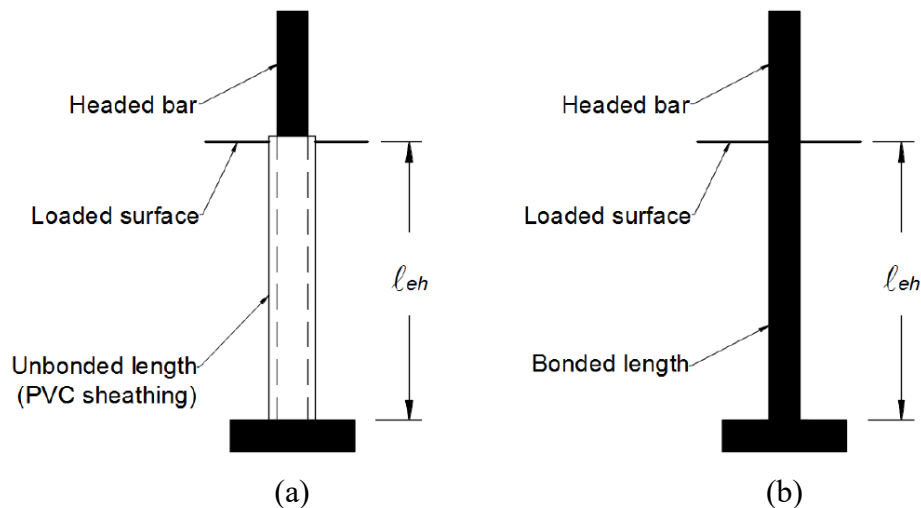


Figure 3.18 Headed reinforcing bars (a) unbonded and (b) bonded embedment length (DeVries et al. 1999)

Choi et al. (2002) conducted 16 tests on headed bars anchored in slabs (Figure 3.19), with embedment lengths ranging from 6.9 to $12.1d_b$. The concrete compressive strength ranged from 3,930 to 5,270 psi. The slab specimens contained headed bars anchored in the middle of the slab

with a clear cover to the bar of 35 in., as well as headed bars anchored close to the slab boundaries with a clear cover to the bar ranging from 1.6 to 4.9 in., as shown in Figure 3.19. The headed bars in the slab specimens were tested individually. During the tests, the support reaction plates were placed away from the headed bars at a distance equal to at least $1.5\ell_{eh}$ from the headed bars, as shown in Figure 3.19. For tests involving individual headed bars, the center-to-center spacing between the bars s required in the descriptive equations [Eq. (3.3) and (3.4)] to calculate anchorage strength is taken as twice of the minimum concrete cover to the center of the headed bar. Headed bars tested by Choi et al. (2002) had net bearing areas A_{brg} ranging from 2.6 to $3.2A_b$, which is less than the minimum net bearing area of $4A_b$ required in ACI 318-19.

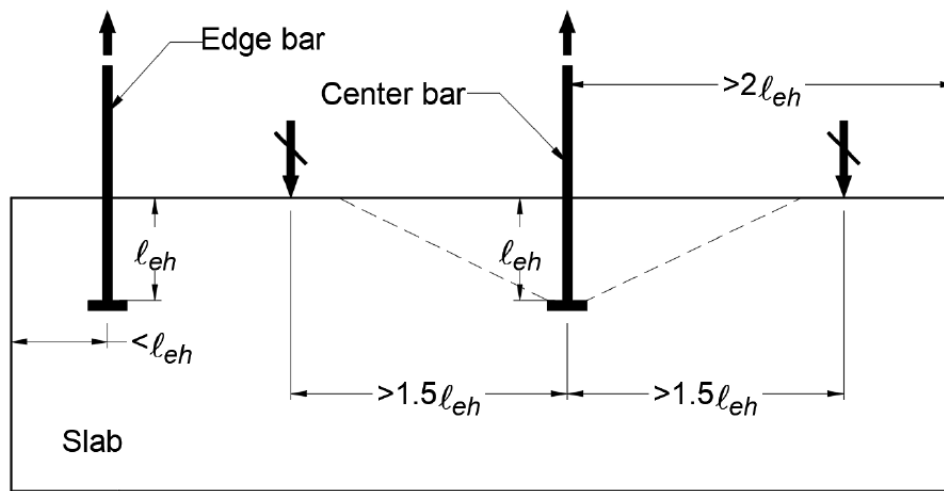
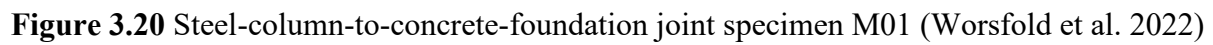


Figure 3.19 Slab specimens (Choi et al. 2002)

Ghimire et al. (2018) tested 32 headed bars anchored in slab specimens with embedment lengths ranging from 6 to 8.5 in. Concrete compressive strength ranged from 4,200 to 8,620 psi. The slab specimens contained two or three headed bars, with the exception of one slab that contained one headed bar anchored in the center of the slab. All headed bars were tested individually. The center-to-center spacing between the bars was at least three times the embedment length of the headed bars to avoid an overlap of the anticipated concrete failure region. Of the 32 tests, 22 had one of the support reaction plates located close to the headed bar at a distance of 10 in. ($1.2\ell_{eh}$ to $1.7\ell_{eh}$), and the other support plate was located far away from the headed bar at a distance of 44.3 in. ($5.2\ell_{eh}$ to $7.4\ell_{eh}$), nine tests had both support plates located outside the

anticipated concrete failure region at a distance ranging from 14.5 to 16.5 in. ($2.3\ell_{eh}$ to $2.8\ell_{eh}$), and one test had both support plates located far away from the headed bars at a distance of 47.5 in. ($5.6\ell_{eh}$). In accordance with Section 17.6.2.1.1 of ACI 318-19, the anticipated concrete failure region is measured as $1.5\ell_{eh}$ radial distance from the centerline of the headed anchors. Headed bars with net bearing areas A_{brg} ranging from 4 to $15A_b$ were tested. Shao et al. (2016) and Ghimire et al. (2018) found that increasing the net bearing area of the head from 3.8 to $9.5A_b$ did not increase the anchorage strength of headed bars; however, the anchorage strength of headed bars increased about 15% for heads with a net bearing area ranging from 13 to $15A_b$. Therefore, the results of the tests with headed bars with net bearing areas ranging from 13 to $15A_b$ are not included in this analysis.

Worsfold et al. (2022) and Worsfold and Mochle (2019, 2022) tested two steel-column-to-concrete-foundation joints located away from foundation edges under reversed cyclic loading with and without parallel tie reinforcement in the foundation to study the failure mechanisms and design requirements. As depicted in Figures (3.20) and (3.21), the test specimens consisted of a steel column (W12x106 ASTM A992 Grade 50) connected to a foundation slab by cast-in-place anchor bolts. The column was subjected to reversed cyclic lateral loads with no axial load other than column self-weight. Four 1.5 in. diameter anchor bolts with heavy hex nuts as heads in the first specimen M01 and with steel plate washers in the second specimen M02, as shown in Figures (3.20) and (3.21), respectively, were cast into the 18 in. thick foundation on each side of the column. The anchor bolts had an effective embedment length from the top of the slab to the bearing surface equal to 14.3 in. The net head bearing areas A_{brg} in specimens M01 and M02 were $1.5A_b$ and $5.5A_b$, respectively. The concrete compressive strengths were 3700 and 3930 psi for specimens M01 and M02, respectively. The nominal yield strength of the anchor bolts was 105,000 psi. Specimen M01 had five perpendicular No. 4 hoops in the joint region, as shown in Figure (3.20), while specimen M02 had No.4 bar parallel ties shaped as 180-degree hooks on the top and heads on the bottom, as shown in Figure (3.21). The parallel tie reinforcement in specimen M02 extended two rows farther on the west side than on the east side of the slab (Figure 3.22), and had no perpendicular hoops around the anchor bolts. A load cell was placed on each anchor bolt to measure the anchorage strength.



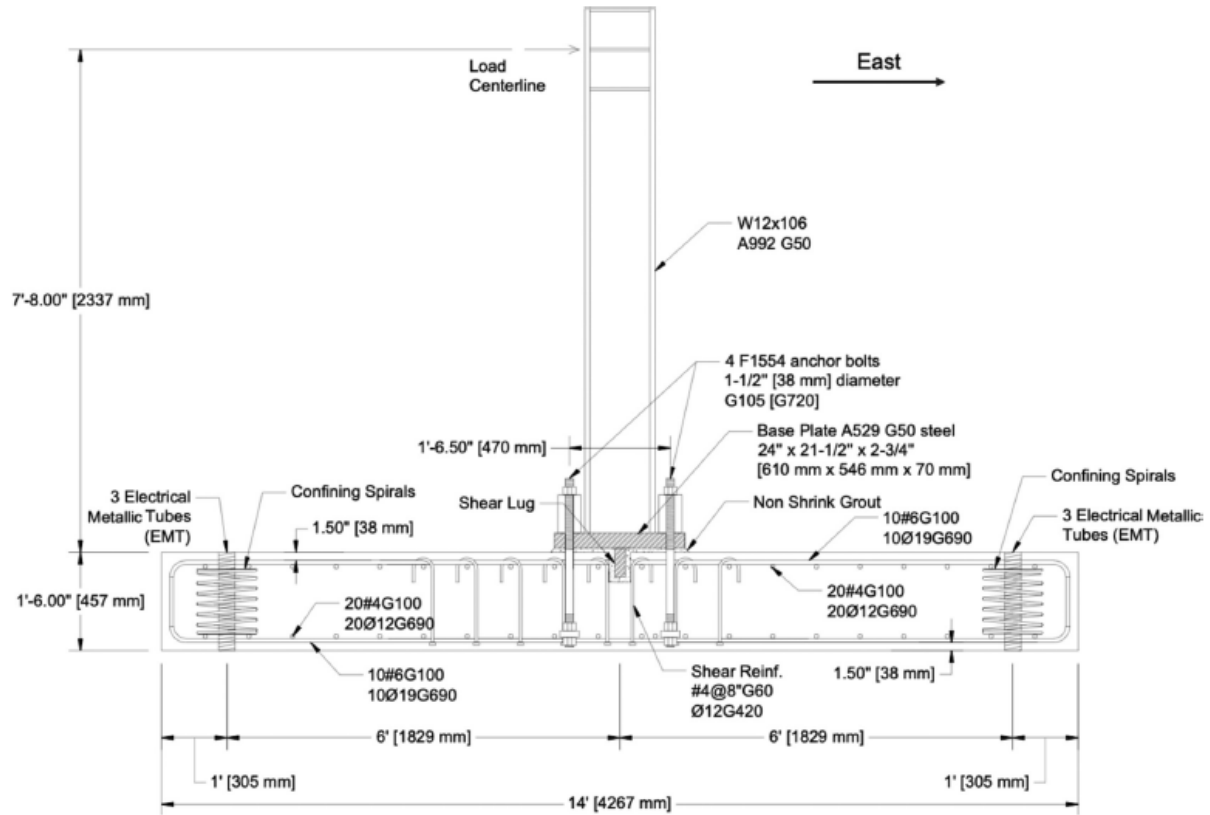


Figure 3.21 Steel-column-to-concrete-foundation joint specimen M02 (Worsfold et al. 2022)

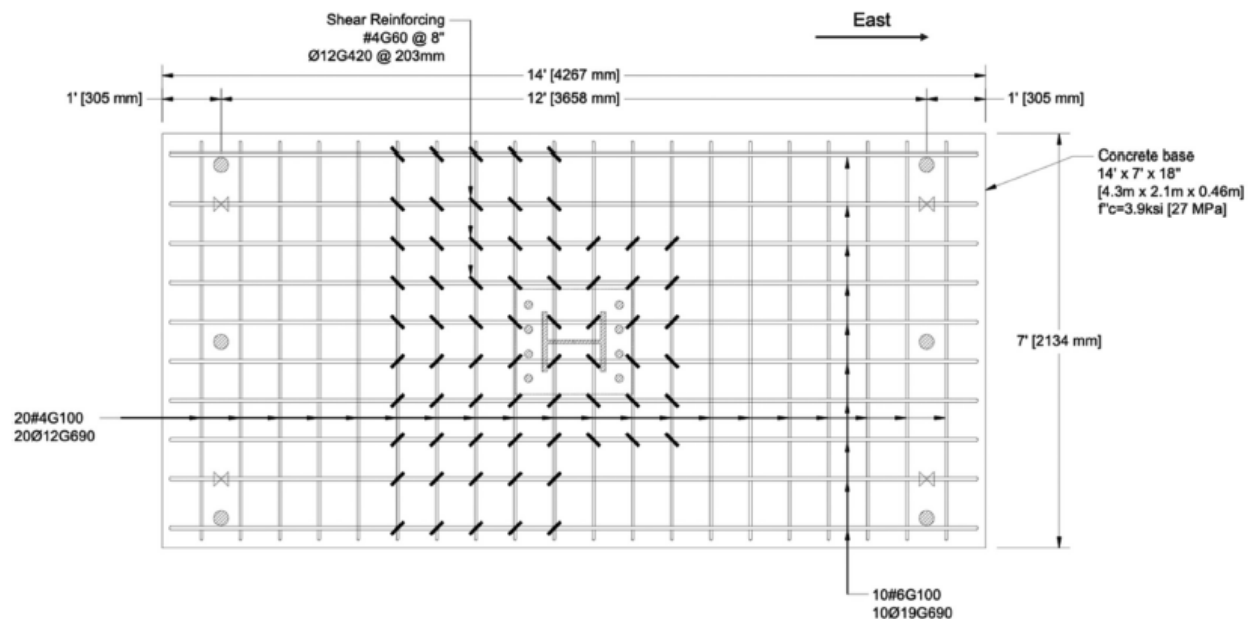


Figure 3.22 Plan view of specimen M02 (Worsfold et al. 2022)

3.2.1.1 Analysis Based on Descriptive Equations, ACI 318-19 Code Provisions, and Proposed Version of Code Provisions

The measured failure loads T on the headed bars tested by DeVries et al. (1999), Choi et al. (2002), Ghimire et al. (2018), Worsfold et al. (2022), and in the current study are compared with the calculated failure loads T_h [based on the descriptive equations, Eq. (3.3) and (3.4)], T_{anc} [based on the anchorage provisions of Chapter 17 of ACI 318-19, Eq. (3.9)], $T_{ACI\ 318}$ [based on the design provisions of Chapter 25 of ACI 318-19, Eq. (3.11)], and T_{calc} [based on the proposed version of the design provisions, as shown in Eq. (3.14)]. A 0.8 reduction factor is applied to the calculated failure load T_h from Eq. (3.3) and (3.4) for headed bars with side cover c_{so} less than $8d_b$ in slab specimens. The effective parallel tie reinforcement A_{tt} used in the descriptive equation, Eq. (3.4), is taken as the total parallel tie reinforcement on all sides of the headed bar(s) within $8d_b$ distance from the center of the headed bar for No. 3 through No. 8 bars or within $10d_b$ for No. 9 through No. 14 bars applying the $0.3A_b$ limit. The measured failure loads T and the calculated failure loads T_h , T_{anc} , $T_{ACI\ 318}$, and T_{calc} , along with the values of the embedment length ℓ_{eh} for specimens tested by DeVries et al. (1999), Choi et al. (2002), and Worsfold et al. (2022) are presented in Table 3.9, with full details provided in Tables C.1 and C.3 of Appendix C. Only headed bars that did not reach the yield strength are included in the analysis. The measured failure loads T and the calculated failure loads T_h , T_{anc} , $T_{ACI\ 318}$, and T_{calc} , along with the specimen properties for headed bars tested in the current study and by Ghimire et al. (2018), are presented in Table 3.1 and 3.2, respectively, with complete details provided in Table B.1 of Appendix B and Table C.2 of Appendix C, respectively.

Table 3.9 Test results for headed bars anchored in slab specimens tested by DeVries et al. (1999), Choi et al. (2002), and Worsfold et al. (2022) and comparisons with anchorage provisions of Chapter 17 of ACI 318-19 [Eq. (3.9)], descriptive equations [Eq. (3.3) and (3.4)], design provisions of Chapter 25 of ACI 318-19 [Eq. (3.11)], and proposed Code provisions [Eq. (3.14)], (a reduction factor of 0.8 is applied to T_h as appropriate ^[1])

Study	Specimen	ℓ_{eh} ^[2] (in.)	T ^{[2][3]} (kips)	T_{anc} (kips)	T_h (kips)	$T_{ACI\ 318}$ (kips)	T_{calc} (kips)	$\frac{T}{T_{anc}}$	$\frac{T}{T_h}$	$\frac{T}{T_{ACI318}}$	$\frac{T}{T_{calc}}$	Remarks
DeVries et al. (1999)	T2B2 ^[1]	9.0	33.3	31.9	32.6	17.7	22.6	1.04	1.02	1.88	1.48	Edge bars in slab specimens
	T2B4 ^[1]	9.0	38.7	31.9	32.6	17.7	22.6	1.21	1.19	2.18	1.71	
	T2B6 ^[1]	9.0	27.4	18.3	32.6	17.7	22.6	1.50	0.84	1.55	1.22	Corner bars in slab specimens
	T2B8 ^[1]	9.0	28.1	18.3	32.6	17.7	22.6	1.53	0.86	1.58	1.25	
Choi et al. (2002)	S16-7db.1	4.4	16.4	26.8	23.9	15.8	18.9	0.61	0.69	1.04	0.87	Center bars in slab specimens
	S16-7db.2	4.4	18.0	26.8	23.9	15.8	18.9	0.67	0.75	1.14	0.95	
	S25-7db.1	6.9	36.0	52.3	44.6	31.2	37.1	0.69	0.81	1.15	0.97	
	S25-7db.2	6.9	33.9	52.3	44.6	31.2	37.1	0.65	0.76	1.09	0.91	
	E16-7db.1 ^[1]	4.4	10.6	13.5	16.2	12.7	11.4	0.78	0.65	0.83	0.93	Edge bars in slab specimens
	E16-7db.2 ^[1]	4.4	10.6	13.5	16.2	12.7	11.4	0.78	0.65	0.83	0.93	
	E19-7db.1 ^[1]	5.2	11.7	16.0	21.1	15.5	15.5	0.73	0.55	0.76	0.76	
	E19-7db.2 ^[1]	5.2	10.8	16.0	21.1	15.5	15.5	0.67	0.51	0.70	0.70	
	E19-7db.3 ^[1]	5.2	17.5	22.4	22.7	15.5	17.9	0.78	0.77	1.13	0.98	
	E19-7db.4 ^[1]	5.2	16.9	22.4	22.7	15.5	17.9	0.75	0.74	1.09	0.94	
	E25-7db.1 ^[1]	6.9	19.6	26.4	29.9	15.6	22.0	0.74	0.65	1.26	0.89	
	E25-7db.2 ^[1]	6.9	20.7	26.4	29.9	15.6	22.0	0.78	0.69	1.33	0.94	
Worsfold et al. (2022)	M01	14.3	66.5	45.9	62.4	46.3	48.3	1.45	1.07	1.44	1.38	Steel column-concrete foundation
	M02	14.3	113.0	47.3	103.9	46.9	78.4	2.39	1.09	2.41	1.44	

^[1] A 0.8 reduction factor is applied when calculating T_h for headed bars with side cover c_{so} less than $8d_b$ in slab specimens

^[2] Values are converted from the SI unit (1 in. = 25.4 mm; 1 psi = 1/145 MPa; and 1 kip = 4.4484 kN)

^[3] T = average peak load (total peak load applied on the specimen divided by the number of headed bars being developed)

Descriptive Equations

The measured failure loads T of the headed bars in slab specimens tested by DeVries et al. (1999), Choi et al. (2002), Ghimire et al. (2018), Worsfold et al. (2022), and in the current study are plotted versus the calculated failure loads T_h [based on the descriptive equations, Eq. (3.3) and (3.4)] in Figure 3.23. The slab specimens tested by DeVries et al. (1999) and Choi et al. (2002)

had a ratio of distance between the center of the headed bars and the inner face of the nearest support reaction to the embedded length, h_{cl}/ℓ_{eh} , greater than 2 and 1.5, respectively (exact values were not reported), while h_{cl}/ℓ_{eh} in specimens tested by Ghimire et al. (2018), Worsfold et al. (2022), and in the current study ranged from 1.24 to 5.6.

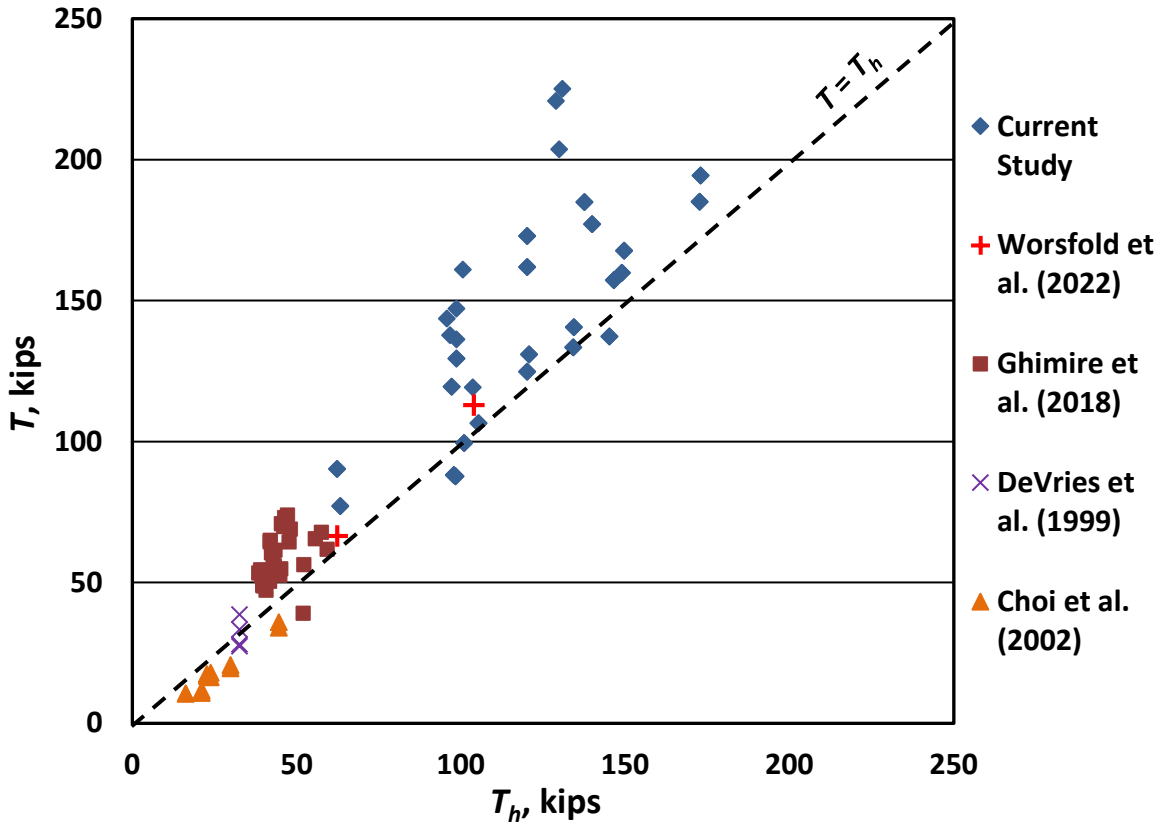


Figure 3.23 Measured force at failure T versus anchorage strength T_h calculated using Eq. (3.3) and (3.4) for slab specimens tested by DeVries et al. (1999), Choi et al. (2002), Ghimire et al. (2018), Worsfold et al. (2022), and in the current study; a reduction factor of 0.8 is applied to T_h for headed bars with concrete cover less than $8d_b$

For the specimens shown in Figure 3.23, the reduction factor of 0.8 for clear cover c_{so} less than $8d_b$ is applied to the four specimens tested by DeVries et al. (1999) and 8 out of 12 specimens tested by Choi et al. (2002). All specimens tested by Ghimire et al. (2018), Worsfold et al. (2022), and in the current study had $c_{so} > 8d_b$. The maximum, minimum, mean, standard deviation (STD), and coefficients of variation (COV) of T/T_h for the headed bars tested by DeVries et al. (1999), Choi et al. (2002), Ghimire et al. (2018), Worsfold et al. (2022) and in the current study are presented in Table 3.10. As shown in the table, all specimens tested by Choi et al. (2002) exhibited

lower anchorage strengths than those calculated by the descriptive equations with T/T_h between 0.51 and 0.81 and an average of 0.69. The values of T/T_h for the four edge and corner bars tested by DeVries et al. (1999) ranged from 0.84 to 1.19; the average for the four specimens is 0.98. The values of T/T_h for the headed bars tested by Ghimire et al. (2018) ranged from 0.75 to 1.57, with an average of 1.30. For the tests by Ghimire et al., only one specimen, which contained a single centrally placed headed bar with h_{cl}/ℓ_{eh} equal to 5.6, had a value of T/T_h less than 1.0. The values of T/T_h for the two specimens tested by Worsfold et al. (2022) are 1.07 and 1.09, with an average of 1.08. For the specimens in the current study, the values of T/T_h ranged from 0.89 to 1.72, with an average of 1.20. The ratio of test to calculated failure load of headed bars T/T_h in beam-column joint specimens tested and used by Shao et al. (2016) to develop the descriptive equations Eq. (3.3) and (3.4) ranged, respectively, from 0.68 to 1.27 with a mean, STD, and COV of 1.00, 0.111, and 0.111 for headed bar specimens without parallel ties and from 0.81 to 1.24 with a mean, STD, and COV of 1.00, 0.095, and 0.095 for headed bar specimens with parallel ties. Overall, the headed bars anchored in the column-foundation joint specimens shown in Tables 3.1, 3.2, 3.9, and the statistical parameters shown in Table 3.10 had values of T/T_h within or above the range of T/T_h for the beam-column joint specimens used to develop the descriptive equations Eq. (3.3) and (3.4), except for five of the edge bar specimens tested by Choi et al. (2002) (shown in Table 3.9). These results indicate that the descriptive equations based on tests of beam-column joints [Eq. (3.3) and (3.4)] are suitable for predicting the anchorage strength of headed bars anchored in slab specimens and, by extension, column-foundation joints. As previously stated, the net bearing areas A_{brg} of the headed bars tested by Choi et al. (2002) ranged from 2.6 to $3.2A_b$, which is less than the minimum net bearing area of $4A_b$ required by ACI 318-19. The low strengths of the specimens tested by Choi et al. (2002) may have been due to the small net bearing area, but specimen M01 tested under reversed cyclic loading by Worsfold et al. (2022) had anchor bolts with a net head bearing area A_{brg} of $1.5A_b$, and had a value of T/T_h equal to 1.07.

Table 3.10 Statistical parameters of T/T_h values for slab specimens tested by DeVries et al. (1999), Choi et al. (2002), Ghimire et al. (2018), Worsfold et al. (2022), and in the current study

Test/Calculated T/T_h ^[1] (a reduction factor of 0.8 is applied to the calculated strength as appropriate ^[2])											
Study [tests]	All	Current Study				Worsfold et al. (2022)	Ghimire et al. (2018)	Choi et al. (2002)		DeVries et al. (1999)	
		Individual headed bars		Multiple headed bars				Center bars	Edge bars	Edge bars	Corner bars
		without parallel tie ^[3]	with parallel tie ^[4]	without parallel tie ^[5]	with parallel tie ^[6]						
Number of specimens	81	6	3	12	10	2	32	4	8	2	2
Max	1.72	1.60	1.72	1.45	1.34	1.09	1.57	0.81	0.77	1.19	0.86
Min	0.51	1.15	1.57	0.89	0.95	1.07	0.75	0.69	0.51	1.02	0.84
Mean	1.16	1.43	1.67	1.16	1.11	1.08	1.30	0.75	0.65	1.10	0.85
STD	0.268	0.154	0.086	0.196	0.116	0.015	0.186	0.049	0.088	0.117	0.015
COV	0.232	0.108	0.052	0.169	0.105	0.014	0.143	0.066	0.135	0.106	0.017
Number of specimens with $T/T_h < 1.0$	20	0	0	3	2	0	1	4	8	0	2

^[1] T_h is calculated based on Eq. (3.3) and (3.4) for specimens without and with parallel tie reinforcement, respectively

^[2] A reduction factor of 0.8 is applied to T_h for headed bars terminating in slab specimens with side cover to the bar $< 8d_b$

^[3] Tests involved individual headed bars without parallel tie reinforcement in the joint region

^[4] Tests involved individual headed bars with parallel tie reinforcement in the joint region

^[5] Tests involved two headed bars loaded simultaneously without parallel tie reinforcement in the joint region

^[6] Tests involved two headed bars loaded simultaneously with parallel tie reinforcement in the joint region

Anchorage Provisions – Chapter 17 of ACI 318-19

To determine the applicability of the anchorage provisions in Chapter 17 of ACI 318-19, the failure loads T on the headed bars in the specimens tested by DeVries et al. (1999), Choi et al. (2002), Ghimire et al. (2018), Worsfold et al. (2022), and in the current study are compared with the calculated failure loads T_{anc} based on the anchorage provisions in Chapter 17 of ACI 318-19, Eq. (3.9). The calculated failure loads T_{anc} , governed by concrete breakout strength N_{cbg} [Eq. (3.6)] or anchorage strength of headed bars provided by anchor reinforcement N_{arg} [Eq. (3.8)].

Figure 3.24 presents the measured failure loads T on the headed bars in slab specimens tested by DeVries et al. (1999), Choi et al. (2002), Ghimire et al. (2018), Worsfold et al. (2022), and in the current study versus the calculated failure loads T_{anc} [based on the anchorage provisions

of Chapter 17 of ACI 318-19, Eq. (3.9)]. The calculated failure load T_{anc} values for the headed bars tested by DeVries et al. (1999), Choi et al. (2002), and Worsfold et al. (2022) are presented in Table 3.9, and for the headed bars tested in the current study and by Ghimire et al. (2018) in Tables 3.1 and 3.2, respectively. The calculated anchorage strengths of these headed bars were governed by the concrete breakout strength [Eq. (3.6), incorporating the modification factor ψ_{mean}] for all specimens.

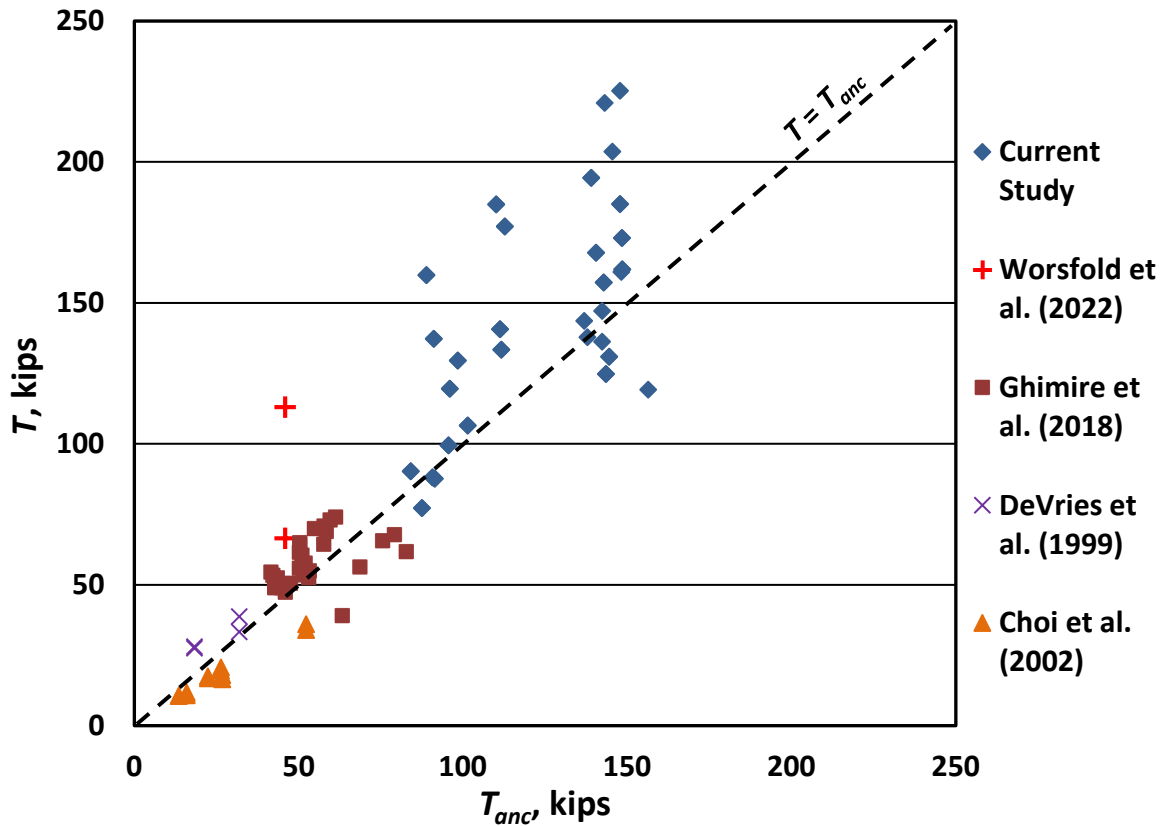


Figure 3.24 Measured force at failure T versus the anchorage strength T_{anc} calculated using Eq. (3.6), incorporating the modification factor ψ_{mean} , for slab specimens tested by DeVries et al. (1999), Choi et al. (2002), Ghimire et al. (2018), Worsfold et al. (2022), and in the current study

As shown in Figure 3.24, the specimens tested by DeVries et al. (1999) and Worsfold et al. (2022) and the majority of the specimens tested by Ghimire et al. (2018) and in the current study exhibited higher anchorage strengths than those calculated based on the concrete breakout strength. In contrast, the specimens tested by Choi et al. (2002) exhibited lower anchorage strengths than calculated by Eq. (3.6). The maximum, minimum, mean, standard deviation (STD),

and coefficients of variation (COV) of T/T_{anc} for the headed bars tested by DeVries et al. (1999), Choi et al. (2002), Ghimire et al. (2018), Worsfold et al. (2022), and in the current study are presented in Table 3.11. As shown in the table, the values of T/T_{anc} for the center bars in slab specimens tested by Choi et al. (2002) ranged from 0.61 to 0.69, with an average of 0.66, and the values of T/T_{anc} for the edge bars tested by Choi et al. (2002) ranged from 0.67 to 0.78, with an average of 0.75. The values of T/T_{anc} for the four edge and corner bars tested by DeVries et al. (1999) ranged from 1.04 to 1.53; the average for the four specimens was 1.32. The headed bars tested by Ghimire et al. (2018) had T/T_{anc} ranging from 0.62 to 1.31, with an average of 1.10; six out of the 32 specimens tested by Ghimire et al. (2018) had values of T/T_{anc} below 1.00 (with values ranging from 0.62 to 0.99). The values of T/T_{anc} for the two specimens tested by Worsfold et al. (2022) are 1.45 and 2.46, with an average of 1.95. For specimens tested in the current study, the values of T/T_{anc} ranged from 0.76 to 1.80, with an average value of 1.20; seven out of the 31 specimens tested in the current study had values of T/T_{anc} below 1.00 (with values ranging from 0.76 to 0.97). As previously mentioned, the net bearing area A_{brg} of the headed bars tested by Choi et al. (2002) ranged from 2.6 to $3.2A_b$, which is less than the minimum net bearing area of $4A_b$ required in ACI 318-19.

Table 3.11 Statistical parameters of T/T_{anc} values for slab specimens for which T_{anc} is governed by concrete breakout tested by DeVries et al. (1999), Choi et al. (2002), Ghimire et al. (2018), Worsfold et al. (2022), and in the current study

Test/Calculated T/T_{anc} ^[1]											
Study [tests]	All	Current Study				Worsfold et al. (2022)	Ghimire et al. (2018)	Choi et al. (2002)		DeVries et al. (1999)	
		Individual headed bars		Multiple headed bars				Center bars	Edge bars	Edge bars	Corner bars
		without parallel tie ^[2]	with parallel tie ^[3]	without parallel tie ^[4]	with parallel tie ^[5]						
Number of specimens	81	6	3	12	10	2	32	4	8	2	2
Max	2.39	1.09	1.54	1.32	1.80	2.39	1.31	0.69	0.78	1.21	1.53
Min	0.61	0.76	1.40	0.87	1.10	1.45	0.62	0.61	0.67	1.04	1.50
Mean	1.13	0.98	1.49	1.05	1.40	1.92	1.10	0.66	0.75	1.13	1.52
STD	0.293	0.116	0.077	0.138	0.227	0.664	0.173	0.032	0.038	0.120	0.026
COV	0.260	0.118	0.052	0.132	0.163	0.346	0.158	0.050	0.051	0.106	0.017
Number of specimens with $T/T_{anc} < 1.0$	25	2	0	5	0	0	6	4	8	0	0

^[1] T_{anc} is calculated using Eq. (3.6), incorporating the modification factor ψ_{mean}

^[2] Tests involved individual headed bars without parallel tie reinforcement in the joint region

^[3] Tests involved individual headed bars with parallel tie reinforcement in the joint region

^[4] Tests involved two headed bars loaded simultaneously without parallel tie reinforcement in the joint region

^[5] Tests involved two headed bars loaded simultaneously with parallel tie reinforcement in the joint region

Design Provisions – Chapter 25 of ACI 318-19

The measured failure load T on the headed bars in slab specimens tested by DeVries et al. (1999), Choi et al. (2002), Ghimire et al. (2018), Worsfold et al. (2022), and in the current study are plotted versus the calculated failure loads $T_{ACI\ 318}$ [based on the design provisions in Chapter 25 of ACI 318-19, Eq. (3.11)] in Figure 3.25. The values of $T_{ACI\ 318}$ for the headed bars tested by DeVries et al. (1999), Choi et al. (2002), and Worsfold et al. (2022) are presented in Table 3.9, and for the headed bars tested in the current study and by Ghimire et al. (2018) are presented in Tables 3.1 and 3.2, respectively.

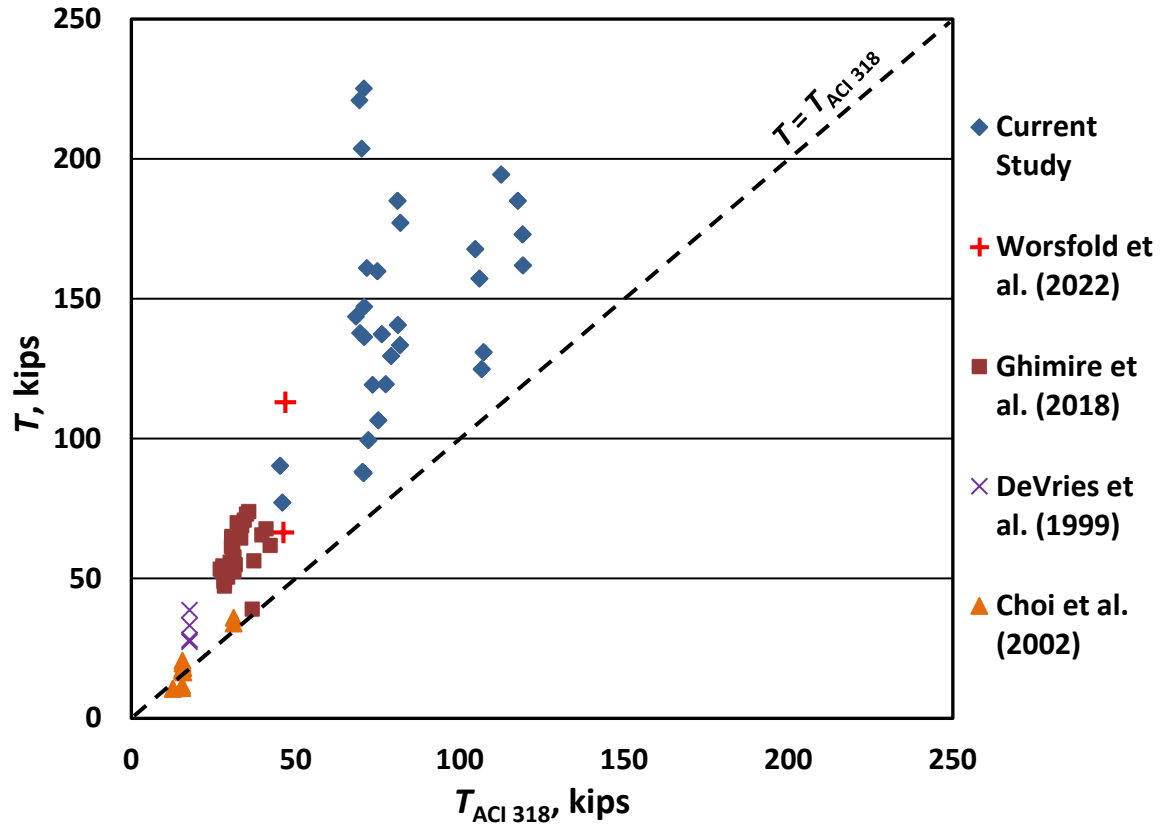


Figure 3.25 Measured force at failure T versus the anchorage strength $T_{ACI\ 318}$ calculated using Eq. (3.11) for slab specimens tested by DeVries et al. (1999), Choi et al. (2002), Ghimire et al. (2018), Worsfold et al. (2022), and in the current study

As shown in Figure 3.25, the specimens tested by DeVries et al. (1999), Ghimire et al. (2018), Worsfold et al. (2022), and in the current study, as well as 8 out of 12 specimens tested by Choi et al. (2002), exhibited higher anchorage strengths than those calculated by the design provisions Eq. (3.11), $T/T_{ACI\ 318} > 1.0$. The maximum, minimum, mean, standard deviation (STD), and coefficient of variation (COV) of $T/T_{ACI\ 318}$ for the headed bars tested by DeVries et al. (1999), Choi et al. (2002), Ghimire et al. (2018), Worsfold et al. (2022) and in the current study are presented in Table 3.12. The values of $T/T_{ACI\ 318}$ for the center bars in slab specimens tested by Choi et al. (2002) ranged from 1.04 to 1.15, with an average of 1.10, and the values of $T/T_{ACI\ 318}$ for the edge bars tested by Choi et al. (2002) ranged from 0.70 to 1.33, with an average of 0.99. The values of $T/T_{ACI\ 318}$ for the four edge and corner bars tested by DeVries et al. (1999) ranged from 1.55 to 2.18; the average for the four specimens was 1.80. The headed bars tested by Ghimire

et al. (2018) had T/T_{ACI318} ranging from 1.06 to 2.17, with an average of 1.83. The values of T/T_{ACI318} for the two specimens tested by Worsfold et al. (2022) are 1.44 and 2.41, with an average of 1.92. For specimens tested in the current study, the values of T/T_{ACI318} ranged from 1.17 to 3.18, with an average value of 1.74. These results indicate that the design provisions in Chapter 25 of ACI 318-19, Eq. (3.11), are conservative, and in most cases very conservative, in predicting the anchorage strength of headed bars anchored in column-foundation joints as expected. The design provisions in Chapter 25 of ACI 318-19, as previously stated, is a modified version of the descriptive equations, Eq. (3.3) and (3.4), with a strength reduction factor of 0.83 built-in, the square root of concrete compressive strength f'_c and ψ_c (defined in Section 3.2) rather than f_{cm} to the 0.24 power as in the descriptive equations, and use the modification factor ψ_p equal to 1 or 1.6 (intermediate values are not permitted) to represent the effect of anchored bar spacing and parallel ties instead of factors that varied as a function of bar spacing and the level of parallel tie reinforcement.

Table 3.12 Statistical parameters of T/T_{ACI318} values for slab specimens tested by DeVries et al. (1999), Choi et al. (2002), Ghimire et al. (2018), Worsfold et al. (2022), and in the current study

Test/Calculated T/T_{ACI318} ^[1]											
Study [tests]	All	Current Study				Worsfold et al. (2018)	Ghimire et al. (2018)	Choi et al. (2002)		DeVries et al. (1999)	
		Individual headed bars		Multiple headed bars				Center bars	Edge bars	Edge bars	Corner bars
		without parallel tie ^[2]	with parallel tie ^[3]	without parallel tie ^[4]	with parallel tie ^[5]						
Number of specimens	81	6	3	12	10	2	32	4	8	2	2
Max	3.18	2.25	3.18	1.99	2.28	2.41	2.17	1.15	1.33	2.18	1.58
Min	0.70	1.62	2.90	1.17	1.48	1.44	1.06	1.04	0.70	1.88	1.55
Mean	1.69	1.99	3.09	1.45	1.81	1.92	1.83	1.10	0.99	2.03	1.57
STD	0.447	0.212	0.159	0.232	0.272	0.689	0.240	0.053	0.240	0.215	0.027
COV	0.265	0.106	0.052	0.161	0.150	0.358	0.131	0.048	0.243	0.106	0.017
Number of specimens with $T/T_{ACI318} < 1.0$	4	0	0	0	0	0	0	0	4	0	0

^[1] T_{ACI318} is calculated using Eq. (3.11)

^[2] Tests involved individual headed bars without parallel tie reinforcement in the joint region

^[3] Tests involved individual headed bars with parallel tie reinforcement in the joint region

^[4] Tests involved two headed bars loaded simultaneously without parallel tie reinforcement in the joint region

^[5] Tests involved two headed bars loaded simultaneously with parallel tie reinforcement in the joint region

Proposed Code Provisions

The measured failure load T on the headed bars in slab specimens tested by DeVries et al. (1999), Choi et al. (2002), Ghimire et al. (2018), Worsfold et al. (2022), and in the current study are plotted versus the calculated failure loads T_{calc} [based on the proposed development length provisions, Eq. (3.14)] in Figure 3.26. The values of T_{calc} for the headed bars tested by DeVries et al. (1999), Choi et al. (2002), and Worsfold et al. (2022) are presented in Table 3.9, and for the headed bars tested in the current study and by Ghimire et al. (2018) are presented in Tables 3.1 and 3.2, respectively.

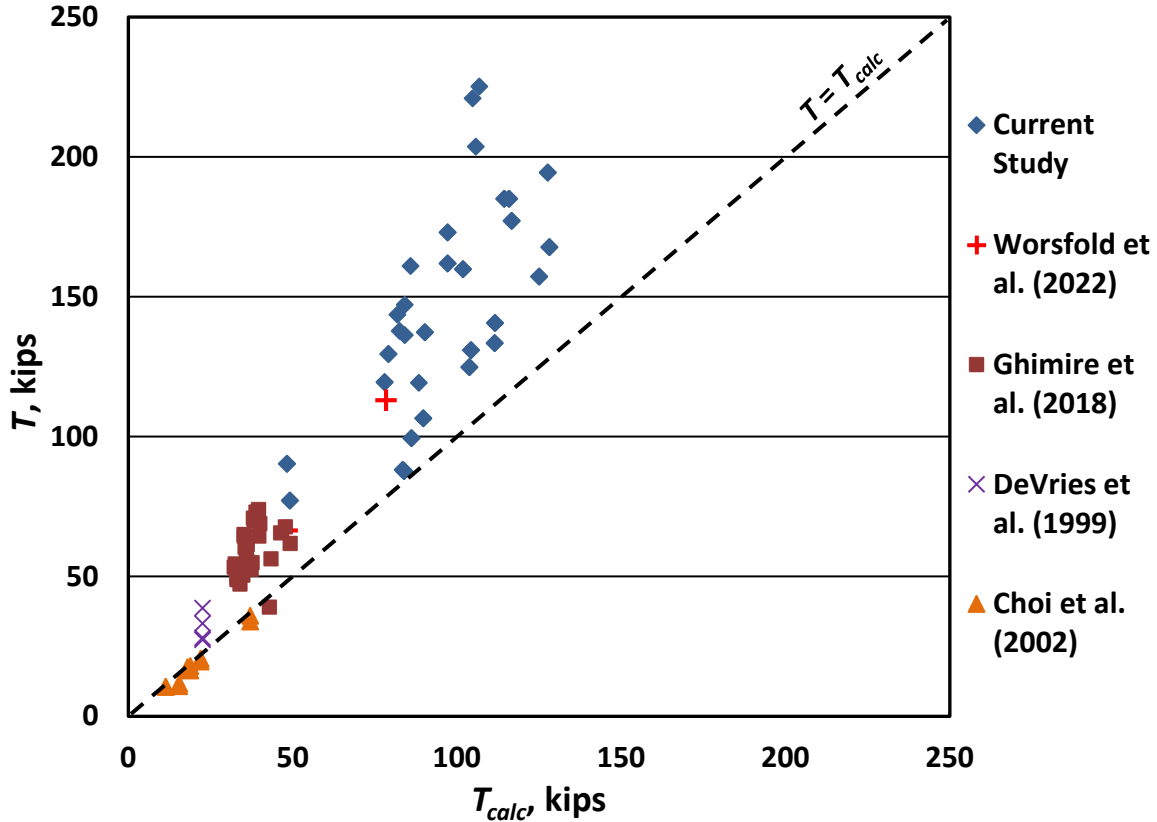


Figure 3.26 Measured force at failure T versus the anchorage strength T_{calc} calculated using Eq. (3.14) for slab specimens tested by DeVries et al. (1999), Choi et al. (2002), Ghimire et al. (2018), Worsfold et al. (2022), and in the current study

As shown in Figure 3.26, the specimens tested by DeVries et al. (1999), Ghimire et al. (2018) [except one specimen with h_{cl}/ℓ_{eh} equal to 5.6], Worsfold et al. (2022), and in the current study had higher anchorage strengths than those calculated using Eq. (3.14). In contrast, the specimens tested by Choi et al. (2002) had lower anchorage strengths than those calculated using Eq. (3.14). The maximum, minimum, mean, standard deviation (STD), and coefficient of variation (COV) of T/T_{calc} for the headed bars tested by DeVries et al. (1999), Choi et al. (2002), Ghimire et al. (2018), Worsfold et al. (2022) and in the current study are presented in Table 3.13. The values of T/T_{calc} for the center bars in slab specimens tested by Choi et al. (2002) ranged from 0.87 to 0.97, with an average of 0.93, and the values of T/T_{calc} for the edge bars tested by Choi et al. (2002) ranged from 0.70 to 0.98, with an average of 0.88. The values of T/T_{calc} for the four edge and corner bars tested by DeVries et al. (1999) ranged from 1.22 to 1.71; the average for the four

specimens is 1.41. The headed bars tested by Ghimire et al. (2018) had T/T_{calc} ranging from 0.91 to 1.88, with an average of 1.56. For the tests by Ghimire et al., only one specimen, which contained a single centrally placed headed bar with h_{cl}/ℓ_{eh} equal to 5.6, had a value of T/T_{calc} less than 1.0. The values of T/T_{calc} for the two specimens tested by Worsfold et al. (2022) are 1.38 and 1.44, with an average of 1.41. For specimens tested in the current study, the values of T/T_{calc} ranged from 1.04 to 2.11, with an average value of 1.48.

Table 3.13 Statistical parameters of T/T_{calc} values for slab specimens tested by DeVries et al. (1999), Choi et al. (2002), Ghimire et al. (2018), Worsfold et al. (2022), and in the current study

Test/Calculated T/T_{calc} ^[1]											
Study [tests]	All	Current Study				Worsfold et al. (2022)	Ghimire et al. (2018)	Choi et al. (2002)		DeVries et al. (1999)	
		Individual headed bars		Multiple headed bars				Center bars	Edge bars	Edge bars	Corner bars
		without parallel tie ^[2]	with parallel tie ^[3]	without parallel tie ^[4]	with parallel tie ^[5]						
Number of specimens	81	6	3	12	10	2	32	4	8	2	2
Max	2.11	1.88	2.11	1.87	1.62	1.44	1.88	0.97	0.98	1.71	1.25
Min	0.70	1.35	1.93	1.04	1.20	1.38	0.91	0.87	0.70	1.48	1.22
Mean	1.43	1.67	2.05	1.41	1.41	1.41	1.56	0.93	0.88	1.59	1.23
STD	0.310	0.180	0.106	0.287	0.144	0.045	0.219	0.044	0.100	0.169	0.021
COV	0.217	0.108	0.052	0.203	0.102	0.032	0.140	0.048	0.113	0.106	0.017
Number of specimens with $T/T_{calc} < 1.0$	13	0	0	0	0	0	1	4	8	0	0

^[1] T_{calc} is calculated using Eq. (3.14)

^[2] Tests involved individual headed bars without parallel tie reinforcement in the joint region

^[3] Tests involved individual headed bars with parallel tie reinforcement in the joint region

^[4] Tests involved two headed bars loaded simultaneously without parallel tie reinforcement in the joint region

^[5] Tests involved two headed bars loaded simultaneously with parallel tie reinforcement in the joint region

3.2.1.2 Comparison Between the Descriptive Equations, ACI 318-19 Code Provisions, and Proposed Code Provisions

The comparisons between the descriptive equations developed by Shao et al. (2016) Eq. (3.3) and (3.4), the provisions in Chapters 17 and 25 of ACI 318-19. Eq. (3.9) and (3.11),

respectively, and the proposed Code provisions. Eq. (3.14) are presented in this section. The four methods to predict the failure load of the headed bars anchored in a simulated column-foundation joint are compared. As previously stated, the descriptive equations were developed to give an average ratio of test-to-calculated failure load equal to 1.0 for beam-column joint specimens. In this analysis, the effective parallel tie reinforcement A_{tt} used in the descriptive equation, Eq. (3.4), is defined as the total parallel tie reinforcement within $8d_b$ radial distance from the center of the headed bar for No. 3 through No. 8 bars or within $10d_b$ for No. 9 through No. 14 bars and is not limited to a single side, as is the case in beam-column joints, as is the case in Chapter 25 of ACI 318-19. The anchorage provisions in Chapter 17 of ACI 318-19 are based on the 5% fractile. In this case, a modification factor (ψ_{mean}), 1.33, is used to convert the 5% fractile value to a mean value. The design provisions in Chapter 25 of ACI 318-19 are a modified version of the descriptive equations, Eq. (3.3) and (3.4), with a strength reduction factor, ϕ , of 0.83 built-in, the square root of concrete compressive strength f'_c and ψ_c (defined in Section 3.2) rather than f_{cm} to the 0.24 power as in the descriptive equations, and use the modification factor ψ_p equal to 1 or 1.6 (intermediate values are not permitted) to represent the effect of anchored bar spacing and parallel ties instead of factors that varied as a function of bar spacing and the level of parallel tie reinforcement. Therefore, anchorage strengths calculated based on these design provisions are expected to be conservative. Finally, the proposed Code provisions are also based on the descriptive equations, Eq. (3.3) and (3.4), with a strength reduction factor, ϕ , of 0.83 built-in, but with a more accurate representation of the effect of the concrete strength, confining reinforcement, and the center-to-center spacing between the headed bars. Therefore, the anchorage strength calculated based on proposed Code provisions is expected to be conservative as well, but not as conservative as the provisions in ACI 318-19. The results for the headed bars tested in the current study (Table 3.1) are used in this comparison.

Figure 3.27 shows the average values of T/T_h , T/T_{anc} , $T/T_{ACI\ 318}$, and T/T_{calc} for tests with two headed bars loaded simultaneously without and with parallel tie reinforcement [Slab Specimens 6, 7 and 10 [(2@8.2)11-5-S5.5-7#11-0-12.75], Slab Specimens 12 and 14 [(2@6.8)14-5-B4.2-7#11-0-12.75], Slab Specimens 8, 9 and 11 [(2@8.2)11-5-S9.2-7#11-6#4-12.75], and Slab Specimens 13 and 15 [(2@6.8)14-5-B4.2-7#11-6#4-12.75], where T is the measured anchorage

strength on the headed bar at failure, T_h is the calculated anchorage strength of the headed bar [based on the descriptive equations, Eq. (3.3) and (3.4)], T_{anc} is the calculated anchorage strength of the headed bar [based on the anchorage provisions of Chapter 17 of ACI 318-19, Eq. (3.9)], $T_{ACI 318}$ is the calculated anchorage strength of the headed bar [based on the design provision in Chapter 25 of ACI 318-19, Eq. (3.11)], and T_{calc} is the calculated anchorage strength of the headed bar [based on the proposed Code provisions, Eq. (3.14)]. The specimen details and test results of the twenty tests used in this comparison are presented in Table 3.1. As shown in Figure 3.27, the average values of T/T_h for tests with two headed bars loaded simultaneously without and with parallel tie reinforcement are nearly identical at 1.12 and 1.11, respectively, indicating that the descriptive equations [Eq. (3.3) and (3.4)] provide a consistent and somewhat conservative representation of headed bars anchored in a region that is larger than a beam-column connection.

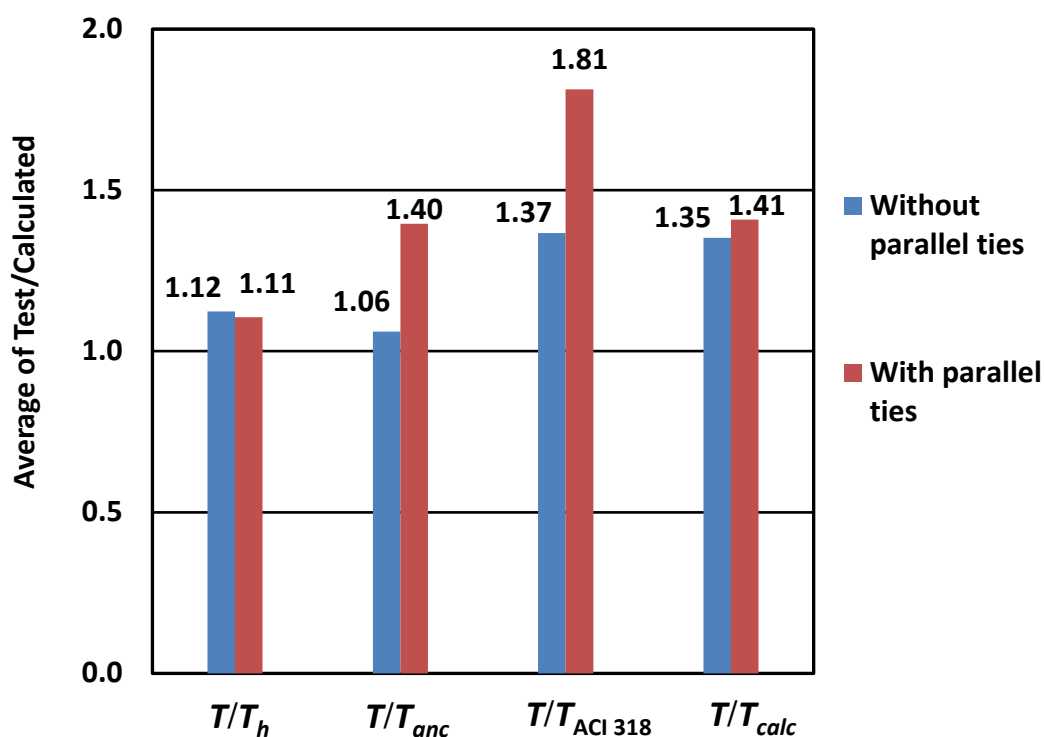


Figure 3.27 Average values of T/T_h , T/T_{anc} , $T/T_{ACI 318}$, and T/T_{calc} for tests involving two headed bars without and with parallel tie reinforcement, Slab Specimens 6, 7 and 10 [(2@8.2)11-5-S5.5-7#11-0-12.75], Slab Specimens 12 and 14 [(2@6.8)14-5-B4.2-7#11-0-12.75], Slab Specimens 8, 9 and 11 [(2@8.2)11-5-S9.2-7#11-6#4-12.75], and Slab Specimens 13 and 15 [(2@6.8)14-5-B4.2-7#11-6#4-12.75]

The average values of T/T_{anc} for tests involving two headed bars loaded simultaneously without and with parallel tie reinforcement in the joint region are 1.06 and 1.40, respectively. Student's t-test shows that the difference in the average values of T/T_{anc} for two headed bars tested simultaneously without and with parallel tie reinforcement in the joint region is statistically significant, with $p = 0.0012$. Because the anchorage provisions of Chapter 17 of ACI 318-19, [Eq. (3.9)] T_{anc} account for the contribution of concrete and parallel tie reinforcement (anchor reinforcement) separately, with only the stronger of the two controlling the strength. On the other hand, the descriptive equations (T_h) account for the contribution of both parallel tie reinforcement and concrete compressive strength on the anchorage strength of headed bars, and because T_{anc} for these specimens is governed by concrete breakout and does not include the contribution of the parallel tie reinforcement within the joint region in these tests, this difference is expected.

The average values of T/T_{ACI318} for tests including two headed bars loaded simultaneously without and with parallel tie reinforcement in the joint region are 1.37 and 1.81, respectively, a difference that is statistically significant, with $p = 0.00032$. The higher values of 1.81 results at least in part to the fact that the ACI design provisions take into account the contribution of parallel tie reinforcement for beam-column joints, but not for column-foundation joints.

The average values of T/T_{calc} for tests involving two headed bars loaded simultaneously without and with parallel tie reinforcement in the joint region are 1.35 and 1.41, respectively. Student's t-test shows that the difference in the average values of T/T_{calc} for two headed bars tested simultaneously without and with parallel tie reinforcement in the joint region is not statistically significant, with $p = 0.574$. These results indicate that proposed Code provisions [Eq. (3.14)] are conservative and consistent for this case if the contribution of parallel ties can be counted.

Summary

The anchorage provisions in Chapter 17 and the design provisions in Chapter 25 of ACI 318-19 Equations (3.9) and (3.11), respectively, do not accurately capture the effect of parallel tie reinforcement on the anchorage strength of headed bars tested with parallel tie reinforcement within the joint region. On the other hand, the descriptive equations [Eq. (3.3) and (3.4)] and the proposed Code provisions [Eq. (3.14)] accurately capture the effect of parallel tie reinforcement on the anchorage strength. In these tests, T_{anc} is governed by the concrete breakout strength N_{cbg}

[Eq. (3.6), incorporating the modification factor ψ_{mean}], which does not account for the contribution of anchor reinforcement to anchorage strength. That is, the anchorage provisions in Chapter 17 of ACI 318-19 [Eq. (3.9)] T_{anc} account for the contribution of concrete and parallel tie reinforcement (anchor reinforcement) separately, with only the stronger of the two controlling the strength. In contrast, the descriptive equations [Eq. (3.3) and (3.4)] T_h account for the contribution of both parallel tie reinforcement and concrete to anchorage strength. The design provisions in Chapter 25 of ACI 318-19 [Eq. (3.11)] T_{ACI318} do not consider the effect of parallel tie reinforcement for other than beam-column joints or the spacing between headed bars when the headed bars are spaced at a center-to-center distance less than $6d_b$. On the other hand, the Code provisions as proposed here [Eq. (3.14)] account for the contribution of parallel tie reinforcement and the effect of the center-to-center spacing between the headed bars on the anchorage strength.

3.3 RECOMMENDED CHANGES TO CHAPTERS 17 AND 25 OF ACI 318-19

Based on the analysis of the data presented in this chapter and the observations described in Sections 3.2.1.1 and 3.2.1.2, the following changes are recommended for ACI 318.

- 1- The anchorage provisions in Chapter 17 of ACI 318-19 do not accurately predict the anchorage strength of headed bars tested when parallel tie/anchor reinforcement is used. The anchorage provisions account for the contribution of concrete and parallel tie reinforcement (anchor reinforcement) separately, with only the stronger of the two controlling the strength. Therefore, the ACI 318 Code should consider including provisions that combine the contributions of concrete strength and parallel tie reinforcement.
- 2- The contributions of concrete strength and parallel tie reinforcement are combined in the descriptive equations [Eq. (3.3) and (3.4)]. Based on the analysis presented in this chapter, the descriptive equations [Eq. (3.3) and (3.4)] accurately capture the effect of parallel tie reinforcement and the contribution of concrete strength to the anchorage strength of headed bars. Therefore, a version of the descriptive equations [Eq. (3.3) and (3.4)] could be used within the anchorage provisions in Chapter 17 of the ACI 318 Code.

- 3- The design provisions in Chapter 25 of ACI 318-19 [Eq. (3.10)] do not consider the contribution of parallel tie reinforcement to the development of headed bars anchored in members other than beam-column joints. Furthermore, the design provisions in Chapter 25 of ACI 318-19 ignore the contribution of parallel tie reinforcement when headed bars are spaced at a center-to-center distance equal to or greater than $6d_b$. However, the analysis presented by Shao et al. (2016) for beam-column joints and in this chapter for column-foundation joints shows that the effect of parallel tie reinforcement is real even for widely-spaced headed bars. Therefore, the design provisions in Chapter 25 of ACI 318-19 should be further modified to accurately represent the effect of parallel tie reinforcement, headed bar spacing, and concrete strength.
- 4- Based on the analysis presented in Sections 3.2.1.1 and 3.2.1.2, the proposed Code provisions [Eq. (3.12) and (3.13)] accurately capture the effect of parallel tie reinforcement on the anchorage strength of headed bars. Therefore, the ACI 318 Code should consider including proposed Code provisions [Eq. (3.12) and (3.13)] in the next version. Section 3.3.1 addresses the proposed changes in Chapter 25 of ACI 318-19.

3.3.1 Proposed Changes in Chapter 25 of ACI 318-19

Based on the analysis presented in this chapter and the summary presented in Sections 3.2.1.2 and 3.3, proposed changes to Chapter 25 of ACI 318-19 are provided in this section. The original text of the Code is presented in black, while proposed code and commentary changes are shown in red underlined or ~~strikeout~~.

25.4.4 *Development of headed deformed bars in tension*

25.4.4.1 Use of a head to develop a deformed bar in tension shall be permitted if conditions (a) through (f) are satisfied:

- (a) Bar shall conform to 20.2.1.6
- (b) Bar size shall not exceed No. 11
- (c) Net bearing area of head A_{brg} shall be at least ~~4~~ A_b
- (d) Concrete shall be normalweight

- (e) Clear cover for bar shall be at least $2d_b$
- (f) Center-to-center spacing between bars shall be at least $3d_b$

R25.4.4 Development of headed deformed bars in tension

R25.4.4.1 As used in this section, development describes cases in which the force in the bar is transferred to the concrete through a combination of a bearing force at the head and bond forces along the bar. In contrast, Chapter 17 anchorage provisions describe cases in which the force in the bar is transferred through bearing to the concrete at the head alone. Headed bars are limited to those types that meet the criteria in 20.2.1.6 for Class HA heads.

The provisions for headed deformed bars were formulated with due consideration of the provisions for anchorage in Chapter 17 (Shao et al. 2016). Chapter 17 contains provisions for headed anchors related to the individual failure modes of concrete breakout, side-face blowout, and pullout. These failure modes were considered in the formulation of 25.4.4.2. The restrictions to maximum bar size of No. 11 and normalweight concrete are based on a lack of data for larger bars or lightweight concrete (Thompson et al. 2005, 2006a,b; Shao et al. 2016). ~~The upper limit of 60,000 psi on f_y that appeared prior to the 2019 Code has been removed.~~

For bars in tension, heads allow the bars to be developed in a shorter length than required for standard hooks, but otherwise perform in a similar manner (Thompson et al. 2005, 2006a,b; Shao et al. 2016). The head is considered to be part of the bar for the purposes of satisfying the specified cover requirements in 20.5.1.3 and aggregate size requirements of 26.4.2.1(a)(5).

Headed bars with $A_{brg} < 4A_b$ have been used in practice, but their performance is not accurately represented by the provisions in 25.4.4.2, and they should be used only with designs that are supported by test results under 25.4.5. These provisions do not address the design of studs or headed stud assemblies used for shear reinforcement.

25.4.4.2 Development length ℓ_{dt} for headed deformed bars in tension shall be the longest of (a) through (c):

$$(a) \quad \frac{\left(\frac{f_y \psi_e \psi_p \psi_o \psi_c}{75 \sqrt{f'_c}} \right) d_b^{1.5}}{\left(\frac{f_y \psi_e \psi_p \psi_o}{600 f'_c{}^{0.25}} \right) d_b^{1.5}} \quad \text{with } \psi_e, \psi_p, \text{ and } \psi_o, \text{ and } \psi_c \text{ given in 25.4.4.3}$$

and where the value of f'_c used to calculate ℓ_{dt} shall not exceed 16,000 psi

(b) $8d_b$

(c) 6 in.

R25.4.4.2 The provisions for developing headed deformed bars give the length of bar, ℓ_{dt} , measured from the critical section to the bearing face of the head, as shown in Fig. R25.4.4.2a. The provisions are primarily based on tests of simulated beam-column joints and have been verified up to concrete compressive strengths of 16,000 psi and bar stresses at failure up to 150,000 psi (Shao et al. 2016, Ghimire et al. 2019).

If longitudinal headed deformed bars from a beam, slab, or corbel terminate in a supporting member, such as the column shown in Fig. R25.4.4.2b, the bars should extend through the joint to the far face of the confined core of the supporting member, allowing for cover and avoidance of interference with column reinforcement, even though the resulting anchorage length may exceed ℓ_{dt} . Extending the bar to the far side of the column core helps engage the entire joint in resisting the anchorage forces and thereby improves the performance of the joint.

If closely spaced headed bars are used, the potential for concrete breakout failure exists. For joints as shown in Fig. R25.4.4.2c and R25.4.4.2d, anchorage strengths will be generally higher if the anchorage length is equal to or greater than $d/1.5$ (Eligehausen 2006b), as shown in Fig. R25.4.4.2c, or by providing reinforcement in the form of hoops and ties to establish a load path in accordance with strut-and-tie modeling principles, as shown in Fig. R25.4.4.2d. Strut-and-tie models should be verified in accordance with Chapter 23. Note that the strut-and-tie models illustrated in Fig. R25.4.4.2c and R25.4.4.2d rely on a vertical strut from a column extending above the joint. Beam-column joints at roof-level and portal frames are vulnerable to joint failure and should be properly detailed to restrain diagonal cracking through the joint and breakout of the bars through the top surface.

For cases where development length cannot be designed in accordance with 25.4.4.2, use of the provisions of Chapter 17 should be considered.

25.4.4.3 For the calculation of ℓ_{dt} , modification factors ψ_e , ψ_p , and ψ_o , ~~and ψ_e~~ shall be in

accordance with Table 25.4.4.3.

Table 25.4.4.3—Modification factors for development of headed bars in tension

Modification factor	Condition	Value of factor
Epoxy ψ_e	Epoxy-coated or zinc and epoxy dual-coated reinforcement	1.2
	Uncoated or zinc-coated (galvanized) reinforcement	1.0
Parallel tie reinforcement ψ_p	For No. 11 and smaller bars with $A_{tr} \geq 0.3A_{hs}$ or $s^{[1]} \geq 6d_b^{[2,3]}$	1.0
	Other	1.6
<u>Parallel tie reinforcement and headed bar spacing ψ_p ^[3]</u>	<u>$s^{[1]} \geq 3d_b^{[2]}$ When calculating ψ_p, A_{tr}/A_{hs} shall not exceed 0.3 and s/d_b shall not exceed 8</u>	<u>$\frac{1}{4} \left(7 - 10 \frac{A_{tr}}{A_{hs}} - 0.5 \frac{s}{d_b} + \frac{A_{tr}}{A_{hs}} \frac{s}{d_b} \right)$</u>
Location ψ_o	For headed bars: (1) Terminating inside column core with side cover to bar ≥ 2.5 in.; or (2) With side cover to bar $\geq 6d_b$	1.0
	Other	1.25
Concrete strength ψ_e	For $f'_e < 6000$ psi	$f'_e/15,000 + 0.6$
	For $f'_e \geq 6000$ psi	1.0

^[1] s is minimum center-to-center spacing of headed bars

^[2] d_b is nominal diameter of headed bar.

^[3] Refer to 25.4.4.5.

R25.4.4.3 The epoxy factor 1.2 is based conservatively on the value used for epoxy-coated standard hooks. The location factor ψ_o accounts for the confinement provided by the reinforcement within columns and large side cover for other members.

The factor ψ_p for headed reinforcement is similar to the confining reinforcement factor for

hooked bars (Shao et al. 2016). Like confining reinforcement for hooked bars, parallel ties are more effective for more closely-spaced headed bars, and the effects of increasing the area of parallel ties and increasing the spacing of headed bars are not directly additive. Unlike hooked bars, ~~however,~~ test results indicate that only tie or hoop reinforcement parallel to headed bars contributes to anchorage strength and reduces development length (Thompson et al. 2005, 2006a,b).

25.4.4.4 For beam column joints, the total cross-sectional area of parallel tie reinforcement A_{tt} shall consist of ties or stirrups oriented parallel to ℓ_{dt} and located within $8d_b$ of the centerline of the headed bar toward the middle of the joint, where d_b is the nominal diameter of the headed bar.

R25.4.4.4 Reinforcement oriented parallel to the development length of the headed bars, located within the region defined in 25.4.4.4 (Fig. R25.4.4.4) contributes to anchorage strength in proportion to its area (Shao et al. 2016). This reinforcement serves to tie concrete near the head to concrete on the other side of the failure surface, thus mobilizing additional anchorage strength. With the exception of vertical joint reinforcement in the form of stirrups that are well anchored to the far side of the joint, reinforcement oriented perpendicular to the development length has been shown in a number of cases to be ineffective in improving the anchorage of headed deformed bars (Thompson et al. 2005, 2006a,b). Both legs of individual stirrups and ties parallel to the headed bars contribute to A_{tt} .

25.4.4.5 For anchorages other than in beam-column joints, parallel tie reinforcement, A_{tt} , shall ~~not be considered, taken as the total parallel tie reinforcement located on all sides of the headed bars within an $8d_b$ radial distance from the centerline of the headed bars and ψ_p shall be taken as 1.0 provided the spacing is at least $6d_b$.~~

R25.4.4.5 ~~No evidence is available regarding the effect of parallel reinforcement on the development length of headed bars except in beam-column joints~~ For members other than beam-column joints, test results indicate that the total cross-section area of parallel tie reinforcement A_{tt}

located on all sides of headed bars within $8d_b$ of the centerline of headed bars, not limited to a single side as is the case in beam-column joints, contribute to anchorage strength.

CHAPTER 4: ANALYSIS OF BEAM-COLUMN JOINT SPECIMENS WITH BEAM BARS ANCHORED WITH HOOKS SUBJECTED TO REVERSED CYCLIC LOADING

4.1 INTRODUCTION

An analysis of exterior beam-column joint specimens containing hooked bars tested under reversed cyclic loading is presented in this chapter. The results of 146 specimens from 24 studies were analyzed using descriptive equations for anchorage strength and design provisions for the development length of hooked bars proposed by Ajaam et al. (2017), presented in detail in Section 1.3.2. The effects of test parameters, including embedment length, concrete compressive strength, center-to-center spacing between the hooked bars, bar size, and confining reinforcement within the joint region on the performance of the beam-column joints subjected to reversed cyclic loading are discussed.

This chapter includes the results of exterior beam-column joint specimens tested under reversed cyclic loading by Hanson and Connor (1967), Hanson (1971), Megget (1974), Uzumeri (1977), Lee et al. (1977), Scribner (1978), Paulay and Scarpas (1981), Ehsani and Wight (1982), Kanada et al. (1984), Zerbe and Durrani (1985), Ehsani et al. (1987), Ehsani and Alameddine (1991), Kaku and Asakusa (1991), Tsonos et al. (1992), Pantelides et al. (2002), Chutarat and Aboutaha (2003), Hwang et al. (2005), Lee and Ko (2007), Chun et al. (2007), Tsonos (2007), Kang et al. (2010), Chun and Shin (2014), Hwang et al. (2014), and Choi and Bae (2019). Complete details of these studies are presented in Appendix D.

4.2 ANALYSIS BASED ON PROPOSED DESCRIPTIVE AND DESIGN EQUATIONS

Test results of 146 exterior beam-column joint specimens subjected to reversed cyclic loading are analyzed using descriptive equations for anchorage strength and design provisions for the development length of hooked bars based on monotonic loading. The analysis is conducted to investigate the applicability of these equations to joints subjected to reversed cyclic loading.

4.2.1 Descriptive Equations and Design Provisions Proposed by Ajaam et al. (2017)

Ajaam et al. (2017) developed descriptive equations for anchorage strength and design provisions for the development length of hooked bars, as described in Section 1.3.2, based on test

results of 353 exterior beam-column joint specimens subjected to monotonic loading. Equations (4.1) and (4.2) are the descriptive equations for the anchorage strength of hooked bars without and with confining reinforcement, respectively.

$$T_h = \left(294 f_{cm}^{0.295} \ell_{eh}^{1.0845} d_b^{0.47} \right) \left(0.0974 \frac{c_{ch}}{d_b} + 0.3911 \right) \quad (4.1)$$

$$\text{with } \left(0.0974 \frac{c_{ch}}{d_b} + 0.3911 \right) \leq 1.0$$

$$T_h = \left(294 f_{cm}^{0.295} \ell_{eh}^{1.0845} d_b^{0.47} + 55050 \left(\frac{A_{th}}{n} \right)^{1.0175} d_b^{0.73} \right) \left(0.0516 \frac{c_{ch}}{d_b} + 0.6572 \right) \quad (4.2)$$

$$\text{with } \left(0.0516 \frac{c_{ch}}{d_b} + 0.6572 \right) \leq 1.0$$

where T_h is the anchorage strength of a hooked bar (lb) equal to the product of the area of a hooked bar, A_b , and the bar stress at anchorage failure, f_s ; f_{cm} is the measured concrete compressive strength (psi); ℓ_{eh} is the embedment length of the hooked bar (in.); d_b is the diameter of the hooked bar (in.); c_{ch} is the center-to-center spacing between hooked bars (in.); A_{th} is the total cross-sectional area of all parallel confining reinforcement located within $8d_b$ of the top of the hooked bars for No. 3 through No. 8 bars or within $10d_b$ for No. 9 through No. 11 bars (in.²), as shown in Figure (4.1); and n is the number of hooked bars being developed in tension.

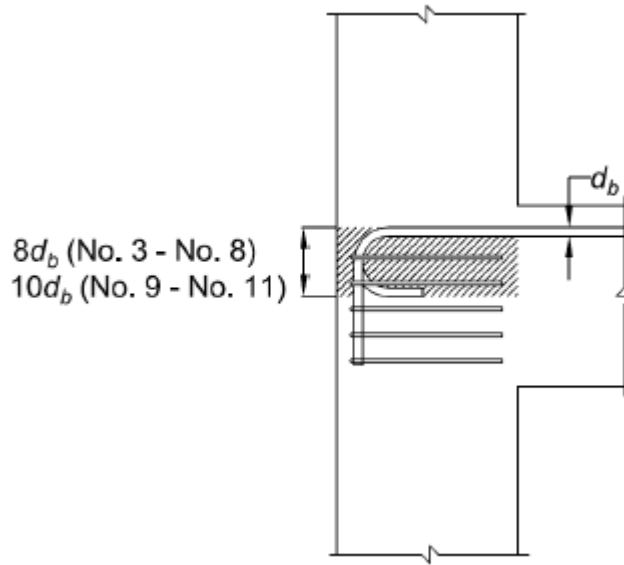


Figure 4.1 Effective confining reinforcement for hooked bars within the joint region of beam-column joints suggested by Ajaam et al. (2017)

Ajaam et al. (2017) developed design provisions [Eq. (4.3)] for the development length of hooked bars based on the descriptive equations [Eq. (4.1) and (4.2)]. The design provisions incorporate a strength reduction factor of 0.81 to ensure that no more than 5% of the specimens used to develop the equation have a ratio of test-to-calculated failure load less than 1.0.

$$\ell_{dh} = 0.003 \frac{f_y \psi_e \psi_{cs} \psi_o}{\lambda f_c^{0.25}} d_b^{1.5} \quad (4.3)$$

where ℓ_{dh} is the development length of a hooked bar in tension (in.) not less than the greater of $8d_b$ and 6 in.; f_y is the specified yield strength of the hooked bar (psi); ψ_e is a modification factor for epoxy coated or zinc and epoxy dual-coated reinforcement; ψ_{cs} is a modification factor for confining reinforcement and bar spacing; ψ_o is a modification factor for bar location; λ is a factor for lightweight concrete; f_c is the specified concrete compressive strength (psi); d_b is the diameter of the hooked bar (in.).

The proposed design provisions apply to hooked bars with yield strengths up to 120,000 psi and concrete compressive strengths up to 16,000 psi. The modification factor ψ_e is equal to 1.2 for epoxy-coated or zinc and epoxy dual-coated reinforcement and 1.0 for uncoated or zinc-coated (galvanized) reinforcement, and is retained from the current code provisions; the factor ψ_o is equal to 1.0 for hooked bars terminating inside a column core with clear side cover to the bar ≥ 2.5 in., or terminating in a supporting member with side cover to the bar $\geq 6d_b$; in other cases, ψ_o is taken as 1.25. Values for the confining reinforcement and bar spacing factor ψ_{cs} are calculated using Table 4.1. The factor λ is equal to 0.75 for lightweight concrete and 1.0 for normalweight concrete and is retained from the current code provisions.

Table 4.1 Modification factor ψ_{cs} for confining reinforcement, expressed as ratio of area of confining reinforcement, A_{th} , to area of hooked bars, A_{hs} , and center-to center bar spacing, c_{ch} ^[1]

Confinement level	f_y	c_{ch}	
		$2d_b$	$\geq 6d_b$
$\frac{A_{th}}{A_{hs}} \geq 0.2$ ^[2] or $\frac{A_{th}}{A_{hs}} \geq 0.4$ ^[3]	60,000	0.6	0.5
	120,000	0.66	0.55
No confining reinforcement	all	1.0	0.6

^[1] ψ_{cs} may be linearly interpolated for spacing or yield strengths not listed

^[2] Confining reinforcement parallel to straight portion of bar

^[3] Confining reinforcement perpendicular to straight portion of bar

4.2.2 Exterior Beam-Column Joints

The performance of 146 exterior beam-column joint specimens subjected to reversed cyclic loading is examined in this section using the descriptive equations for the anchorage strength and design provisions for the development length of hooked bars. Relevant details of the beam-column joint specimens are presented in Table 4.2, and complete details are presented in Appendix C. Table 4.2 includes the key parameters of the test specimens: f_y is the measured yield strength of the hooked bars; c_{so} is the clear concrete cover to the bar; ℓ_{eh} is the embedment length of the hooked bar; ℓ_{ehy} is the embedment length required to yield the hooked bar; d is the distance from the centroid of the tension bar to the extreme compression fiber of the beam; M_n is the nominal flexural strength of the test beam; M_{peak} is the peak moment applied to the test beam; V_p is the peak joint shear applied at the beam-column joint; V_n is the nominal joint shear strength; $\delta_{0.8 peak}$ is the drift ratio at drop to 80% of the peak load, where the drift is defined as the ratio of displacement at the loading point in the direction of the load to the distance between the loading point and center of the beam-column joints; T' is the estimated test failure load on the hooked bar calculated using Eq. (4.4).

The appropriate descriptive equation, Eq. (4.1) or (4.2), is used to calculate the embedment length required to yield a hooked bar based on the measured (not specified) yield strength, by

solving for ℓ_{eh} and replacing T_h with $A_b f_y$. The nominal flexural strength M_n of the test beam is also calculated based on the measured yield strength (Darwin and Dolan 2021). When calculating the nominal flexural strength, compression reinforcement is not considered unless the member is over-reinforced, as was the case for specimens I, I-A, and V tested by Hanson and Connor (1967); specimens 9 through 12 tested by Scribner (1978); all specimens tested by Pantelides et al. (2002); T3-600 tested by Hwang et al. (2014); and H0.7S, H1.0S, H0.7U, and H1.0U tested by Chun and Shin (2014), which were analyzed as doubly reinforced sections. The peak moment applied to the test beam M_{peak} is calculated at the beam-column joint interface, which is also the critical section for the hooked bars in tension.

Table 4.2 Detail of exterior beam-column joint specimens tested under reversed cyclic loading

Study ^[1]		Specimen	Bar Size ^[2]	f_y (ksi)	f_{cm} (psi)	c_{so} (in.)	$\frac{c_{ch}}{d_b}$	$\frac{A_{th}}{A_{hs}}$	ℓ_{eh} (in.)	ℓ_{ehy} (in.)
1	Hanson and Connor (1967)	I ^[3]	No. 9	51.6	3470	3.0	2.3	0.30	13.5	11.2
		I-A ^[3]	No. 9	47.8	3200	3.0	2.3	0.17	13.5	10.8
		II	No. 9	48.3	3650	3.0	2.3	0.30	13.5	10.3
		V ^{[3][4]}	No. 9	51.0	3300	3.0	2.3	0.00	13.5	16.6
		V-A ^[4]	No. 9	49.8	5420	3.0	2.3	0.00	13.5	16.4
2	Hanson (1971)	1 ^[5]	No. 8	63.1	5500	3.0	2.7	0.38	13.5	11.8
		3 ^[5]	No. 8	64.1	5200	3.0	2.7	0.21	13.5	12.1
		4	No. 8	63.4	5380	3.0	2.7	0.14	13.5	12.6
		5	No. 8	65.0	5230	3.0	2.7	0.21	13.5	12.2
3	Megget (1974)	Unit A	D25	54.7	3200	3.3	2.7	0.68	12.6	11.7
4	Uzumeri (1977)	1 ^{[4][5]}	No. 9	50.3	4460	3.5	3.0	0.00	13.0	15.6
		2 ^[4]	No. 9	50.6	4510	3.5	3.0	0.00	13.0	15.7
		3 ^[5]	No. 9	50.8	3920	3.5	3.0	0.29	13.0	11.5
		4 ^[5]	No. 9	50.6	4490	3.5	3.0	0.53	13.0	11.1
		5 ^{[4][5]}	No. 9	50.4	4630	2.0	4.4	0.00	13.0	16.2
		6	No. 9	51.1	5250	2.0	4.4	0.93	13.0	12.6
		7	No. 9	51.1	4460	2.0	4.4	0.53	13.0	13.1
		8	No. 9	51.1	3820	2.0	2.9	0.70	13.0	15.1
5	Lee et al. (1977)	1	No. 6	52.5	4200	2.4	3.3	1.00	9.4	8.6
		2	No. 6	48.6	4200	2.4	3.3	1.00	9.4	7.9
		3	No. 6	48.7	4100	2.4	3.3	0.23	9.4	8.0
		4	No. 6	48.9	4000	2.4	3.3	0.23	9.4	8.1
		5	No. 6	50.9	3600	2.4	3.3	1.00	9.4	8.7
		6	No. 6	51.6	3600	2.4	3.3	0.23	9.4	8.8
		7	No. 6	47.5	3700	2.4	3.3	0.23	9.4	8.0
		8	No. 6	48.2	4200	2.4	3.3	0.23	9.4	7.9

^[1] Values given in SI units are converted to in.-lb (1 in. = 25.4 mm; 1 psi = 1/145 MPa; and 1 kip = 4.4484 kN); notations used in these studies are described in Appendix A

^[2] Bar sizes are presented in SI and in.-lb as reported in the original studies

^[3] Analyzed as a doubly reinforced section to calculate the nominal flexural strength M_n ; all other specimens are analyzed as a single reinforced

^[4] Specimens did not contain confining reinforcement parallel to the hooked bars within the joint region

^[5] Specimens had transverse beams on one or both sides of the test beam. These transverse beams meet the dimensional requirements of Sections 18.8.4 and 15.2.8 of ACI 318-19 and Section 4.3 of ACI 352R-02 to be considered effective in increasing the joint shear strength

^[6] Specimens had $d/\ell_{eh} > 1.5$

Table 4.2 Cont. Detail of exterior beam-column joint specimens tested under reversed cyclic loading

Study ^[1]		Specimen	$\frac{\ell_{eh}}{\ell_{ehy}}$	$\frac{d}{\ell_{eh}}$	M_n (kip.in.)	M_{peak} (kip.in.)	$\frac{M_{peak}}{M_n}$	$\frac{V_p}{V_n}$	$\delta_{0.8 peak}$ ^[7]	$\frac{T'}{T_h}$
1	Hanson and Connor (1967)	I ^[3]	1.21	1.33	3018	3384	1.12	0.91	0.043	1.12
		I-A ^[3]	1.24	1.33	2796	2976	1.06	0.83	0.057	1.06
		II	1.32	1.33	2892	3036	1.05	0.80	0.035	1.04
		V ^{[3][4]}	0.81	1.33	2964	2640	0.89	0.73	0.051	1.11
		V-A ^[4]	0.82	1.33	3156	3372	1.07	0.95	0.021	1.32
2	Hanson (1971)	1 ^[5]	1.15	0.62	3229	3374	1.04	0.72	0.060	1.04
		3 ^[5]	1.11	0.62	3253	3662	1.13	0.80	0.035	1.12
		4	1.08	0.62	3234	3638	1.13	0.99	0.030	1.12
		5	1.10	0.62	3294	3614	1.10	0.98	0.045	1.09
3	Megget (1974)	Unit A	1.07	1.25	1923	1944	1.01	1.01	0.175	1.01
4	Uzumeri (1977)	1 ^{[4][5]}	0.83	1.35	2340	2475	1.06	0.63	0.033	1.29
		2 ^[4]	0.83	1.35	2352	2419	1.03	0.76	0.021	1.26
		3 ^[5]	1.13	1.35	2340	2588	1.11	0.69	0.055	1.10
		4 ^[5]	1.17	1.35	2352	2700	1.15	0.73	0.095	1.14
		5 ^{[4][5]}	0.80	1.35	2364	2531	1.07	0.60	0.016	1.36
		6	1.03	1.35	2412	2700	1.12	0.84	0.061	1.11
		7	0.99	1.35	2400	2813	1.17	0.87	0.063	1.18
		8	0.86	1.35	3132	3263	1.04	1.13	0.045	1.19
5	Lee et al. (1977)	1	1.09	0.85	332	372	1.12	0.80	0.042	1.11
		2	1.18	0.85	310	349	1.12	0.75	0.055	1.12
		3	1.17	0.85	310	314	1.01	0.69	0.042	1.01
		4	1.16	0.85	310	360	1.16	0.80	0.055	1.16
		5	1.08	0.85	317	382	1.20	0.89	0.059	1.20
		6	1.06	0.85	321	371	1.16	0.87	0.062	1.15
		7	1.17	0.85	300	361	1.20	0.83	0.060	1.20
		8	1.19	0.85	308	355	1.15	0.77	0.058	1.15

^[1] Values given in SI units are converted to in.-lb (1 in. = 25.4 mm; 1 psi = 1/145 MPa; and 1 kip = 4.4484 kN); notations used in these studies are described in Appendix A

^[3] Analyzed as a doubly reinforced section to calculate the nominal flexural strength M_n ; all other specimens are analyzed as a single reinforced

^[4] Specimens did not contain confining reinforcement parallel to the hooked bars within the joint region

^[5] Specimens had transverse beams on one or both sides of the test beam. These transverse beams meet the dimensional requirements of Sections 18.8.4 and 15.2.8 of ACI 318-19 and Section 4.3 of ACI 352R-02 to be considered effective in increasing the joint shear strength

^[6] Specimens had $d/\ell_{eh} > 1.5$

^[7] Drift ratio at drop to 80% of the peak load

Table 4.2 Cont. Detail of exterior beam-column joint specimens tested under reversed cyclic loading

Study ^[1]		Specimen	Bar Size ^[2]	f_y (ksi)	f_{cm} (psi)	c_{so} (in.)	$\frac{c_{ch}}{d_b}$	$\frac{A_{th}}{A_{hs}}$	ℓ_{eh} (in.)	ℓ_{ehy} (in.)
6	Scribner (1978)	1	No. 6	48.9	4950	1.0	6.9	0.75	11.0	6.3
		2	No. 6	48.9	5050	1.0	6.9	0.75	11.0	6.2
		3	No. 6	48.9	4940	1.5	2.8	0.67	10.5	7.9
		4	No. 6	48.9	4950	1.5	2.8	0.67	10.5	7.9
		5	No. 6	52.7	3680	1.0	6.9	0.75	11.0	7.4
		6	No. 6	52.7	4080	1.0	6.9	0.75	11.0	7.2
		7	No. 6	52.7	3840	1.5	2.8	0.67	10.5	9.2
		8	No. 6	52.7	3920	1.5	2.8	0.67	10.5	9.1
		9 ^[3]	No. 8	60.2	5130	2.4	2.1	0.25	16.6	15.1
		10 ^[3]	No. 8	60.2	5210	2.4	2.1	0.25	16.6	15.0
		11 ^[3]	No. 8	60.2	4730	2.4	2.1	0.25	16.6	15.4
		12 ^[3]	No. 8	60.2	4760	2.4	2.1	0.25	16.6	15.4
7	Paulay and Scarpas (1981)	Unit 1	D20	42.9	3280	3.4	4.4	0.48	16.6	5.8
		Unit 2	D20	42.9	3260	3.4	4.4	0.25	16.6	5.8
		Unit 3	D20	42.9	3900	3.4	4.4	0.33	16.6	5.5
8	Ehsani and Wight (1982)	2 ^[6]	No. 7	48.0	5070	2.4	3.5	0.11	7.4	9.6
		4 ^[6]	No. 7	48.0	6470	2.4	3.5	0.22	7.4	8.4
9	Kanada et al. (1984)	U40L ^[4]	D19	56.2	3530	2.4	2.8	0.00	9.0	13.2
		U41L	D19	56.2	3870	2.4	2.8	0.22	9.0	9.8
		U42L	D19	56.2	4370	2.4	2.8	0.33	9.0	9.5
		U41S ^[6]	D19	56.2	3870	2.4	2.8	0.22	6.0	9.8
		U42S ^[6]	D19	56.2	4370	2.4	2.8	0.33	6.0	9.5
		U20L ^[4]	D19	56.2	3870	2.4	8.4	0.00	9.0	8.8
		U21L	D19	56.2	4370	2.4	8.4	0.45	9.0	7.5
		U21S ^[6]	D19	56.2	3870	2.4	8.4	0.45	6.0	7.8
		U22S ^[6]	D19	56.2	4370	2.4	8.4	0.67	6.0	7.5
		R41L	D19	56.2	3140	2.4	2.8	0.22	9.0	10.4
		R42S ^[6]	D19	56.2	3140	2.4	2.8	0.33	6.0	10.4

^[1] Values given in SI units are converted to in.-lb (1 in. = 25.4 mm; 1 psi = 1/145 MPa; and 1 kip = 4.4484 kN); notations used in these studies are described in Appendix A

^[2] Bar sizes are presented in SI and in.-lb as reported in the original studies

^[3] Analyzed as a doubly reinforced section to calculate the nominal flexural strength M_n ; all other specimens are analyzed as a single reinforced

^[4] Specimens did not contain confining reinforcement parallel to the hooked bars within the joint region

^[5] Specimens had transverse beams on one or both sides of the test beam. These transverse beams meet the dimensional requirements of Sections 18.8.4 and 15.2.8 of ACI 318-19 and Section 4.3 of ACI 352R-02 to be considered effective in increasing the joint shear strength

^[6] Specimens had $d/\ell_{eh} > 1.5$

Table 4.2 Cont. Detail of exterior beam-column joint specimens tested under reversed cyclic loading

Study ^[1]		Specimen	$\frac{\ell_{eh}}{\ell_{ehy}}$	$\frac{d}{\ell_{eh}}$	M_n (kip.in.)	M_{peak} (kip.in.)	$\frac{M_{peak}}{M_n}$	$\frac{V_p}{V_n}$	$\delta_{0.8 peak}$ ^[7]	$\frac{T'}{T_h}$
6	Scribner (1978)	1	1.75	0.78	343	481	1.41	0.70	0.060	1.40
		2	1.76	0.78	343	498	1.45	0.72	0.058	1.44
		3	1.32	0.96	590	706	1.20	0.88	0.047	1.19
		4	1.32	0.96	747	818	1.10	1.03	0.063	1.09
		5	1.49	0.78	356	453	1.27	0.76	0.066	1.26
		6	1.53	0.78	360	468	1.30	0.74	0.061	1.29
		7	1.14	0.96	710	751	1.06	1.07	0.060	1.05
		8	1.15	0.96	743	809	1.09	1.14	0.061	1.08
		9	1.10	0.73	2472	2508	1.01	1.15	0.076	1.01
		10	1.10	0.73	2520	2592	1.03	1.18	0.084	1.02
		11	1.08	0.73	2472	2501	1.01	1.19	0.052	1.01
		12	1.08	0.73	2520	2539	1.01	1.18	0.053	1.00
7	Paulay and Scarpas (1981)	Unit 1	2.86	1.30	2418	3118	1.29	0.61	0.032	1.28
		Unit 2	2.86	1.29	3481	4385	1.26	0.90	0.038	1.25
		Unit 3	3.00	1.30	2418	3340	1.38	0.61	0.035	1.37
8	Ehsani and Wight (1982)	2 ^[6]	0.77	1.93	1747	1860	1.06	1.18	0.038	1.27
		4 ^[6]	0.88	1.93	1776	2400	1.35	1.35	0.056	1.39
9	Kanada et al. (1984)	U40L ^[4]	0.68	1.45	1129	885	0.78	0.63	0.033	1.19
		U41L	0.91	1.45	1143	1172	1.02	0.79	0.038	1.11
		U42L	0.95	1.45	1160	1165	1.00	0.74	0.033	1.06
		U41S ^[6]	0.61	2.17	1143	631	0.55	0.43	0.014	0.88
		U42S ^[6]	0.63	2.17	1160	690	0.59	0.44	0.020	0.92
		U20L ^[4]	1.02	1.45	608	651	1.07	0.44	0.011	1.07
		U21L	1.19	1.45	613	684	1.12	0.43	0.020	1.11
		U21S ^[6]	0.77	2.17	608	495	0.81	0.33	0.022	1.03
		U22S ^[6]	0.79	2.17	613	573	0.94	0.36	0.030	1.15
		R41L	0.86	1.45	1110	1022	0.92	0.77	0.038	1.06
		R42S ^[6]	0.58	2.17	1110	664	0.60	0.50	0.018	1.00

^[1] Values given in SI units are converted to in.-lb (1 in. = 25.4 mm; 1 psi = 1/145 MPa; and 1 kip = 4.4484 kN); notations used in these studies are described in Appendix A

^[3] Analyzed as a doubly reinforced section to calculate the nominal flexural strength M_n ; all other specimens are analyzed as a single reinforced

^[4] Specimens did not contain confining reinforcement parallel to the hooked bars within the joint region

^[5] Specimens had transverse beams on one or both sides of the test beam. These transverse beams meet the dimensional requirements of Sections 18.8.4 and 15.2.8 of ACI 318-19 and Section 4.3 of ACI 352R-02 to be considered effective in increasing the joint shear strength

^[6] Specimens had $d/\ell_{eh} > 1.5$

^[7] Drift ratio at drop to 80% of the peak load

Table 4.2 Cont. Detail of exterior beam-column joint specimens tested under reversed cyclic loading

Study ^[1]		Specimen	Bar Size ^[2]	f_y (ksi)	f_{cm} (psi)	c_{so} (in.)	$\frac{c_{ch}}{d_b}$	$\frac{A_{th}}{A_{hs}}$	ℓ_{eh} (in.)	ℓ_{ehy} (in.)
9	Kanada et al. (1984)	R21L	D19	56.2	3140	2.4	8.4	0.45	9.0	8.3
		R21S ^[6]	D19	56.2	3140	2.4	8.4	0.45	6.0	8.3
10	Zerbe and Durrani (1985)	J1 ^[6]	No. 6	60.0	5710	3.0	2.3	0.45	7.8	7.7
		J2 ^{[5][6]}	No. 6	60.0	5650	3.0	2.3	0.45	7.8	7.7
		J3 ^[6]	No. 6	60.0	5780	3.0	2.3	0.45	7.8	7.7
		J4 ^{[5][6]}	No. 6	60.0	5940	3.0	2.3	0.45	7.8	7.6
		J5 ^{[5][6]}	No. 6	60.0	5610	3.0	2.3	0.45	7.8	7.7
		J6 ^{[5][6]}	No. 6	60.0	5690	3.0	2.3	0.45	7.8	7.7
11	Ehsani et al. (1987)	1	No. 6	70.0	9380	2.4	5.2	0.36	10.8	8.3
		2	No. 6	70.0	9760	2.4	5.2	0.36	10.8	8.2
		3 ^[6]	No. 6	70.0	9380	2.4	4.1	0.36	9.2	8.8
		4 ^[6]	No. 7	62.0	9760	2.4	3.5	0.27	9.3	9.8
		5 ^[6]	No. 7	48.0	6470	2.4	3.5	0.22	8.6	8.4
12	Kaku and Asakusa (1991)	1	D13	56.7	4510	1.6	3.3	0.22	7.7	5.3
		2	D13	56.7	6050	1.6	3.3	0.22	7.7	4.9
		3	D13	56.7	6050	1.6	3.3	0.22	7.7	4.9
		4	D13	56.7	6480	1.6	3.3	0.06	7.7	5.1
		5	D13	56.7	5320	1.6	3.3	0.06	7.7	5.4
		6	D13	56.7	5860	1.6	3.3	0.06	7.7	5.2
		7	D13	56.7	4670	1.6	3.3	0.22	7.7	5.3
		8	D13	56.7	5970	1.6	3.3	0.22	7.7	4.9
		9	D13	56.7	5890	1.6	3.3	0.22	7.7	5.0
		10	D13	56.7	6440	1.6	3.3	0.06	7.7	5.1
		11	D13	56.7	6080	1.6	3.3	0.06	7.7	5.2
		12	D13	56.7	5090	1.6	3.3	0.06	7.7	5.4
		13	D13	56.7	6730	1.6	3.3	0.22	7.7	4.8
		14	D13	56.7	5950	1.6	3.3	0.06	7.7	5.2

^[1] Values given in SI units are converted to in.-lb (1 in. = 25.4 mm; 1 psi = 1/145 MPa; and 1 kip = 4.4484 kN); notations used in these studies are described in Appendix A

^[2] Bar sizes are presented in SI and in.-lb as reported in the original studies

^[3] Analyzed as a doubly reinforced section to calculate the nominal flexural strength M_n ; all other specimens are analyzed as a single reinforced

^[4] Specimens did not contain confining reinforcement parallel to the hooked bars within the joint region

^[5] Specimens had transverse beams on one or both sides of the test beam. These transverse beams meet the dimensional requirements of Sections 18.8.4 and 15.2.8 of ACI 318-19 and Section 4.3 of ACI 352R-02 to be considered effective in increasing the joint shear strength

^[6] Specimens had $d/\ell_{eh} > 1.5$

Table 4.2 Cont. Detail of exterior beam-column joint specimens tested under reversed cyclic loading

Study ^[1]		Specimen	$\frac{\ell_{eh}}{\ell_{ehy}}$	$\frac{d}{\ell_{eh}}$	M_n (kip.in.)	M_{peak} (kip.in.)	$\frac{M_{peak}}{M_n}$	$\frac{V_p}{V_n}$	$\delta_{0.8 peak}$ ^[7]	$\frac{T'}{T_h}$
9	Kanada et al. (1984)	R21L	1.09	1.45	600	664	1.11	0.50	0.022	1.10
		R21S ^[6]	0.73	2.17	600	495	0.82	0.37	0.022	1.10
10	Zerbe and Durrani (1985)	J1 ^[6]	1.01	1.63	1216	1287	1.06	0.85	0.053	1.05
		J2 ^{[5][6]}	1.00	1.63	1214	1518	1.25	1.01	0.052	1.24
		J3 ^[6]	1.01	1.63	1216	1320	1.09	0.87	0.053	1.08
		J4 ^{[5][6]}	1.02	1.63	1900	2079	1.09	1.35	0.05	1.09
		J5 ^{[5][6]}	1.00	1.63	2221	2244	1.01	1.49	0.051	1.01
		J6 ^{[5][6]}	1.00	1.63	2546	2211	0.87	1.46	0.052	0.86
11	Ehsani et al. (1987)	1	1.30	1.47	1729	2170	1.26	0.61	0.062	1.25
		2	1.32	1.47	2041	2666	1.31	0.74	0.064	1.30
		3 ^[6]	1.04	1.57	1663	1984	1.19	0.82	0.060	1.19
		4 ^[6]	0.94	1.55	2290	2232	0.97	0.91	0.058	1.03
		5 ^[6]	1.02	1.67	2101	2280	1.09	1.05	0.065	1.08
12	Kaku and Asakusa (1991)	1	1.44	1.04	335	427	1.27	0.83	0.055	1.27
		2	1.56	1.04	341	430	1.26	0.73	0.065	1.26
		3	1.56	1.04	338	374	1.10	0.63	0.065	1.10
		4	1.51	1.04	334	412	1.23	0.67	0.060	1.23
		5	1.43	1.04	332	380	1.14	0.68	0.055	1.14
		6	1.47	1.04	340	360	1.06	0.62	0.052	1.06
		7	1.46	1.04	335	428	1.28	0.82	0.060	1.27
		8	1.56	1.04	335	419	1.25	0.71	0.063	1.25
		9	1.55	1.04	335	406	1.21	0.69	0.068	1.21
		10	1.51	1.04	334	418	1.25	0.68	0.059	1.25
		11	1.48	1.04	334	397	1.19	0.67	0.048	1.19
		12	1.41	1.04	336	357	1.06	0.66	0.053	1.06
		13	1.61	1.04	339	360	1.06	0.58	0.065	1.06
		14	1.48	1.04	334	389	1.16	0.66	0.045	1.16

^[1] Values given in SI units are converted to in.-lb (1 in. = 25.4 mm; 1 psi = 1/145 MPa; and 1 kip = 4.4484 kN); notations used in these studies are described in Appendix A

^[3] Analyzed as a doubly reinforced section to calculate the nominal flexural strength M_n ; all other specimens are analyzed as a single reinforced

^[4] Specimens did not contain confining reinforcement parallel to the hooked bars within the joint region

^[5] Specimens had transverse beams on one or both sides of the test beam. These transverse beams meet the dimensional requirements of Sections 18.8.4 and 15.2.8 of ACI 318-19 and Section 4.3 of ACI 352R-02 to be considered effective in increasing the joint shear strength

^[6] Specimens had $d/\ell_{eh} > 1.5$

^[7] Drift ratio at drop to 80% of the peak load

Table 4.2 Cont. Detail of exterior beam-column joint specimens tested under reversed cyclic loading

Study ^[1]		Specimen	Bar Size ^[2]	f_y (ksi)	f_{cm} (psi)	c_{so} (in.)	$\frac{c_{ch}}{d_b}$	$\frac{A_{th}}{A_{hs}}$	ℓ_{eh} (in.)	ℓ_{ehy} (in.)
12	Kaku and Asakusa (1991)	15	D13	56.7	5760	1.6	3.3	0.06	7.7	5.2
		16	D13	56.7	5420	1.6	3.3	0.22	7.7	5.1
13	Ehsani and Alameddine (1991)	LL8 ^[6]	No. 8	66.3	8600	3.0	2.2	0.57	10.5	11.4
		LH8 ^[6]	No. 8	66.3	8600	3.0	2.2	0.76	10.5	11.4
		HL8 ^[6]	No. 9	64.2	8600	3.0	1.9	0.45	10.5	13.1
		HH8 ^[6]	No. 9	64.2	8600	3.0	1.9	0.60	10.5	13.1
		LL11 ^[6]	No. 8	66.3	10700	3.0	2.2	0.57	10.5	10.8
		LH11 ^[6]	No. 8	66.3	10700	3.0	2.2	0.76	10.5	10.8
		HL11 ^[6]	No. 9	64.2	10700	3.0	1.9	0.45	10.5	12.3
		HH11 ^[6]	No. 9	64.2	10700	3.0	1.9	0.60	10.5	12.3
		LL14 ^[6]	No. 8	66.3	13700	3.0	2.2	0.57	10.5	10.1
		LH14 ^[6]	No. 8	66.3	13700	3.0	2.2	0.76	10.5	10.1
		HH14 ^[6]	No. 9	64.2	13700	3.0	1.9	0.60	10.5	11.5
14	Tsonos et al. (1992)	S1 ^[6]	D14	70.3	5360	0.7	10.7	0.33	6.5	5.9
		S2 ^[6]	D12	76.7	3770	0.7	6.3	0.30	6.5	5.9
		S6' ^[6]	D14	70.3	4200	0.7	3.6	0.16	6.5	7.6
15	Pantelides et al. (2002)	2 ^{[3][4]}	No. 9	65.9	6700	1.9	2.1	0.00	16.1	15.6
		4 ^{[3][4]}	No. 9	65.9	5940	1.9	2.1	0.00	16.1	16.1
		5 ^{[3][4]}	No. 9	65.9	5370	1.9	2.1	0.00	16.1	16.6
		6 ^{[3][4]}	No. 9	65.9	5820	1.9	2.1	0.00	16.1	16.2
16	Chutarat and Aboutaha (2003)	Specimen I	No. 8	70.0	4000	3.3	2.8	0.76	12.8	14.2
17	Hwang et al. (2005)	0T0 ^[4]	No. 8	62.4	9760	4.0	2.5	0.00	13.7	11.5
		3T44	No. 8	62.4	11140	4.0	2.5	0.76	13.7	9.8
		1B8	No. 8	63.1	8960	4.0	2.5	0.50	13.7	10.5
		3T3	No. 8	62.4	10010	4.0	2.5	0.21	13.7	10.0

^[1] Values given in SI units are converted to in.-lb (1 in. = 25.4 mm; 1 psi = 1/145 MPa; and 1 kip = 4.4484 kN); notations used in these studies are described in Appendix A

^[2] Bar sizes are presented in SI and in.-lb as reported in the original studies

^[3] Analyzed as a doubly reinforced section to calculate the nominal flexural strength M_n ; all other specimens are analyzed as a single reinforced

^[4] Specimens did not contain confining reinforcement parallel to the hooked bars within the joint region

^[5] Specimens had transverse beams on one or both sides of the test beam. These transverse beams meet the dimensional requirements of Sections 18.8.4 and 15.2.8 of ACI 318-19 and Section 4.3 of ACI 352R-02 to be considered effective in increasing the joint shear strength

^[6] Specimens had $d/\ell_{eh} > 1.5$

Table 4.2 Cont. Detail of exterior beam-column joint specimens tested under reversed cyclic loading

Study ^[1]		Specimen	$\frac{\ell_{eh}}{\ell_{ehy}}$	$\frac{d}{\ell_{eh}}$	M_n (kip.in.)	M_{peak} (kip.in.)	$\frac{M_{peak}}{M_n}$	$\frac{V_p}{V_n}$	$\delta_{0.8 peak}$ ^[7]	$\frac{T'}{T_h}$
12	Kaku and Asakusa (1991)	15	1.46	1.04	333	397	1.19	0.69	0.060	1.19
		16	1.52	1.04	334	432	1.29	0.77	0.055	1.29
13	Ehsani and Alameddine (1991)	LL8 ^[6]	0.92	1.62	3027	3517	1.16	0.89	0.055	1.25
		LH8 ^[6]	0.92	1.62	3027	3402	1.12	0.86	0.061	1.21
		HL8 ^[6]	0.80	1.62	3637	3708	1.02	1.02	0.043	1.24
		HH8 ^[6]	0.80	1.62	3637	3743	1.03	1.02	0.063	1.25
		LL11 ^[6]	0.98	1.62	3118	3020	0.97	0.71	0.056	0.99
		LH11 ^[6]	0.98	1.62	3081	4018	1.30	0.86	0.064	1.33
		HL11 ^[6]	0.85	1.62	3845	3731	0.97	0.89	0.041	1.12
		HH11 ^[6]	0.85	1.62	3872	4089	1.06	0.94	0.063	1.22
		LL14 ^[6]	1.04	1.62	3112	3701	1.19	0.72	0.060	1.18
		LH14 ^[6]	1.04	1.62	3112	3780	1.21	0.73	0.064	1.21
		HH14 ^[6]	0.91	1.62	3830	4084	1.07	0.84	0.054	1.16
14	Tsonos et al. (1992)	S1 ^[6]	1.09	1.67	348	452	1.30	0.66	0.065	1.29
		S2 ^[6]	1.10	1.67	404	465	1.15	0.82	0.030	1.15
		S6' ^[6]	0.85	1.67	646	666	1.03	1.11	0.035	1.21
15	Pantelides et al. (2002)	2 ^{[3][4]}	1.03	0.84	2932	3005	1.02	1.11	0.025	1.02
		4 ^{[3][4]}	1.00	0.84	2932	3100	1.06	1.21	0.018	1.06
		5 ^{[3][4]}	0.97	0.84	2932	3000	1.02	1.24	0.025	1.05
		6 ^{[3][4]}	0.99	0.84	2932	2950	1.01	1.17	0.028	1.01
16	Chutarat and Aboutaha (2003)	Specimen I	0.90	1.19	2848	3344	1.17	1.19	0.074	1.30
17	Hwang et al. (2005)	0T0 ^[4]	1.18	1.11	2794	3229	1.16	0.69	0.060	1.16
		3T44	1.40	1.11	2817	3447	1.22	0.69	0.087	1.22
		1B8	1.30	1.11	2807	4069	1.45	0.91	0.060	1.44
		3T3	1.36	1.11	2798	3666	1.31	0.78	0.100	1.30

^[1] Values given in SI units are converted to in.-lb (1 in. = 25.4 mm; 1 psi = 1/145 MPa; and 1 kip = 4.4484 kN); notations used in these studies are described in Appendix A

^[3] Analyzed as a doubly reinforced section to calculate the nominal flexural strength M_n ; all other specimens are analyzed as a single reinforced

^[4] Specimens did not contain confining reinforcement parallel to the hooked bars within the joint region

^[5] Specimens had transverse beams on one or both sides of the test beam. These transverse beams meet the dimensional requirements of Sections 18.8.4 and 15.2.8 of ACI 318-19 and Section 4.3 of ACI 352R-02 to be considered effective in increasing the joint shear strength

^[6] Specimens had $d/\ell_{eh} > 1.5$

^[7] Drift ratio at drop to 80% of the peak load

Table 4.2 Cont. Detail of exterior beam-column joint specimens tested under reversed cyclic loading

Study ^[1]		Specimen	Bar Size ^[2]	f_y (ksi)	f_{cm} (psi)	c_{so} (in.)	$\frac{c_{ch}}{d_b}$	$\frac{A_{th}}{A_{hs}}$	ℓ_{eh} (in.)	ℓ_{ehy} (in.)
17	Hwang et al. (2005)	2T4	No. 8	62.4	10300	4.0	2.5	0.13	13.7	10.5
		1T44	No. 8	62.4	10560	4.0	2.5	0.25	13.7	9.9
		3T4	No. 8	71.2	10910	4.0	2.5	0.38	15.5	11.3
		2T5	No. 8	71.2	11110	4.0	2.5	0.20	15.5	11.3
		1T55	No. 8	71.2	10110	4.0	2.5	0.39	15.5	11.5
18	Tsonos (2007)	A1 ^[6]	D10	73.0	5080	1.0	4.7	0.36	6.5	4.4
		E1 ^[6]	D14	72.0	3190	0.9	5.0	0.24	6.4	7.7
		E2 ^[6]	D14	72.0	5080	0.9	10.0	0.37	6.4	6.2
		G1 ^[6]	D14	72.0	3190	0.9	5.0	0.12	6.4	7.9
19	Chun et al. (2007)	JC-1	D22	58.4	8950	3.4	3.4	0.09	15.8	8.2
		JC-2	D22	58.4	8720	3.4	3.4	0.05	13.9	8.5
		WC ^[4]	D25	62.5	8180	2.1	6.6	0.00	15.7	12.0
		JC-No. 11-1	D36	66.4	4760	6.0	4.3	0.51	18.9	17.9
20	Lee and Ko (2007)	S0	D22	66.0	4730	4.6	2.3	0.28	21.0	11.0
		W0	D22	66.0	4190	8.6	2.3	0.46	13.1	11.4
21	Kang et al. (2010)	Jk ^[6]	D19	67.0	4200	2.6	5.2	0.25	11.3	7.8
22	Hwang et al. (2014)	T1-400	D22	75.4	4640	4.5	3.7	0.38	19.6	11.6
		T2-600	D22	103.0	4640	4.5	3.7	0.67	19.6	15.9
		T3-600 ^[3]	D25	92.1	4290	4.5	3.3	0.51	19.6	18.0
23	Chun and Shin (2014)	H0.7S ^[3]	D19	70.8	3710	3.0	2.3	0.29	9.0	9.4
		H1.0S ^[3]	D19	70.8	3710	3.0	2.3	0.58	9.0	9.4
		H1.5S ^[6]	D19	70.8	3710	3.0	2.3	0.58	9.0	9.4
		H2.0S ^[6]	D19	70.8	3830	3.0	2.3	0.58	9.0	8.6
		H2.5S ^[6]	D19	70.8	3830	3.0	2.3	0.58	9.0	8.6
		H0.7U ^[3]	D19	70.8	3710	3.0	2.3	0.19	9.0	9.5
		H1.0U ^[3]	D19	70.8	3710	3.0	2.3	0.38	9.0	9.4
24	Choi and Bae (2019)	JTR-0-BTR	D25	68.4	7950	3.1	4.6	1.01	8.3	10.3
		JNR-0-BTR ^[4]	D25	68.4	7950	3.1	4.6	0.00	8.3	12.6
		JTR-0-BNR	D25	68.4	7950	3.1	4.6	1.01	8.3	10.3

^[1] Values given in SI units are converted to in.-lb (1 in. = 25.4 mm; 1 psi = 1/145 MPa; and 1 kip = 4.4484 kN); notations used in these studies are described in Appendix A

^[2] Bar sizes are presented in SI and in.-lb as reported in the original studies

^[3] Analyzed as a doubly reinforced section to calculate the nominal flexural strength M_n ; all other specimens are analyzed as a single reinforced

^[4] Specimens did not contain confining reinforcement parallel to the hooked bars within the joint region

^[6] Specimens had $d/\ell_{eh} > 1.5$

Table 4.2 Cont. Detail of exterior beam-column joint specimens tested under reversed cyclic loading

Study ^[1]		Specimen	$\frac{\ell_{eh}}{\ell_{ehy}}$	$\frac{d}{\ell_{eh}}$	M_n (kip.in.)	M_{peak} (kip.in.)	$\frac{M_{peak}}{M_n}$	$\frac{V_p}{V_n}$	$\delta_{0.8 peak}$ ^[7]	$\frac{T'}{T_h}$
17	Hwang et al. (2005)	2T4	1.30	1.11	2803	3498	1.25	0.73	0.075	1.24
		1T44	1.38	1.11	2808	3363	1.20	0.69	0.080	1.19
		3T4	1.37	0.98	3185	3599	1.13	0.63	0.070	1.13
		2T5	1.38	0.98	3189	3767	1.18	0.66	0.070	1.18
		1T55	1.34	0.98	3168	3649	1.15	0.67	0.070	1.15
18	Tsonos (2007)	A1 ^[6]	1.47	1.64	359	454	1.26	0.73	0.045	1.26
		E1 ^[6]	0.84	1.66	486	558	1.15	1.14	0.060	1.37
		E2 ^[6]	1.04	1.66	348	438	1.26	0.71	0.065	1.26
		G1 ^[6]	0.82	1.66	486	494	1.02	1.01	0.040	1.25
19	Chun et al. (2007)	JC-1	1.93	1.10	2328	3195	1.37	0.49	0.045	1.37
		JC-2	1.64	1.24	4204	4983	1.19	0.80	0.070	1.18
		WC ^[4]	1.31	0.84	4726	5611	1.19	0.53	0.053	1.19
		JC-No. 11-1	1.05	0.90	4567	4912	1.08	0.61	0.054	1.07
20	Lee and Ko (2007)	S0	1.90	0.76	2275	3075	1.35	0.59	0.065	1.35
		W0	1.15	1.22	2241	2857	1.27	0.59	0.055	1.27
21	Kang et al. (2010)	Jk ^[6]	1.43	1.73	2177	2721	1.25	0.55	0.035	1.24
22	Hwang et al. (2014)	T1-400	1.69	0.87	3878	4658	1.20	0.78	0.032	1.20
		T2-600	1.23	0.90	3807	4844	1.27	0.75	0.038	1.27
		T3-600 ^[3]	1.09	0.90	4282	5403	1.26	0.83	0.048	1.26
23	Chun and Shin (2014)	H0.7S ^[3]	0.95	0.6	492	612	1.24	1.18	0.100	1.30
		H1.0S ^[3]	0.95	1.0	984	1080	1.10	1.03	0.070	1.15
		H1.5S ^[6]	0.95	1.7	1728	1752	1.01	0.91	0.050	1.06
		H2.0S ^[6]	1.04	2.4	2484	2760	1.11	0.82	0.070	1.11
		H2.5S ^[6]	1.04	3.0	3216	3252	1.01	0.71	0.050	1.01
		H0.7U ^[3]	0.95	0.6	492	576	1.17	1.12	0.100	1.23
		H1.0U ^[3]	0.95	1.0	984	1020	1.04	0.97	0.070	1.08
24	Choi and Bae (2019)	JTR-0-BTR	0.81	1.45	1221	1275	1.04	0.70	0.044	1.26
		JNR-0-BTR ^[4]	0.66	1.45	1221	1080	0.88	0.59	0.019	1.38
		JTR-0-BNR	0.81	1.45	1221	1221	1.00	0.67	0.047	1.21

^[1] Values given in SI units are converted to in.-lb (1 in. = 25.4 mm; 1 psi = 1/145 MPa; and 1 kip = 4.4484 kN); notations used in these studies are described in Appendix A

^[3] Analyzed as a doubly reinforced section to calculate the nominal flexural strength M_n ; all other specimens are analyzed as a single reinforced

^[4] Specimens did not contain confining reinforcement parallel to the hooked bars within the joint region

^[6] Specimens had $d/\ell_{eh} > 1.5$

^[7] Drift ratio at drop to 80% of the peak load

Because of the effect of joint shear on the performance of beam-column joints subjected to reversed cyclic loading, including potential effects on the anchorage performance of hooked bars, beam-column joint specimens with a ratio of peak joint shear to nominal joint shear strength $V_p/V_n \leq 1.0$ and those with $V_p/V_n > 1.0$ are initially examined separately. The nominal joint shear strength V_n is calculated as $12\sqrt{f'_c}A_j$ in accordance with Section 18.8.4.3 of ACI 318-19, where A_j is the effective cross-sectional area within the beam-column joint in a plane parallel to the hooked bars calculated in accordance with Section 15.4.2.4 of ACI 318-19 and f'_c is concrete compressive strength. The nominal joint shear strength V_n is also calculated in accordance with Section 4.3 of ACI 352R-02, with a 15,000 psi upper limit on f'_c . The peak and nominal joint shear strength values are given in Table C.4 of Appendix C. The effect of joint shear strength on the anchorage performance of the hooked bar is discussed in Sections 4.2.2.1 and 4.2.2.2.

Figure 4.2 shows the plot of the ratio of the peak moment M_{peak} to the nominal flexural strength M_n versus the ratio of the actual embedment length of the hooked bar ℓ_{eh} to the embedment length required to yield the bar ℓ_{ehy} . Linear trendlines for specimens with $\ell_{eh}/\ell_{ehy} \leq 1.0$ and $\ell_{eh}/\ell_{ehy} \geq 1.0$ are shown in the figure. Figure 4.2 only includes specimens with $V_p/V_n \leq 1.0$ (0.43 to 1.00). Beam-column joint specimens with a ratio of effective beam depth to embedment length $d/\ell_{eh} > 1.5$ were not included when Ajaam et al. (2017) developed the descriptive and design equations, Eq. (4.1) through (4.3). Therefore, beam-column joint specimens tested under reversed cyclic loading that had $d/\ell_{eh} > 1.5$ are not included in Figure 4.2 and are analyzed independently in Section 4.2.2.3. Beam-column joint specimens included in Figure 4.2 had a ratio of d/ℓ_{eh} ranging from 0.6 to 1.5. In Figure 4.3, the ratio of the peak moment M_{peak} to the nominal flexural strength M_n is plotted versus the ratio of the actual embedment length of the hooked bar ℓ_{eh} to the embedment length required to yield the bar ℓ_{ehy} for specimens with $V_p/V_n > 1.0$ (1.01 to 1.24).

The beam-column joint specimens were considered to have performed satisfactorily if they met two criteria: first, the ratio of measured peak moment to nominal flexural strength (M_{peak}/M_n) was greater than or equal to 1.0, and second, the reduction in peak moment was $\leq 20\%$ at the end of the first complete cycle at 3.5% drift, where the drift is defined as the ratio of displacement at the loading point in the direction of the load to the distance between the loading point and center of the beam-column joints. The values of the drift ratio at drop to 80% from the peak load ($\delta_{0.8peak}$)

are given in Table (4.2). ACI 374.1-05, Section 9.1.3 utilizes similar acceptance criteria for weak beam-strong column connections, with the exception that the peak moment reduction could be up to 25% at the end of the third complete cycle at 3.5% drift. The acceptance criteria used in this study were used by Kang et al. (2009) for beam-columns joints in which the beam bars were anchored using heads. The results presented in Figures 4.2 and 4.3 are discussed next.

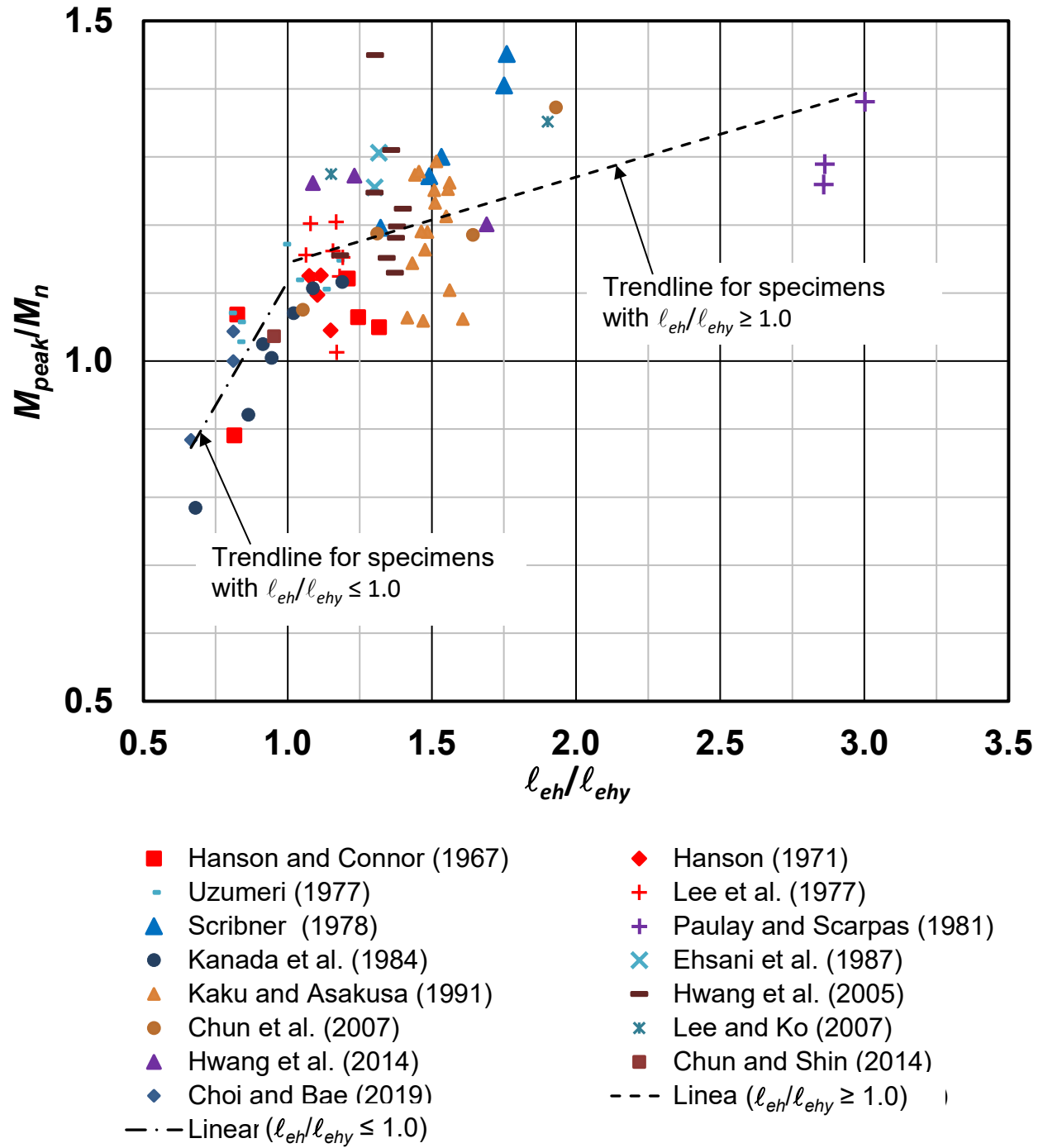


Figure 4.2 M_{peak}/M_n versus l_{eh}/l_{ehy} for specimens with $d/l_{eh} \leq 1.5$ and $V_p/V_n \leq 1.0$. M_{peak}/M_n is the ratio of peak moment to nominal flexural strength, and l_{eh}/l_{ehy} is the ratio of embedment length to the embedment length required to yield the hooked bar calculated using the descriptive equations developed by Ajaam et al. (2017), Eq. (4.1) and (4.2)

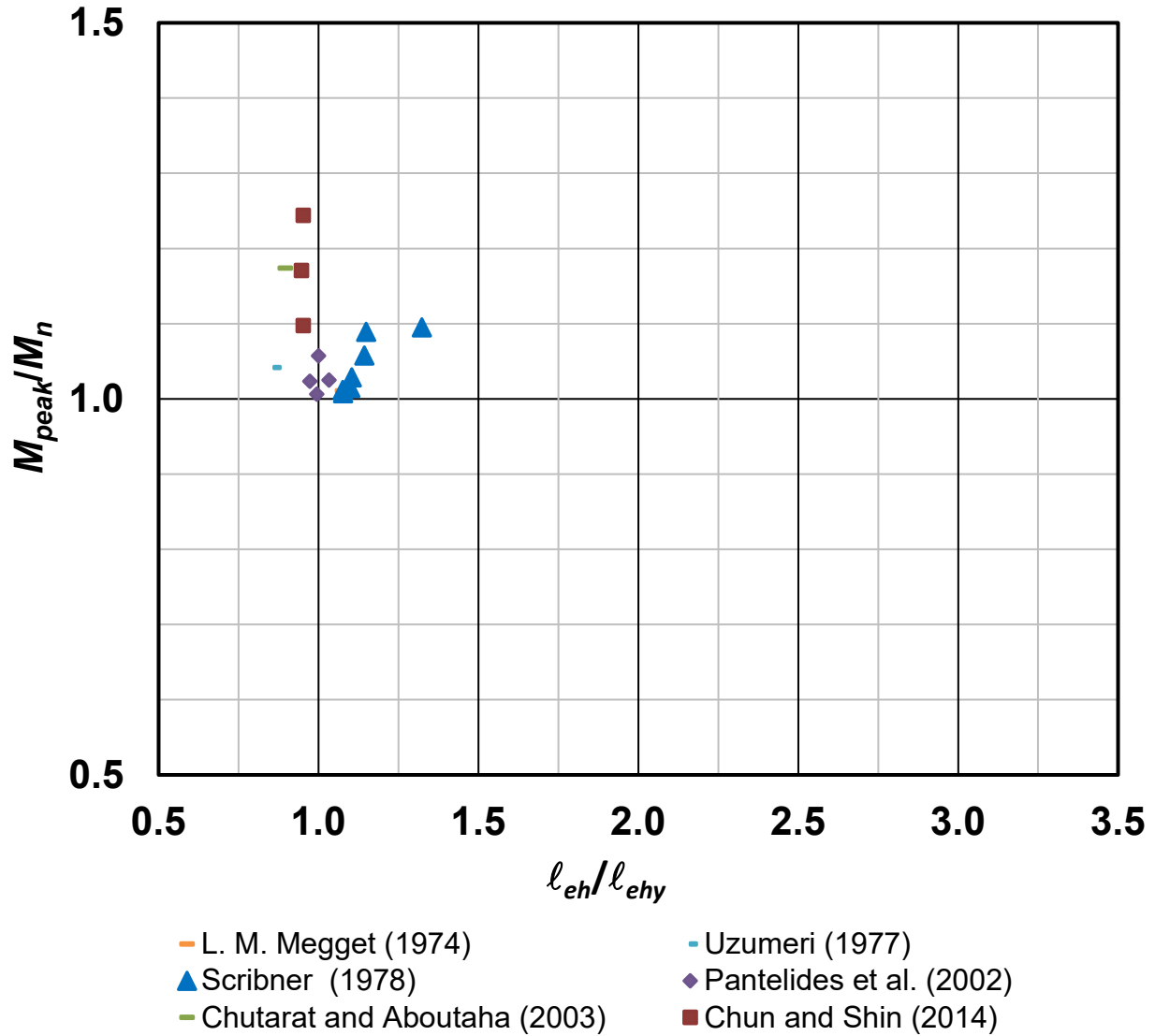


Figure 4.3 M_{peak}/M_n versus ℓ_{eh}/ℓ_{ehy} for specimens with $d/\ell_{eh} \leq 1.5$ and $V_p/V_n > 1.0$. M_{peak}/M_n is the ratio of peak moment to nominal flexural strength, and ℓ_{eh}/ℓ_{ehy} is the ratio of embedment length to the embedment length required to yield the hooked bar calculated using the descriptive equations developed by Ajaam et al. (2017), Eq. (4.1) and (4.2)

4.2.2.1 Specimens with $d/\ell_{eh} \leq 1.5$ and $\ell_{eh}/\ell_{ehy} < 1.0$

The descriptive equations, Eq. (4.1) and (4.2), were developed using exterior beam-column joint specimens with $d/\ell_{eh} \leq 1.5$ under monotonic loading (Ajaam et al. 2017). In this section, the applicability of those equations to beam-column joint specimens with $d/\ell_{eh} \leq 1.5$ and $\ell_{eh}/\ell_{ehy} < 1.0$ subjected to reversed cyclic loading is evaluated.

Twenty-one of the exterior beam-column joint specimens with $d/\ell_{eh} \leq 1.5$ subjected to reversed cyclic loading contained hooked bars with actual embedment lengths, ℓ_{eh} , less than that required to yield the hooked bar, ℓ_{ehy} , calculated using Eq. (4.1) or (4.2). Out of the 21 specimens, 14 had a ratio of peak joint shear to nominal joint shear strength $V_p/V_n \leq 1.0$ and seven had $V_p/V_n > 1.0$. Hooked bar sizes ranged from No. 6 (D19) to No. 9 (D29), with yield strengths ranging from 49,800 to 70,800 psi. Concrete compressive strengths ranged from 3,140 to 7,950 psi. The concrete side cover to the hooked bar ranged from 1.7 to $3.9d_b$ (2 to 3.5 in.), and center-to-center spacing between the hooked bars ranged from 2.1 to $4.6d_b$ (1.8 to 4.9 in.). Confining reinforcement within the joint region parallel to the straight portion of the hooked bars ranged from none to eight No. 4 hoops. Twelve specimens contained confining reinforcement parallel to the straight portion of the hooked bars within the joint region and nine contained none. Two specimens tested by Uzumeri (1977), Specimens 1 and 5 with $\ell_{eh}/\ell_{ehy} < 1.0$, contained transverse beams perpendicular to the test beam at the joint. The transverse beams in those specimens had widths greater than $\frac{3}{4}$ of the effective joint width, which is defined in accordance with Section 15.4.2.4 of ACI 318-19 as the minimum of column width, beam width plus joint depth, and twice the perpendicular distance from the longitudinal axis of the beam to the nearest side face of the column. Therefore, these transverse beams satisfy the minimum dimensional requirement to be considered effective in increasing the joint shear strength in accordance with Section 18.8.4.3 of ACI 318-19, and the nominal joint shear strength (V_n) of these specimens, as calculated in accordance with Section 18.8.4.3 of ACI 318-19, is $15\sqrt{f'_c}A_j$, where A_j is the effective cross-sectional area within the beam-column joint in a plane parallel to the hooked bars calculated in accordance with Section 15.4.2.4 of ACI 318-19.

As shown in Figure 4.2, the trendline for the 14 specimens with $\ell_{eh}/\ell_{ehy} < 1.0$ exhibits an increase in M_{peak}/M_n with an increase in ℓ_{eh}/ℓ_{ehy} , as would be expected. This agrees with the findings by Ajaam et al. (2017) that increasing the embedment length increased the anchorage strength of the hooked bars. Figure 4.3 shows the data for the seven specimens with $\ell_{eh}/\ell_{ehy} < 1.0$ and $V_p/V_n > 1.0$. In this case, no trend is observed for values of ℓ_{eh}/ℓ_{ehy} between 0.86 and 0.99 and values of M_{peak}/M_n between 1.01 and 1.24. Due to the small number of specimens with $\ell_{eh}/\ell_{ehy} < 1.0$ and $V_p/V_n > 1.0$, it is hard to draw any conclusions for this case.

Out of 21 specimens with $\ell_{eh}/\ell_{ehy} < 1.0$, shown in Figures 4.2 and 4.3, four had values of

M_{peak}/M_n less than 1.0. Two of these four specimens had M_{peak}/M_n equal to 0.78 and 0.88 and ℓ_{eh}/ℓ_{ehy} equal to 0.68 and 0.66, respectively, while the other two had M_{peak}/M_n equal to 0.89 and 0.92 and ℓ_{eh}/ℓ_{ehy} equal to 0.81 and 0.86, respectively. These specimens experienced joint deterioration and exhibited diagonal cracks within the joint region, similar to that observed by Ajaam et al. (2017) for simulated exterior beam-column joint specimens tested under monotonic loading. None of these four specimens displayed flexural hinging within the beam, most likely due to inadequate embedment lengths to yield the bars. Of the remaining 17 specimens where $M_{peak}/M_n \geq 1.0$ with ℓ_{eh}/ℓ_{ehy} ranging between 0.8 and 0.99, six specimens—specimen V-A tested by Hanson and Connor (1967), specimens 1, 2 and 5 tested by Uzumeri (1977), and specimens 5 and 6 tested by Pantelides et al. (2002)—showed a 20% reduction in the peak moment at less than 3.5% (1.6 to 3.3%) drift, and the remaining 11 specimens had a reduction in the peak moment of less than 20% at 3.5% drift. Twelve of the seventeen specimens exhibited flexural hinging within the beam, while the remaining five specimens, specimens 1, 2, and 5 tested by Uzumeri (1977), and specimens 5 and 6 tested by Pantelides et al. (2002), failed in the joint region due to the absence of confining reinforcement in the joint. Figures 4.2 and 4.3 show conclusively that the descriptive equations Eq. (4.1) and (4.2) are applicable for members subjected to reversed cyclic loading as well as monotonic loading.

4.2.2.2 Specimens with $d/\ell_{eh} \leq 1.5$ and $\ell_{eh}/\ell_{ehy} \geq 1.0$

Specimens with embedment lengths adequate to yield the hooked bars ($\ell_{eh}/\ell_{ehy} \geq 1.0$) are expected to show post-yield behavior, which is characterized by a slight increase in anchorage strength as embedment length increases due to strain hardening of the steel. The descriptive equations, Eq. (4.1) and (4.2), are used to examine beam-column joint specimens with $\ell_{eh}/\ell_{ehy} \geq 1.0$ subjected to reversed cyclic loading to see if such post-yield behavior is observed in these specimens.

The results for the beam-column joint specimens with d/ℓ_{eh} and $\ell_{eh}/\ell_{ehy} \geq 1.0$ are shown in Figures 4.2 and 4.3 (65 with $V_p/V_n \leq 1.0$ in Figure 4.2 and 10 with $V_p/V_n > 1.0$ in Figure 4.3). ℓ_{eh}/ℓ_{ehy} ranged from 1.02 to 3.0 for the joints with $V_p/V_n \leq 1.0$ and 1.0 to 1.32 for the joints with $V_p/V_n > 1.0$. Hooked bar sizes ranged from No. 4 (D13) to No. 11 (D36), with yield strengths

ranging from 42,900 to 103,000 psi. Concrete compressive strengths ranged from 3,140 to 11,140 psi. The concrete side cover on the hooked bars ranged from 1.4 to $9.8d_b$ (1.03 to 8.6 in.), and center-to-center spacing between the hooked bars ranged from 2.1 to $8.4d_b$ (1.7 to 6.6 in.). Confining reinforcement within the joint region parallel to the straight portion of the hooked bars ranged from none to 8 No. 3 or No. 4 hoops. Out of 75 specimens, 70 contained confining reinforcement parallel to the straight portion of the hooked bars within the joint region, and five specimens did not. Four specimens with $\ell_{eh}/\ell_{ehy} \geq 1.0$, two tested by Hanson (1971), Specimens 1 and 3, and two tested by Uzumeri (1977), Specimens 3 and 4, contained transverse beams perpendicular to the test beam at the joint. The transverse beams in these specimens had widths greater than $\frac{3}{4}$ of the effective joint width, which is defined in accordance with Section 15.4.2.4 of ACI 318-19 as the minimum of column width, beam width plus joint depth, and twice the perpendicular distance from the longitudinal axis of the beam to the nearest side face of the column. Because these transverse beams satisfy the minimum dimensional requirement to be considered effective in increasing the joint shear strength in accordance with Section 18.8.4.3 of ACI 318-19, the nominal joint shear strength (V_n) of these specimens is $15\sqrt{f'_c}A_j$, as described in Section 4.2.2.1. In all cases, joints with $\ell_{eh}/\ell_{ehy} \geq 1.0$ had values of $M_{peak}/M_n \geq 1.0$.

In Figure 4.2, the trendline for the 65 specimens with $\ell_{eh}/\ell_{ehy} \geq 1.0$ shows an increase in M_{peak}/M_n with an increase in embedment length, but at a significantly lower rate of change than the trendline for specimens with $\ell_{eh}/\ell_{ehy} < 1.0$. This is consistent with the hooked bars yielding and strain hardening for $\ell_{eh} \geq \ell_{ehy}$. Out of the 65 specimens, 59 exhibited less than a 20% reduction in the peak moment at about 3.5% drift, while the remaining specimens, Specimen 4 tested by Hanson (1971), Unit 1 tested by Paulay and Scarpas (1981), Specimens U20L, U21L, and R21L tested by Kanada et al. (1984), and Specimen T1-400 tested by Hwang et al. (2014), exhibited a 20% reduction in the peak moment at less than 3.5% (1.1 to 3.2%) drift.

Figures 4.4 and 4.5 provide an understanding of the relationship between M_{peak}/M_n and V_p/V_n for beam-column joint specimens subjected to reversed cyclic loading with $\ell_{eh}/\ell_{ehy} < 1.0$ and $\ell_{eh}/\ell_{ehy} \geq 1.0$. In Figure 4.4, the relationship between V_p/V_n and ℓ_{eh}/ℓ_{ehy} for specimens with $d/\ell_{eh} \leq 1.5$ is presented. Overall, as ℓ_{eh}/ℓ_{ehy} increases, V_p/V_n decreases. This is likely due to the fact that as the embedment length increases, the column depth increases, resulting in a higher nominal joint

shear strength V_n , which reduces V_p/V_n and improves the response of the specimen to reversed cyclic loading. For specimens with $d/\ell_{eh} \leq 1.5$ and $\ell_{eh}/\ell_{ehy} \geq 1.0$, M_{peak}/M_n is plotted versus V_p/V_n in Figure 4.5. The apparent downward trend in M_{peak}/M_n with increasing V_p/V_n in the figure suggests that the increase in M_{peak}/M_n with increasing ℓ_{eh}/ℓ_{ehy} may be related to V_p/V_n , at least to some extent. Reduced M_{peak}/M_n is obviously associated with joint deterioration during cyclic loading at higher V_p/V_n values.

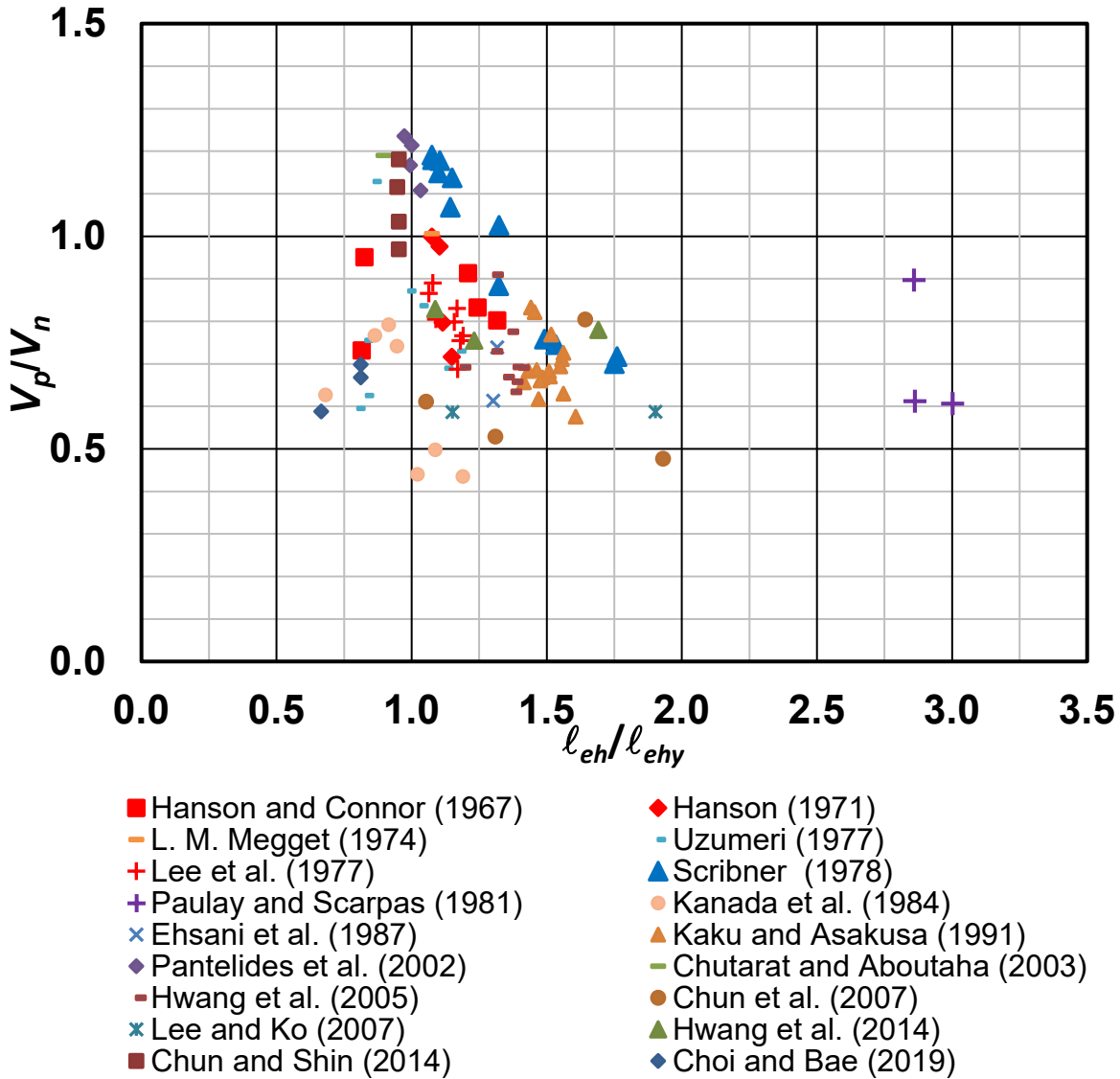


Figure 4.4 V_p/V_n versus ℓ_{eh}/ℓ_{ehy} for specimens with $d/\ell_{eh} \leq 1.5$. V_p/V_n is the ratio of peak joint shear to nominal joint shear strength, and ℓ_{eh}/ℓ_{ehy} is the ratio of embedment length to the embedment length required to yield the hooked bar calculated using the descriptive equations developed by Ajaam et al. (2017), Eq. (4.1) and (4.2)

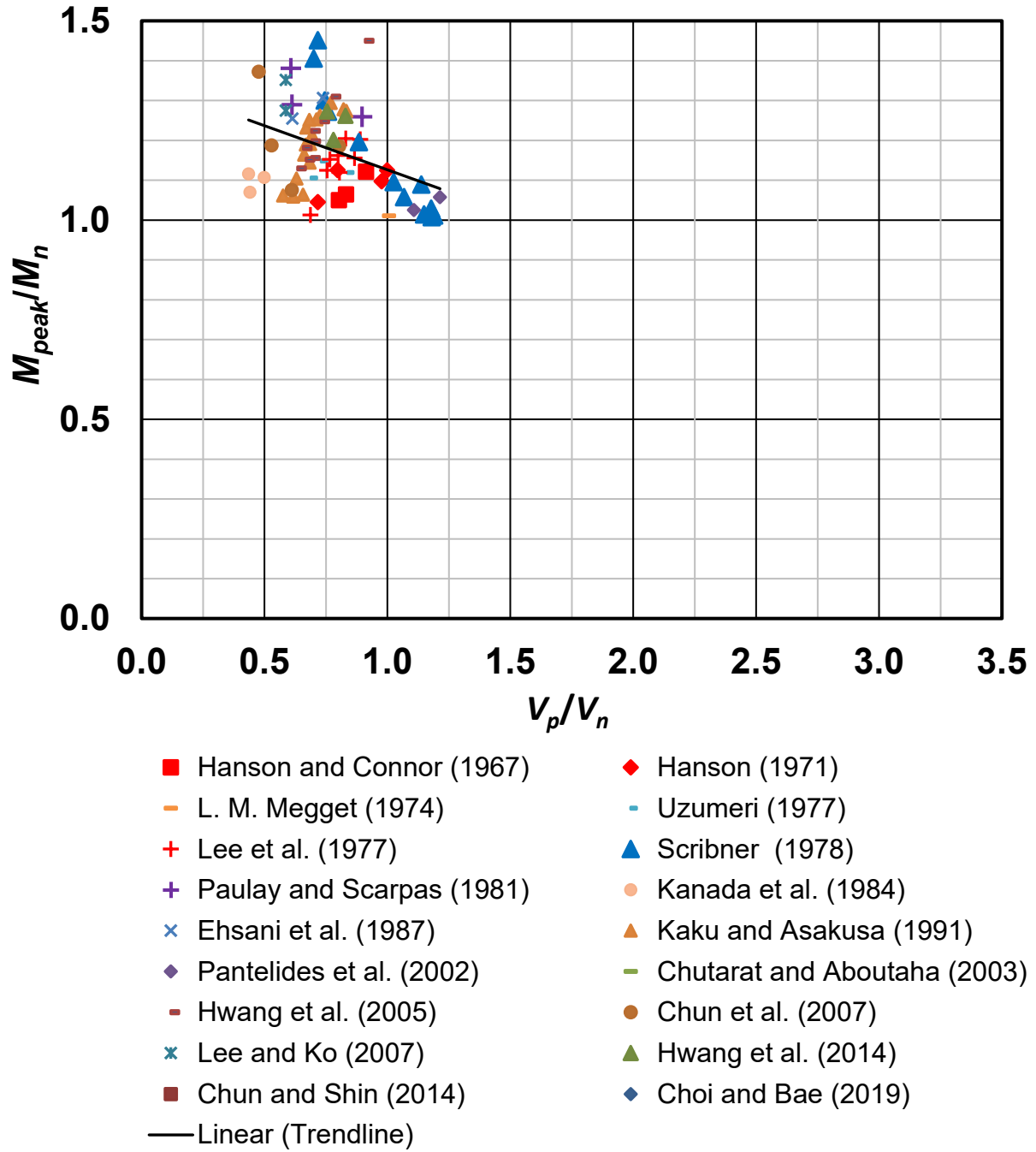


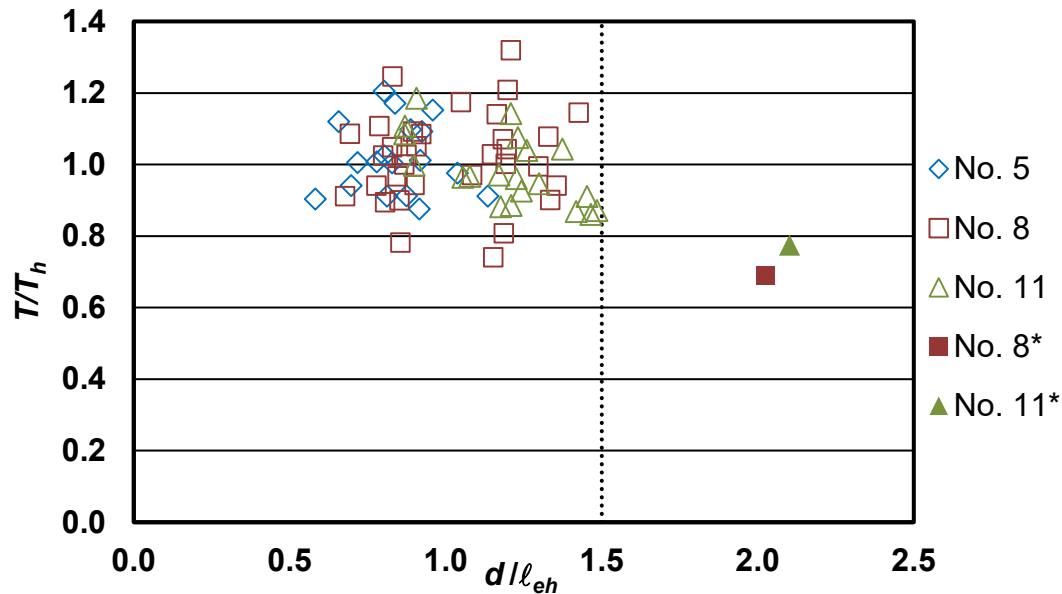
Figure 4.5 M_{peak}/M_n versus V_p/V_n for specimens with $d/\ell_{eh} \leq 1.5$ and $\ell_{eh}/\ell_{ehy} \geq 1.0$. M_{peak}/M_n is the ratio of peak moment to nominal flexural strength, and V_p/V_n is the ratio of peak joint shear to nominal joint shear strength

4.2.2.3 Specimens with $d/\ell_{eh} > 1.5$

Ajaam et al. (2017) found that exterior beam-column joint specimens with a ratio of

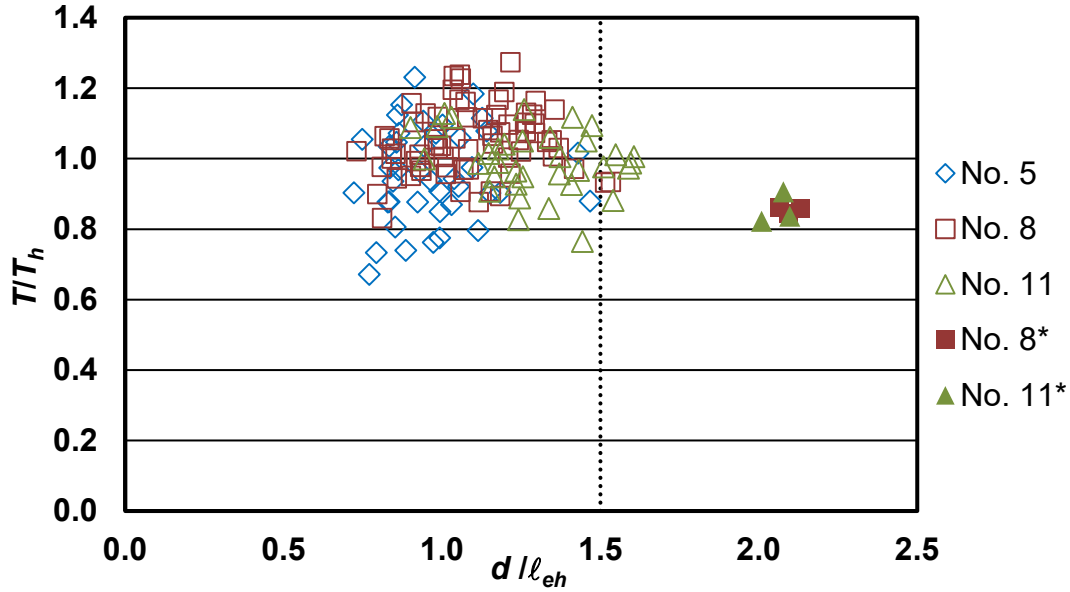
effective beam depth to embedment length $d/\ell_{eh} > 1.5$ exhibited lower anchorage strengths on average than specimens with $d/\ell_{eh} \leq 1.5$. This observation matches Commentary Section R25.4.4.2 of ACI 318-19 for headed bars, which states that “anchorage strengths will be generally higher if the anchorage length is equal to or greater than $d/1.5$.” Specimens with $d/\ell_{eh} > 1.5$ were not used in the development of the descriptive equations, Eq. (4.1) and (4.2). Beam-column joint specimens subjected to reversed cyclic loading with $d/\ell_{eh} > 1.5$ are examined in this section to investigate if the joint performance was affected.

Figures 4.6 and 4.7 show the test-to-calculated strength ratio T/T_h versus d/ℓ_{eh} for specimens tested by Ajaam et al. (2017) under monotonic loading without and with confining reinforcement, respectively. T is the average peak load (total peak load applied on the specimen divided by the number of hooked bars being developed), and T_h is the anchorage strength of a hooked bar calculated using the descriptive equations, Eq. (4.1) and (4.2).



* Specimens not used to develop the descriptive equations [Eq. (4.1) and (4.2)]

Figure 4.6 Ratio of test-to-calculated bar force at failure T/T_h versus ratio of effective beam depth to embedment length d/ℓ_{eh} for specimens without confining reinforcement [T_h is calculated using Eq. (4.1)] (Ajaam et al. 2017)



* Specimens not used to develop the descriptive equations [Eq. (4.1) and (4.2)]

Figure 4.7 Ratio of test-to-calculated bar force at failure T/T_h versus ratio of effective beam depth to embedment length d/ℓ_{eh} for specimens with confining reinforcement [T_h is calculated using Eq. (4.2)] (Ajaam et al. 2017)

As shown in Figures 4.6 and 4.7, the anchorage strengths of monotonically-loaded specimens with $d/\ell_{eh} > 1.5$ average 32 and 19%, respectively, lower than the specimens with $d/\ell_{eh} \leq 1.5$. As was observed by Ajaam et al. (2017), the presence of confining reinforcement reduces the impact of having $d/\ell_{eh} > 1.5$ on anchorage strength.

The ratio of effective beam depth to embedment length d/ℓ_{eh} for 39 of the 135 beam-column joint specimens that were subjected to reversed cyclic loading (see Table 4.2) was greater than 1.5, with values ranging from 1.55 to 3.01. These included two specimens tested by Ehsani and Wight (1982), six specimens tested by Kanada et al. (1984), six specimens tested by Zerbe and Durrani (1985), three specimens tested by Ehsani et al. (1987), 11 specimens tested by Ehsani and Alameddine (1991), three specimens tested by Tsonos et al. (1992), four specimens tested by Tsonos (2007), one specimen tested by Kang et al. (2010), and three specimens tested by Chun and Shin (2014). Of the 39 specimens, 17 had $\ell_{eh}/\ell_{ehy} \geq 1.0$, and the remaining 22 had $\ell_{eh}/\ell_{ehy} < 1.0$. Concrete compressive strengths ranged from 3,140 to 13,700 psi. The hooked bar sizes ranged from No. 3 (D10) to No. 9 (D29), with yield strengths ranging from 48,000 to 76,700 psi. Concrete side cover to the hooked bar and minimum center-to-center spacing between the hooked bars

ranged from 1.3 to $4.0d_b$ (0.7 to 3.0 in.) and 1.9 to $10.7d_b$ (1.8 to 6.3 in.), respectively. Out of the 39 specimens, six specimens tested by Kanada et al. (1984) contained hooked bars terminated at 50% of the column depth; nine specimens, six tested by Zerbe and Durrani (1985), two tested by Ehsani and Wight (1982), and one tested by Kang et al. (2010) contained hooked bars terminated at 64% of the column depth; 17 specimens, three tested by Ehsani et al. (1987), 11 tested by Ehsani and Alameddine (1991), and three tested by Chun and Shin (2014) contained hooked bars terminated at 75% of the column depth; and the remaining seven specimens, three tested by Tsonos et al. (1992) and four tested by Tsonos (2007) contained hooked bars terminated at 83% of the column depth.

The values of the joint confining reinforcement ratio A_{th}/A_{hs} are presented in Table 4.2 and repeated here in Table 4.3. Out of the 39 specimens, the 17 with $\ell_{eh}/\ell_{ehy} \geq 1.0$ had A_{th}/A_{hs} ranging from 0.22 to 0.76, and the 22 specimens with $\ell_{eh}/\ell_{ehy} < 1.0$ had A_{th}/A_{hs} ranging from 0.11 to 0.76. Again, as a reminder, A_{th} for Eq. (4.2) is defined as the area of confining reinforcement within $8d_b$ of the top of the hooked bars for No. 3 through No. 8 bars or within $10d_b$ for No. 9 through No. 11 bars, not $15d_b$ as defined in ACI 318-19, where d_b is the diameter of the hooked bar. As shown in Table 4.3, 36 specimens had values of A_{th}/A_{hs} greater than the upper limit of 0.2 on A_{th}/A_{hs} allowed in Eq. (4.2), and three specimens had values of A_{th}/A_{hs} less than or equal to 0.2. The effect of d/ℓ_{eh} and confining reinforcement within the joint region on the performance of the 39 specimens is discussed next.

Table 4.3 Detail of exterior beam-column joint specimens tested under reversed cyclic loading with $d/\ell_{eh} > 1.5$

Study ^[1]	Specimen	Bar Size ^[2]	f_y (ksi)	f_{cm} (psi)	$\frac{A_{th}}{A_{hs}}$	ℓ_{eh} (in.)	ℓ_{ehy} (in.)	$\frac{\ell_{eh}}{\ell_{ehy}}$	$\frac{d}{\ell_{eh}}$
Ehsani and Wight (1982)	2 ^[6]	No. 7	48.0	5070	0.11	7.4	9.6	0.77	1.93
	4 ^[6]	No. 7	48.0	6470	0.22	7.4	8.4	0.88	1.93
Kanada et al. (1984)	U41S ^[6]	D19	56.2	3870	0.22	6.0	9.8	0.61	2.17
	U42S ^[6]	D19	56.2	4370	0.33	6.0	9.5	0.63	2.17
	U21S ^[6]	D19	56.2	3870	0.45	6.0	7.8	0.77	2.17
	U22S ^[6]	D19	56.2	4370	0.67	6.0	7.5	0.79	2.17
	R42S ^[6]	D19	56.2	3140	0.33	6.0	10.4	0.58	2.17
	R21S ^[6]	D19	56.2	3140	0.45	6.0	8.3	0.73	2.17
Zerbe and Durrani (1985)	J1 ^[6]	No. 6	60.0	5710	0.45	7.8	7.7	1.01	1.63
	J2 ^{[5][6]}	No. 6	60.0	5650	0.45	7.8	7.7	1.00	1.63
	J3 ^[6]	No. 6	60.0	5780	0.45	7.8	7.7	1.01	1.63
	J4 ^{[5][6]}	No. 6	60.0	5940	0.45	7.8	7.6	1.02	1.63
	J5 ^{[5][6]}	No. 6	60.0	5610	0.45	7.8	7.7	1.00	1.63
	J6 ^{[5][6]}	No. 6	60.0	5690	0.45	7.8	7.7	1.00	1.63
Ehsani et al. (1987)	3 ^[6]	No. 6	70.0	9380	0.36	9.2	8.8	1.04	1.57
	4 ^[6]	No. 7	62.0	9760	0.27	9.3	9.8	0.94	1.55
	5 ^[6]	No. 7	48.0	6470	0.22	8.6	8.4	1.02	1.67
Ehsani and Alameddine (1991)	LL8 ^[6]	No. 8	66.3	8600	0.57	10.5	11.4	0.92	1.62
	LH8 ^[6]	No. 8	66.3	8600	0.76	10.5	11.4	0.92	1.62
	HL8 ^[6]	No. 9	64.2	8600	0.45	10.5	13.1	0.80	1.62
	HH8 ^[6]	No. 9	64.2	8600	0.60	10.5	13.1	0.80	1.62
	LL11 ^[6]	No. 8	66.3	10700	0.57	10.5	10.8	0.98	1.62
	LH11 ^[6]	No. 8	66.3	10700	0.76	10.5	10.8	0.98	1.62
	HL11 ^[6]	No. 9	64.2	10700	0.45	10.5	12.3	0.85	1.62
	HH11 ^[6]	No. 9	64.2	10700	0.60	10.5	12.3	0.85	1.62
	LL14 ^[6]	No. 8	66.3	13700	0.57	10.5	10.1	1.04	1.62
	LH14 ^[6]	No. 8	66.3	13700	0.76	10.5	10.1	1.04	1.62
	HH14 ^[6]	No. 9	64.2	13700	0.60	10.5	11.5	0.91	1.62

^[1] Values given in SI units are converted to in.-lb (1 in. = 25.4 mm; 1 psi = 1/145 MPa; and 1 kip = 4.4484 kN); notations used in these studies are described in Appendix A

^[2] Bar sizes are presented in SI and in.-lb as reported in the original studies

^[5] Specimens had transverse beams on one or both sides of the test beam. These transverse beams meet the dimensional requirements of Sections 18.8.4 and 15.2.8 of ACI 318-19 and Section 4.3 of ACI 352R-02 to be considered effective in increasing the joint shear strength

^[6] Specimens had $d/\ell_{eh} > 1.5$

Table 4.3 Cont. Detail of exterior beam-column joint specimens tested under reversed cyclic loading with $d/\ell_{eh} > 1.5$

Study ^[1]	Specimen	Bar Size ^[2]	f_y (ksi)	f_{cm} (psi)	$\frac{A_{th}}{A_{hs}}$	ℓ_{eh} (in.)	ℓ_{ehy} (in.)	$\frac{\ell_{eh}}{\ell_{ehy}}$	$\frac{d}{\ell_{eh}}$
Tsonos et al. (1992)	S1 ^[6]	D14	70.3	5360	0.33	6.5	5.9	1.09	1.67
	S2 ^[6]	D12	76.7	3770	0.30	6.5	5.9	1.10	1.67
	S6' ^[6]	D14	70.3	4200	0.16	6.5	7.6	0.85	1.67
Tsonos (2007)	A1 ^[6]	D10	73.0	5080	0.36	6.5	4.4	1.47	1.64
	E1 ^[6]	D14	72.0	3190	0.24	6.4	7.7	0.84	1.66
	E2 ^[6]	D14	72.0	5080	0.37	6.4	6.2	1.04	1.66
	G1 ^[6]	D14	72.0	3190	0.12	6.4	7.9	0.82	1.66
Kang et al. (2010)	Jk ^[6]	D19	67.0	4200	0.25	11.3	7.8	1.43	1.73
Chun and Shin (2014)	H1.5S ^[6]	D19	70.8	3710	0.58	9.0	9.4	0.95	1.7
	H2.0S ^[6]	D19	70.8	3830	0.58	9.0	8.6	1.04	2.4
	H2.5S ^[6]	D19	70.8	3830	0.58	9.0	8.6	1.04	3.0

^[1] Values given in SI units are converted to in.-lb (1 in. = 25.4 mm; 1 psi = 1/145 MPa; and 1 kip = 4.4484 kN); notations used in these studies are described in Appendix A

^[2] Bar sizes are presented in SI and in.-lb as reported in the original studies

^[6] Specimens had $d/\ell_{eh} > 1.5$

An approach for beam-column joints with $d/\ell_{eh} > 1.5$ is recommended by Section R25.4.4.2 of the Commentary of ACI 318R-19, which, in addressing a similar case for headed bars, recommends “providing reinforcement in the form of hoops and ties to establish a load path in accordance with strut-and-tie modeling principles.” To evaluate specimens subjected to reversed cyclic loading with $d/\ell_{eh} > 1.5$ and check if there was sufficient confining reinforcement within the joint region, anchorage strengths of hooked bars with d/ℓ_{eh} greater than 1.5 are calculated using the strut-and-tie modeling approach. In this approach, all confining reinforcement within the joint region (not the effective confining reinforcement A_{th} , as presented in Section 4.2.1) is assumed, for simplicity, to serve as a single tie with a total force of $f_{ytr}A_v$, as shown in Figure 4.8, where f_{ytr} is the yield strength of the confining reinforcement (ksi) and A_v is the total area of confining reinforcement parallel to the hooked bar (in.²). This tie is used to transfer the force in the hooked bars nT' to the compression region of the beam, where n is the number of hooked bars in tension, and T' is the estimated peak force (kips) in each hooked bar. The force in the hooked bar in beam-column joint specimens subjected to reversed cyclic loading was not directly measured during the tests. Therefore, Eq. (4.4) is used to approximate the peak force in each hooked bar T' .

$$T' = \frac{M_{peak}}{M_n} A_b f_y \quad (4.4)$$

where M_{peak} is the peak moment calculated at the beam-column joint interface (kip-in.); M_n is the nominal flexural strength of the main beam (kip-in.); A_b is the area of a hooked bar (in.²); and f_y is the yield strength of the hooked bar (ksi).

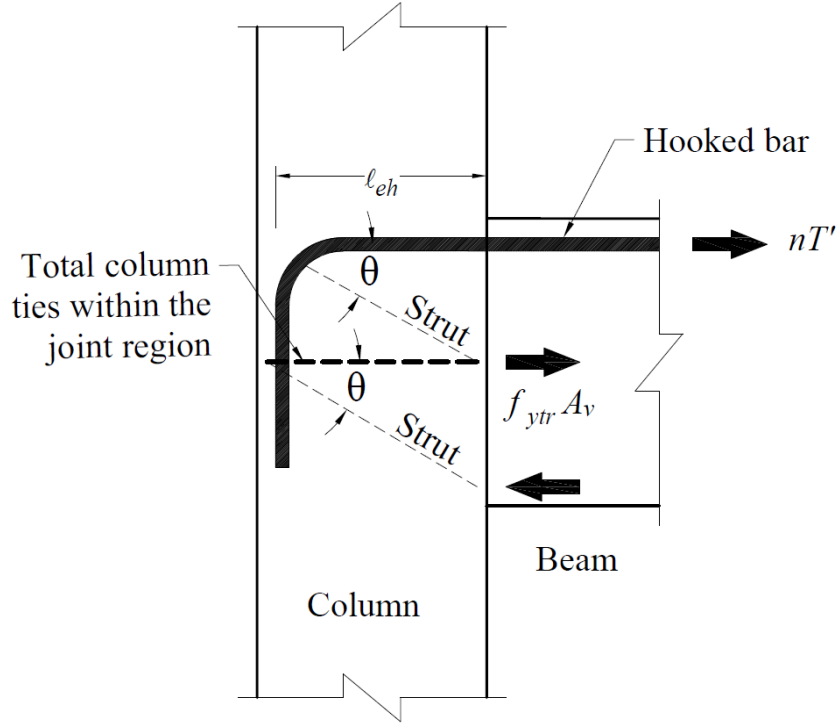


Figure 4.8 Load transfer within the beam-column joint based on the strut-and-tie mechanism (column longitudinal reinforcement and beam compression reinforcement are not shown for clarity)

In this analysis, specimens with $f_{ytr} A_v$ greater than or equal to nT' are considered to have adequate confining reinforcement within the joint region to transfer load using the strut-and-tie mechanism. The summary results of the evaluation of the 39 specimens with $d/\ell_{eh} > 1.5$ are presented in Table 4.4, and details of the specimens are provided in Table C.4 of Appendix C. Only four of the 39 specimens had $f_{ytr} A_v$ values greater than or equal to nT' as required by a strut-and-tie model, one tested by Ehsani and Alameddine (1991) [LH8] and three tested by Chun and Shin (2014) [H1.5S, H2.0S, and H2.5S]. These four specimens, with values of d/ℓ_{eh} ranging from 1.62 to 3.0, had values of ℓ_{eh}/ℓ_{ehy} between 0.88 and 0.90 and M_{peak}/M_n values between 1.01 and

1.12, with a peak moment reduction of less than 20% at 3.5% drift. This observation indicates that beam-column joint specimens with d/ℓ_{eh} greater than 1.5 (up to 3.0) containing a sufficient amount of confining reinforcement within the joint region, as determined by the strut-and-tie modeling approach, performed satisfactorily under reversed cyclic loading. The performance of other specimens with $f_{ytr}A_v < nT'$ is discussed next.

Figure 4.9 shows M_{peak}/M_n plotted versus ℓ_{eh}/ℓ_{ehy} for specimens with $d/\ell_{eh} > 1.5$. For comparison, trendlines for specimens with $d/\ell_{eh} \leq 1.5$ are shown in the figure, along with trendlines for specimens with $d/\ell_{eh} > 1.5$. As shown in the figure, for specimens with $\ell_{eh}/\ell_{ehy} < 1.0$, the trendline for the 22 specimens with $d/\ell_{eh} > 1.5$ crosses and goes above the trendline for specimens with $d/\ell_{eh} \leq 1.5$ as ℓ_{eh}/ℓ_{ehy} approaches 1.0, whereas for specimens with $\ell_{eh}/\ell_{ehy} \geq 1.0$, the trendline for the 17 specimens with $d/\ell_{eh} > 1.5$ is above and parallel to the trendline for specimens with $d/\ell_{eh} \leq 1.5$. All specimens with $\ell_{eh}/\ell_{ehy} \geq 1.0$, including those that did not have enough confining reinforcement to transfer bar force to the compression region of the beam based on the strut-and-tie model approach ($f_{ytr}A_v < nT'$), had values of $M_{peak}/M_n \geq 1.0$ and showed no more than a 20% reduction in the peak moment at 3.5% drift. These observations indicate that given $\ell_{eh} > \ell_{ehy}$, the performance of specimens, including those with $f_{ytr}A_v < nT'$, under reversed cyclic loading was not substantially affected in cases where d/ℓ_{eh} was greater than 1.5 (up to the maximum value of 3.0).

Table 4.4 Test parameters for exterior beam-column joint specimens containing hooked bars with $d/\ell_{eh} > 1.5$ and tested under reversed cyclic loading

Study ^[1]	Specimen	Bar Size ^[2]	f_y (ksi)	f_{cm} (psi)	$\frac{d}{\ell_{eh}}$	f_{ytr} (ksi)	A_v (in. ²)	nT' (kips)	$\frac{f_{ytr} A_v}{nT'}$
Ehsani and Wight (1982)	2	No. 7	48.0	5070	1.93	63.4	0.80	170.8	0.30
	4	No. 7	48.0	6470	1.93	63.4	1.20	214.0	0.36
Kanada et al. (1984)	U41S	D19	56.2	3870	2.17	43.0	0.39	54.8	0.31
	U42S	D19	56.2	4370	2.17	43.0	0.59	59.0	0.43
	U21S	D19	56.2	3870	2.17	43.0	0.39	40.4	0.42
	U22S	D19	56.2	4370	2.17	43.0	0.59	46.4	0.54
	R42S	D19	56.2	3140	2.17	43.0	0.59	59.4	0.42
	R21S	D19	56.2	3140	2.17	43.0	0.39	40.9	0.41
Zerbe and Durrani (1985)	J1	No. 6	60.0	5710	1.63	77.0	1.20	111.8	0.83
	J2 ^[3]	No. 6	60.0	5650	1.63	77.0	1.20	132.0	0.70
	J3	No. 6	60.0	5780	1.63	77.0	1.20	114.6	0.81
	J4 ^[3]	No. 6	60.0	5940	1.63	77.0	1.20	115.5	0.80
	J5 ^[3]	No. 6	60.0	5610	1.63	77.0	1.20	106.7	0.87
	J6 ^[3]	No. 6	60.0	5690	1.63	77.0	1.20	191.7	0.48
Ehsani et al. (1987)	3	No. 6	70.0	9380	1.57	63.4	1.20	183.7	0.41
	4	No. 7	62.0	9760	1.55	63.4	1.20	181.3	0.42
	5	No. 7	48.0	6470	1.67	63.4	1.20	187.5	0.41
Ehsani and Alameddine (1991)	LL8	No. 8	66.3	8600	1.62	64.8	2.40	243.4	0.64
	LH8	No. 8	66.3	8600	1.62	64.8	3.60	235.5	1.00
	HL8	No. 9	64.2	8600	1.62	64.8	2.40	261.8	0.59
	HH8	No. 9	64.2	8600	1.62	64.8	3.60	264.3	0.88
	LL11	No. 8	66.3	10700	1.62	64.8	2.40	202.9	0.77
	LH11	No. 8	66.3	10700	1.62	64.8	3.60	273.2	0.85
	HL11	No. 9	64.2	10700	1.62	64.8	2.40	249.2	0.62
	HH11	No. 9	64.2	10700	1.62	64.8	3.60	271.2	0.86
	LL14	No. 8	66.3	13700	1.62	64.8	2.40	249.2	0.62
	LH14	No. 8	66.3	13700	1.62	64.8	3.60	254.5	0.92
	HH14	No. 9	64.2	13700	1.62	64.8	3.60	273.8	0.85
Tsonos et al. (1992)	S1	D14	70.3	5360	1.67	71.7	0.47	43.6	0.77
	S2	D12	76.7	3770	1.67	71.7	0.47	46.4	0.72
	S6'	D14	70.3	4200	1.67	71.7	0.47	69.1	0.49

^[1] Values given in SI units are converted to in.-lb (1 in. = 25.4 mm; 1 psi = 1/145 MPa; and 1 kip = 4.4484 kN); notations used in these studies are described in Appendix A

^[2] Bar sizes are presented in SI and in.-lb as reported in the original studies

^[3] Specimens had transverse beams on one or both sides of the test beam. These transverse beams meet the dimensional requirements of Section 18.8.4 of ACI 318-19 and Section 4.3 of ACI 352R-02 to be considered effective in increasing the joint shear strength

Table 4.4 Cont. Test parameters for exterior beam-column joint specimens containing hooked bars with $d/\ell_{eh} > 1.5$ and tested under reversed cyclic loading

Study ^[1]	Specimen	Bar Size ^[2]	f_y (ksi)	f_{cm} (psi)	$\frac{d}{\ell_{eh}}$	f_{ytr} (ksi)	A_v (in. ²)	nT' (kips)	$\frac{f_{ytr}A_v}{nT'}$
Tsonos (2007)	A1	D10	73.0	5080	1.64	78.0	0.44	45.0	0.76
	E1	D14	72.0	3190	1.66	78.0	0.44	59.2	0.58
	E2	D14	72.0	5080	1.66	78.0	0.44	43.3	0.79
	G1	D14	72.0	3190	1.66	78.0	0.18	52.5	0.26
Kang et al. (2010)	JK	D19	67.0	4200	1.73	83.0	0.88	147.4	0.50
Chun and Shin (2014)	H1.5S	D19	70.8	3710	1.70	66.7	3.00	126.3	1.58
	H2.0S	D19	70.8	3830	2.40	66.7	4.20	138.5	2.02
	H2.5S	D19	70.8	3830	3.00	66.7	5.40	126.0	2.86

^[1] Values given in SI units are converted to in.-lb (1 in. = 25.4 mm; 1 psi = 1/145 MPa; and 1 kip = 4.4484 kN); notations used in these studies are described in Appendix A

^[2] Bar sizes are presented in SI and in.-lb as reported in the original studies

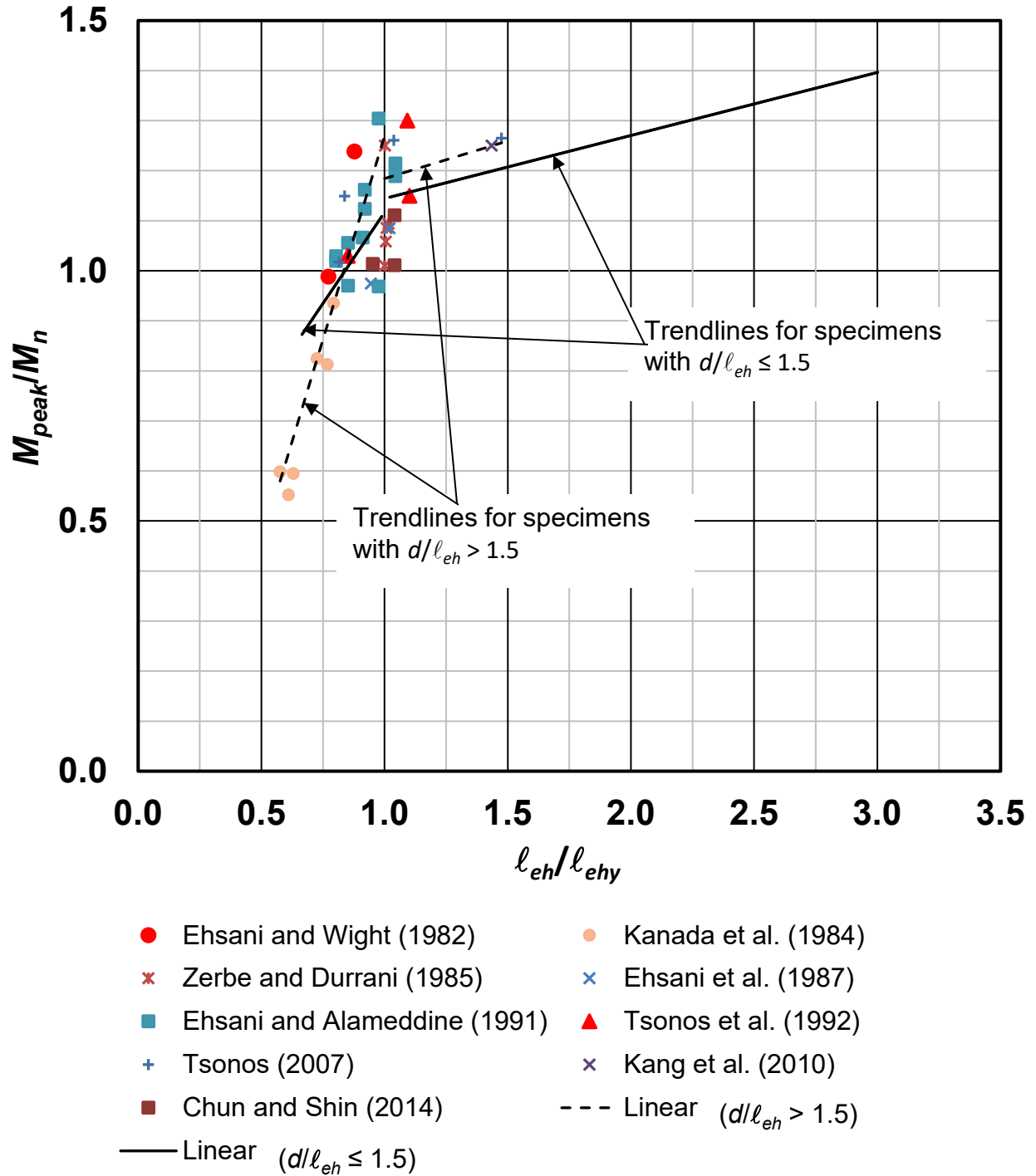


Figure 4.9 M_{peak}/M_n versus ℓ_{eh}/ℓ_{ehy} for specimens with $d/\ell_{eh} > 1.5$. M_{peak}/M_n is the ratio of peak moment to nominal flexural strength, and ℓ_{eh}/ℓ_{ehy} is the ratio of embedment length to the embedment length required to yield the hooked bar calculated using the descriptive equations developed by Ajaam et al. (2017), Eq. (4.1) and (4.2)

4.2.2.4 Applicability of Descriptive Equations to Predict Anchorage Strength of Hooked Bars Anchored in Members Subjected to Reversed Cyclic Loading

The applicability of the descriptive equations developed by Ajaam et al. (2017) for the anchorage strength of hooked bars in beam-column joints tested under monotonic loading to predict the anchorage strength of hooked bars anchored in members subjected to reversed cyclic loading is investigated in this section. The descriptive equations, Eq. (4.1) and (4.2), are presented in detail in Section 4.2.1. In this investigation, the bar forces at failure in beam-column joint specimens subjected to reversed cyclic loading evaluated in this chapter and shown in Table 4.5 are compared with the bar forces predicted by the descriptive equations. The force in the hooked bars at failure T' is estimated using Eq. (4.4), and the anchorage strength T_h is calculated using the descriptive equations, Eq. (4.1) and (4.2). The descriptive equations give an average ratio of test-to-calculated failure load for beam-column joint specimens tested under monotonic loading equal to 1.0. Therefore, the descriptive equations can be considered to have accurately predicted the anchorage strength of hooked bars subjected to reversed cyclic loading if the average ratio of test to calculated bar force at failure is greater than or equal to 1.0. As mentioned earlier in Section 4.2.2, beam-column joint specimens with a ratio of effective beam depth to embedment length $d/\ell_{eh} > 1.5$ were not included when Ajaam et al. (2017) developed the descriptive equations, Eq. (4.1) and (4.2). Therefore, only beam-column joint specimens with $d/\ell_{eh} \leq 1.5$ (ranging from 0.6 to 1.5) were included in this investigation. As found earlier in Sections 4.2.2.1 and 4.2.2.2, the anchorage performance of the hooked bars in beam-column joints subjected to reversed cyclic loading was affected by high joint shear. Therefore, only beam-column joint specimens with the ratio of peak joint shear (V_p) to nominal joint shear strength (V_n) less than or equal to 1.0 (V_p/V_n ranging from 0.43 to 1.00) were included in this investigation. To this end, the test results of 79 exterior beam-column joint specimens (shown in Table 4.5) tested under reversed cyclic loading with $d/\ell_{eh} \leq 1.5$ and $V_p/V_n \leq 1.0$ are used in this evaluation.

Table 4.5 Detail of exterior beam-column joint specimens tested under reversed cyclic loading with $d/\ell_{eh} \leq 1.5$ and $V_p/V_n \leq 1.0$ used in this evaluation and comparisons with descriptive equations, Eq. (4.1) and (4.2)

Study ^[1]		Specimen	Bar Size ^[2]	f_y (ksi)	f_{cm} (psi)	$\frac{\ell_{eh}}{\ell_{ehy}}$	T' (kips)	T_h (kips)	$\frac{T'}{T_h}$
1	Hanson and Connor (1967)	I ^[3]	No. 9	51.6	3470	1.21	57.9	51.9	1.12
		I-A ^[3]	No. 9	47.8	3200	1.24	50.9	48.0	1.06
		II	No. 9	48.3	3650	1.32	50.7	48.6	1.04
		V ^{[3][4]}	No. 9	51.0	3300	0.81	45.4	40.8	1.11
		V-A ^[4]	No. 9	49.8	5420	0.82	53.2	40.4	1.32
2	Hanson (1971)	1 ^[5]	No. 8	63.1	5500	1.15	52.1	50.1	1.04
		3 ^[5]	No. 8	64.1	5200	1.11	57.0	50.9	1.12
		4	No. 8	63.4	5380	1.08	56.3	50.3	1.12
		5	No. 8	65.0	5230	1.10	56.3	51.6	1.09
4	Uzumeri (1977)	1 ^{[4][5]}	No. 9	50.3	4460	0.83	53.2	41.2	1.29
		2 ^[4]	No. 9	50.6	4510	0.83	52.0	41.3	1.26
		3 ^[5]	No. 9	50.8	3920	1.13	56.2	51.1	1.10
		4 ^[5]	No. 9	50.6	4490	1.17	58.1	50.9	1.14
		5 ^{[4][5]}	No. 9	50.4	4630	0.80	54.0	39.6	1.36
		6	No. 9	51.1	5250	1.03	57.2	51.3	1.11
		7	No. 9	51.1	4460	0.99	59.9	50.8	1.18
5	Lee et al. (1977)	1	No. 6	52.5	4200	1.09	25.9	23.2	1.11
		2	No. 6	48.6	4200	1.18	24.0	21.5	1.12
		3	No. 6	48.7	4100	1.17	21.7	21.5	1.01
		4	No. 6	48.9	4000	1.16	25.0	21.6	1.16
		5	No. 6	50.9	3600	1.08	26.9	22.5	1.20
		6	No. 6	51.6	3600	1.06	26.2	22.8	1.15
		7	No. 6	47.5	3700	1.17	25.2	21.0	1.20
		8	No. 6	48.2	4200	1.19	24.4	21.3	1.15

^[1] Values given in SI units are converted to in.-lb (1 in. = 25.4 mm; 1 psi = 1/145 MPa; and 1 kip = 4.4484 kN); notations used in these studies are described in Appendix A

^[2] Bar sizes are presented in SI and in.-lb as reported in the original studies

^[3] Analyzed as a doubly reinforced section to calculate the nominal flexural strength M_n ; all other specimens are analyzed as a single reinforced

^[4] Specimens did not contain confining reinforcement parallel to the hooked bars within the joint region

^[5] Specimens had transverse beams on one or both sides of the test beam. These transverse beams meet the dimensional requirements of Section 18.8.4 of ACI 318-19 and Section 4.3 of ACI 352R-02 to be considered effective in increasing the joint shear strength

Table 4.5 Cont. Detail of exterior beam-column joint specimens tested under reversed cyclic loading with $d/\ell_{eh} \leq 1.5$ and $V_p/V_n \leq 1.0$ used in this evaluation and comparisons with descriptive equations, Eq. (4.1) and (4.2)

Study ^[1]		Specimen	Bar Size ^[2]	f_y (ksi)	f_{cm} (psi)	$\frac{\ell_{eh}}{\ell_{ehy}}$	T' (kips)	T_h (kips)	$\frac{T'}{T_h}$
6	Scribner (1978)	1	No. 6	48.9	4950	1.75	30.2	21.6	1.40
		2	No. 6	48.9	5050	1.76	31.2	21.6	1.44
		3	No. 6	48.9	4940	1.32	25.7	21.6	1.19
		5	No. 6	52.7	3680	1.49	29.5	23.3	1.26
		6	No. 6	52.7	4080	1.53	30.1	23.3	1.29
7	Paulay and Scarpas (1981)	Unit 1	D20	42.9	3280	2.86	27.0	21.1	1.28
		Unit 2	D20	42.9	3260	2.86	26.3	21.1	1.25
		Unit 3	D20	42.9	3900	3.00	28.9	21.1	1.37
9	Kanada et al. (1984)	U40L ^[4]	D19	56.2	3530	0.68	19.5	16.4	1.19
		U41L	D19	56.2	3870	0.91	25.4	22.9	1.11
		U42L	D19	56.2	4370	0.95	24.9	23.6	1.06
		U20L ^[4]	D19	56.2	3870	1.02	26.6	24.8	1.07
		U21L	D19	56.2	4370	1.19	27.7	25.0	1.11
		R41L	D19	56.2	3140	0.86	22.9	21.7	1.06
		R21L	D19	56.2	3140	1.09	27.5	25.0	1.10
11	Ehsani et al. (1987)	1	No. 6	70.0	9380	1.30	38.7	30.9	1.25
		2	No. 6	70.0	9760	1.32	40.2	30.9	1.30
12	Kaku and Asakusa (1991)	1	D13	56.7	4510	1.44	14.2	11.2	1.27
		2	D13	56.7	6050	1.56	14.1	11.2	1.26
		3	D13	56.7	6050	1.56	12.3	11.2	1.10
		4	D13	56.7	6480	1.51	13.7	11.2	1.23
		5	D13	56.7	5320	1.43	12.7	11.2	1.14
		6	D13	56.7	5860	1.47	11.8	11.2	1.06
		7	D13	56.7	4670	1.46	14.2	11.2	1.27
		8	D13	56.7	5970	1.56	13.9	11.2	1.25
		9	D13	56.7	5890	1.55	13.5	11.2	1.21
		10	D13	56.7	6440	1.51	13.9	11.2	1.25
		11	D13	56.7	6080	1.48	13.2	11.2	1.19

^[1] Values given in SI units are converted to in.-lb (1 in. = 25.4 mm; 1 psi = 1/145 MPa; and 1 kip = 4.4484 kN); notations used in these studies are described in Appendix A

^[2] Bar sizes are presented in SI and in.-lb as reported in the original studies

^[4] Specimens did not contain confining reinforcement parallel to the hooked bars within the joint region

Table 4.5 Cont. Detail of exterior beam-column joint specimens tested under reversed cyclic loading with $d/\ell_{eh} \leq 1.5$ and $V_p/V_n \leq 1.0$ used in this evaluation and comparisons with descriptive equations, Eq. (4.1) and (4.2)

Study ^[1]		Specimen	Bar Size ^[2]	f_y (ksi)	f_{cm} (psi)	$\frac{\ell_{eh}}{\ell_{ehy}}$	T' (kips)	T_h (kips)	$\frac{T'}{T_h}$
12	Kaku and Asakusa (1991)	12	D13	56.7	5090	1.41	11.8	11.2	1.06
		13	D13	56.7	6730	1.61	11.8	11.2	1.06
		14	D13	56.7	5950	1.48	13.0	11.2	1.16
		15	D13	56.7	5760	1.46	13.3	11.2	1.19
		16	D13	56.7	5420	1.52	14.4	11.2	1.29
17	Hwang et al. (2005)	0T0 ^[4]	No. 8	62.4	9760	1.18	56.9	49.3	1.16
		3T44	No. 8	62.4	11140	1.40	60.3	49.5	1.22
		1B8	No. 8	63.1	8960	1.30	72.3	50.1	1.44
		3T3	No. 8	62.4	10010	1.36	64.5	49.5	1.30
		2T4	No. 8	62.4	10300	1.30	61.5	49.4	1.24
		1T44	No. 8	62.4	10560	1.38	59.0	49.5	1.19
		3T4	No. 8	71.2	10910	1.37	63.6	56.5	1.13
		2T5	No. 8	71.2	11110	1.38	66.4	56.5	1.18
		1T55	No. 8	71.2	10110	1.34	64.8	56.5	1.15
19	Chun et al. (2007)	JC-1	D22	58.4	8950	1.93	48.1	35.2	1.37
		JC-2	D22	58.4	8720	1.64	41.6	35.1	1.18
		WC ^[4]	D25	62.5	8180	1.31	58.6	49.4	1.19
		JC-No. 11-1	D36	66.4	4760	1.05	111.4	104.0	1.07
20	Lee and Ko (2007)	S0	D22	66.0	4730	1.90	53.5	39.8	1.35
		W0	D22	66.0	4190	1.15	50.5	39.8	1.27
22	Hwang et al. (2014)	T1-400	D22	75.4	4640	1.69	54.3	45.5	1.20
		T2-600	D22	103.0	4640	1.23	78.6	62.0	1.27
		T3-600 ^[3]	D25	92.1	4290	1.09	91.8	73.0	1.26
23	Chun and Shin (2014)	H1.0U	D19	70.8	3710	0.95	32.3	29.8	1.08
24	Choi and Bae (2019)	JTR-0-BTR	D25	68.4	7950	0.81	56.4	44.8	1.26
		JNR-0-BTR ^[4]	D25	68.4	7950	0.66	47.8	34.7	1.38
		JTR-0-BNR	D25	68.4	7950	0.81	54.0	44.8	1.21

^[1] Values given in SI units are converted to in.-lb (1 in. = 25.4 mm; 1 psi = 1/145 MPa; and 1 kip = 4.4484 kN); notations used in these studies are described in Appendix A

^[2] Bar sizes are presented in SI and in.-lb as reported in the original studies

^[3] Analyzed as a doubly reinforced section to calculate the nominal flexural strength M_n ; all other specimens are analyzed as a single reinforced

^[4] Specimens did not contain confining reinforcement parallel to the hooked bars within the joint region

Fourteen beam-column joint specimens tested under reversed cyclic loading with $d/\ell_{eh} \leq 1.5$ and $V_p/V_n \leq 1.0$ used in this evaluation had $\ell_{eh}/\ell_{ehy} < 1.0$. Concrete compressive strengths

ranged from 3,140 to 7,950 psi. Hooked bar sizes ranged from No. 6 (D19) to No. 9 (D29), with yield strengths ranging from 49,800 to 70,800 psi. The concrete side cover to the hooked bar ranged from 1.8 to $3.9d_b$ (2 to 3.5 in.), and center-to-center spacing between the hooked bars ranged from 2.3 to $4.6d_b$ (1.8 to 4.9 in.). The embedment length of the hooked bars ranged from 8.3 to $12d_b$ (8.3 to 13.5 in.). Statistical parameters, including maximum, minimum, mean, standard deviation (STD), and coefficient of variation (COV), of T'/T_h for the specimens with $\ell_{eh}/\ell_{ehy} < 1.0$ are presented in Table 4.6. For comparison, the statistical parameters of T'/T_h for the beam-column joint specimens tested under monotonic loading and used by Ajaam et al. (2017) to develop the descriptive equations, Eq. (4.1) and (4.2), are also presented in Table 4.6, where T is the measured average bar force at failure (total peak load carried by the specimen divided by the number of hooked bars being developed). The values of T'/T_h for the 14 specimens with $\ell_{eh}/\ell_{ehy} < 1.0$ ranged between 1.06 and 1.38 with a mean, standard deviation (STD), and coefficient of variation (COV) of 1.20, 0.110, and 0.091, respectively, as shown in Table 4.6. The ratio of test to calculated failure load of hooked bars T'/T_h in the specimens tested and used by Ajaam et al. (2017) to develop descriptive equations, Eq. (4.1) and (4.2), ranged from 0.74 to 1.32 with a mean, STD, and COV of 1.00, 0.115, and 0.115, and from 0.67 to 1.27 with a mean, STD, and COV of 1.00, 0.112, and 0.112, respectively. These findings indicate that the descriptive equations successfully capture the anchorage behavior of the hooked bars with $\ell_{eh}/\ell_{ehy} < 1.0$ subjected to reversed cyclic loading.

Table 4.6 Statistical parameters for test-to-calculated ratio in beam-column joint specimens with $\ell_{eh}/\ell_{ehy} < 1.0$ tested under reversed cyclic loading and in beam-column joint specimens tested under monotonic loading and used by Ajaam et al. (2017) to develop the descriptive equations, Eq. (4.1) and (4.2)

Test/Calculated	T'/T_h	T/T_h	
Statistical Parameters	Specimens tested under reversed cyclic loading with $\ell_{eh}/\ell_{ehy} < 1.0$	Specimens tested and used by Ajaam et al. (2017) to develop Eq. (4.1)	Specimens tested and used by Ajaam et al. (2017) to develop Eq. (4.2)
Max	1.38	1.32	1.27
Min	1.06	0.74	0.67
Mean	1.20	1.00	1.00
STD	0.110	0.115	0.112
COV	0.091	0.115	0.112
Number of specimens	14	88	149

A similar analysis was carried out on specimens with $\ell_{eh}/\ell_{ehy} \geq 1.0$ that were subjected to reversed cyclic loading. Sixty-five beam-column joint specimens tested under reversed cyclic loading with $d/\ell_{eh} \leq 1.5$ and $V_p/V_n \leq 1.0$ used in this evaluation had $\ell_{eh}/\ell_{ehy} \geq 1.0$. Concrete compressive strengths ranged from 3,140 to 11,140 psi. Hooked bar sizes ranged from No. 4 (D13) to No. 11 (D36), with yield strengths ranging from 42,900 to 103,000 psi. The concrete side cover to the hooked bar ranged from 1.4 to $9.8d_b$ (1.03 to 8.6 in.), and center-to-center spacing between the hooked bars ranged from 2.3 to $8.4d_b$ (1.7 to 6.6 in.). The embedment length of the hooked bars ranged from 11.5 to $24d_b$ (7.7 to 21.0 in.). All the sixty-five specimens with $\ell_{eh}/\ell_{ehy} \geq 1.0$ had $M_{peak}/M_n \geq 1.0$. The statistical parameters, including maximum, minimum, mean, standard deviation (STD), and coefficient of variation (COV), of T'_{mod}/T_h for the specimens with $\ell_{eh}/\ell_{ehy} \geq 1.0$ are presented in Table 4.7. T'_{mod} is the modified bar force at failure T' corresponding to the value of M_{peak}/M_n projected on the line $\ell_{eh}/\ell_{ehy} = 1.0$ line by extending a line parallel to the trend line for specimens with $\ell_{eh}/\ell_{ehy} \geq 1.0$, as shown in Figure 4.10 for one specimen, and calculated using Eq. (4.5). The anchorage strength of the hooked bar T_h is calculated using the descriptive equations, Eq. (4.1) and (4.2), corresponding to $\ell_{eh} = \ell_{ehy}$ as for T'_{mod} .

$$T'_{\text{mod}} = \left(\frac{M_{\text{peak}}}{M_n} \right)_{\text{mod}} A_b f_y \quad (4.5)$$

$$\text{with } \left(\frac{M_{\text{peak}}}{M_n} \right)_{\text{mod}} = \frac{M_{\text{peak}}}{M_n} - 0.126 \left(\frac{\ell_{eh}}{\ell_{ehy}} - 1 \right)$$

where the coefficient of 0.126 is the slope of the trendline for specimens with $\ell_{eh}/\ell_{ehy} \geq 1.0$ in Figure 4.10. An example of calculating $(M_{\text{peak}}/M_n)_{\text{mod}}$ is shown graphically in Figure 4.10.

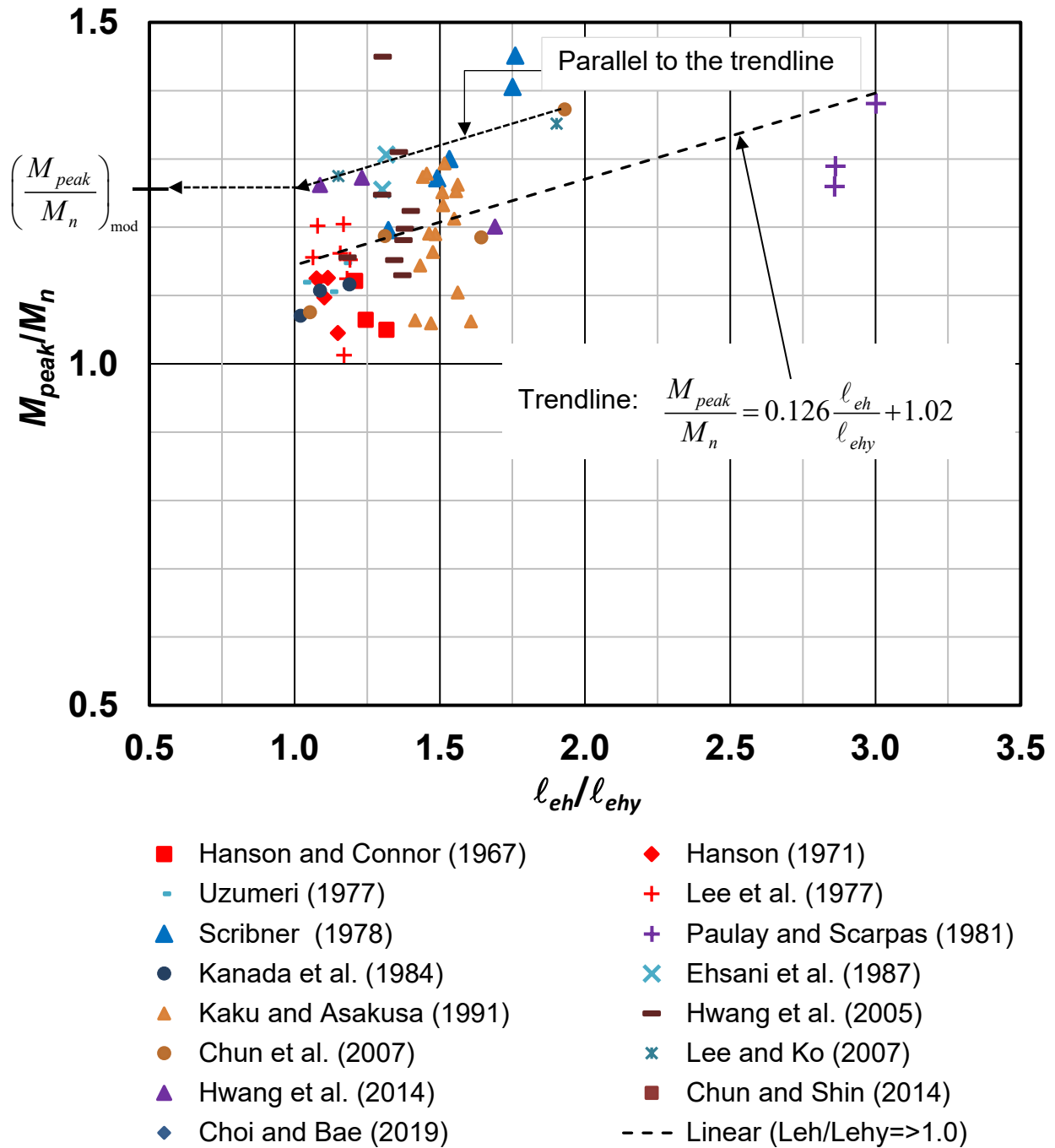


Figure 4.10 M_{peak}/M_n versus ℓ_{eh}/ℓ_{ehy} for beam-column joint specimens with $\ell_{eh}/\ell_{ehy} \geq 1.0$. The value of M_{peak}/M_n for one specimen is projected on the line $\ell_{eh}/\ell_{ehy} = 1.0$ line by extending a line parallel to the trend line for specimens with $\ell_{eh}/\ell_{ehy} \geq 1.0$

The values of T'_{mod}/T_h for the 65 beam-column joint specimens with $\ell_{eh}/\ell_{ehy} \geq 1.0$ (presented in Table 4.8) ranged between 0.98 and 1.41 with a mean, STD, and COV of 1.14, 0.087,

and 0.076, respectively, as shown in Table 4.7. As mentioned earlier that the ratio of test to calculated failure load of hooked bars T/T_h in the specimens tested and used by Ajaam et al. (2017) to develop the descriptive equations, Eq. (4.1) and (4.2), ranged from 0.74 to 1.32 with a mean, STD, and COV of 1.00, 0.115, and 0.115, and from 0.67 to 1.27 with a mean, STD, and COV of 1.00, 0.112, and 0.112, respectively, as shown in Table 4.6. These results indicate that the descriptive equations conservatively capture the anchorage behavior of the hooked bars with $\ell_{eh}/\ell_{ehy} \geq 1.0$ subjected to reversed cyclic loading.

Table 4.7 Statistical parameters for T'_{mod}/T_h in beam-column joint specimens with $\ell_{eh}/\ell_{ehy} \geq 1.0$ tested under reversed cyclic loading

Test/Calculated	T'_{mod}/T_h
Statistical Parameters	Specimens tested under reversed cyclic loading with $\ell_{eh}/\ell_{ehy} \geq 1.0$
Max	1.41
Min	0.98
Mean	1.14
STD	0.087
COV	0.076
Number of specimens	65

Table 4.8 Detail of exterior beam-column joint specimens tested under reversed cyclic loading with $d/\ell_{eh} \leq 1.5$, $V_p/V_n \leq 1.0$, and $\ell_{eh}/\ell_{ehy} \geq 1.0$ used in this evaluation and comparisons with descriptive equations, Eq. (4.1) and (4.2)

Study ^[1]		Specimen	Bar Size ^[2]	f_y (ksi)	f_{cm} (psi)	$\frac{\ell_{eh}}{\ell_{ehy}}$	T'_{mod} (kips)	T_h (kips)	$\frac{T'_{mod}}{T_h}$
1	Hanson and Connor (1967)	I ^[3]	No. 9	51.6	3470	1.21	56.5	51.9	1.09
		I-A ^[3]	No. 9	47.8	3200	1.24	49.4	48.0	1.03
		II	No. 9	48.3	3650	1.32	48.8	48.6	1.00
2	Hanson (1971)	1 ^[5]	No. 8	63.1	5500	1.15	51.2	50.1	1.02
		3 ^[5]	No. 8	64.1	5200	1.11	56.3	50.9	1.11
		4	No. 8	63.4	5380	1.08	55.9	50.3	1.11
		5	No. 8	65.0	5230	1.10	55.7	51.6	1.08
4	Uzumeri (1977)	3 ^[5]	No. 9	50.8	3920	1.13	55.4	51.1	1.08
		4 ^[5]	No. 9	50.6	4490	1.17	57.0	50.9	1.12
		6	No. 9	51.1	5250	1.03	57.0	51.3	1.11
5	Lee et al. (1977)	1	No. 6	52.5	4200	1.09	25.6	23.2	1.1
		2	No. 6	48.6	4200	1.18	23.6	21.5	1.1
		3	No. 6	48.7	4100	1.17	21.2	21.5	1.0
		4	No. 6	48.9	4000	1.16	24.6	21.6	1.1
		5	No. 6	50.9	3600	1.08	26.7	22.5	1.2
		6	No. 6	51.6	3600	1.06	26.1	22.8	1.1
		7	No. 6	47.5	3700	1.17	24.7	21.0	1.2
		8	No. 6	48.2	4200	1.19	23.9	21.3	1.1
6	Scribner (1978)	1	No. 6	48.9	4950	1.75	28.2	21.6	1.3
		2	No. 6	48.9	5050	1.76	29.2	21.6	1.3
		3	No. 6	48.9	4940	1.32	24.9	21.6	1.1
		5	No. 6	52.7	3680	1.49	28.1	23.3	1.2
		6	No. 6	52.7	4080	1.53	28.6	23.3	1.2
7	Paulay and Scarpas (1981)	Unit 1	D20	42.9	3280	2.86	22.0	21.1	1.05
		Unit 2	D20	42.9	3260	2.86	21.4	21.1	1.02
		Unit 3	D20	42.9	3900	3.00	23.6	21.1	1.12

^[1] Values given in SI units are converted to in.-lb (1 in. = 25.4 mm; 1 psi = 1/145 MPa; and 1 kip = 4.4484 kN); notations used in these studies are described in Appendix A

^[2] Bar sizes are presented in SI and in.-lb as reported in the original studies

^[3] Analyzed as a doubly reinforced section to calculate the nominal flexural strength M_n ; all other specimens are analyzed as a single reinforced

^[4] Specimens did not contain confining reinforcement parallel to the hooked bars within the joint region

^[5] Specimens had transverse beams on one or both sides of the test beam. These transverse beams meet the dimensional requirements of Section 18.8.4 of ACI 318-19 and Section 4.3 of ACI 352R-02 to be considered effective in increasing the joint shear strength

Table 4.8 Cont. Detail of exterior beam-column joint specimens tested under reversed cyclic loading with $d/\ell_{eh} \leq 1.5$, $V_p/V_n \leq 1.0$, and $\ell_{eh}/\ell_{ehy} \geq 1.0$ used in this evaluation and comparisons with descriptive equations, Eq. (4.1) and (4.2)

Study ^[1]		Specimen	Bar Size ^[2]	f_y (ksi)	f_{cm} (psi)	$\frac{\ell_{eh}}{\ell_{ehy}}$	T'_{mod} (kips)	T_h (kips)	$\frac{T'_{mod}}{T_h}$
9	Kanada et al. (1984)	U20L ^[4]	D19	56.2	3870	1.02	26.5	24.8	1.07
		U21L	D19	56.2	4370	1.19	27.1	25.0	1.09
		R21L	D19	56.2	3140	1.09	27.2	25.0	1.09
11	Ehsani et al. (1987)	1	No. 6	70.0	9380	1.30	37.5	30.9	1.21
		2	No. 6	70.0	9760	1.32	39.0	30.9	1.26
12	Kaku and Asakusa (1991)	1	D13	56.7	4510	1.44	13.6	11.2	1.21
		2	D13	56.7	6050	1.56	13.3	11.2	1.19
		3	D13	56.7	6050	1.56	11.5	11.2	1.03
		4	D13	56.7	6480	1.51	13.0	11.2	1.17
		5	D13	56.7	5320	1.43	12.1	11.2	1.09
		6	D13	56.7	5860	1.47	11.1	11.2	1.00
		7	D13	56.7	4670	1.46	13.6	11.2	1.22
		8	D13	56.7	5970	1.56	13.2	11.2	1.18
		9	D13	56.7	5890	1.55	12.7	11.2	1.14
		10	D13	56.7	6440	1.51	13.2	11.2	1.19
		11	D13	56.7	6080	1.48	12.6	11.2	1.13
		12	D13	56.7	5090	1.41	11.3	11.2	1.01
		13	D13	56.7	6730	1.61	11.0	11.2	0.98
		14	D13	56.7	5950	1.48	12.3	11.2	1.10
		15	D13	56.7	5760	1.46	12.6	11.2	1.13
		16	D13	56.7	5420	1.52	13.7	11.2	1.22
17	Hwang et al. (2005)	0T0 ^[4]	No. 8	62.4	9760	1.18	55.8	49.3	1.13
		3T44	No. 8	62.4	11140	1.40	57.8	49.5	1.17
		1B8	No. 8	63.1	8960	1.30	70.4	50.1	1.41
		3T3	No. 8	62.4	10010	1.36	62.3	49.5	1.26
		2T4	No. 8	62.4	10300	1.30	59.6	49.4	1.21
		1T44	No. 8	62.4	10560	1.38	56.7	49.5	1.14

^[1] Values given in SI units are converted to in.-lb (1 in. = 25.4 mm; 1 psi = 1/145 MPa; and 1 kip = 4.4484 kN); notations used in these studies are described in Appendix A

^[2] Bar sizes are presented in SI and in.-lb as reported in the original studies

^[3] Analyzed as a doubly reinforced section to calculate the nominal flexural strength M_n ; all other specimens are analyzed as a single reinforced

^[4] Specimens did not contain confining reinforcement parallel to the hooked bars within the joint region

Table 4.8 Cont. Detail of exterior beam-column joint specimens tested under reversed cyclic loading with $d/\ell_{eh} \leq 1.5$, $V_p/V_n \leq 1.0$, and $\ell_{eh}/\ell_{ehy} \geq 1.0$ used in this evaluation and comparisons with descriptive equations, Eq. (4.1) and (4.2)

Study ^[1]		Specimen	Bar Size ^[2]	f_y (ksi)	f_{cm} (psi)	$\frac{\ell_{eh}}{\ell_{ehy}}$	T'_{mod} (kips)	T_h (kips)	$\frac{T'_{mod}}{T_h}$
17	Hwang et al. (2005)	3T4	No. 8	71.2	10910	1.37	60.9	56.5	1.08
		2T5	No. 8	71.2	11110	1.38	63.8	56.5	1.13
		1T55	No. 8	71.2	10110	1.34	62.4	56.5	1.10
19	Chun et al. (2007)	JC-1	D22	58.4	8950	1.93	44.0	35.2	1.25
		JC-2	D22	58.4	8720	1.64	38.7	35.1	1.10
		WC ^[4]	D25	62.5	8180	1.31	56.7	49.4	1.15
		JC-No. 11-1	D36	66.4	4760	1.05	110.7	104.0	1.06
20	Lee and Ko (2007)	S0	D22	66.0	4730	1.90	49.0	39.8	1.23
		W0	D22	66.0	4190	1.15	49.7	39.8	1.25
22	Hwang et al. (2014)	T1-400	D22	75.4	4640	1.69	50.4	45.5	1.11
		T2-600	D22	103.0	4640	1.23	76.8	62.0	1.24
		T3-600 ^[3]	D25	92.1	4290	1.09	91.0	73.0	1.25

^[1] Values given in SI units are converted to in.-lb (1 in. = 25.4 mm; 1 psi = 1/145 MPa; and 1 kip = 4.4484 kN); notations used in these studies are described in Appendix A

^[2] Bar sizes are presented in SI and in.-lb as reported in the original studies

^[3] Analyzed as a doubly reinforced section to calculate the nominal flexural strength M_n ; all other specimens are analyzed as a single reinforced

^[4] Specimens did not contain confining reinforcement parallel to the hooked bars within the joint region

The estimated hooked bar forces at failure T'_{mod} for the 65 exterior beam-column joint specimens tested under reversed cyclic loading with $d/\ell_{eh} \leq 1.5$, $V_p/V_n \leq 1.0$, and $\ell_{eh}/\ell_{ehy} \geq 1.0$ are plotted versus the calculated failure loads T_h [based on the descriptive equations, Eq. (4.1) and (4.2)] in Figure 4.11. The broken line represents equality, where the calculated and the estimated hooked bar forces at failure are equal. The solid line is the trend line for the data. As shown in the figure, the trend line is above and close to the broken line, indicating that the descriptive equations, Eq. (4.1) and (4.2), provide a somewhat conservative estimate of the anchorage strength of hooked bars with and without confining reinforcement in beam-column joint specimens subjected to reversed cyclic loading.

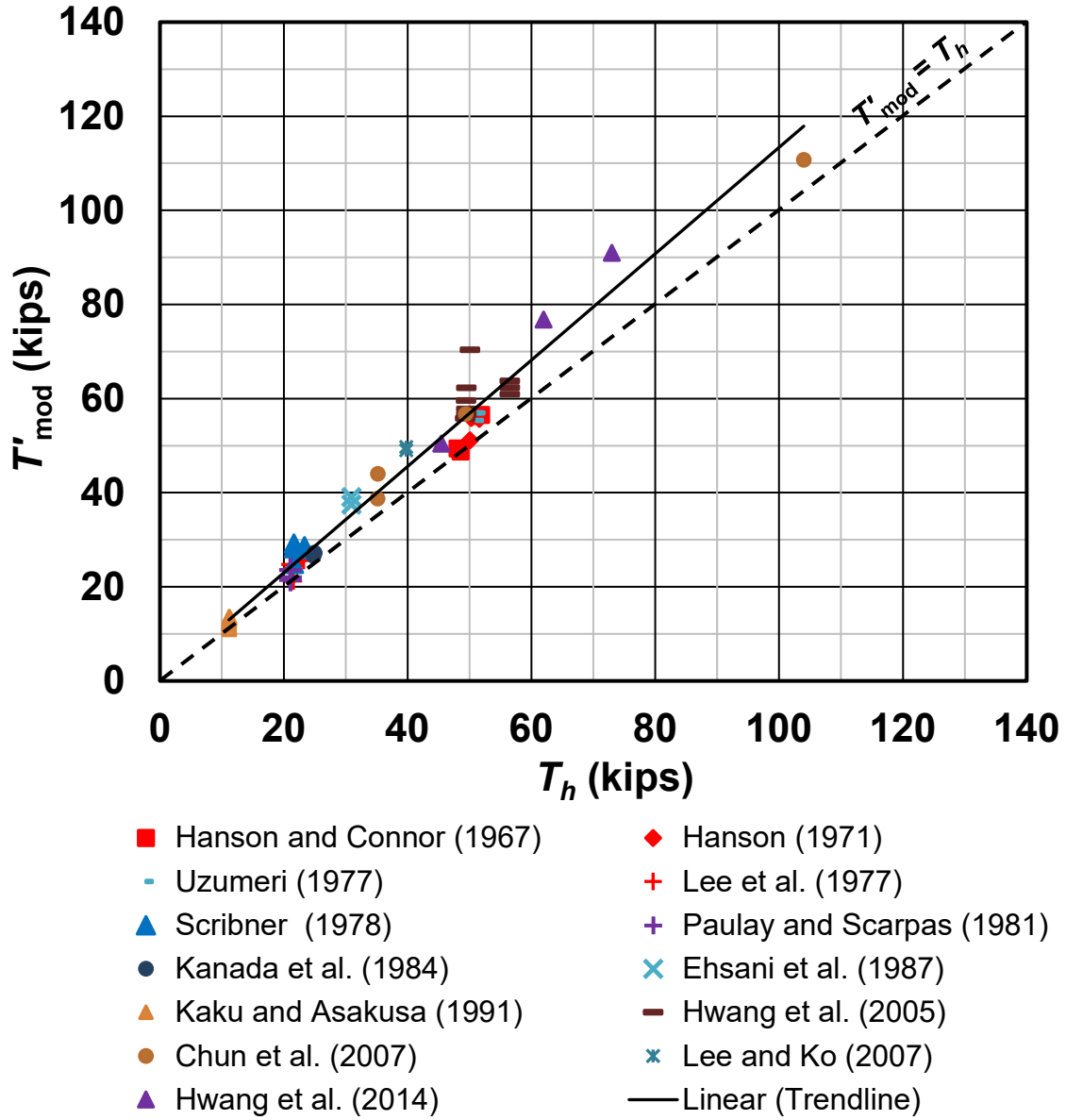


Figure 4.11 Estimated hooked bar force at failure T'_{mod} versus hooked bar force T_h [based on the descriptive equations, Eq. (4.1) and (4.2)] for specimens with $d/\ell_{eh} \leq 1.5$, $V_p/V_n \leq 1.0$, and $\ell_{eh}/\ell_{ehy} \geq 1.0$.

In summary, of the 146 beam-column joint specimens tested under reversed cyclic loading in the database, 65 satisfied the criteria of having $d/\ell_{eh} \leq 1.5$, $V_p/V_n \leq 1.0$, and $\ell_{eh}/\ell_{ehy} \geq 1.0$. These specimens, on average, satisfied the requirements for minimum strength and deformation capacity, with $M_{peak}/M_n \geq 1.0$ and $\delta_{0.8peak} \geq 3.5\%$. According to the results of the analyses presented in this chapter, it is concluded that the descriptive equations developed for beam-column joint specimens

tested under monotonic loading, which serve as the basis for the development length provisions for hooked bars in ACI 318-19, are sufficient for determining the required embedment length of hooked bars in beam-column joints subjected to reversed cyclic loading.

4.3 GUIDELINES AND RECOMMENDATIONS FOR CHAPTER 18 OF ACI 318-19

As mentioned in Sections 1.1 and 1.6.3, the development length provisions for hooked bars in tension under reversed cyclic loading in Section 18.8.5.1 of ACI 318-19 were derived directly from the development length provisions for non-seismic (monotonic) loading (Section 25.4.3.1) that existed in ACI 318 Building Codes prior to 2019. Even though the development length provisions (Section 25.4.3.1) were updated in ACI 318-19 based on the comprehensive study conducted at KU using specimens tested under monotonic loading (Sperry et al. 2015a,b, 2017a,b, 2018, Ajaam et al. 2017, 2018, Yasso et al. 2017), the Code design provisions for the development length of hooked bars in tension subjected to reversed cyclic loading remained unchanged. This has resulted in provisions allowing development lengths for hooked bars designed in accordance with Chapter 18 to be *shorter* than those needed for gravity load by Chapter 25, as shown in Section 4.3.1, which is an odd situation. The analyses in this chapter were performed to examine the suitability of applying the development length requirements of 25.4.3 to the design of hooked bars subjected to reversed cyclic stress. Those analyses show that the descriptive equations developed by Ajaam et al. (2017), Eq. (4.1) and (4.2), for the anchorage strength of hooked bars in beam-column joints tested under monotonic loading are suitable for predicting the anchorage strength of hooked bars anchored in members subjected to reversed cyclic loading. These findings strongly suggest that a single approach be used in ACI 318 for calculating the development length of hooked bars anchored in members subjected to gravity and seismic loading using Section 25.4.3.1 of ACI 318-19. Section 4.3.2 addresses the proposed changes in Chapter 18 of ACI 318-19.

4.3.1 Comparison Between the Development Lengths of Hooked Bars Required for Seismic and Non-Seismic (Gravity) Loading (Chapter 18 vs. 25 of ACI 318-19)

The development length provisions for hooked bars in tension under *non-seismic (gravity) loading* (Section 25.4.3.1 of ACI 318-19) and under reversed cyclic loading (Section 18.8.5.1 of

ACI 318-19) are described in Sections 1.6.2 and 1.6.3, respectively. In accordance with Section 25.4.3.1 of ACI 318-19, the development length of a standard hooked bar in tension, ℓ_{dh} , for non-seismic (gravity) loading is given in Eq. (4.6), with ℓ_{dh} not less than the greater of $8d_b$ and 6 in., while, in accordance with Section 18.8.5.1 of ACI 318-19, the development length of a standard hooked bar in tension, ℓ_{dh} , for No. 11 and smaller bars embedded in beam-column joints in special moment frames with capability of sustaining reversed cyclic loading is given in Eq. (4.7), with ℓ_{dh} not less than the maximum of $8d_b$ and 6 in. for normalweight concrete and $10d_b$ and 7.5 in. for lightweight concrete.

$$\ell_{dh} = \left(\frac{f_y \Psi_e \Psi_r \Psi_o \Psi_c}{55 \lambda \sqrt{f'_c}} \right) d_b^{1.5} \quad (4.6)$$

$$\ell_{dh} = \frac{f_y d_b}{65 \lambda \sqrt{f'_c}} \quad (4.7)$$

where ℓ_{dh} is the development length of a hooked bar in tension (in.); f_y is the specified yield strength of the hooked bar (psi); d_b is the hooked bar diameter (in.); f'_c is the specified concrete compressive strength (psi); Ψ_e is a factor based on the presence or absence of a coating on the bars, equal to 1.2 for epoxy-coated or zinc and epoxy dual-coated reinforcement and 1.0 for uncoated or zinc-coated (galvanized) reinforcement; Ψ_r is a confining reinforcement factor equal to 1.0 for No. 11 and smaller hooked bars spaced at a center-to-center distance not less than $6d_b$ and for hooked bars with A_{th}/A_{hs} not less than 0.4, where A_{th} is the total cross-sectional area of ties or stirrups confining hooked bars (in.²) and A_{hs} is the total cross-sectional area of hooked bars being developed at a critical section (in.²); otherwise, Ψ_r is equal to 1.6; Ψ_o is the bar location factor equal to 1.0 for No. 11 and smaller hooked or headed bars anchored within a column core with side cover not less than 2.5 in. or in other members with side cover not less than $6d_b$; otherwise, Ψ_o is equal to 1.25; Ψ_c is the concrete strength factor equal to $f'_c/15,000 + 0.6$ if f'_c is less than 6000 psi and equal to 1.0 if f'_c is greater than or equal to 6000 psi; λ is a lightweight concrete factor equal to 0.75 for lightweight concrete and 1.0 for normalweight concrete. The modification factors in Eq. (4.6) are defined in Table 25.4.3.2 of ACI 318-19.

By way of an example, the development lengths of hooked bars ℓ_{dh} designed in accordance with the provisions in Chapter 25 are compared with those designed in accordance with Chapter 18 of ACI 318-19 for No. 8 and No. 11 bars with a yield strength of 60,000 psi cast in concrete with a compressive strength of 6000 psi: The modification factors in Eq. (4.6) are taken as 1.0. Comparing the values of ℓ_{dh} calculated using Eq. (4.6) and (4.7), it is found that the development lengths of No 8 and No. 11 hooked bars required for seismic loading according to Eq. (4.7) are 85% and 71%, respectively, of those required for *gravity loading* alone according to Eq. (4.6). Because the development lengths of hooked bars designed in accordance with Chapter 18 are shorter than those needed for gravity load by Chapter 25, the Code change presented in Section 4.3.2 is clearly warranted.

4.3.2 Proposed Changes in Chapter 18 of ACI 318-19

Based on the analysis presented in this chapter and the summary conclusions given in Section 4.3, proposed changes to Chapter 18 of ACI 318-19 are provided in this section. The original text of the Code is presented in black, while proposed code and commentary changes are shown in red underlined or ~~strikeout~~.

18.8.5 Development length of bars in tension

18.8.5.1 For bar sizes No. 3 through No. 11 terminating in a standard hook, ℓ_{dh} shall be calculated by Eq. (18.8.5.1), but ℓ_{dh} shall be at least the greater of **$8d_b$** and 6 in. for normalweight concrete and at least the greater of **$10d_b$** and 7-1/2 in. for lightweight concrete, but ℓ_{dh} shall not be less than the development length requirements of Section 25.4.3.

$$\ell_{dh} = f_y d_b / (65\lambda\sqrt{f'_c}) \quad (18.8.5.1)$$

The value of λ shall be 0.75 for concrete containing lightweight aggregate and 1.0 otherwise.

The hook shall be located within the confined core of a column or of a boundary element, with the hook bent into the joint.

R18.8.5 Development length of bars in tension

R18.8.5.1 The design provisions for the development of standard hooked bars for beam-

column joints under reversed cyclic loading Eq. (18.8.5.1) first appeared in Appendix A of ACI 318-83 Building Code, with no changes in the current ACI 318-19 provisions. Eq. (18.8.5.1), however, by itself does not provide an adequate development length in all cases, especially for larger bars.

Minimum embedment length in tension for deformed bars with standard hooks is determined using Eq. (18.8.5.1), ~~which is based on the requirements of 25.4.3~~ but not less than the requirements of 25.4.3. The embedment length of a bar with a standard hook is the distance, parallel to the bar, from the critical section (where the bar is to be developed) to a tangent drawn to the outside edge of the hook. The tangent is to be drawn perpendicular to the axis of the bar (refer to Table 25.3.1).

The requirement for the hook to project into the joint is to improve development of a diagonal compression strut across the joint. The requirement applies to beam and column bars terminated at a joint with a standard hook.

18.8.5.3 For bar sizes No. 3 through No. 11, ℓ_d , the development length in tension for a straight bar, shall be at least the greater of (a) and (b):

(a) 2.5 times the length in accordance with 18.8.5.1, ~~without the requirements of Section 25.4.3~~, if the depth of the concrete cast in one lift beneath the bar does not exceed 12 in.

(b) 3.25 times the length in accordance with 18.8.5.1, ~~without the requirements of Section 25.4.3~~, if the depth of the concrete cast in one lift beneath the bar exceeds 12 in.

R18.8.5.3 Minimum development length in tension for straight bars is a multiple of the length indicated by 18.8.5.1, ~~without the requirements of 25.4.3~~. Section 18.8.5.3(b) refers to top bars. Lack of reference to No. 14 and No. 18 bars in 18.8.5 is due to the paucity of information on anchorage of such bars subjected to load reversals simulating earthquake effects.

CHAPTER 5: SUMMARY AND CONCLUSIONS

5.1 SUMMARY

Hooked and headed reinforcing bars are commonly used as a means of shortening development length of reinforcing bars, but a limited amount of previous research has resulted in restrictions on their use in practice. This study included two phases: In the first phase, 31 tests of simulated column-foundation joints were conducted to investigate the anchorage strength and behavior of large and high-strength headed bars. The work involved 15 specimens, each with one to three simulated column-foundation joints. The main variables were distance between the anchored headed bar and the compression reaction, number of headed bars tested simultaneously (1 or 2), size of the headed bars (No. 11 or No. 14), center-to-center spacing between headed bars loaded simultaneously (3.2 or $8.2d_b$), amount of parallel tie reinforcement within the joint region (zero to six No. 4 closed stirrups), and concrete compressive strength ($5,060$ to $14,470$ psi). The embedment length of the headed bars ranged from $12\frac{5}{8}$ to 14 in. The stresses in the headed bars at failure ranged from $41,800$ to $144,400$ psi. The net bearing area of the headed bars ranged from 4.2 to $9.2A_b$. This phase also included an evaluation of tests on headed bars tested in simulated column-foundation joints by DeVries et al. (1999), Choi et al. (2002), and Ghimire et al. (2018), and on anchor bolts tested in steel column-concrete foundation joints by Worsfold et al. (2022). The test results of the current and previous studies were compared with anchorage strengths based on the descriptive equations for headed bars developed at the University of Kansas by Shao et al. (2016), the anchorage provisions in Section 17.6.2 of ACI 318-19 with a strength reduction factor equal to 1.0 , the design provisions in Section 25.4.4 of ACI 318-19, and proposed code provisions. Recommended changes to Chapters 17 and 25 of ACI 318-19 were presented.

The second phase of the study involved the analysis of test results from 24 studies that included 146 exterior beam-column joint specimens subjected to reversed cyclic loading. Key variables included embedment lengths of the hooked bars (6 to 21 in.), concrete compressive strength ($3,140$ to $13,700$ psi), center-to-center spacing between the hooked bars (1.75 to 6.5 in.), bar size (No. 3 to No. 9), and confining reinforcement within the joint region parallel to the straight portion of the hooked bars (none to nine hoops spaced at 1.25 to 6.0 in.). The yield strength of the hooked bars ranged from $42,900$ to $103,000$ psi. Concrete side cover ranged from 0.7 to 8.6 in.

Column axial compressive load applied during the test ranged from zero to $0.25A_gf'_c$, where A_g is the column cross-sectional area (in.²) and f'_c is the nominal concrete compressive strength (psi). The data from these tests are analyzed using the equations developed by Ajaam et al. (2017) at the University of Kansas for beam-column joints tested under monotonic loading to investigate the applicability of the equations to predict the anchorage strength of hooked bars anchored in members subjected to reversed cyclic loading. This analysis is used, in turn, to propose a change in Section 18.8.5.1 of ACI 318 to require the use of Section 25.4.3 of ACI 318 to establish the minimum development length ℓ_{dh} for hooked bars anchored in joints for frames subjected to seismic loading. Proposed changes to Chapter 18 of ACI 318-19 were presented.

5.2 CONCLUSION

Based on the test results and analysis presented in this report, the following conclusions can be drawn:

1. Anchorage strength of headed bars anchored in column-foundation joints is improved by parallel tie reinforcement located on all sides of the headed bars, a contribution that is not included in the provisions of ACI 318-19.
2. Test results of simulated column-foundation joint specimens tested under monotonic loading show that the distance between the headed bar and the compression reaction (nearest support reaction), with a test range of up to 2.79 times the embedment length, has no effect on the anchorage strength. The anchorage strength of headed bars decreased, however, for the two specimens in which the distance between the headed bar and compression reaction equaled 5.3 and 5.6 times the embedment length.
3. Similar to observations for beam-column joints, the anchorage strength of headed bars anchored in simulated column-foundation joints decreases as the center-to-center spacing decreases below $8d_b$.
4. The descriptive equations developed based on tests of beam-column joints are suitable for predicting the anchorage strength of headed bars anchored in column-foundation joints.
5. The anchorage strength of headed bars with net bearing areas of 2.6 to $3.2A_b$ tested under monotonic loading is lower than that of the headed bars with a minimum net bearing area

of $4A_b$. Results from a single specimen tested under reversed cyclic loading with anchor bolts having a net head bearing area of $1.5A_b$, however, gave a similar strength to headed bars with bearing areas above $4A_b$.

6. The anchorage provisions in Chapter 17 of ACI 318-19 do not accurately predict the anchorage strength of headed bars tested when parallel tie/anchor reinforcement is used because the anchorage provisions account for the contribution of concrete and parallel tie reinforcement (anchor reinforcement) separately, with only the stronger of the two controlling the strength. Therefore, the ACI 318 Code should consider including provisions that combine the contributions of concrete strength and parallel tie reinforcement.
7. The descriptive equations developed by Shao et al. (2016) accurately capture the effect of parallel tie reinforcement and the contribution of concrete strength to the anchorage strength of headed bars in column-foundation joints. Therefore, a version of the descriptive equations could be used within the anchorage provisions in Chapter 17 of the ACI 318 Code.
8. The design provisions in Chapter 25 of ACI 318-19 should be further modified to accurately represent the effect of parallel tie reinforcement in connections other than beam-column joints.
9. The proposed Code provisions accurately capture the effect of parallel tie reinforcement on the anchorage strength of headed bars. Therefore, ACI 318-19 Code should consider including the proposed Code provisions in the next version.
10. The descriptive equations developed by Ajaam et al. (2017) for the anchorage strength of hooked bars in beam-column joints tested under monotonic loading, which serve as the basis for the development length provisions for hooked bars in ACI 318-19, are suitable for predicting the anchorage strength of hooked bars anchored in members subjected to reversed cyclic loading.
11. The current code provisions for the development length of hooked bars in tension under reversed cyclic loading in earthquake resistant structures (Section 18.8.5.1 of ACI 318-19) were derived directly from the development length provisions for non-seismic loading (Section 25.4.3.1) that existed in ACI 318 Building Codes before 2019. Even though the

development length provisions for monotonic loading (Section 25.4.3.1) were modified in the 2019 Code, the code design provisions for the development length of hooked bars in tension under cyclic loading did not change. This has resulted in provisions allowing development lengths for hooked bars designed in accordance with Chapter 18 to be *shorter* than those needed for gravity load by Chapter 25. Changes in Chapter 18 of ACI 318-19 are proposed that require the use of Section 25.4.3 of ACI 318 to establish the minimum development length ℓ_{dh} for hooked bars anchored in members subjected to seismic loading.

12. The test results of exterior beam-column joint specimens tested under reversed cyclic loading show that the distance between the hooked bars and compression reaction (compression region of the beam), with a test range of up to 3.0 times the embedment length, had no effect on the anchorage strength.

5.3 FUTURE WORK

In the current investigation, a maximum of two headed bars were tested simultaneously in simulated column-foundation joints. It is suggested that additional tests be conducted on groups of three or four headed bars loaded simultaneously.

The maximum bar size of headed bars evaluated in the current study is No. 14. There is interest, however, in using larger No. 18 headed bars. Therefore, it is recommended that tests be performed to investigate the anchorage strength of No. 18 headed bars in simulated column-foundation joints without and with parallel tie reinforcement.

In the current and previous studies, headed bars were investigated in normalweight concrete; there is no information regarding headed bars tested in lightweight concrete. As a result, the development length provisions of ACI 318-19 are only permitted for use with headed bars in normalweight concrete. To understand headed bar anchorage behavior and permit their use in lightweight concrete, tests are recommended.

REFERENCES

ACI Committee 318, 1983, *Building Code Requirements for Structural Concrete (ACI 318-83) and Commentary (ACI 318R-83)*, American Concrete Institute, Farmington Hills, Michigan, 111 pp.

ACI Committee 318, 1999, *Building Code Requirements for Structural Concrete (ACI 318-99) and Commentary (ACI 318R-99)*, American Concrete Institute, Farmington Hills, Michigan, 369 pp.

ACI Committee 318, 2002, *Building Code Requirements for Structural Concrete (ACI 318-02) and Commentary (ACI 318R-02)*, American Concrete Institute, Farmington Hills, Michigan, 443 pp.

ACI Committee 318, 2005, *Building Code Requirements for Structural Concrete (ACI 318-05) and Commentary (ACI 318R-05)*, American Concrete Institute, Farmington Hills, Michigan, 430 pp.

ACI Committee 318, 2008, *Building Code Requirements for Structural Concrete (ACI 318-08) and Commentary (ACI 318R-08)*, American Concrete Institute, Farmington Hills, Michigan, 465 pp.

ACI Committee 318, 2011, *Building Code Requirements for Structural Concrete (ACI 318-11) and Commentary (ACI 318R-11)*, American Concrete Institute, Farmington Hills, Michigan, 503 pp.

ACI Committee 318, 2014, *Building Code Requirements for Structural Concrete (ACI 318-14) and Commentary (ACI 318R-14)*, American Concrete Institute, Farmington Hills, Michigan, 520 pp.

ACI Committee 318, 2019, *Building Code Requirements for Structural Concrete (ACI 318-19) and Commentary (ACI 318R-19)*, American Concrete Institute, Farmington Hills, Michigan, 624 pp.

ACI Committee 352, 2002, *Recommendation for Design of Beam-Column Connections in Monolithic Reinforced Concrete Structures (ACI 352R-02, reapproved 2010)*, American Concrete Institute, Farmington Hills, Michigan, 38 pp.

ACI Committee 349, 2006, *Code Requirements for Nuclear Safety Related Concrete Structures (ACI 349-06)*, American Concrete Institute, Farmington Hills, Michigan, 157 pp.

ACI Committee 408, 2003, *Bond and Development of Straight Reinforcement in Tension (ACI 408R-03)*, American Concrete Institute, Farmington Hills, Michigan, 49 pp.

Ajaam, A., Darwin, D., and O'Reilly, M., 2017, "Anchorage Strength Reinforcing Bars with Standard Hooks," *SM Report No. 125*, University of Kansas Center for Research, Inc., Lawrence, Kansas, Apr., 346 pp.

Ajaam, A., Yasso, S., Darwin, D., O'Reilly, M., and Sperry, J., 2018, "Anchorage Strength of Closely Spaced Hooked Bars," *ACI Structural Journal*, Vol. 115, No. 4, July, pp. 1143-1152

ASTM A615, 2016, *Standard Specification for Deformed and Plain Carbon-Steel Bars for Concrete Reinforcement (ASTM A615/A615M-16)*, ASTM International, West Conshohocken, PA, 8 pp.

ASTM A615, 2020, *Standard Specification for Deformed and Plain Carbon-Steel Bars for Concrete Reinforcement (ASTM A615/A615M-20)*, ASTM International, West Conshohocken, PA, 8 pp.

ASTM A706, 2016, *Standard Specification for Deformed and Plain Low-Alloy Steel Bars for Concrete Reinforcement (ASTM A706/A706M-16)*, ASTM International, West Conshohocken, PA, 7 pp.

ASTM A970, 2016, *Standard Specification for Headed Steel Bars for Concrete Reinforcement (ASTM A970/A970M-16)*, ASTM International, West Conshohocken, PA, 9 pp.

ASTM A970, 2017, *Standard Specification for Headed Steel Bars for Concrete Reinforcement (ASTM A970/A970M-17)*, ASTM International, West Conshohocken, PA, 9 pp.

ASTM A1035, 2015, *Standard Specification for Deformed and Plain, Low-Carbon, Chromium, Steel Bars for Concrete Reinforcement (ASTM A1035/A1035M-15)*, ASTM International, West Conshohocken, PA, 7 pp.

Bashandy, T. R., 1996, "Application of Headed Bars in Concrete Members," *Ph.D. dissertation*, University of Texas at Austin, Austin, TX, Dec., 303 pp.

Choi, D.-U., Hong, S.-G., and Lee, C.-Y., 2002, "Test of Headed Reinforcement in Pullout," *KCI Concrete Journal*, Vol. 14, No. 3, Sep., pp. 102-110.

Choi, D.-U., 2006, "Test of Headed Reinforcement in Pullout II: Deep Embedment," *International Journal of Concrete Structures and Materials*, Vol. 18, No. 3E, Aug., pp. 151-159.

Choi, C., and Bae, B., 2019, "Effectiveness of Steel Fiber as Hoops in Exterior Beam-to-Column Joints under Cyclic Loading," *ACI Structural Journal*, Vol. 116, No. 2, Mar., pp. 205-220.

Chutarat, N., and Aboutaha, R., 2003, "Cyclic Response of Exterior Reinforced Concrete Beam-Column Joints Reinforced with Headed Bars Experimental Investigation," *ACI Structural Journal*, Vol. 100, No. 2, Mar.-Apr., pp. 259-264.

Chun, S., Lee, S., Kang, T., Oh, B., and Wallace, J., 2007, "Mechanical Anchorage in Exterior Beam-Column Joints Subjected to Cyclic Loading," *ACI Structural Journal*, Vol. 104, No. 1, Jan.-Feb., pp. 102-112.

Chun, S. C., Oh, B., Lee, S. H., and Naito, C. J., 2009, "Anchorage Strength and Behavior of Headed Bars in Exterior Beam-Column Joints," *ACI Structural Journal*, Vol. 106, No. 5, Sep.-Oct., pp. 579-590.

Chun, S., and Shin, Y., 2014, "Cyclic Testing of Exterior Beam-Column Joints with Varying Joint Aspect Ratio," *ACI Structural Journal*, Vol. 111, No. 3, May-June, pp. 693-704.

Craig, R., Mahadev, S., Patel, C., Viteri, M., and Kertesz, C., 1984, "Behavior of Joints Using Reinforced Fibrous Concrete," Fiber Reinforced Concrete, SP 81, *American Concrete Institute*, Detroit, MI, pp. 125-167.

Darwin, D., and Dolan, C. W., 2021, *Design of Concrete Structures*, 16th ed., McGraw-Hill, New York, 880 pp.

DeVries, R. A., 1996, "Anchorage of Headed Reinforcement in Concrete," *PhD Dissertation*, The University of Texas at Austin, Austin, Texas, Dec., 314 pp.

DeVries, R. A., Jirsa, J. O., and Bashandy, T., 1999, "Anchorage Capacity in Concrete of Headed Reinforcement with Shallow Embedments," *ACI Structural Journal*, Vol. 96, No. 5, Sep.-Oct., pp. 728-736.

Ehsani, M., and Alameddine, F., 1991, "Design Recommendations for Type 2 High-Strength Reinforced Concrete Connections," *ACI Structural Journal*, Vol. 88, No. 3, May-June, pp. 227-291.

Ehsani, M., and Wight, J., 1982, "Behavior of External Reinforced Concrete Beam to Column Connections Subjected to Earthquake Type Loading," *Report No. NSF/CEE-82099*, University of Michigan, Department of Civil Engineering, Ann Arbor, MI, July, 270 pp.

Ehsani, M., Moussa, A., and Vallenilla, C., 1987, "Comparison of Inelastic Behavior of Reinforced Ordinary- and High-Strength Concrete Frames," *ACI Structural Journal*, Vol. 84, No. 2, Mar.-Apr., pp. 161-169.

Eligehausen, R., Mällée, R., and Silva, J., 2006b, "*Anchorage in Concrete Construction*," Ernst & Sohn (J. T. Wiley), Berlin, Germany, May, 380 pp.

Fishburn, C. D., 1947, (iley), Berlid Slip Under Load of Bent-Bar Anchorages and Straight Embedments in Haydite Concrete, *ACI Journal*, Proceedings Vol. 44, Dec., pp. 289-305.

Fuchs, W., Eligehausen, R., and Breen, J. E., 1995, "Concrete Capacity Design (CCD) Approach for Fastening to Concrete," *ACI Structural Journal*, Vol. 92, No. 1, Jan.-Feb., pp. 73-94.

Fujii, S., and Morita, S., 1991, "Comparison Between Interior and Exterior RC Beam-Column Joint Behavior," Design of Beam-Column Joints for Seismic Resistance, SP 123-6, *American Concrete Institute*, Detroit, MI, pp. 145-165.

- Ghimire, K., Darwin, D., and O'Reilly, M., 2018, "Anchorage of Headed Reinforcing Bars in Concrete," *SM Report* No. 127, University of Kansas Center for Research, Inc., Lawrence, KS, Jan., 278 pp.
- Ghimire, K., Shao, Y., Darwin, D., and O'Reilly, M., 2019a, "Conventional and High-Strength Headed Bars—Part 1: Anchorage Tests," *ACI Structural Journal*, Vol. 116, No. 3, May, pp. 255-264.
- Ghimire, K., Shao, Y., Darwin, D., and O'Reilly, M., 2019b, "Conventional and High-Strength Headed Bars—Part 2: Data Analysis," *ACI Structural Journal*, Vol. 116, No. 3, May, pp. 265-272.
- Ghimire, K. P., Darwin, D., and Lepage, A., 2021, "Headed Bars in Beam-Column Joints Subjected to Reversed Cyclic Loading," *ACI Structural Journal*, Vol. 118, No. 3, May, pp. 27-33.
- Hamad, B., Jirsa, J., and D'Abreu de Paulo, N., 1993, "Anchorage Strength of Epoxy-Coated Hooked Bars," *ACI Structural Journal*, Vol. 90, No. 2, Mar.-Apr., pp. 210-217.
- Hanson, N., and Connor, H., 1967, "Seismic Resistance of Reinforced Concrete Beam-Column Joints," *Journal of the Structural Division*, Vol. 93, ST 5, Oct., pp. 535-560.
- Hanson, N., 1971, "Seismic Resistance of Concrete frames with grade 60 reinforcement," *Journal of the Structural Division*, ASCE, Vol. 97, ST6, June, pp. 1685-1700.
- Hribar, J. A. and Vasko, R. C., 1969, "End Anchorage of High Strength Steel Reinforcing Bars," *ACI Journal*, Proceedings Vol. 66, Nov., pp. 875-883.
- Hwang, H., Park, H., Choi, W., Chung, L., and Kim, J., 2014, "Cyclic Loading Test for Beam-Column Connections with 600 MPa (87 ksi) Beam Flexural Reinforcing Bars," *ACI Structural Journal*, Vol. 111, No. 4, July-Aug., pp. 913-924.
- Hwang, S., Lee, H., Liao, T., Wang, K., and Tsai, H., 2005, "Role of Hoops on Shear Strength of Reinforced Concrete Beam-Column Joints," *ACI Structural Journal*, Vol. 102, No. 3, May-June, pp. 445-453.
- Kanada, K., Kondo, G., Fujii, S., and Morita, S., 1984, "Relation Between Beam Bar Anchorage and Shear Resistance at Exterior Beam-Column Joints," *Transactions of the Japan Concrete Institute*, V. 6, pp. 433-440.
- Kaku, T., and Asakusa, H., 1991, "Ductility Estimation of Exterior Beam-Column Subassemblies in Reinforced Concrete Frames," Design of Beam-Column Joints for Seismic Resistance, SP 123-7, *American Concrete Institute*, Detroit, MI, pp. 167-185.
- Kang, T., Ha, S., and Choi, D., 2010, "Bar Pullout Tests and Seismic Tests of Small-Headed Bars in Beam-Column Joints," *ACI Structural Journal*, Vol. 107, No. 1, Jan.-Feb., pp. 32-42.

Lee, H., and Ko, J., 2007 “Eccentric Reinforced Concrete Beam-Column Connections Subjected to Cyclic Loading in Principal Directions,” *ACI Structural Journal*, Vol. 104, No. 4, July-Aug., pp. 459-467.

Lee, D. N., Wight, J. K., and Hanson, R. D., 1976, “Original and Repaired Reinforced Concrete Beam-Column Subassemblages Subjected to Earthquake Type Loading,” *Report No. UMEE 76S4*, University of Michigan, Department of Civil Engineering, Ann Arbor, MI, Apr., 206 pp.

Lee, D. N., Wight, J. K., and Hanson, R. D., 1976, “RC Beam-Column Joints Under Large Load Reversals,” *Journal of the Structural Division*, Vol. 103, ST12, Oct., pp. 2337-2350.

Marques, J. L., and Jirsa, J. O., 1975, “A Study of Hooked Bar Anchorages in Beam-Column Joints,” *ACI Journal*, Proceedings Vol. 72, No. 5, May-Jun., pp. 198-209.

Megget, L., 1974, “Cyclic Behavior of Exterior Reinforced Concrete Beam-Column Joints,” *Bulletin of the New Zealand National Society for Earthquake Engineering*, Vol. 7, No. 1, Mar., pp. 27-47.

McMackin, P. J., Slutter, R. G., and Fisher, J. W., 1973, “Headed Steel Anchor under Combined Loading,” *AISC Engineering Journal*, Vol. 10, No. 2, Apr.-Jun., pp. 43-52.

Minor, J. and Jirsa, J., 1975, “Behavior of Bent Bar Anchorages,” *ACI Journal*, Proceedings Vol. 72, No. 4, Apr., pp. 141-149.

Nilforoush, R., Nilsson, M., and Elfgren, L., 2017, “Experimental Evaluation of Tensile Behaviour of Single Cast-in-Place Anchor Bolts in Plain and Steel Fibre-Reinforced Normal- and High-Strength Concrete,” *Engineering Structures*, Vol. 147, pp. 195-206.

Pantelides, C., Clyde, C., and Reaveley, L., 2002, “Performance-Based Evaluation of Reinforced Concrete Building Exterior Joints for Seismic Excitation,” *Earthquake Engineering Research Institute, Earthquake Spectra*, Vol. 18, No. 3, Aug., pp. 449-480.

Paulay, T., and Scarpas, A., 1981, “The Behavior of Exterior Beam-Column Joints,” *Bulletin of the New Zealand National Society for Earthquake Engineering*, Vol. 14, No. 3, Sep., pp. 131-144.

Ramirez, J. and Russell, B., 2008, “Transfer, Development, and Splice Length for Strand/reinforcement in High-strength Concrete,” *Transportation Research Board, National Research Council*, Washington, D.C., 99-120 pp.

Soroushian, P., Obaseki, K., Nagi, M., and Rojas, M., 1988, “Seismic Excitation in Exterior Beam-Column Connections,” *ACI Structural Journal*, Vol. 85, No. 3, May-Jun., pp. 269-276.

Shao, Y., Darwin, D., O'Reilly, M., Lequesne, R. D., Ghimire, K., and Hano, M., 2016, “Anchorage of Conventional and High-Strength Headed Reinforcing Bars,” *SM Report No. 117*, University of Kansas Center for Research, Inc., Lawrence, KS, Aug., 334 pp.

Sperry, J., Al-Yasso, S., Searle, N., DeRubeis, M., Darwin, D., O'Reilly, M., Matamoros, A., Feldman, L., Lepage, A., Lequesne, R., and Ajaam, A., 2015a, "Anchorage of High-Strength Reinforcing Bars with Standard Hooks," *SM Report* No. 111, University of Kansas Center for Research, Inc., Lawrence, Kansas, June, 243 pp.

Sperry, J., Darwin, D., O'Reilly, M., and Lequesne, R., 2015b, "Anchorage Strength of Conventional and High-Strength Hooked Bars in Concrete," *SM Report* No. 115, University of Kansas Center for Research, Inc., Lawrence, Kansas, Dec., 266 pp.

Sperry, J., Yasso, S., Searle, N., DeRubeis, M., Darwin, D., O'Reilly, M., Matamoros, A., Feldman, L., Lepage, A., Lequesne, R., and Ajaam, A., 2017a, "Conventional and High-Strength Hooked Bars—Part 1: Anchorage Tests," *ACI Structural Journal*, Vol. 114, No. 1, Jan.-Feb., pp. 255-265.

Sperry, J., Darwin, D., O'Reilly, M., Lequesne, R., Yasso, S., Matamoros, A., Feldman, L., and Lepage, A., 2017b, "Conventional and High-Strength Hooked Bars—Part 2: Data Analysis," *ACI Structural Journal*, Vol. 114, No. 1, Jan.-Feb., pp. 267-276.

Sperry, J., Darwin, D., O'Reilly, M., Lepage, A., Lequesne, R., Matamoros, A., Feldman, L., Yasso, S., Searle, N., DeRubeis, M., and Ajaam, A., 2018, "Conventional and High-Strength Steel Hooked Bars: Detailing Effects," *ACI Structural Journal*, Vol. 115, No. 1, Jan., pp. 247-257.

Stoker, J. R., Boulware, R. L., Crozier, W. F., and Swirsky, R. A., 1974, "Anchorage Devices for Large Diameter Reinforcing Bars," *Report* No. CA-DOT-TL-6626-1-73-30, Transportation Laboratory, California Division of Highways, Sacramento, California, Sep., 63 pp.

Scribner, C. F., 1978, "Delaying Shear Strength Decay in Reinforced Concrete Flexural Members under Large Load Reversals," *Report* No. UME 78R2, University of Michigan, Department of Civil Engineering, Ann Arbor, MI, May, 221 pp.

Tsonos, A., Tegos, I., and Penelis, G., 1992, "Seismic Resistance of Type 2 Exterior Beam-Column Joints Reinforced with Inclined Bars," *ACI Structural Journal*, Vol. 89, No. 1, Jan.-Feb., pp. 3-12.

Tsonos, A., 2007, "Cyclic Load Behavior of Reinforced Concrete Beam-Column Subassemblages of Modern Structures," *ACI Structural Journal*, Vol. 104, No. 4, July-Aug., pp. 468-478.

Uzumeri, S., 1977, "Strength and Ductility of Cast-In-Place Beam-Column Joints," *Reinforced Concrete Structures in Seismic Zones*, SP 53-12, American Concrete Institute, Farmington Hills, MI, pp. 293-350.

Viest, I. M., 1956, "Investigation of Stud Shear Connectors for Composite Concrete and Steel T-Beams," *Journal of American Concrete Institute*, Vol. 27, No. 8, Apr., pp. 875-892.

Yasso, S., Darwin, D., and O'Reilly, M., 2017, "Anchorage Strength of Standard Hooked Bars in Simulated Exterior Beam-Column Joints," *SM Report* No. 124, University of Kansas Center for Research, Inc., Lawrence, Kansas, Apr., 307 pp.

Yasso, S., Darwin, D., and O'Reilly, M. O., 2021, "Effects of Concrete Tail Cover and Tail Kickout on Anchorage Strength of 90-Degree Hooks," *ACI Structural Journal*, Vol. 118, No. 6, Nov. 2021, pp. 227-236 .

Zerbe, H., and Durrani, A., 1985, "Effect of a Slab on The Behavior of Exterior Beam to Column Connections," *Report* No. 30, Department of Civil Engineering, Rice University, Houston, Texas, Mar., 159 pp.

Zuo, J., and Darwin, D., 1998, "Bond Strength of High Relative Rib Area Reinforcing Bars," *SM Report* No. 46, University of Kansas Center for Research, Inc., Lawrence, Kansas, Jan., 350 pp.

APPENDIX A: NOTATION

A_b	Cross-sectional area of an individual headed or hooked deformed bar
A_{brg}	Net bearing area of the head of headed deformed bar calculated as the gross head area minus the bar area if there is no obstruction. However, the net bearing area of the head is calculated as the gross head area minus the maximum area of the obstruction adjacent to the head if there is an obstruction
A_g	Gross cross-sectional area of column in exterior beam-column joint
A_{hs}	Total cross-sectional area of headed or hooked deformed bars being developed (nA_b)
A_j	Effective cross-sectional area within the beam-column joint in a plane parallel to the hooked bars (Section 4.2.2)
A_{Nc}	Projected concrete failure area of group of headed bars
A_{Nco}	Projected concrete failure area of a single headed bar ($9\ell_{eh}^2$)
A_{st}	Total cross-sectional area of reinforcement perpendicular to the headed bar within a $1.5\ell_{eh}$ radial distance from the center of the bar
A_{tr}	Cross-sectional area of a single leg of confining reinforcement (or anchor reinforcement) parallel to the headed or hooked bar within the joint region
A_{tt}	Total cross-sectional area of all confining reinforcement parallel to headed bars being developed and located within $8d_b$ of the top or bottom of the test bars for No. 3 through No. 8 hooked bars or within $10d_b$ for No. 9 through No. 11 hooked bars
A_{th}	Total cross-sectional area of all confining reinforcement parallel to hooked bars being developed and located within $8d_b$ of the top or bottom of the test bars for No. 3 through No. 8 hooked bars or within $10d_b$ for No. 9 through No. 11 hooked bars
A_v	Total cross-sectional area of confining reinforcement parallel to the hooked bar ($N_{total} A_{tr,i}$) assumed to serve as a single tie (Section 4.2.2.3)
b_b	Width of beam in exterior beam-column joints
b_c	Width of column in exterior beam-column joints
b_j	Effective width of beam-column joint perpendicular to the hooked bars in tension calculated based on Section 15.4.2.4 of ACI 318-14
$b_{j,ACI 352}$	Effective width of beam-column joint perpendicular to the hooked bars in tension calculated based on Section 4.3.1 of ACI 352R-02
c_{a1}	Minimum distance from the center of the headed bar to the edge of concrete
c_{a2}	Minimum distance from the center of the headed bar to the edge of concrete in the direction perpendicular to c_{a1}
c_{bc}	Clear cover measured from the back of the head to the back of the member
c_{ch}	Center-to-center spacing between adjacent headed or hooked bars
c_{so}	Clear cover measured from the headed or hooked bar to the nearest free concrete face of the member within the anchorage region

d	Distance from the centroid of the tension bar to the extreme compression fiber of the beam in exterior joints; diameter of the head (Table 2.3)
d'	Distance from the centroid of the compression bar to the extreme compression fiber of the beam in exterior joints
d_b	Nominal diameter of the headed or hooked bar
f'_c	Specified compressive strength of concrete
f_{cm}	Measured compressive strength of concrete
f_{su}	Stress in the headed bar at failure
f_y	Measured yield strength of the headed or hooked bar
$f_{ytr,l}$	Measured yield strength of confining reinforcement (hoops) parallel to the headed or hooked bar within the joint region
h_b	Depth of beam in exterior beam-column joints
h_c	Depth of column in exterior beam-column joints
h_{cl}	Distance between the center of headed bar to the inner face of the nearest support plate (Figures 1.34 and 3.8)
h_{ef}	Embedment length of the anchor (Sections 1.4 and 1.7.1)
k_c	Coefficient for concrete breakout strength in tension
ℓ_{dh}	Development length in tension of deformed bar or deformed wire with a standard hook, measured from outside end of hook, point of tangency, toward critical section
ℓ_{dt}	Development length in tension of headed deformed bar, measured from the critical section to the bearing face of the head
ℓ_{eh}	Embedment length measured from the critical section to the bearing face of the head; Embedment length measured from the critical section to the back of the hook
ℓ_{ehy}	Embedment length required to yield the hooked bars calculated using the descriptive equations, Eq. (4.1) and (4.2)
M_{peak}	Peak moment at critical section of hooked bars in beam-column joints subjected to reversed cyclic loading
M_n	Nominal flexural strength of beam in exterior beam-column joints
n	Number of headed bars loaded simultaneously in tension; number of hooked bars at the tension face of the beam in exterior beam-column joints
N	Number of legs of effective confining reinforcement A_{tt} or A_{th} in the joint region
N_{ar}	Nominal anchorage strength of a single headed bar based on anchor reinforcement
N_{arg}	Nominal anchorage strength of a group of headed bars based on anchor reinforcement
N_b	Basic concrete breakout strength of a single headed bar in tension
N_{cb}	Nominal concrete breakout strength of a single headed bar in tension
N_{cbg}	Nominal concrete breakout strength of a group of headed bars in tension
N_{sb}	Nominal side-face blowout strength of a single headed bar in tension
N_{sbg}	Nominal side-face blowout strength of a group of headed bars in tension

N_{total}	Total number of legs of confining reinforcement within a beam-column joint
N_{tr}	Total number of legs of anchor reinforcement parallel to the headed bars within $0.5\ell_{eh}$ radial distance from the center of the bar
p	Probability value from student t-test
s	Center-to-center spacing between adjacent headed bars
s_{tr}	Center-to-center spacing of confining reinforcement (hoops) within the joint region
T	Test failure load on a headed bar
T'	Estimated test failure load on a hooked bar in beam-column joints subjected to reversed cyclic loading calculated using Eq. (4.4)
T'_{mod}	Modified bar force T' in beam-column joint specimens with $\ell_{eh} \geq \ell_{ehy}$ calculated using Eq. (4.5)
T_{anc}	Nominal anchorage strength of each headed bar in tension governed by concrete breakout, or anchor reinforcement, calculated using Eq. (3.9) based on anchorage design provisions in Chapter 17 of ACI 318-19
T_{ACI318}	Anchorage strength of a headed bar calculated using Eq. (3.11) based on design provisions in Chapter 25 of ACI 318-19
T_{calc}	Anchorage strength of a headed bar calculated using Eq. (3.14) based on proposed Code provisions
T_c	Anchorage strength of a headed or hooked bar without confining reinforcement in Eq. (1.2), (1.4) and (1.7); contribution of concrete to anchorage strength of a headed or hooked bar
T_h	Anchorage strength of a headed or hooked bar with confining reinforcement in Eq. (1.3), (1.5) and (1.8); anchorage strength of a headed or hooked bar calculated using descriptive equations in Sections 3.2 and 4.2.1
T_N	Normalized load on a headed bar at failure calculated using Eq. (3.1) and (3.2)
t	Thickness of the head (Tables 2.3)
V_n	Nominal joint shear strength calculated in accordance with the joint shear strength requirements of Section 18.8.4 of ACI 318-19
$V_{n,ACI352}$	Nominal joint shear strength calculated in accordance with Section 4.3 of ACI 352R-02
V_p	Peak joint shear applied at the beam-column joint
w/c	Water-to-cement ratio by weight
$\delta_{0.8peak}$	Drift ratio at drop to 80% from the peak load
ψ_{cs}	Factor used to modify development length based on confining reinforcement and bar spacing
ψ_e	Factor used to modify development length based on reinforcement coating
$\psi_{ec,N}$	Factor used to modify tensile strength of anchors based on eccentricity of applied loads
$\psi_{ed,N}$	Factor used to modify tensile strength of anchors based on proximity to edges of concrete member

$\psi_{c,N}$	Factor used to modify tensile strength of anchors based on presence or absence of cracks in concrete
$\psi_{cp,N}$	factor used to modify tensile strength of postinstalled anchors intended for use in uncracked concrete without supplementary reinforcement to account for the splitting tensile stresses due to installation
ψ_o	Factor used to modify development length based on bar location within member
ψ_p	Factor used to modify development length for headed bars based on parallel tie reinforcement
ψ_r	Factor used to modify development length for hooked bars based on confining reinforcement
θ	Strut angle in beam-column joints (Figure 4.8)
λ, λ_a	Modification factor to reflect the reduced mechanical properties of lightweight concrete relative to normalweight concrete of the same compressive strength

Acronym list

ACI	American Concrete Institute
ASTM	American Society of Testing and Materials - International
COV	Coefficient of Variation
MAX	Maximum
MIN	Minimum
SG	Specific Gravity
SN	Specimen Number
SSD	Saturated Surface Dry
STD	Standard Deviation

APPENDIX B: DETAILS OF SLAB SPECIMENS TESTED IN THE CURRENT STUDY

B.1 STRESS-STRAIN CURVES FOR HEADED BARS

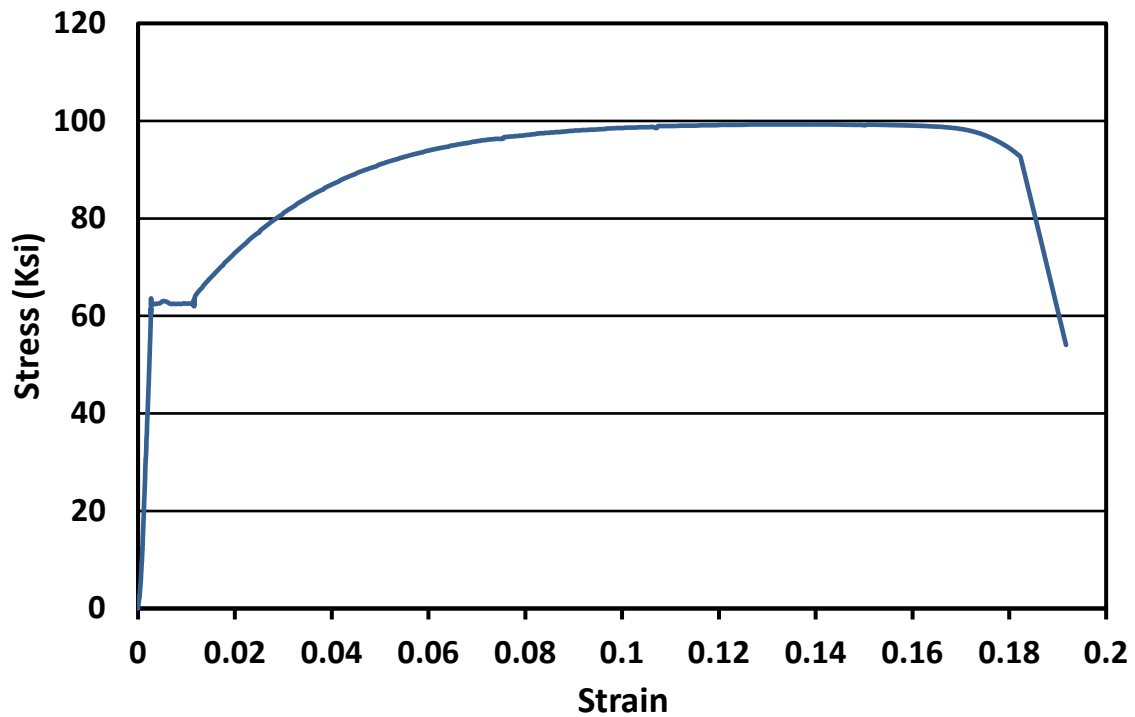


Figure B.1 Stress-strain curve for No. 4 bar (A615 steel)

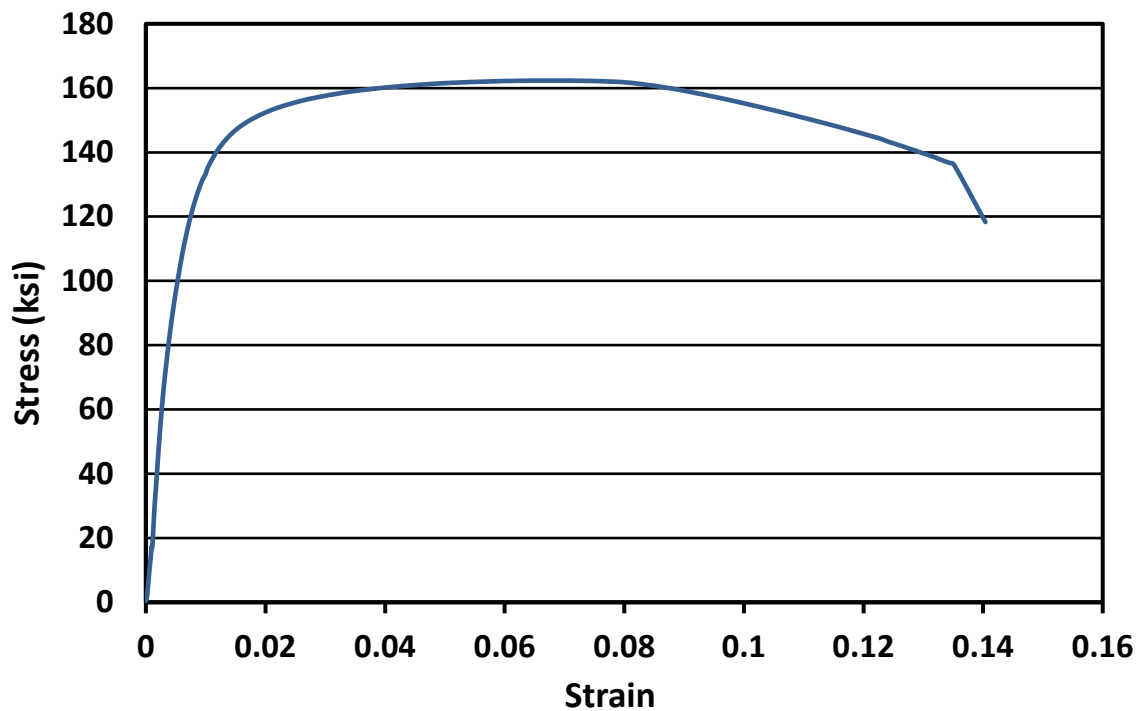


Figure B.2 Stress-strain curve for No. 11 headed bar (A1035 steel)

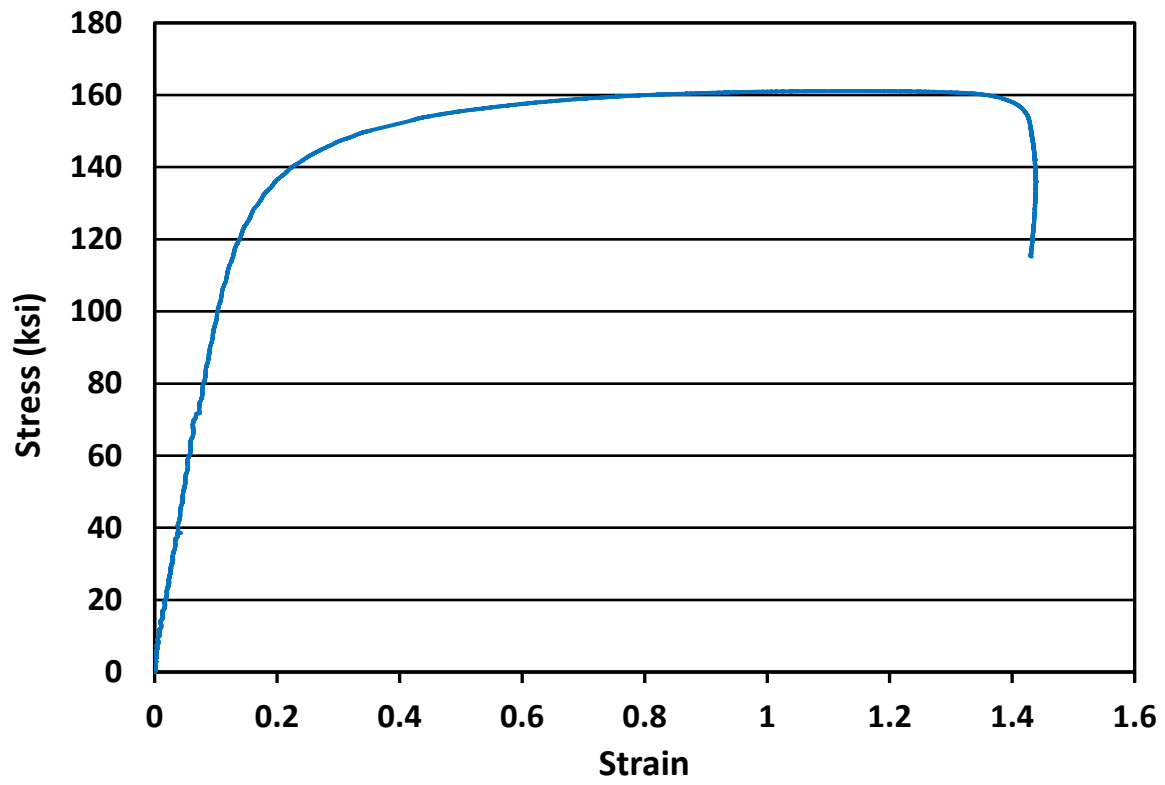


Figure B.3 Stress-strain curve for No. 14 headed bar (A1035 steel)

B.2 SCHEMATICS OF SLAB SPECIMENS

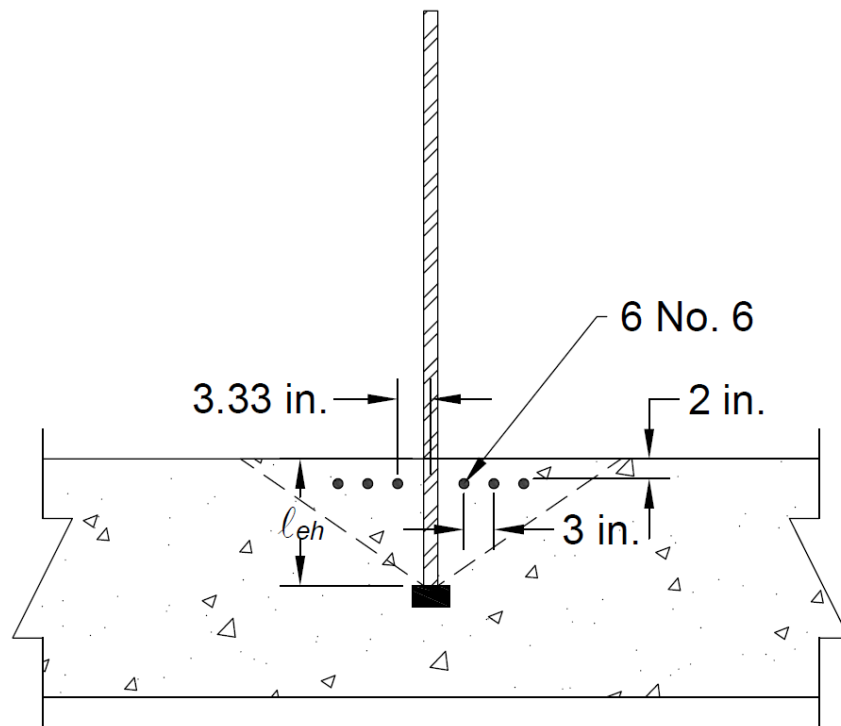


Figure B.4 Cross-section view of slab specimen 11-5-S5.5-6#6-0-12.75 with no parallel ties

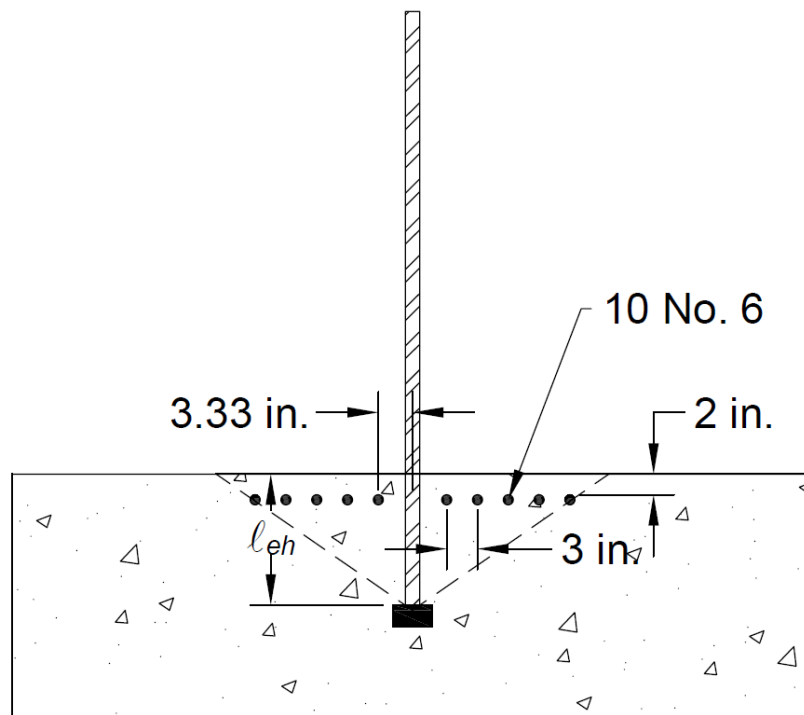


Figure B.5 Cross-section view of slab specimen 11-5-S5.5-10#6-0-12.75 with no parallel ties

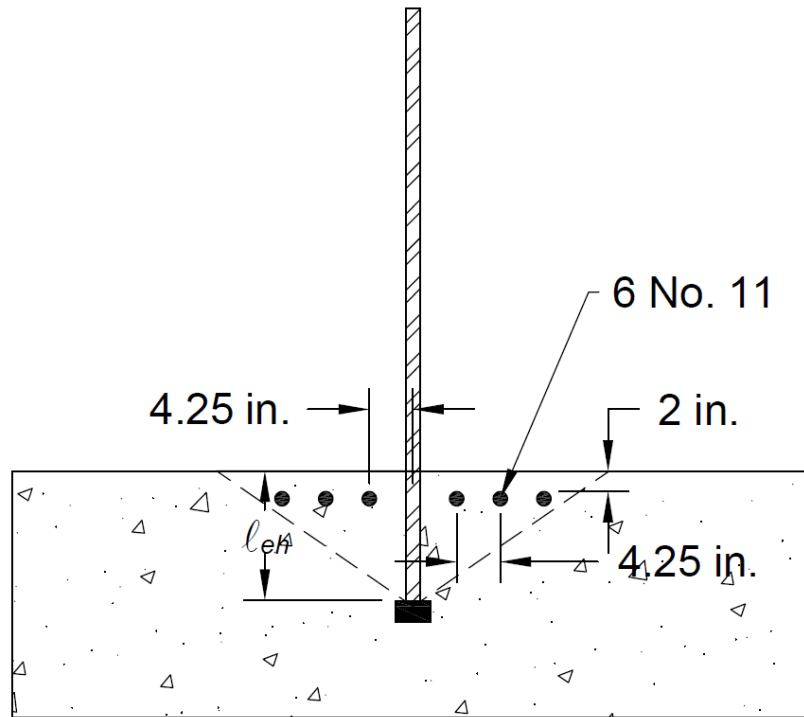


Figure B.6 Cross-section view of slab specimen 11-5-S5.5-6#11-0-12.75 with no parallel ties

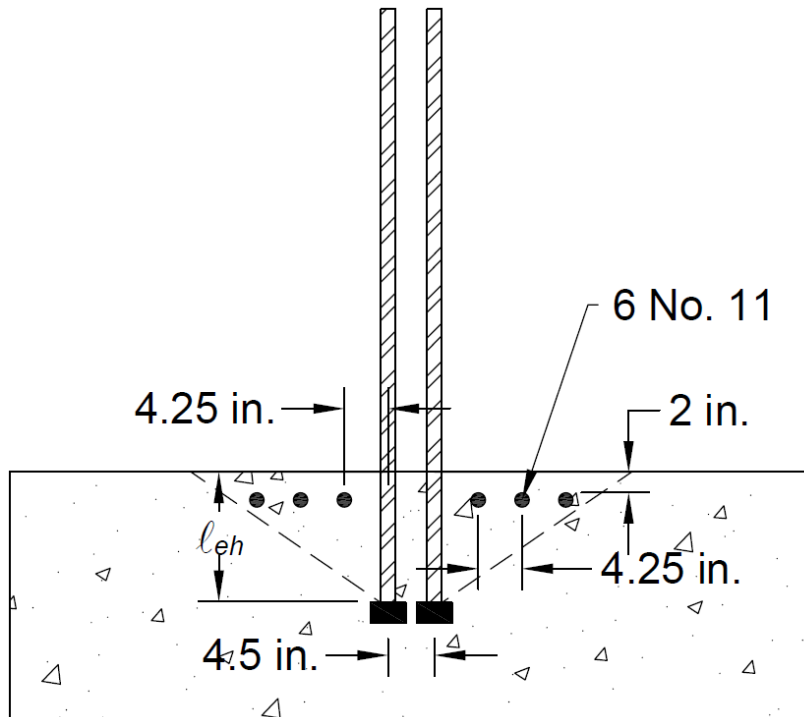


Figure B.7 Cross-section view of slab specimen (2@3.2)11-5-S5.5-6#11-0-12.75 with no parallel ties

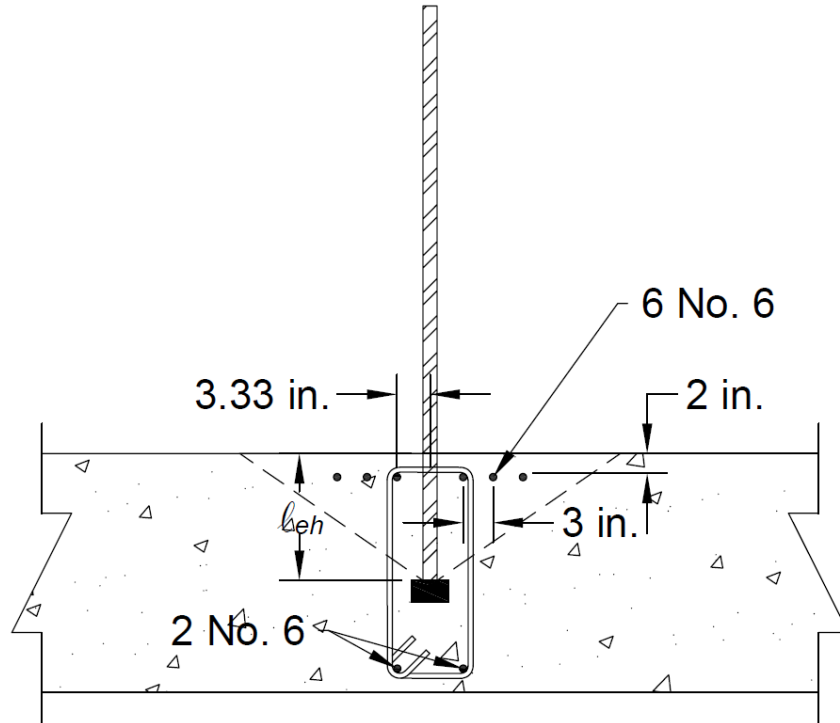


Figure B.8 Cross-section view of slab specimen 11-5-S5.5-6#6-2#4-12.75 with parallel ties

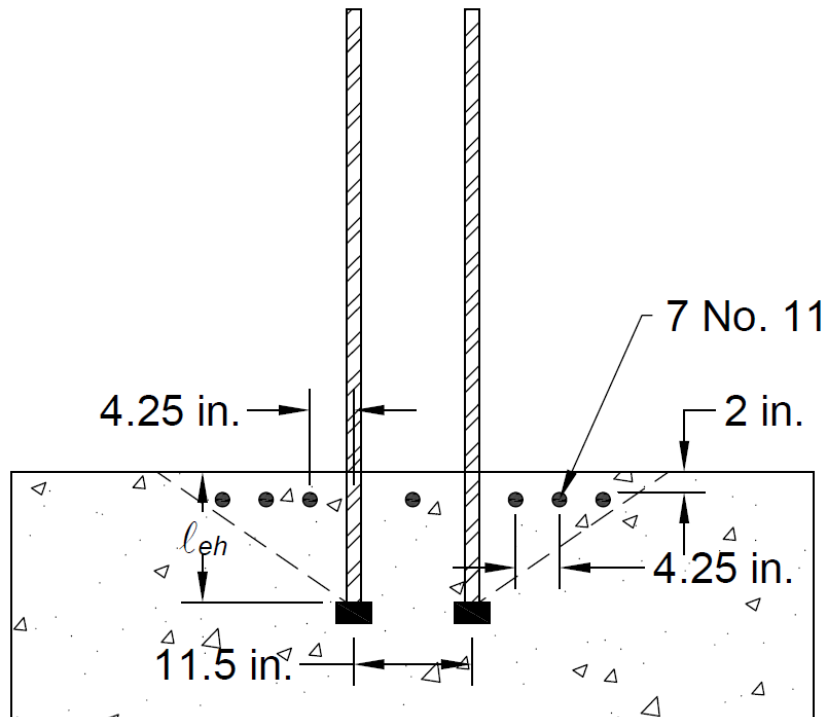


Figure B.9 Cross-section view of slab specimens (2@8.2)11-5-S5.5-7#11-0-12.75, (2@8.2)11-15-S9.2-7#11-0-12.75, (2@6.8)14-5-B4.2-7#11-0-12.75, and (2@6.8)14-15-B4.2-7#11-0-12.75 with no parallel ties

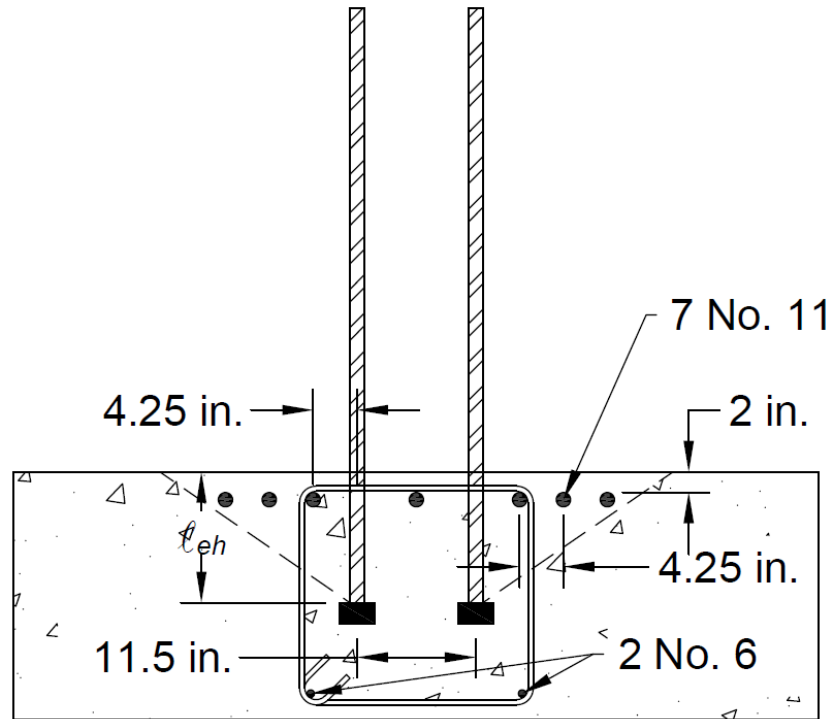


Figure B.10 Cross-section view of slab specimens (2@8.2)11-5-S9.2-7#11-3#4-12.75, (2@8.2)11-5-S9.2-7#11-6#4-12.75, (2@8.2)11-15-S9.2-7#11-3#4-12.75, (2@8.2)11-15-S9.2-7#11-6#4-12.75, (2@6.8)14-5-B4.2-7#11-3#4-12.75, (2@6.8)14-5-B4.2-7#11-6#4-12.75, (2@6.8)14-15-B4.2-7#11-3#4-12.75, and (2@6.8)14-15-B4.2-7#11-6#4-12.75 with parallel ties

B.3 TEST RESULTS AND SPECIMENS CONSTRUCTED AND TESTED IN THE CURRENT STUDY

Table B.1 Detail of slab specimens^[1]

Specimens ^[2]			Head Type ^[3]	$\frac{A_{brg}}{A_b}$	A_{st} (in. ²)	$\frac{A_{st}}{A_b}$	c_{bc} (in.)	c_{ch} ^[4] (in.)	c_{so} (in.)	ℓ_{eh} (in.)
SN	Description	Head								
1	11-5-S5.5-6#6-0-12.75	A	S5.5	5.5	2.64	1.69	7.9	38.0	18.3	13.38
	11-5-S5.5-6#6-0-12.75	B	S5.5	5.5	2.64	1.69	7.9	38.0	18.3	13.13
	11-5-S5.5-6#6-0-12.75	C	S5.5	5.5	2.64	1.69	8.1	78.0	38.3	13.38
2	11-5-S5.5-10#6-0-12.75	A	S5.5	5.5	4.40	2.82	7.9	64.5	31.5	13.38
	11-5-S5.5-10#6-0-12.75	B	S5.5	5.5	4.40	2.82	8.5	64.5	31.5	12.75
3	11-5-S5.5-6#11-0-12.75 ^[5]	A	S5.5	5.5	9.36	6.00	7.6	78.0	38.3	13.63
4	(2@3.2)11-5-S5.5-6#11-0-12.75	A1	S5.5	5.5	9.36	6.00	7.8	4.5	31.5	13.50
		A2	S5.5	5.5	9.36	6.00	7.8	4.5	31.5	13.50
	(2@3.2)11-5-S5.5-6#11-0-12.75	B1	S5.5	5.5	9.36	6.00	7.9	4.5	31.5	13.38
		B2	S5.5	5.5	9.36	6.00	7.9	4.5	31.5	13.38
5	11-5-S5.5-6#6-2#4-12.75	A	S5.5	5.5	2.64	1.69	8.3	38.0	18.3	13.00
	11-5-S5.5-6#6-2#4-12.75	B	S5.5	5.5	2.64	1.69	8.1	38.0	18.3	12.88
	11-5-S5.5-6#6-2#4-12.75	C	S5.5	5.5	2.64	1.69	8.4	78.0	38.3	13.13
6	(2@8.2)11-5-S5.5-7#11-0-12.75	A1	S5.5	5.5	10.92	7.00	7.8	11.5	32.5	13.50
		A2	S5.5	5.5	10.92	7.00	7.8	11.5	32.5	13.50
	(2@8.2)11-5-S5.5-7#11-0-12.75	B1	S5.5	5.5	10.92	7.00	7.2	11.5	32.5	14.06
		B2	S5.5	5.5	10.92	7.00	7.2	11.5	32.5	14.06
7	(2@8.2)11-5-S5.5-7#11-0-12.75	A1	S5.5	5.5	10.92	7.00	8.0	11.5	32.5	13.25
		A2	S5.5	5.5	10.92	7.00	8.0	11.5	32.5	13.25
	(2@8.2)11-5-S5.5-7#11-0-12.75	B1	S5.5	5.5	10.92	7.00	7.9	11.5	32.5	13.31
		B2	S5.5	5.5	10.92	7.00	7.9	11.5	32.5	13.31
8	(2@8.2)11-5-S9.2-7#11-3#4-12.75	A1	S9.2	9.2	10.92	7.00	7.1	11.5	32.5	13.13
		A2	S9.2	9.2	10.92	7.00	7.1	11.5	32.5	13.13
	(2@8.2)11-5-S9.2-7#11-6#4-12.75	B1	S9.2	9.2	10.92	7.00	7.3	11.5	32.5	13.00
		B2	S9.2	9.2	10.92	7.00	7.3	11.5	32.5	13.00
9	(2@8.2)11-5-S9.2-7#11-3#4-12.75	A1	S9.2	9.2	10.92	7.00	7.0	11.5	32.5	13.25
		A2	S9.2	9.2	10.92	7.00	7.0	11.5	32.5	13.25
	(2@8.2)11-5-S9.2-7#11-6#4-12.75	B1	S9.2	9.2	10.92	7.00	6.9	11.5	32.5	13.38
		B2	S9.2	9.2	10.92	7.00	6.9	11.5	32.5	13.38

^[1] Notation described in Appendix A

^[2] Multiple headed bars in a single specimen loaded individually are denoted by letters A, B, and C, and grouped headed bars loaded simultaneously are denoted with a number after a common letter (A1, A2); specimen dimensions shown in Figures 2.2 through 2.10

^[3] Details of heads provided in Section 2.1.2

^[4] c_{ch} for tests with individual headed bars is taken as twice of the minimum concrete cover to the center of the bar [that is, $c_{ch} = 2 \times (c_{so} + d_b/2)$]

^[5] Specimen contained a single centrally placed headed bar

Table B.1 Cont. Detail of slab specimens ^[1]

Specimens ^[2]			f_{cm}	f_{su}	h_{cl}	$\frac{h_{cl}}{\ell_{eh}}$	A_{tt}	$\frac{A_{tt}}{A_{hs}}$	T_{peak}	T_{total}	T
SN	Description	Head	(psi)	(psi)	(in.)		(in. ²)		(kips)	(kips)	(kips)
1	11-5-S5.5-6#6-0-12.75	A	5060	94.3	24.7	1.85	0.0	0.0	147.1	-	147.1
	11-5-S5.5-6#6-0-12.75	B		88.3	24.7	1.88	0.0	0.0	137.8	-	137.8
	11-5-S5.5-6#6-0-12.75	C		87.3	24.7	1.85	0.0	0.0	136.3	-	136.3
2	11-5-S5.5-10#6-0-12.75	A	5490	103.2	19.7	1.47	0.0	0.0	161.0	-	161.0
	11-5-S5.5-10#6-0-12.75	B		92.1	19.7	1.55	0.0	0.0	143.7	-	143.7
3	11-5-S5.5-6#11-0-12.75 ^[5]	A	5740	76.4	71.4	5.24	0.0	0.0	119.2	-	119.2
4	(2@3.2)11-5-S5.5-6#11-0-12.75	A1	5550	54.2	19.7	1.46	0.0	0.0	84.6	180.5	90.3
		A2		61.5	19.7	1.46	0.0	0.0	95.9		
	(2@3.2)11-5-S5.5-6#11-0-12.75	B1	6190	41.9	19.7	1.47	0.0	0.0	65.3	154.3	77.2
		B2		57.1	19.7	1.47	0.0	0.0	89.0		
5	11-5-S5.5-6#6-2#4-12.75	A	5810	130.6	24.7	1.90	0.8	0.51	203.7	-	203.7
	11-5-S5.5-6#6-2#4-12.75	B		141.6	24.7	1.92	0.8	0.51	220.9	-	220.9
	11-5-S5.5-6#6-2#4-12.75	C		144.4	24.7	1.88	0.8	0.51	225.2	-	225.2
6	(2@8.2)11-5-S5.5-7#11-0-12.75	A1	5370	58.5	19.7	1.46	0.0	0.0	91.3	199.0	99.5
		A2		69.0	19.7	1.46	0.0	0.0	107.7		
	(2@8.2)11-5-S5.5-7#11-0-12.75	B1		57.6	19.7	1.40	0.0	0.0	89.8	213.0	106.5
		B2		79.0	19.7	1.40	0.0	0.0	123.2		
7	(2@8.2)11-5-S5.5-7#11-0-12.75	A1	5110	54.3	19.7	1.49	0.0	0.0	84.7	176.2	88.1
		A2		58.7	19.7	1.49	0.0	0.0	91.5		
	(2@8.2)11-5-S5.5-7#11-0-12.75	B1		60.1	19.7	1.48	0.0	0.0	93.7	175.3	87.7
		B2		52.3	19.7	1.48	0.0	0.0	81.6		
8	(2@8.2)11-5-S9.2-7#11-3#4-12.75	A1	7950	83.6	19.7	1.50	0.8	0.26	130.4	267.0	133.5
		A2		87.5	19.7	1.50	0.8	0.26	136.5		
	(2@8.2)11-5-S9.2-7#11-6#4-12.75	B1		122.1	19.7	1.52	1.6	0.51	190.4	370.0	185.0
		B2		115.1	19.7	1.52	1.6	0.51	179.6		
9	(2@8.2)11-5-S9.2-7#11-3#4-12.75	A1	7680	88.8	19.7	1.49	0.8	0.26	138.6	281.3	140.7
		A2		91.5	19.7	1.49	0.8	0.26	142.7		
	(2@8.2)11-5-S9.2-7#11-6#4-12.75	B1		114.9	19.7	1.47	1.6	0.51	179.3	354.2	177.1
		B2		112.1	19.7	1.47	1.6	0.51	174.9		

^[1] Notation described in Appendix A

^[2] Multiple headed bars in a single specimen loaded individually are denoted by letters A, B, and C, and grouped headed bars loaded simultaneously are denoted with a number after a common letter (A1, A2); specimen dimensions shown in Figures 2.2 through 2.10

^[3] Details of heads provided in Section 2.1.2

^[4] c_{ch} for tests with individual headed bars is taken as twice of the minimum concrete cover to the center of the bar [that is, $c_{ch} = 2 \times (c_{so} + d_b/2)$]

^[5] Specimen contained a single centrally placed headed bar

Table B.1 Cont. Detail of slab specimens ^[1]

Specimens ^[2]			T_{anc}	T_h	$T_{ACI\ 318}$	T_{calc}	$\frac{T}{T_{anc}}$	$\frac{T}{T_h}$	$\frac{T}{T_{ACI\ 318}}$	$\frac{T}{T_{calc}}$	Ψ_o
SN	Description	Head	(kips)	(kips)	(kips)	(kips)					
1	11-5-S5.5-6#6-0-12.75	A	142.3	98.6	70.9	84.1	1.03	1.49	2.07	1.75	1.0
	11-5-S5.5-6#6-0-12.75	B	137.9	96.7	69.6	82.5	1.00	1.42	1.98	1.67	1.0
	11-5-S5.5-6#6-0-12.75	C	142.3	98.6	70.9	84.1	0.96	1.38	1.92	1.62	1.0
2	11-5-S5.5-10#6-0-12.75	A	148.3	100.6	71.7	85.8	1.09	1.60	2.25	1.88	1.0
	11-5-S5.5-10#6-0-12.75	B	136.9	95.7	68.3	81.8	1.05	1.50	2.10	1.76	1.0
3	11-5-S5.5-6#11-0-12.75 ^[5]	A	156.4	103.6	73.4	88.4	0.76	1.15	1.62	1.35	1.0
4	(2@3.2)11-5-S5.5-6#11-0-12.75	A1	84.1	62.2	45.3	48.3	1.07	1.45	1.99	1.87	1.0
		A2									
	(2@3.2)11-5-S5.5-6#11-0-12.75	B1	87.5	63.3	46.0	49.1	0.88	1.22	1.68	1.57	1.0
		B2									
5	11-5-S5.5-6#6-2#4-12.75	A	145.5	129.9	70.1	105.8	1.40	1.57	2.90	1.93	1.0
	11-5-S5.5-6#6-2#4-12.75	B	143.1	128.9	69.5	104.7	1.54	1.71	3.18	2.11	1.0
	11-5-S5.5-6#6-2#4-12.75	C	147.8	130.9	70.8	106.8	1.52	1.72	3.18	2.11	1.0
6	(2@8.2)11-5-S5.5-6#11-0-12.75	A1	95.6	101.0	72.2	86.1	1.04	0.99	1.38	1.16	1.0
		A2									
	(2@8.2)11-5-S5.5-6#11-0-12.75	B1	101.4	105.2	75.1	89.7	1.05	1.01	1.42	1.19	1.0
		B2									
7	(2@8.2)11-5-S5.5-6#11-0-12.75	A1	90.8	97.9	70.4	83.5	0.97	0.90	1.25	1.06	1.0
		A2									
	(2@8.2)11-5-S5.5-6#11-0-12.75	B1	91.4	98.4	70.7	83.9	0.96	0.89	1.24	1.04	1.0
		B2									
8	(2@8.2)11-5-S9.2-7#11-3#4-12.75	A1	111.7	134.2	81.8	111.4	1.19	0.99	1.63	1.20	1.0
		A2									
	(2@8.2)11-5-S9.2-7#11-6#4-12.75	B1	110.2	137.6	81.0	114.4	1.68	1.34	2.28	1.62	1.0
		B2									
9	(2@8.2)11-5-S9.2-7#11-3#4-12.75	A1	111.3	134.4	81.1	111.5	1.26	1.05	1.73	1.26	1.0
		A2									
	(2@8.2)11-5-S9.2-7#11-6#4-12.75	B1	112.8	139.9	81.9	116.7	1.57	1.27	2.16	1.52	1.0
		B2									

^[1] Notation described in Appendix A

^[2] Multiple headed bars in a single specimen loaded individually are denoted by letters A, B, and C, and grouped headed bars loaded simultaneously are denoted with a number after a common letter (A1, A2); specimen dimensions shown in Figures 2.2 through 2.10

^[3] Details of heads provided in Section 2.1.2

^[4] c_{ch} for tests with individual headed bars is taken as twice of the minimum concrete cover to the center of the bar [that is, $c_{ch} = 2 \times (c_{so} + d_b/2)$]

^[5] Specimen contained a single centrally placed headed bar

Table B.1 Cont. Detail of slab specimens ^[1]

Specimens ^[2]			Head Type ^[3]	$\frac{A_{brg}}{A_b}$	A_{st} (in. ²)	$\frac{A_{st}}{A_b}$	c_{bc} (in.)	c_{ch} ^[4] (in.)	c_{so} (in.)	ℓ_{eh} (in.)
SN	Description	Head								
10	(2@8.2)11-15-S9.2-7#11-0-12.75	A1	S9.2	9.2	10.92	7.00	7.6	11.5	32.5	12.69
		A2	S9.2	9.2	10.92	7.00	7.6	11.5	32.5	12.69
	(2@8.2)11-15-S9.2-7#11-0-12.75	B1	S9.2	9.2	10.92	7.00	7.5	11.5	32.5	12.75
		B2	S9.2	9.2	10.92	7.00	7.5	11.5	32.5	12.75
11	(2@8.2)11-15-S9.2-7#11-3#4-12.75	A1	S9.2	9.2	10.92	7.00	7.5	11.5	32.5	12.75
		A2	S9.2	9.2	10.92	7.00	7.5	11.5	32.5	12.75
	(2@8.2)11-15-S9.2-7#11-6#4-12.75	B1	S9.2	9.2	10.92	7.00	7.6	11.5	32.5	12.63
		B2	S9.2	9.2	10.92	7.00	7.6	11.5	32.5	12.63
12	(2@6.8)14-5-B4.2-7#11-0-12.75	A1	B4.2	4.2	10.92	4.85	6.6	11.5	32.4	13.00
		A2	B4.2	4.2	10.92	4.85	6.6	11.5	32.4	13.00
	(2@6.8)14-5-B4.2-7#11-0-12.75	B1	B4.2	4.2	10.92	4.85	6.5	11.5	32.4	13.13
		B2	B4.2	4.2	10.92	4.85	6.5	11.5	32.4	13.13
13	(2@6.8)14-5-B4.2-7#11-3#4-12.75	A1	B4.2	4.2	10.92	4.85	6.6	11.5	32.4	13.00
		A2	B4.2	4.2	10.92	4.85	6.6	11.5	32.4	13.00
	(2@6.8)14-5-B4.2-7#11-6#4-12.75	B1	B4.2	4.2	10.92	4.85	6.9	11.5	32.4	12.75
		B2	B4.2	4.2	10.92	4.85	6.9	11.5	32.4	12.75
14	(2@6.8)14-15-B4.2-7#11-0-12.75	A1	B4.2	4.2	10.92	4.85	6.5	11.5	32.4	13.13
		A2	B4.2	4.2	10.92	4.85	6.5	11.5	32.4	13.13
	(2@6.8)14-15-B4.2-7#11-0-12.75	B1	B4.2	4.2	10.92	4.85	6.5	11.5	32.4	13.13
		B2	B4.2	4.2	10.92	4.85	6.5	11.5	32.4	13.13
15	(2@6.8)14-15-B4.2-7#11-3#4-12.75	A1	B4.2	4.2	10.92	4.85	6.3	11.5	32.4	13.38
		A2	B4.2	4.2	10.92	4.85	6.3	11.5	32.4	13.38
	(2@6.8)14-15-B4.2-7#11-6#4-12.75	B1	B4.2	4.2	10.92	4.85	6.8	11.5	32.4	12.88
		B2	B4.2	4.2	10.92	4.85	6.8	11.5	32.4	12.88

^[1] Notation described in Appendix A

^[2] Multiple headed bars in a single specimen loaded individually are denoted by letters A, B, and C, and grouped headed bars loaded simultaneously are denoted with a number after a common letter (A1, A2); specimen dimensions shown in Figures 2.2 through 2.10

^[3] Details of heads provided in Section 2.1.2

^[4] c_{ch} for tests with individual headed bars is taken as twice of the minimum concrete cover to the center of the bar [that is, $c_{ch} = 2 \times (c_{so} + d_b/2)$]

^[5] Specimen contained a single centrally placed headed bar

Table B.1 Cont. Detail of slab specimens ^[1]

Specimens ^[2]			f_{cm}	f_{su}	h_{cl}	$\frac{h_{cl}}{\ell_{eh}}$	A_{tt}	$\frac{A_{tt}}{A_{hs}}$	T_{peak}	T_{total}	T
SN	Description	Head	(psi)	(psi)	(in.)		(in. ²)		(kips)	(kips)	(kips)
10	(2@8.2)11-15-S9.2-7#11-0-12.75	A1	14470	79.7	19.7	1.55	0.0	0.00	124.3	249.6	124.8
		A2		80.3	19.7	1.55	0.0	0.00	125.3		
	(2@8.2)11-15-S9.2-7#11-0-12.75	B1		86.2	19.7	1.55	0.0	0.00	134.5	261.9	131.0
		B2		81.7	19.7	1.55	0.0	0.00	127.4		
11	(2@8.2)11-15-S9.2-7#11-3#4-12.75	A1	14140	100.4	19.7	1.55	0.8	0.26	156.6	314.5	157.3
		A2		101.2	19.7	1.55	0.8	0.26	157.9		
	(2@8.2)11-15-S9.2-7#11-6#4-12.75	B1	14080	107.9	19.7	1.56	1.6	0.51	168.4	335.5	167.8
		B2		107.1	19.7	1.56	1.6	0.51	167.1		
12	(2@6.8)14-5-B4.2-7#11-0-12.75	A1	6040	54.0	19.9	1.53	0.0	0.00	121.5	239.0	119.5
		A2		52.2	19.9	1.53	0.0	0.00	117.5		
	(2@6.8)14-5-B4.2-7#11-0-12.75	B1	6180	57.4	19.9	1.51	0.0	0.00	129.1	259.0	129.5
		B2		57.7	19.9	1.51	0.0	0.00	129.9		
13	(2@6.8)14-5-B4.2-7#11-3#4-12.75	A1	5440	61.8	19.9	1.53	1.2	0.27	139.0	274.6	137.3
		A2		60.3	19.9	1.53	1.2	0.27	135.6		
	(2@6.8)14-5-B4.2-7#11-6#4-12.75	B1	5480	72.9	19.9	1.56	2.4	0.53	164.0	319.8	159.9
		B2		69.2	19.9	1.56	2.4	0.53	155.8		
14	(2@6.8)14-15-B4.2-7#11-0-12.75	A1	14030	76.1	19.9	1.51	0.0	0.00	171.2	346.0	173.0
		A2		77.7	19.9	1.51	0.0	0.00	174.8		
	(2@6.8)14-15-B4.2-7#11-0-12.75	B1	14050	71.3	19.9	1.51	0.0	0.00	160.5	323.8	161.9
		B2		72.6	19.9	1.51	0.0	0.00	163.3		
15	(2@6.8)14-15-B4.2-7#11-3#4-12.75	A1	13190	81.2	19.9	1.48	1.2	0.27	182.6	370.1	185.1
		A2		83.3	19.9	1.48	1.2	0.27	187.5		
	(2@6.8)14-15-B4.2-7#11-6#4-12.75	B1	13020	86.7	19.9	1.54	2.4	0.53	195.0	388.8	194.4
		B2		86.1	19.9	1.54	2.4	0.53	193.8		

^[1] Notation described in Appendix A

^[2] Multiple headed bars in a single specimen loaded individually are denoted by letters A, B, and C, and grouped headed bars loaded simultaneously are denoted with a number after a common letter (A1, A2); specimen dimensions shown in Figures 2.2 through 2.10

^[3] Details of heads provided in Section 2.1.2

^[4] c_{ch} for tests with individual headed bars is taken as twice of the minimum concrete cover to the center of the bar [that is, $c_{ch} = 2 \times (c_{so} + d_b/2)$]

^[5] Specimen contained a single centrally placed headed bar

Table B.1 Cont. Detail of slab specimens ^[1]

Specimens ^[2]			T_{anc}	T_h	$T_{ACI\ 318}$	T_{calc}	$\frac{T}{T_{anc}}$	$\frac{T}{T_h}$	$\frac{T}{T_{ACI\ 318}}$	$\frac{T}{T_{calc}}$	Ψ_o
SN	Description	Head	(kips)	(kips)	(kips)	(kips)					
10	(2@8.2)11-15-S9.2-7#11-0-12.75	A1	143.5	120.2	106.7	103.7	0.87	1.04	1.17	1.20	1.0
		A2									1.0
	(2@8.2)11-15-S9.2-7#11-0-12.75	B1	144.5	120.8	107.2	104.2	0.91	1.08	1.22	1.26	1.0
		B2									1.0
11	(2@8.2)11-15-S9.2-7#11-3#4-12.75	A1	142.9	146.5	105.9	125.0	1.10	1.07	1.48	1.26	1.0
		A2									1.0
	(2@8.2)11-15-S9.2-7#11-6#4-12.75	B1	140.6	149.7	104.7	128.1	1.19	1.12	1.60	1.31	1.0
		B2									1.0
12	(2@6.8)14-5-B4.2-7#11-0-12.75	A1	96.0	97.2	77.4	77.9	1.24	1.23	1.54	1.53	1.0
		A2									1.0
	(2@6.8)14-5-B4.2-7#11-0-12.75	B1	98.5	98.7	79.0	79.1	1.32	1.31	1.64	1.64	1.0
		B2									1.0
13	(2@6.8)14-5-B4.2-7#11-3#4-12.75	A1	91.1	145.2	76.3	99.6	1.51	0.95	1.80	1.38	1.0
		A2									1.0
	(2@6.8)14-5-B4.2-7#11-6#4-12.75	B1	88.9	149.0	74.9	101.8	1.80	1.07	2.13	1.57	1.0
		B2									1.0
14	(2@6.8)14-15-B4.2-7#11-0-12.75	A1	148.4	120.1	119.1	97.1	1.17	1.44	1.45	1.78	1.0
		A2									1.0
	(2@6.8)14-15-B4.2-7#11-0-12.75	B1	148.5	120.2	119.2	97.2	1.09	1.35	1.36	1.67	1.0
		B2									1.0
15	(2@6.8)14-15-B4.2-7#11-3#4-12.75	A1	147.8	172.6	117.7	127.8	1.25	1.07	1.57	1.45	1.0
		A2									1.0
	(2@6.8)14-15-B4.2-7#11-6#4-12.75	B1	139.0	172.9	112.5	127.6	1.40	1.12	1.73	1.52	1.0
		B2									1.0

^[1] Notation described in Appendix A

^[2] Multiple headed bars in a single specimen loaded individually are denoted by letters A, B, and C, and grouped headed bars loaded simultaneously are denoted with a number after a common letter (A1, A2); specimen dimensions shown in Figures 2.2 through 2.10

^[3] Details of heads provided in Section 2.1.2

^[4] c_{ch} for tests with individual headed bars is taken as twice of the minimum concrete cover to the center of the bar [that is, $c_{ch} = 2 \times (c_{so} + d_b/2)$]

^[5] Specimen contained a single centrally placed headed bar

APPENDIX C: TEST RESULTS AND SPECIMENS FROM OTHER STUDIES INCLUDED IN THE CURRENT STUDY

C.1 SLAB SPECIMENS TESTED BY DEVRIES ET AL. (1999) AND CHOI ET AL. (2002)

Table C.1 Data for specimens tested by DeVries et al. (1999) and Choi et al. (2002) ^[1]

Study	Specimen	Bar size ^[2]	A_b (in. ²)	$\frac{A_{brg}}{A_b}$	A_{hs} (in. ²)	A_{Nc} (in. ²)	A_{tr} (in. ²)	A_{tt} (in. ²)	$\frac{A_{st}}{nA_b}$
DeVries et al. (1999)	T2B2	D20	0.49	6.9	0.49	420	0	0	0.0
	T2B4	D20	0.49	6.9	0.49	420	0	0	0.4
	T2B6	D20	0.49	6.9	0.49	241	0	0	0.0
	T2B8	D20	0.49	6.9	0.49	241	0	0	0.4
Choi et al. (2002)	S16-7db.1	D16	0.31	3.2	0.31	175	0	0	0
	S16-7db.2	D16	0.31	3.2	0.31	175	0	0	0
	S25-7db.1	D25	0.79	3.0	0.79	427	0	0	0
	S25-7db.2	D25	0.79	3.0	0.79	427	0	0	0
	E16-7db.1	D16	0.31	3.2	0.31	112	0	0	0
	E16-7db.2	D16	0.31	3.2	0.31	112	0	0	0
	E19-7db.1	D19	0.44	2.6	0.44	165	0	0	0
	E19-7db.2	D19	0.44	2.6	0.44	165	0	0	0
	E19-7db.3	D19	0.44	2.6	0.44	206	0	0	0
	E19-7db.4	D19	0.44	2.6	0.44	206	0	0	0
	E25-7db.1	D25	0.79	3.0	0.79	275	0	0	0
	E25-7db.2	D25	0.79	3.0	0.79	275	0	0	0

^[1] Columns arranged in alphabetical order of notation; notation described in Appendix A

^[2] Bar sizes are presented in SI as reported in the original studies

Table C.1 Cont. Data for specimens tested by DeVries et al. (1999) and Choi et al. (2002) ^[1]

Study	Specimen	$\frac{A_u}{A_{hs}}$	$\frac{c_{ch}^{[3]}}{d_b}$	$\frac{c_{so}}{d_b}$	$d_b^{[4]}$ (in.)	$f_{cm}^{[4]}$ (ksi)	f_{su} (ksi)	$f_y^{[4]}$ (ksi)	$\ell_{eh}^{[4]}$ (in.)
DeVries et al. (1999)	T2B2	0	5.1	2.0	0.79	4790	67.9	80.3	9.0
	T2B4	0	5.1	2.0	0.79	4790	78.9	80.3	9.0
	T2B6	0	5.1	2.0	0.79	4790	56.0	80.3	9.0
	T2B8	0	5.1	2.0	0.79	4790	57.3	80.3	9.0
Choi et al. (2002)	S16-7db.1	0	114.4	56.7	0.625	5270	52.9	60.9	4.4
	S16-7db.2	0	113.4	56.2	0.625	5270	58.0	60.9	4.4
	S25-7db.1	0	71.1	35.1	1	5270	45.5	60.9	6.9
	S25-7db.2	0	70.9	34.9	1	5270	43.0	60.9	6.9
	E16-7db.1	0	6.0	2.5	0.625	5270	34.1	60.9	4.4
	E16-7db.2	0	6.0	2.5	0.625	5270	34.1	60.9	4.4
	E19-7db.1	0	7.0	3.0	0.75	3930	26.6	52.2	5.2
	E19-7db.2	0	7.0	3.0	0.75	3930	24.5	52.2	5.2
	E19-7db.3	0	14.0	6.5	0.75	3930	39.9	52.2	5.2
	E19-7db.4	0	14.0	6.5	0.75	3930	38.3	52.2	5.2
	E25-7db.1	0	5.9	2.5	1	5270	24.8	60.9	6.9
	E25-7db.2	0	5.9	2.5	1	5270	26.2	60.9	6.9

^[1] Columns arranged in alphabetical order of notation; notation described in Appendix A

^[3] c_{ch} for tests with individual headed bars is taken as twice of the minimum concrete cover to the center of the bar [that is, $c_{ch} = 2 \times (c_{so} + d_b/2)$]

^[4] Values are converted from the SI unit (1 in. = 25.4 mm; 1 psi = 1/145 MPa; and 1 kip = 4.4484 kN)

Table C.1 Cont. Data for specimens tested by DeVries et al. (1999) and Choi et al. (2002) ^[1]

Study	Specimen	N	N_{ar} (kips)	N_{cb} (kips)	N_{sb} (kips)	N_{tr}	n	$S_{tr}^{[4]}$ (in.)	$T^{[4]}$ (kips)	T_{anc} (kips)
DeVries et al. (1999)	T2B2	0	0.0	24.0	40.9	0	1	-	33.3	31.9
	T2B4	0	0.0	24.0	40.9	0	1	-	38.7	31.9
	T2B6	0	0.0	13.8	40.9	0	1	-	27.4	18.3
	T2B8	0	0.0	13.8	40.9	0	1	-	28.1	18.3
Choi et al. (2002)	S16-7db.1	0	0.0	20.2	-	0	1	-	16.4	26.8
	S16-7db.2	0	0.0	20.2	-	0	1	-	18.0	26.8
	S25-7db.1	0	0.0	39.4	-	0	1	-	36.0	52.3
	S25-7db.2	0	0.0	39.4	-	0	1	-	33.9	52.3
	E16-7db.1	0	0.0	10.2	-	0	1	-	10.6	13.5
	E16-7db.2	0	0.0	10.2	-	0	1	-	10.6	13.5
	E19-7db.1	0	0.0	12.1	-	0	1	-	11.7	16.0
	E19-7db.2	0	0.0	12.1	-	0	1	-	10.8	16.0
	E19-7db.3	0	0.0	16.9	-	0	1	-	17.5	22.4
	E19-7db.4	0	0.0	16.9	-	0	1	-	16.9	22.4
	E25-7db.1	0	0.0	19.9	-	0	1	-	19.6	26.4
	E25-7db.2	0	0.0	19.9	-	0	1	-	20.7	26.4

^[1] Columns arranged in alphabetical order of notation; notation described in Appendix A

^[4] Values are converted from the SI unit (1 in. = 25.4 mm; 1 psi = 1/145 MPa; and 1 kip = 4.4484 kN)

Table C.1 Cont. Data for specimens tested by DeVries et al. (1999) and Choi et al. (2002) ^[1]

Study	Specimen	T_h (kips)	$T_{ACI\ 318}$ (kips)	T_{calc} (kips)	$\frac{T}{T_{anc}}$	$\frac{T}{T_h}$	$\frac{T}{T_{ACI\ 318}}$	$\frac{T}{T_{calc}}$	ψ_o	Remarks
DeVries et al. (1999)	T2B2	32.6	17.7	22.6	1.04	1.02	1.88	1.48	1.25	Edge bars in slab specimens
	T2B4	32.6	17.7	22.6	1.21	1.19	2.18	1.71	1.25	
	T2B6	32.6	17.7	22.6	1.50	0.84	1.55	1.22	1.25	Corner bars in slab specimens
	T2B8	32.6	17.7	22.6	1.53	0.86	1.58	1.25	1.25	
Choi et al. (2002)	S16-7db.1	23.9	15.8	18.9	0.61	0.69	1.04	0.87	1.0	Center bars in slab specimens
	S16-7db.2	23.9	15.8	18.9	0.67	0.75	1.14	0.95	1.0	
	S25-7db.1	44.6	31.2	37.1	0.69	0.81	1.15	0.97	1.0	
	S25-7db.2	44.6	31.2	37.1	0.65	0.76	1.09	0.91	1.0	
	E16-7db.1	16.2	12.7	11.4	0.78	0.65	0.83	0.93	1.25	Edge bars in slab specimens
	E16-7db.2	16.2	12.7	11.4	0.78	0.65	0.83	0.93	1.25	
	E19-7db.1	21.1	15.5	15.5	0.73	0.55	0.76	0.76	1.25	
	E19-7db.2	21.1	15.5	15.5	0.67	0.51	0.70	0.70	1.25	
	E19-7db.3	22.7	15.5	17.9	0.78	0.77	1.13	0.98	1.25	
	E19-7db.4	22.7	15.5	17.9	0.75	0.74	1.09	0.94	1.25	
	E25-7db.1	29.9	15.6	22.0	0.74	0.65	1.26	0.89	1.25	
	E25-7db.2	29.9	15.6	22.0	0.78	0.69	1.33	0.94	1.25	

^[1] Columns arranged in alphabetical order of notation; notation described in Appendix A

C.2 SLAB SPECIMENS TESTED AT THE UNIVERSITY OF KANSAS

Table C.2 Data for slab specimens tested by Ghimire et al. (2018) ^[1]

SN	Specimens		$\frac{A_{brg}}{A_b}$	A_{st} (in. ²)	$\frac{A_{st}}{A_b}$	c_{bc} (in.)	c_{ch} ^[3] (in.)	c_{so} (in.)	$\frac{d}{\ell_{eh}}$
	Description	Headed bar ^[2]							
1	8-5-T9.5-8#5-6 ^[4]	A	9.5	1.02	1.29	7.0	48	23.5	1.48
	8-5-T9.5-8#5-6 ^[4]	B	9.5	1.02	1.29	6.8	48	23.5	1.44
2	8-5-T4.0-8#5-6	A	4.0	0	0	6.5	48	23.5	1.38
	8-5-T4.0-8#5-6	B	4.0	0	0	7.5	48	23.5	1.55
3	8-5-F4.1-8#5-6 ^[4]	A	4.1	1.02	1.29	7.6	48	23.5	1.63
	8-5-F4.1-8#5-6 ^[4]	B	4.1	1.02	1.29	7.6	48	23.5	1.63
4	8-5-F9.1-8#5-6 ^[4]	A	9.1	1.02	1.29	7.9	48	23.5	1.71
	8-5-F9.1-8#5-6 ^[4]	B	9.1	1.02	1.29	8.0	48	23.5	1.69
5	8-5-F4.1-2#8-6	A	4.1	0	0	9.0	48	23.5	1.96
	8-5-F9.1-2#8-6	B	9.1	0	0	9.0	48	23.5	1.96
6	8-5-T4.0-2#8-6	A	4.0	0	0	8.9	48	23.5	1.93
	8-5-T9.5-2#8-6	B	9.5	0	0	8.9	48	23.5	1.90
7	8-8-O12.9-6#5-6	A	13.0	0	0	8.8	48	23.5	1.79
	8-8-O9.1-6#5-6	B	9.1	0	0	8.8	48	23.5	1.89
8	8-8-S6.5-6#5-6	A	6.5	0	0	8.6	48	23.5	1.78
	8-8-O4.5-6#5-6	B	4.5	0	0	8.5	48	23.5	1.86
9	8-5-S14.9-6#5-6	A	15.0	0	0	8.5	48	23.5	1.84
	8-5-S6.5-6#5-6	B	6.5	0	0	8.5	48	23.5	1.75
10	8-5-O12.9-6#5-6	A	13.0	0	0	8.4	48	23.5	1.73
	8-5-O4.5-6#5-6	B	4.5	0	0	8.5	48	23.5	1.77
11	8-5-S9.5-6#5-6	A	9.5	0	0	8.5	48	23.5	1.79
	8-5-S9.5-6#5-6	B	9.5	0	0	8.6	48	23.5	1.83
12	8-5-F4.1-6#5-6 ^[5]	-	4.1	0	0	6.6	48	23.5	5.73
13	8-5-F4.1-0-6	A	4.1	0	0	12.0	32	15.5	2.49
	8-5-F4.1-0-6	B	4.1	0	0	12.0	32	15.5	2.91
	8-5-F4.1-2#5-6	C	4.1	0.62	0.78	12.0	32	15.5	2.74
14	8-5-F4.1-4#5-6	A	4.1	1.24	1.57	12.0	32	15.5	3.00
	8-5-F4.1-4#5-6	B	4.1	1.24	1.57	12.0	32	15.5	2.98
	8-5-F4.1-4#5-6	C	4.1	1.24	1.57	12.0	32	15.5	2.70
15	8-5-F4.1-6#5-6	A	4.1	1.86	2.35	12.0	32	15.5	2.89
	8-5-F4.1-6#5-6	B	4.1	1.86	2.35	12.0	32	15.5	2.72
	8-5-F4.1-6#5-6	C	4.1	1.86	2.35	12.0	32	15.5	2.65

^[1] Notation described in Appendix A; all specimens contained No. 8 headed bars

^[2] Multiple headed bars in a single specimen loaded individually are denoted by letters A, B, and C

^[3] c_{ch} for tests with individual headed bars is taken as twice of the minimum concrete cover to the center of the bar [that is, $c_{ch} = 2 \times (c_{so} + d_b/2)$]

^[4] In addition to 8 No. 5 bars as reinforcement perpendicular to the headed bar, specimens contained No. 4 bars spaced at 12 in. in a direction perpendicular to the No. 5 bars

^[5] Specimen contained a single centrally placed headed bar

Table C.2 Cont. Data for slab specimens tested by Ghimire et al. (2018) ^[1]

Specimens			f_{cm} (psi)	f_{su} (psi)	h_{cl} (in.)	ℓ_{eh} (in.)	$\frac{h_{cl}}{\ell_{eh}}$	T (kips)	T_{anc} (kips)
SN	Description	Headed bar ^[2]							
1	8-5-T9.5-8#5-6 ^[4]	A	7040	83.0	10.5	8.00	1.31	65.6	75.6
	8-5-T9.5-8#5-6 ^[4]	B	7040	85.8	10.5	8.25	1.27	67.8	79.2
2	8-5-T4.0-8#5-6	A	7040	78.2	10.5	8.50	1.24	61.8	82.8
	8-5-T4.0-8#5-6	B	7040	71.3	10.5	7.50	1.40	56.3	68.6
3	8-5-F4.1-8#5-6 ^[4]	A	5220	87.2	10.5	7.44	1.41	68.9	58.4
	8-5-F4.1-8#5-6 ^[4]	B	5220	81.5	10.5	7.38	1.42	64.4	57.7
4	8-5-F9.1-8#5-6 ^[4]	A	5220	88.5	10.5	7.13	1.47	69.9	54.8
	8-5-F9.1-8#5-6 ^[4]	B	5220	69.5	10.5	7.00	1.50	54.9	53.3
5	8-5-F4.1-2#8-6	A	7390	81.5	10.5	6.00	1.75	64.4	50.3
	8-5-F9.1-2#8-6	B	7390	82.3	10.5	6.00	1.75	65.0	50.3
6	8-5-T4.0-2#8-6	A	7390	76.6	10.5	6.06	1.73	60.5	51.1
	8-5-T9.5-2#8-6	B	7390	73.0	10.5	6.13	1.71	57.7	52.0
7	8-8-O12.9-6#5-6	A	8620	100.0	9.8	6.25	1.56	79.0	57.8
	8-8-O9.1-6#5-6	B	8620	89.7	10.5	6.25	1.68	70.9	57.8
8	8-8-S6.5-6#5-6	A	8620	92.4	10.0	6.38	1.57	73.0	59.6
	8-8-O4.5-6#5-6	B	8620	93.7	10.8	6.50	1.65	74.0	61.3
9	8-5-S14.9-6#5-6	A	4200	78.2	10.3	6.50	1.58	61.8	42.8
	8-5-S6.5-6#5-6	B	4200	62.3	10.0	6.50	1.54	49.2	42.8
10	8-5-O12.9-6#5-6	A	4200	66.3	10.0	6.63	1.51	52.4	44.1
	8-5-O4.5-6#5-6	B	4200	63.4	10.1	6.50	1.56	50.1	42.8
11	8-5-S9.5-6#5-6	A	4200	61.9	10.3	6.50	1.58	48.9	42.8
	8-5-S9.5-6#5-6	B	4200	69.0	10.1	6.38	1.59	54.5	41.6
12	8-5-F4.1-6#5-6 ^[5]	-	4200	49.5	47.3	8.44	5.60	39.1	63.3
13	8-5-F4.1-0-6	A	5180	63.9	15.0	6.50	2.31	50.5	47.5
	8-5-F4.1-0-6	B	5180	61.9	17.0	6.25	2.72	48.9	44.8
	8-5-F4.1-2#5-6	C	5180	77.8	17.0	6.75	2.52	61.5	50.3
14	8-5-F4.1-4#5-6	A	5180	67.6	16.8	6.00	2.79	53.4	42.1
	8-5-F4.1-4#5-6	B	5180	66.3	17.0	6.13	2.78	52.4	43.5
	8-5-F4.1-4#5-6	C	5460	67.7	17.0	6.75	2.52	53.5	51.6
15	8-5-F4.1-6#5-6	A	5460	59.8	17.0	6.25	2.72	47.3	46.0
	8-5-F4.1-6#5-6	B	5460	70.8	16.8	6.63	2.53	55.9	50.2
	8-5-F4.1-6#5-6	C	5460	66.6	17.0	6.88	2.47	52.6	53.1

^[1] Notation described in Appendix A; all specimens contained No. 8 headed bars

^[2] Multiple headed bars in a single specimen loaded individually are denoted by letters A, B, and C

^[4] In addition to 8 No. 5 bars as reinforcement perpendicular to the headed bar, specimens contained No. 4 bars spaced at 12 in. in a direction perpendicular to the No. 5 bars

^[5] Specimen contained a single centrally placed headed bar

Table C.2 Cont. Data for slab specimens tested by Ghimire et al. (2018) ^[1]

Specimens			T_h	$T_{ACI\ 318}$	T_{calc}	$\frac{T}{T_{anc}}$	$\frac{T}{T_h}$	$\frac{T}{T_{ACI\ 318}}$	$\frac{T}{T_{calc}}$	Ψ_o
SN	Description	Headed bar ^[2]	(kips)	(kips)	(kips)					
1	8-5-T9.5-8#5-6 ^[4]	A	55.8	39.8	46.3	0.87	1.18	1.65	1.42	1.0
	8-5-T9.5-8#5-6 ^[4]	B	57.5	41.0	47.8	0.86	1.18	1.65	1.42	1.0
2	8-5-T4.0-8#5-6	A	59.3	42.3	49.2	0.75	1.04	1.46	1.26	1.0
	8-5-T4.0-8#5-6	B	52.2	37.3	43.4	0.82	1.08	1.51	1.30	1.0
3	8-5-F4.1-8#5-6 ^[4]	A	48.2	33.6	40.0	1.18	1.43	2.05	1.72	1.0
	8-5-F4.1-8#5-6 ^[4]	B	47.8	33.3	39.6	1.12	1.35	1.93	1.62	1.0
4	8-5-F9.1-8#5-6 ^[4]	A	46.1	32.2	38.3	1.28	1.52	2.17	1.82	1.0
	8-5-F9.1-8#5-6 ^[4]	B	45.2	31.6	37.6	1.03	1.21	1.74	1.46	1.0
5	8-5-F4.1-2#8-6	A	41.9	30.6	35.2	1.28	1.54	2.11	1.83	1.0
	8-5-F9.1-2#8-6	B	41.9	30.6	35.2	1.29	1.55	2.13	1.85	1.0
6	8-5-T4.0-2#8-6	A	42.4	30.9	35.5	1.18	1.43	1.96	1.70	1.0
	8-5-T9.5-2#8-6	B	42.9	31.2	35.9	1.11	1.35	1.85	1.61	1.0
7	8-8-O12.9-6#5-6	A	45.4	34.4	38.1	1.37	1.74	2.30	2.08	1.0
	8-8-O9.1-6#5-6	B	45.4	34.4	38.1	1.23	1.56	2.06	1.86	1.0
8	8-8-S6.5-6#5-6	A	46.4	35.1	38.9	1.23	1.57	2.08	1.88	1.0
	8-8-O4.5-6#5-6	B	47.3	35.8	39.6	1.21	1.57	2.07	1.87	1.0
9	8-5-S14.9-6#5-6	A	39.8	28.4	33.1	1.44	1.55	2.18	1.87	1.0
	8-5-S6.5-6#5-6	B	39.8	28.4	33.1	1.15	1.24	1.73	1.49	1.0
10	8-5-O12.9-6#5-6	A	40.6	28.9	33.7	1.19	1.29	1.81	1.55	1.0
	8-5-O4.5-6#5-6	B	39.8	28.4	33.1	1.17	1.26	1.77	1.51	1.0
11	8-5-S9.5-6#5-6	A	39.8	28.4	33.1	1.14	1.23	1.72	1.48	1.0
	8-5-S9.5-6#5-6	B	39.0	27.8	32.5	1.31	1.40	1.96	1.68	1.0
12	8-5-F4.1-6#5-6 ^[5]	-	52.0	36.8	42.9	0.62	0.75	1.06	0.91	1.0
13	8-5-F4.1-0-6	A	41.8	29.3	34.9	1.06	1.21	1.72	1.45	1.0
	8-5-F4.1-0-6	B	40.2	28.2	33.5	1.09	1.22	1.73	1.46	1.0
	8-5-F4.1-2#5-6	C	43.5	30.4	36.2	1.22	1.41	2.02	1.70	1.0
14	8-5-F4.1-4#5-6	A	38.5	27.1	32.2	1.27	1.39	1.97	1.66	1.0
	8-5-F4.1-4#5-6	B	39.4	27.7	32.9	1.20	1.33	1.89	1.59	1.0
	8-5-F4.1-4#5-6	C	44.0	30.7	36.7	1.04	1.22	1.75	1.46	1.0
15	8-5-F4.1-6#5-6	A	40.7	28.4	34.0	1.03	1.16	1.67	1.39	1.0
	8-5-F4.1-6#5-6	B	43.2	30.1	36.0	1.11	1.29	1.86	1.55	1.0
	8-5-F4.1-6#5-6	C	44.9	31.2	37.4	0.99	1.17	1.68	1.41	1.0

^[1] Notation described in Appendix A; all specimens contained No. 8 headed bars

^[2] Multiple headed bars in a single specimen loaded individually are denoted by letters A, B, and C

^[4] In addition to 8 No. 5 bars as reinforcement perpendicular to the headed bar, specimens contained No. 4 bars spaced at 12 in. in a direction perpendicular to the No. 5 bars

^[5] Specimen contained a single centrally placed headed bar

C.3 SLAB SPECIMENS TESTED AT THE UNIVERSITY OF CALIFORNIA, BERKELEY

Table C.3 Data for slab specimens tested by Worsfold et al. (2022) ^[1]

Specimens		A_b	$\frac{A_{brg}}{A_b}$	A_{tt}	$\frac{A_{tt}}{A_{hs}}$	c_{ch}	c_{so}	d_b	f_{cm}
SN	Description	(in. ²)		(in. ²)		(in.)	(in.)	(in.)	(psi)
1	M01	1.77	1.5	0.0	0.00	5.0	33.75	1.5	3700
2	M02	1.77	5.5	3.2	0.45	5.0	33.75	1.5	3930

^[1] Columns arranged in alphabetical order of notation; notation described in Appendix A

Table C.3 Cont. Data for slab specimens tested by Worsfold et al. (2022) ^[1]

Specimens		f_{su}	h_{cl}	ℓ_{eh}	$\frac{h_{cl}}{\ell_{eh}}$	T	T_{anc}	T_h
SN	Description	(psi)	(in.)	(in.)		(kips)	(kips)	(kips)
1	M01	37.6	21.3	14.3	1.49	66.5	45.9	62.4
2	M02	63.9	21.3	14.3	1.49	113.0	47.3	103.9

^[1] Columns arranged in alphabetical order of notation; notation described in Appendix A

Table C.3 Cont. Data for slab specimens tested by Worsfold et al. (2022) ^[1]

Specimens		$T_{ACI\ 318}$	T_{calc}	$\frac{T}{T_{anc}}$	$\frac{T}{T_h}$	$\frac{T}{T_{ACI\ 318}}$	$\frac{T}{T_{calc}}$	ψ_o
SN	Description	(kips)	(kips)					
1	M01	46.3	48.3	1.45	1.07	1.44	1.38	1.00
2	M02	46.9	78.4	2.39	1.09	2.41	1.44	1.00

^[1] Columns arranged in alphabetical order of notation; notation described in Appendix A

C.4 EXTERIOR BEAM-COLUMN JOINT SPECIMENS

Table C.4 Data for exterior beam-column joint specimens tested under reversed cyclic loading ^[1]

Study		Specimen	Bar Size ^[2]	A_b (in. ²)	A_{hs} (in. ²)	A_{tr} (in. ²)	A_{th} (in. ²)	$\frac{A_{th}}{A_{hs}}$	A_v (in. ²)	b_b (in.)
1	Hanson and Connor (1967)	I ^[3]	No. 9	1.00	4.00	0.20	1.20	0.30	2.00	12.0
		I-A ^[3]	No. 9	1.00	4.00	0.11	0.66	0.17	1.10	12.0
		II	No. 9	1.00	4.00	0.20	1.20	0.30	2.00	12.0
		III ^[7]	No. 9	1.00	4.00	0.20	1.20	0.30	2.00	12.0
		IV ^[7]	No. 9	1.00	4.00	0.20	1.20	0.30	2.00	12.0
		V ^{[3][4]}	No. 9	1.00	4.00	0.00	0.00	0.00	0.00	12.0
		V-A ^[4]	No. 9	1.00	4.00	0.00	0.00	0.00	0.00	12.0
2	Hanson (1971)	1 ^[5]	No. 8	0.79	3.16	0.20	1.20	0.38	2.40	12.0
		3 ^[5]	No. 8	0.79	3.16	0.11	0.66	0.21	1.10	12.0
		4	No. 8	0.79	3.16	0.11	0.44	0.14	0.88	12.0
		5	No. 8	0.79	3.16	0.11	0.66	0.21	1.32	12.0
3	Megget (1974)	Unit A	D25	0.79	2.37	0.20	1.60	0.68	2.40	10.0
4	Uzumeri (1977)	1 ^{[4][5]}	No. 9	1.00	3.00	0.00	0.00	0.00	0.00	12.0
		2 ^[4]	No. 9	1.00	3.00	0.00	0.00	0.00	0.00	12.0
		3 ^[5]	No. 9	1.00	3.00	0.11	0.88	0.29	0.88	12.0
		4 ^[5]	No. 9	1.00	3.00	0.20	1.60	0.53	1.60	12.0
		5 ^{[4][5]}	No. 9	1.00	3.00	0.00	0.00	0.00	0.00	15.0
		6	No. 9	1.00	3.00	0.20	2.80	0.93	3.20	15.0
		7	No. 9	1.00	3.00	0.20	1.60	0.53	1.60	15.0
		8	No. 9	1.00	4.00	0.20	2.80	0.70	3.20	15.0
5	Lee et al. (1977)	1	No. 6	0.44	0.88	0.11	0.88	1.00	0.88	8.0
		2	No. 6	0.44	0.88	0.11	0.88	1.00	0.88	8.0
		3	No. 6	0.44	0.88	0.05	0.20	0.23	0.20	8.0
		4	No. 6	0.44	0.88	0.05	0.20	0.23	0.20	8.0
		5	No. 6	0.44	0.88	0.11	0.88	1.00	0.88	8.0
		6	No. 6	0.44	0.88	0.05	0.20	0.23	0.20	8.0
		7	No. 6	0.44	0.88	0.05	0.20	0.23	0.20	8.0
		8	No. 6	0.44	0.88	0.05	0.20	0.23	0.20	8.0

^[1] Columns arranged in alphabetical order of notation; notation described in Appendix A; values given in SI units are converted to in.-lb (1 in. = 25.4 mm; 1 psi = 1/145 Mpa; and 1 kip = 4.4484 kN)

^[2] Bar sizes are presented in SI and in.-lb as reported in the original studies

^[3] Analyzed as a doubly reinforced section to calculate the nominal flexural strength M_n ; all other specimens are analyzed as a single reinforced

^[4] Specimens did not contain confining reinforcement parallel to the hooked bars within the joint region

^[5] Specimens had transverse beams on one or both sides of the test beam. These transverse beams meet the dimensional requirements of Sections 18.8.4 and 15.2.8 of ACI 318-19 and Section 4.3 of ACI 352R-02 to be considered effective in increasing the joint shear strength

^[6] Specimens had $d/\ell_{eh} > 1.5$

^[7] Specimens had column to beam flexural strength ratio, M_R , less than 1.2

Table C.4 Cont. Data for exterior beam-column joint specimens tested under reversed cyclic loading ^[1]

Study		Specimen	b_c (in.)	b_j (in.)	$b_{j,ACI 352}$ (in.)	c_{ch} (in.)	$\frac{c_{ch}}{d_b}$	c_{so} (in.)	$\frac{c_{so}}{d_b}$	d
1	Hanson and Connor (1967)	I ^[3]	15.0	15.0	13.5	2.6	2.3	3.0	2.7	17.9
		I-A ^[3]	15.0	15.0	13.5	2.6	2.3	3.0	2.7	17.9
		II	15.0	15.0	13.5	2.6	2.3	3.0	2.7	17.9
		III ^[7]	12.0	12.0	12.0	2.6	2.3	1.5	1.3	17.9
		IV ^[7]	12.0	12.0	12.0	2.6	2.3	1.5	1.3	17.9
		V ^{[3][4]}	15.0	15.0	13.5	2.6	2.3	3.0	2.7	17.9
		V-A ^[4]	15.0	15.0	13.5	2.6	2.3	3.0	2.7	17.9
2	Hanson (1971)	1 ^[5]	15.0	15.0	13.5	2.7	2.7	3.0	3.0	18.0
		3 ^[5]	15.0	15.0	13.5	2.7	2.7	3.0	3.0	18.0
		4	15.0	15.0	13.5	2.7	2.7	3.0	3.0	18.0
		5	15.0	15.0	13.5	2.7	2.7	3.0	3.0	18.0
3	Megget (1974)	Unit A	13.0	13.0	11.5	2.7	2.7	3.3	3.3	15.7
4	Uzumeri (1977)	1 ^{[4][5]}	15.0	15.0	13.5	3.4	3.0	3.5	3.1	17.6
		2 ^[4]	15.0	15.0	13.5	3.4	3.0	3.5	3.1	17.6
		3 ^[5]	15.0	15.0	13.5	3.4	3.0	3.5	3.1	17.6
		4 ^[5]	15.0	15.0	13.5	3.4	3.0	3.5	3.1	17.6
		5 ^{[4][5]}	15.0	15.0	15.0	4.9	4.4	2.0	1.8	17.6
		6	15.0	15.0	15.0	4.9	4.4	2.0	1.8	17.6
		7	15.0	15.0	15.0	4.9	4.4	2.0	1.8	17.6
		8	15.0	15.0	15.0	3.3	2.9	2.0	1.8	17.6
5	Lee et al. (1977)	1	8.0	8.0	8.0	2.5	3.3	2.4	3.2	8.0
		2	8.0	8.0	8.0	2.5	3.3	2.4	3.2	8.0
		3	8.0	8.0	8.0	2.5	3.3	2.4	3.2	8.0
		4	8.0	8.0	8.0	2.5	3.3	2.4	3.2	8.0
		5	8.0	8.0	8.0	2.5	3.3	2.4	3.2	8.0
		6	8.0	8.0	8.0	2.5	3.3	2.4	3.2	8.0
		7	8.0	8.0	8.0	2.5	3.3	2.4	3.2	8.0
		8	8.0	8.0	8.0	2.5	3.3	2.4	3.2	8.0

^[1] Columns arranged in alphabetical order of notation; notation described in Appendix A; values given in SI units are converted to in.-lb (1 in. = 25.4 mm; 1 psi = 1/145 Mpa; and 1 kip = 4.4484 kN)

^[2] Bar sizes are presented in SI and in.-lb as reported in the original studies

^[3] Analyzed as a doubly reinforced section to calculate the nominal flexural strength M_n ; all other specimens are analyzed as a single reinforced

^[4] Specimens did not contain confining reinforcement parallel to the hooked bars within the joint region

^[5] Specimens had transverse beams on one or both sides of the test beam. These transverse beams meet the dimensional requirements of Sections 18.8.4 and 15.2.8 of ACI 318-19 and Section 4.3 of ACI 352R-02 to be considered effective in increasing the joint shear strength

^[6] Specimens had $d/\ell_{ch} > 1.5$

^[7] Specimens had column to beam flexural strength ratio, M_R , less than 1.2

Table C.4 Cont. Data for exterior beam-column joint specimens tested under reversed cyclic loading ^[1]

Study		Specimen	$\frac{d}{\ell_{eh}}$	d' (in.)	d_b (in.)	$f_{cm}^{[8]}$ (psi)	$f_{cm}^{[9]}$ (psi)	f_y (ksi)	$f_{ytr,l}$ (ksi)	$f_{ytr,l} A_v$ (kips)
1	Hanson and Connor (1967)	I ^[3]	1.33	2.1	1.128	5720	3470	51.6	46.6	93.2
		I-A ^[3]	1.33	2.1	1.128	5330	3200	47.8	52.8	58.1
		II	1.33	2.1	1.128	5960	3650	48.3	54.8	109.6
		III ^[7]	1.33	2.1	1.128	4940	3200	48.2	49.2	98.4
		IV ^[7]	1.33	2.1	1.128	3490	3480	49.9	50.5	101.0
		V ^{[3][4]}	1.33	2.1	1.128	5420	3300	51.0	0.0	0.0
		V-A ^[4]	1.33	2.1	1.128	5240	5420	49.8	0.0	0.0
2	Hanson (1971)	1 ^[5]	0.62	2.0	1	5610	5500	63.1	66.8	160.3
		3 ^[5]	0.62	2.0	1	5340	5200	64.1	73.5	80.9
		4	0.62	2.0	1	5240	5380	63.4	73.5	64.7
		5	0.62	2.0	1	5420	5230	65.0	73.5	97.0
3	Megget (1974)	Unit A	1.25	2.4	1	3200	3200	54.7	46.0	110.4
4	Uzumeri (1977)	1 ^{[4][5]}	1.35	2.4	1.128	4460	4460	50.3	0.0	0.0
		2 ^[4]	1.35	2.4	1.128	4510	4510	50.6	0.0	0.0
		3 ^[5]	1.35	2.4	1.128	3920	3920	50.8	62.0	54.6
		4 ^[5]	1.35	2.4	1.128	4490	4490	50.6	55.0	88.0
		5 ^{[4][5]}	1.35	2.4	1.128	4630	4630	50.4	0.0	0.0
		6	1.35	2.4	1.128	5250	5250	51.1	51.8	165.8
		7	1.35	2.4	1.128	4460	4460	51.1	53.0	84.8
		8	1.35	2.4	1.128	3820	3820	51.1	53.0	169.6
5	Lee et al. (1977)	1	0.85	2.0	0.75	4200	4200	52.5	56.4	49.6
		2	0.85	2.0	0.75	4200	4200	48.6	56.4	49.6
		3	0.85	2.0	0.75	4100	4100	48.7	39.6	7.9
		4	0.85	2.0	0.75	4000	4000	48.9	39.6	7.9
		5	0.85	2.0	0.75	3600	3600	50.9	56.4	49.6
		6	0.85	2.0	0.75	3600	3600	51.6	39.6	7.9
		7	0.85	2.0	0.75	3700	3700	47.5	39.6	7.9
		8	0.85	2.0	0.75	4200	4200	48.2	39.6	7.9

^[1] Columns arranged in alphabetical order of notation; notation described in Appendix A; values given in SI units are converted to in.-lb (1 in. = 25.4 mm; 1 psi = 1/145 Mpa; and 1 kip = 4.4484 kN)

^[3] Analyzed as a doubly reinforced section to calculate the nominal flexural strength M_n ; all other specimens are analyzed as a single reinforced

^[4] Specimens did not contain confining reinforcement parallel to the hooked bars within the joint region

^[5] Specimens had transverse beams on one or both sides of the test beam. These transverse beams meet the dimensional requirements of Sections 18.8.4 and 15.2.8 of ACI 318-19 and Section 4.3 of ACI 352R-02 to be considered effective in increasing the joint shear strength

^[7] Specimens had column to beam flexural strength ratio, M_R , less than 1.2

^[8] Column concrete compressive strength

^[9] Beam concrete compressive strength

Table C.4 Cont. Data for exterior beam-column joint specimens tested under reversed cyclic loading ^[1]

Study		Specimen	h_b (in.)	h_c (in.)	ℓ_{dh} (in.)	$\frac{\ell_{dh}}{d_b}$	ℓ_{eh} (in.)	$\frac{\ell_{eh}}{d_b}$	ℓ_{ehy} (in.)	$\frac{\ell_{ehy}}{d_b}$
1	Hanson and Connor (1967)	I ^[3]	20.0	15.0	12.6	11.2	13.5	12.0	11.2	9.9
		I-A ^[3]	20.0	15.0	13.2	11.7	13.5	12.0	10.8	9.6
		II	20.0	15.0	11.7	10.4	13.5	12.0	10.3	9.1
		III ^[7]	20.0	15.0	15.3	13.6	13.5	12.0	13.8	12.2
		IV ^[7]	20.0	15.0	17.3	15.3	13.5	12.0	15.7	14.0
		V ^{[3][4]}	20.0	15.0	20.7	18.3	13.5	12.0	16.6	14.7
		V-A ^[4]	20.0	15.0	20.4	18.0	13.5	12.0	16.4	14.5
2	Hanson (1971)	1 ^[5]	20.0	15.0	12.8	12.8	13.5	13.5	11.8	11.8
		3 ^[5]	20.0	15.0	13.1	13.1	13.5	13.5	12.1	12.1
		4	20.0	15.0	15.4	15.4	13.5	13.5	12.6	12.6
		5	20.0	15.0	13.3	13.3	13.5	13.5	12.2	12.2
3	Megget (1974)	Unit A	18.1	15.0	12.7	12.7	12.6	12.6	11.7	11.7
4	Uzumeri (1977)	1 ^{[4][5]}	20.0	15.0	19.8	17.6	13.0	11.5	15.6	13.8
		2 ^[4]	20.0	15.0	19.9	17.6	13.0	11.5	15.7	13.9
		3 ^[5]	20.0	15.0	13.2	11.7	13.0	11.5	11.5	10.2
		4 ^[5]	20.0	15.0	12.7	11.3	13.0	11.5	11.1	9.8
		5 ^{[4][5]}	20.0	15.0	20.9	18.6	13.0	11.5	16.2	14.4
		6	20.0	15.0	14.6	12.9	13.0	11.5	12.6	11.1
		7	20.0	15.0	15.2	13.5	13.0	11.5	13.1	11.7
		8	20.0	15.0	16.9	14.9	13.0	11.5	15.1	13.4
5	Lee et al. (1977)	1	10.0	11.0	9.0	12.0	9.4	12.5	8.6	11.5
		2	10.0	11.0	8.3	11.1	9.4	12.5	7.9	10.6
		3	10.0	11.0	8.4	11.2	9.4	12.5	8.0	10.7
		4	10.0	11.0	8.5	11.3	9.4	12.5	8.1	10.8
		5	10.0	11.0	9.1	12.1	9.4	12.5	8.7	11.6
		6	10.0	11.0	9.2	12.3	9.4	12.5	8.8	11.8
		7	10.0	11.0	8.4	11.2	9.4	12.5	8.0	10.7
		8	10.0	11.0	8.3	11.0	9.4	12.5	7.9	10.5

^[1] Columns arranged in alphabetical order of notation; notation described in Appendix A; values given in SI units are converted to in.-lb (1 in. = 25.4 mm; 1 psi = 1/145 Mpa; and 1 kip = 4.4484 kN)

^[2] Bar sizes are presented in SI and in.-lb as reported in the original studies

^[3] Analyzed as a doubly reinforced section to calculate the nominal flexural strength M_n ; all other specimens are analyzed as a single reinforced

^[4] Specimens did not contain confining reinforcement parallel to the hooked bars within the joint region

^[5] Specimens had transverse beams on one or both sides of the test beam. These transverse beams meet the dimensional requirements of Sections 18.8.4 and 15.2.8 of ACI 318-19 and Section 4.3 of ACI 352R-02 to be considered effective in increasing the joint shear strength

^[6] Specimens had $d/\ell_{eh} > 1.5$

^[7] Specimens had column to beam flexural strength ratio, M_R , less than 1.2

Table C.4 Cont. Data for exterior beam-column joint specimens tested under reversed cyclic loading ^[1]

Study		Specimen	$\frac{\ell_{eh}}{h_c}$	$\frac{\ell_{eh}}{\ell_{dh}}$	$\frac{\ell_{eh}}{\ell_{ehy}}$	M_n (kip.in.)	M_{peak} (kip.in.)	$\frac{M_{peak}}{M_n}$	N	N_{total}
1	Hanson and Connor (1967)	I ^[3]	0.9	1.07	1.21	3018	3384	1.12	3	5
		I-A ^[3]	0.9	1.02	1.24	2796	2976	1.06	3	5
		II	0.9	1.15	1.32	2892	3036	1.05	3	5
		III ^[7]	0.9	0.88	0.98	2820	2616	0.93	3	5
		IV ^[7]	0.9	0.78	0.86	2952	2892	0.98	3	5
		V ^{[3][4]}	0.9	0.65	0.81	2964	2640	0.89	0	0
		V-A ^[4]	0.9	0.66	0.82	3156	3372	1.07	0	0
2	Hanson (1971)	1 ^[5]	0.9	1.06	1.15	3229	3374	1.04	3	6
		3 ^[5]	0.9	1.03	1.11	3253	3662	1.13	3	5
		4	0.9	0.88	1.08	3234	3638	1.13	2	4
		5	0.9	1.02	1.10	3294	3614	1.10	3	6
3	Megget (1974)	Unit A	0.8	0.99	1.07	1923	1944	1.01	4	6
4	Uzumeri (1977)	1 ^{[4][5]}	0.9	0.66	0.83	2340	2475	1.06	0	0
		2 ^[4]	0.9	0.65	0.83	2352	2419	1.03	0	0
		3 ^[5]	0.9	0.98	1.13	2340	2588	1.11	4	4
		4 ^[5]	0.9	1.02	1.17	2352	2700	1.15	4	4
		5 ^{[4][5]}	0.9	0.62	0.80	2364	2531	1.07	0	0
		6	0.9	0.89	1.03	2412	2700	1.12	7	8
		7	0.9	0.86	0.99	2400	2813	1.17	4	4
		8	0.9	0.77	0.86	3132	3263	1.04	7	8
5	Lee et al. (1977)	1	0.9	1.04	1.09	332	372	1.12	4	4
		2	0.9	1.13	1.18	310	349	1.12	4	4
		3	0.9	1.12	1.17	310	314	1.01	2	2
		4	0.9	1.10	1.16	310	360	1.16	2	2
		5	0.9	1.03	1.08	317	382	1.20	4	4
		6	0.9	1.02	1.06	321	371	1.16	2	2
		7	0.9	1.12	1.17	300	361	1.20	2	2
		8	0.9	1.13	1.19	308	355	1.15	2	2

^[1] Columns arranged in alphabetical order of notation; notation described in Appendix A; values given in SI units are converted to in.-lb (1 in. = 25.4 mm; 1 psi = 1/145 Mpa; and 1 kip = 4.4484 kN)

^[2] Bar sizes are presented in SI and in.-lb as reported in the original studies

^[3] Analyzed as a doubly reinforced section to calculate the nominal flexural strength M_n ; all other specimens are analyzed as a single reinforced

^[4] Specimens did not contain confining reinforcement parallel to the hooked bars within the joint region

^[5] Specimens had transverse beams on one or both sides of the test beam. These transverse beams meet the dimensional requirements of Sections 18.8.4 and 15.2.8 of ACI 318-19 and Section 4.3 of ACI 352R-02 to be considered effective in increasing the joint shear strength

^[6] Specimens had $d/\ell_{eh} > 1.5$

^[7] Specimens had column to beam flexural strength ratio, M_R , less than 1.2

Table C.4 Cont. Data for exterior beam-column joint specimens tested under reversed cyclic loading ^[1]

Study		Specimen	<i>n</i>	<i>nT'</i> (kips)	<i>s_{tr}</i> (in.)	<i>T_h</i> (kips)	<i>T'</i> (kips)	<i>T'</i> _{mod} (kips)	$\frac{T'}{T_h}$	$\frac{T'_{mod}}{T_h}$
1	Hanson and Connor (1967)	I ^[3]	4	231.4	4.5	51.9	57.9	56.5	1.12	1.09
		I-A ^[3]	4	203.5	4.5	48.0	50.9	49.4	1.06	1.03
		II	4	202.8	4.5	48.6	50.7	48.8	1.04	1.00
		III ^[7]	4	178.9	4.5	47.5	44.7	-	0.94	-
		IV ^[7]	4	195.5	4.5	43.6	48.9	-	1.12	-
		V ^{[3][4]}	4	181.7	0.0	40.8	45.4	-	1.11	-
		V-A ^[4]	4	212.8	0.0	40.4	53.2	-	1.32	-
2	Hanson (1971)	1 ^[5]	4	208.4	3.2	50.1	52.1	51.2	1.04	1.02
		3 ^[5]	4	228.0	4.0	50.9	57.0	56.3	1.12	1.11
		4	4	225.4	5.3	50.3	56.3	55.9	1.12	1.11
		5	4	225.4	3.2	51.6	56.3	55.7	1.09	1.08
3	Megget (1974)	Unit A	3	131.0	2.0	43.4	43.7	43.4	1.01	1.00
4	Uzumeri (1977)	1 ^{[4][5]}	3	159.6	0.0	41.2	53.2	-	1.29	-
		2 ^[4]	3	156.1	0.0	41.3	52.0	-	1.26	-
		3 ^[5]	3	168.5	3.0	51.1	56.2	55.5	1.10	1.08
		4 ^[5]	3	174.3	3.0	50.9	58.1	57.2	1.14	1.12
		5 ^{[4][5]}	3	161.9	0.0	39.6	54.0	-	1.36	-
		6	3	171.6	1.8	51.3	57.2	57.0	1.11	1.11
		7	3	179.6	3.0	50.8	59.9	-	1.18	-
		8	4	212.9	1.8	44.8	53.2	-	1.19	-
5	Lee et al. (1977)	1	2	51.7	1.25	23.2	25.9	25.6	1.11	1.10
		2	2	48.1	1.25	21.5	24.0	23.6	1.12	1.10
		3	2	43.4	3.00	21.5	21.7	21.2	1.01	0.99
		4	2	50.0	3.00	21.6	25.0	24.6	1.16	1.14
		5	2	53.9	1.25	22.5	26.9	26.7	1.20	1.19
		6	2	52.5	3.00	22.8	26.2	26.1	1.15	1.14
		7	2	50.3	3.00	21.0	25.2	24.7	1.20	1.18
		8	2	48.9	3.00	21.3	24.4	23.9	1.15	1.12

^[1] Columns arranged in alphabetical order of notation; notation described in Appendix A; values given in SI units are converted to in.-lb (1 in. = 25.4 mm; 1 psi = 1/145 Mpa; and 1 kip = 4.4484 kN)

^[2] Bar sizes are presented in SI and in.-lb as reported in the original studies

^[3] Analyzed as a doubly reinforced section to calculate the nominal flexural strength M_n ; all other specimens are analyzed as a single reinforced

^[4] Specimens did not contain confining reinforcement parallel to the hooked bars within the joint region

^[5] Specimens had transverse beams on one or both sides of the test beam. These transverse beams meet the dimensional requirements of Sections 18.8.4 and 15.2.8 of ACI 318-19 and Section 4.3 of ACI 352R-02 to be considered effective in increasing the joint shear strength

^[6] Specimens had $d/\ell_{eh} > 1.5$

^[7] Specimens had column to beam flexural strength ratio, M_R , less than 1.2

Table C.4 Cont. Data for exterior beam-column joint specimens tested under reversed cyclic loading ^[1]

Study		Specimen	V_n (kips)	$V_{n,ACI 352}$ (kips)	V_p (kips)	$\frac{V_p}{V_n}$	$\delta_{0.8 peak}$	ψ_o
1	Hanson and Connor (1967)	I ^[3]	204.2	183.8	186.4	0.91	0.043	1.00
		I-A ^[3]	197.0	177.3	163.9	0.83	0.057	1.00
		II	208.4	187.6	167.2	0.80	0.035	1.00
		III ^[7]	151.7	151.7	144.1	0.95	0.029	1.25
		IV ^[7]	127.6	127.6	159.3	1.25	0.082	1.25
		V ^{[3][4]}	198.8	178.9	145.4	0.73	0.051	1.00
		V-A ^[4]	195.4	175.8	185.8	0.95	0.021	1.00
2	Hanson (1971)	1 ^[5]	252.8	227.5	181.1	0.72	0.060	1.00
		3 ^[5]	246.6	222.0	196.6	0.80	0.035	1.00
		4	195.4	175.9	195.3	1.00	0.030	1.00
		5	198.8	178.9	194.0	0.98	0.045	1.00
3	Megget (1974)	Unit A	131.9	117.0	132.8	1.01	0.175	1.00
4	Uzumeri (1977)	1 ^{[4][5]}	225.4	202.9	140.9	0.63	0.033	1.00
		2 ^[4]	181.3	163.2	136.9	0.76	0.021	1.00
		3 ^[5]	211.3	190.2	145.7	0.69	0.055	1.00
		4 ^[5]	226.2	203.5	165.1	0.73	0.095	1.00
		5 ^{[4][5]}	229.6	229.6	136.7	0.60	0.016	1.25
		6	195.6	195.6	163.7	0.84	0.061	1.25
		7	180.3	180.3	157.1	0.87	0.063	1.25
		8	166.9	166.9	188.4	1.13	0.045	1.25
5	Lee et al. (1977)	1	68.4	68.4	55.1	0.80	0.042	1.25
		2	68.4	68.4	51.6	0.75	0.055	1.25
		3	67.6	67.6	46.5	0.69	0.042	1.25
		4	66.8	66.8	53.3	0.80	0.055	1.25
		5	63.4	63.4	56.4	0.89	0.059	1.25
		6	63.4	63.4	54.9	0.87	0.062	1.25
		7	64.2	64.2	53.3	0.83	0.060	1.25
		8	68.4	68.4	52.4	0.77	0.058	1.25

^[1] Columns arranged in alphabetical order of notation; notation described in Appendix A; values given in SI units are converted to in.-lb (1 in. = 25.4 mm; 1 psi = 1/145 Mpa; and 1 kip = 4.4484 kN)

^[2] Bar sizes are presented in SI and in.-lb as reported in the original studies

^[3] Analyzed as a doubly reinforced section to calculate the nominal flexural strength M_n ; all other specimens are analyzed as a single reinforced

^[4] Specimens did not contain confining reinforcement parallel to the hooked bars within the joint region

^[5] Specimens had transverse beams on one or both sides of the test beam. These transverse beams meet the dimensional requirements of Sections 18.8.4 and 15.2.8 of ACI 318-19 and Section 4.3 of ACI 352R-02 to be considered effective in increasing the joint shear strength

^[6] Specimens had $d/\ell_{eh} > 1.5$

^[7] Specimens had column to beam flexural strength ratio, M_R , less than 1.2

Table C.4 Cont. Data for exterior beam-column joint specimens tested under reversed cyclic loading ^[1]

Study		Specimen	Bar Size ^[2]	A_b (in. ²)	A_{hs} (in. ²)	A_{tr} (in. ²)	A_{th} (in. ²)	$\frac{A_{th}}{A_{hs}}$	A_v (in. ²)	b_b (in.)
6	Scribner (1978)	1	No. 6	0.44	0.88	0.11	0.66	0.75	0.66	8.0
		2	No. 6	0.44	0.88	0.11	0.66	0.75	0.66	8.0
		3	No. 6	0.44	1.32	0.11	0.88	0.67	1.10	8.0
		4	No. 6	0.44	1.32	0.11	0.88	0.67	1.10	8.0
		5	No. 6	0.44	0.88	0.11	0.66	0.75	0.66	8.0
		6	No. 6	0.44	0.88	0.11	0.66	0.75	0.66	8.0
		7	No. 6	0.44	1.32	0.11	0.88	0.67	1.10	8.0
		8	No. 6	0.44	1.32	0.11	0.88	0.67	1.10	8.0
		9	No. 8	0.79	3.16	0.20	0.80	0.25	1.60	10.0
		10	No. 8	0.79	3.16	0.20	0.80	0.25	1.60	10.0
		11	No. 8	0.79	3.16	0.20	0.80	0.25	1.60	10.0
		12	No. 8	0.79	3.16	0.20	0.80	0.25	1.60	10.0
7	Paulay and Scarpas (1981)	Unit 1	D20	0.49	2.92	0.18	1.40	0.48	2.80	14.0
		Unit 2	D20	0.49	3.90	0.12	0.97	0.25	1.46	14.0
		Unit 3	D20	0.49	2.92	0.12	0.97	0.33	1.95	14.0
8	Ehsani and Wight (1982)	1 ^[7]	No. 7	0.60	3.60	0.20	0.40	0.11	0.80	10.2
		2 ^[6]	No. 7	0.60	3.60	0.20	0.40	0.11	0.80	10.2
		3 ^[7]	No. 7	0.60	3.60	0.20	0.80	0.22	1.20	10.2
		4 ^[6]	No. 7	0.60	3.60	0.20	0.80	0.22	1.20	10.2
9	Kanada et al. (1984)	U40L ^[4]	D19	0.44	1.77	0.00	0.00	0.00	0.00	10.2
		U41L	D19	0.44	1.77	0.10	0.39	0.22	0.39	10.2
		U42L	D19	0.44	1.77	0.10	0.59	0.33	0.59	10.2
		U41S ^[6]	D19	0.44	1.77	0.10	0.39	0.22	0.39	10.2
		U40L ^[4]	D19	0.44	1.77	0.10	0.59	0.33	0.59	10.2
		U20L ^[4]	D19	0.44	0.88	0.00	0.00	0.00	0.00	10.2
		U21L	D19	0.44	0.88	0.10	0.39	0.45	0.39	10.2
		U21S ^[6]	D19	0.44	0.88	0.10	0.39	0.45	0.39	10.2

^[1] Columns arranged in alphabetical order of notation; notation described in Appendix A; values given in SI units are converted to in.-lb (1 in. = 25.4 mm; 1 psi = 1/145 Mpa; and 1 kip = 4.4484 kN)

^[2] Bar sizes are presented in SI and in.-lb as reported in the original studies

^[3] Analyzed as a doubly reinforced section to calculate the nominal flexural strength M_n ; all other specimens are analyzed as a single reinforced

^[4] Specimens did not contain confining reinforcement parallel to the hooked bars within the joint region

^[5] Specimens had transverse beams on one or both sides of the test beam. These transverse beams meet the dimensional requirements of Sections 18.8.4 and 15.2.8 of ACI 318-19 and Section 4.3 of ACI 352R-02 to be considered effective in increasing the joint shear strength

^[6] Specimens had $d/\ell_{eh} > 1.5$

^[7] Specimens had column to beam flexural strength ratio, M_R , less than 1.2

Table C.4 Cont. Data for exterior beam-column joint specimens tested under reversed cyclic loading^[1]

Study		Specimen	b_c (in.)	b_j (in.)	$b_{j,ACI 352}$ (in.)	c_{ch} (in.)	$\frac{c_{ch}}{d_b}$	c_{so} (in.)	$\frac{c_{so}}{d_b}$	d
6	Scribner (1978)	1	8.0	8.0	8.0	5.2	6.9	1.0	1.4	8.6
		2	8.0	8.0	8.0	5.2	6.9	1.0	1.4	8.6
		3	8.0	8.0	8.0	2.1	2.8	1.5	2.0	10.1
		4	8.0	8.0	8.0	2.1	2.8	1.5	2.0	10.1
		5	8.0	8.0	8.0	5.2	6.9	1.0	1.4	8.6
		6	8.0	8.0	8.0	5.2	6.9	1.0	1.4	8.6
		7	8.0	8.0	8.0	2.1	2.8	1.5	2.0	10.1
		8	8.0	8.0	8.0	2.1	2.8	1.5	2.0	10.1
		9	12.0	12.0	11.0	2.1	2.1	2.4	2.4	12.1
		10	12.0	12.0	11.0	2.1	2.1	2.4	2.4	12.1
		11	12.0	12.0	11.0	2.1	2.1	2.4	2.4	12.1
		12	12.0	12.0	11.0	2.1	2.1	2.4	2.4	12.1
7	Paulay and Scarpas (1981)	Unit 1	18.0	18.0	16.0	3.5	4.4	3.4	4.3	21.7
		Unit 2	18.0	18.0	16.0	3.5	4.4	3.4	4.3	21.5
		Unit 3	18.0	18.0	16.0	3.5	4.4	3.4	4.3	21.7
8	Ehsani and Wight (1982)	1 ^[7]	11.8	11.8	11.0	3.1	3.5	2.4	2.7	15.9
		2 ^[6]	11.8	11.8	11.0	3.1	3.5	2.4	2.7	14.3
		3 ^[7]	11.8	11.8	11.0	3.1	3.5	2.4	2.7	15.9
		4 ^[6]	11.8	11.8	11.0	3.1	3.5	2.4	2.7	14.3
9	Kanada et al. (1984)	U40L ^[4]	11.8	11.8	11.0	2.1	2.8	2.4	3.2	13.0
		U41L	11.8	11.8	11.0	2.1	2.8	2.4	3.2	13.0
		U42L	11.8	11.8	11.0	2.1	2.8	2.4	3.2	13.0
		U41S ^[6]	11.8	11.8	11.0	2.1	2.8	2.4	3.2	13.0
		U42S ^[6]	11.8	11.8	11.0	2.1	2.8	2.4	3.2	13.0
		U20L ^[4]	11.8	11.8	11.0	6.3	8.4	2.4	3.2	13.0
		U21L	11.8	11.8	11.0	6.3	8.4	2.4	3.2	13.0
		U21S ^[6]	11.8	11.8	11.0	6.3	8.4	2.4	3.2	13.0

^[1] Columns arranged in alphabetical order of notation; notation described in Appendix A; values given in SI units are converted to in.-lb (1 in. = 25.4 mm; 1 psi = 1/145 Mpa; and 1 kip = 4.4484 kN)

^[2] Bar sizes are presented in SI and in.-lb as reported in the original studies

^[3] Analyzed as a doubly reinforced section to calculate the nominal flexural strength M_n ; all other specimens are analyzed as a single reinforced

^[4] Specimens did not contain confining reinforcement parallel to the hooked bars within the joint region

^[5] Specimens had transverse beams on one or both sides of the test beam. These transverse beams meet the dimensional requirements of Sections 18.8.4 and 15.2.8 of ACI 318-19 and Section 4.3 of ACI 352R-02 to be considered effective in increasing the joint shear strength

^[6] Specimens had $d/\ell_{eh} > 1.5$

^[7] Specimens had column to beam flexural strength ratio, M_R , less than 1.2

Table C.4 Cont. Data for exterior beam-column joint specimens tested under reversed cyclic loading ^[1]

Study		Specimen	$\frac{d}{\ell_{eh}}$	d' (in.)	d_b (in.)	f_{cm} ^[8] (psi)	f_{cm} ^[9] (psi)	f_y (ksi)	$f_{ytr,l}$ (ksi)	$f_{ytr,l} A_v$ (kips)
6	Scribner (1978)	1	0.78	1.3	0.75	4950	4950	48.9	75.5	49.8
		2	0.78	1.3	0.75	5050	5050	48.9	75.5	49.8
		3	0.96	1.8	0.75	4940	4940	48.9	75.5	83.1
		4	0.96	1.8	0.75	4950	4950	48.9	75.5	83.1
		5	0.78	1.3	0.75	3680	3680	52.7	75.5	49.8
		6	0.78	1.3	0.75	4080	4080	52.7	75.5	49.8
		7	0.96	1.8	0.75	3840	3840	52.7	75.5	83.1
		8	0.96	1.8	0.75	3920	3920	52.7	75.5	83.1
		9	0.73	1.8	1	5130	5130	60.2	75.5	120.8
		10	0.73	1.8	1	5210	5210	60.2	75.5	120.8
		11	0.73	1.8	1	4730	4730	60.2	75.5	120.8
		12	0.73	1.8	1	4760	4760	60.2	75.5	120.8
7	Paulay and Scarpas (1981)	Unit 1	1.30	2.4	0.79	3280	3280	42.9	47.3	132.6
		Unit 2	1.29	2.6	0.79	3260	3260	42.9	46.0	66.9
		Unit 3	1.30	2.4	0.79	3900	3900	42.9	46.0	89.2
8	Ehsani and Wight (1982)	1 ^[7]	2.15	3.0	0.875	4870	4870	48.0	63.4	50.7
		2 ^[6]	1.93	3.0	0.875	5070	5070	48.0	63.4	50.7
		3 ^[7]	2.15	3.0	0.875	5930	5930	48.0	63.4	76.1
		4 ^[6]	1.93	3.0	0.875	6470	6470	48.0	63.4	76.1
9	Kanada et al. (1984)	U40L ^[4]	1.45	2.0	0.75	3530	3530	56.2	0.0	0.0
		U41L	1.45	2.0	0.75	3870	3870	56.2	42.7	16.8
		U42L	1.45	2.0	0.75	4370	4370	56.2	42.7	25.2
		U41S ^[6]	2.17	2.0	0.75	3870	3870	56.2	42.7	16.8
		U42S ^[6]	2.17	2.0	0.75	4370	4370	56.2	42.7	25.2
		U20L ^[4]	1.45	2.0	0.75	3870	3870	56.2	0.0	0.0
		U21L	1.45	2.0	0.75	4370	4370	56.2	42.7	16.8
		U21S ^[6]	2.17	2.0	0.75	3870	3870	56.2	42.7	16.8

^[1] Columns arranged in alphabetical order of notation; notation described in Appendix A; values given in SI units are converted to in.-lb (1 in. = 25.4 mm; 1 psi = 1/145 Mpa; and 1 kip = 4.4484 kN)

^[4] Specimens did not contain confining reinforcement parallel to the hooked bars within the joint region

^[5] Specimens had transverse beams on one or both sides of the test beam. These transverse beams meet the dimensional requirements of Sections 18.8.4 and 15.2.8 of ACI 318-19 and Section 4.3 of ACI 352R-02 to be considered effective in increasing the joint shear strength

^[6] Specimens had $d/\ell_{eh} > 1.5$

^[7] Specimens had column to beam flexural strength ratio, M_R , less than 1.2

^[8] Column concrete compressive strength

^[9] Beam concrete compressive strength

Table C.4 Cont. Data for exterior beam-column joint specimens tested under reversed cyclic loading^[1]

Study		Specimen	h_b (in.)	h_c (in.)	ℓ_{dh} (in.)	$\frac{\ell_{dh}}{d_b}$	ℓ_{eh} (in.)	$\frac{\ell_{eh}}{d_b}$	ℓ_{ehy} (in.)	$\frac{\ell_{ehy}}{d_b}$
6	Scribner (1978)	1	10.0	12.0	7.1	9.5	11.0	14.6	6.3	8.4
		2	10.0	12.0	7.1	9.4	11.0	14.6	6.2	8.3
		3	12.0	12.0	8.2	11.0	10.5	14.0	7.9	10.6
		4	12.0	12.0	8.2	11.0	10.5	14.0	7.9	10.6
		5	10.0	12.0	8.2	11.0	11.0	14.6	7.4	9.8
		6	10.0	12.0	8.0	10.7	11.0	14.6	7.2	9.5
		7	12.0	12.0	9.5	12.6	10.5	14.0	9.2	12.2
		8	12.0	12.0	9.4	12.5	10.5	14.0	9.1	12.2
		9	14.0	18.0	16.0	16.0	16.6	16.6	15.1	15.1
		10	14.0	18.0	15.9	15.9	16.6	16.6	15.0	15.0
		11	14.0	18.0	16.3	16.3	16.6	16.6	15.4	15.4
		12	14.0	18.0	16.3	16.3	16.6	16.6	15.4	15.4
7	Paulay and Scarpas (1981)	Unit 1	24.0	18.0	6.4	8.1	16.6	21.1	5.8	7.4
		Unit 2	24.0	18.0	6.4	8.2	16.6	21.1	5.8	7.4
		Unit 3	24.0	18.0	6.1	7.8	16.6	21.1	5.5	7.0
8	Ehsani and Wight (1982)	1 ^[7]	18.9	11.8	12.1	13.9	7.4	8.5	10.1	11.5
		2 ^[6]	17.3	11.8	12.0	13.7	7.4	8.5	9.6	11.0
		3 ^[7]	18.9	11.8	9.4	10.8	7.4	8.5	9.2	10.5
		4 ^[6]	17.3	11.8	9.2	10.5	7.4	8.5	8.4	9.6
9	Kanada et al. (1984)	U40L ^[4]	15.0	11.8	16.4	21.8	9.0	12.0	13.2	17.6
		U41L	15.0	11.8	10.1	13.4	9.0	12.0	9.8	13.1
		U42L	15.0	11.8	9.8	13.0	9.0	12.0	9.5	12.7
		U41S ^[6]	15.0	11.8	10.1	13.4	6.0	8.0	9.8	13.1
		U42S ^[6]	15.0	11.8	9.8	13.0	6.0	8.0	9.5	12.7
		U20L ^[4]	15.0	11.8	10.4	13.9	9.0	12.0	8.8	11.7
		U21L	15.0	11.8	8.4	11.2	9.0	12.0	7.5	10.1
		U21S ^[6]	15.0	11.8	8.7	11.6	6.0	8.0	7.8	10.4

^[1] Columns arranged in alphabetical order of notation; notation described in Appendix A; values given in SI units are converted to in.-lb (1 in. = 25.4 mm; 1 psi = 1/145 Mpa; and 1 kip = 4.4484 kN)

^[2] Bar sizes are presented in SI and in.-lb as reported in the original studies

^[3] Analyzed as a doubly reinforced section to calculate the nominal flexural strength M_n ; all other specimens are analyzed as a single reinforced

^[4] Specimens did not contain confining reinforcement parallel to the hooked bars within the joint region

^[5] Specimens had transverse beams on one or both sides of the test beam. These transverse beams meet the dimensional requirements of Sections 18.8.4 and 15.2.8 of ACI 318-19 and Section 4.3 of ACI 352R-02 to be considered effective in increasing the joint shear strength

^[6] Specimens had $d/\ell_{eh} > 1.5$

^[7] Specimens had column to beam flexural strength ratio, M_R , less than 1.2

Table C.4 Cont. Data for exterior beam-column joint specimens tested under reversed cyclic loading ^[1]

Study		Specimen	$\frac{\ell_{eh}}{h_c}$	$\frac{\ell_{eh}}{\ell_{dh}}$	$\frac{\ell_{eh}}{\ell_{ehy}}$	M_n (kip.in.)	M_{peak} (kip.in.)	$\frac{M_{peak}}{M_n}$	N	N_{total}
6	Scribner (1978)	1	0.9	1.55	1.75	343	481	1.41	3	3
		2	0.9	1.55	1.76	343	498	1.45	3	3
		3	0.9	1.27	1.32	590	706	1.20	4	5
		4	0.9	1.27	1.32	747	818	1.10	4	5
		5	0.9	1.33	1.49	356	453	1.27	3	3
		6	0.9	1.37	1.53	360	468	1.30	3	3
		7	0.9	1.11	1.14	710	751	1.06	4	5
		8	0.9	1.11	1.15	743	809	1.09	4	5
		9	0.9	1.04	1.10	2472	2508	1.01	2	4
		10	0.9	1.04	1.10	2520	2592	1.03	2	4
		11	0.9	1.02	1.08	2472	2501	1.01	2	4
		12	0.9	1.02	1.08	2520	2539	1.01	2	4
7	Paulay and Scarpas (1981)	Unit 1	0.9	2.59	2.86	2418	3118	1.29	2	4
		Unit 2	0.9	2.59	2.86	3481	4385	1.26	2	3
		Unit 3	0.9	2.71	3.00	2418	3340	1.38	2	4
8	Ehsani and Wight (1982)	1 ^[7]	0.6	0.61	0.74	2394	2040	0.85	1	2
		2 ^[6]	0.6	0.62	0.77	1882	1860	0.99	1	2
		3 ^[7]	0.6	0.79	0.81	2457	2520	1.03	2	3
		4 ^[6]	0.6	0.80	0.88	1938	2400	1.24	2	3
9	Kanada et al. (1984)	U40L ^[4]	0.8	0.55	0.68	1129	885	0.78	0	0
		U41L	0.8	0.89	0.91	1143	1172	1.02	2	2
		U42L	0.8	0.92	0.95	1160	1165	1.00	3	3
		U41S ^[6]	0.5	0.59	0.61	1143	631	0.55	2	2
		U42S ^[6]	0.5	0.61	0.63	1160	690	0.59	3	3
		U20L ^[4]	0.8	0.86	1.02	608	651	1.07	0	0
		U21L	0.8	1.07	1.19	613	684	1.12	2	2
		U21S ^[6]	0.5	0.69	0.77	608	495	0.81	2	2

^[1] Columns arranged in alphabetical order of notation; notation described in Appendix A; values given in SI units are converted to in.-lb (1 in. = 25.4 mm; 1 psi = 1/145 Mpa; and 1 kip = 4.4484 kN)

^[2] Bar sizes are presented in SI and in.-lb as reported in the original studies

^[3] Analyzed as a doubly reinforced section to calculate the nominal flexural strength M_n ; all other specimens are analyzed as a single reinforced

^[4] Specimens did not contain confining reinforcement parallel to the hooked bars within the joint region

^[5] Specimens had transverse beams on one or both sides of the test beam. These transverse beams meet the dimensional requirements of Sections 18.8.4 and 15.2.8 of ACI 318-19 and Section 4.3 of ACI 352R-02 to be considered effective in increasing the joint shear strength

^[6] Specimens had $d/\ell_{eh} > 1.5$

^[7] Specimens had column to beam flexural strength ratio, M_R , less than 1.2

Table C.4 Cont. Data for exterior beam-column joint specimens tested under reversed cyclic loading^[1]

Study		Specimen	<i>n</i>	<i>nT'</i> (kips)	<i>s_{tr}</i> (in.)	<i>T_h</i> (kips)	<i>T'</i> (kips)	<i>T'</i> _{mod} (kips)	$\frac{T'}{T_h}$	$\frac{T'_{mod}}{T_h}$
6	Scribner (1978)	1	2	60.5	1.75	21.6	30.2	28.2	1.40	1.30
		2	2	62.5	1.75	21.6	31.2	29.2	1.44	1.35
		3	3	77.2	1.50	21.6	25.7	24.9	1.19	1.15
		4	3	70.7	1.50	21.6	23.6	22.7	1.09	1.05
		5	2	59.0	1.75	23.3	29.5	28.1	1.26	1.20
		6	2	60.3	1.75	23.3	30.1	28.6	1.29	1.23
		7	3	73.6	1.50	23.3	24.5	24.1	1.05	1.04
		8	3	75.8	1.50	23.3	25.3	24.8	1.08	1.07
		9	4	193.0	2.00	47.7	48.3	47.7	1.01	1.00
		10	4	195.7	2.00	47.7	48.9	48.3	1.02	1.01
		11	4	192.5	2.00	47.7	48.1	47.7	1.01	1.00
		12	4	191.7	2.00	47.7	47.9	47.5	1.00	0.99
7	Paulay and Scarpas (1981)	Unit 1	6	161.7	4.3	21.1	27.0	22.0	1.28	1.05
		Unit 2	8	210.6	5.9	21.1	26.3	21.4	1.25	1.02
		Unit 3	6	173.2	4.3	21.1	28.9	23.6	1.37	1.12
8	Ehsani and Wight (1982)	1 ^[7]	6	179.6	4.4	22.1	29.9	-	1.35	-
		2 ^[6]	6	170.8	3.9	22.4	28.5	-	1.27	-
		3 ^[7]	6	218.9	3.3	25.1	36.5	-	1.45	-
		4 ^[6]	6	214.0	3.0	25.7	35.7	-	1.39	-
9	Kanada et al. (1984)	U40L ^[4]	4	77.8	0.0	16.4	19.5	-	1.19	-
		U41L	4	101.7	3.9	22.9	25.4	-	1.11	-
		U42L	4	99.7	2.0	23.6	24.9	-	1.06	-
		U41S ^[6]	4	54.8	3.9	15.6	13.7	-	0.88	-
		U42S ^[6]	4	59.0	2.0	16.1	14.8	-	0.92	-
		U20L ^[4]	2	53.1	0.0	24.8	26.6	26.5	1.07	1.07
		U21L	2	55.4	3.9	25.0	27.7	27.1	1.11	1.09
		U21S ^[6]	2	40.4	3.9	19.5	20.2	-	1.03	-

^[1] Columns arranged in alphabetical order of notation; notation described in Appendix A; values given in SI units are converted to in.-lb (1 in. = 25.4 mm; 1 psi = 1/145 Mpa; and 1 kip = 4.4484 kN)

^[2] Bar sizes are presented in SI and in.-lb as reported in the original studies

^[3] Analyzed as a doubly reinforced section to calculate the nominal flexural strength M_n ; all other specimens are analyzed as a single reinforced

^[4] Specimens did not contain confining reinforcement parallel to the hooked bars within the joint region

^[5] Specimens had transverse beams on one or both sides of the test beam. These transverse beams meet the dimensional requirements of Sections 18.8.4 and 15.2.8 of ACI 318-19 and Section 4.3 of ACI 352R-02 to be considered effective in increasing the joint shear strength

^[6] Specimens had $d/\ell_{eh} > 1.5$

^[7] Specimens had column to beam flexural strength ratio, M_R , less than 1.2

Table C.4 Cont. Data for exterior beam-column joint specimens tested under reversed cyclic loading ^[1]

Study		Specimen	V_n (kips)	$V_{n,ACI\ 352}$ (kips)	V_p (kips)	$\frac{V_p}{V_n}$	$\delta_{0.8\ peak}$	ψ_o
6	Scribner (1978)	1	81.1	81.1	56.8	0.70	0.060	1.25
		2	81.9	81.9	58.7	0.72	0.058	1.25
		3	81.0	81.0	71.5	0.88	0.047	1.25
		4	81.1	81.1	83.1	1.03	0.063	1.25
		5	69.9	69.9	53.0	0.76	0.066	1.25
		6	73.6	73.6	54.8	0.74	0.061	1.25
		7	71.4	71.4	76.2	1.07	0.060	1.25
		8	72.1	72.1	82.1	1.14	0.061	1.25
		9	185.6	170.2	213.3	1.15	0.076	1.25
		10	187.1	171.5	220.4	1.18	0.084	1.25
		11	178.3	163.4	212.2	1.19	0.052	1.25
		12	178.8	163.9	211.1	1.18	0.053	1.25
7	Paulay and Scarpas (1981)	Unit 1	222.4	197.8	136.1	0.61	0.032	1.00
		Unit 2	221.9	197.4	199.1	0.90	0.038	1.00
		Unit 3	242.6	215.8	147.2	0.61	0.035	1.00
8	Ehsani and Wight (1982)	1 ^[7]	116.6	108.7	131.5	1.13	0.038	1.25
		2 ^[6]	119.0	110.9	140.3	1.18	0.038	1.25
		3 ^[7]	128.7	119.9	162.4	1.26	0.053	1.25
		4 ^[6]	134.4	125.3	181.0	1.35	0.056	1.25
9	Kanada et al. (1984)	U40L ^[4]	99.4	92.8	62.3	0.63	0.033	1.25
		U41L	104.1	97.2	82.5	0.79	0.038	1.25
		U42L	110.6	103.2	82.0	0.74	0.033	1.25
		U41S ^[6]	104.1	97.2	44.4	0.43	0.014	1.25
		U42S ^[6]	110.6	103.2	48.6	0.44	0.020	1.25
		U20L ^[4]	104.1	97.2	45.8	0.44	0.011	1.25
		U21L	110.6	103.2	48.1	0.43	0.020	1.25
		U21S ^[6]	104.1	97.2	34.8	0.33	0.022	1.25

^[1] Columns arranged in alphabetical order of notation; notation described in Appendix A; values given in SI units are converted to in.-lb (1 in. = 25.4 mm; 1 psi = 1/145 Mpa; and 1 kip = 4.4484 kN)

^[2] Bar sizes are presented in SI and in.-lb as reported in the original studies

^[3] Analyzed as a doubly reinforced section to calculate the nominal flexural strength M_n ; all other specimens are analyzed as a single reinforced

^[4] Specimens did not contain confining reinforcement parallel to the hooked bars within the joint region

^[5] Specimens had transverse beams on one or both sides of the test beam. These transverse beams meet the dimensional requirements of Sections 18.8.4 and 15.2.8 of ACI 318-19 and Section 4.3 of ACI 352R-02 to be considered effective in increasing the joint shear strength

^[6] Specimens had $d/\ell_{eh} > 1.5$

^[7] Specimens had column to beam flexural strength ratio, M_R , less than 1.2

Table C.4 Cont. Data for exterior beam-column joint specimens tested under reversed cyclic loading ^[1]

Study		Specimen	Bar Size ^[2]	A_b (in. ²)	A_{hs} (in. ²)	A_{tr} (in. ²)	A_{th} (in. ²)	$\frac{A_{th}}{A_{hs}}$	A_v (in. ²)	b_b (in.)
9	Kanada et al. (1984)	U22S ^[6]	D19	0.44	0.88	0.10	0.59	0.67	0.59	10.2
		R41L	D19	0.44	1.77	0.10	0.39	0.22	0.39	10.2
		R42S ^[6]	D19	0.44	1.77	0.10	0.59	0.33	0.59	10.2
		R21L	D19	0.44	0.88	0.10	0.39	0.45	0.39	10.2
		R21S ^[6]	D19	0.44	0.88	0.10	0.39	0.45	0.39	10.2
10	Zerbe and Durrani (1985)	J1 ^[6]	No. 6	0.44	1.76	0.20	0.80	0.45	1.20	10.0
		J2 ^{[5][6]}	No. 6	0.44	1.76	0.20	0.80	0.45	1.20	10.0
		J3 ^[6]	No. 6	0.44	1.76	0.20	0.80	0.45	1.20	10.0
		J4 ^{[5][6]}	No. 6	0.44	1.76	0.20	0.80	0.45	1.20	10.0
		J5 ^{[5][6]}	No. 6	0.44	1.76	0.20	0.80	0.45	1.20	10.0
		J6 ^{[5][6]}	No. 6	0.44	1.76	0.20	0.80	0.45	1.20	10.0
		J7 ^[7]	No. 6	0.44	1.76	0.20	0.80	0.45	1.20	12.0
11	Ehsani et al. (1987)	1	No. 6	0.44	2.20	0.20	0.80	0.36	1.20	11.8
		2	No. 6	0.44	2.20	0.20	0.80	0.36	1.20	11.8
		3 ^[6]	No. 6	0.44	2.20	0.20	0.80	0.36	1.20	10.2
		4 ^[6]	No. 7	0.60	3.00	0.20	0.80	0.27	1.20	10.2
		5 ^[6]	No. 7	0.60	3.60	0.20	0.80	0.22	1.20	10.2
12	Kaku and Asakusa (1991)	1	D13	0.20	0.79	0.04	0.18	0.22	0.35	6.3
		2	D13	0.20	0.79	0.04	0.18	0.22	0.35	6.3
		3	D13	0.20	0.79	0.04	0.18	0.22	0.35	6.3
		4	D13	0.20	0.79	0.01	0.04	0.06	0.09	6.3
		5	D13	0.20	0.79	0.01	0.04	0.06	0.09	6.3
		6	D13	0.20	0.79	0.01	0.04	0.06	0.09	6.3
		7	D13	0.20	0.79	0.04	0.18	0.22	0.35	6.3
		8	D13	0.20	0.79	0.04	0.18	0.22	0.35	6.3
		9	D13	0.20	0.79	0.04	0.18	0.22	0.35	6.3

^[1] Columns arranged in alphabetical order of notation; notation described in Appendix A; values given in SI units are converted to in.-lb (1 in. = 25.4 mm; 1 psi = 1/145 Mpa; and 1 kip = 4.4484 kN)

^[2] Bar sizes are presented in SI and in.-lb as reported in the original studies

^[3] Analyzed as a doubly reinforced section to calculate the nominal flexural strength M_n ; all other specimens are analyzed as a single reinforced

^[4] Specimens did not contain confining reinforcement parallel to the hooked bars within the joint region

^[5] Specimens had transverse beams on one or both sides of the test beam. These transverse beams meet the dimensional requirements of Sections 18.8.4 and 15.2.8 of ACI 318-19 and Section 4.3 of ACI 352R-02 to be considered effective in increasing the joint shear strength

^[6] Specimens had $d/\ell_{eh} > 1.5$

^[7] Specimens had column to beam flexural strength ratio, M_R , less than 1.2

Table C.4 Cont. Data for exterior beam-column joint specimens tested under reversed cyclic loading ^[1]

Study		Specimen	b_c (in.)	b_j (in.)	b_j , ACI 352 (in.)	c_{ch} (in.)	$\frac{c_{ch}}{d_b}$	c_{so} (in.)	$\frac{c_{so}}{d_b}$	d
9	Kanada et al. (1984)	U22S ^[6]	11.8	11.8	11.0	6.3	8.4	2.4	3.2	13.0
		R41L	11.8	11.8	11.0	2.1	2.8	2.4	3.2	13.0
		R42S ^[6]	11.8	11.8	11.0	2.1	2.8	2.4	3.2	13.0
		R21L	11.8	11.8	11.0	6.3	8.4	2.4	3.2	13.0
		R21S ^[6]	11.8	11.8	11.0	6.3	8.4	2.4	3.2	13.0
10	Zerbe and Durrani (1985)	J1 ^[6]	12.0	12.0	11.0	1.8	2.3	3.0	4.0	12.6
		J2 ^{[5][6]}	12.0	12.0	11.0	1.8	2.3	3.0	4.0	12.6
		J3 ^[6]	12.0	12.0	11.0	1.8	2.3	3.0	4.0	12.6
		J4 ^{[5][6]}	12.0	12.0	11.0	1.8	2.3	3.0	4.0	12.6
		J5 ^{[5][6]}	12.0	12.0	11.0	1.8	2.3	3.0	4.0	12.6
		J6 ^{[5][6]}	12.0	12.0	11.0	1.8	2.3	3.0	4.0	12.6
		J7 ^[7]	12.0	12.0	12.0	1.8	2.3	3.0	4.0	12.6
11	Ehsani et al. (1987)	1	13.4	13.4	12.6	3.9	5.2	2.4	3.2	15.9
		2	13.4	13.4	12.6	3.9	5.2	2.4	3.2	15.9
		3 ^[6]	11.8	11.8	11.0	3.1	4.1	2.4	3.2	14.4
		4 ^[6]	11.8	11.8	11.0	3.1	3.5	2.4	2.7	14.4
		5 ^[6]	11.8	11.8	11.0	3.1	3.5	2.4	2.7	14.4
12	Kaku and Asakusa (1991)	1	8.7	8.7	7.5	1.7	3.3	1.6	3.2	8.0
		2	8.7	8.7	7.5	1.7	3.3	1.6	3.2	8.0
		3	8.7	8.7	7.5	1.7	3.3	1.6	3.2	8.0
		4	8.7	8.7	7.5	1.7	3.3	1.6	3.2	8.0
		5	8.7	8.7	7.5	1.7	3.3	1.6	3.2	8.0
		6	8.7	8.7	7.5	1.7	3.3	1.6	3.2	8.0
		7	8.7	8.7	7.5	1.7	3.3	1.6	3.2	8.0
		8	8.7	8.7	7.5	1.7	3.3	1.6	3.2	8.0
		9	8.7	8.7	7.5	1.7	3.3	1.6	3.2	8.0

^[1] Columns arranged in alphabetical order of notation; notation described in Appendix A; values given in SI units are converted to in.-lb (1 in. = 25.4 mm; 1 psi = 1/145 Mpa; and 1 kip = 4.4484 kN)

^[2] Bar sizes are presented in SI and in.-lb as reported in the original studies

^[3] Analyzed as a doubly reinforced section to calculate the nominal flexural strength M_n ; all other specimens are analyzed as a single reinforced

^[4] Specimens did not contain confining reinforcement parallel to the hooked bars within the joint region

^[5] Specimens had transverse beams on one or both sides of the test beam. These transverse beams meet the dimensional requirements of Sections 18.8.4 and 15.2.8 of ACI 318-19 and Section 4.3 of ACI 352R-02 to be considered effective in increasing the joint shear strength

^[6] Specimens had $d/\ell_{ch} > 1.5$

^[7] Specimens had column to beam flexural strength ratio, M_R , less than 1.2

Table C.4 Cont. Data for exterior beam-column joint specimens tested under reversed cyclic loading ^[1]

Study		Specimen	$\frac{d}{\ell_{eh}}$	d' (in.)	d_b (in.)	f_{cm} ^[8] (psi)	f_{cm} ^[9] (psi)	f_y (ksi)	$f_{ytr,l}$ (ksi)	$f_{ytr,l} A_v$ (kips)
9	Kanada et al. (1984)	U22S ^[6]	2.17	2.0	0.75	4370	4370	56.2	42.7	25.2
		R41L	1.45	2.0	0.75	3140	3140	56.2	42.7	16.8
		R42S ^[6]	2.17	2.0	0.75	3140	3140	56.2	42.7	25.2
		R21L	1.45	2.0	0.75	3140	3140	56.2	42.7	16.8
		R21S ^[6]	2.17	2.0	0.75	3140	3140	56.2	42.7	16.8
10	Zerbe and Durrani (1985)	J1 ^[6]	1.63	2.4	0.75	5710	5710	60.0	77.0	92.4
		J2 ^{[5][6]}	1.63	2.4	0.75	5650	5650	60.0	77.0	92.4
		J3 ^[6]	1.63	2.4	0.75	5780	5780	60.0	77.0	92.4
		J4 ^{[5][6]}	1.63	2.4	0.75	5940	5940	60.0	77.0	92.4
		J5 ^{[5][6]}	1.63	2.4	0.75	5610	5610	60.0	77.0	92.4
		J6 ^{[5][6]}	1.63	2.4	0.75	5690	5690	60.0	77.0	92.4
		J7 ^[7]	1.63	2.4	0.75	5900	5900	60.0	77.0	92.4
11	Ehsani et al. (1987)	1	1.47	3.0	0.75	9380	9380	70.0	63.4	76.1
		2	1.47	3.0	0.75	9760	9760	70.0	63.4	76.1
		3 ^[6]	1.57	2.9	0.75	9380	9380	70.0	63.4	76.1
		4 ^[6]	1.55	2.9	0.875	9760	9760	62.0	63.4	76.1
		5 ^[6]	1.67	2.9	0.875	6470	6470	48.0	63.4	76.1
12	Kaku and Asakusa (1991)	1	1.04	0.7	0.5	4510	4510	56.7	36.3	12.7
		2	1.04	0.7	0.5	6050	6050	56.7	36.3	12.7
		3	1.04	0.7	0.5	6050	6050	56.7	36.3	12.7
		4	1.04	0.7	0.5	6480	6480	56.7	40.7	3.6
		5	1.04	0.7	0.5	5320	5320	56.7	40.7	3.6
		6	1.04	0.7	0.5	5860	5860	56.7	40.7	3.6
		7	1.04	0.7	0.5	4670	4670	56.7	36.3	12.7
		8	1.04	0.7	0.5	5970	5970	56.7	36.3	12.7
		9	1.04	0.7	0.5	5890	5890	56.7	36.3	12.7

^[1] Columns arranged in alphabetical order of notation; notation described in Appendix A; values given in SI units are converted to in.-lb (1 in. = 25.4 mm; 1 psi = 1/145 Mpa; and 1 kip = 4.4484 kN)

^[4] Specimens did not contain confining reinforcement parallel to the hooked bars within the joint region

^[5] Specimens had transverse beams on one or both sides of the test beam. These transverse beams meet the dimensional requirements of Sections 18.8.4 and 15.2.8 of ACI 318-19 and Section 4.3 of ACI 352R-02 to be considered effective in increasing the joint shear strength

^[6] Specimens had $d/\ell_{eh} > 1.5$

^[7] Specimens had column to beam flexural strength ratio, M_R , less than 1.2

^[8] Column concrete compressive strength

^[9] Beam concrete compressive strength

Table C.4 Cont. Data for exterior beam-column joint specimens tested under reversed cyclic loading ^[1]

Study		Specimen	h_b (in.)	h_c (in.)	ℓ_{dh} (in.)	$\frac{\ell_{dh}}{d_b}$	ℓ_{eh} (in.)	$\frac{\ell_{eh}}{d_b}$	ℓ_{ehy} (in.)	$\frac{\ell_{ehy}}{d_b}$
9	Kanada et al. (1984)	U22S ^[6]	15.0	11.8	8.4	11.2	6.0	8.0	7.5	10.1
		R41L	15.0	11.8	10.6	14.1	9.0	12.0	10.4	13.8
		R42S ^[6]	15.0	11.8	10.6	14.1	6.0	8.0	10.4	13.8
		R21L	15.0	11.8	9.1	12.2	9.0	12.0	8.3	11.0
		R21S ^[6]	15.0	11.8	9.1	12.2	6.0	8.0	8.3	11.0
10	Zerbe and Durrani (1985)	J1 ^[6]	15.0	12.0	8.0	10.6	7.8	10.3	7.7	10.3
		J2 ^{[5][6]}	15.0	12.0	8.0	10.6	7.8	10.3	7.7	10.3
		J3 ^[6]	15.0	12.0	7.9	10.6	7.8	10.3	7.7	10.2
		J4 ^{[5][6]}	15.0	12.0	7.9	10.5	7.8	10.3	7.6	10.2
		J5 ^{[5][6]}	15.0	12.0	8.0	10.7	7.8	10.3	7.7	10.3
		J6 ^{[5][6]}	15.0	12.0	8.0	10.6	7.8	10.3	7.7	10.3
		J7 ^[7]	15.0	12.0	7.9	10.5	7.8	10.3	7.6	10.2
11	Ehsani et al. (1987)	1	18.9	13.4	9.0	12.0	10.8	14.4	8.3	11.1
		2	18.9	13.4	8.9	11.9	10.8	14.4	8.2	10.9
		3 ^[6]	17.3	11.8	9.5	12.6	9.2	12.3	8.8	11.8
		4 ^[6]	17.3	11.8	10.7	12.3	9.3	10.6	9.8	11.3
		5 ^[6]	17.3	11.8	9.2	10.5	8.6	9.8	8.4	9.6
12	Kaku and Asakusa (1991)	1	8.7	8.7	5.2	10.4	7.7	15.4	5.3	10.7
		2	8.7	8.7	4.8	9.7	7.7	15.4	4.9	9.8
		3	8.7	8.7	4.8	9.7	7.7	15.4	4.9	9.8
		4	8.7	8.7	6.6	13.2	7.7	15.4	5.1	10.2
		5	8.7	8.7	6.9	13.8	7.7	15.4	5.4	10.7
		6	8.7	8.7	6.7	13.5	7.7	15.4	5.2	10.4
		7	8.7	8.7	5.2	10.3	7.7	15.4	5.3	10.6
		8	8.7	8.7	4.9	9.7	7.7	15.4	4.9	9.9
		9	8.7	8.7	4.9	9.7	7.7	15.4	5.0	9.9

^[1] Columns arranged in alphabetical order of notation; notation described in Appendix A; values given in SI units are converted to in.-lb (1 in. = 25.4 mm; 1 psi = 1/145 Mpa; and 1 kip = 4.4484 kN)

^[2] Bar sizes are presented in SI and in.-lb as reported in the original studies

^[3] Analyzed as a doubly reinforced section to calculate the nominal flexural strength M_n ; all other specimens are analyzed as a single reinforced

^[4] Specimens did not contain confining reinforcement parallel to the hooked bars within the joint region

^[5] Specimens had transverse beams on one or both sides of the test beam. These transverse beams meet the dimensional requirements of Sections 18.8.4 and 15.2.8 of ACI 318-19 and Section 4.3 of ACI 352R-02 to be considered effective in increasing the joint shear strength

^[6] Specimens had $d/\ell_{eh} > 1.5$

^[7] Specimens had column to beam flexural strength ratio, M_R , less than 1.2

Table C.4 Cont. Data for exterior beam-column joint specimens tested under reversed cyclic loading ^[1]

Study		Specimen	$\frac{\ell_{eh}}{h_c}$	$\frac{\ell_{eh}}{\ell_{dh}}$	$\frac{\ell_{eh}}{\ell_{ehy}}$	M_n (kip.in.)	M_{peak} (kip.in.)	$\frac{M_{peak}}{M_n}$	N	N_{total}
9	Kanada et al. (1984)	U22S ^[6]	0.5	0.71	0.79	613	573	0.94	3	3
		R41L	0.8	0.85	0.86	1110	1022	0.92	2	2
		R42S ^[6]	0.5	0.56	0.58	1110	664	0.60	3	3
		R21L	0.8	0.98	1.09	600	664	1.11	2	2
		R21S ^[6]	0.5	0.65	0.73	600	495	0.82	2	2
10	Zerbe and Durrani (1985)	J1 ^[6]	0.6	0.97	1.01	1216	1287	1.06	2	3
		J2 ^{[5][6]}	0.6	0.97	1.00	1214	1518	1.25	2	3
		J3 ^[6]	0.6	0.98	1.01	1216	1320	1.09	2	3
		J4 ^{[5][6]}	0.6	0.98	1.02	1900	2079	1.09	2	3
		J5 ^{[5][6]}	0.6	0.97	1.00	2221	2244	1.01	2	3
		J6 ^{[5][6]}	0.6	0.97	1.00	1218	2211	1.82	2	3
		J7 ^[7]	0.6	0.98	1.01	2869	2211	0.77	2	3
11	Ehsani et al. (1987)	1	0.8	1.20	1.30	1729	2170	1.26	2	3
		2	0.8	1.21	1.32	2041	2666	1.31	2	3
		3 ^[6]	0.8	0.97	1.04	1663	1984	1.19	2	3
		4 ^[6]	0.8	0.87	0.94	2290	2232	0.97	2	3
		5 ^[6]	0.7	0.93	1.02	2101	2280	1.09	2	3
12	Kaku and Asakusa (1991)	1	0.9	1.48	1.44	335	427	1.27	2	4
		2	0.9	1.59	1.56	341	430	1.26	2	4
		3	0.9	1.59	1.56	338	374	1.10	2	4
		4	0.9	1.17	1.51	334	412	1.23	2	4
		5	0.9	1.11	1.43	332	380	1.14	2	4
		6	0.9	1.14	1.47	340	360	1.06	2	4
		7	0.9	1.49	1.46	335	428	1.28	2	4
		8	0.9	1.58	1.56	335	419	1.25	2	4
		9	0.9	1.58	1.55	335	406	1.21	2	4

^[1] Columns arranged in alphabetical order of notation; notation described in Appendix A; values given in SI units are converted to in.-lb (1 in. = 25.4 mm; 1 psi = 1/145 Mpa; and 1 kip = 4.4484 kN)

^[2] Bar sizes are presented in SI and in.-lb as reported in the original studies

^[3] Analyzed as a doubly reinforced section to calculate the nominal flexural strength M_n ; all other specimens are analyzed as a single reinforced

^[4] Specimens did not contain confining reinforcement parallel to the hooked bars within the joint region

^[5] Specimens had transverse beams on one or both sides of the test beam. These transverse beams meet the dimensional requirements of Sections 18.8.4 and 15.2.8 of ACI 318-19 and Section 4.3 of ACI 352R-02 to be considered effective in increasing the joint shear strength

^[6] Specimens had $d/\ell_{eh} > 1.5$

^[7] Specimens had column to beam flexural strength ratio, M_R , less than 1.2

Table C.4 Cont. Data for exterior beam-column joint specimens tested under reversed cyclic loading ^[1]

Study		Specimen	n	nT' (kips)	s_{tr} (in.)	T_h (kips)	T' (kips)	T'_{mod} (kips)	$\frac{T'}{T_h}$	$\frac{T'_{mod}}{T_h}$
9	Kanada et al. (1984)	U22S ^[6]	2	46.4	2.0	20.1	23.2	-	1.15	-
		R41L	4	91.4	3.9	21.7	22.9	-	1.06	-
		R42S ^[6]	4	59.4	2.0	14.8	14.9	-	1.00	-
		R21L	2	54.9	3.9	25.0	27.5	27.2	1.10	1.09
		R21S ^[6]	2	40.9	3.9	18.5	20.5	-	1.10	-
10	Zerbe and Durrani (1985)	J1 ^[6]	4	111.8	3.0	26.5	27.9	27.9	1.05	1.05
		J2 ^{[5][6]}	4	132.0	3.0	26.5	33.0	33.0	1.24	1.24
		J3 ^[6]	4	114.6	3.0	26.5	28.7	28.6	1.08	1.08
		J4 ^{[5][6]}	4	115.5	3.0	26.5	28.9	28.8	1.09	1.09
		J5 ^{[5][6]}	4	106.7	3.0	26.5	26.7	26.7	1.01	1.01
		J6 ^{[5][6]}	4	91.7	3.0	26.5	22.9	22.9	0.86	0.86
		J7 ^[7]	4	81.4	3.0	26.5	20.3	20.3	0.77	0.8
11	Ehsani et al. (1987)	1	5	193.3	3.5	30.9	38.7	37.5	1.25	1.21
		2	5	201.2	3.5	30.9	40.2	39.0	1.30	1.26
		3 ^[6]	5	183.7	2.2	30.9	36.7	36.6	1.19	1.18
		4 ^[6]	5	181.3	2.5	35.3	36.3	-	1.03	-
		5 ^[6]	6	187.5	2.5	28.9	31.3	31.2	1.08	1.08
12	Kaku and Asakusa (1991)	1	4	56.7	2.0	11.2	14.2	13.6	1.27	1.21
		2	4	56.2	2.0	11.2	14.1	13.3	1.26	1.19
		3	4	49.2	2.0	11.2	12.3	11.5	1.10	1.03
		4	4	54.9	2.0	11.2	13.7	13.0	1.23	1.17
		5	4	50.9	2.0	11.2	12.7	12.1	1.14	1.09
		6	4	47.2	2.0	11.2	11.8	11.1	1.06	1.00
		7	4	56.9	2.0	11.2	14.2	13.6	1.27	1.22
		8	4	55.8	2.0	11.2	13.9	13.2	1.25	1.18
		9	4	54.0	2.0	11.2	13.5	12.7	1.21	1.14

^[1] Columns arranged in alphabetical order of notation; notation described in Appendix A; values given in SI units are converted to in.-lb (1 in. = 25.4 mm; 1 psi = 1/145 Mpa; and 1 kip = 4.4484 kN)

^[2] Bar sizes are presented in SI and in.-lb as reported in the original studies

^[3] Analyzed as a doubly reinforced section to calculate the nominal flexural strength M_n ; all other specimens are analyzed as a single reinforced

^[4] Specimens did not contain confining reinforcement parallel to the hooked bars within the joint region

^[5] Specimens had transverse beams on one or both sides of the test beam. These transverse beams meet the dimensional requirements of Sections 18.8.4 and 15.2.8 of ACI 318-19 and Section 4.3 of ACI 352R-02 to be considered effective in increasing the joint shear strength

^[6] Specimens had $d/\ell_{eh} > 1.5$

^[7] Specimens had column to beam flexural strength ratio, M_R , less than 1.2

Table C.4 Cont. Data for exterior beam-column joint specimens tested under reversed cyclic loading ^[1]

Study		Specimen	V_n (kips)	V_n , ACI 352 (kips)	V_p (kips)	$\frac{V_p}{V_n}$	$\delta_{0.8 peak}$	Ψ_o
9	Kanada et al. (1984)	U22S ^[6]	110.6	103.2	40.3	0.36	0.030	1.25
		R41L	93.9	87.6	71.9	0.77	0.038	1.25
		R42S ^[6]	93.9	87.6	46.7	0.50	0.018	1.25
		R21L	93.9	87.6	46.7	0.50	0.022	1.25
		R21S ^[6]	93.9	87.6	34.8	0.37	0.022	1.25
10	Zerbe and Durrani (1985)	J1 ^[6]	130.6	119.7	110.9	0.85	0.053	1.00
		J2 ^{[5][6]}	162.4	148.8	130.8	0.81	0.052	1.00
		J3 ^[6]	131.4	120.4	113.8	0.87	0.053	1.00
		J4 ^{[5][6]}	133.2	122.1	179.2	1.35	0.050	1.00
		J5 ^{[5][6]}	161.8	148.3	193.4	1.20	0.051	1.00
		J6 ^{[5][6]}	162.9	149.4	190.6	1.17	0.052	1.00
		J7 ^[7]	132.7	132.7	190.6	1.44	0.050	1.00
11	Ehsani et al. (1987)	1	208.7	196.2	128.0	0.61	0.062	1.25
		2	212.9	200.2	157.2	0.74	0.064	1.25
		3 ^[6]	161.8	150.9	133.2	0.82	0.060	1.25
		4 ^[6]	165.1	153.9	149.8	0.91	0.058	1.25
		5 ^[6]	134.4	125.3	141.6	1.05	0.065	1.25
12	Kaku and Asakusa (1991)	1	60.5	52.2	50.3	0.83	0.055	1.25
		2	70.0	60.5	50.8	0.73	0.065	1.25
		3	70.0	60.5	44.1	0.63	0.065	1.25
		4	72.5	62.6	48.6	0.67	0.060	1.25
		5	65.7	56.7	44.8	0.68	0.055	1.25
		6	68.9	59.5	42.5	0.62	0.052	1.25
		7	61.5	53.1	50.5	0.82	0.060	1.25
		8	69.6	60.1	49.5	0.71	0.063	1.25
		9	69.1	59.7	47.9	0.69	0.068	1.25

^[1] Columns arranged in alphabetical order of notation; notation described in Appendix A; values given in SI units are converted to in.-lb (1 in. = 25.4 mm; 1 psi = 1/145 Mpa; and 1 kip = 4.4484 kN)

^[2] Bar sizes are presented in SI and in.-lb as reported in the original studies

^[3] Analyzed as a doubly reinforced section to calculate the nominal flexural strength M_n ; all other specimens are analyzed as a single reinforced

^[4] Specimens did not contain confining reinforcement parallel to the hooked bars within the joint region

^[5] Specimens had transverse beams on one or both sides of the test beam. These transverse beams meet the dimensional requirements of Sections 18.8.4 and 15.2.8 of ACI 318-19 and Section 4.3 of ACI 352R-02 to be considered effective in increasing the joint shear strength

^[6] Specimens had $d/\ell_{eh} > 1.5$

^[7] Specimens had column to beam flexural strength ratio, M_R , less than 1.2

Table C.4 Cont. Data for exterior beam-column joint specimens tested under reversed cyclic loading ^[1]

Study		Specimen	Bar Size ^[2]	A_b (in. ²)	A_{hs} (in. ²)	A_{tr} (in. ²)	A_{th} (in. ²)	$\frac{A_{th}}{A_{hs}}$	A_v (in. ²)	b_b (in.)
12	Kaku and Asakusa (1991)	10	D13	0.20	0.79	0.01	0.04	0.06	0.09	6.3
		11	D13	0.20	0.79	0.01	0.04	0.06	0.09	6.3
		12	D13	0.20	0.79	0.01	0.04	0.06	0.09	6.3
		13	D13	0.20	0.79	0.04	0.18	0.22	0.35	6.3
		14	D13	0.20	0.79	0.01	0.04	0.06	0.09	6.3
		15	D13	0.20	0.79	0.01	0.04	0.06	0.09	6.3
		16	D13	0.20	0.79	0.04	0.18	0.22	0.35	6.3
		17 ^[7]	D13	0.20	0.79	0.04	0.18	0.22	0.35	6.3
		18 ^[7]	D13	0.20	0.79	0.04	0.18	0.22	0.35	6.3
13	Ehsani and Alameddine (1991)	LL8 ^[6]	No. 8	0.79	3.16	0.20	1.80	0.57	2.40	12.5
		LH8 ^[6]	No. 8	0.79	3.16	0.20	2.40	0.76	3.60	12.5
		HL8 ^[6]	No. 9	1.00	4.00	0.20	1.80	0.45	2.40	12.5
		HH8 ^[6]	No. 9	1.00	4.00	0.20	2.40	0.60	3.60	12.5
		LL11 ^[6]	No. 8	0.79	3.16	0.20	1.80	0.57	2.40	12.5
		LH11 ^[6]	No. 8	0.79	3.16	0.20	2.40	0.76	3.60	12.5
		HL11 ^[6]	No. 9	1.00	4.00	0.20	1.80	0.45	2.40	12.5
		HH11 ^[6]	No. 9	1.00	4.00	0.20	2.40	0.60	3.60	12.5
		LL14 ^[6]	No. 8	0.79	3.16	0.20	1.80	0.57	2.40	12.5
		LH14 ^[6]	No. 8	0.79	3.16	0.20	2.40	0.76	3.60	12.5
		HH14 ^[6]	No. 9	1.00	4.00	0.20	2.40	0.60	3.60	12.5
14	Tsonos et al. (1992)	S1 ^[6]	D14	0.24	0.48	0.08	0.16	0.33	0.47	7.9
		S2 ^[6]	D12	0.18	0.53	0.08	0.16	0.30	0.47	7.9
		S3 ^[7]	D12	0.18	0.70	0.08	0.16	0.22	0.47	7.9
		S4 ^[7]	D14	0.24	0.95	0.08	0.16	0.16	0.47	7.9
		S5 ^[7]	D14	0.24	0.95	0.08	0.16	0.16	0.47	7.9

^[1] Columns arranged in alphabetical order of notation; notation described in Appendix A; values given in SI units are converted to in.-lb (1 in. = 25.4 mm; 1 psi = 1/145 Mpa; and 1 kip = 4.4484 kN)

^[2] Bar sizes are presented in SI and in.-lb as reported in the original studies

^[3] Analyzed as a doubly reinforced section to calculate the nominal flexural strength M_n ; all other specimens are analyzed as a single reinforced

^[4] Specimens did not contain confining reinforcement parallel to the hooked bars within the joint region

^[5] Specimens had transverse beams on one or both sides of the test beam. These transverse beams meet the dimensional requirements of Sections 18.8.4 and 15.2.8 of ACI 318-19 and Section 4.3 of ACI 352R-02 to be considered effective in increasing the joint shear strength

^[6] Specimens had $d/\ell_{eh} > 1.5$

^[7] Specimens had column to beam flexural strength ratio, M_R , less than 1.2

Table C.4 Cont. Data for exterior beam-column joint specimens tested under reversed cyclic loading ^[1]

Study		Specimen	b_c (in.)	b_j (in.)	b_j , ACI 352 (in.)	c_{ch} (in.)	$\frac{c_{ch}}{d_b}$	c_{so} (in.)	$\frac{c_{so}}{d_b}$	d
12	Kaku and Asakusa (1991)	10	8.7	8.7	7.5	1.7	3.3	1.6	3.2	8.0
		11	8.7	8.7	7.5	1.7	3.3	1.6	3.2	8.0
		12	8.7	8.7	7.5	1.7	3.3	1.6	3.2	8.0
		13	8.7	8.7	7.5	1.7	3.3	1.6	3.2	8.0
		14	8.7	8.7	7.5	1.7	3.3	1.6	3.2	8.0
		15	8.7	8.7	7.5	1.7	3.3	1.6	3.2	8.0
		16	8.7	8.7	7.5	1.7	3.3	1.6	3.2	8.0
		17 ^[7]	8.7	8.7	7.5	1.7	3.3	1.6	3.2	8.0
		18 ^[7]	8.7	8.7	7.5	1.7	3.3	1.6	3.2	8.0
13	Ehsani and Alameddine (1991)	LL8 ^[6]	14.0	14.0	13.3	2.2	2.2	3.0	3.0	17.0
		LH8 ^[6]	14.0	14.0	13.3	2.2	2.2	3.0	3.0	17.0
		HL8 ^[6]	14.0	14.0	13.3	2.2	1.9	3.0	2.7	17.0
		HH8 ^[6]	14.0	14.0	13.3	2.2	1.9	3.0	2.7	17.0
		LL11 ^[6]	14.0	14.0	13.3	2.2	2.2	3.0	3.0	17.0
		LH11 ^[6]	14.0	14.0	13.3	2.2	2.2	3.0	3.0	17.0
		HL11 ^[6]	14.0	14.0	13.3	2.2	1.9	3.0	2.7	17.0
		HH11 ^[6]	14.0	14.0	13.3	2.2	1.9	3.0	2.7	17.0
		LL14 ^[6]	14.0	14.0	13.3	2.2	2.2	3.0	3.0	17.0
		LH14 ^[6]	14.0	14.0	13.3	2.2	2.2	3.0	3.0	17.0
		HH14 ^[6]	14.0	14.0	13.3	2.2	1.9	3.0	2.7	17.0
14	Tsonos et al. (1992)	S1 ^[6]	7.9	7.9	7.9	5.9	10.7	0.7	1.3	10.8
		S2 ^[6]	7.9	7.9	7.9	3.0	6.3	0.7	1.5	10.8
		S3 ^[7]	7.9	7.9	7.9	2.0	4.2	0.7	1.5	10.8
		S4 ^[7]	7.9	7.9	7.9	2.0	3.6	0.7	1.3	10.8
		S5 ^[7]	7.9	7.9	7.9	2.0	3.6	0.7	1.3	10.8

^[1] Columns arranged in alphabetical order of notation; notation described in Appendix A; values given in SI units are converted to in.-lb (1 in. = 25.4 mm; 1 psi = 1/145 Mpa; and 1 kip = 4.4484 kN)

^[2] Bar sizes are presented in SI and in.-lb as reported in the original studies

^[3] Analyzed as a doubly reinforced section to calculate the nominal flexural strength M_n ; all other specimens are analyzed as a single reinforced

^[4] Specimens did not contain confining reinforcement parallel to the hooked bars within the joint region

^[5] Specimens had transverse beams on one or both sides of the test beam. These transverse beams meet the dimensional requirements of Sections 18.8.4 and 15.2.8 of ACI 318-19 and Section 4.3 of ACI 352R-02 to be considered effective in increasing the joint shear strength

^[6] Specimens had $d/\ell_{ch} > 1.5$

^[7] Specimens had column to beam flexural strength ratio, M_R , less than 1.2

Table C.4 Cont. Data for exterior beam-column joint specimens tested under reversed cyclic loading ^[1]

Study		Specimen	$\frac{d}{\ell_{eh}}$	d' (in.)	d_b (in.)	f_{cm} ^[8] (psi)	f_{cm} ^[9] (psi)	f_y (ksi)	$f_{ytr,l}$ (ksi)	$f_{ytr,l} A_v$ (kips)
12	Kaku and Asakusa (1991)	10	1.04	0.7	0.5	6440	6440	56.7	40.7	3.6
		11	1.04	0.7	0.5	6080	6080	56.7	40.7	3.6
		12	1.04	0.7	0.5	5090	5090	56.7	40.7	3.6
		13	1.04	0.7	0.5	6730	6730	56.7	36.3	12.7
		14	1.04	0.7	0.5	5950	5950	56.7	40.7	3.6
		15	1.04	0.7	0.5	5760	5760	56.7	40.7	3.6
		16	1.04	0.7	0.5	5420	5420	56.7	36.3	12.7
		17 ^[7]	1.04	0.7	0.5	5760	5760	56.7	36.3	12.7
		18 ^[7]	1.04	0.7	0.5	5900	5900	56.7	36.3	12.7
13	Ehsani and Alameddine (1991)	LL8 ^[6]	1.62	3.0	1	8600	8600	66.3	64.8	155.4
		LH8 ^[6]	1.62	3.0	1	8600	8600	66.3	64.8	233.1
		HL8 ^[6]	1.62	3.0	1.128	8600	8600	64.2	64.8	155.4
		HH8 ^[6]	1.62	3.0	1.128	8600	8600	64.2	64.8	233.1
		LL11 ^[6]	1.62	3.0	1	10700	10700	66.3	64.8	155.4
		LH11 ^[6]	1.62	3.0	1	10700	10700	66.3	64.8	233.1
		HL11 ^[6]	1.62	3.0	1.128	10700	10700	64.2	64.8	155.4
		HH11 ^[6]	1.62	3.0	1.128	10700	10700	64.2	64.8	233.1
		LL14 ^[6]	1.62	3.0	1	13700	13700	66.3	64.8	155.4
		LH14 ^[6]	1.62	3.0	1	13700	13700	66.3	64.8	233.1
		HH14 ^[6]	1.62	3.0	1.128	13700	13700	64.2	64.8	233.1
14	Tsonos et al. (1992)	S1 ^[6]	1.67	1.0	0.55	5360	5360	70.3	71.7	33.5
		S2 ^[6]	1.67	1.0	0.47	3770	3770	76.7	71.7	33.5
		S3 ^[7]	1.67	1.0	0.47	2750	2750	76.67	71.7	33.5
		S4 ^[7]	1.67	1.0	0.55	3040	3040	70.3	71.7	33.5
		S5 ^[7]	1.67	1.0	0.55	3620	3620	70.3	71.7	33.5

^[1] Columns arranged in alphabetical order of notation; notation described in Appendix A; values given in SI units are converted to in.-lb (1 in. = 25.4 mm; 1 psi = 1/145 Mpa; and 1 kip = 4.4484 kN)

^[4] Specimens did not contain confining reinforcement parallel to the hooked bars within the joint region

^[5] Specimens had transverse beams on one or both sides of the test beam. These transverse beams meet the dimensional requirements of Sections 18.8.4 and 15.2.8 of ACI 318-19 and Section 4.3 of ACI 352R-02 to be considered effective in increasing the joint shear strength

^[6] Specimens had $d/\ell_{eh} > 1.5$

^[7] Specimens had column to beam flexural strength ratio, M_R , less than 1.2

^[8] Column concrete compressive strength

^[9] Beam concrete compressive strength

Table C.4 Cont. Data for exterior beam-column joint specimens tested under reversed cyclic loading ^[1]

Study		Specimen	h_b (in.)	h_c (in.)	ℓ_{dh} (in.)	$\frac{\ell_{dh}}{d_b}$	ℓ_{eh} (in.)	$\frac{\ell_{eh}}{d_b}$	ℓ_{ehy} (in.)	$\frac{\ell_{ehy}}{d_b}$
12	Kaku and Asakusa (1991)	10	8.7	8.7	6.6	13.2	7.7	15.4	5.1	10.2
		11	8.7	8.7	6.7	13.4	7.7	15.4	5.2	10.3
		12	8.7	8.7	7.0	14.0	7.7	15.4	5.4	10.9
		13	8.7	8.7	4.7	9.4	7.7	15.4	4.8	9.6
		14	8.7	8.7	6.7	13.4	7.7	15.4	5.2	10.4
		15	8.7	8.7	6.8	13.5	7.7	15.4	5.2	10.5
		16	8.7	8.7	5.0	9.9	7.7	15.4	5.1	10.1
		17 ^[7]	8.7	8.7	4.9	9.8	7.7	15.4	5.1	10.3
		18 ^[7]	8.7	8.7	4.9	9.7	7.7	15.4	5.1	10.2
13	Ehsani and Alameddine (1991)	LL8 ^[6]	20.0	14.0	12.3	12.3	10.5	10.5	11.4	11.4
		LH8 ^[6]	20.0	14.0	12.3	12.3	10.5	10.5	11.4	11.4
		HL8 ^[6]	20.0	14.0	14.4	12.7	10.5	9.3	13.1	11.6
		HH8 ^[6]	20.0	14.0	14.4	12.7	10.5	9.3	13.1	11.6
		LL11 ^[6]	20.0	14.0	11.7	11.7	10.5	10.5	10.8	10.8
		LH11 ^[6]	20.0	14.0	11.7	11.7	10.5	10.5	10.8	10.8
		HL11 ^[6]	20.0	14.0	13.6	12.1	10.5	9.3	12.3	10.9
		HH11 ^[6]	20.0	14.0	13.6	12.1	10.5	9.3	12.3	10.9
		LL14 ^[6]	20.0	14.0	11.0	11.0	10.5	10.5	10.1	10.1
		LH14 ^[6]	20.0	14.0	11.0	11.0	10.5	10.5	10.1	10.1
		HH14 ^[6]	20.0	14.0	12.8	11.3	10.5	9.3	11.5	10.2
14	Tsonos et al. (1992)	S1 ^[6]	11.8	7.9	6.3	11.4	6.5	11.8	5.9	10.8
		S2 ^[6]	11.8	7.9	6.0	12.6	6.5	13.8	5.9	12.5
		S3 ^[7]	11.8	7.9	7.0	14.9	6.5	13.8	7.4	15.6
		S4 ^[7]	11.8	7.9	8.9	16.1	6.5	11.8	8.6	15.5
		S5 ^[7]	11.8	7.9	8.5	15.5	6.5	11.8	8.2	14.8

^[1] Columns arranged in alphabetical order of notation; notation described in Appendix A; values given in SI units are converted to in.-lb (1 in. = 25.4 mm; 1 psi = 1/145 Mpa; and 1 kip = 4.4484 kN)

^[2] Bar sizes are presented in SI and in.-lb as reported in the original studies

^[3] Analyzed as a doubly reinforced section to calculate the nominal flexural strength M_n ; all other specimens are analyzed as a single reinforced

^[4] Specimens did not contain confining reinforcement parallel to the hooked bars within the joint region

^[5] Specimens had transverse beams on one or both sides of the test beam. These transverse beams meet the dimensional requirements of Sections 18.8.4 and 15.2.8 of ACI 318-19 and Section 4.3 of ACI 352R-02 to be considered effective in increasing the joint shear strength

^[6] Specimens had $d/\ell_{eh} > 1.5$

^[7] Specimens had column to beam flexural strength ratio, M_R , less than 1.2

Table C.4 Cont. Data for exterior beam-column joint specimens tested under reversed cyclic loading ^[1]

Study		Specimen	$\frac{\ell_{eh}}{h_c}$	$\frac{\ell_{eh}}{\ell_{dh}}$	$\frac{\ell_{eh}}{\ell_{ehy}}$	M_n (kip.in.)	M_{peak} (kip.in.)	$\frac{M_{peak}}{M_n}$	N	N_{total}
12	Kaku and Asakusa (1991)	10	0.9	1.17	1.51	334	418	1.25	2	4
		11	0.9	1.15	1.48	334	397	1.19	2	4
		12	0.9	1.10	1.41	336	357	1.06	2	4
		13	0.9	1.63	1.61	339	360	1.06	2	4
		14	0.9	1.14	1.48	334	389	1.16	2	4
		15	0.9	1.13	1.46	333	397	1.19	2	4
		16	0.9	1.54	1.52	334	432	1.29	2	4
		17 ^[7]	0.9	1.57	1.49	338	304	0.90	2	4
		18 ^[7]	0.9	1.58	1.50	330	205	0.62	2	4
13	Ehsani and Alameddine (1991)	LL8 ^[6]	0.8	0.85	0.92	3027	3517	1.16	3	4
		LH8 ^[6]	0.8	0.85	0.92	3027	3402	1.12	4	6
		HL8 ^[6]	0.8	0.73	0.80	3637	3708	1.02	3	4
		HH8 ^[6]	0.8	0.73	0.80	3637	3743	1.03	4	6
		LL11 ^[6]	0.8	0.90	0.98	3118	3020	0.97	3	4
		LH11 ^[6]	0.8	0.90	0.98	3081	4018	1.30	4	6
		HL11 ^[6]	0.8	0.77	0.85	3845	3731	0.97	3	4
		HH11 ^[6]	0.8	0.77	0.85	3872	4089	1.06	4	6
		LL14 ^[6]	0.8	0.96	1.04	3112	3701	1.19	3	4
		LH14 ^[6]	0.8	0.96	1.04	3112	3780	1.21	4	6
		HH14 ^[6]	0.8	0.82	0.91	3830	4084	1.07	4	6
14	Tsonos et al. (1992)	S1 ^[6]	0.8	1.03	1.09	348	452	1.30	1	3
		S2 ^[6]	0.8	1.09	1.10	404	465	1.15	1	3
		S3 ^[7]	0.8	0.92	0.88	504	524	1.04	1	3
		S4 ^[7]	0.8	0.73	0.76	616	480	0.78	1	3
		S5 ^[7]	0.8	0.76	0.80	634	532	0.84	1	3

^[1] Columns arranged in alphabetical order of notation; notation described in Appendix A; values given in SI units are converted to in.-lb (1 in. = 25.4 mm; 1 psi = 1/145 Mpa; and 1 kip = 4.4484 kN)

^[2] Bar sizes are presented in SI and in.-lb as reported in the original studies

^[3] Analyzed as a doubly reinforced section to calculate the nominal flexural strength M_n ; all other specimens are analyzed as a single reinforced

^[4] Specimens did not contain confining reinforcement parallel to the hooked bars within the joint region

^[5] Specimens had transverse beams on one or both sides of the test beam. These transverse beams meet the dimensional requirements of Sections 18.8.4 and 15.2.8 of ACI 318-19 and Section 4.3 of ACI 352R-02 to be considered effective in increasing the joint shear strength

^[6] Specimens had $d/\ell_{eh} > 1.5$

^[7] Specimens had column to beam flexural strength ratio, M_R , less than 1.2

Table C.4 Cont. Data for exterior beam-column joint specimens tested under reversed cyclic loading ^[1]

Study		Specimen	<i>n</i>	<i>nT'</i> (kips)	<i>s_{tr}</i> (in.)	<i>T_h</i> (kips)	<i>T'</i> (kips)	<i>T'</i> _{mod} (kips)	$\frac{T'}{T_h}$	$\frac{T'_{mod}}{T_h}$
12	Kaku and Asakusa (1991)	10	4	55.7	2.0	11.2	13.9	13.2	1.25	1.19
		11	4	53.0	2.0	11.2	13.2	12.6	1.19	1.13
		12	4	47.4	2.0	11.2	11.8	11.3	1.06	1.01
		13	4	47.3	2.0	11.2	11.8	11.0	1.06	0.98
		14	4	51.8	2.0	11.2	13.0	12.3	1.16	1.10
		15	4	53.0	2.0	11.2	13.3	12.6	1.19	1.13
		16	4	57.6	2.0	11.2	14.4	13.7	1.29	1.22
		17 ^[7]	4	39.9	2.0	11.2	10.0	9.2	0.89	0.8
		18 ^[7]	4	27.7	2.0	11.2	6.9	6.2	0.62	0.6
13	Ehsani and Alameddine (1991)	LL8 ^[6]	4	243.4	3.5	48.6	60.9	-	1.25	-
		LH8 ^[6]	4	235.5	2.3	48.6	58.9	-	1.21	-
		HL8 ^[6]	4	261.8	3.5	52.7	65.5	-	1.24	-
		HH8 ^[6]	4	264.3	2.3	52.7	66.1	-	1.25	-
		LL11 ^[6]	4	202.9	3.5	51.4	50.7	-	0.99	-
		LH11 ^[6]	4	273.2	2.3	51.4	68.3	-	1.33	-
		HL11 ^[6]	4	249.2	3.5	55.6	62.3	-	1.12	-
		HH11 ^[6]	4	271.2	2.3	55.6	67.8	-	1.22	-
		LL14 ^[6]	4	249.2	3.5	52.6	62.3	62.0	1.18	1.18
		LH14 ^[6]	4	254.5	2.3	52.6	63.6	63.3	1.21	1.20
		HH14 ^[6]	4	273.8	2.3	59.1	68.5	-	1.16	-
14	Tsonos et al. (1992)	S1 ^[6]	2	43.6	2.5	16.8	21.8	21.6	1.29	1.28
		S2 ^[6]	3	46.4	2.5	13.5	15.5	15.3	1.15	1.13
		S3 ^[7]	4	55.9	2.5	12.1	14.0	-	1.15	-
		S4 ^[7]	4	52.3	2.5	13.1	13.1	-	1.00	-
		S5 ^[7]	4	56.4	2.5	13.7	14.1	-	1.03	-

^[1] Columns arranged in alphabetical order of notation; notation described in Appendix A; values given in SI units are converted to in.-lb (1 in. = 25.4 mm; 1 psi = 1/145 Mpa; and 1 kip = 4.4484 kN)

^[2] Bar sizes are presented in SI and in.-lb as reported in the original studies

^[3] Analyzed as a doubly reinforced section to calculate the nominal flexural strength M_n ; all other specimens are analyzed as a single reinforced

^[4] Specimens did not contain confining reinforcement parallel to the hooked bars within the joint region

^[5] Specimens had transverse beams on one or both sides of the test beam. These transverse beams meet the dimensional requirements of Sections 18.8.4 and 15.2.8 of ACI 318-19 and Section 4.3 of ACI 352R-02 to be considered effective in increasing the joint shear strength

^[6] Specimens had $d/\ell_{eh} > 1.5$

^[7] Specimens had column to beam flexural strength ratio, M_R , less than 1.2

Table C.4 Cont. Data for exterior beam-column joint specimens tested under reversed cyclic loading ^[1]

Study		Specimen	V_n (kips)	$V_{n,ACI\ 352}$ (kips)	V_p (kips)	$\frac{V_p}{V_n}$	$\delta_{0.8\ peak}$	ψ_o
12	Kaku and Asakusa (1991)	10	72.2	62.4	49.3	0.68	0.059	1.25
		11	70.2	60.6	46.9	0.67	0.048	1.25
		12	64.2	55.5	42.1	0.66	0.053	1.25
		13	73.8	63.8	42.5	0.58	0.065	1.25
		14	69.4	59.9	45.9	0.66	0.045	1.25
		15	68.3	59.0	46.8	0.69	0.060	1.25
		16	66.3	57.3	51.0	0.77	0.055	1.25
		17 ^[7]	68.3	59.0	35.8	0.52	0.070	1.25
		18 ^[7]	69.2	59.7	24.2	0.35	0.040	1.25
13	Ehsani and Alameddine (1991)	LL8 ^[6]	218.1	206.4	193.4	0.89	0.055	1.00
		LH8 ^[6]	218.1	206.4	188.4	0.86	0.061	1.00
		HL8 ^[6]	218.1	206.4	221.8	1.02	0.043	1.00
		HH8 ^[6]	218.1	206.4	221.6	1.02	0.063	1.00
		LL11 ^[6]	243.3	230.3	172.9	0.71	0.056	1.00
		LH11 ^[6]	243.3	230.3	210.0	0.86	0.064	1.00
		HL11 ^[6]	243.3	230.3	217.5	0.89	0.041	1.00
		HH11 ^[6]	243.3	230.3	229.5	0.94	0.063	1.00
		LL14 ^[6]	275.3	260.5	197.3	0.72	0.060	1.00
		LH14 ^[6]	275.3	260.5	200.2	0.73	0.064	1.00
		HH14 ^[6]	275.3	260.5	232.1	0.84	0.054	1.00
14	Tsonos et al. (1992)	S1 ^[6]	54.5	54.5	36.2	0.66	0.065	1.25
		S2 ^[6]	45.7	45.7	37.3	0.82	0.030	1.25
		S3 ^[7]	39.0	39.0	42.0	1.08	-	1.25
		S4 ^[7]	41.0	41.0	38.5	0.94	-	1.25
		S5 ^[7]	44.8	44.8	42.7	0.95	-	1.25

^[1] Columns arranged in alphabetical order of notation; notation described in Appendix A; values given in SI units are converted to in.-lb (1 in. = 25.4 mm; 1 psi = 1/145 Mpa; and 1 kip = 4.4484 kN)

^[2] Bar sizes are presented in SI and in.-lb as reported in the original studies

^[3] Analyzed as a doubly reinforced section to calculate the nominal flexural strength M_n ; all other specimens are analyzed as a single reinforced

^[4] Specimens did not contain confining reinforcement parallel to the hooked bars within the joint region

^[5] Specimens had transverse beams on one or both sides of the test beam. These transverse beams meet the dimensional requirements of Sections 18.8.4 and 15.2.8 of ACI 318-19 and Section 4.3 of ACI 352R-02 to be considered effective in increasing the joint shear strength

^[6] Specimens had $d/\ell_{eh} > 1.5$

^[7] Specimens had column to beam flexural strength ratio, M_R , less than 1.2

Table C.4 Cont. Data for exterior beam-column joint specimens tested under reversed cyclic loading^[1]

Study		Specimen	Bar Size ^[2]	A_b (in. ²)	A_{hs} (in. ²)	A_{tr} (in. ²)	A_{th} (in. ²)	$\frac{A_{th}}{A_{hs}}$	A_v (in. ²)	b_b (in.)
14	Tsonos et al. (1992)	S6 ^[7]	D14	0.24	0.95	0.08	0.16	0.16	0.47	7.9
		S6' ^[6]	D14	0.24	0.95	0.08	0.16	0.16	0.47	7.9
15	Pantelides et al. (2002)	2 ^{[3][4]}	No. 9	1.00	4.00	0.00	0.00	0.00	0.00	12.0
		4 ^{[3][4]}	No. 9	1.00	4.00	0.00	0.00	0.00	0.00	12.0
		5 ^{[3][4]}	No. 9	1.00	4.00	0.00	0.00	0.00	0.00	12.0
		6 ^{[3][4]}	No. 9	1.00	4.00	0.00	0.00	0.00	0.00	12.0
16	Chutarat and Aboutaha (2003)	Specimen I	No. 8	0.79	3.16	0.20	2.40	0.76	3.20	14.0
17	Hwang et al. (2005)	0T0 ^[4]	No. 8	0.79	3.16	0.00	0.00	0.00	0.00	12.6
		3T44	No. 8	0.79	3.16	0.20	2.40	0.76	3.60	12.6
		1B8	No. 8	0.79	3.16	0.79	1.58	0.50	1.58	12.6
		3T3	No. 8	0.79	3.16	0.11	0.66	0.21	0.99	12.6
		2T4	No. 8	0.79	3.16	0.20	0.40	0.13	0.80	12.6
		1T44	No. 8	0.79	3.16	0.20	0.80	0.25	0.80	12.6
		3T4	No. 8	0.79	3.16	0.20	1.20	0.38	1.80	12.6
		2T5	No. 8	0.79	3.16	0.31	0.62	0.20	1.24	12.6
		1T55	No. 8	0.79	3.16	0.31	1.24	0.39	1.24	12.6
18	Tsonos (2007)	A1 ^[6]	D10	0.12	0.49	0.04	0.18	0.36	0.44	7.9
		E1 ^[6]	D14	0.24	0.72	0.04	0.18	0.24	0.44	7.9
		E2 ^[6]	D14	0.24	0.48	0.04	0.18	0.37	0.44	7.9
		G1 ^[6]	D14	0.24	0.72	0.04	0.09	0.12	0.18	7.9
19	Chun et al. (2007)	JC-1	D22	0.60	2.40	0.11	0.22	0.09	0.44	13.8
		JC-2	D22	0.60	4.80	0.11	0.22	0.05	0.44	13.8
		WC ^[4]	D25	0.79	3.95	0.00	0.00	0.00	0.00	31.5
		JC-No. 11-1	D36	1.56	4.68	0.20	2.40	0.51	2.40	17.7
20	Lee and Ko (2007)	S0	D22	0.60	2.40	0.11	0.66	0.28	0.99	12.0
		W0	D22	0.60	2.40	0.11	1.10	0.46	1.65	12.0

^[1] Columns arranged in alphabetical order of notation; notation described in Appendix A; values given in SI units are converted to in.-lb (1 in. = 25.4 mm; 1 psi = 1/145 Mpa; and 1 kip = 4.4484 kN)

^[2] Bar sizes are presented in SI and in.-lb as reported in the original studies

^[3] Analyzed as a doubly reinforced section to calculate the nominal flexural strength M_n ; all other specimens are analyzed as a single reinforced

^[4] Specimens did not contain confining reinforcement parallel to the hooked bars within the joint region

^[5] Specimens had transverse beams on one or both sides of the test beam. These transverse beams meet the dimensional requirements of Sections 18.8.4 and 15.2.8 of ACI 318-19 and Section 4.3 of ACI 352R-02 to be considered effective in increasing the joint shear strength

^[6] Specimens had $d/\ell_{eh} > 1.5$

^[7] Specimens had column to beam flexural strength ratio, M_R , less than 1.2

Table C.4 Cont. Data for exterior beam-column joint specimens tested under reversed cyclic loading^[1]

Study		Specimen	b_c (in.)	b_j (in.)	$b_{j,ACI352}$ (in.)	c_{ch} (in.)	$\frac{c_{ch}}{d_b}$	c_{so} (in.)	$\frac{c_{so}}{d_b}$	d
14	Tsonos et al. (1992)	S6 ^[7]	7.9	7.9	7.9	2.0	3.6	0.7	1.3	10.8
		S6' ^[6]	7.9	7.9	7.9	2.0	3.6	0.7	1.3	10.8
15	Pantelides et al. (2002)	2 ^{[3][4]}	12.0	12.0	12.0	2.4	2.1	1.9	1.7	13.6
		4 ^{[3][4]}	12.0	12.0	12.0	2.4	2.1	1.9	1.7	13.6
		5 ^{[3][4]}	12.0	12.0	12.0	2.4	2.1	1.9	1.7	13.6
		6 ^{[3][4]}	12.0	12.0	12.0	2.4	2.1	1.9	1.7	13.6
16	Chutarat and Aboutaha (2003)	Specimen I	16.0	16.0	15.0	2.8	2.8	3.3	3.3	15.2
17	Hwang et al. (2005)	0T0 ^[4]	16.5	16.5	14.6	2.5	2.5	4.0	4.0	15.1
		3T44	16.5	16.5	14.6	2.5	2.5	4.0	4.0	15.1
		1B8	16.5	16.5	14.6	2.5	2.5	4.0	4.0	15.1
		3T3	16.5	16.5	14.6	2.5	2.5	4.0	4.0	15.1
		2T4	16.5	16.5	14.6	2.5	2.5	4.0	4.0	15.1
		1T44	16.5	16.5	14.6	2.5	2.5	4.0	4.0	15.1
		3T4	17.7	17.7	15.2	2.5	2.5	4.0	4.0	15.1
		2T5	17.7	17.7	15.2	2.5	2.5	4.0	4.0	15.1
		1T55	17.7	17.7	15.2	2.5	2.5	4.0	4.0	15.1
18	Tsonos (2007)	A1 ^[6]	7.9	7.9	7.9	1.8	4.7	1.0	2.5	10.6
		E1 ^[6]	7.9	7.9	7.9	2.8	5.0	0.9	1.6	10.6
		E2 ^[6]	7.9	7.9	7.9	5.5	10.0	0.9	1.6	10.6
		G1 ^[6]	7.9	7.9	7.9	2.8	5.0	0.9	1.6	10.6
19	Chun et al. (2007)	JC-1	16.7	16.7	15.3	3.0	3.4	3.4	3.9	17.3
		JC-2	16.7	16.7	15.3	3.0	3.4	3.4	3.9	17.3
		WC ^[4]	31.5	31.5	31.5	6.6	6.6	2.1	2.1	13.1
		JC-No. 11-1	25.6	25.6	21.7	6.1	4.3	6.0	4.3	17.1
20	Lee and Ko (2007)	S0	16.0	16.0	14.0	2.0	2.3	4.6	5.2	16.0
		W0	24.0	24.0	16.0	2.0	2.3	8.6	9.8	16.0

[1] Columns arranged in alphabetical order of notation; notation described in Appendix A; values given in SI units are converted to in.-lb (1 in. = 25.4 mm; 1 psi = 1/145 Mpa; and 1 kip = 4.4484 kN)

[2] Bar sizes are presented in SI and in.-lb as reported in the original studies

[3] Analyzed as a doubly reinforced section to calculate the nominal flexural strength M_n ; all other specimens are analyzed as a single reinforced

[4] Specimens did not contain confining reinforcement parallel to the hooked bars within the joint region

[5] Specimens had transverse beams on one or both sides of the test beam. These transverse beams meet the dimensional requirements of Sections 18.8.4 and 15.2.8 of ACI 318-19 and Section 4.3 of ACI 352R-02 to be considered effective in increasing the joint shear strength

[6] Specimens had $d/\ell_{eh} > 1.5$

[7] Specimens had column to beam flexural strength ratio, M_R , less than 1.2

Table C.4 Cont. Data for exterior beam-column joint specimens tested under reversed cyclic loading ^[1]

Study		Specimen	$\frac{d}{\ell_{eh}}$	d' (in.)	d_b (in.)	f_{cm} ^[8] (psi)	f_{cm} ^[9] (psi)	f_y (ksi)	$f_{ytr,l}$ (ksi)	$f_{ytr,l} A_v$ (kips)
14	Tsonos et al. (1992)	S6 ^[7]	1.67	1.0	0.55	4780	4780	70.3	71.7	33.5
		S6' ^[6]	1.67	1.0	0.55	4200	4200	70.3	71.7	33.5
15	Pantelides et al. (2002)	2 ^{[3][4]}	0.84	2.4	1.128	6700	6700	65.9	0.0	0.0
		4 ^{[3][4]}	0.84	2.4	1.128	5940	5940	65.9	0.0	0.0
		5 ^{[3][4]}	0.84	2.4	1.128	5370	5370	65.9	0.0	0.0
		6 ^{[3][4]}	0.84	2.4	1.128	5820	5820	65.9	0.0	0.0
16	Chutarat and Aboutaha (2003)	Specimen I	1.19	2.8	1	4000	4000	70.0	53.0	169.6
17	Hwang et al. (2005)	0T0 ^[4]	1.11	2.6	1	9760	9760	62.4	0.0	0.0
		3T44	1.11	2.6	1	11140	11140	62.4	72.2	260.0
		1B8	1.11	2.6	1	8960	8960	63.1	63.1	99.7
		3T3	1.11	2.6	1	10010	10010	62.4	68.3	67.6
		2T4	1.11	2.6	1	10300	10300	62.4	72.2	57.8
		1T44	1.11	2.6	1	10560	10560	62.4	72.2	57.8
		3T4	0.98	2.6	1	10910	10910	71.2	63.2	113.8
		2T5	0.98	2.6	1	11110	11110	71.2	68.0	84.3
		1T55	0.98	2.6	1	10110	10110	71.2	68.0	84.3
18	Tsonos (2007)	A1 ^[6]	1.64	1.2	0.39	5080	5080	73.0	78.0	34.2
		E1 ^[6]	1.66	1.2	0.55	3190	3190	72.0	78.0	34.2
		E2 ^[6]	1.66	1.2	0.55	5080	5080	72.0	78.0	34.2
		G1 ^[6]	1.66	1.2	0.55	3190	3190	72.0	78.0	13.7
19	Chun et al. (2007)	JC-1	1.10	2.4	0.875	8950	8950	58.4	55.7	24.5
		JC-2	1.24	2.4	0.875	8720	8720	58.4	55.7	24.5
		WC ^[4]	0.84	2.6	1	8180	8180	62.5	0.0	0.0
		JC-No. 11-1	0.90	2.8	1.41	4760	4760	66.4	72.5	174.0
20	Lee and Ko (2007)	S0	0.76	2.0	0.875	4730	4730	66.0	68.0	67.3
		W0	1.22	2.0	0.875	4190	4190	66.0	68.0	112.2

^[1] Columns arranged in alphabetical order of notation; notation described in Appendix A; values given in SI units are converted to in.-lb (1 in. = 25.4 mm; 1 psi = 1/145 Mpa; and 1 kip = 4.4484 kN)

^[3] Analyzed as a doubly reinforced section to calculate the nominal flexural strength M_n ; all other specimens are analyzed as a single reinforced

^[4] Specimens did not contain confining reinforcement parallel to the hooked bars within the joint region

^[6] Specimens had $d/\ell_{eh} > 1.5$

^[7] Specimens had column to beam flexural strength ratio, M_R , less than 1.2

^[8] Column concrete compressive strength

^[9] Beam concrete compressive strength

Table C.4 Cont. Data for exterior beam-column joint specimens tested under reversed cyclic loading ^[1]

Study		Specimen	h_b (in.)	h_c (in.)	ℓ_{dh} (in.)	$\frac{\ell_{dh}}{d_b}$	ℓ_{eh} (in.)	$\frac{\ell_{eh}}{d_b}$	ℓ_{ehy} (in.)	$\frac{\ell_{ehy}}{d_b}$
14	Tsonos et al. (1992)	S6 ^[7]	11.8	7.9	7.9	14.4	6.5	11.8	7.6	13.7
		S6' ^[6]	11.8	7.9	8.2	14.9	6.5	11.8	7.6	13.9
15	Pantelides et al. (2002)	2 ^{[3][4]}	16.0	18.0	32.4	28.7	16.1	14.3	15.6	13.8
		4 ^{[3][4]}	16.0	18.0	33.4	29.6	16.1	14.3	16.1	14.3
		5 ^{[3][4]}	16.0	18.0	34.2	30.3	16.1	14.3	16.6	14.7
		6 ^{[3][4]}	16.0	18.0	33.5	29.7	16.1	14.3	16.2	14.4
16	Chutarat and Aboutaha (2003)	Specimen I	18.0	16.0	15.3	15.3	12.8	12.8	14.2	14.2
17	Hwang et al. (2005)	0T0 ^[4]	17.7	16.5	17.9	17.9	13.7	13.7	11.5	11.5
		3T44	17.7	16.5	10.7	10.7	13.7	13.7	9.8	9.8
		1B8	17.7	16.5	11.4	11.4	13.7	13.7	10.5	10.5
		3T3	17.7	16.5	11.0	11.0	13.7	13.7	10.0	10.0
		2T4	17.7	16.5	13.4	13.4	13.7	13.7	10.5	10.5
		1T44	17.7	16.5	10.9	10.9	13.7	13.7	9.9	9.9
		3T4	17.7	17.7	12.3	12.3	15.5	15.5	11.3	11.3
		2T5	17.7	17.7	12.4	12.4	15.5	15.5	11.3	11.3
		1T55	17.7	17.7	12.5	12.5	15.5	15.5	11.5	11.5
18	Tsonos (2007)	A1 ^[6]	11.8	7.9	4.3	10.9	6.5	16.5	4.4	11.2
		E1 ^[6]	11.8	7.9	7.7	14.0	6.4	11.6	7.7	13.9
		E2 ^[6]	11.8	7.9	6.5	11.9	6.4	11.6	6.2	11.2
		G1 ^[6]	11.8	7.9	8.7	15.8	6.4	11.6	7.9	14.3
19	Chun et al. (2007)	JC-1	19.7	19.7	10.7	12.2	15.8	18.0	8.2	9.3
		JC-2	19.7	19.7	11.7	13.4	13.9	15.9	8.5	9.7
		WC ^[4]	15.7	23.6	14.8	14.8	15.7	15.7	12.0	12.0
		JC-No. 11-1	19.9	20.5	21.8	15.5	18.9	13.4	17.9	12.7
20	Lee and Ko (2007)	S0	18.0	24.0	11.6	13.2	21.0	24.0	11.0	12.6
		W0	18.0	16.0	11.9	13.6	13.1	15.0	11.4	13.0

^[1] Columns arranged in alphabetical order of notation; notation described in Appendix A; values given in SI units are converted to in.-lb (1 in. = 25.4 mm; 1 psi = 1/145 Mpa; and 1 kip = 4.4484 kN)

^[2] Bar sizes are presented in SI and in.-lb as reported in the original studies

^[3] Analyzed as a doubly reinforced section to calculate the nominal flexural strength M_n ; all other specimens are analyzed as a single reinforced

^[4] Specimens did not contain confining reinforcement parallel to the hooked bars within the joint region

^[5] Specimens had transverse beams on one or both sides of the test beam. These transverse beams meet the dimensional requirements of Sections 18.8.4 and 15.2.8 of ACI 318-19 and Section 4.3 of ACI 352R-02 to be considered effective in increasing the joint shear strength

^[6] Specimens had $d/\ell_{eh} > 1.5$

^[7] Specimens had column to beam flexural strength ratio, M_R , less than 1.2

Table C.4 Cont. Data for exterior beam-column joint specimens tested under reversed cyclic loading^[1]

Study		Specimen	$\frac{\ell_{eh}}{h_c}$	$\frac{\ell_{eh}}{\ell_{dh}}$	$\frac{\ell_{eh}}{\ell_{ehy}}$	M_n (kip.in.)	M_{peak} (kip.in.)	$\frac{M_{peak}}{M_n}$	N	N_{total}
14	Tsonos et al. (1992)	S6 ^[7]	0.8	0.82	0.86	656	518	0.79	1	3
		S6' ^[6]	0.8	0.79	0.85	646	666	1.03	1	3
15	Pantelides et al. (2002)	2 ^{[3][4]}	0.9	0.50	1.03	2932	3005	1.02	0	0
		4 ^{[3][4]}	0.9	0.48	1.00	2932	3100	1.06	0	0
		5 ^{[3][4]}	0.9	0.47	0.97	2932	3000	1.02	0	0
		6 ^{[3][4]}	0.9	0.48	0.99	2932	2950	1.01	0	0
16	Chutarat and Aboutaha (2003)	Specimen I	0.8	0.83	0.90	2848	3344	1.17	3	4
17	Hwang et al. (2005)	0T0 ^[4]	0.8	0.76	1.18	2794	3229	1.16	0	0
		3T44	0.8	1.27	1.40	2817	3447	1.22	4	6
		1B8	0.8	1.19	1.30	2807	4069	1.45	1	1
		3T3	0.8	1.24	1.36	2798	3666	1.31	2	3
		2T4	0.8	1.02	1.30	2803	3498	1.25	1	2
		1T44	0.8	1.26	1.38	2808	3363	1.20	2	2
		3T4	0.9	1.26	1.37	3185	3599	1.13	2	3
		2T5	0.9	1.25	1.38	3189	3767	1.18	1	2
		1T55	0.9	1.24	1.34	3168	3649	1.15	2	2
18	Tsonos (2007)	A1 ^[6]	0.8	1.52	1.47	359	454	1.26	2	5
		E1 ^[6]	0.8	0.83	0.84	486	558	1.15	2	5
		E2 ^[6]	0.8	0.98	1.04	348	438	1.26	2	5
		G1 ^[6]	0.8	0.74	0.82	486	494	1.02	1	2
19	Chun et al. (2007)	JC-1	0.8	1.48	1.93	2328	3195	1.37	1	2
		JC-2	0.7	1.19	1.64	4204	4983	1.19	1	2
		WC ^[4]	0.7	1.06	1.31	4726	5611	1.19	0	0
		JC-No. 11-1	0.9	0.87	1.05	4567	4912	1.08	3	3
20	Lee and Ko (2007)	S0	0.9	1.81	1.90	2275	3075	1.35	2	3
		W0	0.8	1.10	1.15	2241	2857	1.27	2	3

^[1] Columns arranged in alphabetical order of notation; notation described in Appendix A; values given in SI units are converted to in.-lb (1 in. = 25.4 mm; 1 psi = 1/145 Mpa; and 1 kip = 4.4484 kN)

^[2] Bar sizes are presented in SI and in.-lb as reported in the original studies

^[3] Analyzed as a doubly reinforced section to calculate the nominal flexural strength M_n ; all other specimens are analyzed as a single reinforced

^[4] Specimens did not contain confining reinforcement parallel to the hooked bars within the joint region

^[5] Specimens had transverse beams on one or both sides of the test beam. These transverse beams meet the dimensional requirements of Sections 18.8.4 and 15.2.8 of ACI 318-19 and Section 4.3 of ACI 352R-02 to be considered effective in increasing the joint shear strength

^[6] Specimens had $d/\ell_{eh} > 1.5$

^[7] Specimens had column to beam flexural strength ratio, M_R , less than 1.2

Table C.4 Cont. Data for exterior beam-column joint specimens tested under reversed cyclic loading^[1]

Study		Specimen	n	nT' (kips)	s_{tr} (in.)	T_h (kips)	T' (kips)	T'_{mod} (kips)	$\frac{T'}{T_h}$	$\frac{T'_{mod}}{T_h}$
14	Tsonos et al. (1992)	S6 ^[7]	4	53.0	2.5	14.8	13.3	-	0.90	-
		S6' ^[6]	4	69.1	2.5	14.3	17.3	-	1.21	-
15	Pantelides et al. (2002)	2 ^{[3][4]}	4	270.2	0.0	65.9	67.5	67.3	1.02	1.02
		4 ^{[3][4]}	4	278.7	0.0	65.9	69.7	-	1.06	-
		5 ^{[3][4]}	4	269.7	0.0	64.0	67.4	-	1.05	-
		6 ^{[3][4]}	4	265.2	0.0	65.5	66.3	-	1.01	-
16	Chutarat and Aboutaha (2003)	Specimen I	4	259.7	3.1	50.1	64.9	-	1.30	-
17	Hwang et al. (2005)	0T0 ^[4]	4	227.8	0.0	49.3	56.9	55.8	1.16	1.13
		3T44	4	241.2	3.8	49.5	60.3	57.8	1.22	1.17
		1B8	4	289.0	6.3	50.1	72.3	70.4	1.44	1.41
		3T3	4	258.2	3.8	49.5	64.5	62.3	1.30	1.26
		2T4	4	245.9	5.7	49.4	61.5	59.6	1.24	1.21
		1T44	4	236.1	6.3	49.5	59.0	56.7	1.19	1.14
		3T4	4	254.2	3.8	56.5	63.6	60.9	1.13	1.08
		2T5	4	265.8	5.7	56.5	66.4	63.8	1.18	1.13
		1T55	4	259.2	6.3	56.5	64.8	62.4	1.15	1.10
18	Tsonos (2007)	A1 ^[6]	4	45.0	2.0	8.9	11.2	10.7	1.26	1.20
		E1 ^[6]	3	59.2	2.0	14.4	19.7	-	1.37	-
		E2 ^[6]	2	43.3	1.9	17.2	21.7	21.6	1.26	1.25
		G1 ^[6]	3	52.5	3.9	14.0	17.5	-	1.25	-
19	Chun et al. (2007)	JC-1	4	192.5	5.9	35.2	48.1	44.0	1.37	1.25
		JC-2	8	332.5	5.9	35.1	41.6	38.7	1.18	1.10
		WC ^[4]	5	293.1	0.0	49.4	58.6	56.7	1.19	1.15
		JC-No. 11-1	3	334.3	4.7	104.0	111.4	110.7	1.07	1.06
20	Lee and Ko (2007)	S0	4	214.1	3.9	39.8	53.5	49.0	1.35	1.23
		W0	4	202.0	3.9	39.8	50.5	49.7	1.27	1.25

^[1] Columns arranged in alphabetical order of notation; notation described in Appendix A; values given in SI units are converted to in.-lb (1 in. = 25.4 mm; 1 psi = 1/145 Mpa; and 1 kip = 4.4484 kN)

^[2] Bar sizes are presented in SI and in.-lb as reported in the original studies

^[3] Analyzed as a doubly reinforced section to calculate the nominal flexural strength M_n ; all other specimens are analyzed as a single reinforced

^[4] Specimens did not contain confining reinforcement parallel to the hooked bars within the joint region

^[5] Specimens had transverse beams on one or both sides of the test beam. These transverse beams meet the dimensional requirements of Sections 18.8.4 and 15.2.8 of ACI 318-19 and Section 4.3 of ACI 352R-02 to be considered effective in increasing the joint shear strength

^[6] Specimens had $d/\ell_{eh} > 1.5$

^[7] Specimens had column to beam flexural strength ratio, M_R , less than 1.2

Table C.4 Cont. Data for exterior beam-column joint specimens tested under reversed cyclic loading^[1]

Study		Specimen	V_n (kips)	$V_{n,ACI 352}$ (kips)	V_p (kips)	$\frac{V_p}{V_n}$	$\delta_{0.8 peak}$	ψ_o
14	Tsonos et al. (1992)	S6 ^[7]	51.4	51.4	41.5	0.81	-	1.25
		S6' ^[6]	48.2	48.2	53.4	1.11	0.035	1.25
15	Pantelides et al. (2002)	2 ^{[3][4]}	212.2	212.2	235.1	1.11	0.025	1.25
		4 ^{[3][4]}	199.8	199.8	242.5	1.21	0.018	1.25
		5 ^{[3][4]}	189.9	189.9	234.7	1.24	0.025	1.25
		6 ^{[3][4]}	197.7	197.7	230.8	1.17	0.028	1.25
16	Chutarat and Aboutaha (2003)	Specimen I	194.3	182.1	231.2	1.19	0.074	1.00
17	Hwang et al. (2005)	0T0 ^[4]	324.2	285.6	224.1	0.69	0.060	1.00
		3T44	346.3	305.1	239.4	0.69	0.087	1.00
		1B8	310.6	273.7	282.6	0.91	0.060	1.00
		3T3	328.2	289.2	254.5	0.78	0.100	1.00
		2T4	333.0	293.3	242.8	0.73	0.075	1.00
		1T44	337.1	297.0	233.6	0.69	0.080	1.00
		3T4	393.4	336.5	249.5	0.63	0.070	1.00
		2T5	397.0	339.7	261.2	0.66	0.070	1.00
		1T55	378.7	324.0	253.1	0.67	0.070	1.00
18	Tsonos (2007)	A1 ^[6]	53.0	53.0	38.9	0.73	0.045	1.25
		E1 ^[6]	42.0	42.0	47.8	1.14	0.060	1.25
		E2 ^[6]	53.0	53.0	37.6	0.71	0.065	1.25
		G1 ^[6]	42.0	42.0	42.3	1.01	0.040	1.25
19	Chun et al. (2007)	JC-1	373.9	340.9	178.3	0.48	0.045	1.00
		JC-2	369.0	336.4	296.7	0.80	0.070	1.00
		WC ^[4]	807.4	807.4	426.7	0.53	0.053	1.25
		JC-No. 11-1	433.6	366.9	265.0	0.61	0.054	1.00
20	Lee and Ko (2007)	S0	316.8	277.2	186.0	0.59	0.065	1.00
		W0	298.3	198.9	175.0	0.59	0.055	1.00

^[1] Columns arranged in alphabetical order of notation; notation described in Appendix A; values given in SI units are converted to in.-lb (1 in. = 25.4 mm; 1 psi = 1/145 Mpa; and 1 kip = 4.4484 kN)

^[2] Bar sizes are presented in SI and in.-lb as reported in the original studies

^[3] Analyzed as a doubly reinforced section to calculate the nominal flexural strength M_n ; all other specimens are analyzed as a single reinforced

^[4] Specimens did not contain confining reinforcement parallel to the hooked bars within the joint region

^[5] Specimens had transverse beams on one or both sides of the test beam. These transverse beams meet the dimensional requirements of Sections 18.8.4 and 15.2.8 of ACI 318-19 and Section 4.3 of ACI 352R-02 to be considered effective in increasing the joint shear strength

^[6] Specimens had $d/\ell_{eh} > 1.5$

^[7] Specimens had column to beam flexural strength ratio, M_R , less than 1.2

Table C.4 Cont. Data for exterior beam-column joint specimens tested under reversed cyclic loading ^[1]

Study		Specimen	Bar Size ^[2]	A_b (in. ²)	A_{hs} (in. ²)	A_{tr} (in. ²)	A_{th} (in. ²)	$\frac{A_{th}}{A_{hs}}$	A_v (in. ²)	b_b (in.)
21	Kang et al. (2010)	Jk ^[6]	D19	0.44	1.76	0.11	0.44	0.25	0.88	17.7
22	Hwang et al. (2014)	T1-400	D22	0.60	4.20	0.20	1.60	0.38	2.40	13.8
		T2-600	D22	0.60	2.40	0.20	1.60	0.67	2.40	13.8
		T3-600 ^[3]	D25	0.79	3.16	0.20	1.60	0.51	2.40	13.8
23	Chun and Shin (2014)	H0.7S ^[3]	D19	0.44	1.76	0.20	0.51	0.29	0.60	9.8
		H1.0S ^[3]	D19	0.44	1.76	0.20	1.02	0.58	1.80	9.8
		H1.5S ^[6]	D19	0.44	1.76	0.20	1.02	0.58	3.00	9.8
		H2.0S ^[6]	D19	0.44	1.76	0.20	1.02	0.58	4.20	9.8
		H2.5S ^[6]	D19	0.44	1.76	0.20	1.02	0.58	5.40	9.8
		H0.7U ^[3]	D19	0.44	1.76	0.11	0.33	0.19	0.33	9.8
		H1.0U ^[3]	D19	0.44	1.76	0.11	0.66	0.38	0.99	9.8
24	Choi and Bae (2019)	JTR-0-BTR	D25	0.79	1.58	0.20	1.60	1.01	1.60	9.8
		JNR-0-BTR ^[4]	D25	0.79	1.58	0.00	0.00	0.00	0.00	9.8
		JTR-0-BNR	D25	0.79	1.58	0.20	1.60	1.01	1.60	9.8

^[1] Columns arranged in alphabetical order of notation; notation described in Appendix A; values given in SI units are converted to in.-lb (1 in. = 25.4 mm; 1 psi = 1/145 Mpa; and 1 kip = 4.4484 kN)

^[2] Bar sizes are presented in SI and in.-lb as reported in the original studies

^[3] Analyzed as a doubly reinforced section to calculate the nominal flexural strength M_n ; all other specimens are analyzed as a single reinforced

^[4] Specimens did not contain confining reinforcement parallel to the hooked bars within the joint region

^[5] Specimens had transverse beams on one or both sides of the test beam. These transverse beams meet the dimensional requirements of Sections 18.8.4 and 15.2.8 of ACI 318-19 and Section 4.3 of ACI 352R-02 to be considered effective in increasing the joint shear strength

^[6] Specimens had $d/\ell_{eh} > 1.5$

^[7] Specimens had column to beam flexural strength ratio, M_R , less than 1.2

Table C.4 Cont. Data for exterior beam-column joint specimens tested under reversed cyclic loading ^[1]

Study		Specimen	b_c (in.)	b_j (in.)	$b_{j,ACI 352}$ (in.)	c_{ch} (in.)	$\frac{c_{ch}}{d_b}$	c_{so} (in.)	$\frac{c_{so}}{d_b}$	d
21	Kang et al. (2010)	Jk ^[6]	17.7	17.7	17.7	3.9	5.2	2.6	3.5	19.4
22	Hwang et al. (2014)	T1-400	19.7	19.7	16.7	3.3	3.7	4.5	5.1	17.1
		T2-600	19.7	19.7	16.7	3.3	3.7	4.5	5.1	17.7
		T3-600 ^[3]	19.7	19.7	16.7	3.3	3.3	4.5	4.5	17.6
23	Chun and Shin (2014)	H0.7S ^[3]	12.0	12.0	10.9	1.8	2.3	3.0	3.9	5.4
		H1.0S ^[3]	12.0	12.0	10.9	1.8	2.3	3.0	3.9	9.4
		H1.5S ^[6]	12.0	12.0	10.9	1.8	2.3	3.0	3.9	15.3
		H2.0S ^[6]	12.0	12.0	10.9	1.8	2.3	3.0	3.9	21.2
		H2.5S ^[6]	12.0	12.0	10.9	1.8	2.3	3.0	3.9	27.1
		H0.7U ^[3]	12.0	12.0	10.9	1.8	2.3	3.0	3.9	5.4
		H1.0U ^[3]	12.0	12.0	10.9	1.8	2.3	3.0	3.9	9.4
24	Choi and Bae (2019)	JTR-0-BTR	11.8	11.8	10.8	4.6	4.6	3.1	3.1	12.1
		JNR-0-BTR ^[4]	11.8	11.8	10.8	4.6	4.6	3.1	3.1	12.1
		JTR-0-BNR	11.8	11.8	10.8	4.6	4.6	3.1	3.1	12.1

^[1] Columns arranged in alphabetical order of notation; notation described in Appendix A; values given in SI units are converted to in.-lb (1 in. = 25.4 mm; 1 psi = 1/145 Mpa; and 1 kip = 4.4484 kN)

^[2] Bar sizes are presented in SI and in.-lb as reported in the original studies

^[3] Analyzed as a doubly reinforced section to calculate the nominal flexural strength M_n ; all other specimens are analyzed as a single reinforced

^[4] Specimens did not contain confining reinforcement parallel to the hooked bars within the joint region

^[5] Specimens had transverse beams on one or both sides of the test beam. These transverse beams meet the dimensional requirements of Sections 18.8.4 and 15.2.8 of ACI 318-19 and Section 4.3 of ACI 352R-02 to be considered effective in increasing the joint shear strength

^[6] Specimens had $d/\ell_{ch} > 1.5$

^[7] Specimens had column to beam flexural strength ratio, M_R , less than 1.2

Table C.4 Cont. Data for exterior beam-column joint specimens tested under reversed cyclic loading ^[1]

Study		Specimen	$\frac{d}{\ell_{eh}}$	d' (in.)	d_b (in.)	f_{cm} ^[8] (psi)	f_{cm} ^[9] (psi)	f_y (ksi)	$f_{ytr,l}$ (ksi)	$f_{ytr,l} A_v$ (kips)
21	Kang et al. (2010)	Jk ^[6]	1.73	1.8	0.75	4200	4200	67.0	83.0	73.0
22	Hwang et al. (2014)	T1-400	0.87	2.6	0.875	4640	4640	75.4	64.7	155.2
		T2-600	0.90	2.0	0.875	4640	4640	103.0	64.7	155.2
		T3-600 ^[3]	0.90	2.1	1	4290	4290	92.1	64.7	155.2
23	Chun and Shin (2014)	H0.7S ^[3]	0.60	2.5	0.75	5050	3710	70.8	66.7	40.0
		H1.0S ^[3]	1.04	2.4	0.75	5050	3710	70.8	66.7	120.1
		H1.5S ^[6]	1.70	2.4	0.75	5050	3710	70.8	66.7	200.1
		H2.0S ^[6]	2.35	2.4	0.75	6990	3830	70.8	66.7	280.1
		H2.5S ^[6]	3.01	2.4	0.75	6990	3830	70.8	66.7	360.2
		H0.7U ^[3]	0.60	2.5	0.75	5050	3710	70.8	62.4	20.6
		H1.0U ^[3]	1.04	2.4	0.75	5050	3710	70.8	62.4	61.8
24	Choi and Bae (2019)	JTR-0-BTR	1.45	2.6	1	7950	7950	68.4	58.0	92.8
		JNR-0-BTR ^[4]	1.45	2.6	1	7950	7950	68.4	0.0	0.0
		JTR-0-BNR	1.45	2.6	1	7950	7950	68.4	58.0	92.8

^[1] Columns arranged in alphabetical order of notation; notation described in Appendix A; values given in SI units are converted to in.-lb (1 in. = 25.4 mm; 1 psi = 1/145 Mpa; and 1 kip = 4.4484 kN)

^[3] Analyzed as a doubly reinforced section to calculate the nominal flexural strength M_n ; all other specimens are analyzed as a single reinforced

^[4] Specimens did not contain confining reinforcement parallel to the hooked bars within the joint region

^[6] Specimens had $d/\ell_{eh} > 1.5$

^[7] Specimens had column to beam flexural strength ratio, M_R , less than 1.2

^[8] Column concrete compressive strength

^[9] Beam concrete compressive strength

Table C.4 Cont. Data for exterior beam-column joint specimens tested under reversed cyclic loading ^[1]

Study		Specimen	h_b (in.)	h_c (in.)	ℓ_{dh} (in.)	$\frac{\ell_{dh}}{d_b}$	ℓ_{eh} (in.)	$\frac{\ell_{eh}}{d_b}$	ℓ_{ehy} (in.)	$\frac{\ell_{ehy}}{d_b}$
21	Kang et al. (2010)	Jk ^[6]	21.3	17.7	8.4	11.2	11.3	15.0	7.8	10.5
22	Hwang et al. (2014)	T1-400	19.7	21.7	12.5	14.3	19.6	22.4	11.6	13.3
		T2-600	19.7	21.7	17.1	19.5	19.6	22.4	15.9	18.2
		T3-600 ^[3]	19.7	21.7	19.4	19.4	19.6	19.6	18.0	18.0
23	Chun and Shin (2014)	H0.7S ^[3]	7.9	12.0	9.7	12.9	9.0	12.0	9.4	12.6
		H1.0S ^[3]	11.8	12.0	9.7	12.9	9.0	12.0	9.4	12.6
		H1.5S ^[6]	17.7	12.0	9.7	12.9	9.0	12.0	9.4	12.6
		H2.0S ^[6]	23.6	12.0	8.9	11.9	9.0	12.0	8.6	11.5
		H2.5S ^[6]	29.5	12.0	8.9	11.9	9.0	12.0	8.6	11.5
		H0.7U ^[3]	7.9	12.0	10.1	13.4	9.0	12.0	9.5	12.7
		H1.0U ^[3]	11.8	12.0	9.7	12.9	9.0	12.0	9.4	12.6
24	Choi and Bae (2019)	JTR-0-BTR	14.8	11.8	11.6	11.6	8.3	8.3	10.3	10.3
		JNR-0-BTR ^[4]	14.8	11.8	16.2	16.2	8.3	8.3	12.6	12.6
		JTR-0-BNR	14.8	11.8	11.6	11.6	8.3	8.3	10.3	10.3

^[1] Columns arranged in alphabetical order of notation; notation described in Appendix A; values given in SI units are converted to in.-lb (1 in. = 25.4 mm; 1 psi = 1/145 Mpa; and 1 kip = 4.4484 kN)

^[2] Bar sizes are presented in SI and in.-lb as reported in the original studies

^[3] Analyzed as a doubly reinforced section to calculate the nominal flexural strength M_n ; all other specimens are analyzed as a single reinforced

^[4] Specimens did not contain confining reinforcement parallel to the hooked bars within the joint region

^[5] Specimens had transverse beams on one or both sides of the test beam. These transverse beams meet the dimensional requirements of Sections 18.8.4 and 15.2.8 of ACI 318-19 and Section 4.3 of ACI 352R-02 to be considered effective in increasing the joint shear strength

^[6] Specimens had $d/\ell_{eh} > 1.5$

^[7] Specimens had column to beam flexural strength ratio, M_R , less than 1.2

Table C.4 Cont. Data for exterior beam-column joint specimens tested under reversed cyclic loading ^[1]

Study		Specimen	$\frac{\ell_{eh}}{h_c}$	$\frac{\ell_{eh}}{\ell_{dh}}$	$\frac{\ell_{eh}}{\ell_{ehy}}$	M_n (kip.in.)	M_{peak} (kip.in.)	$\frac{M_{peak}}{M_n}$	N	N_{total}
21	Kang et al. (2010)	Jk ^[6]	0.6	1.33	1.43	2177	2721	1.25	2	4
22	Hwang et al. (2014)	T1-400	0.9	1.57	1.69	3878	4658	1.20	2	3
		T2-600	0.9	1.15	1.23	3807	4844	1.27	2	3
		T3-600 ^[3]	0.9	1.01	1.09	4282	5403	1.26	2	3
23	Chun and Shin (2014)	H0.7S ^[3]	0.8	0.93	0.95	492	612	1.24	1	1
		H1.0S ^[3]	0.8	0.93	0.95	984	1080	1.10	2	3
		H1.5S ^[6]	0.8	0.93	0.95	1728	1752	1.01	2	5
		H2.0S ^[6]	0.8	1.01	1.04	2484	2760	1.11	2	7
		H2.5S ^[6]	0.8	1.01	1.04	3216	3252	1.01	2	9
		H0.7U ^[3]	0.8	0.89	0.95	492	576	1.17	1	1
		H1.0U ^[3]	0.8	0.93	0.95	984	1020	1.04	2	3
24	Choi and Bae (2019)	JTR-0-BTR	0.7	0.72	0.81	1221	1275	1.04	4	4
		JNR-0-BTR ^[4]	0.7	0.52	0.66	1221	1080	0.88	0	0
		JTR-0-BNR	0.7	0.72	0.81	1221	1221	1.00	4	4

^[1] Columns arranged in alphabetical order of notation; notation described in Appendix A; values given in SI units are converted to in.-lb (1 in. = 25.4 mm; 1 psi = 1/145 Mpa; and 1 kip = 4.4484 kN)

^[2] Bar sizes are presented in SI and in.-lb as reported in the original studies

^[3] Analyzed as a doubly reinforced section to calculate the nominal flexural strength M_n ; all other specimens are analyzed as a single reinforced

^[4] Specimens did not contain confining reinforcement parallel to the hooked bars within the joint region

^[5] Specimens had transverse beams on one or both sides of the test beam. These transverse beams meet the dimensional requirements of Sections 18.8.4 and 15.2.8 of ACI 318-19 and Section 4.3 of ACI 352R-02 to be considered effective in increasing the joint shear strength

^[6] Specimens had $d/\ell_{eh} > 1.5$

^[7] Specimens had column to beam flexural strength ratio, M_R , less than 1.2

Table C.4 Cont. Data for exterior beam-column joint specimens tested under reversed cyclic loading ^[1]

Study		Specimen	<i>n</i>	<i>nT'</i> (kips)	<i>s_{tr}</i> (in.)	<i>T_h</i> (kips)	<i>T'</i> (kips)	<i>T'</i> _{mod} (kips)	$\frac{T'}{T_h}$	$\frac{T'_{mod}}{T_h}$
21	Kang et al. (2010)	Jk ^[6]	4	147.4	4.7	29.6	36.9	35.2	1.24	1.19
22	Hwang et al. (2014)	T1-400	7	380.4	3.9	45.4	54.3	50.4	1.20	1.11
		T2-600	4	314.4	3.9	62.0	78.6	76.8	1.27	1.24
		T3-600 ^[3]	4	367.1	3.9	73.0	91.8	91.0	1.26	1.25
23	Chun and Shin (2014)	H0.7S ^[3]	4	155.0	3.0	29.8	38.8	-	1.30	-
		H1.0S ^[3]	4	136.8	3.0	29.8	34.2	-	1.15	-
		H1.5S ^[6]	4	126.3	3.0	29.8	31.6	-	1.06	-
		H2.0S ^[6]	4	138.5	3.0	31.3	34.6	34.5	1.11	1.10
		H2.5S ^[6]	4	126.0	3.0	31.3	31.5	31.3	1.01	1.00
		H0.7U ^[3]	4	145.9	3.0	29.6	36.5	-	1.23	-
		H1.0U ^[3]	4	129.2	3.0	29.8	32.3	-	1.08	-
24	Choi and Bae (2019)	JTR-0-BTR	2	112.8	2.4	44.8	56.4	-	1.26	-
		JNR-0-BTR ^[4]	2	95.5	0.0	34.7	47.8	-	1.38	-
		JTR-0-BNR	2	108.1	2.4	44.8	54.0	-	1.21	-

^[1] Columns arranged in alphabetical order of notation; notation described in Appendix A; values given in SI units are converted to in.-lb (1 in. = 25.4 mm; 1 psi = 1/145 Mpa; and 1 kip = 4.4484 kN)

^[2] Bar sizes are presented in SI and in.-lb as reported in the original studies

^[3] Analyzed as a doubly reinforced section to calculate the nominal flexural strength M_n ; all other specimens are analyzed as a single reinforced

^[4] Specimens did not contain confining reinforcement parallel to the hooked bars within the joint region

^[5] Specimens had transverse beams on one or both sides of the test beam. These transverse beams meet the dimensional requirements of Sections 18.8.4 and 15.2.8 of ACI 318-19 and Section 4.3 of ACI 352R-02 to be considered effective in increasing the joint shear strength

^[6] Specimens had $d/\ell_{eh} > 1.5$

^[7] Specimens had column to beam flexural strength ratio, M_R , less than 1.2

Table C.4 Cont. Data for exterior beam-column joint specimens tested under reversed cyclic loading ^[1]

Study		Specimen	V_n (kips)	$V_{n,ACI 352}$ (kips)	V_p (kips)	$\frac{V_p}{V_n}$	$\delta_{0.8 peak}$	ψ_o
21	Kang et al. (2010)	Jk ^[6]	244.1	244.1	134.0	0.55	0.035	1.00
22	Hwang et al. (2014)	T1-400	348.4	296.2	271.8	0.78	0.032	1.00
		T2-600	348.4	296.2	262.9	0.75	0.038	1.00
		T3-600 ^[3]	335.1	284.8	277.8	0.83	0.048	1.00
23	Chun and Shin (2014)	H0.7S ^[3]	122.8	111.5	145.0	1.18	0.100	1.00
		H1.0S ^[3]	122.8	111.5	127.0	1.03	0.070	1.00
		H1.5S ^[6]	122.8	111.5	112.0	0.91	0.050	1.00
		H2.0S ^[6]	144.5	131.2	118.0	0.82	0.070	1.00
		H2.5S ^[6]	144.5	131.2	102.0	0.71	0.050	1.00
		H0.7U ^[3]	122.8	111.5	137.0	1.12	0.100	1.00
		H1.0U ^[3]	122.8	111.5	119.0	0.97	0.070	1.00
24	Choi and Bae (2019)	JTR-0-BTR	149.2	136.8	104.2	0.70	0.044	1.00
		JNR-0-BTR ^[4]	149.2	136.8	87.8	0.59	0.019	1.00
		JTR-0-BNR	149.2	136.8	99.7	0.67	0.047	1.00

^[1] Columns arranged in alphabetical order of notation; notation described in Appendix A; values given in SI units are converted to in.-lb (1 in. = 25.4 mm; 1 psi = 1/145 Mpa; and 1 kip = 4.4484 kN)

^[2] Bar sizes are presented in SI and in.-lb as reported in the original studies

^[3] Analyzed as a doubly reinforced section to calculate the nominal flexural strength M_n ; all other specimens are analyzed as a single reinforced

^[4] Specimens did not contain confining reinforcement parallel to the hooked bars within the joint region

^[5] Specimens had transverse beams on one or both sides of the test beam. These transverse beams meet the dimensional requirements of Sections 18.8.4 and 15.2.8 of ACI 318-19 and Section 4.3 of ACI 352R-02 to be considered effective in increasing the joint shear strength

^[6] Specimens had $d/\ell_{eh} > 1.5$

^[7] Specimens had column to beam flexural strength ratio, M_R , less than 1.2

APPENDIX D: SUMMARY OF STUDIES ON BEAM-COLUMN JOINT SPECIMENS TESTED UNDER REVERSED CYCLIC LOADING

This study includes an analysis of the results of 146 exterior beam-column joint specimens containing hooked bars tested under reversed cyclic loading by Hanson and Connor (1967), Hanson (1971), Megget (1974), Uzumeri (1977), Lee et al. (1977), Scribner (1978), Paulay and Scarpas (1981), Ehsani and Wight (1982), Kanada et al. (1984), Zerbe and Durrani (1985), Ehsani et al. (1987), Ehsani and Alameddine (1991), Kaku and Asakusa (1991), Tsonos et al. (1992), Pantelides et al. (2002), Chutarat and Aboutaha (2003), Hwang et al. (2005), Lee and Ko (2007), Chun et al. (2007), Tsonos (2007), Kang et al. (2010), Chun and Shin (2014), Hwang et al. (2014), and Choi and Bae (2019). The specimens contained hooked bars ranging in size from No. 3 to No. 9, with peak bar stresses ranging from 42,900 to 103,000 psi, and concretes with compressive strengths ranging from 3,140 to 13,700 psi. A detailed summary of these studies is presented in this appendix.

Hanson and Connor (1967)

Hanson and Connor (1967) tested seven exterior beam-column joint specimens to determine the required joint reinforcement to maintain ultimate capacity for cast-in-place beams and columns subjected to reversed cyclic loading. The principle variables were column size, column load, and the amount of confining reinforcement in the joint. Four and two No. 9 hooked bars were used as top and bottom beam longitudinal reinforcement, respectively, anchored in the column. Concrete compressive strength and the yield strength of hooked bars ranged from 3,200 to 5,420 psi and from 47,800 to 51,600 psi, respectively. The center-to-center spacing between the hooked bars was $2.3d_b$ (2.6 in.), and the clear side concrete cover to the bar was $2.7d_b$ (3.0 in.). The embedment length of the hooked bars was $12d_b$ (13.5 in.). Hanson and Connor found that confining reinforcement (hoops) is required for exterior beam-column joints. In addition, they concluded that hoops are not required for exterior joints that are confined on at least three sides by beams or spandrels of approximately equal depth and meet the ACI 318 requirements for the concrete strength required to transfer the column load through the joint. Hanson and Connor found that properly designed and detailed exterior beam-column joints can resist moderate earthquakes without losing strength.

Hanson (1971)

Hanson (1971) tested five beam-column joint specimens to investigate the behavior of Grade 60 No. 8 hooked reinforcement anchored in beam-column joint specimens subjected to reversed cyclic loading. The five beam-column joints represented assemblies from different locations in a frame made up of 12 in. \times 20 in. beams and 15 in. \times 15 in. columns. Concrete compressive strengths ranged from 5200 to 5500 psi, and the yield strength of the hooked bars ranged from 63,100 to 65,000 psi. The center-to-center spacing between the hooked bars was $2.7d_b$ (2.7 in.), and the clear side concrete cover to the bar was $3.0d_b$ (3.0 in.). The embedment length of the hooked bars was $13.5d_b$ (13.5 in.). A constant axial load of 640 kips, $\frac{1}{3}$ of the column capacity, was applied on all specimens except specimen 5; a constant load of 320 kips, $\frac{1}{6}$ the column capacity, was used on specimen 5. Hanson found that the presence of confining reinforcement in the joint region improves the anchorage strength of hooked bars and controls the joint shear distortion and cracking. Hanson concluded that Grade 60 hooked reinforcing bars are suitable for use in structures designed to develop ductile behavior.

Megget (1974)

Megget (1974) tested two exterior beam-column joint specimens to investigate the effect of the presence of transverse beam stubs on the behavior of the external beam-column joints. The two specimens were identical, except one had transverse beam stubs on both sides of the main test beam, and the other did not. Concrete compressive strength and the yield strength of hooked bars were 3,200 psi and 54,700 psi, respectively. The center-to-center spacing between the No. 8 hooked bars was $2.7d_b$ (2.7 in.), and the clear side concrete cover to the hooked bar was $3.3d_b$ (3.3 in.). The embedment length of the hooked bars was $12.6d_b$ (12.6 in.). Six No. 4 hoops were used as confining reinforcement within the joint region. A constant axial load of 44 kips was applied to the specimens throughout the test. Megget found that the presence of transverse beam stubs significantly contributes to the confinement of the joint core concrete and causes a plastic hinge to form in the main beam rather than in the beam-column joint region.

Uzumeri (1977)

Uzumeri (1977) tested eight exterior beam-column joint specimens to investigate the effects of the amount of confining reinforcement and the presence of transverse beam stub on the

behavior of beam-column joints subjected to reversed cyclic loading. The transverse beam stub was located only on one side of the column in four specimens, whereas the other four had no transverse beam stub. Three of the eight specimens had no confining reinforcement, and the remaining five included confining reinforcement ranging from four to eight No. 3 or No. 4 hoops in the joint region. A constant axial load of 520 kips was applied to the column throughout the test. Concrete compressive strength and the yield strength of the No. 9 hooked bars ranged from 3,820 to 5,250 psi and 50,300 to 51,100 psi, respectively. The center-to-center spacing between the hooked bars ranged from 2.9 to $4.4d_b$ (3.3 to 4.9 in.), and the clear side concrete cover to the hooked bar ranged from 1.8 to $3.1d_b$ (2.0 to 3.5 in.). The embedment length of the hooked bars was $11.5d_b$ (13.0 in.). Uzumeri found that the presence of confining reinforcement in beam-column joints increased the anchorage strength and ductility of the beam-column joints subjected to reversed cyclic loading. Uzumeri observed that, within the limitations of the tests, the presence of the transverse beam stub on one side of the beam-column joints showed no significant effect on the behavior of beam-column joint specimens tested under reversed cyclic loading.

Lee et al. (1977)

Lee et al. (1977) tested eight exterior beam-column joint specimens with two design procedures and loading conditions to investigate the behavior of exterior beam-column joints subjected to reversed cyclic loading. The beam-column joints were designed using two criteria: the first is referred to as Type 1 design using the ACI 318-71 for non-seismic conditions, and the second design is referred to as Type 2 design using the ACI 318-71 and the ACI 352 Recommendations for Seismic Conditions. The amount of transverse reinforcement in the specimens was the main difference between the two designs. Three of the eight specimens were designed in accordance with the Type 1 design procedure and the remaining five were designed following the Type 2 design procedure. The main parameters were the amount of confining reinforcement within the joint region, the magnitude of axial load on the column, and the severity of loading. Two displacement patterns (9 and 12 cycles) were used to obtain different degrees of damage during testing. The displacement patterns were meant to simulate the type of displacements the beam-column joints may be subjected to during moderate and severe earthquakes. Of the eight specimens, two were subjected to the displacement pattern representing

a moderate earthquake loading, and the remaining six were subjected to the displacement pattern representing a severe earthquake loading. Four specimens had a constant axial load of 40 kips applied to the column throughout the test, while the others had zero axial loads. Specimens contained No. 2 or No. 3 bars (hoops) spaced at 3 or 1.25 in., respectively, as confining reinforcement within the joint region. Beam and column cross-section dimensions for all specimens were 8×10 in. and 8×11 in., respectively. Concrete compressive strengths ranged from 3,600 to 4,200 psi. The No. 6 hooked bars with a yield strength ranging from 47,500 to 52,500 psi were used as longitudinal beam reinforcing bars. The center-to-center spacing between the hooked bars was $3.3d_b$ (2.5 in.), and the clear side concrete cover to the hooked bar was $3.2d_b$ (2.4 in.). The embedment length of the hooked bars was $12.5d_b$ (9.4 in.). Lee et al. found that the joints for specimens with axial loads of 40 kips were stiffer than those without axial loads. They observed that Type 2 design specimens performed better during testing and had less load degradation than Type 1 design specimens. Lee et al. concluded that the additional transverse reinforcement in Type 2 designed specimens provided better confinement for the beam core, resulting in less strength degradation and more energy dissipation during the test.

Scribner (1978)

Scribner (1978) tested 12 exterior beam-column joint specimens to evaluate the effect of intermediate longitudinal reinforcement in preventing shear strength and stiffness deterioration in beam-column joints subjected to reversed cyclic loading. The main variables were the presence of intermediate longitudinal bars in half of the specimens and the amount of confining reinforcement within the joint region. Intermediate longitudinal bars consisted of four No. 2, No. 3, or No. 4 bars placed in two layers at approximately the third points between tension and compression reinforcement of the beam. The 12 specimens were divided into two groups. Group 1 consisted of eight specimens tested using No. 6 hooked bars as beam longitudinal reinforcement. The column cross-section dimensions for all specimens in group 1 were 8×12 in., whereas the beam cross-section dimensions were a width of 8 in. and a height of 10 or 12 in. Group 2 consisted of four specimens tested with No. 8 hooked bars as beam longitudinal reinforcement. The dimensions of the beam and the column cross-section for all specimens in group 2 were 10×14 in. and 12×18 in., respectively. Constant axial loads of 40 and 100 kips were applied to the columns in groups 1

and 2, respectively, throughout the test. Confining reinforcement of No. 3 and No. 4 bars were used in the joint region in groups 1 and 2, respectively. Concrete compressive strengths ranged from 3,680 to 5,210 psi, and the yield strength of hooked bars ranged from 48,900 to 60,200 psi. The center-to-center spacing between the hooked bars ranged from 2.1 to $6.9d_b$ (2.1 to 5.2 in.), and the clear side concrete cover to the hooked bar ranged from 1.4 to $2.4d_b$ (1.0 to 2.4 in.). The embedment length of the hooked bars ranged from 14.0 to $16.6d_b$ (10.5 to 16.6 in.). Scribner found that the presence of the intermediate longitudinal reinforcement increased the energy dissipation capacity of the exterior beam-column joints and prevented significant strength and stiffness decay during reversed cyclic loading. Scribner also observed that the presence of the intermediate longitudinal reinforcement and confining reinforcement limited shear strength decay.

Paulay and Scarpas (1981)

Paulay and Scarpas (1981) tested three exterior beam-column joint specimens to study the effect of confining reinforcement in the joint region and the presence of intermediate column bars on the anchorage strength and behavior of the exterior beam-column joints subjected to reversed cyclic loading. The intermediate column bars were placed on the sides of the beam longitudinal hooked bars used as vertical joint shear reinforcement. A constant axial load of $0.05 f'_c A_g$ was applied to specimens 1 and 3 throughout the test, while specimen 2 was subjected to a load of $0.15 f'_c A_g$, where f'_c is the design concrete compressive strength and A_g is the cross-section area of the column. Specimen 1 had confining reinforcement in accordance with the New Zealand code requirements, whereas specimens 2 and 3 had 50% of the amount of confining reinforcement recommended in New Zealand. Measured concrete compressive strengths ranged from 3,260 to 3,900 psi, and the yield strength of the No. 6 (D20) hooked bars was 42,900 psi. The center-to-center spacing between the hooked bars was $4.4d_b$ (3.5 in.), and the clear side concrete cover to the hooked bar was $4.3d_b$ (3.4 in.). The embedment length of the hooked bars was $21.1d_b$ (16.7 in.). Paulay and Scarpas found that specimens with approximately 50% of the recommended confining reinforcement performed satisfactorily. As a result, they concluded that the confining reinforcement required to carry the joint design shear force in exterior beam-column joints could be considerably decreased.

Ehsani and Wight (1982)

Ehsani and Wight (1982) tested 12 exterior beam-column joint specimens to study the effect of confining reinforcement within the joint region and the presence of transverse beams and slab on the anchorage strength and behavior of exterior beam-column joints subjected to reversed cyclic loading. The main parameters were the flexural strength ratio (the flexural capacity of the columns to that of the beams), ranging from 1.1 to 2.0, percentage of the confining reinforcement within the joint region, ranging from 0.86% to 1.86%, and joint shear stress, either $10\sqrt{f'_c}$ or $14\sqrt{f'_c}$, where f'_c is the design concrete compressive strength (4000 psi). Six of the 12 specimens had transverse beams and a slab, while the others did not. Measured concrete compressive strengths ranged from 3,470 to 6,470 psi, and the yield strength of the No. 7 hooked bars was 48,000 psi. A constant axial load of 80 kips was applied to the specimens throughout the test. Ehsani and Wight concluded that the flexural strength ratio for exterior beam-column joints without and with transverse beams and a slab should be greater than 1.4 and 1.2, respectively, to ensure that plastic flexural hinges form in beams rather than columns. They discovered that to delay the rapid deterioration of joint concrete, the joint shear stress should be less than or equal $12\sqrt{f'_c}$. Ehsani and Wight observed that the larger percentage of confining reinforcement within the joint region improved the behavior of the exterior beam-column joints.

Kanada et al. (1984)

Kanada et al. (1984) tested 16 exterior beam-column joint specimens under reversed cyclic loading to investigate the relationship between the anchorage capacity and the joint shear strength. Of the 16 specimens, 13 had No. 6 bars with 90° standard hooks, and three had No. 6 bars with heads as beam longitudinal reinforcement. The primary variables examined were the anchorage of beam bars to the column, amount of confining reinforcement within the joint region, and percentage of beam bars. No axial load was applied to the specimens. Concrete compressive strengths ranged from 3,140 to 4,370 psi, and the yield strength of hooked bars was 56,200 psi. The center-to-center spacing between the hooked bars ranged from $2.8d_b$ (2.1 to 6.3 in.), and the clear side concrete cover to the hooked bar was $3.2d_b$ (2.4 in.). The embedment length of the hooked bars ranged from $8d_b$ (6 to 9 in.). Kanada et al. observed that it was more accurate to take the effective joint depth equal to the projected development length of hooked beam bars to

calculate the joint shear. Kanada et al. concluded that the main function of the confining reinforcement in the joint region is to delay the deterioration of the joint core concrete and to strengthen the inclined compression strut under large reversed cyclic loading.

Zerbe and Durrani (1985)

Zerbe and Durrani (1985) tested seven exterior beam-column joint specimens to investigate the effect of transverse beams, with and without a slab, on the performance of exterior beam-column joints subjected to reversed cyclic loading. Three of the seven specimens did not have a slab and acted as reference specimens, and the remaining four contained slabs with different widths. Concrete compressive strengths ranged from 5,610 to 5,940 psi, and the yield strength of the No. 6 hooked bars was 60,000 psi. The center-to-center spacing between the hooked bars was $2.3d_b$ (1.75 in.), and the clear side concrete cover to the hooked bar was $4d_b$ (3 in.). The embedment length of the hooked bars was $10.3d_b$ (7.8 in.). Zerbe and Durrani concluded that the contribution of a slab must be considered in the flexural strength of beams to avoid the possible formation of plastic hinges in columns instead of in beams in exterior beam-column joints. They suggested that the lateral confinement, which is primarily provided by the transverse beams, is responsible for the increased strength and stiffness of joints with transverse beams. They recommended that the beam longitudinal reinforcement be terminated in a stub outside the joint core to avoid steel congestion in the exterior joint.

Ehsani et al. (1987)

Ehsani et al. (1987) examined five exterior beam-column joint specimens to investigate the effect of different shear stress levels on beam-column joints constructed with high-strength concrete and compared the results with a similar specimen constructed with normal-strength concrete. The main variable was joint shear stress, which ranged between $7.52\sqrt{f'_c}$ and $12.84\sqrt{f'_c}$, where f'_c is the measured concrete compressive strength (psi). A constant axial load ranging from 30 to 86 kips was applied to the columns. Concrete compressive strengths ranged from 6,470 to 9,760 psi, and the yield strength of the No. 6 and No. 7 hooked bars ranged from 48,000 to 70,000 psi. The center-to-center spacing between the hooked bars ranged from 3.5 to $5.2d_b$ (3.1 to 3.9 in.), and the clear side concrete cover to the hooked bar ranged from 2.7 to $3.2d_b$ (2.3 to 2.4 in.). The embedment length of the hooked bars ranged from 9.8 to $14.4d_b$ (8.6 to 10.8 in.). Ehsani

et al. suggested that the maximum permitted joint shear stress should be a function of the concrete compressive strength but provided no specifics. They also indicated that the shear stress factors provided by ACI 352R-85 should be modified before they can be safely applied to beam-column joints designed with high-strength concrete, but again provided no specifics. Ehsani et al. found that even in the presence of high flexural strength ratios, high joint shear stresses significantly reduce the energy-absorption capability of beam-column joints. Ehsani et al. also observed that specimens with lower joint shear stresses could withstand more cycles of loading, which ultimately resulted in more severe damage to the concrete, exposing the bars that then buckled.

Ehsani and Alameddine (1991)

Ehsani and Alameddine (1991) tested 12 exterior beam-column joint specimens to investigate the effects of joint shear stress and confining reinforcement within the joint region on the behavior of high-strength reinforced concrete beam-column joints subjected to reversed cyclic loading. The main variables were concrete compressive strength, ranging from 8,600 to 13,700 psi, joint shear stress, 1100 or 1400 psi, and the amount of confining reinforcement within the joint region, 4 or 6 No. 4 hoops. A constant axial load was applied to the columns ranging from 50 to 136 kips. The yield strength of the No. 8 and No. 9 hooked bars ranged from 64,200 to 66,300 psi. The center-to-center spacing between the hooked bars ranged from 1.92 to $2.17d_b$ (2.17 in.), and the clear side concrete cover to the hooked bar was 3 in., and the embedment length of the hooked bars was 10.5 in. Ehsani and Alameddine concluded that the joint shear stress and the confining reinforcement within the joint region are the key factors in achieving adequate strength and ductility of the joint. In addition, they observed that a column to beam flexural strength ratio of at least 1.4 is essential in helping formation of a plastic hinge in the beam rather than the column. Ehsani and Alameddine found that the deterioration of the joint concrete was delayed significantly and the cyclic load carrying capacity of the specimens was more stable throughout the test in beam-column joint specimens subjected low joint shear stress, on the order of $12\sqrt{8000}$ (≈ 1100 psi). They observed that increasing the confining reinforcement in the joint region provides additional confinement for the joint concrete and delays joint deterioration. Ehsani and Alameddine observed that by increasing the confining reinforcement and decreasing the joint shear stress, slippage or pullout of the hooked bars was reduced or delayed.

Kaku and Asakusa (1991)

Kaku and Asakusa (1991) tested 18 reinforced concrete exterior beam-column joint specimens under reversed cyclic loading. The specimens were designed so that either the beam or the column bars yielded prior to joint shear failure. The main variables were column axial load, amount of confining reinforcement within the joint region, and the presence of intermediate column bars. Concrete compressive strengths ranged from 4,510 to 6,730 psi, and the yield strength of the No. 4 hooked bars was 56,700 psi. The center-to-center spacing between the hooked bars was $3.3d_b$ (1.7 in.), and the clear side concrete cover to the hooked bar was $3.2d_b$ (1.6 in.). The embedment length of the hooked bars was $15.4d_b$ (7.7 in.). A constant axial load was applied to the columns ranging from 0 to 81 kips. Kaku and Asakusa found that the ductility of the exterior beam-column joints increased as the column axial load and the amount of confining reinforcement within the joint region increased. They also observed that the presence of intermediate column bars increased the ductility of the specimens.

Tsonos et al. (1992)

Tsonos et al. (1992) tested 20 exterior beam-column joint specimens to investigate the behavior of external beam-column joints constructed with inclined column longitudinal reinforcing bars within the joint and tested under reversed cyclic loading. Figure D.1 shows schematic drawings of exterior beam-column joints with conventional and nonconventional column longitudinal reinforcing bars. The main variables were the number of inclined reinforcing bars, the ratio of the column-to-beam flexural strength, and the joint shear stress. The 20 specimens tested in eight series. In six series, the first specimen in each series was constructed with conventional column longitudinal reinforcement, while the second specimen was constructed with four crossed, inclined bars bent diagonally across the joint core, as shown in Figure D.1. Another series had two specimens constructed with conventional column longitudinal reinforcement and one specimen constructed with four crossed, inclined bars bent diagonally across the joint core. The last series had five specimens constructed with conventional column longitudinal reinforcement, two of which were cast with fiber-reinforced concrete containing 1.0 percent by volume of steel fibers. Concrete compressive strengths ranged from 3,770 to 5,360 psi, and the yield strength of the No. 4 (D14) hooked bars ranged from 70,300 to 76,700 psi. The center-to-

center spacing between the hooked bars ranged from 3.6 to $10.7d_b$ (1.97 to 5.91 in.), and the clear side concrete cover to the hooked bar ranged from 1.3 to $1.5d_b$ (0.71 in.). The embedment length of the hooked bars ranged from 11.8 to $13.8d_b$ (6.5 in.). Tsonos et al. found that the use of crossed inclined reinforcing bars (nonconventional column longitudinal reinforcing bars) in the joint region is one of the most efficient methods to improve the seismic resistance of exterior beam-column joints. They reported that external beam-column joints with crossed inclined reinforcing bars exhibited high strength and no significant degradation after reaching their maximum capacity and that the presence of crossed inclined reinforcing bars introduces an additional new mechanism of shear transfer. Tsonos et al. found that both exterior beam-column joints, conventionally reinforced and with crossed inclined reinforcing bars, performed satisfactorily with low joint shear stress and high column-beam flexural strength ratios.

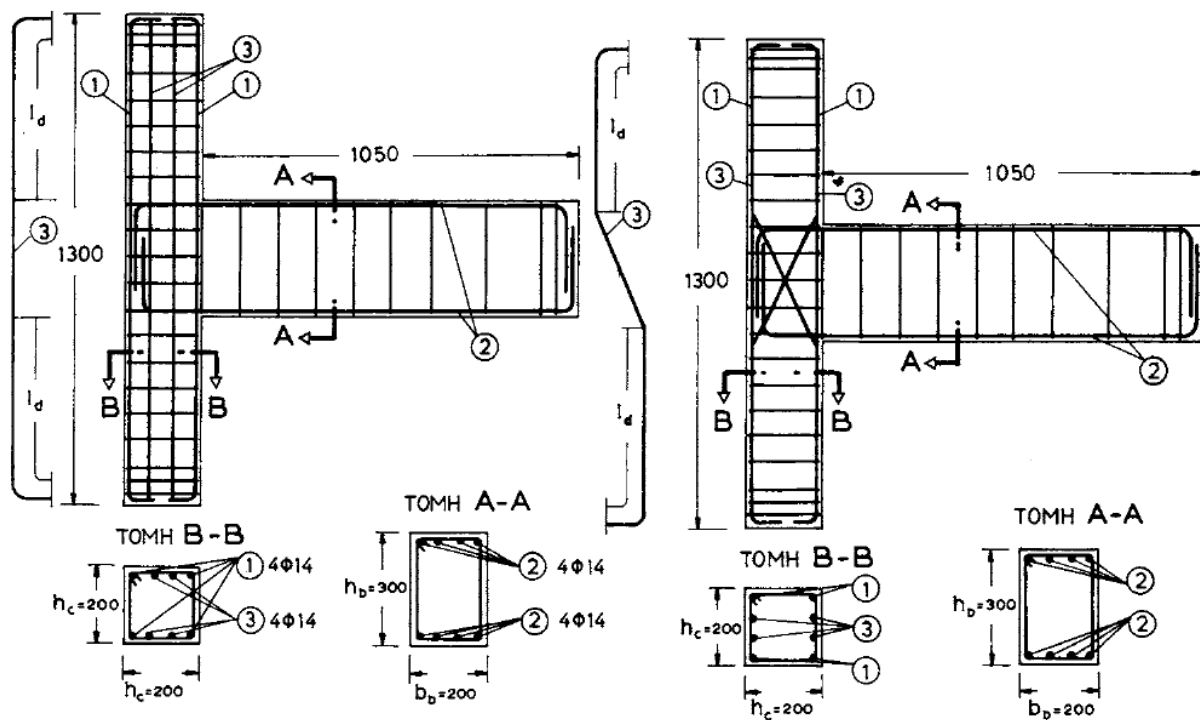


Figure D.1 Schematic drawings of exterior beam-column joints with conventional and nonconventional column longitudinal reinforcing bars (Tsonos et al. 1992)

Pantelides et al. (2002)

Pantelides et al. (2002) tested four exterior beam-column joint specimens under reversed cyclic loading. They examined the performance of the specimens in terms of lateral load capacity,

drift ratio (ratio of displacement at the loading point in the direction of the load to the distance between the loading point and the beam-column joint's center), axial load, joint shear stress, ductility, and residual strength. Two column axial load levels ($0.1f'_cA_g$ and $0.25f'_cA_g$) were used to investigate their effect on the performance of the joints subjected to reversed cyclic loading, where f'_c is the design concrete compressive strength (psi) and A_g is the cross-section area of the column. There was no confining reinforcement within the joint region. All specimens had the same dimensions and detailing. The width and depth of the beams were 12 and 16 in., respectively. Four No. 9 hooked reinforcing bars were used as beam top and bottom longitudinal reinforcement. The column width was 12 in., and the depth was 18 in. The column was reinforced with eight No. 7 bars evenly distributed around the perimeter. Concrete compressive strengths ranged from 5,370 to 6,700 psi, and the yield strength of the No. 9 hooked bars was 65,900 psi. The center-to-center spacing between the hooked bars was $2.1d_b$ (2.4 in.), and the clear side concrete cover to the hooked bar was $1.7d_b$ (1.9 in.). The embedment length of the hooked bars was $14.3d_b$ (16.1 in.). Pantelides et al. found that specimens with lower axial loads were 1.7 times more ductile than those with higher column axial loads. The specimens subjected to the higher axial load dissipated 20% less energy than those subjected to the smaller level of axial load. In addition, Pantelides et al. discovered that yielding of the beam longitudinal bars began at drift ratios of 0.5 to 0.6% for specimens with the $0.1f'_cA_g$ axial column load, while for specimens with the $0.25f'_cA_g$ axial load, yielding did not begin until drift ratios of 0.7 to 1%.

Chutarat and Aboutaha (2003)

Chutarat and Aboutaha (2003) tested four exterior beam-column joint specimens with hooked bars as the main beam longitudinal reinforcement under reversed cyclic loading to investigate a practical solution for relocating potential beam plastic hinge regions by the use of straight-headed bars, as shown in Figure D.2. Two of the four specimens were tested with additional straight-headed bars and two without the additional bars. The straight-headed bars extended 20 in. into the beam for specimens with a relocated beam plastic hinge region, as shown in Figure D.2. The concrete compressive strength ranged from 4,000 to 4,800 psi, and the yield strength of the No. 8 hooked bars was 70,000 psi. The center-to-center spacing between the hooked bars was $2.8d_b$ (2.8 in.), and the clear side concrete cover to the hooked bar was $3.3d_b$ (3.3 in.).

The embedment length of the hooked bars was $12.8d_b$ (12.8 in.). Chutarat and Aboutaha concluded that the beam plastic hinge region can be successfully moved from the column face to an exact predetermined location using straight-headed bars. They found that specimens with straight-headed bars developed a beam plastic hinge away from the face of the column near the head of the straight-headed bars, and the specimens developed their ultimate strength by fracture of the beam longitudinal bars.

Figure D.2 Schematic drawings of exterior beam-column joints with and without straight-headed bars (Chutarat and Aboutaha 2003)

Hwang et al. (2005) tested nine exterior beam-column joint specimens to investigate the effect of confining reinforcement within the joint region on the shear strength and behavior of exterior beam-column joints subjected to reversed cyclic loading. The main parameters were the quantity and detailing of the confining reinforcement within the joint region. In all specimens, shear reinforcement in the beam and columns was sufficient to prevent shear failure outside the joint. Concrete compressive strengths ranged from 8,960 to 11,140 psi, and the yield strength of the No. 8 hooked bars ranged from 62,400 to 71,200 psi. The center-to-center spacing between the

hooked bars was $2.5d_b$ (2.5 in.), and the clear side concrete cover to the hooked bar was $4d_b$ (4 in.). The embedment length of the hooked bars ranged from 13.7 to $15.5d_b$ (13.7 to 15.5 in.). Hwang et al. concluded that the primary role of the confining reinforcement within the joint region is to carry shear as a tension tie and to constrain the width of the crack. They also found that less confining reinforcement within the joint region with wider spacing could be used without significantly affecting the performance of the beam-column joints. Hwang et al. observed that confining reinforcement within the joint region effectively restrained the deterioration of exterior beam-column joints subjected to reversed cyclic loading.

Lee and Ko (2007)

Lee and Ko (2007) tested five exterior beam-column joint specimens to investigate the effect of the eccentricity between the beam and column centerline on the performance of exterior beam-column joints subjected to reversed cyclic loading. The exterior beam-column joints were constructed with one concentric or eccentric beam framing into a rectangular column in the strong or weak direction, as shown in Figure D.3. The main variables were the lateral loading directions and the eccentricity between the beam and column centerlines. As shown in Figure D.3, the five specimens are designated as S0, S50 (Series S), W0, W75, and W150 (Series W). The first character of the designation (S or W) represents one south or west beam framing into the rectangular column in either the strong or weak direction. Two concentric (S0 and W0) and three eccentric (S50, W75, and W150) joints were tested. The column had dimensions of 16×24 in. and was reinforced with 12 No. 7 longitudinal bars distributed evenly around the cross-section. The beam was 12×18 in. and reinforced with four No. 7 longitudinal bars at both the top and bottom. Concrete compressive strengths ranged from 4,190 to 4,730 psi, and the yield strength of hooked bars was 66,000 psi. The center-to-center spacing between the hooked bars was $2.3d_b$ (2.0 in.), and the clear side concrete cover to the hooked bar ranged from 5.2 to $9.8d_b$ (4.6 to 8.6 in.). The embedment length of the hooked bars ranged from 15 to $24d_b$ (13.1 to 21.0 in.). A constant axial load $0.1f'_cA_g$ was applied to the columns, where f'_c is the design concrete compressive strength and A_g is the area of column cross-section. Lee and Ko found that the joint shear capacity of a rectangular joint is greater in the strong direction than in the weak direction. They observed that specimens subjected to lateral loading in the strong direction were capable of supporting the

complete formation of a beam plastic hinge, whereas specimens with the joint shear acting along the weak direction of the column exhibited significant damage at the joints. Lee and Ko concluded that the joint eccentricity between the centerlines of the beam and the column had a detrimental effect on the performance of the beam-column joints subjected to reversed cyclic loading. They found that little effect on the performance of beam-column joints for a joint eccentricity of $b_c/8$, where b_c is the width of the column, but observed significant reductions in the strength, ductility, and energy dissipation capacity when the eccentricity increased to $b_c/4$.

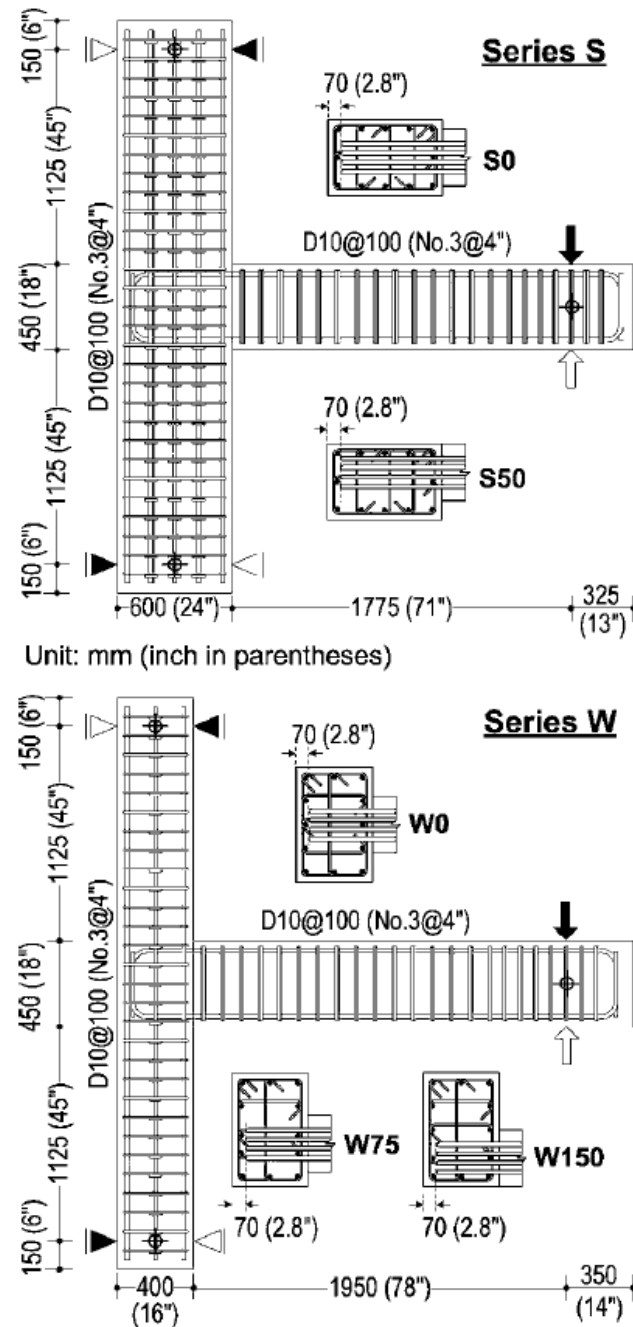


Figure D.3 Schematic drawings of exterior beam-column joints with one concentric or eccentric beam (Lee and Ko 2007)

Chun et al. (2007)

Chun et al. (2007) investigated the effect of the anchorage type (hooked or headed bars) and the bar size on the anchorage strength of exterior joint specimens subjected to reversed cyclic loading. Seven exterior and five knee beam-column joints and two wide-beam-to-wall joint specimens were tested. Concrete compressive strengths ranged from 4,760 to 8,950 psi. Beam

reinforcement consisted of D22 (No. 7), D25 (No. 8), or D36 (No. 11) hooked and headed bars with actual yield strengths ranging between 58,450 and 67,880 psi. The center-to-center spacing between the longitudinal reinforcing bars of the beam ranged from 3 to $6.6d_b$ (3.4 to 6.6 in.), and the clear side concrete cover to the bar ranged from 2.1 to $4.3d_b$ (1.9 to 6 in.). The embedment lengths of the anchored bars ranged from 12.3 to $18d_b$ (13.9 to 18.9 in.). The joints were designed and constructed in accordance with the ACI 352R-02 requirements for Type 1 and Type 2 joints. Type 1 joints are designed for non-seismic requirements and do not take into account significant inelastic deformation, whereas Type 2 joints are designed for seismic loading and take into account deformation due to load reversals into the inelastic range. A constant column axial load of 110 kips ($0.05A_gf'_c$) was applied to the specimens containing No. 7 and No. 8 bars, where f'_c is the design concrete compressive strength and A_g is the gross cross-sectional area of the column. The test specimens were designed based on a strong column-weak beam to ensure yielding of the anchored bars. The specimens were loaded to five drift levels corresponding to 1, 2, 4, 8, and 12 times the displacement at first yield, with three cycles per drift level, except for the specimens containing No. 11 bars, which were loaded monotonically while increasing the drift level from 0.5 to 10%. The first drift level was selected to be within an elastic range in all cases. Chun et al. found that exterior beam-column joint specimens constructed with headed and hooked bars and tested under reversed cyclic loading showed similar hysteretic behavior. Specimens with both hooked and headed bars maintained the peak load at approximately 4% drift and 80% of the peak load at 3.5% drift.

Tsonos (2007)

Tsonos (2007) tested four exterior beam-column joint specimens to study the performance of the joints subjected to reversed cyclic loading. The main parameters were the column-beam flexural strength ratio, amount of confining reinforcement within the joint region, and joint shear stress. The cross-sectional dimensions of the four specimens were identical, but the reinforcement ratios varied. The beam dimensions were 8×12 in., and the column dimensions were 8×8 in. Three specimens (E_1 , E_2 , and G_1) had the same longitudinal column reinforcement, eight No. 4 bars, whereas the fourth specimen (A_1) consisted of eight No. 3 bars distributed evenly around the column cross-section. Specimens E_1 and G_1 had three No. 4 hooked bars each as top and bottom

beam reinforcement, while specimens A₁ and E₂ had four No. 3 hooked bars and two No. 4 hooked bars as top and bottom beam reinforcement, respectively. The longitudinal beam reinforcement was chosen to produce low joint shear stresses in specimens A₁ and E₂, and high joint shear stresses in specimens E₁ and G₁. Confining reinforcement within the region ranged from 2 to 5 No. 2 hoops. The specimens were subjected to a constant axial load of 45 kips throughout the test. Concrete compressive strengths ranged from 3,190 to 5,080 psi, and the yield strength of hooked bars ranged from 72,000 to 73,000 psi. The center-to-center spacing between the hooked bars ranged from 4.7 to 10.0 d_b (1.8 to 5.5 in.), and the clear side concrete cover to the hooked bars ranged from 1.6 to 2.5 d_b (0.9 to 1.0 in.). The embedment length of the hooked bars ranged from 11.6 to 16.5 d_b (6.4 to 6.5 in.). Tsonos found that specimens with low joint shear stresses showed satisfactory performance, and failed in beam flexural, while specimens with high joint shear stress performed poorly and exhibited joint shear failure.

Kang et al. (2010)

Kang et al. (2010) tested two exterior beam-column joint specimens to investigate the seismic behavior of the anchored bars in exterior beam-column joints subjected to reversed cyclic loading. One specimen contained No. 6 bars with a 90-degree hook and the other contained bars of the same size with a head as beam longitudinal reinforcing bars, as shown in Figure D.4. Both beam-column joint specimens contained four No. 6 (D19) anchored bars as top and bottom beam reinforcement anchored in the column with an embedment length of 15 d_b . The joint region contained 4 No. 3 (D10) hoops as confining reinforcement. Concrete compressive strengths were 4200 psi and 4220 psi for specimens with hooked and headed bars, respectively, and the yield strengths of the hooked and headed bars were 66,700 psi and 69,750 psi, respectively. No axial load was placed on the columns. The specimens were loaded to drift levels of 0.4 to 3.5%, with three cycles at each drift level. Kang et al. discovered that both specimens behaved in a relatively ductile manner failed by beam flexural yielding. The specimens reached the peak loads at drifts of 2 to 2.5% and maintained that maximum load until about 3.58% drift for specimens with headed bars, whereas for specimens with hooked bars, after reaching the peak load, subsequently dropped to 80% of the peak load at 3.46% drift.

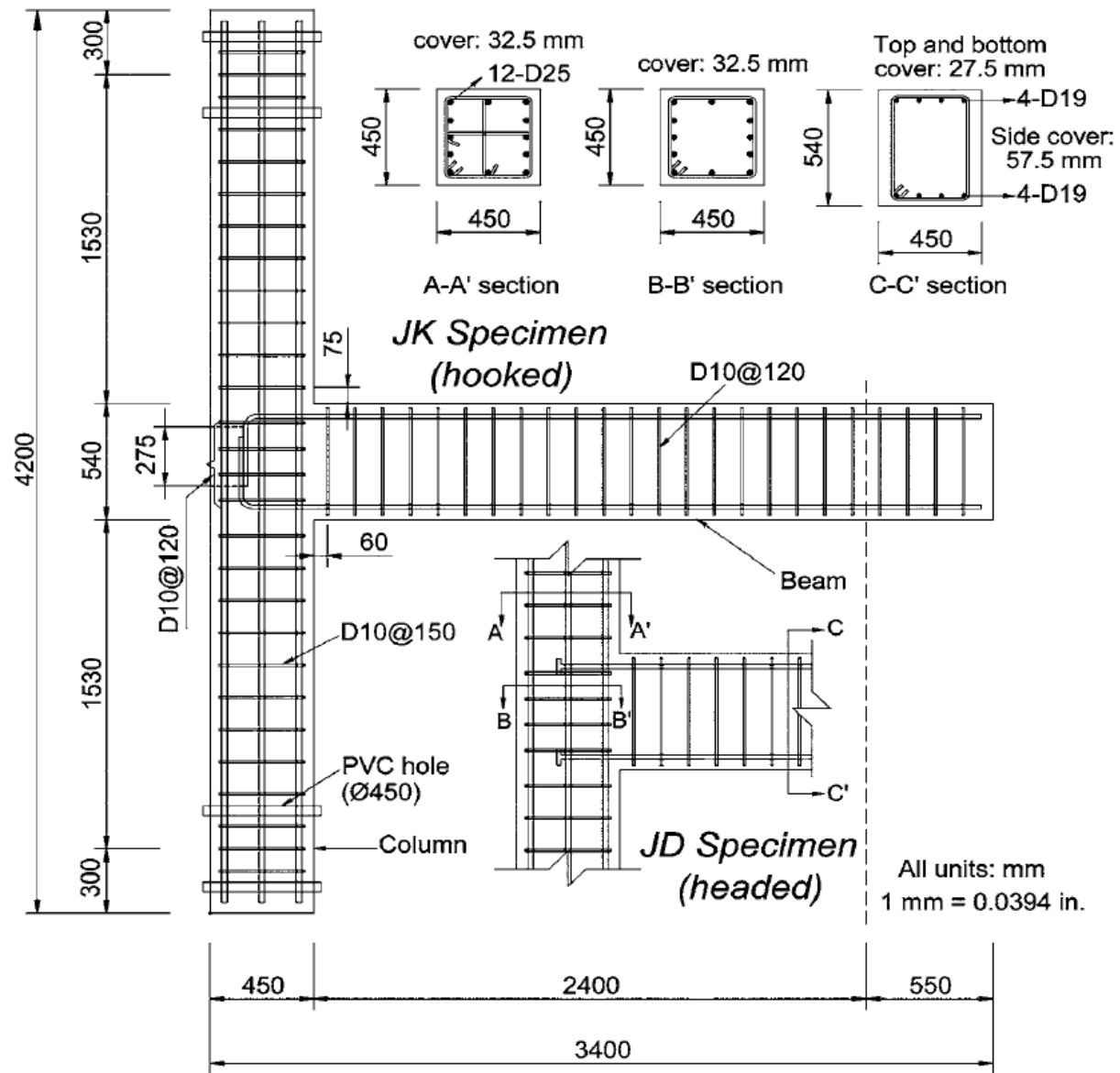


Figure D.4 Detail of exterior beam-column joint specimens containing hooked and headed bars (Kang et al. 2010)

Chun and Shin (2014)

Chun and Shin (2014) tested 14 exterior beam-column joint specimens to examine the effect of joint aspect ratio (beam depth to column depth) and confining reinforcement on the anchorage strength of hooked and headed bars in exterior beam-column joints subjected to reversed cyclic loading. The main variables were the joint aspect ratio (0.67 to 2.5), the amount of confining reinforcement within the joint region (four specimens with joint aspect ratios of 0.67 and 1.0 had two-thirds of the confining reinforcement required by ACI 352 and the remaining 10,

with joint aspect ratios of 1.5, 2.0 and 2.5, had the full amount of the confining reinforcement required by ACI 352), and anchorage type for the beam bars (hooks or heads). Seven of the 14 exterior beam-column joints contained standard 90° hooked bars, and seven had headed bars as the longitudinal reinforcement of the beam. The specimens had a 12 × 12 in. column and a 9.8 in. wide beam; total beam depths ranged from 7.9 to 29.5 in. depending on the joint aspect ratio. Ten of the specimens contained confining reinforcement consisting of three legs - two D13 (No. 4) legs in the form of a hoop and one D10 (No. 3) leg in the form of a cross tie – spaced at 3 in. within the joint region, in accordance with the joint confining reinforcement requirements of Section 4.2.2.2 of ACI 352R-02. In the other four specimens also had three legs spaced at 3 in., but the hoop was reduced to a D10 (No. 3), resulting in two-thirds of the confining reinforcement required in Section 4.2.2.2 of ACI 352R-02. The top and bottom bars for the beam reinforcing bars consisted of four and three D19 (No. 6) bars, respectively. The center-to-center spacing between the longitudinal reinforcing bars of the beam was $2.3d_b$ (1.75 in.), and the clear side concrete cover to the bar was $3.9d_b$ (3.0 in.). The embedment length of the bars in all specimens was $12d_b$ (9 in.). Concrete compressive strengths were between 3,710 and 3,830 psi. No column axial load was applied during the test.

The peak moments were 1.1% to 24% greater than the nominal moment capacity based on the yield strengths of the beam reinforcement. All specimens maintained their peak load at a 3.5% drift ratio. Specimens with joint aspect ratios less than or equal to 1.0 failed by flexural hinging at the beam away from the joint with limited joint damage. Specimens with joint aspect ratios equal to or greater than or equal to 1.5 failed by hinging at the column, with extensive joint deterioration characterized by substantial spalling of the joint cover concrete. As the joint aspect ratio increased, the joint damage increased while beam damage decreased. Chun and Shin found that for joint aspect ratios less than or equal to 1.0, joints with less confining reinforcement (two-thirds of the confining reinforcement required by ACI 352) exhibited similar behavior to the joints designed in accordance with ACI 352R-02. Chun and Shin discovered that there was no significant difference in failure modes, moment-drift relation, joint distortion, and energy dissipation between specimens with hooked bars or headed bars.

Hwang et al. (2014)

Hwang et al. (2014) tested three exterior beam-column joint specimens to evaluate the performance of exterior beam-column joints constructed with high-strength (87,000 psi) beam flexural reinforcement under reversed cyclic loading. The main parameters were the diameter and the yield strength of the beam longitudinal reinforcing bars. The specimens had beam and column cross-sectional dimensions of 350×500 mm (14×20 in.) and 500×550 mm (20×22 in.), respectively. Four legs (two hoops) of D13 (No. 4) spaced at 100 mm (4 in.) were used as confining reinforcement within the joint region in all three specimens. Concrete compressive strengths ranged from 4,290 to 4,640 psi, and the yield strength of hooked bars ranged from 75,400 to 103,000 psi. The diameter of the hooked bars ranged from D19 to D25 (No. 6 to No. 8), as shown in Figure D.5. The center-to-center spacing between the hooked bars ranged from 3.25 to $3.71d_b$ (3.25 in.), and the clear side concrete cover to the hooked bars ranged from 4.5 to $5.1d_b$ (4.5 in.). The embedment length of the hooked bars ranged from 19.6 to $22.4d_b$ (19.6 in.). No axial load was applied to the column. Hwang et al. found that due to insufficient hooked bar development length in compression, concrete cover spalling and punching occurred at the location of the beam bottom bars in the exterior face of the column, in addition to the concrete crushing at the beam bottom. Hwang et al. concluded that the load-carrying capacities of exterior beam-column joints subjected to reversed cyclic loading with high-strength (87,000 psi) beam flexural reinforcement agreed with the predicted nominal strengths.

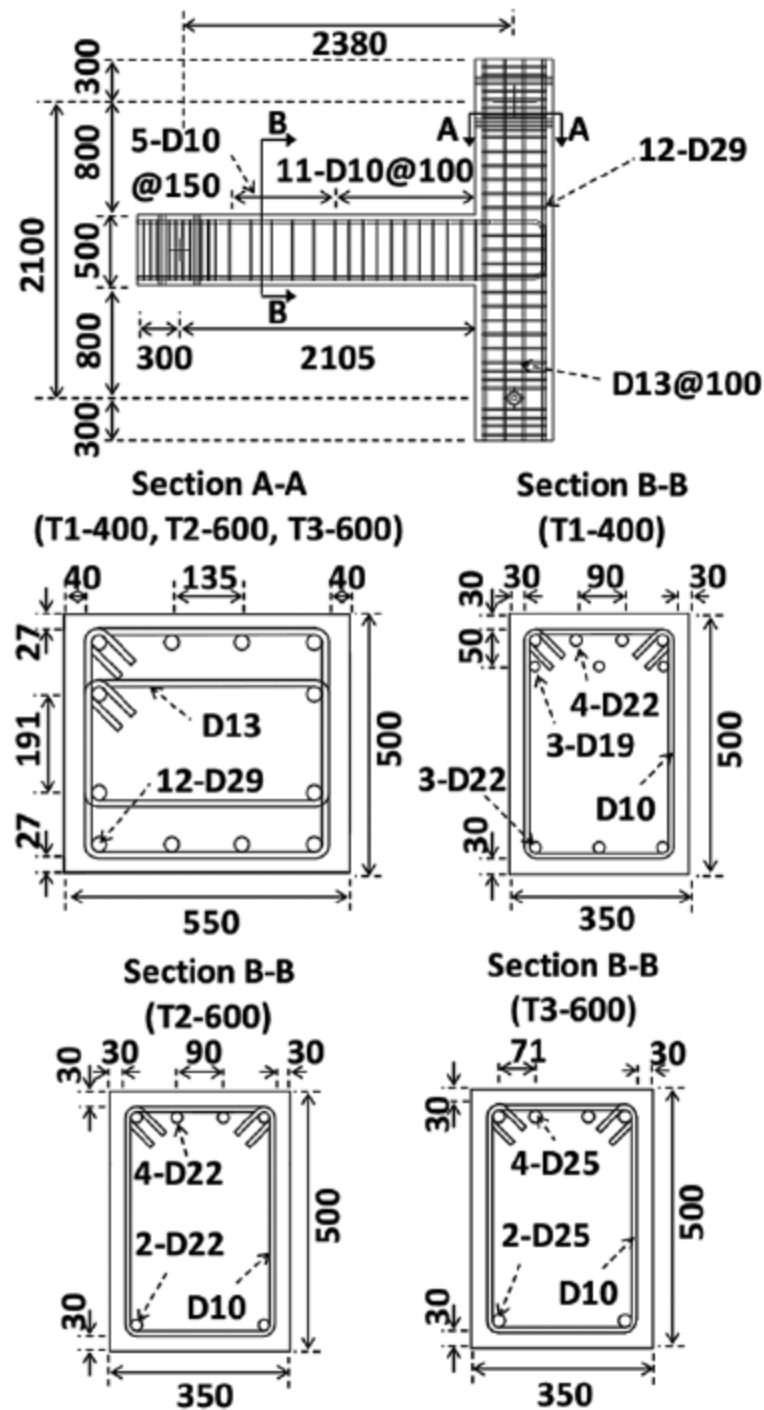


Figure D.5 Detail of exterior beam-column joint specimens (Hwang et al. 2014)

Choi and Bae (2019)

Choi and Bae (2019) tested seven exterior beam-column joint specimens to investigate the effect of steel fibers on the anchorage strength and behavior of exterior beam-column joints

subjected to reversed cyclic loading. The main parameters were the presence of steel fibers, the amount of confining reinforcement within the joint region, and the spacing between the confining reinforcement in the beam. Of the seven specimens, four had steel fibers with and without the presence of confining reinforcement within the joint region, and three did not; of the three specimens without steel fibers, two had confining reinforcement within the joint region and one had none. A constant axial load of $0.1f'_cA_g$ was applied to the column throughout the test, where f'_c is the design concrete compressive strength and A_g is the area of column cross-section. The beam and column cross-sectional were, respectively, 250×375 mm (10×15 in.) and 300×300 mm (12×12 in.). Confining reinforcement within the joint region consisted of two legs (a hoop) of D13 (No. 4) spaced at 60 mm (2.4 in.). The concrete compressive strength was 7,950 psi, and the yield strength of the hooked bars was 68,400 psi. Two D25 (No. 8) hooked bars were used as longitudinal beam reinforcing bars at the top and bottom of the beam. The center-to-center spacing between the hooked bars was $4.6d_b$ (4.6 in.), and the clear side concrete cover to the hooked bar was $3.1d_b$ (3.1 in.). The embedment length of the hooked bars was $8.3d_b$ (8.3 in.). Choi and Bae found that steel fibers increase joint strength even when no hoops are present. They also observed that the bond strength between reinforcement and concrete in the joint region increased as the steel fiber content increased, but the rate of increase in strength decreased with increasing steel fiber content. Choi and Bae discovered that using an adequate quantity of steel fibers in exterior beam-column joints can change the mode of failure from joint shear failure to beam flexural failure.

